

Vera Murgul
Zdenka Popovic *Editors*

International Scientific
Conference Energy
Management of Municipal
Transportation Facilities
and Transport EMMFT 2017



Advances in Intelligent Systems and Computing

Volume 692

Series editor

Janusz Kacprzyk, Polish Academy of Sciences, Warsaw, Poland
e-mail: kacprzyk@ibspan.waw.pl

About this Series

The series “Advances in Intelligent Systems and Computing” contains publications on theory, applications, and design methods of Intelligent Systems and Intelligent Computing. Virtually all disciplines such as engineering, natural sciences, computer and information science, ICT, economics, business, e-commerce, environment, healthcare, life science are covered. The list of topics spans all the areas of modern intelligent systems and computing.

The publications within “Advances in Intelligent Systems and Computing” are primarily textbooks and proceedings of important conferences, symposia and congresses. They cover significant recent developments in the field, both of a foundational and applicable character. An important characteristic feature of the series is the short publication time and world-wide distribution. This permits a rapid and broad dissemination of research results.

Advisory Board

Chairman

Nikhil R. Pal, Indian Statistical Institute, Kolkata, India

e-mail: nikhil@isical.ac.in

Members

Rafael Bello Perez, Universidad Central “Marta Abreu” de Las Villas, Santa Clara, Cuba

e-mail: rbellop@uclv.edu.cu

Emilio S. Corchado, University of Salamanca, Salamanca, Spain

e-mail: escorchado@usal.es

Hani Hagrass, University of Essex, Colchester, UK

e-mail: hani@essex.ac.uk

László T. Kóczy, Széchenyi István University, Győr, Hungary

e-mail: koczy@sze.hu

Vladik Kreinovich, University of Texas at El Paso, El Paso, USA

e-mail: vladik@utep.edu

Chin-Teng Lin, National Chiao Tung University, Hsinchu, Taiwan

e-mail: ctlin@mail.nctu.edu.tw

Jie Lu, University of Technology, Sydney, Australia

e-mail: Jie.Lu@uts.edu.au

Patricia Melin, Tijuana Institute of Technology, Tijuana, Mexico

e-mail: epmelin@hafsamx.org

Nadia Nedjah, State University of Rio de Janeiro, Rio de Janeiro, Brazil

e-mail: nadia@eng.uerj.br

Ngoc Thanh Nguyen, Wroclaw University of Technology, Wroclaw, Poland

e-mail: Ngoc-Thanh.Nguyen@pwr.edu.pl

Jun Wang, The Chinese University of Hong Kong, Shatin, Hong Kong

e-mail: jwang@mae.cuhk.edu.hk

More information about this series at <http://www.springer.com/series/11156>

Vera Murgul · Zdenka Popovic
Editors

International Scientific
Conference Energy
Management of Municipal
Transportation Facilities
and Transport EMMFT 2017



 Springer

Editors

Vera Murgul
Moscow State University of Civil
Engineering
Moscow
Russia

Zdenka Popovic
Department of Roads, Airports
and Railways, Faculty of Civil
Engineering
University of Belgrade
Belgrade
Serbia

ISSN 2194-5357

ISSN 2194-5365 (electronic)

Advances in Intelligent Systems and Computing

ISBN 978-3-319-70986-4

ISBN 978-3-319-70987-1 (eBook)

<https://doi.org/10.1007/978-3-319-70987-1>

Library of Congress Control Number: 2017959627

© Springer International Publishing AG 2018

This work is subject to copyright. All rights are reserved by the Publisher, whether the whole or part of the material is concerned, specifically the rights of translation, reprinting, reuse of illustrations, recitation, broadcasting, reproduction on microfilms or in any other physical way, and transmission or information storage and retrieval, electronic adaptation, computer software, or by similar or dissimilar methodology now known or hereafter developed.

The use of general descriptive names, registered names, trademarks, service marks, etc. in this publication does not imply, even in the absence of a specific statement, that such names are exempt from the relevant protective laws and regulations and therefore free for general use.

The publisher, the authors and the editors are safe to assume that the advice and information in this book are believed to be true and accurate at the date of publication. Neither the publisher nor the authors or the editors give a warranty, express or implied, with respect to the material contained herein or for any errors or omissions that may have been made. The publisher remains neutral with regard to jurisdictional claims in published maps and institutional affiliations.

Printed on acid-free paper

This Springer imprint is published by Springer Nature

The registered company is Springer International Publishing AG

The registered company address is: Gewerbestrasse 11, 6330 Cham, Switzerland

Preface

The nineteenth international scientific conference Energy Management of Municipal Transportation Facilities and Transport EMMFT 2017 took place in Khabarovsk on 10–13 April 2017.

The conference was hosted by Far Eastern State Transport University, Russia.

Far Eastern State Transport University has an 80-year-long history and prepares high-qualified specialists in transport engineering. It takes one of the leading positions among the country's technical universities in the rating of the Ministry of Education and Science of Russia.

Far Eastern State Transport University annually hosts international scientific conferences. This year the authors from several countries submitted approximately 800 qualified papers to EMMFT 2017 conference. The conference included several workshops.

Within the conference, the participants discussed a wide range of scientific and research issues including Russian and foreign experience of managing multimodal transportation, improving the efficiency of functionality of locomotives, electric locomotives, traction substations, electrical substations, relay protection and automation devices and power-factor correction units. The speakers shared their opinions on using renewable energy sources, problems of mathematical and simulation modelling of electromagnetic processes of electrical power objects and systems, aspects of cost reduction for fuel-and-power resources, theoretical aspects of energy management, development of transport infrastructure, modern organizational and technological solutions in construction, new approaches in the field of management, analysis and monitoring in transport sector.

Discussions about relevant application and theoretical problems of present-day energy management significantly contribute not only to the increase in effectiveness of modern vocational education, but also to the development of applied scientific researches aimed at efficiency enhancement of transport and energetics functioning.

All papers passed a four-stage review. The first stage consisted in the examination for compliance with the subject of conference. At the second stage, all papers were thoroughly checked for plagiarism. Acceptable minimum of originality was 90%. The third stage involved the review by a native speaker for acceptable English

language. At the same time, papers were checked by a technical proofreader. The fourth stage involved a scientific review made by at least three reviewers. If opinions of the reviewers were radically different, additional reviewers were appointed. We did not use “Potential Reviewers” recommended by authors. After the review had been accomplished, 300 qualified papers were accepted.

The members of our organizing committee express their deep gratitude to the crew of journal “Advances in Intelligent Systems and Computing” and to editorial department Springer International Publishing AG for publication of Selected Papers of conference EMMFT 2017.

We also accord special thanks to our project coordinator Mr. Arulmurugan Venkatasalam for his instant responses to our questions, great support, participation and entering into all the nuances of our work. We appreciate his help in preparation for our EMMFT 2017 conference volume.

Zdenka Popovic
Vera Murgul

Organization

On the Organizing Committee of the Conference Were

Sergei Kudriavtcev	Far Eastern State Transport University, Russia
Vera Murgul	Moscow State University of Civil Engineering, Russia
Arkadii Edigarian	Far Eastern State Transport University, Russia
Zdenka Popovic	University of Belgrade, Serbia
Andrey Pustovgar	Moscow State University of Civil Engineering, Russia
Olga Kalinina	Peter the Great St. Petersburg Polytechnic University, Russia

On the Scientific Committee of the Conference Were

Sergei Kudriavtcev	Far Eastern State Transport University, Russia
Andrey Pustovgar	Moscow State University of Civil Engineering, Russia
Igor V. Ilyin	Peter the Great Saint-Petersburg Polytechnic University, Russia
Zdenka Popovic	University of Belgrade, Serbia
Miroslav Premrov	University of Maribor, Slovenia
Vitaly Sergeev	Peter the Great St. Petersburg Polytechnic University, Russia
Olga Kalinina	Peter the Great St. Petersburg Polytechnic University, Russia
Angela Mottaeva	Moscow State University of Civil Engineering, Russia
Tanja Mihalič	Ljubljana University, Slovenia
Boštjan Kovačič	University of Maribor, Slovenia
Rok Kamnik	University of Maribor, Slovenia
Tjaša Štrukelj	University of Maribor, Slovenia
Simona Sternad	University of Maribor, Slovenia
Zabukovšek	
Smiljana Zajec	Ljubljana University, Slovenia

Manfred Esser	CEO-GET Information Technology GmbH, Germany
Andrii Bieliatynskyi	National Aviation University, Ukraine
Vera Murgul	Moscow State University of Civil Engineering, Russia
Aleksey Adamtsevich	Moscow State University of Civil Engineering, Russia
Liubov Shilova	Moscow State University of Civil Engineering, Russia
Ewa Więcek-Janka	Poznan University of Technology, Poznan, Poland
Tadeusz Mikołajczyk	University of Technology and Life Sciences in Bydgoszcz, Poland
Tomas Hanak	Brno University of Technology, Czech Republic
Anatolijs Borodinecs	Riga Technical University, Latvia
Luís Bragança	University of Minho, Portugal
Paulo Cachim	University of Aveiro, Portugal
Milorad Jovanovski	Ss. Cyril and Methodius University in Skopje, Macedonia
Milan Veljkovic	Lulea University of Technology, Sweden
Biljana Stamatovic	Donja Gorica University of Donja Gorica, Montenegro
Petya Dankova	University of Economics, Varna, Bulgaria
Stanislav V. Vlasevskii	Far Eastern State Transport University, Russia
Valerii N. Li	Far Eastern State Transport University, Russia
Slobodan Ognjenovic	Ss. Cyril and Methodius University in Skopje, Macedonia
Ivana Barišić	University of Osijek, Croatia
Jaroslav Matuška	University of Pardubice, Czech Republic

Contents

Electric Power Systems and Electromechanical Systems	
Interaction Phenomenon Between Train, Track and Bridge	3
Zdenka Popović, Luka Lazarević, Milica Vilotijević, and Nikola Mirković	
Improvement of Current Collection System with a Rigid Current Distributor for Overhead Transport	12
Oleg Sidorov, Vladimir Goryunov, Valery Tomilov, and Ilya Salya	
Improvement of the Methodology for Improvement of the Turn-to-Turn Short Circuit Detection in the Driving Motor Anchor Winding	24
Viktor Kharlamov, Pavel Shkodun, and Ignat Shestakov	
Selection and Validation of the Mathematical Model for the Solution of the Optimization Problem of Fuel Cost Efficiency Improvement of the Locomotive Diesel Engines	31
Alexandr Anisimov and Vitaly Chetvergov	
Improvement of Traction Rolling Stock Energy Efficiency Analysis System	48
Elena Sidorova and Svetlana Podgornaya	
Simulation of Wear Processes of the Monorail Electrical Transport Current Collector Contact Elements	59
Oleg Sidorov and Victor Philippov	
Determination of the Electrical Locomotive Energy Efficiency to Evaluate Its Repair Quality	69
Sergei Shantarenko, Mikhail Kapustyan, and Oleg Supchinsky	

Application of Magnetic Wedges for Stator and Rotor Slots of DC Motors	76
Viktor Kharlamov, Yuriy Moskalev, and Denis Popov	
Intelligent Automated System for the Monitoring of Railway Areas with a Low Transport Process Energy Efficiency	83
Vasily Cheremisin, Mikhail Nikiforov, Alexey Kashtanov, and Sergey Ushakov	
Intelligent Traction Power Supply System	91
Vasilii Zakaryukin, Andrey Kryukov, and Aleksandr Cherepanov	
Mathematical Model of Multiphase Power Transmission Line	100
Vasilii Zakaryukin, Andrey Kryukov, and Aleksandr Cherepanov	
Basis for Local Methods of Insulation Hardening of Traction Rolling Stock Electrical Machines	109
Anatoliy Khudonogov, Evgeny Dulskiy, and Pavel Ivanov	
Technology of Electric Power Efficient Use in Transport	120
Tatyana Alekseeva, Natalya Ryabchyonok, and Leonid Astrakhantsev	
Development of Scientific-and-Experimental Stand to Study Operating Processes of New Transistor Converter of Alternating Current Locomotive	134
Oleg Melnichenko, Aleksey Linkov, and Dmitry Yagovkin	
Strengthening Design for Weak Base Using Geomaterials on “Amur” Automobile Road Section	145
Sergey Kudryavtsev, Tatiana Valtseva, Elena Goncharova, and Aleksey Kazharsky	
The False Tripping of Relay Protection in Parallel Lines: Finding Cause and Solution Methods	154
Pavel Pinchukov and Svetlana Makasheva	
Improving Methods for Reliability Assessment of Electric Power Systems	162
Pavel Pinchukov and Svetlana Makasheva	
Research of Deicing Processes by Means of Electrodynamic Method	170
Sergei Sukhorukov, Vyacheslav Soloviev, and Olga Malysheva	

A Mathematical Model of the Estimated Cases for Designing a Multimodal Transport Network 177
 Natalia Nesterova, Vladimir Anisimov, Sergey Goncharuk, and Aleksandr Anisimov

Assessment of the Fatigue Durability of the Rolling Contact 184
 Alexey Beskopylny, Nikolay Onishkov, and Viktor Korotkin

Power Distribution Control in the Transmission of the Perspective Wheeled Tractor with Automated Gearbox 192
 Roman Didikov, Roman Dobretsov, and Yuriy Galyshev

Stress-Strain State and Plasticity Reserve Depletion on the Lateral Surface of Workpiece at Various Contact Conditions During Upsetting 201
 Volodymyr Kukhar, Viktor Artiukh, Andrey Butyrin, and Andrii Prysiashnyi

Analysis of Stress Conditions of Rolling Stand Elements 212
 Viktor Artiukh, Vladlen Mazur, and Andrey Butyrin

Researching of the Stress-Strain State of the Open-Type Press Frame Using of Elastic Compensator of Errors of “Press-Die” System 220
 Elena Balalayeva, Viktor Artiukh, Volodymyr Kukhar, Olga Tuzenko, Vladyslav Glazko, Andrii Prysiashnyi, and Vadim Kankhva

Online Energy-Efficient Train Traffic Adjustments 236
 Boris Davydov and Vadim Gopkalo

Development of Transport Infrastructure

Needs and Possibilities of Development of the Macedonian Motorways 247
 Slobodan Ognjenovic, Tamara Narezhnaya, Zlatko Zafirovski, and Ivana Nedevska

Transport Complex of Primorye as a Factor of the Economic Status of the Region 256
 Tatyana Miroshnikova and Natalia Taskaeva

Modeling the Duration of Works During the Scheduling of Construction of the Transport Infrastructure Facility 265
 Marina Romanovich, Wang Ziyue, and Shi Peiyu

Modified Method for Calculation of Vehicles Residual Lifetime with Regard of the Impact Factors Variability 273
 Nadezhda Sevryugina

Particularities of Public-Private Partnership Mechanisms Application for Implementation of Construction Megaprojects of Transport Infrastructure Development	282
Alexandr Orlov	
Assessment of the Level of Balance of the Development of the Regional Transport Systems in the Russian Federation	289
Violetta Politi	
The Priority Directions of Public Transport Transit Hubs Development on Commuter Railways	299
Denis Vlasov, Nina Danilina, and Anna Shagimuratova	
Management and Economic Performance of Sustainable Transport	310
Olga Shirokova and Lev Shirokov	
The Risk-Based Approach to Rating the Competitiveness of Transport Enterprises in the System of Economic Security	318
Elena Karanina, Olesya Ryazanova, and Alexander Timin	
Methodological Approach to the Pricing of Construction Investment Projects for Road Construction in the Context of Sustainable Development	326
Khuta Gumba and Svetlana Uvarova	
Sea Transport of the Kamchatka Region: The Analysis, Tendencies and Mechanism of the Effective Development	334
Tatyana Miroshnikova and Natalia Taskaeva	
Location-Based Potential for the Development of Cruise and Yachting Industries in the Protected Region of the Kotor Municipality	345
Nikola Konjević and Goran Radović	
The Development of Underground Construction as a Way to Improve the Organization of Traffic	356
Ekaterina Utkina, Kirill Pshennikov, and Natalia Braila	
Organizational-Technological Solutions, Risks and Reliability of the Preparatory Period of the Renovation of Territories	367
Vitaliy Chulkov, Arkadiy Kiselev, Garrik Maloyan, and Anatoly Efimenko	

Energy Efficiency: Energy Saving Solutions for Transportation Facilities

The Study of Compact Convective Stream Formed by Use of Recessed Floor Convection Heaters with Natural Air Circulation 379
 Viktor Pukhkal and Voldemar Taurit

Analysis of the Strength Characteristics of Internal Sprayed Protective Coatings of Pipelines to Improve Energy Efficiency 391
 Vladimir Orlov, Ilya Averkeev, and Alexey Pelipenko

Outlooks for Building Solar Charging Infrastructure for Self-propelled Electric Vehicles 402
 Liubov Shilova, Dmitry Solovyev, and Aleksey Adamtsevich

Deformation Monitoring of Road Transport Structures and Facilities Using Engineering and Geodetic Techniques 410
 Ekaterina Kuzina and Vladimir Rimshin

Thermal Properties of the Building with Low Energy Consumption (LEB) 417
 Elena Statsenko, Anastasia Ostrovaia, Tatiana Musorina, and Natalia Sergievskaya

Energy Efficiency Upgrading of Enclosing Structures of Mass Housing of the Soviet Union 432
 Eliza Gumerova, Olga Gamayunova, and Tatiana Meshcheryakova

Energy Efficiency of Structural Regulation of Stress-Related Characteristics of Concrete 440
 Igor Bezhgodov and Elena Dmitrenko

Transport Interchange Hubs Under the Conditions of the Far North 446
 Ilya Dunichkin

Adjustment of Energy Strategy of Russia to Specific Nature of Far North: Analytic Hierarchy Process 453
 Irina Zaychenko, Svetlana Gutman, and Olga Kalinina

Energy-Efficient Lighting Systems Design in Industrial Premises of Motor Transport Enterprise 463
 Irina Romanova and Petr Romanov

Thermal Resistance and Accumulation of Heat by the Wall Construction	473
Daria Zaborova, Tatiana Musorina, Anna Selezneva, and Andrey Butyrin	
Experimental Study of Thermal Stability of Building Materials	482
Daria Zaborova, Gabriel Vieira, Tatiana Musorina, and Andrey Butyrin	
Measures of Improving the Accuracy of the Calculation of Energy Efficiency and Energy Saving of Construction Transport Infrastructure	490
Olga Poddaeva, Alexander Kubenin, and Dmitry Gribach	
Choice of Thermal Protection of an Office Building of the Transport Infrastructure by Economic Reasons	498
Elena Malyavina and Anastasya Frolova	
The Study of Flat Convective Stream Formed by Use of Recessed Flood Convection Heaters with Natural Air Circulation in High Height Rooms with Continuous Glassing	512
Viktor Pukhkal	
Problems of Energy Efficiency When Design of Construction Objects for Transport Infrastructure	520
Ekaterina Fomina, Natalia Kozhukhova, Alexander Fomin, and Elena Voitovich	
The Issues of Energy-Efficiency Increase of Three-Layer Reinforced Concrete Plate Constructions	529
Alexey Belyaev, Grigory Nesvetaev, and Dmitry Mailyan	
Energy-Efficient Reinforced Concrete Columns Made of Concrete, Grade B90...B140	536
Dmitry Mailyan, Vladimir Aksenov, and Nikolay Aksenov	
Review of Heat Pumps Application Potential in Cold Climate	543
Raimonds Bogdanovičs, Anatolijs Borodinecs, Aleksandrs Zajacs, and Kristīne Šteinerte	
Chlorella Microalga Biomass Cultivation for Obtaining Energy in Climatic Conditions of St. Petersburg	555
Natalia Politaeva, Tatiana Kuznetsova, Yulia Smyatskaya, Iryna Atamaniuk, and Elena Trukhina	

Energy Performance Simulation and Evaluation of Various Construction Types for a Residential Building (International ODOO Project) 563
 Norbert Harmathy, Jenő Kontra, Vera Murgul, and Zoltán Magyar

Calculation of Heat Energy Consumption by a Typical Historical Building with a Courtyard 577
 Aleksandr Gorshkov and Vera Murgul

Employment of Skirting Board Heating Water System in Accommodation 592
 Kirill Sukhanov and Anatoly Smirnov

Transport Buildings and Structures

Effect of the Structural Characteristics on Frost Resistance of Concrete 601
 Lev Alimov, Victor Voronin, Oksana Larsen, and Vasiliy Korovyakov

Concrete Waste Recycling and Re-use of Shielding Wall Materials After Decommissioning of Fusion Reactors 608
 Andrey Pustovgar, Aleksey Adamtsevich, and Liubov Shilova

Solving Problems of Distribution Network Tracing: Example of Gas Distribution Using the Search Optimization Methodology 615
 Aleksej Klochko, Victor Zhila, and Asmik Klochko

Stabilization of Low Bearing Soil Using Fly Ash and Chemical Additive Polybond 625
 Mirjana Vukićević, Veljko Pujević, and Miloš Marjanović

Evaluation of the Effectiveness of the Creation of Antifiltration Curtains in Hydroelectric Power Plant in Syria 634
 Konstantin Mordvintsev and Yaser Abd Alwahab

Research on Long-Term Strength of Glass-Fiber Reinforced Concrete 640
 Antonina Ryabova, Alexey Kharitonov, Larisa Matveeva, Nina Shangina, and Yuri Belentsov

Foundation Deformations Modeling in Underworking and Hydroactivated Rocks	647
Peter Dolzhikov, Albert Prokopov, and Vladimir Akopyan	
Subminiature Eddy-Current Transducers for Conductive Materials and Layered Composites Research	655
Sergey Dmitriev, Alexey Ishkov, Alexander Katasonov, Vladimir Malikov, and Anatoly Sagalakov	
Influence of the Longitudinal Compressive Force on Parametric Vibrations and Dynamic Stability of Thin-Walled Above-Ground Steel Oil Pipelines with Large Diameter	666
Vladimir Sokolov and Igor Razov	
Methodology of Monitoring of Hydrocarbon Transportation Hydraulic Reliability	679
Maria Zemenkova	
Trenchless Technology Application of Protective Coatings That Provide Energy Savings Associated with Transport of Water via Pipelines	689
Vladimir Orlov and Sergey Zotkin	
The Neural Modeling for the Assessment of Hazardous Hydro Meteorological Phenomena Including the Case of the Providing a Sustainable Work (Reliability) on Transport	700
Larisa Haritonova	
The Principles of the Layout and Evaluation of Systems for Protection from Dust Pollution of the Air	710
Natalia Sergina, Tatyana Kondratenko, Maxim Nikolenko, and Sergey Pushenko	
Blasting Operations in Conditions of Buildings and Facilities Reconstruction	720
Denis Synitsyn	
Methodology of Comprehensive Slope Stability Evaluation Based on Engineering Geodesy and Soil Mechanics Methods for the Road Engineering Application	729
Vladimir Simonyan	
Fire Resistance of Prefabricated Monolithic Reinforced Concrete Slabs of “Marko” Technology	739
Ekaterina Nedviga, Natalia Beresneva, Marina Gravit, and Angelina Blagodatskaya	

Mechanization of Technological Processes Assembly of Threaded Joints 750
 Anatoly Drozdov and Vitaliy Stepanov

Modeling of Movement the Flowable Building Load in the Operating Vessel of Vehicle 760
 Evgeny Plavelsky and Rashid Sharapov

The Interaction of Piles in Double-Row Pile Retaining Walls in the Stabilization of the Subgrade 769
 Anatoly Buslov and Vladimir Margolin

Reasonability of Application of Slags from Metallurgy Industry in Road Construction 776
 Natalia Kozhukhova, Nikolay Kadyshchev, Alla Cherevatova, Elena Voitovich, and Kirill Lushin

Problems of Fire Extinguishing in Buildings of the Transport Transit Hubs Using Carbon Dioxide and Gaseous Chladones 783
 Dmitry Korolchenko and Andrey Pigurin

Railway/Road Level Crossing Design – Aspect of Safety and Environment 791
 Milica Vilotijević, Luka Lazarević, and Zdenka Popović

Building Platforms of Polymer Matrix Based Composite Construction Materials for Transportation Facilities 801
 Andrey Glasunov, Victor Bobryashov, Victor Bobryashov, and Nikolay Bushuev

Finite Element Modeling of the Creep of Shells of Revolution Under Axisymmetric Loading 808
 Anton Chepurnenko, Natalia Neumerzhitskaya, and Michael Turko

Increase of Fire Resistance Limits of Building Structures of Oil-and-Gas Complex Under Hydrocarbon Fire 818
 Marina Gravit, Eliza Gumerova, Alexey Bardin, and Vitaly Lukinov

Experimental Determination of Permeability Coefficient 830
 Gulnara Gabitova, Daria Zaborova, and Sergey Barinov

Photoelasticity-Based Study of Stress-Strain State in the Area of the Plain Domain Boundary Cut-Out Area Vertex 837
 Lyudmila Frishter

Simulation of Blast Load on a Reinforced Concrete Slab in the Time Domain 845
 Galina Kravchenko, Dmitry Kostenko, and Sergey Tsurikov

The Modified Fiber Cement Panels for Civil Construction	852
Rustem Mukhametrakhimov and Liliya Lukmanova	
Designs from Innovative Materials in Transport Construction	859
Alexandr Kvitko and Viktor Shendrik	
Task for a Prestressed Reinforced Concrete Cylinder with External Reinforcement and Cylinder Optimization by Varying the Modulus of Elasticity	869
Serdar Yazyev, Mukhtar Bekkiev, Evgeniy Peresyppkin, and Mikhail Turko	
Cracking in Reinforced Concrete Structures of Buildings at Seismic Exposure	877
Mukhtar Bekkiev, Sergey Skuratov, Evgeniy Peresyppkin, and Dmitry Vysokovsky	
Optimization of the Solution of a Plane Stress Problem of a Polymeric Cylindrical Object in Thermoviscoelastic Statement	885
Lyubov Trush, Stepan Litvinov, Nadezhda Zakieva, and Salis Bayramukov	
Optimization of the Thick-Walled Sphere by the Energy Method on the Basis of the Strength Criterion of P. Balandin	894
Serdar Yazyev, Sergey Skuratov, Valery Bondarenko, and Svetlana Yazyeva	
Forecasting the Strength of an Adhesive Bond Over a Long Period of Time	902
Stepan Litvinov, Alexander Zhuravlev, Salis Bajramukov, and Serdar Yazyev	
MSW Landfills Reclamation Based on Monitoring of Biogas Emissions	908
Vladimir Maslikov, Alexander Chusov, Viacheslav Zhazhkov, and Olga Vasilyeva	
Mathematical Simulation of Flood Management by Hydro Systems with Temporarily Flooded Reservoirs	915
Roman Davydov, Valery Antonov, Dmitry Molodtsov, and Anatoliy Trebukhin	
Functional Model That Evaluates the Impact of Hydrotechnical Works and Facilities on a Water Object	921
Alexander Shishkin, Alexander Chusov, Marina Epifanova, and Dmitriy Silka	

Assessment of the Subsurface Fire-Fighting System Pipeline Impact on the Tank Stress State During the Foundation Settlement . . . 936
 Alexander Tarasenko, Petr Chepur, and Alesya Gruchenkova

Justification of the Most Rational Jack Method in the Corroded Tank 944
 Mikhail Tarasenko and Alexander Tarasenko

The Investigation of Freezing and Thawing Processes of Metal Foundations Ground of Pipelines 953
 Sergey Kudryavtsev, Vyacheslav Kovshun, and Aleksandra Mut

Sizing the Residual Deformation of Metal Structures in the Tank After Shell Replacement 962
 Alexander Tarasenko, Petr Chepur, and Alesya Gruchenkova

Numerical-and-Analytical Method of Estimation Insulated Glass Unit Deformations Caused by Climate Loads 970
 Pavel Stratiy

Statistical Test Data Evaluation of Track Rutting in Stone Mastic Asphaltic Concrete 980
 Dmitry Yastremsky, Tatiana Abaidullina, and Petr Chepur

Mathematical Models of the Output of Major Pollutants in the Process of Burning Water Fuel Oil Emulsions in Boiler Plants 987
 Viktor Katin, Vladimir Kosygin, Midkhat Akhtiamov, and Igor Vol'khin

Method of Evaluation of Ground Frost Heaving Pressure on Ice-Ground Barrier of an Underground Construction and Well Strengthening Walls 998
 Vyacheslav Kim and Marina Kim

Comparative Analysis of the Simplest Finite Elements of Plates in Bending 1009
 Vladimir Agapov and Roman Golovanov

The Influence of Cement Plant on the Atmospheric Pollution with Microscale Particulate Matter in Spassk-Dalny Town (Primorsky Region, Russia) – Particle Size Analysis 1017
 Aleksei Kholodov, Sergey Ugay, Vladimir Drozd, Svetlana Gulkova, and Kirill Golokhvast

Estimation of Practical Significance for Application of Composite Pipes in Comparison with Metal and Polymer Materials	1024
Konstantin Stroganov, Alexander Fedyukhin, Tatiana Stepanova, and Oleg Derevianko	
Autodesk Revit and Robot Structural Analysis in Design of Framed Buildings	1036
Rustam Gilemkanov, Ruslan Bagautdinov, and Vadim Kankhva	
Determination of Environmental Impact Factors of Flood Control Hydrosystems with Temporarily Filled Self-regulating Reservoirs	1046
Alexander Chusov, Vladimir Maslikov, Dmitry Molodtsov, and Olga Manukhina	
Comparative Analysis of Alternative Solutions of Excavation for Section of Hydropower Tunnel HPP “Dabar”	1055
Uroš Mirković, Slobodan Radovanović, Ljubo Divac, Nikola Mirković, Nikola Obradović, and Zdenka Popović	
Evaluation of Surface Deformations of Rolling Mills Stands Elements Resulting from Horizontal Forces Acting at Rolling	1065
Victor Artiukh, Vladlen Mazur, and Elena Nidziy	
Low-Temperature Swirl Burning as Technological Method of Simultaneous Decrease in Emissions of Nitrogen and Sulfur Oxides (Part 1. Principles, Organization and Mathematical Model of Furnace Process)	1074
Aleksey Trinchenko and Aleksandr Paramonov	
Low-Temperature Swirl Burning as Technological Method of Simultaneous Decrease in Emissions of Nitrogen and Sulfur Oxides (Part 2. Results of Modeling, Their Practical Implementation and Analysis)	1083
Aleksey Trinchenko and Aleksandr Paramonov	
Problems of Magnesium Oxide Wallboard Usage in Construction	1093
Marina Gravit, Olga Zybina, Artem Vaititckii, and Anna Kopytova	
Additive Technologies in Construction of Temporary Housing for Victims of Natural Disasters and Other Emergencies	1102
Alexander Lanko	

Management, Analysis, Monitoring, Organizational and Technological Solutions

Management and Monitoring of Urban Environment in the Integrated Development of Underground Space 1111
Galina Romanova, Michael Pleshko, Marina Rossinskaya, Nelli Saveleva, and Alexander Pankratenko

Integrated Approach to the Improvement of the Information Support of Management During the Transporting and Distribution of Heat 1125
Natalia Verstina and Evgeny Evseev

Methodic Approach to Energy Costs Reduction on the Basis of the Energy Service Contract 1136
Tatiana Meshcheriakova and Natalia Verstina

Influence of the Sustainable Development of the Fuel Power Complex on the Formation of Competitiveness of the Region 1151
Angela Mottaeva and Jasmina Četković

Organizational-Technological Reliability of Monolithic Construction 1160
Alexander Ginzburg, Alina Bolotova, Andrey Dolganov, Ivan Vedyakov, and Michael Vaynshteyn

Automation of Roof Construction Management by Means Artificial Neural Network 1168
Azary Lapidus and Alexander Makarov

Organization of Concrete Works on the Bases of the Information System of Tracking 1177
Alexander Ginzburg, Sophia Kozhevnikova, Alexander Afanas'ev, and Vitaliy Stepanov

Information Support for the Operational Management of the Construction Organization 1186
Nataly Knyazeva, Vitaliy Chulkov, and Mark Abelev

Production Skills and the PC in Training of Students 1194
Il'ja Cipurskij

Labor Management in Organizational Structures of Russian Energy Enterprises 1204
Natalia Zotkina, Miroslava Gusarova, and Anna Kopytova





Enterprise Architecture Analysis for Energy Efficiency of Saint-Petersburg Underground	1214
Igor Ilin, Anastasia Levina, and Oxana Iliashenko	
The Energy Saving Motivation of Certain Categories of Personnel in the Company	1224
Anna Minnullina and Rais Abdrazakov	
The Problems of Market Orientation of Russian Innovative Products (Electric Cars as a Case Study)	1234
Svetlana Bozhuk and Natal'ya Pletneva	
Automation of Calculations for Selecting Construction Equipment Purchasing Techniques	1243
Zalina Tuskaeva, Gevork Aslanov, and Zalina Alikova	
Analysis of the Reproduction of Generating Capacities of Electric Power Industry of the Russian Federation	1254
Lyubov Manukhina	
Green (Ecological) Marketing in Terms of Sustainable Development and Building a Healthy Environment	1265
Boban Melovic, Slavica Mitrovic, Biljana Rondovic, and Irina Alpackaya	
Quality as a Determinant of the Customer's Satisfaction on the Mobile Communication Market	1282
Boban Melović, Biljana Rondović, Slavica Mitrović, and Vitaly Shoshinov	
Methodological Approaches to a Substantiation Resurso - and Energetically Effective Economic Model of Object of Placing of a Waste	1296
Edward Tshovrebov, Evgeniy Velichko, and Andrey Shevchenko	
Analysis of Factors, Defining Software Development Approach	1306
Igor Ilin, Aleksandr Lepekhin, Anastasia Levina, and Oksana Iliashenko	
Human Capital Management as Innovation Technologies for Municipal Organization	1315
Olga Kalinina and Olga Valebnikova	
Financial Literacy as a Driver for Responsible Energy Consumption	1323
Mariia Sigova, Inna Kruglova, Marina Vlasova, and Irina Shashina	

**Matrix Tool for Efficiency Assessment of Production of Building
Materials and Constructions in the Digital Economy 1333**
Tamara Kuladzhi, Aleksandr Babkin, and Said-Alvi Murtazaev

Author Index. 1347

Electric Power Systems and Electromechanical Systems

Interaction Phenomenon Between Train, Track and Bridge

Zdenka Popović^(✉) , Luka Lazarević , Milica Vilotijević ,
and Nikola Mirković 

University of Belgrade, Bulevar kralja Aleksandra, 73, 11000 Belgrade, Serbia
zdenka@grf.bg.ac.rs

Abstract. The paper presents principle of track/bridge interaction in the case of temperature gradient, breaking and acceleration of railway vehicles. Influence of different bridge structures to the bridge expansion length was analysed for the purpose of expansion joint avoiding in CWR track. This would lead to the reduction of noise and vibration emission from railway traffic and maintenance activities, which is especially important in the urban environment. Additional stresses in track were considered according to the type of track and bridge deck, type of bridge bearings, as well as bridge support stiffness. Conclusion of this paper provides basic stances that could be used for the calculation of different railway bridge structures. The aim of the paper is providing the basis for improvement of the existing technical regulations in the field of railway infrastructure, as well as its harmonisation with EU regulations.

Keywords: Railway · Track/bridge interaction · Bridge expansion length
Sustainable railway transport

1 Introduction

The modern construction of the track implies continuously welded rails (CWR), thus providing a continuous running table (upper surface of the rail head). The track with CWR is standard track structure that is used on embankment, bridge or in tunnel.

The increase in design speed leads to the increase in share of engineering structures (tunnels, viaducts, bridges) on railway line, due to the large radii of horizontal curves and limited longitudinal slope on the conventional railways, as well as the need to protect the environment from the adverse effects of rail traffic [11, 12].

This paper presents the principles of track/bridge interaction, which leads to occurrence of stresses in the rails. The choice of track and bridge structures has an important role in the design and dimensioning, as well as maintenance of both railway track and bridge.

Displacement of bridge deck leads to the generation of forces in CWRs [7–9]. These displacements occur on both unloaded track (due to the temperature influence) and loaded track (Fig. 1).

Additional pressure/tension forces occur in CWRs due to the longitudinal displacement of the bridge. Figure 2 shows the longitudinal displacements of the bridge due to the acceleration and braking of the railway vehicles, as well as the temperature

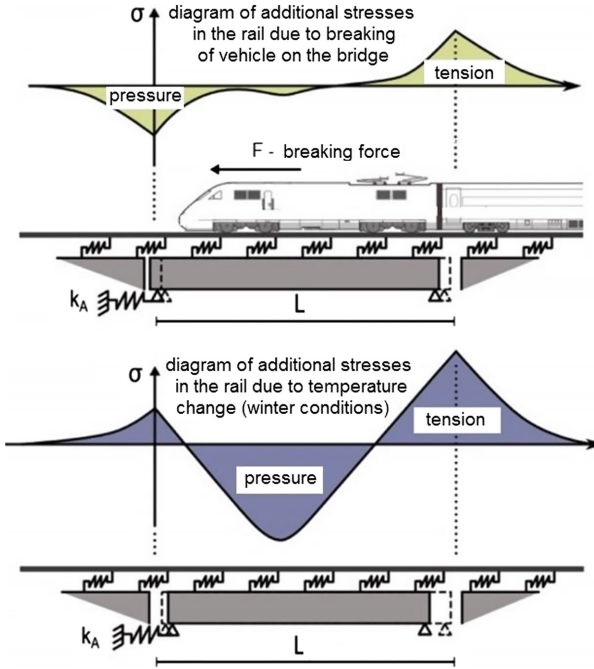


Fig. 1. Additional stresses in the CWR due to the bridge deck displacement.

changes in the bridge deck. In addition, Fig. 2 shows longitudinal displacements which are specific for concrete bridges - influence of creep and shrinkage of concrete.

In addition, bridge deck bends under the load from rail traffic, which leads to the rotation of the bridge deck ends. This further leads to the longitudinal displacement contributing to the increase of forces in CWRs (Fig. 3).

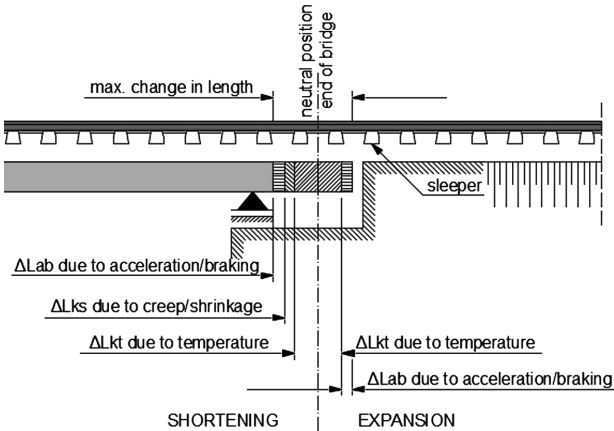


Fig. 2. Change in length of the bridge deck above the movable bearing at the bridge end [6].

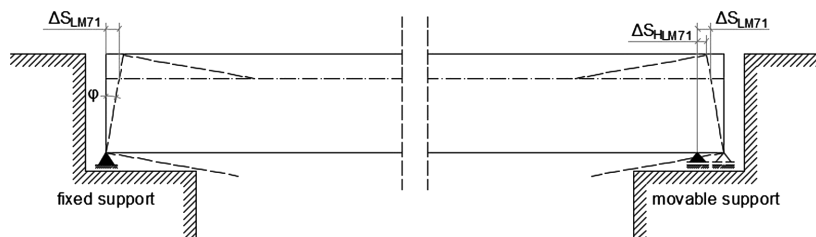


Fig. 3. Rotation of the bridge deck ends due to the bending in a vertical plane under the load from rail traffic [6].

2 Specificities of the Bridges with Continuously Welded Rails in Track

The track with CWRs on the bridge presents the modern track superstructure, which is applied on the conventional railways (speeds up to 200 km/h) and on high speed lines. This track structure provides favorable technical and economic effects, as well as a significant improvement in driving comfort and protection of the environment from noise and vibration. Cost efficiency of the CWR track is the most evident in reducing maintenance costs, extending the service life of the railway superstructure and substructure, as well as reducing traction costs and environmental protection costs.

According to the measuring and analysis of the noise emission from rail traffic, it was determined that the most significant share has the noise generated in the wheel/rail contact. For this reason, it is essential to maintain continuity of the running table - avoidance of fishplate joints, as well as expansion joints. The noise from the power unit is only relevant for the low-speed domain (e.g. in stations). On the other hand, aerodynamic noise is dominant in the high-speed domain.

CWR installation reduces the unevenness that presents excitation for noise and vibration in wheel/rail contact. This is of great importance in the urban environment, where noise (irritating, undesirable sound) negatively influences the quality of life, work performance and human health. Installation of welded joint instead of fishplate joint reduces the noise level in the wheel/rail contact by around 5 dB. Better results could be achieved by application of flash butt welding comparing to thermite welding. Professional welding and maintenance are the main assumptions for the previous statement.

Maintenance of fishplate joints presents about 30–50% of the total maintenance activities. Application of continuous welding of the rails leads to the significant decrease in costs of track and vehicle maintenance. Furthermore, this leads to the decrease in time for conducting of the maintenance activities, which influence the increase of track availability for railway traffic.

Replacement of fishplate joints with welded joints leads to significant extension of rail service life (20–30% longer service life).

The basic specificity of the CWR track is that rail dilatation is not possible during temperature changes (comparing to the rail temperature during final welding). Therefore, significant axial forces and stresses occur in CWR. The stress σ is constant in the

middle section of CWR (L_2 length, Fig. 4). The axial force due to the temperature changes in the CWR could be calculated using Eq. (1).

$$F = E \cdot A \cdot \alpha \cdot \Delta T \quad (1)$$

F - axial force in CWR due to temperature changes, E - Young's modulus (elastic modulus) for the rail steel, A - cross-sectional area of the rail, α - coefficient of thermal expansion for the rail steel, ΔT - change in the rail temperature relative to the reference or laying temperature. If there are fishplate joints at the both ends of CWR, the resistance at the end of CWR is equal to the resistance of the fishplate joint σ_R . On the other hand, if there are expansion joints at the both ends of CWR, then these ends could move freely - the resistance at the both ends equal zero. Stress in CWR changes linearly in the expansion zone (approx. $L_1 = 150$ m), as it is shown in Fig. 4.

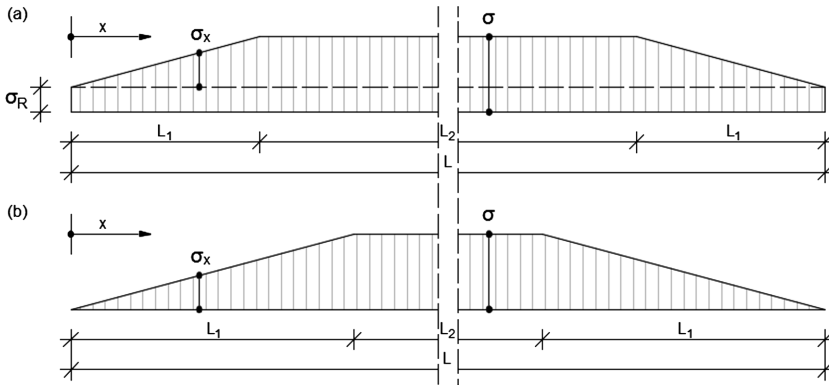


Fig. 4. Diagram of stresses due to the temperature change in continuously welded rails in the case of: fishplate joints (a) and expansion joints (b) on both ends.

When the temperature in CWR is greater than the reference or laying temperature, there occurs axial pressure force in CWR. During extreme summer temperatures, the pressure force in CWR with fishplate joints on both ends (case (a) in Fig. 4) could lead to track buckling. Figure 5 shows different cross-sections of railway bridges with a ballasted track in concrete trough, which is suitable solution for prevention of the track buckling.

It should be noted that slab track is stable in both longitudinal and lateral direction during extreme summer temperatures (Fig. 6).

The tension force occurs in CWRs during the winter and could cause rail breakage. For this reason, it is important to use rail fastening with a sufficient longitudinal resistance of rail in sleeper, in order to control the rail gap in case of rail breakage during the winter conditions. According to technical regulations, rail fastening should provide longitudinal rail resistance not less than 7 kN [2, 4, 15] when measured by the procedure in EN 13146-1 [2]. For use in category D fastening systems ($V \geq 250$ km/h), the longitudinal rail resistance should not be less than 9 kN [2, 4, 15]. On structures such as

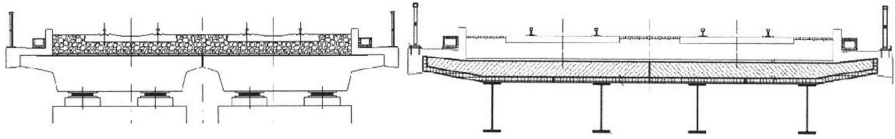


Fig. 5. Examples of railway bridge cross-sections with ballasted track in concrete trough [10].

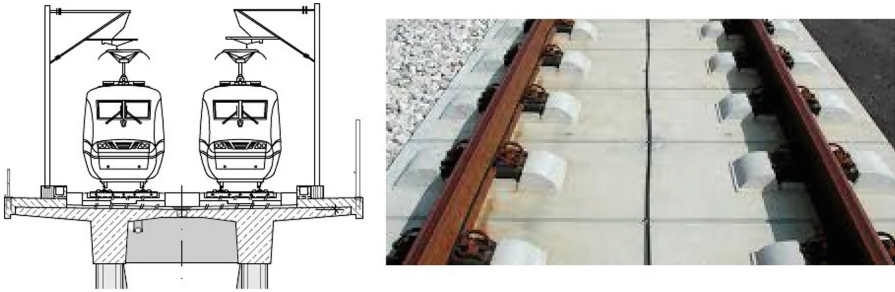


Fig. 6. An example of a cross-section of railway bridge with a slab track (left) and slab track construction (right).

long bridges, the longitudinal force transmitted between the track and the structure may be calculated by the method in EN 1991-2 [1]. According to appropriate calculation, the minimum requirement for longitudinal resistance may be reduced on long bridges.

Figure 7 shows longitudinal resistance for fastening system W 14, according to laboratory tests at TU Munich [5], which were carried out in accordance with [2]. Figure 7 clearly shows that the actual resistance to the longitudinal displacement is greater than the required value according to [2].

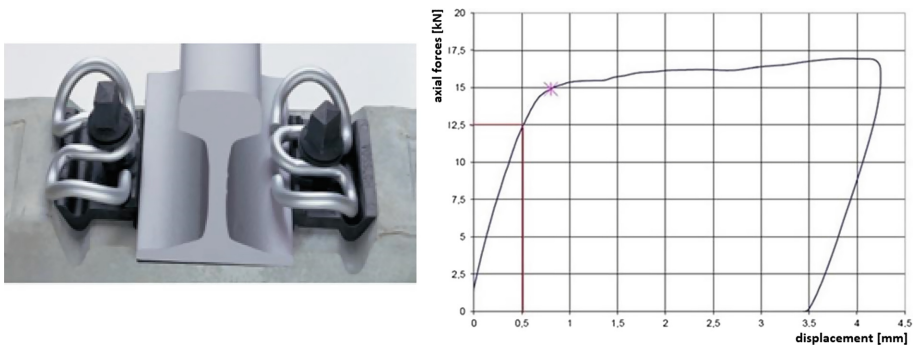


Fig. 7. W 14 rail fastening system before and after installation (left) and longitudinal displacements/axial force diagram (right) [2].

On the other hand, the resistance to the longitudinal displacement of the rail is generally greater than resistance of sleeper in ballast (Fig. 8).

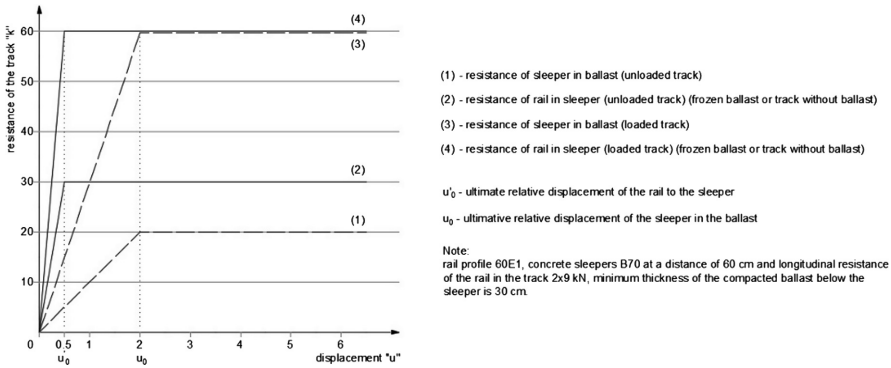


Fig. 8. Longitudinal resistance as a function of the longitudinal displacement of the rail according to [7].

In the case of unloaded track, the resistance of the rail in sleeper is greater comparing to resistance of sleeper in ballast (Fig. 8). In addition, in the case of winter temperatures, some rail fastening systems could have greater resistance of sleeper in frozen ballast comparing to the resistance of rail in sleeper. For calculation of axial forces in CWR due to the temperature change, resistance of sleepers in ballast is representative for the unloaded track (except when the ballast is frozen). For calculation of axial forces in CWR due to the braking and acceleration of railway vehicles, resistance of sleepers in ballast is representative for the loaded track (except when the ballast is frozen), as it is shown in Fig. 8.

As opposed to the elastic fastening system, rigid rail fastening systems have decreasing clamping force and resistance of rail in sleeper over time [13]. Rigid rail fastening systems are usually complemented with rail anti-creep anchors, which are laid in the track before and after the bridge.

3 Bridge Structure as an Element of Track Substructure

The railway bridge represents a deformable structure that causes the displacement of the track with CWRs. Therefore, this is the reason to discuss the track/bridge interaction. The forces transferred to the track with CWRs lead to the additional forces in the track and/or in the bridge bearings, and the displacement of the track and bridge deck. Bridge deck displacement leads to the track displacement and generates additional force in the track and indirectly leads to the force in the bridge bearings.

The parameters of the bridge structure that influence to the stresses in the track with CWRs are: bridge expansion length, bridge span length, support stiffness, deck bending stiffness and height of the bridge deck.

3.1 Span and Expansion Length of the Bridge

Based on the recommendations in UIC Code 774-3 [7], the maximum expansion length of the bridge deck with CWR track without expansion joints should be:

- for steel bridges with ballasted track (maximum length of the deck with the fixed bearing in the middle: $2 \times 60 = 120$ m),
- for concrete or composite bridges with ballasted track (maximum length of the deck with the fixed bearing in the middle: $2 \times 90 = 180$ m).

In the case of ballastless track a specific evaluation should be performed [7].

Figure 9 shows the possible position of the expansion joint in the track on the bridge [3], as well as the reduction of the pressure stress in CWR. However, according to the available possibilities, the installation of expansion joints should be avoided, since they represent a discontinuity on the running table, thus affecting the increase in dynamic forces, reducing comfort and increasing the maintenance costs of track, vehicles and a bridge.

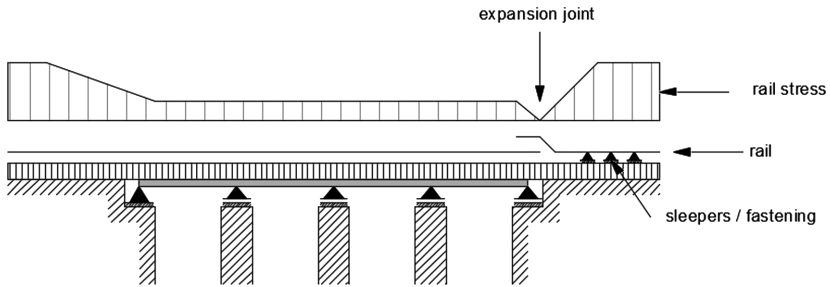


Fig. 9. Expansion joint in the track on the bridge above the movable bearing at the bridge end.

3.2 Stiffness of Bridge Supports Including Foundation

The stiffness of the support K influences the longitudinal displacement of the bridge deck and it could be determined using Eq. 2.

$$K = \frac{H}{\sum \delta_i} \text{ [kN/cm]} \quad (2)$$

where $\delta_i = \delta_p + \delta_F + \delta_h + \delta_a$, δ_p - displacement of the head of the support due to elastic deformation, δ_F - displacement at the head of the support due to rotation of the foundation, δ_h - displacement of the support due to the horizontal displacement of the foundation, δ_a - relative displacement between the upper and lower parts of the bearing.

3.3 Bending Stiffness and Height of the Bridge Deck

The vertical load due to the railway traffic on the bridge causes large track/bridge interaction forces [8, 9], since the deformations of the bridge deck during bending lead

to the longitudinal displacement of the upper edge of the deck end (Fig. 3). The interaction depends primarily on the flexibility and position of the neutral axis of the bridge deck, but it is influenced by the stiffness of the fixed elastic support and by the height of the bridge deck.

4 Conclusion

The choice of track and bridge structures has an important role in the design and dimensioning, as well as maintenance of both railway track and bridge and protection of the environment.

Obviously, the simply-supported bridge deck is not suitable as a static system for railway bridges, since it has larger displacements at the bridge ends due to the higher bridge deck. From this aspect, the application of the continuous deck with a fixed middle support, is the much more favourable solution for the railway bridges (the lower bridge deck height).

The stiffness of the bridge supports should be adjusted according to the permitted stresses in the rails. The smaller stiffness of the supports causes the larger displacement of the bridge structure, and therefore higher stresses in continuously welded rails. On the other hand, the large support stiffness influences negatively to the dynamic characteristics of the bridge by increasing the frequency of the free oscillation of the bridge and seismic force. The optimum stiffness of the rail bridge supports should meet both criteria [14].






Acknowledgement. This work was supported by the Ministry of Education and Science of the Republic of Serbia through the research project No. 36012: “Research of technical-technological, staff and organization capacity of Serbian Railway, from the viewpoint of current and future European Union requirements”.

References

1. CEN/TC 250: EN 1991-2:2003. Eurocode 1: actions on structures. Part 2: traffic loads on bridges (2003)
2. CEN/TC 256: EN 13146-1:2002. Railway applications. Track, test methods for fastening systems - part 1: determination of longitudinal rail restraint (2002)
3. CEN/TC 256: EN 13232-8:2007+A1. Railway applications. Track – switches and crossings – part 8: expansion devices (2007)
4. CEN/TC 256: EN 13481-2:2012. Railway applications. Track - performance requirements for fastening systems - part 2: fastening systems for concrete sleepers (2012)
5. Freudenstein, S.: Forschungsbericht, Prüfung des Schienenbefestigungssystems, vol. 14, pp. 13481–13482 (2014)
6. Freystein, H.: Interaktion Gleis/Brücke – Stand der Technik und Beispiele. Ernst & Sohn Verlag für Architektur und technische Wissenschaften GmbH & Co. KG, vol. 3, pp. 220–231 (2010)
7. International Union of Railways. UIC Code 774-3. Track/Bridge Interaction Recommendations for calculation. Paris (2001)

8. International Union of Railways. UIC Code 776-1. Loads to be considered in railway bridge design. Paris (2006)
9. International Union of Railways. UIC Code 776-2. Design requirements for rail-bridges based on interaction phenomena between train. Track and bridge. Paris (2009)
10. Muncke, M., Freystein, H., Schollmeier, P.: Entwerfen von Bahnanlagen. Eurailpress, Hamburg (2005). ISBN 3-7771-0333-0
11. Popović, Z., Lazarević, L., Brajović, L., Vilotijević, M.: The importance of rail inspections in the urban area-aspect of head checking rail defects. *Procedia Eng.* **117**, 596–608 (2015)
12. Popović, Z., Lazarević, L., Vukićević, M., Vilotijević, M., Mirković, N.: The modal shift to sustainable railway transport in Serbia. In: *MATEC Web of Conferences*, vol. 106, p. 05001 (2017)
13. Republika Srbija: Pravilnik o projektovanju rekonstrukcije i izgradnje određenih elemenata železničke infrastrukture pojedinih magistralnih železničkih pruga. *Sl. glasnik RS* (2012)
14. Salatić, R., Mirković, N.: Connection between superstructure and substructure concrete bridges with aspect seismic isolation of construction. *Zbornik radova*, p. 5 (2017)
15. Vilotijević, M., Popović, Z., Lazarević, L.: Test methods and requirements for fastening systems for concrete sleepers. *Build. Mater. Struct.* **60**(2), 33–48 (2017)

Improvement of Current Collection System with a Rigid Current Distributor for Overhead Transport

Oleg Sidorov¹ , Vladimir Goryunov² , Valery Tomilov¹  ,
and Ilya Salya¹ 

¹ Omsk State University, Marx av., 35, Omsk 644046, Russia
tomilov_omsk@mail.ru

² Omsk State Technical University, Mira Ave., 11, Omsk 644050, Russia

Abstract. Conventional power supply systems for overhead transport have disadvantages of self-aligning contact pair geometry which limit the rolling stock operation speed due to poor current collection quality. At Omsk State Railway University new systems with a rounded contact surface were proposed. The calculations of the interface of this current collection system based on Lagrange second kind equations demonstrate satisfactory results at higher speeds. The calculation results are confirmed experimentally.

Keywords: Monorail · Current · Transport

1 Introduction

Monorail transport systems are operated in dozens countries of the world [1]. Until now an extensive operation experience of the systems for electrical power supply to the rolling stock [2–13]. Studies [14–17] devoted to this subject point to its relevance.

Power-supply system for overhead, monorail transport is, as a rule, a contact current collection system consisting of rigid encompassing current distributors, as shown in Fig. 1(a). The said system contains flat operating facets and has major disadvantages, including speed limitation to 60 km/h. In case of lateral vibrations and inclinations of the contact element relative to the rigid current distributor the specific pressure onto the contacting surfaces increases, the contact spot reduces, arcing and burnouts are produced which significantly reduces the current collection quality. Significant wear of the contact surfaces is observed in increased speeds.

At Omsk State Railway University works on the current collection system with rigid current distributors are underway. Correction of the disadvantages above may be attained by changing the contact pair geometry and consequently, – contact surface. The said technical solution is implemented at Omsk State Railway University. The rigid current distributor of the proposed current collection system is a half-pipe and a contact element interacting with the internal surface of the half-pipe (Fig. 1(b)). The cross-section of the contact element operating surface is an arc of the radius r smaller than internal surface of current distributor R .

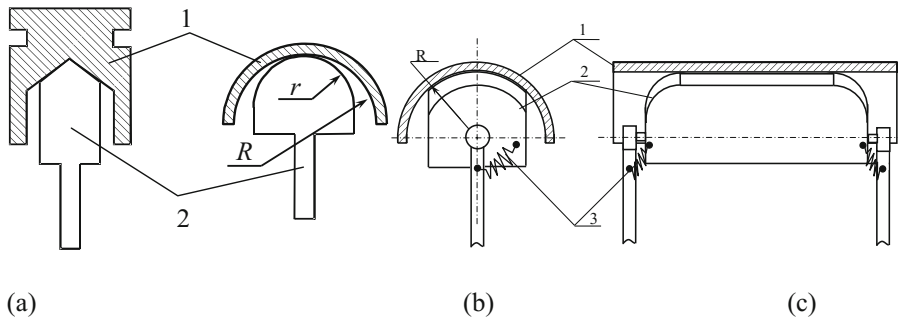


Fig. 1. Monorail transport current collection systems (a) – existing one; (b), (c) – improved ones: 1 – current distributor; 2 – contact element; 3 – flexible shunt.

An advantage of the system proposed also consists in improved dynamic characteristics of the current distributors due to the reduction of the slack of the current distributor with a smaller weight.

To provide a larger contact area regardless of the inclinations and turns of the interfacing surfaces the rigid current distributor 1 and current collector 2 may be made with equal rounding radii (Fig. 1(c)). Current collector 2 of the current distributor is installed with the possibility of rotating around its axis coinciding with the rounding center of the contact surfaces of the rigid current distributor 1 and current collector 1 of the current distributor. For the current transfer flexible shunt 3 is used. Centre of gravity of the current collector 1 of the current distributor is located on its rotation axis or lower.

2 Experimental Section

To evaluate the current collector serviceability there are different methods to calculate the current collector interface with catenaries. At the stage of new devices' design more and more often simplified methods are used, particularly, models with a small number of degrees of freedom, with external harmonic impact from the current distributor (of sinusoid shape).

The main objective of the calculations is the determination of the contact pressure FP , as the main indicator of the current collection quality. Dynamic characteristic is understood as the dependence of the maximum and minimum contact pressure in the span on the rolling stock speed (frequency of vertical vibrations of the current distributor contactor).

The design diagram is provided in Fig. 2. For calculations the following admissions were made: the current distributor is adopted absolutely rigid; the current distributor slack trajectory is selected sinusoid; the amplitudes of horizontal and vertical displacement amplitudes of the current distributor base are equal to zero (the crew influence is absent); there are no breaks of the distributor current conductor; there is no viscous friction in the current distributor hinges; there is no aerodynamic impact on the

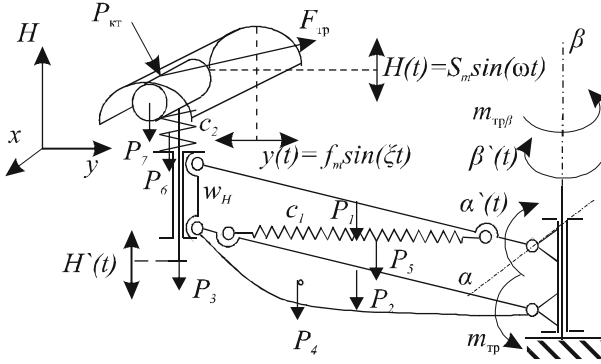


Fig. 2. Design diagram of the level current distributor with a C-shaped contact element.

current conductor; the current conductor has no disturbed butt welds; there is no pressure re-distribution between slack and leading parts of the contact element.

The design diagram (Fig. 2) has three degrees of freedom. To identify the position of the current distributor elements three generalized coordinates are required: H – vertical displacement of the contact element; α – rotation angle of the current conductor levers in the vertical plane; β – rotation angle of the current conductor levers in the horizontal plane.

For the equation system in question Lagrange equation of second kind look as follows:

$$\begin{cases} \frac{d}{dt} \left(\frac{\partial T}{\partial \dot{H}} \right) - \frac{\partial T}{\partial H} + \frac{\partial E}{\partial H} = Q_H; \\ \frac{d}{dt} \left(\frac{\partial T}{\partial \dot{\alpha}} \right) - \frac{\partial T}{\partial \alpha} + \frac{\partial E}{\partial \alpha} = Q_\alpha; \\ \frac{d}{dt} \left(\frac{\partial T}{\partial \dot{\beta}} \right) - \frac{\partial T}{\partial \beta} + \frac{\partial E}{\partial \beta} = Q_\beta, \end{cases} \quad (1)$$

where T is the kinetic energy of the mechanical system;

E – potential energy;

Q_H – generalized force along the generalized coordinate H ;

Q_α – generalized force along the generalized coordinate α ;

Q_β – generalized force along the generalized coordinate β .

Axis H is directed vertically upwards. Axis α is perpendicular to the lever rotation axis in the vertical plane. Axis β is in the horizontal plane.

The following forces are applied to the system: P_1 – weight of the lower lever, P_2 – upper lever, P_3 – carriage weight, P_4 – current-conducting cable weight. P_5 – pressure spring weight, P_6 – secondary cushioning spring weight, P_7 – contact element weight, F_P – perturbing force bringing the contact element in motion, F_{tr} – force of the sliding friction of the contact element on the current distributor surface, W_H – dry friction during the contact element displacement relative to the carriage, $M_{w\alpha}$ and $M_{w\beta}$ – dry friction in the current distributor hinges along axes α and β , respectively.

The system kinetic energy is calculated as per the following equation:

$$T = \sum_{i=1}^7 T_i \quad (2)$$

where T_i is the kinetic energy of the current distributor i^{th} element.

The current distributor upper and lower rods are involved in the complex movement: transient rotary movement around the vertical axis of the current distributor base (Fig. 2) with the angular speed β and relative rotary movement around the current distributor horizontal axis perpendicular to the figure plane with the angular speed α .

The kinetic energy of the upper rod is calculated using the following equation:

$$T_1 = \frac{1}{2} \left(J_{1\alpha} \dot{\alpha}^2 + J_{1\beta} \dot{\beta}^2 \right) \quad (3)$$

where $J_{1\alpha}$ is the moment of inertia of the current distributor upper rod in the vertical rotation plane:

$$J_{1\alpha} = \frac{1}{3} m_1 l^2 \quad (4)$$

$J_{1\beta}$ – the moment of inertia of the current distributor upper rod in the horizontal rotation plane:

$$J_{1\beta} = \frac{1}{3} m_1 (l \cdot \cos \alpha)^2 \quad (5)$$

Kinetic energy of other elements is calculated similarly. Contact element and carriage spring have a more complex movement, they move with the following speed:

$$V_7 = \sqrt{\dot{H}^2 + l^2 \cdot \dot{\alpha}^2 \cdot \sin^2 \alpha + l^2 \cdot \dot{\beta}^2 \cdot \cos^2 \alpha} \quad (6)$$

Potential energy is calculated using the following equation:

$$E = \sum_{i=1}^7 E_i + \sum_{i=1}^2 E_{sp,i} \quad (7)$$

where E_i is the potential energy of the current distributor structure i^{th} element in the field of forces of gravity;

$E_{sp,i}$ – potential energy of the current distributor i^{th} spring in the field of elastic forces.

Generalized force for the current collection element includes contact pressure force F_P , the vector of which is shown in Fig. 3.

Force F_P is the resulting of two forces:

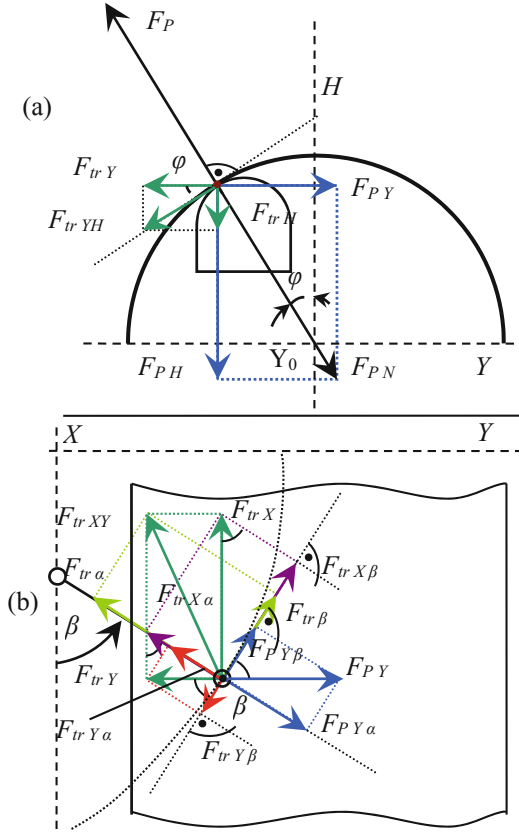


Fig. 3. Design diagram to determine the generalized forces.

$$F_P = \sqrt{F_{PY}^2 + F_{PH}^2} \quad (8)$$

where F_{PH} is the vertical force bringing the contact element in motion along the vertical;

F_{PY} – horizontal.

From Fig. 3(a) it is seen that:

$$F_{PH} = F_P \cdot \cos \varphi \quad (9)$$

$$F_{PY} = F_P \cdot \sin \varphi \quad (10)$$

Rough surfaces of the current distributor and contact element are not an ideal constraint. The force of friction F_{tr} is directed opposite to the contact element movement and in module is equal to:

$$F_{tr} = f \cdot N = f \cdot F_P \tag{11}$$

where f is the coefficient of friction of sliding.

Geometrically (Fig. 3) the resulting force of the sliding friction F_{tr} is equal to the sum of two forces:

$$F_{tr} = \sqrt{F_{trX}^2 + F_{trYH}^2} \tag{12}$$

where F_{trX} is the longitudinal force of the sliding friction produced as a result of the rolling stock movement;

F_{trYH} – transverse force of the sliding friction produced as a result of the movement of the contact element relative to the current conductor.

The calculation admits the possibility of accounting for the forces of friction (along and across the current conductor) with different coefficients f : μ – along the current conductor, η – across the current conductor, including the latter:

$$F_{trX} = \mu \cdot F_P \tag{13}$$

$$F_{trYH} = \eta \cdot F_P \tag{14}$$

The projection of the longitudinal force of sliding friction F_{trX} onto the tangent to the circular trajectory (Fig. 3(b)), of generalized coordinate β :

$$F_{trX\beta} = \mu \cdot F_P \cdot \sin \beta \tag{15}$$

The same force, as shown in Fig. 4, affects the current distributor rods along the generalized coordinate α , and its projection is equal to:

$$F_{trX\alpha} = \mu \cdot F_P \cdot \cos \beta \tag{16}$$

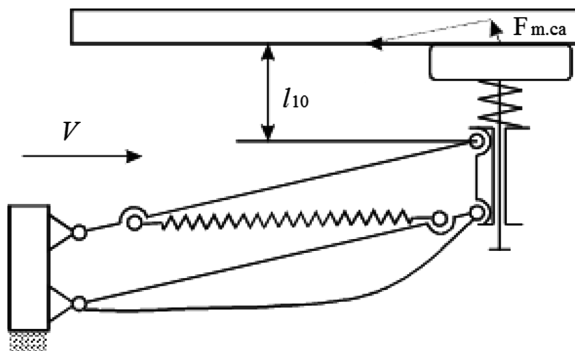


Fig. 4. Action of the force of sliding friction on the first current distributor facing the engine.

The force F_{trYH} may be decomposed to the geometric sum of forces F_{trY} and F_{trH} :

$$F_{trYH} = \sqrt{F_{trY}^2 + F_{trH}^2} \quad (17)$$

where F_{trY} is the force of sliding friction acting in the horizontal plane;

F_{trH} – the force of sliding friction acting on the contact in the vertical plane.

From Fig. 3(a) we can see:

$$F_{trH} = F_{trYH} \cdot \sin \varphi \quad (18)$$

$$F_{trY} = F_{trYH} \cdot \cos \varphi \quad (19)$$

The projection of force F_{trY} on the tangent line to the trajectory of the movement of the contact element centre is, similar to F_{pY} (Fig. 3(b)), the force acting on the rods along the generalized coordinate β . Based on the above, the projection:

$$F_{trY\beta} = F_{trY} \cdot \cos \beta \quad (20)$$

The same force acts on the current distributor force along the generalized coordinate α , and its projection is equal to:

$$F_{trY\alpha} = F_{trY} \cdot \sin \beta \quad (21)$$

The resulting forces of the sliding friction acting along generalized coordinates α and β (Fig. 3(b)), respectively:

$$F_{tr\alpha} = F_{trX\alpha} + F_{trY\alpha} \quad (22)$$

$$F_{tr\beta} = F_{trX\beta} - F_{trY\beta} \quad (23)$$

The sum of the set forces of sliding friction F_{tr} on the possible movement of the system points corresponding to the generalized possible movement, for example $d\alpha$, respectively, is equal to:

$$\Sigma \partial A_\alpha = \partial A_\alpha (M_{\omega\alpha}) + \partial A_\alpha (F_{pY\alpha}) + \partial A_\alpha (F_{tr\alpha}) \quad (24)$$

Generalized forces Q_i are proportion factors attached to di , in the equations determining dA .

After the determination of the partial derivatives and their substitution to the equation system (1) final Lagrange equations were produced; solving these equations it is possible to obtain the functions of angles of inclination of the current distributor levers α and β as function of time. Knowing this function, at the next stage the contact pressure curve is calculated which is used to find minimum and maximum value for a specific speed. Having obtained their values for a specific speed range the current distributor dynamic characteristic is built up.

In the calculation the admission of the continuous movement of the current conductor element on the current distributor is made, i.e., forces pressing the current conductor to the current distributor are always larger than the forces trying to separate it from the current distributor. The expression for the movement of the contact element shown in Fig. 5, is derived from the equation of circumference:

$$(H - H_c)^2 + (Y - Y_c)^2 = r^2 \quad (25)$$

where $(H_c; Y_c)$ is the coordinate of the centre of circle, i.e., the centre of current distributor with the radius r ; $(H; Y)$ – coordinates of the point belonging to the circle, i.e., position of the contact element centre relative to the current distributor.

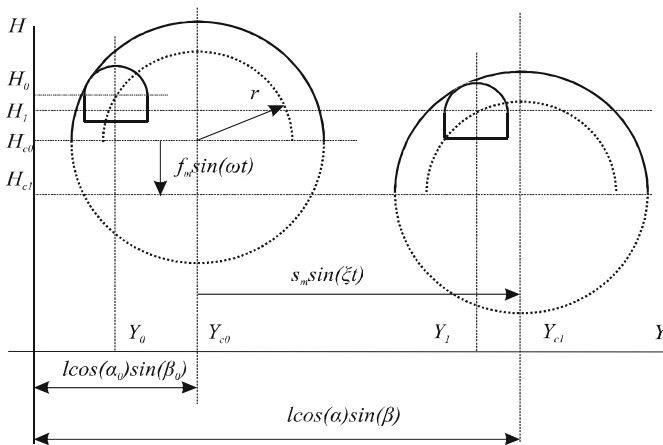


Fig. 5. Design diagram of the contact element movement determination.

Coordinate H_c is the function which expresses the slack of the current distributor having sinusoid shape in the calculation:

$$H_c = H_{c0} + f_m \cdot \sin(\omega \cdot t - 90) \quad (26)$$

where H_{c0} is the initial coordinate of the height of the current distributor centre relative to the adopted coordinate system;

f_m – amplitude of the current distributor vertical vibrations;

t – time;

ω – frequency of the current distributor vertical vibrations:

$$\omega = 2 \cdot \pi \cdot \frac{V}{l} \quad (27)$$

V – rolling stock speed;

L – current distributor span length

Coordinate Y_c is the function expressing the value of the current distributor horizontal deflection having sinusoid shape in the calculation:

$$Y_c = Y_{c0} + s_m \cdot \sin(\xi \cdot t) \quad (28)$$

where s_m is the amplitude of the current distributor horizontal vibrations;

Y_{c0} – initial position of the current distributor centre in the horizontal plane (Fig. 5), which may be expressed as follows:

$$Y_{c0} = l \cdot \cos \alpha_0 \cdot \sin \beta_0 \quad (29)$$

ξ – frequency of the current distributor horizontal vibrations:

$$\xi = 2 \cdot \pi \cdot \frac{V}{n \cdot l} \quad (30)$$

N – number of the spans deflecting to the same side

Intermediate position of the contact element in the horizontal plane:

$$Y = l \cdot \cos \alpha \cdot \sin \beta \quad (31)$$

Based on the above, the expression for the contact element movement (25) will look as follows:

$$H = H_{c0} + f_m \cdot \sin(\omega \cdot t - 90) + \sqrt{R^2 - (l \cdot \cos \alpha \cdot \sin \beta - Y_c)^2} \quad (32)$$

The current collector element speed and acceleration shall be calculated as the first and second derivatives of the Eq. (32), respectively.

3 Results and Discussion Section

The calculation of the resulting equation system is made in MathCAD software. For the following basic data the contact pressure curve was built: $f_m = 1$ mm; $s_m = 10$ mm; $V = 20$ m/s; $l = 2$ m.

This mathematical model enables accounting for the horizontal vibrations occurring in this contact surface shape. Accounting for the generalized coordinate β enables tracing the movement of the current collection point across the surface of the interfacing pair, evaluation of the contact pressure force as the sum of the horizontal and vertical impact, and separately.

Upon the simulation results the current distributor with a larger-radius contact element (up to the difference $R - r = 5$ mm) has higher critical speeds, without current distributor welds. With this radii difference the current distributor is self-centered relative to the current conductor faster.

The calculation demonstrates that at the rolling stock speeds up to 1 m/s the contact element moves along the current distributor trajectory due to the force of sliding friction, slightly lagging behind it.

It is necessary to point out that at the angle β_0 over 2° , under the action of the force of sliding friction along the current distributor the current distributor medium position moves towards this angle. At more intensive current distributor vibrations the contact pressure substantially depends on the horizontal component and the application point FP significantly moves along the current distributor and contact element.

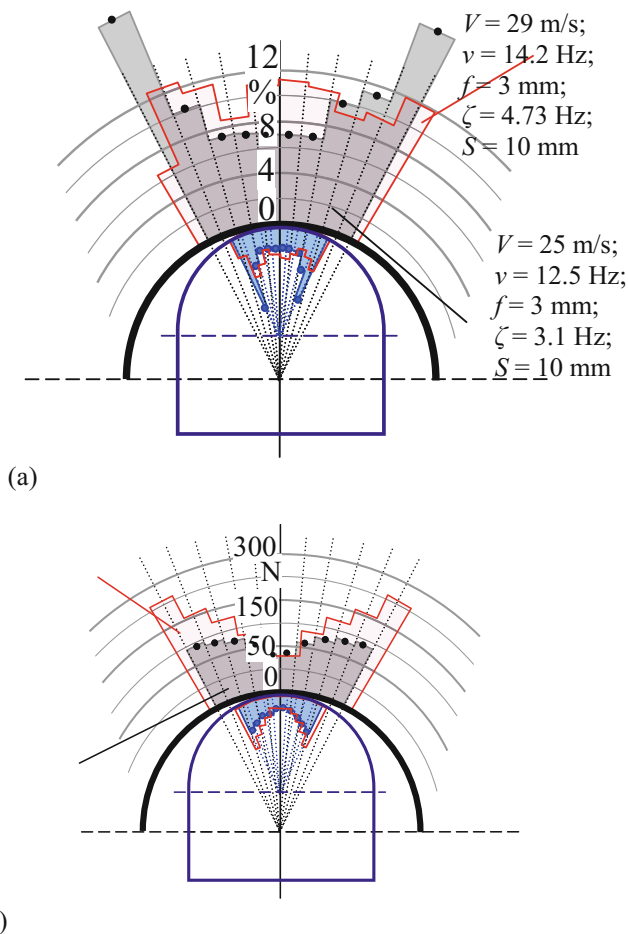


Fig. 6. (a) Diagram of the distribution density of the movement of the contact element along the current distributor; (b) The diagram of distribution of average values of the contact pressure

Envelopes of the maximum and minimum contact pressures do not display the point of the force application in the contact. To predict the contact pair wear it is supposed to evaluate the time of positioning of the contact element by the diagram of the deviation distribution density, and the impact degree shall be evaluated by the diagram of average contact pressures. Evaluation of the contact pair serviceability and current collection system characteristics in the conditions maximum close to real-life ones was performed on a 20-m line test bed designed and implemented at the laboratory in Omsk State Railway University. The contact pair visual appearance is provided in Fig. 8(a). The overall view of the current collection system on the line test bed with the rolling unit is provided in Fig. 8(b). This test bed was used to measure dynamic, wear and load characteristics of the current distributor. Besides, impact processes on deregulated current distributor welds were studied (Figs. 6 and 7).

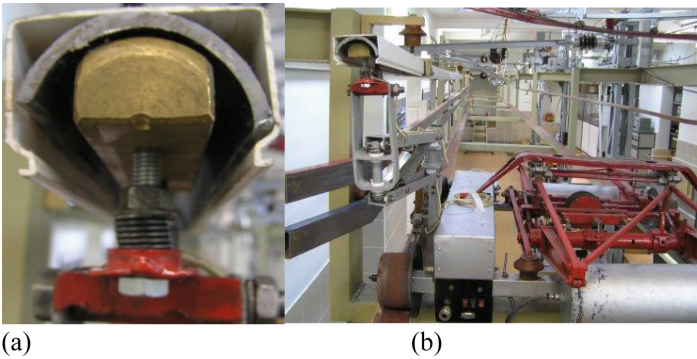


Fig. 7. (a) Visual appearance of the contact pair; (b) Overall view of the line test bed

4 Conclusions

The existing current collection systems with a rigid current distributor having flat contact facets of encompassing type do not ensure reliability, especially in high speeds.

At Omsk State Railway University current collection system with rounded contact surfaces were proposed. The engineering solutions are protected with patents.

The developed mathematical model of the current conductor interface with the current distributor enables selecting optimum parameters of the contact surfaces of the current distributor and current conductor.

At Omsk State Railway University a methodology of experimental study of the new current collection system using line test bed was proposed.

The results of the theoretical and experimental studies have acceptable convergence. The divergence does not exceed 10%. Please note that the first paragraph of a section or subsection is not indented. The first paragraphs that follows a table, figure, equation etc. does not have an indent, either.

Subsequent paragraphs, however, are indented.

References

1. Tomilov, V., Jakovlev, V.: Device features current collection foreign monorail systems. *J. Transsib Railway Stud.* **4**(8), 49–57 (2011). (Omsk State Transport University, Omsk)
2. Sidorov, O., Tarasenko, A.: Improvement current collectors monorail transport for high speeds. *J. Transsib Railway Stud.* **4**(28), 108–115 (2016) (Omsk: Omsk State Transport University)
3. Sidorov, O., Smerdin, A.: New technologies of current collection research for the high-speed railways by omsk state transport university. *Vestnik VELNII* **1**(75), 29–38 (2017). (Novocherkassk: OJSC “VELNII”)
4. Sidorov, O., Philippov, V.: Method of prediction elements wear contact pairs monorail electric vehicles. *Sci. J. Modern High Technol.* **2**, 441–446 (2016). (Penza: ID «Academia Estestvoznaniya»)
5. Sidorov, O., Stupakov, S.: Construction of a mathematical model of wear of contact pairs of electric current collection devices taking into account the effect of temperature factors. *Electricity supply of railways: Interuniversity thematic collection of scientific papers* (Omsk: Omsk State Transport University), pp. 46–50 (2016)
6. Sidorov, O., Philippov, V.: The issue of forecasting elements wear contact pairs devices electric rolling current collection. *Int. J. Appl. Fundam. Res.* **12**, 1393–1397 (2015). (Penza: ID «Academia Estestvoznaniya»)
7. Sidorov, O., Tomilov, V.: Improvement of the research laboratory “Overhead contact line, power lines and current collectors” OSTU. *Eltrans-2015* (St. Petersburg: Emperor Alexander I St. Petersburg State Transport University), p. 70 (2015)
8. Sidorov, O., Stupakov, S.: Studies of the electromechanical wear of contact pairs in the current collection devices of electric transports. *J. Friction Wear* **5**, 511–517 (2015). (Gomel: V.A. Belyi Metal-Polymer Research Institute of National Academy of Sciences of Belarus)
9. Sidorov, O., Tomilov, V.: New current collection research technologies for high speed railway. In: *Materials of the 8th International Symposium for Transportation Universities in Europe and Asia* (Nanjing: Nanjing Institute of Railway Technology), pp. 46–49 (2015)
10. Sidorov, O., Philippov, V.: Construction of mathematical models of mechanical wear contact pairs devices current collection. *J. Transsib Railway Stud.* **2**(18), 36–40 (2014). (Omsk: Omsk State Transport University)
11. Sidorov, O., Stupakov, S.: Construction of mathematical models of electromechanical wear of contact pair device current collection. *Vestnik SibADI* **1**(35), 103–108 (2014). (Omsk: Siberian State Automobile and Highway Academy)
12. Sidorov, O., Stupakov, S.: Construction of mathematical models mechanical wear contact pairs devices current collection. *Vestnik SibADI* **3**(31), 97–101 (2013). (Omsk: Siberian State Automobile and Highway Academy)
13. Sidorov, O., Goryunov, V.: Dynamic models choice for pantographs of highspeed railway transport. In: *Dynamics of Systems, Mechanisms and Machines (Dynamics)*, pp. 1–4 (2016). (Omsk: Omsk State Technical University)
14. Pavlov, V., Smerdin, A.: Electric current collection system. *Eltrans-2013* (St. Petersburg: Emperor Alexander I St. Petersburg State Transport University), pp. 35–36 (2013)
15. Smerdin, A., Meshcheryakov, V.: Electric current collection system. *Eltrans-2013* (St. Petersburg: Emperor Alexander I St. Petersburg State Transport University), p. 34 (2013)
16. Smerdin, A., Golubkov, A.: Linear stand for the investigation of the interaction of a current collector with a contact wire *Eltrans-2015* (St. Petersburg: Emperor Alexander I St. Petersburg State Transport University.), p. 17 (2015)
17. Tyurnin, P., Mironos, N.: *Vestnik of the Railway Research Institute* (Moscow: JSC VNIIZhT), vol. 6, pp. 365–370

Improvement of the Methodology for Improvement of the Turn-to-Turn Short Circuit Detection in the Driving Motor Anchor Winding

Viktor Kharlamov^(✉) , Pavel Shkodun , and Ignat Shestakov 

Omsk State Transport University, Karl Marx Ave., 35, Omsk 644046, Russia
emoe@omgups.ru

Abstract. The article provides results of the application of the wave response method to detect turn-to-turn short circuit in the anchor winding of the DC driving motor. Experimental angular characteristics of the wave response diagnostic parameters for damaged anchor windings are provided. Coefficient enabling determination of the anchor winding turn-to-turn insulation status in the DC driving motor is proposed.

Keywords: DC driving motor · Diagnosis · Wave response · Insulation

1 Introduction

One of the key factors determining rolling stock and DC motors' performance quality is the reliability of its elements [1, 2]. It is known from the operation experience that electrical motors are most susceptible to damage, hereby their performance degrades due to the winding insulation ageing [3, 4]. DC motor turn-to-turn insulation damage accounts for up to a half of all the faults identified. Electrical influence on the insulation is due to overvoltage during the motor operation and may result in the insulation destruction or delamination. Mechanical damage may be due to the driving motor mechanical load, unbalancing, frequent starts and stops, electrical motor elements wear [5]. Chemical effect is manifested during the insulation operation in high humidity, acid environment, it may also be due to dirt inside the motor. Thermal influence [6] is mostly due to the start torques and overloads during the operation, for example, in case of the train long ascents along the slopes. Environment is capable of exerting serious impact on the insulation state: in this respect, there are numerous factors – from the air dustiness degree to the motor operation elevation above the sea level etc. Numerous researchers and research teams have completed works on the development and improvement of various methods for the evaluation of the electrical machine winding insulation technical status, including DC machines [7–17]. Hence, DC motor insulation status monitoring is an important and topical problem requiring development of modern methodologies for the evaluation of turn-to-turn insulation state.

2 Experimental Section

As the method used to evaluate the driving motor turn-to-turn insulation state in this study the wave response method is selected [18–20]. Its advantages include safety (due to the use of low-voltage diagnostic pulse source), processability (no need to disassemble the machine) and diagnostic signal information value. Wave response method is based on the short duration low amplitude pulse supply to the winding followed by the analysis of the parameters of the attenuating oscillatory process initiated in the winding. In order to implement the wave response method a portable microcontroller device implementing the functions required for the function measurement has been developed. The schematic diagram of the device developed is provided in Fig. 1. During the device design STM32F746G series microcontroller ensuring the test algorithm, information input and output was used. The device is supplied from lithium batteries. To control the device a touch-screen display used for the information output is provided. To connect the measurement cables from the brushes of the motor in question a connector is provided. To evaluate the state of the driving motor anchor winding turn-to-turn insulation measurements in quasi-stationary mode are necessary: after cranking to some angle the anchor is fixed in a standstill position and record the wave response. If there is a short circuit in the anchor winding, the wave response parameters will substantially differ both in amplitude and in frequency.

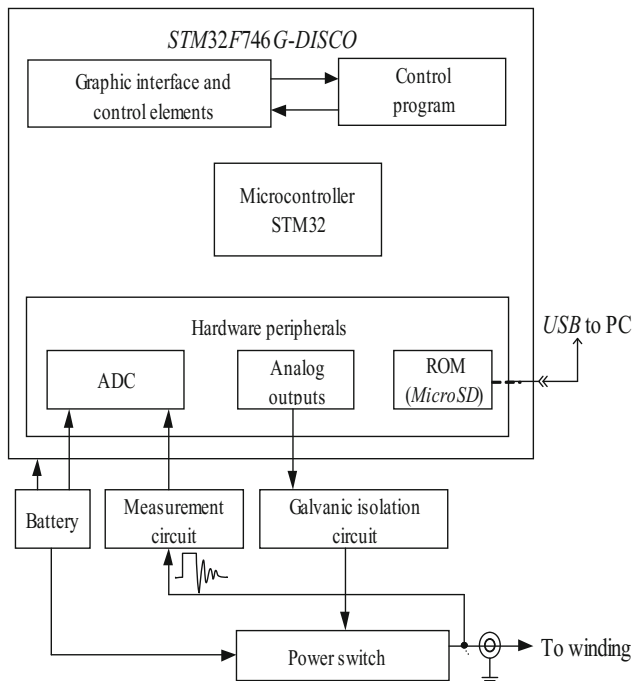


Fig. 1. Microcontroller device block diagram.

During the research the wave response implementations for different series of driving motors (Fig. 2), wave response basic implementation existence areas (Fig. 3) were obtained (here curves a and b are the main existence areas of the wave response basic implementations, curve c – ground fault state), also angular diagrams of the wave response amplitude and period vs. the anchor angular position with the turn-to-turn short circuit in the anchor winding have been obtained (see an example in Fig. 4).

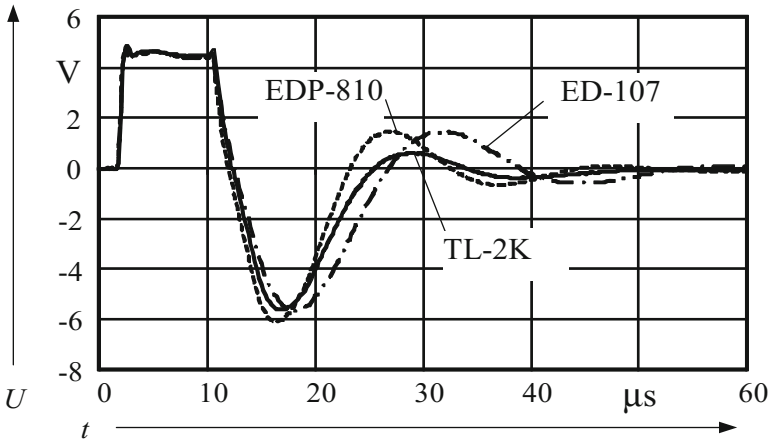


Fig. 2. Wave response shape for different electrical motors.

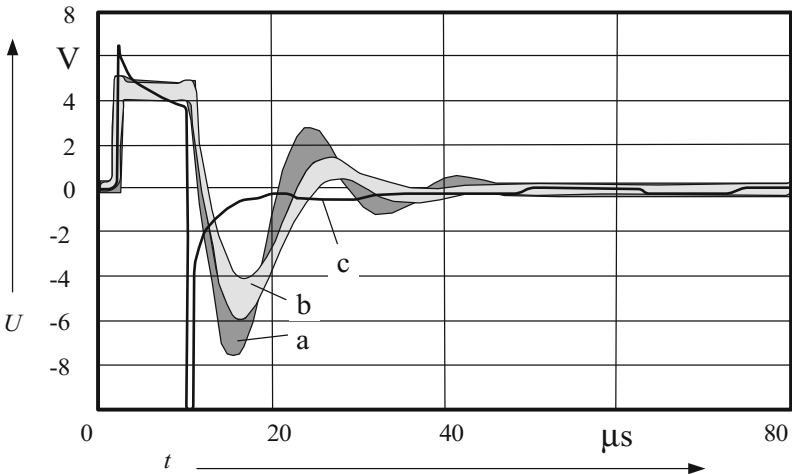


Fig. 3. Wave response basic implementation existence areas for EDP-810 electrical motor

The results of the research conducted demonstrate that the shape of curves of the wave response amplitude and period is symmetrical and is linked to the number of the machine poles. This fact enables limiting the required angle to which the motor anchor

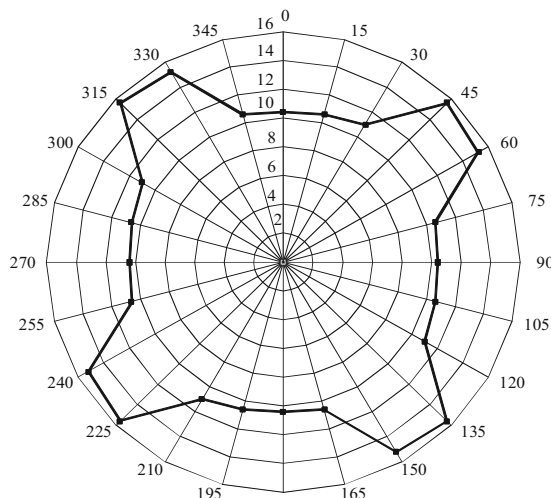


Fig. 4. Curve of wave response vs. the anchor angular position for P31M electrical motor

should be cranked to evaluate the presence of the turn-to-turn short circuit using the pole pitch value. If there are no substantial insulation faults during the electrical motor tests, the signal received is compared with the reference signal and the statement of the absence of damage and motor anchor winding serviceable state is produced.

To evaluate the insulation state it is proposed to calculate the diagnostic coefficient which is calculated using the following equation:

$$K = 1 \frac{A_2}{T_2} / \frac{A_1}{T_1} \quad (1)$$

where A_1 , T_1 is the “full amplitude” and period of the first basic implementation of the wave response, A_2 , T_2 – “full amplitude” and period of the second basic implementation of the wave response.

The proposed coefficient K enables simultaneous accounting for the variation of the amplitude and period of the wave response two implementations.

3 Results

Figure 4 provides examples of the wave response obtained for the anchor windings of two electrical motors.

The wave response (see Fig. 5, curve a) was obtained for the anchor winding of the electrical motor with the favourable storage and operation conditions. The three remaining implementations were recorded for the anchor winding of the machine with a knowingly compromised state of the turn-to-turn insulation in its serviceable state (see Fig. 5, curve b) and with the short circuit between two conductors in one slot (see Fig. 5, curve c) and in two different slots (see Fig. 5, curve d), respectively. Noteworthy is the

fact that the wave response implementations (see Fig. 5, curves c, d) were obtained in the anchor position when the maximum difference of the frequency and amplitude of the values obtained is recorded. In Table 1 the main parameters of the said wave response implementations as well as K coefficient calculation results are summarized.

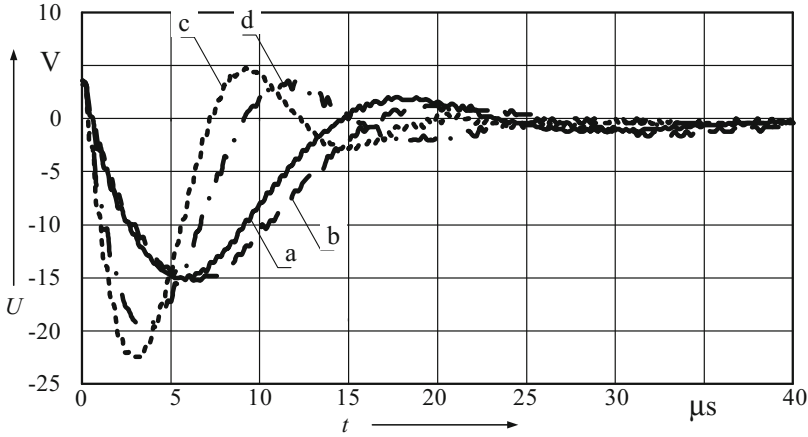


Fig. 5. Wave response implementations as function of the insulation state.

K coefficient value increase characterizes turn-to-turn short circuit in the anchor winding and this value reduction is an evidence of the developing damages and insulation quality compromise resulting from the insulation material degradation process. Negative K values demonstrate the insulation quality compromise, hereby, the insulation capacitance value of the winding in question increases due to the insulation structural variations caused by the bad storage conditions. The capacitance increase results in the increased wave response period as compared to the reference value and negative result of the K value calculation.

Table 1. Wave response implementation parameters.

Parameter	Response code			
	a	b	c	d
“Full amplitude” of the wave response first period A_1 (A_2), V	18.0	17.0	23.0	27.5
Wave response period T , μ s	22.8	26.9	16.8	14.4
K coefficient value, units	–	–0.249	0.423	0.587

4 Discussion

K values obtained during the anchor cranking from an arbitrary position to small angles are of low diagnostic value. K coefficient variation degree may be used to judge the insulation damage obviousness degree. There are cases when extreme points

correspond to the brush overlapping the shorted turns. This nature of the K value variations is observed in all the types of the driving motors studied. As a criterion to identify turn-to-turn short circuits the K coefficient variation by 10% or more in case of the anchor cranking by a certain angle θ , or the result of its comparison with the reference value may be used.

5 Conclusions

1. The selected wave response method enables reliable diagnosis of the turn-to-turn short circuit in the motor anchor winding.
2. The “ideal implementations” obtained may be used as references to evaluate the degree of the DC motor anchor winding turn-to-turn insulation degradation.
3. The proposed K coefficient enables simultaneous accounting for the variation in the amplitude and period of the wave response two implementations and evaluation of the damage or integrity degree of the DC motor anchor winding turn-to-turn insulation.

References

1. Glinka, T.: Investigations of electrical machines in industry. Research and Development Centre of Electrical Machines Komel, Katowice (2002)
2. Durocher, D., Feldmeier, G.: Future control technologies in motor diagnostics and system wellness. In: Conference Record Annual IEEE Pulp Paper Industry Technical Conference, pp. 98–106 (2003)
3. Jones, D., Jowett, J., Thomson, S., Danner, D.: Megger: Guide to Diagnostic Insulation Testing Above 1 kV, 2nd edn. (2002)
4. Zhang, P., Du, Y., Habetler, T., Bin, L.: A survey of condition monitoring and protection methods for medium-voltage induction motors. *IEEE Trans. Indus. Appl.* **47**(1), 34–46 (2011)
5. Stashko, V., Gubin, I.: Simulation of seasonal operating induction machines insulation condition using wave transient process parameters. *Polzunovskiy vestnik* **1**, 51–56 (2002)
6. Toliyat, H., Nandi, S., Choi, S., Meshgin-Kelk, H.: Electric Machines-Modeling Condition Monitoring and Fault Diagnosis, pp. 117–118. CRC Press, Taylor & Francis Group, Boca Raton (2013)
7. Grubic, S., Aller, J., Lu, B., Habetler, T.: A survey on testing and monitoring methods for stator insulation systems of low-voltage induction machines focusing on turn insulation problems. *IEEE Trans. Industr. Electron.* **12**, 4127–4136 (2008)
8. Polak, A.: The use of DC current to testing condition of the insulation of electrical machines. *Przegląd Elektrotechniczny* **1**, 123–131 (2013)
9. Decner, A., Glinka, T., Polak, A.: Diagnostic tests method of turn to turn insulation. *Zeszyty Problemowe – Maszyny Elektryczne* **79**, 103–106 (2008)
10. Sebok, M., Gutten, M., Kucera, M.: Diagnostics of electric equipments by means of thermovision. *Przegląd Elektrotechniczny* **87**(10), 313–317 (2011)

11. Glowacz, A., Glowacz, A., Glowacz, Z.: Recognition of thermal images of direct current motor with application of area perimeter vector and Bayes classifier. *Measur. Sci. Rev.* **15** (3), 119–126 (2015)
12. Henao, H., Capolino, G., Fernandez-Cabanas, M., Filippetti, F., Bruzzese, C., Strangas, E., Pucsa, R., Riera-Guasp, M., Hedayati-Kia, S.: Trends in fault diagnosis for electrical machines: a review of diagnostic techniques. *IEEE Industr. Electron. Mag.* **8**(2), 31–42 (2014)
13. Grubic, S., Restrepo, J., Aller, J., Bin, L., Habetler, T.: A new concept for online surge testing for the detection of winding insulation deterioration in low-voltage induction machines. *IEEE Trans. Indus. Appl.* **47**(5), 2051–2058 (2011)
14. Schemmel, F., Bauer, K., Kaufhold, M.: Reliability and statistical lifetime-prognosis of motor winding insulation in low-voltage power drive systems. *IEEE Electr. Insul. Mag.* **25** (4), 6–13 (2009)
15. Gyftakis, K., Kavanagh, D., Sumislawska, M., Howey, D., McCulloch, M.: Dielectric characteristics of electric vehicle traction motor winding insulation under thermal ageing. *IEEE Trans. Ind. Appl.* (2015)
16. Decner, A., Polak, A.: Wear estimation criteria of turn to turn insulation in Notebooks Problems – Electrical Machines 81/2009. Research and Development Centre of Electrical Machines Komel, Katowice (2002)
17. Cusido, J., Rosero, J., Ortega, J., Garcia, A., Romeral, L.: Induction motor fault detection by using wavelet decomposition on dq0 components. In: *Proceedings of IEEE International Symposium on Industrial Electronics*, vol. 3, pp. 2406–2411 (2006)
18. Vorobev, N., Vorobjeva, S., Suhankin, G., Gertsen, N.: Methods and devices for testing of induction machines insulation. *Polzunovskiy vestnik* **2**(2), 261–269 (2011)
19. Griбанov, A., Khomutov, S.: Improving reliability of supply transformers insulation testing using spectral analysis of transient process parameters in same voltage phase windings. *Polzunovskiy vestnik* **4**, 54–61 (2009)
20. Griбанov, A., Khomutov, S.: Mathematical simulation of testing signal in state assessment process by low-voltage impulses. *Polzunovskiy vestnik* **2**, 232–238 (2010)

Selection and Validation of the Mathematical Model for the Solution of the Optimization Problem of Fuel Cost Efficiency Improvement of the Locomotive Diesel Engines

Alexandr Anisimov^(✉)  and Vitaly Chetvergov 

Omsk State Transport University, Karl Marx av., 35, 644046 Omsk, Russia
anisimovas1971@mail.ru

Abstract. In the article issues of mathematical simulation of the working processes of the locomotive diesel engines are discussed. Mathematical model for the calculation of the fuel combustion process in the diesel engine cylinder is proposed. The mathematical model enables the optimization of the internal combustion engines converted to gas-diesel cycle operation, using the specific fuel consumption and acceptable thermal and dynamic loads on the sleeve assembly. It is demonstrated under which conditions the use of the gas fuel blended with the diesel fuel will be economically advantageous in the locomotive diesel engines. To evaluate the hydro-carbon fuel blend application efficiency in the locomotive power units it was proposed to use a consolidated efficiency criterion as the sum of dimensionless particular efficiency criteria characterizing the variation of the fuel cost efficiency and quantity of the fuel incomplete combustion products.

Keywords: Diesel engine · Hydrocarbon fuel · Mathematical simulation
Experiment planning · Fuel Saving

1 Introduction

Monitoring and control action on the engineering and economic performance of self-propelled locomotives in the operation are possible in case of using different on-board and fixed instrumentation systems currently widely introduced in the locomotive fleet. These systems are primarily aimed at the maximum accurate measurement of the fuel consumption from the locomotive fuel tank. The locomotive power unit and equipment parameters to be monitored are, mostly, recorded parameters and the set of these parameters is not exhaustive. Besides, on-board and fixed instrumentation systems and central complexes for the monitoring, diagnosis and locomotive technical state tuning require a large number of primary signal converters, rather a long time for the pre-operation activities and expensive equipment. A number of smart complexes do not have sufficient mathematical and software support of the analytical methods for the evaluation of the locomotive engineering and economic characteristics.

In this situation it is necessary to continue the improvement of the locomotive diesel engines' thermodynamic parameters and economic characteristics monitoring in

order to improve their cost efficiency and utilization, including in case of using hydrocarbon fuels alternative to the diesel fuel in the locomotive diesel engines [1–6].

2 Materials and Methods

Monitoring of the thermodynamic parameters of the diesel engine working cycle may be based on the so-called “virtual” indicator diagram in order to identify indicator and effective cycle indicators for all the possible operation modes of the locomotive diesel engine. The fuel combustion law may be set by a number of dependencies proposed by Neuman et al. [7, 8].

Due to the fact that locomotive diesel engines have rather a large power at the diesel engine average specific speed, substantial dimensions of the sleeve assembly, high values of the boost pressure and compression degree for the combustion laws, pilot check for their applicability is necessary. For this purpose experimental data on the heat emission rates from the pilot indicator diagrams of PD1 M and 2A-5D49 locomotive diesel engines were used.

For example, combustion process in these diesel engines very well follows the law expressed by Wiebe fuel burnout equation

$$x = 1 - e^{-6,908 \left(\frac{\varphi}{\varphi_2} \right)^{m+1}} \quad (1)$$

and abstract combustion rate

$$w_0 = -6,908(m+1) \left(\frac{\varphi}{\varphi_z} \right)^m e^{-6,908 \left(\frac{\varphi}{\varphi_2} \right)^{m+1}} \quad (2)$$

where m is the combustion nature indicator, $-$ the parameter describing the nature of variation of the relative density of effective centres during the combustion as function of time; φ_z – combustion time.

The resulting curves of the theoretical burnout dependencies $x = F(\varphi)$ and combustion rate $x = F(\varphi)$ and $w_\varphi = dx/d\varphi$ (Figs. 1 and 2) demonstrate that the calculated values of the fuel combusted and combustion rate well match the experimental data and Wiebe burnout equation may be used for other types of locomotive diesel engines.

The main difficulty in the calculation of the heat released by the working medium to the cylinder walls consists in the determination of the heat-transfer coefficient. Simultaneously, it is the heat transfer which enables the determination of such an important indicator as the fuel combustion efficiency coefficient. Currently the best-proven equation for the calculation of heat-transfer coefficient is the one proposed by professor Woschni [9], looking as follows:

$$\alpha_{summ} = 127.9D^{-0.2}T_g^{-0.53}P_g^{0.8} \left[C_1C_m + C_2 \frac{V_h T_a}{P_a V_a} (P_g - P_{g0}) \right]^{0.8} \quad (3)$$

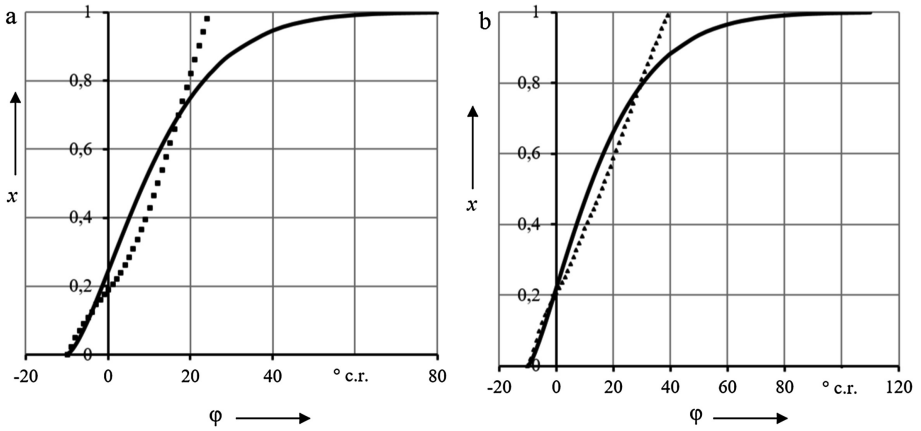


Fig. 1. Pilot and theoretical (solid line) characteristics of the fuel combustion law: a – 2A-5D49 diesel engine, b – PD1M diesel engine.

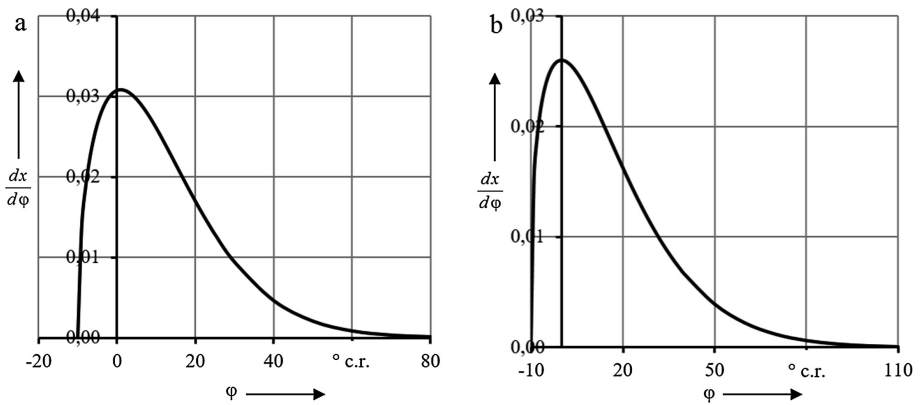


Fig. 2. Theoretical characteristic of the fuel burnout rate: a – 2A-5D49 diesel engine, b – PD1M diesel engine.

where T_g is the working medium temperature, K; c_m – average piston speed, m/s; $C_1 = 2.28 + 0.308w_\tau/c_m$; $C_2 = 0.00324$; V_h – cylinder working volume, m^3 ; T_a – working medium temperature at the compression process start, K; P_a – working medium pressure at the compression process start, bar; V_a – working medium volume at the compression process start, m^3 ; P_g – working medium pressure inside the cylinder during the combustion, bar; P_{g0} – working medium pressure inside the cylinder without the combustion process, bar.

Later the Eq. (3) describing heat-exchange processes in the direct injection diesel engine combustion chamber was converted by Hohenberg to look as follows [9]:

$$\alpha_{summ} = 130V_{\varphi}^{-0.06}T_g^{-0.4}P_g^{0.8}[c_m + 1.4]^{0.8} \quad (4)$$

where $V_{\varphi} = \pi D^3/6$ – is the current cylinder volume, m^3 ; D – is the conditional sphere diameter accounting for the influence of the time-variable volume on the gas flow in the cylinder.

Update of the proposed mathematical model of the working cycle enables calculating the fuel combustion efficiency coefficient for each combustion process interval, without taking its average value as it was adopted in the earlier models by other authors. Besides, in the mathematical model the influence of the fuel combustion product components, gas temperature excessive air coefficient and share of the fuel combusted on the heat-transfer factor is introduced [10].

Therefore, the diesel engine working cycle mathematical model based on the fuel combustion rate and heat-exchange inside the engine combustion chamber enables the determination of the current and maximum values of pressure and temperature and respective crankshaft rotation angles, maximum rate of the gas pressure increase inside the cylinder and gas work during the combustion process with the maximum approximation to the engine actual working cycle. Subsequently, as a result of the updated calculation of the combustion process expansion process, indicative and effective data of the locomotive diesel working cycle are calculated.

If Wiebe combustion law is used, the values of the formal parameters (combustion time φ_z , combustion nature indicator m , share of the fuel combusted x_z) are not known in advance during the update of the combustion process, only their variation intervals are known. In this case, it is proposed to use a combination of Grinevetski-Mazing and Wiebe methods for diesel engine thermal calculation [7, 8]. This approach provides setting the type and parameters of the fuel burnout law, variations of the working medium pressure and temperature during the working cycle, variations of the internal energy of the working medium inside the cylinder and heat-exchange with the cylinder walls during the piston displacement for any hydrocarbon fuel and design operation mode of the diesel engine.

3 Results

At the first stage of the simulation of the diesel engine working cycle using Grinevetski-Mazing method the maximum combustion pressure inside the cylinder at the set value of the gas pressure increase at the heat-supply isochore section is calculated. At the second stage the working cycle mathematical model is updated using Wiebe method by means of sequential calculation of the combustion efficiency coefficient, specific combustion heat used and working medium pressure and temperature during the heat burnout for each crankshaft rotation angle (Figs. 3 and 4).

The final result of the formal parameters of the fuel burnout equation is represented by the minimum values which in the absolute deviation of the cycle maximum combustion pressure determined using mathematical calculation as per Wiebe method and the value obtained on Grinevetski-Mazing method. The effective cycle average pressure is compared with the pressure value determined by the power, shaft rotation

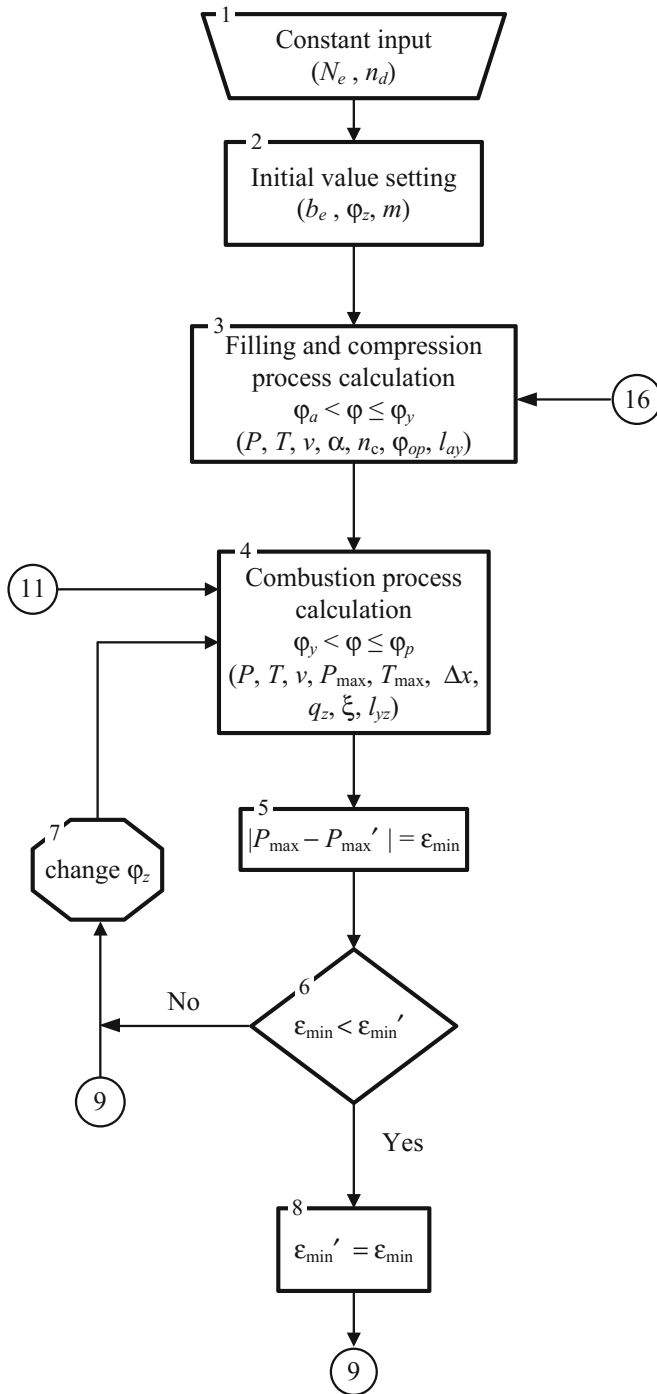


Fig. 3. Working cycle calculation algorithm for the turbocharger diesel engine.

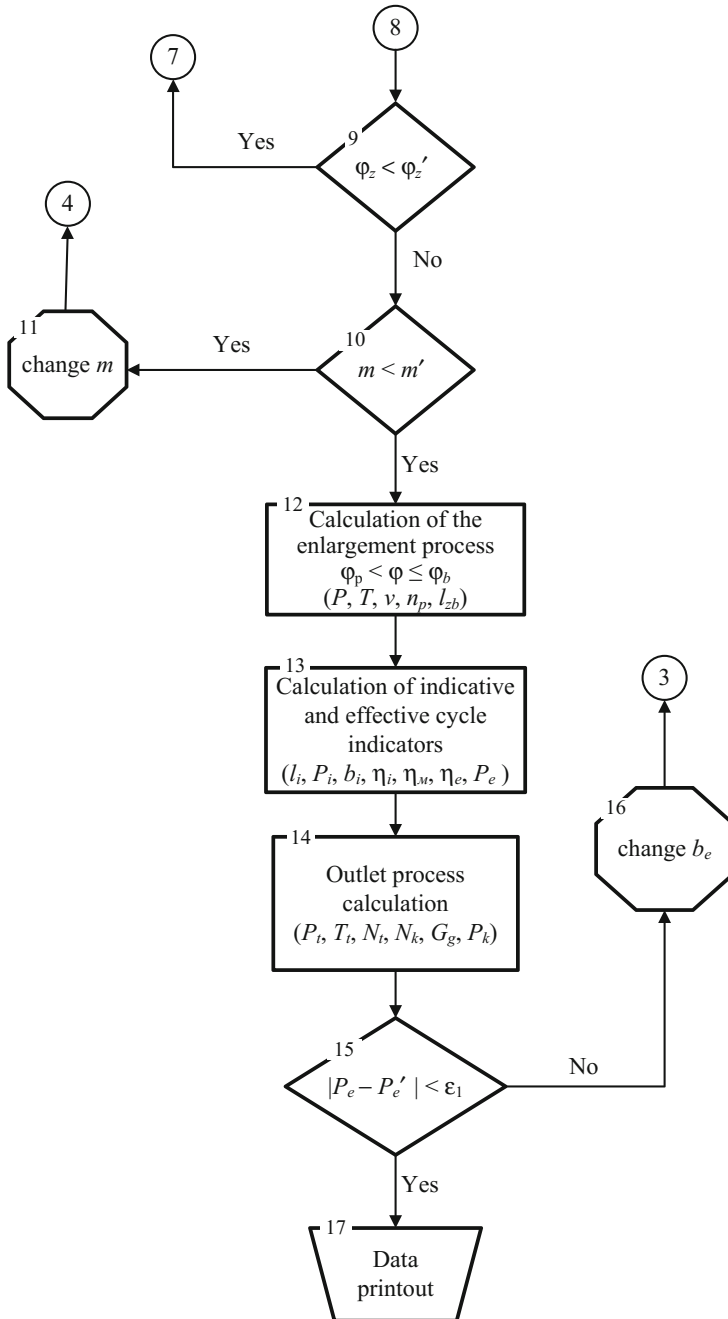


Fig. 4. Working cycle calculation algorithm for the turbocharger diesel engine.

frequency and the engine design parameters and then, if the convergence condition is not met, the value of the specific fuel consumption set at the calculation start is updated. For 1A-5D49 diesel engine curves of the gas pressure and temperature variation during the fuel combustion, burnout characteristics and fuel combustion rate by the crankshaft rotation angle are built (Fig. 5a).

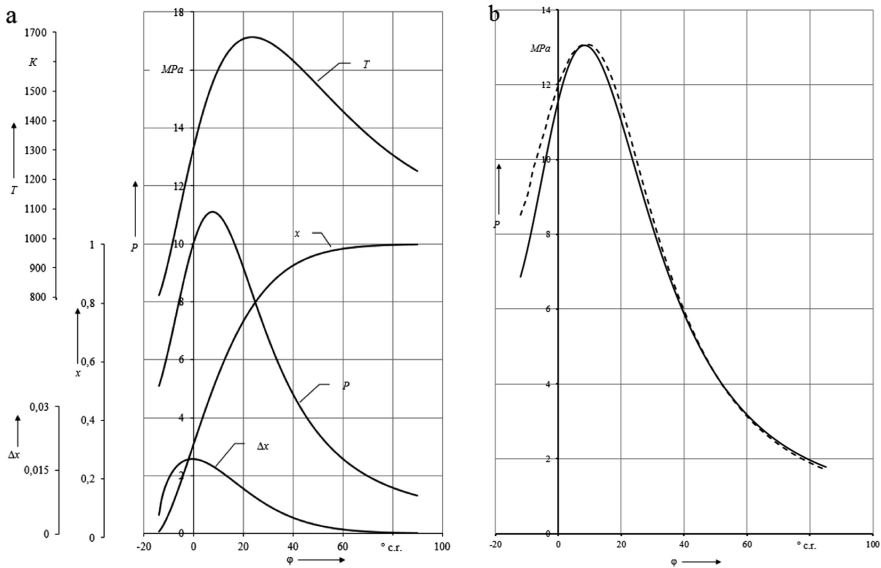


Fig. 5. Fragment of the indicative diagram for D49 diesel engine working cycle combustion process).

The results of the combustion process mathematical simulation were compared with the experimental data using indicative diagrams obtained during the factory tests of 2A-5D49 diesel engines which were calibrated on the rated power mode (Fig. 5b). The diagram shows a good match of experimental and calculated (solid line) values of the gas pressure during the combustion. The average divergence does not exceed 4%.

Thermal and dynamic processes in the internal combustion engines, as a rule, cannot be described using linear regression functions. To improve their description accuracy it is necessary to use higher order mathematical models which results in the need of using orthogonal composite experiment planning. To study the efficiency of the fuel blend application in locomotive diesel engines simulation modeling principles were used [11].

Table 1 provides some results of the working cycle simulation modeling for 2A-5D49 loco-motive diesel engine operating in the rated-power mode on diesel fuel blended with natural gas ($\alpha = 2.071$, $n_d = 1000 \text{ min}^{-1}$, $\varphi_z = 93^\circ$ crankshaft rotation, $m = 0.92$).

Table 1. Results of the working cycle parameter simulation modeling for 2A-5D49 diesel engine operating on diesel fuel and natural gas blend.

Parameter	Simulation experiment results by the experiment number								
	1	2	3	4	5	6	7	8	9
Pz, MPa	10.13	10.14	14.26	14.28	12.46	12.44	14.27	10.13	12.45
Tz, K	1684	1678	1855	1848	1759	1766	1852	1681	1762
l, kJ/kg	637	640	682	684	672	670	683	639	671
Pe, MPa	1.51	1.52	1.62	1.62	1.59	1.59	1.62	1.52	1.59
b, kg/kWh	0.204	0.204	0.199	0.199	0.200	0.200	0.199	0.204	0.200

Obviously, the analysis of the fuel blend application efficiency in locomotive engines should be better performed using both efficiency parameters and diesel engine operation parameters characterizing thermal and dynamic stress of the diesel engine units and assemblies.

Using the methodology above regression coefficients for the equations characterizing the connections between average effective pressure (Pe, MPa), maximum combustion pressure (Pz, MPa), maximum combustion temperature (Tz, K), specific effective fuel consumption (be, kg/(kWh)) and diesel fuel supply timing advance angle x1 and percentage of the alternative additive x2 for rated-power (design) operation mode of the locomotive power unit were calculated:

$$P_e = 1.1672 + 0.2535x_1 + 0.0291x_2 - 0.6025x_1^2 - 0.0005x_2^2 \quad (5)$$

$$T_z = 1420.228 + 251.2084x_1 + 19.7958x_2 - 0.125x_1x_2 - 661.875x_1^2 - 0.2248x_2^2 \quad (6)$$

$$P_z = 4.628 + 1.8499x_1 + 0.4234x_2 + 0.0014x_1x_2 - 4.6065x_1^2 - 0.0043x_2^2 \quad (7)$$

$$b_e = 0.199 + 0.0245x_1 + 0.0005x_2 + 0.0002x_1x_2 - 0.075x_1^2 - 0.00002x_2^2 \quad (8)$$

The optimization calculation results are provided in Fig. 6.

Analysis of the results obtained shows that extreme points for the maximum power characteristics (average effective pressure, maximum combustion temperature, maximum cycle work) and maximum cost efficiency characteristics (specific effective fuel consumption) for the fuel types in question do not coincide. Maximum values for the fuel blend are in the area of fuel supply timing advance angle 44 – 49° crankshaft rotation to UDC. Hereby, the pressure and temperature values are somewhat overstated relative to the rated values. Maximum of the average effective pressure corresponds to the fuel supply timing advance angle about 30° crankshaft rotation to UDC, and minimum value of the specific effective fuel consumption – about 17° crankshaft rotation to UDC. Average effective pressure and specific effective fuel consumption are close to the locomotive engine nameplate values. For all the characteristics the maximum values correspond to the additive percentage in the fuel blend equal to 17.1 – 20.8%. Striving for the minimization of the specific fuel consumption by the fuel supply timing advance angle results in the need of increasing maximum combustion pressure and temperature values relative to the nameplate data.

Therefore, during the optimization problem solution it is appropriate to select the cycle average effective pressure as the key parameter characterizing the diesel engine operation because it is determined not by the diesel engine operation output parameters but also by the cycle indicative operation calculated by the parameters of the simulated indicative diagram and which, alongside with the specific fuel consumption evaluates the locomotive operation work efficiency.

Application of hydrocarbon fuel blend (mixture of gas and diesel fuel) in the locomotive diesel engines will be of substantial advantage in the operation conditions if the price of the gas additive to the diesel fuel is substantially lower than the diesel fuel price.

To attain the locomotive operation mode chart in the train service at the selected traffic section the total heat emitted from the fuel blend combustion must correspond to the heat at each position of the locomotive driver position obtained in diesel cycle. Hereby, the gas supply control system must be set up in such a way that the diesel engine power at each position of the locomotive driver controller corresponded to the rated (nameplate) data.

For this purpose it is proposed to use the law of diesel fuel and alternative additive (natural gas, butane/propane) supply setting up the dependence of the value of the supplied diesel fuel ignition portion and the heat-generating gas portion ensuring the required diesel engine power at the set locomotive driver controller position (Fig. 6).

During the locomotive diesel engine operation in gas/diesel fuel cycle we admit that the value of the diesel fuel ignition portion is 20% of the rated consumption and

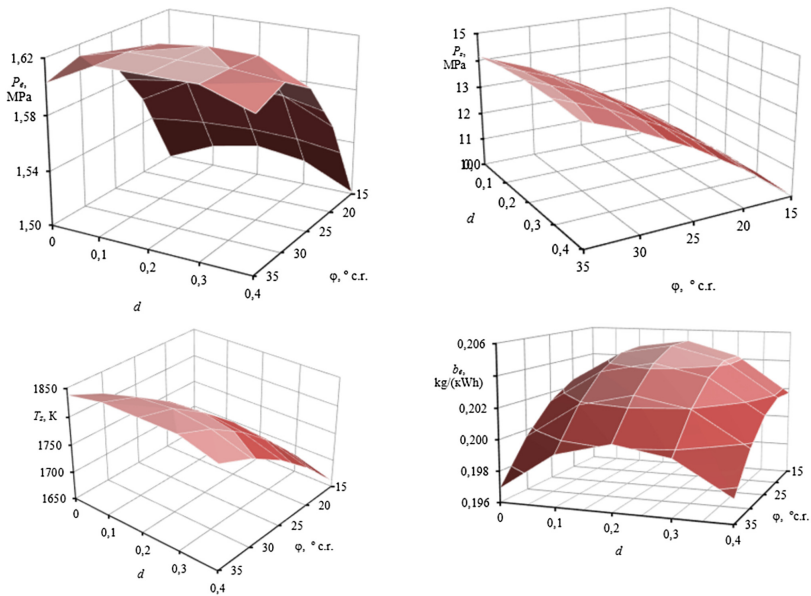


Fig. 6. Dependence of the average effective pressure, maximum combustion pressure and temperature and specific fuel consumption vs. quantity of the additive in the fuel blend and fuel supply timing advance angle for 2A-5D49 diesel engine.

remains virtually unchanged for all the locomotive driver controller positions. Diesel engine power increase from the third position is attained at the expense of the gas supply increase.

The heat to be produced in the diesel engine during the combustion of any types of hydrocarbon fuel in order to implement the operation chart in the locomotive train operation in case of the locomotive engine operation on diesel fuel –

$$Q_{\Sigma} = \sum_{i=0}^{P_k} Q_{\Sigma_i} = \sum_{i=0}^{P_k} B_i t_i H_u^{(d)} \quad (9)$$

in case of the locomotive engine operation on fuel blend

$$Q_{\Sigma} = \sum_{i=0}^{P_k} Q_{\Sigma_i} = \sum_{i=0}^2 B_d^{(i)} t_i H_u^{(d)} + \sum_{i=3}^{15} B_g^{(i)} t_i H_u^{(g)} \quad (10)$$

where $B_d^{(i)}$, $B_g^{(i)}$ are, respectively, diesel fuel and gas hourly flow rate on the its position of the locomotive engine driver controller, kg/h; t_i – diesel engine operation time share on the i th position of the locomotive engine driver controller, h; $H_u^{(d)}$, $H_u^{(g)}$ – respectively, diesel fuel and gas lower heating value, kJ/kg.

The calculation results on Eqs. (9) and (10) are provided in Table 2, based on which it is possible to conclude that regardless of the fuel blend type, regardless of the heat capacity, its combustive components, the total heat quantity must comply with the heat quantity on each locomotive driver controller position obtained during the diesel-fuel cycle operation. This condition must be met, and, obviously, the gas injection control system must be set up to make the diesel engine power on each i th position of the locomotive driver controller be in compliance with the rated, nameplate, values.

The fuel blend flow rate is determined based on its combustion heat, attainment of the diesel engine rated power at the driver controller position as well as based on the cost of different fuel types – monetary costs for the train work completion (Table 3). The calculations completed demonstrate that the conversion of commercial locomotive diesel engines to gas/diesel cycle in case of butane-propane mixture are the additive to the diesel fuel will ensure cost reduction per unit of the work completed by 50%, and natural gas application – by about 44%.

The working cycle calculation in case of work on different types of hydrocarbon fuel blend for the diesel engine rated-power operation mode demonstrated that the combustion pressure line position in the indicative diagram for all the fuel blends is virtually the same. The working fluid temperature at the end of the combustion process for fuel blends is in terms of its value close to the temperature of the diesel fuel combustion products. The fuel combustion rate for all the fuel blends is a bit lower than diesel fuel burnout rate.

The use fuel blends as per the previously proposed law of the fuel blend injection will result in the change of the fuel blend components in the diesel engine cylinder and element chemical composition of the combustive blend which will result in the change

Table 2. Heat distribution by the driver controller positions in case of combustion of different hydrocarbon fuels in diesel and gas/diesel cycles.

Driver controller position	Driver controller position operation time, hrs	Heat, kJ	Heat distribution (kJ) in case of working cycle implementation for 2A-5D49 diesel engine				
			Diesel cycle	Gas/diesel cycle			
				Diesel fuel	Diesel fuel + CH ₄	Diesel fuel	Diesel fuel + C ₄ H ₁₀ + C ₃ H ₈
0	4.37	3383599	3383599	0	3383599	0	
1	0.13	461490	461490	0	461490	0	
2	0.22	1286227	1286227	0	1286227	0	
3	0.27	2113594	2113594	535043	1578551	535043	
4	0.40	3832989	3832989	2338594	1494394	1494394	
5	0.34	3795523	3795523	1987805	1807718	1807718	
6	0.32	4035031	4035031	1870875	2164156	1870875	
7	0.34	4744524	4744524	1987805	2756719	1987805	
8	0.57	8682239	8682239	3332497	5349742	3332497	
9	0.60	9887704	9887704	3507891	6379813	3507891	
10	0.80	14192913	14192913	4677189	9515725	4677189	
11	0.44	8390880	8390880	2572454	5818426	2572454	
12	0.34	6980707	6980707	1987805	4992902	1987805	
13	0.19	4218785	4218785	1110832	3107952	1110832	
14	1.29	31197630	31197630	7541967	23655663	7541967	
15	3.58	95185660	95185660	20930419	74255241	20930419	
Total		2.02·10 ⁸	2.02·10 ⁸	60556000	1.42·10 ⁸	60556000	
			95185660			95185660	

Table 3. Heat distribution by the driver controller positions and total utilities costs' distribution in case of diesel engine operation in diesel and gas/diesel cycles.

Driver controller position number	Fuel flow rate (kg) by the driver controller positions in case of working cycle implementation for 2A-5D49 diesel engine				
	Diesel cycle	Gas/diesel cycle			
	Diesel fuel	Diesel fuel + CH ₄		Diesel fuel + (C ₄ H ₁₀ + C ₃ H ₈)	
Diesel fuel		CH ₄	Diesel fuel	C ₄ H ₁₀ + C ₃ H ₈	
0	78.66	79.43	0	79.43	0
1	10.74	10.83	0	10.83	0
2	29.9	30.19	0	30.19	0
3	50.04	37.06	10.44	37.06	11.58
4	90.28	54.90	29.16	54.90	32.34
5	89.82	46.66	35.27	46.66	39.12
6	94.54	43.92	42.23	43.92	46.83
7	112.21	46.66	53.79	46.66	59.66
8	204.99	78.23	104.38	78.23	115.77
9	230.25	82.35	124.48	82.35	138.06
10	335.42	109.80	185.66	109.80	205.93
11	199.16	60.39	113.52	60.39	125.91
12	164.34	46.66	97.42	46.66	108.05
13	97.2	26.08	60.64	26.08	67.26
14	726.82	177.05	461.55	177.05	511.92
15	2210.29	491.34	1448.81	491.34	1606.92
Total, kg	4724.66	1391.55	2767.35	1391.55	3069.35
Total, RUR	142685	42025	43171	42025	28913
Total per Trip, RUR	142685	85196		70938	

of equilibrium equations and thermodynamic parameters of the different fuel blends' burnout process.

The thermal calculation results obtained, accounting for the fuel element components enabled the application of equilibrium composition for the calculation of the combustion products in the diesel engine cylinder for different fuel types [12].

Graphs of the fuel blend combustion product quantity in the diesel engine exhaust gases vs. the locomotive driver controller position are provided in Fig. 7.

Based on the provided dependencies of the quantity of fuel blend combustion products in the diesel engine exhaust gases it is possible to conclude that the application of diesel and gas fuel blend in the diesel engines enables substantial reduction of a large quantity of soot in the exhaust gases in the entire load range, which, undoubtedly, will promote a larger fuel carbon burnout completeness.

To evaluate the efficiency of the use of fuel blends in the diesel engines for each type of fuel blend a generalized efficiency criterion was worked out as the sum of

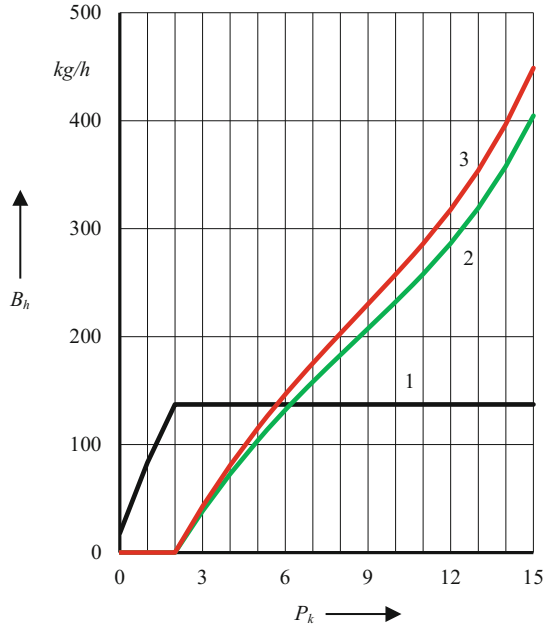


Fig. 7. Law of diesel and gas fuel supply for the working cycle implementation in 2A-5D49 Diesel engine: 1 – Diesel fuel; 2 – Natural gas; 3 – Butane-propane.

dimensionless particular efficiency criteria characterizing the variation of fuel cost efficiency $R_{b_e}^{(j)}$ and quantity of the fuel incomplete combustion products quantity $R_C^{(j)} + R_{CO}^{(j)}$ over the diesel engine working cycle:

$$R_0^{(j)} = \frac{1}{3} \left(a_{b_e} R_{b_e}^{(j)} + a_C R_C^{(j)} + a_{CO} R_{CO}^{(j)} \right) \quad (11)$$

where a_{b_e} , a_C , a_{CO} are the weight coefficients of the particular efficiency criteria.

During the optimization problem solution using Eq. (11) at the first optimization stage the generalized criterion R_0 is minimized, i.e. specific mass emissions of the incomplete combustion products as well as specific fuel flow rate by the power unit using fuel blend are minimized (Fig. 8).

The significance of the particular criteria of the incomplete combustion products is determined by the degree of compliance of the parameters of the diesel engine in question with the existing rates for the toxicity of the exhaust gases (rates EURO-2, EURO-3 etc.).

In order to implement this principle of the weight coefficient selection it is proposed to admit a_{b_e} weight coefficient equal to one ($a_{b_e} = 1$), and to determine a_C , a_{CO} weight coefficients as the ratio of the actual emission of toxic components of the diesel engine exhaust gases $e_{C_{dt}}$, $e_{CO_{dt}}$ to the limiting emission values determined by the exhaust gases toxicity rates for specific diesel engines e_{C_g} , e_{CO_g} . With the exact correspondence

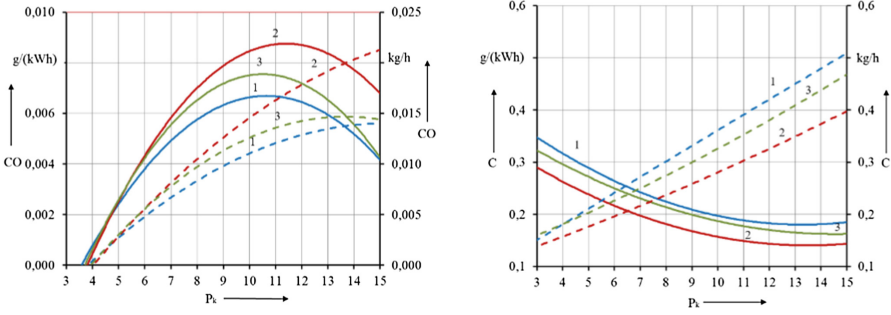


Fig. 8. Graphs of specific (solid line) and mass (dotted line) quantity of co (carbon oxide) and C (soot) in the exhaust gases of 2A-5D49 diesel engine vs. driver controller position: 1 – Diesel fuel; 2 – Diesel fuel and natural gas (CH₄) blend; 3 – Diesel fuel and butane-propane mixture blend (50% C₄H₁₀ + 50% C₃H₈).

of the emissions of the toxic components of exhaust gases of the diesel engine to the toxicity rates, i.e. on condition $e_C = e_{C_g}$, $e_{CO} = e_{CO_g}$ the weigh coefficients a_C , a_{CO} are also equal to one and particular criteria $R_{b_e}^{(j)}$, $R_C^{(j)}$, $R_{CO}^{(j)}$ become equal.

At the first stage of the evaluation of the use fuel blends in the locomotive diesel engines it is appropriate to admit that if $R_0^{(j)} = 1$, then fuel blend application is appropriate provided that each of the particular criteria used does not exceed one.

Bearing in mind the variable operation mode of the locomotive power unit it is appropriate to select the following items as the particular criteria:

Ratio of the hourly fuel flow rate by the locomotive diesel engine operating on fuel blend to similar characteristics of the diesel engine operating on diesel fuel;

Ratio of the quantity of the rated components of incomplete fuel combustion in the fuel blend combustion products over the selected time interval to similar characteristics of the diesel engine operating on diesel fuel.

If the condition (11) is met, it is necessary to additionally (optimization stage 2) use economic criterion which will enable evaluating operation costs for fuel based on inevitable fuel blend price variation.

Particular efficiency criteria included in the equation are determined for each fuel blend type based on the operation modes of the diesel locomotives:

$$R_{b_e}^{(j)} = \frac{\sum_{i=0}^{P_k} t_i b_{e_i}^{(j)} N_{e_i}^{(j)}}{\sum_{i=0}^{P_k} t_i b_{e_i}^{(d)} N_{e_i}^{(d)}} \tag{12}$$

$$R_C^{(j)} = \frac{\sum_{i=0}^{P_k} t_i m_{C_i}^{(j)} b_{e_i}^{(j)} N_{e_i}^{(j)}}{\sum_{i=0}^{P_k} t_i m_{C_i}^{(d)} b_{e_i}^{(d)} N_{e_i}^{(d)}} \tag{13}$$

Table 4. Results of the diesel engine operation parameters calculations, particular and generalized efficiency criteria in case of using fuel blends for 2A-5D49 diesel engine.

P _k	Diesel fuel				Diesel fuel + Natural gas				R _{b_e} ^(j)	R _C ^(j)	R _{CCO} ^(j)	R ₀ ^(j)
	N _e , kW	b _e , kg/(kW/h)	C _i , kg/h	CO _i , kg/(kW/h)	N _e , kW	b _e , kg/(kW/h)	C _i , kg/h	CO _i , kg/(kW/h)				
0	53	0.602	0.572	0.000042	54	0.585	0.433	7.02E-08	0.988	0.748	0.001667	0.579
1	178	0.527	0.516	0.000056	181	0.534	0.392	9.69E-08	1.031	0.783	0.001786	0.605
2	311	0.470	0.464	0.000075	316	0.487	0.353	1.34E-07	1.053	0.801	0.001872	0.619
3	452	0.425	0.416	0.000101	460	0.443	0.318	1.84E-07	1.060	0.809	0.001933	0.624
4	602	0.388	0.372	0.000136	612	0.404	0.285	2.55E-07	1.057	0.810	0.001979	0.623
5	760	0.357	0.332	0.000183	773	0.368	0.256	3.51E-07	1.047	0.806	0.002012	0.618
6	927	0.329	0.296	0.000246	943	0.335	0.229	4.85E-07	1.035	0.801	0.002040	0.612
7	1102	0.306	0.264	0.000331	1120	0.307	0.206	6.69E-07	1.020	0.794	0.002064	0.605
8	1285	0.284	0.236	0.000444	1307	0.282	0.185	9.23E-07	1.007	0.790	0.002091	0.600
9	1477	0.266	0.212	0.000598	1502	0.260	0.168	1.27E-06	0.996	0.787	0.002123	0.595
10	1677	0.249	0.192	0.000804	1706	0.243	0.153	1.76E-06	0.991	0.790	0.002167	0.594
11	1886	0.235	0.176	0.001080	1918	0.229	0.142	2.42E-06	0.992	0.797	0.002226	0.597
12	2103	0.223	0.164	0.001453	2138	0.219	0.133	3.35E-06	1.000	0.811	0.002304	0.605
13	2328	0.213	0.156	0.001953	2368	0.213	0.128	4.62E-06	1.017	0.831	0.002404	0.617
14	2562	0.205	0.152	0.002627	2605	0.210	0.125	6.37E-06	1.042	0.857	0.002528	0.634
15	2800	0.200	0.152	0.003532	2847	0.202	0.126	8.79E-06	1.028	0.849	0.002559	0.627

$$R_{CO}^{(j)} = \frac{\sum_{i=0}^{P_k} t_i m_{CO_i}^{(j)} b_{e_i}^{(j)} N_{e_i}^{(j)}}{\sum_{i=0}^{P_k} t_i m_{CO_i}^{(d)} b_{e_i}^{(d)} N_{e_i}^{(d)}} \quad (14)$$

In Eqs. 12-13 it is designated: $b_{e_i}^{(d)}$, $b_{e_i}^{(j)}$ – specific fuel flow rate by the diesel engine on the i th position of the locomotive driver controller (the locomotive operating, respectively, on diesel and j th fuel blend), kg/(kWh); $N_{e_i}^{(d)}$, $N_{e_i}^{(j)}$ – effective power of the diesel engine on the i th position of the locomotive driver controller (the locomotive operating, respectively, on diesel and j th fuel blend), kW; $m_{C_i}^{(d)}$, $m_{C_i}^{(j)}$, $m_{CO_i}^{(d)}$, $m_{CO_i}^{(j)}$ – respectively, specific quantity of carbon, carbon oxide on the i th position of the locomotive driver controller (the locomotive operating, respectively, on diesel and j th fuel blend), kg/(kWh).

During the implementation of the methodology proposed the weight coefficients a_C , a_{CO} were determined as the ratio of the effective emission of these components in the exhaust gases of the diesel engine operating on fuel blend to the limiting emission values determined by the diesel engines' toxicity rates. The values of weight coefficients are adopted equal to one because the actual emissions of the exhaust gas components were not measured.

The results of the diesel engine operation parameters calculations, particular and generalized efficiency criteria in case of using fuel blends consisting of diesel fuel and 20% natural gas, are provided in Table 4.

4 Conclusions

Using the results of the calculations performed it is possible to conclude that the application of fuel blends in the locomotive diesel engines results in the reduction of the total quantity of incomplete fuel combustion products. Some increase of the diesel engine specific fuel flow rate is due to, mostly, fuel blend combustion heat reduction, theoretical air quantity required to burn a unit of fuel blend, excessive air coefficient and working medium heat for the diesel engine cycle working processes.

The study results provides enable setting the quantity of alternative additives to the diesel fuel, calculating the cost of the work unit produced during the combustion of different hydrocarbon fuel blends in the locomotive diesel engine cylinders as well as solving a number of problems related to the selection of multi-fuel engine setup parameters, evaluation of dynamic effort and thermal stress of the diesel engine parts, methods of cost efficiency improvement and reduction of the engines' negative environmental impact.

The final decision of the locomotive power units' conversion parameters for simultaneous operation on diesel fuel and fuel blends must be made upon results of the comprehensive studies accounting for the variations of power, economics, dynamic characteristics of the diesel engine and type and quantity of the additive to the diesel fuel.

References

1. <http://www.springer.com/lncs> (2016)
2. Ablaev, A.: Receiving motor fuel from renewable raw materials in Russia. *Veh. Flex-fuel* **5** (5), 73–76 (2008)
3. Orsik, L., Sorokin, N., Fedorenko, V.: Bioenergetics: international experience and development forecasts. In: Fedorenko, V. (eds). *Rosinformagroteh FGNU, Moscow* (2008)
4. Devyanin, S.: Vegetable Oils and Fuel on Their Basis for Diesel Engines. Publishing center of FGCU HPE MGAU, Moscow (2008)
5. Markov, V., Gayvoronskiy, A., Grehov, L.: The Work of the Diesels on Nonconventional Fuels. *Legion-Supply, Moscow* (2008)
6. Fofanov, G.: Alternative fuels for rolling stock of railway transport. In: Fofanova, G. (ed.) *Works Ojsc Vniizht. Intekst, Moscow* (2008)
7. Kavtaradze, R.: Thermophysical Processes in Diesel Engines Converted to Natural Gas and Hydrogen. MSTU Bauman Moscow State Technical University, Moscow (2011)
8. Volodin, A.: Complex analysis of thermodynamic, economic and environmental performance of diesel locomotive engines in operation. Omsk State Transport University (2011)
9. Kavtaradze, R.: Special chapter: Textbook for universities. In: *Theory of Piston Engines*, p. 720. MSTU Bauman Moscow State Technical University, Moscow (2008)
10. Kavtaradze, R.: Local Heat Transfer in Reciprocating Engines: Tutorial, p. 472. MSTU Bauman Moscow State Technical University, Moscow (2007)
11. Anisimov, A.: Calculation relationship heats working at combustion of mixed fuels combustion in the cylinder of a diesel locomotive engines. *J. Transsib Railway Stud.* **1**, 8–14 (2014)
12. Semenov, B.: Engineering Experiment in Industrial Engineering, Thermal Engineering and Teplotekhnologijah. Yuri Gagarin State Technical University of Saratov, Saratov (2009)
13. Anisimov, A.: Calculation of the composition of combustion in the cylinder of a diesel engine running on gazodizel cyclea. *J. Transsib Railway Stud.* **1**, 2–6 (2015)

Improvement of Traction Rolling Stock Energy Efficiency Analysis System

Elena Sidorova  and Svetlana Podgornaya  

Omsk State Transport University, pr. Marksa, 35, Omsk 644046, Russia
ps.light@mail.ru

Abstract. Utilities use efficiency improvement is a key task in the energy strategy of Russia. In the conditions of demand growth and constant utilities' price increase correctly organized energy use management is necessary. A critical part in the rate-setting and prediction accuracy improvement in terms of fuel and utilities use for the train traction is allocated to the realistic analysis of the traction rolling stock energy efficiency relative to the previously attained values at the expense of the operation factors' variation. As new locomotive series appear, heavy-weight cargo train traffic develop, passenger train speed increase, innovative equipment and technologies are implemented etc., the degree of various indicators' influence on the utilities' consumption is re-distributed. The purpose of this article is the development of methods for the traction rolling stock energy efficiency variation evaluation at the expense of operation factor set variation.

Keywords: Fuel and utilities · Train traction · Energy efficiency
Specific Energy Use · Analysis · Traction rolling stock

1 Introduction

Every year demand for energy grows so the development of energy-saving technologies enabling solving global economic growth and energy security problems is becoming more and more urgent. Efficient and harmonized use of fuel and utilities is currently one of the top-priority tasks of our country's energy strategy [1]. Railway transport is among the most energy-intensive industries of Russia's economy having a significant energy-saving potential. More than three quarters of the total energy use scope on the railway network is spent on the train traction [2]. Harmonized business administration in this area is impossible without correct organization of fuel and energy use, determination of the demand in utilities corresponding to the present-day engineering development level, organization of the transportation technological process and scope of the work completed.

High performance of Russian Railways JSC activities at the expense of the Company technological upgrade and innovative development is attained by means of increasing energy efficiency and resource-saving technologies' implementation. The main indicator of the railway transportation process energy efficiency is fuel and utilities specific consumption [3]. Structural departments of Russian Railways JSC set technically justified planned rates of the specific energy consumption (SEC) per unit of

the work completed, including statistical average values of operation factors highlighting rolling stock performance indicators and its efficiency utilization, track peculiarities and a number of other factors determining the energy use efficiency [3, 4].

A critical part in the rate-setting and prediction accuracy improvement in terms of fuel and utilities use for the train traction is allocated to the realistic analysis of the traction rolling stock energy efficiency relative to the previously attained values at the expense of the operation factors' variation [3–7]. As new locomotive series appear, heavy-weight cargo train traffic develop, passenger train speed increase, innovative equipment and technologies are implemented etc., the degree of various indicators' influence on the utilities' consumption is re-distributed. The purpose of this article is the development of methods for the traction rolling stock energy efficiency variation evaluation at the expense of operation factor set variation.

2 Experimental Section

Train traction SEC for the entire department bob is determined using the following equation:

$$b_{ob} = \frac{\sum_j b_j \cdot A_j + b_{MR} \cdot \frac{L_{MR}}{100}}{\sum_j A_j}, \quad (1)$$

where b_j , A_j are, respectively, specific utilities consumption, kWh/10.000 km gross and hauling work, 10.000 km gross, in the j^{th} motion type (except maneuver work);

$b_{MR}L_{MR}$ are, respectively, specific utilities consumption, kWh/100 locomotive•km and locomotive conditional run, km, on maneuver work.

b_{ob} value is influenced by a number of operation factors [7, 8]. Analysis of the data and structure of operation and statistics reports of Russian Railways JSC for all the railways and operation locomotive depots for 2009–2014 enabled development of a list of indicators to be accounted for the determination of indicators concerning the energy use for the train traction and for the identification of the reasons for the change thereof. They include:

- train average weight;
- freight car average per-axle load;
- average operating speed;
- service speed factor;
- freight car empty run ratio;
- structure of hauling work by traffic types, by work areas, by locomotive series;
- locomotive downtime awaiting work without locomotive crew;
- locomotive light run;
- number of delays by the red traffic light;
- number of unscheduled stops;
- number of cases of traffic across speed-limit areas;
- passenger train make time;

- specific energy costs in business traffic, shunting service, during downtime, awaiting work without locomotive crew, during locomotive light run;
- recovered energy scope;
- ambient air temperature (in winter);
- specific recovery value;
- implementation (efficiency variation) of energy-saving equipment on the locomotives and new train driving technologies.

All these factors should be better classified based on their physical essence, accounting specific features and peculiarities of energy use influence (Fig. 1).

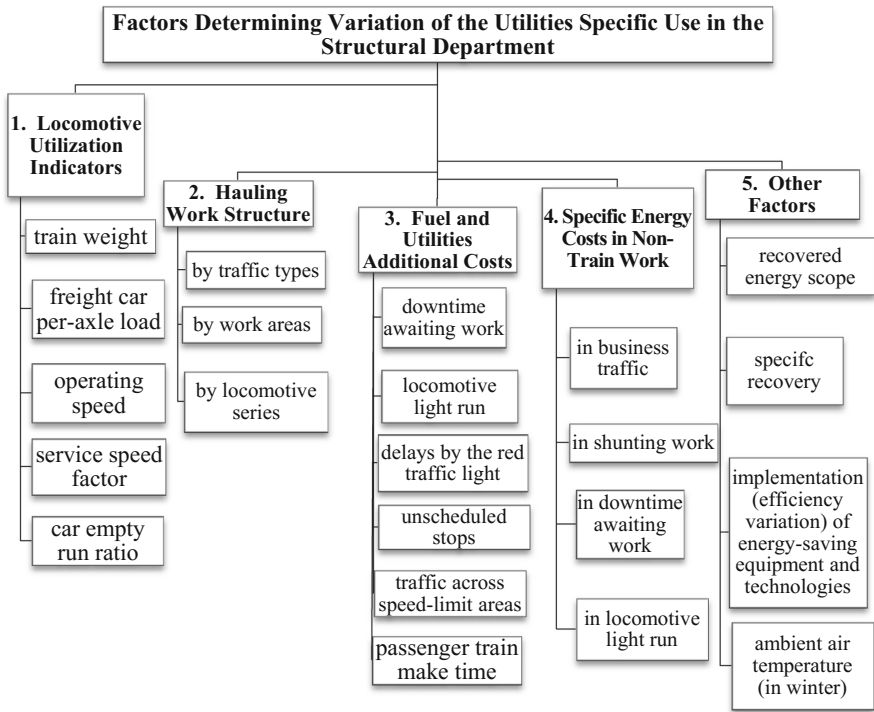


Fig. 1. Classification of factors determining SEC variation for the train traction

It is worth mentioning that the methodology of analysis of fuel and utilities consumption for the train traction which was used in the 1990s [9] provided the evaluation of effect of a number of indicators which cannot be reliably accounted for using report data, or their variation (and, consequently, effect on the fuel and utilities consumption change) throughout the period in question is negligible. They include:

- percentage of cars with rollers (most of the rolling stock wheel pairs are equipped with roller bearings);

- percentage of passenger cars equipped with air conditioning system (there are no report data on the air conditioning system running time in each mode);
- percentage of continuous welded rail tracks in freight and passenger traffic (this indicator exceeds a half of the total railway track length and is increasing every year);
- equivalent grade variation (its value does not change for a long time);
- additional saving in freight and passenger traffic (the technology of such saving determination is not clear);
- non-design factor in freight and passenger traffic (its values differ for different companies, however, formal guidelines on the realistic evaluation of this factor for a specific department and operation area of the locomotive crew are not available).

For the reasons above, the factors above should be neglected during the analysis of the energy use variation.

Besides, a number of parameters, for example, variation of rail tractive effort, technical state and locomotive efficiency, locomotive adhesive weight are included in the mathematical equations determining locomotive utilization indicators' impact on the SEC [7, 9, 10]. For this reason it is not reasonable to study the impact of each individual factor on the SEC, especially, bearing in mind the fact that the calculation of reliable values for the locomotive fleet in operation is problematic and ambiguous.

The main area in the analysis of the traction rolling stock energy efficiency at the department is the evaluation of the difference between the SEC actual delta Δb_{ob}^{fakt} and respective design value of the SEC total delta due to the operation factors' variation Δb_{ob}^{rasch} in the report period relative to the base period. The preceding calendar period similar to the report period is selected as base period [11]. The said values are determined using the following equations:

$$\Delta b_{ob}^{fakt} = b_{ob}^{otch} - b_{ob}^{baz}, \quad (2)$$

where b_{ob}^{otch} , b_{ob}^{baz} are train traction SEC for the entire department, respectively, in the report and base period, determined by the statistical data using the following Eq. (1);

$$\Delta b_{ob}^{rasch} = \sum_n \Delta b_n, \quad (3)$$

where Δb_n is the SEC variation due to the variation of the nth factor in the report period relative to the base period.

Δb_n values are calculated using statistical data for each factor stated in Fig. 1 in the following order.

SEC variation due to the variation of the i^{th} indicator of the locomotive utilization in the j^{th} traffic type is calculated using the following equation:

$$\Delta b_{ij} = b_j^{baz} \cdot \frac{\Delta X_{ij} \cdot \beta_{ij} \cdot \gamma A_j^{otch}}{10000}, \quad (4)$$

where b_j^{baz} is the SEC in the j^{th} traffic type in the base period;

ΔX_{ij} – delta due to the variation of the i^{th} indicator in the j^{th} traffic type in the report period relative to the base period, engineering units;

β_{ij} – effect factor of the variation of the i^{th} indicator on the fuel and utilities specific use in the j^{th} traffic type, %. For detailed description of β_{ij} calculation – see proceedings [9–15];

γA_j^{otch} – percentage of work in the j^{th} traffic type from the total work in the department in the report period, %.

SEC delta due to the hauling work variation by the traffic types is determined using the following equation:

$$\Delta b_{VD} = \sum_j b_j^{\text{baz}} \cdot \frac{(\gamma A_j^{\text{otch}} - \gamma A_j^{\text{baz}})}{100}, \quad (5)$$

where γA_j^{baz} is the work percentage in the j^{th} traffic type from the total work in the department in the base period.

SEC delta due to the transportation scope structure variation by the work areas and locomotive series

$$\Delta b_{kj} = \sum_k b_{kj}^{\text{baz}} \cdot \frac{(\gamma A_{kj}^{\text{otch}} - \gamma A_{kj}^{\text{baz}}) \cdot \gamma A_j^{\text{otch}}}{10000}, \quad (6)$$

where k is the energy efficiency analysis category (work area or locomotive series);

b_{kj}^{baz} – SEC on the k^{th} energy efficiency analysis in the j^{th} traffic type in the base period;

$\gamma A_{kj}^{\text{otch}}, \gamma A_{kj}^{\text{baz}}$ – percentage of work completed on the k^{th} energy efficiency analysis in the j^{th} traffic type, from the total work on the traffic type, respectively, in the report and base periods.

Additional costs of the fuel and utilities shall be determined using the following equations:

From the locomotive downtime awaiting work (including shunting work) –

$$\Delta b_{\text{ozh},j} = \sum_s b_{\text{ozh},s,j}^{\text{baz}} \cdot \frac{(T_{\text{ozh},s,j}^{\text{otch}} - T_{\text{ozh},s,j}^{\text{baz}})}{A^{\text{baz}}}, \quad (7)$$

where $b_{\text{ozh},s,j}^{\text{baz}}$ is the SEC per hour of the locomotive downtime awaiting work without locomotive crew of the s^{th} series in the j^{th} traffic type in the base period, kWh(kg)/h;

$T_{\text{ozh},s,j}^{\text{otch}}, T_{\text{ozh},s,j}^{\text{baz}}$ – locomotive downtime awaiting work without locomotive crew of the s^{th} series in the j^{th} traffic type, respectively, in the report and base periods, hrs;

A^{baz} – total work at the department in all traffic types in the base period.

Due to the locomotive light run delta (including shunting work) –

$$\Delta b_{rez,j} = \sum_s b_{rez,sj}^{baz} \cdot \frac{(L_{rez,sj}^{otch} - L_{rez,sj}^{baz})}{100 \cdot A^{baz}}, \quad (8)$$

where $b_{rez,sj}^{baz}$ is the SEC of the s^{th} series locomotives during light run in the j^{th} traffic type or in shunting work in the base period, kWh (kg)/100 locomotive•km;

$L_{rez,sj}^{otch}$, $L_{rez,sj}^{baz}$ – the s^{th} series locomotives during light run in the j^{th} traffic type or in shunting work, respectively, in the report and base periods, locomotive•km.

Due to the change in the number delays by the red traffic light, unscheduled stops, cases of traffic across speed-limit areas (in all the traffic types, except shunting work) –

$$\Delta b_{ij} = b_{ij}^{norm} \cdot \frac{(X_{ij}^{otch} - X_{ij}^{baz})}{A^{baz}}, \quad (9)$$

where b_{ij}^{norm} is the SEC average rated value per unit of the i^{th} analyzed indicator in the j^{th} traffic type, kWh (kg)/unit;

X_{ij}^{otch} , X_{ij}^{baz} – value of the i^{th} analyzed indicator in the j^{th} traffic type, respectively, in the report and base periods, engineering units.

From the delta of the train make time in passenger traffic (in long-range and short-range traffic) –

$$\Delta b_{nag} = b_{nag}^{norm} \cdot \frac{(T_{nag}^{otch} - T_{nag}^{baz}) \cdot \gamma A_{ps}^{otch} \cdot 0.6}{A^{baz}}, \quad (10)$$

where b_{nag}^{norm} is the SEC average rated value per one minute of the train make time, kWh (kg)/min;

T_{nag}^{otch} , T_{nag}^{baz} – total train make time in passenger traffic, respectively, in the report and base periods, hrs;

γA_{ps}^{otch} – percentage of the total passenger traffic work in the department in the report period.

The SEC delta due to the variation in the recovery energy scope in all traffic types, except shunting work, is determined using the following equation:

$$\Delta b_{rek,j} = \frac{B_{rek,j}^{baz} - B_{rek,j}^{otch}}{A^{baz}}, \quad (11)$$

where $B_{rek,j}^{baz}$, $B_{rek,j}^{otch}$ is the recovery energy scope in the j^{th} traffic type, respectively, in the report and base periods, kWh.

The SEC delta due to the temperature change in the report period relative to the base period is determined by the months of Quarters 1 and 4 using the following equations:

In all traffic types, except shunting work –

$$\Delta b_{\tau_j} = b_j^{baz} \cdot \frac{(t^{baz} - t^{otch}) \cdot \beta_{\tau_j} \cdot \gamma A_j^{otch}}{10000}, \tag{12}$$

in shunting work –

$$\Delta b_{\tau_{man}} = b_{man}^{baz} \cdot \frac{(t^{baz} - t^{otch}) \cdot \beta_{\tau_{man}} \cdot L_{man}^{otch}}{10000 \cdot A^{otch}}, \tag{13}$$

where t^{baz} , t^{otch} is the monthly average ambient temperature in the base and report periods, °C;

b_{man}^{baz} – SEC in shunting work in the base period;

L_{man}^{otch} – total run in the shunting work in the report period;

β_{τ_j} , $\beta_{\tau_{man}}$ – factors of the temperature change effect on the fuel and utilities specific use, respectively, in the j^{th} traffic type and in shunting work, % [16].

3 Results and Discussion Section

In order to validate the methodology above numerous calculations of the SEC variation for Russian Railways JSC departments at different data integration levels over different time periods were performed. As an example, Fig. 2 provides decomposition of the factors affecting the SEC change in freight traffic on electrical traction at N railway in

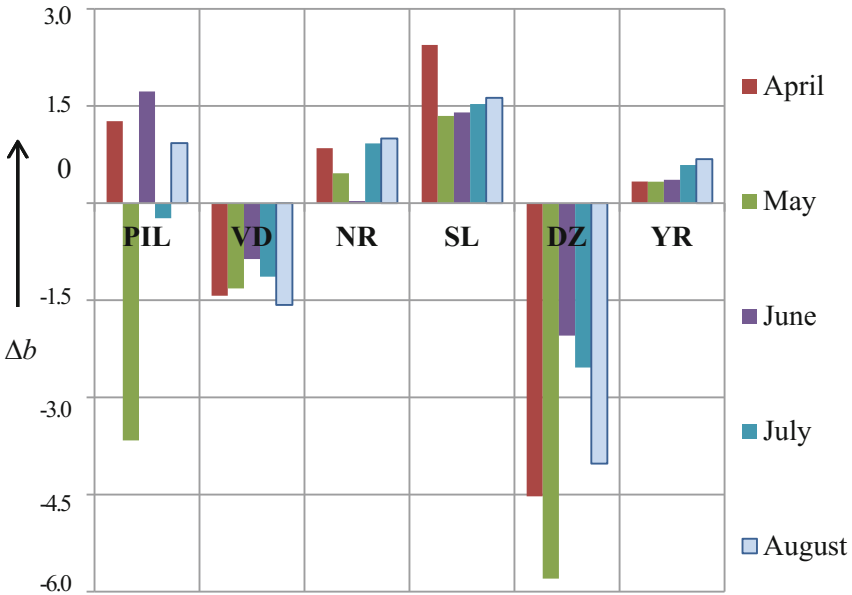


Fig. 2. Decomposition of the factors affecting the change of the utilities specific use in N railway in 2016

April–August 2016. In this figure the following legend is used: PIL – locomotive utilization indicators; VD – hauling work structure change by the traffic types, NR – by the work areas, SL – by the locomotive series; DZ – fuel and utilities additional costs; YR – specific recovery.

The approach to the analysis of the fuel and utilities use for the train traction proposed by the authors is implemented in the Methodology [11] implemented in the Russian railways network, however, it lacks equations to determine a number of factors from groups 4 and 5 (see Fig. 1). To account for the effect of the variation in specific energy costs on the SEC change the following equations are recommended:

In business traffic –

$$\Delta b_{b_{hoz}} = (b_{hoz}^{otch} - b_{hoz}^{baz}) \cdot \frac{\gamma A_{hoz}^{otch}}{100}, \quad (14)$$

where b_{hoz}^{otch} , b_{hoz}^{baz} are SEC in business traffic, respectively, in the report and base periods; γA_{hoz}^{otch} – percentage of business traffic work relative to the total work in the department over the report period.

In shunting work –

$$\Delta b_{b_{man}} = (b_{man}^{otch} - b_{man}^{baz}) \cdot \frac{L_{ob}^{baz}}{100 \cdot A^{baz}}, \quad (15)$$

where b_{man}^{otch} is the SEC in shunting work in the report period;

L_{ob}^{baz} – total run during shunting work in the base period.

The SEC variation due to the change of specific energy costs per one hour of the locomotive downtime awaiting work in the j^{th} traffic type is determined using the following equation:

$$\Delta b_{b_{ozh,j}} = (b_{ozh,j}^{otch} - b_{ozh,j}^{baz}) \cdot \frac{T_{ozh,j}^{baz}}{A^{baz}}, \quad (16)$$

where $b_{ozh,j}^{otch}$ is the SEC per one hour of the locomotive downtime awaiting work without the locomotive crew in the j^{th} traffic type in the report period;

$T_{ozh,j}^{baz}$ – the locomotive downtime awaiting work without the locomotive crew in the j^{th} traffic type in the base period.

The SEC variation due to the change of specific energy recovery in each j^{th} traffic type (except shunting work) is calculated as follows:

$$\Delta b_{b_{rek,j}} = (b_{rek,j}^{otch} - b_{rek,j}^{baz}) \cdot \frac{\gamma A_j^{otch}}{100}, \quad (17)$$

where $b_{rek,j}^{baz}$, $b_{rek,j}^{otch}$ is the specific recovery in the j^{th} traffic type, respectively, in the base and report periods.

Recently, in the railway network, to improve energy efficiency of the utilities use innovative equipment and technologies have been implemented, potential of the

technological process energy efficiency improvement has been used [17–21]. The data of the International Energy Agency (IEA) on the railway transport energy efficiency in the recent years enable making conclusions that in some countries the physical performance of energy-saving activities are improved faster than in Russia. This is primarily due to the fact that the energy use reduction potential in Russian railways has in many respects been utilized (natural limit of the existing technologies' use efficiency has been attained), and its further reduction is possible only at the expense of implementation of innovative, high-end technologies and cost effective equipment and technologies for all the activities of Russian Railways JSC [1].

In 2015 the implementation of energy-saving activities in Russian Railways JSC departments resulted in the reduction of the specific fuel and utilities consumption for train traffic relative to 2014 – for diesel engine locomotives by 2.0%, for electrically-driven traffic – by 1.2% [22]. These indicators were attained, among other things, by making the rated values of energy costs for the traction more stringent at the expense of regenerative braking application efficiency improvement, locomotive fleet upgrade, introduction of energy-optimum train traffic schedule, implementation of utility-saving technologies etc. In this connection it was proposed to extend the traction energy costs analysis methodology with the equation for the calculation of the fuel and utilities specific use due to the implementation (efficiency variation) of energy-saving equipment on the locomotives and new train driving technologies, lubrication performance change in the wheel-to-rail contact zone:

$$\Delta b_{sber.i} = \frac{\Delta B_{sber.i}^{baz} - \Delta B_{sber.i}^{otch}}{A^{otch}}, \quad (18)$$

where $\Delta B_{sber.i}^{baz}$, $\Delta B_{sber.i}^{otch}$ is the value of the fuel and utilities use variation at the expense of implementation (efficiency variation) of the i^{th} energy-saving aid or technology, respectively, in the base and report periods, kWh (kg); is determined using the following equation:

$$\Delta B_{sber.i} = \frac{B_{sber.i} \cdot \delta_{sber.i}}{100 - \delta_{sber.i}}, \quad (19)$$

where $B_{sber.i}$ is the total fuel and utilities consumption on the locomotives using the i^{th} energy-saving aid or technology in the period in question;

$\delta_{sber.i}$ – fuel and utilities saving value at the expenses of using the i^{th} energy-saving aid or technology, %; determined using respective methodologies regulating their application [23, 24].

Realistic analysis of the traction rolling stock energy efficiency variation due to the variation of the effect of the operation factors is the basis for the rate-setting accuracy improvement and fuel and utilities train traffic use prediction which, in its turn, will enable working out strategy and tactics of further railway transport development in the area of energy saving; justifying planned SEC rates, implementing monitoring over the observance thereof, identifying opportunities for the transport process efficiency improvement, evaluating the performance of Russian Railways JSC, its departments and staff.

4 Conclusions

1. Factors determining the value of the traction rolling stock energy efficiency indicator were studied, their classification based on their physical essence, accounting specific features and peculiarities of energy use influence was proposed.
2. Methodology for the analysis of variation of the specific use of fuel and utilities due to the variation of operation factors was presented, including new equations for this process accounting for specific energy costs in non-train activities, as well as implementation (efficiency variation) performance of energy saving equipment on the locomotives and new train driving technologies.

References

1. Development Strategy of Russian Railways Holding for the period until 2030, Approved by the decree of Russian Railways of 14/12/2016, p. 2537
2. Gapanovich, V.A., Avilov, V.D., Ivanov, B.I., et al.: Energy saving in railway transport. Moscow, "Intekhenergo-Izdat", "Teploenergetik", pp. 304 (2014)
3. Order of JSCo Russian Railways from 17/09/2007. 1808 p. "On planning and normalizing the consumption of fuel and energy resources for the traction of trains in JSCo "Russian Railways"
4. Postol, B.G.: The normalization of fuel consumption and electric energy for the traction of trains for a trip, Khabarovsk (2001)
5. Muginshtein, L.A., Molchanov, A.I., Vinogradov, S.A., Popov, K.M., Shkolnikov, E.N.: Modern methodology of technical regulation of fuel and energy resources consumption by locomotives for traction of trains. VMG-Print, Moscow, p. 141 (2014)
6. Galiev, I.I., Nekhaev, V.A., Gorbachev, A.N., et al.: Resource-saving technologies in the structural subdivisions of the West Siberian Railway, pp. 234–256 (2005)
7. Methodology for analyzing the results of consumption of fuel and energy resources for traction of trains CTD-26 Approved by Order of the Ministry of Railways of the Russian Federation of 20/06/1997
8. Vyalkova, S.O.: Eng. Theory Pract. **10**(23), 26–31 (2013). Part 1
9. Sidorova, E.A., Podgornaya, S.O.: Transp. Urals **1**(48), 41–45 (2016)
10. Sidorova, E.A., Podgornaya, S.O.: Izvestiia Transsiba **2**(26), 112–118 (2016)
11. Methodology for the analysis and forecasting of fuel consumption for traction of trains, Approved by the decree of Russian Railways of 26/12/2014, 512
12. Sidorova, E.A., Vyalkova, S.O.: Increase of energy efficiency of land transport systems, pp. 88–95 (2014)
13. Sidorova, E.A., Vyalkova, S.O.: Innovative projects and technologies in education, industry and transport, pp. 36–42 (2015)
14. Sidorova, E.A., Vyalkova, S.O.: Fundamental and applied studies in the modern world, pp. 56–61 (2015)
15. Vyalkova, S.O.: Priority research directions: from theory to practice, pp. 55–59 (2015)
16. Methodology for assessing the effect of ambient air temperature on fuel and energy resources consumption on the traction of trains, Approved by the decree of Russian Railways of 02/04/2012, p. 640
17. Cheremisin, V.T., Nikiforov, M.M.: Izvestiia Transsiba **2**(14), 75–84 (2013)
18. Ivanov, B.I.: Energy Saving **8**, 4–9 (2013)

19. Sharapov, A.A.: *Locomotive* **3**(687), 5–6 (2014)
20. Igin, V.N.: *Railway Transp.* **10**, 53–56 (2015)
21. Cheremisin, V.T., Nikiforov, M.M., Vilgelm, A.S.: *Izvestiia Transsiba* **1**(25), 60–70 (2016)
22. http://ir.rzd.ru/static/public/ruSTRUCTURE_ID=32 (Date of circulation 4 March 2017)
23. Order 2538p of JSCo “Russian Railways” of 28/10/2008 “On methodological recommendations for calculating the economic efficiency of new equipment, technology, intellectual property objects and rationalization proposals” (as amended by Russian Railways Decree No. 2288p of 10/11/2009)
24. Order 1998p of JSCo “Russian Railways” of 09/10/2012 “On Approval of the Methodology for Evaluating the Energy Efficiency of the Application of Lubrication of the Wheel-Rail Contact”

Simulation of Wear Processes of the Monorail Electrical Transport Current Collector Contact Elements

Oleg Sidorov  and Victor Philippov 

Omsk State Transport University, Marx av., 35, 644046 Omsk, Russia
fvm-omgups@mail.ru

Abstract. The article discusses the issues of physical simulation of the wear process of the contact pairs of the monorail electrical transport current collectors. Phenomena arising in the sliding contact during the interaction of the contact elements with the rigid current distributor are described. The simulation was performed on the reciprocating unit imitating impacts typical for the real-life operation conditions, particularly, in the increased humidity and dustiness environment. Based on the study results recommendations on the selection of the optimum combination of the contact element and current distributor materials are provided.

Keywords: Monorail transport · Contact pair · Contact element · Wear Contact pressure · Electrical sliding contact

1 Introduction

Currently in Russia works are underway to develop new types of electrical rolling stock (ERS) designed for high speeds and increased current loads; new types of overhead monorail electrical transport are commissioned.

Electrical energy is transferred to the ERS through the sliding contact for which reason the contact pair elements function in increased electromechanical wear conditions [1].

Wear reduction and current collection device service life extension may be provided using different methods, including by means of selection of such materials for the contact pair which to the fullest extent meet the current collection quality conditions [2, 3].

Omsk State Railway University has accumulated a substantial experience in the development and study of the current collecting devices of monorail transport system with the practical embodiment during the improvement of the current collectors and current distributors at Moscow Monorail Road.

Currently works are underway on the design of overhead monorail transports for different regions of Russia, China, Kazakhstan and other countries in which the conditions require accounting for a wider range of factors affecting the electrical sliding contact. In this connection the study methodology accounting for the increased humidity and dustiness in the contact zone is topical.

The development of new or upgrade of the existing current collectors require substantial number of studies. One of these studies is the study of wear of the current collector contact pairs for which physical and models or tribopairs, tests of real-life objects on special-purpose test beds, on test grounds and in real-life operation are performed.

2 Experimental Section

To solve the problems related to the current collector improvement and development at Omsk State Railway University experimental complex which enables comprehensive studies of the current collectors of underground railways, trunk-line and monorail electrical transport [4].

The studies of the current distributor performance provides static, dynamic, strength, fatigue wear, thermal, aerodynamic, climatic, service life and environmental tests [5]. For the study implementation using the units of the complex methodologies for the evaluation of individual operation parameters of the current distributors and complex impacts of external factors on the current distributor were worked out.

One of the main test beds for the wear study of the monorail transport current collector contact pairs is the reciprocal type unit (Fig. 1), to which the following modules may be connected: module for the simulation of the current conductor butt weld, module for the study of atmospheric phenomena impacts on the electrical sliding contact, module for the simulation of the rolling stock dynamic impact; module for the study of the force of friction in the sliding contact etc.

The basic mechanical part of the unit includes bed frame on which guides connected with the bearers on sliding carriage 4 attached on them. On the carriage contact element 3 is fastened interfacing with the current distributor Sect. 1, fastened on the isolating plate 2. Reciprocal movement of the carriage 4 is performed using rotation drive 5, connected with the carriage using rod 8 [6].

The electrical part of the unit contains a transformer, ballast resistor R_b , measurement shunt R_s and current conducting cables with the ends connected to the current collector and current distributor, respectively.

To ensure reliability of the data array obtained during the tests an algorithm for the implementation and processing of the experimental data developed based on the experiment planning theory provisions was developed. The experiment conditions depend on the parameters and characteristics of the measurement equipment, study object and experimental unit. It is also necessary to account for the human factor the impact of which is manifested through accidental errors and mistakes during the measurements. The final experiment will result in the final relationships documented as charts or tables [7, 8]. Further processing of the graphic or table data and prediction of the study object service life is performed using respective mathematical models.

The experimental studies were performed on the unit above as per the relevant methodology for each combination of the contact pair materials. The main characteristics of the materials in question are provided in Table 1.

Processing and analysis if the experimental data array received demonstrated that in case of electrical current flow in the contact the wear intensity dependence on the

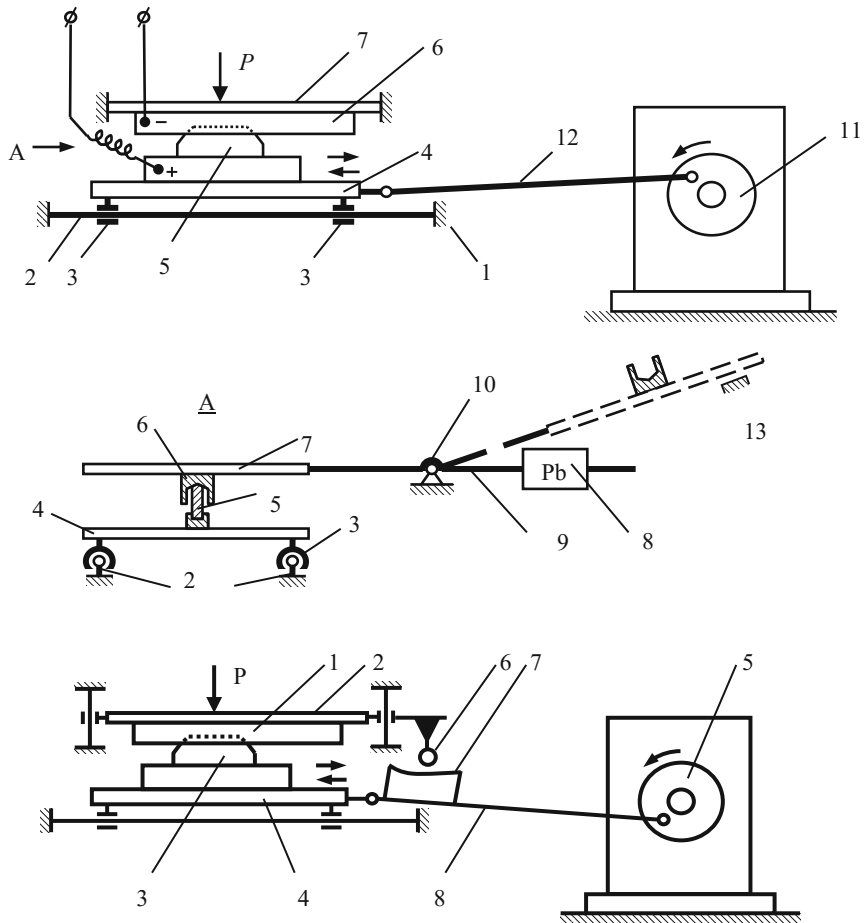


Fig. 1. Reciprocal unit.

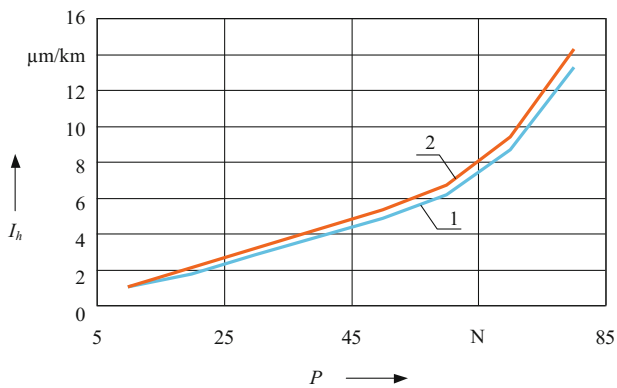


Fig. 2. Copper graphite contact element wear intensity: 1 – unidirectional movement; 2 – reciprocal movement.

Table 1. Characteristics of the materials in question.

Parameter	Hardness, HB	Density, g cm ⁻³	Specific heat, J/(kg K)	Resistivity, μ Ω m
Contact element material				
PMG*	23.45	6.270	518	12
Graphite*	20.18	5.720	720	28
Bronze	72.47	7.514	385	10
Steel	170.52	8.256	462	14
Metal ceramics*	129.04	9.508	444	29

*Legend:

PMG – contact element of copper-graphite composite made using powder metallurgy method;
 Graphite – carbon inserts, grade B for trunk line electrical rolling stock current collector;
 Metal ceramics – metal ceramic iron-based overlays.

contact pressure for all the elements distinctly becomes U-shaped with minimum wear in the pressure range from 40 to 60 N [22].

The analysis of the wear intensity curves obtained showed that the rational combination of the tribopair materials is metal ceramic contact element/BrNCK Alloy Current distributor pair for which the recommended contact pressure range (on the contact element wear minimum) is 50 N.

3 Results and Discussion Section

The objective of the contact pair wear of the current collection devices in monorail electrical transport due to the contact mechanical pressure is the selection of the materials which in the best way comply with the tribo-compatibility, score resistance and wear resistance specifications.

Studies were performed for the contact element materials provided in Table 1; current distributor material – BrNCK brass alloy. The study result review demonstrates that based on the tribosystem elements' wear due to the contact pressure in different study modes (reciprocal and unidirectional movement) has similar shape but the contact pair element wear values are different. Figure 2 shows the dependencies of wear of copper-graphite contact element as function of sliding contact pressure. These rules are manifested for other contact element materials.

In the course of the long-term interaction of the contact pair elements in reciprocal movement under normal environment conditions [8] fine disperse wear particles are produced in the friction zone, these particles have surfactant properties (selective carry-over), or are abrasive particles. The abrasive is charged into softer metal, its particles are not completely removed out of the contact area and later the interaction of the charged surface results in the increased roughness of both surfaces and their intensive wear [13]. The unit unidirectional movement process implementation enables obtaining the wear process picture adequate to the current collector contact pair real-life operation conditions. However, the studies performed in the unit reciprocal movement enable shortening of the experiment time, and then the data obtained may be adjusted respectively.

The ambient air humidity increase results in a minor reduction of the contact pair material wear values.

Further studies of the contact pair materials above (see Table 1) were performed with the current load: on alternating current, on direct current with anode and cathode polarization of the contact element as per the methodology provided in [11].

It is noteworthy that the maximum current in the contact pair is 500 A per duel (standard) current collector with two current distributors. For this reason the current load per one current distributor is 250 A.

Figure 3 provides U-shaped wear curves of the copper graphite and metal ceramics contact elements' wear, hereby the following legend is adopted: 1 – on direct current (anode polarization contact element); 2 – on direct current (cathode polarization contact element); 3 – on alternating current.

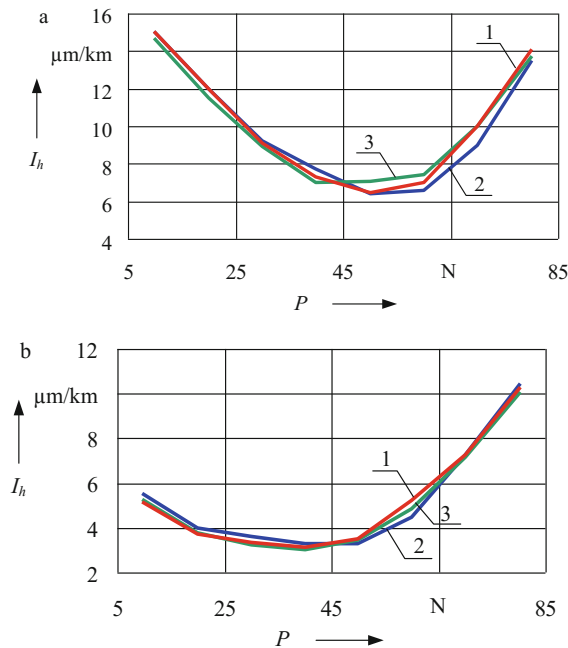


Fig. 3. Electromechanical wear intensity: a- copper graphite composite contact element; b- metal ceramics contact element.

If the current density increases the friction pair element contact wear intensity is reduced. This phenomenon is due to a new factor arising in the contact area – a quasi-liquid lubricating layer (current lubrication effect) [14]. However, this effect may be evaluated only in arc-free current collection, i.e., in the optimum value of the mechanical pressure in the contact, relative air humidity of 50% and minimum values of the environment dustiness.

The material wear with the current load is determined by numerous external factors: current type (alternating or direct), current rate (or density), current polarity (anode or

cathode polarization of the contact element), environment humidity, fine disperse abrasive particles in the air [15].

The material wear curve shape with the current load in the contact takes up U-like shape, both in alternating and direct current. Besides, for all the materials in question, minor bias of the minimum wear towards higher pressure values in case of direct current flow in the contact compared with the minimum wear in case of alternating current flow is observed [16].

During the comparison of the wear curves of anode- and cathode-polarization contact elements the following may be pointed out:

- for anode-polarized metal ceramic contact elements the minimum wear value is lower than for cathode-polarized ones;
- for anode-polarized copper graphite contact elements the minimum wear value is higher than for cathode-polarized ones.

The graphite contact element wear value virtually does not depend on the current type and contact element polarization [17].

Values of the wear of the materials in question at minimum, maximum and average value of the pressure range at the value of the current flow of 250 A are provided in Table 2.

Table 2. Contact element material wear.

Pressure, N	PMG	Bronze	Steel	Graphite	Metal ceramics
<i>Alternating current</i>					
10	14.6	10.8	8.9	24.2	5.2
50	7.05	4.9	2.9	13.8	3.4
80	13.7	10.2	7.4	28.1	10.1
<i>Direct current</i>					
10	15.6/15.0	14.3/13.2	10.1/9.7	25.2/25.7	5.1/5.5
50	6.2/6.4	5.9/5.7	3.1/2.98	13.9/13.9	3.5/3.3
80	14.1/13.3	11.2/10.5	7.8/8.1	29.1/30.5	10.3/10.4

In Table 2 for the direct current the numerator is the wear value for anode-polarized contact element, in the denominator – for cathode-polarized one.

Of special wear are metal ceramic contact element wear research. Experimental studies reveal that during the interaction (without current in the contact) the metal ceramic element undergoes intensive wear and abrasive particles are produced the hardness of which is comparable with the current distributor material hardness. The abrasive particles produced concentrate on various sections of the contact area which results in the current distributor surface destruction and, consequently, to the intensive abrasive wear thereof.

However, the wear picture changes during the current flow in the contact. Substantial reduction of the abrasive quantity in the contact is observed already at the current value of 10 A [18]. For metal ceramics – BrNCK alloy contact pair aspects

pertaining to synergy phenomena occur, particularly, occurrence (like in solid lubricant use) of the quasi-liquid lubricating layer. The said factor is due to the destruction of the large wear fractions as a result of the contact pair elements' surface layer temperature reduction in case of current load (Fig. 4). This phenomenon substantially reduces the wear of the said contact pairs [19]. The contact spot state study demonstrates that graphite is present in the friction area (Fig. 5), which results in the boundary lubrication effect. This phenomenon results in the reduced friction factor and wear.

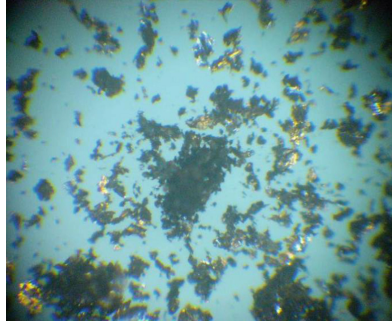


Fig. 4. Fine disperse wear fraction produced during the current flow in the contact.

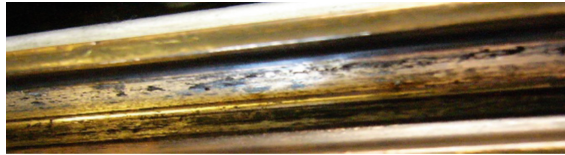


Fig. 5. Graphite lubrication formation in the friction area on the current distributor during the interaction with an iron-based metal ceramic contact element.

In real-life operation conditions the ambient humidity increase results in the current collection quality compromise resulting from the condensate formation on the current distributor which results in increased sparking and arcing [20, 21].

The ambient humidity increase to 98% has changed the minimum wear values for the materials in question compared with the basic values. This is due to the fact that minimum wear is observed at the contact pressure values characterized by the absence (or minimum) of sparking. At low pressure values electrical erosion component in all the materials in question increases which is due to the increased sparking and arcing in increased humidity conditions (Fig. 6).

As per the methodology [8], in the contact area air dustiness (number of fine disperse abrasive particles) was increased to 200 mg/m^3 .

The material wear studies were performed under the current load (alternating and direct current with different contact element polarization). The study results for copper graphite and metal ceramic contact elements are provided in Fig. 7, numbers designate



Fig. 6. Sparking in PMG-current distributor tribopair contact in increased humidity.

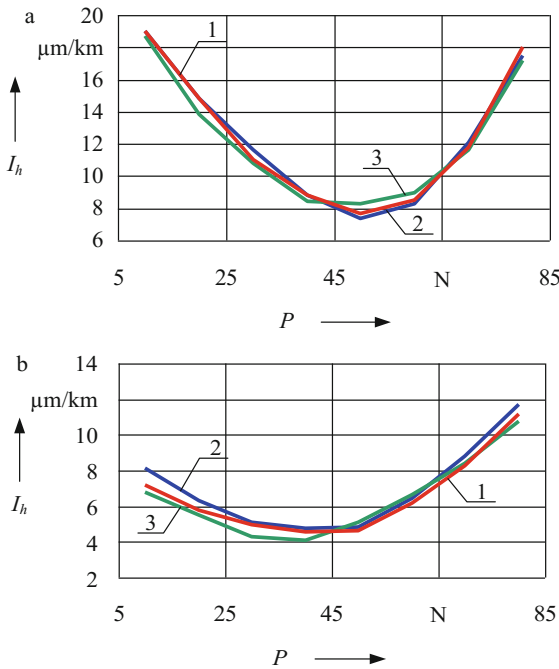


Fig. 7. Electromechanical wear intensity curves with the ambient air dustiness: a – for copper graphite contact element; b – for metal ceramic contact element.

the wear curves: 1 – direct current (anode polarized contact element); 2 – direct current (cathode polarized contact element); 3 – alternating current.

Wear studies demonstrate that during the copper graphite contact element interaction with the current distributor in increased ambient air dustiness grooves from fine disperse particles appear on the copper graphite contact element (Fig. 8). Besides, intensive sparking is observed (Fig. 9).



Fig. 8. Grooves from fine disperse particles on the copper graphite contact element.

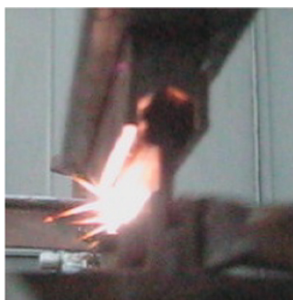


Fig. 9. Intensive sparking during the work of copper graphite contact element-current distributor tribopair in increased air dustiness.

In case of using metal ceramic contact elements the arcing substantially reduces and the grooves are not distinct.

4 Conclusions

Processing and analysis of the experimental data array received demonstrated that in case of electrical current flow in the contact the wear intensity dependence on the contact pressure for all the elements distinctly becomes U-shaped with minimum wear in the pressure range from 40 to 60 N [22].

The analysis of the wear intensity curves obtained showed that the rational combination of the tribopair materials is metal ceramic contact element/BrNCK Alloy Current distributor pair for which the recommended contact pressure range (on the contact element wear minimum) is 50 N.

References

1. Stupakov, S., Sidorov, O., Philippov, V.: Modelling of electromechanical wear of contact pairs of current pickup devices electric transport. *Frict. Lubr. Mach. Mec.* **4**, 23–30 (2012)
2. Sidorov, O.: Studies of the electromechanical wear of contact pairs in the current collection devices of electric transports. *J. Frict. Wear* **5**, 390–394 (2015)
3. Sidorov, O., Stupakov, S.: Methods for studying the wear of contact pairs of monorail electric transport current collection devices. OSTU, Omsk (2009)

4. Stupakov, S., Philippov, V.: The simulation of wear of contact pairs of current collection devices of monorail electric vehicles. *Izvestia Transsiba* **3**(7), 43–52 (2011)
5. Tucker, R., Miller, A.: Low stress abrasion and adhesive wear testing. Device for investigating the sliding contact between the current collector and the contact wire. *ASTM STP* **615**, 68–90 (1975)
6. Sidniaev, N., Vilisova, N.: Device for investigating the sliding contact between the current collector and the contact wire. In: *Introduction to the Theory of Experimental Design*, vol. 463 (2011)
7. Stepanova, E.: Introduction to the theory of experimental design. In: *Basics of Processing the Results of Measurements*, vol. 95 (2014)
8. Chichinadze, A.: *Basics of Processing the Results of Measurements. Friction, Wear and Lubrication*. Mashinostroenie, Moscow (2003)
9. Stupakov, S., Sidorov, O.: Friction, wear and lubrication. Research and forecasting of wear of contact pairs of current collector systems with a rigid current conductor, p. 173 (2012)
10. Russian Standard GOST 8.050-73: Reference conditions for linear and angular measurements (1988)
11. Myshkin, N.: *Electrical Contacts*. Dolgoprudny (2008)
12. Avilov, V.: Electrical contacts. *Railw. Transp.* **11**, 69–71 (2010)
13. Sidorov, O., Kharlamov, V., Shkodun, P.: Study of sliding contact in electric machines contact current collector systems with a rigid current lead. *Marshrut*, Moscow (2006)
14. Sidorov, O.: Prediction of wear of contact pairs of current-carrying monorail electric vehicles. *Elektromekhanika* **5**, 76–80 (2011)
15. Biesenack, H., Pintscher, F.: Kontakt zwischen Fahrdrabt und Schleifleiste-Ausgangspunkte zur Bestimmung des elektrischen Verschleißes. *Elektrische Bahnen* **3**, 138–146 (2005)
16. Sidorov, O.: On the issue of reducing wear and increasing the level of the contact insertion of urban electric vehicles. Increasing the efficiency of operation of collector electromechanical energy converters IX, pp. 76–80 (2013)
17. Sidorov, O.: Experimental studies of wear of contact pairs of current-collecting devices. In: *Materials of the Fourth All-Russian Scientific-Practical Conference with International Participation*, vol. 2, pp. 8–11 (2013)
18. Sidorov, O.: Methods for estimating the wear of contact pairs of electric current collection devices. In: *Theses of the Reports of the Seventh International Symposium*, pp. 81–82 (2013)
19. Philippov, V., Frolova, O.: Modeling the interaction of contact pairs of monorail electric transport current collection devices. *Mathematical modeling and calculation of units and devices of railway transport objects*, pp. 50–53 (2012)
20. Stupakov, S., Philippov, V.: Methods for estimating the wear of contact pairs of current collector devices based on tribological studies. *Innovative projects and new technologies in education, industry and transport*, pp. 235–246 (2012)
21. Stupakov, S., Philippov, V.: Modeling of wear of contact pairs of electrical transport monorail. *Transport Urala* **2**(29), 87–91 (2011)

Determination of the Electrical Locomotive Energy Efficiency to Evaluate Its Repair Quality

Sergei Shantarenko^(✉) , Mikhail Kapustyan ,
and Oleg Supchinsky 

Omsk State Transport University, Karl Marx Ave., 35, 644046 Omsk, Russia
nauka@omgups.ru

Abstract. The article is dedicated to the urgent problems of resource saving and energy efficiency of the railway rolling stock. The methodology of the electrical locomotive repair quality evaluation based on the locomotive energy efficiency indicator is proposed. Constraining units and key parameters affecting additional energy losses determined depending on the electrical locomotive repair quality are singled out. The article provides the results of the locomotive energy efficiency indicator calculations for a number of locomotive series.

Keywords: Repair quality · Energy efficiency · Energy efficiency indicator
Rolling stock · Electrical locomotive

1 Introduction

One of the key areas in the railway transport energy efficiency improvement [1–5] are the activities to improve the locomotive fleet technical state which is substantially influenced by the quality of the maintenance and repair activities [6].

Technical state of the units and assemblies in which during the operation in case of their parameters and characteristics variation additional power losses may occur in many ways affects the electrical locomotive energy efficiency. Therefore, the electrical locomotive repair quality may be determined by the level of the additional energy losses in the units, assemblies and assembly elements occurring in case of violation of the engineering and technological parameter tolerances set in the repair documents. Electrical locomotive quality repair is a crucial factor of the railway transportation process reliability and safety [7]. Currently in Russian Railways the locomotive fleet is repaired by servicing companies in the servicing locomotive depots and at the locomotive repair plants. The main objective of these companies is the assurance of the company driving rolling stock availability with the economically justified financial costs level [8]. The repair quality is characterized by the engineering, technological and economic indicators, one of the key ones being the energy efficiency of the locomotive repaired.

2 Experimental Section

To determine the repair quality in terms of the electrical locomotive energy efficiency the energy efficiency indicator (EEA_{EL}) was selected and justified which is determined based on the technological parameters of the units and assemblies received during the repair and documented in the reports and electronic certificate of the electrical locomotive [9]. To determine the electrical locomotive energy efficiency indicator it is necessary to account for only those performance characteristics and technological parameters determined during its repair or post-repair diagnosis. Losses due to the operation modes are not accounted for [10]. It is proposed to evaluate the quality of the electrical locomotive repair from the energy efficiency prospective using the locomotive energy efficiency calculated as the ratio of the experimentally calculated efficiency value to the control calculation value [11]:

$$EEA_{EL} = \frac{\eta_{EC}}{\eta_{CC}} \quad (1)$$

where η_{EC} is the experimentally calculated efficiency determined based on post-repair parameters of the units and assemblies as per the repair documents;

η_{CC} – control calculation efficiency adopted based on the manufacturer’s certificate data for this series locomotives.

The locomotive efficiency during the driving motor operation at full power at the speed corresponding to the locomotive long-term operation mode and at the rated voltage on the current collector should be not less than:

- 0.860 for alternating current;
- 0.875 for direct current [12].

The efficiency is reduced due to the power loss growth in the driving motors, in converters, including transformers, smoothing reactors, exciters in case of independent or compound excitation; power losses during the electrical power consumption by the auxiliary machines and other users of the auxiliary circuits due to their technical state worsening (Fig. 1) [13, 14].

In the hourly mode the power loss in the driving motors is 5–6% of the locomotive active power; converter losses, including transformers, smoothing reactors, exciters in case of independent or compound excitation, are 4–5.5%; power losses in case of electricity use by the auxiliary machines and other auxiliary circuit users are 3–5.5%. In their turn, transformer losses are 1.5–2.0%, in the converter themselves –1.0–1.5%, in the smoothing reactors –1.5–2.0%. The total losses are 13–16%.

Power losses caused by the locomotive proper motion resistance are normally accounted for in the power consumption for the train motion in general, i.e., conditionally classified as the net work, where the net work is the work on the locomotive wheel rim. However, one should bear in mind that the wheel rim power, i.e. product of the rail tractive effort and the train speed is in effect larger by the value of the wheel friction work power during the sliding along the rail surface. In the normal mode of the so-called elastic sliding the losses do not exceed 0.5%.

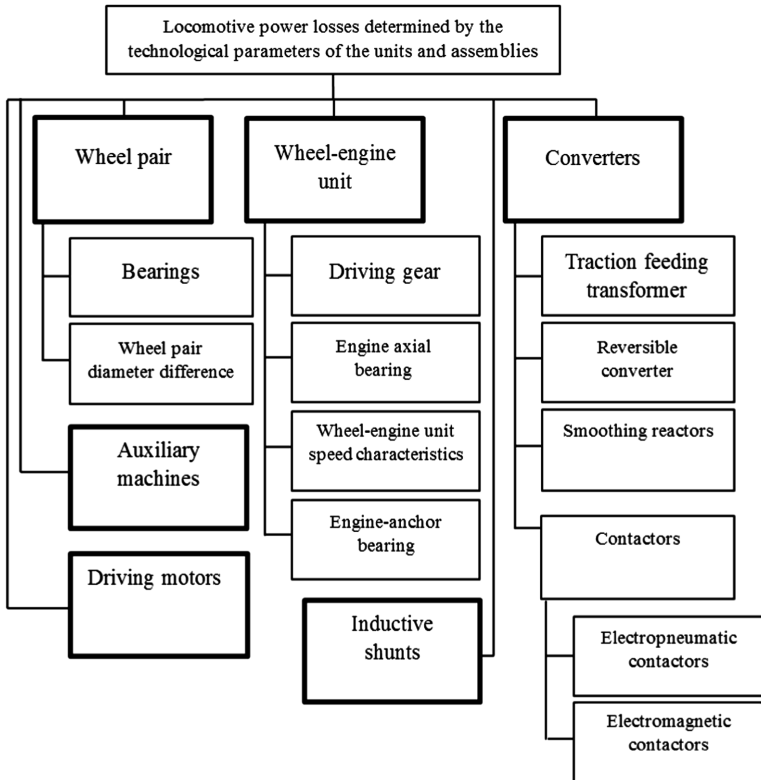


Fig. 1. Loss determination block diagram.

Therefore, the following technological parameters affect the locomotive energy efficiency:

- radial gap in the journal bearing and motor anchor bearings;
- side gap in the driving gear;
- diameter difference of the wheel pair treads;
- driving motor rotation frequency;
- dimension controlling the dip of the upper and lower power contacts (as per the drawing and after the wear);
- power contact break;
- power contact dip;
- power contact pressing (initial and final);
- idle voltage on the driving transformer secondary windings;
- voltage drop at each arm of the rectifier-inverter;
- air consumption for the cool-down of the inductive shunts, smoothing reactors.

During the repair in the locomotive elements, units and assemblies additional power losses due to the deviation of their technical parameters and characteristics from the manufacturer's values set in the design documents may occur which reduces its

efficiency. Additional power losses depend on the units' and assemblies' technical parameter and characteristic tolerances set in the repair documents: the higher are the tolerances, the more significant the power losses may be.

The locomotive post-repair experimentally calculated efficiency is

$$\eta_{EC} = \eta_{CC} - \frac{\sum_i \Delta P_i}{P_{EL}} \quad (2)$$

where ΔP_i are the predicted additional power losses in the i th locomotive assembly determined based on the technical parameters and characteristics of this assembly after the repair completed as recorded in the repair documents;

P_{EL} – long-term mode power on the locomotive motor shafts for the locomotive series in question.

For the locomotive series in question total predicted additional power losses are determined when all the tolerances for the repair of individual units and assemblies set in the regulatory documents are met but hereby the losses in each unit or assembly are maximum

$$\Delta P_{max} = \sum_i \Delta P_i^{max} \quad (3)$$

To determine the total power losses calculation and analysis method is used. The calculation and analysis method is based on the determination of the electrical power use components for the entire product or for the component parts thereof with the subsequent summation thereof [15].

At such additional loss level the experimentally calculated efficiency η_{EC} and energy efficiency indicator EEA_{EL} will have minimum values:

$$\eta_{EC}^{min} = \eta_{CC} - \frac{\Delta P_{max}}{P_{EL}} \quad (4)$$

$$EEA_{EL}^{min} = \frac{\eta_{EC}^{min}}{\eta_{CC}} \quad (5)$$

For each locomotive series the EEA_{EL}^{min} has its own value due to the design peculiarities. To evaluate the repair quality obtained through calculation the energy efficiency indicator EEA_{EL} is compared with EEA_{EL}^{min} calculated for this locomotive series.

When the EEA_{EL} is smaller than EEA_{EL}^{min} , the repair quality from the energy efficiency prospective is considered unsatisfactory. In this case additional repair activities on the units with the largest predicted power losses is required.

3 Results and Discussion Section

The application object of the methodology proposed are long-range cargo and passenger DC and AC locomotives operated in Russian Railways. EEA_{EL} is calculated for the locomotive after TP-3 routine repair or repair of similar scope and ready for the operation handover.

This methodology validation in the servicing locomotive depots and repair plants demonstrated that to calculate the energy efficiency indicator a large number of parameter values (from 100 to 150 parameters for one locomotive section, depending on the design features) measured during the locomotive repair and after it shall be used. Apart from this, some parameters, such as contactor pressing force, are not recorded in the reports; it is merely stated that they are within the rated limits.

This approach does not enable speaking of the possible practical application of the methodology proposed and the mathematical calculation complicated by a large number of parameter inputs significantly complicates the EEA_{EL} determination process computerization.

Further studies demonstrated that in the present-day locomotives 15–20% of the total energy is used for auxiliary needs (auxiliary equipment, converters etc.) is used in direct current, and 25–30% – in alternating current. Most of the electrical energy (70–85%) used by the locomotive is due to driving motors and in the wheel-motor units is converted into mechanical energy of the wheel pair rotation and driving effort for the train motion.

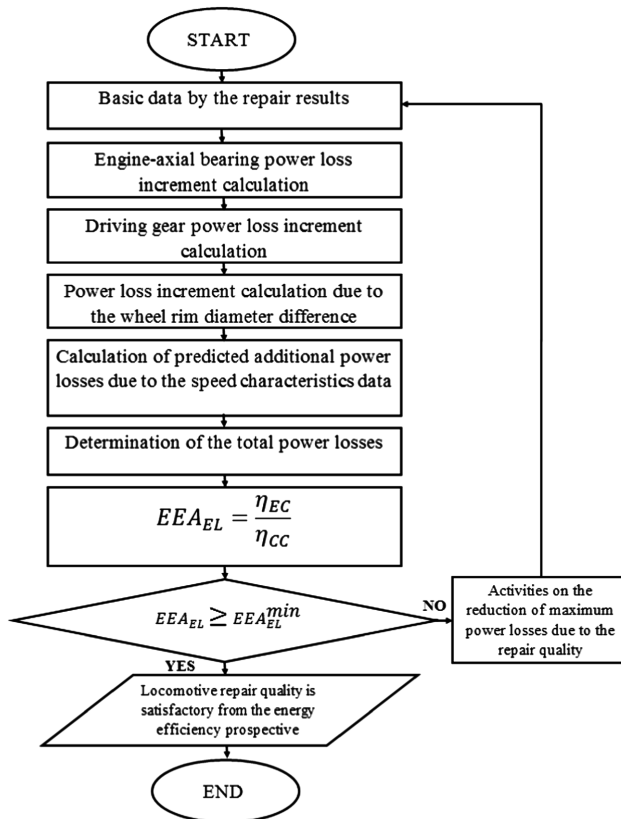


Fig. 2. EEA_{EL} determination algorithm.

Therefore, for the EEA_{EL} calculation it is necessary to account for the additional power losses related to the post-repair parameters of the locomotive following units and assemblies: motor-axial bearings, driving gear, wheel pairs and driving motors (speed characteristics) [16].

EEA_{EL} determination algorithm based on the loss increment evaluation in the locomotive mechanical system constraining units is provided in Fig. 2.

To validate the methodology proposed and calculate the locomotive energy efficiency indicator data collection and input into the Locomotive Energy Passport was arranged in the locomotive plants and servicing locomotive depots of Locomotive Technologies LLC and STM-Service LLC.

4 Conclusions

Based on the EEA_{EL} calculation data obtained for 2ES6, 2ES5C, EP2C series locomotives (Table 1) by means of pilot operation of the Locomotive Energy Passport it is possible to make the conclusion that the updated methodology of the locomotive energy efficiency indicator calculation is operable and may be used to evaluate the locomotive repair quality.

Table 1. EEA_{EL} calculation results for pilot operation.

Locomotive	Date	EEA_{EL}	EEA_{EL}^{\min}
2ES5C No.110-1	26.12.2016	0.997	0.993
2ES5C No.110-2	27.12.2016	0.996	0.993
2ES5C No.119-1	27.12.2016	0.994	0.993
2ES5C No.119-2	27.12.2016	0.997	0.993
2ES6 No.235-1	26.12.2016	0.999	0.994
2ES6 No.237-2	21.11.2016	0.999	0.994
2ES6 No.315-1	12.12.2016	0.997	0.976
2ES6 No.315-2	09.12.2016	0.996	0.976
2ES6 No.323-1	26.12.2016	0.996	0.976
2ES6 No.323-2	26.12.2016	0.996	0.976
EP2C No.029	18.01.2017	0.997	0.986
EP2C No.148	20.12.2016	0.997	0.986
EP2C No.153	15.12.2016	0.999	0.986
EP2C No.174	21.12.2016	0.997	0.986
EP2C No.179	07.12.2016	0.998	0.986
EP2C No.183	15.12.2016	0.998	0.986

The methodology proposed may also be used for the locomotive state monitoring using the energy efficiency indicator variations during the operation. Besides, with the further accumulation and classification of the data concerning the energy efficiency indicator variation trends there appears the possibility of EEA_{EL} comparison with the

actual data of the locomotive operation energy efficiency data to identify the reasons of the electrical energy over-use and taking follow-up measures to correct the situation. Besides, the methodology proposed may be used to evaluate the repair quality of individual limiting units of the mechanical equipment as well as for the prediction of their residual service life based on the data of the energy efficiency indicator variations.

References

1. Gapanovich, V.: Increase Energy Effic. *Railway Transp.* **2**, 12–16 (2012)
2. Mlinarić, T., Ponikvar, K.: Energy efficiency of railway lines promet. *Traffic Transp.* **3**, 187–193 (2011)
3. Alzhanov, B.: Energy efficiency of electric locomotives. *World Transp.* **1**, 56–63 (2009)
4. Andryushchenko, A.: Increase of power efficiency of passenger electric locomotives with an asynchronous traction drive. *News Petersburg Univ. Commun. Sci.* **4**, 5–14 (2015)
5. Nachigin, V.: Reserves for improving the energy efficiency of locomotives in processing heterogeneous information. *Her. SAGUTU* **5**, 24–30 (2015)
6. Shantarenko, S.: Quality of repair and energy efficiency of electric locomotives. *Bull. Rostov State Univ. Commun.* **1**, 46–53 (2015)
7. Jastremskas, V.: System for the maintenance of locomotive operational reliability. In: *Proceedings of the 6th International Scientific Conference Transbaltica*, pp. 98–102 (2009)
8. Shantarenko, S.: Technological audit as a tool to ensure the operational reliability of locomotives. *News Transsib.* **4**, 63–69 (2011)
9. Batko, W., Borkowski, B., Glocki, K.: Application of database systems in machine diagnostic monitoring. *Maint. Reliab.* **1**, 7–10 (2008)
10. Kurbasov, A.: The operational efficiency of electric locomotives as an indicator of the efficiency of their use. *Transp. Russ. Fed.* **3–4**, 39–41 (2012)
11. Shantarenko, S.: Calculation of the index of energy efficiency of electric locomotives for assessing the quality of their repair. *Increase of energy efficiency of land transport systems*, pp. 280–285 (2014)
12. Russian Standard GOST R 55364-2012: Electric locomotives General specifications. Moscow (2013)
13. Buzmakova, L.: Technique of diagnostics of rectifier-inventory converters of electric locomotives of an alternating current. *Electr. Eng.* **2**, 24–27 (2016)
14. Sklyar, A.: Diagnostics system of electric equipment of traction rolling stock Sklyar. *Operational reliability of locomotive fleet and increase of traction efficiency*, pp. 59–67 (2014)
15. Nikiforov, M.: Application of the calculation-analytical method for comparative evaluation of energy efficiency of freight electric locomotives. *Operational reliability of the locomotive fleet and increasing the traction efficiency*, pp. 143–149 (2014)
16. Shantarenko, S., Kapustyan, M., Obrivalin, A.: Estimation of power losses in the nodes of the crew part of electric locomotives. *News Transsib* **3**, 62–68 (2015)

Application of Magnetic Wedges for Stator and Rotor Slots of DC Motors

Viktor Kharlamov^(✉) , Yuriy Moskalev , and Denis Popov 

Omsk State Transport University, 35 Karl Marx Ave., Omsk 644046, Russia
emoe@omgups.ru

Abstract. The article considers the issue of ferromagnetic wedge application efficiency for the anchor and main pole slots in DC motors. Magnetic field simulation results using finite element method as exemplified by the commercial DC motor are provided. The findings obtained are analyzed for the cases with and without the ferromagnetic wedges. The change of the machine magnetic flux value is evaluated.

Keywords: DC motor · Magnetic flux pulsation · Magnetic slot wedge
Finite element method

1 Introduction

Electromechanical converter energy performance improvement is a topical area in scientific research. Energy performance improvement of high power motors which also include rolling stock motors is of special importance. Motor high energy performance guarantees operation and capital expenses reduction. This electrical machinery energy performance improvement is especially urgent due to the utilities' price growth. Reliability and efficiency improvement should be attained without noticeable increase of the electrical machine fabrication costs. One of the possible ways to improve the electrical machinery efficiency is the application of ferromagnetic slot wedges [1–19].

It enables magnetic loss reduction due to the magnetic flux pulsation reduction in the stator and rotor core teeth pulsation reduction (air gap induction distribution curve improvement), air gap magnetic reluctance and, consequently, magnetization current and electrical losses reduction [13, 14]. Currently, in Russia in different industry and transport branches DC electrical machines are still used due to their good starting and control characteristics, despite their known disadvantages. DC commutator motors are used as driving motors both in railway transport (on electrical locomotives and trains), and in mine dump trucks, on urban passenger transport etc. Magnetic wedges for electrical motor slots are made in a way minimizing eddy currents in them, for example, using iron powder [18]. These wedges are made as plates reinforced with four layers of fiberglass cloth of glass-magnet-dielectric mass consisting of epoxy resin, hardener and iron powder [5, 7, 9, 16]. This material magnetic permeability of this material at the manufacture stage may be adjusted by modifying the iron powder to other components ratio [17, 19].

Let us analyze DC motor magnetic system using magnetic wedges which may replace paper laminate and cloth laminate slot wedges.

2 Experimental Section. Materials and Methods

This work makes use of finite element method implemented in FEMM software [20–22] enabling calculation of two-dimensional image of the magnetic field lines distribution and calculation results export for the analysis in other programs. Finite element method is a widely used to solve problems of magnetic field simulation in the systems with complex geometry and different magnetic permeability in different areas. For simulation purposes the parameters of commercial DC series-wound driving motor (power – 800 kW and rated power – 980 A). For the calculation the driving motor magnetic system is reviewed in one cross-section. The machine slot skewing is not accounted for. Geometric dimensions, steel grades, magnetization curves and other parameters required for simulation are adopted as stated in the design documents and reference data.

3 Results and Discussion Section

The magnetic field calculation without the magnetic slots in the core slots gives the result shown in Fig. 1.

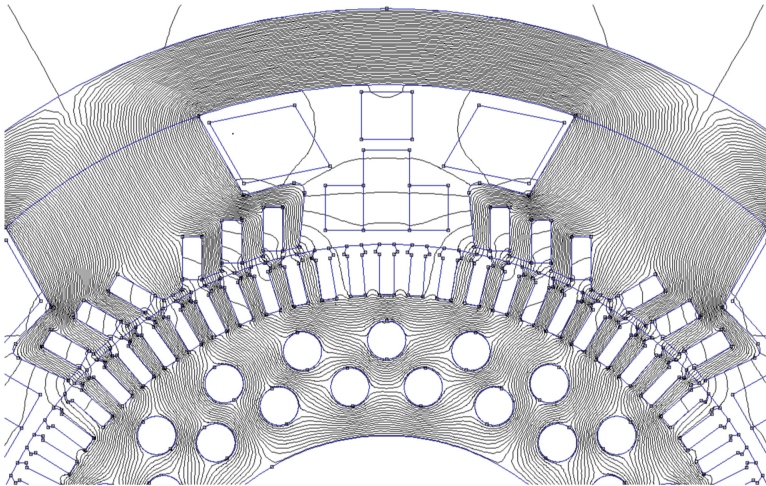


Fig. 1. Magnetic field line distribution for the case without magnetic wedges.

The magnetic induction distribution in one pole pitch along the anchor surface is provided in Fig. 2(a).

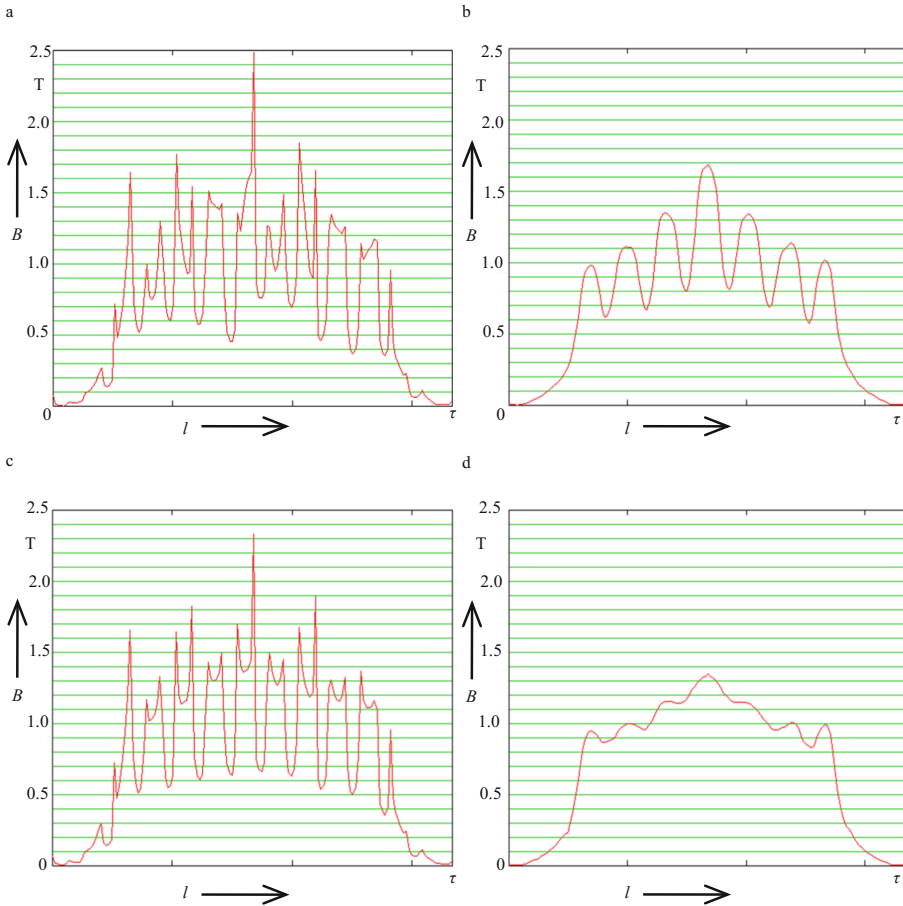


Fig. 2. Induction distribution along the pole pitch: (a) without magnetic wedges; (b) with magnetic wedges in the anchor slots; (c) with magnetic wedges in the main pole slots; (d) with magnetic wedges in the anchor and main pole slots.

As we can see from Fig. 2(a) the magnetic induction under the main pole is distributed in a substantially non-uniform manner. Hereby, at the teeth edges there are areas of significant saturation. In the induction curve there are harmonics due to the teeth of both the anchor core and main poles. The results of the magnetic field induction distribution calculation along one pole pitch on the anchor surface with the magnetic wedges in the anchor slots only is provided in Fig. 2(b). As we can see from Fig. 2(b), the magnetic induction under the main pole with the magnetic wedges in the anchor slots only is distributed in a more uniform manner than in the case without the magnetic wedges.

At the tooth edges there are no substantially saturated areas. In the induction curve the harmonic due to the main poles' teeth is distinctly observed. The calculated

magnetic field induction distribution long one pole pitch on the anchor surface in the case with the magnetic wedges in the main pole slots only is shown in Fig. 2(c).

As we can see from Fig. 2(c) the magnetic induction under the main pole with the magnetic wedges in the main pole slots only is distributed in a more uniform manner than in the case without the magnetic wedges (Fig. 2(a)), however, in a less uniform manner than with the magnetic wedges in the anchor slots.

On the teeth edges there are substantially saturated areas. In the induction curve the harmonic due to the anchor teeth is distinctly seen.

The magnetic field calculation with the magnetic wedges in place simultaneously in the anchor and main pole slots yields the result of the induction distribution along one pole pitch on the anchor surface, as provided in Figs. 2(d) and 3.

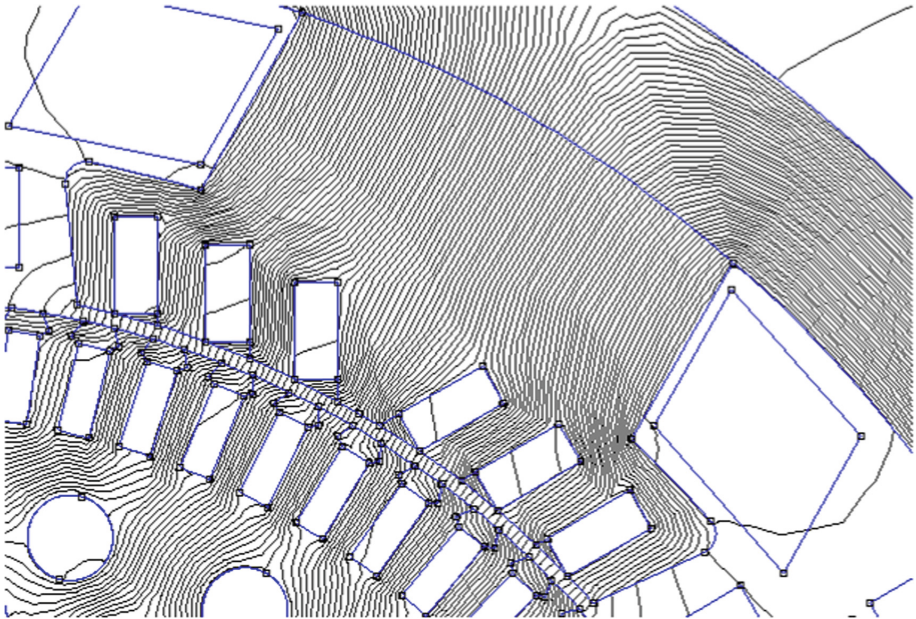


Fig. 3. Magnetic field line distribution with magnetic wedges both in the anchor slots and in the main pole slots.

As may be seen from Figs. 2(d) and 3, the magnetic induction under the main pole with the magnetic wedges in place simultaneously in the anchor slots and main pole slots is distributed in a more uniform manner. Along the pole pitch the induction distribution is close to sinusoid law. On the teeth edges there are no areas with substantial saturation. In the induction curve harmonics due to the anchor and main pole teeth are rather mildly manifested.

The magnetic induction distribution curves along the pole pitch provided in Fig. 2 enable evaluation of the magnetic flux variation with the magnetic wedge introduction into this machine as the ratio of the reduced function integrals:

$$\frac{\Phi'}{\Phi} = \frac{\int_0^{\tau} (B'(l))dl}{\int_0^{\tau} (B(l))dl} \quad (1)$$

where Φ is the machine main pole magnetic flux without magnetic wedges in place;
 Φ' – the machine main pole magnetic flux with magnetic wedges in place both in the anchor slots and in the main pole slots;

L – point coordinate on the anchor surface;

B – magnetic induction in the respective points of one pole pitch in the machine without magnetic wedges in place;

B' – magnetic induction in the respective points of one pole pitch in the machine with magnetic wedges in place both in the anchor slots and in the main pole slots.

Due to the fact that the magnetic system calculation using finite element method enables obtaining results as a numerical series, the Eq. (1) calculation is reduced to finding the following ratio:

$$\frac{\Phi'}{\Phi} = \frac{\sum_{i=1}^N B'_i}{\sum_{i=1}^N B_i} \quad (2)$$

where i is the number of the point in which the magnetic field induction value is found,
 N – number of points on the calculated curve.

The calculation of Eq. (2) for the curves in Fig. 2(a) and (d) provides the following result:

$$\frac{\Phi'}{\Phi} \approx 1.018$$

Therefore, the magnetic wedges' application enables enhancing the magnetic flux of the driving motor in question by approximately 1.8%, other machine parameters being equal, due to the increased tooth area magnetic conductivity.

4 Conclusions

The simulation conducted using finite element method as exemplified by the specific driving motor shows that the magnetic wedge application enables, to a significant degree, getting rid of the known disadvantages of the open-slot wedges.

A more uniform induction distribution under the main pole (Fig. 2(d)), enables simplifying the machine design due to the waiving the slot skewing in the anchor core which will also reduce the main pole field effect on the anchor winding section switching process. Advantages of this engineering solution application in the driving motor will consist in the following positive effects:

- increased electromagnetic torque and electromotive force (EMF) of the anchor winding with the retained values of the anchor current and excitation current due to the magnetic flux increase;
- reduced magnetic losses due to the induction pulsation;
- the machine switching improvement.

The data obtained from the magnetic field simulation using finite element method are mostly harmonized with the known proceedings of other authors, they also do not contradict the physical processes in the electrical machine.





The findings from the research conducted may be used in machine-building during the design of new DC driving motors. Hereby, to improve a specific motor performance it is necessary to determine the optimum value of the ferromagnetic wedges' magnetic permeability value and the shape of these wedges.

References

1. Donato, G., Capponi, F., Caricchi, F.: Influence of magnetic wedges on the no-load performance of axial flux permanent magnet machines. In: IEEE International Symposium Industrial Electronics (ISIE), 2010 (2010)
2. Simburger, H.: Technical report: Investigation of Metal Powder Filled, Glass Fiber Reinforced Resin, used as Slot Wedge in Electrical Engineering Industry, Vienna University of Technology, Vienna Austria (2010)
3. Belhadi, M., Krebs, G., Marchand, C., Hannoun, H., Mininger, X.: Evaluation of a switched reluctance motor with magnetic slot wedges. In: International Conference on Electrical Machines, Berlin, Germany, pp. 150–155 (2014)
4. Li, R.: Improvements in energy efficiency of induction motors by the use of magnetic wedges. In: Petroleum and Chemical Industry Conference, 2011 Record of Conference Papers Industry Applications Society 58th Annual IEEE, pp. 1–6, 19–21 (2011)
5. Tessarolo, A., Luise, F., Bortolozzi, M., Mezzarobba, M.: New magnetic wedge design for enhancing the performance of open-slot electric machines. In: IEEE Conference Publications in Electrical Systems for Aircraft, Railway and Ship Propulsion (ESARS) (2012)
6. Wang, S., Zhao, Z., Yuan, L., Wang, B.: Investigation and analysis of the influence of magnetic wedges on high voltage motors performance. In: IEEE Vehicle Power and Propulsion Conference (VPPC), Harbin, China (2008)
7. Dems, M., Komeza, K., Sykulski J.: Analysis of effects of magnetic slot wedges on characteristics of large induction motor. In: ISEF 2011, Funchal, Portugal (2011)
8. Milojkovic, Z., Ban, D., Petrinic, M., Studir, J., Polak J.: Application of magnetic wedges for stator slots of hydrogenerators. Cigre Session, SCA1, A1-101, Croatia (2010)
9. Dems, M., Komezai, K., Sykulski, J.: Analysis of effects of magnetic slot wedges on characteristics of large induction motor. *Prz. Elektrotech. (Electr. Rev.)* **88**(7b), 73–77 (2012). ISSN 0033-2097
10. Cha, J., Kim, R., Choi, J., Yun J.: A study of the characteristic of the high-voltage induction motor considering the magnetic wedge effect with poles. In: Electrical Machines and Systems ICEMS, pp. 122–124 (2015)
11. Li, W., et al.: Influence of magnetic wedge on electromagnetic field distribution of permanent magnet traction motor. In: 2015 International Conference on Electrical Systems for Aircraft, Railway, Ship Propulsion and Road Vehicles (ESARS), Aachen, pp. 1–5 (2015)

12. Petričić, M., Tvorčić, S., Car, S.: The effects of pole number and rotor wedge design on unbalanced magnetic pull of the synchronous generator. In: 2014 International Conference on Electrical Machines (ICEM), Berlin, pp. 316–322 (2014)
13. Delaere, K., Belmans, R., Hameyer, K.: Influence of rotor slot wedges on stator currents and stator vibration spectrum of induction machines: a transient finite-element analysis. *IEEE Trans. Magn.* **39**, 1492–1494 (2003)
14. Zhu, Z., Wu, L., Xia, Z.: An accurate subdomain model for magnetic field computation in slotted surface-mounted permanent magnet machines. *IEEE Trans. Magn.* **46**(4), 1100–1115 (2010)
15. Besnerais, J.: Reduction of magnetic noise in PWM-supplied induction machines – low-noise design rules and multi-objective optimization, Ph.D. dissertation, Ecole Centrale de Lille, France (2008)
16. Besnerais, J., Fasquelle, A., Pelle, J., Harmand, S., Hecquet, M., Lanfranchi, V., Brochet, P., Randria, A.: Multiphysics modeling: electro-vibro-acoustics and heat transfer of induction machines. In: International Conference on Electrical Machines (ICEM 2008), Villamura, Portugal (2008)
17. Oberretl, K.: Iron losses, flux pulsation and magnetic slot wedges in squirrel cage motors. *Electr. Eng.* **82**(6), 301–311 (2001)
18. Doronin, A.Y.: Patent 2525425/24-07 Russian Federation, MPK H02K3/48. Magnetic wedge for mounting the windings in the slots of magnetic core of electrical machine. Applicant for a Patent and Patent Holder is State Educational Institution of Higher Education Omsk State Transport University, № 668043; Stated. 19.09.1977; Released 15.06.1979. Bul. №22
19. Chumak, V.: Development, implementation and operation experience of magnetic wedges into a powerful asynchronous motors and synchronous generators. *Ukr. hydropower* **4**, 4–10 (2010)
20. <http://www.femm.info>. Accessed 27 Aug 2017
21. Meeker, D.: Improvised open boundary conditions for magnetic finite elements. *IEEE Trans. Magn.* **49**(10), 5243–5247 (2013)
22. Meeker, D.: Improvised asymptotic boundary conditions for electrostatic finite elements. *IEEE Trans. Magn.* **50**(6), 7400609 (2014)

Intelligent Automated System for the Monitoring of Railway Areas with a Low Transport Process Energy Efficiency

Vasily Cheremisin , Mikhail Nikiforov  ^(✉), Alexey Kashtanov ,
and Sergey Ushakov 

Omsk State Transport University, Karl Marx av., 35, Omsk 644046, Russia
nikiforovmm@rambler.ru

Abstract. The article provides principles for the evaluation of the energy utilization efficiency for the train traction at the sections of electrified railways of arbitrary length using time-synchronized data of the automatic electricity billing systems installed on the contact network feeders of the traction substations and electrically driven rolling stock as well as satellite system rolling stock location data are used. Restrictions of the existing measurement systems and data processing of the electricity utilization for the train traction are listed. Identification areas of the bottlenecks with reduced energy efficiency in the traction power supply system, train driving technology, train traffic organization are demonstrated. Results of the pilot operation of the electrical power accounting subsystem on the contact network DC traction substation feeders are provided. Expected scientific and practical results of the system proposed are identified.

Keywords: Traction power supply system · Electrrolling stock
Transportation process · Accounting of the electric power · Energy efficiency

1 Introduction

One of the priorities of Russian Railways JSC is energy efficiency improvement of its core activities – transportation process [1]. A large part of the known organization and engineering activities on the train traction energy efficiency improvement has already been developed and is implemented at the railway network [2] or requires such significant capital investments that make them economically inappropriate.

There is also a number of factors related to the organization of the train traction electrical power accounting organization [3], preventing further substantial improvement of the train traction energy efficiency indicators at Russian Railways JSC at the expense of development and implementation of organization activities. As far as the engineering support of the electrical power accounting on the electrical rolling stock is concerned, the existing systems have the following disadvantages:

- low accuracy class;
- high sensitivity threshold;

- absence of satellite navigation system GPS/GLONASS;
- absence of wireless data transmission;
- vulnerability of unauthorized external intervention with their operation.

Besides, at the DC railway test ground there are no electrical power accounting on the contact network feeders. As far as the data processing is concerned, the Automated System for the Centralized Driver Route Processing (COMM) has the following disadvantages:

COMM data source is routes of the train drivers stating only total use and return of the electrical power on the trip which restricts a more detailed analysis of the electrical rolling stock power use and search for the saving opportunities;

It does not enable obtaining information of the electrical power use efficiency by the electrical rolling stock on the days' results for prompt response purposes;

Manual information input from the driver's route which results in numerous errors in the statistical reports and, consequently, unreliable information of the electrical power accounting and inadequate rate-setting of the electricity use.

Therefore, for further reduction of the electricity use and loss for the train traffic a new tool for the search and elimination of the local low-efficiency sections is required. This tool may be the Automated System for the Transportation Process Energy Efficiency Monitoring (ASMEPP) which ensures energy efficiency evaluation of the joint operation of traction energy use and electrical rolling stock.

2 Experimental Section

ASMEPP concept provides joint processing of the electrical parameter synchronous measurements on the feeders of the contact network of traction substations and electrical rolling stock in the boundaries of the arbitrary railway section using satellite and geoinformation technologies of the electrical rolling stock positioning [4, 5], which enables prompt and sufficiently reliable determination of the electrical power use for the train traffic and development of the system of control actions to improve it. The ASMEPP operation is possible in the boundaries of individual inter-substation zones, tariff zones, locomotive crew operation areas, in the boundaries of the railways as well as any other arbitrary sections.

ASMEPP ensures evaluation of the electrical power use efficiency for the train traction in the boundaries of the set railway section on the following key indicators:

- electrical power losses in the traction substation equipment – traction-feeding transformers and reversible converters;
- specific electrical power use for the train traction by the traction substation meters;
- electrical energy losses in the traction network;
- specific electrical power use for the train traction by the electrical rolling stock meters;
- electrical power use per each unit of electrical rolling stock in the boundaries of the area in question.

Processing of synchronous measurements of the electricity use variations on the contact network feeders and on the electrical rolling stock in combination with the train traffic schedule data will enable evaluation of:

- Utilization ratio of the adjacent traction substations;
- Scope of electrical power transfer in the boundaries of inter-substation zones;
- Efficiency of regenerative braking application and regeneration energy use;

Engineering and economic effects produced in case of energy-optimum train traffic schedule implementation, application of new electrical locomotives and, consequently, new weight rates, heavy-weight train driving, upgrade of the traction power-supply system equipment etc.

Works on the development and implementation of ASMEPP include the following stages [6]:

- (1) Setting of the project objective and tasks;
- (2) Development of the system creation philosophy;
- (3) Development of ASMEPP elements' specifications;
- (4) Status review of the existing engineering facilities for its potential use within the ASMEPP system;
- (5) Development of ASMEPP concept;
- (6) Development of methodological base and its algorithmization;
- (7) Engineering implementation of ASMEPP elements.

All the ASMEPP internal elements may be conditionally divided into hardware and software ones (Fig. 1).

ASMEPP software includes:

Data bases containing characteristics of the traction power supply system and electric rolling stock (equipment on the traction substations, electrical parameters of the traction network in different configurations, traction and braking characteristics of different series of electrical locomotives and electrical trains operated at the section etc.);

Calculation module to determine the actual module for the determination of the actual indicators or the transportation process energy efficiency;

Simulation modeling module of the modes of the joint system of electrical power supply and electrical rolling stock;

Logical module for the analysis of actual values of the controlled parameters obtained and comparison with the rated values;

Module for the control action production.

Hardware to be implemented for the ASMEPP commissioning includes automatic systems for the electrical energy accounting on contact network feeders (ASUE FKS) and on electric rolling stock (ASUE EPS) as well as geo-positioning units based on the satellite navigation systems GLONASS/GPS.

It is worth mentioning that for the implementation of all the ASMEPP functions it is necessary to use the data of external systems, such as Automated System for the Commercial Billing of Electrical Power (ASKUE) of the traction substations, Auto-mated System of the Train Sheet Record and Analysis GID "Ural", the data of the

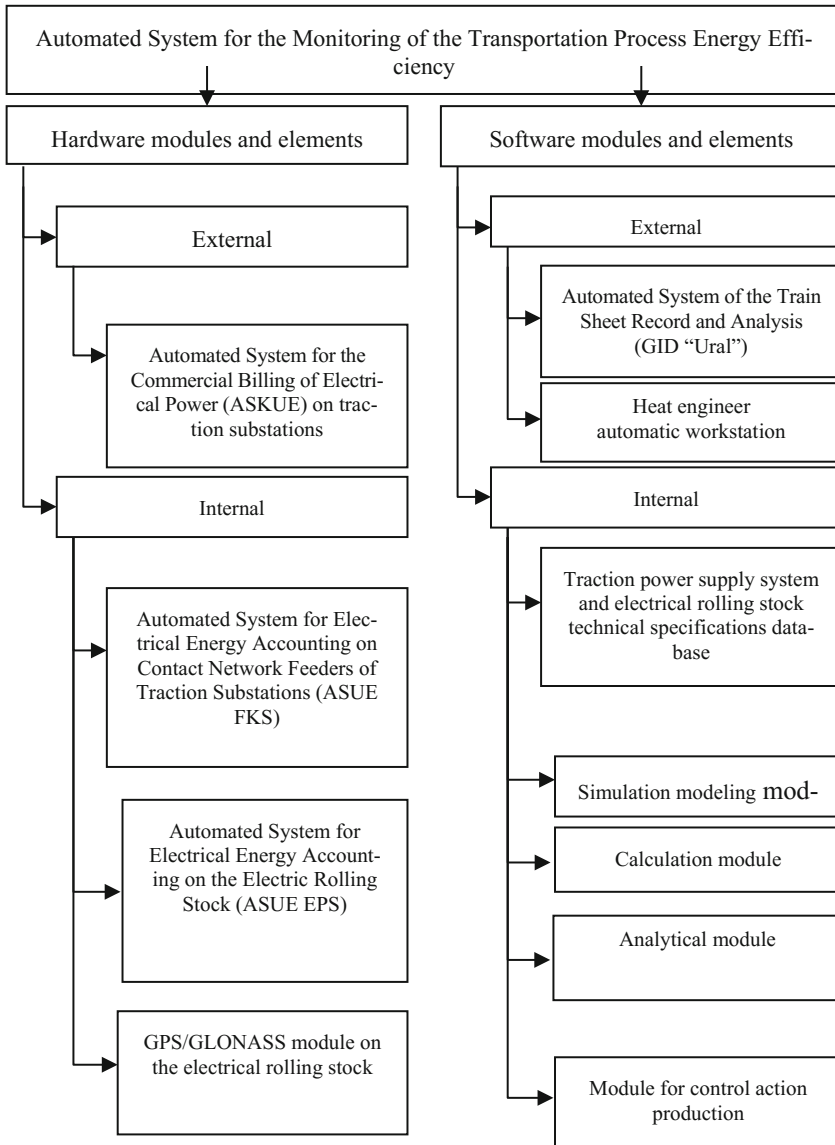


Fig. 1. Modules and elements used in ASMEPP

software system for the accounting, analysis and rate-setting of the energy resource utilization for the train traction used in locomotive depots (Heat Engineer Automated Workstation). The use of the basic data from various systems to determine design (rated) and actual indicators of the transportation process energy efficiency is provided in Table 1.

Table 1. Basic data for the determination of the transportation process energy efficiency

Transportation process energy efficiency indicators		Basic data					
		Traction substation ASKUE	ASUE FKS	ASUE EPS	GID “Ural”	Heat engineer automatic workstation	DB of traction electricity supply and electrical rolling stock
Losses in the traction substation equipment	design	+					+
	actual	+	+				
Specific use by the traction substation meters	design	+			+		
	actual		+		+		
Losses in the traction network	design	+			+	+	+
	actual		+	+			
Specific use by the electrical rolling stock meters	design				+	+	+
	actual			+	+		
Electric energy used by train for single trip	design				+	+	+
	actual			+	+		

3 Experimental Section

Based on the experimental studies performed and simulation modeling of a large number of railway sections methods for the evaluation of electrical energy losses in the traction substation equipment to be used in ASMEPP operation in traction substation [7] and traction network [8] equipment as well as method for the determination of the electrical energy use on electrical rolling stock in the boundaries of the arbitrary section [9] were developed and patented.

Further automatic system of the electrical energy accounting for the DC traction substation contact network feeders was developed [10]. Pilot implementation of the electrical energy accounting system on contact network feeders of the traction sub-station was performed on one of the sections of Sverdlovsk Railway. The structure of the ASUE FKS implemented, functions of its elements and their specifications as well as engineering and economic effect evaluation are provided in [11].

Based on the results of ASUE FKS pilot operation at Sverdlovsk Railway pilot test ground first the following results were obtained:

Dependence of the electrical energy losses in the traction network as function of non-uniformity of the voltage levels at the busbars of the adjacent DC traction sub-stations;

Load distribution of the traction substation converters, including in the conditions of contact-free automatic voltage control devices (BARN) [12];

Evaluation of the electrical energy losses in the transformer equipment in case of parallel operation of similar-type transformers and transformers of different types;

Experimental evaluation of the electrical energy losses in the converters of DC traction substations [13].

One of the most urgent issues in the area of the train traction energy efficiency improvement in the recent years has been extension of the test ground of regenerative braking application and regeneration energy application efficiency.

Results of the environmental experiments and mathematical simulation performed in West Siberian and Sverdlovsk Railways provided in [14] demonstrated that ASMEPP implementation will enable efficient determination of the boundaries of regenerative braking application sections for all types of electrical rolling stock in a wide range of weight rates. The data obtained using ASMEPP will enable, based on the algorithms developed, reliable determination of engineering [15] and economic [16] efficiency of regenerative braking application efficiency and regeneration energy use.

4 Conclusions

Implementation of ASMEPP in the Russian railways network will enable obtaining the following results:

- expansion of theoretical knowledge of the processes underway in the traction electricity supply system and electrical rolling stock;
- methodological justification of the principles of monitoring of use and losses of the electrical energy for the train traction and traction substation contact network feeders using GLONASS technology for the determination of the electrical rolling stock location;
- generation of the data base to build a real mathematical model of the traction power-supply system followed by the building of Smart Grid intellectual network the work of which will be aimed at the electricity use efficiency improvement;
- Engineering solutions for the building of intellectual automatic system for the efficiency monitoring of the transportation process;
- algorithms for the processing and analysis of the information obtained as a result of synchronous measurements of the electrical parameters on the electrical rolling stock and feeders of the traction substation contact network;
- complex of scientifically justified control actions in the traction electricity supply system and on the electrical rolling stock aimed at the transportation process energy efficiency improvement.
- principles for the creation of automatic system for the management decision-making support.

Expected economic effect from the implementation of the automatic system for the monitoring of energy efficiency of the transportation process at the railway net-work is 1–2% of the electrical energy use for the train traction at the expense of the following factors:

- reduction of the electrical energy use for the train traction at the expense of the implementation of the recommendations obtained from the protocols of daily monitoring of the railway section energy efficiency;
- reduction of electrical energy “unbalance” in the traction network to the level of technological losses and, consequently, occurrence of the possibility of waiving “un-balance” term by replacing it with common term “technological losses”, hereby the “commercial” component of the “unbalance” will be virtually liquidated;
- reduction of the engineering losses in the traction network due to the improvement of the traction electricity supply system operation modes and train traffic organization upon the results of the transportation process energy efficiency daily monitoring;
- quality improvement of the planning and rate setting of the electrical energy use for the train traction;
- automatic control of obtaining key indicators on the use of the electrical energy for the train traction without experts’ involvement, which, in its turn will enable productivity and operation convenience improvement of all the departments and services involved;
- provision of prompt reception of the data on the energy use for making decisions on the energy efficiency improvement, including, automatic generation of protocols on the transportation process energy efficiency on railway arbitrary sections, including the traction electricity supply system operation.

References

1. Energy strategy of Russian Railways Holding for the period till 2020 and on prospect till 2030, Moscow, p. 76 (2016)
2. Cheremisin, V., Nikiforov, M.: Evaluation of the potential for improving the energy efficiency of the traction power supply system. *Izv. Transsiba* **2**, 75–84 (2013)
3. Shkolnikov, E., Cheremisin, V., Ushakov, S.: The commercial accounting of electric energy on the electrrolling stock. *Zheleznodorozhniy Transp.* **8**, 50–54 (2016)
4. Cheremisin, V., Pashkov, D., Ushakov, S.: The automated monitoring of power overall performance of the electrrolling stock of JSC «RZhd». *Izv. Transsiba* **3**, 87–91 (2014)
5. Cheremisin, V., Pashkov, D., Nikiforov, M.: Concept of traction power supply and electrrolling stock JSC «RZhd» power system effectiveness monitoring. In: Increase in Power Efficiency of Land Transport Systems: Materials of the International Scientific and Practical Conference, Omsk, pp 7–14. OSTU, Omsk (2014)
6. Cheremisin, V., Ushakov, S., Pashkov, D., Nikiforov, M.: Stages of transportation process energy efficiency automated system monitoring realization. *Zheleznodorozhniy Transp.* **3**, 45–49 (2015)

7. Kashtanov, A., Nezevak, V., Nikiforov, M., Ushakov, S., Cheremisin, V.: Method for determining technological losses of electric power for traction in traction substations of railway transport direct current. Patent for Invention RUS 2573098 (2014)
8. Kashtanov, A., Nezevak, V., Nikiforov, M., Ushakov, S., Cheremisin, V.: Method for determination technological losses of electric energy in traction network of railway transport. Patent for Invention RUS 2572797 (2014)
9. Kashtanov, A., Nezevak, V., Nikiforov, M., Pashkov, D., Ushakov, S., Cheremisin, V.: Method for determining the consumption of electrical energy by an electric rolling stock within the limits of an arbitrary recording area. Patent for Invention RUS 2559408
10. Cheremisin, V., Chizhma, S., Nikiforov, M., Lavruhin, A., Malyutin, A., Okishev, A., Plotnikov, Yu., Degtyareva, A.: Block of monitoring and accounting of electric energy. Patent for Use-ful Model RUS 165423 (2015)
11. Cheremisin, V., Kashtanov, A., Nikiforov, M.: Increase of electric traction power efficiency at introduction of electric energy monitoring on feeders of contact network. *Transp. Urala* **2**, 67–70 (2015)
12. Nezevak, V., Nikiforov, M.: Increase of electric traction power efficiency at introduction of electric energy monitoring on feeders of contact network. In: *Transport Infrastructure of the Siberian Region: Materials of the Sixth International Scientific and Practical Conference, Irkutsk*, vol. 1, pp 613–617. IrGUPS, Irkutsk (2015)
13. Nikiforov, M., Plotnikov, Yu.: Experimental assessment of losses of electric energy in converting units of traction substations of a direct current due to application ASAEP FCN. In: *Devices and Methods of Measurements, Quality Control and Diagnostics in the Industry and on Transport: Materials of the Second All-Russian Scientific and Technical Conference with the International Participation, Omsk*, pp. 234–241. OSTU, Omsk (2016)
14. Cheremisin, V., Nikiforov, M., Kashtanov, A., Vilgelm, A.: Increase of recuperative braking power efficiency at sites of a direct current. In: *In-crease Of Recuperative Braking Power Efficiency at Sites of a Direct Current*, OSTU, Omsk, pp. 176 (2016)
15. Cheremisin, V., Nikiforov, M., Vilgelm, A.: Methodology for evaluating the energy efficiency of regenerative braking application and energy recovery. *Izv. Transsiba* **1**, 60–70 (2016)
16. Cheremisin, V., Nikiforov, M., Vilgelm, A.: Method of regenerative braking and energy recovery use cost-effectiveness calculating. *Transp. Urala* **3**, 95–99 (2016)

Intelligent Traction Power Supply System

Vasilii Zakaryukin¹ , Andrey Kryukov^{1,2}  ,
and Aleksandr Cherepanov¹ 

¹ Irkutsk State Transport University,
Chernishevsky st., 15, Irkutsk 664074, Russia
and_kryukov@mail.ru

² Irkutsk National Research Technical University,
Lermontova st., 83, Irkutsk 664074, Russia

Abstract. The control of operating conditions of traction power supply systems can be done by combination of controlled reactive power sources, energy storage systems, active harmonic conditioners, and distributed generators. Simulation modeling shows that the facilities intended to control the operating conditions of traction power supply systems make it possible to stabilize voltage in the network, improve power quality at the buses of traction substations, and decrease power losses.

Keywords: Railway electric system · Operating control · Simulation modeling

1 Introduction

With the rapid pace of economic development by the year 2030 the electricity consumption in Russia will double against 2000 according to the maximum forecast variant. It is impossible to provide such levels of electricity production without a system approach to the following problems [1]:

- creation of a new technological platform for the energy industry;
- an integrating role to be assigned to the electric network;
- installation of active equipment in the networks to control electric power system operation and create an adaptive control system on their basis;
- application of new information technologies and fast computation systems for state estimation and control;
- improvement of the efficiency of using energy resources and energy saving.

All in all the electric power industry should acquire a new quality of control and make a transition to an intelligent electric power system (IEPS) with active adaptive network (AAN).

The IEPS with AAN includes the following segments [1, 2]:

- all types of electricity sources including distributed generation;
- different types of consumers that take part in the control of power quality and reliability of power system;

- electric networks of various voltages and functions that are capable to change parameters and topology according to the current conditions; to control voltage at nodal points, which minimizes losses while maintaining the standard values of power quality indices and to meter electric energy at substations;
- control system for all operating conditions with full-scale information support.

2 Statement of the Problem

Creation of an IEPS with AAN requires the development and implementation of new equipment and technologies [1, 2] that are presented in the diagram (Fig. 1).

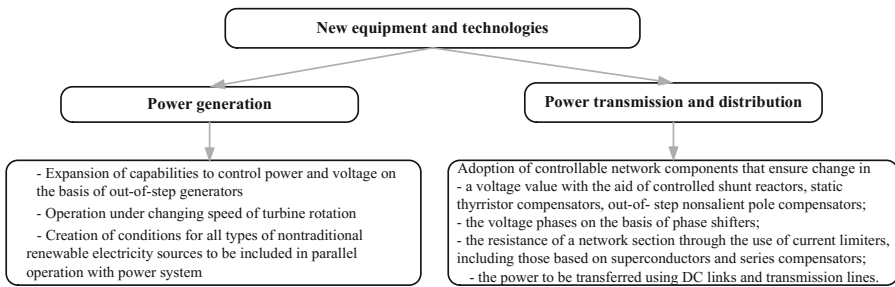


Fig. 1. Equipment and technologies required to implement IEPS with AAN

Besides, it is planned to connect energy storages that are based on different physical principles, and use compact equipment at substations. Additionally, there are plans to use compact multi-circuit transmission lines with high transfer capabilities that are mounted on the multifaceted metallic towers. An effective way to improve reliability will be the use of complex systems for diagnosing the equipment and monitoring its life cycle in the future.

Operation of IEPS with AAN requires creation of well-developed information, communication and control systems [1, 2] (Fig. 2). Control of IEPS ANN should be based on the following principles:

- the use of measuring devices that employ digital principles of data acquisition, processing and transfer;
- the creation of universal on-line systems for all operating conditions that optimize normal electric power system (EPS) conditions, reveal inadmissible deviations and switch emergency control systems.

In the last years distributed generation plants have been widely applied in electricity generation. This leads to changes in the technologies for control of electricity transmission and distribution as well as in the structure of distribution networks. The arising problems can be solved by creating smart grids that have the functions of self-diagnosing and automated decision making on control of operating conditions [3].

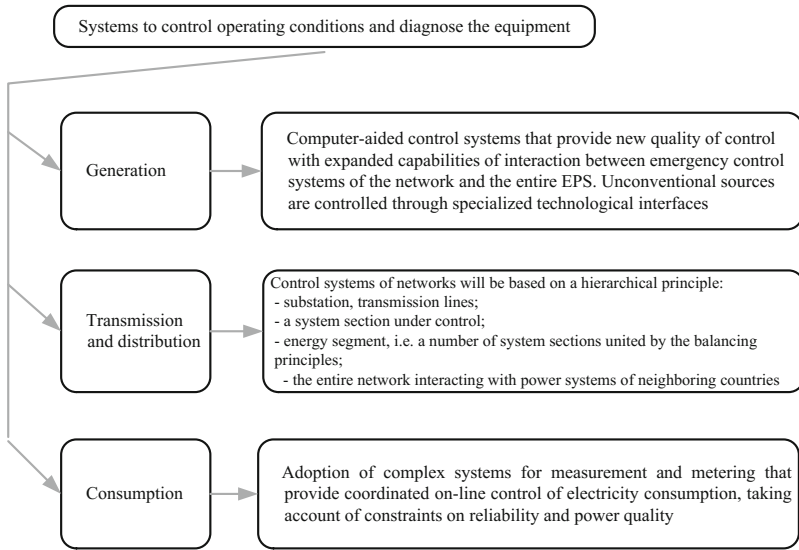


Fig. 2. Operating and diagnosing system

The most accurate definition of the smart grid concept is given in [4]. The authors of [4] take smart grid to mean fully self-controlled and self-restoring electric power system that has a network topology and includes the following components:

- conventional energy sources as well as distributed generation including those based on unconventional renewable energy sources;
- electric networks;
- all types of industrial, transport and residential consumers of electricity.

Operating conditions in such a network are controlled in real time on the basis of a unified information network.

3 Structure and Functions of Intelligent Traction Power Supply System

Russian railway transport is a large consumer of energy resources. On the whole the network of railways consumes annually up to 5...6% of electric power generated in the Russian Federation. The train traction requires about 80% of electric power consumed by the railway. Besides, up to 20 billion kW·h of electric power is transmitted by power supply systems of railways to non-transport consumers. In electric networks feeding railway traction substations, as well as in traction power supply systems the mentioned problems appear in full measure and they can be solved on the basis of the technologies of IEPS with AAN and smart grid. Application of such technologies is particularly

urgent in Eastern Siberia and the Far East, where the backbone network is directly connected with railway traction substations [5]. Because of a sizable volume of sharply variable nonlinear single-phase traction load the power quality indices in these networks essentially exceed the permissible values. The structure of intelligent traction power supply system (ITPSS) is presented in Fig. 3.

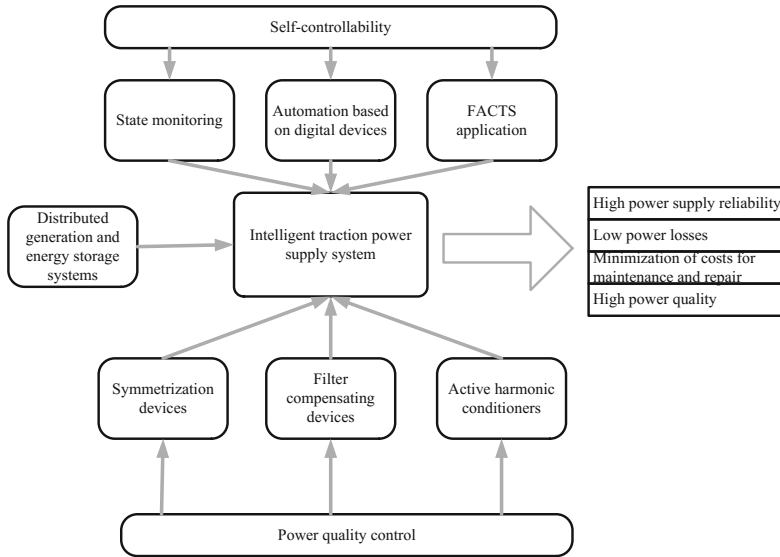


Fig. 3. Structure of intelligent TPSS

Besides of traditional equipment ITPSS consists of the following segments:

- developed measuring devices which monitor the state of power facilities including the devices operating on-line;
- automatic controllers designed on the basis of digital technologies;
- controlled reactive power sources designed on the basis of flexible alternating current transmission systems (FACTS) concept;
- distributed generation plants and energy storage systems;
- complex of devices for power quality improvement.

Introduction of ITPSS will make it possible to solve the following important applied problems:

- assurance of high reliability of traction power supply of trains and power supply to non-traction and non-transport consumers;
- minimization of power losses in TPSS and its operation expenses;
- improvement of power quality in TPSS and at the interfaces of feeding EPS.

Irkutsk State Transport University conducts comprehensive studies aiming to solve the problems arising at traction power supply system (TPSS) design [6–11]. Because of

a limited volume of the paper it is impossible to describe fully the results of conducted studies. Therefore, the present paper pays man attention to improvement of power quality and reduction of power losses based on the technologies of intelligent EPS with AAN and smart grid.

4 Results and Discussion Section

4.1 Stabilization of Voltage Level in Traction Networks

Possibilities for application of controlled reactive power sources (RPS) to voltage stabilization in traction networks were analyzed for the railway test area that included eight inter-substation zones and nine 1×25 kV. traction substations of TPSS. Voltage variations in the current collecting device of the even train with a mass of 6300 tons for the maximum capacity 10 MVar of RPS at the contact net switching point are presented in Fig. 4. The Figure shows that application of RPSs results in the pronounced decrease in the range of voltage deviations in the current collecting devices of electric locomotives.

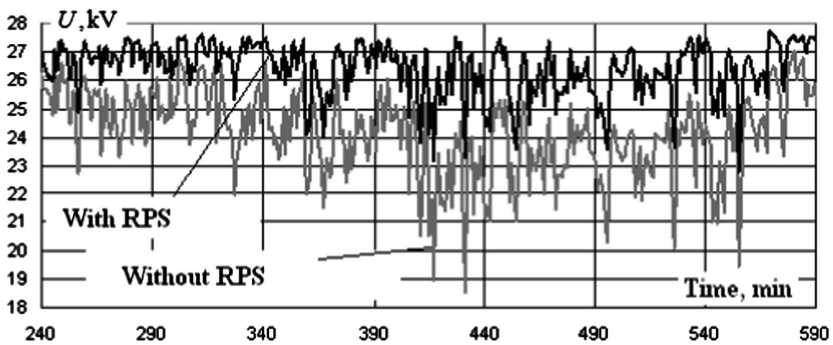


Fig. 4. Voltage variations of 6300 tons train

Stabilization of the voltage level in the networks of non-traction consumers of railway transport on the basis of reactive power sources with the distributed generators (DG) equipped with automatic voltage regulators is illustrated in Fig. 5. The Figure presents the results of modeling operating network conditions in the area of power supply to non-traction consumers [12].

Voltage deviates to the greatest extent at the 0.4 kV buses of the remote step-down substation for phase B; at heavy train movement uphill the voltage falls to 160...170 V for a short time. DG plant at this substation with the reactive power control limits ± 480 kvar is efficient, raising the minimum voltage by 24 V, and on an average by 17 V.

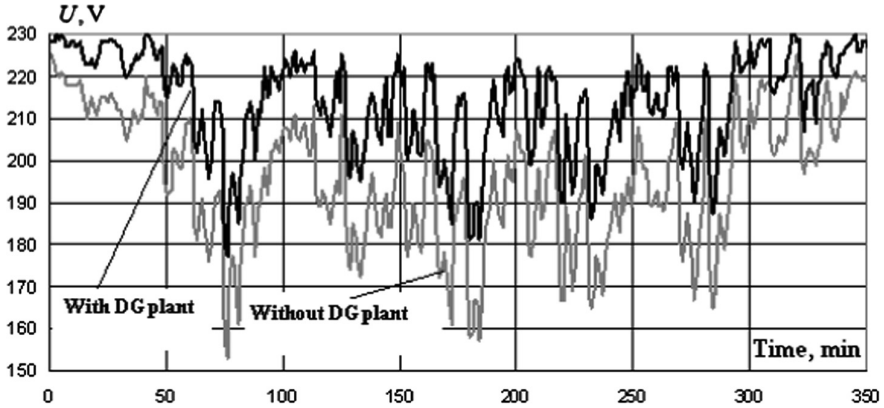


Fig. 5. Changes in the phase voltage of the step-down substation at train movement

4.2 Decrease in Power Losses in Traction Networks

Simulation modeling applied to the real railway test area has made it possible to establish that installation of the controlled reactive power sources allows the decrease of power losses in traction networks by 20...30%, and the minor decrease of transformer losses. From the standpoint of decreasing the losses the variant of RPS installation at the contact net switching point is more favorable than RPS installation at the traction substation. Modeling has showed that the use of RPSs at the switching point leads to reduction of losses on an average by 0.6% of total power consumption by trains in the inter-substation zone as compared to their use at the traction substation.

4.3 Decrease in Voltage Deviations at the Buses of Traction Substations

The application of controlled reactive power sources equipped with high harmonic filters makes it possible to improve the following power quality indices:

- to decrease voltage deviations at buses of traction substations;
- to decrease voltage unbalance at traction substations;
- to decrease current and voltage waveform distortion (non-sinusoidally).

Thanks to the use of controlled fast reactive power sources (with the response time of about 5...20 ms) it is possible to significantly reduce voltage fluctuations.

The reduction in voltage deviations and fluctuations is achieved by decreasing the range of changes in currents consumed at 27.5 kV traction substations (Fig. 6).

Voltage deviations and fluctuations can be lowered by using energy storages that allow a significant improvement in the indices characteristic of unsteady operating conditions of traction power supply systems [7].

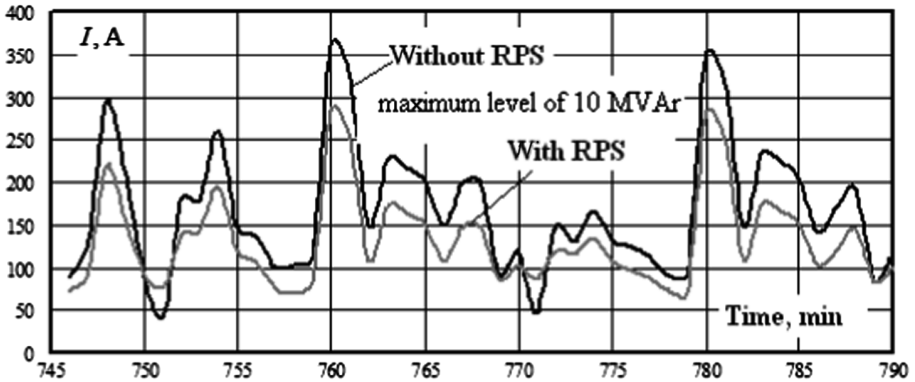


Fig. 6. Currents of contact net feeder of the traction substations with moving of 72 train pairs

4.4 Decrease in Voltage Unbalance and Non-sinusoidality at Buses of Traction Substations

Using phase-controlled reactive power sources, it is possible to halve the voltage unbalance factor k_{2U} at supply voltage buses of traction substations (Fig. 7). The degree of unbalance decrease depends on the amount of traffic, short-circuit capacity, and the presence of steep slopes in the inter-substation zones.

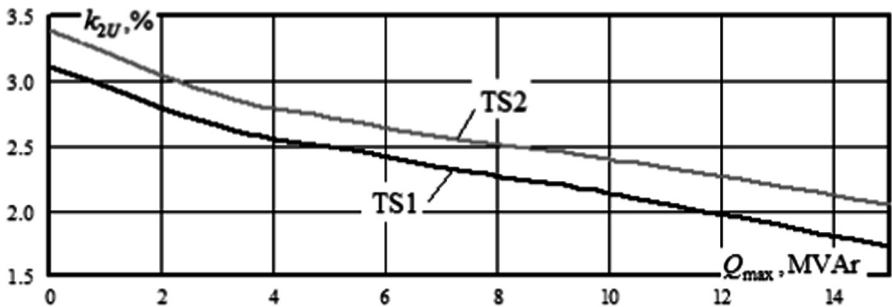


Fig. 7. Relationship between maximum value of the voltage unbalance factor and the limit Q_{max} of regulating the RPS capacity

One of the most efficient ways to reduce non-sinusoidality is to use active harmonic conditioners [13, 14]. Using the MATLAB system, the authors of [14] modeled an active harmonic conditioner installed at a traction substation. Under the operating conditions, when the filter was not used, the current waveform distortion factor in the arm of the traction substation reached 26%. The use of the active harmonic conditioner decreased the current waveform distortion factor up to 5.3%.

The active harmonic conditioners are reasonable to apply not only for stabilizing voltage quality indices for high harmonics at the voltage of 110–220 kV and 6–10 kV, but also for reducing the current waveform distortion in traction winding.

5 Conclusions




1. The problems of power quality and energy efficiency improvement in traction networks can be solved by creating intelligent traction power supply systems on the basis of smart grid and active adaptive network technologies.
2. The most effective ways to use modern technical means for the control of operating conditions of traction power supply systems are to combine controlled reactive power sources, energy storage systems, active harmonic conditioners, and distributed generators.
3. The authors used the simulation modeling to show that the facilities intended to control the operating conditions of traction power supply systems make it possible to stabilize voltage in the network, improve power quality at the buses of traction substations, and decrease power losses.

References

1. Dorofeyev, V.V.: Smart grids in electric power industry. <http://www.energyland.info/analytic-show-45305>. Accessed 13 Sep 2011
2. Dorofeyev, V.V., Makarov, A.A.: Active adaptive network as a new quality of the UPS of Russia. *Energoekspert* **4**, 29–34 (2009)
3. Kobets, B.B., Volkova, I.O.: Innovative Development of Electric Power Industry on the Basis of Smart Grid Concept. Information and Analysis Centre, Moscow, p. 208 (2010)
4. Smart Power Grids – Talking about Revolution. IEEE Emerging Technology Portal (2000)
5. Zakaryukin, V.P., Kryukov, A.V., Abramov, N.A.: Electro energetic technological control in east Siberia railway. In: *Energy of Russia in XXI century: Development Strategy – Eastern Vector*. CD-ROM Proceedings, p. 3–10 (2010)
6. Kryukov, A.V., Zakaryukin, V.P., Astashin, S.M., Stepanov, A.D.: *Mathematical Analysis of Results of Thermal Mapping for Traction Substations: Monograph*. Irkutsk, p. 135 (2006)
7. Zakaryukin, V.P., Kryukov, A.V., Raevsky, N.V., Yakovlev, D.A.: *Modeling and Forecasting of Electricity Consumption Processes in Railway Transport: Monograph*. Transbaikalian Institute of Railway Transport, Chita, p. 114 (2006)
8. Kryukov, A.V., Zakaryukin, V.P., Astashin, S.M. (eds.): *Control of Operating Conditions of Traction Power Supply Systems: Monograph*. Publishing Department of Irkutsk State University of Railway Transport Engineering, Irkutsk, p. 104 (2009)
9. Kryukov, A.V., Zakaryukin, V.P., Abramov, N.A.: *Situation Control of Operating Conditions of Traction Power Supply Systems: Monograph*. Publishing Department of Irkutsk State University of Railway Transport Engineering, Irkutsk, p. 123 (2010)
10. Kryukov, A.V., Zakaryukin, V.P., Sokolov, V.Yu.: *Modeling of Power Supply Systems with Massive Current Leads: Monograph*. LAP LAMBERT Academic Publishing GmbH & Co. KG, Dudweiler Landstraße 99, 66123, Saarbrücken, Germany, p. 90 (2011)

11. Kryukov, A.V., Zakaryukin, V.P., Abramov, N.A.: Control of Traction Power Supply Systems. Contingency Approach: Monograph. LAP LAMBERT Academic Publishing GmbH & Co. KG, Dudweiler Landstraße 99, 66123, Saarbrücken, Germany, p. 128 (2011)
12. Kryukov, A.V., Zakaryukin, V.P., Arsentiev, M.O.: Use of distributed generation technologies in railway transport. *Sovrem. Tekhnologii. Sist. Analiz. Modelirovaniye* **3** (19), 81–87 (2008)
13. Courault, J.: Modern technologies for the improvement of power quality during power supply and distribution [electronic resource]. *Nov. elektrotek.* **1**(31) (2005). (in Russian). <http://news.elteh.ru/arh>
14. Ushakov, V.A., Mashutin, S.N.: Filtering of High Harmonics of the Current of Electric Locomotives in Traction Power Supply Systems. *Politransportnye Sistemy.* Siberian Federal University, Krasnoyarsk, pp. 49–54 (2007)

Mathematical Model of Multiphase Power Transmission Line

Vasilii Zakaryukin¹ , Andrey Kryukov^{1,2} ,
and Aleksandr Cherepanov¹ 

¹ Irkutsk State Transport University,
Chernishevsky st., 15, Irkutsk 664074, Russia
and_kryukov@mail.ru

² Irkutsk National Research Technical University,
Lermontova st., 83, Irkutsk 664074, Russia

Abstract. A method of electric power system modeling has been proposed, which includes multiphase power transmission lines. The method is based on application of phase coordinates and equivalent lattice circuits from RLC-elements connected in complete graph schemes.

Keywords: Power supply systems · Multiphase transmission line
Mode modeling

1 Introduction

Some properties of multi-phase power line cause the increase of interest to it [1–9]. Also cost of multiphase line is higher than 3-phase as signed in [1], the results of the researches [2–6] evidence that by increasing of the number of power transmission line (PTL) phases it is possible to increase reliability of power supply, power transmission efficiency, and reduce ecological impact of PTL on the environment. Using multiphase PTL, the needed transmission line capability may be provided with a lower voltage class.

For modeling of multiline system some authors use single line performance as in [3] or matrix model [6, 7]. But these models have some difficulties in non-adequate modeling in asymmetric modes or high complexity for using. Methods of multiphase transformers modeling was published in [8, 9]. These transformer's models were made by number of single-phase transformers that not allow adequate modeling of asymmetric modes.

Effective instrument for modeling of multiline system is made in Irkutsk State Transport University [10], allowing to calculate appropriate electromagnetic fields creating by multiphase line [11]. Appliance of this instrument for multiphase system modeling describes in this paper.

2 Materials and Methods

For practical use of multiphase PTL it is required to develop adequate algorithms of electric power system (EPS) modeling, which include such power transmission lines. These algorithms may be implemented on the basis of the methods of multiphase

electric system modeling worked out in Irkutsk State Transport University, based on application of phase coordinates and equivalent lattice circuits from RLC-elements connected in complete graph scheme [10]. Calculations in phase coordinates allow determining electromagnetic field (EMF) intensities near the multi wire PTL [11].

This article presents the results of modeling of 6-phase and 12-phase power transmission lines.

3 Results and Discussion

3.1 Results of 6-Phase PTL Modelling

Modeling has been carried out based on the software “Fazonord-Quality” developed in Irkutsk State Transport University [10], as applied to the 6-phase PTL circuit with wire voltage relating to the ground $220/\sqrt{3}$ kV (Fig. 1). In order to compare with standard transmission lines, modeling of 3-phase PTL 500 kV has been carried out, which has comparable capability. A full transposition of the 6-phase PTL wires has been presumed, and absence of transposition of PTL-500. Wire coordinates are shown on Fig. 2. Vector diagrams of the 6-phase PTL voltages are shown on Fig. 3.

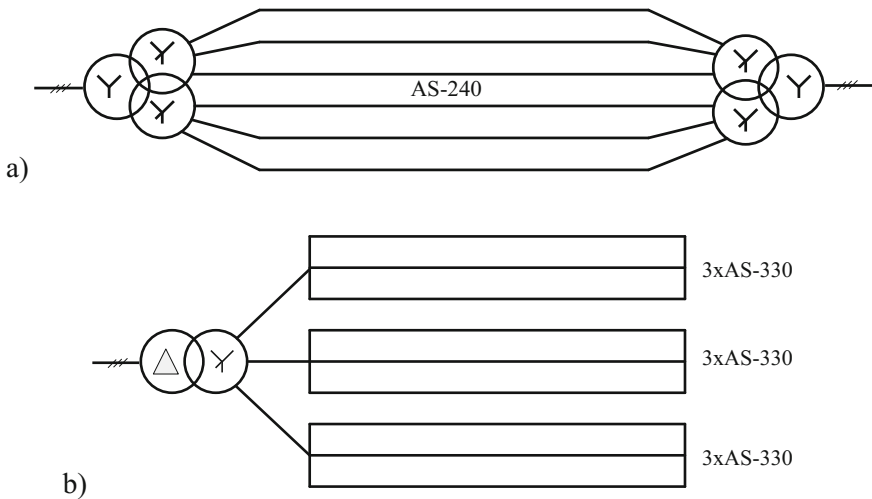


Fig. 1. PTL circuits: (a) 6-phase line; (b) 3-phase line

Having considered the vector diagrams shown on Fig. 3, one may conclude that in the 6-phase system there are three sets of linear voltages with modules equal to U_{PH} , $\sqrt{3}U_{PH}$, $2U_{PH}$, where U_{PH} – a phase voltage module.

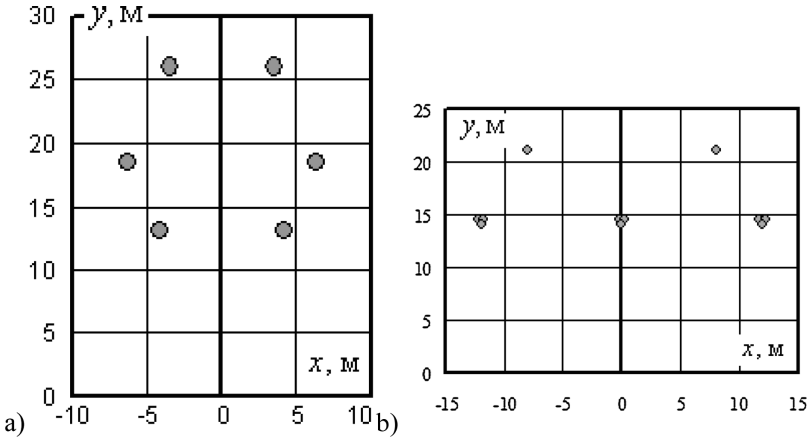


Fig. 2. Wire arrangement coordinates: (a) 6-phase PTL; (b) 3-phase PTL

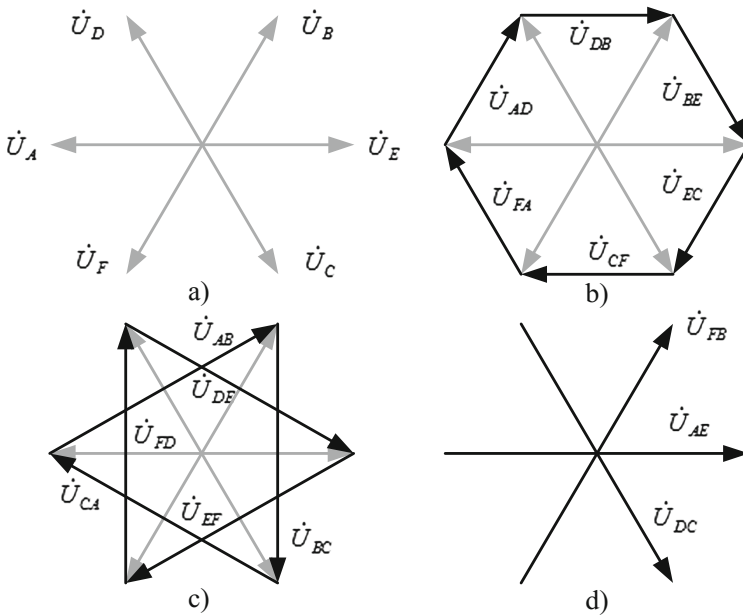


Fig. 3. Vector diagrams of 6-phase line voltages.

Due to linear voltages $U_L = 2U_{PH}$ a higher capability of the 6-phase PTL is provided compared to the standard 3-phase one of a similar voltage class. The results of computer modeling are below which prove the conclusion. Calculated schemes formed by the software “Fazonord-Quality” are given on Fig. 4. Modeling results are illustrated on Figs. 5, 6, 7, 8, 9 and 10.

Based on the modeling results one can make the following conclusions:

1. The 6-phase PTL with wire voltage relating to the ground $220/\sqrt{3}$ kV has capability comparable with a similar value for a standard PTL 500 kV.
2. Construction of 6-phase line with the above mentioned parameters needs twice less wire materials then 500 kV line.
3. Power losses allocated to one Ohm of wire resistance for the 6-phase PTL 7...9 times higher than that of the 3-phase PTL 500 kV.
4. The 6-phase PTL creates much less electromagnetic field intensities compared to the 3-phase line 500 kV. Maximum level of electric field intensity of the 6-phase PTL is approximately 6 times less, and that of the magnetic field is one and a half time less.
5. Negative sequence factor at the receiver end of the 6-phase PTL is much lower than a similar value for PTL 500 kV; without transposition of the 6-phase line wires this factor equals to 0.02% at the load of 400 MW. Therefore, for the 6-phase PTL at symmetric wire arrangement there may be no need to construct expensive transposition supports.

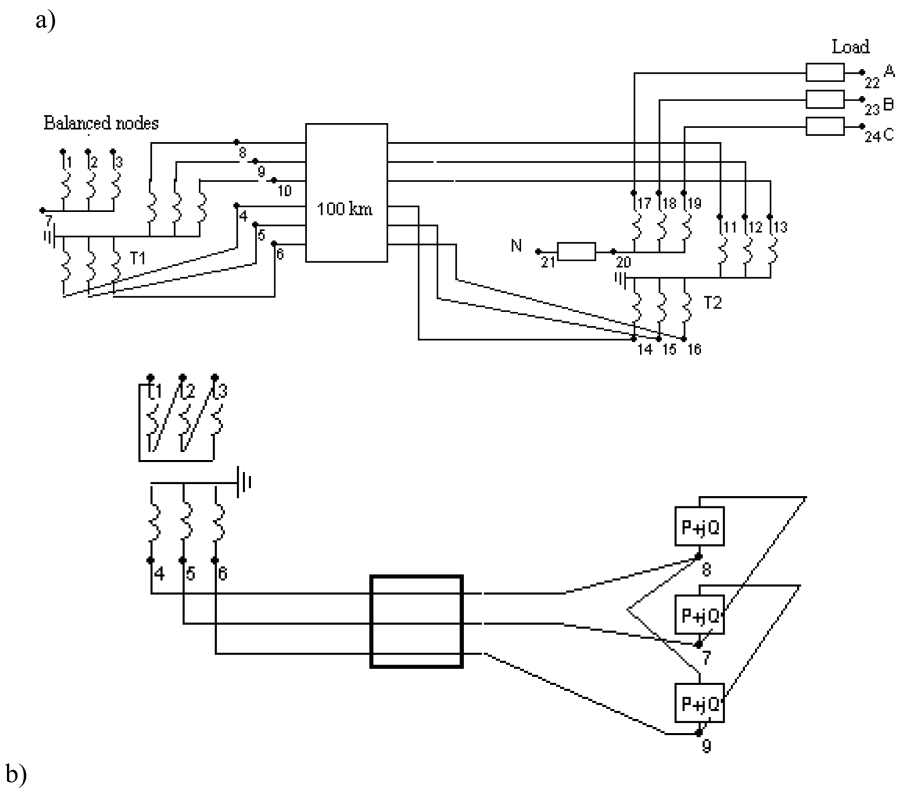


Fig. 4. Calculated schemes: (a) 6-phase line; (b) 3-phase line

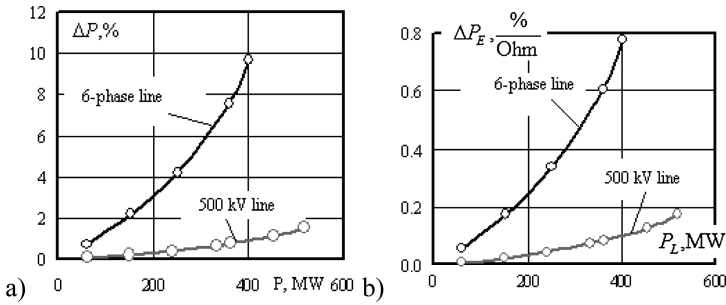


Fig. 5. Losses of transmitted power: (a) power losses calculated in the software system “Fazonord”; (b) power losses on 1 Ohm of PTL wire active resistance

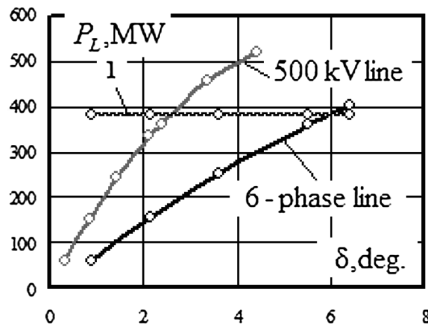


Fig. 6. Power-angle diagram; 1 – heating limit of AC-240 6-phase line

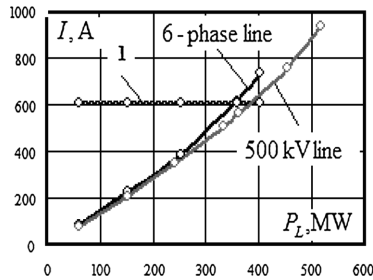


Fig. 7. Currents in PTL phases; 1 – heating limit of AC-240 6-phase line

3.2 Results of 12-Phase PTL Modelling

Modeling with software “Fazonord-Quality” was made to the 12-phase PTL circuit with wire voltage relating to the ground $220/\sqrt{3}$ kV (Fig. 11). In order to compare with standard power transmission methods, a 3-phase PTL 500 kV modeling has been conducted, which has comparable capability (Fig. 1b). Wire arrangement coordinates are shown on Fig. 12.

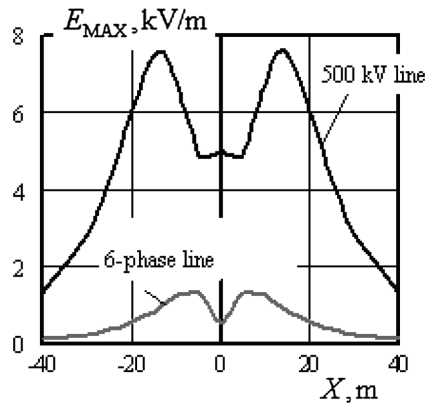


Fig. 8. Electric field at the height of 1.8 m

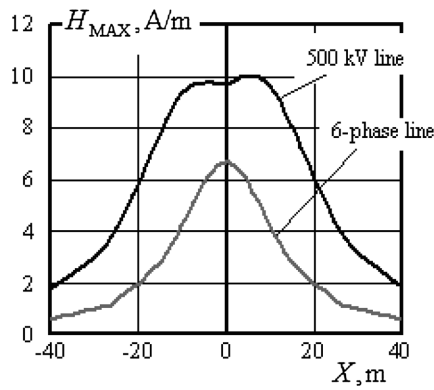


Fig. 9. Magnetic field at the height of 1.8 m

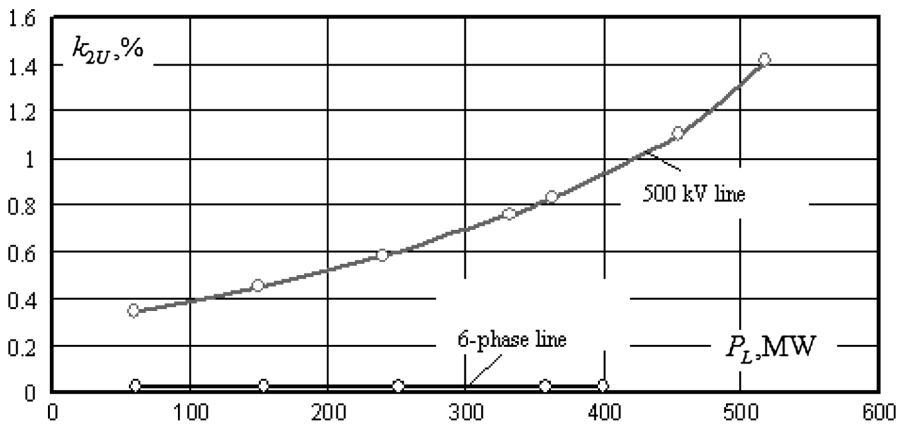


Fig. 10. Negative sequence factor

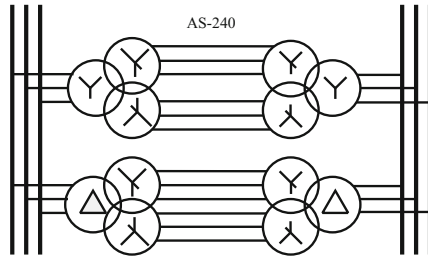


Fig. 11. Twelve-phase PTL diagram

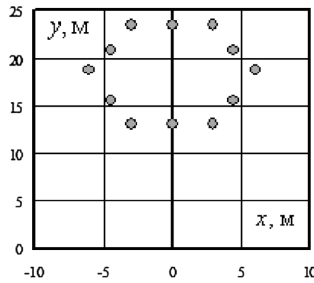


Fig. 12. Twelve-phase PTL wire arrangement coordinates

Calculated circuit formed by means of the software “Fazonord-Quality” is shown on Fig. 13. Computer modeling results are illustrated on Figs. 14, 15, 16 and 17.

The 12-phase PTL with wire voltage relating to the ground $220/\sqrt{3}$ kV has capability comparable with standard PTL 500 kV.

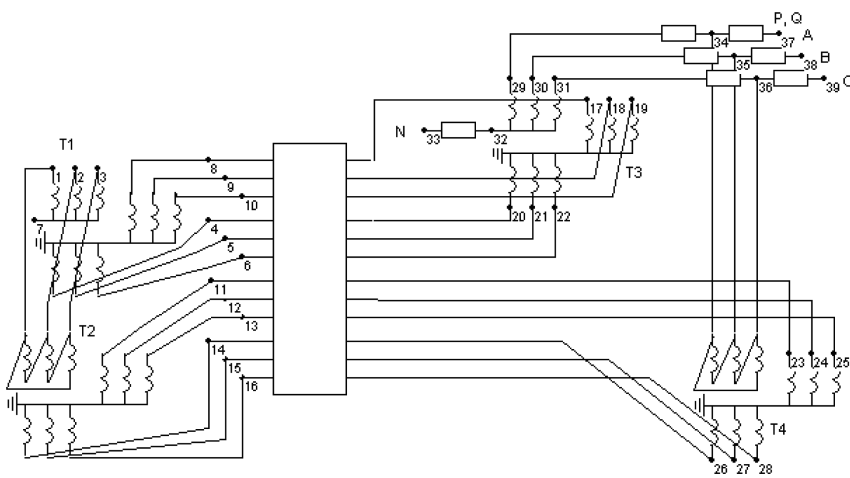


Fig. 13. Calculated circuit of 12-phase line

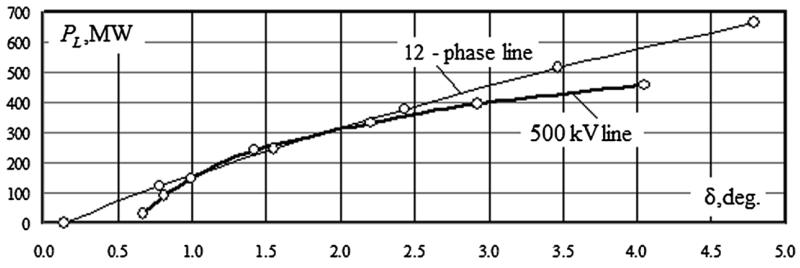


Fig. 14. Power-angle diagram

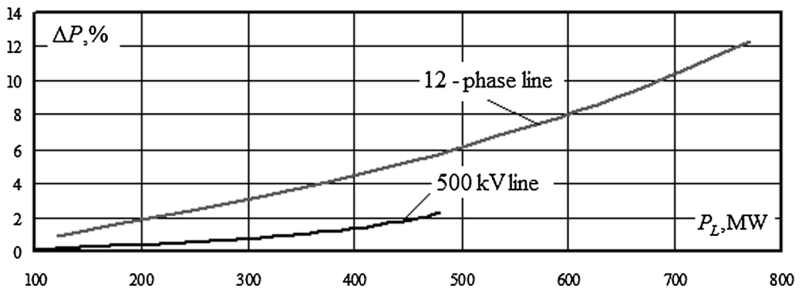


Fig. 15. Losses of transmitted power

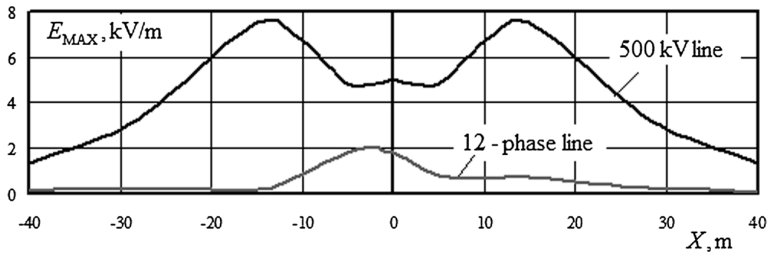


Fig. 16. Electric field at the height of 1.8 m

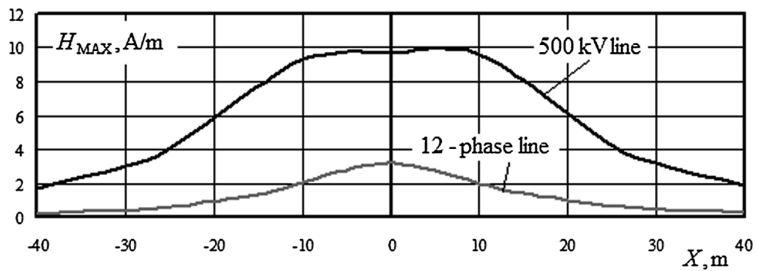


Fig. 17. Magnetic field at the height of 1.8 m

Power losses for the 12-phase PTL are slightly higher than that of the 3-phase PTL 500 kV.

The 12-phase PTL creates much less electromagnetic field intensities compared to the 3-phase line 500 kV. Maximum level of electric field intensity of the 12-phase PTL is 3.5 times less, and magnetic field intensity is 4 times less.

4 Conclusions

The obtained results evidence that multiphase PTL have a number of advantages over standard structures; however, they are behind the latter as for the loss level. Consequently, a final choice of power transmission method should be made on the basis of technical and economic assessment provided that a required level of power supply reliability is insured.

References

1. Beutel, A., Britten, A., Motloun, T.: Proceedings of the 16th International Symposium on High Voltage Engineering, vol. C23, p. 6 (2009)
2. Liu, G., Zhou, X., Zhan, C., Li, X.: Four phase power transmission and the power transformer. *Trans. China Electro Tech. Soc.* **0120**(4), 9–14 (2005)
3. Husain, Z., Singh, R., Tiwari, S.: Proceedings of the 6th WSEAS International Conference on Applications of Electrical Engineering, pp. 246–250 (2007)
4. Singh, T.C., Ram, K.R., Ram, B.V.S., Subramanyam, P.S.: Investigation on transient stability of six-phase transmission system and proposal for integrating with smart grid. *Int. J. Eng. Sci. (IJES)* 31–40 (2014)
5. Tripathi, V.K., Bharadwaj, A.K.: Performance evaluation of multi-phase transmission lines. *Int. J. Adv. Eng. Sci. Technol.* **3**(2), 57–64 (2014). ISSN 2319-1120
6. Xianda, D.: Exploring Six-Phase Transmission Lines for Increasing Power Transfer with Limited Right of Way. Arizona State University, 142 p. (2012)
7. Group D: A report to the line protection subcommittee of the power system relay committee of the IEEE power and energy society (2014)
8. Julian, A., Oriti, G.: Energy Conversion Congress and Exposition, pp. 1658–1665 (2010)
9. Somashekar, B., Chandrasekhar, B., Livingston, D.: Modeling and simulation of three to nine phase using special transformer connection. *Int. J. Emerg. Technol. Adv. Eng.* **3**(6), 629–638 (2013). ISSN 2250-2459
10. Kryukov, A., Zakaryukin, V.: Methods of joint modeling of traction and AC railway power supply systems: monograph. Irkutsk State Transport University, Irkutsk, p. 170 (2011)
11. Kryukov, A., Zakaryukin, V., Buyakova, N.: Electromagnetic environment at railway transport facilities: monograph. Irkutsk State Transport University, Irkutsk, 130 p. (2011)

Basis for Local Methods of Insulation Hardening of Traction Rolling Stock Electrical Machines

Anatoliy Khudonogov , Evgeny Dulskiy  , and Pavel Ivanov 

Irkutsk State Transport University, 15, Chernishevsky st., Irkutsk 664074, Russia
E. Dulskiy@mail.ru

Abstract. The article concerns issues connected with improvement of traction rolling stock electrical machines (TRS EMs) reliability using local methods of insulation hardening by means of infrared (thermal) radiation during repair and manufacturing processes. Reasons for low reliability of advanced electric locomotives EMs with commutator traction electrical motors (TEMs) have been analyzed. The low reliability of electrical machines is associated with a low resource of winding insulation. The existing methods of restoration of insulation are not able to adequately provide high-quality hardening of insulation in the process of depot and factory repair. On the basis of Irkutsk state University of Railways has set up a scientific laboratory for the study of effective ways of hardening the insulation in the repair process based on the use of energy thermal (infrared) radiation. Laboratory and production researches confirming efficiency of the proposed methods have been carried out. Methods and industrial plants on hardening the insulation of TRS EMs of various types have been developed on the basis of experimental data. In conjunction with the company “Elinar” (the largest supplier of electrical insulating materials across the network of JSC “RZD”) has conducted studies on the effectiveness of the proposed methods in comparison with the currently used, based on the use of convection.

Keywords: Insulation · Reliability · Electrical machines

1 Introduction

One of the most important tasks of railway transport in Russia is a necessity to provide reliable work of traction rolling stock. Long-term analysis of traction rolling stock reliability shows that the most damageable component is an electrical machine.

Summarized data submitted by “Zheldorremmash” over the period from 1994 till 2004 reflects the reliability of locomotives and multiple-unit rolling stock (MURS) [1, 2]. Electrical machines of locomotives account for 53% of the total number of failures, electrical equipment accounts for 25%, mechanical equipment accounts for 20%, brake and pneumatic equipment accounts for 2%. Electrical machines of electric trains account for 28% of the total number of failures, mechanical equipment accounts for 33.6%, electrical equipment accounts for 39.2%. Electrical machines of diesel-electric locomotives account for 42% of the total number of failures, electrical equipment accounts for 28%, mechanical equipment accounts for 16%, diesel accounts for 12%,

and brake and pneumatic equipment accounts for 2%. Nowadays the statistics is almost unchanged although there is an intensive re-equipping with new locomotives and MURS.

The number of unplanned repairs due to TRS EMs failures for some series of new locomotives exceeds the number of the previous series repairs. Freight two-unit sixteen-wheel mainline electric locomotives of “Ermak” series with commutator traction motors have arrived at alternating current railways and electric locomotives of “Donchak” (2ES4K) and “Sinara” (2ES6) series have arrived at direct current railways. The electric locomotives of VL80 and VL10 series have been replaced with these electric locomotives.

Until recently, the electric locomotives with TEMs of NB-418K6 type of the electric locomotives VL80 (with all indexes) and NB-412K of the electric locomotives VL60 (with all indexes) equipped with closed heads of armature coils have been the most popular at East Siberian Railway. These electric locomotives have been limited in power. Starting with TEMs of NB-514 series of electric locomotives VL85, production

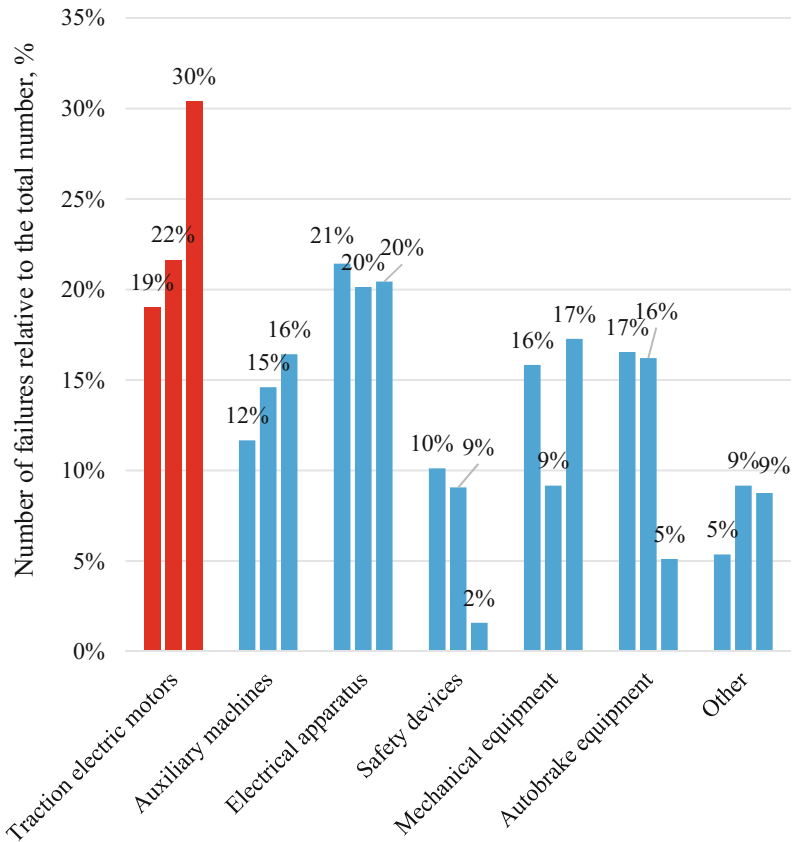


Fig. 1. Diagram of failures and damages of TEMs elements in electric locomotives of “Ermak” series per 2012–2015.

of armature windings with open head ends began to provide the power increase. This led to significant decrease in reliability of TEMs of these series in comparison with TEMs with closed heads of armature coils.

Nowadays, about 600 electric locomotives are located at East Siberian Railway. One of the advanced electric locomotive is “Ermak” – E5K, 2ES5K, 3ES5K. Statistically, in recent years TEMs (Fig. 1) head the list of electric locomotives equipment of “Ermak” series in relation to number of unplanned repairs [3, 4]. As the statistical data show, the weakest element of TEMs in these electric locomotives is an insulation of windings (Fig. 2). As the diagram shows, insulation failures account for about 40% of all TEMs failures.

About 575 direct current electric freight locomotives of 2ES6 series “SINARA” have been produced by “Ural Locomotives LLC”. These locomotives are maintained in “Sinara-Transport Machines–Service” (STM-Service). Analysis of operational reliability and causes of failures in electrical machines of this series is contained in studies prepared by members of “Rolling stock of electric railways” and “Technologies of transport engineering and repair of rolling stock” faculties of Omsk State Transport University [5, 6].

Figure 3 gives the statistical data on electrical equipment failures in electric locomotive 2ES6 “Sinara”. EMs of electric locomotives of these series take one of the leading positions concerning the number of failures (Fig. 3).

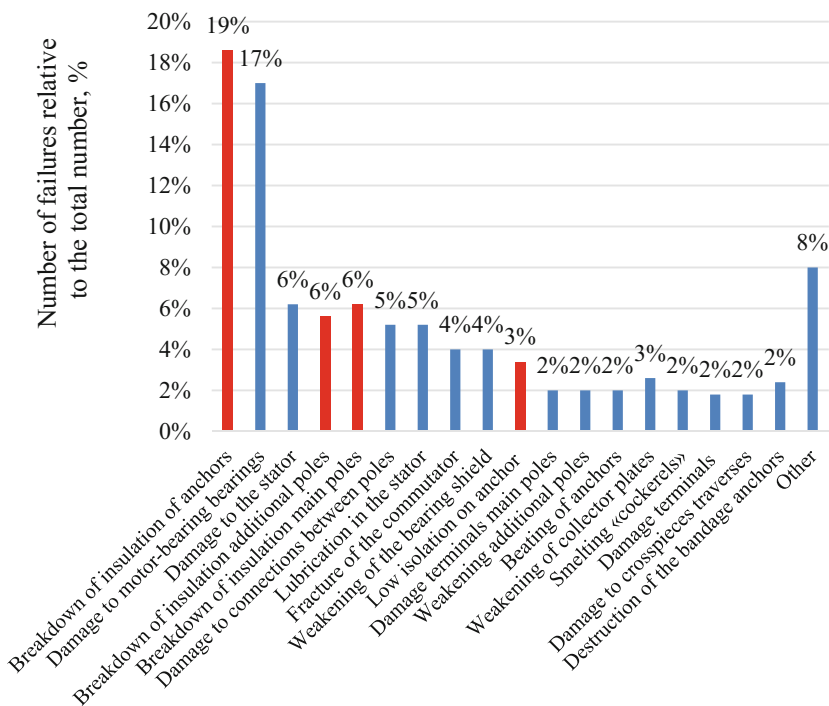


Fig. 2. Diagram of failures of EM elements in electric locomotives of “Ermak” series per 2015

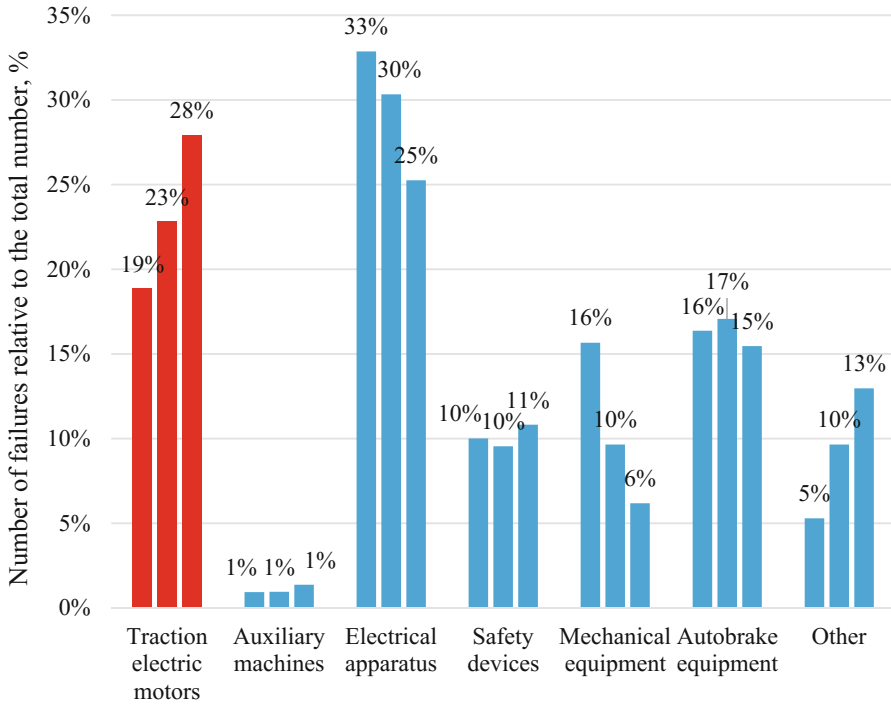


Fig. 3. Diagram of equipment failures in electric locomotives of 2ESC6 series “Sinara” per 2012–2015.

Thus, technical state analysis of 2ES6 electric freight locomotives fleet shows that the number of failures and unplanned repair remains high.

Also, causes of low reliability indexes are connected with low operation life of TEM insulation of CTK 810U1, EDP 810U1, and EK810Ch (Fig. 4). Insulation failures account for about 50% of all TEMs failures.

Electrical machines (EMs) of traction rolling stock (TRS) refer to fully-stressed equipment. Despite the constantly taken measures of constructive and engineering nature, the level of electric machines damageability during their operation remains sufficiently high with regard to the complex effect of thermal, electromagnetic, mechanical, and climatic factors during manufacturing and repair. This is evidenced by statistical data on reliability of commutator TEMs units.

Advanced technologies on production of commutator traction electrical motors based on varnish- or compound-impregnated insulation with following drying in convection electrical ovens allow to increase operating life of frames for the run up to 5 mln km [7]. But the same technologies can increase operating life of armatures not more than by 1 mln km of run. So, there is a problematic situation connected with operating mode and execution of insulating structures.

The necessity of forced ventilation and commutator TEMs protection from external attacks requires almost complete insulation of TEMs units for their protection.

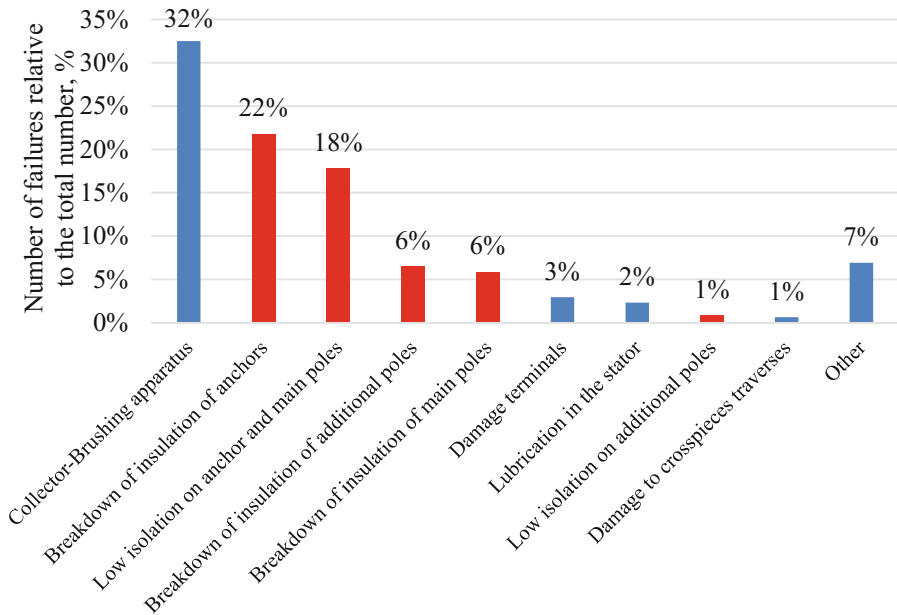


Fig. 4. Diagram of EM elements failures in electric locomotives of 2ES6 series “Sinara” per 2015.

This complicates the internal aerodynamics of the machine, since the inlet and outlet elbows for venting air have to be placed in the upper part. This leads to a significantly uneven heating of the armature windings: they are cooled more intensively from the side of air entrance than from the opposite side. The temperature difference of individual windings is 12–32%. Theoretical studies and calculations found that windings along the machine length are heated unevenly with maximum temperature at the air outlet. Figure 5 gives curves of temperature rise of armature windings for TEM NB-418K6 with the capacity of 740 kW with closed heads of coils and TEM NB-514 with the capacity of 780 kW with open heads of coils.

Curves of temperature rise in these motors armatures in case of mutual changes in their load currents are shown here as well [8]. However, placement of inlet and outlet elbows in the traction electrical motors ventilation system in the same plane leads not only to significant uneven heating of armature winding but also to excessive moistening of insulation of armature winding ends at the side opposite to commutator (at the side of air egress from the outlet elbow). The situation becomes more complicated when end shield without ventilation holes is installed in the way of moisture air. Up to 10 litres of water may be collected in the frame during operation of traction electrical motors in regions with high absolute air humidity. Uneven heating and excessive moistening of armature winding insulation will lead to local decrease in reliability of traction electrical motor.

In this case, the overhang ends of windings are least protected from ingress of moisture. Due to the overhang ends structural features, moisture can enter the slot

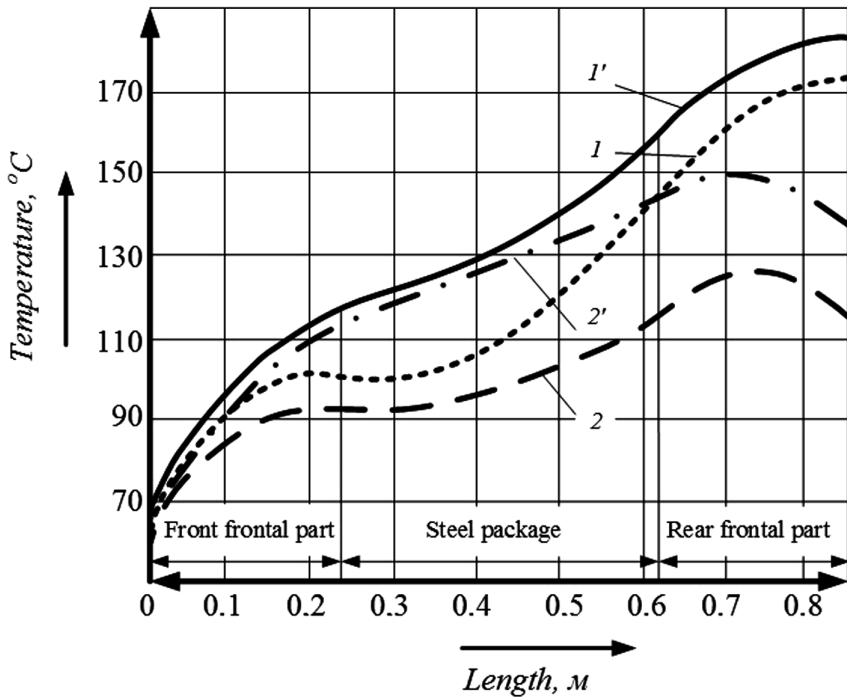
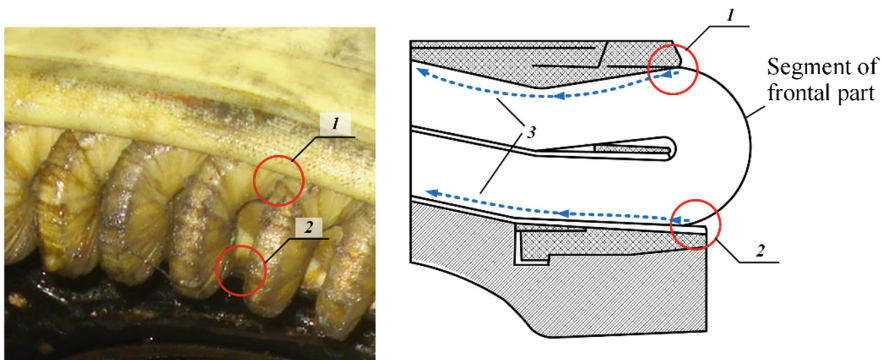


Fig. 5. Curves of temperature rise in armature windings of TEM NB-418K6 with closed (1 – at $P_h = 790$ kW and 1' – at $P_h = 835$ kW) and NB-514 with open heads of coils (2 and 2' – at the same power)

insulation under the permanent influence of dynamic forces on TEMs during operation and lead to electrical breakdown (Fig. 6) [9].



1, 2 – areas of probable penetration of moisture, 3 – motion of moisture into the slot depth

Fig. 6. Places of moisture penetration at the TEM armature winding head end

The research objective is to increase reliability of insulating structures of TRS EMs by means of their hardening using thermal radiation.

To increase EMs reliability during manufacturing and repair it is necessary to implement local methods for hardening of insulating structures using thermal radiation.

In addition to insulation hardening, while increasing the electric and mechanical strength it is necessary to provide the sufficient level of plasticity for insulation protection from impact of vibration stresses.

2 Materials and Methods

To assess the efficiency of thermal radiation during manufacturing and repair process of TRS EMs, the experimental studies have been carried out in two stages.

The first stage includes preparation of polymeric insulation samples on the basis of compound PK-21 applied during impregnation of TRS EM insulation, on the basis of different-time drying using convection method and thermal radiation.

The second stage includes determination of binding material soluble part in the prepared samples.

To provide an objective assessment and reliability of experimental studies concerning comparison of drying methods of TRS EMs insulation, 6 identic blank parts representing sheets made of foil with thickness of 0.2 mm and dimensions of 14.5 mm × 12 mm have been prepared. The compound PK-21 has been cast into mold to the depth of 5 mm. The weight of sample was 50 g including the weight of compound of 45 g and weight of the mold of 5 g.

Three samples have been installed into the convection electrical oven of Locomotive repair plant (Ulan-Ude) and have been dried within 4 h (sample No. 1), 6 h (sample No. 2), and 8 h (sample No. 3) at the temperature of 160 °C (Fig. 7).



Fig. 7. Samples installation into the convection oven

To provide reliability of drying process, when each sample had been taken from oven, the time of other samples drying was suspended till the oven reached the temperature of 160 °C; it was checked by diagram of oven air space heating.

The other three samples have been dried at the experimental-laboratory stand for TRS EM insulation drying by means of thermal radiation [9].

The samples have been exposed to thermal radiation within 1 h (sample No. 4), 2 h (sample No. 5), and 3 h (sample No. 6) at the continuous infrared power supply. The temperature at the compound surface has been 160 °C just like in the oven during drying by means of convection method.

Methods of determination of binding material soluble part content in the compound have been developed and approved by GC “Elinar” – a leading supplier of electrical insulation for Russian Railways. Methods are based on the samples extraction in Soxhlet extractor.

3 Results

The results of studies on determining the efficiency of proposed methods of TRS EM insulation hardening in comparison with standard method are given in Table 1.

Table 1. Results of studies on determination of binding material soluble part content in samples.

Type of heating and its duration	Degree of cure	Soluble part, %
oven 160 °C – 8 h (1)	78.0	22.0
oven 160 °C – 8 h (2)	75.9	24.1
oven 160 °C – 6 h (1)	72.5	27.5
oven 160 °C – 6 h (2)	77.0	23.0
IR; 160 °C – 1 h	80.7	19.3
IR; 160 °C – 2 h	97.6	2.4
IR; 160 °C – 4 h	95.2	4.8

In Table 1: oven – convection heating (standard technology); IR – infrared heating (proposed technology).

As the table shows, use of thermal heating sufficiently reduces duration of impregnating material curing process. At that, degree of cure is notably higher after heating by means of thermal radiation; this indicates the efficiency of the proposed method.

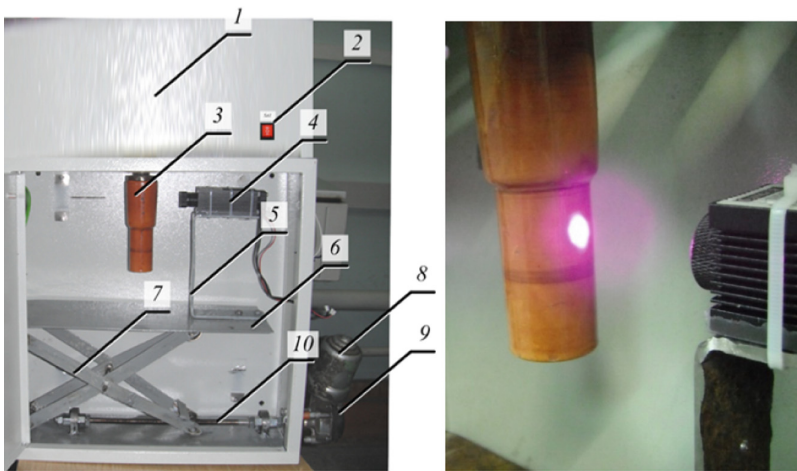
On the basis of experiments carried out to assess the efficiency of thermal radiation during manufacturing and repair of TRS EMs as well as experiments carried out to determine quantitative indexes of insulation (electric strength, hardness) obtained as a result of hardening by means of thermal radiation [10], new methods of TRS EM insulation drying using thermal radiation have been proposed [11–13].

High-accuracy modeling of the insulation hardening process by means of thermal radiation using computer technologies of engineering analysis based on the finite-element method [14] allows to adjust operation of industrial plants with high precision.

4 Discussion

One of the latest developments of Irkutsk State University of Railways scientists is the method of polymeric insulation drying by means of coherent radiation – using energy of infrared laser (iraser). Iraser has a very narrow band of radiation (almost identical wavelength) and high intensity (hundreds of times greater than standard IR emitters have) in the point area.

Figure 8 shows an experimental-and-production plant for small-sized parts drying by means of IR-laser (via example of TEM brushholder stud drying).



- 1 – body; 2 – control switch; 3 – stud of brushholder;
 4 – IR emitter; 5 – support of IR emitter; 6 – plate of hoisting device;
 7 – rack of hoisting device; 8 – electric motor; 9 – gear box;
 10 – infeed screw

Fig. 8. Experimental-and-production plant for drying of TEM brushholder brackets studs in electric locomotives by means of IR-laser

5 Conclusions

Based on the results of studies, the following conclusions can be drawn:

- content of soluble part after treatment by thermal radiation is 6...8 times lower in comparison with convection ovens;
- degree of samples cure after treatment by thermal radiation is 30% higher in comparison with convection ovens;
- intensity of IR-radiation provides degree of cure 97.6 in case of heating within 2 h in comparison with degree of cure 78.0 in case of heating in oven within 8 h; at that, the difference in soluble part is about 10 times greater in case of IR heating;

- proposed methods of insulation hardening by means of thermal radiation allow to increase breakdown voltage by 45%;
- local application of iraser during the process of insulation hardening for the most wearable places (including coil ends) provides significant increase in quality and strength-plasticity ratio owing to the possibility of complete control.




Acknowledgments. Thus, the proposed methods of hardening insulation can significantly reduce the time for the technological processes of drying, and also improve the quality of insulation and its reliability in general.

References

1. Sbornik dokladov i soobshchenii nauchno-tekhnicheskoi konferentsii «Povyshenie resursa tyagovykh elektrodvigatelei» pod obshchei redaktsiei d.t.n. Osyayeva, A.T., Moscow, p. 127 (2004)
2. Khudonogov, A.M., Lytkina, E.M., Dul'skii, E.Yu.: Innovatsionnaya tekhnologiya povysheniya nadezhnosti i prodleniya resursa elektricheskikh mashin tyagovogo podvizhnogo sostava [Tekst]. *Sovremennye tekhnologii, Sistemnyi analiz, Modelirovanie* 4(36), 102–108 (2012)
3. Khudonogov, A.M., Dul'skii, E.Yu.: Analiz nadezhnosti tyagovykh elektricheskikh mashin elektrovozov serii «ERMAK» [Tekst]. In: *Problemy transporta Vostochnoi Sibiri. Sbornik trudov Chetvertoi Vserossiiskoi nauchno-prakticheskoi konferentsii studentov, aspirantov i molodykh uchenykh fakul'tetov «Transportnye sistemy» i «Sistemy obespecheniya transporta»*, chap. 1, pp. 20–24. IrGUPS, Irkutsk (2013)
4. Smirnov, V.P.: Nepreryvnyi kontrol' temperatury predel'no nagruzhennogo oborudovaniya elektrovoza [Tekst]: avtoref. dis. ... dokt, tekhn, nauk, 05.22.07, Irkutsk, p. 320 (2005)
5. Yurasov, O.D.: Analiz neplanovykh remontov elektricheskikh mashin elektrovozov serii 2ES6 v servisnom lokomotivnom depo Moskovka [Tekst]. In: *Ekspluatatsionnaya nadezhnost' lokomotivnogo parka i povyshenie effektivnosti tyagi poezdov. Materialy vtoroi vserossiiskoi nauchno-tekhnicheskoi konferentsii s mezhdunarodnym uchastiem*, pp. 235–242. OmGUPS, Omsk (2014)
6. Sotnikov, S.G., Smirnov, V.A.: Analiz ekspluatatsionnoi nadezhnosti i prichin povrezhdaiemosti elektricheskikh apparatov elektrovozov 2ES6, 2ES10 [Tekst]. In: *Ekspluatatsionnaya nadezhnost' lokomotivnogo parka i povyshenie effektivnosti tyagi poezdov. Materialy vtoroi vserossiiskoi nauchno-tekhnicheskoi konferentsii s mezhdunarodnym uchastiem*, pp. 49–53. OmGUPS, Omsk (2014)
7. Dul'skii, E.Yu.: Energoaudit bezrazbornoi tekhnologii remonta magnitnoi sistemy tyagovykh dvigatelei elektrovozov [Tekst]. *Mir transporta*, pod red, Levin, B.A. i dr, Moskva: izd-vo MKZhT MPS Rossii 3(41), 168–171 (2012)
8. Lytkina, E.M.: Povyshenie effektivnosti kapsulirovaniya izolyatsii lobovykh chastei obmotok tyagovykh dvigatelei elektrovozov infrakrasnym izlucheniem [Tekst]: avtoref. dis. ... kand. tekhn, nauk, 05.22.07, Irkutsk, p. 205 (2011)
9. Khudonogov, A.M., Lytkina, E.M., Dul'skii, E.Yu.: Osnovy lokal'nogo metoda prodleniya resursa izolyatsii elektricheskikh mashin tyagovogo podvizhnogo sostava teplovym izlucheniem [Tekst]. *Izvestiya Transsiba* 1(17), 26–30 (2014)

10. Dul'skii, E.Yu.: Sovershenstvovanie tekhnologii vosstanovleniya izolyatsii elektricheskikh mashin tyagovogo podvizhnogo sostava pri depovskom remonte [Tekst]: dis. ... kand. tekhn. nauk, Irkutsk, 190 p. (2014)
11. Lytkina, E.M., Dul'skii, E.Yu., Khudonogov, A.M.: Spektral'no-ostsilliruyushchii sposob propitki izolyatsii lobovykh chastei obmotok vrashchayushchikhsya elektricheskikh mashin i ustroystvo dlya ego realizatsii. Patent Rossii № 2515267, 2012, Patent RF № 2012157499/07, 26 Dec 2012, Byul **13** (2012)
12. Khudonogov, A.M., Lytkina, E.M., Dul'skii, E.Yu., Ivanov, P.Yu., Garev, N.N., Vyzhimova, V.N.: Selektivnyi sposob sushki uvlazhnennoi ili propitannoi izolyatsii obmotok yakorya tyagovykh elektricheskikh mashin i ustroystvo dlya ego realizatsii. Patent Rossii № 2525296, 2012, Patent RF № 2012143541/07, 11 Oct 2012, Byul **11** (2012)
13. Lytkina, E.M., Dul'skii, E.Yu., Khudonogov, A.M.: Infrakrasno-konvektivno-vakuumnyi sposob sushki izolyatsii obmotok magnitnoi sistemy ostova tyagovoi elektricheskoi mashiny i ustroystvo dlya ego realizatsii. Patent Rossii № 2569337, 2012. Patent RF № 2012145098/07, 23 Oct 2012, Byul **12** (2012)
14. Dul'skii, E.Yu.: Modelirovanie rezhimov IK-energopodvoda v tekhnologii prodleniya resursa tyagovykh elektricheskikh mashin s ispol'zovaniem metoda konechnykh elementov [Tekst]. Vestnik: IrGTU **12**(83), 258–263 (2013)
15. Dul'skii, E.Yu.: Sovershenstvovanie tekhnologii vosstanovleniya pal'tsev shchetkoderzhateli elektricheskikh mashin tyagovogo podvizhnogo sostava [Tekst]. In: Transportnaya infrastruktura Sibirskogo regiona: Materialy shestoi mezhdunarodnoi nauchno-prakticheskoi konferentsii 2016 g, pp. 510–513. Izd-vo IrGUPS, Irkutsk (2016)

Technology of Electric Power Efficient Use in Transport

Tatyana Alekseeva^(✉) , Natalya Ryabchyonok ,
and Leonid Astrakhantsev 

Irkutsk State Transport University,
Chernyshevskogo St., 15, Irkutsk 664074, Russia
talecseeva@rbcmail.ru

Abstract. Shortcomings of educational process of specialists training for development, manufacture of equipment and technology for use of electric power in transport, which hinder the further development of high-technology equipment, have been revealed. A new theory of power processes in electrical circuits with semiconductor power regulators has been developed. Practicability of continuous use of electric potential of power sources for electric traction instead of known switching regulators of traction electric drive power has been proved. It has been proposed to regulate the power of vehicles by changing the input electric resistance of the traction electric drive to ensure high power efficiency, power saving and electromagnetic compatibility of transport with the power supply system.

Keywords: Duration · Voltage switching regulators · Power · Device
Electric power accumulator · Power consumer

1 Introduction

The world production of semiconductor power regulators for various purposes, which are widely used in many sectors of economy to improve the quality of technological processes, labor productivity, power saving, changes in electrical power parameters and for solving other problems, is characterized by pulse methods of transferring electrical power from sources to consumers [1, 2]. Currently, while controlling power and power flow by means of power switching regulators, power efficiency is reduced and electromagnetic compatibility of the electric power system elements is disturbed with increasing degree of power regulation; the possibility of reducing power losses during generation, transfer and use of electric power by vehicles is not realized.

The research is aimed at identifying the cause of the existing problem in the power system, improving the content of the educational process of educational institutions, justifying a new parameter of power control and promising directions for the further development of vehicles power regulators.

2 Materials and Methods

The law of motion and power distribution in elastic media of various physical nature was discovered by Professor Umov [3] in 1874 and formalized in relation to the electromagnetic field by Professor Poynting [4] in 1884 (1). The law is currently applied not only for the analysis of stationary power modes, but also for modes of power regulation in the electric power system. For arbitrary volume V , bounded by surface S , the electromagnetic field varies with time t (1). Within the volume V there are conducting bodies and the medium is homogeneous and isotropic; there are no external power sources, the reflected wave is absent.

$$-\oint (\vec{E} \cdot \vec{H}) dS = \oint (\vec{\delta} \cdot \vec{E}) dV + \oint (\vec{H} \cdot \frac{\partial \vec{B}}{\partial t} + \vec{E} \cdot \frac{\partial \vec{D}}{\partial t}) dV, \quad (1)$$

where \vec{E}, \vec{H} – electric-field vector and magnetic field vector, respectively, caused by the action of external forces in the process of power generation;

$\vec{\delta}$ – conduction current density vector;

\vec{B} – magnetic induction vector;

\vec{D} – electrical displacement vector.

Within the volume V there are conducting bodies and the medium is homogeneous and isotropic; there are no external power sources, the reflected wave is absent. Part of electric potential of the power source (1) is used to irreversibly transform electrical power into other type of power and, with the help of the second integral of the right-hand side of the equation; another part of electric potential is used to change the electromagnetic power. Duration of irreversible transformation of electrical power into other type of power due to reactive elements is decreased by time φ twice for the period T of the alternating voltage u (Fig. 1).

From Fig. 1, it follows that transformation of electrical power into thermal power is carried out by pulses; during a pause φ between pulses, the source electrical voltage u is not used for irreversible transformation of electrical power into thermal power. With the help of electrical power, thermal power is generated in the resistor due to rms current I and part of rms voltage of the power source $U \cdot \cos\varphi$. When the power source voltage U is continuously used to generate thermal power in the resistor R , the current can be consumed from the power source less than the current I . Thus, pulse transformation of electrical power into other type of power due to reactive elements is accompanied by reduction in duration of the irreversible transformation of electrical power into thermal power and decrease in power efficiency of the electric power system.

Ideally, when work of the external forces of the power source to provide the electric field strength \vec{E} and the magnetic field strength \vec{H} varies in accordance with the volume of power consumed, the left-hand side of Eq. (1) is equal to the right-hand side. Seasonal, daily cycles of change in power of power consumers with the help of switching devices allow changing generator power, technology, production output and transmission of power to reduce power losses and ensure power saving.

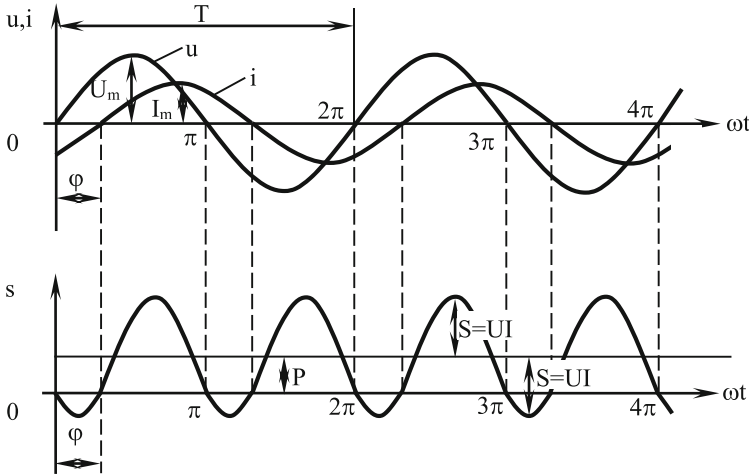


Fig. 1. Time diagrams of instantaneous values of u , i , s in electrical circuit with elements R and L .

At present, to control technological processes and power saving, the flow of power in electrical circuits is interrupted by means of contact switching devices with the duration of electricity consumption cycle measured in hours and minutes. During these time intervals, it is often impossible to change work of external forces in the process of generating electricity. In practice, during cycles with duration of 1 h or less, change in the mode of generating sources operation is caused by difficulties of technological realization, inertia of equipment, performance of work to ensure standard electric power parameters or unjustified power losses when power equipment is withdrawn from economic mode of operation. Semiconductor power regulators (SPRs) with duration of the cycle of conducting and non-conducting state of power semiconductor power devices (SPDs), measured in milliseconds or in microseconds, are manufactured in Russia and abroad. For these reasons, in the modes of pulsed flow control, the left-hand side of Eq. (1) is greater than the right-hand side. Therefore, in the balance of power (2) justified by the theory of power processes [5, 6], which is studied in educational institutions, active power P_1 , shear power Q_1 and distortion power T are contained in the right-hand side of Eq. (2). This theory is used by specialists in development, manufacture and operation of controllable rectifiers, inverters [2, 7], electric power recuperators, 4qS-converters, DC switching converters, voltage regulators and other SPRs.

$$S_G = \sqrt{P_1^2 + Q_1^2 + T^2}. \tag{2}$$

The symbols P_1 , Q_1 usually means active and reactive power generated by the fundamental harmonic of voltage and current. The distortion power T is equal to the product of effective value of the fundamental harmonic of voltage by the sum of effective values of harmonics of current except for the fundamental harmonic. Incorrect

application of spectral analysis to justify the known power characteristics causes insuperable contradictions in the educational process [8] and directs specialists to develop, manufacture and use additional equipment or complicate the structure of SPRs for power Q1, T elimination. Due to the pauses in the process of pulse transmission of electrical power from sources to consumers with the help of SPR, as well as due to reactive elements, the duration of its irreversible transformation into other type of power is reduced. Since this factor is not taken into account by expressions (1, 2), therefore, the Umov-Pointing theorem has been corrected and the theory of power processes in electrical circuits with semiconductor devices has been developed [9–11]. If switching equipment (SE) that interrupts the power flow entering the closed volume V is used and operation of external forces in the power source during the pause is performed, then work and change in the electromagnetic field power in the volume V are performed by means of the source power only during the conducting state of the SE power elements (Fig. 2).

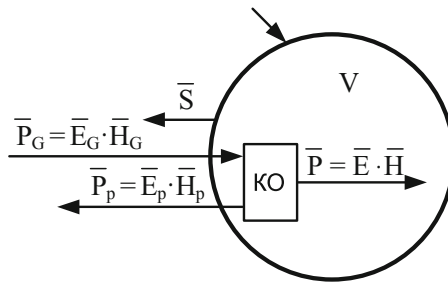


Fig. 2. Powers of pulse power flow.

The Pointing vector \vec{P} enters the volume V during the conductive state of the SE force elements which is part of the vector \vec{P}_G and the other part of this vector \vec{P}_p does not enter the volume V during the nonconducting state of the SE force elements. Then, taking into account change in the duration of the irreversible transformation of electrical power into other type of power due to the pulse regulation of the power flow with the help of SE, Eq. (1) takes the following form:

$$-\left[\oint (\vec{E}_G \cdot \vec{H}_G) d\vec{S} - \oint (\vec{E}_p \cdot \vec{H}_p) d\vec{S} \right] = \oint (\vec{\delta} \cdot \vec{E}) dV + \oint \left(\vec{H} \cdot \frac{\partial \vec{B}}{\partial t} + \vec{E} \cdot \frac{\partial \vec{D}}{\partial t} \right) dV, \tag{3}$$

where $\vec{E}_G \vec{H}_G$ – is the electric-field vector and magnetic field vector, respectively, caused by the action of external forces in the process of power generation;

\vec{E}_p, \vec{H}_p – is the electromagnetic field vectors caused by operation of external forces in the process of generating power during the non-conducting state of the switching equipment power elements;

\vec{E}_C, \vec{H}_C – is the electromagnetic field vectors caused by operation of external forces in the process of generating power during the conducting state of the switching equipment power elements.

The second integral in the left-hand side of Eq. (3) takes into account change in the switching equipment of duration of the irreversible transformation of electrical power into other type of power.

With transition from vector values in Eq. (3) to their scalar values, the power balance (4) takes the following form:

$$\sqrt{S_G^2 - \Delta S^2} = \sqrt{P^2 + Q^2}. \quad (4)$$

Change in the electrical potential at the terminals of electrical power consumers by means of SPRs can be determined using Kirchhoff's second law (5).

$$u_G(t) - u_p(t) = u_c(t), \quad (5)$$

where $u_G(t)$ – is the instantaneous value of the power source voltage;

$u_p(t)$ – is the instantaneous value of the power source voltage during the non-conducting state of the SPR semiconductor power devices;

$u_c(t)$ – the instantaneous value of the power source voltage during the conducting state of the SPR semiconductor power devices.

Instantaneous values of voltage and current can be expanded in Fourier series [12].

$$\sum_{k=0}^n u_{Gk}(k\omega t) - \sum_{k=0}^n u_{pk}(k\omega t) = \sum_{k=0}^n u_{ck}(k\omega t), \quad (6)$$

where $\sum_{k=0}^n u_{Gk}(k\omega t)$ – is the instantaneous value of voltage of the k-harmonic at the SPR input;

$\sum_{k=0}^n u_{pk}(k\omega t)$ – is the instantaneous value of voltage of the k-harmonic at the SPR input during the SPD non-conducting state;

$\sum_{k=0}^n u_{ck}(k\omega t)$ – is the instantaneous value of voltage of the k-harmonic at the SPR input during the SPD conducting state;

k – is the number of the Fourier series components, integers;

n – is the number of the last harmonic counted;

$\omega - 0$ is the angular frequency of the fundamental harmonic component of voltage at the SPR input.

Under the influence of voltage $\sum_{k=0}^n u_{ck}(k\omega t)$, during the conducting state of the power regulator SPD, the current flows in the electric circuit.

$$i(t) = \sum_{k=0}^n i_k(k\omega t), \quad (7)$$

where $i_k(k\omega t)$ – is the instantaneous value of current of the k-th component of the Fourier series at the SPR input.

The instantaneous values of power at the SPR input can be obtained by multiplying the left-hand and right-hand parts of expressions (6) and (7):

$$\begin{aligned} & \sum_{k=0}^n u_{Gk}(k\omega t) \cdot \sum_{k=0}^n i_k(k\omega t) - \sum_{k=0}^n u_{pk}(k\omega t) \cdot \sum_{k=0}^n i_k(k\omega t) \\ & = \sum_{k=0}^n u_{ck}(k\omega t) \cdot \sum_{k=0}^n i_k(k\omega t). \end{aligned} \quad (8)$$

Depending on the force elements, structure and principle of SPR operation, the components of the Fourier series and their values in expression (8) change. In expression (8), the sums of the products of constant components of the series into harmonic components with frequency $k\omega$ and the sum of the products of harmonic components of different frequencies are equal to zero. Thus, the instantaneous value of the total power at the SPR input can be written in the following form.

$$S_G(t) = \sum_{k=0}^n u_{Gk}(k\omega t) \cdot \sum_{k=0}^n i_k(k\omega t). \quad (9)$$

The total power at the SPR input can be calculated from the formula

$$S_G = U \cdot I, \quad (10)$$

where U, I – is the effective values of the voltage, current at the SPR input.

The component of the instantaneous power at the SPR input during the SPD non-conducting state can be denoted in the left-hand side of the expression (8) as $\Delta S(t)$:

$$\Delta S(t) = \sum_{k=0}^n u_{pk}(k\omega t) \cdot \sum_{k=0}^n i_k(k\omega t). \quad (11)$$

Since expression (11) contains products of the similar components of the Fourier series, then one more component of the total power at the SPR input expressed in terms of the effective values of voltage and current, is equal to

$$\Delta S = \sqrt{\sum_{k=0}^n U_{pk}^2 \cdot I_k^2} = U_p \cdot I, \quad (12)$$

where U_{pk} – is the effective value of voltage of the k th component of the Fourier series at the power regulator input during the non-conductive state of SPD;

I_k – the effective value of the similar k -harmonic of current at the SPR input;

U_p – the rms voltage at the SPR input during the non-conducting state of SPD.

The power ΔS represents the component of total power at the input of power regulator characterizing the part of sources electrical power that cannot be transformed into the other type of power, or it is impossible to provide power interchange by means of this part of power because voltage U_p is applied to the power regulator during nonconducting state of its power components. The sign ΔS means potential or passive power, it appears in electric power system at the pulse transmission of power flow from source to consumer. Since rms voltage U_p is not used for execution of work by means of electrical power during space in the power flow, then rms current I exceeds minimum current (active current) that would be consumed from power sources if rms voltage U was entirely used at the input of power regulator. i.e. equal in value additional current will be consumed from power sources both due to spaces in electrical

power flow and due to reactive components in electric power system [13, 14], if equal reduction in duration of irreversible transformation of electrical power into the other type of power occurs.

The instantaneous value of total power at the SPR input during the conducting state of SPD is as follows:

$$s_{Gc}(t) = u_0 \cdot i_0 + \sum_{k=1}^n u_{ck}(k\omega t) \cdot \sum_{k=1}^n i_k(k\omega t). \quad (13)$$

Each k-harmonic in the expression (13) may be resolved into cosine and sine components.

The cosine component of voltage k-harmonic amplitude may be found from the formula:

$$U_{km} \cdot \cos \psi_{uk} = \frac{1}{\pi} \int_0^{2\pi} u(k\omega t) \cdot \sin(k\omega t) \cdot d(k\omega t), \quad (14)$$

where U_{km} – is an amplitude of sinusoidal components of voltage with various frequencies $k\omega$;

ω – is an angular frequency of the first harmonic voltage;

ψ_{uk} – is a primary phase of k-harmonic voltage.

The sine component of voltage k-harmonic amplitude may be found from the formula:

$$U_{km} \cdot \sin \psi_{uk} = \frac{1}{\pi} \int_0^{2\pi} u(k\omega t) \cdot \cos(k\omega t) \cdot d(k\omega t). \quad (15)$$

To find the primary phase of voltage k-harmonic, divide the expression (15) by expression (14):

$$\operatorname{tg} \psi_k = \frac{U_{km} \cdot \sin \psi_{uk}}{U_{km} \cdot \cos \psi_{uk}} = \frac{\frac{1}{\pi} \int_0^{2\pi} u(k\omega t) \cdot \cos(k\omega t) \cdot d(k\omega t)}{\frac{1}{\pi} \int_0^{2\pi} u(k\omega t) \cdot \sin(k\omega t) \cdot d(k\omega t)}. \quad (16)$$

Using expressions similar to formulas (14–16) it is possible to calculate cosine and sine components of amplitude I_{km} and primary phases ψ_{ik} of k-harmonics of current.

Shear angle of k-harmonic of current towards the same k-harmonic of voltage is as follows:

$$\varphi_k = \psi_{uk} \cdot \psi_{ik}. \quad (17)$$

The product of constant components and the products of cosine components of the row (13) in the whole form an average value of the total power at the SPR input (18).

$$P = U_{c0} \cdot I_0 + \sum_{k=1}^n U_{ck}(k\omega t) \cdot I_k, \quad (18)$$

where U_{c0} , U_{ck} – are average value of voltage and actual value of k-harmonic voltage at the SPR input during SPD conducting state;

I_0 , I_k – are average value of current and actual value of k-harmonic current at the SPR input.

The products of sine harmonical components of the row (13) form components of the instantaneous power at the SPR input (19) commonly referred to as reactive power Q .

$$Q = \mp \sqrt{\sum_{k=1}^n U_{ck}^2 \cdot I_k^2} = U_p \cdot I. \quad (19)$$

An argument φ_S of the total power and electrical resistance at the SPR input may be calculated from the formula:

$$\varphi_S = \arctg \frac{\mp \sqrt{\sum_{k=1}^n U_{ck}^2 \cdot I_k^2}}{U_{c0} \cdot I_0 + \sum_{k=1}^n U_{ck}(k\omega t) \cdot I_k}. \quad (20)$$

The expressions (19, 20) for calculation of reactive power and argument of total power, electrical resistance at the SPR input are obtained for the first time and allow to consider reactive powers of harmonical components, to assess nature of input electrical resistance if the reactive components are present in electrical circuits with nonsinusoidal voltages and currents. The basic theory of electrical circuits [15–17] gives formulas to calculate the total power and active power in electrical circuits with nonsinusoidal voltages and currents only.

Considering (10–20) from the expression (4) it is possible to detect reasons for present disadvantages of SPRs and to define prospective directions for technical solutions to provide efficient operation of electric power system.

$$\sqrt{U^2 \cdot I^2 - U_p^2 \cdot I^2} = \sqrt{P^2 + Q^2}. \quad (21)$$

$$I = \frac{\sqrt{P^2 + Q^2}}{\sqrt{U^2 - U_p^2}}. \quad (22)$$

Rms current in the electric power system (22) depends on rms voltage, operation carried out by electrical power, and changes in duration of irreversible transformation of electrical power into the other type of power.

Various SPRs produced in Russia and abroad for manufacturing processes control change duration of sources electrical power use. Thus, the efficiency of electric power system decreases and electromagnetic compatibility of its elements is disturbed when degree of control over power P increases by means of increase in U_p .

Powers may be calculated with high accuracy from the formulas (10–19) using advanced computer programs. In practice, it is possible to measure values using devices, to calculate components of the expression (4) using readings of these devices, and to check the power balance.

The analytic expression of power factor K_M allowing assessment of efficiency of electrical power to carry out operation considering reactive components and switching equipment in electrical circuit (23) will be obtained if the left and right parts of the expression (4) are squared and if ΔS is transferred into the right part of equation.

$$\begin{aligned} K_M &= \frac{P}{S_G} = \frac{P}{\sqrt{P^2 + Q^2 + \Delta S^2}} \cdot \frac{\sqrt{P^2 + Q^2}}{\sqrt{P^2 + Q^2}} = \frac{\sqrt{P^2 + Q^2}}{\sqrt{P^2 + Q^2 + \Delta S^2}} \cdot \frac{P}{\sqrt{P^2 + Q^2}} \\ &= K_C \cdot K_Q, \end{aligned} \quad (23)$$

where $K_C = \frac{\sqrt{P^2 + Q^2}}{\sqrt{P^2 + Q^2 + \Delta S^2}}$ – factor considering change made by switching equipment in duration of use of sources electrical power for operation execution;

$K_Q = \frac{P}{\sqrt{P^2 + Q^2}}$ – factor considering change made by reactive components of electrical circuit in duration of irreversible transformation of electrical power into the other type of power.

3 Results

According to Ohm's law, rms current in electrical circuit may be changed by means of change in value and nature of input electrical resistance of SPR with load instead of generally used pulse transmission of power flow from source to consumer by means of well-known voltage regulators [18]. Duration of electrical power irreversible transformation into the other type of power per power consumption cycle will not be reduced by switching equipment if power is controlled by means of change in electrical resistance of the electric power system components. The efficiency of various technical solutions for control over power of consumers by means of change in electrical resistance and disadvantages of well-known pulse power regulators confirm the validity of analytical expressions (4–23) for physical processes analysis in the electric power system. The power balance (4) is checked by means of mathematical modeling in Matlab environment in electrical circuits of alternating (Fig. 3) and direct (Fig. 4) currents with semiconductor regulators of voltage and resistive load R. Geometric difference between total power S_G and power ΔS is equal to active power P and does not depend on method of regulators SPD pulse control. If the power source voltage is 100 V, 50 V will be used for electrical power transformation into thermal power of resistor R, and the other part of source voltage $U_P = 86$ V will be applied to regulators SPDs during their nonconducting state. The same results are obtained [19] using semiconductor regulators with packet control of voltage, with pulse-frequency modulation and pulse-width modulation of voltage.

Power control by means of decrease in duration of electrical power irreversible transformation into the other type of power and formation of UP causes significant harmonic distortions of instantaneous current waveform. Current waveform distortion factor is calculated using unit THD signal Harmonic $K_i = 0.93$ (Figs. 3 and 4). In the examples $\Delta S = 4300$ VA, thus the power factor is equal to $K_M = 0.5$ in alternating

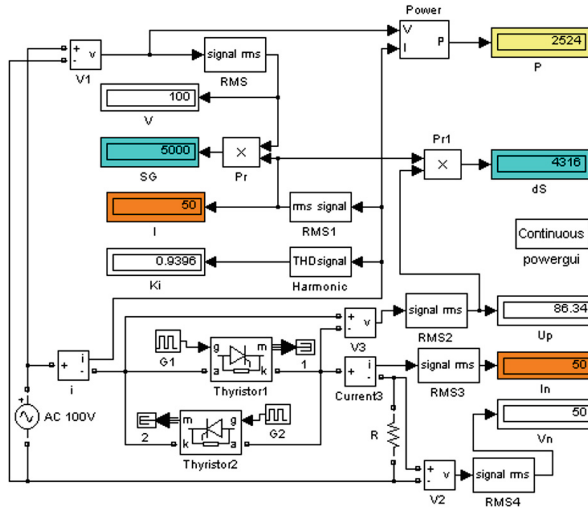


Fig. 3. Mathematical model of power processes in alternating current electrical circuit.

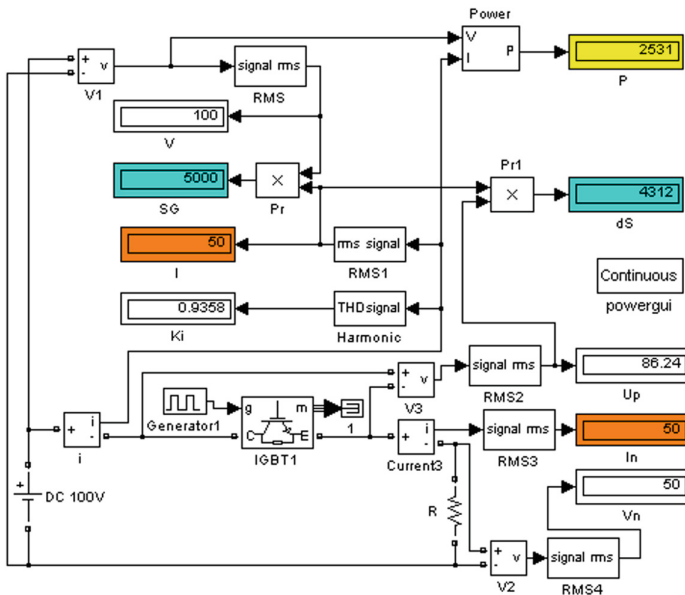


Fig. 4. Mathematical model of power processes in direct current electrical circuit.

current circuit and in direct current circuit due to nonconducting state of semiconductor devices and decrease in duration of use of sources electrical power for generation of thermal power in resistor R.

In case of pulse-phase control of thyristors (Fig. 3) with lagging or advanced angle of control at the input of voltage regulator with resistive load, varmeter shows shear capacity $Q1$ with negative or positive sign. From the expression (19) and results of researches [20] it follows that angle of shear φ_k of every k -harmonic of current I_k towards the same k -harmonic of voltage U_{ck} is equal to zero, thus it is not correct to call shear capacity a reactive power.

By means of changes in electrical resistance value and nature, the power regulators continuously transfer power flow from source to consumer and take on feature of electrical variator that changes the ratio of currents at the input and output depending on the ratio of voltages at the variator input and output. Nowadays power regulators do not possess such feature (Figs. 3 and 4). Mathematical model of power processes at the operation of electrical semiconductor variator (ESV) is given in the Fig. 5.

From the expression (22) it follows that active power $P = 2500$ W at total use of voltage $U = 100$ V may be obtained by means of twofold decrease in rms current at the ESV input in comparison with pulse voltage regulators using increase in input electrical resistance of power regulator with load. Power $\Delta S = 0$, and power factor $KM = 1$. Its high power efficiency and electromagnetic compatibility are present in the whole range of power control without application of additional equipment for compensation of shear capacity $Q1$ and distortion power T . The feature of electrical variator in the example (Fig. 5) is obtained by means of continuous and total use of power source electrical potential. In combination with throttle D_p that excludes power source loading with pulse current, intermediate storage of power C acts as a filter. Harmonic distortions of instantaneous current waveform ($K_i = 0.1$) are decreased by variator, thus harmonic distortions of voltage waveform in the electric power supply system will be less than the normal level permitted by GOST.

The test stand for examination of power regulator with smooth variation in input electrical resistance of electrical drive has been manufactured in Irkutsk State University of Railways. Obtained oscillograms (Fig. 6) of voltage (curve 1) and current (curve 2) at the developed power regulator input confirm the active nature of input electrical resistance of electrical drive and its electromagnetic compatibility with electric power supply system. Oscillograms are obtained in the mode of electrical drive power control when the current of 2.5 A flows in electrical motor windings and the current of 0.5 A is consumed from the main. Using advanced power characteristic, mathematical modeling of control over TEM НБ-514Б power in Simulink environment of MATLAB computer program has been carried out by means of developed regulator during “Ermak” electric locomotive motion with the speed of 5 km/h and rated tractive effort [21]. The current of 820 A flows in electrical motor windings, the current of 113.7 A flows at the power regulator input from the secondary winding of traction transformer. It means that regulator possesses ESV feature. The distortion factor of voltage curve harmonicity at the locomotive collector is less than normally acceptable limit in the whole range of locomotive power control.

While improving the power factor and increasing the electric locomotive efficiency with ESV at the same power of traction motors of 5538 kW, the power losses in overhead system are reduced by 29.5% compared to the power losses at the locomotive operation with pulsed SPRs. The construction is considerably simplified and the costs on ESV production are reduced in comparison with analogues of domestic and foreign manufacture.

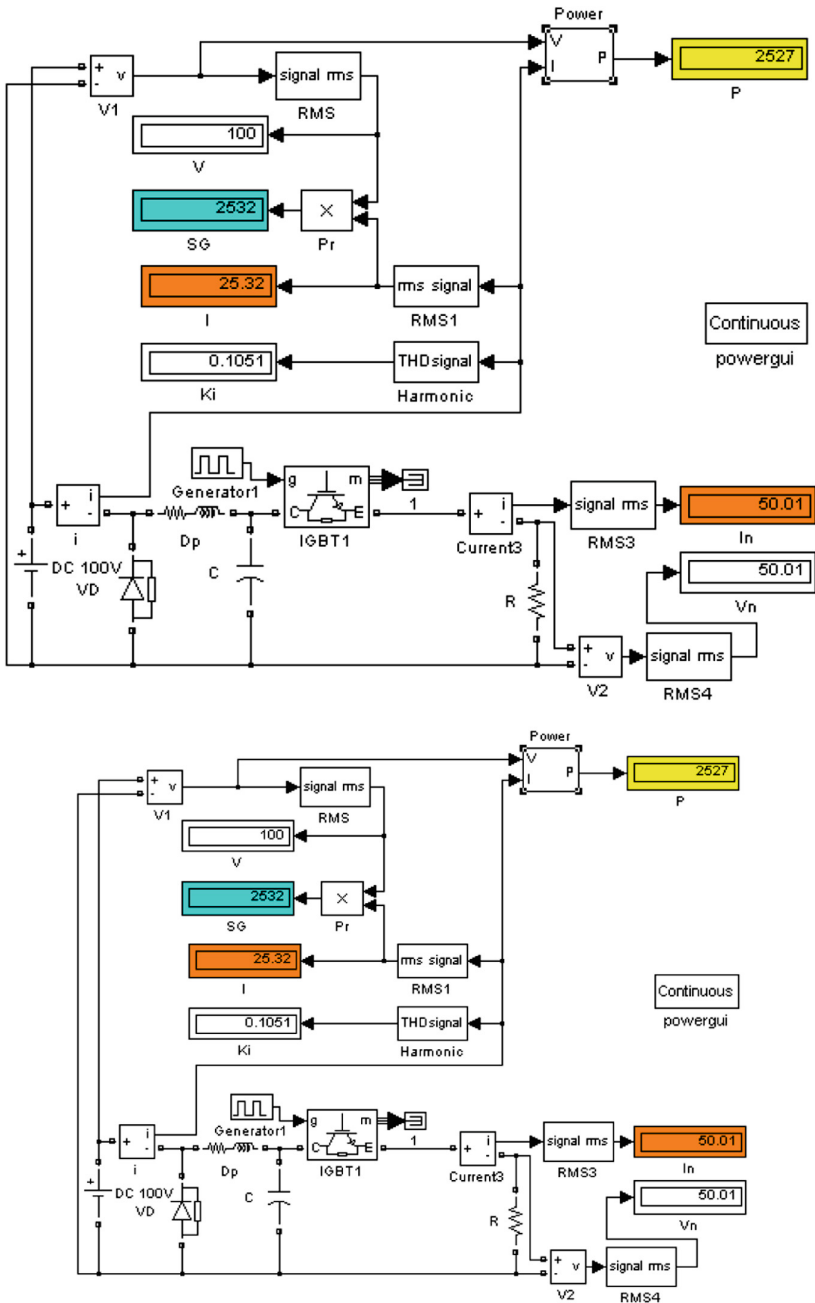


Fig. 5. Mathematical model of electrical semiconductor variator operation with resistive load.

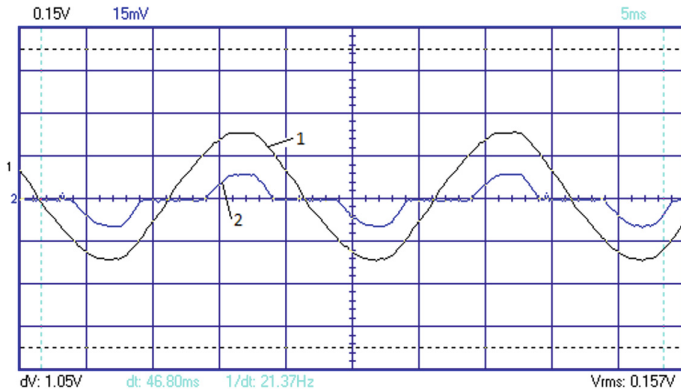


Fig. 6. Oscillograms of voltage and current at the electrical drive input.

4 Conclusion

Thus, fulfillment of the condition of effective use of the power sources electrical potential for traction solves the tasks of energy saving and electromagnetic compatibility of vehicles as evidenced by experimental research and mathematical modeling. ESV feature acquires special value when used to control the traction drive power of urban electrical transport and electric vehicles. Production of new-generation semiconductor power regulators is possible on the basis of educational process improvement in educational institutions.

References

1. Zheleznye dorogi mira **10**, 9–40 (1997)
2. Taigel'ketter, I.: Moshchnyi preobrazovatel' na IGBT-tranzistorakh dlya primeneniya nazheleznodorozhnom podvizhnom sostave, 50 p. Siemens AG, Myunkhen (2000)
3. Umov, N.A.: Izbrannye sochineniya, 571 p. Moscow - Leningrad, Gostekhizdat (1950)
4. Poynting, J.H.: On the transfer of energy in the electromagnetic field. *Philosactions Roy. Soc. Lond.* **175**, 343–361 (1884)
5. Maevskii, O.A.: Energeticheskie kharakteristiki ventil'nykh preobrazovatelei, 320 p. Energiya, Moscow (1978)
6. Zinov'ev, G.S.: Pryamye metody rascheta energeticheskikh pokazatelei ventil'nykh preobrazovatelei, 219 p. Izd-vo Novosibirskogo gosudarstvennogo universiteta, Novosibirsk (1990)
7. Burkov, A.T.: Elektronika i preobrazovatel'naya tekhnika, 307 p. UMTs ZhDT, Moscow (2015)
8. Alekseeva, T.L., Ryabchenok, N.L., Astrakhantsev, L.A.: Sovremennye problemy professional'nogo obrazovaniya: opyt i puti resheniya: Materialy Pervoi Vserossiiskoi nauch.-prakt. In: konf. s mezhdunarodnym uchastiem, pp. 44–48 (2016)
9. Ryabchenok, N.L., Alekseeva, T.L., Astrakhantsev, L.A.: Fundamental'nye i prikladnye problemy nauki. In: Materialy VII Mezhdunarodnogo simpoziuma, vol. 1, pp. 255–264 (2012)

10. Alekseeva, T.L., Ryabchenok, N.L., Astrakhantseva, N.M., Astrakhantsev, L.A.: Elektronnye preobrazovateli dlya resursosbergayushchikh tekhnologii, 240 p. IrGUPS, Irkutsk (2010)
11. Ryabchenok, N.L., Alekseeva, T.L., Yakobchuk, K.P., Astrakhantsev, L.A.: (2015). http://www.rusnauka.com/42_PRNT_2015/Tecnic/5_202603.doc.htm
12. Vlasova, E.A.: Ryady, 615 p. MGTU im N.E. Baumana, Moscow (2006)
13. Alekseeva, T.L., Ryabchenok, N.L., Astrakhantseva, N.M., Astrakhantsev, L.A.: (2015)
14. Sovremennyye tekhnologii. Sistemnyi analiz. Modelirovanie **3**(47), 181–186
15. Alekseeva, T.L., Ryabchenok, N.L., Astrakhantsev, L.A.: Byulleten' nauchnykh rabot Bryanskogo filiala MIIT **4**, 22–25 (2013)
16. Teoreticheskie osnovy elektrotekhniki, 544 p. Vysshaya shkola, Moscow (1976)
17. Bessonov, L.A.: Teoreticheskie osnovy elektrotekhniki, 638 p. Vysshaya shkola, Moscow (1996)
18. Demirchan, K.S., Neiman, L.R., Korovkin, N.V.: Teoreticheskie osnovy elektrotekhniki, 431 p. Piter, Saint-Petersburg (2009)
19. Astrakhantsev, L.A., Alekseeva, T.L., Ryabchenok, N.L.: Evraziiskii Soyuz Uchenykh **6** (15), 22–25 (2015)
20. Alekseeva, T.L., Ryabchenok, N.L., Astrakhantseva, N.M., Astrakhantsev, L.A.: Elektronnye (2010)
21. Preobrazovateli dlya resursosbergayushchikh tekhnologii, 240 p. IrGUPS, Irkutsk
22. Alekseeva, T.L., Ryabchenok, N.L.: Universum: Tekhnicheskie nauki: elektronnyi nauchnyi zhurnal **11**(32), 25–30 (2016)
23. Vorotilkin, A.V., Mikhal'chuk, N.L., Ryabchenok, N.L., Alekseeva, T.L.: Mir Transporta **6**, 62–76 (2015)

Development of Scientific-and-Experimental Stand to Study Operating Processes of New Transistor Converter of Alternating Current Locomotive

Oleg Melnichenko^(✉) , Aleksey Linkov ,
and Dmitry Yagovkin 

Irkutsk State Transport University, 15, Chernishevsky st., Irkutsk 664074, Russia
olegmelnval@mail.ru

Abstract. The article deals with various aspects of experimental stand construction for studying the operating processes of thyristor and transistor reversible converters of alternating current locomotive in the traction mode. Two types of reversible converter main circuit execution are provided at the stand – on the basis of thyristors and on the basis of transistors with specified technical features. The elements of electrical and mechanical equipment are listed in each circuit of converter, functions of these elements are explained. The article considers examples of thyristor and transistor converters operation in the mode of rectifier (the mode of locomotive traction) at the upper bands of regulation (the second band, the third one) where the rectifier operation differs from the first band. The oscillograms of converters operating processes are represented as current and voltage curves in the primary winding of transformer and in the circuit of rectified current of load (traction motor). Their comparison is given as well. Based on the results of comparative tests of thyristor and transistor converters operation in the rectifier mode at the upper bands of regulation, an experimental dependence of the electric locomotive power factor on changes in band voltage has been obtained. The comparative assessment of energy efficiency of converters operation has been provided by means of its power factor measurement for half-value (0.5) and total value (1.0) of regulation band voltage.

Keywords: Locomotive · Transistor · Power factor

1 Introduction

In the 1960s semiconductor rectifiers, thyristors, and the first power transistors were developed. This allowed creation of the controlled rectifiers to extend the potential of electrical drive control. Several generations of reversible converters (RCs) have been developed on the basis of thyristors. These converters are still used for electric rolling stock (ERS). The converters may provide the power factor (PF) of not more than 0.84 in the traction mode at the design [1–4] load. In the 1990s high-powered transistor-diode modules were developed in the sphere of converter equipment [1].

Previously the scientists of Irkutsk State University of Railways have offered RC development on the basis of IGBT transistors for ERS with commutator traction electrical motors (TEMs) to provide high values of the power factor [5, 6].

2 Description of Experimental Stand

The article contains description of stand for simulation of electric locomotive RS operation in the traction mode at the upper bands of regulation. Operation of rectifier at the upper bands and thus electromagnetic processes are slightly different from processes in RC at the first band of regulation. Figure 1 shows the functional flow diagram of RC experimental stand for electric locomotive in the traction mode with thyristors and IGBT transistors.

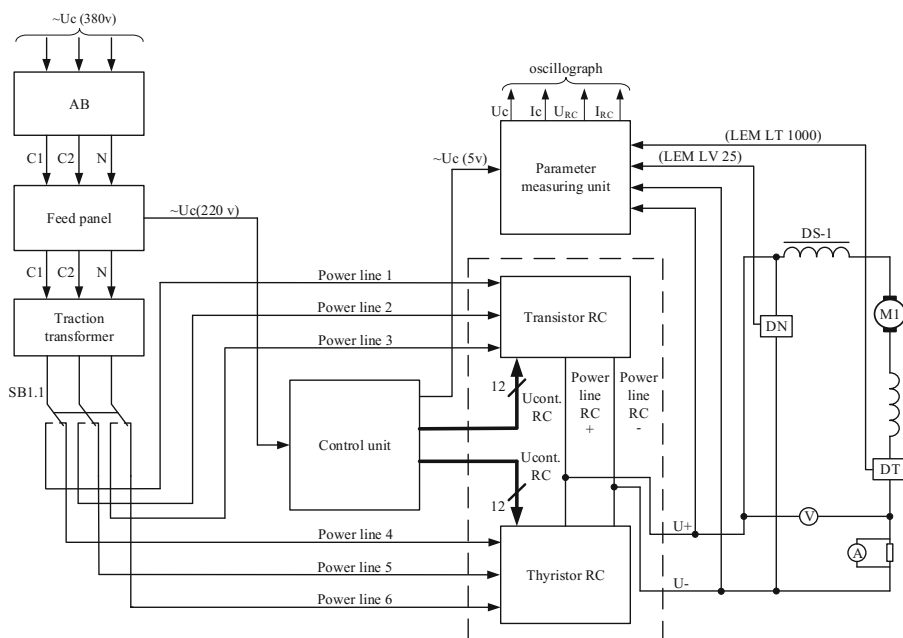


Fig. 1. Functional flow diagram of RC experimental stand for electric locomotive in the traction mode using thyristors and IGBT transistors

Wheels-and-motors unit (WMU) with traction motor NB-514 is used as a load to provide the most suitable studying of electromagnetic processes of thyristor and transistor RCs operation.

The stand allows studying of various RC operation modes and algorithms of their control, carrying out of measurements of power factor, active, reactive, and total power, alternating voltage and current, rectified voltage and load current. The stand allows detection of dependence using obtained results as well.

To simplify the stand structure and its control system, the simulation of three regulation bands is provided instead of four ones provided at the real electric locomotive. The only difference is in the scale of voltage amplitude at each band. At the same time, the diagram of each band provides all necessary physical characteristics of electromagnetic processes represented at the real electric locomotive. Voltage increase during transfer to the upper band is carried out by means of series connection of all secondary windings of the traction transformer (TT) starting from the winding 4-3. Figure 2 shows the electrical circuit diagram of RC experimental stand for electric locomotive in the traction mode using thyristors and IGBT transistors.

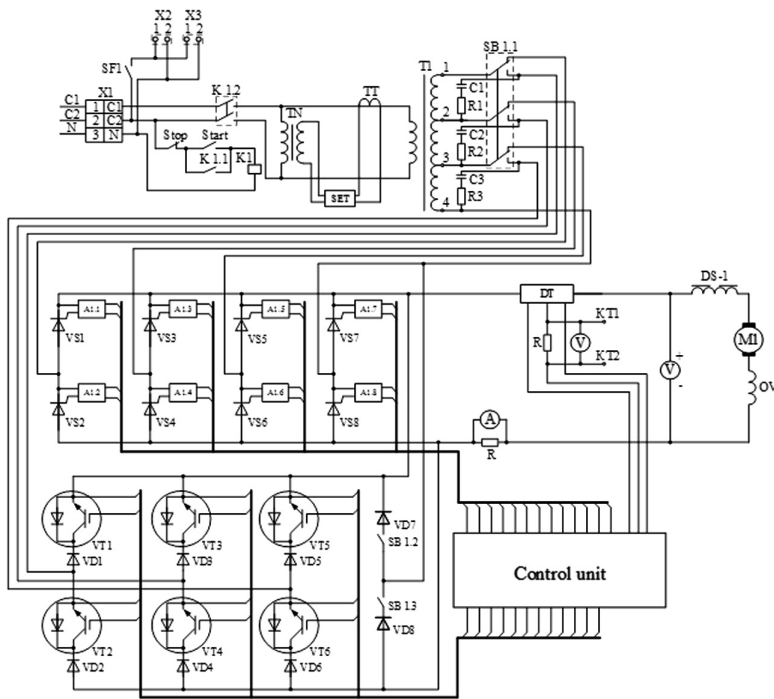


Fig. 2. Electrical circuit diagram of RC stand for electric locomotive in the traction mode using thyristors and IGBT transistors

As Fig. 1 shows, the stand includes two various circuits of RCs to be selected by means of the packet-type switch SB1. Each arm of thyristor RC contains one thyristor of T153-630-20 type. Arms of transistor RC consist of IGBT transistors of CM1000HA-24H type. In each arm of transistor RC, the transistor CM1000HA-24H is connected in series with diode of D253-1600-22 type. The throttle DS-1 necessary for rectified current ripple smoothing in the traction motor circuit is connected to the output circuit of RC. The traction transformer of OSZM-16 380/65 type is used in the stand. The transformer contains one primary winding with the voltage of 380 V and three secondary windings with voltage of 65 V each.

To control the combined RC, the special control system has been developed. The system provides various algorithms of control. The voltage of control unit is ~ 220 V. The main view of experimental stand for studying the electric locomotive RC operation is given in Fig. 3.

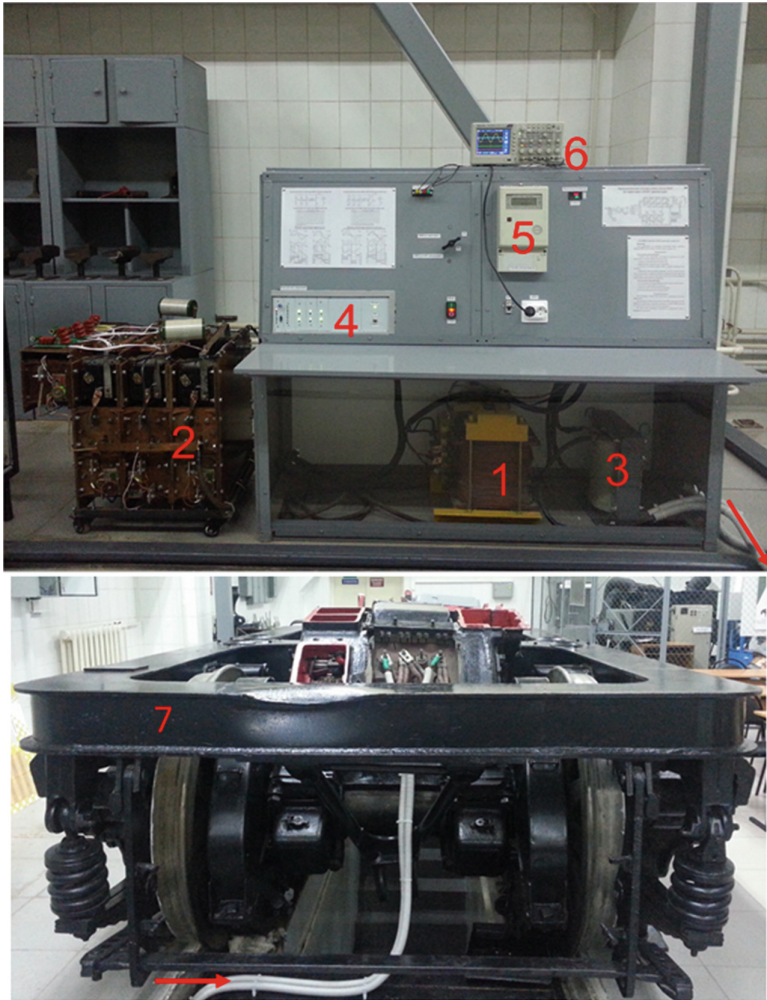


Fig. 3. Experimental stand for RC operation studying

The stand includes the following units:

- simulator of the traction transformer (1);
- combined RC (2) is designed for single-phase alternating current rectifying into the direct one and for smooth control of rectified voltage at the traction motor;
- smoothing inductor (3) is designed for TEM rectified current ripples reduction;

- control unit (CU) of RC (4) consists of processor unit, keys unit, drivers unit, feed panel with indicator;
- counter SET-1 M.01 M (5) is designed for measurement of power factor, active, reactive, and total powers;
- oscillograph Tektronix TDS 2024C (6) is designed for graphic representation of waveforms of transformer primary winding voltage and current, RC voltage and current as well as for obtained results saving to USB-storage device with possibility of data transfer to PC and further data processing;
- load (7) of WMU of VL85 electric locomotive with NB-514 traction motor.

Figure 4 shows the combined RC including the following elements: IGBT transistor (1); diode (2); thyristor (3); discharge diode arm (4); snubber circuit (5, 6).

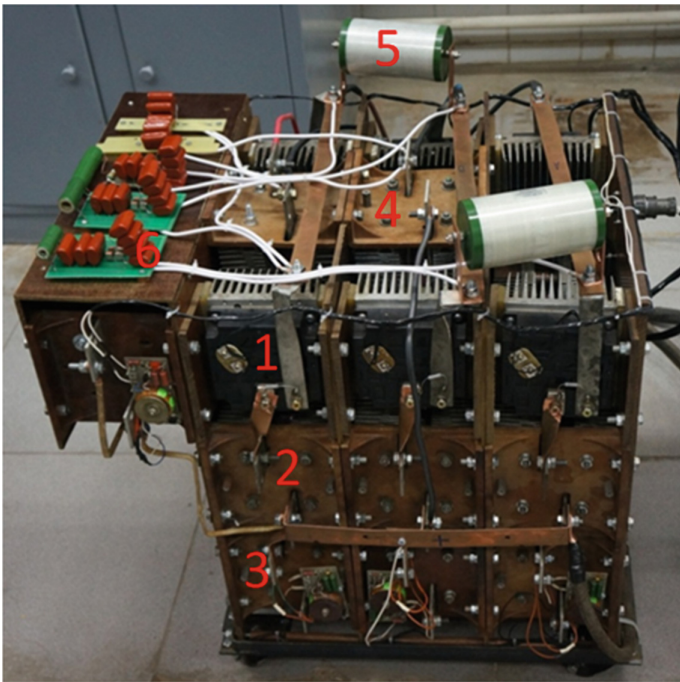


Fig. 4. Combined reversible converter

Figure 5 shows the feed panel with indicator. The panel includes the following elements: 1 – processor unit designed for generation of pulses to control RC arms; 2 – keys unit designed for distribution of control pulses over the thyristor RC arms; 3, 4, 5 – drivers designed for IGBT transistors control and for galvanic isolation of power circuit and control circuit; 6 – panel of CU switching on/off with indicators.



Fig. 5. Feed panel with indicator. Combined RC

3 Operating Processes of Thyristor and Transistor Rectifiers and Their Control Algorithms

Figure 6 shows the control algorithms of thyristor and transistor RCs. As can be seen, regulation starts from the rightmost arms in accordance with diagram given in Fig. 2. The diode arms VD7 and VD8 operate during the whole regulatory process and act as a discharge diode arm as well. The discharge diode arm is designed for maintenance of current in motors when arms of transistor RC do not operate.

The algorithm of control over thyristor rectifier arms by the example of the second band is as follows: during the first voltage half-cycle (closed arrow) the control pulse with phase uncontrolled angle α_0 is fed to the arm VS7, the control pulse with phase angle of delay α_{03} is fed to the arm VS6, and the control pulse with phase controlled angle α_p is fed to the arm VS4. During the second voltage half-cycle (stroke arrow) the control pulse with phase uncontrolled angle α_0 is fed to the arm VS8, the control pulse with phase angle of delay α_{03} is fed to the arm VS5, and the control pulse with phase controlled angle α_p is fed to the arm VS3.

The algorithm of control over transistor rectifier arms by the example of the second band is as follows: during the first voltage half-cycle (closed arrow) the diode arm VD7 comes into operation from the very beginning of regulation, the control pulse with phase uncontrolled angle α_w is fed to the arm VT6, the control pulse with phase controlled angle α_{reg} is fed to the arm VT4. During the second voltage half-cycle (stroke arrow) the diode arm VD8 comes into operation from the very beginning of regulation, the control pulse with phase uncontrolled angle α_w is fed to the arm VT5, the control pulse with phase controlled angle α_{reg} is fed to VT3.

During comparison tests at the stand of thyristor and transistor rectifiers operation at the upper bands of rectified voltage regulation, the oscillograms of voltage and current in the primary winding of transformer, rectified voltage and current in the traction motor circuit as well as values of locomotive power factors in the mode of traction, for Figs. 7, 8, 9 and 10 have been obtained at the half of second (Fig. 7) and third (Fig. 9) bands of regulation as well as total second (Fig. 8) and third (Fig. 10) bands of regulation.

Bands	Half-cycle	Algorithms of thyristor RCs operation							
		VS1	VS2	VS3	VS4	VS5	VS6	VS7	VS8
1	→	—	—	—	—	—	α_p	α_p	—
	←---	—	—	—	—	α_p	—	—	α_p
2	→	—	—	—	α_p	—	α_{03}	α_0	—
	←---	—	—	α_p	—	α_{03}	—	—	α_0
3	→	—	α_p	—	α_{03}	—	—	α_0	—
	←---	α_p	—	α_{03}	—	—	—	—	α_0
Bands	Half-cycle	Algorithms of transistor RCs operation							
		VT1	VT2	VT3	VT4	VT5	VT6	VD7	VD8
1	→	—	—	—	—	—	α_{reg}	+	—
	←---	—	—	—	—	α_{reg}	—	—	+
2	→	—	—	—	α_{reg}	—	α_w	+	—
	←---	—	—	α_{reg}	—	α_w	—	—	+
3	→	—	α_{reg}	—	α_w	—	—	+	—
	←---	α_{reg}	—	α_w	—	—	—	—	+

Fig. 6. Algorithms of thyristor and transistor RCs operation

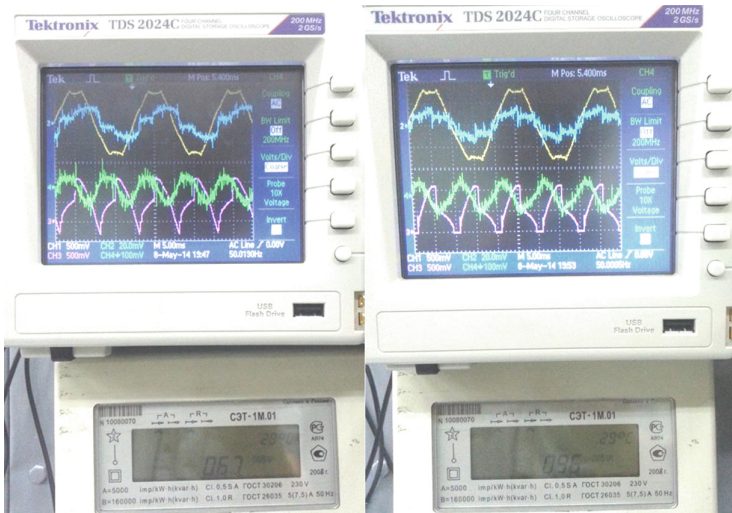


Fig. 7. Oscillograms and power factor of thyristor -0.67 (a) and transistor -0.96 (b) RCs obtained at the experimental stand in the traction mode at the 1.5 band of regulation

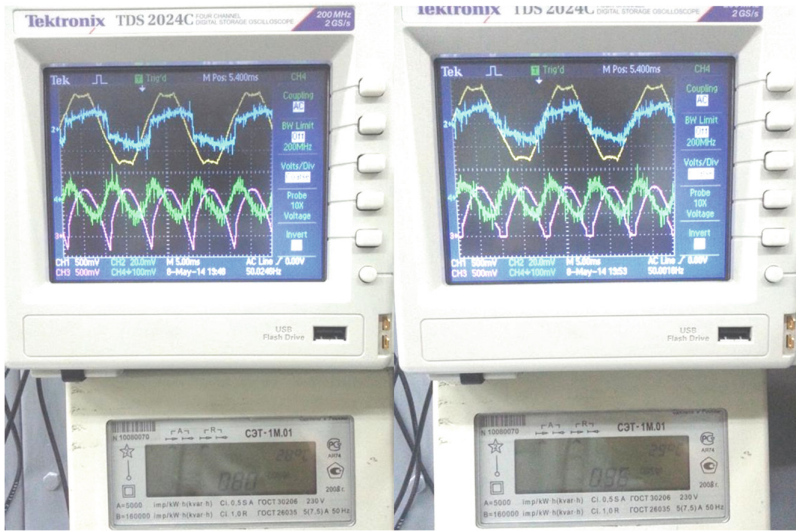


Fig. 8. Oscillograms and power factor of thyristor -0.80 (a) and transistor -0.96 (b) RCs obtained at the experimental stand in the traction mode at the 2nd band of regulation

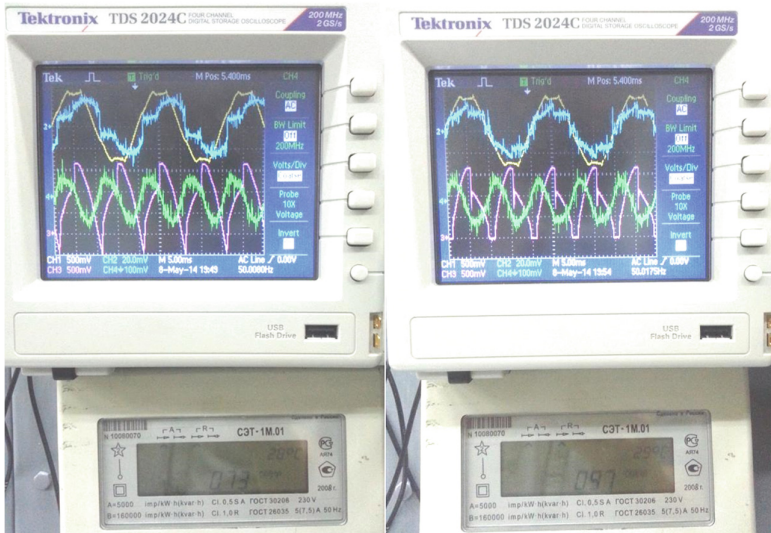


Fig. 9. Oscillograms and power factor of thyristor -0.73 (a) and transistor -0.97 (b) RCs obtained at the experimental stand in the traction mode at the 2.5 band of regulation

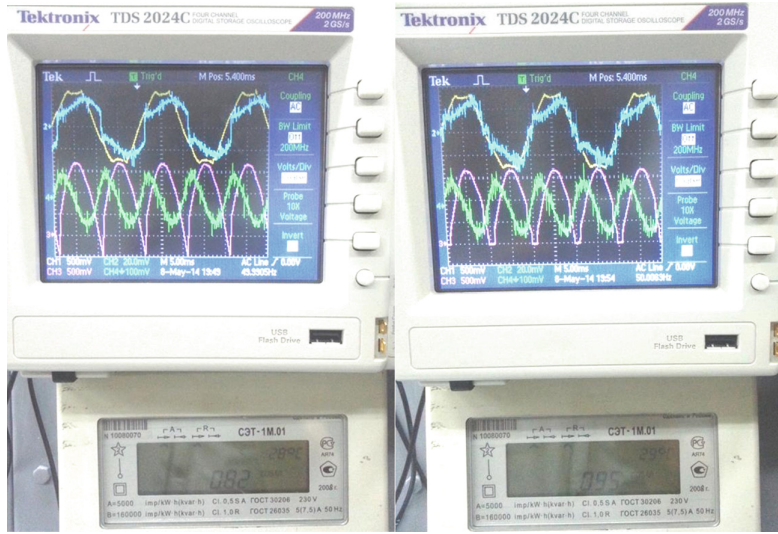


Fig. 10. Oscillograms and power factor of thyristor -0.82 (a) and thyristor -0.95 (b) RCs obtained at the experimental stand in the traction mode at the 3rd band of regulation

4 Results of Studies Carried Out at the Experimental Stand

Analyzing the obtained oscillograms, it can be concluded that low power factor of the thyristor rectifier is due to the fact that thyristors open in the second half of the half cycle (Figs. 7a, 8a, 9a and 10a). Besides, the inductive nature of the load causes an additional phase shift of the transformer primary current in relation to its voltage. In transistor converter it is proposed to carry out opening of the arms with leading in time in relation to maximum voltage (Figs. 7b, 8b, 9b and 10b). This partially compensates for the phase shift introduced by inductive nature of the load and causes significantly higher power factor [5, 6].

The diode arms VD7 and VD8 connected in parallel to the rectified current circuit of the transformer allow to maintain the motors current during the period of time between IGBT transistors switching off and switching on when the voltage half-cycle changes.

Figure 11 gives an experimental dependence of electric locomotive power factor for thyristor and transistor rectifiers in the traction mode for three bands of regulation implemented at the experimental stand.

The graph shows that during the whole process of rectified voltage increase, the transistor converter power factor is significantly higher than the thyristor converter power factor, and can reach 0.95 in the end of band.

Comparison of power factors values for thyristor and transistor rectifiers in the electric locomotive traction mode for three bands of regulation is given in Table 1.

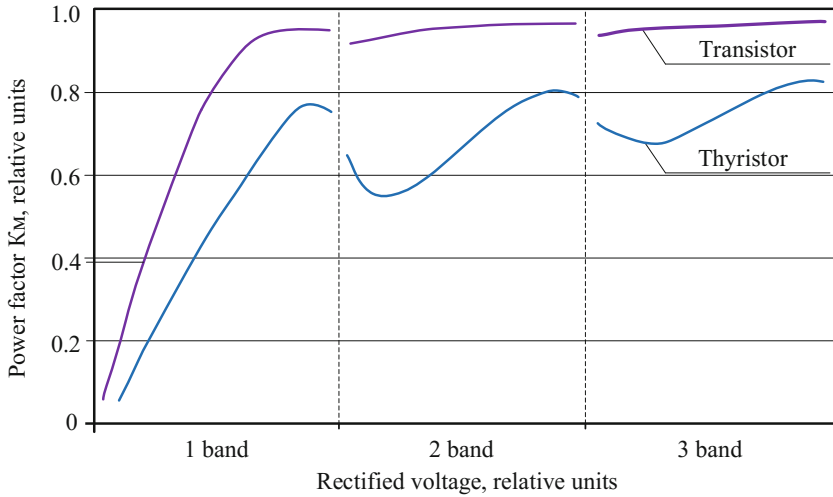


Fig. 11. Electric locomotive power factor vs rectified voltage in the traction mode for thyristor and transistor rectifiers during the whole regulation process

Table 1. Power factors of thyristor and transistor rectifiers in all bands of regulation

Band	Power factor		Difference, %
	Thyristor RC	Transistor RC	
0.5	0.45	0.83	84
1	0.74	0.95	28
1.5	0.67	0.96	43
2	0.8	0.96	20
2.5	0.73	0.96	32
3	0.82	0.95	16

5 Conclusion

Based on the results of studies, the following conclusions can be drawn:





- power factor at the half (0.5) of the first band of regulation for thyristor converter is 0.45, for transistor converter is 0.83, the latter is greater by 84%;
- power factor at (1.0) the first band of regulation for thyristor converter is 0.74, for transistor converter is 0.95, the latter is greater by 28%;
- power factor at the half (1.5) of the second band of regulation for thyristor converter is 0.67, for transistor converter is 0.96, the latter is greater by 43%;
- power factor at (2.0) the second band of regulation for thyristor converter is 0.8, for transistor converter is 0.96, the latter is greater by 20%;
- power factor at the half (2.5) of the third band of regulation for thyristor converter is 0.73, for transistor converter is 0.96, the latter is greater by 32%;

- power factor at (3.0) the third band of regulation for thyristor converter is 0.82, for transistor converter is 0.95, the latter is greater by 16%.

References

1. Gruzov, V.L.: Ventil'nye preobrazovateli: uchebnoe posobie. Vologda, p. 94 (2002)
2. Tikhmenev, B.N.: Elektrovozy peremennogo toka s tiristornymi preobrazovatelyami. In: Tikhmenev, B.N., Kuchumov, V.A. (eds.) Moscow, Transport, p. 312 (1988)
3. Tikhmenev, B.N.: Podvizhnoi sostav elektrifitsirovannykh zheleznykh dorog. In: Tikhmenev, B.N., Trakh-tman, L.M. (eds.) Moscow, Transport, p. 362 (1980)
4. Tushkanov, B.A., Pushkarev, N.G., Pozdnyakova, L.A.: Elektrovoz VL85: Rukovodstvo po ekspluatatsii. Moscow, p. 480 (1992)
5. Portnoi, A.Y., Mel'nichenko, O.V., Shramko, S.G., Poluyanov, A.G.: Patent na izobretenie 2498490 Rossiiskaya Federatsiya, MPK H02 M, H02P, G05F, B60L. Mnogozonnyi vypryamitel'no-invertornyi preobrazovatel' i sposob upravleniya preobrazovatelem. zayavitel' i patentoobladatel' FGBOU VPO «Irkutskii gos-udarstvennyi universitet putei soobshcheniya» . № 2012114982/07; zayavl. 16.04.2012, 31, p. 7 (2013)
6. Yagovkin, D.A., Mel'nichenko, O.V., Portnoi, A.Y.: Razrabotka novogo energosberegayushchego algoritma upravleniya VIP elektrovoza na IGBT modulyakh. Vestnik Instituta podvizhnogo sostava, pod red. Stetsyuka, A.E. i Gamoli, Y.A., Khabarovsk, DVGUPS 5, pp. 17–24 (2013)

Strengthening Design for Weak Base Using Geomaterials on “Amur” Automobile Road Section

Sergey Kudryavtsev^(✉) , Tatiana Valtseva , Elena Goncharova ,
and Aleksey Kazharsky 

Far Eastern State Transport University,
47 Seryshev St., Khabarovsk 680021, Russia
prn@festu.khv.ru

Abstract. The design of a variable hardness is developed for preventing deformations in the line facilities built on sections with different stability. The results of geotechnical modeling are presented with the example of Zabaykalsky highway section. This highway is constructed in the harsh environments and complex engineering-geological conditions on seasonal freezing soils. The sections with different stability and a culvert are located there. The design includes installation of geosynthetic material layers. The amount and location of the geogrid layers depends on the base stiffness. The structural behavior modeling with the geotechnical software complex « FEM models » gives a design assessment. Some constructional measures are taken as a result of the modeling to provide an exploitation reliability of the highway engineering solutions.

Keywords: Deformations · Geotechnical modeling · Geosynthetic material

1 Introduction

The building of constructions in northern regions of the Far East is always connected with a high degree of seasonal freezing risk. This especially refers to a line transport structures which require a high level of reliability and responsibility as seen in studies [1, 2].

As researches show [3–6] one of the rational solutions for the main issues which is connected with a construction of facilities in the areas with complex geological and climatic conditions is reasonable usage of modern geosynthetic material properties.

Such materials are capable of providing long-term stable operation of facilities made of local building materials. This can be seen in the works [7–9]. So, the properties of such geosynthetics materials must fully comply with the demands of conditions of their work in the structures and provide a long lifespan as well as high quality as discussed in the study [10].

The projected section of the road is located within starting complex. It is part of the regional Krasnokamensk-Maciejewski road. The road is of regional significance in the Krasnokamensk area and Trans-Baikal Territory. The existing Krasnokamensk - Maciejowski road is built in sections at different times.

Almost all the area under construction lies outside the existing road. The problem of a sufficiently short section which located from picket 137+00 to picket 138+00 is the combination of different stiffness. The section of the starting complex has a culvert. It is a three-pointer pipe made of the corrugated metal. It has a diameter of two meters. This pipe located on picket 137+50 m at the end of section which has a weak base. The strengthening design is located entirely on the weak base and joins the culvert at the picket 137+00.

Having reviewed the works [11, 12] additional structural element has been developed to ensure a smooth transition from one construction to another. It has variable stiffness on the entire length of a weak base. The element of variable stiffness is arranged at the top of the embankment across the all width of a passage connecting the junction area of constructions with different stiffness.

This element provides a variable stiffness in the longitudinal direction as it is made of integral biaxial geogrid meshes. The biaxial geogrid E'GRID 4040L is placed at the different levels with crushed stone of 40–70 mm fraction.

A superimposition of the design axis and the culvert axis is necessary for the most efficient operation of the variable hardness design. All the major elements of the variable stiffness design are shown in Figs. 1, 2, 3 and 4.

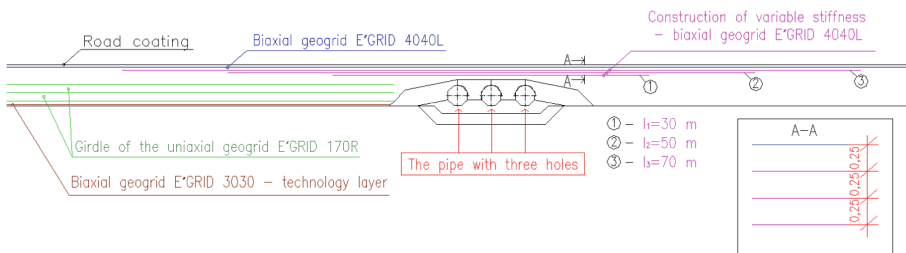


Fig. 1. Longitudinal section of embankment with element of variable stiffness; axis on picket 137+50.

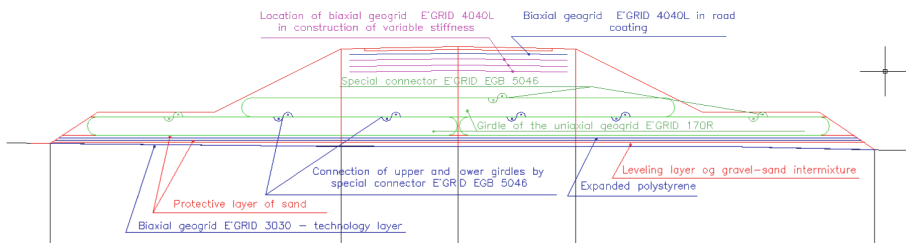


Fig. 2. Variable stiffness design outside pipe zone strengthened with geotechnical gird.

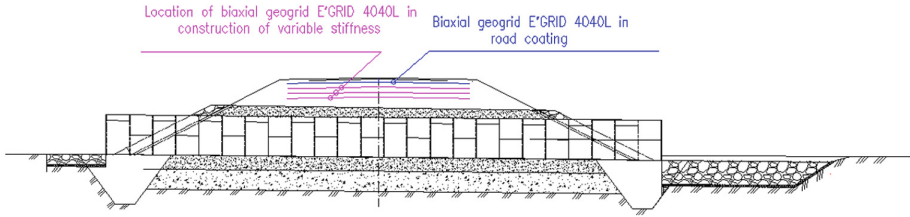


Fig. 3. Variable stiffness design in pipe area.

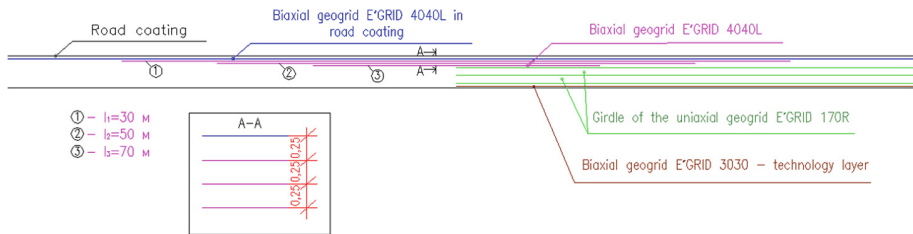


Fig. 4. Longitudinal section of embankment with element of variable stiffness; axis on picket 136+82.

2 Methods of Numerical Modeling

As discussed in the works [13–15], it is necessary to perform a calculation. The design geotechnical modeling was performed using software package «FEM models», which was developed by geotechnical engineers from Saint-Petersburg.

The elastic-plastic model with the yield criterion was used to describe the work of variable stiffness design. This elastic-plastic model was chosen because its parameters can be taken from existing material of engineering and geological surveys.

Numerical methods are in good correspondence with the traditional engineering methods of calculating the settlement in such formulation. They provide accurate description of deformations in structures. Figure 5 shows a scheme of determining the theoretical stresses in the elastic-plastic model of the soil.

The ultimate stresses in the tension field are restricted by the tensile strength σ_p .

Area I in the tension field is restricted by the stress $\sigma_3 = \sigma_p$, while in the compression area it is restricted by the Coulomb strength criterion according to:

$$\sigma_1 = R_c + \sigma_3 \text{ctg}\psi \tag{1}$$

where R_c is the uniaxial compression strength.

The element stiffness matrixes and the ones for the whole system are formed once and stay the same in the procedure of elastic-plastic solution. The load is applied in small portions as it happens in its real sequence in nature.

If the point M occurs within the limits of the elastic region I, it means the element is in the elastic state and there is no need to correct the stresses.

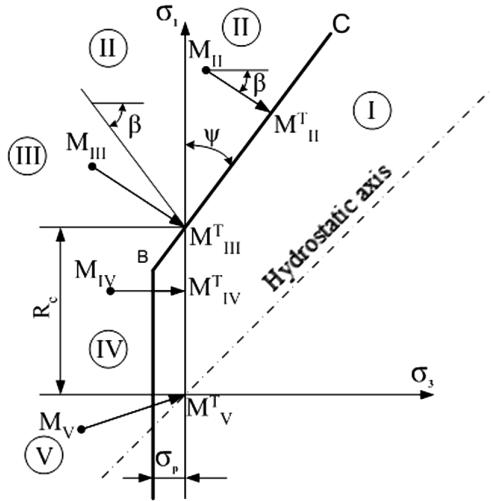


Fig. 5. Scheme of determining theoretical stresses in elastic-plastic model of soil.

If the point M occurs beyond the yield behavior contour, the theoretical stresses are calculated in the following order. If the point of total stress occurs in the area II (the basic plastic zone), the theoretical point lies at the intersection of the plastic yield and the right line.

If the point of total strength occurs in area III, the element breaks in the direction of the stress, while the stresses go down to the level of the soil strength to the uniaxial compression.

For the area IV where the stresses do not go beyond the uniaxial compression strength, the parameters are the following. Finally, for the area V where the element is broken, the parameters are the following:

In the FEM Models program the natural stress state is substituted by the hydro engineering tensor for pressing the soil of the “characteristic volume” that is summarized with the actual stresses in situ:

$$\{\sigma_{1,3}\} = \{\sigma_{1,3}^F\} + \{\sigma_{1,3}^G\} \tag{2}$$

The assumption reflects a real picture of the natural stress state in weak soils.

The used method and the software package «FEM models» are developed by the authors for the projects under construction in Russia and the Far East.

Application of the methods and approaches for the calculation and design of geotechnical structures using software package «FEM models» show its accurate and objective performance in the most rational calculations of geotechnical constructions. This can be seen from the works [16–19].

3 Results of Numerical Simulation

On the basis of numerical modeling the close to real picture of the vertical deformation for the variable stiffness design is obtained.

The numerical models of the design of variable stiffness with the axis on the picket 137+50 on the Krasnokamensk - Maciejewski road section are shown in Figs. 6, 7 and 8.

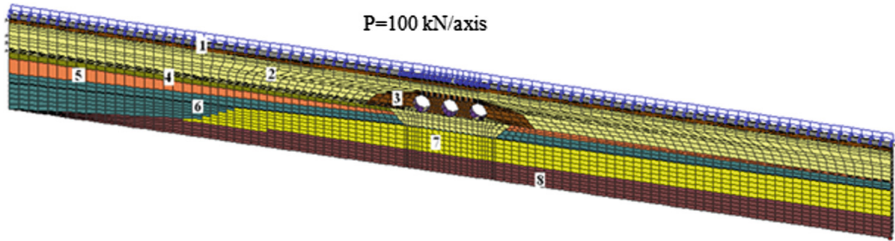


Fig. 6. Numerical model of soil structure: 1 – pavement; 2 – crushed stone and sandy loam; 3 – grassy ground; 4 – silt loam; 5 – loam heavy silty; 6 – loam heavy silty; 7 – loam heavy, silty, solid; 8 – sand gravel, water-saturated.

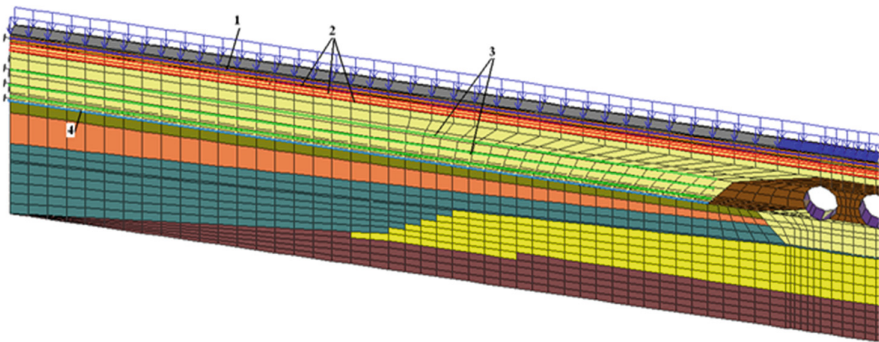


Fig. 7. Scheme of strengthening construction with variable stiffness design: 1 – biaxial geogrid E'GRID 4040L in pavement; 2 – biaxial geogrid E'GRID 4040L in variable stiffness design; 3 – meshes of uniaxial geogrid E'GRID 170R; 4 – biaxial geogrid E'GRID 3030 (technological layer).

The numerical models of the design of variable stiffness with the axis on the picket 136+82 on the Krasnokamensk - Maciejewski road section are shown in Figs. 9, 10 and 11.

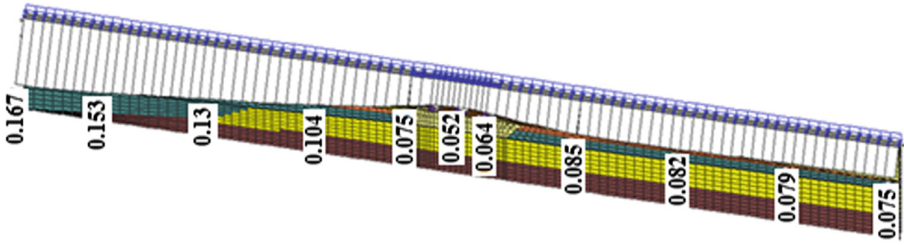


Fig. 8. Curve of vertical deformation on construction surface of with variable stiffness design, m.

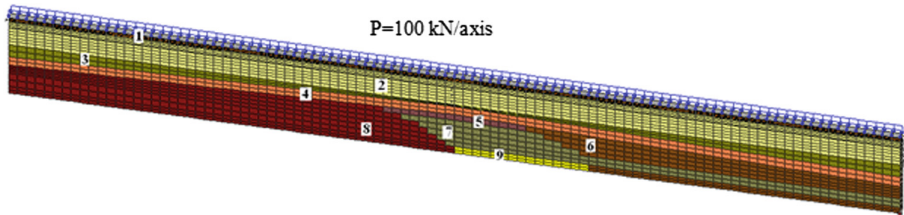


Fig. 9. Numerical model of soil structure: 1 – pavement; 2 – crushed stone with a sandy loam placeholder; 3 – silt loam; 4 – loam heavy silty; 5 – loam heavy silty; 6 – loam silty, light, frozen; 7 – loam silty, light, frozen; 8 – grussy soil with loamy filler, frozen; 9 – clay with gravel up to 15%, frozen.

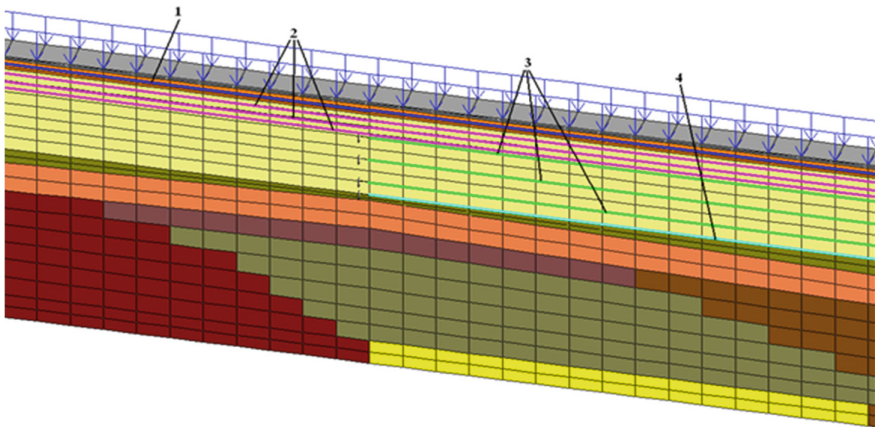


Fig. 10. Scheme of strengthening construction with variable stiffness design: 1 – biaxial geogrid E'GRID 4040L in pavement; 2 – biaxial geogrid E'GRID 4040L in variable stiffness design; 3 – meshes the uniaxial geogrid E'GRID 170R; 4 – biaxial geogrid E'GRID 3030 (technological layer).

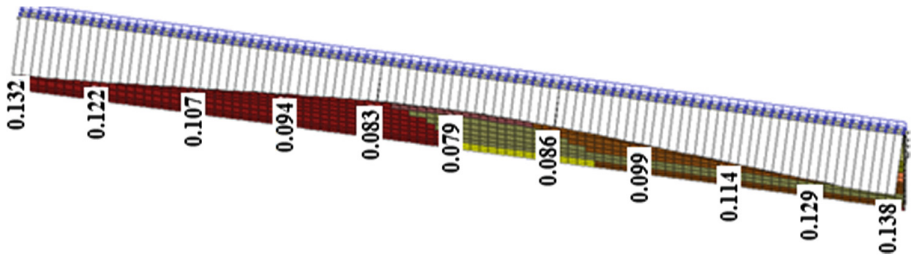


Fig. 11. Curve of vertical deformation on construction surface with variable stiffness design, m

4 Conclusions

1. The results of the numerical simulation of structures with element of variable hardness showed a smooth change in hardness at the surface facilities
2. This element avoids sharp deformations of road
3. Smooth change of hardness provides normative technical condition of road during using it in places of sharp changing in stiffness of adjacent structures
4. High strength of construction with elements of geosynthetic materials ensures the integrity of the road as well as the safe use of this section of the road
5. All this technical solutions have theoretical and laboratory proofs, as well as extensive experience of the practical application for strengthening roadbed and for a weak base with the use of modern high-tech geosynthetics materials.



References

1. Berestyanyy, Y., Valtseva, T., Kudryavtcev, S., Fedorenko, E.: Using geomaterials when reconstructing Yakutsk-Magadan road. *Roads. Innov. Constr.* (29), 96–100 (2013)
2. Berestyanyy, Y., Valtseva, T., Kudryavtcev, S., Mikhailin, R.: Using geotechnical materials in structures when constructing roads in snow region of Russia. In: II International Symposium “Physics, chemistry and snow mechanics”, Yuzhno-Sakhalinsk, pp. 96–100 (2013)
3. Berestyanyy, Y., Goncharova, E., Kudryavtcev, S., Mikhailin, R., Valtseva, T.: Motorway structures reinforced with geosynthetic materials in polar regions of Russia. In: The 24rd International Off-shore (Ocean) and Polar Engineering Conference, Korea, pp. 502–506 (2014)
4. Valtseva, T., Goncharova, E., Kudryavtcev, S., Mikhailin, R.: Using designs of variable rigidity on weak soils roads in the Russian far east. In: The 6th International Geotechnical Symposium on Disasters Mitigation in Special Geoenvironmental Conditions, Indian Institute of Technology, Madras, pp. 409–412. India (2015)
5. Berestyanyy, Y., Valtseva, T., Kudryavtcev, S.: Geomaterial impact on bearing capability of the embankment. In: Proceedings of the 44th All-National Scientific Conference “Modern Technologies to Railway Transport and Industry”. Khabarovsk, no. 1, pp. 24–27 (2006)

6. Berestyanyy, Y., Kudryavtcev, S., Valtseva, T., Barsukova, N.: Practice of use of positive properties of geosynthetic materials on building objects in severe climatic conditions of the far east of Russia. In: *The 1st International Conference On New Developments in Geoenvironmental and Geotechnical Engineering*, pp. 423–427. University of Incheon, Korea (2006)
7. Berestyanyy, Y., Kudryavtcev, S., Valtseva, T., Chylichkov, V., Tsvigunov, D.: Rational designs of the railway road-bed of thawing permafrost soils in condition of the Far East. In: *8th International Symposium on Cold Region Development. ISCORD 2007*, Tampere, Finland, pp. 37–38 (2007)
8. Berestyanyy, Y., Kudryavtcev, S., Valtseva, T.: Laboratory researches behavior geogrid reinforced embankment body. In: *Geotechnical Engineering, Ground Improvement and Geosynthetics for Human Security and Environmental Preservation*, Thailand, pp. 493–500 (2007)
9. Berestyanyy, Y., Kudryavtcev, S., Valtseva, T., Mikhailin, R.: The survey results of strengthening embankment and the ballast layer for heavy train. In: *The 4th International Scientific Conference on Modern Problems of Projecting, Construction and Railway Road Exploitation*, Moscow, Readings devoted to Shakhunyants, G.M., pp. 116–121 (2007)
10. Berestyanyy, Y., Kudryavtcev, S., Valtseva, T.: Research of railway embankment design on thaw permafrost. In: *International Conference on Cryogenic Resources in Polar and Mountain Regions. Conditions and perspectives of permafrost engineering*, Tyumen, pp. 113–116 (2008)
11. Berestyanyy, Y., Kudryavtcev, S., Fedorenko, E., Valtseva, T., Mikhailin, R.: Development of geotechnical solutions for deformation stabilization on the “Amur” (Chita-Khabarovsk) automobile road. In: *Proceedings of the Russian National and International Conference on Scientific and Technical Cooperation of APR-Countries in XXI Century*, no. 2, pp. 24–27 (2009)
12. Berestyanyy, Y., Kudryavtcev, S., Fedorenko, E., Valtseva, T., Mikhailin, R.: Research and development of rational structure of pavement using integral geogrid for section of Chita – Khabarovsk highway. In: *3rd International Geotechnical Symposium on Geotechnical Engineering for Disaster Prevention and Reduction*, Harbin Institute of Technology, Harbin, China, pp. 18–25 (2009)
13. Berestyanyy, Y., Goncharova, E., Kudryavtcev, S., Mikhailin, R., Valtseva, T.: Geosynthetic materials in designs of highways in cold regions of Far East. In: *14th Conference on Cold Regions Engineering*, Duluth, Minnesota, USA, pp. 45–48 (2009)
14. Berestyanyy, Y., Kudryavtcev, S., Fedorenko, E., Valtseva, T., Goncharova, E., Mikhailin, R.: Rational designs of motorways with use of integrated geosynthetic materials for northern territories of Russian far east. In: *Materials of the IX International Symposium on Cold Regions Development*, Yakutsk, p. 120 (2010)
15. Berestyanyy, Y., Kudryavtcev, S., Fedorenko, E., Valtseva, T., Mikhailin, R.: The survey results of strengthening embankment designs using modern methods of numerical modeling of effective geosynthetic materials. In: *Proceedings of the Second Regional Scientific Conference on Problems of Railroad And Motorway Embankment in Siberia*, Novosibirsk, pp. 37–47 (2011)
16. Berestyanyy, Y., Valtseva, T., Mikhailin, R.: Geotechnical cartridges for embankment strengthening. *Track and its facilities* (6), 34–35 (2011)
17. Berestyanyy, Y., Kudryavtcev, S., Fedorenko, E., Valtseva, T., Goncharova, E., Mikhailin, R.: Use of geosynthetic materials on weak besses in highways of the far east Russia. In: *International Symposium on Geosynthetics Technology*, Seoul, South Korea, pp. 117–125 (2011)

18. Berestyanyy, Y., Kudryavtcev, S., Valtseva, T., Goncharova, E., Mikhailin, R.: Motorway structures reinforced with geosynthetic materials in polar regions of Russia. In: The 24rd International Offshore (Ocean) and Polar Engineering Conference, Bussan, Korea, pp. 502–506 (2014)
19. Kudryavtcev, S., Kazharsky, A., Goncharova, E., Valtseva, T., Kotenko, Z.: Thermophysical feasibility of railway embankment design on permafrost when projecting side tracks. In: 15th International Scientific Conference “Under-ground Urbanisation as a Prerequisite for Sustainable Development”, St. Petersburg, Russia. *Procedia Engineering*, no. 165, pp. 1080–1086 (2016)

The False Tripping of Relay Protection in Parallel Lines: Finding Cause and Solution Methods

Pavel Pinchukov^(✉)  and Svetlana Makasheva 

Far Eastern State Transport University,
Seryshev Street, 47, Khabarovsk 680021, Russia
dee@festu.khv.ru

Abstract. This paper deals with electromagnetic processes occurring in case of LG fault for parallel lines of different voltage levels (from 6 to 35 kV) and their relay protection operation. The most probable cause of false tripping of relay protection devices in parallel less nominal voltage line in case of LG fault in a higher nominal voltage line is considered. Created and patented device for allowing eliminating the false tripping of relay protection is described. The paper contains detailed vector diagrams that may be useful not only for engineers and researchers in the field of relay protection, but for everyone who are interested in evaluating the interference level or in selecting and applying any devices protection measures.

Keywords: Single line to ground (LG) fault · Isolated neutral
Relay protection · Electromagnetic compatibility

1 Introduction

Medium voltage (in Russia - starting from 6 and reaching up to 35 kV) power distribution networks are used for distribution in urban and rural areas. Also, these electric networks are commonly used for providing train movement system in Russia and other countries [1–3, 19]. They are characterized by significant degree of line's branching and sophisticated configuration [3].

Often in the construction of these lines there is a shortage of territory occupied by them, which leads to the necessity of placing parallel lines of different voltage level on common transmission poles. This close arrangement requires more attention to the electromagnetic compatibility of these lines and their equipment. In fact, the results of the electromagnetic influence are manifested as induced currents and voltages in environmental space and on adjacent objects that may pose a serious threat to maintenance staff and equipment, including relaying system [4, 5].

Furthermore, lines 6–35 kV are still used isolated neutral type, which is characterized by the possibility of the single line to ground fault [1–3, 6–8]. This type of circuits constitutes the majority of all circuits in power networks. Commonly known, that about 75–80% of all circuiting in transmission and distribution lines accounted for LG faults [7–12].

Statistical analysis of power outages in parallel lines located at one pole shows that in case of LG fault in a higher voltage line taking place a non-correct operation of relay protection devices in parallel lower voltage line [11]. As a result, the relay protection device disables smaller voltage line despite the fact that it is not required. This phenomena is known as a false tripping, incorrect or superfluous operation of relay protection devices [9–11, 13].

2 Materials and Methods

In this study, we used empirical and theoretical research methods, based on analysis of statistics of relay protection superfluous operation and failures that occurred in medium voltage power distribution networks at Far Eastern region of Russia during last 5 years [12].

2.1 Methods and Main Points of Research

Applied to the case of LG fault in parallel different nominal voltage lines, we want to find answers to the following questions:

1. Which phenomena are occurring in the lines and how the line relaying devices react on them?
2. Can the electromagnetic interference from one line to be the cause of superfluous operation of relay protection devices in another one?
3. How we can to eliminate the false tripping of relay protection in case of single line to ground fault in parallel lines?

Sequential decision assigned tasks will help clearly understand the causes of the phenomena and will give an idea about the methods of solving the problem.

2.2 Vector Analysis of the Processes Occurring in Parallel Lines During LG Fault in One of Them

If a network has isolated neutral, it means that this network is not tied to ground using a galvanic connection. The emergence of LG fault can be stable (dead short-circuit), or through intermittent earth arc. Isolated neutral has capacitors, formed by wire itself and ground. Capacitance of such a capacitor is small, however lines are long also and can sum quite high capacitance values.

For the following analysis of the relay protection behavior on parallel lines, the different use cases have to be distinguished. Therefore, the different operating states of parallel lines have to be considered. Next, we analyzed 3 cases of LG fault in one of two parallel lines given that:

1. nominal voltages of both lines are equal;
2. nominal voltages of lines are different and LG fault occurs in a less voltage line;
3. nominal voltage of lines are different and LG fault occurs in higher voltage line.

The different operating states of the parallel lines are also relevant for the behavior of the protection devices, whereby the only one of following states have to be considered, namely, both parallel lines are in operation.

2.2.1 Nominal Voltages of Both Lines are Equal and the LG Fault Occurs in One of Them

A Fig. 1 gives the scheme of power distribution system including two parallel lines of the same voltage. For example, LINE 1 and LINE 2 at Fig. 1 have a voltage of 10 kV.

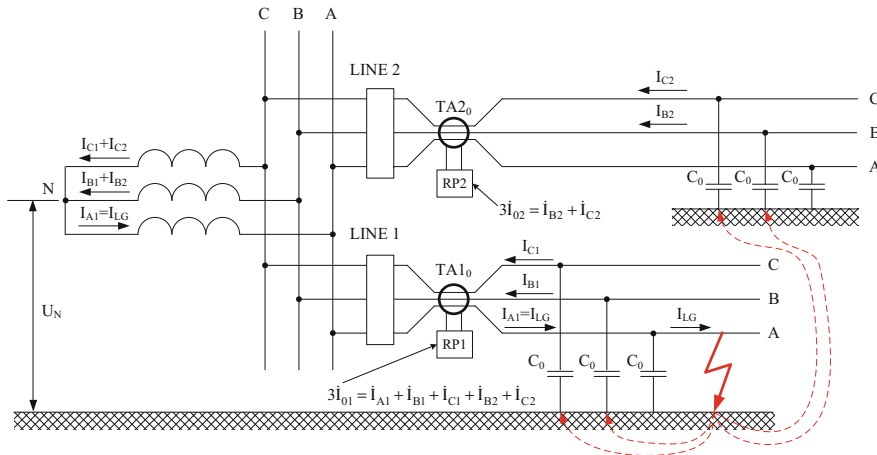


Fig. 1. The single phase to ground fault in isolated three-phase system where ILG is discharge current due to capacitance of healthy phases.

When the LG fault occurs in ungrounded (isolated) three-phase LINE 1 in phase A, the phase voltage of the faulty phase UA is reduced to the ground potential as the capacitance of the faulty line is discharged at the fault location. A charging current IC occurs between these phase-to-ground capacitances, which will continue to flow via the fault path while it remains.

As we can see at Fig. 1, when the LG fault occurs in LINE 1, the phase-to-ground voltage each of the other two healthy phases UB (or UC) rises by times. In each of two healthy phases at LINE 1 their capacities relative to ground (C0) increase the faulty phase current ILG. At once, in LINE 1 the zero sequence current and the zero sequence voltage are formed, as shown at Fig. 2(a).

Importantly that the zero sequence current vector lagging behind the zero sequence voltage vector due to the capacitive nature of zero sequence current, as shown on Fig. 2 (a). The angle between zero sequence current vector and zero sequence voltage vector is 90°. Relay protection in LINE 1 is triggered when that all four conditions are present, namely:

- the zero sequence voltage;
- the zero sequence current;

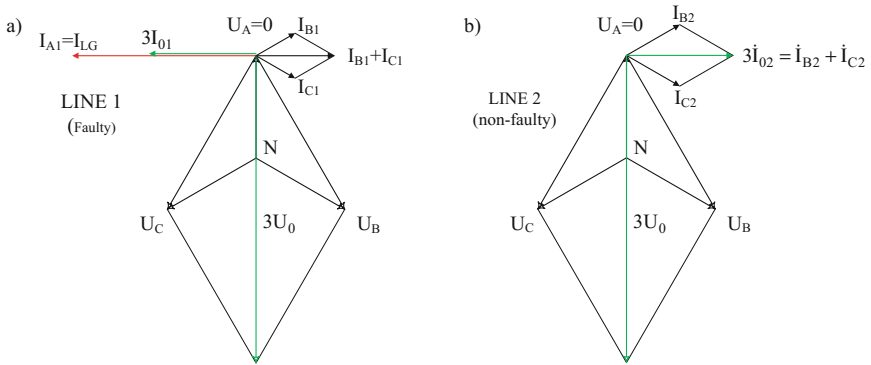


Fig. 2. The phasor diagram during LG fault in LINE 1; (b) the phasor diagram during LG fault in LINE 1 for non-faulty LINE 2.

- the angle between them is 90° ;
- the zero sequence current vector lagging behind the “zero sequence” voltage vector.

This correct operation of relay protection switch off the faulty LINE 1 and LG fault is liquidated. For relay protection of parallel LINE 2 there are no the above triggering condition number four, as we can see at Fig. 2(b). Therefore the non-faulty LINE 2 keeps working. The superfluous operation of relay protection devices is absent in LINE 2.

2.2.2 Nominal Voltages of Both Lines are Equal and the LG Fault Occurs in One of Them

A Fig. 3 gives the scheme of power distribution system including two parallel lines of different nominal voltage. For example, voltage of LINE 1 is 10 kV and voltage of LINE 2 is 35 kV.

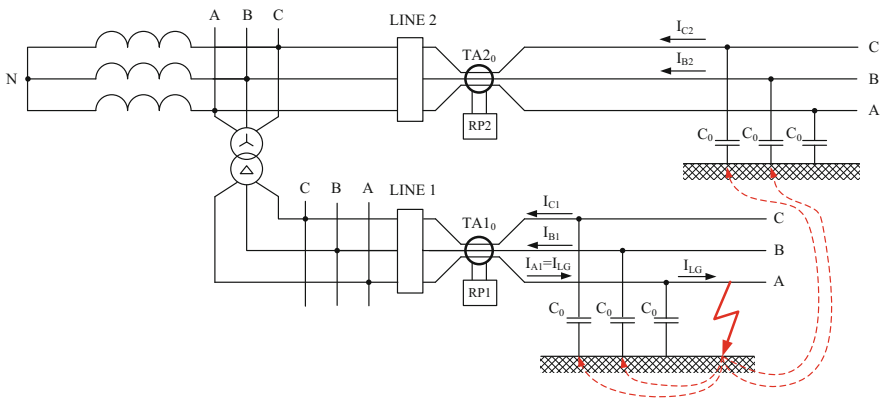


Fig. 3. The LG fault is occurs in one of two parallel lines, which has a less voltage.

When single-phase to ground fault occurs in phase A of LINE 1, physical processes occurring in LINE 1 are the same as described above for the case of lines with the same nominal voltages. Correct operation of relay protection switch off the faulty LINE 1 and LG fault is liquidated.

At the same time in the intact LINE 2, which has higher nominal voltage, the zero sequence voltage of LINE 1 creates an electric field in surrounding space. The electric field induces in LINE 2 a voltage, which is significantly less than the phase voltages of LINE 2, which does not violate their symmetry. Phase voltage system of LINE 2 is still symmetrical, so the zero-sequence voltage of LINE 2 is not created. Because in LINE 2 for its relay protection the condition number 1 of the four above conditions is absent, that relay protection is not triggered and the non-faulty LINE 2 keeps working. The superfluous operation of relay protection devices is absent in LINE 2.

2.2.3 Nominal Voltages of Lines are Different and LG Fault Occurs in Higher Voltage Line

A Fig. 4 shows the power distribution system including two parallel lines of different voltage levels: LINE 1 is 10 kV and LINE 2 is 35 kV. LG fault occurs in phase A of LINE 2.

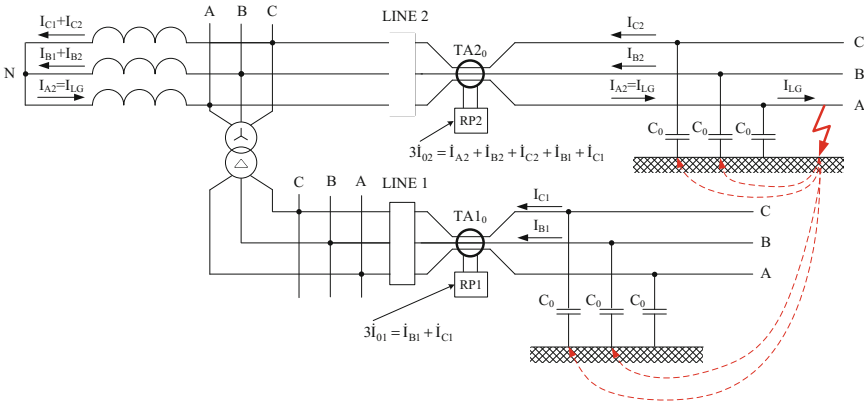


Fig. 4. The LG fault is occurs in one of two parallel lines, which has a higher nominal voltage.

When single-phase ground fault occurs in phase A of LINE 2, physical processes occurring in LINE 2 are the same as described above for the case of lines with the same nominal voltages as we can see at Fig. 5(b). Correct operation of relay protection switch off the faulty LINE 2 and LG fault in it is liquidated.

At the same time in the non-faulty LINE 1, which has a less nominal voltage ($10 < 35$ kV), the zero sequence voltage of LINE 2 creates an electric field in surrounding space. The electric field induces in LINE 1 a voltage, which is significantly more than the phase nominal voltages of LINE 1, as shown at Fig. 5(a). The symmetry

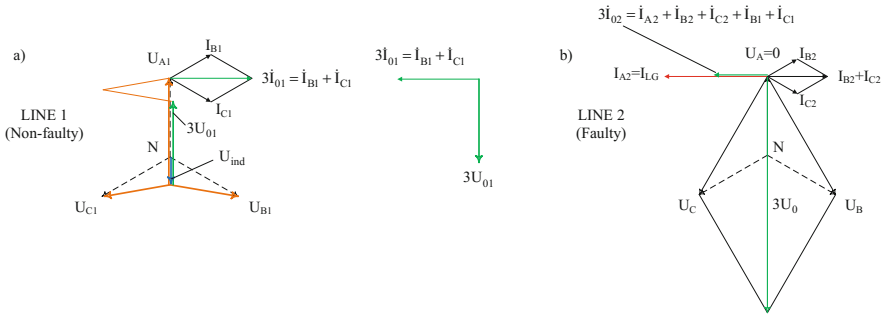


Fig. 5. The phasor diagram during LG fault in LINE 2 for non-faulty LINE 1; (b) the phasor diagram during LG fault in LINE 2.

of the LINE 1 phase voltage is broken and the zero sequence voltage is formed in this non-faulty line. Condition number one of four above conditions is present.

The zero sequence current in the non-faulty LINE 1 is formed by longitudinal phase capacitance and flows in the direction from the end of LINE 1 through the busbar of substation going to the point of LG fault. Condition number two of four above conditions is also present. Because the zero sequence current in non-faulty LINE 1 has a capacitive nature, it lags behind the zero sequence voltage of LINE 1 by 90°. That means that the third and the fourth conditions are also present. Relay protection of LINE 1 switch off the non-faulty line. The superfluous operation of relay protection devices is present in LINE 1.

3 Results

Vector analysis results indicate that the superfluous operation of relay protection devices are present only in case when the nominal voltages of lines are different and LG fault occurs in higher nominal voltage line. Despite the apparent similarity of electromagnetic processes occurring during the LG fault in parallel lines, we found one significant difference. It is a significant electromagnetic influence from the higher nominal voltage line to less nominal voltage line during the LG fault, as shown at Fig. 5(a).

The induced voltage from faulty line of higher nominal voltage causes the breaking symmetry of phase voltages system in healthy (non-faulty) less nominal voltage line. This effect gives rise to the zero sequence voltage in the non-faulty line, as the result all four conditions for relay protect operations are presented. It is the main cause of false tripping of non-faulty line relay protection devices.

This phenomenon is not observed in the case of fault lines of less or equal nominal voltage, as we can see at Figs. 1–3, because the induction voltage from faulty line has a much less value than the nominal voltage of these line and cannot break the symmetry of the phase voltages system in non-faulty line.

Thus, the breaking of the phase voltages symmetry in the non-faulty less nominal voltage lines, as a result of electromagnetic influence of the faulty higher nominal

voltage line, leads to the appearance of the zero sequence voltage in the non-faulty line. Next, the specified sequence of events leads to incorrect or superfluous operation of relay protection devices in case of LG faults.

4 Discussion

Now that we have identified and clarified the distinguishing feature of incorrect operation of relay protection devices in case of LG faults, we can solve the problem by several ways. In the first, we can take any measures to eliminate the electromagnetic interference per se, or, in the second, we can take any measures, regardless of presence of electromagnetic interference. Now, the first way, namely, the task of reducing the electromagnetic interference in distribution and transmission power networks has been well studied. For example, three main ways to prevent the electromagnetic interference are suggested as shown in [20]:

1. Suppress the emission at its source (in other words, suppress the emission of the zero sequence voltage in higher nominal voltage line when the LG fault in it occurs);
2. Make the coupling path as inefficient as possible (in our case, to destroy an electric field in surrounding space);
3. Make the receptor less susceptible to the emission (to protect line of less nominal voltage by, for example, placing the line in a metal enclosure (a shield) will serve to reduce the efficiency of the coupling path).

The complex task reducing the electromagnetic interference should be solved with a view to minimizing costs, but it is very difficult for operating lines. The authors do not rule out the possibility of the search for an effective way to ensure the electromagnetic compatibility of parallel lines in the future, but in the present we have used another way. The second way for eliminating the relay protection devices incorrect operation in case of LG faults comprises a usage of device, which can detect the above-described characteristics of LG fault mode [21].

The device for protection lines with isolated neutral [21] allows timely to switch off the damaged line of higher nominal voltage in case of LG fault in it, and also does not allows switch off the intact parallel line of less This prevents interruption of electricity supply lines of less nominal voltage. In addition, besides saving money, it increases the reliability of the consumers, which is particularly important for transport power network system.

5 Conclusions

Obtained results leads to the following conclusions:



- the most probably cause of superfluous operation of relay protection devices in case of LG fault in parallel different nominal voltage lines is found;

- different ways to resolve the problem of superfluous operation of relay protection devices in case of LG fault in parallel different nominal voltage lines are considered;
- created and patented by authors device for protection lines with isolated neutral is proposed.

References

1. The Innovative Digest of JSC “Russian Railways”
2. Ter-Oganov, E., Pyshkin, A.: Railway Electrification System, Ekaterinburg, Russia (2014)
3. Transmission and Distribution Lines. IMIA WGP 069 (10). IMIA Conference, Berlin (2010)
4. Chitashvili, Y., Makasheva, S.: Study of Electromagnetic Compatibility of Electric Networks. Scientific, Technical and Economic Cooperation Between Asia and Pacific Countries in the XXI Century, T. 1, pp. 100–104 (2014)
5. Luo, Y., Chen, R., Zhu, Y., Cheng, J., Wei, W.: Analysis of magnetic field intensity and induced current under live working based on charge simulation method. In: MATEC Web of Conferences, vol. 22, p. 02009 (2015)
6. Kütt, L., Järvik, J.: Analysis on faulty phase grounding in medium-voltage networks with isolated neutral. In: Lahtmets (ed) 8th International Symposium “Topical Problems in the Field of Electrical and Power Engineering. Doctoral School of Energy and Geotechnology”. II: Pärnu, Estonia, 11.01–16.01, Rein, Tallinn, pp. 281–284 (2010)
7. Wang, L.L: The fault causes of overhead lines in distribution network. In: MATEC Web of Conferences, vol. 61, p. 02017 (2016)
8. Power Outage Annual Report. Blackout Tracker United States Annual Report (2015)
9. Gelfand, Y.: Relay Protection of Electric Networks, 2nd edn., Moscow, Soviet Union, (1987)
10. Shalin, A., Trofimov, A.: Efficiency of relay protection of power system. In: 2007 International Forum on Strategic Technology, IFOST, Ulaanbaatar, pp. 371–375 (2007)
11. Capenko, E.: Grounded fault in networks 6–35 kV, Moscow, Soviet Union, (1986)
12. Pinchukov, P., Makasheva, S.: The issue of malfunction of parallel line relay protection. Transp. Asia Pac. Reg. **4**(9), 18–21 (2016)
13. Rules for Electrical Installation Design (Russian Electrical Code), Part 3.2. Relay Protection, 7th edn., Moscow, Russia (2003)
14. Gurevich, V.: Power Supply Devices and Systems of Relay Protection, vol. 264. CRC Press (Taylor & Francis Group), Boca Raton (2013)
15. Nam, S., Kang, S.H., Ahn, S.J., Choi, J.H.: Single line-to-ground fault location based on unsynchronized phasors in automated ungrounded distribution systems. Electr. Power Syst. Res. **86**, 151–157 (2012)
16. Zoran, N., Stojanović, N., Milenko, B., Djurić, B.: An algorithm for directional earth-fault relay with no voltage inputs. Electr. Power Syst. Res. **96**, 144–149 (2013)
17. Sahu, S., Sharma, A.: Detection of fault location in transmission lines using wavelet transform. J. Eng. Res. Appl. **3**(5), 149–151 (2013)
18. El-Zonkoly, A.: Fault diagnosis in distribution networks with distributed generation. Smart Grid Renew. Energy **2**, 1–11 (2011)
19. Pritchard, C., Hensler, T.: Test and analysis of protection behaviour on parallel lines with mutual coupling. In: 2014 APS, pp. 1–9 (2014)
20. Paul, C.: Introduction to Electromagnetic Compatibility. 2nd edn. USA, vol. 102 (2006)
21. Pinchukov, P., Makasheva, S.: Device for protection lines with isolated neutral. Utility model patent number RU № 168130 (2016)

Improving Methods for Reliability Assessment of Electric Power Systems

Pavel Pinchukov^(✉)  and Svetlana Makasheva 

Far Eastern State Transport University,
Seryshev Street, 47, Khabarovsk 680021, Russia
dee@festu.khv.ru

Abstract. This paper deals with the basic methods for calculating reliability of electric power systems. The alternative method for determining the probability of system's failure is offered. The principle is based on a new "compact" recording of possible routes which provide the electric power system operability. For calculating reliability parameters of the system the method of exceptions and the method of decomposition are used.

Keywords: Reliability · Electric power system · Route
Method of decomposition

1 Introduction

Reliability is one of the major requirements for any type of system, especially for such a complicated system as the electric power system. Commonly known, that electric power systems are very complex and highly integrated. It consists of a large number of elements and has an extensive internal and external communications [1–3].

Reliability generally describes the continuity of electric service to customers, which depends both on the availability of sufficient generation resources to meet demand and on the ability of the transmission and distribution system to deliver the power. The reliability of the electric power system is determined by how it is operated in the face of the reliability-threatening events to which it is subjected. Some of these factors can be managed, at least to a degree, by planning and preparing for routine events that the electric power system is expected to withstand. Others events are less manageable, including infrequent, yet catastrophic storms, which stress the electric power system beyond expectations [4–6].

Historically, though, the analysis of reliability has emphasized the generation aspect, especially at the system level. In part, this is because transmission systems have been designed with sufficient excess capacity to merit the assumption that generated power could always be delivered, anywhere. However, as transmission systems are being more fully utilized due to a combination of economic pressures, demand growth, interconnections between territories, and difficulties in siting new lines, transmission is playing an increasingly important role in system reliability. Now the integrity of the electric power supply system is specifically analyzed in terms of security [2–4, 6, 7]. Failure in any part of the electric power system can cause interruptions of supply to end

users. Electric power system reliability is increasingly a concern to the power industry and society at large [2–10].

Reliability of electric power system is a property to perform the predetermined function in a given volume under certain operating conditions [10]. At the present time there are a large number of adequate economic and mathematical models of electric power system reliability, electric grids and transmission reliability models, and model of system failures, which were suggested by lot of authors during last decade [5, 8, 9, 11]. Using these models we can analytically determinate the main power engineering and economic indicators which characterizing the reliability of power system operation.

2 Materials and Methods of Electric Power System Reliability Calculation

For increase of accuracy of calculation we need to take into account a large number of the initial information to such as the configuration of electric network, placement of generating capacities and electrical loads, electrical operating modes, and steady state stability of electric network operation, as well as configurations of daily and annual load curves of consumers.

We analyzed the advantages and disadvantages considered above models and as a result, we found that despite the significant advantages, we can mark some them disadvantages such as: (1) a large number of elements (2) their schemes drawing bulkiness (3) increased demands on computer resources.

In order to minimize time and simplify the calculations, as well as to minimize errors associated with the need to input a large amount of background information, perspective is the search for new compact methods of reliability assessment for electric power system, which can to allow to determine the system probability in a simpler form.

2.1 Fundamental Provisions

Power system reliability means the probability that an electric power system can perform a required function under given conditions for a given time interval [10]. Reliability analysis of power systems traditionally attempts to answer three fundamental questions (in analogy to risk analysis [12]):

1. What can go wrong?
2. How likely is it to happen?
3. What are the consequences?

Answering fundamental questions outlined above, we expect specific numerical parameters, called reliability indicators. A reliability indicator is an observable or computable quantity that provides insight into the level of reliability of a system in a particular context. It can be used, ex-ante, to formulate a reliability criterion used for reliability management or alternatively to assess, ex-post, the reliability level of a system [9, 10, 12].

In terms of maintainability of electric power system all its elements can be divided on the repairable item and the non-repairable item [10, 13]. The item (or entity, system, etc.), which under these conditions after a failure may be returned to the state in which it can execute the desired function is called the repairable item. “These conditions” may include climatic, technical or economic circumstances. Important, that the item, which is repairable under the conditions of the same data may be a non-repairable other conditions.

Conversely, an item, which under these conditions after a failure may be returned to the state in which it can execute the desired function is called the non-repairable item. And also, in analogy to the repairable item, the item, which is the data non-repairable in some circumstances, may be repairable under other conditions [10, 13].

One of the main numerical parameters of non-repairable systems, also of repairable system at a given time interval, is the reliability.

Reliability $R(t_1, t_2)$ is a probability of performing a required function under given conditions in the time interval (t_1, t_2) , which may be written in the general form [10]:

$$R(t) = R\{T \geq t\} \quad (1)$$

The “T” component in Eq. (1) represents a time of system continuous operation before the first failure. This function most fully determines the system reliability and reliability of its separate elements. In practice it can be determined if the statistics (performance) data on failures:

$$R(t) = \frac{N_0 - n(t)}{N_0} \quad (2)$$

The component N_0 in Eq. (2) is the initial number of researched elements and the component $n(t)$ is the number of items that failed during time t .

Reliability assessment of any type of system (including the electric power system) is the calculation of the probability of up state operation of the equivalent circuit. The equivalent circuit of a real system consists of some of its elements (sub-items), and each of them will be stored as the probability of uptime. Therefore, the correctness of the compiled equivalent circuit and the adequacy of its application to calculation methods depend largely on the accuracy of the results.

2.2 Example of the Complicated Equivalent Circuit

When the reliability of a complicated system consisting of a large number of elements is analyzed, as a rule, all the information about the reliability of performance, structure and functional interaction is known. In order to standardize the calculation of the reliability theory, these objects are replaced with the reliability block diagram (equivalent circuit), consisting of n elements (items) that are functionally related to each other.

If the connection between elements in the considered system do not form series-parallel connection, the reliability assessment for such a scheme leads to difficulty in its transformation. An example of such a complex scheme is shown below at Fig. 1.

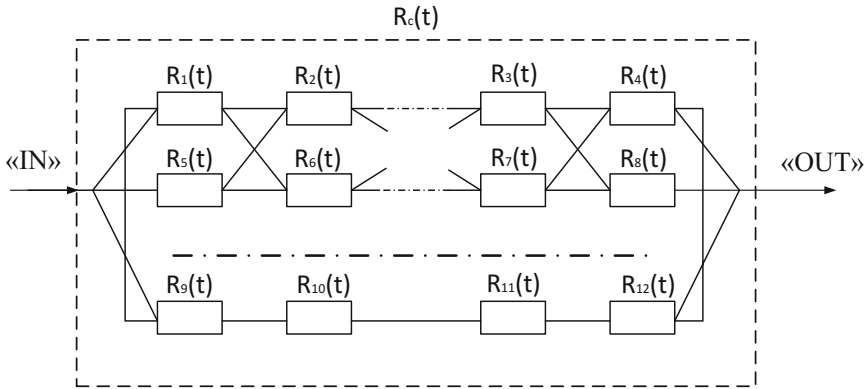


Fig. 1. The structural diagram of the reliability of a complex system.

Systems of this type as shown at Fig. 1 is called the bridging type, i.e. systems comprising elements are connected in wye (T or star) or delta (triangle or mesh). In practice, such scheme connection of electric power system components are widespread as the schemes of switchgear, substation and power plants circuits [13–16].

In most cases, for reliability assessment of uptime for non-renewable systems commonly use method of complete group of events [14] and exceptions item method [15, 16].

2.3 The Method of Complete Group of Events and the Exceptions Item Method

The method of complete group of events is a classic reception sorting variants item states. In other words, at any given moment every item can take only one of two operating states (up state or non-operating state). Therefore, the system has a number of possible states of an equal 2^n , where n means the number of its items. Then, from the obtained set up state system status are selected and next the probability of staying the system in them are determined.

The exceptions item method allows the system consisting of “ n ” items spread out on two systems. Each of these systems the number of elements less than the original system, as shown at Fig. 2.

The peculiarity of this method is that the calculation is carried out in two steps. In the block diagram excluded one or more elements, which form crosslinks. Then two extreme cases are considered:

1. when the selected items completely reliable (they replaced by a permanent bond);
2. when these elements are totally unreliable (between two nodes is a gap).

For two received structural schemes the probability of uptime are determined R_{\max} (in first case) and R_{\min} (in second case).

The resulting reliability of the system R_{res} is determined by the equation [15]:

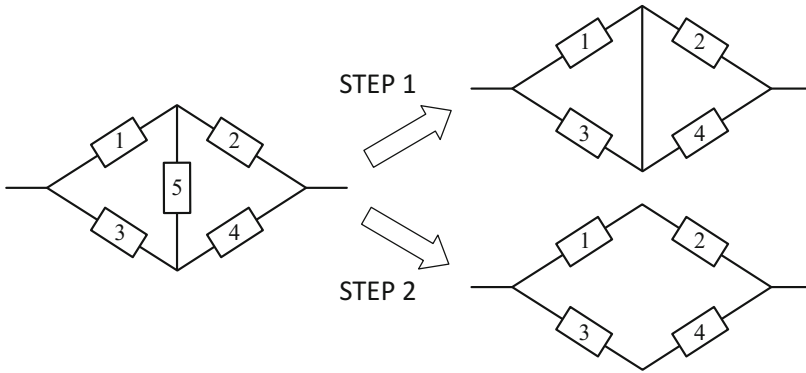


Fig. 2. The exceptions item method and steps of exception cross-link scheme

$$R_{res} = R_{min} + (R_{max} - R_{min}) \cdot R_{ei} \tag{3}$$

The component in Eq. (3) is a reliability of excepted item.

Both of the above methods is not very convenient to use because of a large number of items due to the bulkiness and complexity of circuitry changes step-by-step and scheme cumbersome. To minimize the time and to optimize the calculation procedure may offer methods to determine the probability of failure of the system in a simpler form.

2.4 The Method of Exceptions and the Method of Decomposition

The method of exceptions based on the fact that in the original data is perceived by a table describing all the possible routes (the way in which the consumer can get the power in the circuit diagram). Next to the recorded routes is carried out independent combinations of the system states [13].

Let us show at Fig. 3 this method on the example of the system with a bridge circuit, i.e. system with a complex compound of elements previously shown at Fig. 1.

The Fig. 3 gives the original scheme and its equivalent table of routes. Vertical Roman numerals show the possible routes, horizontally numbers of every item are marked.

The notation for a compact recording are used as:

1. the dot mark means an arbitrary item the state (serviceability or failure) at a given time, the probability of the state is equal to 1;
2. the line mark means the item up state; this i-number item reliability is equal $R_i(t)$

Route defined by one of the plurality of options, i.e. a plurality of such combinations, consisting of zeros and (or) units, in which the availability of the system, and each option corresponds to one state of the system [14].

For scheme at Fig. 3 if they are made common event elements operability for the following variant matches: (1 and 4) or (2 and 5) or (1 and 3 and 5) or (2 and 3 and 4), it means the whole system operability [17].

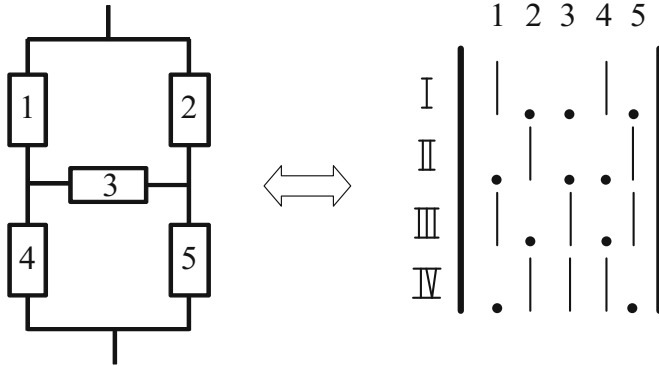


Fig. 3. The original scheme and equivalent table of routes

For the independence of these routes must be written all the combinations, leaving the originals. By the method of exceptions the number of combinations will be as $2^3 + 2^3 + 2^2 + 2^2 = 24$.

At the same time, by the method of complete group of events, the number of combinations will be $2^5 = 32$.

Omitting the intermediate calculations the systems state are:

10010, 11010, 10110, 10011, 11110, 11011, 10111, 01001, 01011, 01101, 11001, 01111, 11101, 10101, 11111, 01110

Assigning probability and transforming the formula, we get a result:

$$\begin{aligned}
 R(t) = & R_1(t) \cdot R_4(t) + R_2(t) \cdot R_5(t) + R_2(t) \cdot R_3(t) \cdot R_4(t) + R_1(t) \cdot R_3(t) \cdot R_5(t) \\
 & - R_1(t) \cdot R_2(t) \cdot R_3(t) \cdot R_5(t) - R_1(t) \cdot R_2(t) \cdot R_4(t) \cdot R_5(t) \\
 & - R_1(t) \cdot R_2(t) \cdot R_3(t) \cdot R_4(t) - R_2(t) \cdot R_3(t) \cdot R_4(t) \cdot R_5(t) \\
 & - R_1(t) \cdot R_3(t) \cdot R_4(t) \cdot R_5(t) + 2 \cdot R_1(t) \cdot R_2(t) \cdot R_3(t) \cdot R_4(t) \cdot R_5(t) \quad (4)
 \end{aligned}$$

As we can see, in the proposed method is not required drawn appropriate scheme that minimizes the time the process of rendering $R(t)$ and reduces the probability of error. For convenience in the proposed method the paired independence of routes can be used.

The method of decomposition is an analogue of the exceptions item method. As a way of a decomposition here is used not the equivalent scheme but table of equivalent routes. Further follow conversion of the table and reduce the number of columns in the table.

This method is also effective and is applicable to systems with complex communication elements. It is as well as elimination method requires no additional drawing of the equivalent circuit. We apply the exception a method for calculating the same of the initial circuit as previously discussed [16] and show it at Fig. 4.

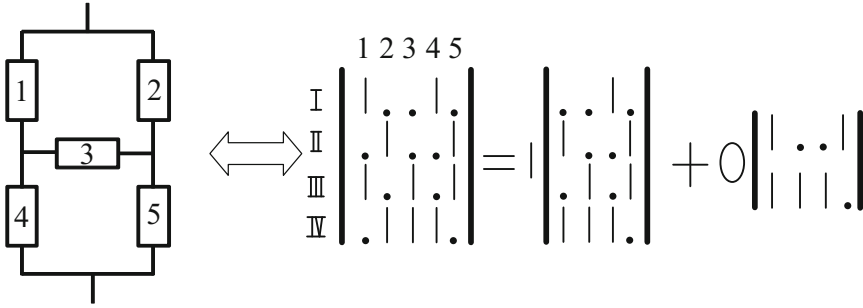


Fig. 4. The method of decomposition

The resulting conversion of each table defines corresponding scheme (in the case of items operating state and if the first element faulted). Decomposing the same way each table, we arrive at an independent combinations:

1111; 11101; 1101; 11001; 1011; 10101; 1001; 0111; 01101; 010.1

As we can see, the total number of combinations is identical with that obtained by the method of exceptions. Depending on the number of items and the complexity of their connection, the effectiveness of electric power system reliability calculation is greatly enhanced when integrated use of both of the proposed methods.

3 Results

Application the method of exceptions and the method of decomposition as a way of reducing the number of states considered system is proposed. As follows from the results of reliability calculation of a complicated electric power system using each of these methods to replace classical methods (the method of complete group of events and the exceptions item method) can significantly reduce the number of system states which should be calculated.

As reviewed in our example, the number of system states, which should be calculated according to the classical methods of calculation were 32 states. In case of using the proposed methods it was reduced to 24 states. Thus, the number of the produced calculations is decreased by approximately thirty percent.

4 Discussion

The new compact form for recording possible routes, which help to reduce the probability of an arithmetical error during calculation is proposed. In emergency situations and rejection of any item in the electric power system is urgently needed to make operational reliability calculation weakened power system while maintaining the accuracy of the calculation. This makes it possible to develop an action plan to ensure the consumers by electricity in the current emergency situation.

5 Conclusions




Obtained results leads to the following conclusions:

1. the new “compact” recording type of possible states of the electric power system, which is proposed by authors, provides the visibility, clarity of perception and improve the information understanding;
2. due to the application the method of exceptions and the method of decomposition the amount of reliability calculations of electric power systems is significantly (by approximately 30%) reduced while maintaining the assessment accuracy. note that the first paragraph of a section or subsection is not indented. The first paragraphs that follows a table, figure, equation etc. does not have an indent, either.

References

1. Bayliss, C.: Transmission and Distribution Electrical Engineering. 2nd edn., vol. 1003 (2014)
2. Meier, A.: Electric Power Systems: A Conceptual Introduction, 328 p. Wiley-IEEE Press (2006)
3. Transmission and Distribution Lines. IMIA WGP 069 (10). IMIA Conference, Berlin (2010)
4. Larsen, P., LaCommare, K., Eto, J., Sweeney, J.: Assessing Changes in the Reliability of the US Electric Power System, Lawrence Berkeley National Laboratory, pp. 95, USA (2015)
5. Moreno, R., Pudjianto, D., Strbac, G.: Integrated reliability and cost-benefit-based standards for transmission network operation. Proc. Inst. Mech. Eng., Part O: J. Risk Reliab. **226**(1), 75–87 (2012)
6. Power Outage Annual Report. Blackout Tracker United States Annual Report (2015)
7. Gurevich, V.: Power Supply Devices and Systems of Relay Protection, vol. 264. CRC Press (Taylor & Francis Group), Boca Raton (2013)
8. Piaszeck, S., Wenzel, L., Wolf, A.: Regional diversity in the costs of electricity outages: results for German counties, HWWI Research Paper 142 (2013)
9. Kovalev, G., Lebedeva, L.: Reliability assessment model of electric power systems in long-term operation planning. RT&A # 04 (35), vol. 9, pp. 14–28 (2014)
10. Russian Federation National Standard № 27.002-2009. Dependability in technics. Terms and definitions. (IEC 60050 (191):1990-12 (NEQ)), Moscow, Russia (2011)
11. Nepomnyashchiy, V.: Reliability model and system blackout development model of complex electrical networks of power systems. In: Proceedings of the Conference of St. Petersburg Power Tech 2005, St. Petersburg, Russia (2005)
12. Kjølle, G., Jakobsen, S., Baldursson, F., Galant, S., Haarla, L.: Generally accepted reliability principle with uncertainty modelling and through probabilistic risk assessment (GARPUR) D1.1. state of the art on reliability assessment in power systems (2014)
13. Polovko, A., Gurov, S.: Fundamentals of Reliability Theory, 2nd edn, p. 704. Russia, St. Petersburg (2006)
14. Koryakovtzev, S.: Fundamentals of reliability theory, p. 120, Moscow (2011)
15. Shemetov, A.: Reliability of power supply, vol. 141, Magnitogorsk, Russia (2007)
16. Zanevsky, A., Pinchukov, P.: To the question of improving the methods of calculating power supply systems reliability. Scientific and technical and economic cooperation between Asia-Pacific countries in the XXI century, vol. 1, pp. 62–66 (2014)
17. Gmurman, V.: The theory of probability and mathematical statistics, p. 479, Moscow, Russia (2003)

Research of Deicing Processes by Means of Electrodynamic Method

Sergei Sukhorukov¹(✉) , Vyacheslav Soloviev¹ ,
and Olga Malysheva² 

¹ Komsomolsk-na-Amure State Technical University, Lenin Prospect, 27,
Komsomolsk-on-Amur 681013, Russia
sergei.svan@gmail.com

² Far Eastern State Transport University,
Seryshev st., 47, Khabarovsk 680021, Russia

Abstract. The article deals with the problem of deicing of power line wires. Routine methods of power line wire deicing are notable for low energy efficiency and long time needed for wire's cleaning. Research objective consists in model-based studying of power line wire's deicing process by means of electrodynamic method. In the article, a short review with the reference of disadvantages of existing power line wire's deicing methods are described. An electrodynamic method, based on combined effect on ice layer, is outlined. A short description of mathematical model used at the investigation process is shown. The model allows to calculate the parameters of three parallel sub processes of deicing: melting of a thin ice layer on the "wire-ice" boundary, destruction of ice coating on separate fragments and shaking off the fractured ice coating elements by inertial forces. Three cases were considered during investigation. The relationship between the required pulse ratio during change of thickness of the melted ice layer, and pulse size at different ambient temperatures is defined. The relationship between length of cracked ice cylinder fragment and ice coating thickness and size of pulses supplied to the line is defined. The energy consumption for clean-up of the line by electrodynamic method is defined. This energy consumption is compared with energy consumption of ice melting. The results of numerical experiment are shown and conclusions are made.

Keywords: Ice · Mathematical model · Energy efficiency
Electrodynamic method · Numerical experiment · Power lines

1 Introduction

Nowadays electric power is one of the most widely used and popular energy resources, which can provide the function ability of industrial, accommodation and social facilities in the very remote points of the world. The power is transferred through power transmission lines networks from the generation points to end users. The main part of these power transmission lines is represented by overhead power transmission lines. Significant part of such lines is located in hard-to-reach regions with severe climatic conditions not only in Russia, but also abroad. Maintenance of these transmission lines

is associated with emergency situation risk, caused by ice and frost deposits on the wire due to low temperatures and high air humidity [1, 2]. Recovery from an accident caused by ice and wind loads is a time consuming, expensive and labor-intensive process.

The above said determines the importance and applicability of the challenge related to development and improvement of deicing means for power transmission lines.

At the present time the methods based on thermal effect on the ice layer, i.e. melting by high amperage direct or alternate current is mostly used for deicing of the power lines wires [3]. The main disadvantages of such approach are high power consumption, expensive and long-time clean-up. In addition, in most cases the melting requires the disconnection of the line affecting the continuity of power supply.

The significant part of researches in the field of deicing of power lines wires is focused on optimization of melting conditions and patterns [4–6], as well as on use of controlled ice melting rectifiers [7–9]. It is necessary to stress that such an approach is featured by low power saving potential and clean-up time reduction.

Besides of ice melting the different electromechanical and robotized devices for mechanic clean-up of wire are developed and tested [10–14]. However the general disadvantages of such devices are their expensiveness, need of qualified maintenance personnel and limited field of application, i.e. most of these devices are oriented at wire clean-up within one span.

As an alternative approach the use of the methods has been proposed, which base on combined effect on ice layer. One of such alternatives is a use of combined electrodynamic method based on simultaneous application of thermal and mechanical effect on ice [15]. In such case the destruction of ice coating on separate fragments occurs due to bending under mechanical oscillations of the frosted wire. For excitation of the wire oscillations the periodic Ampere force is applied to pair of parallel wires, which is caused by current pulse flow through the wires. Thereafter the resulting ice fragments are shaken off the wire. In such case the current flows through the wire producing a thermal energy, which causes melting of a thin ice layer on the “wire-ice” boundary. This results in sudden reduction of adhesion between the wire and ice fragments [16, 17] and reduces deicing energy.

Such an approach reduces a clean-up time mainly due to mechanical ice destruction, and reduces the clean-up energy, as this method does not require melting of big amounts of ice.

2 Materials and Methods

While research of the proposed method the mathematical description of physical processes appearing during deicing by electrodynamic method has been developed [18, 19]. During development of mathematical description the entire deicing process has been figuratively divided into three parallel subprocesses - melting of thin ice horizon on the boundary with a wire, splitting of the ice coating into fragments and shaking of the fragments from the wire.

The following assumptions have been considered during development of the mathematical description:

- generally accepted representation of the ice coating as perfect hollow cylinder with internal diameter equal to wire outside diameter and volume corresponding to deposited ice volume has been used;
- ice deposits within the span are uniform by ice density and structure;
- the wire in section is represented as perfect circle without adhesive coating;
- temperature of the wire and ice are similar at the moment of clean-up.

The obtained mathematical description allowed to generate a Matlab Simulink model, calculating the process parameters appearing during application of electrodynamic method of power lines deicing.

The output data for model calculation are the following:

- span geometries;
- wire type and structure;
- ice layer thickness;
- mechanical properties of ice (density, strength, heat conductivity) [20];
- main physical constants.

During calculations the model allows to determine:

- amount of energy required for heating and melting of thin layer of ice on “wire-ice” boundary;
- required frequency and ratio of pulses, supplied to line;
- intensity of stress acting on wire and ice coating;
- length of cracked fragments of ice cylinder;
- total amount of energy consumed while clean-up.

While application of the obtained mathematical model several series of numerical experiments have been performed. During these experiments the interrelationships of various power lines deicing process parameters have been studied.

Three main cases have been studied. For the first case the change of ambient temperature in initial model parameters has been made. Considering the accepted assumptions, the initial ice temperature was equal to air temperature. For each temperature a cycle of calculations has been performed. As a result of these calculations a surface has been obtained, which represents relationship between the required pulse ratio during change of thickness of the melted ice layer and size of pulses. Temperature variation range was from -2 to 10 °C with step of 1 °C. The thickness of the melted ice layer changed within $0.1 \dots 0.5$ mm with step of 0.05 mm. Current pulse size, flown through the wires, changed within $1000 \dots 2000$ A with step of 20 A.

The second series of calculations focused on study of relationship between length of cracked ice cylinder fragment $l_{i.cyl.}$ and ice coating thickness and size of pulses supplied to the line. Pulse variation range used for this series of calculations is equal to the first case reviewed. The ice coating thickness changed during the calculations within $5 \dots 30$ mm with step of 5 mm.

The third part of study with use of the developed model focused on determination of energy consumed during clean-up.

At this step the following model output parameters changed: ice wall thickness and clean-up time. Thereafter we conducted the calculations during which the energy

volume required for clean-up by electrodynamic method has been determined. To compare with the existing approach we calculated an amount of energy required for ice melting for each thickness. The melting process was considered as perfect with design performance factor equal to one. For each selected ice wall thickness the size of pulses required for electrodynamic method has been determined by use of mathematical model of wire oscillation under periodic Ampere force within plane of loads with 5... 10% reserve. To check sufficiency of the developed mathematical model and to confirm the functionality of the proposed electrodynamic method, we conducted the experimental study using physical model at a scale of 1:40. Experimental methods and results are specified in [21].

3 Results

The results of the calculations performed on the model at the first case a family of surfaces has been obtained, which is shown on Fig. 1. Considering the limited possible pulse ratio size which cannot exceed one, the resulting surfaces are limited by level $\gamma = 1$.

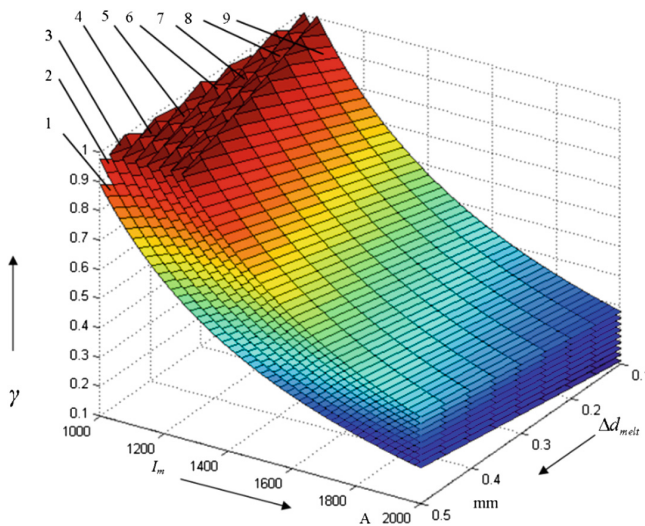


Fig. 1. Family of surfaces representing relationship between the required pulse ratio during change of thickness of the melted ice layer, and pulse size at different ambient temperatures

1 – surface at temperature $t_2 = -2$ °C; 2 – surface at temperature $t_2 = -3$ °C; 3 – surface at temperature $t_2 = -4$ °C; 4 – surface at temperature $t_2 = -5$ °C; 5 – surface at temperature $t_2 = -6$ °C; 6 – surface at temperature $t_2 = -7$ °C; 7 – surface at temperature $t_2 = -8$ °C; 8 – surface at temperature $t_2 = -9$ °C; 9 – surface at temperature $t_2 = -10$ °C;

Graph of the resulting surface of second series of calculations is shown on Fig. 2.

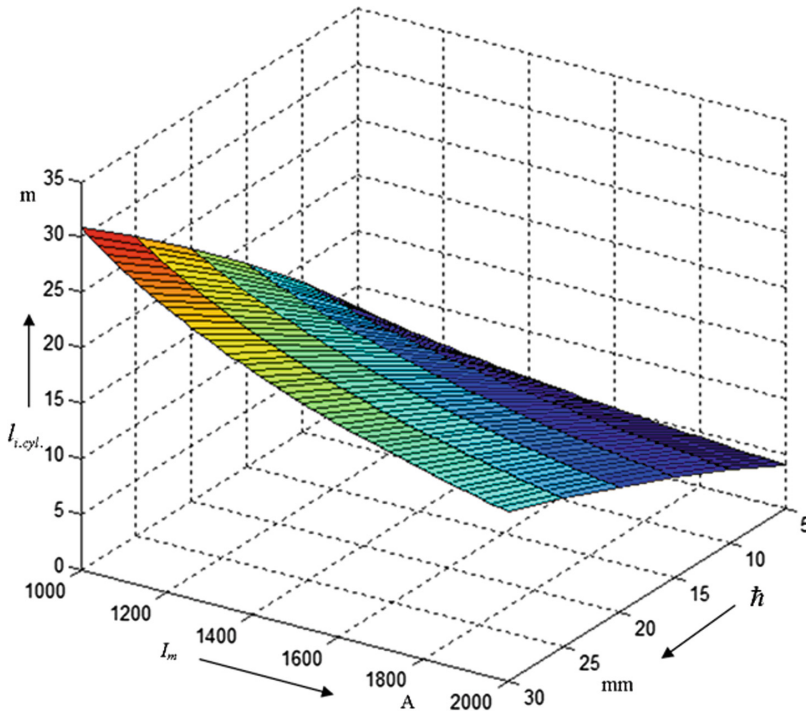


Fig. 2. Surface representing relationship between length of cracked ice cylinder fragment and ice coating thickness and size of pulses supplied to the line

The numerical results of third part of study are shown in Table 1.

Table 1. Results of calculation of energy consumption for clean-up of 1 km of the line by electrodynamic method and ice melting.

Ice thickness, mm	Weight of ice on the wire, kg/km	Approximate clean-up time by electrodynamic method, min	Pulse size using electrodynamic method, A	Energy consumption during melting, MJ/km	Energy consumption using electrodynamic method, MJ/km	Energy saving using electrodynamic method, %
5	571.14	3	850	194.50	32.1	83.50
10	1425.03	5	1300	485.29	116.8	75.93
15	2561.65	8	1800	872.37	340	61.03
20	3981.03	12	2400	1355.74	963	28.97
25	5683.14	15	2800	1935.39	1650	14.75

Comparison of the mathematical model results with experimental study results shows that the deviation of theoretical data from the experimental data does not exceed 5%, if sleet is missing, and 10% in case the ice uniformly covers the wire.

4 Discussion

The conducted study with use of developed mathematical model shows that the proposed electrodynamic method is more effective than traditional ice melting from the perspective of energy consumption. However in case of increasing the ice wall thickness the effectiveness of this method is decreasing, and cost and complexity of equipment required for this method rise steeply. In addition, application of significant load to wire in case of thick or extra thick ice walls may result in exceeding of the applicable wire strength followed by wire break. This fact confirms again that moment of ice formation shall be determined first, and after that all necessary deicing measures shall be taken as soon as possible.

Figure 1 shows, that the required pulse ratio increase while increasing ambient temperature at the constant pulse size. It is associated with both effects: increasing of quantity of heat required for heating ice and increasing of rate of heat exchange with ambient air.

5 Conclusions





In this work model-based studying of power line wire's deicing process by means of electrodynamic method is made. The relationship between the required pulse ratio during change of thickness of the melted ice layer, and pulse size at different ambient temperatures is defined. The relationship between length of cracked ice cylinder fragment and ice coating thickness and size of pulses supplied to the line is defined. The energy consumption for clean-up of the line by electrodynamic method is defined. Energy efficiency of electrodynamic method in comparison with traditional ice melting is shown.

References

1. http://forca.ru/instrukcii-po-ekspluatacii/vl/ekspluataciya-vozdushnyh-linii-elektroperedachi_4.html. Accessed 21 Aug 2017
2. Sukhorukov, S.: Innovative control technologies, Odesa (2013)
3. Standard instructions on operation of overhead transmission lines under 35–800 kV: RD 34.20.504-94: appr. by Electrical Power Network Department of Russian Academy of Education "Unified Electrical System of Russia" on 19.09.1994, appl. since 01.01.1996, vol. 200 (2003)
4. Zasytkin, A.: Integral evaluation of overhead transmission lines deicing methods efficiency. Universities' reports, Electromekhanika, vol. 4, pp. 42 – 45 (2013)
5. Zasytkin, A.: Calculation tables for selection and analysis of overhead transmission lines deicing patterns: study guide. Novocheerkassk. YuRGU (NPU), vol. 102, (2013)

6. Figurnov, Y.: Successful deicing conditions on uninsulated transmission line. *Electricity* **8**, 21–27 (2013)
7. <http://elvpr.ru/preobrazotechnic/gololed/V-TPPD-14k-U1.php>. Accessed 21 Aug 2017
8. <http://www.energy-t.ru/vipryamitel-dlya-plavki-gololeda.html>. Accessed 27 Aug 2017
9. <http://www.ielectro.ru/news51718/index.html>. Accessed 17 Aug 2017
10. Almayev, M.: Electromechanical vibration transmission-lines deicing unit. Collection of scientific works of finalists among post-graduate students and young scientists in the field of industrial power saving, Novocherkassk, Ministry of Education and Science of the Russian Federation, South-Russian State Technical University (NPI). Novocherkassk, Lik, pp. 3–5 (2010)
11. <http://roboting.ru/957-robot-expliner-inspektiruet.html>. Accessed 04 Aug 2017
12. <http://roboting.ru/1253-robot-linescout-na-liniyax-yelektroperedach.html>. Accessed 04 Aug 2017
13. Pat. 93184 Russian Federation, MPK N 02 G 7/16. Transmission lines deicing unit. Sattarov, R.R., Ismagilov, F.R., Almayev, M.A., applicant for patent and patenter Federal State Educational Institution of Higher Professional Education “Ufa State Aviation Technical University”. no. 2009142495/22, appl. on 17.11.09, publ. on 20.04.2010, Bul. no. 11
14. Pat. 2142188 Russian Federation, MPK N 02 G 7/16. Transmission lines deicing unit. Khairullin, I.K., Ismagilov, F.R., Khairullin, T.I., Ismagilov, R.F., applicant for patent and patenter Federal State Educational Institution of Higher Professional Education “Ufa State Aviation Technical University” № 98108193/09 appl. on 21.04.1998, publ. on 21.04.1998
15. Pat. 2442256 S1 Russian Federation, MPK N 02 G 7/16. Transmission lines deicing method. Kozin, V.M., Solovyev, V.A., Orlov, D.A., Sukhorukov, S.I., Malykh, K.S., applicant for patent and patenter Federal State Educational Institution of Higher Professional Education “Amur State University of Humanities and Pedagogy” № 2010144485/07, appl. on 29.10.2010; publ. on 10.02.2012, Bul. no. 4, p. 4, ill
16. Goldstein, R.: Adhesive strength of ice deposits on steel structure elements. *Novosibirsk State University Reporter. Series: Mathematics, mechanics, informatics*, vol. 12, no. 4 (2012)
17. Matsumoto, K.: Fundamental study on adhesion of ice to cooling solid surface. *Int. J. Refrig* **30**, 851–860 (2007)
18. Sukhorukov, S.: Mathematical model of destruction of ice coating on power transmission lines by electrodynamic method. *Electricity*, № 7, pp. 61–65, Moscow (2016)
19. Sukhorukov, S.: Physical basis of power transmission wires deicing by electrodynamic. In: *MATEC Web of Conferences: The 2nd International Youth Forum “Smart Grids”*, vol. 19 (2014)
20. Petrov, I.G.: Selection of the most expectable values of mechanical properties of ice. In: *Works of AA NII*, b.331, no. 7, pp. 4–41 (1976)
21. Sukhorukov, S.: Evaluation of possibilities of transmission line wires deicing by electrodynamic method. *Inform. Control Syst.* (2), 148–158 (2014). (Blagoveschensk)

A Mathematical Model of the Estimated Cases for Designing a Multimodal Transport Network

Natalia Nesterova¹ , Vladimir Anisimov¹ ,
Sergey Goncharuk¹ , and Aleksandr Anisimov² 

¹ Far Eastern State Transport University, Serysheva st. 47,
Khabarovsk 680021, Russia
anisvl@mail.ru

² Skolkovo Innovation Center, Skolkovo Institute of Science and Technology,
Building 3, Moscow 143026, Russia

Abstract. The article substantiates the relevance of development of multi-modal transport network for the strategic objectives of Unified transport network of Russia. Also, explains the need for a methodology of designing changes of landmark appearance and network capacity. We further provide a brief overview of the works, dedicated to solving this problem. Lastly, we consider mathematical model with different estimated cases, defining options for the required traffic volume and options for designing schemes of multimodal transport network appearance, that can vary under different scenarios of socio-economic development of the region, taking into account the impact on the decision-making factors.

Keywords: Multimodal transport network · Multimodal transport corridor
Transport corridor

1 Introduction

Transport infrastructure is one of the basic foundations of the socio-economic development of the country. According to the Transport Strategy of the Russian Federation for the period up to 2030 [1] (further Transport Strategy) developing of Unified Transport Network (UTN) should provide “satisfaction of the needs for innovative socially-oriented development of the economy in high-quality competitive transport services”.

For Russia, which occupies a huge area and has a lack of transport sufficiency, the development of UTN has special significance. The high cost of development of new and reconstruction of existing transport communications leads to the need to define priority objects from the UTN that solves effectively the task of the Transport Strategy. These include the realization of the transit potential of the Russian Federation and hydrocarbon exports to APR. To solve this problem in [2, 3] proposes to allocate from the unified transport network (UTN) multimodal transportation network (MTN), as a set of multi-modal transport corridors (MTC), consisting of a multi-modal transport

nodes and transport links of the various modes of transport, to address the strategic objectives of UTN development on the main transit and export routes.

Development of MTN allows to achieve one of the main objectives of the Transport Strategy - “the formation of a solid foundation for a successful integration of Russia into the global transport system, expansion of access of Russian transport providers to foreign markets, strengthening of Russia’s role in shaping the international transport policy and transform the export of transport services into one of the largest sources of income of the country” [1]. The transport system of Russia has a number of competitive advantages to achieve this goal, but changes in the economic situation and the political situation in the world reveal a number of problems, which considerably complicate the integration of the transport complex of Russia in the global transportation system.

The foregoing confirms the complexity and urgency of the development of a multimodal transport network for solving strategic UTN tasks of Russia. In addition, it proves the need to establish a methodology of designing landmark shape and capacity changes of MTN under different scenarios of socio-economic development of the country and its regions.

2 Materials and Methods

Investigation of various issues of development of transport networks, polygons, lines, objects as one mode of transport are devoted to the works of many scientists [2–23]. In [16–20] provides an overview of the development of systems for different modes of transport.

In [21] results are presented from document- and literature studies examining how the concepts of sustainability and sustainable development (economical, ecological and social) are used in the process of developing main transport corridors in the European Union. In [21] highlight that the concept of sustainable development is used in a multifaceted way, sometimes indicating the overarching goal of sustainability, sometimes indicating certain dimensions, and sometimes referring to conducting efforts in a sustainable way.

In [22] assess infrastructure and operational status of two important intermodal transport corridors linking North-East and Central Asia namely: Korea–China–Central Asia; and Korea–China–Mongolia–Russian Federation. Is used time–cost–distance approach to assess and compare the performance of intermodal transport corridors. Based on the findings in [22] are defined challenges for the development and operation of intermodal transport corridors in North-East and Central Asia. The recommendations about improvement of physical infrastructure and minimization of nonphysical barriers are offered to increase operational effectiveness of corridors of transportation with use of several means of transport.

In [23] elaborates on the definitions of inter and multi-modal transport, as well as their differences in terms of performance. A survey of the barriers, both internal and external, to an efficient intermodal transport is included followed by an analysis of the advantages and disadvantages of combining rail transport with the other transport modes. Transshipment technologies for efficient freight service and some examples of freight rail corridors between sea and inland terminals are presented. The integration

between air and rail transport is discussed and the potential synergies between air and high-speed rail services are emphasised.

In studies [4–23] proposes models, methods, and techniques for solving specific problems of the organization MTC functioning, forecasting their development, assessing the effectiveness of the implementation of MTC projects. Integrated use of the proposed models, methods, and techniques to solve the problems of formation, functioning and development of multi-modal transport network as a set of MTC is only possible by their development within the framework of a unified methodology.

In [3, 24] gives an explanation of the development of a unified design methodology MTN.

The analysis of scientific papers on the development of UTN allowed:

- to select the object of study – a multimodal transport network and its elements;
- to define subject of investigation – designing the development of MTN;
- to set the purpose of the study – creation of the MTN design methodology under different scenarios of socio-economic development of the country and its regions, taking into account the factor of the initial information uncertainty.

The following problems are solved for the implementation of the objectives of the study.

Elaborated the concept of design methodology MTN [25], which is a continuation of existing research in the field of railway transport infrastructure development on multimodal level. The concept is seen as a system of views and philosophies that form the master plan to identify key objectives and action sequences in achieving the objectives of the study. This approach is presented in the form of three pillars: informational, conceptual and methodological. Informational basis determines the amount of data to describe the external and internal factors affecting the formation, operation, and development of MTN. Conceptual – models and methods used to solve development problems MTN. Methodological framework includes a methodology and determines the sequence of solving the problem under investigation.

In [26] analyzed the existing terms and approaches to the problem, formulated the concept of “multimodal transport network”, given its rationale, proposed systematical technical description and a four-leveled decomposition of MTN appearance. In [27] summarized the existing interpretation of the terms “transport corridor”, “international transport corridor” and “multi-modal transport corridor”.

In [28] proposed and considered the systemic presentation of the main MTN elements – multimodal transport unit (MTU), transport node (TN) and a multi-modal transport node (MTN). On the basis of [26–28], using the theory of systems, we developed the model of MTN, its subsystems, and its elements, as well as processes of their functioning and development [3, 29, 30]. Using a four-level decomposition of MTN and combining into a single strategy the results of the solution for local MTN objects development, this model could serve as a mathematical basis for the methodology of designing. To evaluate the effectiveness on a plurality of criteria based on [31, 32] suggested a Balanced Scorecard (BSC). BSC, reflecting the quality of the strategy and linking the strategic management with operational on the basis of key performance indicators and the causal relationships between them, determines the direction of shape and power changes of MTN to achieve the objectives of its development and operating.

In accordance with the objective of development and functioning of MTN, the strategy should meet transport demand, so the appointment of possible measures to change the shape and power facilities of MTN we need to compare their current and possible power facilities with the required traffic volume.

3 Results

Estimated cases are used in the methodology of designing MTN for identifying options for the required traffic volume and design schemes of shape under different scenarios of socio-economic development of the region, taking into account the external and internal factors that give rise to the uncertainty of the initial information.

The external factors include:

- climatic;
- economic (economic interests of the participating states and private investors, the possibility of expanding economic and infrastructure links between the participants of the project, the conditions of rational distribution of productive forces, financial and credit policies, etc.);
- political (political situation in the countries of the region under study);
- social (changes in people's behavior, social conflicts, migration, etc.)

The internal factors:

- reliability of MTN and its objects (the technical condition of the existing transport communications MTN, technology of transport processes, provision of human resources and their level of training);
- the cost of obtaining additional information about the technical condition of objects MTN;
- human factor.

Effective management of development project requires taking into account influence of the factors mentioned above. To this end, on the basis of socio-economic analysis of the study region and the economic and political analysis of the international situation forms the estimated cases (Fig. 1).

$$RS = \{RS_{i_{rs}}\}, \quad (1)$$

$$RS_{i_{rs}} = \{scr_{i_{scr}}, VG_{i_{vg}}, Rsch_{i_{Rsch}}\}, \quad (2)$$

where $scr_{i_{scr}} = \{G_{i_{scr}}, A_{i_{scr}}, K_{i_{scr}}\}$, $i_{scr} \in \{1, 2, \dots, n_{scr}\}$ – a scenario of socio-economic development of the region under study, including the required traffic volume $G_{i_{scr}}$ without account of traffic flows on MTN, the transportation tariffs $A_{i_{scr}}$, possible investments $K_{i_{scr}}$; $VG_{i_{vg}}$ – variants of required traffic volumes on MTN; – $Rsch_{i_{Rsch}}$ design scheme MTN shape.

According to the scenario define variants for loading objects of MTN with traffic with some billing period and direction of movement

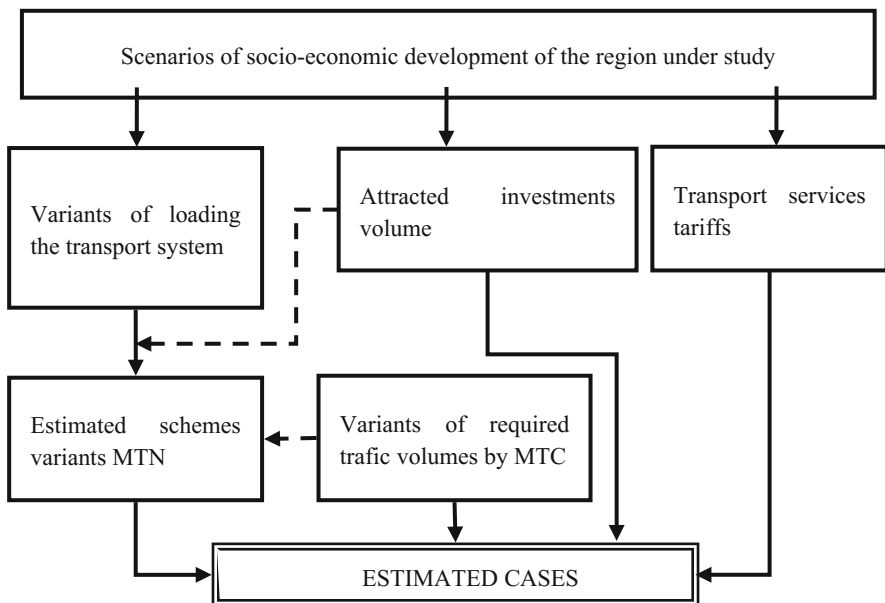


Fig. 1. The circuit forming settlement cases.

$$G_{i_{scr}} = \{G_{i_{vg}}^{g^o}(t)\}, \tag{3}$$

$$G_{i_{vg}}^{g^o}(t) = \sum_{dir(g^o)} G_{i_{scr}}^{g^o, dir(g^o)}(t), \tag{4}$$

where $dir(g^o)$ – direction of movement of transport streams on MTN object.

Required traffic volume of each multimodal transport corridor $MTC_{i_{MTC}}$ with the billing period and the directions of movement set by next variables:

$$VG = \{VG_{i_{vg}}\}, i_{vg} = \overline{1, n_{vg}} \tag{5}$$

$$VG_{i_{vg}} = \{G_{i_{vg}, tp}^{i_{MTC}, dir_{i_{MTCY} \rightarrow j_{MTCY}}}(t)\}, \tag{6}$$

$$tp = \overline{1, n_{tp}}, i_{MTCY}, j_{MTCY} \in \overline{1, n_{MTCY}}, i_{MTCY} \neq j_{MTCY},$$

where $G_{i_{vg}, tp}^{i_{MTC}, dir_{i_{MTCY} \rightarrow j_{MTCY}}}(t)$ – the predicted traffic on the billing period for category tp in direction $dir_{i_{MTCY} \rightarrow j_{MTCY}}$ on i -th MTN for i_{vg} variant; tp – category of transport flow: coal, ore, oil, wood, grain, container (TEU), passengers etc.

Then, according to (5) and (6) loading the MTN object with traffic flow for multimodal transportation corridors by variant will be determined by the following model

$$G_{i_{vg}}^{g^o}(t) = \sum_{i_{MTC}=1}^{n_{MTC}} \sum_{tp=1}^{n_{tp}} \sum_{dir} G_{i_{vg,tp}}^{i_{MTC},dir}(t), \quad (7)$$

$$dir \in \{dir_{i_{MTY}-j_{MTY}} \mid i_{MTY}, j_{MTY} \in \overline{1, n_{MTY}}, i_{MTY} \neq j_{MTY}\},$$

Thus, the total loading of MTN object with required traffic volume is determined by

$$G_{p(i_{rs})}^{g^o}(t) = \sum_{dir(g^o) \in dir} G_{i_{scr}}^{g^o, dir(g^o)}(t) + G_{i_{vg}}^{g^o}(t), \quad (8)$$

$$dir \in \{dir_{i_{MTY}-j_{MTY}} \mid i_{MTY}, j_{MTY} \in \overline{1, n_{MTY}}, i_{MTY} \neq j_{MTY}\}.$$

Possible schemes of MTN shape $\{Rsch_{i_{Rsch}}\}$ formed by the method described in [33], depending on the scenarios of socio-economic development of the region under study and variants of required traffic volume on MTN.

4 Conclusions

Suggested mathematical model for generating estimated cases is used in the methodology of designing of multimodal transport network to identify possible options for the required traffic volume and the corresponding schemes design of MTN shape depending on different scenarios of socio-economic development of the region and traffic requirements of the multimodal transport corridors. In each case, the design expert forms the field of effective strategies for staged changes in shape and power of MTN, which makes it possible by taking into account the influence of factors that give rise to uncertainty of the initial information.

References

1. Transport Strategy of the Russian Federation for the Period Through to 2030 (enacted by Russian Federation government decree No. 1734-r on 22 November 2008)
2. Goncharuk, S., Anisimov, V., Nesterova, N., Lebedeva, N.: Methodological foundation for designing stage-by-stage development of layout and capacity of multimodal transportation network. In: Proceedings of Far Eastern State Transport University, Khabarovsk, p. 227 (2012)
3. Nesterova, N., Goncharuk, S., Anisimov, V., Anisimov, A., Shvartfeld, V.: Set-theoretic model of strategies of development for objects of multimodal transport network. *Procedia Eng.* **165**, 1547–1555 (2016)
4. Svintsov, E.: Regional transport studies in modern conditions, 301 p. Marshrut, Moscow (2005)
5. Sazonov, S., Kudryavtsev, E., Wu, Z.: *Far Eastern Affairs*, vol. 2, pp. 47–58 (2012)
6. http://ec.europa.eu/transport/themes/infrastructure_en. Accessed 22 July 2017
7. http://europa.eu/rapid/press-release_MEMO-14-525_en.htm. Accessed 22 July 2017
8. http://www.unece.org/trans/theme_infrastructure.html. Accessed 25 July 2017

9. Korolyova, E.: Organizational-economic bases of functioning of transport corridors DrScThesis (2000)
10. Morozov, V.: Methodology of organization of functioning of international transportation corridors on the basis of the cluster approach with the use of multimodal logistics centers DrScThesis (2010)
11. Drożdżiel, P., Buková, B., Brumerčíková, E.: *Transp. Probl.* **104**, 5–13 (2015)
12. Goncharenko, E.: The Russian sections of international transportation corridors as an object of economic research. Ph.D. thesis (2015)
13. Tchumlyakov, K., Tchumlyakova, D.: *Bull. Transp. Inf.* **11**(245), 8–13 (2015)
14. Macheret, D.: *Soiskatel – Suppl. World Transp. J.* **1**(9), 58–61 (2015)
15. Kovalev, S.: *Soiskatel – Suppl. World Transp. J.* **1**(9), 62–67 (2015)
16. Shapoval, D.: *Tech. Technol. Constr.* **1**(5), 8 (2016)
17. Bykov, Y., Vasilyev, A., Fadeeva, V.: *Transp. Urals* **1**(44), 53–56 (2015)
18. Nesterova, N., Goncharuk, S., Anisimov, V., Anisimov, A.: Strategy development management of Multimodal Transport Network. In: *MATEC Web of Conferences*, vol. 86, p. 05024 (2016)
19. Nesterova, N., Anisimov, V., Goncharuk, S.: About the forming and development of multimodal transport network, Design of the development of a regional network of Railways, *Izdatelstvo DVGUPS, Khabarovsk*, pp. 39–48 (2016)
20. Anisimov, V.: Theory and practice of design of the development of a regional network of Railways taking into account change of shape and capacity of stations and hubs, Dissertation for the degree of Doctor of Engineering, 380. *DVGUPS, Khabarovsk, MIIT* (2005)
21. Oberg, M., Nilsson, K., Johansson, C.: *Transp. Res. Procedia* **25**, 3694–3702 (2017)
22. Regmi, M., Hanaoka, S.: *Res. Transp. Bus. Manag.* **5**, 27–37 (2012)
23. Reis, V., Meier, J., Pace, G., Palacin, R.: *Res. Transp. Econ.* **41**(1), 17–30 (2013)
24. Anisimov, V., Nesterova, N., Bondarenko, N., Goncharuk, S.: Conceptual proposals for the development of innovative project of advancement of the ITC «Asia pacific – Europe» for the realization of transit potential of Russia. *Mod. Technol. Syst. Anal. Model.* **1**(49), 166–170 (2016)
25. Nesterova, N.: The concept of methodology design study of multimodal transportation development. *Des. Develop. Reg. Netw. Railways* **4**, 55–61 (2016)
26. Nesterova, N.: Multimodal transport network as part of a united transport system of the country and its regions. *Volga Reg. Transp. Herald* **1**(55), 66–74 (2016)
27. Nesterova, N.: To a question of multimodal transport corridors. *Volga Reg. Transp. Herald* **2**(56), 70–75 (2016)
28. Nesterova, N.: Research of basic elements of multimodal transport network. *Mod. Technol. Syst. Anal. Model.* **2**(50), 173–179 (2016)
29. Nesterova, N., Anisimov, V.: Set-theoretical model of multimodal transport network. *Transp. Urals* **2**(49), 26–29 (2016)
30. Anisimov, V., Nechiporuk, M.: Interaction model for railroad and sea transportation to improvement of multimodal transportation efficiency. *Izvestiya PGUPS* **3**(40), 9–15 (2014)
31. Nesterova, N., Anisimov, V.: Balanced scorecard for evaluation of multimodal transportation network development strategies. *Izvestiya PGUPS* **2**(47), 197–205 (2016)
32. Nechiporuk, M., Anisimov, V.: Regarding the use of balanced scorecard in modeling of interaction between rail and sea transport in a multimodal transport hub. *Transp. Urals* **3**(42), 13–17 (2014)
33. Nesterova, N.: Multimodal transportation network shape forming. *Modern Technol. Syst. Anal. Model.* **3**(51), 146–153 (2016)

Assessment of the Fatigue Durability of the Rolling Contact

Alexey Beskopylny¹, Nikolay Onishkov¹,
and Viktor Korotkin²

¹ Don State Technical University,
sq. Gagarin, 1, Rostov-on-Don 344010, Russia
besk-an@yandex.ru

² South Federal University,
Bolshaya Sadovaya Str. 105/42, Rostov-on-Don 344006, Russia

Abstract. The phenomenon of reducing the contact strength of conjugate parts under conditions of pseudo-pure rolling and (or) the effect of oscillating forces of small amplitudes is considered. This work is to analyze the effect on the level of strength of differential slip in the contact area. Surface contact disruptions are initially localized in the region of minimum slip velocities of the conjugate surfaces; the allowable stresses for the pulsating contact mode are much lower than for the apparently less favorable “rolling with slip” regime. The conditions initiating the fracture were investigated on the basis of the experimental material and the determination of tangential loads in the rolling contact in the presence of cohesion and slip on the basis of minimization of the Kalker functional over Spector-Fedorenko. The localization of the fracture zones corresponds to the boundaries of the separation of these regions, where the concentration of shearing frictional stresses takes place.

Keywords: Fatigue · Contact strength · Novikov gears

1 Introduction

Questions of contact fatigue life, despite intensive research, remain relevant. Wear, pitting, “gray spotting”, deep chipping - is not a complete list of negative results of contact interaction. Annual economic losses from the destruction of the contacting elements of machine parts and mechanisms in the eighties of the last century in the USA reached 50 billion dollars [1, 2] and only increased. Pitting (Fig. 1) - surface dyeing of contacting surfaces - the main type of failure gears, whose need only in the automotive industry is estimated at tens of billions per year.

Pitting, as a rule, occurs in closed gears operating in an oil bath. In the initial stage, they are localized in the zone adjacent to the linking pole. In the surface layer, the presence of micro defects is inevitable, which are also the risks of instrumental processing. Under the influence of the oil pressure, which is pressed into the micro cracks by a conjugate tooth, a crack develops and then the particles of the material are discolored. On the working surface, shells are formed, which over time cover a large part of the tooth. In open gears, due to the lack of liquid lubricant, this kind of

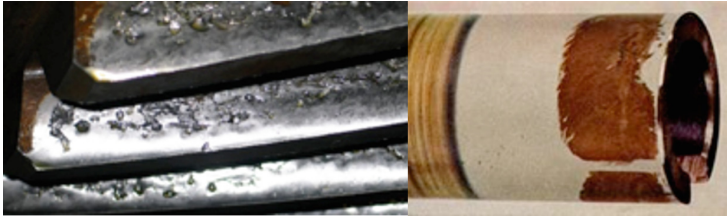


Fig. 1. A typical kind of surface chipping (pitting) and fretting corrosion

destruction is not observed. No less urgent is the problem of fretting wear (fretting corrosion) - a common type of wear, which accompanies the work of many contact joints subjected to small tangential displacements during operation. These include numerous bolted, riveted, pin, keyed, lock joints, interference connections, rolling bearings, electrical contacts, fuel assemblies of power nuclear reactors, ropes, even medical implants.

Despite the external difference in the processes-rolling contact in the first case and the cyclic relative motion of extremely small amplitude between densely planted surfaces-in the second, many of the factors initiating their destruction have a common basis. Principles of contact interaction formed the basis for testing materials for determining their mechanical characteristics and diagnostics of structures [3, 4].

2 Materials and Methods

It is generally recognized that the zones of “pure rolling” (pole) are potentially the most dangerous. Questions of the strength of the pseudo pure rolling zones of contacting bodies refer to the region of the least investigated in contact problems. And there is no common opinion about the reasons. So in [5] as one of the factors marks the wear of the adjacent near-pole sections of contacting surfaces leading to the appearance in the pole of a peculiar “mound”. In [6] a continuum damage mechanics-based elastic-plastic FE model developed to quantify the rolling contact fatigue (RCF) life of refurbished bearings made from case carburized steel is presented. But in any case, the modes “pure rolling”, “rolling with external tangential force”, “rolling with slip”, “pulsating contact” for which a significant (up to 35%) the difference of the maximum permissible stress is recommended, and the lower level is corresponding to the regime of “pulsating contact”. Since the geometry of the contacting bodies and the material do not change, it can be assumed that these differences are a consequence of the kinematic features of the contact.

The “rolling with slip” regime assumes the presence of a geometric slip of interacting bodies, as absolutely rigid. In other cases, there is none. In connection with this, experiments are of interest [7, 8]. Figure 2 shows the graph of the change in the contact longevity from the level of the external tangential load T_{Σ} when a stationary cylindrical specimen $d_1 = 9.32$ mm is rolled over by a ball $d_2 = 10.32$ mm under the conditions of the braking effect caused by the profile of the outer ring pressed to the ball.

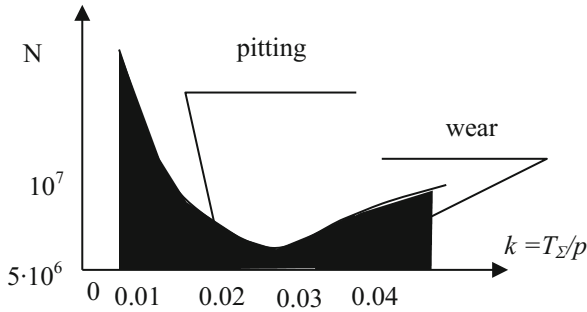


Fig. 2. Durability of contact damage depending on the external tangential load ($P = 1670 \text{ N}$)

Attention is drawn to the nature of the dependence $N = N(T_\Sigma)$. An increase in the rolling resistance coefficient $k = T_\Sigma/P$ where P is the external normal load, leads to a certain reduction in durability by the pitting criterion until a certain point. But further increase of this coefficient, on the contrary - to a certain increase in it, with a simultaneous change in the nature of the destruction. Deterioration becomes the factor limiting durability.

Two points are of interest. The first is the reason of the increase in T_Σ , under the assumption of the presence of Coulomb friction. The second is the reason for the increase in durability at $0.03 < k < 0.04$ in the conditions of invariability of the nature of destruction.

These questions have already been the subject of research in papers, in particular in [9], the continuation of which is the present article. It was assumed that the main “contributors” to the value of the coefficient of rolling resistance of steel parts are:

1. Slip on the contact area.
2. Elastic hysteresis and micro plastic deformations.
3. Losses in the lubricant.

In these experiments, the lubricant was applied sporadically, and its influence was not taken into account. The resistance due to the elastic hysteresis T_g is determined primarily by the value of the normal load. For the case of a ball rolling along the plane (according to Taybour): $T_r = 2 \text{ Pa an}/3\pi R$, where α is the coefficient of losses due to hysteresis at the corresponding stress level; a is a semi axis of the contact spot; R is the radius of the ball.

3 Results

The elastic constants of interacting bodies are the same, which allows us to separate the contact problem itself, i.e. the problem of determining the shape of the contact area and the distribution of pressures from the problem of studying the stress state. In the presence of external tangential loads, this is necessary and possible. In the coordinate system with the contact surface of the bodies lying in the XOY plane (the Z axis is

directed along the normal to the surface), the jumps of the elastic displacements of the interacting bodies 1 and 2, expressed through surface stresses, have the structure [10]:

$$\begin{aligned}
 U_{x1} - U_{x2} &= K\varphi_1(\sigma_z) + \psi_2(\tau_{xz}, \tau_{yz}); \\
 U_{y1} - U_{y2} &= K\varphi_2(\sigma_z) + \psi_2(\tau_{xz}, \tau_{yz}); \\
 U_{z1} - U_{z2} &= \varphi_3(\sigma_z) + K\psi_2(\tau_{xz}, \tau_{yz});
 \end{aligned}
 \tag{1}$$

where $K = [(1 - 2\mu_1)/G_1 - (1 - 2\mu_2)/G_2]/2\pi$; μ_1 and μ_2 , G_1 and G_2 - respectively, the Poisson's coefficients and the shear moduli of the materials of the contacting bodies.

It is obvious that for $\mu_1 = \mu_2$ and $G_1 = G_2$, $K = 0$, and the discontinuity in the normal displacements that determines the contact area depends only on the normal load. This gives the basis for the loss from hysteresis to be regarded as a constant value.

The coefficient of friction f when rolling lubricated steel surfaces is, of course, a variable. But these fluctuations are in the range of 20 ... 30 per cent and it is unrealistic to explain the change of T_Σ in several times.

Residual deformations can lead to a change in the nature of the contact: instead of "rolling the ball along the cylinder" - "rolling the ball along the adjacent trench", which does not exclude the appearance of alternating slip and, consequently, a certain decrease in T_Σ . Such an effect can not be excluded if we take into account the residual deformations - δ , which (according to Palmgren) with point contact of steel bodies with hardness $H = (63 \dots 65)$ HRC are:

$$\delta = 1.25 \cdot 10^{-7} P^2 (k_{11} + k_{12}) (k_{21} + k_{22}) / d_2 \tag{2}$$

where k_{11} , k_{12} , k_{21} , k_{22} - principal curvatures; d_2 - diameter of the rolling specimen.

When the hardness decreases, the deformations increase sharply. The experiments were carried out with hardness of bodies $H = (61 \dots 62)$ HRC. The total magnitude of the tangential load may change, which, however, does not explain the behavior of the $N = N(T_\Sigma)$ dependence at $P = \text{const}$.

Analyzing the results of experiments, under the assumption of the presence of Coulomb friction, the change in T , can be related to the presence of slip within the instantaneous contact spot. The inevitable breaking under the load of the conditions of "pure" rolling leads to the appearance within the contact area E of regions with zero and nonzero relative slip velocities of the s -regions of adhesion E_0 and slippage E_+ : $E = E_+ \cup E_0$

$$T_\Sigma = \Sigma T_0 + \Sigma T_+ \leq f P \Sigma.$$

The case $T\Sigma = f P \Sigma$ corresponds to complete slippage.

Within the present work, tangential loads in the rolling contact were detected in the presence of slip and cohesion on the basis of the variational approach [10], in accordance with which the problem reduces to minimizing the Kalker functional [11], which

is interpreted as the principle of minimizing the dispersion of additional energy on the actual velocity field.

$$\int_E [f P |s| (\tau) - \tau(s)(\tau)] dx dy \quad (3)$$

at $\forall(x, y) \in E_+; \tau_+ = f P(s/|s|); \forall(x, y) \in E_0; \tau_+ \leq f P$.

$$\mathbf{s} = -\mathbf{VB}(\tau) + \mathbf{v} \quad (4)$$

where V - characteristic rolling speed; $\mathbf{B}_{(\tau)}$ - component of slip velocities due to elastic deformations of bodies; \mathbf{v} - speed of slippage of bodies, as absolutely rigid.

4 Discussion

In spite of the assumptions made in the cited papers: the lateral rotation of the ball, the rigidity of the system, which was inevitable by the braking method, was not taken into account, and the friction coefficient f was assumed constant; for E_+ and E_0 , they qualitatively confirmed the tendency of the increase in the slip region and the tangential load T_Σ depending on The degree of inhibition. Thus, for $f = 0.045$; $P_\Sigma = 1670H$; $v = 0.262$ m/s; $\Omega = 26.67$ 1/s (orbital velocity), the following results are obtained.

1. $\omega = 24.085$ 1/s - the angular velocity of rotation of the ball around its own axis; $v \rightarrow 0$; $E_+ \rightarrow 0$; formally - "pure rolling".
2. $\omega = 23.943$ 1/s; $v = 0.735 \cdot 10^{-3}$ m/s; $T_+ = 0.63fP_\Sigma$; $T_0 = 0.16fP_\Sigma$; $T_\Sigma = 0.79fP_\Sigma$.
3. $\omega = 23.208$ 1/s; $v = 0.453 \cdot 10^{-2}$ m/s; $T_+ = T_\Sigma = 1.0fP_\Sigma$; $E_0 \rightarrow 0$ is the total slippage.

The braking of the rolling element leads to a decrease in the angular velocity of rotation of the ball around its own axis with the same orbital rotation. $v = 0.5 (\Omega d_1 - \omega d_2)$. With decreasing ω , the slip velocity increases, which leads to the degeneration of the region E_0 (see Fig. 3) and an increase in T_Σ : $\lim_{E_0 \rightarrow 0} T_\Sigma = 1.0fP_\Sigma$. Thus, it seems logical that a change in the rolling resistance coefficient is a consequence of the degeneration of the adhesion regions and the transition of the "rolling with external tangential load" regime to the "rolling with slip" regime.

If the change in the magnitude of the tangential load at a constant normal stress is due to the presence and variation within the instantaneous contact patch of the slip and adhesion regions, the process of destruction of the surfaces may be associated not only (and not so much) with the magnitude of the tangential frictional stresses - but also with the concentration of these stresses near the interfaces of the regions E_+ and E_0 . In the experiments [12] (pulsating contact "ball-plane") in the central zone of the contact area, where the pressures are maximum, traces of instrumental surface treatment remain. Areas of destruction with traces of fusion are localized closer to the periphery of the site. In the experiments discussed above, the primary cracks had an enveloping arc character. In all cases, the defective zones corresponded to the expected boundaries for the separation of the slip and bond regions.

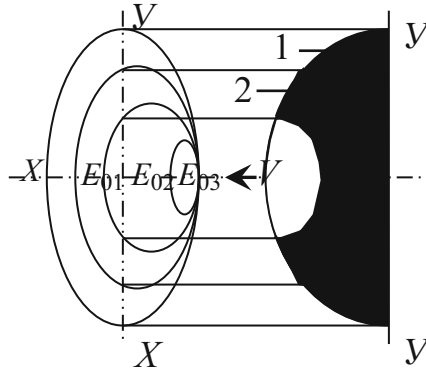


Fig. 3. Degeneration of the adhesion region with increasing slip velocity: $v = \text{const}$; $v_1 < v_2 < v_3$.

In [12, 13], similar damage occurred under the action of a purely normal load, which is in good agreement with the experiments discussed above.

It is known that sliding of conjugate surfaces even in micro volumes begins only after having passed the stage of elastic and elastic-plastic displacement. Then $\text{grad } \tau$ will in many respects be determined by the position of the interfaces of the zones. Let the region E_0 be sufficiently large at the initial position, as shown in Fig. 4. Let us consider the change in the tangential stresses in the degeneracy of the cohesion region (Fig. 5). In position 1, the interfaces E_0 and E_+ correspond to zones of contact with relatively small specific loads (both normal and tangential). The constriction of E_0 leads not only to a certain increase in T_Σ , but also to the displacement of the interfaces into the region of increased pressures, determining the increase of $\text{grad } \tau$ -position 2. However, with a further increase in the velocity v , the region of adhesion, degenerating, again exits its boundaries to the periphery of the contact spot, and the effect of concentrating shearing stresses is reduced.

Such a change in $\text{grad } \tau$ quite clearly corresponds to a change in the durability of the samples in the interval of variation of the rolling resistance coefficient “k” from 0.01 to 0.04 (Fig. 2).

The influence of residual deformations can be affected in two ways - as a reduction in the effective contact stresses due to a more dense contact of the contacting surfaces, and an increase in the influence of tangents - as a result of the appearance of alternating slip in the contact area. In [2] for samples [9] with a normal load $P\Sigma = 1670$ H, a residual (according to the Palmgren) deformation $\delta = 0.030$ mm (at $P_\Sigma = 2340$ H $\delta = 0.057$ mm). This shows - as a result of plastic run-in, after several dozen cycles, there are grounds to regard contact as “rolling the ball along an adjacent trench”. In this case, the contact area is divided into three subregions (Fig. 5) - central, where slip is positive, and two external ones with negative slip. The boundaries of separation are zero-slip lines of y_{so} . Near these lines, the direction of the tangential stresses changes to the opposite, which naturally increases the effect of their concentration. The total tangential load is reduced, but there is a “hard shock” of the tangential stresses in the contact of the rolling bearings noted by a number of authors

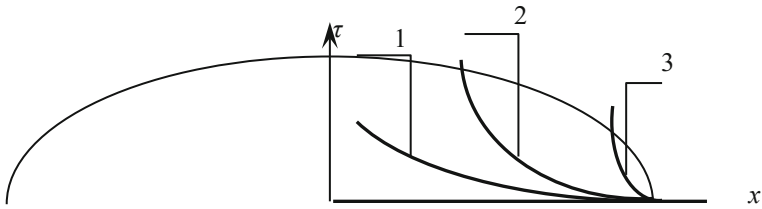


Fig. 4. The change *grad* τ as the coupling region degenerates

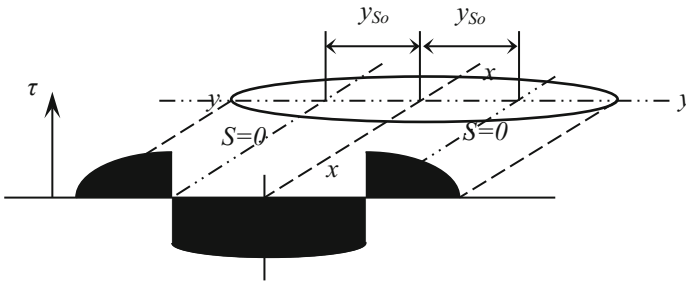


Fig. 5. The distribution of tangential stresses with alternating slip

5 Conclusion

The Kalker functional assumes rolling under conditions of dry friction. However, the appearance of pitting centers in the near-pole zone of the lagging surface is in qualitative agreement with the possible interface between the E_+ and E_0 regions in gears operating with the presence of a lubricant. Wear of peripheral areas (by Ignatisev) is certainly an aggravating “additive”, and a flash of the coefficient of friction (according

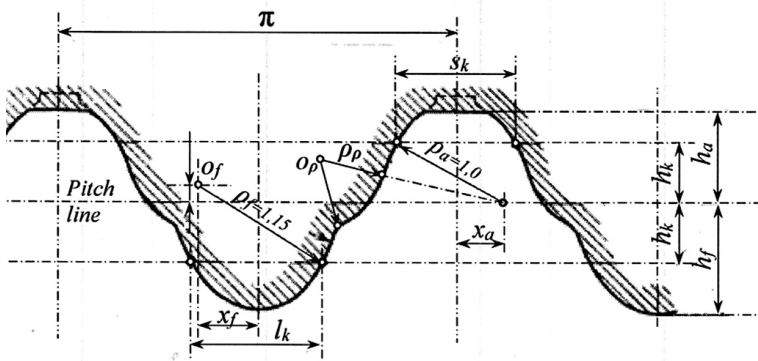


Fig. 6. The initial contour of Novikov gears with two lines of engagement DLZ1.0-0.15 (all sizes in fractions of the normal module)

to Trubin) may turn out to be some analog of a “hard blow”. But in any case, the contact area in which there is no geometric slip is potentially dangerous.

In involute gearing, the transition of the slip velocity “through zero” with a change in direction is inevitable. The attempt to pull the pole out of the engagement process is not realistic, because for traditional designs, a positive gear shift $x_f \geq 1.0$ is required, which is unacceptable by sharpening (even without counting other factors). This problem is practically absent in Novikov transmissions of the type GOST 30224-96 or DLZ 1.0-0.15 (Fig. 6), in which the circumpolar zone has a concave profile (in the initial contour - the arc radius ρ_p) and is fundamentally excluded from the engagement process.

According to the contact strength, all known designs of these transmissions exceed the equivalent involutes by two or more times, and where there are no rigid axial dimensions, and the support nodes can perceive significant axial forces, their application is uniquely justified.

References

1. Korotkin, V.I., Onishkov, N.P., Kharitonov, Y.D.: Novikov Gearing: Achievements and Developments, pp. 1–249 (2011)
2. Korotkin, V.I., Onishkov, N.P., Kharitonov, Y.D.: *Handb. Eng. J.* **6**, 11–17 (2015)
3. Beskopylny, A.N., Veremeenko, A.A., Yazyev, B.M.: *MATEC* **106**, 04004 (2017)
4. Chepurnenko, A.S., Andreev, V.I., Beskopylny, A.N., Jazyev, B.M.: *MATEC* **67**, 06059 (2016)
5. Ignatisev, R.M.: *Russ. Eng. Res.* **9**, 59–61 (2005)
6. Paulson, N.R., Golmohammadi, Z., Walvekar, A.A.: *Tribol. Int.* **115**, 348–364 (2017)
7. Wang, W.J., Lewis, S.R., Lewis, R., He, C.G., Liu, Q.Y.: *Wear* **376–377(B)**, 1892–1900 (2017)
8. Burbank, J., Woyd, M.: *Wear* **360–361**, 29–37 (2016)
9. Korotkin, V.I., Kolosova, E.M., Onishkov, N.P.: University News. North-Caucasian Region. Technical Science Series, vol. 3, pp. 57-63 (2011)
10. Goldshtein, R.V., Zazovski, A.F., Spector, A.A., Fedorenko, R.P.: Institut Mechanical Problems RAN Russia, pp. 1–67 (1979)
11. Kalker, J.J.: *Trans. ASME J. Appl. Mech.* **38**, part 1, 875–880
12. Tyler, J.C., Burton, R.A., Ku, P.M.: *Trans. ASLE* **6**, 255 (1963)
13. Beskopylny, A.N., Liapin, A.A., Andreev, V.I.: *MATEC* **117**, 00018 (2017)

Power Distribution Control in the Transmission of the Perspective Wheeled Tractor with Automated Gearbox

Roman Didikov^(✉) , Roman Dobretsov , and Yuriy Galyshev 

Peter the Great St. Petersburg Polytechnic University,
Politekhnicheskaya str., 29, St. Petersburg 195251, Russia
Didikov-r@yandex.ru

Abstract. The article suggests a mathematical model, describing the motion of a tractor with hinged frame and the power distribution mechanism in the transmission, on the basis of Routh equation. The authors completed analysis of possible power distribution mechanism application solutions in the transmission of the tractor, evaluated different packaging solutions for the power distribution mechanism in the tractor transmission. The authors proposed methodology to determine the parameters of the inter-wheel power distribution mechanism, which is used as a part of the 4th drawback category tractor transmission. Kinematic scheme solutions for such mechanism are proposed. The authors evaluated the effect of power distribution mechanism on the resistance torque in a steering mechanism of the tractor with a hinged frame.

Keywords: Transport · Wheeled tractor · Automated gearbox

1 Introduction

In the ideal case, possibility to control the power flows in the transmission allows to optimize the power input to each wheel of the traction-transport or transport vehicles, considering the actual driving conditions. For the wheeled tractor with two or more driven axles the task of the power distribution between driven axles resolved by installation of the geared clutch which is used to engage an additional axle. Such clutch can be embedded in the automatic gearbox casing or can be a separate unit of the transmission.

Power distribution between driven axles requires installation of the special power distribution mechanism. The simplest example of such a mechanism is an inter-wheel differential.

Tractors, which utilize the cornering principle through turning of the steered wheels have little demand in the power distribution control. In the transmission of tractors, utilizing the skid steering principle (at first it is tracked vehicles) such function is realized with a steering mechanism. Tractors with a hinged frame which utilize the cornering function through the turning of the frame sections in the motion plane are not equipped with such mechanisms. The demand to control the power distribution at least between the wheels of the front driven axle for the vehicles of such construction does

exist as far as purely kinematic turning requires generation of great efforts with the hydraulic cylinders, turning the sections. As well it is demanded to have improved ride and handling and driving stability in the transport mode and to minimize the corridor, occupied by the chassis when making a turn. With the statements above we justify the timeliness of the idea to develop the power distribution mechanism for the wheeled tractor with a hinged frame.

2 Literature Review

Analysis of the modern literature sources and of the existing tractor designs [1, 2] has shown that devices that allow to realize different algorithms of operation (i.e. to quantitatively and qualitatively control the power distribution between the wheels) are not used. That can be explained by the fact that manufacturers has objectives to reduce the cost of the tractor an at the same time there is no direct request to have such function from the customer – agricultural and farming industry.

In the adjacent industries of the mechanical engineering, which are concerned with the manufacturing of the tracked transport vehicles and automobiles, significant experience of design, manufacturing and exploitation of the power distribution mechanisms which utilize complex operational algorithms has been accumulated.

For the tracked vehicles, the mechanism with a similar function is presented as a turning mechanism. The theoretical basis has been formed and efficient design solutions of steering drives has been tried out as well for turning mechanisms [3]. The researches take place in the present state of the art [3–8]. Methods to determine the parameters of the turning mechanism [3–5] are used as a basis in presented researches.

Automotive industry is characterized with a big variety of the power distribution mechanisms [10–15]. Modern construction of such mechanism [14, 15] allow operation with the electronic control systems. There are no publications, which describe methods of parameters determination for such mechanism, except author’s proposals, presented in [16–18].

We can conclude that in the modern scientific literature has formed prerequisites for development of the tractor and transport-traction (technological) power distribution mechanisms theory. The purpose of this research – determination of the scheme solution (in perspective – development of proto unit) of the power distribution mechanism for the 4th drawback category tractor. Examined objectives and tasks – development of the mathematical model of the cornering tractor which take into account operation of the power distribution mechanism; determination of mechanism parameters; search of the kinematic scheme solutions and development of the approaches for realization of at least one scheme as a proto construction.

3 Materials and Methods

Following hypothesis are taken into account for tractor turning process modeling, the purpose of which is to assess the influence of the power distribution mechanism operation on the motion process:

- cornering of the two-axle tractor with hinged frame take place in the horizontal plane; tractor is influenced with the force and the action direction, value and the coordinates of the force application point are known;
- original task is started in non-holonomic formulation;
- ground area is deformable, characteristics are isotropic and defined through rolling resistance coefficients and adhesion coefficients with the ground; longitudinal reactive forces on the wheels are considered as a direct proportion to normal reactions;
- tractor tires are pneumatic, deformable, tire slip angle is taken into account; transversal reaction on the wheel and slip angle linked with a direct proportional dependence; the proportion coefficient is taken based on literature sources.

The modeling of the cornering is made through comprising of the Routh equation, describing the dynamics of the mechanic system (E. Routh about 1876 y.). Traditional for transport vehicles motion theory simplifications considered (fundamental theories of N.A. Zabavnikov, E.Ya. Ageykin, M.G. Bekker, I. Rokar, J. Wong et al., published in the second half of XX century).

Simplified homonymic model of the side cornering of the vehicle used, which does not take into account the deformation of the ground surface and tires. Such type of models are used in the transport vehicles motion theory for initial evaluations and calculations.

The power distribution mechanism synthesis issue is not considered within the research scope. Structural design solution of the tractor is based on the solutions, applied on the tractor K-700, but significantly differentiate due to introduction of the new power distribution mechanism for the front driven axle.

4 Results

Key results of the research:

- proposed the mathematical model of the cornering two-axle tractor with a hinged frame, which allow to evaluate the influence of the power distribution mechanism in cornering process;
- defined the values for key external parameters of the power distribution mechanism and the calculation method explained;
- proposed a power distribution mechanism kinematic scheme, satisfying the calculated values of the external parameters.

5 Discussion

Different approaches can be realized to package the power distribution mechanism in the transmission of the two-axle wheeled tractor of the 4th drawback category. On the Fig. 1 presented the most simple packaging solution when the mechanism is installed instead of the symmetrical geared differential or analogous device.

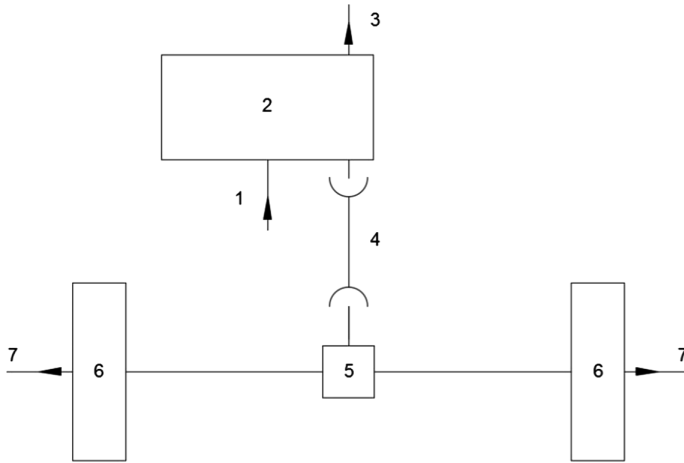


Fig. 1. Generalized scheme of the wheeled tractor transmission with front axle power distribution control: 1 – power input from the engine; 2 – automatic gearbox; 3 – power output to the rear axle; 4 – cardan drive; 5 – power distribution mechanism; 6 – wheel reduction gear; 7 – power output to the driven wheels.

Another packaging solution can be realized which considers the parallel power stream. Such solution is reflected in the research [19]. It is more complex solution and it requires much greater modification of the transmission than first solution.

Utilization of the packaging solution reflected on the Fig. 1 allow to vary the traction force ratio on the wheels on the front driven axle and influence the resistance torque of the steering unit. Normally, the tractor is used in the transport mode when the rear axle is not engaged. In such mode it is crucial to have appropriate ride and handling which is demanded by the safety requirements on the public roads and other reasons as well.

The tractor with hinged frame, moving in the horizontal plane can be mathematically described by the Routh equation. Related calculation scheme is reflected on the Fig. 2:

$$\frac{d}{dt} \left(\frac{\partial T}{\partial \dot{q}_k} \right) - \frac{\partial T}{\partial q_k} = Q_k + R_k, k = 1, 2, \dots, n \quad (1)$$

In the equation T - kinetic energy of the system; q_k - generalized coordinate; Q_k - generalized force, corresponding to k -th generalized coordinate and derived from elementary work expression; R_k - generalized reaction force of the nonholonomic or kinematic-force link, corresponding to k -th generalized coordinate; n - number of generalized coordinates.

According to calculation scheme on the Fig. 2, tractor location is defined by eight generalized coordinates: x_0 and y_0 - coordinates of the vertical joint 0 relatively to the origin of coordinates for the chosen system of axis XOY ; v and Θ - rear frame section longitudinal axis alteration angle relative to OX coordinate axis and the angle between sections respectively; ψ_{11} and ψ_{12} , ψ_{21} and ψ_{22} - corresponding wheels turning angle.

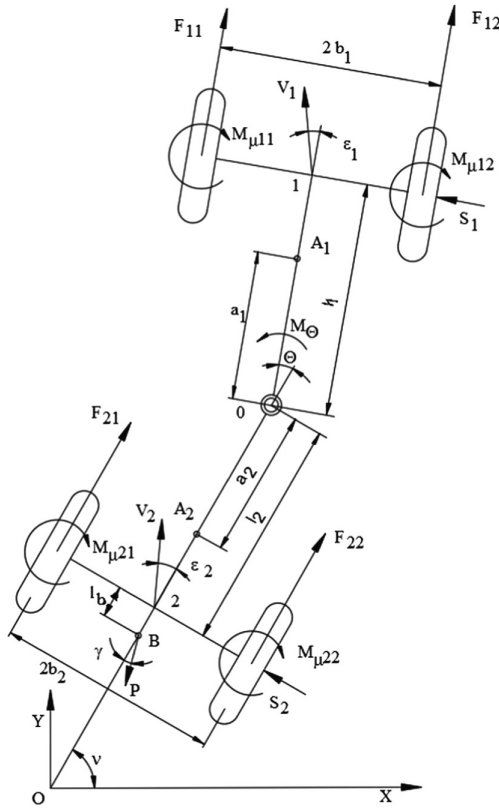


Fig. 2. Scheme of forces, acting to the moving tractor when cornering.

Other nomenclature on the Fig. 2: F_{11} and F_{12} , F_{21} and F_{22} - longitudinal forces, acting on corresponding wheels; $2b_1$ and $2b_2$ - width of the front and rear axle track; S_1 and S_2 - transversal forces for the front and rear axes; A_1 and A_2 - centers of gravity for the front and rear sections; a_1 and a_2 - distance from the hinge joint 0 to the gravity centers of each section, measured along longitudinal axis; l_1 and l_2 - distance from the joint 0 to axle axis (points 1 and 2); l_b - distance from the rear axle center to point B (point of traction force P_b on hook application); γ - P_b force line alteration from the longitudinal axis of the rear section; M_Θ - torque, generated by hydraulic cylinders of the steering mechanism.

Solution of the Routh equation allowing, in particular, to get expression for M_Θ calculation:

$$M_\Theta = m_1 a [-\ddot{x}_0 \sin(v + \Theta) + \ddot{y}_0 \cos(v + \Theta)] + (J_1 + m_1 a_1^2) (\ddot{v} + \ddot{\Theta}) + M_{\mu 11} + M_{\mu 12} + b_1 (F_{11} - F_{12}) - l_1 S_1 \tag{2}$$

Following nomenclature is used in the dependence above: J_1 - front section momentum of inertia; \ddot{x}_0 and \ddot{y}_0 , \ddot{v} and $\ddot{\Theta}$ - linear and angular acceleration for corresponding coordinates.

Expression above contains elements, characterizing dynamic and static components of the M_{Θ} . Calculations and data from literature sources allow to assume, that under cornering conditions without slippage, static component is not less than a half of M_{Θ} value.

According to data from sources [4, 5], turning resistance moment can be defined through the dependence:

$$M_{\mu ij} = \chi L \mu_{ij} G_{ij} \quad i = 1, 2 \quad j = 1, 2 \tag{3}$$

Here $\chi = 0.25 \dots 0.33$ – coefficient, taking into consideration the shape of the tyre contact patch; $L = 0.6$ – length of the tractor tyres contact patch; μ_{ij} and G_{ij} - coefficient of cornering resistance on the given ground and load on the wheel.

Transversal forces can be defined based on the I. Rokar hypothesis:

$$S_i = K_{yi} G_i, \quad i = 1, 2$$

Here K_{yi} - cornering coefficient of tyre for particular axle; G_i - load on axle. Approach for K_{yi} determination is based on calculation data, presented in literature sources. For indicative calculations, values from the range 0.2...0.3 can be taken, that represent the turning at the limit when the lateral slippage starts.

Values $(F_{11} - F_{12})$ depend on specifics of the power distribution mechanism operation, installed on the front axle. In case if standard type differential applied, the difference equal to zero. Power distribution mechanism with ratio $u_M = F_{12}/F_{11} > 1$ allow to get $(1 - u_M) < 0$, thus to reduce M_{Θ} value. The maximum value of u_M can be defined if to take an assumption, that the tractions force on the surpassing wheel is achieving the adhesion limit, while the slower wheel is overcoming the rolling resistance. Under the statistically average conditions u_M achieve the value of not less than 3...3.5.

On the other hand the ratio has to meet the conformity principle for steering mechanism and power distribution mechanism operation: under conditions of turning with the minimum radius there must be no slippage. Such approach has been utilized by authors in the research [17].

Inter-side ratio and the minimum turning radius of the sections are linked according to expressions [17]:

$$u_M = (2\rho_{\min} + 1)/(2\rho_{\min} - 1), \tag{4}$$

where $\rho_{\min} = R_{\min}/(2b_1)$, R_{\min} - minimal turning radius of the section.

For calculation value $R_{\min} = 5.3$ m we get $u_M = 1.44$. This value corresponds with the ratios $u_{O1} = 1.22$ and $u_{O1} = 0.84$ from the driving link to the output link of the mechanism.

Traditional kinematic schemes synthesis approaches for planetary gear with two degrees of freedom for given values u_{O1} and u_{O1} allow to get solution, but the mechanism will have great radial size. Introduction of additional planetary gear with constant ratio has been proposed to reduce radial size. Therefore the range of kinematic schemes can be developed with required ratios and acceptable radial sizes. On the Fig. 3 presented a calculation scheme for one of the mechanisms.

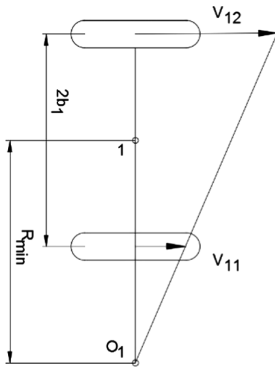


Fig. 3. Calculation scheme for determination of power distribution mechanism ratio

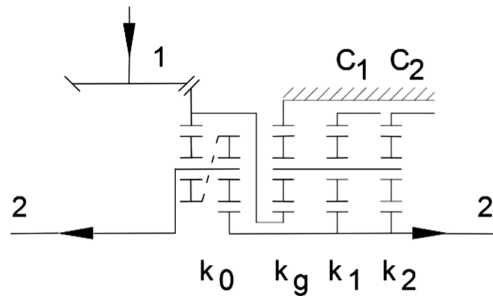


Fig. 4. Variant of the power distribution mechanism kinematic scheme: 1 – power input from the cardan shaft; 2 – power output to the driven wheels; C1 and C2 - control elements; k – kinematic parameters for the rows

For the scheme on Fig. 4 the following kinematic parameters has been obtained: $k_0 = 2$; $k_g = (-2.5)$; $k_1 = (-1.868)$; $k_2 = (-3.167)$.

Based on educated estimates, utilization of the mechanism with inter-side ratio of 1.44 allow to reduce the static component of the resistance torque, overcoming with the hydraulic steering mechanism almost by 1.5 times, under statistical average conditions.

Gradual change of the inter-side ratio can be achieved with the pressure pulse-width modulation in the hydraulic drive of the control elements (brakes) in the power distribution mechanism [7, 8, 17].

Results of the research submitted to Federal Institute of Industrial Property and positive decision granted for the patent of invention in April 2017.

6 Conclusions

1. The load on the steering plungers of the hydraulic steering unit can be reduced by up to 10-15% and the ride and handling performance in the transport mode can be improved through application of the power distribution mechanism;
2. Methodology for determination of the power distribution mechanism external parameters can be used for transport and traction-transport wheeled vehicles of different purpose and utilizing different cornering control methods;

- In order to reduce the overall size and improve reliability and the life of the mechanism, it is purposeful to use the materials and technologies, developed for the steering mechanisms of the high-speed tracked vehicles.

7 Acknowledgement





The present research work has been carried out with financial support from the Ministry of Education and Science of the Russian Federation in the frames of the federal targeted program “Research and Development in the Priority Areas for the Development of Science and Technology Sector of the Russian Federation for 2014–2020” pursuant to the project: “The Design Of The New Model Series Of Automated Boxes Change Gears For Agricultural And Road-Building Equipment In The Range Of 140–440 kW, Adapted For Use In Complex Systems Unmanned Tractor”(Unique Project Identifier RFMEFI57816X0213).

References

- Sharipov, V.M.: Calculation and Design of a Tractor. Mashinostroenie, Moscow (2009)
- Kartushin, G.K., Bazhenov, S.P.: Design, Basic Theory, Calculation and Testing of Tractors. Agropromizdat, Moscow (2001)
- Wong, J.Y.: Theory of Ground Vehicles, 3rd edn (2001)
- Shelomov, V.B.: Theory of Motion of a Multi-Purpose Tracked and Wheeled Vehicles. Polytechnic university publishing, Saint-Petersburg (2013)
- Shelomov, V.B., Dobretsov, R.Y.: Tracked vehicle engine and turning drive mechanism friction element slipping power. Sci.-Tech. J. St. Petersburg State Polytechnic University **N2-2**, 87–89 (2010)
- Galyshv, Y.V.: Researches and projects of St. Petersburg State Polytechnic University scientists in the field of defense equipment. Sci.-Tech. J. St. Petersburg State Polytechnic University **N1**, 26–32 (2014)
- Galyshv, Y.V., et al.: Closed loop turning control system in the tracked vehicles. Sci.-Tech. J. St. Petersburg State Polytechnic University **N3-2**, 201–208 (2014)
- Dobretsov, R.Y.: Friction Type Turning Mechanism in the Double Stream Transmission of the Tracked Vehicle, pp. 121–124. Polytechnic University publishing, St. Petersburg (2014)
- Demidov, N.N., et al.: Tracked Vehicles: the Nonlinear Steering Mechanism, pp. 898–912. Polytechnic university publishing, St. Petersburg (2016)
- Karunin, A.L., et al.: Automobile design. Chassis. Mashinostroenie, Moscow (1987)
- Kravets, V.N.: Vehicle Theory. N. Novgorod, NGTU (2007)
- Gladov, G.I., Lobanov, S.A.: Differentials with controlled torque distribution on the wheels. “Automob. Ind.” J. **N5**, 36–40 (2004)
- Bosch: Automotive Handbook. “Za rulem” publishing, Moscow (2004)
- http://www.irs.kit.edu/download/131213_GC_TorqueVectoring_ZF_Handout.pdf. Accessed 24 July 2015
- Ushiroda, Y., Sawase, K., Takahashi Suzuki, K., Manabe, K.: Development of Super AYC «Technical review». №15, pp. 73–76 (2003)
- Didikov, R.A., Dobretsov, R.Y.: Regarding the kinematic schemes choice issue for the geared power distribution mechanism. “Automob. Ind.” J. **N9**, 12–14 (2014). Moscow

17. Didikov, R.A., Dobretsov, R.Y., Rusinov, R.V.: Regarding possibility to apply hydraulic drive in the power distribution mechanism. Bull. Soc. Automot. Eng. **N5**(100), 30–32 (2016)
18. Didikov, R.A.: Methods of power balance equitation components definition for the power distribution mechanism in the vehicle. Bull. Siberian State Automob. Highw. Acad., SibADI **N4**(50), 61–63 (2016)
19. Didikov, R.A., Dobretsov, R.Y., Galyshev, Y.V.: Kinematic scheme variants of the double stream transmission for the perspective tractor with automatic gearbox: prospects of the 6th Russian applied research conference with international participation. Rubtsovsk Industrial University publishing, pp. 113–120 (2016)

Stress-Strain State and Plasticity Reserve Depletion on the Lateral Surface of Workpiece at Various Contact Conditions During Upsetting

Volodymyr Kukhar^{1,2} , Viktor Artiukh^{1,2} ,
Andrey Butyrin^{2,3} , and Andrii Prysiashnyi¹ 

¹ Pryazovskiy State Technical University,
Universytetskaya str., 7, Mariupol 87500, Ukraine
artiukh@mail.ru

² Peter the Great St. Petersburg Polytechnic University,
Polytechnicheskaya str., 29, 195251 Saint-Petersburg, Russia

³ Moscow State University of Civil Engineering,
Yaroslavskoe shosse, 26, Moscow 129337, Russia

Abstract. The stress-strain state and the indices of the plasticity reserve depletion on the lateral surface of workpieces at the site of the greatest barreling after upsetting with dry and lubricated dies are compared in paper. The estimation of the calculation results by methods of the plasticity flow and deformation theory was done. It was found that the application of lubricants to the contact surfaces of workpieces at upsetting reduces the depletion of plasticity reserve, which prevents to the formation of conditions for the formation of surface damages. A comparative analysis shows that the value of the index of depletion of plasticity reserve at upsetting determined with using the strain theory by 20...25% less than those calculated on the plastic flow theory.

Keywords: Upsetting · Barreling · Stress-strain state
Depletion of plasticity reserve · Lubricant

1 Introduction

The problem of the stress-strain state valuation, especially in terms of the development of new technological processes, is very complex and important. The plasticity of the material under specified conditions is the main characteristic for the selection of the technological transitions and largely depends on the deformation temperature and implements schemes of stress-strain state. The knowledge of the plasticity reserve index allows setting the right deformation modes and exclude of surface and internal discontinuities in the workpiece.

2 Analysis of Researches and Publications

Typically, while upsetting with flat dies, the defects appear on a free lateral surface at the site of the maximal barreling [1–3]. Forming and stress-strain state depends not only from the compression ratio, but also from contact conditions, initial shape and

material of workpiece, forces of the systems, temperature and strain rate [3–8]. This barreling phenomenon can be considered as a method of useful application of non-uniform deformation of the workpiece in order to set the form of the workpiece closer to the shape of a finished forging [9, 10]. To determine the stress-strain state at upsetting by theoretical methods there engineering method, slip-line method, variation methods, finite elements method etc. are applied the most [11–14]. Fundamentals of research on depletion of plasticity reserve are given in works [15–17]. The use of different criteria for evaluation of index of plasticity reserve depletion, damage accumulation based on tensor and nonlinear models did not show essential differences in the results for the hot-forming of ductile materials [18–23].

However, these methods do not take into account the dependence of metal plasticity from the stress-strain state, temperature, and surface conditions at upsetting billets or workpieces accurately. Particularly, the relevance was shown in the works [24, 25] at the present stage of development of the theory and technology of metal forming processing, solving problems of determination of deformation conditions without any damage in the real production process with the formulation of the boundary conditions based on the study of contact interaction of deformable material with a solid tool. The upsetting of workpieces is used as a universal test on material deformability (workability) [26–28], to study of damages behavior in metal-forming processes [29, 30]. It is often the label applied to the lateral surface in areas of maximum barrelling [25–28] or using the various configurations dies [31, 32].

To assess of stress-strain state by analytical methods were developed plastic flow theory and the finite strain theory [11, 12]. The quantitative difference between the results of different approaches has not yet been established and will be a new scientific and practical knowledge required to evaluate the stress-strain state, residual life and the choice of forming sequence.

3 The Purpose of the Research

The work objective was to determine the stress-strain states on the lateral surface of the upset workpieces at different deformation modes, and contact conditions on the basis of the phenomenological theory of plasticity with tensor analysis in Cartesian coordinates.

Material of the research. The index of plasticity reserve depletion was determined by the phenomenological theory of failure. For monotonic process the stress state index (K) as well as Lode coefficient (ν) remain unchanged i.e.

$$K = \sigma/T = \text{const}; \nu = \text{const} \quad (1)$$

where σ is the average hydrostatic stress;

T – shear stress intensity.

In the given point ($a_0 \times b_0$ square) on the lateral surface of the specimen, the main stress axis σ_n (Fig. 1) and the main directions of logarithmic deformations ε_n and strain rate ξ_n coincide with the axis of the cylindrical coordinate system, which corresponds to the conditions of the monotonious process. For the points located on the horizontal

axis of symmetry the main logarithmic deformations and strain rate at any point in time $d\tau$ is defined as

$$\bar{\varepsilon}_\theta = \ln \frac{d_n}{d_0}; \quad \bar{\varepsilon}_z = \ln \frac{b_n}{b_0} \quad \text{and} \quad \xi_\theta = \frac{d\bar{\varepsilon}_\theta}{d\tau}; \quad \xi_z = \frac{d\bar{\varepsilon}_z}{d\tau} \quad (2)$$

The stress state at the free lateral surface of the specimen can be determined by using one of the theories:

- the plastic flow theory (PFT):

$$\sigma_n - \sigma = \frac{2T(H; \lambda)}{H} \cdot \xi_n; \quad (n = 1, 2, 3); \quad (3)$$

where σ_n – the main components of the stress tensor; $T(H; \lambda)$ – shear stress intensity, which depends (at constant temperature) upon the intensity of shear-strain rate (H) and index: $\lambda = \int_0^t H d\tau$.

- deformational theory (DT):

$$\sigma_n - \sigma = \frac{2T(\bar{G})}{G} \varepsilon_n; \quad (n = 1, 2, 3) \quad (4)$$

where $T(\bar{G})$ – shear stress intensity as a function of the logarithmic strain intensity (\bar{G}).

At the conditions of monotonous process of plastic forming, according to the volume constancy law (continuity of deformation), we obtain $\bar{\varepsilon}_p = -(\bar{\varepsilon}_z + \bar{\varepsilon}_\theta)$.

In the main axes ($z; \theta; \rho$) of stress, normal to the free surface $\sigma_p = 0$. Using this condition, in the plastic flow theory, we have:

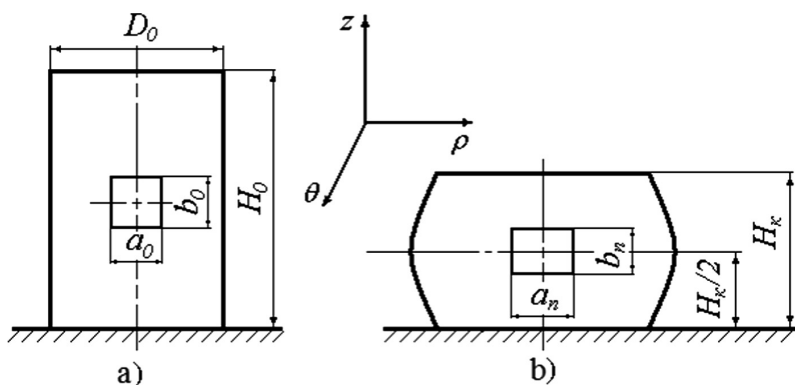


Fig. 1. Coordinate grid on free lateral surface of initial (a) and upsetting (b) workpiece (specimen).

$$\sigma = -\frac{2T}{H} \xi_\rho; \quad \sigma_z = \frac{2T}{H} (\xi_z - \xi_\rho); \quad \sigma_\theta = \frac{2T}{H} (\xi_\theta - \xi_\rho); \quad n = \rho; \quad \theta; \quad z. \quad (5)$$

Similarly to the deformation theory:

$$\sigma = -\frac{2T}{G} \bar{\varepsilon}_\rho; \quad \sigma_z = \frac{2T}{G} (\bar{\varepsilon}_z - \bar{\varepsilon}_\rho); \quad \sigma_\theta = \frac{2T}{G} (\bar{\varepsilon}_\theta - \bar{\varepsilon}_\rho). \quad (6)$$

Stiffness factor of the stress state scheme for the deformation theory (K_ε) and for the plastic flow theory (K_ξ) introduced correspondingly:

$$K_\varepsilon = \frac{\sigma}{T} = -\frac{2\bar{\varepsilon}_\rho}{G} \quad \text{and} \quad K_\xi = \frac{\sigma}{T} = -\frac{2\xi_\rho}{H}. \quad (7)$$

The intensity of the logarithmic strain (under the conditions of the monotonic process):

$$\bar{G} = 2\sqrt{\bar{\varepsilon}_\theta^2 + \bar{\varepsilon}_\theta\bar{\varepsilon}_z + \bar{\varepsilon}_z^2}. \quad (8)$$

The intensity of the shear strain rate (H) at any particular time (τ_n) is given by:

$$H = 2\sqrt{\xi_\theta^2 + \xi_\theta\xi_z + \xi_z^2} = 2\frac{\varepsilon}{\Delta\varepsilon_{\text{mid}}} \sqrt{\Delta\bar{\varepsilon}_{\theta,n}^2 + \Delta\bar{\varepsilon}_{z,n}^2 + \Delta\bar{\varepsilon}_{\theta,n}\Delta\bar{\varepsilon}_{z,n}}, \quad (9)$$

where

$$\xi_\theta = \frac{d\bar{\varepsilon}_\theta}{d\tau} = \frac{\Delta\bar{\varepsilon}_\theta}{\Delta\tau} = \frac{c}{\Delta\varepsilon_{\text{mid}}} \Delta\bar{\varepsilon}_\theta; \quad \xi_z = \frac{c}{\Delta\bar{\varepsilon}_z}; \quad c = \text{const.} \quad (10)$$

In finite difference form we suggest the following notation:

$$\Delta\bar{\varepsilon}_{\theta,n} = \frac{\bar{\varepsilon}_{\theta;n+1} - \bar{\varepsilon}_{\theta;n-1}}{2}; \quad \Delta\bar{\varepsilon}_{z,n} = \frac{\bar{\varepsilon}_{z;n+1} - \bar{\varepsilon}_{z;n-1}}{2}. \quad (11)$$

We determine the $\Delta\varepsilon_{\text{mid}} = c \cdot \Delta\tau$ dimension assuming that the strain rate $V = \text{const}$; then $\Delta h = V \cdot \Delta\tau$, as a result:

$$\frac{\Delta h}{h} = \varepsilon_{\text{mid}} = \frac{V}{h_0} \tau = c\tau. \quad (12)$$

Hence Lode ratios on the deformation theory:

$$v_{\varepsilon,n} = \frac{2\bar{\varepsilon}_{\rho,n} - \bar{\varepsilon}_{\theta,n} - \bar{\varepsilon}_{z,n}}{\bar{\varepsilon}_{\theta,n} - \bar{\varepsilon}_{z,n}}; \quad \bar{\varepsilon}_{\rho,n} > \bar{\varepsilon}_{\theta,n}, \quad (13)$$

and the flow theory:

$$v_{\xi,n} = \frac{2\xi_{p,n} - \xi_{\theta,n} - \xi_{z,n}}{\xi_{\theta,n} - \xi_{z,n}} = \frac{3(\Delta\bar{\varepsilon}_{\theta,n} + \bar{\varepsilon}_{z,n})}{\Delta\bar{\varepsilon}_n + \Delta\bar{\varepsilon}_{z,n}}. \quad (14)$$

The deformation index according to the flow theory can also be determined without calculating the constants c and $\Delta\varepsilon_{\text{mid}}$:

$$\begin{aligned} \lambda &= \int_0^{\tau=\tau_n} H d\tau = \sum_{\tau=0}^{\tau=n} \Delta\tau \cdot H = \sum_{\tau=0}^{\tau=n} 2 \frac{c}{\Delta\varepsilon_{\text{mid}}} \sqrt{\Delta\bar{\varepsilon}_{\theta,n}^2 + \Delta\bar{\varepsilon}_{z,n}^2 + \Delta\bar{\varepsilon}_{\tau,n} + \Delta\bar{\varepsilon}_{\theta,n}} = \\ &= \sum_{\varepsilon_{\text{mid}}=0}^{\varepsilon_{\text{mid}}=n} 2 \sqrt{\Delta\bar{\varepsilon}_{\theta,n}^2 + \Delta\bar{\varepsilon}_{z,n}^2 + \Delta\bar{\varepsilon}_{\theta,n} + \Delta\bar{\varepsilon}_{z,n}}; \end{aligned} \quad (15)$$

According to the theory of deformation, λ is equal to the intensity of logarithmic strain \bar{G} . The difference between the \bar{G} value and the λ value gives an indication of the non-monotonicity process index, the greater the inequality $\lambda > \bar{G}$, the more non-monotonic the process is.

Dependencies (7) and (15) make it possible at any particular time $\tau = \tau_n$ to determine K and λ and to build a curve of stress and strain progression history: $\lambda = \lambda_{\tau}$. Comparison of v_{ξ} with v_{ε} values at any stage of $\tau = \tau_n$ deformation, also gives an idea about the rejection of the deformation process at the point of interest from monotony. The index of plasticity reserve depletion was calculated after performing experimental research on deformation theory (Ψ_{DT}) and on the plasticity flow theory (Ψ_{PFT}), correspondingly:

$$\Psi_{DT} = \frac{\lambda}{\bar{G}} \quad \text{and} \quad \Psi_{TPF} = \int_0^{\tau} \frac{H d\tau}{\lambda_p}, \quad (16)$$

where λ_p – the critical index of deformation at a given value $K = \sigma/T$.

With the known λ_p and H values the plasticity reserve depletion is determined by a formula for the deformation theory and correspondingly the theory of flow:

$$\Psi_{DT} = \frac{\bar{G}}{\lambda_{\rho}(K_{\varepsilon})} \quad \text{and} \quad \Psi_{PFT} = \int_0^t \frac{H dt}{\lambda_{\rho}(K_{\xi})} = \int_0^t \frac{\lambda}{\lambda_{\rho}(K_{\xi})} \quad (17)$$

The upsetting of over-alloyed hard-to-form steel forging ingot was formed at a temperature of 900 °C was simulated during the experiment. The specimens material was Pb-Sb (up to 6% Sb) alloy. The conditions of simulation obeyed to the principles of similarity for approximate isothermal process how it was determined by A. Il'yushin, that will allow to determine the average ratings of stress-strain state characteristics. 1:20 scale of modeling reflects the shape and dimensions of forging ingots with a ratio of height to diameter of about two [33]. The material was previously pressed with an extrusion ratio 5.06 to obtain the exact size of the diameter of the

workpiece and qualitative lateral surface. The end surfaces of models (specimens) were put through a lathe. The height of specimens was presented by $H_0 = 80$ mm, the diameter by $D_0 = 40$ mm (Fig. 2).

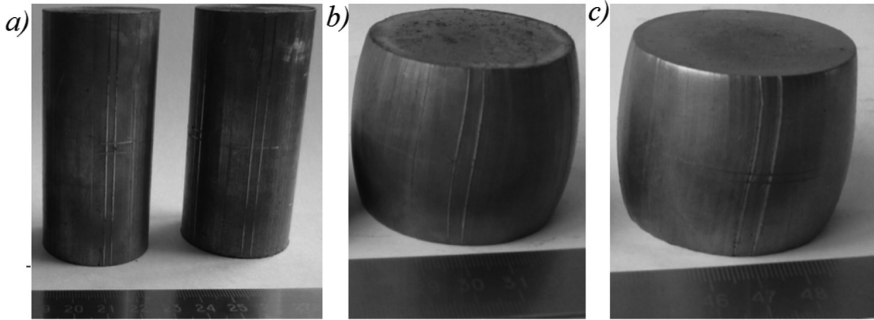


Fig. 2. Specimens before upsetting (a), after upsetting with dry (b) and greased (c) flat dies.

Prior to the upsetting the lateral surface of the specimen was covered by grid (Fig. 1) with cell 3×3 mm. The initial size of the specimen was measured with a 0.005 mm caliper. Before the upsetting the contact surfaces of flat dies were degreased with acetone. The first lot of specimen was upset with rough dry flat dies, the second lot was deformed with plates with contact surfaces which were greased with machine oil. The upsetting was carried out with a universal testing machine UMM-10 (0,1 MN) at stages with $\varepsilon_{mid} \cdot 100\% = [(H_0 - H_k)/H_0] \cdot 100\% = 10, 20, 30, 40$ and 50%, upsetting indices, τ time of deformation and the size of the grid cells on the lateral surface were recorded after every compression.

The data for the peripheral area of the rapid steel ($C = 0.73 \dots 0.8\%$, $Mo = 1\%$, $W = 17 \dots 18.5\%$, $V = 1 \dots 1.4\%$, $Si \leq 0.5\%$, $Mn \leq 0.5\%$, $Ni \leq 0.4\%$, $Cr = 3.8 \dots 4.4\%$) ingot at temperature of 900 °C was used to determine λ_p . The λ_p dependence upon the stressed state scheme was determined by the regression equation:

$$\lambda_p = b_0 + b_1 K_{\xi} + b_2 K_{\xi}^2, \tag{18}$$

where $b_0 = 2.95$, $b_1 = -5.92$, $b_2 = 3.09$ – regression coefficient.

Based on the above-discussed methods for determining the stress-strain state and index of plasticity reserve depletion algorithms and calculations of indicators were performed: $\bar{\varepsilon}_z$; $\bar{\varepsilon}_\theta$; $\bar{\varepsilon}_\rho$; $K_{\bar{\varepsilon}}$; \bar{G} ; $v_{\bar{\varepsilon}}$; Ψ_{DT} ; ξ_z ; ξ_θ ; ξ_ρ ; H ; λ ; K_{ξ} ; v_{ξ} ; λ_p ; Ψ_{PFT} . Particular attention while the construction of curves is paid to $\bar{\varepsilon}_z$; $\bar{\varepsilon}_\theta$; $\bar{\varepsilon}_\rho$ values. After the curves adjustment, the condition was tested: $\bar{\varepsilon}_z + \bar{\varepsilon}_\theta + \bar{\varepsilon}_\rho = 0$. Having analyzed the calculation results, it was possible to estimate the possibility of metal discontinuity at given upsetting conditions.

The dependencies were built according to the obtained results: $\bar{G} = f(\varepsilon_{mid})$ (Fig. 3), $K_{\bar{\varepsilon}} = f(\varepsilon_{mid})$ (Fig. 4), $v = f(\varepsilon_{mid})$ (Fig. 5), $\Psi = f(\varepsilon_{mid})$ (Fig. 6).

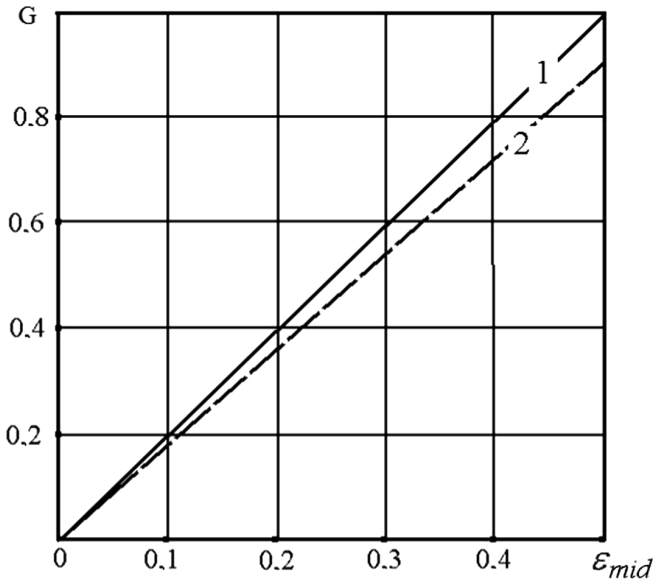


Fig. 3. The dependence of the deformation intensity \bar{G} on the deformation index ϵ_{mid} during the upsetting with dry (1) and greased (2) flat dies

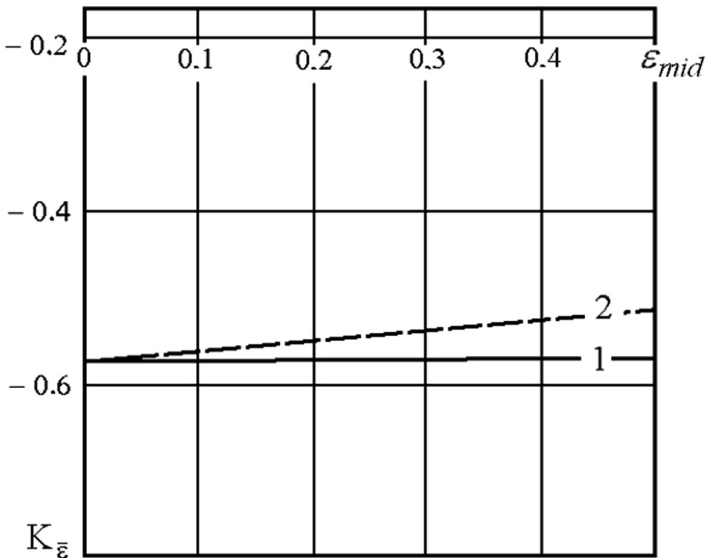


Fig. 4. Stiffness factor of the stress state scheme during upsetting with dry (1) and greased (2) flat dies.

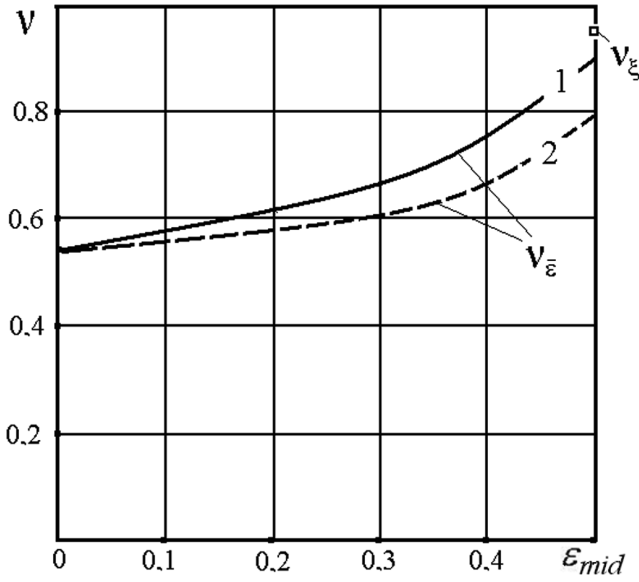


Fig. 5. The dependence of the Lode ratio v on the deformation index ϵ_{mid} during upsetting with dry (1) and greased (2) flat dies.

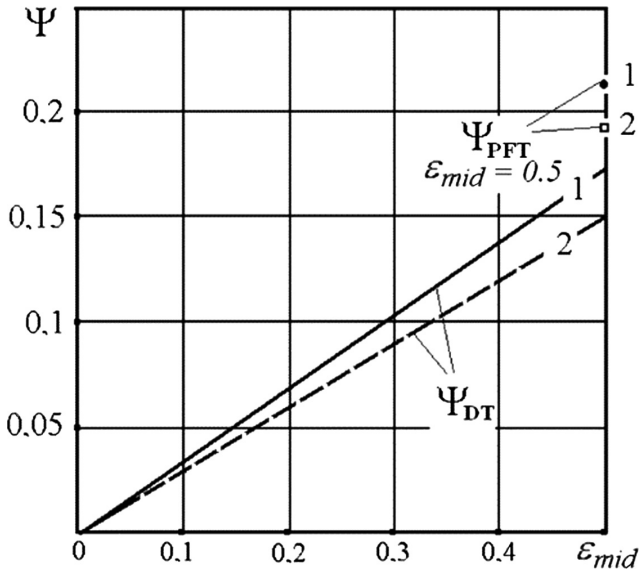


Fig. 6. The dependence of the plasticity reserve depletion Ψ on the deformation index ϵ_{mid} during upsetting with dry (1) and greased (2) flat dies.

Since the deformation theory does not take into account the load history, Ψ_{DT} , v_ε values, etc. were determined at all stages of deformation. The calculations according to the theory of plasticity flow determined Ψ_{PFT} value only after the last upsetting, which is why the v_ε and Ψ_{PFT} values represented with dots on Figs. 5 and 6, correspondingly.

Analyzing the obtained data presented in the form of graphs, it becomes clear that the change in the surface condition affects the stress-strain state and plasticity reserve depletion. The graphs on Fig. 5 show that the upsetting process is non-monotonic and local deformation index is greater rather than with the absence of greasing at the lateral surface, which is also confirmed by graphs on Figs. 3 and 6. The use of lubricant drops the plasticity reserve Ψ by 4...5% when $\varepsilon_{mid} \rightarrow 50\%$ (see Fig. 5).

Figure 4 shows that the upsetting with dry flat dies changes the scheme of stressed state. It is in all stages tougher than at upsetting with lubricated flat dies. Consequently, application of lubricants will help to provide a better surface of the workpiece for upsetting and better correction of surface defects.

The graph on Fig. 6 shows that the data about plasticity reserve depletion, defined by the deformation theory, is slightly less than by the plastic flow theory. This is due to the fact that the deformation theory does not take into account the load history.

The obtained data shows, that it is impossible to compare the results of upsetting with various temperatures without including the stress state, because in this case there are differences in the time at surface conditions, which can result in barrel distortion and different K_ε exponent values.

4 Conclusions

1. The greasing of the contact surfaces of workpieces is soften the stress-state scheme and favors to the monotony of upsetting process.
2. The usage of lubricants on the contact surfaces when drafting the workpieces modestly reduces the plasticity reserve depletion, which prevents from appearance of the conditions for formation of surface defects.
3. The index value of the plasticity reserve depletion at upsetting, defined by the deformation theory, are 20...25% less than those calculated on the plastic flow theory.

Acknowledgement. The reported study was funded by RFBR according to the research project №16-08-00845a «Verification and development of models of inelastic deformation at the passive loading». The authors declare that there is no conflict of interest regarding the publication of this paper.

References

1. Altinbalik, T.: An experimental study of barreling and FEM based simulation in cold upsetting of aluminum. *Int. J. Modern Manuf. Technol.* **III**(1), 9–14 (2011)
2. Baskaran, K., Narayanasamy, R., Arunachalam, S.: Effect of friction factor on barreling in elliptical shaped billets during cold upset forging. *J. Mater. Sci.* **42**, 7630 (2007). <https://doi.org/10.1007/s10853-007-1900-7>

3. Narayanasamy, R., Thaheer, A., Baskaran, K.: Comparison of barreling unlubricated truncated cone billets during cold upset forging of metals. *Indian J. Eng. Mater. Sci.* **13**, 202–208 (2006)
4. Narayan, S., Rajeshkannan, A.: Some aspects of barreling in sintered plain carbon steel powder metallurgy preforms during cold upsetting. *Mater. Res.* **15**(2), 291–299 (2012). <https://doi.org/10.1590/S1516-14392012005000029>
5. Altinbalik, T., Yilmaz, C.: An upper bound analysis and determination of the barreling profile in upsetting. *Indian J. Eng. Mater. Sci.* **18**, 416–424 (2011)
6. Mihalevich, V., Dobranjuk, Y., Trach, E.: Formozmina bichnoyi poverhni tsilindrychnykh zagotovok pid chas visesymetrychnogo osadzhennja. *Visnik NTU «KhPI»* **42**(1015), 126–131 (2013). <http://archive.kharkiv.org/view/35620>
7. Kajtoch, J.: Strain in the upsetting process. *Metall. Foundry Eng.* **33**(1), 51–61 (2007)
8. Mazur, V., Artiukh, V., Matarneh, M.: Horizontal force during rolling as indicator of rolling technology and technical conditions of main rolling equipment. *Procedia Eng.* **165**, 1722–1730 (2016). <https://doi.org/10.1016/j.proeng.2016.11.915>
9. Kukhar, V., Burko, V., Prysiaznyi, A., Balalayeva, E., Nahnibeda, M.: Development of alternative technology of dual forming of profiled workpiece obtained by buckling. *East-Eur. J. Enterp. Technol.* **3/7**(81), 53–61 (2016). <http://doi.org/10.15587/1729-4061.2016.72063>. ISSN 1729-3774
10. Kukhar, V., Artiukh, V., Serduik, O., Balalayeva, E.: Form of gradient curve of temperature distribution of lengthwise the billet at differentiated heating before profiling by buckling. *Procedia Eng.* **165**, 1693–1704 (2016). <https://doi.org/10.1016/j.proeng.2016.11.911>. ISSN 1877-7058
11. Lubliner, J.: *Plasticity theory*. University of California at Berkeley (2005)
12. Unksov, E., Johnson, W., Kolmogorov, V.: The theory of plastic deformation of metals. In: Unksov, E., Ovchinnikov, A. (eds.) *Engineering*, Moscow (1983)
13. Zbankov, I., Markov, O., Perig, A.: Rational parameters of profiled workpieces for an upsetting process. *Int. J. Adv. Manuf. Technol.* **71**(5–8), 865–872 (2014). <https://doi.org/10.1007/s00170-014-5727-5>
14. Shapoval, A., Mos'pan, D., Dragobetskii, V.: Ensuring high performance characteristics for explosion-welded bimetals. *Metallurgist* **60**(3), 313–317 (2016). <https://doi.org/10.1007/S11015-016-0292-9>
15. Ogorodnikov, V.: Methods of transport vehicle velocity determination according to its failures as a result of traffic accidents. In: *Proceedings of the International Ukrainian-Japanese Conference on Scientific and Industrial Cooperation*. Odes'kiy national'nyi politehnicnyi universytet, pp. 135–136 (2013)
16. Sivak, I., Savulyak, V., Chorna, J.: Construction of plasticity diagrams on the basis of limit forming during upsetting process. *Buletinul institutului politehnic din IAȘI* **5**, 209–216 (2011)
17. Mihalevich, V., Kraevskiy, V., Dobranyuk, Y.: Analytical research of residual resource model during material diagnostics. *Machine Building and Transport. Naukovi pratsi VNTU* **1**, 1–6 (2008)
18. Wong, M., Li, D., Wang, F., Zang, X., Li, X., Xiao, H., Du, F., Zang, F., Jiang, Z.: Analysis of laminated crack defect in the upsetting process of heavy disk-shaped forgings. *Eng. Fail. Anal.* **59**, 197–210 (2016)
19. Blumenstein, V., Ferranti, A.: Calculation and justification parameters of strengthening technology to produce drill rig shaft gear on the basis of mechanics of technological inheritance. In: *Coal in 21st Century: Mining, Processing and Safety*, pp. 265–272 (2016). http://www.atlantis-press.com/php/download_paper.php?id=25861476

20. Beygelzimer, Ya., Shevelev, A.: On the development of fracture models for metal forming. *Russ. Metall. (Metally)* **5**, 452–456 (2003)
21. Kukhar, V.: Producing of elongated forgings with sharpened end by rupture with local heating of the workpiece method. *Metall. Min. Ind.* **6**, 122–132 (2015). <http://www.metaljournal.com.ua/assets/Journal/MMI-6/016-Kukhar.pdf>
22. Strugov, S., Ivanov, V., Sherkunov, V.: Comparison of methods of stress-strain state estimation in the upset of a cylindrical workpiece. *Bull. South Ural State Univ. Ser. Metall.* **16**(4), 140–146 (2016). <https://doi.org/10.14529/met160416>
23. Blumenstein, V., Petrenko, K.: Influence of roller burnishing parameters on depletion of plasticity reserve. In: *Materials of VII International Scientific and Practical Conference on Innovations in Mechanical Engineering, ISPCIME 2015*, pp. 12–17 (2016). <http://doi.org/10.1088/1757-899X/126/1/01201>
24. Gharaibeh, N., Matarneh, M., Artyukh, V.: Loading decrease in metallurgical machines. *Res. J. Appl. Sci. Eng. Technol.* **8**(12), 1461–1464 (2014)
25. Radic, N., Krasnik, M., Trifkovic, S.: Numerical analysis of upsetting cylinder using FEM with experimental verification. *Infoteh-Jahorina* **10**(C-1), 239–243 (2011)
26. Kivivuori, S.: Simulation of cold formability for cold forming processes. In: *Advanced Knowledge Application in Practice* (2010). ISBN: 978-953-307-141-1
27. Rajeshkannan, A.: Workability studies on cold upsetting of sintered copper alloy preforms. *Mater. Res.* **13**(4), 457–464 (2010)
28. ASTM International. Standard test methods of compression testing of metallic materials at room temperature. Standard E9-09, ASTM International (2009). <http://doi.org/10.1520/E0009-09>
29. Foster, A., Lin, J., Farrugia, D., Dean, T.: A test for evaluating the effects of stress-states on damage evolution with specific application to the hot rolling of free cutting steels. *Int. J. Damage Mech.* **20**, 113–129 (2011). <https://doi.org/10.1177/1056789509343077>
30. Christiansen, P., Hattel, J., Bay, N., Martins, P.: Modelling of damage during hot forging of ingots. In: *The 5th International Conference, STEELSIM 2013*, pp. 1–13 (2013)
31. Markov, O., Perig, A., Markova, M., Zlygoriev, V.: Development of a new process for forging plates using intensive plastic deformation. *Int. J. Adv. Manuf. Technol.* **83**(9–12), 2159–2174 (2016). <https://doi.org/10.1007/s00170-015-8217-5>
32. Ivanisevic, A., Vilotic, D., Plancak, M., Kacmarcik, I., Movrin, D., Milutinovic, M., Skakun, P.: Contact stresses and forming load in upsetting of prismatic billets by V-shape dies. *J. Technol. Plast.* **37**(2), 133–140 (2012)
33. Paderni, A., Lissignoli, A., Bettoni, P., Scholz, H., Biebricher, U., Franz, H.: Large ESP forging ingots and their quality in production. In: *2nd International Conference, ICRF 2014*, pp. 1–10 (2014)

Analysis of Stress Conditions of Rolling Stand Elements

Viktor Artiukh¹✉, Vladlen Mazur², and Andrey Butyrin³

¹ Peter the Great St. Petersburg Polytechnic University,
Polytechnicheskaya str., 29, 195251 Saint-Petersburg, Russia
artiukh@mail.ru

² LLC “Saint-Petersburg Electrotechnical Company”,
Pushkin, Parkovaya str., 56, 196603 Saint-Petersburg, Russia

³ Moscow State University of Civil Engineering,
Yaroslavskoe shosse, 26, 129337 Moscow, Russia

Abstract. A technical solution is offered in order to prevent wear/breaking of contact surfaces of rolling stand elements which affected by horizontal impacts during rolling. On the basis of results of suggested mathematical models stress calculations a material is proposed for lining straps of rolls chocks of a quarto reverse 4-hi rolling stand of 3000 thick plate rolling mill shop (PJSC «MMPP n. Illich») for their industrial application.

Keywords: Horizontal impact · Rolling mill · Mathematical model
Stress calculation

1 Introduction

In order to prevent rolling mill housings and rolls chocks from wear/breaking towards rolling direction (horizontal direction) facing strips and lining straps were developed. Flat contact surfaces of rolls chocks, lining straps, facing strips and housings are heavily loaded elements of rolling stands. Good conditions of flat contact surfaces are important for quality of rolled metal and values of dynamic forces acting on equipment [1–3]. Moreover, revamp or replacement of the aforementioned rolling stands elements is expansive procedure [4].

Previously engineers, technologists and design engineers only discussed selection of hardness and strength of materials of lining straps and facing strips and methods of their installation [5–7]. At present, following different materials of lining straps of rolling stands are used:

- steel [8, 9];
- bimetallic (double-layer, rigid outer surface and soft inside surface) [10].

Usage experience of that lining straps and facing strips shows that:

- big wear values and smaller durability are typical for steel ones;
- cold-hardening of the soft inside surfaces and increased wear of flat contact surfaces of chocks/housings are typical for bimetallic ones.

In addition, during last time engineers consider necessity to reduce horizontal forces acting on housings and chocks during rolling and damping of rolls chocks oscillations [11, 12].

The next step in studying of horizontal forces during sheet rolling was definition of stress conditions of thick strip reversing 4-hi roughing rolling stand elements of 3000 thick plate rolling mill shop of PJSC «MMPP n. Illich» (Mariupol city, Ukraine). Von Mises stresses were calculated during rolling in a system consisted of:

- bottom work roll (BWR) chock from operator side, material steel “30XГCΦЛ” according to CIS State standard (SS) 977-75;
- facing strip, material steel 080 M 46 according to B.S. 970;
- hydraulic cylinder (HC) for BWR pressing, material steel “25X2M1Φ” according to CIS SS 20072-74;
- enough part of housing, material steel 161 grade 430 according to B.S. 1504 (76).

FEM mathematical model (MM) was created (refer to Fig. 1) and it was loaded by horizontal force $F = 2MH$ [12]. Conditions of contact surfaces interactions, materials properties and geometry of the aforementioned elements of rolling stand are actual according to scientific and practical suggestions [13–15] that helped to design mesh with great accuracy.

FEM calculations of two different MMs were done:

- lining strap and facing strip are from steel 080 M 46 according to B.S. 970;
- lining strap and facing strip are from bimetallic steel (outer surface is from rigid steel 65Г according to CIS SS 20072-74 and soft inside surface is from soft steel Cr3 according to CIS SS 380-94).

General view of MM with Mesh for FEM calculation is shown on Fig. 2.

Results of Von Mises stresses calculations of MM with lining strap and facing strip from steel 080 M 46 are shown on Figs. 3, 4, 5, 6 and 7.

Results of Von Mises stresses calculations of two different MMs are shown in Table 1.

As it is shown in Table 1, maximum Von Mises stresses values are lower than yield stresses of corresponding steel grades but their values are enough for arise of contact surfaces wear. Furthermore, use of steel 080 M 46 or bimetallic steel gives approximately the same results of Von Mises stresses.

Working conditions of the rolling stand in such situation can be improved by installation of shock absorber between lining strap and BWR chock. Polyurethane lining strap instead of steel one can be used to reduce the horizontal force and improve its distribution by contact surfaces.

To confirm the practicability of suggested technical solution a loading of MM with facing strip from steel 080 M 46 and lining strap from polyurethane. Its calculation results of Von Mises stresses are shown on Figs. 8, 9, 10 and 11.

During FEM calculations of lining strap from energy-efficient materials e.g. polyurethane it is important to know experimentally defined maximum value of lining strap possible compression when there is no residual deformation. Experimentally defined maximum value of polyurethane lining strap possible compression is $\delta^* = 0.70$ mm in this case and design of lining strap. Compressive stresses in

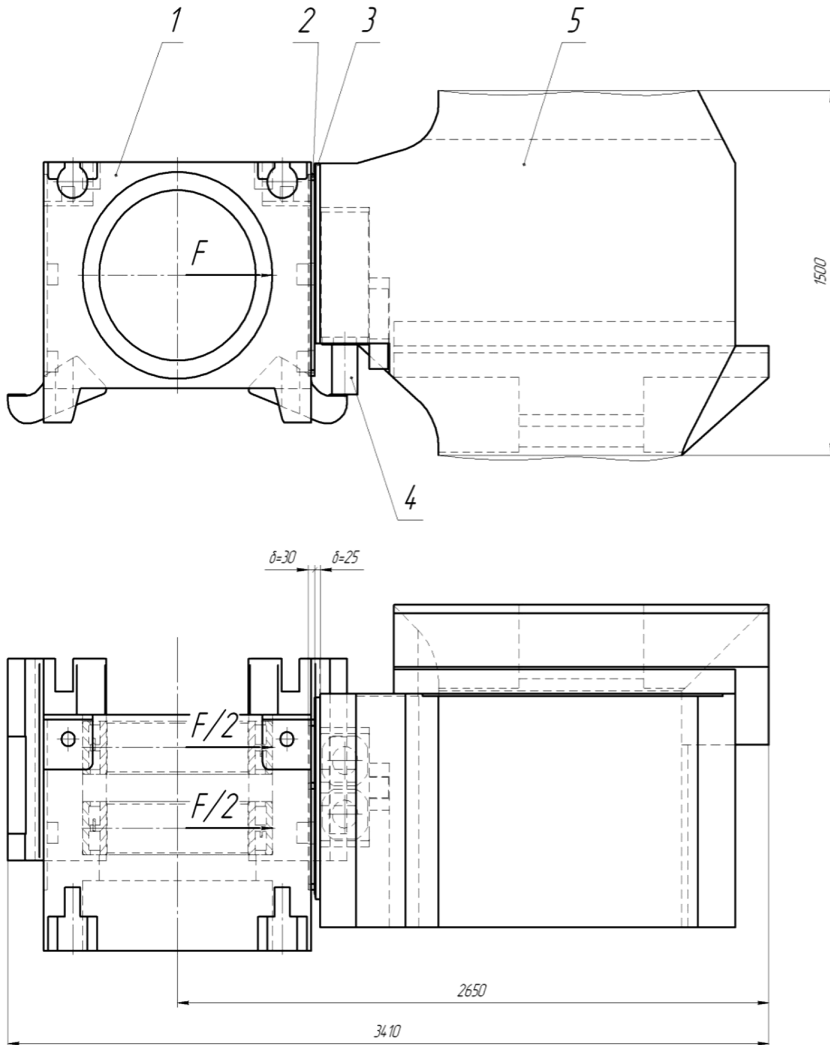


Fig. 1. Loading scheme of MM by horizontal force: 1 – BWR chock from operator side; 2 – lining strap; 3 – facing strip; 4 – HC for BWR pressing; 5 – housing.

polyurethane lining strap of MM are shown on Fig. 12. Compression of polyurethane lining strap subjected to act of horizontal force $F = 2\text{MN}$ (refer to Fig. 1) is shown on Fig. 13.

During such loading of lining strap from polyurethane grade Adiprene L-167:

- maximum compressive stress of polyurethane lining strap is $\sigma = 7,856 \text{ MPa}$ (refer to Fig. 12) and maximum permissible stress compressive stress is $[\sigma] = 15 \text{ MPa}$;

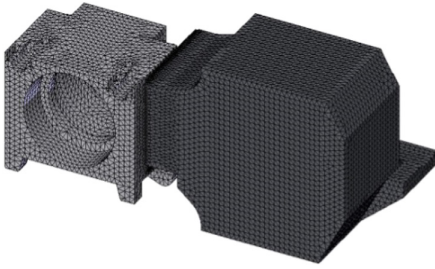


Fig. 2. General view of MM with mesh chock.

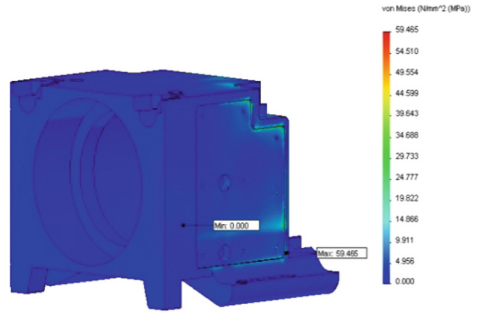


Fig. 3. FEM calculation results of BWR from operator side.

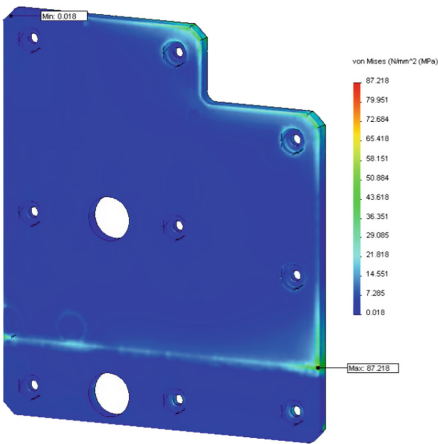


Fig. 4. FEM calculation results of lining strap from steel 080 M 46.

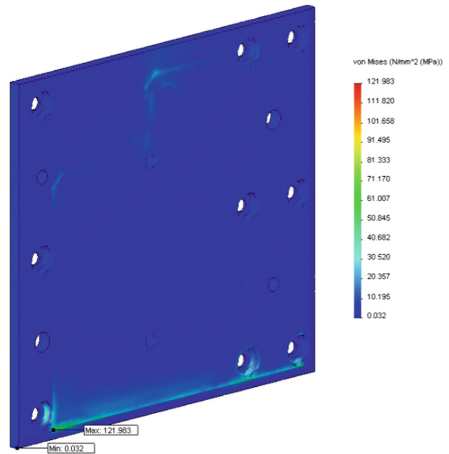


Fig. 5. FEM calculation results of facing strip from steel 080 M 46.

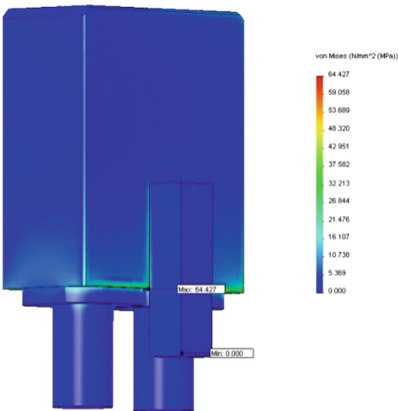


Fig. 6. FEM calculation results of HC for BWR pressing.

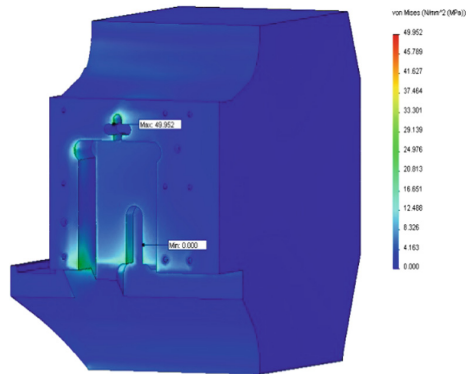


Fig. 7. FEM calculation results of housing.

Table 1. Maximum Von Mises stresses calculated in rolling stand elements.

Steel of lining strap/facing strip	BWR chock, MPa	Lining strap, MPa	Facing strip, MPa	HC for BWR pressing, MPa	Housing, MPa
080 M 46	59.465	87.218	121.983	64.427	49.952
Bimetallic	57.525	88.340	111.464	65.144	46.425

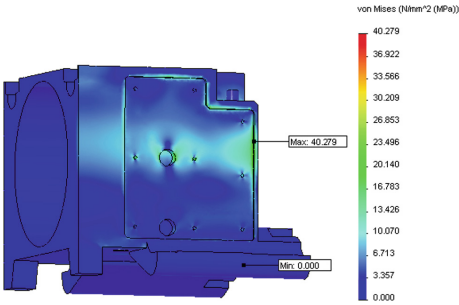


Fig. 8. FEM calculation results of BWR chock from operator side when polyurethane lining strap is used.

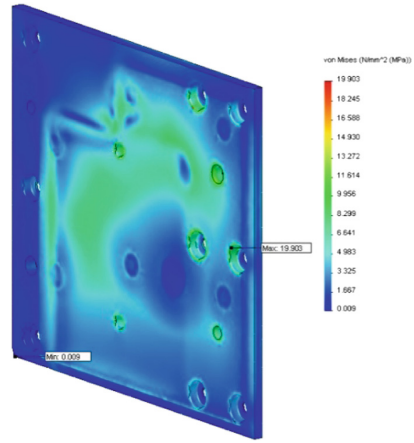


Fig. 9. FEM calculation results of facing strip from steel 080 M 46 when polyurethane lining strap is used.

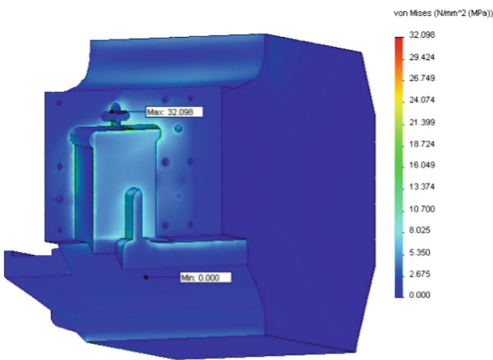


Fig. 10. FEM calculation results of when polyurethane lining strap is used.

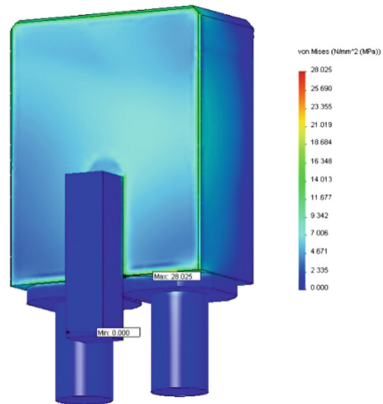


Fig. 11. FEM calculation results of housing HC for BWR pressing when polyurethane lining strap is used.

- maximum theoretical compression of polyurethane lining strap towards direction of the horizontal force is $\delta = 0.18$ mm (refer to Fig. 13) that is acceptable because $\delta \leq \delta^*$ according to condition of its use and rolling of good quality metal.

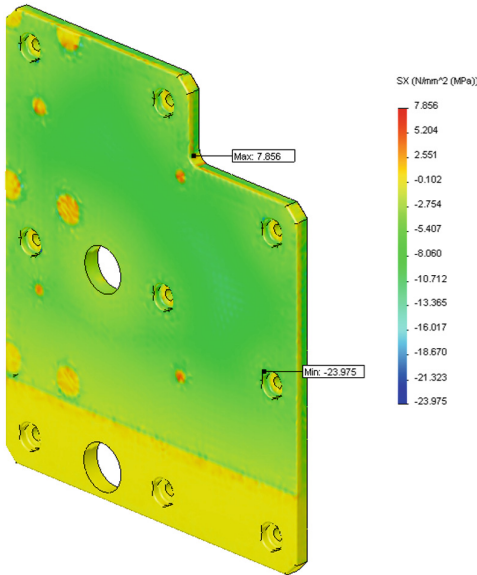


Fig. 12. FEM calculation results of compression of compressive stress in strap polyurethane lining strap.

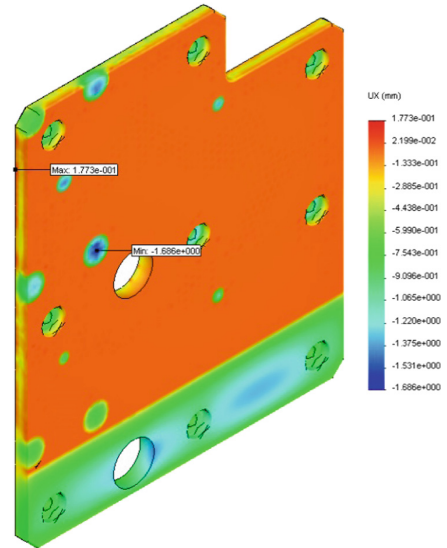


Fig. 13. FEM calculation results of polyurethane lining.

Done FEM calculation of MM has proved possibility to install polyurethane lining straps from polyurethane grade Adiprene L-167 on chocks of top work roll (TWR) and BWR of the thick strip reversing 4-hi roughing rolling stand of 3000 thick plate rolling mill shop. Percentage reduction of Von Mises stresses when polyurethane lining strap is used compared to usage of steel lining strap are given in Table 2.

In accordance with aforementioned information and figures in Table 2 it is reasonable to use lining strap from polyurethane grade Adiprene L-167 on chocks of TWR and BWR.

Table 2. Percentage reduction of maximum Von Mises stresses calculated in MM elements when lining strap from polyurethane grade Adiprene L-167 is used compared to MMs where steel lining strap is used.

Steel grade	BWR chock, %	Lining strap, %	Facing strip, %	HC for BWR pressing, %	Housing, %
080 M 46	32.3	90.86	83.68	56.5	35.74
Bimetallic	29.98	90.97	82.14	56.98	30.86

Set of lining strap from polyurethane grade Adiprene L-167 was installed on chocks of TWR and BWR of thick strip reversing 4-hi roughing rolling stand elements of 3000 thick sheet rolling mill shop of PJSC «MMPP n. Illich». It was working for more than 24 month that can be described as successful result.

During operation of lining straps from polyurethane their shrink became from 0.5 to 1.5 mm because of wear, horizontal force and friction with particles of scale. That shrink can be easily revamped by use of thin steel sheet between contact surfaces of TWR/BWR chocks and their lining straps. To the point, there was no wear of TWR/BWR chocks surfaces under lining straps. Moreover, there was reduction of housings facing strips wear (together with set of TWR and BWR with chocks equipped with polyurethane lining straps there were two sets with steel lining straps).

Suggested technical solution is protected by patent of Ukraine [16].

Use of polyurethane lining straps on back-up rolls chocks is a perspective solution [17–20].








The reported study was funded by RFBR according to the research project №16-08-00845a «Verification and development of models of inelastic deformation at the passive loading». The authors declare that there is no conflict of interest regarding the publication of this paper.

References

1. Mazur, V., Artyukh, V., Artyukh, G., Takadzhi, M.: Current views on the detailed design of heavily loaded components for rolling mills. *Eng. Des.* **37**(1), 26–29 (2012)
2. Matarneh, M., Gharaibeh, N., Artyukh, V.: Effectiveness of flexible pin type couplings. *Int. J. Eng. Sci. Innov. Technol. (IJESIT)* **4**(2), 1–7 (2015)
3. Bolshakov, V.: Features of operation of roughing stands main drive lines of hot rolling mill 1680. *Prot. Metall. Mach. Breakdowns* **4**, 15–24 (1999)
4. Bolshakov, V.: Features of dynamic loads in main drive lines of rolling stands of rolling mill 1700. *Prot. Metall. Mach. Breakdowns* **2**, 25–32 (1997)
5. Sorochan, E., Artiukh, V., Melnikov, B., Raimberdiyev, T.: Mathematical model of plates and strips rolling for calculation of energy power parameters and dynamic loads. In: *MATEC Web of Conferences*, vol. 73, p. 04009 (2016)
6. Artiukh, V., Mazur, V., Prakash, R.: Increasing hot rolling mass of steel sheet products. In: *Solid State Phenomena*, vol. 871, pp. 3–8 (2016)
7. Mazur, V., Artiukh, V., Matarneh, M.: Horizontal force during rolling as indicator of rolling technology and technical conditions of main rolling equipment. *Procedia Eng.* **165**, 1722–1730 (2016)
8. Korolyov, A.: *Rolling Stands and Equipment of Rolling Mills*. Metallurgy, Moscow (1981)
9. Celikov, A.: *Machines and Aggregates of Metallurgical Plants*. Metallurgy, Moscow (1988)
10. Alexandrov, I.: Reconstruction of rolling stands by means of bimetallic lining straps. *Metal Casting Ukraine* **3**, 51–52 (2004)
11. Artiukh, V., Mazur, V., Pokrovskaya, E.: Influence of strip bite time in work rolls gap on dynamic loads in strip rolling stands. In: *MATEC Web of Conferences*, vol. 86, p. 01030 (2016)
12. Ishenko, A.: Experimental analysis of impact forces acting on housings of rolling stands of thick sheet rolling mills. *Steel* **5**, 56–58 (2009)

13. Alyamovskiy, A.: SolidWorks/COSMOSWorks. Engineering analysis by FEM. DMK Press, Moscow (2004)
14. Belevich, A.: Study of technological and design parameters of helical rolling stands by means of modern FEM systems. Universities News: Nonferrous Metallurgy, vol. 9, pp. 32–35 (2002)
15. Kaplun, A.: ANSYS in hands of engineer. In: Practical Handbook. Editorial URSS, Moscow (2003)
16. Artiukh, V.: Patent 42803 of Ukraine, MPK B21B 13/00. Elastic Lining Strap of Rolling Stand Chock (2009)
17. Gharaibeh, N., Matarneh, M., Artyukh, V.: Loading decrease in metallurgical machines. Res. J. Appl. Sci. Eng. Technol. **8**(12), 1461–1464 (2014)
18. Al-Quran, F., Matarneh, M., Artukh, V.: Choice of elastomeric material for buffer devices of metallurgical equipment. Res. J. Appl. Sci. Eng. Technol. **4**(11), 1585–1589 (2012)
19. Artiukh, V., Karlushin, S., Sorochan, E.: Peculiarities of mechanical characteristics of contemporary polyurethane elastomers. Procedia Eng. **117**, 938–944 (2015)
20. Artiukh, V., Raimberdiyev, T., Mazur, V.: Use of CAE-systems at evaluation of shock absorbers for metallurgical equipment. In: MATEC Web of Conferences, vol. 53, p. 01039 (2016)

Researching of the Stress-Strain State of the Open-Type Press Frame Using of Elastic Compensator of Errors of “Press-Die” System

Elena Balalayeva¹ , Viktor Artiukh² , Volodymyr Kukhar¹ ,
Olga Tuzenko¹ , Vladyslav Glazko¹ , Andrii Prysiashnyi¹ ,
and Vadim Kankhva³ 

¹ Priazovskyi State Technical University,
Universytetska, 7, Mariupol 87500, Ukraine

² St. Petersburg State Polytechnical University,
Polytechnicheskaya, 29, Saint-Petersburg 195251, Russia
artiukh@mail.ru

³ Moscow State University of Civil Engineering,
Yaroslavskoe Shosse, 26, Moscow 129337, Russia

Abstract. The calculating of stress-strain state in the frame of the open crank press using finite element method which allows algorithmizing the process of selecting an elastic compensator of required configuration with specified performance characteristics was designed. Solid models of elastic compensators with various designs are built. Their use is enables to determine the dependences of gap and stress-strain state of the frame in the certain indicative points of the frame from the shape and characteristics of the compensator. A comparison of theoretical and experimental data for the calculation of the stress-strain state of the frame of open crank press with elastic compensators working was made. It was found that the using of compensators reduces the angular deformation in the frame by 10...24%, and the tensile stress – by 6...42%.

Keywords: Elastic compensator · Polyurethane plate · «press-die» system
Crank press · Stress-strain state · Finite-element modeling

1 Introduction

Technological operations of sheet-forming on crank presses are accompanied by distortions of the slide and deformation of the frame, which decreases of tool life working and deteriorates conditions of its exploitation. Durability of dies of open presses (with C-shaped frame) is 2...3 times lower than close presses (with U-shaped frame). Open press frames have lower hardness than close press frames that lead to large angular deformations, which are transmitted to the punching unit and reduce the precision of the forming details. The accuracy of ‘press-die’ systems are affected from misalignment of the slide axis to press table surface in the loaded state, from distortion in the gaps between press and slide guides, as well as cumulative errors of the punching unit. There are several directions of the development of technical solutions to reduce errors in the

'press-die' system and increase the accuracy of the sheet-formed metal products. The most efficient is the use of compensating elements installed between the slider and the upper die plate. The most perspective and cost-effective compensators of 'press-die' system errors are considered devices based on elastic (more often polyurethane) elements, however, it requires a separate justification. Despite the availability of calculation methods of certain types of elastic compensators, their impact on the stress-strain state of the press and dies details has not been studied yet. Explanation of the positive effect requires theoretical and experimental studies of joint deformation of presses with elastic compensators at technological loads. The establishment of new, previously unknown patterns of influence of constructions of elastic compensators on the stress-strained state of the main press parts (for example, the frame as a deformation indicator) allows choosing the type, shape, size and hardness parameters of these devices scientifically based. This ensures operational efficiency of the equipment and compensators, reduction of costs for preliminary design and project works, improving quality indicators of formed parts. Consequently, establishing a correlation between the design parameters of elastic compensators and the stress-strain state and the opening of the frame of open presses is an urgent scientific and practical task.

2 The Analysis of Recent Investigations and Publications

Constructions of pipelines provide compensating devices (stuffing box, lens, bellows expansion joints, as well as U-shaped and Z-shaped portions) to compensate for thermal elongation and external loads. Misalignment of transmission shafts eliminates the use of different types of couplings that ensure torque transmission even under significant misalignment angles. The wear of sealing elements of hydraulic and pneumatic equipment systems is compensated by pressure relief valves by the reserve pressure developed by the pumps or of the compressors accordingly.

Modern numerical control (NC) systems provide automatic correction for tool wear at processing, and some of them even take into account the wear of the bedplate rails and the elastic deformation of the system, "frame-device-tool-part" [5, 6]. Installation of modern machining equipment is often made on the elastic "cushions" to eliminate external vibration influence on machining accuracy and reduce errors in the guide surfaces with errors of "hard" first assembly on anchors. Geometric accuracy in operation is one of the main criteria of efficiency of production equipment [7]. Its parameters are mainly dependent on frame errors. To determine the design parameters of the compensating devices, it is necessary to determine deformation magnitude and direction of these body parts of industrial equipment.

The frames of many technological machines perform a mounting function. Press frames serve not only for the installation of nodes, but also for the power circuit. Therefore, they are exposed to significant loads. The most difficult stress-strain state is experienced by open C-frames of press-forging equipment [8]. Deformation of the frames of this type is reduced when designed by differentiated increase in their sections to increase the rigidity in the opening direction [8]. In other cases, it has been proposed the hardening of the C-shaped frames by installing additional ties [10]. The same authors propose the wedge compensation of opening the frames of this type. Analysis

of stress-strain state of the C-shaped frame presses and optimization of their design is reflected in works [11, 12].

The analysis of stress-strain state of the “press-die” system, and the frame press deformation during hot die-forging of aircraft engine parts were studied in works [13, 14]. Researchers [15, 16] are analyzed the stress state of the C-shaped frames of rotary tablet presses and calculation of strain in them. Similar studies were carried out for the C-shaped hydraulic clamps [17]. There are two basic approaches to eliminate the influence of deformation of the C-shaped type frame on the alignment of “press-die” system. The first approach is the closure of open C-shaped type frames with using the ties [8, 18], which greatly reduces its deformation. A second approach for solving the skew problem is to eliminate the misalignment between the upper and lower basing plates with various additional devices or elements. These devices or parts are called “compensators”. A further alternative approach to reducing of errors of the “press-die” system can be die-free [19] and impression-free [20] methods of metal-forming.

The main purpose of installing a skew compensator in forging equipment is to ensure the transfer of the operating force from basic die elements, which have lost alignment as a result of deformation of the frame, to coaxial (parallel) basic die surfaces. Slider skew causes to the additional and uneven pressure on the guide elements of the press and the press dies. This requires additional costs to providing a hardening of guide elements by surfacing, by surface deformation, by use of composites or other methods [21, 22].

The patent search shows that one of the first compensator models for press equipment is a design patented by Rode in 1931 [23]. This device was a unit of the springs, which were drawing in the bottom plate of the press in order to equalize the not parallel ones regarding the upper plate. Although such constructions were developed later as well [24], their main disadvantages are size and the need for significant alteration of the press.

Further development of the spring compensators can be considered compact spring units installed in the die-space of the press and consisting, for example, of a set of cup springs [25]. While such devices do not require significant alterations of press design and their dimensions are substantially smaller than previously proposed variants, but their application is limited by the size of free space.

The design of skew compensator shaped with sealed steel flat elastic elements [26] is interesting. The main advantage is the compactness and the disadvantages include a relatively high complexity of manufacturing.

Instead of conventional spring compensators for press equipment recently been proposed autonomous gas springs [27], but their reliability is questionable because of the inevitable leaks of working environment during operation. The devices based on elastic elements collected in steel digit form hulls have greater reliability [28].

A separate group of compensators can be considered hydraulic device for leveling elements of presses. The design of hydraulic leveling of the upper plate (slider) is presented in [29]. Variants of hydraulic compensators for the lower press plate are proposed in [30, 31]. General disadvantages of such devices are size, difficulty of maintenance and relatively low reliability.

Various designs of ball compensators are quite common [32]. Their operating principle is the redistribution of metal balls in a closed space between two moving surfaces. These compensators are reliable and relatively small.

The task of compensating skews do well spherical compensators [33]. Their advantage can be regarded as significant deviation from the permissible angles of alignment, and the major drawbacks are the difficulty in manufacturing and lack of cushioning effect.

All of these devices in one way or another have their drawbacks: size, structural and technological complexity, low reliability. The absence of all these shortcomings determines the prospects of elastic polymer compensators. Let's consider the examples of construction of such elastic elements.

Interesting decision on compensation of deformation of bending press frame (bulldozers) was not only suggested by Gasparini [34], but also put into mass production by the same name company. In this construction the elastomeric material acts as a matrix component and not only eliminates a skew, but spring back effect as well. The elastic compensators can be used both as compensation for a plunger skew [35], and as compensation for matrix skew [36].

The material of the elastic compensator can be as rubber as other elastic polymers. However, the most promising are the polyurethanes of different brands. This is due to their high fatigue resistance, good elastic properties, ease of handling and availability. But their choice as a material for compensating elements of equipment is complicated by wide range of functional properties of the polyurethanes from various manufacturers. Recommendations for optimization of this choice are based on laboratory studies [37]. Method of calculating the optimum design parameters is discussed in [38]. The same group of scientists proposed an automated method of calculation for the reconfigurable polyurethane compensators, taking into account the errors of "press-and-die" system [39].

So, on the basis of the above, we can conclude that today polyurethane compensators are optimal for use in the pressing equipment, in addition for them there have been developed and successfully applied the techniques of choosing materials and design parameters. However, the influence of design parameters to reduce of stresses and strains in the base elements of presses has not been studied yet. This complicates selection of refined designs compensators and assesses of the service life of the press equipment.

3 The Purpose and Objectives of the Study

The purpose of this study is to develop a method for calculating the stress-strain state of an open frame crank press considering the various structures of the elastic compensating elements, which are located between the bearing surfaces of the slider and the top of the die plates.

3.1 The Materials and Results of the Investigation

Methods of Finite-Element Modeling

For mathematical description of the stress-strain state of the frame of open type crank press is used the finite element method. The system of resolving equations of motion of the mechanical environment for the case is built on the basis of the variational principle of d'Alembert-Lagrange. Layers of the press frame are broken down into finite elements. According to the principle of d'Alembert-Lagrange, at each time point the elementary work of external static forces, including the drag forces and internal forces in any possible movement of the system is zero, that is:

$$\sum_{i=1}^n \left[\iint_S \{\delta \varepsilon\}^T \{\sigma\} dS + \iint_S \{\delta u\}^T [b] \{\dot{u}\} dS + \iint_S \{\delta u\}^T \{p\} dS - \{\delta w\}^T \{f(t)\} \right] = 0, \quad (1)$$

where i – number of finite elements;

n – the number of finite elements;

S – finite element area;

δ – the operator of variation;

$\{\varepsilon\}$ and $\{\sigma\}$ – vectors of relative deformations and stresses;

$\{u\}$ and $\{w\}$ – vectors of displacement of the arbitrary point and displacement of nodes of finite element;

$\{p\}$ – vector of surface pressures;

$\{f(t)\}$ – vector of external forces;

$[b]$ – matrix of resistance coefficients;

t – time.

Since the components of the vector of the displacement nodes $\{w\}$ are independent, and their variations are arbitrary, the final expression takes the form:

$$[B]\{\dot{w}\} + ([C] - [P])\{w\} = \{f(t)\} + \{f_0\}. \quad (2)$$

Thus, we got a system from n vector equations. The system is solved numerically by an implicit unconditionally stable scheme using finite element and SOLID92 SOLID95 of software package ANSYS. In the process of numerical solution are calculated the components of displacement vector and equivalent stresses according to Mises.

To calculate the stress-strain state of the frame of open-type crank press with force of 0.16MN (Fig. 1a) was built its solid model (Fig. 1b). At the characteristic points 1–8 (Fig. 2) were fixed the indicators of the stress-strain state: the components of the stress tensor, stress intensity, the equivalent stress. After placing the load on the frame in a pattern corresponding to the scheme of technological process were got the following characteristics of stress: the components of the stress tensor σ_x , σ_y , σ_z ; stress intensity σ_i ; the equivalent stress σ_e (as Mises). We consider the elastic compensators of three different designs. The first construction (Fig. 3a) was a polyurethane plate of 14 mm in height and the size of 220 × 140 mm, the second one (Fig. 3b) and third one (Fig. 3c)

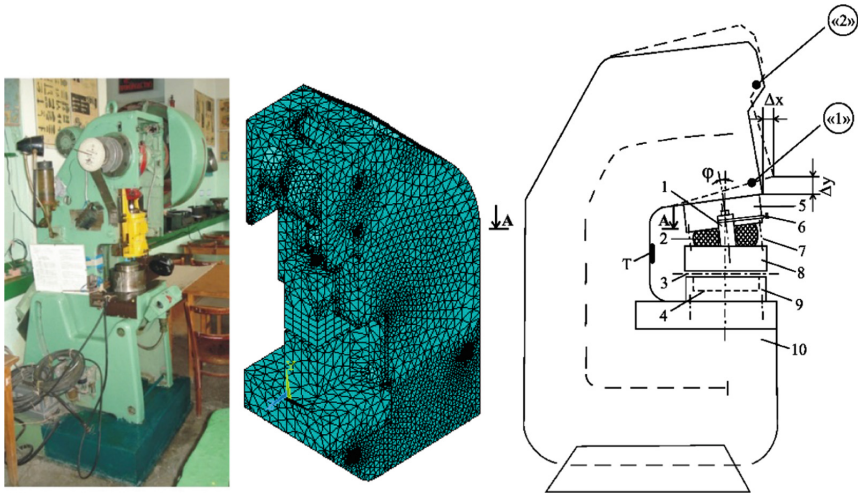


Fig. 1. Photo of open-type crank press, its solid model; scheme of mounting the upper die plate to a press slider. 1 – shank; 2 – compensator; 3 – die line connector; 4 – circuit of a formed product; 5 – slider; 6 – fixing pin; 7 – fasteners; 8 – upper plate; 9 – lower plate; 10 – frame; φ – skew angle of the slider; “1” and “2” – displacement measurement point (Δ); Δx and Δy – horizontal and vertical movement; T – electrical strain gauges.

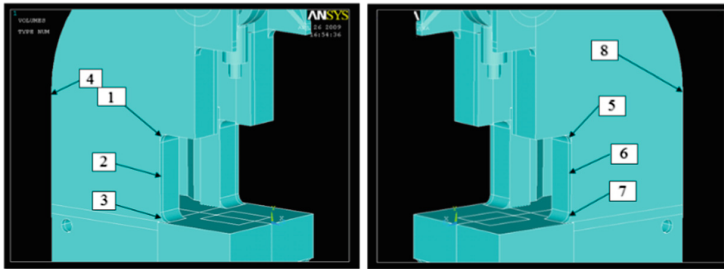


Fig. 2. Model of open-type crank press. 1, 5 – points on the upper bending radius of the press racks; 2, 6 – points on mid-height of press racks; 3, 7 – points on the lower bending radius of the press racks; 4, 8 – points on the bending radius of the frame on rear side of the press.

constructions are complemented with holes. Moreover, compensators (b) and (c) were placed in two ways: as a more rigid side as a less rigid one to the press frame.

Previously were constructed solid models of considered compensators that have been imported into software package ANSYS. Were constructed finite element models of the compensators, an example of which is shown in Fig. 4. The following properties of the material were set, corresponding to the polyurethane brand SKU-PFL-100: the modulus of elasticity $E = 69 \text{ MPa}$, Poisson’s ratio $\mu = 0.49$ Then set the move of nodes at the upper plane $\Delta 1$ and $\Delta 2$ (on the lower surface of the compensator they were taken as zero) as the boundary conditions.

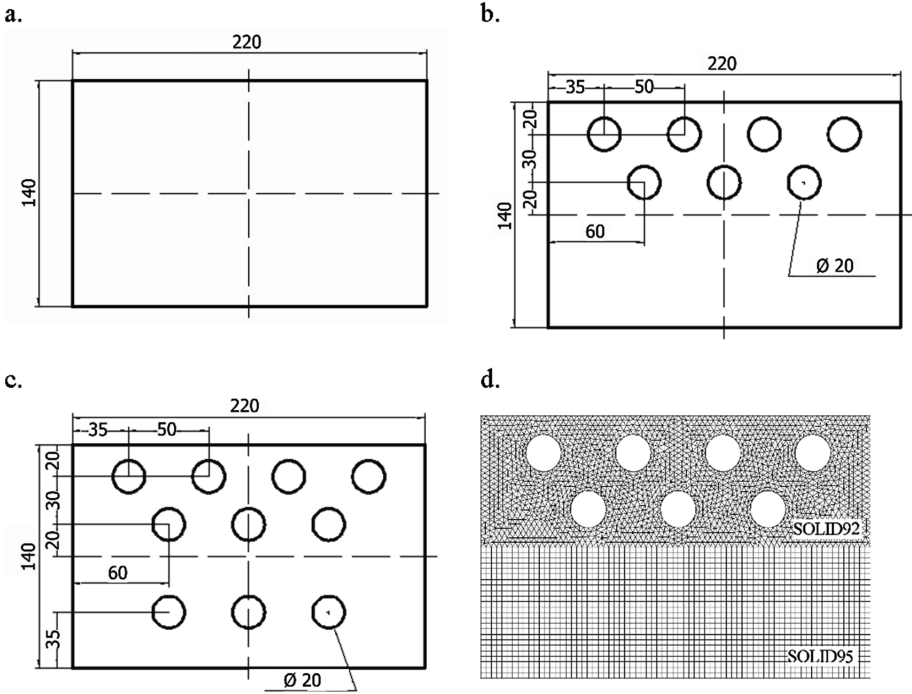


Fig. 3. (a) Construction of polyurethane compensators without holes, (b) with 7 holes, (c) with 10 holes; (d) finite element mesh on the upper surface of the compensator.

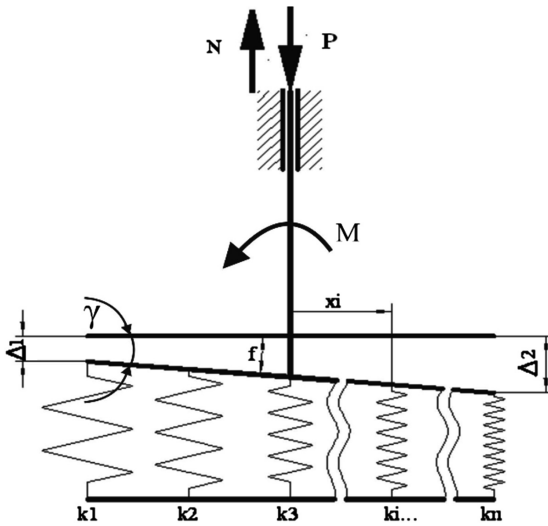


Fig. 4. Model compensator of uneven hardness given angular deformation of the frame.

The task with the compensator selection with necessary properties was that angular deformation of the elastic element with predetermined force P was equal to angular deformations of the frame. In this case, the model parameters were determined by the method described below.

Step 1. Was noted that before loading the additional bending moment M and the overall reaction at the rigidity nodes N of the compensator are equal to 0 ($M = 0, N = 0$).

Step 2. Was set the press load P .

Step 3. Was calculated the components of the stress tensor $\sigma_x, \sigma_y, \sigma_z, \gamma_{xy}, \gamma_{zy}, \gamma_{xz}$; stress intensity σ_i ; equivalent stress σ_e (as Mises). As a result, was received a corner deformation value for the frame γ for set M and P .

Step 4. Was calculated the moving of nodes of the upper plane Δ_1 and Δ_2 for a given angular deformation of the frame γ .

Step 5. To construct a finite element model of the compensator was determined k_i – the rigidity of the i -th finite element; Δ_i – moving of i -th finite element; x_i – distance from the axis of load application to i -th finite element.

Step 6. Was calculated values of equivalent displacement response A and the additional bending moment M occurring at a given value of the angular deformation γ . The computational model of the compensator based on the angular deformation of the frame is shown schematically in Fig. 4.

The value of equivalent displacement reactions with respect to the load axis was calculated as:

$$A = \sum_{i=1}^n N_i \cdot x_i / N, \tag{3}$$

where $N_i = k_i \cdot \Delta_i$ – the reaction occurring in rigidity nodes of the compensator;

N – The overall reaction to the rigidity nodes of the compensator.

Additional bending moment is given by:

$$M = \sum_{i=1}^n N_i \cdot x_i. \tag{4}$$

Step 7. In view of the calculated additional torque M re-determined angular deformation of the frame γ .

Step 8. If the overall reaction N did not coincide with the magnitude of the load P to an accuracy of 1%, then we went to step 2 and commit the next iteration in the loop. In different way fixed indicators of stress-strain states in points 1...8 of the press frame and built the graphs.

The Results of Finite Element Modeling

Based on the developed finite element model the method of calculation angular deformities (Fig. 6a) and tensile stresses (Fig. 6b) were defined.

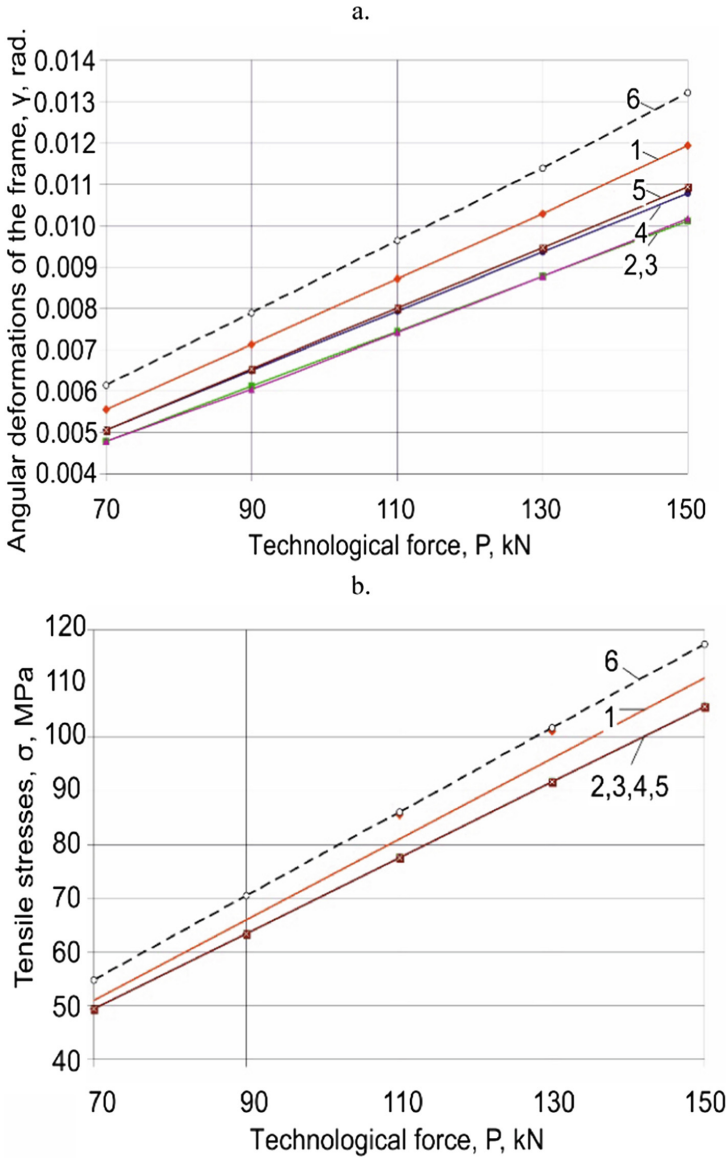


Fig. 5. Charts on (a) angular deformation dependencies of the press frame and (b) tensile stresses in the dangerous section of the technological forces using elastic compensators. 1 – compensator without holes; 2 – compensator with 7 holes deployed less rigid side to the press frame; 3 – compensator with 7 holes deployed more rigid side to the press frame; 4 – compensator with 10 holes deployed less rigid side to the press frame; 5 – compensator with 10 holes deployed more rigid side to the press frame; 6 – without compensator.

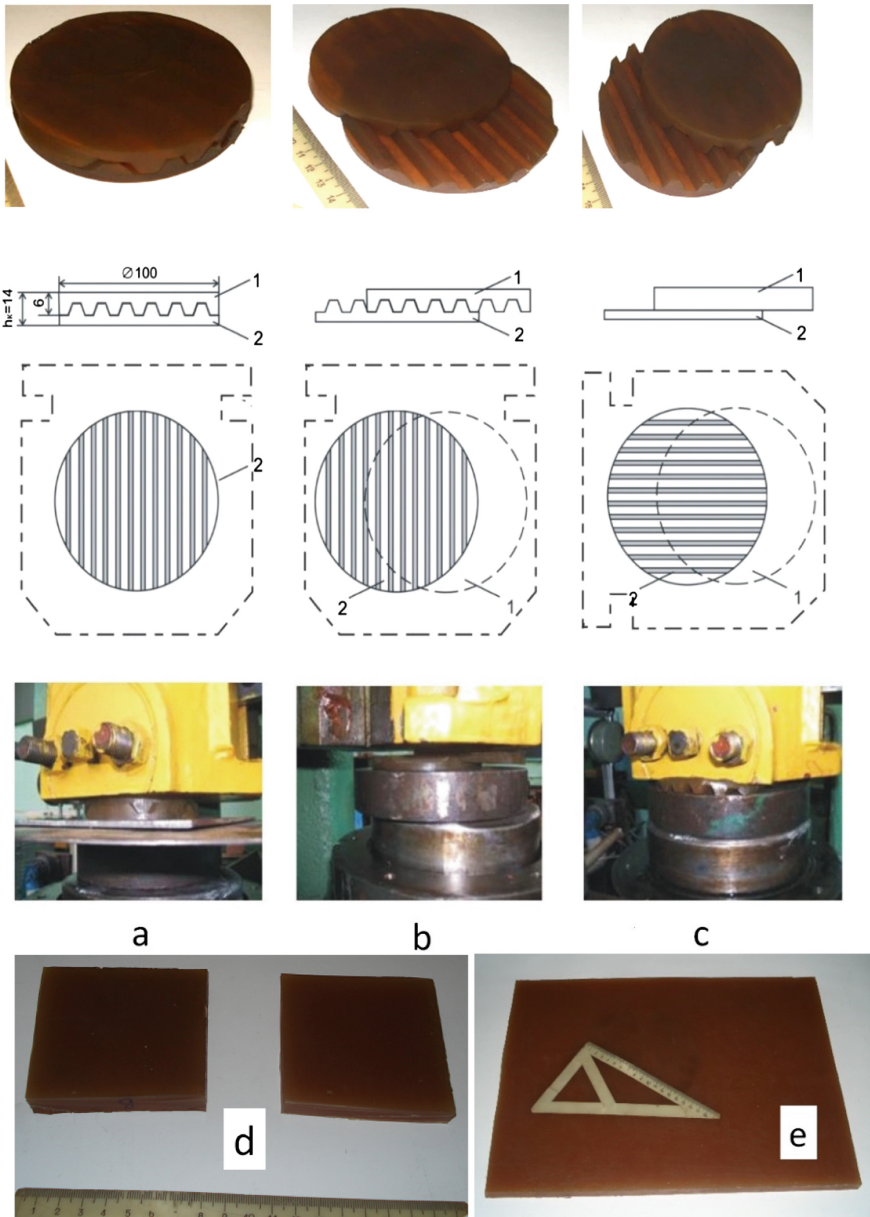


Fig. 6. The design of the two-layer embossed compensator (a) in the closed form, (b) when expanded transversely and (c) along a press table; the design of a flat plate-compensator with dimensions (d) 81×76 mm and (e) 190×220 mm. 1 – the upper plate; 2 – the lower plate.

The modeling results shown in Fig. 5a showed that the use of compensator No. 1 reduces angular deformation of the frame by 10%, the use of compensators No. 2 and 3 – by 22%, compensators No. 4 and No. 5 – by 17% compared to the loading of the press without a compensator.

Thus, it was confirmed that the most effective is the use of elastic compensators No. 2 and No. 3 (with 7 holes), which provides the greatest equivalent torque reaction.

The analysis of the dependences shown in Fig. 5b shows that the use of elastic compensator No. 1 allows reducing tensile stresses in the dangerous section, defined by points “2” and “6”, by 6%, and the use of compensators No. 2, No. 3, No. 4 and No. 5 – by 10% on average compared to the work of the press without the compensator.

Thus, it was found that the most effective is the use of compensators with 7 holes, accompanied by the implementation of the maximum torque equivalent response.

Comparison of Modeling and Experimental Results

Experimentally was investigated the dependence of displacements Δ and stresses σ in the press frame on force P by applying mechanical strain measurement techniques and electrical strain measurement.

For the experiment was used the following equipment (see Fig. 1c.): the crank press with an open frame with nominal force of 0.16MN; hydraulic loader; wire resistance strain gauges, taken from the same batch included in the Wheatstone bridge; strain gauge amplifier; millimeter; the calibration beam of equal resistance.

The opening of the frame was recorded by mechanical strain gauges represented as dial indicators in characteristic points “1” and “2” (see. Fig. 1c) in a horizontal Δx and vertical Δy directions, and total displacement was calculated as $\Delta = \sqrt{\Delta x^2 + \Delta y^2}$. The

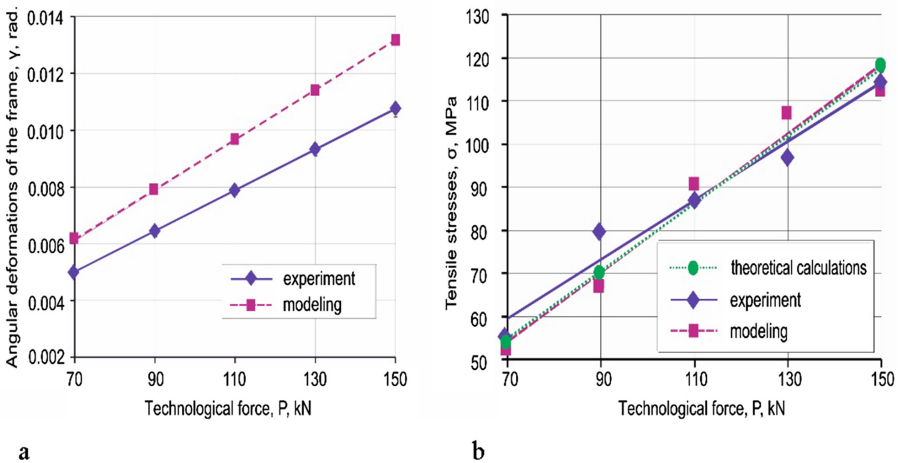


Fig. 7. Graphs of dependence of (a) the angular deformations of the frame γ and (b) tensile stress σ on the process of the force P at the press work without compensator.

stress in the dangerous section of the frame (section A-A, see Fig. 1c) was recorded using electrical strain gauges (T) included in the half-bridge Wheatstone circuit, amplifier and milliammeter.

Was performed a draft of polyurethane samples in the form of a two-layer embossed plates $\varnothing 100$ mm and tooth height of the relief of 6 mm (Fig. 6), as well as a flat rectangular compensator-plates with 14 mm height and size of 81×76 mm 190×220 mm.

Figure 7a shows the comparison of the angular deformations of the frame from technological strength, obtained by experimental testing and finite element simulation of the press without a compensator. The increase of process load from 70kN to 150kN leads to the increase in the value of the angular deformation of experimental data – from 0.0050 rad to 0.0099 rad, for the simulation – from 0.0061 rad to 0.0132 rad.

Figure 7b shows the comparison of the dependences of tensile stresses on technological strength point in the characteristic point “2” (see. Fig. 2) obtained by theoretical calculations, experimental testing and finite element simulation of the press without the use of a compensator. Increasing the process load from 70kN to 150kN leads to increasing the tensile stress from 54.7 MPa to 117.4 MPa for theoretical data, from 55.5 MPa to 115.0 MPa for experiment data and from 52.5 MPa to 112 MPa 5 MPa for simulation. Thus, the results of modeling a stress-strain state of the frame of an open crank press are confirmed by theoretical calculations and experimental data. The value of the relative error in the determination of the angular deformation of the frame and tensile stresses in the dangerous section does not exceed 15%.

Also was investigated the dependence of the angular deformation and tensile stresses in the press frame on the form factors of elastic compensators of various types at a given load process (Fig. 7).

Solid physical models of compensators were considered. The form factor is defined as

$$F = F_{\text{lat}}/F_{\text{bear}}, \quad (5)$$

where F_{lat} – is free lateral surface area of the compensator;

F_{bear} – is bearing surface area of the compensator.

Graph of dependence of the angular deformation and tensile stresses in the press frame on the form factors of elastic compensators are shown in Fig. 8.

The analysis of the dependencies (see. Fig. 8) has shown that the most effective in terms of reducing the angular deformation and tensile stresses in the press frame is the use of two-layer embossed compensators (No. 4, No. 5, No. 6). Thus, the most effective among flat compensators with variable rigidity is a compensator with 7 holes (No. 2), among two-layer embossed compensators – a compensator disclosed along the press table (No. 4), and among the flat-plate compensators – a plate-compensator with 190×220 mm (No. 7).

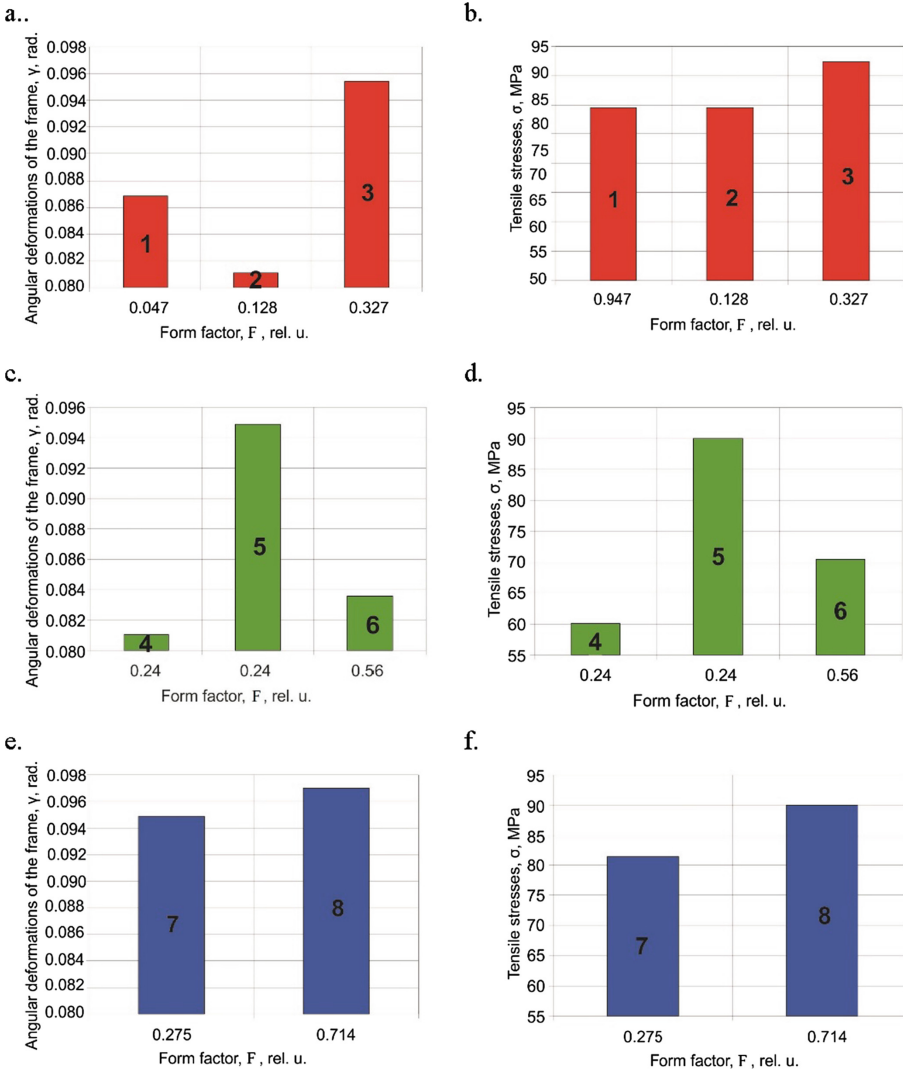


Fig. 8. Histograms of dependences of angular deformation and tensile stresses on the form factors for the compensators of (a, b) variable rigidity (solid models), (c, d) two-layer embossed compensators (physical model), (d, e) flat compensators (physical model) at $P = 0.12$ MN.

4 Conclusions

1. The method of calculating the stress-strain state in the frame of the open crank press using finite element analysis ANSYS was designed. Solid models of the press frame and elastic compensators of different forms were built. The developed method allows algorithmizing the process of selecting an elastic compensator of required configuration with specified performance characteristics.

2. Based on the developed finite element models and methods of calculating the stress-strain state of the press frame, when working with elastic compensators of various shapes, the angular deformation and tensile stresses have been calculated. It is shown that by using elastic compensators of variable stiffness the angular deformation of the frame is reduced by 10...22%, and the tensile stress – by 6...10%.
3. It was found that the installation of elastic compensators more rigid side to the rear of the press reduces the elastic deformations in the frame, and the installation of less rigid – reduces the bending stresses in the guide columns of a punching unit.
4. It was found that the most effective among the flat compensators with variable rigidity is a compensator with 7 holes, among two-layer embossed compensators – a compensator disclosed along the press table, and among flat compensators – a plate-compensator of 190 × 220 mm. Moreover, among the considered solid and physical models of compensators most effective in terms of reducing the angular deformation and tensile stresses in the press frame is the use of two-layer embossed compensators.
5. It has been shown that the stress-strain state simulation of the frame of open crank press is confirmed by theoretical calculations and experimental data. The value of the relative error in the determination of the angular deformation of the frame and the tensile stress at the dangerous section does not exceed 15%.

The reported study was funded by RFBR according to the research project № 16-08-00845a «Verification and development of models of inelastic deformation at the passive loading». The authors declare that there is no conflict of interest regarding the publication of this paper.

References

1. Norton, R.: *Machine Design: An Integrated Approach*. Pearson Prentice Hall, Upper Saddle River (2006)
2. Smith, D.: *Why Press Slide out of Parallel Problems Affect Part Quality and Available Tonnage*. Society of Manufacturing Engineers, Dearborn (1988)
3. Bringmann, B.: *Improving Geometric Calibration Methods for Multi-Axis Machining Centers by Examining Error Interdependencies Effects*. ETH, Zürich (2007)
4. Dasgupta, A., Pecht, M.: Material failure mechanisms and damage models. *IEEE Trans. Reliab.* **40**(5), 531–536 (1991). <https://doi.org/10.1109/24.106769>
5. Belforte, G., Bona, B., Canuto, E., Donati, F., Ferraris, F., Gorini, I., Morei, S., Peisino, M., Sartori, S.: Coordinate measuring machines and machine tools self-calibration and error correction. *Ann. CIRP* **36**(1), 359–364 (1987)
6. Ni, J.: CNC machine accuracy enhancement through real-time error compensation. *J. Manuf. Sci. Eng.* **119**(4B), 717 (1997). <https://doi.org/10.1115/1.2836815>
7. Schwenke, H., Knapp, W., Haitjema, H., Weckenmann, A., Schmitt, R., Delbressine, F.: Geometric error measurement and compensation of machines. *CIRP Ann. Manuf. Technol.* **57**(2), 660–675 (2008). <https://doi.org/10.1016/j.cirp.2008.09.008>
8. Dan, I., Cioara, R.: Methods to increase the rigidity of the c-frame of a press. *AMM Appl. Mech. Mater.* **371**, 183–187 (2013). <https://doi.org/10.4028/www.scientific.net/amm.371.183>

9. Cioara, R., Dan, I.: Combined constructive solutions for increasing cast c-frame stiffness of mechanical presses. *AMM Appl. Mech. Mater.* **657**, 455–459 (2014). <https://doi.org/10.4028/www.scientific.net/amm.657.455>
10. Raz, K., Cechura, M., Chval, Z., Zahalka, M.: Improvement of mechanical press productivity and accuracy by compensation of frame opening. In: 10th International DAAAM Baltic Conference “INDUSTRIAL ENGINEERING”, vol. 1, pp. 82–85 (2015)
11. Bi, D., Liu, D., Chu, L., Zhang, J.: Finite element analysis on frame-type hydraulic press. *AMR Adv. Mater. Res.* **199–200**, 1623–1628 (2011). <https://doi.org/10.4028/www.scientific.net/amr.199-200.1623>
12. Chauhan, H., Bambhanian, M.: Design & analysis of frame of 63 ton power press machine by using finite element method. *IJAR Indian J. Appl. Res.* **3(7)**, 285–288 (2011). <https://doi.org/10.15373/2249555x/july2013/88>
13. Ou, H., Lan, J., Armstrong, C., Price, M.: An FE simulation and optimization approach for the forging of aeroengine components. *J. Mater. Process. Technol.* **151(1–3)**, 208–216 (2014). <https://doi.org/10.1016/j.jmatprotec.2004.04.042>
14. Ou, H., Armstrong, C.: Evaluating the effect of press and die elasticity in forging of aerofoil sections using finite element simulation. *Finite Elem. Anal. Des.* **42(10)**, 856–867 (2006). <https://doi.org/10.1016/j.finel.2006.01.006>
15. Arango, I., Pineda, F.: Design of CNC turret punch for small batches production, *Ingenieria y Desarrollo. Universidad del Norte* **30(1)**, 79–100 (2012)
16. Altaf, S., Hoag, S.: Deformation of the stokes B2 rotary tablet press: quantitation and influence on tablet compaction. *J. Pharm. Sci.* **84(3)**, 337–343 (1995). <https://doi.org/10.1002/jps.2600840314>
17. Markowski, T., Mucha, J., Witkowski, W.: FEM analysis of clinching joint machine’s c-frame rigidity. *Eksploatacja i Niezawodność – Maintenance and reliability* **15(1)**, 51–57 (2013)
18. Maeda, N., Itakura, H., Yagi, T.: U.S. Patent No. 4,434,646. U.S. Patent and Trademark Office, Washington, DC (1984)
19. Kukhar, V.: Producing of elongated forgings with sharpened end by rupture with local heating of the workpiece method. *Metall. Min. Ind.* **6**, 122–132 (2015)
20. Kukhar, V., Burko, V., Prysiaznyi, A., Balalayeva, E., Nyhnibeda, M.: Development of alternative technology of dual forming of profiled workpiece obtained by buckling. *Eastern-Eur. J. Enterp. Technol.* **3(7(81))**, 53–61 (2016). <https://doi.org/10.15587/1729-4061.2016.72063>
21. Shapoval, A., Mos’pan, D., Dragobetskii, V.: Ensuring high performance characteristics for explosion-welded bimetals. *Metallurgist* **60(3)**, 313–317 (2016). <https://doi.org/10.1007/S11015-016-0292-9>
22. Dragobetskii, V., Shapoval, A., Mospan, D., Trotsko, O., Lotous, V.: Excavator bucket teeth strengthening using a plastic explosive deformation. *Metall. Min. Ind.* **4**, 363–368 (2015)
23. Rode, F.: U.S. Patent No. 1,827,440. U.S. Patent and Trademark Office, Washington, DC (1931)
24. Harper, H.: U.S. Patent No. 3,200,508. U.S. Patent and Trademark Office, Washington, DC (1965)
25. Yoshida, T., Toyoda, D.: U.S. Patent Application 0,327,115 (2013)
26. Harper, B., Bajorek, C.: U.S. Patent 7,320,584. U.S. Patent and Trademark Office, Washington, DC (2008)
27. Wallis, B.: U.S. Patent 5,197,718. U.S. Patent and Trademark Office, Washington, DC (1993)

28. Aoshima, K., Baba, K.: U.S. Patent 7,243,521. U.S. Patent and Trademark Office, Washington, DC (2007)
29. Carrieri, L.: U.S. Patent 4,272,980. U.S. Patent and Trademark Office, Washington, DC (1981)
30. Seki, S., Aoshima, K.: U.S. Patent 4,635,466. U.S. Patent and Trademark Office, Washington, DC (1987)
31. Yoshikawa, E.: U.S. Patent 5,339,665. U.S. Patent and Trademark Office, Washington, DC (1994)
32. Brams, P.: U.S. Patent 5,858,422. U.S. Patent and Trademark Office, Washington, DC (1999)
33. Bordignon, A., Bordignon S.: US Patent Application 0,008,628 (2015)
34. Gasparini, L.: U.S. Patent 6,519,996. U.S. Patent and Trademark, Washington, DC (2003)
35. Casolari, F.: European Patent EP1403017-A3. European Patent Office, Modena (2005)
36. Frost, D., Lutkemeyer, O., Koster, J.: European Patent EP2990192-A1. European Patent Office, Bochum (2016)
37. Artiukh, V., Karlushin, S., Sorochan, E.: Peculiarities of mechanical characteristics of contemporary polyurethane elastomers. *Procedia Eng.* **117**, 938–944 (2015). <https://doi.org/10.1016/j.proeng.2015.08.180>
38. Kukhar, V., Balalayeva, E., Tuzenko, A., Burko, V.: Calculation of universal elastic compensator applied to the pressing-extrusion operations. *Multi. J. Res. Eng. Technol.* **2**(3), 593–604 (2015)
39. Balalayeva, E., Kukhar, V., Hrushko, O.: The Computer-Aided Method of Calculation of Universal Elastic Rotary Compensator for the “Press-and-Die” System Errors of Crank Press for Drawing-Forming Operations. *HCTL Open Science and Technology Letters (STL)* (2014). ISSN 2321–6980, ISBN 978-1-62951-779-7

Online Energy-Efficient Train Traffic Adjustments

Boris Davydov  and Vadim Gopkalo 

Far Eastern State Transport University, 47 Serysheva st., Khabarovsk 680021,
Russian Federation
dbi@rambler.ru, vng@yandex.ru

Abstract. High quality dispatching ensures a good level of train punctuality and reduces operating costs. The main savings come from reduction of the traction energy consumption. The paper considers the issues of creating an adequate energy model, which is needed for efficient adjustment of train traffic. The authors develop a methodology for the meso-modeling and optimal traffic control. We describe two types of operational management such as regulation of a single train speed profile and the services flow control. Optimization criterion is the minimum energy rate. Detailed study of the traction energy consumption dynamics is carried out using correlation analysis. The main revealed regularities are: the correlation between the energy consumption and the relief increases with heaviness of path and falls when an unplanned delays occur. The conclusions obtained make it possible to improve the traction energy consumption model.

Keywords: Train traffic · Online adjustments · Energy consumption Modeling · Optimal decision making

1 Introduction

Adjustments of train traffic are made in order to eliminate deviations from the schedule that have already occurred or are possible in the near future. These deviations from the normal process lead to the train lateness and to overruns of energy and money. You must have a high-quality dispatching to reduce the level of losses. Such an adaptive management involves elaboration of the optimal schedule adjustments, as well as the precise and timely implementation.

Most of the current literature explores the problem of finding the rescheduling solutions, which are optimized according to the criterion of punctuality the train traffic. This approach is valid for the control of passenger trains and of freight services are moving according to hard schedule. It is often used operational adjustment, which significantly increase energy consumption for traction. There are a few articles that examine the problem of reducing energy consumption while maintaining a high level of punctuality. Obviously, this problem needs an additional study.

There is an intense flow of mixed passenger and freight trains on many conventional rail mainline of Russia, China, the United States and other countries. It is known that requirement on the accurate schedule execution when driving freight train is much

weaker than in the traveling of passenger train. Schedule of ordinary freight trains contains large time supplements which compensate for random perturbations. Time reserve appears in periods when there is little of random obstacles to the train traffic. This fund should be used to save energy resource.

Modelling of train traffic is the most important part of operational rescheduling process. The major part of research in the field of traffic modelling is devoted to solving the problem of train delays minimizing. There is a lack of models that predict evolution of the train traffic situation and determine the optimal adjustment based on energy criterion. The present paper is devoted to solving the issues of traffic modelling that allows eliminating this drawback.

The principles underlying the dispatching adjustments are provided in Sect. 3 after an analytical literature review (Sect. 2). We present a brief description of methods for operational traffic management from the perspective of reducing energy consumption for train traction. The main provisions of modeling which are focused on the economic assessment of train traffic are addressed in Sect. 4. Here we formulate the new general form of criterion for search the optimal dispatching decision. We declare that the main part of the current operating costs determined by the amount of traction energy. In Sect. 5, we study a thin dynamics of energy consumption for train traction.

The requirement for precise execution the schedule of freight trains is much weaker than for the travel of passenger trains. Large time margins that compensate the random disturbances are included in the timetable of ordinary freight trains. Often there is a time reserve when a little amount of random obstacles to the train movement arises. This reserve should be used to save energy resource.

Modelling of train traffic is the most important part of operational rescheduling process. The major part of research in the field modelling is devoted to solving the problem of train delay minimizing. There is a lack of models that predict the development of train situation and determine the best adjustments based on energy criterion. The present paper considers the issues that allow eliminating this drawback.

Beyond, the principles underlying the dispatch operational adjustments outlines after an analytical review of the literature (Sect. 2). The examined types of control reduce energy consumption. The meso-model of traffic that helps to describe the process of delay propagation is proposed in Sect. 4 of the paper. We also formulate the general form of objective function for search the optimal dispatching decision. The final Sect. 5 carries detailed analysis of dynamics the energy consumption. Fast dynamics of traction energy is studied in order to obtain the regularities that are used in the consumption volume forecast.

2 Literature Review

Most of the published work on the problem of operative train traffic rescheduling is based on deterministic models of functioning the railway section. The paper [1] provides an extensive overview of recovery models and algorithms for real-time railway rescheduling. The paper deals with the problem of passenger orientation when searching for the optimal traffic adjustments.

The main types of problems that are solved in the process of searching for optimal adjustments are conflict detection and resolution (CDR) and train speed coordination (TSC) [2–5]. In these problems, the best order of trains movement determined on the condition that arise the deviations from their schedule (delays), which lead to conflicts. Most of the works explores the algorithms that make corrections of the passenger train traffic on busy line. Typically, it is considered the total value of delay of all trains in a given time period. Authors, that attempt to use economic indicators of quality of passing the passenger flow, one way or another interprets the volume of delays. The decisions for rescheduling, which minimize delays of the trains, are calculated by constructing the discrete models of movement and use of integer or partially integer linear programming [for example, 6, 7].

Local punctuality in the freight flow movement recedes into the background. Here you want to use other criteria, adequate economic interests of the company - train traffic operator. The analysis shows that the operating costs for passing trains or part of the rail operator profits may be used as a criterion that corresponds to the freight trains traffic on the section. Formulation of such the economic criterion is made in [8].

Only a small number of works devoted to solving the problem of reducing both the energy consumption and the costs through efficient operational traffic management. As an example, we present the paper [9], the authors of which are exploring this problem for suburban passenger traffic. Many papers have been published [e.g. 10, 11] which address to the creation the trajectory of the train, providing a minimum energy consumption. Rational allocation of the extra time between the elementary path segments is provided by the technique of timetable adjustment that aims to fuel economy.

3 Options for Operative Adjustment the Train Schedule

Operative traffic management of the freight train flow is significantly different from that which is used during the passage of passenger train packet. It is not necessary to provide a local unconditional punctuality of freight trains when occasional delays occur. You only need to exclude the effect of knock-ons to reduce the losses of railway capacity and operational costs. It is not necessary to follow the schedule with high accuracy on each section, since there are biggest margins to the running and dwell times of freight trains. We understand that you only need to guarantee the macro-punctuality of freight trains that is compliance of the exact arrival time at the destination, where the consignment is to be delivered.

Operational adjustment of speed profile the single train is the first adjustment option which aims to reduce energy consumption in the case of unscheduled stops. Here we believe the main type of maneuver that is carried out to prevent unscheduled stop is timely speed reduction of following train (see Fig. 1). Train 2 resets the speed at the point A when receiving information on short stopping the preceding train. The reduced speed value is maintained until the train 1 will get out at the safe interval Δ_{sch} that is prescribed by the schedule. Herewith you need to solve the following problem. It is necessary to choose such a speed v'_2 of the train 2 that it not to get into the zone of impact the yellow aspect after receiving a signal of the train 1 stopping. This is

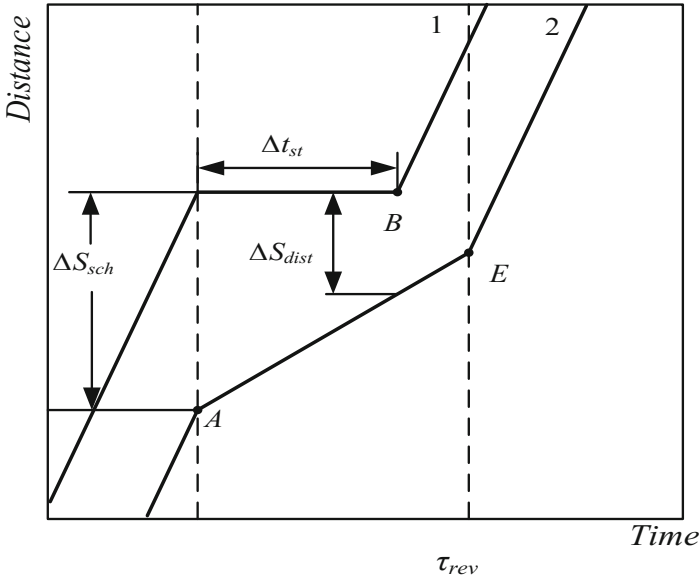


Fig. 1. Fragment of adjusted schedule in case of unplanned stop

achieved when current value of the headway Δs at closest approach of both trains exceeds the overall length Δs_{app} of two block sections.

If the headway is equal to $\Delta s_{sch} = v \Delta t_{sch}$ (where v is the planned speed) then complied the following condition: $\Delta s > \Delta s_{dist}$. This condition is satisfied when you are set the certain train speed value:

$$v'_2 < \frac{\Delta s_{dist}}{\Delta t_{st}} \left(\frac{\Delta s_{sch}}{\Delta s_{dist}} - 1 \right) \tag{1}$$

During a slow traveling mode, the driver can apply the optimal speed trajectory. This would result in savings of amount at least 50 kWh when moving passenger train and more than 100 kWh for heavy freight train traveling.

The intensity of the freight train flow undergoes a significant change from one hour to another. The reasons for this are the variations in the freight traffic volume and technology features of the railway operator, as well as planned and unplanned interruptions of the train travel. There are additional reserves, primarily time, which should be used to improve the efficiency of traffic on sites and processing at stations in intervals when the trains' flow decreases. When the flow rate increases, the nature of operational dispatch management must change towards ensuring the passage of the maximum possible number of trains, even with the operating cost overruns. Described kinds of functioning the railway section may be characterized as the economical (cost-effective) and the intensive operational mode respectively.

Prevention of conflicts between trains during period of disturbances is a major problem of operative traffic management. Rescheduling in different flows of trains may

have a certain type. The main requirement for dispatching is to ensure the accuracy of the arrivals and the quality of the transfer process if is regulated the flow of passenger trains. The same requirements apply also to freight trains, are moving on a hard schedule. These conditions assume the use of a control strategy in which the manager detects and resolves every conflict individually. This framework we call the strategy of local management.

At the main railway with mixed traffic, there are the periods when are moving large packets of conventional freight trains. Quite often there are periods of 2-3 h, when the intensity of freight flow is low. During these periods there are additional time reserves which can help to eliminate many conflicts. An increase the train running time is one of the main methods to reduce the level of delays [8]. The adjusting action is that the dispatcher purposefully assigns the group of trains that travel in economical mode. The example of combination the economical and the intensive modes is illustrated in Fig. 2.

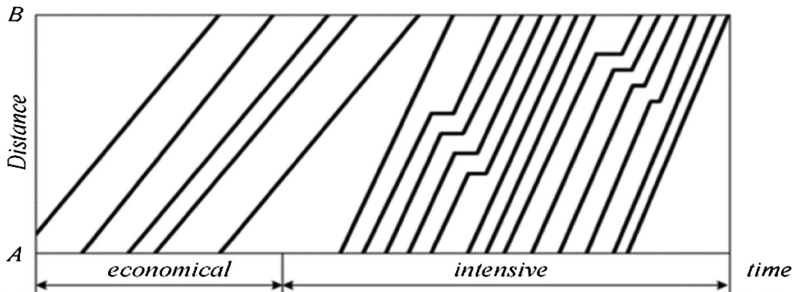


Fig. 2. Fragment of schedule with the economical and intensive train traffic.

We consider the methodology for analyzing the features of train flow and rational choice of a traffic mode as the on-line integral flow adjustment. The paper [12] uses the stochastic model which allows determining the local zone of schedule space in which it is expedient to introduce the economical traffic mode.

4 Traffic Meso-Modelling and Optimization

Model of train traffic are usually represented as a set of operations, each of which has its own duration. Elementary operating times have fixed values when traffic is undisturbed. These elements correspond to fragments of the normative schedule. Running and dwelling times are deviated from planned values when there are influencing factors.

The widespread micro-models of traffic are using block-sections as the elements of permanent way [2]. Such a small specification of the railway infrastructure leads to a large amount of computing for solving the optimization problem. Microscopic approach is valid only in a small number of cases where there is very intense commuter train traffic. Slight deviation from the schedule causes a cascade of knock-ons. More common is the situation on the railway with mixed traffic where conflicts between

trains are relatively rare and the delay propagation process is weakly expressed. In this case, more effective representation is the traffic model of meso-level. Nodes of train traffic graph in maso-model reflect conflicting events only [13].

The example shown in Fig. 3 reflects the delay propagation across the network comprising various types of conflicts on stations and at open tracks. The picture illustrates simplified mesoscopic representation of train traffic. The node 12 describes a train succeeding conflict while each of the nodes 23 and 34 reflect a conflict at the station caused by disturbances of process the passenger transfer.

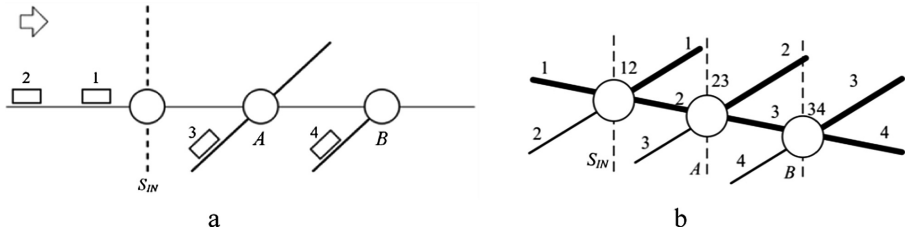


Fig. 3. Fragment of the meso-model illustrating a propagation of delays: (a) trains 3 and 4 come from the lines which differ from previous travel direction of trains 1 and 2; (b) operations which contain secondary delays are denoted in bold.

Dynamic problem for resource placement that includes the power restrictions [14] is the methodological basis to optimize schedule using economic criterion. We formulate the following general form of objective function for the optimal dispatching decision search:

$$\min \sum_{i \in T} \sum_{j \in J} \left(C_{jt}^0 z_{jt} + \sum_{i \in I_i} c_{ij} x_{ij} + \sum_{i \in I_i} C_{ij}^{ocm} x'_{ij} \right) \quad (2)$$

The first term of equ characterize the travel cost which accumulated before train j entry to the controlled site. The second component reflects the costs of a nonstop train pass along the i-th meso-section up to the point of conflict appearance. The third term shows the total losses at occurrence the unscheduled stops. Binary variables and serve to incorporate the relevant components of the train trajectory into computation process the dynamic operational costs. Formulated criterion corresponds to the class of MILP.

Each of conflict is accompanied by increase in the amount of energy that consumed for train traction. Therefore, this value is to be the basis for optimizing the timetable together with the indicator of punctuality. Mainly, it concerns the freight train traffic. The most effective adjusting solutions at the first stage of search are fixed by determining the scenario with minimum number of non-scheduled stops. Thereby the main part of unproductive energy consumption is eliminated (more than 60 per cent). At the second stage, you can make rational choice of the travel time at elementary sections. This problem is solved by redistributing the time margins that are included into the schedule.

In Sect. 5, we study a thin dynamics of energy consumption for train traction. The obtained conformity may be used in the train traffic model considering real circumstances at the site. Updated model is used for improve the prognosis created. It allows you increasing an efficiency of dispatching.

5 Detailed Analysis of Dynamics the Traction Energy Consumption

Power consumption by the train unit is determined not only by value of the mechanical resistance but due to speed features when moving along the site. Current speed value depends on actual condition of the infrastructure and of quality the train control that executes the driver. It is necessary to separate these two impacts during analysis fulfilment to create a correct prediction of consumption, taking into account the likely future deviations from the schedule.

We propose original methodology to check the root of occurrence the energy overruns at the element of train path. This approach allows you to identify the influence of the disturbing factor which leads to exceeding the normative consumption. The factor mentioned is a deviation from the standard trajectory because of driver’s irrational action or presence an obstacle to the train traveling.

The developed approach is based on obtaining data on the traction energy and the implementation of its correlation analysis. Basic regularities determined most fully if you are considering the correlation of energy consumption of the given train unit with the characteristic of the path relief and with the energy function the other trains.

We have investigated in detail the energy consumption by heavy haul trains at the electrified main line. Data on the current energy consumption, the coordinate and train speed were obtained from the onboard electronic recorder. The volume of energy was determined for train travel at elementary sections with different relief characteristics. One of them (type I) has the heavy relief with lengthy grade. Other sections have a more smooth behaviour (types II and III). Measurements were carried out on a large number of the trains the same type. Measured values of power consumption for the different sites are summarized in Table 1.

The values of correlation index calculated for the consumption and the path relief are depicted at the Fig. 4.

Table 1. Power consumption according to heaviness the site relief, kW * h

Site tipe	I	II	III
Length, km	15	40	20
Min	900	1207	641
Average	1112	1559	845
Max	1264	2055	1184

Relief types: I heavy type II facilitated type III light type+

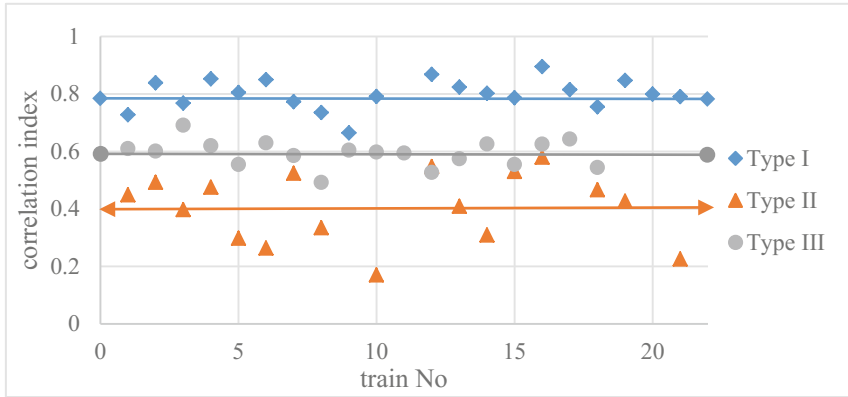


Fig. 4. Correlation index of the energy consumption and the path relief

The data presented at the picture are showing the following regularities. The correlation index rises with increasing severity of the site relief. This is due to the fact, on a site that includes a steep and extended rise there is a very narrow spectrum of options for implementation the traction trajectory.

Drivers use various run trajectories on the light sections so the characteristics of energy consumption by different trains correlate poorly. This explains the great difference in the amount of energy that is spent by the experienced and inexperienced drivers when they have freedom of action during the locomotive control.

The calculated correlation index of the consumption and of the vertical profile of the path is weakened when unscheduled stops arise. Thus, the presence of short stops when train's 22, 23 run at the Sect. 1 reduces the correlation coefficient from 0.8 to 0.5.

6 Conclusions

Optimum dispatching can significantly reduce the consumption of traction energy. Preventive adjustments such as assigning an economical traffic mode and the target train trajectory correction in the event of unscheduled delays are the main actions of operative management. The result of this activity is a significant reduction in consumption mostly by the freight train flow. The proposed methodology of correlation analysis of traction energy can improve the consumption prognosis and provide a tool to assess effective operational dispatch adjustments.





References

1. Cacchiani, V., Huisman, D., Kidd, M., Kroon, L., Toth, P., Veelenturf, L., Wagenaar, J.: Overview of recovery models and algorithms for real-time railway rescheduling. *Transp. Res. Part B* **63**, 15–37 (2014)

2. D'Ariano, A., Pacciarelli, D., Pranzo, M.: A branch and bound algorithm for scheduling trains in a railway network. *Eur. J. Oper. Res.* **183**(2), 643–665 (2007)
3. Quan, L., Dessouky, M., Leachman, R.: Modeling train movements through complex rail networks. *ACM Trans. Model. Comput. Simul.* **14**, 32–76 (2004)
4. Törnquist, J.: Computer-based decision support for railway traffic scheduling and dispatching: a review of models and algorithms. In: *Proceedings of ATMOS*, Palma de Mallorca, Spain (2005)
5. Carey, M., Crawford, I.: Scheduling trains on a network of busy complex stations. *Transp. Res. Part B* **41**, 159–178 (2007)
6. Cordeau, J.-F., Toth, P., Vigo, D.: A survey of optimization models for train routing and scheduling. *Transp. Sci.* **32**(4), 380–404 (1998)
7. Huisman, D., Kroon, L., Lentink, R., Vromans, M.: *Operations research in passenger railway transportation*. Erasmus Research Institute of Management (ERIM). Research Paper № ERS-2005-023-LIS (2005)
8. Davydov B., Dynkin B., Chebotarev V.: Optimal rescheduling for the mixed passenger and freight line. In: *COMPRAIL* (2014)
9. Bocharnikov, Y.V., Tobias, A.M., Roberts, C., Hillmansen, S., Goodman, C.J.: Optimal driving strategy for traction energy saving on DC suburban railways. *IET Electr. Power* **1**(5), 675–682 (2007)
10. Kuznetsova, A.: Optimization of technology of driving freight trains on the stretch, by the criterion of minimum operating costs for the mileage, Ph.D. thesis (2006)
11. Luethi, M.: Evaluation of energy saving strategies in heavily used rail networks by implementing an integrated real-time rescheduling system. *WIT Trans. Built Environ.* **103**, 349–358 (2008)
12. Chebotarev, V., Davydov, B., Godyaev, A.: Stochastic traffic models for the adaptive train dispatching. In: *Proceedings of the First International Scientific Conference “Intelligent information technologies for industry” (IITI 2016)*. *Advances in Intelligent Systems and Computing*, pp. 323–333 (2016)
13. Davydov, B., Chebotarev, V., Kablukova, K.: Adaptive stochastic model for the train rescheduling. In: *7th International Conference on Railway Operations Modelling and Analysis Planning, Simulation and Optimisation Approaches*, Lille, France (2017)
14. Kochetov, U.: Local search methods for discrete location problems, DrSc. thesis (2009)

Development of Transport Infrastructure

Needs and Possibilities of Development of the Macedonian Motorways

Slobodan Ognjenovic¹ , Tamara Narezhnaya² ,
Zlatko Zafirovski¹ , and Ivana Nedevska³ 

¹ Faculty of Civil Engineering, Ss. Cyril and Methodius University in Skopje,
blvd. Partizanski Odredi 24, Skopje 1000, Republic of Macedonia
ognjenovic@gf.ukim.edu.mk

² Moscow State University of Civil Engineering, 26, Yaroslavskoye shosse,
Moscow 129337, Russia

³ Geing Krebs und Kiefer-Skopje, Boris Trajkovski str., Skopje 1000,
Republic of Macedonia

Abstract. The road network has been compared to the human blood circulation since the beginning of its development, the analogy referring to both its function and its hierarchically arranged and branching structure. In other words, the balanced development and the coordinated function, starting from the main arteries (motorways) until to the capillary system (local roads) is a precondition to the overall rationality of the existence and development of the organism (the country) and its vital functions (e.-g economy).

Keywords: Roads · Development · Road network · Maintenance
Annual average daily traffic

1 Foreword

Any deviation from the optimal balance on any side entails similar problems which regularly raise the question: How to distribute the available funds for maintenance and construction of the different levels of road network in order to achieve the maximal approach to the balance of the overall function? The essential criterion for the distribution is the justifiability of the investments, that is, the expected level of profit acquired as related to the expenses and this according to the analysis of the justifiability on the level of certain routes and/or sections, from the viewpoint of the road network as a subsystem of traffic.

2 Present Condition

Pursuant to the data of the Public Enterprise of State Roads of Macedonia, the overall length of the state roads is of 4893.78 km of which 1112.27 km are main roads, 3645.20 km are regional roads, and the branch length is of 38.53 km and 97.98 km on the main and regional roads respectively (Fig. 1). By adding the length of 9258 km, which is the one of the local roads, we obtain the approximate overall length of all the

roads in Macedonia, which is of 14252 km. Additional 132 km of highways are currently under construction: the Demir Kapija-Smokvica road which is around 28 km in length, the road Miladinovci-Shtip (47 km) and Kichevo-Ohrid (57 km). Figure 1 shows the road network of the Republic of Macedonia.

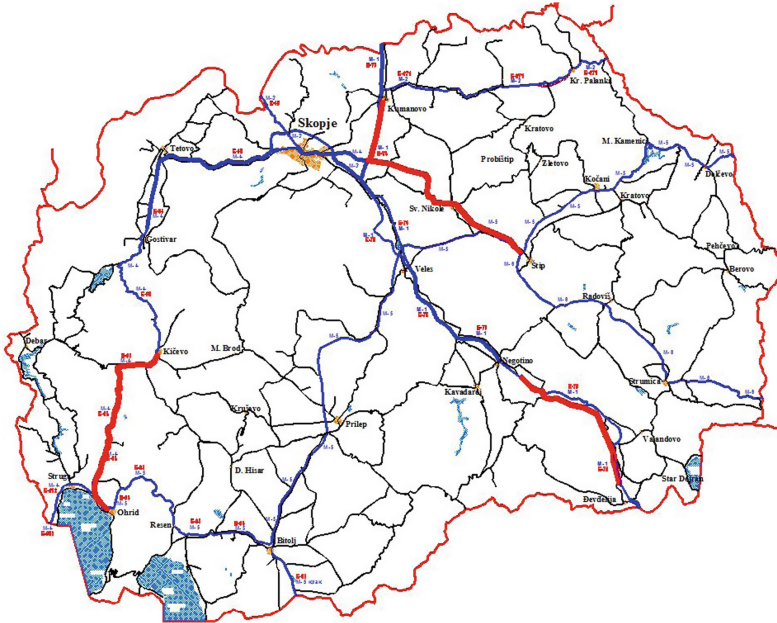


Fig. 1. Road network of the Republic of Macedonia

Figure 2 gives a comparative demonstration of the highway density (number of highway kilometers on 100 km² of the country territory), and a comparative presentation of the motorization (number of registered passenger cars per km of highway, Fig. 3).

Pursuant to the European Road Statistics data of 2012 regarding the highway density related to the territory of the country, Macedonia belongs to the group of countries where the highway density is of medium level, with approximately 960 m on a 100 km² of territory, which is a significantly better indicator than some EU countries (Bulgaria, Poland, Romania etc.). As for the motorization level, Macedonia is the last in Europe regarding the number of registered passenger cars and the length of its highway network, with 1255 cars per kilometer of highway. The example of Poland is especially interesting, as the highway density in that country is very low, meaning that the number of registered cars per highway kilometer is high, although Poland is characterized by a considerable economic growth. In other words, highways are not the key condition; a high-quality network of two-lane roads is perfectly able to support the crucial development of economic activities.

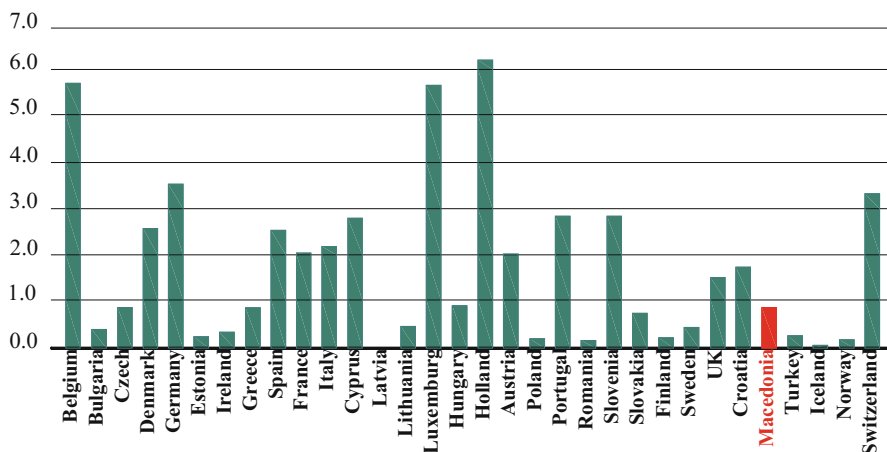


Fig. 2. Highway density in the European countries (km of highway/100 km²). Source: European Road Statistics for 2012

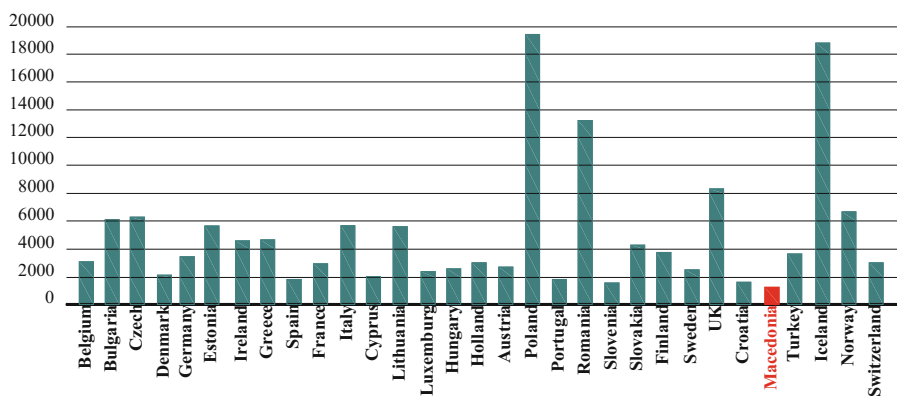


Fig. 3. Registered passenger cars per km of highway in the European countries (1000 passenger cars/km of highway). Source: European Road Statistics for 2012

Supposing that the additional 132 km of highways currently under construction will be completed until 2020 and that the level of motorization will increase at the annual rate of 3%, the length of the Macedonian roads would be of 1473 km on the territory of 100 km², and 973 registered vehicles per kilometer of highway. In that case, the increase of the highway network would be considerably faster than the increase of the motorization level, which could be justifiable only if the entry and transit of foreign vehicles considerably increases in the several years to come.

3 Needs

On the macro level, the overall needs can be approximated though the increase of the number of registered vehicles and the level of their use, as well as the number of trans-border target and transit journeys of foreign registration vehicles. As the vehicles with foreign registration plates which spend some time on Macedonia using the road network for internal movements are not included, the so established needs reflect the lower limits. The level of use by the domestic vehicles, that is, the average annual mileage per vehicle is not an available data, but its approximate value can be indirectly established by the annual fuel consumption for traffic needs (Tables 1 and 2).

Table 1. Total number of registered vehicles in the period 2009–2013 (motorcycles, passenger cars, heavy-duty vehicles, busses)

	2009	2010	2011	2012	2013
Motorcycles	9097	7761	8373	8473	8093
Passenger vehicles	282196	310231	313080	301761	346798
Heavy duty vehicles	27771	28795	27917	26542	30167
Buses	2454	2695	2636	2719	3022
Total	321518	349482	352006	339495	388080

Source: National Bureau of Statistics: Transport and other services 2013

It can be noticed that the number of registered vehicles in 2010 is 8.7% higher than the same number of 2009, and the fuel consumption in 2010 was 4% higher than in 2009. This means that although the number of registered vehicles (exception made for 2012), it seems that the increase of the fuel consumption does not follow that increase. It would be interesting to observe the relation of the number of registered vehicles and the fuel consumption in the period of 2011–2013, but there are no available data thereon. If the increase of the difference between the increase of the number of registered vehicles and the fuel consumption continues, and considering that according to the National Bureau of Statistics of the Republic of Macedonia, the number of the vehicle over 10 years old amounts 78.2%, no increase of the traffic scope can be expected on our highways in the forthcoming period, at least regarding the number of vehicles with Macedonian registration plates. As for the trans-boundary traffic there are no available data on the vehicles with foreign registration plates with transit or target traffic on the territory of Macedonia. But the data on fuel consumption on the level of the rolling fleet of the EU demonstrate that the individual fuel consumption has been decreased from 8.25 l/100 km in 1995 to 7.2 l/100 km in 2010 (Energy Efficiency Trends in the Transportation in Europe, 2012). Also, the completion of the Romanian and Bulgarian highways and the commissioning of the Egnatia highway in North Greece on the one hand, and the two border crossings in Macedonia and Serbia (entry and exit of the transit traffic through the country), was not accompanied by any significant increase of traffic on our highways.

Table 2. Fuel consumption in the period 2005–2010 (Diesel, LPG, petrol) in tons

	2005	2006	2007	2008	2009	2010
Diesel	184682	189314	218547	223186	247252	266687
LPH	27158	32378	43210	45687	44412	41807
Petrol	116527	106849	113603	117784	123324	123131
Total	328367	328541	375360	386657	414988	431625

The average annual daily traffic (AADT) on the Macedonian highways is shown on Table 3. It is clear that, except on the Glumovo-Tetovo and Tetovo-Gostivar sections, the traffic load is under 10,000 vehicles/day both ways on all other sections. The increased load on these two sections is the direct consequence of the low mobility of the Macedonian population as a whole, the said mobility being increased on a local level, that is, on short relations on the Glumovo-Tetovo-Gostivar area. A similar situation can be observed on the area between Kichevo and Ohrid (where a highway is under construction).

Table 3. AADT on the Macedonian highways (vehicles/day/both ways)

Section	Vehicles of all categories
Border to the Republic of Serbia-Kumanovo	5254
Kumanovo-Miladinovci	8146
Miladinovci-Petrovec	6418
Petrovec-Veles	9213
Veles-Gradsko	5592
Gradsko-Negotino	3942
Demir Kapia-Udovo	4463
Smokvica-Gevgelija	4134
Gevgelija – border to Greece	7377
Skopje-Glumovo	9662
Glumovo-Tetovo	10631
Tetovo-Gostivar	12646
Gostivar-Kichevo	4634
Kichevo-Botun	4480
Botun-Podmolje	4539
Podmolje-Ohrid	9624

The situation is further complicated if an analysis is elaborated concerning the funds invested in regular maintenance. Table 4 gives data on the road maintenance funds on the level of the overall state road network in Macedonia.

Comparatively, the road maintenance funds in some countries in the region and in the European developed countries are given in Tables 5 and 6.

Table 4. Data on the funds invested in the maintenance of the state road network in Macedonia in the period of 2005–2009.

Year	2005	2006	2007	2008	2009
Funds in EUR*	6	4	14	14	12
Average EUR/km	1226	818	2861	2861	2452

* million EUR

Source: European Road Statistics for 2012

Table 5. Data on the funds invested in road maintenance in some EU countries and in our region in the period of 2005–2009 (millions of sue)

	2005		2006		2007		2008		2009	
	EUR*	EUR/km	EUR*	EUR/km	EUR*	EUR/km	EUR*	EUR/km	EUR*	EUR/km
Croatia	242	12740	155	8160	158	8318	168	8844	144	7581
Slovenia	99	14612	140	20664	139	20516	148	21845	155	22879
Bulgaria			108	5582	215	11113	203	10493	69	3566
France	2189	5488	2235	5602	2294	5750	2184	5474	2207	5533
Switzerland	1520	76617	1534	77323	1410	71072	1608	81052		

* million of EUR

Source: European Road Statistics for 2012

Table 6. Length of the national road network in some EU countries and in our region

	Croatia	Slovenia	Bulgaria	France	Switzerland
Length in km	18996	6775	19347	398917	19839

Source: European Road Statistics for 2012

The tables clearly demonstrate that the funds invested in the maintenance of the Macedonian road network are far below the funds invested in the countries of the region, whereas the situation regarding the developed European countries is incomparable.

On the field, this means that winter maintenance of the highways is carried out as per the priority of the Public Enterprise of Makedonija Pat, including the reparation of the potholes, urgent cleaning of landslides, trimming of the grass at the flanks and along the central line, although not regular, renewal of the horizontal signaling. So, not a word about the application of any preventive maintenance measures. Namely, backfilling of cracks or any kind of surface treatment are not carried out on the Macedonian roads.

Rehabilitations are part of the investment maintenance and are subject to the same conditions as those applying to new roads, that is, they are financed through credits and EU funds.

4 Possibilities

The principal benefits upon the construction of highways are the reduced expenses regarding the existing two-line road network, and above all, the time-related expenses of vehicle exploitation and the decrease in the expenses caused by road accidents. The direct income from the pay-tolls will have to cover the investment payment costs, as well as the costs on maintenance and pay-toll collection, control and processing. Of course, the expenses on highway building costs are always higher than those on a two-line roads, above all due to the considerably wider cross-section, the increased costs on expropriation and environment protection, the comfort elements of the site and leveling plan, the de-leveled intersections, the increased number of engineering constructions etc. Considering that the issue of economic justifiability is crucial in decision making, upper and lower limits are defined in many countries referring to the investment justifiability within the designing regulation framework. The Fig. 4 chart is constructed as pursuant to the German and Serbian regulations. The lower limit is primarily established by the investment payment capacity, and the upper limit by the road capacity where the time dependent expenses exponentially increase.

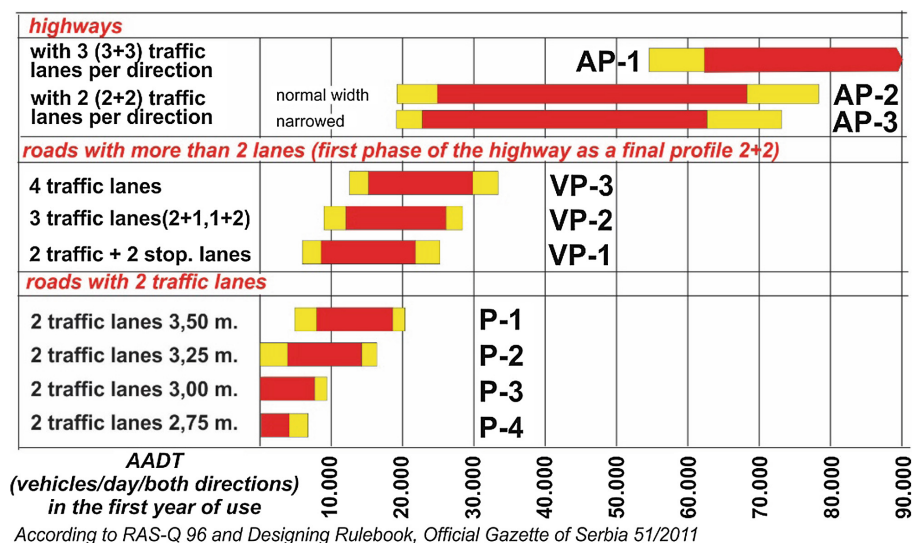


Fig. 4. Limit values of the Average Annual Daily Traffic (AADT) as a basis to the justifiability of the investments in different road types

The low limit of the justifiability for the construction of a highway with two-lanes per direction (AP-2, AP-3, Fig. 4) can be expected at AADT = 22000–25000 vehicles/day/two directions in the first year of exploitation. If this value is compared to the numbers of traffic on the Macedonian highways in 2012 (Table 3) it is clear that no section of the existing highways meets the justifiability criterion. Some of them even

have three times lower traffic loads than the limit ones, and in fact create losses, that is, are prone to create losses that will have to be covered from the national incomes. What is yet more important, this criterion is not met even by the sections under construction. For example, the average load (AADT) of the road under the competence of the Croatian Highways, namely the Rijeka-Zagreb road, of 16,500 vehicles/day/two directions as in compliance with the data of 2012 generates annual losses in the approximate amount of 37,000,000 euro. The data concerning the average AADT of the roads of the Croatian roads (13200) and roads in Serbia (13,700) indicate that these networks under the competence of the respective country, create losses that are not known. The average annual daily traffic on the Macedonian roads for the year 2012 amounts 7702 vehicles/day/both lines. In the region, only Slovenia has a larger traffic scope, with AADT = 29300 vehicles/day/both lines.

It is interesting to note that a high-quality road with two lines (P-1, Fig. 4) has an upper limit of justifiability at AADT = 19000–20000 vehicles/day/both lines, that is, provides for economically acceptable exploitation conditions. This fact is very important when referring to pay-toll roads because, if the road is of a relatively good quality, parallel to a section of a highway, an important part of the users will still use the two-lane road in order to avoid the pay-toll, but the use of the highway by a large number of vehicles will create better conditions.

The multi-line roads (VP-1, VP-2, VP3, Fig. 4) are similar to highways by many important features, and they cover the traffic loads between the two-line roads and the highways. They can be a final solution when it can be confirmed with a relative certainty that no two-line highway per direction (2 + 2) will be necessary on those sections. Upon the staged construction of the highway with two lines per direction, a full-profile construction can be applied per sections when the traffic load approaches the upper load limit, for a two-line road; it is also possible to apply intermediate profile, that is, conditionally said, build half of the profile of a highway on several sections in continuity, so that the scope of the investments can be adjusted to the slower increase of the traffic needs with time. In such a case, all the elements correspond to a final highway profile, by simultaneous pre-investment, for example, in expropriation, undercarriage, drainage, over-road constructions etc. As a consequence, the price of a staged building of a highway amounts 60–65% of the final building costs.

The crucial issue which is most frequently not addressed by the experts is the one of the increase of the traffic needs which are nowadays under the lower limit of justifiability of construction of highway sections. As it can be concluded from the above, it is not realistic to expect any serious increase of the traffic loads, that is, of the AADT, without a serious increase of the economic activities and people's standard, accompanied by some considerable increase in the mobility of the vehicles with domestic registration plates. On the other hand, no serious increase of the transit flows through Macedonia can be expected while there are border crossings where the time needed to control the vehicles, the passengers and the load (two border crossings) importantly increases the overall journey time, especially considering the construction of the highways through Romania and Bulgaria which shall take over an important part of the traffic flows of the vehicles with foreign registration plates.

Considering this, it is not realistic to plan that the Macedonian highway network will reach positive economic effects in the long run in future. In such a situation, which

is not typical only for Macedonia, the budget funds for maintenance and rehabilitation are the first recourse at hand. Thus we are still faced with an impermissibly low level of funds for the maintenance of the existing road network, contributed by the traffic load of the existing highway network, which is considerably below the low limit of justifiability. As each serious concessionary knows the limit values of justifiability very well (Fig. 6), the solution to this situation by issuing concessions for the existing highways will not be simple or easy.

Finally, there is one phenomenon that is, as a rule, characteristic of the medium developed European countries, not only of Macedonia, which is the emotional tendency of the politicians, professionals and the public to always entirely dedicate themselves to new buildings and large projects as highways are, neglecting the same, even maybe higher economic benefits that the country and society can reach by high-quality maintenance and rational reconstruction of all categories of existing roads as pursuant to their contribution to the economic and social development of the country.

As long ago as in 1881, A. Wellington, in his book entitled *Economic Theory of Railway Location* wrote his following attitude: “It is unbelievable and discouraging how much the engineers, their teachers and employers pay attention to the smallest possible detail in the construction of a railway, forgetting more important issues regarding when, where and why to build”

The present text is an attempt to actualize the questions of *When?* and *Why?* by rough and stubborn numerical data. Of course it is also an attempt to reduce the emotional “charge” and limit the intuitive determination as a precondition to a more rational decision-making, at present as well in the future.

References

1. Ognjenovic, S., Ishkov, A., Cvetkovic, D., Peric, D., Romanovich, M.: *Procedia Eng.* **165**, 954–959 (2016). <https://doi.org/10.1016/j.proeng.2016.11.805>
2. Dražić, J., Peško, I., Mučenski, V., Dejić, A., Romanovich, M.: *Procedia Eng.* **165**, 898–905 (2016). <https://doi.org/10.1016/j.proeng.2016.11.790>
3. Jevric, M., Romanovich, M.: *Procedia Eng.* **165**, 1478–1482 (2016). <https://doi.org/10.1016/j.proeng.2016.11.882>
4. Simankina, T., Romanovich, M., Tsvetkov, O.: *MATEC Web of Conferences*, vol. 53, Article Number 01054 (2016). <https://doi.org/10.1051/mateconf/20165301054>
5. Romanovich, R., Vilinskaya, A.: *MATEC Web of Conferences*, vol. 53, Article Number 01052 (2016). <https://doi.org/10.1051/mateconf/20165301052>

Transport Complex of Primorye as a Factor of the Economic Status of the Region

Tatyana Miroshnikova¹  and Natalia Taskaeva² 

¹ Vladivostok State University of Economy and Service, Gogolya str., 41,
Vladivostok 690014, Russia

² Moscow State University of Civil Engineering, Yaroslavskoye Shosse, 26,
Moscow 129337, Russia
natalia.taskaeva@yandex.ru

Abstract. To strengthen the economic and geopolitical status of the Russian Federation in Asia-Pacific region, it is expedient to create a modern multi-functional infrastructure of national importance, including transport and engineering in the coastal zone of Primorsky Krai. This is the Russian center for international cooperation with the countries of Asia-Pacific region (APR) and Asia-Pacific Economic Cooperation (APEC). The article presents some problems, the fleet of the Russian Federation faces, and the probable ways of their solving. The main method of analyzing and researching this issue is a program-targeted approach to solving problems of balancing the interests of all participants in the transport and logistics center in the region. An unconventional financial method for ensuring the reproductive process of fixed assets of sea transport is proposed. In terms of improving the management efficiency of the subject of the federation, the issue of ensuring the renewal and replenishment of ships of maritime transport is urgent and relevant.

Keywords: Transport infrastructure · Road infrastructure · Economic status

1 Introduction

Transportation of Primorsky Krai is represented by all types of transport - rail, road, river and sea, as well as air and pipeline. Maritime transport of the Primorsky Territory is one of the most important branches of its specialization. Seaports of the Primorsky Territory are in fact the trade gate of Russia to the Asia-Pacific region. One of the most important freight-forming factors for the seaports of the region is the position of the ATR as the largest center for the consumption of energy carriers, mineral fertilizers and forests.

The transport complex of the Primorsky Territory of Russian Federation is the leader in the Far East in terms of the volume of public goods turnover. The share of transport services in the gross domestic product of the region is more than two times higher than the average Russian level. Regional modes of transport “specialize” in the performance of certain types of transport. Freight transportation is carried out mainly by rail and road transport; passenger turnover is serviced by railway, road and fast-growing air transport; export-import shipments are carried out mainly by sea and rail.

2 Materials and Methods

The methodology is based on the analytical approach, analysis of dynamics, and realization of comparative analysis. The main method of analyzing research issue is a program-targeted approach to solving problems of balancing the interests of all participants in the transport center.

The cargo turnover of the ports of the Primorsky Territory averages 46.9 million tons. However, the potential of seaports in Primorsky Krai is not fully utilized. Seaside ports are now ready to process additional volumes of oil, coal, and liquefied gas [1].

In January–April, 2017 large and medium-sized organizations engaged in transport activities shipped their own production, performed works and services for 46.9 billion rubles, which in current prices was 100.4% compared to January–April 2016. The volume of freight transported by road transport of large and medium-sized organizations of all types of activities in January–April 2017 amounted to 3868.9 thousand tons (89.7% compared to January–April 2016), cargo turnover - 157.6 million ton-km (91%).

The organizations of maritime transport, excluding microenterprises, transported 439 thousand tons of cargo in foreign navigation (1.7 times less than in January–April 2016), in coastal navigation –440.6 thousand tons (7.4% less). Transportation of passengers by sea transport in January–April 2017 decreased by January–April 2016 by 9.4%, passenger turnover decreased 2.1 times.

The largest share in the structure of transported cargo is the marine mode of transport (40.3%). In dynamics over a five-year period, the share of cargo transported by sea traffic increased by 3.5%. There is a trend towards increased shipping. A steady trend towards growth in traffic volumes has a positive effect, increasing the role of transport in the economy, is ensured by the sale of transport services on the world market through the attraction of foreign transit freight flows [2].

On the territory of Primorsky Krai, there are 6 largest sea ports of the Russian Far East: Vostochny, Vladivostok, Nakhodka, Olga, Posiet, Zarubino.

The development of the transport complex of the urban district will ensure a stable socio-economic growth of the region. One of the tasks of the development of the transport complex is the renewal and expansion of the fleet of vehicles. Three key factors predetermine the expediency of the development of the transport and logistics center: the location in the densely populated Asia-Pacific region, which is an attractive sales market, the advantageous transport position at the intersection of the transit routes, the presence of a large port capable of accepting ships of almost any displacement.

The strategic alternative to the development of the city of Vladivostok is a universal city that combines the functions of a transport, logistics, industrial, tourist regional center, the Far East and international level. This implies the active development of port facilities, roads, railways, air transport. High business activity in such areas as transport, logistics, development of business tourism, active urban policy aimed at the development of the road network in order to optimize traffic flows.

The largest seaports of the Primorsky Territory - Vladivostok, Nakhodka and Posiet in the first four months of 2015 reduced the volume of transshipment. The only port that increased cargo turnover was «Vostochny», which increased cargo turnover by

14.3%. In general, the turnover of the sea ports of the Far-Eastern basin for the four months of this year increased by 2.3% compared to last year's indicator [3].

For January–May, 2017 cargo turnover of ports increased:

By 7.6% of the port of Vostochny and amounted to 29.4 million tonnes, to 7.7% of the port of Nakhodka and amounted to 10.4 million tonnes, to 11.3% of the port of Prigorodnoye and amounted to 7.6 million tonnes, an increase of 18.6% Port of Vladivostok and amounted to 6.7 million tons [3].

For the first five months of 2017, stevedore received 135,378 wagons with coal and sent it for export to the APR countries on 232 ships. For the same period in 2016, 199 ships were handled in the East Port. Recently, the demand for Russian coal in the APR countries has increased again after a slight decline. By the end of 2016, over 23 million tons of coal were transhipped. In 2017, the volume of transshipments continues to increase [3].

For Vladivostok, sustainable development of the sea transport hub is of great importance.

According to the data in Table 1 and Fig. 1, the volume of cargo transshipment in the ports by 2017 was 29.4 million tons, which is 2.5 times higher than in 2010. However, there are a number of factors that impede the effective development of Vladivostok ports [4].

Table 1. Volume of cargo transshipment in ports, million tons

Volume of cargo transshipment in ports, million tons	2010	2011	2012	2013	2014	2017
	11.18	11.8	13.05	14.5	15.3	29.4

Source: Official site of the Association of Russian Sea Commercial Ports <http://www.morport.com>

For Vladivostok, the southern part of Primorsky Krai, which has significant coastal and island territories, the development of land and air transport is clearly not enough. There is no less demand for the development of sea traffic, and its absence inhibits the development of the city and agglomeration. The tourist and recreational potential of the sea city will not be fully revealed without an organized maritime communication. The development of the Vladivostok port's capacities is limited by the fact that the port is surrounded by urban buildings.

For Vladivostok, sustainable development of the sea transport hub is of great importance.

In 2015, the law on the territory of the Freeport of Vladivostok was adopted, which includes all key ports of the south of the Far East from Zarubino to Nakhodka. For residents and non-residents of the Freeport, a number of financial preferences have been granted: for residents of the free port of Vladivostok (SPV). In particular, the amount of insurance contributions for 10 years is 7.6%; Income tax for the first 5 years - 0% (the next 5 years 12%); The property tax for the first 5 years is 0%, and the next 5 years 0.5%; Land tax for the first 5 years - 0% [5]. Forecasting economic indicators based on the results of the introduction of the free port shows by 2025 the following: revenues to the budget - at the level of 97 billion rubles, with budget losses due to preferences at the

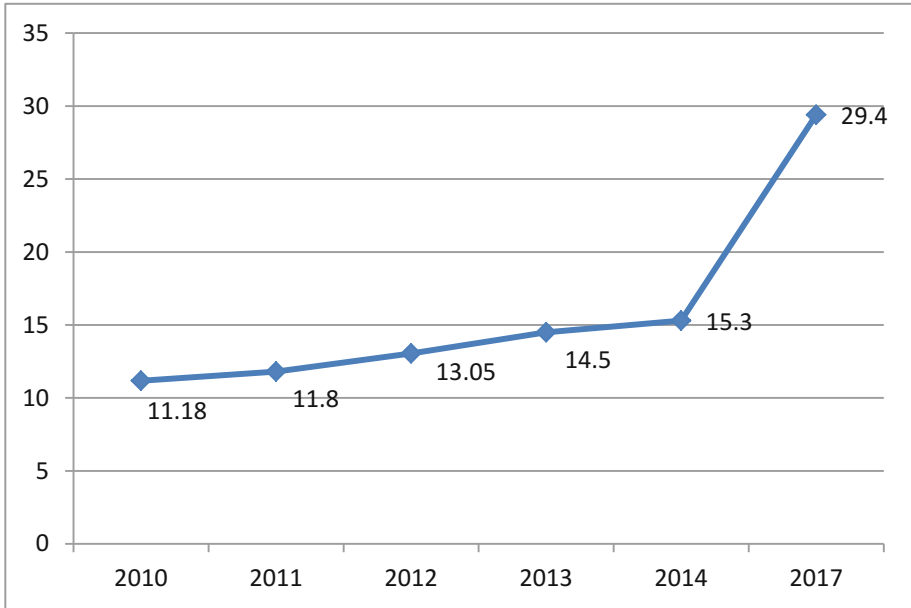


Fig. 1. Volume of cargo transshipment in ports, million tons

level of 31 billion rubles. The main economic effect will come in 2034, when the preferential tax regime for the first residents will cease: losses by this time are projected at 35 billion rubles, and receipts - more than 500 billion rubles. According to our forecasts, the free port regime will contribute to the creation of more than 50,000 new jobs in the first 5 years. By 2034, there will be almost 350,000 new jobs.

In the period 2011–2015, there is a stable negative trend in the volume of expenditures directed to the creation and reproduction of fixed capital, regardless of the state's attempts to increase the investment attractiveness of Primorsky Krai and the Far East as a whole by creating territories for advanced development and a free economic zone in the region.

To assess the results of the free port regime that have been achieved so far, the main statistical indicators of its activity during 2016 have been examined according to official data of reports on the activities of JSC "Corporation for the Development of the Far East", as well as the register of residents of the free port. It should be noted that by the end of 2016 most of the indicators significantly exceeded the planned values for this period. Thus, for example, the number of agreements with residents for the year totaled 118, which indicates a 68.6% percentage of the implementation of the plan. The volume of investments claimed in agreements with residents in 2016 amounted to more than 180 billion rubles, which indicates overfulfillment of the plan by 34%. Exceeding the planned values in 2016 is a good indicator of the implementation of the regime of SPS (free port Vladivostok) [6].

The creation of a free economic zone, according to the preliminary assessment of experts, will contribute to an increase in the inflow of investments into business

activities of Primorsky Krai by 2.5 times. The attraction of foreign investors to the entrepreneurial activities of the free port of Vladivostok is conditioned by the need for effective use of foreign financial and material assets and managerial experience for the development and improvement of the region's economy. For residents of the Free Port of Vladivostok, a free customs zone regime is available. This regime is competitive in comparison with similar forms of supporting the economy in other countries. For example, the established free customs zone regime for residents involves duty-free and tax-free importation, storage and consumption of foreign goods. Free port of Vladivostok provides for a simplified visa order of entry.

The sea terminals of Vladivostok transport hub, the development opportunities of which are primarily connected with overcoming the problems of the port location in the city, form one of the most promising port hubs in the Far East. Here, development involves technical modernization, unloading of the urban transport system, development of logistics and distribution terminals outside the urban areas. Thus, the development of the airport in combination with the further development of the sea and land transport and logistics complex will make Vladivostok one of the key transport hubs of the Asia-Pacific Region.

The implementation of the free port project implies a significant increase in freight turnover. To territorial problems today it is possible to attribute such problem as expansion of territory of a free port on nearby water areas. In the port, it is possible to achieve large volumes of cargo traffic during the construction of a single-point berth. The berth enables to take more ships, increasing the volumes of fuel consumption. A single-point berth can take ships all the year round, regardless of the season, weather conditions and cataclysms. The increase in cargo traffic in the port is possible with the construction of a roadside berth a few miles from the coast. In this case, there is no need to deepen the bottom, investing large amounts of money in upgrading, or improving the port infrastructure. This greatly simplifies the process of calling a vessel into the port, accelerates it, reduces the costs associated with creating a port-point. The increase in cargo traffic is possible with increased patency.

For example, Singapore is a port of world importance, almost 50% of calls of sea vessels provide for their bunkering, both in the roadstead and in its internal part. That is, the construction of the complex in the port water area will contribute to an increase in the total cargo turnover. Vessels entering the port area can be serviced both in the roadstead and near the shore. Carriers in the future will carry out the transshipment of cargo directly near the shore, and bunker in the roadstead. With the construction of a raid berth, the number of ship calls can almost double. Therefore, the construction of the raid complex is an opportunity to increase the portability of the port, and the prospect of its development.

The problem of the transport complex in the region is a significant degree of depreciation of capacities, high cost of operating costs, low investment opportunities of transport companies, low level of development of transport infrastructure, insufficient financing. The most significant restrictions and risks of transport infrastructure development are insufficient funding from budgets of various levels and extra budgetary sources. Based on the official statistics of the Russian Federation, as well as analysis and data published by official bodies of Russia, it can be concluded that in the fishing industry the main problems associated with the state of the fleet.

The structure of the fleet of the Russian Federation is shown in the Fig. 2 [7].

According to the published data of the All-Russian Scientific Research Institute of Fisheries and Oceanology, the number of the fishing fleet of the Russian Federation is

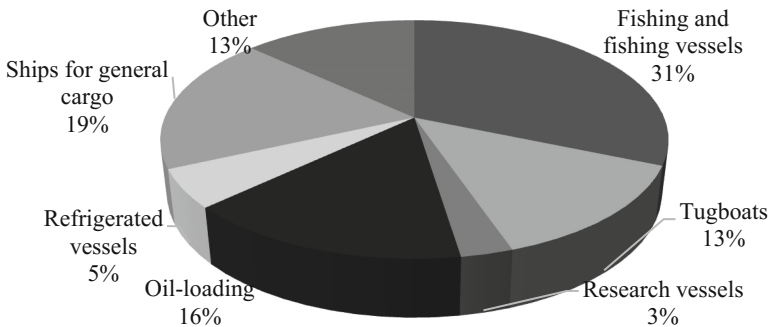


Fig. 2. The structure of the fleet of the Russian Federation.

1888 units [8]. At the time of the study, according to the Russian Maritime Register of Shipping, fishing and fishing vessels occupy about 31% of the fleet of the Russian Federation and occupy the largest volume in the structure of the fleet [9] (Table 2).

The number of vessels under 10 years old has decreased from 60 to 39 units. The share of vessels used in excess of the standard period is 89.2%. According to the results

Table 2. Number and age composition of fishing fleet vessels

Groups of vessels	Quantity	Including by age groups, years				
		Till 5	6–10	11–15	16–20	Over 20
Mining fleet	1888	19	20	81	114	1645
Processing fleet	20	–	–	–	5	15
Transport refrigerators	231	–	–	–	13	218
Research fleet, training	57	1	1	14	10	31
Of all vessels	2196	20	21	95	142	1918

of the survey “Development of the Russian Fish Industry: A Request for Fleet Modernization” conducted by the All-Russian Center of Public Opinion among captains of large-capacity vessels of the Russian fishing fleet, more than 38% of respondents believe that more than 80% of the fleet needs to be replaced, 22% 60–75% of the fleet needs replacement [10].

3 Results

Solving the problem of reproduction of fixed assets requires the implementation of a set of measures. To this end, the authors proposed an algorithm for implementing forfeiting financing for the restoration and development of a fishing fleet [11]. The algorithm for holding a forfeiting deal can be represented in the structural-logical scheme of forfeiting (Fig. 3).

Most enterprises are oriented towards financing leasing schemes, or on the state budget. These are the most traditional sources of financing. Leasing currently plays a decisive role in the development of domestic shipbuilding, fleet renewal and onshore

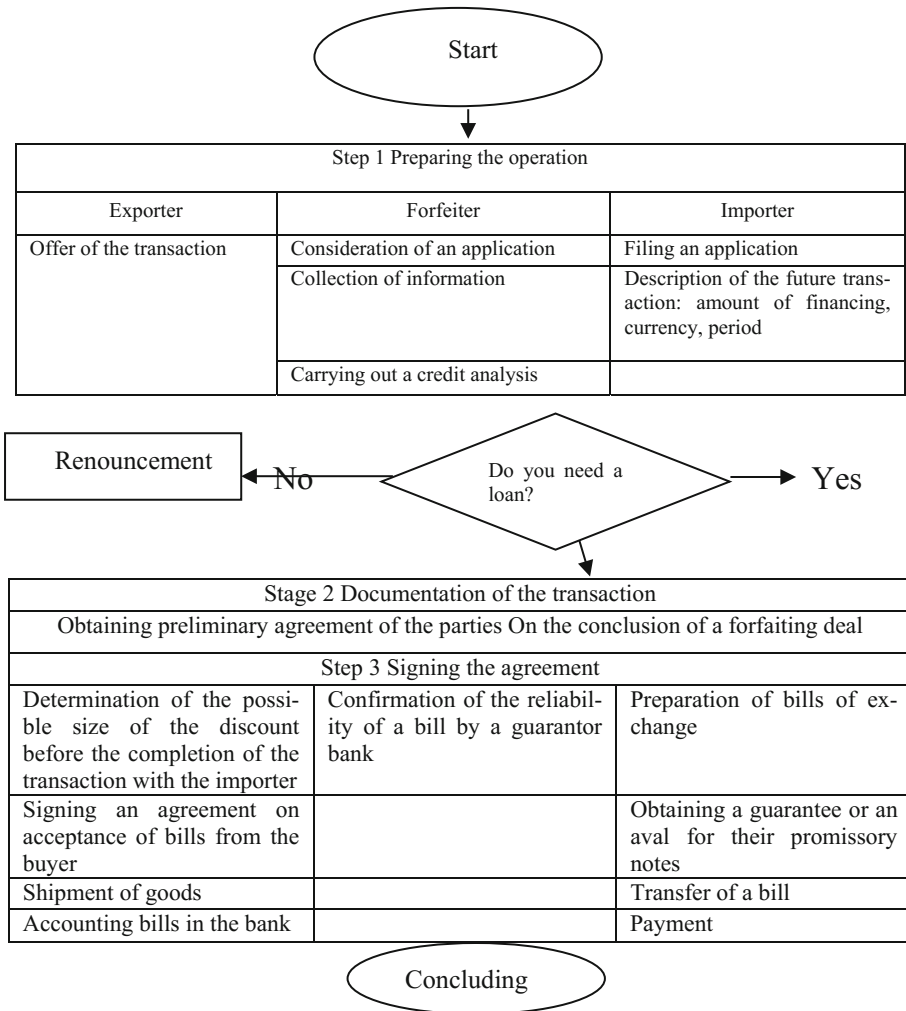


Fig. 3. Algorithm for holding a forfeiting

production facilities. Its application is due to the possibility of applying the method of accelerated depreciation. The acquisition of vessels on leasing terms is a real opportunity to develop and replenish the fleet. However, along with this mechanism, it is necessary to develop other promising schemes for financing fleet renewal. One of such instruments of financial and credit support for fleet development is the use of forfeiting. The loan amount in the case of forfeit financing can be quite high due to the possibility of syndication [12].

4 Discussion

Both methods of lending are unique in their own way and are in demand by the economies of different countries [13–15]. The expediency of using this or that method is determined by the purpose pursued by the creditor (seller, exporter): forfeiting, and leasing are most effective for large enterprises, which pursue the goal of accumulating funds for the implementation of long-term and costly projects. The financial result of a leasing transaction is the positive value of net present value. The financial feasibility of forfeiting is provided by the difference in the value of interest rates for credit resources [16, 17]. We calculated the scheme of the financial-credit support of the reproduction of the fleet of the fish industry of the Far East with the use of forfeiting, leasing, credit and the analyzed obtained results. In calculating the leasing scheme, the cost of the vessel, taking into account the payment of all interest, was \$ 594,276.5. When calculating an alternative forfeiting scheme of financing, by repaying a portfolio of bills and taking them into account at a discount, the vessel's appreciation was \$ 188,052. The scheme of credit financing, providing for the conclusion of the forfeiting agreement, is more effective. Indicators of economic efficiency are calculated on the basis of the table "Cash flow" [18–20]. It should be noted that quantitative estimates of costs and incomes are of a probabilistic nature [21, 25]. In the proposed scheme, the average values of the parameters are given, which may differ from those that are determined during the actual operation of the vessel.



5 Conclusions

The development of the transport complex should be aimed at ensuring sustainable socio-economic growth of the region. The strategic goal of the transport complex development is to bring the transport infrastructure in line with the needs of economic development and to integrate the transport center into the APR countries. Use of modern financial and credit tools for solving problems of reproduction of fixed assets [22–24]. To eliminate the reasons restraining the development of sea traffic, it is necessary: to reduce the cost of construction and operation of ships. To improve technical perfection and adaptability of vessels to operating conditions (modern vessels are required, adapted to solve a complex of tasks, adapted to operating conditions, including climate, seasonality, imbalance of cargo flows); Create an appropriate coastal infrastructure; Further development of the port to the required capacities, including pouring into the sea; Complete withdrawal of the port beyond urban land.

References

1. Miroshnikova, T., Taskaeva, N.: MATEC Web of Conferences, vol. 106, p. 08093 (2017)
2. Social and economic situation of the Kamchatka Territory. <http://kamchatka.gov.ru>. Accessed 27 Nov 2015
3. Kolosov, V.: Water transport, vol. 2, p. 1 (1991)
4. Pimenova, A., Kuzmina, S., Morozova, N., Mottaeva, A.: The functional model approach to the consulting for vertically - integrated construction group. In: MATEC Web of Conferences, p. 07018 (2016). <https://doi.org/10.1051/mateconf/20167307018>
5. Jevric, M., Romanovich, M.: Procedia Eng. **165**, 1478–1482 (2016). <https://doi.org/10.1016/j.proeng.2016.11.882>
6. Gorshkov, A.S., Rymkevich, P.P., Vatin, N.I.: Mag. Civil Eng. **52**(8), 38–48 and 65–66 (2014). <https://doi.org/10.5862/MCE.52.5>
7. Pimenova, A., Kuzmina, S., Morozova, N., Mottaeva, A.: The functional model approach to the consulting for vertically - integrated construction group. In: MATEC Web of Conferences, p. 07018 (2016). <https://doi.org/10.1051/mateconf/20167307018>
8. Grinfeldi, G.I., Gorshkov, A.S., Vatin, N.I.: Adv. Mater. Res. **941–944**, 786–799 (2014). <https://doi.org/10.4028/www.scientific.net/AMR.941-944.786>
9. Hirkovskis, A., Serdjuks, D., Goremikins, V., Pakrastins, L., Vatin, N.I.: Mag. Civil Eng. **57** (5), 86–96 and 116–117 (2015). <https://doi.org/10.5862/MCE.57.8>
10. Saari, J., Sermyagina, E., Kaikko, J., Vakkilainen, E., Sergeev, V.: Energy **113**, 574–585 (2016). <https://doi.org/10.1016/j.energy.2016.06.102>
11. Isaev, S.A., Vatin, N.I., Baranov, P.A., Sudakov, A.G., Usachov, A.Y., Yegorov, V.V.: Mag. Civil Eng. **36**(1), 103–109 (2013). <https://doi.org/10.5862/MCE.36.13>
12. Ognjenovic, S., Ishkov, A., Cvetkovic, D., Peric, D., Romanovich, M.: Procedia Eng. **165**, 954–959 (2016). <https://doi.org/10.1016/j.proeng.2016.11.805>
13. Romanovich, R., Vilinskaya, A.: MATEC Web of Conferences, vol. 53, p. 01052 (2016). <https://doi.org/10.1051/mateconf/20165301052>
14. Nazmeeva, T.V., Vatin, N.I.: Mag. Civil Eng. **62**(2), 92–101 (2016). <https://doi.org/10.5862/MCE.62.9>
15. Romanovich, M., Simankina, T.: Procedia Eng. **165**, 1587–1594 (2016). <https://doi.org/10.1016/j.proeng.2016.11.897>
16. Priadko, I.N., Mushchanov, V.P., Bartolo, H., Vatin, N.I., Rudnieva, I.N.: Mag. Civil Eng. **65**(5), 27–41 (2016). <https://doi.org/10.5862/MCE.65.3>
17. Radovic, G., Murgul, V., Vatin, N.: Appl. Mech. Mater. **641–642**, 634–638 (2014). <https://doi.org/10.4028/www.scientific.net/AMM.641-642.634>
18. Vasilyeva, E., Polyakova, I.: MATEC Web of Conferences, vol. 106, p. 08097 (2017)
19. Polyakova, I., Vasilyeva, E.: Procedia Eng. **165**, 1380–1387 (2016)
20. Polyakova, I., Chibisova, E.: J. Econ. Entrep. **5**(70), 579–582 (2016)
21. Mottaeva, A.: Methodological approaches to identification of clusters in regional economy system. In: MATEC Web of Conferences, p. 08071 (2017). <https://doi.org/10.1051/mateconf/201710608071>
22. Verstina, N., et al.: Int. J. Econ. Fin. Issues **5**(3S), 217–223 (2015)
23. Akimova, E., Knyazev, D.: Int. J. Appl. Eng. **10**, 18 (2015)
24. Stein, E., et al.: Procedia Eng. **165**, 1410–1416 (2016)
25. Rozhentsova, I., Mottaeva, A.: Terms of orientation on customer needs in the housing sector. In: MATEC Web of Conferences, p. 08076 (2017). <https://doi.org/10.1051/mateconf/201710608076>

Modeling the Duration of Works During the Scheduling of Construction of the Transport Infrastructure Facility

Marina Romanovich¹ , Wang Ziyue^{1,2}, and Shi Peiyu^{1,2} 

¹ Peter the Great St. Petersburg Polytechnic University,
Politechnicheskaya St., 29, 195251 St. Petersburg, Russia
p198320@yandex.ru

² China University of Mining and Technology, No. 1, Daxue Road,
Xuzhou 221116, Jiangsu, People's Republic of China

Abstract. The paper considers the scheduling of construction of the transport infrastructure facility – a one-storey building of production and technical complex. The main parameters of the construction process are the duration of construction, cost and quality. These elements are always closely connected and require constant monitoring. In a research various world regulatory bases of labor have been used: Chinese normative base, Unified Norms and Prices (further – UN&P, Russia), “Building Construction Costs with RSMeans Data” (further – RSMeans, United States of America, USA). Different approaches to the calculation of the duration of different types of work and the formation of the construction crew gave different total duration. The result of the study was the possibility of modeling the duration of various types of work, taking into account the change in the quantitative and qualification level of the work crew.

Keywords: Transport infrastructure · Duration of construction
Modeling the duration of works

1 Introduction

Nowadays, the construction industry is highly competitive, construction enterprises want to strengthen market share and obtain much more profit than before. The most effective and concise way is control of duration of works, quality and cost control. As a rule, increasing the duration of construction entails an increase in cost. Therefore, project duration control is enterprise performance of competitiveness, which reflects the enterprise management level. In addition, the project duration control can also reflect the work quality of the project [1].

In terms of quality management system (QMS), it plays a decisive role in the competitiveness of the construction unit in the market as well as the sustainable and healthy development. Of course, the quality control system, cost control and the duration control are inseparable and coordinated [2].

The amount of payment for construction projects in the transport industry is very large. If the cost of the construction project is reduced, it can be explained that both the

labor and the machine are fully useful in the process of construction. This can decrease the amount of unnecessary expenditure and make sure that the construction process is carried out normally [3]. According to the factors of cost control, we can get that the time is a determining factor for cost control. Time, it means opportunity and cost, the acceleration of progress is largely manifested as productivity improvement. Therefore, it is an important goal of cost management that the project should complete in time [4].

The aim of this work is scheduling of construction of the transport infrastructure facility, using world regulatory bases of labor: Chinese normative base, Unified Norms and Prices (further – UN&P, Russia), “Building Construction Costs with RSMMeans Data” (further – RSMMeans, United States of America, USA). This will give an objective assessment of the service of labor and cost in present-day construction project and it is instructive for duration and cost control.

To achieve the aims, it is necessary to solve the following tasks:

1. To calculate the volume of work for construction the transport infrastructure facility – a one-storey building of production and technical complex.
2. To work out schedules using different world regulatory bases of labor and different types of work crew (UN&P, RSMMeans).
3. To analyze the total construction durations of the facility.

2 Materials and Methods

The object of research is the transport infrastructure facility – a one-storey building of production and technical complex, total area of 1396 square meters. The main structural elements of the object:

- Floor System: Precast slab plank, 200 mm thick;
- Bearing Walls: brick (640 mm thick, 2.5 brick);
- Interior Walls: pre-fabricated masonry panels;
- Precast Stairs;
- Plates: Precast Slab plank, 150 mm thick.

According to the technology of construction, the building was divided into three bays: 419, 547, 430 square meters.

The calculation methods included the integration of several methods for computation the duration of individual types of work. For various regulatory bases of labor, duration of construction is defined differently. For UN&P, Russia, the duration of work is determined by the formula 1, for RSMMeans, USA, the duration of work is determined by the formula 2, for China the duration of work is determined by the formula 3 [5]. It is particularly worth noting that all further calculations were performed for the same working conditions, taking into account the necessary technological and constructive solutions. It was assumed that the duration of one shift is 8 h.

$$T = \frac{Q \times H}{8 \times R} \quad (1)$$

$$T = \frac{Q}{D} \tag{2}$$

$$T = \frac{Q}{R \times S \times C} = \frac{Q \times H}{R \times C} \tag{3}$$

where:

- T – duration of work in days;
- Q – volume of work (amount of physical units);
- H – time quota;
- 8 – number of hours in shift;
- R – work crewnumber of workers required to perform this type of work (amount of manpower);
- D – daily output;
- S – coefficient equal to $1/H$;
- C – the number of classes arranged every day.

3 Results

All the volumes of construction work were calculated, the duration of each type of work was determined, the quantitative and professional composition of the work crew was selected. Table 1 shows the calculation of the duration of construction one-storey building of production and technical complex with the application of the regulatory framework of labor UN&P. Table 2 shows the total duration obtained as a result of the integration of the two normative labor bases – UN&P and China frameworks.

Table 1. Duration of works using UN&P framework.

N	Line number	Material	Unit	Q	H	R	T	
1	4-1-7	Floor system: precast slab plank (200 mm)	1 element (up to 10 square meters)	Bay 1	419/42	0.72 + 0.18	5 (installer 4 level-1, 3 level-2, 2 level-1, crane operator 6 level-1)	5
				Bay 2	547/55			7
				Bay 3	430/43			5
2	3-3	Bearing walls: brick (640 mm)	Square meters	Bay 1	519	2.90	$2 \times 5 = 10$ (mason 3 level-2 \times 5)	38
				Bay 2	682			50
				Bay 3	550			40
3	3-12	Interior walls: pre-fabricated masonry panels	Square meters	Bay 1	474	0.77	$2 \times 4 = 8$ (mason 4 level-1, 2 level -1 \times 4)	12
				Bay 2	658			16
				Bay 3	513			13
4	4-1-10	Precast stairs	1 element	Bay 1	6	1.70	5 (installer 4 level-2, 3 level-1, 2 level-1, crane operator 6 level-1)	1.3
				Bay 2	2			0.43
				Bay 3	2			0.43
5	4-1-12	Plates: precast slab plank (150 mm)	1 element	Bay 1	7	2.00	5 (installer 4 level-2, 3 level-1, 2 level-1, crane operator 6 level-1)	1.75
				Bay 2	4			1
				Bay 3	3			0.75

Table 2. Duration of works using integrated UN&P and China frameworks.

N	Line number	Material	Unit	Q		H	S	C	R	T
				Bay	Value					
1	AH0065	Floor system: precast slab plank (200 mm)	Square meters	Bay 1	419	0.236	4.23	4	5	5
				Bay 2	547					7
				Bay 3	430					5
2	AH0050	Bearing walls: brick (640 mm)	Square meters	Bay 1	519	0.800	1.25	1	10	42
				Bay 2	682					55
				Bay 3	550					44
3	AH0239	Interior walls: pre-fabricated masonry panels	Square meters	Bay 1	474	0.480	2.08	2	8	15
				Bay 2	658					20
				Bay 3	513					16
4	AH0218	Precast stairs	Riser	Bay 1	84	0.470	2.13	4	5	1.9
				Bay 2	12					0.28
				Bay 3	12					0.28
5	AH0202	Plates: precast slab plank, (150 mm)	Square meters	Bay 1	16	0.560	1.79	4	5	0.4
				Bay 2	11					0.3
				Bay 3	9					0.25

Table 3 shows the calculation of the duration of construction with the application of the regulatory framework of labor RSMeans. Table 4 shows the total duration obtained as a result of the integration of the two normative labor bases – RSMeans and China frameworks.

Based on the calculations presented in Tables 1, 2, 3 and 4, the construction schedules were constructed according to the critical path method. The total duration of the construction of one-storey building of production and technical complex: 164 days

Table 3. Duration of works using RSMeans framework.

N	Line number	Material	Unit	Q		D	R	T
				Bay	Value			
1	034113500100	Floor system: precast slab plank (200 mm)	Square meters	Bay 1	419	297	C11-9 (1 struc. steel foreman (outside), 6 struc. steel workers, 1 equip. oper. (crane), 1 equip. oper. (oiler))	2
				Bay 2	547			2
				Bay 3	430			2
2	042113400100	Bearing walls: brick (640 mm)	Square meters	Bay 1	519	22.76	D8-5 (3 bricklayers, 2 bricklayer helpers)	23
				Bay 2	682			30
				Bay 3	550			25
3	042520100020	Interior walls: pre-fabricated masonry panels	Square meters	Bay 1	474	72	C11-9 (1 struc. steel foreman (outside), 6 struc. steel workers, 1 equip. oper. (crane), 1 equip. oper. (oiler))	7
				Bay 2	658			10
				Bay 3	513			8
4	034123500020	Precast stairs	Riser	Bay 1	84	75	C 12-6 (1 carpenter foreman (outside), 3 carpenters, 1 laborer, 1 equip. oper. (crane))	2
				Bay 2	12			1
				Bay 3	12			1
5	034113500050	Plates: precast slab plank (150 mm)	Square meters	Bay 1	16	260	C11-9 (1 struc. steel foreman (outside), 6 struc. steel workers, 1 equip. oper. (crane), 1 equip. oper. (oiler))	1
				Bay 2	11			1
				Bay 3	9			1

Table 4. Duration of works using integrated RSMeans and China frameworks.

N	Line number	Material	Unit	Q		H	S	C	R	T
1	AH0065	Floor system: precast slab plank (200 mm)	Square meters	Bay 1	419	0.236	4.23	4	9	3
				Bay 2	547					4
				Bay 3	430					3
2	AH0050	Bearing walls: brick (640 mm)	Square meters	Bay 1	519	0.800	1.25	2	5	42
				Bay 2	682					55
				Bay 3	550					44
3	AH0239	Interior walls: pre-fabricated masonry panels	Square meters	Bay 1	474	0.480	2.08	4	9	7
				Bay 2	658					9
				Bay 3	513					7
4	AH0218	Precast stairs	Riser	Bay 1	84	0.470	2.13	4	6	1.65
				Bay 2	12					0.24
				Bay 3	12					0.24
5	AH0202	Plates: precast slab plank, (150 mm)	Square meters	Bay 1	16	0.560	1.79	4	9	0.25
				Bay 2	11					0.17
				Bay 3	9					0.17

using integrated UN&P and China frameworks; 153 days using integrated RSMeans and China frameworks. The schedules for the construction of the facility and the schedules of the workers' movement are shown in Figs. 1, 2, 3 and 4.

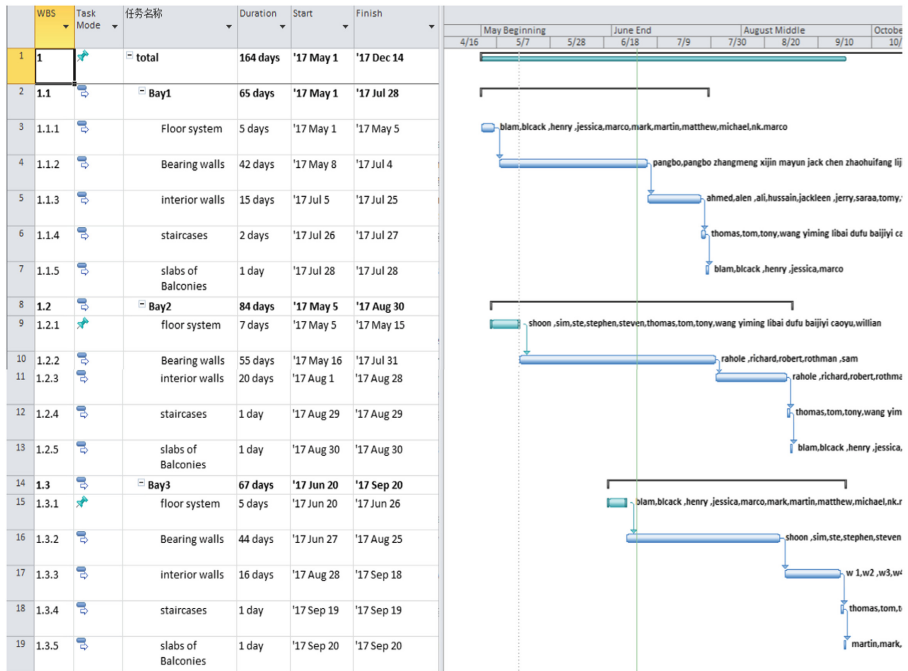


Fig. 1. Schedule of construction one-storey building of production and technical complex with the application of the UN&P and China frameworks.

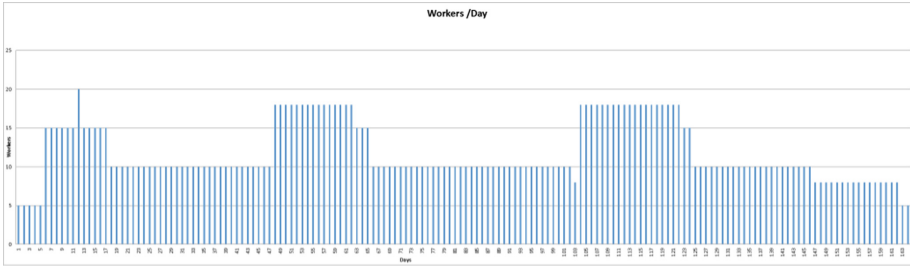


Fig. 2. Schedule of the workers’ movement with the application of the UN&P and China frameworks.

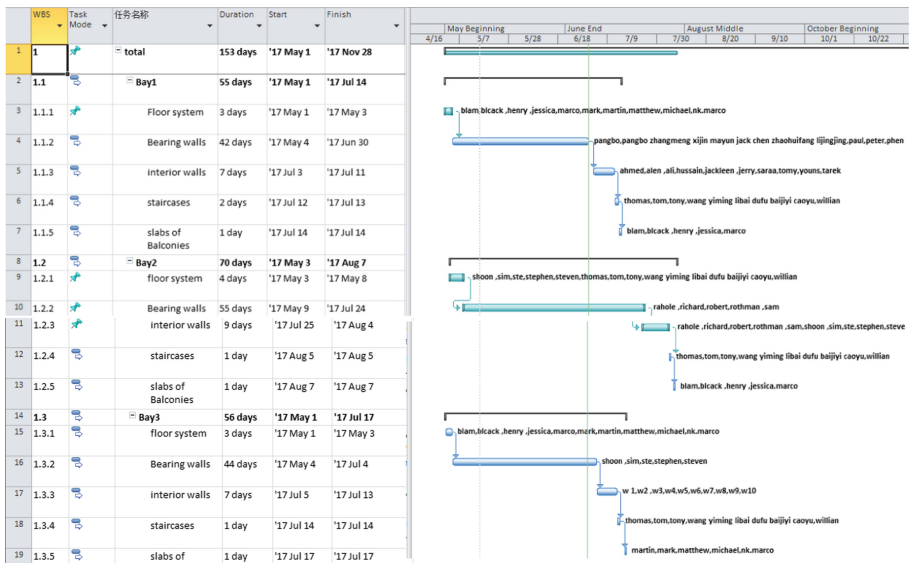


Fig. 3. Schedule of construction one-storey building of production and technical complex with the application of the RSMeans and China frameworks.

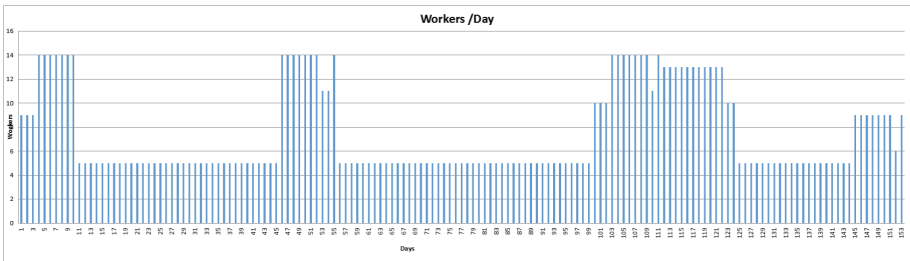


Fig. 4. Schedule of the workers’ movement with the application of the RSMeans and China frameworks.

The coefficient of uneven movement of workers is equal to 1.68 for integrated UN&P and China frameworks and 1.87 for RSMMeans and China frameworks.

4 Discussion

If we elaborate on the principles of forming a construction work crew in the regulatory bases of different countries, it is worth noting the following. The Russian regulatory framework UN&P for labor was created in the eighties of the last century, later it was only partially updated and modernized. The normative documents for any type of work indicate the required composition of workers, with mandatory indication of the level of qualification or grade. The question of modern approaches to assessing the qualifications of workers was considered in [6, 7].

Depending on the scope of work, it forms the final composition of the work crew with the required number of people of the required qualifications. Unlike the Russian regulatory framework, there are no qualification categories in the USA regulatory bases of labor – RSMMeans. In the national publicly accessible RSMMeans database, work crews are already fully formed for each type of construction work and have their code names,

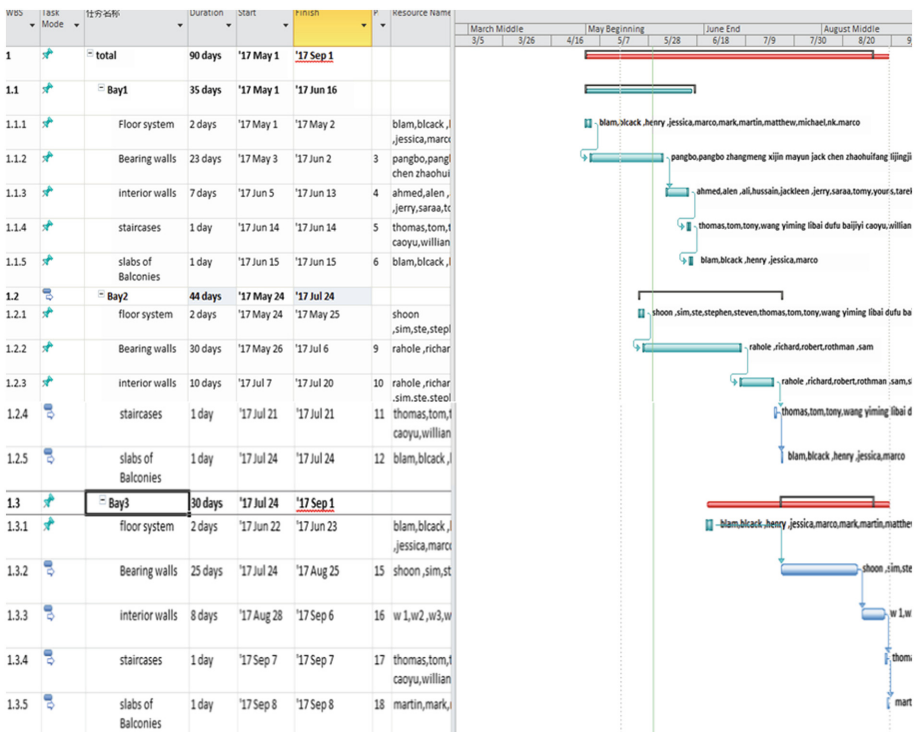


Fig. 5. Schedule of construction one-storey building of production and technical complex with the application of the RSMMeans framework.

for example, C11, D8. To calculate the duration of any work, it is enough to use such parameter as *daily output or labor hours*. It is also worth noting that the largest number of people in the crews formed from the normative base of RSMeans. For example, to install a precast slab plank (200 mm thick), you need a work crew of C11 with 9 people in it, while using the UN&P for the same work you need 5 people, but with different skill levels (see Table 1 and 3, line number 1). In this regard the speed of performance of work with use of the regulatory base of the USA the highest (see Fig. 5). The general duration of construction of the one-storey building of production and technical complex when using the maximum structure of work crew was 90 days.

As for the Chinese regulatory framework, the approach to calculating the duration of construction is fundamentally different from the Russian and USA ones. To determine the duration, different coefficients are used as *the number of classes arranged every day*, i.e. coefficient that takes into account the various professions involved in the performance of a particular type of work. It is interesting to note that there is no pre-formed work crew in the Chinese regulatory databases. Therefore, in this study, the authors were interested in integrating various systems and approaches to determining the duration of construction and the formation of construction crews.

5 Conclusion

The conducted research has shown the possibility of successful integration of various world regulatory bases of labor with the obligatory consideration of similar construction conditions and observance of the fundamental principles of technology and organization of construction. The result of the study was the possibility of modeling the duration of various types of work, taking into account the change in the quantitative and qualification level of the work crew. On the other hand, the issue of the quality of construction works is still open. As mentioned above, despite the shortest period of construction of the facility, the USA regulatory framework does not take into account the qualification level of the workers. The issue of the quality of construction work in the integration of various regulatory bases of labor can become subjects for further research.

References

1. Qi, B.: Project Management. Dalian University of Technology Press, Dalian (1999)
2. Jia, X., Wu, X.: Construction Organization Design Example. China Building Industry Press, Beijing (2003)
3. Lukichev, S., Romanovich, M.: *Procedia Eng.* **165**, 1717–1721 (2016)
4. Du, X., Lu, H.: Construction Enterprise Construction Site Management. China Building Industry Press, Beijing (1997)
5. Qian, K.: Construction Project Quota and Budget. Southeast University Press, Nanjing (2006)
6. Romanovich, M.: *Bull. Irkutsk State Tech. Univ.* **12**, 135–140 (2014)
7. Romanovich, M., Simankina, T., Il'chenko, D.: *Procedia Eng.* **5**, 49–53 (2015)

Modified Method for Calculation of Vehicles Residual Lifetime with Regard of the Impact Factors Variability

Nadezhda Sevryugina^(✉) 

Moscow State University of Civil Engineering,
Yaroslavskoye Sh., 26, 129337 Moscow, Russia
SevryuginaNS@mgsu.ru

Abstract. Transportation infrastructure management methods analysis is provided. Scientific research main focus areas with highlighting future aspects and challenges for regional development are summarized. Transportation management tasks solution comprehensiveness is established, and the gap in insufficiency of the region-specific considerations for priority factors determination is discovered. Purpose of these studies is to determine the applicability of various scientific approaches for multi-factor region-specific circumstances and to elaborate a unified approach capable to eliminate the shortfalls of various methods. Model for solution of this task assumes the identification of parameters as the basic ones with further time lag control, and here the classical methods for outlining the impact factors are applicable, such as: driver; external environment; functional condition maintaining factor (service); randomness of the regional transportation infrastructure functioning peculiarity. Mathematical model for vehicle cost evaluation with regard of the residual lifetime is considered; significance of operation expenses parameter, vehicle mechanism elements wear intensity parameters are substantiated. Modification of basic target function by consideration of operation region-specific impact factors variability, human factor, service quality while maintaining the operability and safety is proposed. Example is given for substantiation of applicability of individual method for vehicle residual lifetime calculation and harmonization of the result with the averaged market value evaluation parameter; future cost intensity of operation for the given time lag, for owners, as well as to evaluate the vehicle operation profitability and the impact level on the region transportation infrastructure.

Keywords: Infrastructure · Vehicle · Lifetime · Operation · Factor · Hazard Human · Costs · Region

1 Introduction

Significance of transport and infrastructure ensuring its efficient functioning can hardly be overestimated not only from the economic development viewpoint, but social significance as well. Multiple researches offer various methods for transportation infrastructure management methods, options for its saturation [1]. Currently, technical means

available to researchers allow to re-orient the universal methods for evaluation of the transportation systems management with regard of factor-specific steady development of particular region. There are widely known respective scientific publications [1, 4–21] aimed at solution of the following problems:

- Transport functional efficiency problem (A.V. Velmozhin, D.P. Velikanov, V.A. Zorin, S.R. Leyderman, I.V. Nikolsky, S.M. Rezer, L.G. Reznik, N.N. Tikhomirov, and others);
- Land transport arrangement and management issues (L.L. Afanasyev, A.I. Vorkut, I.M. Golovnykh, N.N. Gromov, V.A. Gudkov, O.N. Dedmanidze, V.K. Dolya, E. A. Kravchenko, O.N. Larin, R.G. Leontyev, L.B. Mirotin, A.U. Mikhailov, V.A. Persianov, N.A. Troitskaya, I.V. Spirin, and others);
- Land transport functioning economic efficiency issues (L.A. Bronshtein, G.Y. Voloshin, S.N. Glagolev, V.N. Livshits, A.I. Malyshev, M.P. Ulitsky, A.S. Shulman, and others);
- Creation of transportation management and marketing mathematical models (M.E. Antoshvili, G.A. Varelopulo, E.E. Vitvitsky, V.L. Geronimus, A.P. Kozhin, A.N. Novikov, S.A. Panov, E.F. Tikhomirov, and others).

2 Materials and Methods

Functionality of the transportation functioning efficiency in general terms may be represented by the following equation: $ETS = E (\sum R_{ij})$. Analysis of the developed methods demonstrates the commonality of researchers' views of the transportation management efficiency improvement problem, with emphasizing the following basic components: human factor; safety; economic and ecological impact factors; machinery structural improvement qualitative parameters; systematicity and synergy of functioning. Therefore, the transportation management tasks solution comprehensiveness is established, and the gap in insufficiency of the region-specific considerations for priority factors determination is discovered.

In all studies, the transport functioning efficiency is considered as a population of reliability parameters; among them, it is worth emphasizing the vehicle lifetime enshrined by the manufacturer as the theoretically possible one, but in fact implemented with the regard of the impact environment factors during the operation period, i.e. region-specific.

It should be noted that the vehicle lifetime is influenced by the ability to adapt to the operation environment, i.e. its functioning ability and safety expressed by dimensionless value, within the range from 1 to 0, and the tendency to reduce, as time goes. Purpose of these studies is to determine the applicability of various scientific approaches for multi-factor region-specific circumstances and to elaborate a unified approach capable to eliminate the shortfalls of various methods.

Building of logical chain of impact factors has been accomplished within several stages that allowed to outline the category of vehicle in service for a long time with indefinite characteristic of qualitative parameters loss caused by human factor, for example, driving manner, maintenance level in preceding periods. Up to now, there has

been no unified method for evaluation of the human factor impact onto the operability and safety of the vehicle, calculation methods typically are of qualitative evaluation nature, and the quantitative representation is volatile to some extent, however the software resources, modern control, diagnostic, and registration systems enable to obtain a rather accurate value.

It is logical that by creating the transportation management system, when ensuring safety and prevention of accidents, the preferable should be the uncertainty factor in risk of failure and transport safety operation, which is also variable even within some specific region [3, 15].

Model for solution of this task assumes the identification of parameters as the basic ones with further time lag control, and here the classical methods for outlining the impact factors are applicable, such as: driver; external environment; functional condition maintaining factor (service); randomness of the regional transportation infrastructure functioning peculiarity [2, 7, 8, 14].

Calculated parameters should be able to be perceived by the core component of the system - human being, in particular, the owner of the vehicle, and substantiated by psychologically acceptable and alternative time lag, for example, determined as the theoretically fixed period of the vehicle lifecycle end, and expressed in the monetary equivalent of costs need for this vehicle operation.

Cost of the vehicle when considering the residual lifetime (ΔT_{rl}) includes the market value (C_n), normative value of costs for operation, and actual costs for the considered period (T_n, T_e). Mathematical expression can be as follows:

$$C_{rl} = \frac{C_n(T_n - T_e)}{T_n} \tag{1}$$

where $(T_n - T_e) = \Delta T_{rl}$.

According to the experience, determination of normative parameters values is not a problem, but the actual costs for the considered period of operation require acquisition of statistical data continuously, which has not been currently implemented in sufficient manner. Figure 1 shows the diagram that illustrates the spread of the determined calculated market values of the similar type vehicles in various operating conditions, with different mileage and commissioning year [4, 9, 13].

Most of popularity is attributed to the optimization models [7, 8, 11, 14] based on target function:

$$C(T) = \frac{\vartheta_q(T) C_{av} + C_e + C_{cl}}{M} + \sum_i \frac{C_{mi}}{T_{mi}} \rightarrow \min \tag{2}$$

where

- a, b, α - empirical coefficients.
- $\vartheta_q(T)$ - Quantity of repair cycles within the vehicle lifetime before disposal;
- C_{av} - average value of depreciation expenses per one repair cycle of the vehicle;
- C_e - expenses for elimination of failures and malfunctioning during the repair within one repair cycle;

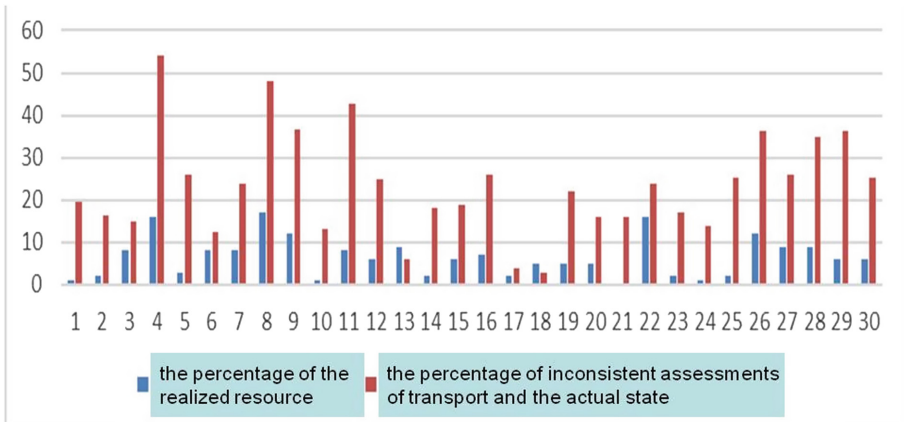


Fig. 1. Basic lifetime parameter deviation spread diagram for the vehicles with different mileage, commissioning year, when determining their market value.

- Ccl - expenses for compensation of losses caused reduced performance and increased consumption of lubrication materials when the vehicle parts become worn out per one repair cycle;
- T - lifetime before the first overhaul;
- Cmi - expenses for maintenance of i vehicles;
- Tmi - maintenance interval.
- M - empirical coefficient that characterizes the vehicle operation intensity:

$M = 1 + k_{rl}[\vartheta(T) - 1]$, where k_{rl} - coefficient equal to the ratio of the vehicle lifetime after overhaul to the new vehicle lifetime.

Basic methods of the reliability theory propose to consider the costs for the vehicle operation through the operation intensity determined by the nature of the functional assemblies coupled parts wearing process, by means of empirical expression of the wearing pattern [2, 7, 8, 11, 14].

Let us give the mathematical description of the impact factors variability:

$I = \alpha(T_{ri})$ - dependence of the wear intensity from the maintenance interval, the calculated expression looks like this:

$$I = bT_{ri}^{\alpha-1}T \tag{3}$$

$C_{cl} = \varphi(I)$ - dependence of the costs for compensation of losses from wear intensity, the calculated expression looks like:

$$C_{cl} = cI^{\beta} \tag{4}$$

or in average specific estimate per 1 h of runtime

$$C_{cl} = cb^\beta T^{(\alpha-1)\beta} T^{\beta-1},$$

where c - coefficient that dependence from the operation mode and vehicle operation conditions;

β - degree parameter stipulated by the coupling structure and functional purpose;

$K_{LT} = \varphi(T)$ - dependence of the lifetime from the vehicle/assembly use intensity, expressed by the utilization coefficient.

Calculated value of the vehicle lifetime according to the provided patterns with regard of the wear factor looks like this:

$$T = \frac{I_p}{bT_{rl}^{\alpha-1}} \tag{5}$$

To consider the impact factors variability, it is proposed to modify the target function (2) by introducing the significance parameters.

$k_r, k_{sc}, k_{op}, k_{siq}$ - core system components impact factors variation coefficient that establish the dependence, respectively: from region-specific circumstances; operation conditions dictated by environment and the driver’s professional skills with regard of his/her mental & physical stability while driving, as well as the service influence quality;

ψ - degree parameter stipulated by the structure safety and coupling functionality.

Below you can find a number of modified models for considering the impact factors in the target function (2).

Model 1 serves for optimization of the lifetime and maintenance intervals. Marginal wear is determined using the criterion if impossibility to ensure its safe functioning for the human-machinery-environment system. During the course of calculation, this value is preset and is not to be optimized [3, 11, 18].

Target function of this model looks like this:

$$C(T) = \frac{\vartheta_q(T)k_r C_{av}}{M} + \frac{k_{sc} k_{op} I_p^\psi}{I_p} bT_{rl}^{\alpha-1} + \frac{C_{cl}}{T_{rl}} k_{siq} \rightarrow \min \tag{6}$$

Optimal lifetime with maintenance with i-th periodicity

$$T_{opt} = \frac{k_r k_{sc} k_{op} I_p^\psi}{k_{siq} bT_{rl}^{\alpha-1}} \tag{7}$$

Model 2 serves for optimization of the lifetime, maintenance intervals, and marginal wear. In this case, model 1 target function is used as the basic one.

This model allows to evaluate the optimal marginal wear value for determination of the criterial risk-factor of impossibility to ensure the safe functioning of the vehicle for human-machinery-environment system.

$$I_{\text{Pop}}^{\psi} = \frac{C_{av}}{e(\psi - 1)} \tag{8}$$

Optimal maintenance periodicity and optimal lifetime are determined using the model 1 target function formula.

Model 3 allows to evaluate the safety of the vehicle recovered functionality in the human-machinery-environment system in case of dangerous situation occurrence caused by the system failure and accomplished service actions aimed at elimination of their consequences.

Let us introduce a notion such as “lifetime after current repair” (T'_r) and “accounting of expenses for elimination of failures and malfunctioning per operation period value”

$$C_{CP} = \frac{e}{\gamma + 1} T^{\gamma + 1} \tag{9}$$

where e, γ - empirical coefficient.

3 Results

This model may be modified extending the impact factors consideration:

- lifetime optimization model by the system failure occurrence risk caused by the elements functional aging.

Target function of this model looks like this:

$$C(T) = \frac{\vartheta_q(T)k_r}{M} \left[\frac{C_{av}}{T'_r} + \frac{e}{\gamma + 1} (T'_r)^{\gamma} \right] + \sum_i \frac{C_{cli}}{T_{cli}} k_{siq} \rightarrow \min \tag{10}$$

Optimal lifetime in case of repair

$$T_{opt} = \left(\frac{C_n}{\vartheta_q(T)} \frac{(\gamma + 1)}{e\gamma} \right)^{\frac{1}{\gamma + 1}} \tag{11}$$

- model for optimization of lifetime, maintenance intervals, and marginal wear of the assembly unit by the system failure risk evaluation parameter that affects safety.

Target function of this model looks like this:

$$C(T) = \frac{\vartheta_q(T)k_r}{M} \left[\frac{C_{av}}{T'_r} + \frac{e}{\gamma + 1} (T'_r)^{\gamma} + k_{sc} k_{op} b^{\psi} T_{rl}^{(\alpha - 1)\psi} T_{mi}^{\psi - 1} \right] + \sum_i \frac{C_{cli}}{T_{cli}} k_{siq} \rightarrow \min \tag{12}$$

Optimal marginal wear

$$I_{\text{Popt}}^\psi = k_{sc} k_{op} b^\psi T_{rl}^{(\alpha-1)\psi} T_{mi}^{\psi-1} k_{siq} \tag{13}$$

By converting the resulting marginal wear expression for ensuring safety into the dimensionless parameter, we obtain the following:

$$I_s = 100 (1 - e^{-K_\Sigma \cdot \psi}) \tag{14}$$

4 Discussion

All afore mentioned discussions allow to obtain the vehicle residual lifetime calculation formula within the given time lag:

$$C_{RL} = \frac{C_N(T_N - T_E)}{T_N} e^{-K_\Sigma \cdot \psi} \tag{15}$$

where

- e - base of the natural logarithm, $e \approx 2.72$;
- K_Σ - comprehensive coefficient for impact factors variability consideration
 $K_\Sigma = k_r k_{sc} k_{op} k_{siq}$;
- ψ - function that depends on the age and actual mileage of the vehicle from the beginning of operation.

Exemplary calculation in graphical form is illustrated on Fig. 2.

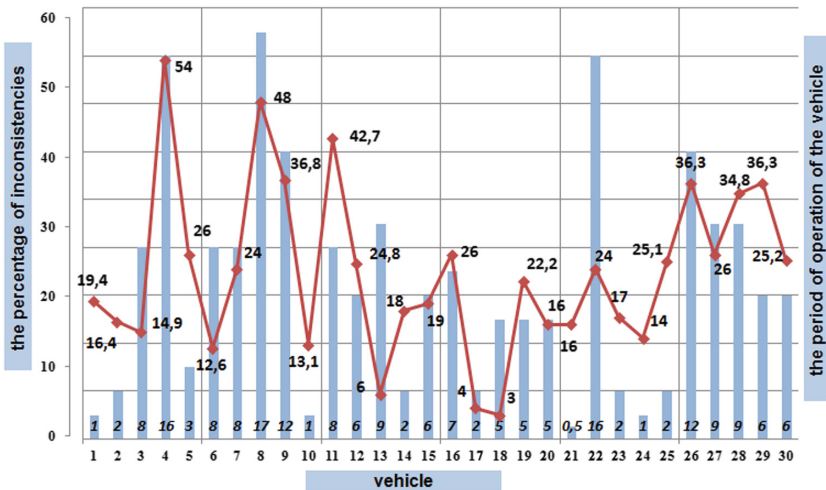


Fig. 2. Plot illustrating the consistency of the vehicle actual condition with the average market value.

5 Conclusions

All afore mentioned discussions allow to propose the individual method for vehicle residual lifetime calculation and harmonization of the result with the averaged market value evaluation parameter; evaluate the future cost intensity of operation for the given time lag, for owners; for production entities - to evaluate the vehicle operation profitability and the impact level on the region transportation infrastructure.

References

1. Abaimov, R., Bahracheva, Y., Vasilyev, A., Konev, A., Kychkin, V., Lezhneva, E., Sevryugina, N., Selivanov, K., Yushkov, V., Ahmednabiev, R. (eds.): Road Transport. Novosibirsk (2013)
2. Andrianov, Y., Krawczynski, V.: Improvement of methods of calculation of depreciation vehicles. Moscow appraiser 3 (2006)
3. Bogomolov, A., Sevryugina, N.: Variational interpretation of the life cycle of technical systems. Constr. Road Mach. **10**, 48–52 (2010)
4. Voitenkov, S., Vitvitskiy, E.: The Management of the truck transportation system of the city: state and prospects. Dyn. Syst. Mech. Mach. **3**(1), 313–320 (2016)
5. Glagolev, S., Sevryugina, N., Konev, A.: Mathematical model of an estimation of efficiency of development of the Territory of the region with the formation of clusters of roadside service. World Transp. Technol. Mach. **3**(42), 121–125 (2013)
6. Glagolev, S., Sevryugina, N.: Efficiency of functioning of the owner-car-service system as result of the choice its accented components. Automot. Ind. **6**, 10–11 (2012)
7. Glagolev, S., Konev, A.: The method of complex evaluation of service quality of road transport on the example of the Belgorod region. Motor Transp. Enterp. **8**, 45–49 (2013)
8. Glagolev, S., Sevryugina, N., Kozlova, N., Konev, A.: The formation of roadside service facilities as a component of the transport and logistics cluster in the overall system of the region innovation development. Motor Transp. Enterp. **11**, 42–44 (2012)
9. Didmanidze, O., Karev, A., Mityaev, G.: On the development prospects of road transport in the agricultural sector. Int. Sci. J. **1**, 53–65 (2016)
10. Evtukov, S., Vorobyov, S., Abyzov, I.: Perspective ways of increase of ecological safety of automobile park of the country. Bull. Civil Eng. **6**(59), 213–215 (2016)
11. Zorin, V.: Bases of Operability of Technical Systems. Academy Press, Moscow (2009)
12. Ishkov, A., Werstine, N., Telichenko, V., Miloradov, N.: The patent for the invention. The diagnostic method of the level of claims person 2444979 (2010)
13. Kruzhhkov, D., Yakimenko, V.: Methods and algorithms of estimation of efficiency of vehicle operation. Sci. Rev. **11**, 142–147 (2016)
14. Novikov, A., Kulev, M.: Analysis of factors influencing the number of points of technical inspection of vehicles in the region. World Transp. Technol. Mach. **4**(27), 3–6 (2009)
15. Novikov, A., Tryastin, A., Kondrashov, S.: Improving the safety of transport of dangerous goods through the use of global navigation satellite systems. In the Collection: Information Technologies and Innovations in Transportation Proceedings of the International Scientific-Practical Conference, pp. 52–57 (2015)
16. Novikov, A., Katunin, A., Kulev, A., Peshekhonov, M.: Comparison of positioning systems and their application in intelligent transportation systems. World Transp. Technol. Mach. **2**(41), 109–113 (2013)

17. Novikov, A., Ivashchuk, O., Vasilieva, V.: Ecological monitoring of the impact of transport on the acoustic environment of the city. *Repair. Recov. Mod.* **6**, 33–34 (2006)
18. Sevryugina, N., Melikhova, S., Volkov, E.: The solution of applied problems of optimization of stability of system “environment-man-technics”. *Mod. Appl. Sci.* **9**(3), 200–207 (2015). <https://doi.org/10.5539/mas.v9n3p200>
19. Telichenko, V., Korol', E., Kagan, P., Borsukov, S., Dmitriev, A., Kurganskaya, N.: Framework for the management of investment and construction programs in the city. Tutorial. ASV, Moscow (2008)
20. Telichenko, V., Korol', E., Khlistunov, M., Zavalishin, S.: Global risks and new security threats of megapolis responsible building objects. In the collection: *City Building Complex and Problems of Life Support of Citizens Collection of Reports of Scientific and Technical Conference*, pp. 211–218 (2005)
21. Telichenko, V., Korol', E.B., Kagan, P., Kulikova, E.: Systemic administration of the trust building programs. *Pricing Manual*. ASV, Moscow (2010)

Particularities of Public-Private Partnership Mechanisms Application for Implementation of Construction Megaprojects of Transport Infrastructure Development

Alexandr Orlov^(✉) 

Moscow State University of Civil Engineering,
Yaroslavskoye shosse, 26, 129337 Moscow, Russia
alor333@gmail.com

Abstract. The present article analyses particularities of public-private partnership mechanisms application for implementation of construction megaprojects in field of transport infrastructure. It is proposed to use public-private partnership mechanisms within toll road construction taking into account both interests of the state and interests of the private capital. Implementation of megaprojects in this field is reasonable using contract form of public-private partnership. Carried out analysis of the problems of public-private partnership mechanisms application in the Russian Federation as well as consideration of the project of construction of the toll road “Moscow – Saint Petersburg” on the section km 543 – km 684 allowed to justify a number of measures of improvement in this field.

Keywords: Transport infrastructure · Toll roads · Construction megaproject
Public-private partnership

1 Introduction

Development of public-private partnership (hereinafter - PPP) in Russia should become one of the main factors of economic growth, especially taking into account limited financial recourses of the state. At the same time, budget investments into the economy should encourage growth of private investments, promote formation of up-to date transport and engineering infrastructure. In Budget Message for 2014–2016 years, optimization of federal budget expenses structure is indicated as one of the main tasks for new budget cycle; and “active usage of PPP mechanisms is directly indicated as one the reserves allowing to attract investments and services of private companies to solve public tasks.

Advantages of the partnership of the state and private business in construction sector and, in particular, in field of transport infrastructure development are confirmed by practice of its application in foreign countries [1–4]. In particular, PPP allows to attract private sector’s financial resources to the industries and fields of activity being in the state’s area of responsibility, to use experience of private structures to improve

efficiency of state property management; it also facilitates implementation of innovative technologies into capital intensive industries.

Implementation of the first PPP projects in modern Russia started comparatively not so long ago, mainly in field of infrastructure (transport, energy, housing and utilities, etc.). At the same time, analysis of the process of their implementation reveals insufficient level of methodical and legal coverage of PPP in Russia which prevents from successful implementation of such projects [5, 6]. In the approved state program “Development of transportation system” (approved by the directive of the Government of the Russian Federation dated 28.12.2012 No. 2600-p), it is stated that contemporary condition of transportation system does not correspond with needs and prospects of the Russian Federation development, and deficit of traffic capacity exists for all types of transport; in connection with it, implementation of PPP mechanisms is especially important for this field.

It should be noted that development transport infrastructure is implemented in many cases in format of construction megaprojects.

Megaprojects are large-scale targeted programs [7] that in some cases contain subprograms combining interests of several co-investors as well as public interests on various management levels (federal, regional, municipal).

Megaprojects include programs of creation of special economic zones, territorial clusters, advanced development zones [8], implementation of complicated infrastructural facilities (for example, construction of toll roads, electric-power facilities, etc.), projects of complex development of territories and development of cities, other large-scale projects with participation of the state. Separately, global projects implemented with participation of several countries can be pointed out [9].

The following peculiarities of megaprojects should be pointed out [10–12]:

- Long period of implementation (usually, at least 5 years);
- High investment value (over USD 1 billion);
- Significant expenses for infrastructure development;
- Availability of large number of participants for project implementation (co-investors) and application of various schemes of financing;
- Influence on social and economic, environmental, demographic and other characteristics of a city, region or country on the whole;
- Participation of the state in megaprojects implementation: in many cases, megaprojects are implemented using PPP mechanisms.

In spite of high degree of development of the problem of PPP projects implementation abroad, this problem requires detailed analysis and generalization from the point of view of specifics of Russian economy. In recent years, there is a heightened interest to this subject in Russian scientific environment. At the same time, available publications are mainly of theoretical, fragmental nature.

In connection with it, conceptual framework and methodology in this field require development, theoretical generalization of the first results of PPP projects implementation in Russia is needed, especially taking into specifics of Russian budget system and peculiarities of institutional environment.

It is also important to reveal the main problems of PPP implementation in the system of selection and assessment of efficiency of construction megaprojects in field

of transport infrastructure using PPP mechanisms and to work our certain proposals to increase efficiency of their implementation.

2 Methodological Fundamentals

In the present article, while analysing specifics of usage of PPP mechanisms for implementation of construction megaprojects of transport infrastructure development and working out proposals and recommendations, the following methods and instruments were used: qualitative scientific analysis, methods of comparison and generalization within review of literature sources according to the article subject, methods of economic analysis of investment and construction projects, including sensitivity analysis, strategic analysis. Worked out recommendations are based on the results of analysis of PPP mechanisms implementation in the construction projects on development of transport infrastructure in Russian conditions.

Within the present article, toll roads [13] were chosen as the study subject; it is justified by the following preconditions:

PPP mechanism supposes availability of interest of a private partner for implementation of construction megaproject. As a rule, such interest is caused by availability of profit component as a result of project implementation. Majority of road construction projects (roads of federal, regional and local significance) don't have such a component, therefore application of PPP mechanisms in these cases is not reasonable. PPP mechanisms gave a good account of themselves in world practice for implementation of construction megaprojects where public interests and private capital interests are combined. At the same time, key task is to take into account interests of all participants of investment process. Projects of toll road construction are that particular case when PPP mechanism application can be reasonable.

Toll road construction is relatively new phenomenon for the Russian Federation. First pilot projects in this direction were implemented in recent years (2014–2017). A number of problems was revealed (considered below in the present article in the clause “Results”) during implementation of such construction projects; it justifies timeliness of the following research in this field.

General approach to the assessment of construction megaproject implementation efficiency worked out by the author earlier [14] supposes, as it was stated above, taking into account public interests and private capital interests. Efficiency of megaproject implementation on the state level (G) is a function of many variables, like efficiency for private capital (I). In this context, both state and private investors strive for maximization of this efficiency (1).

$$\left. \begin{aligned} G &= f(a_1, a_2, a_3 \dots a_n) \rightarrow \max \\ I &= f(b_1, b_2, b_3 \dots b_m) \rightarrow \max \end{aligned} \right\} \quad (1)$$

- a1 ... an – many factors determining efficiency on the state level;
- b1 ... bm – many factors determining efficiency for private capital.

The task of efficiency maximization practically transforms into optimization task when such combination of factors should be found to provide optimal variant of megaproject implementation satisfying all participants.

It is possible to determine qualitatively assessment of factors defining efficiency for private capital. These are such traditional parameters for investment analysis like NPV, IRR, PP, DPP, PI.

Parameters reflecting achievement of the state's purposes and tasks within megaproject depend on the project peculiarities, and for the toll roads they can include:

- Total amount of investment expenses;
- Roads length;
- Road capacity and actual traffic intensity;
- Specific value of investment and operating costs during the whole lifetime of the facility per 1 year;
- Reduction of traffic congestion for alternative (free) roads.

3 Results

As a result of carried out research, it can be concluded that, taking into account variety of forms and models of PPP in the world practice, it is reasonable to classify PPP in the following way. In simplified form, PPP forms can be divided into:

- institutional forms that are mainly of organizational nature; it is reasonable to mention the following forms among them: special economic zones, development institutes, public companies, joint ventures, etc.;
- contract forms of PPP including various types of agreements with investment obligations, concession agreements, production sharing agreements, etc. Specific feature of this form is the fact that, as a rule, agreement is concluded with the purpose of implementation of a separate investment project. In connection with it, while making a classification, specifics of a project approach should be taken into account.

Besides, it should be noted that in the world and Russian practice of transport infrastructure development contract forms of PPP are used, as a rule (implementation of separate projects of transport infrastructure development), and institutional forms play auxiliary role.

As a result of carried out analysis of construction megaprojects implementation in field of transport infrastructure of the Russian Federation, the following problems of PPP development were revealed in this field:

1. in the system of transport infrastructure financing, there is no established algorithm of projects selection for implementation based on public-private partnership providing, among others, determination of reasonability of project implementation based on PPP and complex assessment of its efficiency, including the cases when they are included into federal target programs and program of activity of the Public Company "Avtodor" for a long-term period;

2. competitiveness between potential investors remains extremely low; it negatively influences efficiency of projects implementation based on PPP, including their cost for the state;
3. there is a problem of transaction costs reduction while concluding contracts between the state and private party, especially for conclusion of concession agreements;
4. lack of criteria of financial assessment and projects selection. Taking into account large scale, capital capacity, structural complexity and long terms (over 10 years) of the projects of transport infrastructure construction, assessment of financial efficiency of a project implementation by calculation of a project net present value (NPV), without assessment of influence on the parameter of significant external factors and risks, in case of their occurrence, is insufficient.

As an example, the project “Financing, constriction and operating on a paid basis of highway M-11 “Moscow-Saint Petersburg” on the section km 543 – km 684” was analyzed; its implementation is carried out using PPP mechanism. Key information about the project is provided in the Table 1.

Table 1. Key information about the project

Location	Saint Petersburg, Leningrad region
Construction length	137.5 km
Forecasted intensity	23 000–26 000 cars/day on the section km 543 – km 646
	18 000–21 000 cars/day on the section km 646 – km 684
Road category	1A
Number of lanes	6/4
Project total cost	83.1 billion rubles (in the prices of relevant years)
Public financing	75%
Private financing	25%
Type of contract	Concession agreement with concession grantor payment
Agreement period of validity	27 years
Construction period	2015–2017

The project implementation is being carried out according to the scheme of life cycle contract; it supposes refund of investor’s funds at the account of investment payments from the side of the state.

Results of financial modelling of the construction project are provided in the Table 2.

Having analysed obtained results of financial modelling, the following conclusions can be made:

- the project is characterized by long payback period, at the same time efficiency of the investment project implementation is much higher for the private partner;
- most part of risks of the project implementation is attributable to the public partner because compensation of investment and operating costs is guaranteed to the private partner.

Table 2. Results of financial modelling of the construction project

Parameter	Unit	Private partner	Public partner	Consolidated
Proceeds	Million roubles	182 702.83	504 204.52	504 204.52
Expenses (without depreciation)	Million roubles	-28 801.60	-182 702.83	-28 801.60
Depreciation	Million roubles	-70 426.27	0.00	-69 299.45
Loan interest	Million roubles	-628.30	0.00	0.00
Profit tax	Million roubles	-16 569.33	0.00	-81 220.69
Net profit	Million roubles	66 277.33	321 501.69	324 882.78
Discounting rate	%	9.0	9.0	9.0
FCFE	Million roubles	50 650.58	314 565.94	305 756.05
NPV as of 31.12.2017	Million roubles	2 317.07	27 497.30	26 152.11
IRR	%	9.9	1.0	11.4
Non-discounted payback period	Date	31.12.2026	30.04.2030	30.04.2029
Discounted payback period	Date	30.11.2037	31.01.2037	30.09.2036

- if we refer to the formula (1), proposed PPP scheme is significantly focused on efficiency maximization for the private partner, at the same time efficiency on the level of public partner is not guaranteed: it refers not just to the parameters of economic efficiency but also to other factors, like:
- disinterestedness of the private partner in implementation of innovative solutions on toll road construction and lack of motivation to reduce aggregate expenses for the project implementation and object operating during the whole life cycle;
- lack of connection between a fee received by the private partner and revenue component of the project that significantly depends of carefulness of working out of technical solutions on the conceptual stage. In this example, the project results are extremely sensitive to traffic intensity at the stage of operating.

4 Conclusions

Based on performed analysis of PPP mechanisms in field of transport infrastructure development, the author proposes the following main directions of improvement:

- development of methodological support in field of PPP on federal level, including approval of algorithm of projects selection for implementation based on PPP that can serve as a basis for approval of similar documents on regional and local level;
- increase of transparency of PPP projects implementation, including formation of common open base of projects as well as normative consolidation of the requirements regarding disclosure of information about PPP projects;

- practical choice of PPP mechanisms taking into account interests of both private and public partners. Efficiency for the private partner should be bound to economic efficiency of investment project on the whole;
- for improvement of the instruments for methods of a project financial efficiency, with the purpose to work out and to select the most efficient scenarios of project implementation (with reference to the projects of toll road construction), the author proposes to supplement the assessment with calculation and construction of charts of sensitiveness of the main financial parameter of project efficiency (NPV) to the change of demand to the services of driving on the toll road (traffic intensity while operating).

References

1. Liyanage, C., Villalba-Romero, F.: *Transp. Rev.* **35**(2), 140–161 (2015)
2. Mladenovic, G., Vajdic, N., Wüdsch, B., Temeljotov-Sala, A.: *Built Environ. Proj. Asset Manag.* **3**(2), 228–249 (2013)
3. Macário, R.: *Res. Transp. Econ.* **30**(1), 145–154 (2010)
4. Li, B., Akintoye, A., Edwards, P., Hardcastle, C.: *Constr. Manag. Econ.* **23**(5), 459–471 (2005)
5. Morkovin, D.: *Ind. Econ.* **1**, 4–7 (2016)
6. Tsvetkov, V., Zoidov, K., Medkov, A., Zoidov, Z.: *Financ. Econ.* **5–6**, 7–20 (2015)
7. *PMBOK Guide: A Guide to the Project Management Body of Knowledge*. Newtown Square, PMI, 589 p. (2013)
8. Orlov, A.: *Sci. Surv.* **14**, 315–318 (2015)
9. Ainamo, A., Artto, K., Levitt, R., Orr, R., Scott, W., Tainio, R.: *Scand. J. Manag.* **26**(4), 343–351 (2010)
10. Flyvbjerg, B., et al.: *Megaprojects and Risk an Anatomy of Ambition*, 215 p. Cambridge University Press, Cambridge (2003)
11. Flyvbjerg, B.: *Proj. Manag. J.* **45**(2), 6–19 (2014)
12. Zabrodin, et al.: *Management of Investment Programs and Project Portfolios*, 576 p. Delo ANH, Moscow (2010)
13. Tamayo, J., Vassallo, J., Baeza, M.: *Publ. Money Manag.* **34**(6), 447–451 (2014)
14. Orlov, A.: *MATEC Web of Conferences*, vol. 106, p. 08013 (2017)

Assessment of the Level of Balance of the Development of the Regional Transport Systems in the Russian Federation

Violetta Politi^(✉) 

Moscow State University of Civil Engineering,
Yaroslavskoye shosse, 26, 129337 Moscow, Russia
polity_violca@list.ru

Abstract. This article explores the factors which influence on the balance of development of the regional economy and regional transport systems. New indicator of assessment of the sustainable development “stability of interaction” and the corresponding institutional and synergistic methodological approach was proposed. There was presented a concept of assessment of the level of balanced development of regional transport systems which includes three key criteria: stability, proportionality and adaptability.

Keywords: Regional transport systems · Regional economy
Transport infrastructure

1 Introduction

Main reason for the negative results of the program on reformation of the transport sector of economy of the Russian Federation and the lag in the development of regional transport systems, is rather mismatch and imbalance of market processes and the lack of mechanisms for regulation of the development of the system than the lack of proper support from the state and the legal regulation measures. As a result, there was a violation of interbank production (natural) and cost proportions, irrational consumption of the material and technical resources of the industry, widespread profitableness of transportations and destruction of the network of service enterprises of the transport sector.

2 Methods

Certain groups of criteria which allow to assess the level of balanced development of regional transport systems can be allocated on the basis of the indicators of the socio-economic development of the region and through the usage of the criteria of systemic nature of the management theory and definition of the stability of the economic system.

Firstly, these are the criteria for the balance of the regional transportation system, including positive succession and capacity-building activity. Relying on the system

criteria which were developed with management theory, it can be defined that conscious fulfillment of the succession requirements in the management of the regional transport system means the following:

- development and adherence of the sequence of the stages of reformation of the existing transport system in the Russian Federation;
- proactive institutional, legal and investment provision;
- general support of the changes made by society and authorities of different levels;
- identification of the potential for development of the transport system and its support.

It is necessary to dynamically increase the potential of the transport complex, including the development of the providing infrastructure and different types of transport for the balanced development of the regional socio-economic system as a whole. This is possible at the expense of the appearance of the synergetic effect, which gives new opportunities to the development of the transport network [1].

Secondly, it is required to allocate specific criteria for assessment of the effectiveness of system management. These criteria are designed to assess the achievement of the balance both inside the system and among its individual elements, including the correspondence of goals of the different level, investment interests, harmonization of interests and proportional allocation of resources.

Formation of mechanism for balanced management through the development of transport systems contributes to the harmonization of the targeted interests of its subjects. Consequently, the level of coherence is an indicator of assessment for both negative consequences and conditions for development of the regional transport system. Thirdly, it is necessary to establish criteria which integrate various aspects of functioning and development of transport system, namely, criteria of economic balance. It allows to assess the degree of satisfaction of social needs, balance of production and consumption, economic equilibrium in the subsystems. For assessment of the level of balance of the development of the transport system it is necessary to consider it as a balanced subsystem of a higher order, as a regional socio-economic system and national transportation system. According to the provisions of theory of self-organizing systems and from position of the systems approach, mechanism of management of the balanced development of regional transportation systems of the Russian Federation includes the following starting provisions:

- development of the transport system takes place inside of the more complex self-organizing system, which has its internal aspiration and ability to grow;
- public authorities and enterprises of the transportation system aspire to rule the process of development in the target direction chosen by them;
- modern market conditions are characterized by the absence of subject which has resource capabilities and is able to rule the development of the system exclusively.

Geographical features of many regions of the Russian Federation determine the priority role of transport in the development of the competitive advantages of the territory in terms of their transport potential. So, transport network, which is the tool for achievement of social and economic goals of the region is also an important part of both production and social infrastructures in any region of the Russian Federation.

Dynamically developing economy requires an appropriate transport infrastructure, which is the basis for concentration and specialization of manufacture, demand for services for the transportation of passengers and loads. In turn, the improvement and development of transport infrastructure contributes to the growth of mobility of the working power, goods and resources, expansion of the trade ties and increase of accessibility of many economic regions. Nowadays it is accepted to talk about the concept of the sustainable development which was formulated by the UN working group, within which there are made some attempts to move on to a comprehensive review of the environmental, economic and social aspects of development in the interaction of society with environment. In accordance with this, in the long term prospective, the development of the economy of the country must be conditioned by the principle of sustainable development, which implies the necessity of both present and future generations. In context of the development of transport systems, which are a source of environmental pollution, requirements of sustainable development are particularly relevant. In turn, for sustainable development of regions in Russia it is necessary to create transport and logistics conditions and remove infrastructure constraints with the help of development of the strong federal transport network and formation of the international transport corridors. Consequently, the balance of the interests of the three components, which are nature, society and economy with the help of creation of the conditions, which ensure the possibility of interconnected, internally balanced functioning of this triad. Thus, the solution of the problem of sustainable development of the territory centers around the consideration of this territory as social ecological and economic system, at the same time exploring environmental, social and economic aspects. For achievement of the sustainable development it is necessary it balance interests and demands of all of the components of the social ecological and economic system [2]. Types of sustainability and methodological approaches to the concept of “stability” are given in the Table 1. In this study, author proposes to use the new notion “stability of interaction”, which is applicable to the enterprises of transport sphere and institutional environment, which is presented by the regional economy. At the same

Table 1. Methodological approaches to the essence of the concept of “stability”.

Stability mode	Methodological approach	Founders
Stability of form	Philosophical	G. Hegel, F. Schelling, A.A. Bogdanov
Dynamic stability	Mechanistic	Pierre-Simon Laplace, Joseph-Louis Lagrange, A.M. Lyapunov
Stability of the system	Biological	D. Hume, T. Malthus, G. Spencer
	System	R. Ackoff, L. Von Bertalanffy
	Cybernetic	N. Wiener, W. Ashby, V.M. Glushkov
Stability of equilibrium	Economic	L. Walras, V.V. Leontiev, A. Marshall, P. Samuelson, J. Hicks, K. Arrow
Stability of interaction between industry enterprises and institutional environment	Institutional and synergistic	Author proposes to allocate as a separate type of stability

time, there should be used methodological approach which combines achievement of institutionalism and synergetics [3].

Regional socio-economic system is a combination of economic and social elements, which are limited by legislative institutions and territory within the administrative regional division, interacting with each other in relation to the improvement and development of the condition of every of elements and system as a whole. Regional transport complex is a vital part of the regional economy, which creates basis for an active interaction of all elements of the socio-ecological and economic system, like a blood circulatory system of living organism.

3 Results

Theory of index analysis, the basis for selection of indicators served the concept of sustainable development (Table 1), was applied for integrated assessment of the balanced development of the regional transport complex. Three blocks of system characteristics, which allow to assess the condition of the external and internal environment of the operation of the research object were created for this purpose (Table 2).

Table 2. Summary characteristics index method.

No	Integrated indicators	The components of the complex index
1	The index of regional stability	e index of economic stability of the region
		The social stability index $I_{SOC} = \frac{T_r^v \times T_r^{in} \times T_r^{ser}}{T_r^{in} \times T_r^{uns} \times T_r^{sp}}$
		The index of ecological stability $I_{ECOL} = \frac{T_r^{sc} \times T_r^i}{T_r^{pol}}$
2	Dynamic index characterizing structural adaptation	The index of structural shifts (an index of the effect of changes in the structure of phenomena) $I_S = \frac{\sum x_i^1 f_i^1}{\sum f_i^1} \div \frac{\sum x_i^0 f_i^0}{\sum f_i^0}$
3	Index of adaptability	Growth index of gross regional product $I_{GROW} = \sum_{i=1}^n d_i^g \times g_i$
		A lower index of gross regional product $I_{LOS} = \sum_{j=1}^n d_j^l \times l_j $
		The speed of adaptation $I_{ADT}^i = \frac{t_{adt-1} - t_{adt}}{t_{adt-1}}$

Summary measures of level of balanced development

Multiplicative model $I_{BALANS} = I_{RS} \times I_S \times I_{ADP}$

Additive model $I'_{BALANS} = k_1 I_{RS} + k_2 I_S + k_3 I_{ADP}$

First block of characteristics, described with the index of regional stability I_{RS} , which was designed for assessment of the level of balance of regional economic system. It includes three indicators: index of economic stability; index of social stability; index of environmental stability, and is calculated as the average compound index. So,

$$I_{RS} = \sqrt[3]{I_{ECON} \times I_{SOC} \times I_{ECOL}} \quad (1)$$

where I_{RS} is the regional stability index; I_{ECON} is the index of economic stability; I_{SOC} is the index of social stability; I_{ECOL} is the index of environmental stability.

In turn, the index of economic stability of the development of the region (I_{ECON}) includes the following statistical indicators:

- index of industrial production for the region I_{ip} ;
- index of agricultural production in the region I_{ic} ;
- growth rate of the specific regional indicators (shipped decoctions of own production, work performed and services per capita) T_r^{sp} .

Index can be calculated in the following way:

$$I_{ECON} = I_{ip} \times I_{ic} \times T_r^{sp} \quad (2)$$

Index of social stability of the development of the region (I_{soc}) includes following statistic indicators:

- rate of increase/decrease of the average monthly nominal accrued salary T_r^w ;
- rate of increase/decrease of the real money income of the population T_r^{in} ;
- rate of increase/decrease of the amount of paid services for the population T_r^{ser} ;
- rate of increase/decrease of the level of unemployment T_r^{un} ;
- rate of increase/decrease of the hidden unemployment (quantity of employees who work part-time on the initiative of the employer) T_r^{uns} ;
- rate of increase/decrease of the prices for goods and services T_r^p .

Index can be calculated in the following way:

$$I_{SOC} = \frac{T_r^w \times T_r^{in} \times T_r^{ser}}{T_r^{un} \times T_r^{uns} \times T_r^p} \quad (3)$$

Index of Ecological Stability of the Development of the Region (I_{ECOL}) includes the following statistical indicators:

- rate of growth of the current operational costs for environmental protection T_r^{oc} ;
- rate of growth of investments in key assets directed on the rational usage of the natural resources T_r^i ;
- rate of growth of pollution emissions (to the atmosphere, soil, water environment) T_r^{pol} .

Index can be calculated in the following way:

$$I_{ECOL} = \frac{T_r^{oc} \times T_r^i}{T_r^{pol}} \quad (4)$$

Second block of characteristics is intended to assess the level of balance of the regional economy and internal environment of enterprises, which are the part of the regional

transport system. It includes index of dynamics of adaptation indicators (I_{ADP}), and index of the level of proportionality of development (I_S).

Let us understand the observance of established norms, regulations, proportions, equilibrium of resource characteristics and coordination of relationships inside the system under the proportional development.

From the point of view of congruence of interests and for provision of proportionality of the development of separate elements of the system, important value has an effective allocation of resources between them, which allows to avoid contradictions inside the regional transport system. Maintenance of the necessary proportionality between the individual elements of the resource potential of the transport complex is directed on their efficient usage and on the improvement of distribution of the totality of the resources of the region [4, 5].

Proportionality criteria are intended to assess the following key indicators: manufacturing, labor, finance and investment, customers and competitors, that is, the basic characteristics of the balanced indicators system.

Indicators of assessment of the transport system can be presented as follows:

$$Y = \begin{pmatrix} P_{1i}, P_{2i}, \dots, P_{pi} \\ L_{1i}, L_{2i}, \dots, L_{li} \\ F_{1i}, F_{2i}, \dots, F_{fi} \\ M_{1i}, M_{2i}, \dots, M_{mi} \end{pmatrix} \quad (5)$$

where P is the production (p - number of production and economic indicators); L - labor (l - number of indicators of labor); F - finance and investment (f - number of indicators of capital); M - customers and competitors (m - market factors).

Proportionality means observation of certain proportions between economic indicators. For example, proportions of progressive development for the region, as for a part of national economy (I_S^1), are following:

1. priority development of knowledge-intensive sectors of the economy;
2. rapid growth of the service industries;
3. rapid growth of foreign trade turnover in comparison with growth of production inside the country.

Proportions of the progressive promotion for regional economy as a set of enterprises (I_S^2) reflect such indicators as:

1. positive trend and change of cost of the key assets;
2. outstripping growth of the rates of production and realization of products and services in comparison with the growth of capital;
3. outstripping growth of gross regional product in comparison with growth of amounts of production of the goods and services;
4. priority development of infrastructure;
5. outstripping growth of international traffic in comparison with the growth of domestic traffic.

Determination of proportions (required rates of growth) for transport enterprises in the region (I_S^3), can be defined on the basis of actual and necessary (required) structure of freight and passenger transportations.

It should be noted that the regions of the Russian Federation in general, are characterized by lag in development of the transport infrastructure. So, identification of disproportions in the development of transport infrastructure can be implemented on the basis of the ratio of growth of key indicators for transport enterprises and rates of growth of the regional infrastructure I_S^{inf} .

Thus, estimates of coherence (proportionality) are determined by each level and come down to the single indicator, so-called index of the level of proportionality (coherence) of development:

$$I_S = \sqrt[n]{I_S^1 \times I_S^2 \times \dots \times I_S^n} \quad (6)$$

For final verification of the balance on the studied aggregate of enterprises, namely, in relation to the established proportions, it is recommended to determine the coefficients of Candell and Spearman, values of which will show a violation or compliance of the established regulatory values. Adaptation capabilities are one of the fundamental properties of the organizational system, expressed in the reserve of functional resources, which are spent on maintenance of the balance between organization and the external environment. Therefore, it should be considered that adaptability is one of the key characteristics of the level of balance of economic system [6]. Assessment of adaptive capabilities of the transport complex should be performed on the basis of determination of dynamic index of structural adaptation I_{ADP}

$$I_{ADP} = \frac{I_{\text{grow}}}{I_{\text{los}}} \quad (7)$$

where I_{grow} is the index of growth which characterizes positive changes in the regional transport complex;

I_{los} is the index of losses which characterizes negative changes in the regional transport complex. Indexes of increase (decrease) of the amount of gross regional product, with allocation of the share of the gross regional product created with the branch "Transport and Communication", are calculated by the formulas:

$$I_{\text{GROW}} = \sum_{i=1}^n d_i^g \times g_i \quad (8)$$

$$I_{\text{LOS}} = \sum_{j=1}^n d_j^l \times |l_j| \quad (9)$$

where:

- I, j is the number of economic activities with expected growth/losses of production, respectively;
- d_i^g, d_j^l – is the share of i -th and j -th type of economic activity in gross regional product, respectively;

- g_i, l_i - is the growth/loss of gross regional product, which is created with the help of "Transport and Communications" branch by i and j type of economic activity, respectively.

Additional dynamic characteristic of the level of balance in the development of transport systems is the period of adaptation for the time of which enterprises should renew composition and structure of the property complex. Speed characteristic can be the index of the dynamics of adaptation of enterprises:

$$I_{ADT}^t = \frac{t_{adt-1} - t_{adt}}{t_{adt-1}} \tag{10}$$

t_{adt}, t_{adt-1} - time of adaptation of the transport industry enterprises in the basic and previous period, respectively.

Third block of characteristics includes a composite indicator which allows to assess the level of development of the balance. Integral indicator of the level of the balance of the regional transport system can be presented in the form of the additive model which allows to link three vectors which determine the directions of the sustainable development. They are index of regional stability, index of the proportionality of development, index of the adaptability of transport enterprises.

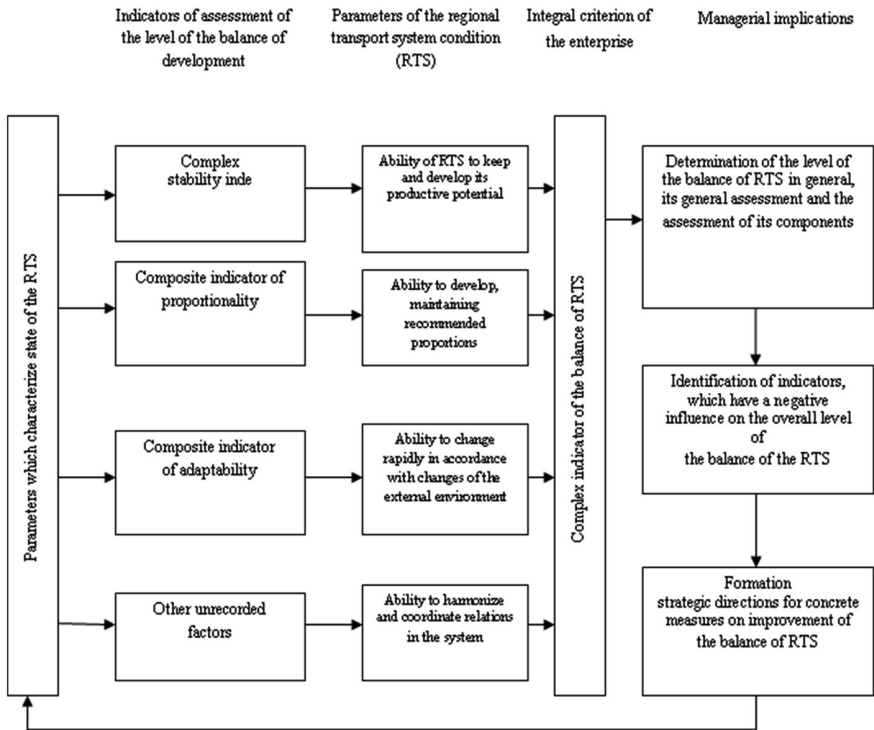


Fig. 1. Scheme of the assessment of level of the balance of development of regional transport system (RTS).

Corresponding managerial decisions on the balance of interests of the transport complex and regional social economic and environment system should become the result of the comprehensive assessment (Fig. 1).

So, methodology for assessment of the level of development of transport complex as a part of regional social ecological and economic system should include three blocks of indicators. They are sustainability of interests (coherence in the development of society, ecology, economy), proportionality (implementation of regulatory proportions and ratios in terms of industry, territory, society, economy and ecology), adaptability (rate of change for achievement of correspondence of the internal and external environment).

Comprehensive index for assessment of the balance of development of the regional transport system can be presented in the following way:

$$I_{BALANS} = I_{RS} \times I_S \times I_{ADP} \tag{11}$$

where I_{RS} is the index of regional stability; I_S is the index of proportionality of development; I_{ADP} is the adaptability index.

4 Discussion

For visual presentation of the index of the balance of the development there can be used a vector diagram, presenting the search index in the vectorial three-dimensional space as a kind of “balance point”:

$$B = f(X_i, Y_i, Z_i) \tag{12}$$

Then the complex indicator can be represented in three-dimensional space as coordinates of this point. Each of planes determines with a set of characteristics of stability (Y), proportionality of development (X), and adaptivity (Z). Thus, the magnitude of the equilibrium index represents a part of the space, limited with the planes (XY, XZ, YZ) (Fig. 2).

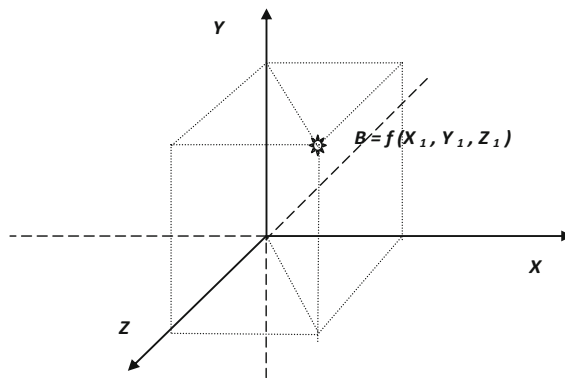


Fig. 2. Index of balance as a result of integration of three groups of indicators.

Formalized expression of the relationship between the proposed vectors of assessment and complex indicator of the level of balance of the regional transport system can be presented as an additive model, which can be solved through transformation (8) on the basis of indicators, so-called, matrix of the priorities:

$$I'_{\text{BALANS}} = k_1 I_{\text{RS}} + k_2 I_{\text{S}} + k_3 I_{\text{ADP}} \quad (13)$$

So, the complex indicator of balance consists of the indicators of sustainability, proportionality and adaptability multiplied on the coefficients of the corresponding indicators. More detailed proposed vector approach and the definition of the priority matrix were not considered in this study.





5 Conclusions

For provision of the harmonic and coordinated development of the transport system on the federal and regional levels, it is necessary to develop and adopt a number of government decisions, for example, the creation of interoperable transport exchanges and self-regulating transport organizations. It can allow the coordination of the work of all participants of the transport process. For increase of the level of balance in the development of regional transport systems, it is also necessary to perform a monitoring, analysis and assessment of the developmental balance factors, namely, coherence, sustainability, adaptability and proportionality.

References

1. Ustinovicus, L., Rasiulis, R., Nazarko, L., Vilutienė, T., Reizgevicus, M.: *Procedia Eng.* **122**, 166–171 (2015)
2. Aurora, A., Teixeira, S., Queirós, A.: *Res. Policy* **45**, 1636–1648 (2016)
3. Isaev, S., Vatin, N., Baranov, P., Sudakov, A., Usachov, A., Yegorov, V.: *Mag. Civil Eng.* **36** (1) (2013)
4. Arseniev, D., Rechinskiy, A., Shvetsov, K., Vatin, N., Gamayunova, O.: *Appl. Mech. Mater.* **635–637**, 2076–2080 (2014)
5. Khmel, V., Zhao, S.: *IATSS Res.* **39**(2), 138–145 (2016)
6. Chirkunova, E., Kireeva, E., Kornilova, A., Pschenichnikova, J.: *Procedia Eng.* **153**, 112–117 (2016)

The Priority Directions of Public Transport Transit Hubs Development on Commuter Railways

Denis Vlasov¹ , Nina Danilina¹  , and Anna Shagimuratova² 

¹ Moscow State University of Civil Engineering,
Yaroslavskoye Sh., 26, Moscow 129337, Russia
{vlasych, nina_danilina}@mail.ru

² Moscow Center of Development Planning of the City, Moscow, Russia

Abstract. The article is devoted to the questions of development of the public transport transit hubs system based on the commuter railways on the example of Moscow city. The vast territory of the city, big quantity of transit hubs and expensiveness of their construction define the actual direction of the research addressed to find such solutions that will provide interests of population, authorities and investors. There is the presentation of new approach which allows to graduate all transport hubs and to select the most attractive both as a transport service for population and object of investment. This approach is based on system analysis, theory of graphs and quantitative method that determine the verification and the correctness of the obtained results. The article presents the theory of the approach, algorithm of calculations and description of the area of results application. The implementation of this scientific approach allows defining the structure of the public transport transit hubs system on the commuter railways in Moscow.

Keywords: Transport transit hub · Commuter railways · Public transport
Urban planning · Graph theory · Qualitative method · Value tree

1 Introduction

The implementation of transport infrastructure projects, is one of the major goals for the sustainable development and formation of a comfortable and safe living environment [1–3].

In Moscow, there is an intensive development of all major elements of the transport infrastructure: road network, off-road transport, on-land passenger transport. The public commuter railway is no exception. As part of the Moscow railway junction development, it is planned the construction of additional main tracks, new stops, the organization of high-speed movement.

Public transport transit hubs (TTH) are most important communication elements for providing relationships between different modes of transport and as well as their spatial interaction with the city structure. In Moscow there are more than 95 stopping points of the commuter railways (not to mention railway stations), which constitute potential development of the urban TTH system. TTH development requires considerable

investment, so the challenge is to improve the urban transport service for the maximum number of passengers minimizing at the same time the municipal costs. Practical experience in the formation of TTH in Moscow shows that the period of their project development is about 2 years, and the cost - about 2–3.5 million euro. Thus, to prepare documentation for land planning needs about 300 million euro.

Consequently, there must be a system approach on how to evaluate the development prospects of different transport hubs and their importance for the population. That is, there is a real need for a method to determine priority railway TTH for their development (reconstruction), taking into account all urban factors [4–6]. Such method will allow to select the hubs that ensure high development potential, optimum conditions for providing transport and technological infrastructure and opportunity to create an environment comfort for the passengers transfer.

2 Material and Method

The objective and application of the needed method is in identifying of priority to be developed transport hubs in the major cities exploiting the existing building.

The elaboration of the proposed method requires the following steps:

1. To develop criteria system for evaluation of the commuter railway TTH.
2. To select method of evaluation.
3. To set the value of each indicator.
4. To find algorithms of initial data revenues (requirements, sources of initial data).
5. To calculate algorithm to determine the total values allowing to compare TPU to each other and to form the program.

To describe the system it is used the classical model railway system on the basis of graph theory [7, 8]. From the perspective of graph theory, the transport network is defined as a graph $G(V, E)$ with the plurality of vertices V , corresponding to TTH, and a plurality of edges E , corresponding to the appropriate sections of the railway track. The stations are numbered from 1 to N , that is, $V = \{1 \dots N\}$, the elements of the plurality of edges E are the pairs (i, j) , responsible for the path areas from the top i to the top j (Fig. 1).

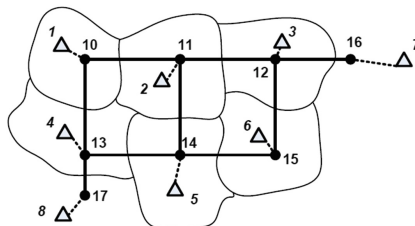


Fig. 1. Transport network graf model.

Solve the problem means to determine the optimal (in terms of city development and investment available) amount of vertices, which will be the priority TTH for the reconstruction. The main indicators related to determining the priority stations are the following: the value of passenger turnover in the station - that is TTH, area urban settings, the indicators of input-output capacity, time to change from rail to other transport modes in the node, the average number of trains passing this lot during a day, etc.

In order to select the priority hubs for the development of the system is necessary to determine criteria for their evaluation, taking into account the urban features of TPU viewing it as an object meant for transport purposes, the occupies nevertheless a large lot of urban area, and the preferences of the passenger as a target services consumer on the given area.

Figure 2 is a practice factor model for TPU development assessment, that includes town planning, transport, technological and socio-economic factors, and ensuring the sustainable development of urban areas and transport complex.

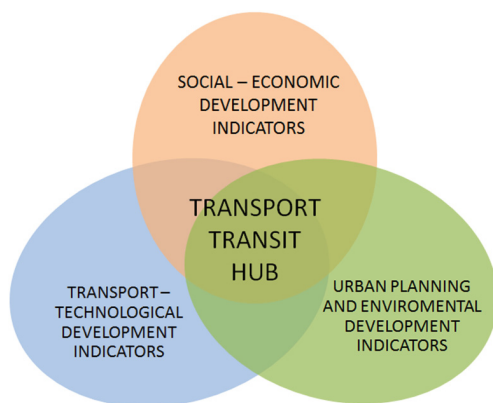


Fig. 2. Factor model for TPU development assessment.

Comprehensive assessment of TTH development it is advisable to carry out using the qualitative method, being in such case the most effective, due to a large number of different evaluation parameters with different units of measurement and significance.

The advantage of qualitative method is in its practical approbation confirmed by a lot of research in the field of architectural design, as well as in its theoretical validity. This method is also used for research in the field of urban development and transport [9].

The result of the elaboration of methodology for TTH development assessing should be the definition of the integral index - the index of the TTH Railway development, which permits to compare the nodes and set them in the ranked list for priority implementation. It is proposed to calculate this Integral index of TTH which is a quantitative mapping of the complex evaluation of the node development, in accordance with the simplified qualitative method - as a weighted arithmetic average of the indicators of the individual properties of the site evaluation and appropriate “ponderability coefficients”.

3 Theory and Calculation

Application of the qualitative method based on system analysis allows to structure the large number of factors, of different significance and functional orientation, in a single evaluation system divided into subgroups [10, 11].

Value tree formally and visually presents a set of properties needed for evaluation. At the initial level, it is proposed to divide the indication values into two main sub-categories: urban planning and socio-economic. Urban planning indicators, in turn, are divided into transport-technological and land use planning indicators that reflect the conditions of land use and area planning characteristics. Socio-economic indicators, in turn, it is proposed to subdivide into social development indicators and marketing indicators that reflect the demand for transport services node. It should be noted that the Value tree is composed for municipal nodes of local significance and may be adjusted in the study of hubs of different functional significance [12, 13].

Drawing the results of Value tree development indicators, in accordance with the assessment rules applied while using the qualitative method, it has been formed the expert group with professional knowledge of the investigated objects aimed to make primary adjustments and identify the set of indicators. As a result, there was elaborated a balanced system of indicators to measure the development of TTH railway, consisting of 96 properties. Upper level of Value tree is represented on Fig. 3, lower level is represented as the table of indicators taking into account different function aspects of the same type of TTH (nods of municipal importance (Table 1)).

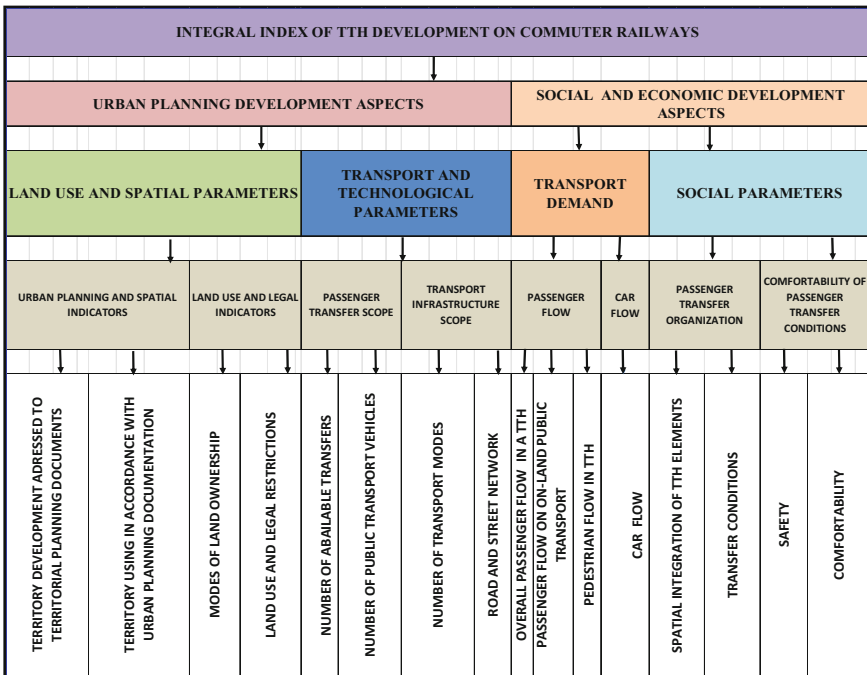


Fig. 3. Upper level of value tree.

Table 1. Total ponder ability coefficient values of the indicators.

№ indicator	Ponder ability	Description of the indicator
	9.05	The number of passenger transfers from rail to other modes
	8.72	The number of individual car on a TTH parking
	8.41	Overall passenger flow in a TTH
	7.50	Passenger flow on-land public transport
	4.57	Average time of transfer between rail and other mode
	4.45	Pedestrians flow in a TTH using its services
	3.56	The traffic capacity of the road network on the territory of a TTH
	2.76	Average distance between boarding platforms
	2.45	Intensity of trains traffic in morning peak hours
	2.37	Proportion of private ownership land area
	2.30	Comfortability of passenger transfer (max density of pedestrian flow)
	2.28	Density of road network in a TTH
	2.27	The number of on-land public transport vehicles
	2.25	The proportion of the reorganized and developed territories
	2.24	Safety conditions for passengers (light and equipment)
	2.16	The proportion of public lands
	1.97	Safety of road and pedestrian intersections
	1.92	The proportion of common areas (road network, green lands, public spaces)
	1.75	Navigation and information support in a TTH
	1.62	The flow of individual cars traffic
	1.46	Permitted use of the territory in accordance with the territorial zoning
	1.40	Zones with special conditions of a territory use
	1.39	Location of residential buildings and areas
	1.38	Length of boarding platforms
	1.37	Limitations on the territory in connection with planned placing of objects of Federal and regional level or are employed for such objects
	1.35	Technical zones of road and engineering zones
	1.34	Proportion of stabilized territories to be saved and landscaped
	1.31	On-land public transport infrastructure objects
	1.21	Location of administrative and trade buildings and areas
	1.11	Proportion of areas with land information on cadastral registration
	1.06	Location of a social and cultural objects
	0.98	Parking of individual transport and Park and Rides
	0.94	Pedestrian communications to boarding platforms
	0.82	The marginal density of the development site
	0.80	Proportion of areas without land information on cadastral registration
	0.79	Kiss and ride parking
	0.77	The main infrastructure elements to ensure comfort transfer of passengers

(continued)

Table 1. (continued)

No indicator	Ponder ability	Description of the indicator
	0.76	The number of boarding platforms
	0.64	Limit high-rise of buildings in a TTH
	0.63	Multifunctional transfer building/rail station
	0.62	Available services in a TTH
	0.57	Accessibility of travel for people with limited and disabled mobility
	0.56	Max. length of rail boarding platform
	0.53	Parking of municipal transport (departmental, taxi, excursions)
	0.44	Parking for people with limited and disabled mobility
	0.41	Bike rents and parking
	0.38	Special services for people with limited and disabled mobility
	0.34	Additional infrastructure elements for comfortability and safety of public transfer

By “ponder ability coefficient” we mean the quantitative evaluation of the given indicator in comparison with other indicators. Determination of this coefficient is made in three stages:

- Stage 1. Defining of ponder ability coefficients of the group.
- Stage 2. Defining of ponder ability coefficients of the level.
- Stage 3. Reducing the number of ponder ability coefficients taken into account.

Determination of ponder ability coefficients of the chosen indicators was carried out by the expert method. Questionnaire survey were carried out among experts from different fields of activity (urban development, transportation, development of planning documentation, management and public service, scientific and educational activities, etc.); different cities an regions of the country (Moscow, St. Petersburg, Tatarstan and Bashkortostan, and others.); different ages, organizations, positions and experience.

Accuracy of the assigned ponder ability coefficients depends on the competence of the experts. To calculate the coefficient of expert’s competence there’ve been developed the criteria for evaluating the competence of the expert commuter and the scale of competence. Expert competence factor is calculated as follows (1):

$$K_j = \sum_{i=1}^g M_i \times R_{ig} \tag{1}$$

- K_j – the coefficient of expert’s competence;
- M_i – ponder ability of the indicators according to the scale of competence;
- R_{ig} – ponder ability, depending on the data expert profiles

Wherein $\sum_{i=1}^g M_i = 1$, and $0 \leq K_{ij} \leq 10$, therefore $0 \leq K_j \leq 10$.

A sufficient number of experts, taking into account the required accuracy and reliability of the results is described by the Eq. 2:

$$N = \frac{t_z^2}{\varepsilon_1^2} \tag{2}$$

where

- N – number of experts;
- t_z – the argument whose value is defined by calculated data tables;
- ε_1 – maximum permissible defined relative error expressed in S shares, definable by the Eq. 3:

$$\varepsilon_1 = \frac{\varepsilon}{S} \tag{3}$$

where

- ε – absolute error;
- S – standard deviation of the assessment.

The total number of expert participants was 47 people. Confidence level of research was not less than 95% maximum permitted relative deviation of 0.3.

As a result of the work done at the first stage, it is approved the structure of value tree of indicators development and determined group ponder ability coefficients of each indicator. At the second stage there were defined the level ponder ability coefficients. The level ponder ability coefficient G_j'' describes the importance of the indicator in relation to any other indicator belonging to the same group and to the same level and to any other indicator, located on the different tier of the tree.

Ponder ability coefficient of the property, located on the j level of the indicators value tree (G_j'') is equal to group ponder ability coefficient of the same indicator (G_j), multiplied by the ponder ability coefficient of corresponding equisetive (common to this group) indicator located in the previous (j-1) tier (G_{j-1}):

$$G_j'' = G_{j-1} \times G_j \tag{4}$$

Ponder ability coefficients are always standardized and vary in the range of $0 \leq G_j'' < 1$. Within each tier of the value tree, it is always provided the condition:

$$\sum G_j'' = 1 \tag{5}$$

where G_j'' - value of the tier ponderability factor.

Reducing the number of accounted ponder ability coefficients is performed on the third stage of calculations. For this purpose, there was fulfilled the audit of performance of the last level indicators of the tree, and the resulting of the calculations of ponder ability coefficients.

Reducing the number of weighting coefficients is performed by the method of aggregation of identical indicators. Total ponder ability coefficient values of the last tier of the value tree for indicators development is presented in Table 1.

4 Results

Determining the integral index of interchange hub is implemented in 6 stages (Fig. 4).

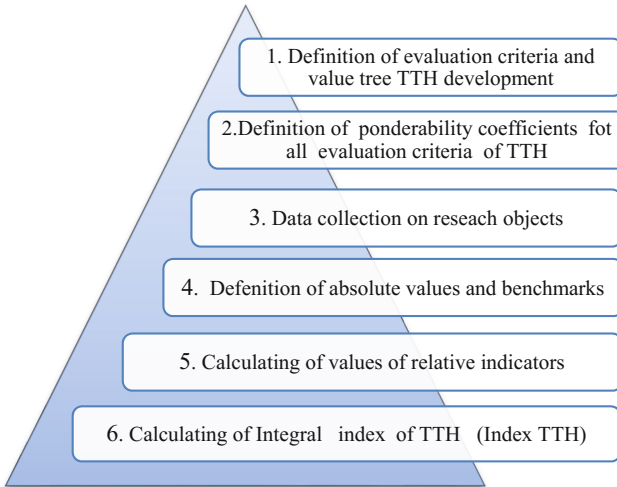


Fig. 4. The stages for determining the index of Railway TTH.

There is developed a form (Table 2) intended to fix the serial data and the development indices calculation results and to determine the grades of Railway TTH (Table 2).

When filling out the form, it should be considered the following:

Column 1 – should state the be the numbers and the name of the indicator

Column 2 – the averaged experts ponderability coefficients of indicators

Column 3 – the reference values of the indicators

Column 4, 7, 10 – the absolute values of indicators

Column 5, 8, 11 – the relative values of the indicators

Column 6 – the values of the indices of transit hubs.

Integral index of TTH (Index TTH) development, which is a quantitative mapping of the complex assessment of site development, it is proposed to count as a weighted arithmetic average of the indicators of the individual properties of the site evaluation and appropriate ponder ability coefficients, according to the formula 6:

$$\text{Index TTH} = \sum_{j=1}^n K_{ij} \times G_j'' \tag{6}$$

where

K_{ij} - relative values of site assessment indicators;

G_j'' - standardized tiered ponderability coefficients of indicators.

Table 2. Evaluation of the priority development of Railway TTH

Number and name of the indicator	$G_j, \%$	P_j^{fl}	Object 1			Object 2			Object 3		
			P_{1j}	K_{1j}	$K_{1j} \times G_j$	P_{2j}	K_{2j}	$K_{2j} \times G_j$	P_{nj}	K_{nj}	$K_{nj} \times G_j$
1											
2											
...											
j-1											
j											
Sum of values	$\Sigma = 100$			$\Sigma = \dots$			$\Sigma = \dots$			$\Sigma = \dots$	
Object grade			I_{p1} Railway TTH		I_{p2} Railway TTH		I_{p3} Railway TTH				

In determining the value of the complex indicator, there should be provided the condition: $0 \leq$ Integral index of TPU ≤ 100 .

The ideal model is a TPU that meets all quality standards and is in sustainable high demand, and which has the maximum potential for urban development of the adjacent territory. According to the results achieved, a transit hub having the largest value of Index of Railway TTH, will have the highest priority in the ranked list as for all of the assessed properties.

5 Discussion

The results achieved by the analysis of the chart and ponder ability coefficients, shows that the indicators line up in sequence “Passenger - territory - infrastructure.” Thus these elements are interrelated and affect each other, forming a system (Fig. 5).

Factors directly associated with the person have the major priority for the assessment of the site development: the number of passengers and turnover, the number of vehicles carrying passengers, the density of pedestrian traffic, variety of the types of transit, the average time and travel distance of the passenger during transit, etc. Such opportunities can be formed by planning parameters of the territory and by its infrastructure [14, 15].

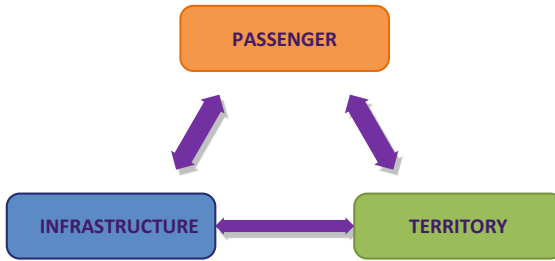


Fig. 5. The scheme of interrelations of the elements of the system “Passenger - Territory - Infrastructure”.

6 Conclusions

Determination of priority directions for the development of TTH transport system is the most important task to improve the efficiency of the transport complex of the largest cities, and make rational management decisions on the financing of the relevant actions. The implementation of urban planning policies for sustainable development will improve the standard of population living and create a comfortable living environment. The developed methodology allows taking into account the needs of passengers, and forms the basis for the system assessment of site development.

References

1. Vlasov, D., Danilina, N.: Sustainable development of transport transit hubs in urban planning. *J. PGS* **9**, 44–49 (2016)
2. Sherbina, E., Slepney, M.: The system of town planning regulations for sustainable development of territories. *Sci. Rev.* **6**, 240–244 (2016)
3. Yao, L., Sun, L., Zhang, Z., Wang, S., Rong, J.: Research on the behavior characteristics of pedestrian crowd weaving flow in transport terminal. *Math. Probl. Eng.* (2012). <https://doi.org/10.1155/2012/264295>
4. Menshutin, A., Vlasov, D., Danilina, N.: The development of intermodal transport services on the basis of geanalytical information. In: *ITM Web of Conferences* (2016). <https://doi.org/10.1051/itmconf/20160801002>
5. Ircham, A., Munawar, I.: Study of key factors determinant choice of rail-based mass transit. *Int. J. Eng. Res. Appl.* **06**(7), 5–10 (2016)
6. Shao Wei, L.: Passenger flow forecast algorithm for urban rail transit. *TELKOMNIKA: Indones. J. Electr. Eng.* **12**(2) (2013). <https://doi.org/10.11591/telkomnika.v12i2.3810>
7. Danilina, N., Vlasov, D.: Aspects of transport transit hubs construction management in coordination with object lifecycle projecting. In: *IPICSE-2016* (2016). <https://doi.org/10.1051/mateconf/2016868605017>
8. Analyse und Bewertung der Qualität von Stationen und Stationsumfeldern des Schienenpersonennahverkehrs. Bericht, Berlin (2014)
9. Steierwald, G., Künne, H., Vogt, W.: *Stadtverkehrsplanung. Grundlagen, Methoden, Ziele*: Bibliografische Information der Deutschen Bibliothek. Springer, Berlin (2005)

10. Shagimuratova, A.: System analysis for determination of priority directions of rail transport-transit hubs development. *J. Gradostroitel'stvo* **2**(42), 63–71 (2016)
11. Setak, M., Abedzadeh, M., Eghbali Zarch, M.: Differential evolution algorithm for multi-commodity and multi-level of service hub covering location problem. *Int. J. Ind. Eng. Comput.* **4**(1), 127–138 (2013)
12. Stjernborg, V., Mattisson, O.: The role of public transport in society—a case study of general policy documents in Sweden. *Sustainability* **8**(11), 11–20 (2016). <https://doi.org/10.3390/su8111120>
13. Valaskova, M., Križanova, A.: The passenger satisfaction survey in the regional integrated public transport system. *Promet (Zagreb)* **20**(6) (2016)
14. Mihajlov, A., Kopylova, T.: Evaluation criteria system of quality of intermodal public transport transit hubs. *Izv. vuzov. Invest. Stroitel'stvo. Nedvizh.* **6**(11), 73–80 (2014)
15. Bahirev, I.: Main transport problems of big cities. *Arhitektura. Stroitel'stvo. Dizajn.* **3**, 60–63 (2008). <https://doi.org/10.7307/ptt.v21i6.1025>

Management and Economic Performance of Sustainable Transport

Olga Shirokova^(✉)  and Lev Shirokov 

Moscow State University of Civil Engineering,
Yaroslavskoye Sh. 26, 129337 Moscow, Russia
shirokovaol@mgsu.ru

Abstract. The paper deals with management issues of the sustainable transport.

We distinguish two aspects of this problem: (1) direct energy use for transportation vehicles; (2) indirect resources costs. Is considered the problem of the sustainable transport as a logical continuation of the problem of sustainable development, initiated by the UN General Assembly. Constructed the model of interaction between the components for the road transport system and the environment. Constructed the criterial for the optimal management of the sustainable transport.

Keywords: Sustainable transport · Energy management · Road system Safety · The optimization criteria

1 Introduction

Energy management of municipal transport services and transport is one of the most important factors in successful modern and efficient development. For the transport of energy management at the system approach is characterized by two aspects. The first aspect is the direct energy consumption for transportation vehicles. The second aspect - is the indirect resource costs, which are determined by society. It is characterized by a number of additional components and inefficient management creates a negative impact, firstly, on the ecology of the environment, and secondly, leads to additional losses as a result of increased accidents and of road accident. Rehabilitation works requires large amounts of energy.

In the category of indirect resource costs is essential acquired issue of sustainable transport as a logical continuation of the problem of sustainable development, which was initiated by the UN General Assembly. The UN has recognized that today, environmental problems have become global, and their solution is important for the sustainable development of all countries. Built World Commission on Environment and Development (WCED) [1] was first convened by the UN in 1983. It formulated the concept of sustainable development as a process of economic and social change in which the exploitation of natural resources, investments, the orientation of technological development aimed at meeting human needs. In accordance with one of the basic principles set out by the Organisation for Economic Co-operation and Development (OECD) at the International Conference in Vancouver in 1996 [2], the

transport system must be designed and operated in such a way as to ensure the safety of all people, improving their quality of life [3].

According to the forecasts of experts of the UN in the absence of effective steps, road traffic injuries will become the fifth leading cause of death in the world. The total number of deaths and injuries resulting from road traffic accidents (RTA) will increase in the period from 2000 to 2020 by about 65% worldwide, and in low- and middle-income countries as a result of road accident deaths could rise to 80% [4, 5].

The aim of the article is to address issues of better governance for the sustainable transport with order to improve safety in the transportation systems on the example of road transport [6, 7]. The model of the interaction of components of the road transport system and the environment, as well as criteria for the optimal management of the sustainable transport.

2 Analysis of the Main Factors Determining Sustainable Transport

Factors determining the sustainable transport can be identified on the basis of consideration of operation of the system of motor vehicles.

The road transport system - a set of transport infrastructure, transport companies and management of systems. The road transport system provides a coordinated development and operation of all types of vehicles in order to meet the needs of road transport at the lowest cost. These include vehicles, drivers, architecture of motor systems, roads and pavements, traffic rules and inspection services, the external environment and its various components, including weather conditions. An analysis of the dynamics of movement in the motor transportation systems allows you to select various dual interacting subsystems: V - TC, TC - D, S - D, D - TC, TC - V and S - TC. Here D – road, TC - vehicle, V - driver, S - the external environment. Description of the properties of these interacting groups is given in [3].

Imagine the homogeneous set of elements that make up the transport system, in the form of a matrixes [8, 9].

The set, which determines the drivers, represent the matrix:

$$V = \left\| V_{ij} \right\|_{(M_v \times N_v)}, V_{ij} \in D_v \tag{1}$$

where V_{ij} - element of the matrix representing the i -th to the driver ($i = 1, \dots, M_v$) of its j -th attribute, i.e., j -th individual characteristics of the driver ($j = 1, \dots, N_v$), D_v – a set of entities such as the driver in a database system or a motor trucking companies.

The set representing the vehicles define the matrix:

$$A = \left\| A_{ij} \right\|_{(M_A \times N_A)}, A_{ij} \in D_A \tag{2}$$

where A_{ij} - element of the matrix representing for the i -th vehicle ($i = 1, \dots, M_A$) of its j -th attribute, i.e., j -th feature type and brand of the vehicle, ($j = 1, \dots, N_A$), D_A – a set of models entity types vehicle in the base trucking system data.

The set representing the main types of maneuvers a variety of vehicles, define the matrix

$$M = \left\| M_{ij} \right\|_{(M_M \times N_M)}, M_{ij} \in D_M \quad (3)$$

where M_{ij} - element of the matrix representing for the i -th maneuver ($i = 1, \dots, M_M$) of its j -th attribute, i.e., j -th characteristic of maneuver ($j = 1, \dots, N_M$), D_M – set of the vehicle maneuvers in the road transport system data base.

The set representing the various ways we define the matrix

$$D = \left\| D_{ij} \right\|_{(M_D \times N_D)}, D_{ij} \in D_D \quad (4)$$

where D_{ij} - element of the matrix representing for the i -th road ($i = 1, \dots, M_D$) of its j -th attribute, i.e., j -th characteristic of the road, ($j = 1, \dots, N_D$), D_D - set of entities type the road for the base of the road transport system data.

The set representing different types of environment, define the matrix

$$S = \left\| S_{ij} \right\|_{(M_S \times N_S)}, S_{ij} \in D_S \quad (5)$$

where S_{ij} - element of the matrix representing for the i -type of environment ($i = 1, \dots, M_S$) of its j -th attribute, i.e., j -th characteristic of this type of an environment, ($j = 1, \dots, N_S$), D_S – a set of entities environment species for the base of the road transport system data.

The set representing the road signs, we define the matrix:

$$Z = \left\| Z_{ij} \right\|_{(M_Z \times N_Z)}, Z_{ij} \in D_Z \quad (6)$$

where Z_{ij} - element of the matrix representing for the i -th mark ($i = 1, \dots, M_Z$) of its j -th attribute, i.e., j -th characteristic of this road sign ($j = 1, \dots, N_Z$), D_Z – set of entities such as road signs for the base of the road transport system data.

The corresponding generalized model of the interaction of the main components of the road transport system is shown in Fig. 1. Information support of the drivers is include automatic system of monitoring of road signs environmental parameters, satellite navigation [10, 11] and dispatching of [12].

Structural diagram of operation of of automotive engineering system creates the possibility of assessing and studying the various factors that determine the quality indicators of the functioning of the road transport system. In the design of the road transport system is necessary to determine tasks of forming matrix of roads D . It requires planning road network graph with all the standards of road safety, formulate requirements to the characteristics of the vehicles represented by the matrix A , planned for the projected road transport system. Modern vehicles speeds, flux densities necessitate automation of monitoring of road signs, certain matrix Z . In order to inform the driver about the parameters of the external environment, determined by matrix S , is required automation of measuring current environmental conditions. Demand are also on-board satellite navigation system.

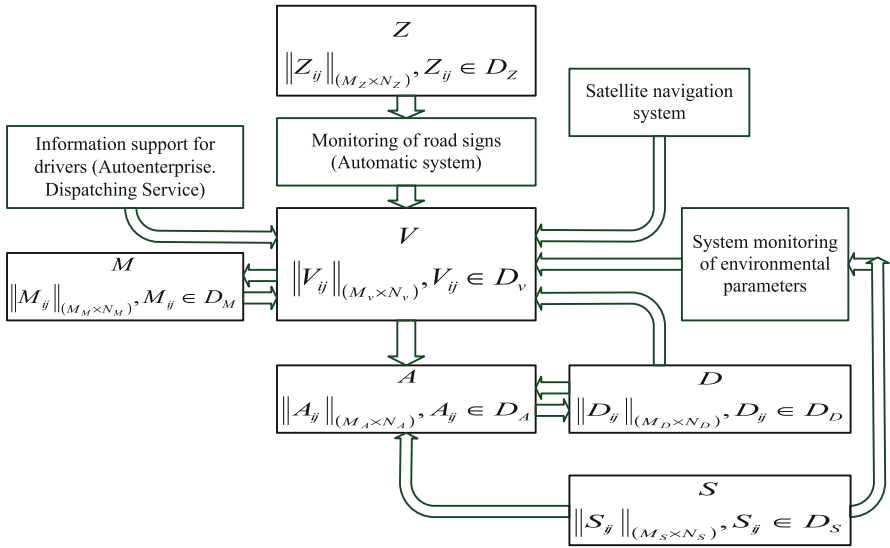


Fig. 1. The model of interaction of the basic components of the road transport system and the environment.

3 Formation of the Criterion for the Optimization Management of the Sustainable Transport

An important factor in optimizing management of the sustainable transport is a solution to the problems of investment projects for road surfaces, automatic and information systems to enhance safety in transport systems, etc. To this end, it is important first of all to consider criteria of optimization [13].

When investing road transportation systems the range of choice of security tools is very wide. These include rational planning transport areas, the construction of “speed bumps”, chicanes, bicycle paths, “security islands”, barriers, pedestrian zones. For highways important to plan the vertical curvature at the bends, the bulge in the cross section. Effective use of road designs that drapes to soften the blow. Most of the signs and road markings can be made retroreflective.

For on-board equipment vehicles are effective automatic systems. Thus, the use of emergency braking system reduces the braking distance by an average of 15–20%. Effective aid system when changing lanes, pedestrian detection system. The use of the detection system allows for a 20% reduction in pedestrian deaths in road accidents and by 30% reduce the risk of serious injury. New perspectives opens the application of information technologies and systems. For example, US developed a system which, along with automatic motorway network provides for control of vehicles on a highway using wireless communications.

To optimize the development of a security project effective use maximin approach at the formation of the optimization criterion. It is characterized by two factors, firstly, the need to ensure the best possible protection of people in an accident, reduce material

and financial losses, and secondly, it is important to complement the best security while minimizing the invested funds. To address the issue of assessing the effectiveness of different means, as well as on their cost to the project specifications require formulation of the of the third problem of the group efficiency selected means [14].

On the basis of the above for the formation of a generalized model of the criterion will present the above means of road safety in the following three groups: (1) road mounted a means of increasing safety (W_1); (2) automatic means of providing security onboard the vehicle (W_2); (3) information technologies and systems to improve security (W_3). Then the sum of the costs of equipment for road safety W_S can be represented as:

$$W_S = W_1 + W_2 + W_3 \quad (7)$$

Elements of (7) are respectively:

$$W_1 = \sum_{i=1}^{N_1} W_{1i} \quad (8)$$

– expenses for complex security tools at road and installation of security tools;

$$W_2 = \sum_{i=1}^{N_2} W_{2i} \quad (9)$$

– expenses for complex security tools for a group of automatic security tools on board the vehicle;

$$W_3 = \sum_{i=1}^{N_3} W_{3i} \quad (10)$$

– expenses for complex security tools for a group of information technology.

The task must be to maximize the safety of road users, ensure maximum safety for the people around them, as well as material values. On the other hand, due to the expenses for a set of security tools should be reduced losses that accompany a variety of accidents. The balance of these two factors [15, 16, 17] requires consideration and accounting at economic and mathematical modeling for the purpose of expenses optimization for safety in an integrated set of optimality criteria.

For the first two of the factors considered based from (8)–(10) can be written

$$W_S^{opt} = \max W_S(W_1, W_2, W_3, P), \quad (11)$$

where P - specified factor the stability of the security.

Factor the stability of the security P in (11) is defined as a vector:

$$P = (S_1, S_2)^T, \tag{12}$$

where the parameter S1 - coefficient of relative accident rate for long and geometrically homogeneous elements of road; S2 - coefficient of relative accident rate for short sections of roads with bridges, crossroads [18, 19].

The second factor losses from traffic accidents based on the a posteriori analysis of accidents in the operation of motor systems can be grouped into the following subsets: (1) loss on the fact of an accident (L1); (2) the expenses of the analysis of the accident and decisions taken (L2); (3) the expenses of further stages of the life cycle for the victims of the accident (L3). Then the amount of loss on an accident LS can be written as

$$L_S = L_1 + L_2 + L_3. \tag{13}$$

In relation (13):

$$L_1 = \sum_{i=1}^{N_1} L_{1i} \tag{14}$$

- loss from accident factors for L1i (i = 1, 2, ..., N1), which include damage to the various of technical facilities and surrounding objects, etc.;

$$L_2 = \sum_{i=1}^{N_2} L_{2i} \tag{15}$$

- expenses related to the accident L2i (i = 1, 2, ..., N2) in the investigation, for litigation, for insurance, etc.;

$$L_3 = \sum_{i=1}^{N_3} L_{3i} \tag{16}$$

- expenses related to the accident L3i (i = 1, 2, ..., N3) for the period of the loss of labor activity of road accident victims, the costs of medical care and treatment.

As a result of expenses at the road safety is natural to consider that the losses in case of accident should be minimized. In accordance with this second factor of economic-mathematical model, taking into account (14)–(16) can be written:

$$L_S^{opt} = \min L_S(L_1 + L_2 + L_3), \tag{17}$$

Based on the above it can be concluded that for the optimization of investing in the development of roads, automatic and information systems to improve traffic safety in road transport systems must take into account two factors. On the one hand, it is necessary to maximize the safety of road users and the expenses for the maximum

safety of other people and material values, and on the other is necessary to collateral damage in an accident will be minimized. Thus, the resulting integrated optimization criterion should be maximin structure. Elements maximin criterion will generate respectively the relations (11) and (17).

$$W_I = Q(\max W_S(W_1, W_2, W_3, P); \min L_S(L_1, L_2, L_3)) \quad (18)$$

In (18) Q - operator of maximin criterion.

Thus, maximin criteria (18) allows the best way to realize the opportunities discussed means of road safety planning project for investment road transport system.

4 Conclusion




The article analyzes the problems of the sustainable transport. Formed a model of the system operation of motor transport on the basis of the interconnected complex matrix arrays. This makes it possible to reveal problems in various areas of the safety of vehicles. Was formulated the task of optimal investment projects to develop advanced the road transport systems with the use of effective means of traffic safety. Was designed a maximin criterion to maximize the safety of designed systems while minimizing losses from the accident. Application the maximin criterion will allow the best way to realize the opportunities existing technical facilities to solve the problems of investment projects for road surfaces, automatic and information systems to enhance safety in transport systems.

References

1. Report of the World Commission on Environment and Development - Our Common Future
2. Towards Sustainable Transportation the Vancouver Conference. Conference organised by the OECD hosted by the Government of Canada Vancouver, British Columbia. Conference highlights and overview of ISSUES. 24–27 March 1996
3. Shirokov, L.A., Shirokova, O.L.: Simulation environment of industrial areas to optimize environmental investments. *Ecol. Urbanized Territories* **2**, 16–22 (2013)
4. Statistical database of the UN Economic Commission for Europe (UNECE)
5. Shirokov, L.A., Shirokova, O.L., Palaguta, K.A.: Investirovanie razrabotok dorozhno-montiruemykh sredstv, avtomaticheskikh i informatsionnykh sistem dlya povysheniya bezopasnosti dvizheniya v avtotransportnykh sistemakh [Investment of the development of road-build means, automatic and informational systems to increase traffic safety in vehicle systems]. In: *Vestnik MGSU [Proceedings of Moscow State University of Civil Engineering]*, vol. 9, pp. 130–145 (2015)
6. Wisniewski, A., Fattakhov, T.: Mortality from road accidents in Russia compared to other countries
7. World report on road traffic injury prevention. *WHO Bull.* **3** (2004)
8. Kremer, N.Sh. (ed.) *Higher Mathematics. UNITY*, 471 p. (2002)
9. Husak, A.A., et al.: *Handbook of higher mathematics. TetraSistems, Mn.*, 640 p. (1999)
10. Solovyov, Yu.A.: Satellite navigation and its applications. *Gyroscopy Navig.* **4**(43), 146 (2003)

11. Rozhkova, M.: Google Android with satellite navigation through Russia. *T-Comm: Telecommun. Transp.* **S4**, 36 (2009)
12. Ivashchenko, A.V., Peisakhovich, D.G.: Proactive scheduling resources 5pl transport operator. *Intell. Innov. Investments* **3**, 153–158 (2013)
13. Shirokov, L.A., Shirokova, O.L.: Packaging automation systems to the specifications of projects in the Internet. *Coll. automation of technological processes and engineering systems*, pp. 80–87 (2006)
14. Karlaftis, M.G., Golias, I.: Effects of road geometry and traffic volumes on rural roadway accident rates. *Accid. Anal.* (2002)
15. Roy, B.: *Multicriteria Methodology for Decision Aiding*. Kluwer Academic Publishers, Dordrecht (1996)
16. Hinloopen, E., Nijkamp, P.: Qualitative discrete multiple criteria choice analysis: the dominant regime method. *Qual. Quantity* **24** (1990)
17. Elvik, R.: *A Framework for a Rational Analysis of Road Safety Problems*. Institute of transport economics, Oslo, Norway (2005)
18. Bryce, J., Flintsch, G., Hall, R.: A multi criteria decision analysis technique for including environmental impacts in sustainable infrastructure management business practices. *Transp. Environ.* **32**, 435–445 (2014)
19. Koorosh, G., Maged, G.: Utilization of infrastructure gateway system (IGS) as a transportation infrastructure optimization tool. *Int. J. Traffic Transp. Eng.* **4**(1), 8–15 (2015)

The Risk-Based Approach to Rating the Competitiveness of Transport Enterprises in the System of Economic Security

Elena Karanina^(✉) , Olesya Ryazanova , and Alexander Timin 

Vyatka State University, Moscow str., 36, Kirov 610000, Russia
kafinanc@yandex.ru

Abstract. The article is dedicated to the applications of risk-based approach. This approach allows assessing the threats. It is necessary for the ranking of competitiveness of small enterprises in the sphere of transport in the system of economic security. The purpose of the study is to test the technique of estimating the level of competitiveness of small enterprises in the sphere of transport. The methodology is based on objective and clear criteria and indicators of potential and risk. Criteria and indicators provide the basis for the formation of integrated information-analytical system of management decisions in investment. Methods of research: economic analysis, integral analysis, averages, ranking, cluster analysis. In the first part of the article, the authors write about economic security of the territory and the role of transport companies in providing it. The second part of the article considers the methodology of research, the main threats to the operations of small enterprises in the sphere of transport and their indicators. In the third part of the paper, the authors present the results of the generated ranking of competitiveness of small enterprises in the sphere of transport in the system of economic security.

Keywords: Competitiveness of transport enterprises
Transport infrastructure · Economic security

1 Introduction

Regional interests are the basis of economic safety of the territory. These include the creation and maintenance of a worthy living standard of the population, the optimal use of accumulated economic potential, the implementation of socio-economic strategy of the region, balance and integrity in the financial system of the state. It is necessary to consider the importance of protection against different threats. Threats are internal and external. Internal threats exist in the region territory. External threats are related to economic policies of government and governments of other regions of the country, foreign countries. Balancing national interests is important.

The economic security of the territory is a constituent element of economic security of the region and the country. Territory is not only coherent socio-economic entity, but also part of the economic system and the subject of the Russian Federation. It is therefore important to balance the interests of the territory, region and national goals. Any area experiencing a powerful effect of national socio-economic trends. However,

the territory has its own unique problems for security. Problem site depends on its features (climate, natural resource endowments, structure of industries, and the national composition of the population). Territory free to decide how to use resources, develop trade, services, infrastructure etc. it is important to preserve a single economic space in the country. It is necessary to ensure the free movement of goods, raw materials, labor, and capital.

System of economic security of the region includes a large number of elements. It includes the following elements [1]:

1. The interests of the territory;
2. The identification of threats to economic security of the territory;
3. Threat assessment of the territory according to various criteria and indicators:
 - Socio-demographic indicators. They reflect the level and quality of life of the population of the territory;
 - Economic indicators. They reflect the ability of the territory's economy to develop;
 - indicators reflecting the situation of food security of the territory;
 - indicators of investment security (credit);
 - Financial indicators. They reflect the stability of the financial system of the territory;
4. Determination of threshold values of indicators and their comparison with the actual data. It is important to determine the critical value. They characterize the security zone of the territory;
5. Improving the territory's economic policy. Development of new effective mechanisms for prevention of threats to economic security of the territory;
6. The protection of economic safety of the territory.

The economic security of the territory is the ability of regional and local authorities to establish effective mechanisms. They ensure the competitiveness of the economy of the territory, the socio-economic stability and sustainable development of the territory. The competitiveness of the territory is a factor of economic security of the region. They can be considered as a system and as part of the system of economic security of the region. Russia's competitiveness and its growth at the present stage of development can take place through the creation of competition between the regions (territories). Thus, the issues of economic development and competitiveness of territories were critical for the country. The competitiveness of the territory is determined primarily by the competitiveness of companies and enterprises. Their result in the competition depends directly on the socio-economic conditions. They reflect the competitive environment. The competitiveness of the territory is characterized by the ability of local producers to exploit the economic potential of the territory. The territory does not have to own rich natural and economic resources.

The competitiveness of the region (territory) is subject to a large number of threats. The main threats are [2]:

- reduction of productivity;
- an increase in the degree of depreciation of fixed assets;

- the lack of private investment;
- the failure of the enterprises;
- the predominance of the extensive development path of the economy;
- The decline in industrial production.

Indicators mentioned threats could serve as follows (respectively):

- index of labor productivity, percentage;
- the level of depreciation of fixed assets, percentage;
- share of own investment, percentage;
- the share of unprofitable enterprises, percentage;
- gains in the number of high-performance workplaces;
- The index of industrial production (IIP), percentage.

In the system, threats to regional competitiveness, it is possible to carry out more detailed analysis of the factors. These factors are considered from the perspective of the investment security (credit) of economic entities of the territory.

The basis of economy of any area today is a small business [3].

Anti-sanctions continues. In these conditions the role and importance of small business in the sphere of transport increases.

2 Materials and Methods

The risk-based approach can be applied to assess threats. It is also used for the ranking of regional competitiveness of small enterprises in the sphere of transport in the system of economic security. The approach developed from the point of view of the territorial aspect. Monoprofile municipal education of the Kirov region considers as the territories.

11 single-industry municipal entities in Kirov region [4] function 1502 of commercial enterprises. Such a number obtained according to formal services (as of 31.12.2015) [5]. These companies belong to different legal forms. These businesses work and receive revenue. 97.07% of businesses are small businesses. Businesses are concentrated in the areas of manufacturing, wholesale and retail trade; the repair of motor vehicles, motorcycles, household goods and personal goods, construction and real estate transactions, rent and services, transportation and storage.

Industry and transport create a “circulatory” system of the country. They affect the economy. This facilitates the interaction of all entities. Transport caters to the needs of business and population in transportation of different cargoes and people. Transport brings together the regions and the country. It connects producers and consumers of goods, products and services. The market and market relations cannot work well without the transport companies. This is an important socio-economic importance for the territory of the state and society. Any disorders in the work of the enterprises of the transport sector can lead to serious negative consequences for the economic security of the territory (region, country).

In the single-industry municipal entities in Kirov region 72 of a small business entity to the transport sector work. They transport goods by specialized and

non-specialized vehicles, road freight transport. They organize regular local and suburban passenger transportation bus transport. They keep other, activities auxiliary to transport.

The risk-based approach to threat assessment and rankings of competitiveness of small enterprises in the sphere of transport in the system of economic security in territorial aspect involves assessing the creditworthiness of small businesses. The evaluation is performed because of objective and clear criteria and indicators of potential and risk. They provide the basis for the formation of integrated information-analytical system of management decision-making in lending and investing. This system needed by all businesses and other stakeholders.

The risk-based approach to threat assessment and rankings of competitiveness of small enterprises in the sphere of transport based on ad hoc indicators. They are calculated based on public data of the accounting (financial) reporting and information and analytical systems. This is a special paid service. They act as a tool to reduce commercial risk. Potential indicators are: return on sales (%), return on equity (%), average number of employees (persons), labour productivity (thousand rubles/person), investment activity (thousand rubles/person), the coefficient of concentration of own investment resources. These indicators denote by x_i . The risk indicators are index of solvency risk, the risk index reliability index scoring, the index of liquidity risk, credit risk, the coefficient of the financial lever. These indicators denote by y_i .

The mechanism of ranking the competitiveness of small enterprises in the sphere of transport in the system of economic security consists in partitioning the objects of study in the parameters of the potential and risk on clusters. Partitioning is the method of scoring. Integral index is defined to assess the competitiveness and ranking of the enterprises within the cluster. The methodology for the rankings of competitiveness of small enterprises in the sphere of transport in the system of economic security can be divided into five main stages:

1. the first stage is the collection of data on transport enterprises. Calculated the metrics. They reflect the efficiency, investment attractiveness for business owners, efficiency of labor, investment activity, and the concentration of private investment resources.
2. The system of risk indicators is formed in the second stage. The main risks of financial and economic activities of transport enterprises associated with the loss of solvency, liquidity, dependence on external sources of funding. The main risk factors [6]: solvency index, the index of reliability index scoring, index of liquidity, credit risk, financial risk (gearing ratio).
3. Processing of indicators is at the third stage. It includes specified pre-processing data if the value is missing or has an incorrect value. Further, all indicators are translated into a single standardized scale. Translation of indicators for businesses are based on formulas of linear scale (1, 2) [7].

$$x_{in}^H = \frac{x'_{in} - x_i^{\min}}{x_i^{\max} - x_i^{\min}} \cdot 99 + 1 \quad (1)$$

$$y_{jn}^H = 100 - \frac{y'_{jn} - y_j^{\min}}{y_j^{\max} - y_j^{\min}} \cdot 99 \tag{2}$$

For the indicator “average number of employees” is a conditional transfer. The result of this conversion, all the indicators become a single dimension (points) and uniform scale changes.

4. The fourth stage is built integral evaluation. It is based on the comparison of the generalized characteristics of the potential and generalized risk. The research objects are divided into clusters by the method of scoring. The integral indicator of assessment of creditworthiness is determined to rank the enterprises within the cluster.

$$X_n = \frac{x_{1n}^H + x_{2n}^H + x_{3n}^H + x_{4n}^H + x_{5n}^H + x_{6n}^H}{6} \tag{3}$$

$$Y_n = \frac{y_{1n}^H + y_{2n}^H + \dots + y_{6n}^H}{6} \tag{4}$$

$$I_n = \sqrt{X_n \times Y_n} \tag{3}$$

It is necessary to assess the purity and correctness of the scoring. A comparative evaluation is carried out by the methods of ward and K-means. This allows us to estimate the coincidence of clusters.

5. On the fifth stage assesses the risk of competitiveness of small businesses to the transport sector. Stakeholders relevant management decisions are taken.

Clusters are formed based on the allocation of four types of potential and three for the level of risk (Table 1).

Table 1. Types of clusters.

Cluster	Feature
1 cluster	High potential-low risk
2 cluster	High potential-moderate risk
3 cluster	High potential-high risk
4 cluster	Moderate potential-low risk
5 cluster	Moderate potential-moderate risk
6 cluster	Moderate potential-high risk
7 cluster	Low potential-low risk
8 cluster	Reduced potential-moderate risk
9 cluster	Reduced potential-high risk
10 cluster	Low potential-low risk
11 cluster	Low potential-moderate risk
12 cluster	Low potential-high risk

Actually part of clusters in practice, may not be formed. The company can not operate successfully with high potential and high risk.

3 Results

The data obtained in Table 2 showed that 31.94% of enterprises refers to the 7th cluster (low potential-low risk) of 29.17% - 8 cluster (moderate potential-moderate risk), 12.50% - 5 cluster (moderate potential-moderate risk).

Table 2. Distribution of subjects of small business in the sphere of transport across clusters in the context of the territories of the Kirov region by the method of scoring units.

Single-industry municipality	Clusters												Total
	1	2	3	4	5	6	7	8	9	10	11	12	
The city of White Kholunitsa	0	0	0	0	1	0	0	2	1	0	1	0	5
The city of Vyatskie Polyany	1	0	0	1	0	1	2	6	2	0	0	0	13
The city of Kirovo-Chepetsk	0	1	0	2	4	0	15	8	1	0	1	0	32
The city of Kirs	0	0	0	0	0	0	0	1	1	0	0	0	2
The town of Luza	0	1	0	0	1	0	0	1	0	0	0	0	3
The city of Omutninsk	0	0	0	0	0	0	3	2	2	0	0	1	8
The city of Urzhum	0	0	0	0	2	0	0	0	0	0	1	1	4
The urban-type settlement of Lokot	0	0	0	0	0	0	1	0	0	0	0	0	1
An urban-type settlement of Krasnaya Polyana	0	0	0	0	0	0	2	1	0	0	0	0	3
An urban-type settlement Murygino	0	0	0	0	0	0	0	0	0	0	0	0	0
Urban village Swifts	0	0	0	0	1	0	0	0	0	0	0	0	1
Total	1	2	0	3	9	1	23	21	7	0	3	2	72
Proportion of clusters %	1.39	2.78	0.00	4.17	12.5	1.39	31.9	29.2	9.72	0.00	4.17	2.78	100

Thus, more than 70% of small businesses to the transport sector of montererry Kirov region have moderate or low capacity low or moderate level of investment risk. Investment of the companies in the clusters is possible. Additional financial resources will enable the business entities to strengthen their capacity and increase business efficiency. Of 2.78% of the enterprises belong to cluster 12 (low potential-high risk) - interest and the level of confidence in these companies should be the smallest. Three companies (or 4.17%) belong to cluster 11 (low potential-moderate risk). Lending (investing) of such enterprises is possible, but must comply with certain conditions and limitations.

Single entity (1.39%) were included in cluster 1. The company timely and completely fulfill their obligations based on high investment potential and efficient operation. To the enterprise of the first cluster belongs LLC “Spetstrans”. It is located in the town of Vyatskie Polyany.

Key indicators of threats to enterprises of the transport act:

- low productivity (41.67% of enterprises employees do not produce minimal income for the business);
- high level of depreciation of fixed assets (low productivity and low profitability of enterprises, disruptions in the transportation system of the region, high level of accidents);
- low share of private investment (businesses transportation need external investment for their development);
- the share of unprofitable enterprises (about one-third (31.94%) of the studied enterprises were unprofitable).

4 Discussion

Transport infrastructure is insufficiently developed in the Kirov region. Enterprise transport will operate at a low efficiency. This seriously restrains the further development of the region, affects the mobility of the population. This reduces its effective employment activity. The study of the potential and risk of transport enterprises gives an estimate of the real situation and the economic security of the territory and the region. By conducting, the rating assessment of the government and municipal authorities will be able to send the necessary forces and means for the economic development of the territory (region). It will provide employment. This will ensure economic growth in General. Investors (creditors) will be able to conduct a preliminary examination of the projects in the enterprises of transport. Their interest is in a high rate of return from investments (minimum risk of capital loss), the balance of the investment (credit) portfolio. The company will satisfy with the help of advanced small business in transportation socially important issues.

5 Conclusions




Thus, capital inflows to the region determined by competitive opportunities of the Russian Federation and prospects of their capacity. Venture capital moves into those areas and areas that provide competitive advantages in the organization of profitable business. The underdevelopment of transport enterprises leads to substantial losses in the region's economy. Each region should assess their threats, and competitive position. They are evaluated on the basis of indicators of capacity and risk. The rankings of enterprises and territories contributes to the attraction of the region in financial resources. This will strengthen the economic security of the territory.

Acknowledgments. The reported study was funded by RFBR according to the research project №17-02-00179.

References

1. Makhanko, G.: Sci. J. Kuban State Agrarian Univ. **105**(01), 236–251 (2015)
2. Karanina, E.: Economic security: state, region, enterprise. Kirov, FGBOU VO “Vyatgu”, 389 p. (2016)
3. The government of the Kirov region. <http://www.ako.kirov.ru>. Accessed 04 Dec 2016
4. The order of the Government of the Russian Federation of 29.07.2014 N 1398-R (edition of 13.05.2016) On approval of the list of monoprofile municipal formations of the Russian Federation (monotowns)
5. Federal state statistics service. <http://kirovstat.gks.ru/>. Accessed 04 Apr 2017
6. Information-analytical system Globas-i. Credinform. <http://www.credinform.ru/ru-RU/globas>. Accessed 01 June 2017
7. Electronic textbook on statistics StatSoft. Cluster analysis. <http://statsoft.ru/home/textbook/default.htm>. Accessed 24 May 2017

Methodological Approach to the Pricing of Construction Investment Projects for Road Construction in the Context of Sustainable Development

Khuta Gumba¹  and Svetlana Uvarova²  

¹ Moscow State University of Civil Engineering,
26, Yaroslavskoye shosse, Moscow 129337, Russia

² Voronezh State Technical University,
Moscovskiy prospect, 14, Voronezh 394026, Russia
uvarova_s.s@mail.ru

Abstract. On the basis of a sound planning and cost determination of construction investment projects for sustainable development of road construction industry, the article suggests a methodological approach to the pricing through the resource approach. The methodology for determining the cost of engineering surveys and road design on the basis of enlarged standards is developed, that will be in demand at the stage of planning and appraisal the development of the road network in the regions. The pricing elements of design and protective archaeological work cost during the construction of highways are figured out. The article provides prospects to implement the suggested methodological approach with the focus on to improve the efficiency and quality of the investment projects for road construction.

Keywords: Road construction · Transport infrastructure · Investment project

1 Introduction

Currently, there is no clearly defined regulatory framework and practice of comprehensive assessment of the cost of investment projects. The state of pricing as well as the budget standard basis, the persisting backlog in the regulatory allocation of the resource cost from their creation and use, which hinders the innovations, are one of the obstacles to sustainable innovative development of the investment and construction complex. There is no mechanism to unite the efforts of the authorities and business in the field of budget valuation [1]. To date, there is a need to improve existing methodological materials to assess the cost of investment projects, taking into account the practical experience of application, as well as changes in economic conditions and legislative framework. The specifics of financing projects on the basis of concession agreements, involving private and foreign capital, are not reflected in the existing developments. A new methodology is required to estimate the cost of large investment projects, financed generally by public funds. It is due to the lack of system pricing rules that one of the most important market mechanisms “price-quality-competition” does not work,

which stimulates innovative activity and provides market motivation to improve the quality of construction products and reduce construction costs. Current pricing system motivates price dynamics with obsolete expensive technologies [2].

One of the most important problem at all stages of the investment cycle is the predictive appraisal of the construction estimate. In terms of the state-run economy, various types of consolidated estimate norms and standards were used such as price lists, consolidated indices of construction cost (CICC), consolidated cost estimate norms (CCEN), and others. In conditions of the development of a market economy, such norms are not sufficient, in addition, the development of consolidated cost estimate norms on a new price level, that correspond to the changes in the economy, engineering and construction technology, requires new methodological approaches [3]. Otherwise, the accuracy of calculations to justify the economic efficiency of investment projects, costs, contract prices and other parameters become too low, while economic and other risks increase significantly.

2 Materials and Methods

Assessing the cost of design and survey, protective archaeological and construction and installation work at various stages of the life cycle of the project is proposed to be carried out in three ways:

- resource method, by developing resource-technological models with allowance for correction and transition coefficients;
- on the basis of the determination of labor efforts (for design, survey and security archaeological work);
- on the basis of consolidated norms, by aggregating the existing prices taking into account inflation rate [4].

A methodology for estimating the cost of design and survey works was suggested in order to improve the pricing system at the design development stage. It is based on the methodology for appraisal of engineering surveys for the construction and reconstruction of highways and structures on them. It also led to creation of a regulatory document of the Federal Road Agency “Rosavtodor”, Methodical recommendations for the cost estimation of design works for the construction (reconstruction) of highways and artificial buildings on them [5]. The main provisions of the methodology can be implemented in appraisal of survey and design work for any type of construction projects as well as in the formation of the starting price of the contract tenders.

The function of the engineering survey cost, performed at the facility, is the following:

$$C = f(Z_i, V_i, U, K_c, F_i) \quad (1)$$

where C_i - the survey cost at the facility; Z_i - expenses for the survey production; V_i - type of required surveys; U - conditions of performance of work; K_c - pricing factors; F_i - factors that complicate the survey production at the facility.

Calculation of the estimated cost of engineering survey of roads is suggested to be carried out through processing statistical information on projects carried out by the design and survey organization. Due to the lack of separate cost accounting for objects of various types of surveys, an algorithm for selecting representative objects has been developed in order to bring the statistical data to a uniform dimension and determine the types of survey costs. The algorithm includes a correlation-regression analysis of survey projects for conducting an analytical grouping of the objects under consideration and excluding the objects with an overestimated or undervalued cost. Correlation analysis allows to identify the main parameters of objects that affect the engineering survey cost, and set the degree of credibility for the choice of representative objects.

Calculation of the engineering survey cost of 1 km of the road formally involves the processing of information about the expenditures of design and survey organizations. Thus, material expenditures are calculated using the correlation and statistical analysis of the data of the balance lists on the credit turnover in quantitative terms. As a result, a list of the basic pricing materials is formed, as well as the criterion for the rest materials (as a percentage of the value of the main materials). Labor costs are determined by analyzing the payroll fund, duty regulations of employees of design and survey organizations, labor standards, as well as the results of expert assessment of working hours depending of the worker profile [6].

In passing from the survey and design cost of 1 formal kilometer to the real conditions for the survey production, there were used dependencies, that have been figured out within the cost analysis of the actually fulfilled projects (Figs. 1 and 2). Thus, the dependence of the design price for 1 km of the road on the length of the section is shown in Fig. 1.

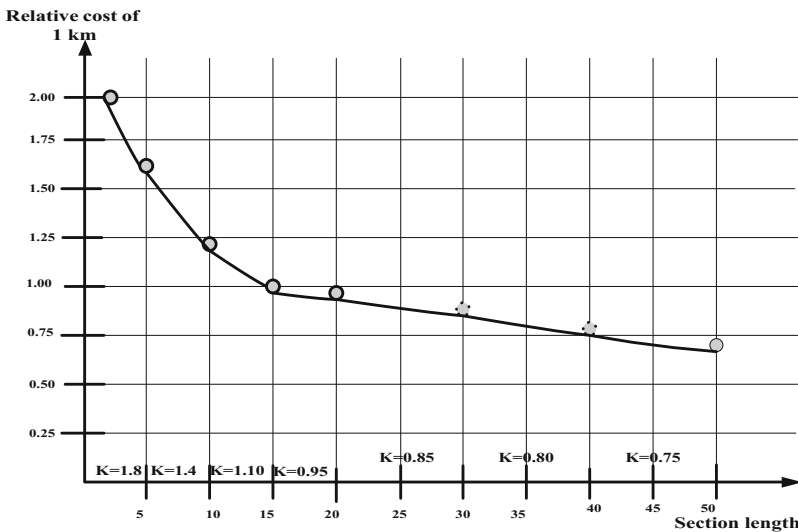


Fig. 1. Dependence of the design cost of 1 km of the road on the section length (for all categories of design complexity)

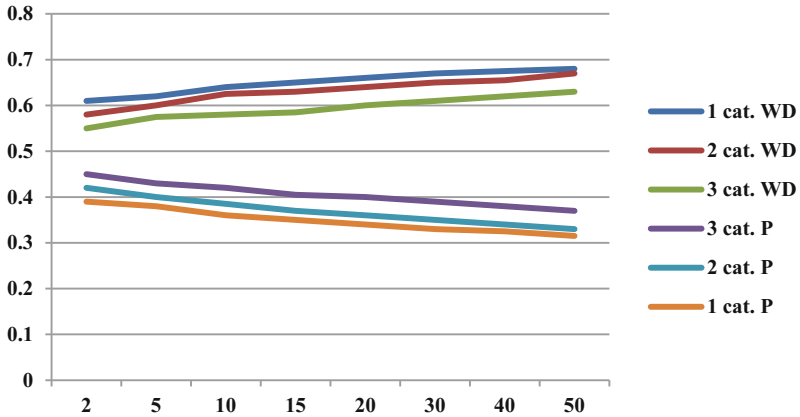


Fig. 2. Dependence of the share in cost at the design stage on the section length (by road category).

3 Results

Due to differences in the stages of surveys, the total cost can be divided into two components: constant and variable. Survey cost is suggested to be determined by the formula:

$$C = \sum_{j=1}^v (a_j + b_j x_j) \quad (2)$$

A constant component of the engineering survey cost of each type includes the cost of the main part of the preparatory and cameral stages. This value is constant relative to the number of kilometers of the road (m² for bridge) that are being surveyed.

The value “b” is a variable component of the cost of the field, preparatory and cameral stages of each type of survey.

Each of the elements of “a” and “b” includes wages with deductions to non-budget funds, the cost of necessary materials, depreciation of equipment, as well as other expenditures, overhead charges and estimated profit.

Calculating the engineering survey costs, pricing and complicating coefficients are taken into account in addition to the basic value.

The flowchart of the algorithm for determining the design and survey cost on the basis of labor efforts is shown in general terms in Fig. 3.

where C_i is the cost of surveys at the facility; Z_i - expenses for the surveys; V_i - type of the required surveys; U - conditions of work performance; K_c - pricing factors; F_i - factors complicating the production of surveys at the facility, O_i - the total of the facility representatives for the i -th type of the design and survey work, Z_w - labor costs for conducting the i -th type of the design and survey work, O_r - the number of main categories of workers engaged in design or survey of the roads; Z_r - labor costs, worker - w., C_{ki} - value, 1 worker - w., Z_m - the amount of material expenses for the

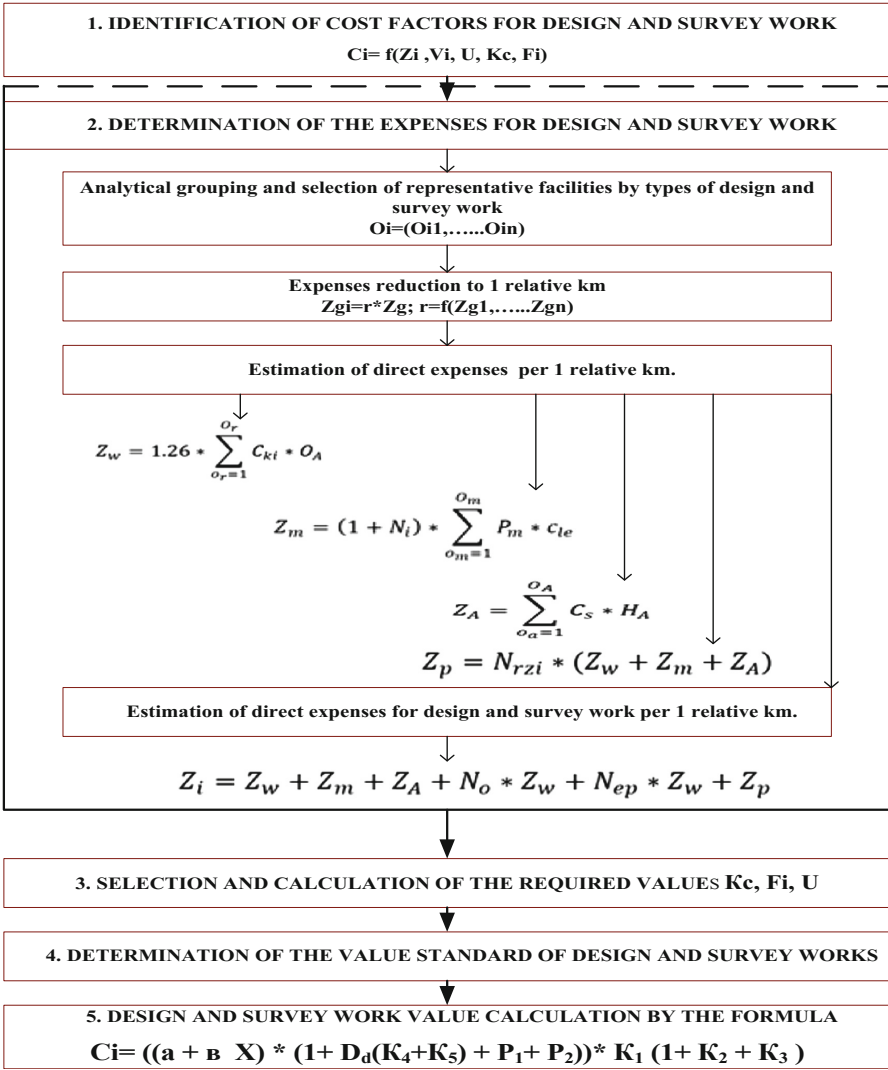


Fig. 3. Flowchart of the algorithm for determining the cost of design and survey works

design or survey work of i-type; O_m - number of the item groups of basic materials; C_{li} - the current price of a unit of material, P_m - the expense of the lth material, N_i - the standard of the cost of other materials (on average, 18–22%); O_A - the number of groups of depreciable assets; C_s - the book value of the property; H_a - the depreciation rate; Z_A - depreciation expenses, Z_p - other expenses for designing or survey work of i-type, N_{rzi} - the standard of other costs (on average, in fact, it is 20–25%), N_o - the standard of the overhead charges, N_{ep} - the normative of the estimated profit in the design or the survey work conduction of the i-type.

The survey cost is calculated by the formula:

$$C_i = ((a + B \cdot X) \cdot (1 + D_d \cdot (K_4 + K_5) + P_1 + P_2)) \cdot K_1 \cdot (1 + K_2 + K_3) \quad (3)$$

where D_d is the relative density of the payroll budget of the survey cost per 1 km of the road (taken to be equal to 0.35).

Calculating the engineering survey costs, pricing and complicating coefficients are considered.

The pricing factors include coefficients that take into account expenditures for external transport, as well as business trips. Amendments P_1 and P_2 are expressed in monetary units and are determined according to the methodology given in [7, 8].

When determining the engineering survey costs, the following coefficients are suggested: K_1 - locality pay rate; K_2 - coefficient for engineering surveys in desert and waterless areas; K_3 - coefficient for engineering surveys in unfavorable climatic conditions; K_4 - the change in the amount of overhead charges; K_5 - the change in the estimated profit; K_6 - adjustment for the inflation rate. Determination of the adjustment factors characterizing the influence of factors, which sophisticate the engineering surveys at the facility, was carried out using the economic statistical approaches - groupings, the mean value calculation, correlation-regression analysis of design organizations - and the coefficients that are used in the reference book of benchmark prices.

The K_1 coefficient is calculated as follows:

$$K_1 = D_{di} \frac{\overline{Z_w - J_s}}{Z_w} + \sum D_z \cdot Y \quad (4)$$

where D_{di} is the relative density of the payroll budget of the survey cost per 1 km of the road (taken to be equal to 0.35); $\overline{Z_w - J_s}$ - average salary of a survey engineer in the region plus bonus paid in the regions of the Extreme North and equated with them; Z_w - average salary in the region of a survey engineer in the basic area (Moscow region); D_z - the share of expenses for individual items of expenditures in the structure of the survey cost; Y - the price index for the i -th type of resource in the analyzed region in comparison with the basic one.

The coefficients K_2 and K_3 are determined by the correlation-regression analysis of their values in the reference book of benchmark prices.

Furthermore, different coefficients can be applied to the cost, that was determined by the formula (3), during the certain types of survey work.

It is possible to avoid the need to consider and determine the correction factors at the development stage of the price norms (a , b), in case the processing data is submitted by a particular design organization.

4 Discussion

Practical implementation of the suggested methodology will allow:

- to determine objectively the design and survey cost by all participants of the construction investment project,
- to estimate the initial price of the design and survey work, appraise the price changes, examine the projects more accurately, with the possibility of accounting for innovative technologies,
- to create a data bank for value of the resources and work specifics in order to keep the estimates updated.

Similarly, it was suggested to determine the design work cost.

The analysis of resource-technology models of the cost for design and survey and protective archaeological work showed that the largest share in the work expenditures falls at labor costs (more than 35% industry average). Therefore, it is considered to be viable to plan and assess the expenses of these works on the basis of labor costs [9, 10].

5 Conclusions

In order to optimize the cost parameters of investment projects, a gradual transition from index methods for calculating the project cost to resource ones is required along with the creation of a monitoring system over the current prices for representative

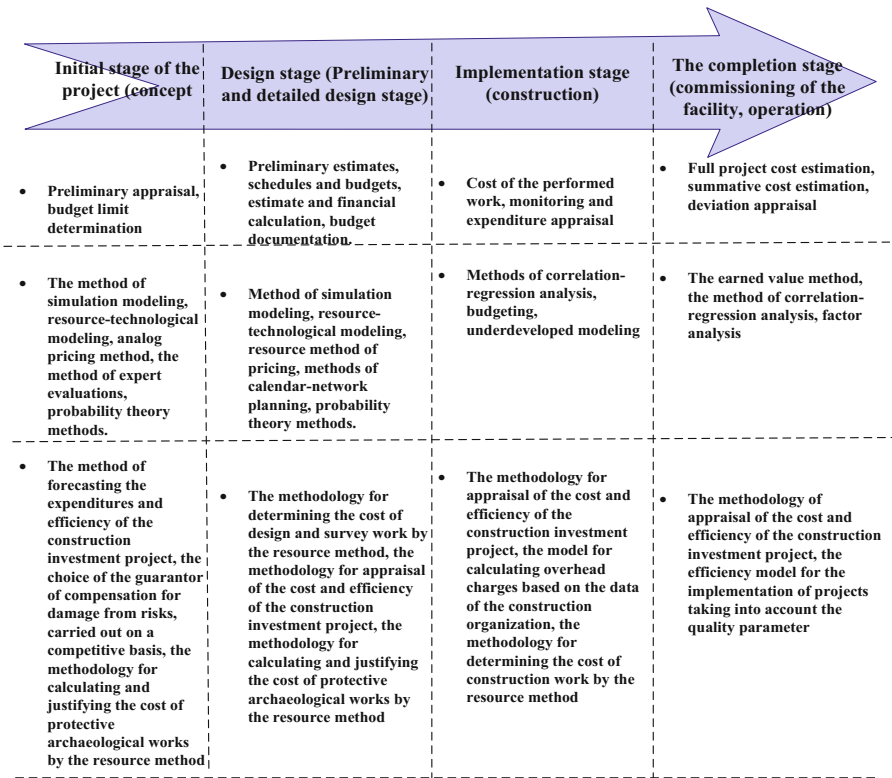


Fig. 4. Methodological approach to pricing of construction investment projects

resources for the project participants. Furthermore, modern information technologies should be implemented to determine prices for construction products and improve the accuracy of estimates at all stages of the investment process. Nevertheless, creation of the resource-technology models to plan the investment volume is vital to cross the budget planning cycle boundaries, what becomes feasible in long-term concession projects.

The corresponding methodological approach to the pricing of construction investment projects (Fig. 4), implemented as a system of interrelated methods, models and algorithms, that is based on the application of a number of methods, contributes to the accuracy increase and integrity of cost calculations at all stages of the project. The choice of the resource method of pricing as a basis of the methodological approach is due to the need for a dynamic adaptation in the estimate and regulatory environment when the technology of working process changes. It also helps to take into account the interests of owners when implementing PPP projects.

Formation of modern standards of pricing, that adequately reflect the real processes of preparation and implementation of the construction investment project, will allow to determine project's efficiency more accurately, competently and reasonably choose a private investor in order to ensure the high quality of infrastructure facilities.

References

1. Belyantseva, O., Uvarova, S.: *Sovremennaya economica: problem i resheniya* **6**, 55–61 (2014)
2. Uvarova, S.: *Vestnik MGSU* **6**, 219–223 (2011)
3. Cataldo, A., Ferrer, J.: *Eur. J. Oper. Res.* **259**(2), 766–777 (2017)
4. Shrestha, K., Shrestha, P.: *Procedia Eng.* **145**, 128–135 (2016)
5. Silka, D., Urazova, K.: *Bull. MGSU* **8**, 171–185 (2015)
6. Tyukova, S.: *Herald ENGECON. Ser. Econ.* **1281**, 96–100 (2009)
7. Larionov, A., Nezhnikova, E.: *Int. J. Appl. Eng. Res.* **6**(11), 4433–4439 (2016)
8. Isaev, S.A., Baranov, P.A., Vatin, N.I., Zhukova, Y.V., Sudakov, A.G.: *Tech. Phys. Lett.* **40**(8), 653–656 (2014)
9. Strelets, K., Vatin, N.: *Rocznik Ochrona Srodowiska* **17**(1), 104–112 (2015)
10. Aggogeri, F., Borboni, A., Merlo, A., Pellegrini, N., Ricatto, R.: Real-time performance of mechatronic PZT module using active vibration feedback control. *Sensors*. **16**(10), article no. 1577 (2016). Switzerland

Sea Transport of the Kamchatka Region: The Analysis, Tendencies and Mechanism of the Effective Development

Tatyana Miroshnikova¹  and Natalia Taskaeva²  

¹ Vladivostok State University of Economy and Service,

Gogolya str., 41, 690014 Vladivostok, Russia

² Moscow State University of Civil Engineering,

Yaroslavskoye Shosse, 26, 129337 Moscow, Russia

natalia.taskaeva@yandex.ru

Abstract. The article deals with the problem of the negative impact of deterioration of the material and technical base of the marine transport fleet of the Kamchatka region for its implementation as a strategically important subject of the Russian Federation. The research methodology involves, in its turn, the use of the historical data and the analysis of different informational sources. Methodology of the content analysis is based on the four types of analysis: vertical, horizontal, comparative and retrospective. The study used an analytical method for the processing of statistical and corporation documentation. The article provides an analysis of the ship calls, quantity and age of the fleet operating in the transport direction in the Kamchatka and carried out an analytical review of the status and trends of marine transport. Based on the research, the Kamchatka region, due to its geographical position, has a high and imperfectly used transport potential. As a solution to the government, it is considered to ensure the relevance of updating and maintenance of maritime vessels, its more appropriate way of functioning.

1 Introduction

One of the most urgent tasks of state regulation of the Russian economy is the equalization of economic conditions for the development of federal regions. In turn, the geographical remoteness of individual regions requires a special mechanism for managing the regional economy. The Far East is a kind of outpost for turning the vector of state attention towards the Asia-Pacific region. The most significant factors are the economic-geographic location, large reserves of natural resources, the presence of an extended sea coast and the outer border as an opportunity for socio-economic cooperation.

Sea transport has a significant impact on the development of the subjects of the Russian Federation, the achievement of geopolitical, economic and social goals. Russia's promising plans for the restoration and construction of port infrastructure directly affect the Kamchatka maritime transport system.

The issue of the formation of an effective mechanism for ensuring the reproduction and development of maritime transport is not adequately represented in regional strategies and targeted programs. Thus, the goal of the study is to identify problem areas in the maritime transport of the Kamchatka Krai by analytical research and develop ways of its effective development.

There are some analysis that were performed during the research:

- historical overview of the sea transport of the region;
- horizontal analysis of the shipping flow in cabotage navigation and ship calls under the Russian flag;
- analysis of the quantitative and age composition of the fleet operating in the Kamchatka direction;
- analytical review of the state and development trends of Kamchatka Krai sea transport;
- analysis of the degree of depreciation of fixed assets in the marine fleet;
- development of potential on the formation of a mechanism for the modernization of transport.

Realization of this potential can give a new impetus to the development of the economy of the Kamchatka Krai. The possible way to solve the problem of the proposal is modernization of the port infrastructure, with the establishment of border crossing points to ensure international transport communications, as well as the creation of a modern transport system in the Arctic zone of the Far East and the transport use of the Northern Sea Route. Kamchatka Krai, through the development of port facilities and the creation of a transport bunkering center, can act as a strategically important subject of the Russian Federation. The realization of effective reproduction of the Kamchatka sea transport infrastructure in the conditions of the development of the processes of federalism, regionalization and international cooperation in the economic space of the Kamchatka Territory will provide an impetus to the development of the regional economy and the realization of the potential of the region in order to meet the economic needs of the region.

2 State-of-the-Art Review

The main part of the flow of goods in Kamchatka belongs to maritime transport and seaports, which provide about 83% of the total freight turnover. In Kamchatka, the main transport hub is the Petropavlovsk-Kamchatsky seaport with a cargo turnover of about 1 million tons of cargo per year, which includes 13 port terminals on the west and east coast of Kamchatka. In 2009 the cargo turnover of the seaport of Petropavlovsk-Kamchatsky was 1030 thousand tons, in 2010–1162.7 thousand tons, in 2011–1063.9 thousand tons [1] Table 1. Sea transport carries out transportation of all types of food, material and technical supplies, fuel. The boundaries of the seaport of Petropavlovsk-Kamchatsky include terminals located in port stations on the coast of the Kamchatka Peninsula. The enterprises of sea transport are the most important link in the transport complex of the Kamchatka Territory. They overload about 300 thousand tons of fish products and more than 350 thousand tons of export-import cargoes per year.

Table 1. Cargo turnover of the seaport of Petropavlovsk-Kamchatsky.

Year	2009	2010	2011	2012	2013	2014	2015
Goods turnover	1030	162.7	1063.9	1208	1194.1	1146.9	987.4

The main part of the flow of goods in Kamchatka belongs to maritime transport and seaports, which provide about 83% of the total freight turnover. In Kamchatka, the main transport hub is the Petropavlovsk-Kamchatsky seaport with a cargo turnover of about 1 million tons of cargo per year, which includes 13 port terminals on the west and east coast of Kamchatka. In 2009, the cargo turnover of the seaport of Petropavlovsk-Kamchatsky was 1030 thousand tons, in 2010–1162.7 thousand tons, in 2011–1063,9 thousand tons [2] Table 1. Sea transport carries out transportation of all types of food, material and technical supplies, fuel. The boundaries of the seaport of Petropavlovsk-Kamchatsky include terminals located in port stations on the coast of the Kamchatka Peninsula. The enterprises of sea transport are the most important link in the transport complex of the Kamchatka Territory. They overload about 300 thousand tons of fish products and more than 350 thousand tons of export-import cargoes per year [3].

Petropavlovsk-Kamchatsky sea commercial port occupies a leading position among economic entities that carry out cargo handling activities in the seaport of Petropavlovsk-Kamchatsky. The largest shipping company in the Kamchatka Territory is Kamchatka Shipping Company (CASCO), which has 4 sea-going vessels with a total deadweight of about 40.000 tons. According to the information-analytical magazine “Marine Fleet”, the company “CASCO” has transferred to the joint activity of the company “Pacific Shipping” six ships. In 2010, the company was established LLC “North-Eastern Shipping Company” and Closed joint-stock company CJSC “Petropavlovsk-Kamchatka Shipping Company”.

Despite the general adaptation of transport to market conditions, the state of the transport system at present cannot be considered optimal, and the level of its development is sufficient.

The current situation with the state of maritime transport presupposes the need to revive the maritime transport of the region. The level of freight turnover is inferior to those of the Soviet period, which is associated with a high degree of depreciation of the fleet. The decline in overall economic activity in the country and in the province, as well as the reorientation of a significant part of external cargo flows to foreign ports, reduced the volumes of freight traffic. In view of the remoteness of Petropavlovsk - Kamchatsky there is a problem of underdevelopment of infrastructure facilities and the costly nature of transportation. The freight turnover of transport has unstable dynamics. In 2012 the volume of transported cargoes by sea transport decreases from 712.7 thousand tons to 640.8 thousand tons [4]. In 2013 610.5 thousand tons of cargo were transported, in 2014 - 541.6 thousand tons of cargo, which indicates a negative dynamics of freight traffic. Goods turnover volume in 2015 made 987.4 thousand tons (–13.9% to a similar index of 2014). The analysis shows that in recent years the cargo turnover of the Port has remained at a level slightly exceeding 1 million tons. The dynamics of cargo turnover at the berths of the port is graphically illustrated in Fig. 1.

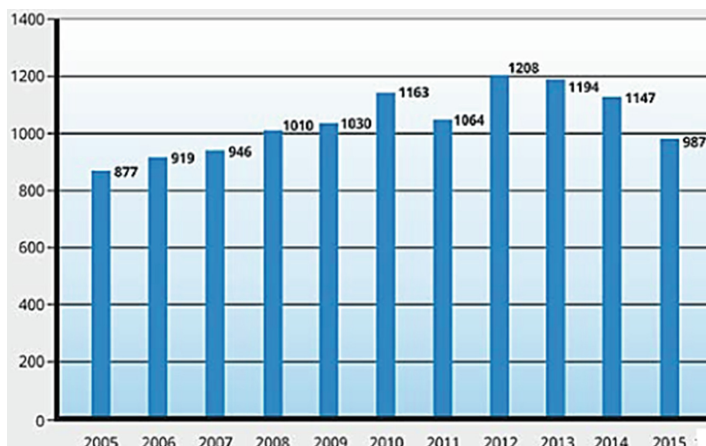


Fig. 1. Dynamics of cargo turnover at the berths of the port [9].

The indicators of the fleet handling in the port indicate the quantitative composition of the transport vessels that enter the bay territory. In 2008 the port handled 222 vessels. The average loading of the vessel was 4556 tons, the employment of the quay wall in the calendar period was 65.5%. (Including under cargo operations - 25.9%). In 2009 the port handled 211 vessels. Occupancy of the quay wall for the calendar period was 54.4% (including under cargo operations - 22.8%). The main areas of coastal cargo: Vladivostok, Vanino, Vostochny. In 2010, 262 vessels were handled at the berths of the port, of which 250 ships were ahead of schedule. Employment of the quay wall for the calendar period was 39.3% (including under cargo operations - 23.9%). The geography of coastal cargo flows traditionally includes the Vladivostok, Sakhalin directions. Carriage of coal was carried out in 2010 from the ports of Sakhalin. In 2011 246 vessels were handled at the port, 229 of them ahead of schedule. The employment of the quay wall for the calendar period was 53.4%.

In 2012 267 vessels were handled at the port, of them 244 ships ahead of schedule. The employment of the quay wall in the calendar period was 50.8% [5].

In 2013 265 vessels were handled. In 2014 the port handled 215 vessels, of which 208 ships were ahead of schedule. The employment of the quay wall for the calendar period was 32.7%.

In 2014 the port handled 215 vessels, of which 208 ships were ahead of schedule. The average loading of the vessel was 5334 tons, while the berthing wall occupied 32.7% (including 22.6% for cargo operations).

In 2015 235 vessels were handled at the port, 232 of them ahead of schedule. The average load of the vessel was 5774 tons.

The number of vessels processed by JSC “Petropavlovsk-Kamchatsky sea trading port” in 2009–2015 is shown in Fig. 2.

Analysis of dynamic changes in the number of vessels processed by JSC “Petropavlovsk-Kamchatsky sea commercial port” confirms the unstable dynamics in

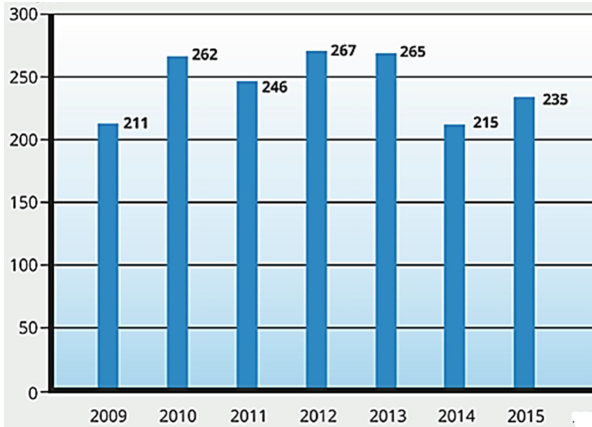


Fig. 2. Number of vessels processed in 2009-2015 JSC “Petropavlovsk-Kamchatsky sea trading port” [9].

the period 2008–2014. There is no stable growth in the indicator. The average annual number of vessels processed is 233 vessels during the period under review.

Table 2 present the main trends in fleet processing indices.

Table 2. Indicators of fleet processing in 2008–2015 JSC “Petropavlovsk-Kamchatsky sea trading port”.

Indicators	2011	%% 2011/2010	2012	%% 2012/2011	2013	2014	%% 2014/2013	2015	%% 2015/2014
Number of processed tons, kt.	1064.0	91.5	1207.6	113.5	11941	1146.9	96.0	987.4	86.1
Number of vessels processed, units	246	93.9	267	108.5	265	215	81.1	235	109.3
The result of the processing of vessels: in time, units	17	242.9	23	135.5	14	7	50.0	3	42.9
Ahead of time, units	229	89.8	244	106.6	251	208	82.9	232	111.5
Non-productive downtimes on port, ships/days	2.06	11.1	1.71	83.0	0.4	2.2	-	8.5	3.86 times
Occupancy of the wharf wall%	53.4	135.9	50.8	95.1	40.1	32.7	81.5	-	-
Including under cargo works%	25.7	107.5	25.9	100.8	26.6	22.6	85.0	-	-

3 Results

Thus, the main problems of development of sea transport are caused by the following reasons:

- Lagging the development of domestic seaports and the organization on their basis of large transport and logistics nodes;
- aging and insufficient replenishment of the sea transport fleet.
- low competitiveness of domestic shipping companies in the world market;
- Inadequate scales of use of modern transport technologies, first of all container, ferry, lighter, roller;

The investment attractiveness of the Kamchatka Territory is limited to a certain extent by imperfection of sea routes. Nevertheless, the region, due to its geographical position, has a high and inadequately used transport potential. The Kamchatka Krai, through the development of port facilities and the creation of a transport bunkering center, can act as a strategically important subject of the Russian Federation, directly determining the state's perspective capabilities in creating an effective international northern transport system as one of its main strong points [6, 7].

The growth of the economy of the Kamchatka Krai can be achieved in those areas where it has real competitive advantages in regional and world markets. In this regard, the establishment of the port and logistics center will ensure the development of the Petropavlovsk-Kamchatsky sea terminal to the international level. The author's vision of the mechanism providing the competitive position of the maritime transport of the region includes:

- The need to update the fleet through the use of non-traditional sources of financing, including forfeiting financing, leasing schemes;
- Planning of alternative locations for port territories, in connection with the deployment of military facilities in Avacha Bay. Alternative places of accommodation can be considered the bay of Morzhovaya and the Russian bay;
- Delineation of bunkering functions, cargo transportation and passenger tourism between port territories as a demonopolization of Petropavlovsk-Kamchatsky commercial seaport;
- Ensuring the transport accessibility of the Kamchatka Peninsula;
- Increase the regularity of transportation and equalization of transport security along the territory of the region;
- The use of the transit potential of the territory of the Kamchatka Peninsula due to the advantage of the geographic location of the Kamchatka Territory;
- Elimination of high indicators of deterioration of transport infrastructure facilities, optimization of production and increase in the volume of transport services;
- Effective improvement of transport services for the population and business entities in hard-to-reach regions with moderate investment due to mass, systemic use of amphibious equipment, both aerial and terrestrial [8, 9].

4 Discussion

According to the table, there is an unstable dynamics of employment of the quay wall of the port, a significant decrease in the indicator occurred in 2010, but by 2012 there has been a positive tendency to increase the berth's busyness. Nevertheless, a fairly low level of employment in 2012, which is 50.8%, remains. Which is lower than the employment level of the quay wall in 2007 (57.1%) by 6.3%. In 2014 the number of vessels handled is reduced compared to 2013 and, accordingly, the berth's employment is only 81.5% compared to the previous year. In 2014 there was a significant decrease in the number of vessels processed (215 units). It should be noted that the decline in the indicator is a negative fact in the operation of the port infrastructure and indirectly characterizes the need to modernize the transport infrastructure.

Priority areas and projects in the field of maritime transport for the development of the transport component of the region are: reconstruction of berths in the seaport of Petropavlovsk-Kamchatsky and its port facilities; A sea checkpoint in Petropavlovsk-Kamchatsky and seasonal checkpoints in port stations; The renewal of the fleet of the region and the organization of sea freight-and-passenger lines along the coast of the Kamchatka Peninsula. The main tasks to be solved are stimulation of domestic demand for passenger and freight transportation, creation of a modern cargo and passenger fleet, improvement and development of the region's transport infrastructure.

In the last 12 years, sea transport by own transport in the region has decreased almost twenty times and is mainly provided by the vessels of the Primorskiy and Far Eastern shipping companies. The location of the Petropavlovsk-Kamchatka sea trading port in the Asia-Pacific region determines the geography of the port's cargo flows. Geography of coastal cargo flows.

Traditionally includes the Vladivostok direction. The Sakhalin direction (the Vanino line) has developed significantly. The transportation of coal in 2009–2010 was carried out from the ports of Sakhalin and Vostochny. The ports of the south of Primorye are potential starting points for the sea transit of Chinese goods to Europe via the Northern Sea Route, as well as to North America. The north-eastern provinces are interested in entering the Russian ports of the south of Primorye. The development of the port of Petropavlovsk-Kamchatsky and the construction of passenger ships will allow the resumption of regular passenger traffic on the Petropavlovsk-Kamchatsky-Vladivostok line, as well as along the coast of the Kamchatka Peninsula.

The current state of the marine transport fleet requires the development of schemes for its renovation. The state of the courts is a decisive factor in the development of the transport complex of the region.

According to the data of the Maritime Transport Development Department, the quantitative composition of the fleet is presented in the following data in Table 3.

According to the table, the transport fleet makes up 18.4% of all maritime transport, which, undoubtedly, can not satisfy all the need to ensure the development of the transport component of the region's economy for further development of the region's potential.

Table 3. Quantitative composition of the fleet operating in the Kamchatka direction.

Title	Units
Non-cargo fleet	
Non-cargo fleet	202
Cargo fleet	
Tugboats	6
Ferry cargo-and-passenger Captain Drabkin	1
Refrigerated vessels	22
Tanker	14
General cargo	10
Universal ships	10
Research vessel	1
Cargo fleet	63

According to the Russian Maritime Register of Shipping, the total number of ships, whose port of registration is Petropavlovsk-Kamchatsky, is 202 units. Of these, the transport fleet is 63 units (31% of the total number of maritime transport), which is insufficient to meet all the need to ensure the development of the transport component of the region's economy for further development of the region's potential. The register book of ships also gives an opportunity to trace the processes of retirement and replenishment of the fleet, since the largest number of vessels was excluded from the register in 2012 (5 units). The most intensive fleet renewal took place in 2013, the fleet of transport fleet was replenished with 3 vessels. Despite the updates in 2013–2015, it should be noted that over the past four years the number of excluded vessels exceeds the added ones by half. Thus, the quantitative composition of the transport fleet is decreasing.

The share of new vessels received in the Kamchatka transport fleet in the period from 2011 to 2015 amounted to only 6 vessels, which is more than 10% of the total number of vessels in this category. Despite the renewal of the park, only 2 vessels out of 6 have an age of less than 20 years. Dynamics of changes in the quantitative composition of the transport fleet for 2011–2015 is presented in Fig. 3.

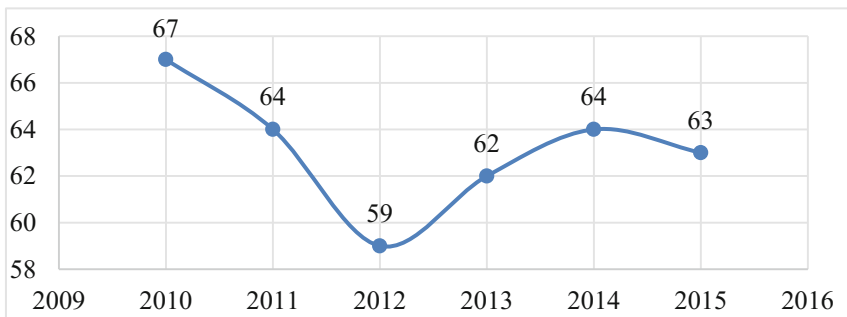


Fig. 3. Dynamics of changes in the quantitative composition of the transport fleet.

Analysis of the age composition of ships is the most urgent task in terms of the emphasis on the average age of ships of the transport fleet. The structure of the age structure of the transport fleet operating in Kamchatsky is shown in Table 4.

Of the total fleet number of 202 units, 63 ships are in maritime transport. At the same time, the age of the ships is from 57 years to 15 years. The weight of vessels with a service life in excess of 30 years is 31%. The share of vessels operating over 50 years is 2%; 40 years old - 5%; Over 30 years –31%; From 20 to 30 years - 47%; Less than 20 years - 10.41%.

The graph shows that the average age of ships falls between 23 and 32 years. The average age of the ships is determined by the weighted average (the weight of the number of vessels corresponding to their age was the weight) is 26.14 years, which confirms the need to update the material and technical base of the transport sector of the economy.

Table 4. Assessment of the state of the transport fleet operating on Kamchatka direction.

Year of construction	1956	1958	1971	1974	1979	1980	1981	1983	1984	1985	1986	1987
Age	57	55	42	39	34	33	32	30	29	28	27	26
Amount	1	1	2	1	1	1	2	2	3	2	2	4
Year of construction	1988	1989	1990	1991	1992	1993	1995	1996	1997	1998		
Age	25	24	23	22	21	20	18	17	16	15		
Amount	1	3	4	5	3	4	2	1	1	1		

The maximum share in the fleet is occupied by refrigerated vessels (22 units) 35%. As part of this group, 14 vessels have a year of construction until 1990.

The share of tankers (14 units) is 22%. As part of this group, 8 vessels have a year of construction until 1990, which indicates a high degree of moral and physical deterioration of sea transport category - tankers.

The share of universal vessels (10 units) in general transport is 16%. As part of this group, 3 vessels have a year of construction until 1990. This indicates that 50% of this group of vessels exceed the normative service life.

As part of the transport fleet there is a cargo-passenger “Kapitan Drabkin” ferry.

By the end of 2013 wear of fixed assets in the marine fleet amounted to more than 70% for certain groups of fixed assets and continues to grow. The state of many technical means of water transport has reached a critical level. A significant part of them is operated outside the normative service life, another, also a significant part, is approaching this deadline. As a result, the safety and economic efficiency of transport operations deteriorates significantly.

The method of determining physical wear should correspond to the type of the object being evaluated. There are the following methods for determining physical depreciation: the regression method; Method of examination; Method of reducing consumer properties; Method of normative age; Modified life method; Method of depreciation; Method of accounting for capital repairs. The method of normative age is applicable for mass evaluation, but it does not take into account ship repairs. The calculation is carried out by the ratio of the actual service life (T_f) to the normative service life (T_n). In accordance with this methodological justification, we will calculate the degree of wear of the transport fleet. Based on the calculation of the average age of vessels of 26.14 years and the standard service life for maritime transport of 20–25 years, the wear amount exceeds the normative 104%.

As part of the implementation of the federal targeted program aimed at the economic and social development of the Far East and Zabaikalye, four self-propelled barges were built for the Kamchatka Territory at the Sosnovsky Shipyard, with a carrying capacity of up to 250 tons. (“Sosnovka-1”, “Sosnovka-2”, “Sosnovka-3”, “Sosnovka-4”). To increase transport accessibility in remote areas, two ships with an air cushion “Arktika-2DK” were built in the city of Omsk, at the request of the Kamchatka Territory, in the city of Omsk. Air cushion ships are a much more advantageous alternative than a helicopter. They are suitable for the transport of goods in the area of unequipped shore, both in open water and in the presence of ice cover.

The icebreaker is used in the most difficult periods, as a rule, at least 3–4 times a year for the wiring of tankers to the Central Heating and Power Plant. The cost of using an icebreaker per hour is 120 thousand rubles, and the time of posting is about 5 h, the cost of a single mooring of the tanker is increased by another 600 thousand rubles. It is effective to use icebreaking hovercraft platforms, the addition of which to icebreakers significantly adds icebreaking capabilities to conventional vessels.

In shallow-water conditions, one of the ways of transporting goods from the vessel to the shore is by using shallow barges, pushers or tugboats. Further, the application of this method requires land transportation from shore to the final intermediate storage. The creation of seasonal stocks and transshipment points on the shore, as well as the construction of the road, cause significant costs. An alternative option is year-round transportation with the help of hovercraft.

Passenger water transport in Kamchatka is in unsatisfactory condition. A significant part of the passenger lines was eliminated due to the overall unprofitability of passenger traffic, aging of the fleet of ships. The ship-repair base of the marine fleet in parallel requires investment. Seasonality of Kamchatka's water transport causes problems in the employment of fleet workers.

5 Conclusions

Using the historical approach and analytical method, the main trends and problems of the development of Kamchatka Krai's maritime transport have been identified. The researched subject of the federation is a region providing security for Russia and representing its geopolitical interests on the eastern border of the country. The ineffective functioning of the transport complex and the deterioration of ships are deterrent factors in realizing the potential of the region's social and economic development.

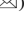
In the process of the study, the reserves for improving the efficiency of Kamchatka's maritime transport have been identified, the establishment of a port and logistics center will ensure the development of marine Terminal Petropavlovsk-Kamchatsky to the international level. Presented is the author's vision of the mechanism, the implementation of elements of which will ensure the competitive position of maritime transport in the region. Within the framework of a simple model of compensatory homeostat, the study examined which resource will facilitate the effective interaction of the subject and the management object at the regional level.

References

1. Miroshnikova, T., Taskaeva, N.: MATEC Web of Conferences, vol. 106, p. 08093 (2017)
2. Stein, E.: *Procedia Eng.* **165**, 1410–1416 (2016)
3. Kolosov, V.: *Water Transp.* **2**, 1 (1991)
4. Kolosov, V.: *Water Transp.* **2**, 2 (1991)
5. Goremikins, V., Rocens, K., Serdjuks, D., Pakrastins, L., Vatin, N.: Cable truss topology optimization for prestressed long-span structure. In: *Advances in Civil Engineering and Building Materials IV*, CEBM 2014 (2015)

6. Romanovich, M., Simankina, T.: *Procedia Eng.* **165**, 1587–1594 (2016). <https://doi.org/10.1016/j.proeng.2016.11.897>
7. Jevric, M., Romanovich, M.: *Procedia Eng.* **165**, 1478–1482 (2016). <https://doi.org/10.1016/j.proeng.2016.11.882>
8. Romanovich, R., Vilinskaya, A.: *MATEC Web of Conferences*, vol. 53, p. 01052 (2016). <https://doi.org/10.1051/mateconf/20165301052>
9. Report of the captain of the seaport of Petropavlovsk-Kamchatsky. The Federal State Institution “Administration of the Seaport of Petropavlovsk-Kamchatsky”. Petropavlovsk-Kamchatsky (2014)

Location-Based Potential for the Development of Cruise and Yachting Industries in the Protected Region of the Kotor Municipality

Nikola Konjević¹  and Goran Radović²  

¹ Adriatic University, Tivat, Montenegro

² Faculty of Architecture, University of Montenegro, Podgorica, Montenegro
rgoran@ac.me

Abstract. This work analyzes the development possibilities connected to the cruising and yachting industries in the area which is under the protection of UNESCO as a World Heritage Site in the Kotor Municipality, Montenegro. At the time of inscribing the territory of Kotor Municipality, i.e. the Bay of Kotor and Bay of Risan area, on the List of World Cultural and Natural Heritage of the United Nations Educational, Scientific and Cultural Organization in September 1979, the key evidence of the universal value of this area was the existence of a harmonious relationship between the natural and man-made cultural and historical agglomerations, which comprise a unique symbiosis and a consistent whole. For centuries, the geographical location, natural, climate and hydrological conditions have been a good basis for the development of the maritime industry—which is a tradition here—so today this area is suitable for the sailing and mooring of watercrafts intended for tourists. The overview of the possible locations for the development of industrial and service activities connected to tourism and the area which is the subject of this paper, in accordance with the limitations due to the area’s status and legal framework, represents the essential part of this paper. For that purpose, the analysis of potential locations for the development of cruise and yachting tourism is of great importance, and at the same time it aims at the protection and integrity of the inherited natural and cultural universal values.

Keywords: Cruise tourism · Yachting industry · Protected area
Cultural and natural values

1 Introduction

The reasons for inscribing the coastal area of the Kotor-Risan Bay in the Bay of Kotor on the UNESCO World Heritage List in 1979 were the extraordinary architectural values of the old town conglomerations, numerous palaces and churches as well as the values of the archaeological locations. The natural and cultural-historical region of Kotor creates a harmonious symbiosis of natural phenomena and architectural heritage. The extraordinary universal value of the cultural and historical area of Kotor is reflected

in the quality of its architecture in the fortified and open towns, villages, palaces and monastery complexes, along with their harmonious integration with the cultivated terraced landscape on the mountainside of high rocky mountains. The natural and cultural-historical region of Kotor provides a unique testimony about the extremely important role which it had played during the centuries in the expansion of the Mediterranean European culture in the Balkans.

Thanks to the attractive facilities which Kotor and its hinterland offer tourists, along with the creation of conditions for the accommodation of tourist vessels, in the last decade Kotor has become a prominent growing destination for tourists who visit Montenegro on cruise ships or yachts.

For that purpose, the most important facilities of the newly constructed infrastructure and port services segment is located in Kotor – with the company “Luka Kotor” JSC (Port of Kotor), through which 535,232 tourists on 487 ships travelled to Montenegro in 2016. In the past four years, the Port of Kotor recorded a total growth of the number of cruise arrivals amounting to a stunning 42%, which is especially pointed out in the analyses by MedCruise. Kotor has become the third most visited port in the Adriatic Sea with 487 ship arrivals in 2016 (18.9% more compared to the previous year), thereby reaching a total number of 536,444 travellers: more than 21.4% compared to 2015. According to the number of ship arrivals, Kotor has been placed on the top 10 list of the busiest ports of the MedCruise association, while it ranks at number 16 in regard to the number of travellers. At the same time, yacht traffic in the Port of Kotor—considered from the aspect of yachts arriving in Montenegro—is more modest. In 2016, a total of 1,674 yachts carrying 8,292 passengers sailed into the Port of Kotor (compared to the previous year, this is a 6% and 14% percent increase in the number of arrivals and the number of passengers respectively).

More significant investments in the vessel accommodation infrastructure were made after the catastrophic earthquake which hit the Montenegrin coast in 1979, resulting in the extension of the wharfage of the Port of Kotor, which created the conditions for the accommodation of higher capacity ships. After that, “Port of Kotor” JSC improved its service through: constructing of the passenger terminal facility; removing the alluvium from the wharfage; improving the intelligence and security facilities and procuring the necessary means and equipment. “Montenegro Public Enterprise for Coastal Zone Management - Budva” was dominantly investing in the recovery of the wharfage in Risan, and with its support and the resources of the local administration, the small old traditional harbours (so-called *mandrač*i) in the Bay of Kotor were recovered as well.

All the activities carried out in the protected Kotor area were planned and based on the principles of sustainable development with the preservation of cultural and historical values and their appropriate cultural and tourism presentation.

2 The Natural and Culture-Historical Region of Kotor

The natural and cultural-historical region of Kotor is a harmonious symbiosis of natural phenomena and architectural heritage. This area includes the part of the Bay of Kotor where it is narrowest (340 m) and cuts most deeply into the mainland (33 km). In terms

of formation, it is a tectonically sunken and flooded river valley and its morphological features (extraordinary vertical segmentation) make it unique in the Mediterranean. It belongs to the Dinaric zone of the holokarst (deep karst), so the most typical karst formations and karst hydrography are prominent in the bay area and its hinterlands.

The southern, eastern and south-western boundaries of the region traverse the slopes of Lovćen and Vrmac, while the south-eastern, northern and north-western boundaries correspond to the boundaries of the national parks Lovćen and Orjen. The surface of the area is 12,000 ha, 2,000 ha of which are made up by the sea. The boundaries of the natural and cultural-historical region from 1979, as determined based on the parameters at that time, cover a total of 12,000 ha of land and 2,600 ha of sea. The boundaries of the natural and cultural-historical region defined in 2010 with new technologies for the purpose of the development of the Management plan for Kotor cover a total of 8,620 ha: 6,120 ha of land and 2,500 ha of the marine surface.

The hydrographical complex consists of the marine surface in the Kotor-Risan Bay (2,600 ha), as an integral whole connected through a narrow passage with the Bay of Kotor and the open sea. The typical formations of karstic hydrography are the karst springs at sea level (Škurda, Gurdić, Ljuta), intermittent springs above sea level (Sopot 33 m), submarine springs on the sea bed (Dražin Vrt, Perast, Sopot). Although the immediate hinterland of the Kotor area (Crkvice 1097 m) is one of the areas with the highest precipitation levels (5,155 mm) in Europe, due to the peculiarity of the karst topography and the underground runoff, the water re-emerges at or below the sea level, which results in the low salinity of the sea water and the lack of water in the area. Another consequence of the vertical segmentation of the area are the climate differences, ranging from a Mediterranean to a mountain climate (subalpine climate). What is also connected to the above is the diversity of vegetation which is characterised by the abundance of different kinds of flora. To name a few, this region is home to the bay laurel (*Laurus nobilis*) as the representative of the Mediterranean (Adriatic-Mediterranean) climate, it is also a rare natural habitat of the oleander (*Nerium oleander*) which grows near Risan, while in the north-western boundary of the region there are plant communities of the pine, Bosnian pine (*Pinus leucodermis*), representing the alpine climate and the endemic flora of the Balkans. Among the endemic species of fauna, the most prominent one is the snail *Clausilia catherensis* which lives on the walls of Kotor.

The Kotor region consists of towns, smaller and bigger villages, which are linked up in an almost uninterrupted chain: Dobrota, Orahovac, Risan, Perast, Morinj, Kostanjica, Stoliv (Gornji and Donji), Prčanj, Muo and Škaljari.

As far as the layout is concerned, the city of Kotor is circumscribed by protective ramparts which descend from the top of the St. Ivan hill (260 m), skirting the two short streams, Škurda and Gurdić, with their movable bridges and the seacoast. This continuous fortification system, which follows the irregular and crisscrossed line of the steeply-sloping range of hills (for about 5 km) is militarily and aesthetically the most important and impressive part of the monumental setting which encircles the town. Out of 30 churches, recorded or preserved in the old town, 4 churches from the Romanesque period are particularly important (St. Luke's, 1195; St. Anne's, probably 1195; St. Mary's, 1222 and St. Paul's, 1266), aside from the cathedral (St. Tripun's, 1166). The urban nucleus of the old town of Kotor is characterised by 12 squares of varying

size whose irregular beauty provides relief from the narrow, closed-in, winding streets. The squares had a specific purpose. The largest and architecturally best designed is the “Place of Arms” near the main gates of the town (the Medieval arsenal), with a series of significant objects, the Medieval “Turrus Torturae”, the “Clock Tower” of 1602, also the unfinished “Prince’s Palace” in Renaissance-Baroque style, and the building in which Yugoslavia’s second permanent theatre was opened at the beginning of the 19th century. Further south is the “Flour Square” with the 17th century “Pima” palace and a series of other 17th and 18th century palaces (Bizanti, Beskuća, Vrakjen, Buća). In the next square, there is the dominant St. Tripun’s Cathedral, first built in the 9th century and entirely renovated in 1166, while its present facade dates from the 17th century, following the disastrous earthquake of 1667. The square is bordered by very harmoniously designed palaces and mansions dating from the 17th to the 19th centuries, whereas a little further to the north you can find a smaller square with the early 18th century Grgurin Palace which now houses the Naval Museum whose exhibits suggestively portray the development of civilization and culture in this region. Three more squares still have links to their former economic functions: “Milk Square”, “Timber Square” and “Salad Square”.

As for Risan, we could say that as the Illyrian and ancient centre of this area it has preserved the remains of 1st to 3rd century buildings and mosaics which are well preserved and exhibited. Perast, as a whole, represents the culmination of the Baroque style on the Yugoslav coast of the Adriatic. Prčanj is a town of maritime traders and warriors with a large number of 17th to 19th century Baroque palaces. Dobrota is a town with several urban centres belonging to individual fraternities and the churches of St. Matthew (originally built in the 13th century, the present church originates from the 17th century) and St. Eustace (18th century), with precious collections of paintings, lace and silverware. The area also includes other very important villages (Gornji Stoliv; Donji Stoliv; Morinj; Kostanjica; Škaljari) and fishing villages (Muo; Orahovac) (Fig. 1).



Fig. 1. Bay of Kotor.

The protected surroundings of the World Heritage Site Kotor is defined according to the fact that the Bay of Kotor is an indivisible region, a single whole with numerous

cohesive factors: the Bay of Kotor with four smaller connected bays, as the geographic factor, its hinterland with similar natural characteristics, the shared history, tradition and heritage. An important feature of the region are the small localities whose houses and palaces link up in series along the seacoast, while the chains, i.e. villages, are intersected by natural green spaces which descend from the slopes all the way to the seacoast. Such a way of constructing and planning spaces and villages resulted in a magnificent symbiosis of the natural surroundings and the man-made elements within it, which is why this region and the entire bay were inscribed on the List of World Natural and Cultural Heritage.

The protected surroundings of the Natural and Cultural-Historical Region of Kotor consists of a part of the maritime zone of the Bay of Kotor with the Bay of Tivat, the Kumbor Gorge and Bay of Herceg Novi including the entrance to the Bay of Kotor with the island of Mamula, Žanjice, Cape Azra and the Ponta Oštra Peninsula, Luštica Peninsula, Tivat and the localities along the coast of the Bay of Tivat, the Tivat Archipelago (the Prevlaka Peninsula, island of St. Mark, island of Our Lady of Grace), the west part of the Vrmac Peninsula, Herceg Novi and the localities along the coast of the Bay of Herceg Novi, the slopes of Mt. Orjen with the neighbouring villages (Ratiševina, Trebesin, Kameno, Podi, Sušćeapan, Sutorina, Malta, Lučići), Kruševice, Ubli, Donji and Gornji Grbalj, the hinterland of Risan (Ledenice and Crkvice), Gornji Orahovac and Zalaze.

3 The Montenegrin Legal Framework in Relation to Cruise and Yachting Tourism and Spatial Planning and Development

In order to analyse the given subject, it is deemed necessary to indicate the set of Montenegrin laws governing this area. Therefore, we shall point out the regulations which govern: relationships connected to cruise and yachting tourism, and spatial planning and development in regard to spaces suitable for carrying out the subject activities.

3.1 Laws from the Area of Cruise and Yachting Tourism

The main law regulating the status of ports which serve for the accommodation of ships and yachts is the Law on Ports. This Law, pursuant to Article 1, governs: the legal status, classification of ports, management, fees, concessions, order, inspection and other issues that are important for ports in Montenegro.

During the adoption of this law, the lawmaker's starting point was to remove the boundaries for a significantly greater participation of the private sector in the performance of activities and funding of the construction and technical and technological improvement of ports. On the basis of already established principles, the functions, responsibilities and rights were divided among the state authorities and the private sector in such a manner that the port's land and infrastructure is state-owned, but that long-term concessions may grant the right to their use to companies which possess a

superstructure and provide port services. Thus, the state limited its role to administrative, regulatory and developmental matters, along with the creation of conditions for a full privatisation of the operational or commercial activities (the landlord organisational model for port management).

Based on the type of maritime traffic, ports can be divided into ports open for international and domestic traffic and ports open for domestic traffic. (Article 6), whereas the division based on the purpose is as follows: (1) trading ports; (2) ports of nautical tourism - marinas; (3) shipbuilding ports; (4) fishing ports (Article 6). With the aim of further elaboration of the legally stipulated norms, the Government adopted the following within its competences: Decree on the conditions which need to be met by ports classified according to the type of maritime traffic and purpose. Decision on the designation of ports for international maritime traffic Proposal of the decree on the manner of maintaining order in ports...

The Government of Montenegro proclaimed the following ports as ports of national importance in the protected region: Trading Port of Kotor, along with the port of nautical tourism of local importance: the Nautical Tourism Centre in Kotor.

The Law on Yachts is the main law on yachts governing: the nationality, identification and registration of yachts in the Register of Yachts, manner of entering, staying and leaving of yachts, as well as the rights and responsibilities connected with the chartering of yachts. On the day when this law entered into force, on 1 January 2008, the provisions on yachts given in the laws of Montenegro and of previous states that Montenegro was a part of ceased to have effect. The starting point at the time of the adoption of this Law was the State's commitment to "(...) create a user-oriented legal framework for the development of nautical tourism in the Republic of Montenegro, which is comparable or better than those in the Mediterranean in terms of convenience (...)".

3.2 The Legal Framework for Spatial Planning and Development

Planning represents the primary, general, framework which can and does influence the methodology of planning. The lawmaker determined that spatial development shall rest on the principles of: "coherent economic, social, ecologic, energy, cultural spatial development of Montenegro; sustainable development; incentives for balanced economic spatial development of Montenegro; economically efficient use and protection of space and natural resources; compliance with European norms and standards; protection of integral values of space; polycentricism; competitiveness and cohesion; decentralization; protection and enhancement of the status of environment; protection of cultural heritage; reconciliation of interests of users of space and priorities for interventions in space; public interest; private interest but not at the disadvantage of public interest; presence of the public in the spatial development proceeding; establishment of space related information system aimed to ensure more efficient spatial development; aseismic planning.

There are four types of planning documents at the state and local administration levels: state planning documents (Spatial Plan of Montenegro; special purpose spatial plan; detailed spatial plan; location study at the state level) and local planning

documents (town-planning scheme passed by the local self-government; detailed urban development plan; urban development design; location study at local level).

Because of its importance, there is a more detailed description of the Special purpose spatial plan for the coastal zone of Montenegro (SPSP CZ), whose development was initiated by the adoption of a corresponding Government Decision (Decision on the development of the special purpose spatial plan for the coastal zone of Montenegro). SPSP CZ is a planning basis for the utilisation, sustainable development, preservation, protection and improvement of the coastal zone of Montenegro.

This region which is comprised of the territories of six Montenegrin municipalities located in the Adriatic has, as a whole, numerous developmental potentials, as well as limitations, which requires a unified planning approach in the future organisation, so the state's priority task is to establish integral management in the Coastal region. Figure 2 shows an excerpt from the Land Use Plan for SPSP CZ which covers the wider zone of the protected region of Kotor.

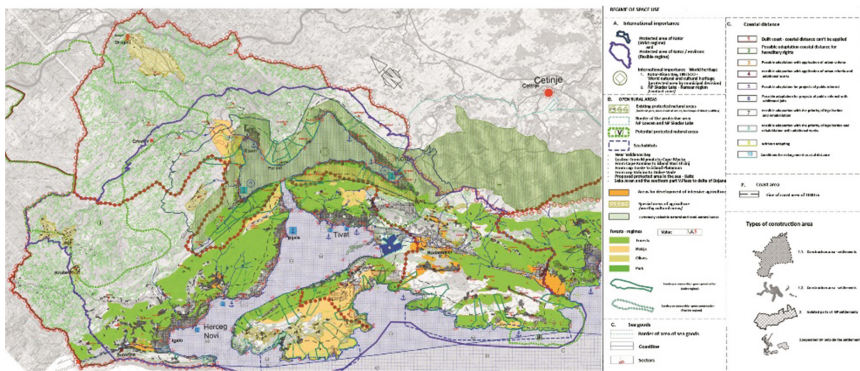


Fig. 2. Excerpt from the Land Use Plan for SPSP CZ.

4 Directed and Controlled Spatial and Coastal Zone Development for the Developmental Function

During the preparation of the above mentioned SPSP CZ, the dominant concept for the future development of the area was the one which can be more closely defined under the term “Cohesion” - Sustainable Development. This commitment stems from the premise “Spatial planning measures must enable the valorisation of the existing potentials of the coastal zone by integrating the maritime and mainland potentials in accordance with the principles of sustainable development; the positioning of the port system should be analysed in terms of planning so that the development is focused on two centres, Bar and Kotor (Bay of Kotor), with the sub-centre Budva (...); the development of the traffic function of the Port of Kotor should be analysed through the establishment of a new, dislocated, passenger terminal outside of Kotor (...); it is necessary to intensify the activities aimed at the development of a basic marina network in Montenegro”.

Regarding the launch of a new location, important innovations are planned for the improvement and restructuring of cruise tourism and the enabling of the creation of a ferry service, by allocation a part of the Port of Kotor traffic to the Lipci locality - port terminal (separate passenger terminal). This is because of two dominant reasons:

- By the construction of the main road M4 (Grahovo - Lipci), this locality got a new, more significant function in the traffic system of Montenegro;
- The Port of Kotor managed the Port of Lipci until the coastal zone was defined as state ownership. In that period, the Port of Lipci served for the unloading of liquid cargo, with a coast 74.60 m long and a plateau with an area of 373 m² and water space with the width of 100 m off the coast. Lipci has the advantage of its historical surroundings, which is important in many ways. The advantage is reflected in: the location's advantages in terms of constructing port infrastructure facilities; development of a new locality function; encouraging the development of surroundings; expansion of the economic utilisation zone of the coastal area; improving investments in the development of new entrepreneurial initiatives; inclusion of the population in the provision of numerous services which will be generated by the new purpose of the space; creation of jobs; establishment of traffic links (international maritime; regional and local roads); contribution to the development and spatial architectural design; recovery of devastated natural and constructed capacities; activation of sufficient unused and abandoned facilities. This rather simple approach of including a new locality on the territory of the Kotor Municipality in the cruising trends can significantly contribute to its development at the micro and macro levels. The micro level refers to the locality of Lipci, while the macro level refers to the logistics-related design for strengthening the port and Kotor as a cruising and stationary tourist destination. Similar solutions are already present in the organisation of the accommodation of cruise ships and tourists in the ports in the Mediterranean, to which Kotor and Montenegro geographically belong.

The accommodation of cruise ships is planned in the Port of Bar as well, where the urban planning documents for the expansion of the port's capacities (expansion of the existing wharfage by approximately 400 m) have been provided, thereby creating a planning basis for the implementation of the necessary capacities for the accommodation of a higher number of larger, i.e. cruise ships.

The arguments for the presented planning commitments can also be found in the fact that the number of cruise ships and especially passengers who come to the Port of Kotor has been continuously growing since 2004 (Fig. 3), and that numerous requests for the booking of berths or mooring in the Port of Kotor cannot be accepted for the next period.

The accommodation of cruise ships is also planned in the Port of Bar, which is located in the south of the Montenegrin coast, where the urban planning documents for the expansion of the port's capacities (expansion of the existing wharfage by approximately 400 m) have been provided, thereby creating a planning basis for the implementation of the necessary capacities for the accommodation of a higher number of larger, i.e. cruise ships.

Marinas, as nautical tourism facilities, represent specialised tourism ports whose water areas are naturally or artificially protected. They are specialised for the

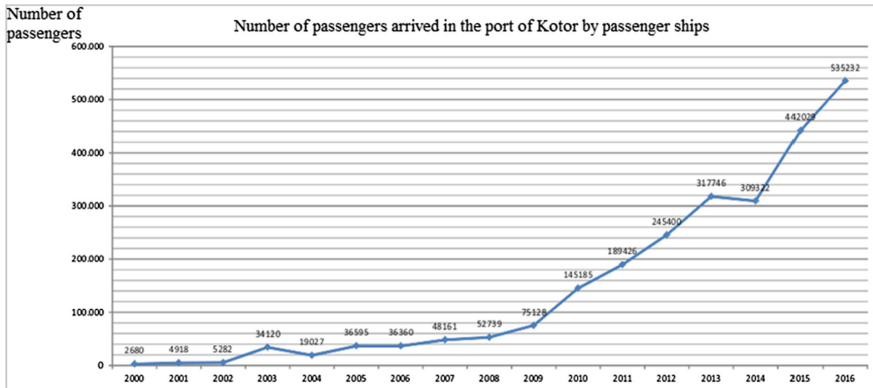


Fig. 3. The total number of passengers on cruise ships in the Port of Kotor for the period 2000–2016. Source: Records of “Port of Kotor” JSC (Konjevic N., Radovic G.).

accommodation, provision of supplies to the crew and tourists, maintaining and equipping nautical tourism vessels, with direct pedestrian access to each berthed vessel which can be used at any moment. Marinas are subject to classification, depending on the level of nautical infrastructure equipment, type, scope and quality of the services they provide, from category one to category five.

The proposed system of marinas in Montenegro tried to take into account the overall needs of Montenegro and of specific local environments to the maximum extent. While respecting those facts, three key criteria were singled out and they should define the priority parts of that system: provision of sustainable development and preservation of ecological balance; avoiding the use of beaches and other important tourism resources; estimated economical justification.

The first criterion purports the behaviour in accordance with basic rule of sustainable development. This means that the basic resource, in this case the Coastal Zone, is used in such a manner which causes minimum changes, thus preserving it for future generations. This rule also purports the need for the protection of the ecological balance, especially in protected and highly vulnerable areas. The second criterion is based on the rule that only those micro locations that do not have some other important economic purpose shall be used for the construction of nautical points, because otherwise it would be uneconomical and could only damage tourism development. Therefore, natural beaches and areas suitable for the construction of hotels and similar facilities were avoided during the selection of sites, while the preferred sites were those where the construction could improve the destination’s image. The third criterion of economical justification is based on rough estimations considering the situation in the region. Exactly because of such criteria, special preference was given to entrepreneurial ventures which imply the transformation of military and industrial complexes and devastated regions into marinas. Namely, after the transformation of sites such as the Boat Repairing Shipyard in Tivat or the military complex in Kumbor into marines, these sites meet all of the three criteria: ecological, because the marina function is less damaging for the environment than the previous function; spatial and tourism, because

the transformation improves the destination image and there are no serious conflicts with other users; economic, because they partly have the infrastructural issue settled (in particular the wharfage).

In addition to these basic criteria for the construction of marinas, some additional ones have also been accepted, in order to define priorities as precisely as possible - maritime conditions, preservation of ecosystems, attractiveness of the location, protection of other resources, position and accessibility, feasibility of the project, attractiveness.

These are the key incentive factors for the marina system development: the coast of Montenegro is very attractive for sailing, it is preserved and mostly unpolluted and represents an insufficiently discovered destination within Europe; neighbouring Croatia already experiences the crowding caused by vessels and considers the introduction of some restrictive measures, which could encourage the boaters to come to Montenegro; the current global trends indicate a constant and large growth of the demand for nautical tourism, in particular for larger yachts, motorboats etc.

In the protected region of Kotor, for the purpose of preserving its environmental and universal values, the larger wharfs and piers need to be executed in accordance with the prescribed preservation and technical solutions and requirements regarding cultural heritage protection and sailing, whereas the perimeters, i.e. edges of the horizontal pedestrian surface and the vertical submerged one, should be made of larger trimmed stone blocks, with rounded edges, and all their visible surfaces should be paved with appropriate stone slabs.

5 Conclusion

Based on the above, we can conclude that when the Kotor Municipality gained the status of a UNESCO protected coastal area, the result was positive in terms of a greater interest shown by tourists for the Region of Kotor and Montenegro. This was especially affirmed on the Mediterranean cruising market where the Port of Kotor managed to take a significant role.


The current condition of the Kotor and Risan Bays, observed from the aspect of constructed and planned infrastructural facilities for cruise and yachting tourism, leads to the conclusion that only one segment of the envisaged contents has been partly implemented in the Bay of Kotor (Port of Kotor), whereas significant interventions in the area (Marina in the Kotor and Risan Bays and a separate passenger terminal in the Lipci locality) have not started yet. Having in mind the positive effects of cruising and cultural tourism in the Bay of Kotor area during the recent years, the leading global cruise and yachting companies are very interested in investing with regard to the planned new contents for the purposes of cruise and yachting tourism.

Apart from the positive results in the development of cruise and yachting tourism, and having in mind the protected universal values of the Kotor-Risan Bay, the development of this type of tourism and industry needs to be planned carefully in order to preserve and not jeopardise the natural and cultural heritage of this area, which is a continuous obligation and duty.

References

1. Archive Records of the Company “Port of Kotor” JSC, Kotor
2. National Commission for UNESCO of Montenegro. Natural and Cultural-Historical Region of Kotor
3. Konjević, N.: Characteristics of the development of cruise tourism in Montenegro. In: Proceedings of the Third International Scientific and Professional Conference – ERAZ 2017, Belgrade (2017)
4. Ministry of Culture, Management Plan for the Natural and Cultural-Historical Region of Kotor (2011)
5. Ministry of Sustainable Development and Tourism. Special Purpose Spatial Plan for the Coastal Zone of Montenegro. Draft, Podgorica (2015)
6. Ministry of Sustainable Development and Tourism. Purpose Spatial Plan for the Coastal Zone of Montenegro. Transport System – analytical and documentation study, Podgorica (2014)

The Development of Underground Construction as a Way to Improve the Organization of Traffic

Ekaterina Utkina, Kirill Pshennikov, and Natalia Braila^(✉) 

Peter the Great St. Petersburg Polytechnic University,
Politechnicheskaya Str., 29, 195251 St. Petersburg, Russia
nashi-n-v@mail.ru

Abstract. Currently, there's a problem with the big population on the earth's surface. This has an extremely negative impact on the transport network of cities and the overall comfort of living. There is a problem to reach in the morning for work, and in the evening home, roads are overloaded with transport in rush hours. In some cities, traffic jams are a constant problem. The construction of intercepting parking facilities near the metro, multi-level roads and other elements of transport infrastructure only lead to temporary improvement. The best solution for this problem is urbanization of the underground space. The purpose of the research was to examine the efficiency of reconstruction of underground structures for new facilities. The study showed that reconstruction of existing underground structures for new appliance is more quick and cheap. In our days there're some objects, which have been restored and now they are amusement parks, shopping centers, etc. Were described the plans for future renovations, which will reduce the density of urban development on the surface of the earth and to repurpose unused underground structures. It was also noted that due to lack of existing underground structures new constructions are often used. There were given some recommendations of the organization and development of the underground space.

Keywords: Underground construction · Traffic · Organization

1 Introduction

Every year, the population in large cities increases, which leads to overcrowding, affecting the way of life of people and the comfort of their living. This problem is relevant in many countries, the most frequent reasons are the absence of land surface areas, terrain features or features of historically developed urban planning. Because of this, further horizontal expansion of the city is impossible.

In Monaco, the population density is 18679 people per square kilometer, when the average density around the world is 53 people per square kilometer. This is the most populous state in 2017. In Russia, the average population density is small and is 9 people per square kilometer, but in large cities, such as Moscow and St. Petersburg, the population density over 4,000 (Table 1).

Table 1. Cities of the world by population density (as of January 2015).

№	Place	City	Country	Population density (per/km ²)
1	1	Calcutta	India	24 252
2	4	Seoul	Republic of Korea	17 164
3	6	Jakarta	Indonesia	15 040
4	15	New York	USA	10 724
5	26	Tokyo	Japan	6 273
6	35	Moscow	Russia	4 814

This problem leads to the search for new effective solutions that allow to reduce the number of people in those areas where it is necessary, while preserving the comfortable living of the population. One of the ways to solve this problem is the urbanization of the underground space, which makes it possible to develop underground areas for people to live, thereby reducing the density of the population living on the surface of the earth.

2 Review of Literature

The problems of urbanization of the underground space are disclosed in the following works [1–5].

In the article Alekseeva and Belyaeva describes the main problems of the distribution of underground space, an approach is proposed for the further division of the urban space for the purposes of a differentiated assessment of its quality [1].

Pustovoitenko and Gavrish consider the problem of forecasting trends in urbanization, and the main factors that affect modern ways of organizing the development of underground construction. They systematise approaches and experience in the development of underground space [2].

In the work of Denisov and Korenkova considers actual problems in the urbanization of large cities [3]. They identify the reasons for the necessary growth in the volume and scale of underground construction in major cities, which are associated with the continuously increasing concentration of the urban population.

A more complete understanding has been achieved in work by Vartanova et al. [4]. They analysed the current problems of urban industrial agglomerations and possible directions for their solution by mastering the underground space of megacities by the example of urbanization in Moscow. Based on the results of the analysis, it is necessary to regulate research, monitoring and control of buildings.

The issue of underground urbanism is affected by many foreign researchers, including QiHu, which presents five problems of using underground space in China and ways of solving them through integrated planning, construction and management [5].

Articles [6–10] consider the prospects for the development of underground space.

Hachtryan in his article considers one of the urgent problems of development of the town-planning industry of St. Petersburg, which will help in solving technical, organisational and legal problems for the development of underground space in dense housing [6].

In the work Labbe considers the principles of development and properties of the architectural approach in the underground space [7]. Also analyses some experiences of the XX century, on the basis of which it is shown that the transition from the development of isolated structures to the related form of urbanism is important.

Pleshanov and Ivanov in his article analyses the benefits of using underground space, and also considers the prospects for using foreign analogues in urban planning [8].

In the work of Korotaeva, on the example of Moscow, examines the main directions and principles of the integrated use of the underground space of the city [9].

Vahaaho in his work considers the prospects of an underground master plan for the entire municipal district of Helsinki [10].

The works [11, 12] consider the development of underground space from the economic point of view.

In the work of Pozelsky the issue of choosing technologies for erecting underground structures that are economically viable is under consideration. The proposed version of the planning of underground construction reduces the work time [11].

Zhou in his article describes the basic principles of the development of underground space, as an economic imperative, in Singapore. He presented the government's economic strategy with specific recommendations for general planning, investment in research and development [12].

Despite the variety of works devoted to the urbanization of the underground space, there are no studies in the field of reconstruction of existing underground structures for public facilities.

3 Purpose of Work

To study the efficiency of reconstruction of underground structures for new uses.

Tasks:

- Identify the merits and demerits of the reconstruction of underground structures.
- Analyse the feasibility of reconstructing underground structures from an economic point of view.
- Perform a comparative analysis of options for new construction and reconstruction for a different functional purpose.

4 Definition, History and Reasons for the Emergence of Underground Urbanistics

Underground urbanism is an area of architecture and town planning, connected with the integrated use of the underground space of cities and other settlements that meet the requirements of urban planning aesthetics, social hygiene, and also technical and economic feasibility.

The development of underground space began from ancient times. A historical example of underground urbanistics can serve as the Egyptian pyramids, in which the

pharaoh's chamber was located beneath the earth, where his remains were found through the dug-out passages.

In ancient times, built a drainage system Cloaca Maxima. The need for sewerage arose because of the need to drain the swampy lowland between Palatine and Capitol Hill. The walls of the canal were laid out of the Gabian stone two meters in length and two meters in width, without the use of cement. With the development of the city, its sewage system also developed, the main part of which was still Cloaca Maxima [28].

In the Middle Ages, cellars began to appear in the castles, which were used as dungeons or storerooms with kitchens. There were also small underground passages connecting buildings or leading from the castle to the forest. The need for underground passageways was due to the fact that in case of an attack they could be used as a way to escape.

Mankind has always strived for a comfortable life, for safety and durability of structures, therefore, in the industrial period with the advent of drilling machines, the construction of railway and transport tunnels began. Two wars served as an impetus for the development of underground construction: underground plants, multi-level shelters and other underground facilities for strategic purposes began to appear [13].

In the 21st century, the issue of developing underground space is more than relevant, since there is a problem of overpopulation of large cities and congestion of land roads. The solution to this problem is found in the development of underground space by building underground cities and transport routes, which will help to reduce the concentration of the population on earth and make life more comfortable. There are already underground cities under China, Canada, Spain, the Crimea and other countries and their parts, where life is no different from life on the "upper level" [26].

5 The Assessment of Underground Urbanization in the World

By 2017, the problems associated with overcrowding on the Earth's surface affect the interests of the whole world. This can be seen in the example of such cities as Moscow, Mexico City, Istanbul, Shanghai, New York and Tokyo [22]. The population of these cities is about 10–17 million people and the density varies between 3–7 thousand people per square kilometer. According to forecasts of scientists, by 2025 in each megalopolis will live 20–35 million people. In such conditions, humanity creates the necessary construction projects, which include large underground objects [23, 27]. The same buildings exist in many cities of Russia, the USA, Japan, China, etc. Such structures as Subway, underground parking, shopping and entertainment complexes - just a small list of existing underground facilities [24].

The growing interest in the development of underground space is explained by its advantages [8] (Fig. 1).

The foregoing words allow us to assert that urbanization of the underground space is the most rational way out, which meets the requirements of modern realities and the possibilities of the latest technologies.

However, despite many advantages, underground urbanization has many social, economic and environmental disadvantages inherent in any complex objects (Fig. 2).

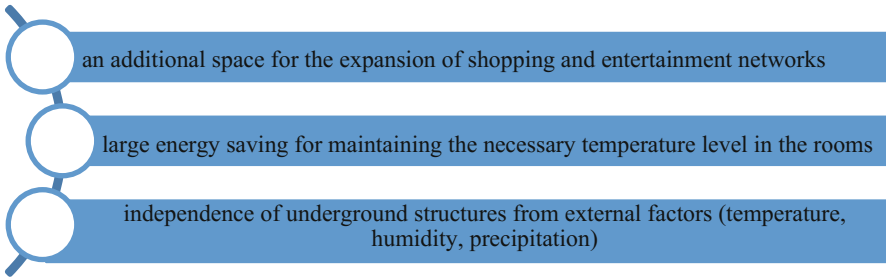


Fig. 1. Main advantages of underground urban planning.

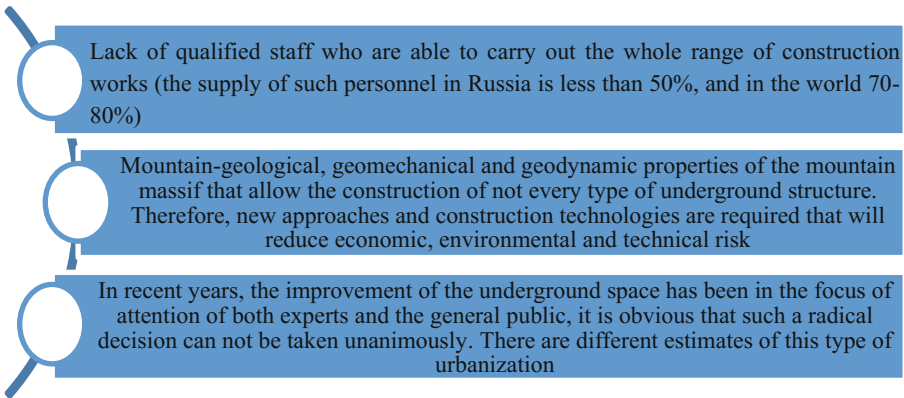


Fig. 2. The main disadvantages of underground urbanistics.

This question is touched upon in the work of Z.S. Adigamova and E.V. Lichnenko, according to which the urban environment has the property of self-exhaustion - at a certain point, infrastructure networks and numerous chains of buildings cease to be cost-effective and require a replacement for something more economical, requiring less resources for maintenance. In addition, they note that the urbanization of the underground space is not a new invention, but it must be brought to a better level than now [14].

Pleshanov, assessing the prospect of the development of underground facilities, focuses not on economic benefits, but on territorial necessity, emphasizing that with an active population growth, it is necessary to use all the space available to a person [8].

Kiran Nash, a BBC journalist, in his article devoted to underground device projects, came to the conclusion that there are a number of historical territories on the surface, the building up of which would not be correct. Thus, the construction of cities inland can also be considered as a way of preserving evidence of the historical memory of humanity [15].

It is impossible not to mention another skeptical point of sight. In the opinion of its adherents, urban underground projects are idealistic and face many challenges in their implementation.

Thus, A.V. Korczak reduces many practical difficulties in implementing ambitious plans to the fact that the countries did not manage to properly prepare for them. For example, this kind of urbanization requires highly qualified specialists who know the features of underground construction and, preferably, have experience in this area. At the same time, there are drawbacks in the legal framework of states - the laws do not regulate the underground environment [25].

Abundantly examined the problem of underground urbanistics and Olga Semyonova, coming to the conclusion that for the development of such projects, a citywide plan is needed, and not separate schemes affecting parts of the city. This is necessary, according to the senior researcher at the Central Research Institute of Urban Development, since the structures should not interfere with the water supply, heating and functioning of each other, while the scheme must be extremely precise, since changing something in the underground structure is a problematic task [16].

Based on the materials of ITA-AITES, the spectrum of possible problems is also quite clearly defined. For example, the need for scrupulous planning because of the lack of an easy, fast and relatively inexpensive ability to transfer parts of the structure. Another argument is that not every geological zone is suitable for underground construction, because of which it may become necessary to go to an increasing depth, and, consequently, to amend the existing project [17].

6 Existing Solutions Used in the Urbanization of the Underground Space

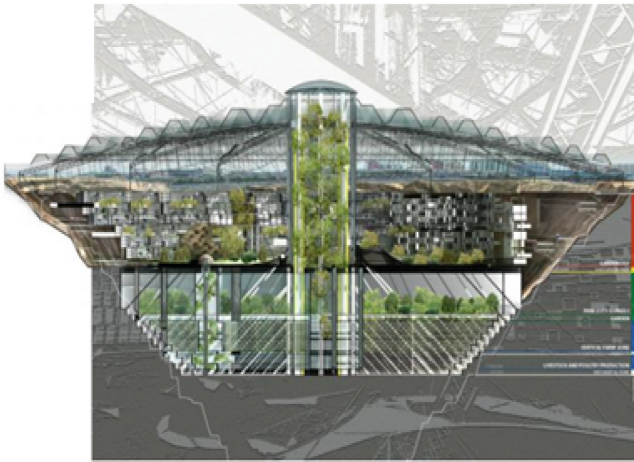
The creation of an underground object is possible by new construction or reconstruction of existing facilities with a change in their functional purpose to the required. These two solutions differ from each other in economic efficiency, time spent on projects, technical solutions and other aspects of construction. In 2017, many underground structures are being reconstructed for new facilities, thereby reducing construction time and financial costs [29].

One of such objects is the amusement park in Romania “Salina Turda”. This entertainment facility was built on the basis of the existing salt mine in the city of Turda in Romania. The mine was in operation from 1075 until the 1930s, and during the Second World War it served as a bomb shelter. In 1992, an amusement park “Salina Turda” was opened there. The park is located at a depth of 122 m below ground and is divided into 16 levels. It was adjusted to the already existing mine planning, minimizing excavation and, consequently, financial costs.

Another example of the reconstruction of underground structures can serve as an underground shopping center “Underground City”, which is part of the infrastructure of the city of Minsk, the capital of Belarus. The given object is a reconstruction of the shopping center that existed at the time at the metro station Partizanskaya, which was sold in 1998 by the Moscow authorities. Within three years, the construction was expanded. Reconstruction of an already existing underground structure allowed to reduce the volume of excavation, which led to significant savings in construction. At the time of 2017 shopping center “Underground City” is located at 2800 square meters. It is also planned to erect the ground part of the shopping center, which will be called “Upper City”.

In the future, it is planned to conduct a number of reconstructions of underground structures for new facilities. This solution of urbanization of the underground space allows not only to reduce the density of buildings on the surface of the earth, but also to redeploy unused underground structures. Reconstruction of existing facilities allows to reduce expenses for the construction of underground facilities, to shorten the terms of works, as well as to increase the economic efficiency of the project, due to a reduction in operating costs, a reduction in the length of engineering communications and fuel and energy resources used for heating and cooling premises [30].

An example of future reconstruction can serve as a project to adapt a quarry in Yakutia to an underground city. It will include three tiers, where agricultural land will be located on the lower level, a forest park zone for air purification will be located on the middle level, and residential and administrative buildings are designed on the upper tier. The population of the underground city will be about 10,000 inhabitants, and the total area will be approximately 3 million square meters (Fig. 3).



Basic concept:
 tier 1: agricultural
 land;
 tier 2: forest park
 area;
 tier 3: housing,
 office buildings.

The population is
 about 10 thousand
 people.

The total area is
 about 3 million
 square meters.

Fig. 3. An example of reconstruction of a quarry - "Eco-city 2020", Mirny, Yakutia.

Because of the features of the technical and economic indicators of the existing quarry and its geographical location, there are a number of problems that the engineers offered their solutions. There is a threat of landslide collapse of slopes, which it was proposed to eliminate with the help of cutting the soil with the formation of a trench in the form of an inverted truncated cone. The problem related to the flooding of the excavation was decided to be eliminated by erecting an anti-filtration curtain along the perimeter of the bottom of the excavation. For the power supply of the underground city, solar batteries with a capacity of 200 MW will be installed, which will adequately meet the needs of the population. This project is energy efficient, since solar energy and heat of the Earth can be used to generate energy.

In China, a project was proposed for an underground city in a non-functioning coal mine. This is one of the countries where the issue of high population density is acute, so the development of underground space is one of the priority tasks of the construction industry in the country. China is the leader in the extraction of coal, so the use of waste coal mines, the volume of which exceeds 30 billion cubic meters for the construction of an underground city is the most rational. The inhabitants of this city with developed infrastructure will be miners, which will significantly improve the quality of life of this category of working class [18].

Analyzing the known solutions of urbanization of the underground space, it was concluded that the reconstruction of existing underground structures with respect to new construction is more attractive. The main factors that ensure the economic efficiency and interestingness of reconstruction are the shorter terms of the works performed, the lower cost, etc [20]. However, the main disadvantage of this urbanization of the underground space is a small number of non-functioning underground structures suitable for the reconstruction project with adaptation to modern needs. Therefore, it is not surprising that at the implementation stage there are projects on the new construction of underground cities in Chicago, Moscow and Amsterdam [21]. For example, in Chicago, an underground city is planned, which includes 100 floors for apartments, offices and parking lots. For its construction it will be necessary to remove 230 million cubic meters of solid soil and come up with an innovative method of ventilation system [19].

7 Recommendations for the Organization of Underground Urbanization

The results of the conducted analysis of the research make it possible to draw some particular conclusions and recommendations on the organisation of underground urbanistics.

First of all, the provision of the necessary level of safety deserves to be noted, since the human resource is the most valuable and health should always be in priority. It is necessary to create an emergency evacuation scheme, to train personnel for possible unplanned situations and to provide each participant with special protective clothing for the construction period. Equally important is providing the territory with sufficient artificial lighting and fire-fighting systems.

Along with this, it should be noted again that the project should not contradict the already existing facilities and approved plans for the urbanization of the underground space. All elements of the project up to heating, water supply, ventilation and electrification must be coordinated with similar networks of other facilities.

In the same way, the obtained material allows us to conclude that it is necessary to perform soil analysis before the plan is approved, since additional supports, improvement of the ground, or even the transfer of the project to another, more favorable terrain may be required.

In connection with the above, it is worth noting the possibility of using different methods of penetration. For example, the method used for transalpine tunnels allows construction in complex geological conditions, when the terrain has radically different properties (including hydrological ones).

Depending on the hydrological conditions, a water regulation system should be chosen. In the case of high hydraulic pressure and/or increased alkalinity of water, which can lead to clogging of the drainage system, the structure must be completely waterproof. If the groundwater table is sufficiently low, then transverse drainage pipes and a special channel are created.

Due to the high cost of construction and engineering support of underground structures, it is necessary to take into account its maintenance. It should initially eliminate errors and inaccuracies in the project, because of which the safety and functioning of the structure can be threatened. It is more correct to calculate and predict in advance the future deformations and other defects that may arise in the design (Table 2).

Table 2. Recommendations for the organization of underground construction.

№	Problem	Solution search
1	Special requirements for the level of security	Development of a rational evacuation plan, high-tech fire-fighting systems, an extremely high degree of personnel training for possible emergencies, etc.
2	Architectural and engineering harmonization with existing buildings	The ground part (if any) must harmoniously fit into the existing building. The design solutions should ensure that they are consistent with similar networks of other facilities
3	The mechanics of an underground object	High-quality performance of all types of engineering surveys. Comprehensive assessment of the interaction of the structures of the object and rocks throughout the depth of penetration. Responsible approach to water regulation. Execution of high-precision calculations in modern software systems, BIM-modeling
4	Construction technology	Substantiation of methods of penetration depending on geological conditions. The choice of optimal and economically and technically sound methods, techniques and technologies of construction works
5	Engineering support. Providing a comfortable stay for people	Development of design solutions for providing the most comfortable lighting, close in quality to sunlight, temperature and humidity conditions, etc. Providing comfort due to architectural solutions, including green spaces. "Psychological" approach to live on the surface
6	Maintenance	The design possibilities of repair and construction works for the construction of a subterranean facility, including those from the point of view of the availability of individual structures

It is also worthwhile to pay attention to such an aspect as the reconstruction of existing facilities, since the specificity of underground urban planning lies in the complexity of the modernisation, and, consequently, in the use of other forms of repair work. It is necessary to create a special solid platform or a safe shield, under which the structure can continue to function [2].

8 Conclusion

The situation with the limited possibility of urbanization of underground space remains an acute problem of any city.

Identifying the merits and demerits of reconstructions of underground structures led to the following conclusions. In the reconstruction of existing facilities for new uses, earthworks are facilitated, thereby reducing financial costs. Thus, the terms of the works are reduced. However, there are very few non-functioning underground structures that are suitable for the reconstruction project. Therefore, it is more expedient, but not more profitable, to build new underground structures.

During analysis of the feasibility of reconstructing underground structures from an economic point of view, it was revealed that underground structures require less maintenance resources than infrastructure networks and numerous building chains. Nevertheless, for the construction of such structures, new approaches and construction technologies are required, which require additional costs. In addition, this type of work requires qualified personnel capable of carrying out the entire complex of mining and construction works.





In this way, the trend of developing underground space is relevant for most cities, but in spite of this, it should be noted that the efficiency of reconstructing underground facilities for new uses is quite high compared to new construction.

References

1. Alekseev, Yu., Belyaev, V.: Underground buildings and structures as a system element of interacting spatial environments of urban development. *Vestnik* **2**, 6–10 (2012)
2. Pustovojtenko, V., Gavrish, O.: Organization of integrated development of the underground space of megacities, vol. 32, pp. 106–110 (2010)
3. Denisov, Yu., Koren'kova, G.: On the need to develop. The underground space of cities, vol. 11, pp. 99–103 (2016)
4. Vartanov, A., Petrov, I., Fedash, A.: The main tendencies of underground construction and development of the subsoil of cities and the problems of designing underground objects in megacities and zones of urban industrial agglomerations, vol. 10, pp. 160–164 (2015)
5. Qihu, Q.: Present state, problems and development trends of urban underground space in China, vol. 55, pp. 280–289 (2016)
6. Hachatryan, V.: Design and development of underground space under buildings in the environment of existing buildings, vol. 6–1, pp. 112–115 (2015)
7. Labbe, M.: Architecture of underground spaces: from isolated innovations to connected urbanism. *Tunn. Undergr. Space Technol.* **55**, 153–175 (2016)

8. Pleshanova, M., Ivanova, A.: Underground construction is below zero, vol. 1, pp. 160–162 (2016)
9. Korotaev, D.: The use of underground space in Moscow, vol. 1, pp. 39–44 (2009)
10. Vahaaho, I.: An introduction to the development for urban underground space in Helsinki, vol. 55, pp. 324–328 (2016)
11. Pozel'skij, E.: Economic effect and reliability of long-term underground structures in the construction of high-rise buildings, vol. 6, pp. 10–11 (2011)
12. Zhou, Y.: Assessment and planning of underground space use in Singapore, vol. 55, pp. 249–256 (2016)
13. Sevryukova, K.: Osnovnye etapy razvitiya podzemnoj urbanistiki (2017). <http://izron.ru/articles/problemy-i-dostizheniya-v-nauke-i-tekhnikе-sbornik-nauchnykh-trudov-po-itogam-mezhdunarodnoy-nauchno-sektsiya-10-stroitelstvo-i-arkhitektura-spetsialnost-05-23-00/osnovnye-etapy-razvitiya-podzemnoj-urbanistiki>
14. Lezina, E.: The current state and prospects for the development of underground urban planning, vol. 5, pp. 71–73 (2015)
15. http://www.bbc.com/russian/society/2015/05/150513_vert_fut_will_we_ever_live_undeground (2017)
16. Semenova, O.: Teoreticheskie problemy gradostroitel'nogo planirovaniya podzemnoj chasti gorodov (2017). <http://www.undergroundexpert.info/stati-i-doklady/item/1788-problemy-planirovaniya>
17. ITA-AITES. Urban underground (2017). <https://www.ita-aites.org/ru/use-of-underground-spaces/underground-planning>
18. Skupov, B.: Vse glubzhe, glubzhe i glubzhe. Strategiya innovacionnogo razvitiya podzemnogo gorodskogo prostranstva (2017). <http://ardexpert.ru/article/4137>
19. Sysoev, A.: Underground city (2017). http://pm-world.ucoz.ru/blog/podzemnyye_goroda/2012-01-24-20
20. Brajla, N., Lazarev, Y., Romanovich, M., Simankina, T., Ulybin, A.: Modern problems of building science. Technol. Technol. **141** (2017)
21. Simankina, T., Brajla, N., Kanyukova, S.: Reclamation trend of underground construction, vol. 165, pp. 1757–1765 (2016)
22. Admiraal, H., Cornaro, A.: Why underground space should be included in urban planning policy. And how this will enhance an urban underground future, vol. 55, pp. 214–220 (2016)
23. Besner, J.: Underground space needs an interdisciplinary approach, vol. 55, pp. 224–228 (2016)
24. <http://russian7.ru/post/commercial/2016/02/21/urbanizaciya-podzemnogo-prostranstva> (2017)
25. <https://www.ita-aites.org/ru/how-to-go-underground/operation/maintenance> (2017)
26. Adigamova, Z., Lihnenko, E.: The development of underground space as a solution to urban urbanization problems, pp. 4–8 (2016)
27. Anoshkin, V.: Modern aspects of underground urban planning, vol. 30, pp. 6–11 (2015)
28. Bazilevich, M., Kozyrenko, N., Ivanova, A.: Typology of underground structures, vol. 1, pp. 133–136 (2011)
29. Belyaev, V.: Comprehensive approach to the development of the underground space of cities as a way to their sustainable development, vol. 9, pp. 109–114 (2014)
30. Belyaev, V.: Urgent tasks of development of the underground space of the capital, vol. 1, pp. 77–79 (2011)

Organizational-Technological Solutions, Risks and Reliability of the Preparatory Period of the Renovation of Territories

Vitaliy Chulkov¹ , Arkadiy Kiselev² , Garrik Maloyan¹ ,
and Anatoly Efimenko¹ 

¹ Moscow State University of Civil Engineering,
Yaroslavskoye Sh. 26, 129337 Moscow, Russia

² Orel State Technical University,
29, Naugorskoe shosse, 302020 Oryol, Russia
kiselev@mail.ru

Abstract. Features of renovation of built-up areas are considered. The main difficulties in carrying out the renovation process are identified. The concept of the constraint factor of the building is defined. A method for analyzing and assessing constraints for selecting optimal organizational and technical solutions for the renovation of territories is proposed. The production of works for the reconstruction of a single object in the conditions of the existing urban development is a complex engineering problem that occurs in any developed city, the history of which totals at least several hundred years. It is associated with numerous restrictions, prohibitions and difficulties created by the city authorities, as well as with the need to use advanced engineering technologies and solutions. Renovation is one of the varieties of this reconstruction.

Keywords: Organizational-technological solutions · Risks · Reliability
Renovation of territories · Reconstruction

1 Introduction

According to the proposal of Vedeneev N.S. and Maklakova T.G. the term “renovation” and its definition of renovation is the compulsory release of the territory to ensure the possibility of new construction, regardless of the degree of safety of the buildings located on it. The term was applied to the construction reconstruction by Resin V.I. in the directive documents of the Government of Moscow. In the theory of reorganization and the basic cycle of reorganization, the reorganization is considered as one of four successive stages [1–3, etc.], regulated by the rules of production [4].

Currently, Moscow is implementing a program for the renovation of individual residential areas. This program replaced the bad experience of spot-building.

The main difference between the renovation projects is their complexity, which means a complete demolition of housing stock, replacement of communications, repair of roads, reconstruction of infrastructure and landscaping [5].

According to Moskomarkhitektura [6], over 45% wear has more than 14% of the city's housing stock. For this part of the fund, the physical depreciation index reaches 55%, which leads to additional costs for maintaining this housing, lowering the comfort level of living and requires the adoption of program measures for the renovation, reconstruction and renovation of existing housing.

The moral and physical deterioration of buildings and communications, the lack of space for new construction and the requirements for more efficient use of the territory - all this contributes to the development of a renovation program, enabling in the near future to take a modern look to many of the "aging" quarters of the city. The purpose of the study was to identify the specifics of organizational and technological solutions for renovating urban areas in constrained conditions. Attempts to address this problem were made more than 10 years ago [7], but at that time they did not find understanding in the administrative-command layer of the Moscow leadership. Today, the implementation of this task is one of the most important socio-economic and strategic goals of the city-planning policy of the Moscow government.

Both the domestic researchers studied the problems of designing the technology and organization of building reconstruction and reconstruction of buildings and structures (Baranovsky A.V., Zolotnitsky N.D., Gendel E.M., Onufriev N.M., Bolshakov V.A., Rogonsky V.V., Kolotilkin B.M., Gusakov A.A., Polyakov E.V., Okon I.P., Budanova N.P., Titova I.A., Ignatyuk M.S., Prokhorkin S.V., Ganiev K.B., Dmitriev M. N., Poryvay G.A., Lapshin E.I., Balk V.A., Dzhililov F.F., Belyakov Yu.I., Redunik A. F., Fedoseenko N.M., Bytko A.I., Frolkin V.T., Sedikh S.V., Frosin A.V., Karsky N.Z., Ivanov R.T., Abramov L.I., Manaenkova E.A., Bolotov V.P., Sataev A.G., Bondar F.I., Yurkin N.M., Zelentsov L.B., Lazarev G.I., Biryukov G.S., Plebukh A.N., Chulkov V. O., Beyer V.E., Belov A.N., Sardaryan T.G., Bashmakov A.N., Rakhimov K.D., Alekseev Yu.V., Aripjanov A.A., Zakharov V.A., Afanasyev A.A., Mokhov A.I., Semechkin A.E., Burdacheva N.A., Ivaschenko A.I., Veykum I.I., Ovchinnikov S.G., Kuznetsov S.V., Golubeva N.N., and others) and foreign experts. They proved that the development of projects for building reconstruction is much more complicated than the design of new construction: multiple additional measurements and surveys of the reconstructed buildings and their premises are necessary, an examination of the suitability of structural elements and individual structures, a study of the layout of schemes of various types of engineering communications, etc.

2 Results and Discussion

One of the problems of organizing the renovation process is that most of the facilities are in close proximity to other buildings, communications, roads, cultural monuments, etc. The planning of work on building reconstruction is often complicated by outdated methods of preparing documentation that certifies the rights of participants in the process of transforming territories into federal and municipal land plots. Norms and rules for the participation of management companies in the exploitation of lands on which renovation objects are located are not always defined.

Departmental disunity, the need to participate in this work of local governments, investors, the population, many organizations and enterprises of different forms of

ownership make this process even more difficult. In addition, special attention should be paid to linking the adopted decisions with innovations in housing policy and in the system of transport and social and infrastructure services to residents.

The system approach to every concrete house, quarter, micro district is important. To date, there is practically no developed scientific, methodological and regulatory framework for analyzing, evaluating and selecting rational options for organizational and technological solutions in the development of renovation projects.

Essential help in optimizing this activity can be the application of special methods of planning, modeling and analysis, based on the extensive use of computer technology.

Obviously, the most important factor influencing the choice of organizational and technical solutions (OTS) is the constraint factor. This is "... the conditions of the existing urban development, suggesting the presence of spatial obstacles on the construction site and the adjacent territory, the restriction on the width, length, height and depth of the working area and underground space, the location of construction machinery and vehicles, the increased degree of construction, Ecological, material risk and, accordingly, enhanced security measures for those working in the construction industry and the living population" [7].

A competent analysis of this factor, carried out at the early stages of preparation of renovation projects, helps to choose the right solutions and, thereby, to reduce costs, reduce deadlines, improve the quality and safety of construction (Fig. 1).

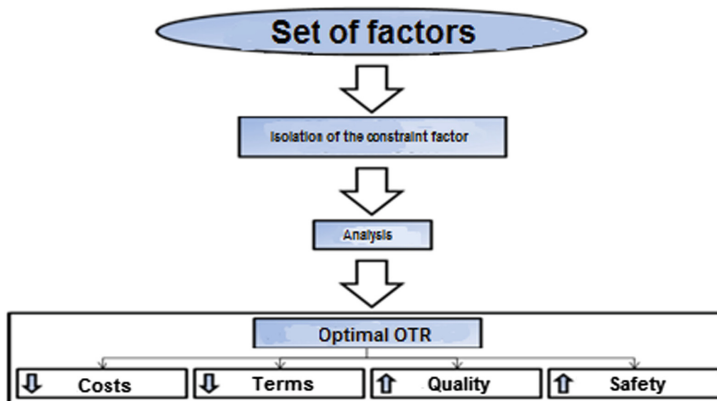


Fig. 1. The choice of optimal OTS based on the analysis of the constraint factor.

The proposed algorithm of analysis is based on the consideration of the constraint factor as an array of effects of individual "objects of influence" on the relevant "subjects of influence" [8] (Kiselev AA, 2010, Fig. 2).

The main significant "objects of influence" (OI):

- operated buildings and structures;
- roads;
- existing communications.

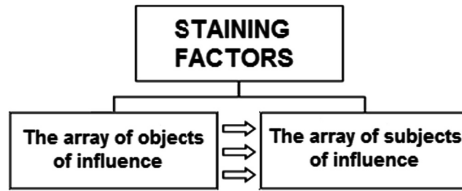


Fig. 2. Separation of the constraint factor into objects and subjects of influence.

“Subjects of influence” (SI) - aspects of organizational and technical solutions, the implementation of which is limited to “objects of influence.” The main ones are:

- the boundaries of the construction site;
- the form of the three-dimensional organization of building (morphological type);
- placement and use of construction and lifting equipment.

Each object of renovation characterizes a unique set of OI and SI.

The result of the analysis of the effect of each OI on each SI is conveniently recorded in the form of a matrix (Fig. 3).

	SI ₁	SI ₂	SI ₃	...	SI _m
OI ₁	1	1	0		1
OI ₂	0	0	1		0
OI ₃	1	0	0		1
...					
OI _n	0	1	0		1

Fig. 3. Impact matrix.

The unit in the matrix means the presence of the effect of OI_i on the corresponding SI_j, and zero means its absence.

Having excluded the links OI_i - SI_j with “zero” influence, we pass to the analysis of significant “single” effects.

Since renovation projects by their definition imply a complete replacement of communications, infrastructure and roads (which in our case are objects of influence), it is important to divide the “eliminated” and “not eliminated” links.

The objects of the final analysis will be “single” “non-removable” links (Fig. 4).

The data obtained during this analysis will help to find the most effective and optimal organizational and technological solutions reflected in the relevant sections of the renovation project, for example, in the development of a construction master plan, drawing up a calendar and network schedules for the production of works.

During the construction of objects the following main stages are distinguished:

- feasibility study;
- design of construction preparation and construction;

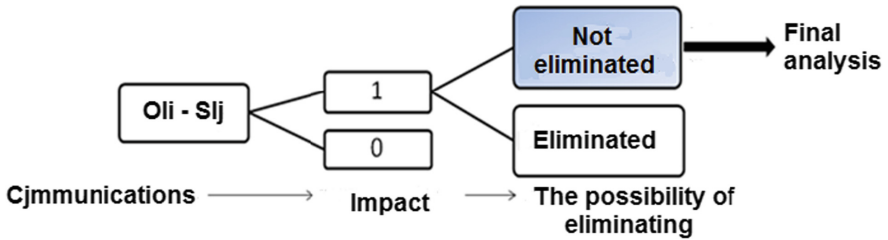


Fig. 4. Algorithm for analysis of relationships of the impact matrix.

- implementation of preparation for the construction of the facility;
- construction of the facility;
- mastering the constructed object.

The development of construction requires an extensive increase in the pace and scope of works of the preparatory phase of construction (PPC), which is decisive in relation to all subsequent stages of the life cycle of a newly constructed or reorganized building project. Methods and methodologies for the development of design solutions for PPC and their quality significantly affect the engineering, technical and economic indicators of the processes of construction. Errors and miscalculations at the design stage of PES with high probability lead to emergence of contingencies, the liquidation of which requires additional labor, material and financial resources in unpredictable volumes.

One of the important criteria of PPC and the construction industry as a whole is organizational and technological reliability (OTR), one of the aspects of which is the consideration of specific features of organizational and technological processes for the construction of a particular facility (the personification of the model of its OTR).

Evaluation of design solutions requires:

- introduction of step-by-step modular consideration (discretization) of organizational and technological processes (works);
- taking into account the specific features of the implementation of the organizational and technological work of PES;
- the ranking of technological processes as their degree of automation increases.

All this allows us to propose a model for a multivariate analysis of the risks of implementing PPC project solutions and minimizing their consequences. The model is a set of eight stages of assessing the risks of the implementation of the design solution of PPC, that is, taking into account input and output criteria obtained at previous stages or defined for future stages of the model:

1. The risks inherent in PPC;
2. Reliability of technological processes of PPC;
3. Risk diagnostics;
4. Means of automation of processes;
5. Methodologies for achieving the required accuracy of results;
6. Means of interpretation of diagnostic results;

7. The means to ensure the reliability of the main processes as algorithms to prevent the risks of the technological processes of the servicing subsystems to ensure the reliability of the main processes;
8. Sledging (documenting and archiving), forming a database of functioning.

The analysis showed that the normative and directive documents of the Russian Federation, domestic and foreign researchers for the synthesis of design solutions and technologies for their implementation in automated systems of PES recommend using as a base model a human-machine (natural-artificial) functional system “man-technology-environment, TTE” [1].

Synthesis of design solutions is possible with step-by-step modular examination of organizational and technological processes. Application of the model of modular (discrete) structuring of organizational and technological processes of PPC provides an increase in the complex reliability of the technological process of the TTE system.

The cycle of “life” of the technological process in the TTE system is a cycle of synthesis of the design solution and consists of three “sistemokvantov” (the term of Sudakov K.V.) Qn, Qfa and Qbz [9].

Qbz is structured into three components (Qdm, Qnpz and Qpa).

Qn and Qfa are respectively the areas of normative work and the “failure” of the TTE system with respect to the Q parameter.

Qbz is the “buffer zone, BZ”, in which the TTE system regularly implements its regulatory functions, but, in the absence of corrective actions, it is guaranteed to pass to Qfa (inaction leads to irreversible consequences).

Qdm is the area of diagnostics and monitoring in the BZ, fixing the disturbing effect, which can bring the TTE system to the Qfa area (to create an abnormal situation) or to identify the tendency of the deviation of the values of the parameter Q in the Qfa domain.

Qnps is the area of the algorithm for preventing an abnormal situation (the transition of the values of the parameter Q to the Qen domain);

Qpa is the local implementation area of the algorithm for preventing an abnormal situation.

An important aspect of the global notion of “reliability” is complex reliability. For the TTE system, this is the average quadratic value of the reliability of each component of the TTE system (human, technical and environmental reliability).

Diagnosis of the current state of the reliability of the operation of the TTE system, monitoring of changes in this state and the impact on this state represent a closed sequence (cycle) of the processes performed, in which the end point of the implementation of the Qnen system and the beginning of the realization of the Qn are taken as the “beginning” or “cycle break point” when it is linearly mapped.

When investigating complex reliability by two parameters, the boundaries of the transition between system-quanta and their components are the achievement by either of the two parameters of the threshold value. Evaluation of the operation of the TTE system by two parameters is not always sufficient. If it is necessary to evaluate the complex reliability for more than two parameters or to enter an additional parameter to evaluate the implementation of the algorithm for preventing an abnormal situation in

two parameters (i.e., creating a system to prevent an abnormal situation for the algorithm being implemented), it is advisable to use the Radishchev-Memke drawing.

An important aspect of the synthesis and analysis of the design solution is the evaluation of its rationality by significant criteria (parameters) determined by the expert group. The design solution is rational if the value of its critical parameters is in the allowable range of values. Allowable and unacceptable threshold values of the selected parameters are advisable to represent in the matrix form (RZ, y).

Comparing the values of the critical parameters of the design solution $U(p)$ with the matrix RZ, y , we can form a conclusion about the rationality of the design solution. Comparison of the last row of the matrix RZ, y with each of the preceding rows by the criterion of “proximity” Zhuravlev Yu.I. Then it is possible to calculate the degree of correlation of the design solution with the threshold values of the critical parameters.

If the synthesized design solution admits risks but is rational, they design a model of an automated system for compensation of risks of the design solution of the PPC based on synthesis and analysis data.

3 Conclusion

When designing design solutions and testing in operating conditions, the following conclusions were made:

1. The analysis of the theory and practice of evaluation, sampling and synthesis in the process of designing and implementing the preparatory stage of the renovation of territories revealed a significant demand for the development of methods and models for the analysis and synthesis of such design solutions that compensate for the risks of performing organizational and technological construction processes and develop models of automated systems on their basis;
2. The proposed model allows to take into account the specific features of the performance of the organizational and technological works of the preparatory stage, to rank the technological processes as the degree of automation increases;
3. The proposed model of modular structuring of organizational and technological processes of the preparatory stage of the renovation of the territory provides the synthesis of organizational solutions and technologies for their implementation (the model of the life cycle of the technological process with the allocation of a specific buffer zone);
4. The proposed concept of analysis and synthesis of design solutions for the organizational and technological work of the preparatory phase in the CAD PPC allows to develop a model of an automated system for compensation of risks;
5. The developed models are used in the synthesis and analysis of design solutions for the preparation of construction, the implementation of preparatory works for renovation in the construction of temporary local roads in the territory of the Republic of TUVA and the Vologda region.

The realized rational variant of the design solution ensured the reduction of the prime cost and the reduction of the terms of the preparatory works for the renovation of housing construction projects in the Irkutsk region, taking into account seismic

uncertainty. The proposed models can be adapted to the synthesis and analysis of design solutions for other stages of housing and industrial construction.

References

1. Chulkov, V.: Reorganization. Organizational-anthropotechnical reliability of construction. SvR-ARGUS, Moscow (2005)
2. Volkov, A., Chulcov, V., Kazaryan, R., Fachratov, A., Kyzina, N., Gazaryan, K.: Components and guidance for construction rearrangement of buildings and structures within reorganization cycles. *Appl. Mech. Mater.* **580–583**, 2281–2284 (2014). <https://doi.org/10.4028/www.scientific.net/AMM.580-583.2281>
3. Volkov, A., Chulcov, V., Kazaryan, R., Gazaryan, R.: Cycle reorganization as a model of dynamics change and development norm in every living and artificial beings. *Appl. Mech. Mater.* **584–586**, 2685–2688 (2014). <https://doi.org/10.4028/www.scientific.net/AMM.584-586.2685>
4. On the approval of the rules for the production of earthwork and construction works, laying and reorganization of engineering networks and communications in Moscow: the Moscow Government Decree of 08.08.2000. №. 603. Collection of the legislation of the Russian Federation
5. <http://www.radiomayak.ru/tvp.html?id=90752&p=10#fl>
6. <http://rway.ru/Bulletines/Item.aspx?id=445>
7. Karaoglanov, V.: Organizational and technological design of the reconstruction of buildings: Diss. Cand. those. Sci. TsNIIOMTP, Moscow (2006)
8. Kiselev, A.: Choice of organizational and technical solutions for the renovation of territories in the conditions of the existing urban development. Management of investment and construction and housing and communal services: International Collection of Scientific Works. MGAKHiS, Moscow (2010)
9. Sudadov, K., Gusakov, A.: Information Models of Functional Systems. The New Millennium Foundation, Moscow (2004)
10. Volkov, A., Sedov, A., Chelyshkov, P.: Usage of building information modelling for evaluation of energy efficiency. *Appl. Mech. Mater.* **409–410**, 630 (2013)
11. Garyaeva, V., Garyaev, N.: Integrated assessment of the technical condition of the housing projects on the basis of computer technology. In: Proceedings International Conference Computing in Civil and Building Engineering (2014)
12. Ginzburg, A., Kachanov, S.: Methodology for building automated systems for monitoring engineering (load-bearing) structures, and natural hazards to ensure comprehensive safety of buildings and constructions. *Int. J. Appl. Eng. Res.* **11**(3), 1660 (2016). Research India Publications
13. Ginzburg, A., Khripushin, A.: Risk management in oil refinery construction projects. *Appl. Mech. Mater.* **411–414**, 2313–2316 (2013)
14. Ginzburg, A., Ryzhkova, A.: Accounting “pure” risks in early stage of investment in construction projects with energy efficient technologies in use. *Appl. Mech. Mater.* **672–674**, 2221 (2014). Trans Tech Publications, Switzerland
15. Kuzina, O.: Components of functional information model of city environment reorganization in interactive mode. In: MATEC Web of Conferences, vol. 73, p. 07013 (2016)
16. Gumerova, E., Gamayunova, O., Shilova, L.: The optimal decision of insulation in cladding structures for energy efficient buildings. In: MATEC Web of Conferences, vol. 106, p. 06020 (2016)

17. Hans-Joachim, B., Abdur Rehman, N., Ignatova E.: Can BIM support better working conditions for low-skilled labor? In: 14th International Conference on Construction Applications of Virtual Reality CONVR 2014, pp. 44–51 (2014)
18. Volkov, A.: General information models of intelligent building control systems: basic concepts, determination and the reasoning. *Appl. Mech. Mater.* **838–841**, 2973 (2014)

Energy Efficiency: Energy Saving Solutions for Transportation Facilities

The Study of Compact Convective Stream Formed by Use of Recessed Floor Convection Heaters with Natural Air Circulation

Viktor Pukhkal^(✉)  and Voldemar Taurit 

Saint Petersburg State University of Architecture and Civil Engineering,
Vtoraja Krasnoarmejskaja ul. 4, St. Petersburg 190005, Russia
pvallll@rambler.ru

Abstract. To prevent an inflow in serviced room zone of descending cold airflow from translucent structures recessed floor convection heaters with natural convection are used. The computational model and recessed floor convection heater's operation simulation in "ANSYS Fluent 14.5" software package with different distances from a glassing to a convection heater are developed. Studies are carried out for "short" heat source given 0.4 relation of convection heater's finned section length to a glassing length relative to each convection heater specified by a possibility of air bleed over convection heater's sidewall. Temperature and velocity fields in the room are calculated. Room's natural convective streams (descending cold airflow near the glassing and ascending warm airflow from the convection heater) are described. The conditions for use of recessed floor convection heaters with natural air circulation are determined.

Keywords: Heating · Residential and public buildings
Recessed floor convection heater · Natural convection

1 Introduction

Descending cold airflows near glass light apertures entering serviced room zone create an undesirable state of microclimate. Heating appliances (convection heaters with natural or forced air circulation) built into the floor (recessed floor convection heaters) are used to prevent cold air inflow [1–10]. The convection heater is placed directly near a glassing or between 80 and 350 mm further from it.

The convection heater's heat flow was determined experimentally and airflows and temperature fields were simulated inside a room with the natural convection heater installed [3]. It was determined that radiant heat flow's share of the convection heater output is less than 1% and therefore radiant heat flow could be neglected during calculations.

The mathematical simulation of temperature and velocity fields inside a room which dimensions are $4 \times 4 \times 2.6$ m with a 2×2.4 m window was performed (Fig. 1). A "BITHERM Floor" natural convection heater (dimensions: $2000 \times 245 \times 55$ mm) was installed inside the room 70 mm further from the glassing. Specific surface heat flow on the glassing was set at $38,4 \text{ W/m}^2$ and a heat flow on an outer wall was set at 8 W/m^2 . Heat element's surface area temperature was assumed to be equal $50 \text{ }^\circ\text{C}$.

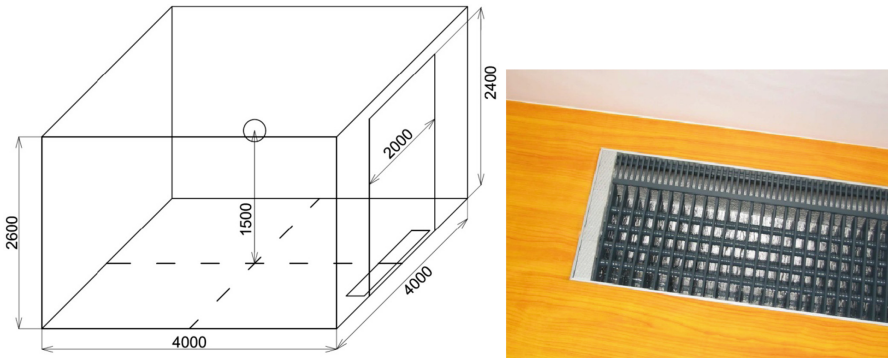


Fig. 1. Room's computational diagram and the convection heater view

It was determined under simulation conditions that heated airflow from convection heater adheres on a glassing surface (Fig. 1). In the upper volume of the room a closed circulation zone with descending cooled airflow is produced when airflow turns and adheres to a ceiling. Room's computational diagram and results of temperature and velocity fields study are shown in Figs. 1, 2 and 3.

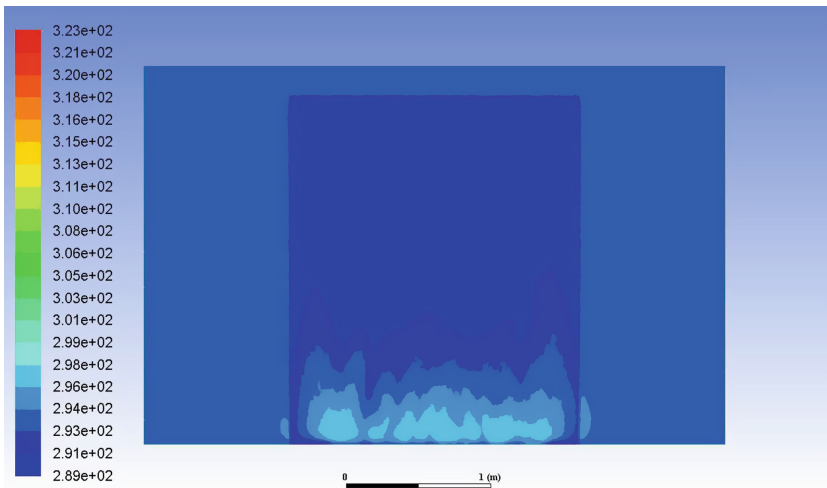


Fig. 2. Temperature field of an inside surface of the outer wall and the glassing

The research allows drawing conclusion that convective airflow from the convection heater developed near a vertical cooled barrier (glassing) has a tendency to adhere. Convection streams' adhesion has not been sufficiently studied. Therefore the study's goal is to obtain qualitative characteristics of convective airflow development in relation to a distance between the glassing and the convection heater. It was determined under simulation conditions that heated airflow from convection heater adheres to glassing surface (Figs. 4 and 5). In the upper volume of the room a closed circulation zone with descending cooled airflow is produced when the flow turns and adheres to the ceiling.

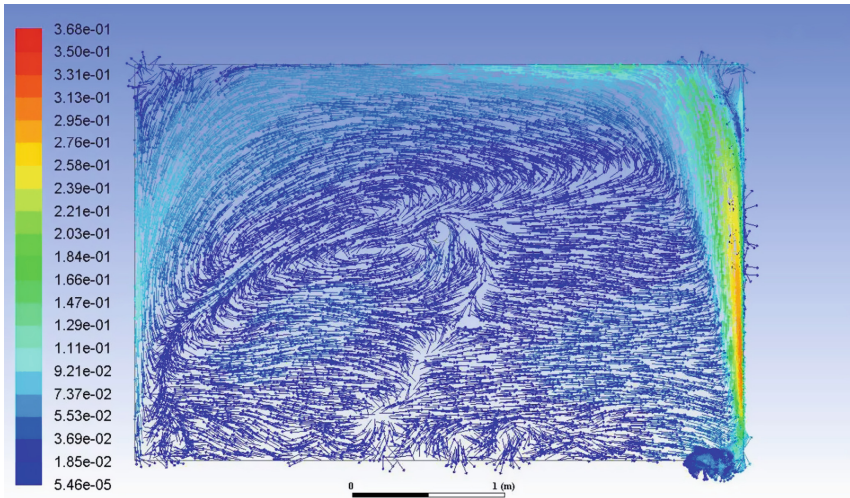


Fig. 3. Velocity field on the convection heater's axis cross-sectioned by perpendicular to the window surface

2 Methods

The simulation of convection heater's operation is performed in "ANSYS Fluent 14.5" software package to take into account actual operating conditions of the recessed floor convection heater and to study in detail velocity and temperature fields' distribution inside the room.

A model room is specified to have dimensions typical for residential and public buildings: width—3 m; depth—6 m; height—3 m (Fig. 4). A window's dimensions are 3×3 m. A KRKP-type convection heater was used for a purpose of modelling [10].

The following conditions were specified during simulation:

- inside surfaces temperature (side walls, floor, ceiling) - plus 18 °C;
- outside air temperature - minus 24 °C;
- glassing's outside surface heat-transfer coefficient - $23 \text{ W}/(\text{m}^2 \cdot \text{K})$;
- glassing's inside surface heat-transfer coefficient - $8 \text{ W}/(\text{m}^2 \cdot \text{K})$;
- glassing's average heat-transfer resistance - $0.685 (\text{m}^2 \cdot \text{K})/\text{W}$;
- heating element's surface temperature – 64.5 °C
- convection heater's heating element position - in the middle of a casing.

During simulation the distance between the glassing and the convection heater (l, mm) was changed from 0 (near glassing) to 500 mm by 100 mm step.

The study assumes that finned section of convection heater's length is related to glassing's length per each convection heater (heat source) – l_{rel} – as 0.4 (short heat source). The 1 m wide room's cell where the convection heater was installed is selected (Fig. 6).

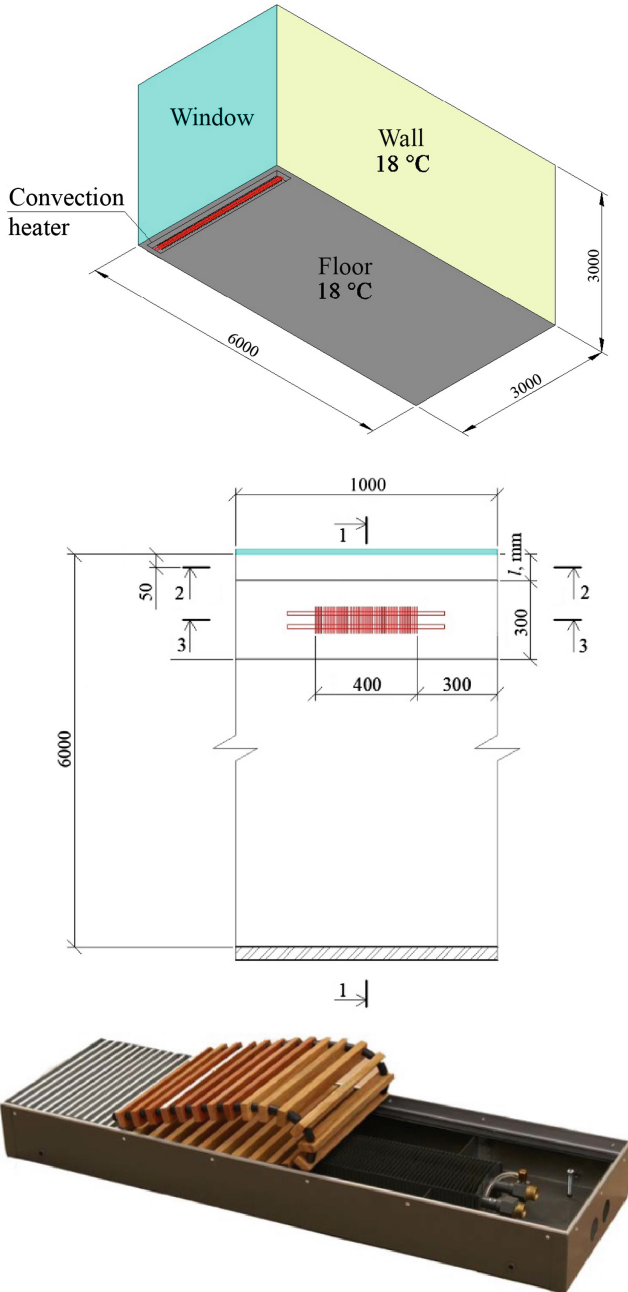


Fig. 4. Room's computational diagram and the convection heater's view

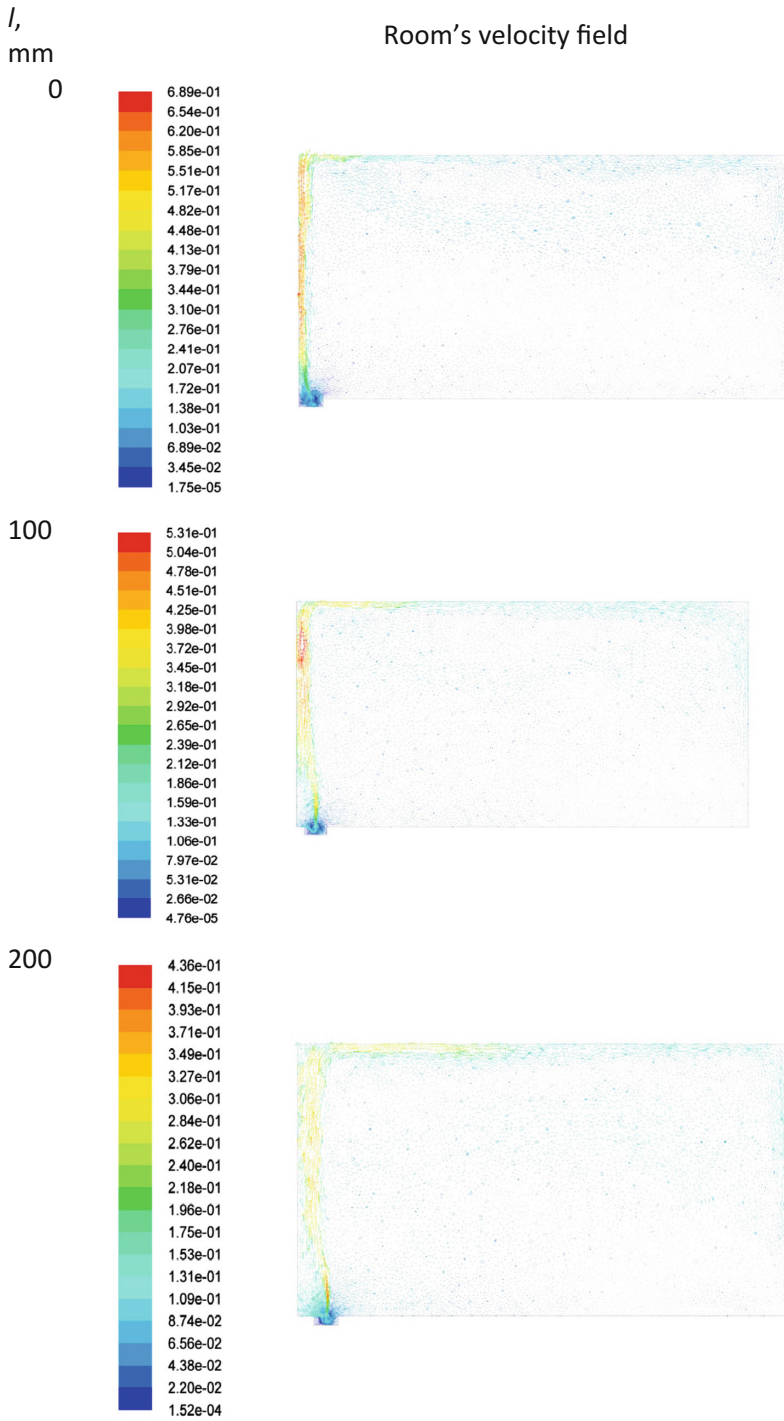


Fig. 5. Room's velocity field simulation result (cross-Section 1-1)

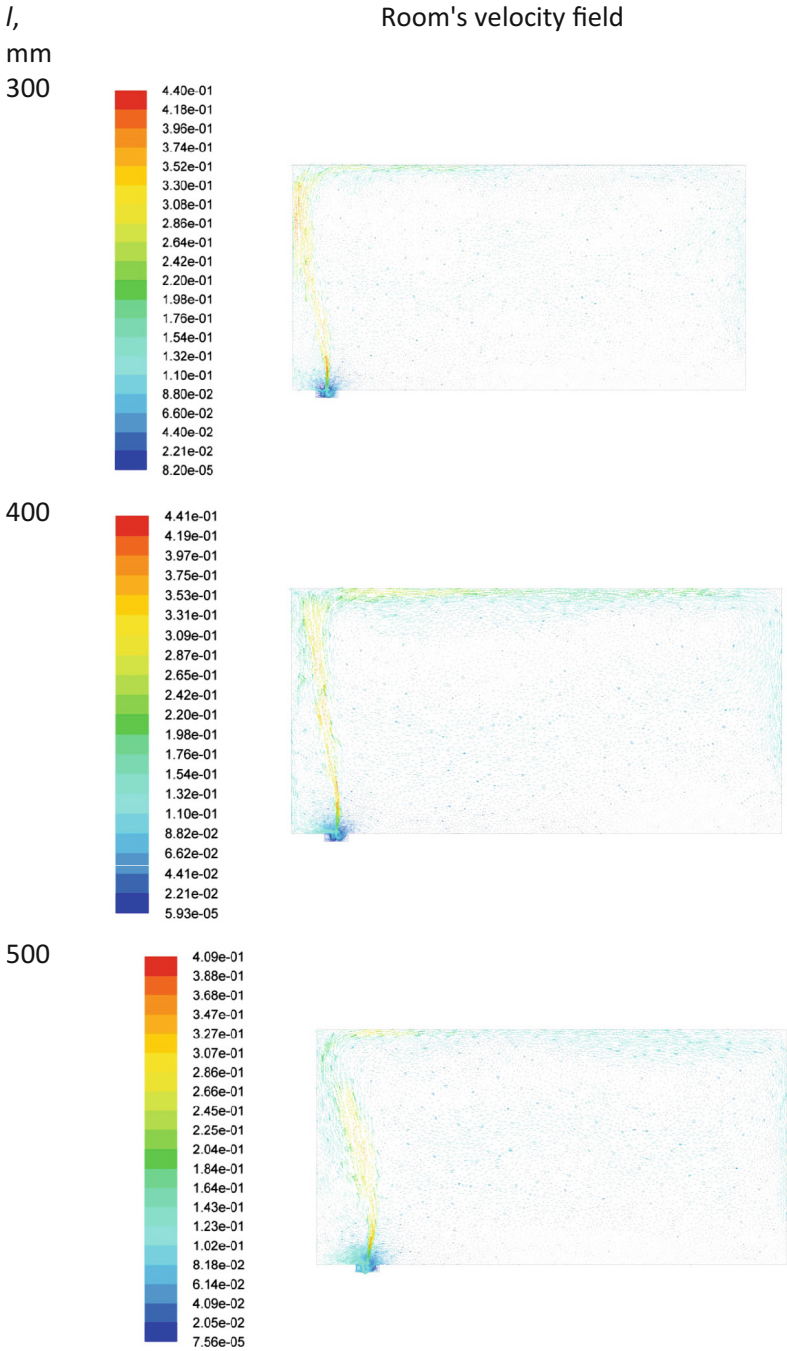


Fig. 5. (continued)

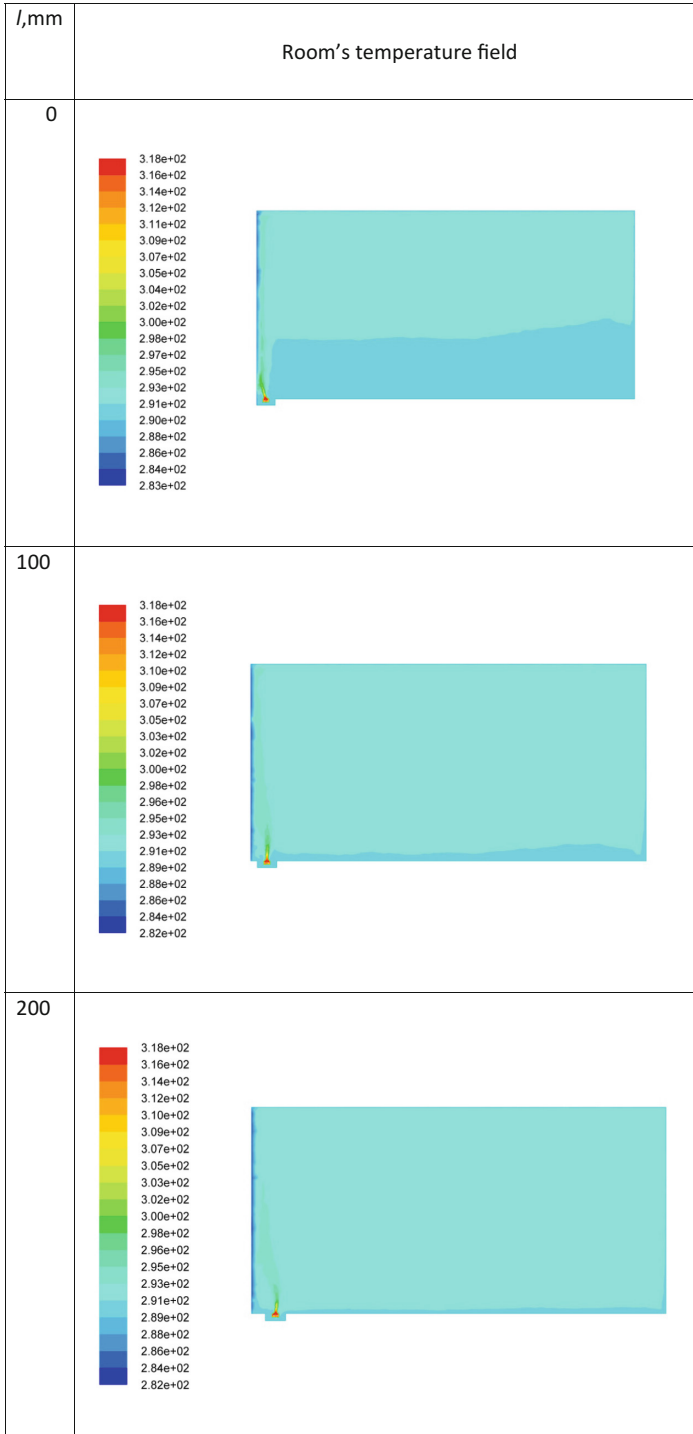


Fig. 6. Room's temperature field simulation results (cross-Section 1-1)

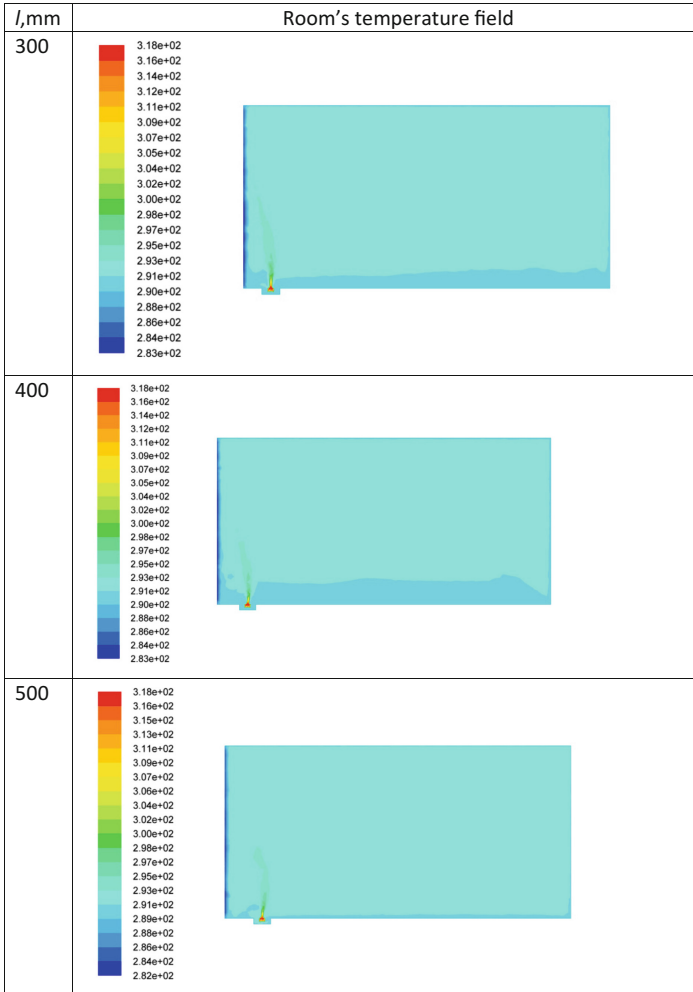


Fig. 6. (continued)

3 Results

Descending convective wall-adjacent flat streams are developed near cooled vertical surface of the glassing under gravitational pull. Conditions of its' formation are largely influenced by adjacent horizontal surfaces (floor, ceiling) and airflow velocity in the room produced by heat source.

Room's velocity and temperature fields' simulation results obtained under variation of distance between the glassing and the convection heater (l mm) are shown on Figs. 5, 6, 7 and 8. These calculations allow estimating a nature of an interaction of descending airflow near glassing and ascending airflow from convection heater under assumed equality of convection heater's heat flow to heat loss through glassing.

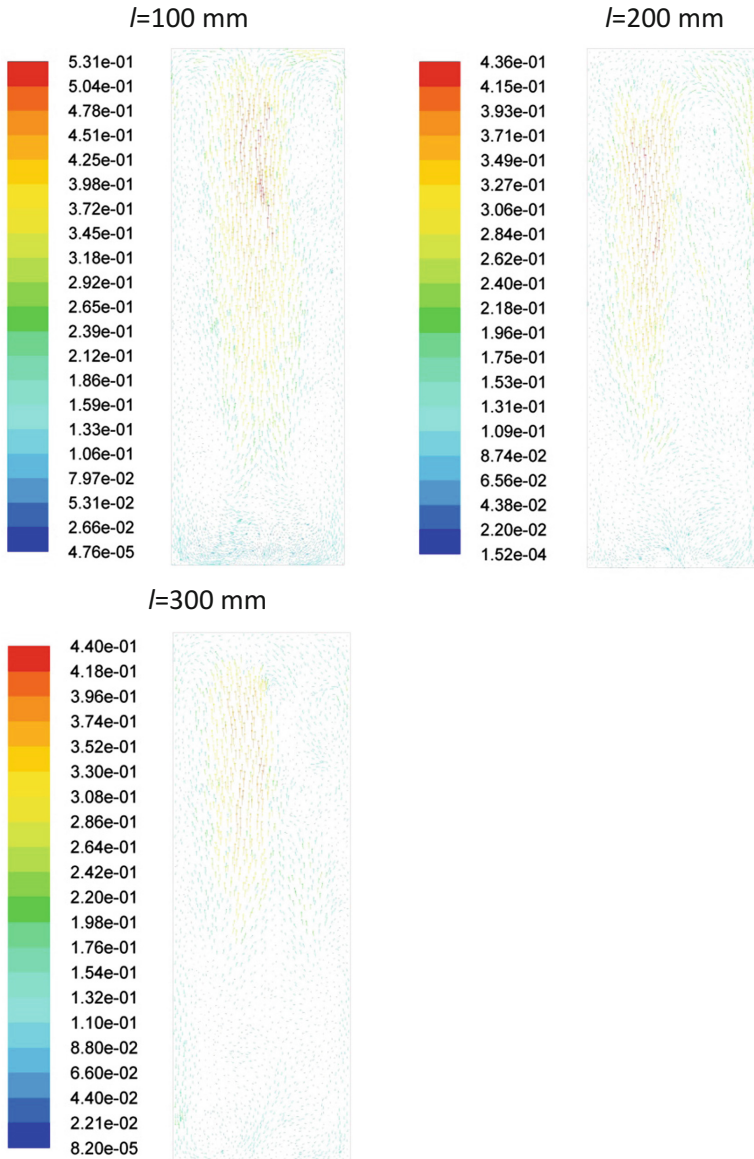


Fig. 7. Room's velocity field simulation results (cross-Section 2-2)

At a distance $l < 400$ mm warm airflow adheres to the glassing. At a distance $l \geq 400$ mm convective stream over heat source touches a barrier only in the upper part of the glassing. When the convection heater is placed between 100 and 300 mm from the glassing a uniform temperature field is produced inside the room (Fig. 6).

In starting section of compact convective stream when $z/b < 1$ (where z – vertical distance from a centre of convection heater's heating element's upper surface, m; b – width

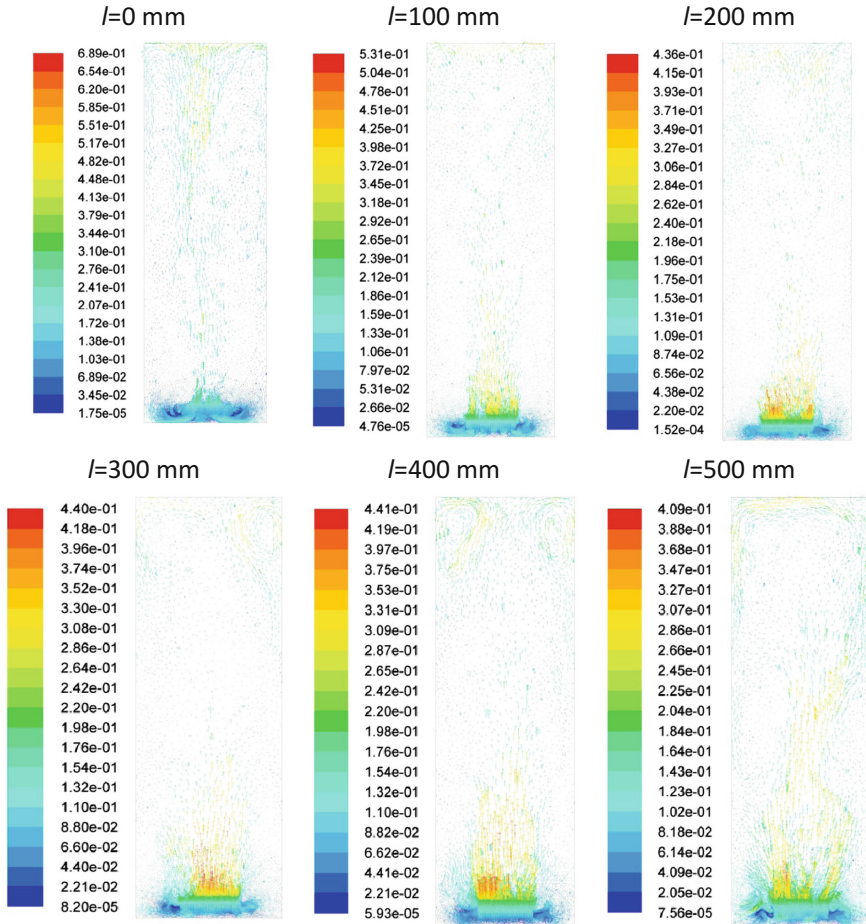


Fig. 8. Room’s velocity field simulation results (cross-Section 3-3)

of convection heater’s heating element) stream’s radius decreases and a vertical wall located near heat emitting element does not prevent bleeding of surrounding air for stream inflow (Figs. 5, 6, 7 and 8).

In main section of the stream when $z/d > 1$ stream’s radius R_{str} begins to increase and stream’s boundary approaches wall’s surface. The space for surrounding air bleeding decreases and pressure difference is produced which causes stream’s axis to curve and then stream adheres to the wall. Compact convective stream’s adherence effect can appear higher than z_{adh} level where stream’s boundary touches the wall. In such case stream’s radius R_{str} becomes equal to a distance Y_0 from the heat source axis to the glassing. After adherence the stream becomes half-restricted and stream’s surface area through which surrounding air’s admixture occurs decreases compared to unrestricted convective stream.

An increase of a distance between the glassing and the convection heater to 500 mm causes vertical formation of closed circulation zones near glassing's surface.

The comparison of the results obtained with the results in [3], which are shown on Fig. 1, indicate that nature of room airflows' circulation and temperature field are specified by dimensions (depth) of the room. The calculation results shown on Figs. 4 and 5 demonstrate that adhering convective stream from the convection heater, when distance between it and the glassing does not exceed 400 mm, rise to room's upper volume where higher temperature zone is formed. The unified circulating airflow does not form in the room but several closed circulation zones are formed instead.

4 Conclusions

1. Recessed floor convection heaters with natural circulation, having heat flow equal to heat loss through the glassing and installed no further than 400 mm from the glassing, produce convective stream adhering to the glassing and protecting the room from descending cold air near the glassing.
2. To eliminate unequal heating of glassing's surface the distance between recessed convection heater and glassing's surface should not be less than 100 mm.
3. It is recommended that the heating element of a floor recessed convection heater with natural air circulation should be installed inside a casing in close contact with a casing's wall proximate to the glassing or in the middle of the casing.
4. The convection heater is to be placed between 100 and 400 mm distance from the glassing.

References

1. Babiak, J., Olesen Bjarne, W., Petráš, D.: Low Temperature Heating and High Temperature Cooling Embedded. Water Based Surface Heating and Cooling Systems. REHVA (2013)
2. Boriskina, I.: Zdaniya i sooruzheniya so svetoprozrachnymi fasadami i krovlyami. Teoreticheskie osnovy proektirovaniya svetoprozrachnykh konstruksii [Buildings and structures with translucent facades and roofings. Theoretical basis of translucent structures design]. Inzhenerno-informatsionnyi Tsentr Okonnykh Sistem, Saint Petersburg, RF (in Russian) (2012)
3. Bašta, J., Legner, T.: Analýza podlahového otopného tělesa. ČVUT v Praze (2017). <http://elvl.cz/onas/pdf/clanek-16.pdf>
4. Composite authors Otopitel'nye pribory i poverkhnosti [Heating devices and surfaces]. Izdatel'skii Tsentr «Akva-Term», Moscow, RF (in Russian) (2012). ISBN: 978-5-905024-04-7
5. Federal'noe agentstvo po tekhnicheskomu regulirovaniyu i metrologii [Federal Agency on Technical Regulation and Metrology] GOST R 53583-2009: Pribory otopitel'nye. Metody ispytanií [Heating appliances. Test methods]. Federal'noe agentstvo po tekhnicheskomu regulirovaniyu i metrologii, Moscow, Russian Federation (2009)
6. Krupnov, B., Krupnov, D.: Otopitel'nye pribory, proizvodimye v Rossii i blizhnem zarubezh'e [Heating devices made in Russia and CIS countries] Izdatel'stvo Assotsiatsii stroitel'nykh vuzov, Moscow. RF (in Russian) (2010)

7. Makhov, L.: Otoplenie [Heating]. Izdatel'stvo Assotsiatsii stroitel'nykh vuzov, Moscow, RF (in Russian) (2014)
8. Mayorov, V.: Peredacha teploty cherez okna [Heat transfer through windows]. Izdatel'stvo ASV, Moscow, RF (in Russian) (2014)
9. Muller, M., Frana, K., Kotek, M., Dancova, P.: The influence of the wall temperature on the flow from the floor convector (experimental results). In: EPJ Web of Conferences, vol. 45 (2013). <https://doi.org/10.1051/epjconf/20134501130>. https://www.epj-conferences.org/articles/epjconf/pdf/2013/06/epjconf_efm2013_01130.pdf
10. Nauchno-tehnicheskaya firma OOO «VITATERM» Rekomendatsii po primeneniyu konvektorov «Gol'fstrim» («Izoterm- TD»), vstraivaemykh v konstruktsiyu pola [Recommendations for use of “Gol'fstrim” (“Izoterm-TD”) convectors which are built into the floor construction]. Second edn. NTF OOO «VITATERM», Moscow, Russian Federation (2008)

Analysis of the Strength Characteristics of Internal Sprayed Protective Coatings of Pipelines to Improve Energy Efficiency

Vladimir Orlov¹(✉) , Ilya Averkeev² , and Alexey Pelipenko¹ 

¹ Moscow State University of Civil Engineering,
Yaroslavl'skoye shosse, 26, 129337 Moscow, Russia
orlov950@yandex.ru

² Polyplastic Group, Ochakovskoe shosse, 18, 119530 Moscow, Russia

Abstract. The most part the RF pipelines require renovation because of their unsatisfactory state. Besides, the pipelines under operation are subject to biological fouling and at the result reduction of the living cross-section of pipes and increase of the hydraulic resistance and improve energy efficiency. One of the methods, which helps to prevent this situation, is application of a sprayed coating to the inner part of a pipeline. Due to many available market proposals, provision has been made of a complex of bench tests aimed at studying strength characteristics and computer simulation of two types of protective coatings to reveal their modifications during a period of time, i.e. Scotchkote 2400 («3M» Company), which is the most popular one and Subcote FLP, which is a prospective development by the NPP “Polyplastic”. Testing has been made at the electromechanical tensile testing machine Instron 3345 and simulation by the «Ansys» automated computer ware of the finite element analysis. The results of the performed tests permitted to determine the recommended coating thickness depending on the pipeline diameter.

Keywords: Pipelines · Trenchless renovation · Sprayed coatings
Scotchkote · Subcote · Wall thickness

1 Introduction

In the RF cities and residential localities, more than 60% of engineering pipeline systems of water supply and sewage are in an unsatisfactory state and need to be renovated and repaired without any delay. It consciously requires an urgent renovation of the pipeline transport [1, 2], that has been also stimulated by the adoption of the Russian RF Federal Law “On water supply and sewage” (№ 416-FZ) [3] in December, 2011.

The above provisions permit to state, that the problem of controlled renovation of water supply systems and their effective operation got the status of a governmental priority.

The questions of a reasonable use of water resources are relevant not only in Russia, but also in all over the world [4–6]. For example, such defects as corrosive and other deposits in the water pipes reduce the living pipe cross-section to 20% and 2–3 times increase the hydraulic resistance by comparison to the design values. To compensate the

pressure losses in the water supply pipelines, it is necessary to increase the pressure in the engineering lines to enable maintenance of the required consumption of the transported media, but it also leads to a higher electric power consumption [7].

To solve the state-of-the art situation, provision may be made of a prompt timely repair and renovation works of the pipeline networks using protective spraying coatings. There are two methods of the pipeline renovation by centrifugal spraying, which are widely used nowadays:

- Non-organic materials (for example, cement-sand mixtures). It prevents corrosion of the metal pipe interior wall and eliminates small fistulas and fissures, but does not increase the bearing capacity of the restored pipelines;
- Polymer materials having a complicated chemical composition, which facilitates a quick polymerization of the coating on the pipe inner walls by filling longitudinal and transversal fistulas and fissures and making possible restoration of the pipeline bearing capacity, in case of their joined functioning with the original pipe [8–10].

The method of application of cement-sand coatings (CSC) is used for renovation of pipelines having the diameter from 70 to 2200 mm and the layer thickness from 4 to 16 mm; the polymer coating method is used for application of polymer coatings for the diameters up to 1200 mm inclusive. The thickness of the polymer coatings shall be associated to the strength calculation and take into account both the state of the pipeline under renovation and the value of exterior and interior loads and effects.

The object of investigation. Sprayed protective polymer coatings, which enable the resource saving effect during renovation of the old pipelines by centrifugal spraying trenchless method.

The subject of investigation. Experimental (bench) research to determine strength indicators of protective polymer coatings.

The target of the work is to find out the strength indices, as well as mathematical relationships, which enable designing and calculation of pipeline networks, when they are subject to a trenchless renovation by sprayed polymer protective coatings. The results of the work shall be reasonably applied in the designing of renovation of the old water supply and water discharge pipelines in the cities and localities to provide a safe and effective operation of municipal engineering water supply and water discharge pipeline.

2 Materials and Methods

Experimental investigations of physical and mechanical properties of Scotchkote 2400 («3M» Company, USA) and Subcote FLP (NPP “Polyplastic”, Russia) materials have been done according to the methods given in the GOST 11262-80 [11] with the electromechanical tensile testing machine Instron 3345.

Calculation and analysis methods enabled reception of physical and mechanical characteristics of Scotchkote 2400 and Subcote FLP coating materials taking into account time simulation of the 50-year operation summer period. They include the maximal tensile strength (σ_{50} , MPa); the Young’s modulus (modulus of elasticity E50,

MPa); density (ρ , kg/m³); the Poisson's ratio (ν); the shear modulus (G_{50} , MPa); the volume elasticity modulus (K_{50} , MPa).

Experimental investigations of physical and mechanical properties of Scotchkote 2400 and Subcote FLP coating materials have been made on a special test bench – “Single column Electromechanical universal tensile testing machine Instron 3345”, in the laboratory of the chair “Water supply and sewage” of NRU MSUCE.

Testing of Scotchkote 2400 and Subcote FLP protective coatings have been made according to the valid procedure stated in the GOST 11262-80 “Plastic. Method of tensile test” [11].

To provide tests on the tensile testing machine in the laboratory of the chair “Water supply and sewage”, 8 identical samples of Scotchkote 2400 coating have been taken in the form of rectangular section stripes having the following parameters: length – 260 mm; width – 25 mm and thickness – 2 mm. To test the Subcote FLP coating, 10 identical samples of this material have been taken in the form of rectangular section stripes having the following parameters: length – 300 mm; width – 25 mm and thickness – 2 mm.

The speed of movement of the tensile testing machine upper crosshead was taken according to the value, which is recommended by GOST 11262-80, and made 5 mm/min. The room temperature during the test made 23 °C.

3 Results and Discussions

The target of investigation of the strength characteristics of interior sprayed protective polymer coatings is to determine the recommended minimal values of the coating thickness to be applied on the worn steel pipeline for renovation of its structural integrity, when its bearing capacity has been broken along some part due to the critical value of the wall thinning. The received values of the coating thickness may be used by a designer for development of a pipeline renovation project or by a builder as a reference information during the pipeline renovation works.

Since during application of the cement-sand coating it does not form a continuous envelope, which may cover the through defects on a pipe and resist itself to the loads and effects in zones of such defects and the wall critical thinning places, this type of coating, as a rule, is not examined as the object of such investigations.

The Scotchkote 169HB coating is not actually used in renovation of pipeline networks in Russia and has been replaced by a more modern coating Scotchkote 2400, which represents the next generation of Scotchkote –type coatings by “3M” Company and is applied all over the world [12, 13]. Thus, the sprayed polymer coatings Scotchkote 2400 and Subcote FLP were taken as the durability investigation.

In total 8 tests of the Scotchkote 2400 coating and 10 tests of Subcote FLP coating have been made (according to the number of samples). During each test, the data of the applied load (F , N) and elongation (x , mm) of the sample have been sent to the PC in the real time.

The test results are given in the Table 1.

It shall be noted, that the rupture of some Scotchkote 2400 coating samples took place in the zone of capturing points of the tensile machine and the results of these tests

Table 1. Results of tension tests of Scotchkote 2400 coating and Subcote FLP

Sample №	Scotchkote 2400				Sample №	Subcote FLP			
	Load (F.N)	Sample tension (σ , MPa)	Elongation (x. mm)	Longitudinal deformation (ϵ , mm/mm)		Load (F.N)	Sample tension (σ , MPa)	Elongation (x. mm)	Longitudinal deformation (ϵ , mm/mm)
0	1520 .31	30.41	2.840	0.0142	1*	1432.80	28.66	3.531	0.0208
1	1493 .21	29.86	2.934	0.0147	2	1865.85	37.32	5.995	0.0353
2*	1491 .55	29.83	2.918	0.0146	3	1766.68	35.33	5.630	0.0331
3	1524 .78	30.50	3.059	0.0153	4	1830.60	36.61	5.551	0.0327
4	1477 .33	29.55	3.039	0.0152	5	1762.30	35.25	5.155	0.0303
5*	1395 .02	27.90	2.735	0.0137	6	1469.05	29.38	4.080	0.0240
6*	1431 .25	28.63	3.000	0.0150	7*	1589.14	31.78	4.649	0.0273
7	1517 .19	30.34	3.161	0.0158	8*	1776.10	35.52	4.905	0.0289
					9	1734.02	34.68	4.964	0.0292
					10	1750.91	35.02	4.965	0.0292

**Note: rupture of the samples № 2, № 5 in the first tests and № 6 № 1, № 7 and № 8 in the second tests took place in the capturing points of the tensile machine – the results of these tests shall be considered as false ones and are not taken into account.*

shall be considered as false ones and are not taken for the further analysis. However, the rupture of 5 samples of the Scotchkote 2400 coating and 7 samples of the Subcote FLP coating took place in the operation zone, and it meets the requirements of Russian Standard GOST 11262-80 concerning the minimum permitted number of samples subject to testing (destroyed in the operation zone).

For general view of the coating, samples according to the tensile test results see Fig. 1.

For average values of the main physical and mechanical characteristics of Scotchkote 2400 and Subcote FLP coatings, which have been received on the basis of the results of the made experimental investigation with the Electromechanical universal tensile testing machine, see Table 2.

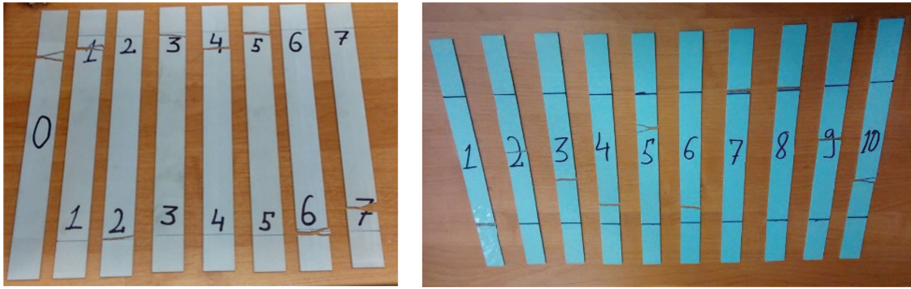


Fig. 1. General view of Scotchkote 2400 and Subcote FLP (from left to right) coating samples after tensile testing

Table 2. Experiment results with the tensile testing machine

Coating	Max. load applied to the sample <i>F</i> , N	Max. tensile strength (σ , MPa)	Max. elongation of the sample (<i>x</i> , mm)	Max. longitudinal deformation (ϵ , mm/mm)
Scotchkote 2400	1506.56	30.13	3.007	0.0150
Subcote FLP	1739.92	34.80	5.191	0.0305

Besides, some necessary physical and mechanical characteristics of Scotchkote 2400 and Subcote FLP coatings have been got by calculation and analysis procedures.

The Young’s modulus (the elastic modulus) is a physical parameter, which characterizes the material properties of resistance to tension/compression in the elastic deformation. The Young’s modulus value (*E*, Mpa) is calculated according to the following Eq. (1):

$$E = \frac{\sigma}{\epsilon} \tag{1}$$

where: σ – tension, which occurs in the sample, (MPa); ϵ – deformation, which occurs in the sample (mm/mm).

The summary Table 3 shows the data of the physical and mechanical characteristics of Scotchkote 2400 and Subcote FLP coatings.

Table 3. Physical and mechanical characteristics of coatings

Characteristics	Characteristics values	
	Scotchkote 2400	Subcote FLP
Maximal tensile strength (maximal tension in the sample), MPa	30.13	34.80
Maximal rupture deformation, mm/mm	0.0150	0.0305
Young’s modulus (elastic modulus), MPa	2008.67	1140.98
Density, kg/m ³	1577	1366
Poisson’s ratio	0.3	0.3

To determine the changes of the Young's modulus (the elastic modulus) of the coatings during a 50-year operation period, provision may be made of the Eq. (2):

$$E = E_0 \left(\frac{b}{\tau} \right)^m, \quad (2)$$

where: E_0 – the initial Young's modulus (the elastic modulus), MPa; τ – operation period, h; $b = 10^{-5}$ h; $m = 0.04$.

The Young's modulus for a 50-year operation period:

-for Scotchkote 2400:

$$E_{50} = 2008.67 \left(\frac{10^{-5}}{438000} \right)^{0.04} = 753.8 \text{ MPa}$$

-for Subcote FLP:

$$E_{50} = 1140.98 \left(\frac{10^{-5}}{438000} \right)^{0.04} = 428.17 \text{ MPa}$$

Then, the shear modulus and the modulus of volume elasticity of the coating have been determined for a 50-year operation period.

The shear modulus (G , MPa) is the ratio of the shear stress to the shear deformation. Having the Young's modulus and the Poisson's ratio, it is possible to calculate G (MPa) according to the following Eq. (3):

$$G = \frac{E}{2(1 + \nu)} \quad (3)$$

Then, the shear modulus for Scotchkote 2400 makes:

$$G_{50} = \frac{753.8}{2(1 + 0.3)} = 289.9 \text{ MPa}$$

and for Subcote FLP it makes:

$$G_{50} = \frac{428.17}{2(1 + 0.3)} = 164.68 \text{ MPa}$$

The modulus of the volume elasticity (K , MPa) characterizes the material property to resist to the overall compression. It shall be determined according to the equation issued from the Young's modulus and the Poisson's ratio (4):

$$K = \frac{E}{3(1 - 2\nu)}, \quad (4)$$

Then, for Scotchkote 2400 we receive the value of the bulk modulus of elasticity:

$$K_{50} = \frac{753.8}{3(1 - 2 \cdot 0.3)} = 628.2 \text{ MPa,}$$

and for Subcote FLP it makes:

$$K_{50} = \frac{428.17}{3(1 - 2 \cdot 0.3)} = 356.81 \text{ MPa,}$$

The lowering of the maximal rupture strength of the coating may be forecast using the manual for designing of technological pipelines made of plastic pipes [14].

The nomogram of the Fig. 2 shows the drop of the fracture resistance of the material R_H of polyvinyl chloride (PVC) pipelines according to the temperature ($^{\circ}\text{C}$) and the pipeline operation period t .

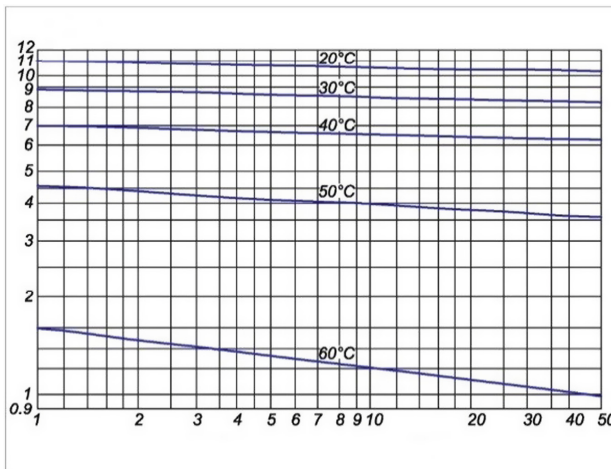


Fig. 2. Nomogram of the resistance drop of the fracture resistance of the material of PVC pipelines (the axis of ordinates shows the fracture resistance of the material R_H , MPa, and the abscissa – the time period, t , year)

On grounds of the nomogram it is possible to state, that the average drop value of the fracture resistance of the material makes $\sim 10\text{--}15\%$ within a 50-year period of the coating exploitation at the operation temperature not higher than 40°C .

The summary Table 4 shows the main physical and mechanical characteristics of Scotchkote 2400 and Subcote FLP coatings at their operation within 50 years.

Mathematical analysis of the investigation results of physical and mechanical characteristics of Scotchkote 2400 and Subcote FLP coatings, as well as determination of their recommended thickness, have been made by modelling in the automated PC medium by «Ansys» finite element analysis. This automated system enables the exact representation of an object according to its geometrical characteristics and the physical and mechanical characteristics of the materials of the object under investigation [15].

Table 4. Physical and mechanical characteristics of the coatings at their operation within 50 years

Characteristics	Characteristics values	
	Scotchkote 2400	Subcote FLP
Maximal tensile strength σ_r , MPa	25.61	29.58
Young’s modulus (the elastic modulus), MPa	753.8	428.17
Density, kg/m ³	1577	1366
Poisson’s ratio	0.3	0.3
Shear modulus, MPa	289.9	164.68
Bulk modulus of elasticity, MPa	628.2	356.81

The PC model of a pipe structure based on the protective coatings permits to investigate their strength properties during a 50-year operation taking into account the critical thinning of the wall of a worn pipeline and the coating operation under different loads and effects (Fig. 3).

At the first step, we determined the values of the minimal residual wall thickness of a steel pipeline, which permits to save its bearing capacity, may bear interior and exterior loads, and effects itself. The minimal values of the coating thickness have been determined at the second stage of the mathematical analysis of the investigation results of physical and mechanical characteristics of Scotchkote 2400 and Subcote FLP coatings.

The Tables 5, 6 and 7 give initial data for modeling strength capacities of a pipe structure coated by Scotchkote 2400 and Subcote FLP during their 50-year operation at different diameters.

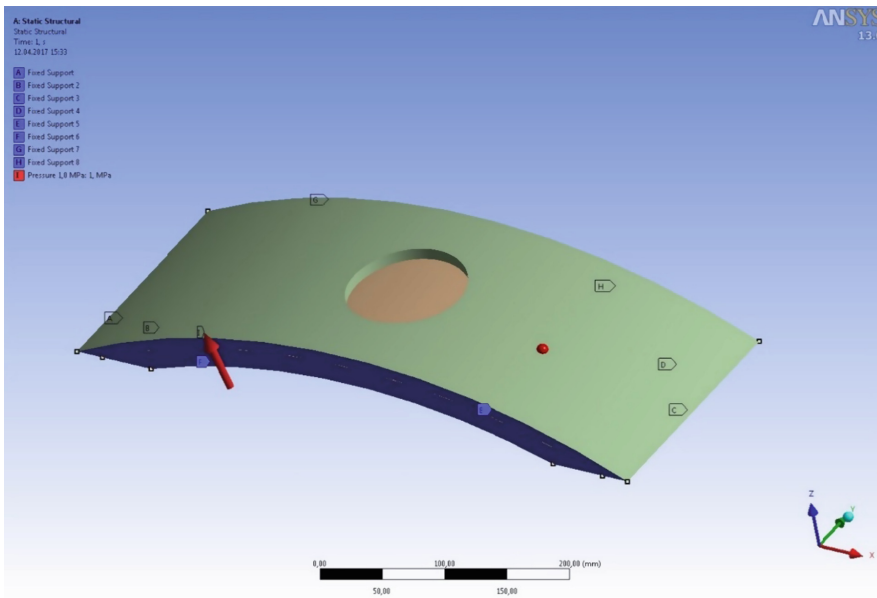


Fig. 3. Model of a pipe structure “steel pipe + protective polymer coating” with applied loads

Table 5. Minimal residual wall thickness of a steel pipeline with the inner diameter from 100 to 450 mm

Diameter, mm	100	150	200	250	300	350	400	450
Minimal residual wall thickness of a pipeline, mm	0.14	0.18	0.22	0.25	0.31	0.37	0.42	0.47

Table 6. Minimal residual wall thickness of a steel pipeline with the inner diameter from 500 to 1200 mm

Diameter, mm	500	600	700	800	900	1000	1200
Minimal residual wall thickness of a pipeline, mm	0.51	0.61	0.72	0.83	0.94	1.04	1.25

Table 7. Initial data for modelling of strength capacities of a pipe structure on the basis of Scotchkote 2400 and Subcote FLP coatings

Data	Examined values
Defect diameter, mm	5–100
Defect area, cm ²	0.2–78.5
Maximal water pressure of the pipe, MPa	1.0
Physical and mechanical characteristics of coatings	See Table 4

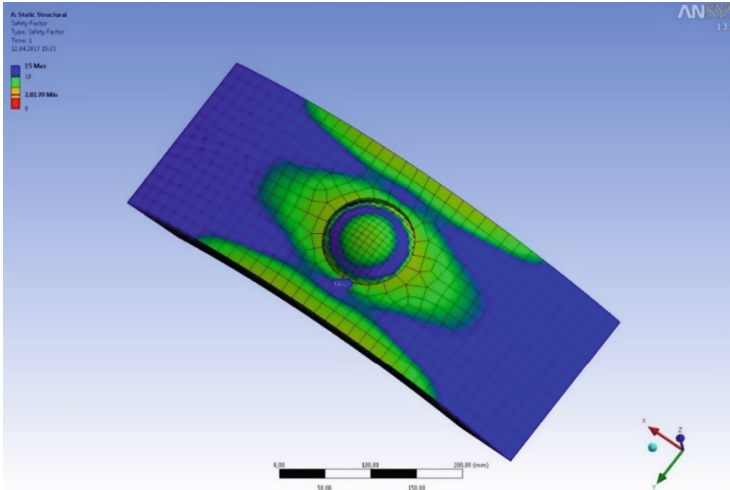


Fig. 4. Graphical presentation of the results of PC calculated model “steel pipe + protective polymer coating”

- maximal equivalent stress σ_e , MPa according to the Eq. (5):

$$\sqrt{\frac{1}{2}[(\sigma_1 - \sigma_2)^2 + (\sigma_3 - \sigma_3)^2 + (\sigma_3 - \sigma_1)^2]}, \text{ MPa} \tag{5}$$

where $\sigma_1, \sigma_2, \sigma_3$ - principal stresses, MPa;

- the safety factor K_z (the ratio of the maximum tensile strength of the material of the coating to its inner appearing maximum equivalent stresses) according to the Eq. (6):

$$K_z = \frac{\sigma_r}{\sigma_e}, \tag{6}$$

For graphical presentation of the results of the calculated model, see Fig. 4.

Table 8. The recommended values of thickness of Scotchkote 2400 and Subcote FLP coatings

Operation period – 50 years Safety factor : $K_z = 2.0$ Maximal pressure in the pipeline: 1.0 MPa				
Size (area) of a through defect or the zone of the wall critical thinning mm ²	~cm ²	Diameter of the defect, which corresponds to the given area, mm	Recommended thickness of the coating, mm	
			Scotchkote 2400	Subcote FLP
≤19.6*	≤0.2*	≤ 5*	1.7*	1.5*
78.5*	0.8*	10*	2.1*	1.8*
314.1	3.1	20	2.9	2.5
706.5	7.1	30	4.3	3.7
1256.6	12.6	40	6.4	5.5
1962.5	19.6	50	8.3	7.2
2827.4	28.3	60	9.8	8.5
3848.4	38.5	70	10.9	9.4
5026.5	50.3	80	11.8	10.2
6361.7	63.6	90	14.0	12.1
7853.9	78.5	100	17.2	14.9

**If the defect of the indicated size goes through, the coating thickness is recommended to be taken not less than 2.75 mm for Scotchkote 2400 and not less than 2.5 mm for Subcote FLP.*

The recommended values of thickness of Scotchkote 2400 and Subcote FLP protective coatings to be used for renovation of steel pipes are presented in the Table 8.

4 Conclusions




A complex analysis of the strength parameters of Scotchkote 2400 and Subcote FLP interior sprayed protective polymer coatings has been made and the values of the wall minimal coating thickness have been received within a wide range of diameters.

When designing renovation of pipeline networks or performing renovation works using Scotchkote 2400 and Subcote FLP sprayed protective polymer coatings, determination of the applied coating thickness is recommended to be taken according to the data of the Table 9, as well as the results of experimental investigations with the electromechanical tensile testing machine and their subsequent processing by computer simulation.

References

1. The State Report State of the sanitary and epidemiological welfare of the population in RF in 2015 (2016)
2. Maslak, V., Nasonkina, N., Sakharovskaya, V., Gutarova, M., Antonenko, S., Nemova, D.: *Procedia Eng.* **117**, 980–989 (2015)
3. Federal Law 2011 On water supply and sewage. № 416-FZ, 65 p., Moscow, Kremlin
4. Huang, Q., Wang, J.: *J. Environ. Econ. Manag.* **82**, 1–16 (2017)
5. Batchelor, C., Rebbly, V., Linstead, C., Dhar, M., Roy, S., May, R.: *J. Hydrol.* **518**, 140–149 (2014)
6. Ahmad, M., Masih, I., Giordano, M.: *Agricult. Ecosyst. Environ.* **187**, 106–115 (2014)
7. Aliofkhazraei, M.: *Developments in Corrosion Protection*. InTech Open Publishers, 698 p. (2014)
8. Wróbel, G., Szymiczek, M., Wierzbicki, Ł.: *J. Mater. Process. Technol.* **157–158**, 637–642 (2004)
9. Pridmore, A.B., Ojdrovic, R.P.: *Rehabilitation of Pipelines Using Fiber-Reinforced Polymer (FRP) Composites*. vol. 1, pp. 17–38 (2015)
10. Bruce, W.A.: *Rehabilitation of Pipelines Using Fiber-Reinforced Polymer (FRP) Composites*, vol. 1, pp. 61–78 (2015)
11. Russian Standard GOST 11262-80 1980
12. Information on: http://www.pwmag.com/water-sewer/structural-cured-in-place-pipe-for-trunk-water-main_o
13. Information on https://infowire.pl/generic/release/315685/technologie-bezwykopowej-renowacji-3m-scotchkote_-2400-nagrodzona-na-konferencji-no-dig-poland-2016
14. SN 550-82 1982 Manual for the Design of Technological Pipelines Made of Plastic Pipes. Moscow, Publishing House of Standards, 33 p.
15. Tsyss, V.G., Sergaeva, M.Yu.: *Procedia Eng.* **152**, 251–257 (2016)

Outlooks for Building Solar Charging Infrastructure for Self-propelled Electric Vehicles

Liubov Shilova¹✉, Dmitry Solovyev²,
and Aleksey Adamtsevich¹

¹ Moscow State University of Civil Engineering,
Yaroslavskoye Sh. 26, 129337 Moscow, Russia
ShilovaLA@mgsu.ru

² Joint Institute for High Temperatures of the Russian Academy of Sciences,
Moscow, Russia

Abstract. The article examines key issues and outlooks for use of recharging photovoltaic stations (PVS) by recharging infrastructure for electric self-propelled vehicles, to be created in Russia. Methodical justification of the use of charging PVS are presented according to the studies of different options for the development of power supply to consumers which are isolated from power systems, including consumers from the remote regions of the Russian Federation. It offers a methodology to design pilot algorithms to validate use of PVS in the electric vehicle recharging infrastructure to be created in some Russian regions; it is used as basis to analyze the potential of different regions for PVS implementation in the electric vehicle recharging infrastructure.

Different approaches are analyzed, and the obtained results allow optimizing the operation and efficiency of the PVS charging taking into account the reduction of environmental impact. The results of the research work allow us to conclude that there is a great potential for using solar energy resources in Russia.

Keywords: Electric vehicle · PVS · Recharging station · RES
Power accumulator battery

1 Introduction

The objective of improving the global environmental situation has taken on particular significance during the recent years. The transportation sector accounts for about 1/3 of total greenhouse gas emissions [1], and so the transition to clean technologies is seen as a vital tool here. Although other environment-friendly vehicle types (such as combustion cell engines, compressed natural gas or hybrid electric vehicles) have been a rising trend, electric vehicles still remain the most promising option in terms of emission control (Fig. 1).

Not only will the growing electric vehicle market be environmentally beneficial, it will also reduce fossil fuel dependence and create new niches for manufacturing and sales of high-end products.

<p>Plug-in electric vehicle (PEV) Ex: NISSAN LEAF</p> <ul style="list-style-type: none"> ⊕ There is no environmental pollution; ⊕ Low operating cost; ⊕ Longer service life; ⊕ Dynamic characteristics and comfort. 	<p>Hybrid EV (HEV, PHEV) Ex: SHEVROLET VOLT</p> <ul style="list-style-type: none"> ⊕ Integration into existing infrastructure; ⊖ Only a partial reduction of emissions.
<p>Fuel cell vehicle (FCEV) Ex: TOYOTA MIRAI</p> <ul style="list-style-type: none"> ⊕ Drastic reduction of emissions; ⊖ High price; ⊖ Low service life; ⊖ Security issues. 	<p>Natural gas vehicle (CNGV) Ex: MERSEDES BENZ Sprinter 316 NGT</p> <ul style="list-style-type: none"> ⊕ Integration into existing infrastructure; ⊖ Only a partial reduction of emissions.

Fig. 1. Advanced environment-friendly vehicles [8].

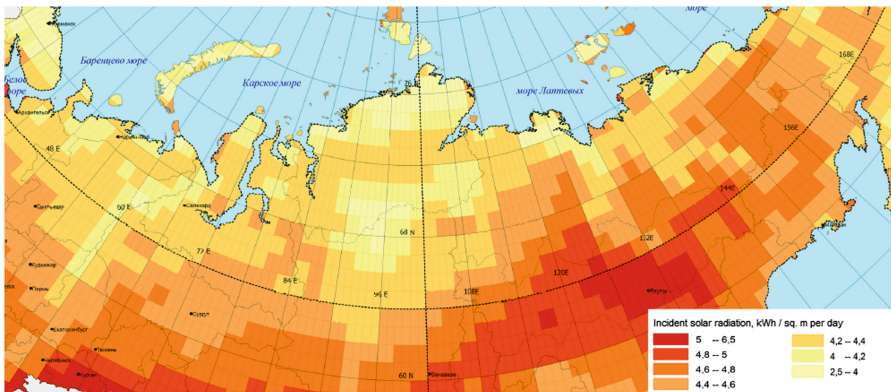


Fig. 2. Solar radiation incidence in Russia [5].

Problems of electric vehicle development and the issues of respective recharging infrastructure that needs to be created have been examined in many studies [11–20].

Major EU nations and the US have declared their intentions to stop the use of internal combustion engines (ICE) altogether by 2050 [2]. Russia has also adopted a series of programs to promote electric vehicles (EV), currently underway in certain regions [3, 4]. Thus it becomes imperative to examine possible engineering options to enable such projects and ensure their viability in the light of the nation's natural and climate conditions, geography, infrastructure and socio-economic specifics.

Intensive use of electric vehicles is unthinkable without a developed battery-charging infrastructure that must be efficient in terms of economy and power generation, able to integrate seamlessly into the available and future power grids. Large-scale use of electric cars will trigger total power consumption, and this is going to call for new power generation facilities. Considering to which extent the electric car is to be involved in the Russian transportation sector [4], researching the effect of the recharging infrastructure for electric vehicles on the grid infrastructure and power consumer quality is becoming an issue of significance. We need to examine the scenario of using systems based on renewable power sources by the recharging infrastructure for electric vehicles in the

light of available resource, estimated growth of the electric car part, and other factors. Considering Russia’s existing solar power potential [5], engineering and operating specifics of photovoltaic stations, and the results of analytical research about regions seen as prospective users of electric cars (and according to [6], these are Russia’s southern and central areas), we deem it reasonable to scrutinize the use of solar power in the infrastructure for electric vehicles.

Unlike thermal power generation that produces most of electric power worldwide, solar batteries are not a serious damaging factor in the environment. In addition, low-output stations placed close to the consumer are easier to build than conventional generating facilities mainly designed for output of at least dozens of megawatts (Fig. 3).

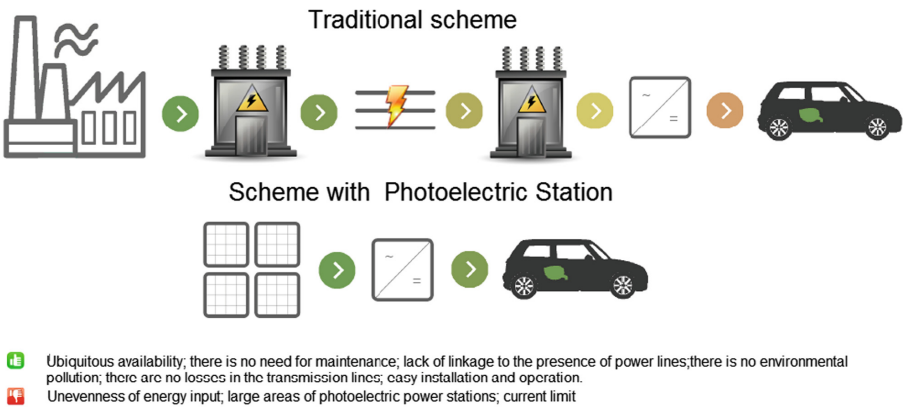


Fig. 3. Key advantages and disadvantages of PVS recharging stations compared to conventional power plants [8].

Major disadvantages of solar power generation include notable circadian and seasonal irregularities of energy inputs, and also fairly large areas needed for photovoltaic systems (PVS), something not feasible normally in an urban area. And yet, international research of the use of PVS as a component in the electric vehicle infrastructure is gaining momentum. To minimize power generation irregularity, such stations may use electric energy storage systems, sometimes relying on past-service life electric car batteries.

2 Methodology

The methodology to select a pilot venue for solar power plants (PVS) as part of EV recharging stations should focus on prospective consumer market with relatively low power loads (up to 5 MW), being also off-the-grid as they are to use standalone power plants and small boiler plants that burn transported fuels as power sources.

Validation of possible PVS use under project options to develop power supply for off-the-grid consumers, including in remote Russian areas, may use the method designed by ISEM SO RAN (R&D Institute for Power Generation, Siberia Branch, Russian Academy of Sciences [9], as schematically illustrated in Fig. 4.

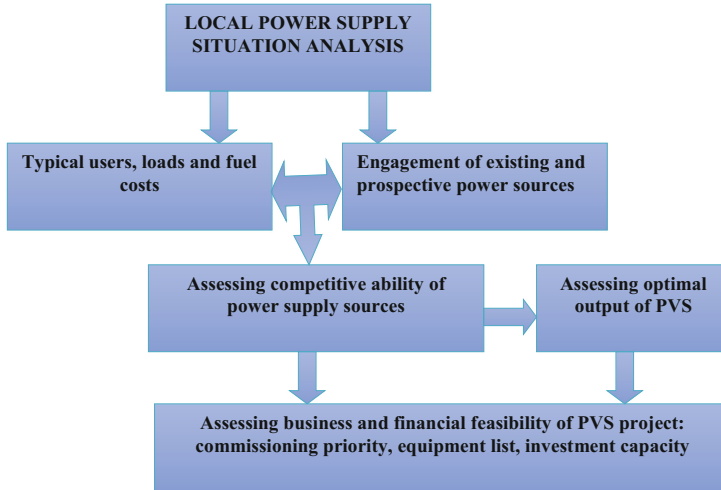


Fig. 4. Diagram of selection sequence for most rational option to integrate a PVS in electric vehicle-recharging infrastructure [9].

The proposed methodology rests on cost correlation analysis (civil construction investments and cost of displaced organic fuel in existing power sources), largely relying on local potential output of solar power resources, as quoted from [5] (Fig. 2).

As its outputs, the proposed methodology produces optimal designed output capacity and respective indicators such as net energy output, investment, and total displaced organic fuel. Such data are found during a simulation of PVS operation as part of a recharging station, to assess business efficiency of the construction project to be used by a specific consumer. In turn, optimal PVS output capacity is determined by the lowest ratio of related investments to the cost of fuel saved by its operation. Given individual nature of data about local potential for solar power production and the wide range of fuel prices depending on consumer location, optimal output capacity of the PVS needs to be custom-calculated based on the specifics of each residential community in Russia. Efficiency of PVS projects is decided by many factors (business, engineering, natural environment), while the methodology helps to evaluate their contributions to and effects on the optimal capacity for the PVS project [10].

Whereas any diagram of power generation by conventional sources, including a hydro plant with its dam pool, is determined by the respective power consumption schedule, the output capacity of a PVS depends on the solar energy patterns in the area. For cyclical and stochastic irregularities in the pattern, even smoothed highs and lows of solar resource density (such as overcast sky), may rise above the magnitude of one,

also failing to match the frequency and phase of the respective power consumer schedule. Therefore, rated output capacity of the PVS for any recharging station should base on a certain averages, and may exceed consumption during its generation peaks. As the base parameter and first efficiency criterion for power supply option and the rated output N of the recharging PVS, we should use its service life, i.e. N consumption period:

$$T = \frac{W_1 - \Delta W_1}{N} \tag{1}$$

where W_1 and ΔW_1 – respectively, generated power, and unused part thereof [10].

Efficiency factor as the ratio of generated (secondary or converted) and primary (used) energy for the PVS is not as unambiguous as that for conventional generation, because the PVS available resource can be typically assumed to be infinite. Evidently, the point of high-efficiency PVS units with advanced technologies, materials and system solutions is to cut costs, including the investment cost component, rather than to save solar energy resources and make the plant more compact.

3 Results and Discussion

In the light of pay time T analysis done herein (see Table 1) to estimate energy output from a typical solaroñ recharging station within the EV recharging infrastructure based on the proposed methodology, we averaged estimates of rational scale of PVS commissioning to serve off-the-grid consumers by aggregate select indicators in the Russian areas deemed to be the most prospective electric car markets: the regions of Stavropol Krai, Belgorod, Leningrad, Moscow, Sverdlovsk, Yaroslavl, Samara and Saratov (see Table 1).

Table 1. Rational scale of PVS operation/commissioning for the EV recharging infrastructure, by output (MW), in certain regions of the Russian Federation. (Source: authors’ calculations.)

Region in Russian Federation	Rational scale of PVS to commission (MW)	Region in Russian Federation	Rational scale of PVS to commission (MW)
Stavropol Krai	12	Sverdlovsk	5
Belgorod	7	Yaroslavl	4
Leningrad	6	Samara	3
Moscow	9	Saratov	3

One needs to bear in mind that solar panels to be used by a PVS rated for 1 MW output, will take the average of 1.5–2 ha of land, with a payback period of about 5 years (for construction project cost of US\$ 1,000 per kilowatt of installed capacity).

The resulting estimates suggest a considerable potential of solar power resources for the EV recharging infrastructure currently built in Russia, and good outlooks for respective low-load off-the-greed consumers.

A storage battery is the cornerstone of any electric vehicle today, and the principal source of energy onboard. Storage batteries used by modern electric cars can accumulate 20 to 85 KWH, enabling 110 to 500 km mileage without recharge; they mainly contain lithium-ion cells, nickel-metal hydride cells being a less common option. Any battery type requires that a certain charging mode procedure be observed, to ensure both safe and lasting service life of the battery as a relatively costly asset.

Most recharging stations at this time are designed to be powered up from the urban AC grid, and made as a high-output power transformer to convert AC to DC that is needed to charge batteries. Such transformers use a specific algorithm ensuring the optimal mode that alternates voltage and current for faster and more complete battery recharge and longer battery life. To fit the proposed algorithm, storage batteries have been actively promoted with the quick-recharge function (receiving 70–80% of total capacity in 40 min); such batteries can seriously reduce the time of the electric vehicle at the recharging station. However, this approach is not the best option if solar energy is used. Because a photovoltaic unit generates direct current, and because the generator is as possibly close to the consumer, it would be reasonable to place the entire system on a DC busbar, as part of an output transformer circuit – in a sense, an analog of the charge controller for standalone solar units. In this scenario, the use of a fast-charge algorithm can be limited by the greatest current of the solar station, which in turn has the constraint of the available area.

The problem can be solved by integrating a dedicated storage unit in the station's structure; this, however, is a major cost item. In a different option, offered by the Israel-based Better-Place [7], discharged onboard batteries are automatically replaced at network stations. This solution fits best the recharging infrastructure of future power grids, harmonizing generation from renewable sources with inherent chaotic distribution that features daytime peaks and night troughs in the urban grid. The station then needs no dedicated storage: as a result, no energy is lost during transfer from such storage to the onboard battery, because the latter is exactly the end product of such recharging station. Obviously, this solution needs batteries of uniform design on all electric cars, as they are to be replaced mechanically. In addition, different owners will have their fairly expensive batteries worn out to different extent; this ultimately will tell on the vehicle's mileage.

4 Conclusions

Solar energy used at recharging stations for electric vehicles in the Russian regions with elaborate conventional generation systems, and most importantly, power grids, may prove costly and unjustified. Environmental effects will also be questionable in the regions with predominant by nuclear and hydro power generation: such technologies produce by far less emissions compared to thermal plants. Moreover, utilizing the surplus power generated during the night trough is more relevant for nuclear plants. At the same time, where thermal plants dominate, solar power can give a perceptible environment effect, enhanced by effects of economy in the regions with undeveloped grids.

As estimated [8], efficient use of recharging stations based on solar generation is possible in Russia in the regions of Stavropol, Belgorod, Leningrad, Moscow, Sverdlovsk, Yaroslavl, Samara, and Saratov. These regions have been selected for pilot projects to implement the electric vehicles program in the Russian Federation [3, 4], and their climate conditions and the existing power supply infrastructure are quite different. In terms of resources for solar generation, Stavropol Krai is the most promising region as regards integration of PVS in the recharging infrastructure for electric vehicles.

References

1. Tie, S., Tan, C.: A review of energy sources and energy management system in electric vehicles. *Renew. Sustain. Energy Rev.* **20**, 82–102 (2013)
2. Homepage of the United Nations Climate Change Conference. <http://www.cop21.gouv.fr/en>. Accessed 22 Aug 2017
3. The official site of the pilot project for the creation of a charging device for electric transport “MOESK-EV”. <http://www.moesk.ru/>. Accessed 22 Aug 2017
4. Homepage of JSC “Rosseti”. Implementing the All-Russian program for developing the charging potential for electric transport. <http://www.rosseti.ru/>. Accessed 22 Aug 2017
5. Andrenko, T., Gabderakhmanova, T., Danilova, O., Ermolenko, G., et al.: Atlas of Renewable Energy Resources on the Territory of Russia. Publishing Center of the Russian Chemical Technical University, D.I. Mendeleev University (2015)
6. Homepage analytical agency “Autostat”. <http://www.autostat.ru/>. Accessed 22 Aug 2017
7. “Better Place”, Wikipedia. https://enA.wikipedia.org/w/index.php?title=Better_Place. Accessed 22 Aug 2017
8. Gabderakhmanova, T., Tarasenko, A.: About the possibilities of using solar energy in the charging infrastructure of electric transport. Moscow State University of Civil Engineering, pp. 1025–1027 (2016)
9. Ivanova, I., Tuguzova, T., Khalgaeva, N.: Determination of the optimal power of a renewable energy source for a consumer isolated from the energy system. In: Proceedings of Russian Academy of Sciences, Power Engineering, vol. 3, pp. 22–28 (2014)
10. Ivanova, I., Koshelev, A., Tuguzova, T., Marchenko, O.: Justification of the use of renewable energy sources. In: Voropay, N. (ed.) Systemic Research in Energy: Retrospective of Scientific Directions SEI-ISEM. Science, Novosibirsk (2010)
11. Hafez, O., Bhattacharya, K.: Optimal design of electric vehicle charging stations considering various energy resources. *Renew. Energy* **107**, 576–589 (2017)
12. Andrenacci, N., Ragona, R., Valenti, G.: A demand-side approach to the optimal deployment of electric vehicle charging stations in metropolitan areas. *Appl. Energy* **182**, 39–46 (2016)
13. Huang, K., Kanaroglou, P., Zhang, X.: The design of electric vehicle charging network. *Transpor. Res. Part D: Transp. Environ.* **49**, 1–17 (2016)
14. Tinton Dwi Atmaja, A.: Energy storage system using battery and ultracapacitor on mobile charging station for electric vehicle. *Energy Procedia* **68**, 429–437 (2015)
15. Arias, M., Bae, S.: Electric vehicle charging demand forecasting model based on big data technologies (Original Research Article). *Appl. Energy* **183**, 327–339 (2016)
16. Chandra Mouli, G., Bauer, P., Zeman, M.: System design for a solar powered electric vehicle charging station for workplaces (Original Research Article). *Appl. Energy* **168**, 434–443 (2016)

17. Sadeghi-Barzani, P., Rajabi-Ghahnavieh, A., Kazemi-Karega, H.: Optimal fast charging station placing and sizing. *Appl. Energy* **125**, 289–299 (2014)
18. Li, S., Huang, Y.: Development of electric vehicle charging corridor for South Carolina (Original Research Article). *Int. J. Transp. Sci. Technol.* **4**(4), 395–411 (2015)
19. Morrissey, P., Weldon, P., O'Mahony, M.: Future standard and fast charging infrastructure planning: an analysis of electric vehicle charging behavior. *Energy Policy* **89**, 257–270 (2016)
20. Bhatti, A.R., Salam, Z., Aziz, M.J.B.A., Yee, K.P., Ashique, R.H.: Electric vehicles charging using photovoltaic: status and technological review. *Renew. Sustain. Energy Rev.* **54**, 34–47 (2016)

Deformation Monitoring of Road Transport Structures and Facilities Using Engineering and Geodetic Techniques

Ekaterina Kuzina^(✉)  and Vladimir Rimshin 

Moscow State University of Civil Engineering,
Yaroslavskoye Sh., 26, Moscow 129337, Russia
kkuzzina@mail.ru

Abstract. Reliability and stability of transport facilities during their maintenance can be ensured by the application of the engineering and geodetic monitoring systems for deformation processes in structures supervision that allows avoiding emergencies. Nowadays, automatic engineering devices are successfully used in order to produce high-precision spatial measurements. Further development of deformation monitoring systems requires the development of software tools for deep analysis of structures based on data. The article considers the methodology and software for deformation monitoring of road transport structures and facilities using geodetic methods during construction, maintenance and reconstruction these structures in order to evaluate their technical availability and to prevent negative impacts on surrounding buildings and structures. In addition, it is reviewed the world's researches on this subject, as well as practical examples of the application this methods.

Keywords: Transport structures and facilities
Geodetic engineering methods · Deformation monitoring

1 Introduction

There has been a huge increase in the construction and reconstruction of transport structures and facilities in the world recently. However, there are some difficulties in the designing, construction, operation and reconstruction of these objects: soil sediments are close to the observed structures, heavy weight, high seismic activity in some areas, natural deterioration processes. It leads to the emergence of deformations that may be both valid and ultimate that cause complete or partial destruction of structures, financial loss and even casualties. Timely inspection and monitoring of structures help to identify deformations in time and maintain its operational capacity and safety.

Many scientists and practical engineers study the theme. For example, Mill et al. in their research work “Geodetic Monitoring of Bridge Deformation Occurring during static load testing” [1] review the question of deformation monitoring by static load loading in designing of bridges. Park et al. in their work “The new approach to health monitoring structures: terrestrial laser scanning” [2] propose to monitor the structures, including transport facilities, with scanners. Soudarissanane et al. [3] suggest to use this

method at the same time. Kutterer et al. [4], Snieder et al. [5] study the problems of safe and modern engineering and geodetic deformation monitoring of transport structures and facilities. In addition, Banerjee et al. [6], Schofield [7], Yang and Myers [8] consider questions and problems of deformation monitoring, including engineering and geodetic methods. Erdélyi et al. study deformation surveys during construction of transport facilities. For example, “Deformation Monitoring of a parabolic structure using TLS“ [9].

Automated monitoring systems that include geodetic engineering methods have a great advantage over other types of monitoring. Through their use, it is possible to save full information on the technical condition of objects between the periods of control measures that can detect and eliminate high-growth deformation processes [10]. Geodetic monitoring system are used with modern geodetic instruments that allow determining displacements of controlled marks [11]. It is levels, total stations, satellite navigation receivers, inclinometers.

Deformation monitoring or deformation survey of road transport structures and facilities should provide obtaining necessary information to assess the impact of new construction or reconstruction on surrounding buildings, structures and utilities, prevention the negative construction impacts on time, as well as monitoring construction works. Deformation survey of road transport structures and facilities, using engineering and geodetic techniques is based on the Codes and the statements of work for design.

The objects of geodetic deformation monitoring are maintenance engineering of existing buildings and structures, receipt objective information about the deformation shape of structures in general, preventing damage propagation in road transport structures and facilities, defect isolation, risk level detection of deflections for the normal buildings and constructions maintenance, calculation of absolute and relative deformation values in structures and its comparison with average admissible numbers, corrective measures implementation, road transport structures and facilities, new construction impact evaluation on surrounding buildings [12].

2 Methods. An Experimental Section

The system of geodetic monitoring used for transport structures is designed to determine the spatial position of the structural elements and their changes in time, geometric parameters, identifying the causes for their changing, the monitored parameters assays for determining the condition of the structure and its elements with the ability for preventing emergencies. Deformation monitoring of road transport structures and facilities, using engineering and geodetic techniques includes the observation system on the relocation of buildings and structures, calculation of absolute and relative deformation values in structures and its comparison with average admissible numbers. Execution the work should comply with the requirements of the State Standards the Codes. The survey analysis frequency in the first instance depends on expected deformations, it should be defined during the project development, and it is based on the statement of work for design. Deformation monitoring cyclicity of road transport structures and facilities is based on the experience of full level testing in Moscow, geological feature and soil persistence within the influence area of construction or renovation.

The deformation monitoring of foundations, underground utility systems and soils around existing structures is performed one time per month. The deformation monitoring using engineering and geodetic techniques is carried out during the construction period and at least one year after its completion. If the conditional stabilization of the deformation occurs after the construction or there is no deformation at all, the monitoring frequency may be revised. On the other hand, if the vertical displacement are close to the ultimate value, the cyclical (frequency) of deformation monitoring should be increased. As well as engineer, efforts to ensure the safety of existing structure in the influenced area of work should be worked out.

In order to determine the deformation marks outside the zone of possible vertical displacement the group of benchmarks consisting of six wall benchmarks should be fixed. In each cycle high-altitude benchmarks position will be monitored. The elevations on a common datum are urban.

Along the perimeter of the area at a height of 0.5–0.8 m from the ground from forty to forty-five deformation marks will be fixed, which is essentially drilled-in to the base of the structure by steel bolts.

A closed traverse is plotted using the geometric levelling method of the Program class II according to the base benchmarks and deformation marks in each cycle of monitoring. After traversing program, for example, Credo_nivelir v1.1 deformation marks are calculated. Vertical displacements of deformation marks are evaluated by the difference of displacements for the each period and for the entire monitoring period [13]. The leveling line is plotted on the same points, which are fixed on the ground with dowels in order to provide conditions for equally accurate measurements and additional control in each monitoring cycle. The length of the directional ray in leveling should not exceed the permissible point 40 m. The error of interior-angle traverse should not be more than a value, which is calculated by formula

$$f_h = 0.5 \text{ mm} * \sqrt{n} \quad (1)$$

where n - number of tripods in the leveling line.

In order to determine horizontal and vertical displacements in the location of road transport structures and facilities base geodetic line is fixed, and its spatial altitude is controlled in each cycle using six marks are fixed outside the influence of possible displacements [4]. The elevations on a common datum are urban and the coordinate system is nominal.

Ten sedimentary marks in the form of reflective membrane, for example, OP-50 are fixed near underground engineering communications on the light poles, which are buried in the ground below its depth of frost (the depth of soil freezing for Moscow is $1.2 \div 1.4$ m according to Construction Norms and Regulations 23-01-99* «Building climatology and geophysics») [14]. In order to control the horizontal and vertical position marks in the form of core samples are set up.

Measurements are performed by a polar method using base geodetic line points basis with a tachymeter Sokkia SET 1X, with an accuracy of determining distances $\pm (3 + 2 \text{ ppm} * D)$ mm, and averaged square error of angles measurement $1''$. Coordinate values and sedimentary marks of heights, which were calculated in the zero measurement cycle, are used as initial values for the horizontal and vertical

displacement of sedimentary marks. The values of the horizontal and vertical displacement of sedimentary marks are determined by the change of coordinates and heights, made in different cycles of measurements.

3 Results

The complex of works on strain sensing in road transport structures and facilities includes checking field work research, measurement of coordinates, the system of ground points and adjusting marks, accuracy estimation of measurements made in a particular cycle, drawing graphics and vertical displacement diagrams, coordinates calculation and technical report preparation.

Test data reduction of vertical displacement and its accuracy estimation are made in the program, for example, Credo_nivelir v1.1. Checking fieldwork research and its evaluation during the making of the traverse are performed in the program, for example, Credo_dat v3.1.

As a result of the office treatment, a catalog of deformation marks and reference frames (Table 1), a summary statement of the sediments (Table 2), a list of elevations and heights of leveling points, Class II (Table 3), characteristics of leveling lines (Table 4), a list for estimating the accuracy of the point heights (Table 5), are obtained.

Table 1. Catalog of deformation marks and reference frames.

Points number	0 cycle	1 cycle	n cycle
1	150.4134	150.4138	
2	150.5448	150.5446	
3	150.4742	150.4738	
4	150.2930	150.2927	
5	150.4975	150.4972	
6	150.3225	150.3223	
7	150.2835	150.2833	
8	150.3343	150.3343	
9	149.9268	149.9283	
10	150.3429	150.3440	
11	150.4833	150.4836	
12	150.5482	150.5484	
13	150.5038	150.5030	
14	150.4895	150.4897	
15	150.3879	150.3881	
16	150.2936	150.2941	
17	150.3811	150.3814	
<i>Reference points</i>			
P _{n1}	150.0000	150.0000	
P _{n2}	149.9248	149.9248	
P _{n3}	149.8930	149.8937	

Table 2. Summary statement of the sediments.

Points number	Cycle number		
	0 cycle	1 cycle	
1	150.4134	0.4	0.4
2	150.5448	-0.2	-0.2
3	150.4742	-0.4	-0.4
4	150.2930	-0.3	-0.3
5	150.4975	-0.3	-0.3
6	150.3225	-0.2	-0.2
7	150.2835	-0.2	-0.2
8	150.3343	0	0
9	149.9268	1.5	1.5
10	150.3429	1.1	1.1
11	150.4833	0.3	0.3
12	150.5482	0.2	0.2
13	150.5038	-0.8	-0.8
14	150.4895	0.2	0.2
15	150.3879	0.2	0.2
16	150.2936	0.5	0.5
17	150.3811	0.3	0.3

Table 3. The list of elevations and heights of leveling points. Class II.

Section number	Name of the levelling mark	Number of tripods	Measured elevation, m	Correction from adjustment mm	Height, m
<i>Process 1</i>					
1	P _{n1}				150
		1	-0.5515	-0.1	
	x ₁				149.448
		1	0.5516	-0.1	
	P _{n1}				150
		2			
<i>Process 2</i>					
1	P _{n1}				150
	P _{n2}	1	-0.0751	0	
	P _{n3}				149.925
		1	-0.0312	0	
	P _{n1}				149.894
		1	0.1063	0	
		3			
<i>Process 3</i>					
1	x ₁				149.448
		1	0.0972	-0.1	
	x ₂				149.546
2		1	-0.2933	-0.1	
	x ₃				149.252
3		1	0.2882	-0.1	
	x ₄				149.54
4		1	0.1036	-0.1	
	X ₆				149.644
		1	-0.2526	-0.1	
	X ₇				149.391
		1	0.0577	-0.1	

Table 4. Characteristics of levelling lines.

Line number	Line name	Class	Number of links	Line discrepancy mm		RMS for 1 tripod in mm
				Received	Allowable	
1	2	3	4	5	6	7
1	$P_{n1} - P_{n1}$	II	2	0.1	0.7	0.2
2	$x_1 - x_1$	II	6	0.8	1.2	0.2
3	$P_{n1} - P_{n1}$	II	3	0.0	0.9	0.2
4	$x_3 - x_3$	II	2	-0.1	0.7	0.2
5	$x_5 - x_5$	II	2	0.3	0.7	0.2

Table 5. List for estimating the accuracy of the point heights.

Point number	Mh, mm
1	2
x_1	0.2
x_2	0.1
x_3	0.2
x_4	0.1
x_5	0.2
P_{n2}	0.1
P_{n3}	0.2

4 Conclusions

In the first place, at the commencement of monitoring, it is necessary to have a clear idea about the amount of information required for control transport objects in order to determine their technical condition, the type of sensors and software for deformation monitoring using geodetic methods. The big advantage of automatic deformation monitoring systems is considered the possibility to add, remove or change certain elements without interrupting the overall process of monitoring [15].






Reliable and safe road transport structures and facilities construction, maintenance and reconstruction can only be achieved with the effective technical monitoring using modern diagnostic techniques of building structures that should to be applied at both construction, reconstruction and maintenance of road transport structures and facilities, as well as the operational phase for reliable forecasting, lifetime assessment and work quality.

References

1. Mill, T., Ellmann, A., Kiisa, M., Idnurm, J., Idnurm, S., Horemuz, M., Aavik, A.: Geodetic monitoring of bridge deformations occurring during static load testing. *Baltic J. Road Bridge Eng.* **10**(1), 17–27 (2015)

2. Park, H.S., Lee, H.M., Adeli, H., Lee, I.A.: New approach for health monitoring of structures: terrestrial laser scanning. *Comput.-Aided Civil Infrastruct. Eng.* **22**(1), 19–30 (2007)
3. Soudarissanane, S., Lindenbergh, R., Menenti, M., Teunissen, P.: Scanning geometry: influencing factor on the quality of terrestrial laser scanning points. *ISPRS J. Photogramm. Remote Sens.* **66**(4), 389–399 (2011)
4. Kutterer, H., Seitz, F., Alkhatib, H., Schmidt, M.: The 1st International Workshop on the Quality of Geodetic Observation & Monitoring Systems (QuGOMS 2011), Munich, Germany, 13–15 April 2011
5. Snieder, R., Hubbard, S., Haney, M., Bawden, G., Hatchell, P., Revil, A.: DOE geophysical monitoring working advanced noninvasive geophysical monitoring. In: *Techniques Group Annual Review of Earth and Planetary Sciences*, pp. 52–63 (2007)
6. Banerjee, D., Chakraborty, S.K., Bhattacharyya, S., Gangopadhyay, A.: Evaluation and analysis of road traffic noise in Asansol: an industrial town of Eastern India. *Int. J. Environ. Res. Publ. Health* **5**, 165–171 (2008)
7. Schofield, W., Breach, M.: *Engineering Surveying of Transport Facilities*, p. 367. Linacre House, Oxford (2007)
8. Yang, Y.M., Myers, J.J.: Live load test results of Missouri’s First high performance concrete superstructure bridge. In: *Transportation Research Board 82nd Annual Meeting*, Washington DC, pp. 89–97 (2003)
9. Erdélyi, J., Kopáček, A., Ilkovičová, L., Lipták, I., Kajánek, P.: Deformation monitoring of a parabolic structure using TLS. In: *Proceedings of “INGEO 2014”*, pp. 75–80 (2014)
10. Erofeev, V., Karpushin, S., Rodin, A., Tretiakov, I., Kalashnikov, V., Moroz, M., Smirnov, V., Smirnova, O., Rimshin, V., Matvievskiy, A.: Physical and mechanical properties of the cement stone based on biocidal Portland cement with active mineral additive. *Solid State Phenomena* **871**, 28–32 (2016)
11. Erofeev, V.T., Zavalishin, E.V., Rimshin, V.I., Kurbatov, V.L., Mosakov, B.S.: Frame composites based on soluble glass. *Res. J. Pharm. Biol. Chem. Sci.* **7**(3), 2506–2517 (2016)
12. Antoshkin, V.D., Erofeev, V.T., Travush, V.I., Rimshin, V.I., Kurbatov, V.L.: The problem optimization triangular geometric line field. *Mod. Appl. Sci.* **9**(3), 46–50 (2015)
13. Erofeev, V.T., Bogatov, A.D., Bogatova, S.N., Smirnov, V.F., Rimshin, V.I., Kurbatov, V. L.: Bioresistant building composites on the basis of glass wastes. *Biosci. Biotechnol. Res. Asia* **12**(1), 661–669 (2015)
14. Bazhenov, Y.M., Erofeev, V.T., Rimshin, V.I., Markov, S.V., Kurbatov, V.L.: Changes in the topology of a concrete porous space in interactions with the external medium. *Eng. Solid Mech.* **4**(4), 219–225 (2016)
15. Chapman, D., Metje, N., Stärk, A.: *Introduction to Tunnel Construction*, p. 417. Spon Press, New York (2010)

Thermal Properties of the Building with Low Energy Consumption (LEB)

Elena Statsenko¹ , Anastasia Ostrovaia¹ ,
Tatiana Musorina¹  , and Natalia Sergievskaya² 

¹ Peter the Great St. Petersburg Polytechnic University,
Politechnicheskaya Str., 29, 195251 St. Petersburg, Russia
tamusorina@mail.ru

² Moscow State University of Civil Engineering,
Yaroslavskoe shosse, 26, 129337 Moscow, Russia

Abstract. Energy saving is one of the important directions in the development of modern technology and energy. The article presents thermal calculation of a building with low energy consumption based on the architectural concept, which was developed earlier. At the same time calculation, can be executed for any terrain and any climatic zone in case of its known climatological data. There are three basic approaches to increase the energy efficiency of modern buildings: level increase of the walling insulation; increasing the efficiency of heating control, ventilation, lighting, air conditioning; the use of renewable energy sources. The maximum effect of power outage savings can be purchased only with the full analysis of space-planning, engineering and design solutions.

Keywords: Energy management · Transport buildings and structures
Energy saving

1 Introduction

The total volumes of new construction in the Russian Federation are increased every year. New buildings and structures are qualitatively different from the buildings constructed before 1995 when the standards for heat insulation have been raised. In most cases, the specific heat energy consumption is less in new building by 30–50% in comparison with the building constructed under the old standards. However, the specific energy consumption in buildings and structures constructed in Russia is notably higher than in other European countries at equitable climatic variables of the outdoor air. Thus, in the Russian Federation remains a lot of energy savings potential in the construction of new buildings.

Reserves for heat energy economy of buildings is:

- high air temperature in the building in the heating season;
- the use of nighttime tariff for electric energy and examples of heat energy storage;
- the use of intermittent heating in administrative and industrial structures;
- an increase of the solar radiance contribution in the heat account of buildings and structures, especially in the regions of Eastern Siberia [1].

Activities for energy saving to the needs HVAC are held in four main areas:

- an increase of heat insulation and tightness of the building outside surface;
- improvement of efficiency of heat supply, heating and ventilation systems;
- the motivation of energy consumers to quality attitude as well as the organization of energy recovery account, the form of the tariffs to payment for energy.

The development of the legal framework was considered the original basis for the transition to an energy-efficient and energy-saving kind of society life in the progressive European countries. It is quite minimal for the actual full-scale implementations in this area. Energy efficiency is an indicator of economic and scientific-technical potential of the society, permitting to estimate the percentage its development. Compare energy efficiency performance of the Russian economy with developed countries shows that the energy density of the Russian GDP (gross domestic product) is in some exceeded than in developed countries. Thus, the energy consumption stage per unit of Russia GDP being compared to approximately 4 times exceeded than in America - a country with high energy armament of material production, life and services. The percentage of electric energy consumption per unit of GDP comparable in Russia is higher than in the United States in 2.5 times, Japan and Germany in 3.6 times. All this shows that significant reserves of economy of energy resources in the Russian Federation can be seen the tune of 40–50% from the necessary consumed energy and fuel [2].

Development in the construction of buildings with low energy consumption in the near future will be the task of the research application in this area. Object of the real research is the project of the building with low energy consumption that is planned to be built in the territory of Peter the Great St. Petersburg Polytechnic University [3].

Object of a research represents the low-rise building developed within demonstration model of buildings with low consuming of energy (Fig. 1). The description of architectural and planning, constructive and engineering solutions of a designed project are provided in article [3]. Constructive solutions of the designed building are agreed with the requirements accepted in standards of Finland [6–11].



Fig. 1. Model of the demonstration house.

Thus in an updated version of the standard joint venture to construction climatology, comparing with the previous version of the standard (SR 23-01-99* “Building climatology”) for most of the settlements, as St. Petersburg and Moscow, design climate conditions have been restated upwards design outdoor air temperature and reduce the duration of heating period [4].

The area where you can dramatically reduce the amount of consumed fuel and as a result, power consumption and emissions into the atmosphere is housing, which according to various estimates consumes from 30 to 40% of all energy resources [5]. It is enough to increase the standards to the level of heat insulation [6], to improve the buildings automation level when adjusting the heat parameters to enter the building, to install the heat reclamation systems of exhaust air [7] and more efficient heating systems.

The first experience in the construction of buildings with ultra-low power consumption conducted by German researcher Wolfgang Feist from the Institute «Institute für Wohnen und Umwelt» and Swedish Professor Bo Adamson from «Lund University» proposed the concept of energy-passive houses [8]. In the 90s in Germany, Darmstadt was finished construction of the first house, marked the beginning of creation of a new construction technology energy-passive buildings. As practice shows, the experience was successful, and in 1996 Dr. Feist (Wolfgang Feist) in Darmstadt founded the Institute of passive house (Passivhaus Institut) due to implementation of the further research development [9]. During the 17 years the institute was built about 15 000 buildings, which correspond to the definition a passive house [10].

Currently, the construction of many important question is the impact of the effect of the level of thermal protection of protecting designs by the amount of heat loss in a building [11]. It is necessary to allocate some of the prominent authors in this area – Tabunshchikov et al. [12–16].

The main legislative acts of the Russian Federation in the field of energy savings are: Russian Federation Presidential Decree of June 04, 2008 № 889, the Federal Law of the Russian Federation of November 23, 2009 № 261-FL, Decree of the Government of the Russian Federation dated 25 January, 2011 № 18.

Biryukov and Dianov in the article [17] claim that all projects of the reconstructed buildings and new buildings shall consider volume “Energy efficiency”. In this volume according to the procedure ordered by territorial norms is calculated index of the heat consumption, which are compared to normative value of this index. Therefore, the procedure of calculation shall have rather high accuracy and to be available to daily project practice.

In foreign countries care of energy saving of resources is also very actual. In normative documents of many countries there are requirements to support of energy efficiency and standards of consuming by buildings of energy which permanently decrease [18, 19].

Taking into account the above work, aimed at reducing the consumption of energy of the existing buildings and constructions and usage of non-traditional sources of energy are represented urgent and having the big scientific, technical and practical significance construction of buildings with low consuming of energy.

Purpose: to prove the necessity of the construction of residential and administrative buildings with low energy consumption.

The following tasks must be solved to achieve this objective:

- To calculate the power of the heating system;
- The calculation of heat energy consumption in the heating season is needed (heating, ventilation, infiltration, home heat losses, solar heat gain, the annual heat energy consumption for heating during the heating season).

2 Materials and Methods

Regional Methodical Documents are harmonized with international standards, in particular with Building Code of Finland, Part D5 [23].

The loss of heat energy of the building by the ventilation heat transfer during the heating period Q_{vent}^y , kW·h/year, should be calculated using the formula according to Regional Methodical Documents (RMD 23-16-2012). Table 1 presents the power calculation of buildings heating systems with required low energy consumption to improve the energy efficiency of buildings (Table 2).

Table 1. Part 1. The power calculation of buildings heating systems with low energy consumption, according to the orientation of the building face on eight rhumbs.

Name of spaces	Protections		n	t _a , °C	t _c , °C	(t _a - t _c), °C	R ₀ ^{cht} , m2·°C/W	1/R ₀ ^{ch} , W/(m2·°C)	Main heat losses	Orientation
	Name	A, m ²								
1	2	3	4	5	6	7	8	9	10	11
LEB	IP	88	1	+20	-24	44	12.0	0.083	323	-
	SW	4.4	1	+20	-24	44	9.0	0.111	22	S
	SW	40.2	1	+20	-24	44	9.0	0.111	197	SW
	SW	22.6	1	+20	-24	44	9.0	0.111	111	SE
	SW	8.3	1	+20	-24	44	9.0	0.111	41	W
	SW	42.0	1	+20	-24	44	9.0	0.111	205	NW
	SW	25.2	1	+20	-24	44	9.0	0.111	123	NE
	EG	3.6	1	+20	-24	44	1.0	1	158	SE
	EG	15.8	1	+20	-24	44	1.0	1	695	NW
	SW	64	1	+20	-24	44	10.0	0.1	282	-
TOTAL for LEB										
vestibule	IP	8.0	1	+15	-24	39	12.0	0.083	26	-
	SW	6.5	1	+15	-24	39	9.0	0.111	28	SE
	SW	8.0	1	+15	-24	39	9.0	0.111	35	NW
	EG	5.0	1	+15	-24	39	1.0	1.0	195	SE
	ED	3.8	1	+15	-24	39	1.0	1.0	148	NE
	SW	5.2	1	+15	-24	39	10.0	0.1	20	-

Table 2. Part 2. The power calculation of buildings heating systems with low energy consumption, according to the orientation of the building face on eight rhumbs (Continue).

Name of space	Orientation	Additional heat losses, β_i					Q_{re} , W	Q_{inf} , W	$Q_{re} + Q_{inf}$, W	Total placement
		To a landmark	To a height	At angles	On the door	$(1 + \sum \beta_i)$				
1	11	12	13	14	15	16	17	18	19	20
LEB	–	–	–	–	–	1.00	323	–	323	2620
	S	0.00	0.00	0.10	0.00	1.1	24	–	24	
	SW	0.00	0.00	0.10	0.00	1.1	216	–	216	
	SE	0.05	0.00	0.10	0.00	1.15	128	–	128	
	W	0.05	0.00	0.10	0.00	1.15	47	–	47	
	NW	0.10	0.00	0.05	0.00	1.15	236	–	236	
	NE	0.10	0.00	0.05	0.00	1.15	142	–	142	
	SE	0.05	0.00	0.10	0.00	1.15	182	45	227	
	NW	0.10	0.00	0.05	0.00	1.15	800	195	995	
	–	–	–	–	–	1.00	282	–	282	
2380								240	2620	
vestibule	–	–	–	–	–	1.00	26	–	26	690
	SE	0.05	0.00	0.10	0.00	1.15	33	–	32	
	NE	0.10	0.00	0.05	0.00	1.15	41	–	40	
	SE	0.05	0.00	0.10	0.00	1.15	195	55	250	
	NE	0.10	0.00	0.05	0.75	1.90	281	39	320	
	–	–	–	–	–	1.00	20	–	20	
TOTAL for vestibule							596	94	690	
TOTAL for building							2976	334	3310	3310

The power calculation of buildings heating systems with low energy consumption:

$$\begin{aligned}
 P_{vent} &= \frac{n \cdot V_{he} \cdot \rho_{in}^{he} \cdot c_{in} \cdot (t_{in} - t_{ex}) \cdot (1 - \eta)}{3600} \\
 &= \frac{0.75 \cdot 400 \cdot 1.3 \cdot 1.0 \cdot (20 + 24) \cdot (1 - 0.72)}{3600} = 1.34(\text{kW}) \quad (1)
 \end{aligned}$$

Aggregate power of buildings heating and ventilation systems: $3.31 + 1.34 = 4.65$ (kW)

2.1 Calculation of Consumption in Buildings of Heat Energy for Heating and Ventilation

Annual consumption of heat energy for heating during the transition and the cold periods of the year Q_{in}^y , kW·h/year, should be calculated using the formula:

$$Q_{in}^y = \left[Q_{re}^y + Q_{vent}^y + Q_{inf}^y - (Q_{dom}^y + Q_{solex}^y) \cdot v_{inertia} \cdot \zeta \right] \cdot \beta_h, \quad (2)$$

Q_{re}^y – a transmission heat losses by the building of heat energy through the enclosing parts during the heating season, kW·h/year;

Q_{vent}^y – the heat losses by the construction due to ventilation heat transfer during the heating season, kW·h/year;

Q_{inf}^y – heat losses by the construction of heat energy due to the infiltration of cold air during the heating season through the enclosing parts, kW·h/year;

- Q_{dom}^y – household heat gain in the apartments and rooms of public purpose during the heating season, kW·h/year;
- Q_{solex}^y – heat gain through the outdoor translucent enclosure structure from solar radiation according to the orientation of the building face on eight rhumbs during heat period, kW·h/year;
- $\nu_{inertia}$ – heat gain reduction coefficient by thermal inertia of the enclosing parts;
- ζ – system effectiveness coefficient of the automatic control flow of heat for space heating;
- β_h – coefficient taking the additional heat consumption by heating system associated with a readability of the nominal heat flux nomenclature number of heating devices, their additional heat losses through the sections for walling radiators, heat loss from the pipes that pass through unheated spaces.

Transmission (through the enclosing parts) heat losses Q_{re}^y , kW·h, should be calculated using the following formula:

$$Q_{re}^y = 0.024 \cdot \left(\frac{A_w}{R_{cit_w}} + \frac{A_{win}}{R_{cit_{win}}} + \frac{A_l}{R_{cit_l}} + \frac{A_{do}}{R_{cit_{do}}} + \frac{A_{\Pi winp}}{R_{cit_{\Pi winp}}} + \frac{A_{overlap}}{R_{cit_{overlap}}} + \frac{A_{a.overlap}}{R_{cit_{a.overlap}}} + \frac{A_{b.overlap}}{R_{cit_{b.overlap}}} + \frac{A_{fl}}{R_{cit_{fl}}} \right) \times HDD \quad (3)$$

- $A_w \cdot R_{cit_w}$ – the area, m², and the calculation value of the reduced total thermal resistance, m²·s/W, of the external wall (with the exception of openings);
- $A_{win} \cdot R_{cit_{win}}$ – the same, the filling of area light (windows and balcony doors, show windows and leaded light);
- 0.024 – scaling factor of transmission waste of the heat energy from W·days in kW·h (1 day = 24 h. 1 W = 0.001 kW);
- HDD – heating season degree-day. °C days, designated for a certain group buildings using the formula:

$$HDD = (t_{in} - t_{he}) \cdot z_{he}, \quad (4)$$

- t_{in} – the calculated mean temperature of the building inside air, °C, taken for thermo technical calculation of building envelope of apartment buildings – 20 °C, public buildings – 18 °C, pre-school institutions – 22 °C, hospitals and health centers, hospitals and boarding schools – 21 °C schools – 20 °C, pool halls baths – 27 °C;
- t_{he}, z_{he} – the mean temperature of the inside air, °C, and period of heating taken for the period with a mean daily temperature of external air is not more than 10 °C - in the design of treatment and prevention, kindergartens, residential care facility, schools, halls and swimming pools and no more than 8 °C - in other cases.

The design temperature of external air in the cold season t_{ex} °C, accepted on the design and construction specifications equal to the average temperature of the coldest five-day week by security 0.92 and a mean temperature of external t_{he} , °C during the heating period, it should be in accordance with Table 3

Table 3. The design temperature of external air in the cold season.

The name locality	Estimated outside air temperature, °C		
	The coldest five days, t_c	Average for heating period t_{he} for buildings	
		Residential and public other than those listed in column 4	Clinics and hospitals, orphanages, kindergartens, schools
1	2	3	4
St. Petersburg	-24	-1.3	-0.4

Estimated air parameters inside the corresponding building types and premises should be taken from Table 4 for the thermotechnical calculation of building envelope.

Duration z_{he} , days, and degree-day HDD , °C-day, heating season for climatic conditions of St. Petersburg should be taken according to Table 5.

Table 4. Estimated temperature, relative humidity and drop point of the air inside the building, taken at the thermal calculations enclosing parts.

Appointment building	The estimated internal temperature t_i , °C	The relative humidity of the internal air φ_i , %	Dew point t_d , °C
1. Residential buildings, hotels, hostels, educational institutions (schools)	20	55	10.7
2. Clinics and hospitals	21	55	11.6
3. Kindergarten	22	55	12.6
4. Other public buildings (or public premises, built in residential buildings), other than those listed in paragraphs 1, 2 and 3 of Table 2	18	55	8.8

Table 5. Degree-day and duration of heating season.

The name locality	HDD, °C·day/duration of the heating period z_{he} , day				
	Appointment building				
	Apartments, hotels and hostels	Community other than those listed in columns 4, 5 and 6	General education schools	Clinics and hospitals, nursing homes	Kindergarten
1	2	3	4	5	6
St. Petersburg	4537/213	4111/213	4733/232	4965/232	5197/232

Construction LEB authors refer to the public with the HDD 4537 °C·d (with an estimated temperature of the air inside the building tin = 20 °C and the duration of the heating period $z_{he} = 213$ days). To place a tambour with an estimated temperature of the indoor air 15 °C, take the HDD $(15 + 0.4) \cdot 232 = 3573$ °C·day.

2.2 Heating

Taking into account the obtained climatological data authors will calculate transmission losses of thermal energy in LEB building:

$$\begin{aligned}
 Q_{re}^y &= 0.024 \cdot \left(\frac{142.7}{9.0} + \frac{19.4}{1.0} + \frac{88.0}{12.0} + \frac{64.0}{10.0} \right) \cdot 4537 + 0.024 \\
 &\quad \cdot \left(\frac{14.5}{9.0} + \frac{5.0}{1.0} + \frac{8.0}{12.0} + \frac{5.2}{10.0} + \frac{3.8}{1.0} \right) \cdot 3573 \\
 &= 6329.1 (\text{kW} \cdot \text{h})
 \end{aligned} \tag{5}$$

2.3 Ventilation

The loss of heat energy of the building by the ventilation heat transfer during the heating period Q_{vent}^y , kW·h/year

$$Q_{vent}^y = 0.0067 \cdot L_{cit} \cdot c_{in} \cdot \rho_{in}^{he} \cdot k_{day} \cdot k_{week} \cdot HDD \cdot (1 - \eta_{rec}), \tag{6}$$

- 0.0067 – scaling factor of duration of the heating period included in the formula for calculating the HDD from days to hours, and heat losses due to ventilation heat transfer kJ in MJ
- L_{cit} – the number of supply air in m³/h accepted for the designed building of equal 300 m³/h
- c_{in} – the mass specific heat of the air taking an equal 1.005 kJ/(kg·°C);
- ρ_{in}^{he} – the mean air density is assumed to be 1.3 kg/m³ for the climatic environment of St. Petersburg;
- k_{day} – daily utilization coefficient of ventilating equipment with mechanical (forced) ventilation, h/24 h, (at unorganized inflow (natural ventilation) k_{day} is accepted equal 1); for example, if the ventilating equipment at mechanical ventilation in office buildings is used for 8 h a day, k_{day} is accepted equal $8/24 = 0.333$
- k_{week} – average weekly coefficient of use of ventilation equipment with mechanical ventilation, days/7 days (at unorganized inflow (natural ventilation) the coefficient k_{week} is accepted equal 1); for example, if the ventilating equipment at mechanical ventilation in office buildings is used 5 days within a week, k_{week} is equal to $5/7 = 0.714$;
- HDD – the same as in the formula (2), °C·days

η_{rec} – energy efficiency ratio of the recovery installation of exhaust air at mechanical ventilation of rooms (for the made design decision η_{rec} the rivers it is accepted equal 0.72).

Substitute the project data into the formula (7):

$$\begin{aligned} Q_{vent}^y &= 0.0067 \cdot 300 \cdot 1.005 \cdot 1.3 \cdot 0.333 \cdot 0.714 \cdot 4537 \cdot (1 - 0.72) \\ &= 789.2(\text{kW} \cdot \text{h}) \end{aligned} \quad (7)$$

2.4 Infiltration

The loss of heat energy of the building by the infiltration of cold air during the heating period through enclosing parts Q_{inf}^y , should be calculated using the formula:

$$Q_{inf}^y = 0.0067 \cdot G_{ieca} \cdot \frac{n_{ieca}}{168} \cdot c_{in} \cdot HDD, \quad (8)$$

0.0067 – it is the same as in the formula (7);

G_{inf} – the number of air infiltration into the building through the building envelope, kg/h; for the designed building – the air coming to the tambour during the day of the heating season;

n_{inf} – number of hours of the accounting of an infiltration within a week, h, equal 168 for buildings with the balanced supply and exhaust ventilation and $168 \cdot (1 - k_{day} \cdot k_{week})$, in which rooms it is supported the space air overpressure an air subtime during action of forced mechanical ventilation;

c_{in} – the same as in the formula (7), kJ/(kg·°C);

HDD – the same as in the formula (2), for the tambour is accepted equal 3573 °C·days.

The number of infiltrating air G_{inf} f, kg/h, coming into the tambour of the room of the public building through fill openings leakages in the belief that they are on the windward side, should be defined by the formula:

$$G_{ieca} = \left(\frac{A_{win}}{R_{inf(win)}^{re}} \right) \cdot \left(\frac{\Delta p_{win}}{10} \right)^{2/3} + \left(\frac{A_{do}}{R_{inf(do)}^{re}} \right) \cdot \left(\frac{\Delta p_{do}}{10} \right)^{1/2}, \quad (9)$$

A_{win}, A_{door} – the windows total area and entrance external doors in the tambour, m²;

$R_{inf(win)}^{re}, R_{inf(door)}^{re}$ – the required resistance to air permeability of windows and exterior doors input, m²·h/kg;

$\Delta p_{win}, \Delta p_{door}$ – the calculated pressure difference of indoor and outdoor air, Pa calculated for windows on a formula

$$\Delta p_{win} = 0.28 \cdot H \cdot (\gamma_{ex} - \gamma_{in}) + 0.03 \cdot \gamma_{ex} \cdot v^2, \quad (10)$$

for external entrance doors to the building on a formula

$$\Delta p_{door} = 0.55 \cdot H \cdot (\gamma_{ex} - \gamma_{in}) + 0.03 \cdot \gamma_{ex} \cdot v^2, \quad (11)$$

In the formulas (9) and (10) the following notation:

- H – the building height (from the floor of the first floor to the top of the exhaust shafts), m;
- γ_{ex} – the relative density of external air accepted for conditions of St. Petersburg of equal 14.02 N/m³;
- γ_{in} – the weight of the indoor air taken equal: for residential buildings, secondary schools, hotels and hostels (with an estimated temperature of the indoor air $t_{in} = 20$ °C) – 11.82 N/m³;
- v – the maximum of the average wind speeds wind at rhumbs January, the repeatability of which is 16% or more, accepted for the climatic conditions in St. Petersburg equal to 4.2 m/s; for buildings more than 60 m v must be multiplied by a coefficient ξ wind speed changes in height accepted according to table 12 RMD 23-16-2012.

Substitute the project data into the formulas (7–11):

- $\Delta p_{win} = 11.7$ Pa;
- $\Delta p_{door} = 15.9$ Pa;
- $R_{inf(win)}^{re} = 5$ m² · h/kg;
- $R_{inf(door)}^{re} = 1.5$ m² · h/kg;
- $G_{inf} = 4.56$ kg/h.

The number of hours of accounting infiltration into the building during the week we will equal 168 because Tambour is not equipped with a mechanical ventilation system.

Authors will calculate by formula (8) heat losses of the building due to the infiltration of cold air:

$$\begin{aligned} Q_{inf}^y &= 0.0067 \cdot G_{inf} \cdot \frac{n_{inf}}{168} \cdot c_{in} \cdot HDD = 0.0067 \cdot 4.56 \cdot 1 \cdot 1.005 \cdot 3573 \\ &= 109.7 \text{ (кIW} \cdot \text{h)}. \end{aligned} \quad (12)$$

2.5 Household Heat Gain

Household heat gain during the heating period Q_{dom}^y , kW·h/year, should be determined using the formula (RMD 23-16-2012):

$$Q_{dom}^y = 0.024 \cdot q_{dom} \cdot z_{he} \cdot A_p, \quad (13)$$

- 0.024 – the same as in the formula (2);
- z_{he} – the same as in the formula (3), days (for the designed building z_{he} 213 days are equal);
- A_p – the calculated area of the building, which is determined in accordance with Construction Norms and Regulations 31-05 as the sum of the areas of all rooms, apart from corridors, tambours, walkways, stairwells, elevator shafts, internal open staircases and ramps, as well as premises for placements of engineering equipment and networks, m^2 (A_p is 92.8 m^2 for of the designed building);
- q_{dom} – the value of household heat emission calculated per 1 m^2 of building area (A_p), W/m^2 , taken:
- by the number of the people who are in the building (at the rate of 90 W/persons – for adult men, $90 \times 0.85 = 76.5$ W/persons – for women, $90 \times 0.75 = 67.5$ W/persons – for children);
 - by the number and capacity of lighting fixtures (based on a fixed power);
 - by the number and capacity of the office equipment and processing equipment (on the basis 10 W/m^2 or based generating capacity).

Facilities for public use without a particular technology are equated to offices. Thus heat gain during the working week (with 8-h working day and 5-day working week) are distributed as follows:

- heat gain from the light – $q_{light} = 25$ W/m^2 of the estimated area using 50% of working hours ($\tau_{light} = 0.5$),
- heat gain from the office equipment $q_{off.e} = 10$ W/m^2 of the estimated area using 40% of working hours ($\tau_{light} = 0.4$).

Then household heat gain q_{dom} per hour for the average day of the heating period may be determined by the formula:

$$q_{dom} = \left(\frac{\sum_{i=1}^n q_{people,i} \cdot n_{people}}{A_p} + q_{light} \cdot \tau_{light} + q_{off.e} \cdot \tau_{off.e} \right) \cdot k_{day} \cdot k_{week}, \quad (14)$$

- $q_{people,i}$ – heat emission from people, W/person;
- n_{people} – the estimated number of people (inhabitants workers, children), persons;
- A_p – the same as in the formula (9), m^2 ;
- q_{light} – the specific heat gain from lighting, W/m^2 ;
- τ_{light} – the ratio of the use duration of lighting during the working day in relation to the total duration of the working day;
- $q_{off.e}$ – heat emission from the office equipment and processing equipment, W/m^2 ;

- $\tau_{off,e}$ – the ratio of the use duration of the office equipment and processing equipment during the working day in relation to the total duration of the working day;
- k_{day}, k_{week} – the same as in the formula (4).

The number of workers in the building is accepted equal of 3.

Then household heat gain per hour for the average day consists of:

$$q_{dom} = \left(\frac{90 \cdot 3}{92.8} + 25 \cdot 0.5 + 10 \cdot 0.4 \right) \cdot 0.333 \cdot 0.714 = 4.6 \left(\frac{\text{kINT}}{\text{m}^2} \right)$$

Consequently, the household heat gain during the heating period are:

$$Q_{dom}^y = 0.024 \cdot q_{dom} \cdot z_{he} \cdot A_p = 0.024 \cdot 4.6 \cdot 213 \cdot 92.8 = 2182.2 \text{ (kINT} \cdot \text{h)}.$$

2.6 Solar Heat Gain

Heat gain through the external translucent external envelope from solar radiation based on the orientation of the facades on eight rhumbs during the heating period Q_{solex}^y , kWh/year, should be determined using the formula (RMD 23-16-2012):

$$Q_{solex}^y = \tau_{win} \cdot k_{win} \cdot \left(\sum_{i=1}^8 A_{win,i} \cdot I_{in,i} \right) + \tau_l \cdot k_l \cdot A_l \cdot I_l, \quad (15)$$

- τ_{win}, τ_l – coefficients taking into account the shadow of the area light according to flat skylights and windows opaque filling components, taken on the design data;
- k_{win}, k_l – coefficients of penetration of solar radiation for the light-transmitting fillings, respectively, windows and flat skylights accepted on passport data of the corresponding light-transmitting products;
- $A_{win,i}$ – the surface area of skylights facades of the building focused on eight areas (skylights staircase-elevator assembly not taken into account), m^2 ;
- A_l – the area of light of flat sky building as well roof windows at an angle to the horizontal of less than 45° , m^2 ;
- $I_{in,i}$ – the average during the heating period the quantity of solar radiation on a horizontal surface with the actual conditions of cloudiness respectively focused on the eight facades of buildings, kWh/m^2 ; for the climatic conditions of St. Petersburg is taken from Table 6;
- I_l – the average during the heating period the quantity of solar radiation on a horizontal surface with the actual conditions of cloudiness, MJ/m^2 ; for the climatic conditions of St. Petersburg is taken equal $253.3 \text{ kW} \cdot \text{h}/\text{m}^2$ (see. Table 6).

Roof windows and skylights are not projected in the building.

The coefficient considering opening windows shading light opaque elements τ_{win} for the received project solutions corresponding to 0.7; the coefficient of relative

penetration of solar radiation for the light transmitting filling k_{win} taken equal to 0.58. Then the heat gain through the external translucent walling from solar radiation based on the orientation of the facades on eight rhumbs during the heating period will be: $Q_{solex}^y = 0.7 \cdot 0.58 \cdot (15.8 \cdot 126.4 + 3.6 \cdot 250.6) = 1177.1(\text{kW} \cdot \text{h})$.

Table 6. The average during the heating period the quantity of solar radiation on a horizontal and vertical surface with the actual conditions of cloudiness.

The name locality	The horizontal surface	Vertical oriented surface:				
		N	NE/NW	E/W	SE/SW	S
St. Petersburg	912 (253.3)	394 (109.4)	455 (126.4)	650 (180.6)	902 (250.6)	1009 (280.3)

2.7 Coefficients

The reduce heat gain coefficient due to thermal inertia of filler structure v_{iex} for the buildings equate to 1. The coefficient of efficiency of the automatic control system of heat supply in ζ heating systems for of the designed building taken equal to 1. The coefficient considering additional thermal consumption by heating system, relating to the readability of the nominal heat flux of the heaters nomenclature number, their additional heat loss through the radiator sections for walling systems, with piping heat losses, following through unheated rooms β_h for this designed building we equate to 1.

3 Results

The annual consumption of heat energy for heating of the projected building during the year heating period

When measuring the amount of heat consumed for heating during the heating period it is recommended to take into account the efficiency of this system of automatic control heating and heat gain through external translucent systems from solar radiation, taking into account the orientation of the building facade to 8 rhumb its intensity at the actual cloud conditions, shading skylights opaque objects and the relative passing it through a light transmitting filling of window spaces [20].

We will substitute the calculated parameters of heat power in the formula (16):

$$\begin{aligned}
 Q_{hp}^y &= [Q_{re}^y + Q_{vent}^y + Q_{inf}^y - (Q_{dom}^y + Q_{solex}^y) \cdot v_{inertia} \cdot \zeta] \cdot \beta_h \\
 &= [6329.1 + 789.2 + 109.7 - (2182.2 + 1177.1) \cdot 1 \cdot 1] \cdot 1 \\
 &= 3868.7(\text{kW} \cdot \text{h}).
 \end{aligned}
 \tag{16}$$

Thus, the heat energy annual consumption for heating and ventilation in the projected building will constitute 3868.7 kWh/year. The specific annual expense of heat energy in the projectable building will constitute:

$$q_{\text{hp}}^y = \frac{Q_{\text{hp}}^y}{A_p} = \frac{3868.7}{92.8} = 41.7 \left(\frac{\text{kW} \cdot \text{h}}{\text{m}^2 \cdot \text{year}} \right). \quad (17)$$

4 Discussion

Papers [18, 23] presents a calculation of the loss of heat through the shell of an apartment building at different levels of thermal insulation of external building envelopes (walls, windows, coating) according to the regulations: Russian Construction Norm and Regulations (SR 50.13330.2012), and the National Building Code of Finland, Part D3. The effect of the level of thermal protection of protecting designs on the magnitude of heat loss, operating costs and the cost of fuel and energy resources during the heating season (10, 30 and 50 years of operation of the building) by the example of a residential apartment building. Recommendations about reduction of payback periods are provided. Articles [21, 22] also is devoted definition of optimum, economically well-founded thickness of a insulant in systems of rear ventilated facades. Are resulted thermotechnical and economic calculations. The optimum thickness of the insulant in the given systems is offered. According to the results of energy audit the analyses of state of energy consumption are provided. The class of energy efficiency is defined. The recommendations and prospective opportunities to save energy and increase power efficiency of “Gidrokorpus-2” are presented as a resume of this article [5]. This article is different from the works presented by the fact that calculation is for low-energy buildings, taking into account the terrain and bred premises.

5 Conclusions

The calculation is for a specific building, which is projected on the territory of Peter the Great St. Petersburg Polytechnic University, takes into account the terrain and layout of the premises. The maximum effect of energy saving can be acquired only in the complete analysis of space-planning, engineering and constructive decisions. Applicable for the project of the building with low consuming of energy:




- The total rate power of heating and ventilation system is 4.65 kW;
- Estimated value of the total thermal energy consumption for heating and ventilation is 3868.7 kWh/ year. The specific annual expenditure of thermal energy makes 41.7 kWh/(m²·year).

References

1. Gorshkov, A., Rymkevich, P., Vatin, N.: Simulation of non-stationary heat transfer processes in autoclaved aerated concrete-walls. *Mag. Civil Eng.* **8**, 38–48 (2014)
2. Vatin, N., Gamayunova, O.: Energy efficiency and energy audit: the experience of the Russian federation and the republic of Belarus. *Adv. Mater. Res.* **2159**, 1065–1069 (2015)
3. Gorshkov, A., Rakova, K., Musorina, T., Tseitin, D., Agishev, K.: Building project with low consumption of thermal energy for heating. *Constr. Unique Build. Struct.* **31**(4), 232–247 (2015)

4. Gorshkov, A., Vatin, N., Nemova, D., Tarasova, D.: The brickwork joints effect on the thermotechnical uniformity of the exterior walls from gas-concrete blocks. *Appl. Mech. Mater.* **725–726**, 3–8 (2015)
5. Vatin, N., Gorshkov, A., Nemova, D., Tarasova, D.: Energy efficiency of facades at major repairs of buildings. *Appl. Mech. Mater.* **633–634**, 991–996 (2014)
6. Vatin, N., Gorshkov, A., Nemova, D., Gamayunova, O., Tarasova, D.: Humidity conditions of homogeneous wall from gas-concrete blocks with finishing plaster compounds. *Appl. Mech. Mater.* **670–671**, 349–354 (2014)
7. Petrichenko, M., Vatin, N., Nemova, D., Olshevskiy, V.: The results of experimental determination of air output and velocity of flow in double skin facades. *Appl. Mech. Mater.* **725–726**, 93–99 (2015)
8. Perlova, E., Platonova, M., Gorshkov, A., Rakova, X.: Concept project of zero energy. *Build. Procedia Eng.* **100**, 1505–1514 (2015)
9. Gorshkov, A., Vatin, N., Nemova, D., Shabaldin, A., Melnikova, L.: Using life-cycle analysis to assess energy savings delivered by building insulation. *Procedia Eng.* **117**, 1080–1089 (2015)
10. Korniyenko, S., Vatin, N., Gorshkov, A.: Thermophysical field testing of residential buildings made of autoclaved aerated concrete blocks. *Mag. Civil Eng.* **4(64)**, 10–25 (2016)
11. Olshevskiy, V., Statsenko, E., Musorina, T., Nemova, D., Ostrovaia, A.: Moisture transfer in ventilated facade structures. In: *MATEC Web of Conferences*, vol. 53, pp. 1–5 (2016)
12. Romanova, A., Rymkevich, P., Gorshkov, A., Stalevich, A., Ginzburg, B.: A new phenomenon - amplitude-modulated free oscillations (beatings) in loaded, highly oriented fibers from semicrystalline polymers. *J. Macromol. Sci. Part B Phys.* **46(3)**, 467–474 (2007)
13. Pukhkal, V.: Humidity conditions for exterior walls insulation (case study of residential housing development in Saint-Petersburg). *Procedia Eng.* **117**, 616–623 (2015). <https://doi.org/10.1016/j.proeng.2015.08.222>
14. Murgul, V.: Special aspects of attic floor warming in historic buildings. In: *MATEC Web of Conferences*, 06001 (2017). <https://doi.org/10.1051/mateconf/201710606001>
15. Perlova, E., Karpova, S., Rakova, X., Bondarenko, E., Platonova, M., Gorshkov, A.: The architectural concept of the building with low energy consumption. *Appl. Mech. Mater.* **725–726**, 1580–1588 (2015)
16. Pukhkal, V., Vatin, N., Murgul, V.: Central ventilation system with heat recovery as one of measures to upgrade energy efficiency of historic buildings. *Appl. Mech. Mater.* **633–634**, 1077–1081 (2014)
17. Murgul, V.: Heat transfer performance uniformity factor for the basement floor made of brick vaults in historic buildings. In: *MATEC Web of Conferences*, 06002 (2017). <https://doi.org/10.1051/mateconf/201710606002>
18. Vatin, N., Petrichenko, M., Nemova, D.: Hydraulic methods for calculation of system of rear ventilated facades. *Appl. Mech. Mater.* **633–634**, 1007–1012 (2014)
19. Pukhkal, V., Murgul, V., Garifullin, M.: Reconstruction of buildings with a superstructure mansard: options to reduce energy intensity of buildings. *Procedia Eng.* **117**, 624–627 (2015). <https://doi.org/10.1016/j.proeng.2015.08.223>
20. Tanner, J., Varela, J., Klingner, R., Brightman, M., Cancino, U.: Seismic testing of autoclaved aerated concrete shearwalls: a comprehensive review. *ACI Struct. J.* **102**, 374–382 (2005)
21. Zemitis, J., Borodinecs, A., Frolova, M.: Measurements of moisture production caused by various sources. *Energy Build.* **127**, 884–891 (2016)
22. Vatin, N., Nemova, D., Rymkevich, P., Gorshkov, A.: Impact of the thermal protection of protecting designs by the amount of heat loss in a building. *Mag. Civil Eng.* **8**, 4–14 (2012)
23. Regional Medical Documents of Saint-Petersburg RMD 23–16–2012. Recommendations about support of energetic efficiency of residential and public buildings

Energy Efficiency Upgrading of Enclosing Structures of Mass Housing of the Soviet Union

Eliza Gumerova¹, Olga Gamayunova¹,
and Tatiana Meshcheryakova²

¹ Peter the Great St. Petersburg Polytechnic University,
Polytechnicheskaya, 29, St. Petersburg 195251, Russia
eliza_gumerova@mail.ru

² Moscow State University of Civil Engineering,
Yaroslavskoe shosse, 26, Moscow 129337, Russia

Abstract. In this article we consider about current state of mass housing of the Soviet Union. The vast majority of houses of that era has the lowest value of noise and thermal insulation. We calculate existing value of thermal resistance of external wall of OD-type building. Moreover, we find the insulation of enclosing structures and conclude that insulation of walls and repair can solve the problem of insufficient heat and sound insulation without demolition of mass housing of the Soviet Union era.

Keywords: Energy management · Energy efficiency
Transport buildings and structures

1 Introduction

The mass housing of the Soviet Union era (the so-called “Khrushchevka”) - the type of low-cost, concrete-paneled or brick three- to five-storied apartment buildings which was built in the USSR from 1950s to 1980s during the time its namesake Nikita Khrushchev directed the Soviet government. These residential houses relate to functional architecture. It is social housing, which people got for free, and planned to be a temporary housing. Subsequently, however, the period of its use is constantly increasing due to insufficient amount of dwelling houses. Distinctive features of mass housing of the Soviet Union era are cramped and uncomfortable apartments and unattractive architecture [1, 2]. The state could provide housing for citizens because of the low cost of construction. In February in 2017 deputies of the Moscow city decided to demolish all the buildings, which remained in the Russian capital. According to the authors of the proposal, the majority of mass housing of the Soviet Union era is unfit for general repair. It is easier to demolish than begin to renovate.

The construction of mass housing of the Soviet Union era began in the 60s of the last century. The principle of design was despite the minimal cost to provide every family for housing. Therefore, initially, there had been brick buildings, but later the construction of prefabricated houses started. It is a small five-storied building without elevator, garbage chute and the attic [3]. The lack of wall insulation is the cause of cold in winter and heat in summer in the apartment.

Most five-storied buildings are still habitable. It is possible to heighten some apartment blocks, meanwhile, to increase the living floor space. In several areas of Moscow designers have already implemented such projects. Despite the simplicity of demolition this type of blocks is still high-quality housing [4]. Therefore, it is necessary to consider alternative options for repair and renovation of the housing.

2 Methods and Materials

2.1 Types of Mass Housing of the Soviet Union Era. Features of Apartment Blocks of Type OD

There are various types of mass housing of the Soviet Union era, they have a certain similarity, but each of them has its own distinctive features.

Type K-7 (in Saint-Petersburg - OD) is one of the first types of industrial housing (years of construction: 1958–1966). It is frame-panel scheme. Apartments have large enough for kitchen, separate bathroom and lavatory. Houses have low noise and thermal insulation. There was a decision to demolish the blocks [5–7].

Type 335 (since 1958) is one of the most widespread types of mass housing of the Soviet Union era. These houses with a prefabricated concrete frame and exterior panel walls (the so-called incomplete frame). The cheapest type of all the panel buildings.

Type 464 also is one of the most widespread types of mass housing of the Soviet Union era (years of construction: 1958–1963). Load-bearing concrete walls with a thickness of 0.35 m which builders pave with ceramic tiles. The apartment blocks have floors from reinforced concrete. Implementation since 1960. The lack of damping of vibration. The design organization “Giprograd” from Kiev developed type 438 (years of construction: 1958–1978). These houses are frameless with spine walls. The foundations were of rubble concrete, and the walls were of brick.

Type 447 (years of construction: 1958–1964) is the most common type throughout the USSR, brick apartment blocks. Due to the thick walls of sand-lime or red brick, these houses are superior in heat and sound insulation not only panel types of mass housing of the Soviet Union era, but also new prefabricated houses. Interior walls in the apartments are not thorough, it allows architectural replanning. They do not refer to demolished types and have an increased service life in comparison with other dwelling houses.

2.2 Features of Apartment Blocks of Type OD

Apartment blocks of type OD was built in 1957–1963. These buildings are in many cities and have an enormous heat loss. In addition to low insulation, there are other significant shortcomings: tiny combined bathrooms and lavatories, thin interior walls with its thickness of only 4 cm, without sound insulating properties.

The frame-panel building;

- Number of floors - 5, 9;
- Height of habitable rooms - 260 cm;
- Apartments - from 1 to 3 living rooms;

- Years of construction – 1959–1964;
- 216 houses of this type in the Nevsky district, Saint-Petersburg

There are two modifications of type OD: OD-4 and OD-6, which differ in a number of sections. Characteristics of the multiple-unit housing projects of type OD are in Table 1.

Table 1. Characteristics of the multiple-unit housing projects.

Type	Quantity			The scope of flats			Living area, sq.m.	Usable space, sq.m.	Volume, m ³
	Sections	Floors	Flats	1-roomed	2-r.	3-r.			
OD-4	4	5	60	10	40	10	1876	2718	9860
OD-6	6	5	90	15	60	15	2844	4077	14790

2.3 Thermotechnical Properties of Enclosed Walls in Buildings of Type OD

In houses of type OD the construction of the outer wall is thin-walled threelayer panels consisting of outer reinforced concrete shell with ribs along the contour, insulation of mineral-wool plate on phenolic binder, aerated concrete, foam glass and internal reinforced cement-sand plaster layer [8, 9].

The characteristics of frost penetration of panels are stains of damp and mould, which protrude on the inner surface of the outer walls while the decreasing outdoor temperature. In some cases rime frost and ice are on the walls during a severe frost [10]. Panels in the buildings of type OD also freeze as on the highest floor, as in any other part of the wall on any floor.

In multilayer walls the cause of freezing is the use of insulation with high humidity, hydration and loss of insulation is because of insufficient thickness.

In some types of houses the specific design features of the joints and deviations from the project also contribute to these processes. For instance, houses of type OD - filling the connector between the panels with heavy concrete.

Winterization of three-layered walls with insulation of mineral wool plate is in replacement of the insulation. In this case builders open the inner layer of the panel and remove the existing insulation [11]. Cleared cavity of wall should be dry and tightly sealed with packages of mineral wool, wrapped in plastic film, which thickness must correspond to the width of the cavity. The opened area with plaster mortar is to apply on mesh which mounted on the reinforcement bars [12, 13]. The faces of ribs are not to destroy while opening the cavity of wall.

Insulation of horizontal joints should be with deleting the raw or sagging insulation, drying the cavity while the replacement of insulation and sealing the joint with concrete in houses with three-layer outer walls [14, 15]. Pre-preparatory works consist in chipping the edge of the panel wall and the concrete sealing of the slab to a depth of 100 mm and a width of about 100 mm (the floor is pre-parsed along the wall), padding of a plaster layer of the wallboard on the plot with a width of 200 mm from the horizontal joint. There is also need in repair the plaster on the grid assigned to

reinforcement bars after laying the insulation and the concreting of chipped corners of the panel and slab concrete. In some cases, if it is impossible to resolve the freezing of the vertical corner joints by the above method, there will be recommendation about bevel of concrete. The bevel should have a triangular cross-section with the dimensions of the legs 25 cm.

Thermotechnical characteristics of materials, which dwelling houses of type OD consist of are in Table 2. Outer walls - reinforced concrete panels with insulation of penokeralit.

Table 2. Thermotechnical characteristics of materials.

Material	Thickness of layer (δ), mm	Density (ρ), kg/m ³	Heat conductivity (λ), W/(m·°C)
Reinforced concrete	300	2500	1.7
Penokeralit	10	500	0.15

Thermal calculation showed that the thermal resistance of the wall $R_0 = 0.4016 \text{ m}^2 \times \text{°C/W}$ is below the required value $R_{\text{req}} = 3.0786 \text{ m}^2 \times \text{°C/W}$. Obviously, in this case, there are two options: either to pick up the insulation for the external walls, or to increase heating costs. The optimal decision is to find the insulation of enclosing structures [16–18].

2.4 A the Selection of Insulation for Improvement Energy Efficiency of Enclosing Structures of Type OD Buildings

There are several options for insulation: insulation with mineral wool, expanded polystyrene, stone wool, etc.

Mineral wool

In fact, the mineral wool is divided into 4 materials:

- glass fibre;
- slag wool;
- rock wool;
- basalt wool.

All four types have similar composition of the mineral wool, however, differ in the length and thickness of fibre [19]. Differences in the structure define material properties. Various types of mineral wool have different heat conductivity, moisture resistance, and resistance to mechanical stress that is why it is significant to understand what the kind of mineral wool project designers need for the certain wall.

Characteristics of the mineral wool

- Is not flammable and able to resist the spread of fire. So it can be used as a vehicle to protect against fire;
- The degree of noise abatement is very high. It may be used as a sound insulation;
- Chemical passivity – high;

- The hygroscopicity is low;
- Shrinkage is very low. The size of the material is almost not changed, so it is possible to avoid occurrence of cold joint.

Water vapour permeability is high. It is disadvantage of the heat retainer. While application it is necessary to install a vapour barrier layer [20, 21].

Foam polystyrene

Foam polystyrene consists of air (98%) [22–24]. The remaining 2% is polystyrene, which is derived from oil. Furthermore it has a small number of modifiers. In particular, it may be flame retardants. Properties of foam polystyrene:

- Does not absorb moisture;
- Resistant to corrosion;
- Defies the effects of microflora and biological agents;
- Almost not combustible. Even if it inflames, there will be much less heat than from the burning wood.

Expanded polystyrene has no limits in applying. It can be used for thermal insulation of ceilings and floors; in addition, it will help to reduce the transmission of impact noise. This insulator is used for winterization the roof.

Stone wool

It is made of gabbro and diabase, the thickness of the fibre is 5–12 μm , and the length is 1.6 cm. This material resembles in its properties the slag wool. However, this material is not prickly, which will be a benefit during installation.

Stone wool absorbs water poorly. So it can be used for heating plating of rooms.

We will calculate the thermal resistance of enclosing structures of buildings of type OD while using the insulation material “ISOVER Warm walls”.

“ISOVER Warm walls” is mineral wool insulation. Thickness: 50, 100 mm. The thermal conductivity 0.036 $\text{W}/(\text{m}\cdot^{\circ}\text{C})$.

The minimal required thermal resistance of the thermal insulation material is calculated by the formula [3]:

$$R_{ins}^{req} = R_{req} - (R_{int} + R_{ext} + \sum R_i) = 3.0786 - 0.4016 = 2.6770 \frac{\text{m}^2 \cdot ^{\circ}\text{C}}{\text{W}} \quad (1)$$

The thickness of insulation layer [3]:

$$\delta_{ins}^{req} = \lambda_{ins} \cdot R_{ins}^{req} = 0.036 \cdot 2.6770 = 0.096 \text{ m} = 96 \text{ mm} \quad (2)$$

If the total thickness of layer is equal to 100 mm, the thermal resistance will be defined by this sum:

$$\begin{aligned} R_0^{ins} &= R_{ins} + R_{ext} + \sum R_i^{ins} \\ &= \frac{1}{8,7} + \frac{1}{23} + 0,18 + \frac{0,1}{0,036} = 3.113 \frac{\text{m}^2 \cdot ^{\circ}\text{C}}{\text{W}} \end{aligned} \quad (3)$$

We can conclude that $R_0 = 3.113 \text{ m}^2 \cdot \text{°C/W} > R_{req0} = 3.0786 \text{ m}^2 \cdot \text{°C/W}$, therefore, we chose the thickness of the insulation correctly.

3 Results

In a similar way we produce a thermal calculation for other heat insulations that can be used to increase thermal resistance of wall structures of residential houses of type OD, and present the results in Table 3.

Table 3. Thermotechnical assessment of application of insulation layers.

The insulation layer	Heat conductivity (λ_{ins}), $\text{W/m}^2 \times \text{°C}$	Required thickness of insulation (δ_{ins}^{req}), mm	Used thickness of insulation (δ_{ins}^{req}), mm	Thermal resistance of wall with insulation (R_0^{ins}), $\text{m}^2 \cdot \text{°C/W}$
ISOVER Warm Walls	0.036	96	100	3.113
URSA TERRA 34 PN	0.034	91	100	3.276
Penoplex Comfort	0.030	81	100	3.668
Knauf Therm Wall PRO	0.042	112	120	3.192
PAROC InWall	0.035	94	100	3.192

Table 3 shows that the best solution will be the use of insulation boards “Penoplex Comfort” while modernization of residential houses of type OD for the aim to improve the thermal insulation of external walls since thermal resistance of the wall with insulation will be $3.668 \text{ m}^2 \cdot \text{°C/W}$.

4 Conclusions

Currently, there is a program of resettlement of inhabitants of the blocks of the industrial construction in Moscow. It involves 1722 five-storey buildings with a total area of 6.3 million square meters: the program includes only the oldest types of houses. It is the panel buildings without balconies and with gas pumps; the significant portion of these blocks was built in the 50s and 60s years of the last century. Such programs exist in other major Russian cities, however, in smaller extent. Every time the authorities debate on whether to demolish or reconstruct.



Insulation of walls and repair can solve the problem of insufficient heat and sound insulation without demolition of mass housing of the Soviet Union era, as well as its insufficient heat and sound insulation can be resolved with, without resorting to the demolition of those buildings.

References

1. Vatin, N., Gamayunova, O., Nemova, D.: Analysis of the real estate market of St. Petersburg. *AMM* **638–640**, 2460–2464 (2014)
2. Vatin, N., Gamayunova, O.: Energy efficiency and energy audit: the experience of the Russian Federation and the Republic of Belarus. *AMR* **1065–1069**, 2159 (2015)
3. Vatin, N., Gamayunova, O.: Choosing the right type of windows to improve energy efficiency of buildings. *AMM* **633–634**, 972–976 (2014)
4. Vatin, N., Gamayunova, O.: Energy saving at home. *AMM* **672–674**, 550–553 (2014)
5. Vatin, N., Gamayunova, O.: The role of the state and citizens in improving energy efficiency. *AMM* **725**, 1493 (2015)
6. Vatin, N., Gamayunova, O., Nemova, D.: An energy audit of kindergartens to improve their energy efficiency. In: *Advances in Civil Engineering and Building Materials IV - Selected and Peer Reviewed Papers from the 2014 4th International Conference on Civil Engineering and Building Materials, 4th CEBM 2014*, pp. 305–308 (2015)
7. Vatin, N., Gamayunova, O., Nemova, D.: Provedenie ehnergoaudita detskih sadov s cel'yu povysheniya ehnergoehffektivnosti [An energy audit of kindergartens with the aim of increasing energy efficiency]. *Constr. Unique Build. Struct.* **9(24)**, 71–83 (2014). (in Russian)
8. Kiryudcheva, A., Shishkina, V., Nemova, D.: Energoehffektivnost' ogradhdayushchih konstrukcij obshchestvennyh zdaniy [The energy efficiency of the walling of public buildings]. *Constr. Unique Build. Struct.* **5(44)**, 19–30 (2016). (in Russian)
9. Tseitin, D., Vatin, N., Nemova, D., Rymkevich, P., Gorshkov, A.: Tekhnikoehkonomicheskoe obosnovanie utepleniya fasadov pri renovacii zhilyh zdaniy pervyh massovyh serij [Feasibility study of facade insulation for renovation of residential buildings of the first mass series]. *Constr. Unique Build. Struct.* **1**, 20–31 (2016). (in Russian)
10. Vilinskaya, A., Nemova, D., Davydova, E., Gnam, P.: Povyslenie klassa ehnergoehffektivnosti obshchestvennogo zdaniya [Upgrade energy efficiency of public buildings]. *Constr. Unique Build. Struct.* **9(36)**, 7–17 (2015). (in Russian)
11. Kopylova, A., Bogomolova, A., Nemova, D.: Vlazhnostnyj rezhim ogradhdayushchej konstrukcii s oblicovkoj silikatnym kirpichom [Humidity conditions of enclosing structure with silicate brick veneer]. *Constr. Unique Build. Struct.* **6**, 74–86 (2015). (in Russian)
12. Vatin, N., Nemova, D., Tarasova, D., Staritsyna, A.: Increase of energy efficiency for educational institution building. *AMR* **953–954**, 854–870 (2014)
13. Nemova, D., Gorshkov, A., Vatin, N., Kashabin, A., Tseytin, D., Rymkevich, P.: V Tekhniko-ehkonomicheskoe obosnovanie po utepleniyu naruzhnyh sten mnogokvartirnogo zhilogo zdaniya s ustrojstvom ventiliruemogo fasada [Feasibility study on warming of external walls of residential buildings with the device of a ventilated facade]. *Constr. Unique Build. Struct.* **11(26)**, 70–84 (2014). (in Russian)
14. Gorshkov, A., Rymkevich, P., Nemova, D., Vatin, N.: Ehkonomicheskaya ehffektivnost' investicij v ehnergoberezenie [Economic efficiency of investments in energy efficiency]. *Inzhenernye sistemy. AVOK - Severo-Zapad* [Eng. Syst. AVOK North – West]. **3**, 32–36 (2014). (in Russian)
15. Vatin, N., Nemova, D., Kazimirova, A., Gureev, K.: Increase of energy efficiency of the building of kindergarten. *AMR* **953–954**, 1537–1544 (2014)
16. Vatin, N., Nemova, D., Murgul, V., Pukhkal, V., Golik, A., Chizhov, E.: Reconstruction of administrative buildings of the 70's: the possibility of energy modernization. *J. Appl. Eng. Sci.* **1**, 37–44 (2014)

17. Gorshkov, A., Nemova, D., Vatin, N.: Formula ehnergoeffektivnosti [The formula of energy efficiency]. *Constr. Unique Build. Struct.* **7**(12), 49–63 (2013). (in Russian)
18. Pukhkal, V.: Humidity conditions for exterior walls insulation (case study of residential housing development in Saint-Petersburg). *Procedia Eng.* **117**, 616–623 (2015). <https://doi.org/10.1016/j.proeng.2015.08.222>. Accessed 19 Aug 2017
19. Gorshkov, A.: Principy ehnergoberezheniya v zdaniyah [The principles of energy efficiency in buildings] *Stroitel'nye materialy, oborudovanie, tekhnologii XXI veka* [Build. Mater. Equip. Technol. XXI Century] **7**, 26–35 (2014). (in Russian)
20. Pukhkal, V., Murgul, V., Garifullin, M.: Reconstruction of buildings with a superstructure mansard: options to reduce energy intensity of buildings. *Procedia Eng.* **117**, 624–627 (2015). <https://doi.org/10.1016/j.proeng.2015.08.223>. Accessed 22 Aug 2017
21. Jakšić, Ž., Trivunić, M., Adamtsevich, A.: Flexibility and adaptability - key elements of end-user participation in living space designing. In: *MATEC Web of Conferences*, vol. 106, p. 01001 (2017). <http://doi.org/10.1051/mateconf/201710601001>. Accessed 22 Aug 2017
22. Gorshkov, A., Muraviev, P., Tarakin, A.: Povyshenie urovnya teploizolyacii naruzhnyh sten maloetazhnogo doma [Increasing the level of insulation of external walls of low-rise houses] *EHnergoberezhenie* [Energy Sav.] **8**, 30–35 (2016). (in Russian)
23. Korniyenko, S., Vatin, N., Gorshkov, A.: Thermophysical field testing of residential buildings made of autoclaved aerated concrete blocks. *Mag. Civil Eng.* **4**(64), 10–25 (2016). (in Russian)
24. Korniyenko, S., Vatin, N., Gorshkov, A.: Analiz teploehnergeticheskikh karakteristik zhilogo zdaniya iz gazobetonnyh blokov [Analysis of thermal power characteristics of a residential building of concrete blocks]. *Constr. Unique Build. Struct.* **12**(51), 45–60 (2016). (in Russian)

Energy Efficiency of Structural Regulation of Stress-Related Characteristics of Concrete

Igor Bezgodov  and Elena Dmitrenko  

Moscow State University of Civil Engineering,
Yaroslavskoye Sh. 26, 129337 Moscow, Russia
DmitrenkoEN@mgsu.ru

Abstract. The article suggests carrying out a wide range research of efficient additives capable of regulating the physical, mechanical and rheological properties of concrete. It also provides experimental studies that prove the ability to solve this problem. Air-entraining agents can be an effective additive to reduce the modulus of elasticity and to increase the limit of the relative compression deformation. The article presents the results of short-term tests for concrete with/without NAR (neutralized air-entraining resin) additive, performed by the method of obtaining the full concrete deformation diagrams. It has shown that the introduction of an NAR additive greatly reduces modulus of elasticity and increases the limit compressive deformability of concrete. In conditions of prolonged load, the creep of pure sand concrete is compared to that of concrete with clay and lime additives. There is quite a significant increase in the creep deformation in concrete with a clay-limestone additive.

Keywords: Concrete · Modified additives · Deformability
Modulus of elasticity · Creep · Structural regulation

1 Introduction

Currently, modified concretes are on the rise. Main concrete modifiers are additives for different purposes [1–3]. The use of additives of certain quality, and in optimal amount allows to manage structure formation processes and to create concrete with desirable properties. Due to using additives, it is possible to control concrete mix properties, concrete setting and hardening, to improve durability, frost resistance, waterproofing, and other properties. Unfortunately, among the many existing additives there are no additives suitable for regulating the stress-related properties of concrete: modulus of elasticity, and ultimate compressive and tensile deformability, and creep.

Meanwhile, in some cases, a low modulus of elasticity and increased deformability can play a positive role in the calculation of concrete and reinforced concrete structures and buildings. For example, the use of high-strength reinforcement in central compression requires increased deformability of concrete, which leads to increased bearing capacity pillars [4, 5]. In conditions of seismic and dynamic impact zones, the structure concrete resists better, having a low modulus of elasticity and increased deformability. In zones of stress concentration, the redistribution of stress slows down the process of cracking. Increased fracture resistance of structures while maintaining a structural

defect index [6] is important for the operation of waterworks. A number of studies [7, 8] have shown that one of the most promising ways of increasing longevity of airfield and road concrete pavements is the use of a variety of modified additives that alter their deformability.

Unfortunately, currently there is no list of such additives and no research results on their effectiveness. This is a cross-sectorial problem of two science disciplines namely of the “Materials” and “Mechanics of solid body deformation.”

2 Materials and Methods

The adjustment of modulus of elasticity and ultimate deformability can proceed in various ways, but the reduction of the modulus of elasticity is not always followed by increasing the limit deformability at compression. In addition, there are cases when in the conditions of short-term loads the limit deformability increase is not observed, and in the conditions of long-term exposure a significant increase in creep has been noted. Therefore, to assess the ultimate deformability is also necessary in the conditions of long-term loading.

It is possible to adjust the elastic limit and deformability module in several ways. Therefore, for example, using large and small low-modulus filler, we can reduce the modulus of elasticity, but not the fact that the limit deformability will increase.

Air-entraining additives used in our industry make possible obtaining materials with air uniformly distributed therein in the form of fine air bubbles, which leads to lower modulus and higher limit deformability.

The introduction of some additives may change the cement crystallization process and cause a change of rheology processes in concrete under load. The complex use of low modulus fillers (gravel and sand), air-entraining additive and an additive which reacts with binder to form more plastic crystals are possible.

It is necessary to identify a potential list of additives, their concentration and the technology of introduction in the concrete mix, as well as to conduct comparative experiments to evaluate the modulus of elasticity and the ultimate deformability at short-term and long-term loading.

If for determining the modulus of elasticity there is a standard procedure, for evaluating the ultimate concrete relative tensile strain corresponding to prism strength, such procedure does not exist in our country, so it is necessary to use pilot plants.

The prediction of the limit relative deformation corresponding to the prism strength as per results of not completed measurements of deformations under standard testing is very difficult because deformations at the last stage of destruction appear differently, depending on the prism strength. At low prism strength values in the section from 0.9 to $1.0R_b$, the deformations can be 30–40% of the ultimate deformation, and for high prism strength values - 15–20%. For determining the maximum relative deformation of concrete at the compression, corresponding to the prism strength, you can use the method proposed in [10].

For comparison of the modulus of elasticity and the ultimate deformability of two concrete compositions which had a similar prism strength, but into the second composition a NAR (neutralized air-entraining resin) additive was introduced in amount of

0.02% of cement mass. Some experiments were performed according to the method of obtaining full concrete compressive strain diagrams at compression. The results of these experiments are in Table 1 and Fig. 1. As seen from Table 1, the modulus value of the concrete with a NAR additive was 23.7% lower, and the maximum relative deformation at compression was by 25.7% higher. By analyzing the curves of Fig. 1, it can be noted, first, that the concrete with a given strength of the prism a descending branch is not available, which is also noted in [9]. Furthermore, the linearity of deformation in the fracture zone in the concrete with a NAR additive is higher.

Table 1. The results of experiments.

Concrete composition	R_b , MPa	$E_b \times 10^3$, MPa	$\varepsilon_{b0} \times 10^{-5}$
1	57.5	37.9	245
2	59.1	28.9	308

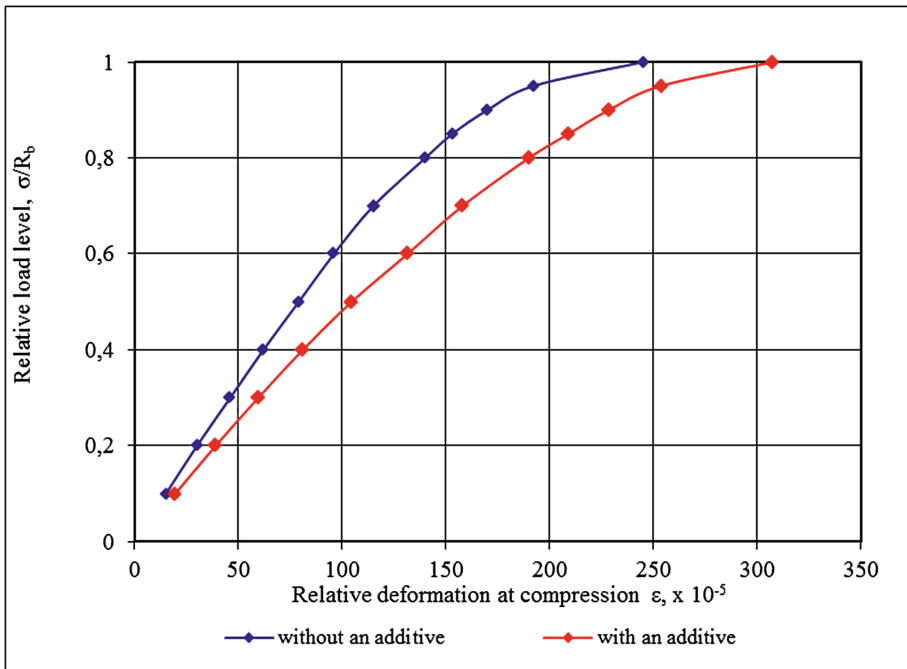


Fig. 1. Full diagrams of concrete deformation with and without SNV additive.

It is known that the sand used in the construction industry for the manufacture of concrete and reinforced concrete structures, should not contain more than 2–3% of clay particles. At the same time, to make the plastic properties of the solution, the clay is allowed to be added to cement-sand mortar in a much greater amount. It is likely that such stringent requirements are essential for high grade concrete, and for the low and

middle concrete classes the impact of clay in the sand is not as strongly affected, although it can have a significant impact on the elastic modulus and the ultimate deformability.

To identify the peculiarities of physical and mechanical characteristics of concrete with the presence of clay particles three series $7.07 \times 7.07 \times 28.0$ cm of prism samples have been prepared. All three series were made of concrete of 1:2.79:4.81 in M500 Portland cement in amount of 261 kg/m^3 , at W/C ratio = 0.69. As a filler fractionated crushed granite 5–10, 10–20 mm and medium size quartz sand was used.

The slump was 1–2 cm. In the first composition, the introduced sand contained clay particles in an amount of 6.8% of sand mass. The second composition was similar, but the sand was decanted and had no clay particles. The third composition was prepared with the presence of clean sand and a clay-lime additive, in ratio of 10:1. The amount of additive was 6% of cement mass. This additive was prepared as follows. Slaked lime and clay powder were mixed and water was added to it until a creamy paste, which was stirred well and subsequently dried at 110°C . Before concreting a required amount of the additive was dissolved in water and introduced into the concrete mix.

The average density value of three series of concrete and ultrasonic velocity were insignificantly different, and were as follows: density of $2.35\text{--}2.37 \text{ g/cm}^3$, and the ultrasonic velocity $4000\text{--}4200 \text{ m/s}$. At that, a third series had higher values of density and ultrasonic velocity.

All three formulations were tested as described in [10] for prism strength, modulus of elasticity and the ultimate deformability under compression, as well as at the level of $0.85R_b$ in the falling-down section. Additionally, these compounds were under prolonged load at a relative level of 0.3 and $0.6R_b$. The experiment lasted 30 days.

3 Results

Comparative experiments on the mechanical and rheological properties are shown in Tables 2, 3 and in Fig. 2. As seen from Table 2, the prism strength values for the three formulations differed little, and modulus of elasticity of concrete in clayey sand dropped by 17.2% compared with the pure sand composition. Comparing the limit deformation corresponding to the prism strength, we can note a significant increase to 23% in the second sand/clay composition in the third composition with the clay-lime additive (by 16%). The values of relative deformations at $0.85R_b$ falling branch were also higher in the second and third composition and exceeded the values obtained in pure sand, by 29 and 33%, respectively.

Table 2. Comparative experiments on the mechanical and rheological properties.

Composition	R_b , MPa	$E_b \times 10^3$, MPa	$\varepsilon_{b0} \times 10^{-5}$	$\varepsilon_{bH}^{-0.85} \times 10^{-5}$
1	28.8	33.7	176	233
2	26.9	27.9	217	301
3	27.1	31.8	204	311

Table 3. Comparative experiments on the mechanical and rheological properties

Composition	$\sigma = 0.3R_b$			$\sigma = 0.6R_b$		
	ϵ_y	$\epsilon_n(30)$	$\Sigma(\epsilon_y + \epsilon_n)$	ϵ_y	$\epsilon_n(30)$	$\Sigma(\epsilon_y + \epsilon_n)$
1	26.5	6.7	33.2	56.7	27.0	83.7
2	31.4	6.6	38.0	66.4	33.0	99.4
3	27.8	11.6	39.4	57.9	55.2	113.1

Figure 2 demonstrates full concrete deformation diagrams of three compositions at the compression. As seen in Fig. 2, plastic properties of the second and the third composition are much higher in comparison with those of the pure sand composition.

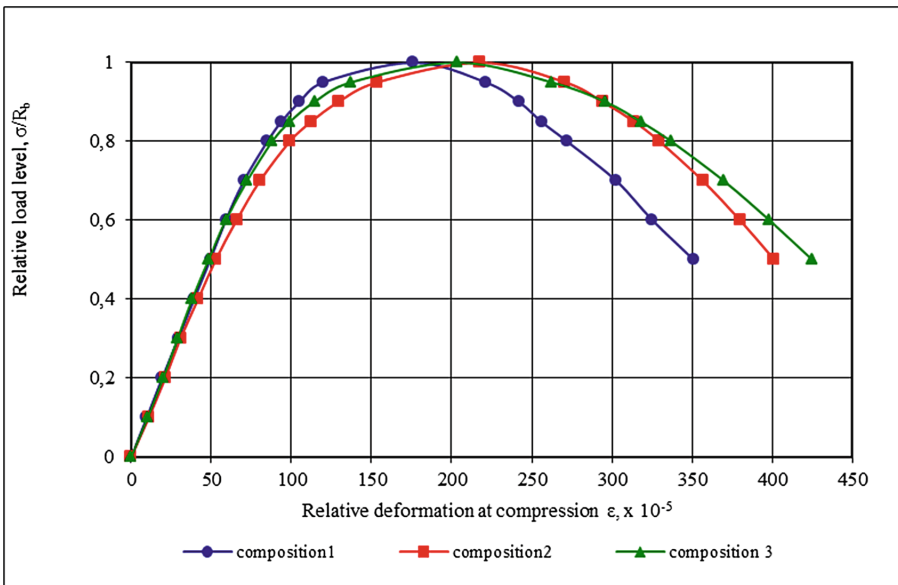


Fig. 2. Full concrete deformation diagrams at the compression.

On comparing the creep deformation, it can be noted that the creep of the second composition with the presence of clay in the sand on the $0.3R_b$ creep level was similar to the that of the first composition, while on the level $0.6R_b$ it increased by 22%. At the same time, the creep of the third composition with the clay-limestone strain, increased on the level of $0.3R_b$ by 73%, and on the level $0.6R_b$ – by 104%. With this, if we compare the elastic deformation at the level of 0.3 and $0.6R_b$, we can note a significant increase in deformations in the second clay/sand composition – by 18.5% at $0.3R_b$ and by 17.1% at $0.6R_b$.


4 Discussion

Thus, the experimental results show that the structural adjustment of physical/mechanical and rheological properties is quite real, and further research is needed in this area in order to identify all the factors that influence the change in the modulus of elasticity, limit deformability and creep. Also necessary is a theoretical basis of capacity of the structural adjustment of physical/mechanical and rheological properties. All this will enable directional regulating the deformation properties of concrete and increasing the level of fracture resistance. The development and research of new types of effective additives for reducing the elastic modulus and increasing the deformability will provide new types of additives to be used in the construction practices that will improve the durability of concrete, reinforced concrete structures and engineering structures erected both of prefabricated and monolithic concrete.

References

1. Russian Standard GOST 24211-91. Additives for concrete. General technical requirements (1992)
2. Kesternich, L.: Additives in Concretes and Mortars: A Training and Reference Manual. Feniks, Rostov-on-don (2007)
3. Bazhenov, Y., Demyanova, V., Kalashnikov, V.: Modified High-Quality Concrete. Publishing House ASV, Moscow (2006)
4. Shchelkunov, V.: Reserves of strength of compressed reinforced concrete elements. *Concr. Reinf. Concr.* **1**, 34–36 (1980)
5. Korkishko, A.: Long-lasting strength of racks reinforced with high-strength reinforcement. *High. Educ. Ser. Build. Archit.* **5**, 15–19 (1980)
6. Bezgodov, I.: On the ratio of strength and deformation characteristics of concrete during compression, stretching and stretching during bending. *Concr. Reinf. Concr.* **2**, 2–5 (2012)
7. Scheinin, A.: Cement for Road and Airfield Pavements. Transport, Moscow (1991)
8. Inozemtsev, S., Korolev, E.: Choosing a mineral carrier nanosized additives for asphalt concrete. *Her. MSUCE* **3**, 158–167 (2014)
9. Bezgodov, I., Levchenko, P.: To a question about the procedure for the preparation of complete concrete deformation diagrams. *Technol. Concr.* **10**, 34–36 (2013)
10. Bezgodov, I.: To the question of limiting the strain of concrete in compression for different classes. *Concr. Reinf. Concr.* **5**, 9–11 (2015)

Transport Interchange Hubs Under the Conditions of the Far North

Ilya Dunichkin^(✉) 

Moscow State University of Civil Engineering,
Yaroslavskoye Sh. 26, 129337 Moscow, Russia
ecse@bk.ru

Abstract. In this article consider the issues of energy efficiency and renewable energy technologies (RES) in the development of the concept of TIH for the Far North conditions. Transport interchange hubs (TIH) are the link that unites the transport infrastructure in a single structural. These unique facilities provide comfortable movement between the different modes of transport, efficient system of foot traffic, creating a ride car parks have an objects of social infrastructure, bring improved environmental performance, and security in general. Today, around the world launched the work on development of space north, are a vivid example of planar transport interchange hubs. Construction is already underway in the most congested areas. And TIH schemes are studied in a place with extreme loads and seasonal effects, the influence of the Sea on the atmosphere. Due to the geographic location of objects in conditions that fall under the definition of the Far North, the load on the design and the building as a whole should be taken into account in the principles and methods of design.

Keywords: Transport hub · The Far North · The Arctic
Transport infrastructure · Port · Railway station · Energy efficiency
Renewable energy sources

1 Introduction

Arctic zone of the Russian Federation is built in the North of Russian and its transport system, so that many of the country's entities have both the Arctic and northern territories. "Far North occupies about 60% of the country with a population of about 6%, and the Arctic regions - 20% and 1.4% respectively," [1]. From the point of view of processes in the field of transport is the most complex area with the highest costs. "Energy resources in northern regions make up 30% of total costs, and in some Arctic areas reach 40%," [2]. Therefore, energy efficiency in transport and its individual elements in the form of a transport interchange hubs (TIH) is the dominant factor affecting the interests of all sectors and levels of government.

2 The Strategy for Transport Development in the North Russian

Infrastructure development in the Far North of Russia in the form of transport hubs (TIH) based on the Strategy of development of the Arctic zone of Russia: “The development of infrastructure related to the construction of new railways, ports, roads,” [3], that mean the production of minerals in the Arctic and migration of the working population. Due to the harsh climatic conditions of the design principles of the infrastructure in the region is developed on the basis of closed systems. There is a lot of major transportation routes, so that the road and passenger traffic are high density because of that the passengers have to wait long transplants. Roads in the region also limited and performed the functions of mainly serve domestic needs. It involves the formation of TIH in the area of logistics facilities. Thus formed three main request of the Arctic logistics and TIH “export of natural raw materials from the region, delivery of goods to the local population and tourism,” [4]. “The development of the Northern Sea Route will add transit flows of goods and passengers emerging transport system and its nodes”. This occurs against the backdrop of the increase since 2000, the share of rail transport in the transport from 33.8 to 37.9%,” [5]. The development of a full-fledged transport system and infrastructure will not only overcome the barriers to the use of transit potential and improve the accessibility of settlements, but also largely eliminate the infrastructure constraints on the growth of mining in the Arctic zone of Russia. It is obvious that without running major railway lines TIH when crossing roads and significant has low prospects of development in the ports of the Arctic coastal infrastructure. “At present, Russia has unique transport and logistics capabilities, which, thanks to the natural assumptions may significantly contribute to its transformation into a competitive transit country with a developed service industry and service economy, and for the realization of this objective would require the TIH on new principles” [6]. Large transport and logistics hub for trunk and international traffic, as well as new labor becomes a passenger seaport “Murmansk”. This means that the promising of Murmansk TIH will be formed in the system of land-sea, and should have developed planning structure.

3 Prerequisites and Best Practices for Developing a TIH

Relevance of TIH is paramount in the development of the Far North and the territories of the Russian Federation equal to them, as long as in the construction are solved the following problems:

1. There is a reduction of a travelling time by an average of 10–20%;
2. Reduce the load on the car in central areas of the settlement;
3. Improving the quality of passenger service conditions for the transplant, due to the possibility of ensuring regulatory compliance for maximum passenger density TIH in accordance with SNIP 2.07.01-89 * “City. Planning and construction of urban and rural areas”;

4. Reducing the time between when transplanting transport network entities between the external and internal transport in the average settlement for 15–30 min;
5. There is a distinction between transport and passenger flows;
6. The availability of public transportation for people with limited mobility;
7. Environmental friendliness and relatively safe;
8. Efficient use of space settlement.

For example, consider the TIH in Matsumoto (Japan), which is an integrated unit of regional importance, it is composed of the railway station and bus station, which takes both regional and city buses. In its structure there are public parking and a large shopping mall. On the periphery of the site there are three open intercept parking, used by locals. The basis planning structure of the railway station is a walking platform that connects two parts of the city, located along the railway. “Communication with the station stopping point and taxi rank, located on the forecourt, is carried out on the pedestrian gallery system, which protect passengers from precipitation translucent constructions” [7].

In general, if we talk about The system of Japanese TIH, it deserves close study, and “best practices to ensure the comfort of passengers transplant in a fairly harsh weather conditions - not only the full study, but also the introduction in leveling and design practice of urban development” [8], taking into account domestic achievements in the development of transparent constructions for the Russian climate conditions, “showing the differences in the approaches to the number of analytical methods of calculating deflections glasses”, [9].

4 Specifics Conditions for TIH in the Arctic

The importance of design decisions transport hubs (TIH) is due to the critical situation in the cities of the far north, caused years of delay in the development of transport infrastructure (underdeveloped network of roads, lack of urban facilities to accommodate passenger service transport and storage). As an emergency measure proposed development of the settlements of the Arctic zone, where an important place is given to the construction of the TIH. “There is an option of transport facilities, developed in spontaneous mode, cannot cope with their obsolete structures with loads and impacts of severe climate,” [10]. The urgency of the TIH in the far north is determined by:

1. The need to involve the economic turnover remote, underdeveloped, areas located in adverse climatic zones;
2. The need for exploration and commercial development of new mineral, fossil, as well as internal labor migration;
3. It is expedient to use shift method for the development of already discovered deposits;
4. The objectives of the resettlement areas included in the strategic state interests (border protection, placement and redeployment of troops, etc.);
5. Protective functions for the population from the harsh climate;
6. Maintenance of external migration processes;
7. Needs for tourism development;

8. Research and internal labor migration;
9. Implementation of the transit of raw materials through the region and external labor migration;
10. The fulfillment of social guarantees.

According to the “Strategy of development of the Arctic zone of Russia and national security for the period up to 2020” on the implementation for the development of the Arctic program only from the federal budget will allocate more than 160 billion Rubles, so the construction of transport hubs in the Far North fulfills a major role in further development of the region.

The main problems that faced in order to achieve these objectives, of course, harsh climatic conditions and due to the complexity of transport accessibility of facilities. “The solution of the transport problem is possible only with the coordinated work on the development of the entire transport system in the Arctic region, which will include road, rail, air, river and sea transport” (Fig. 1).

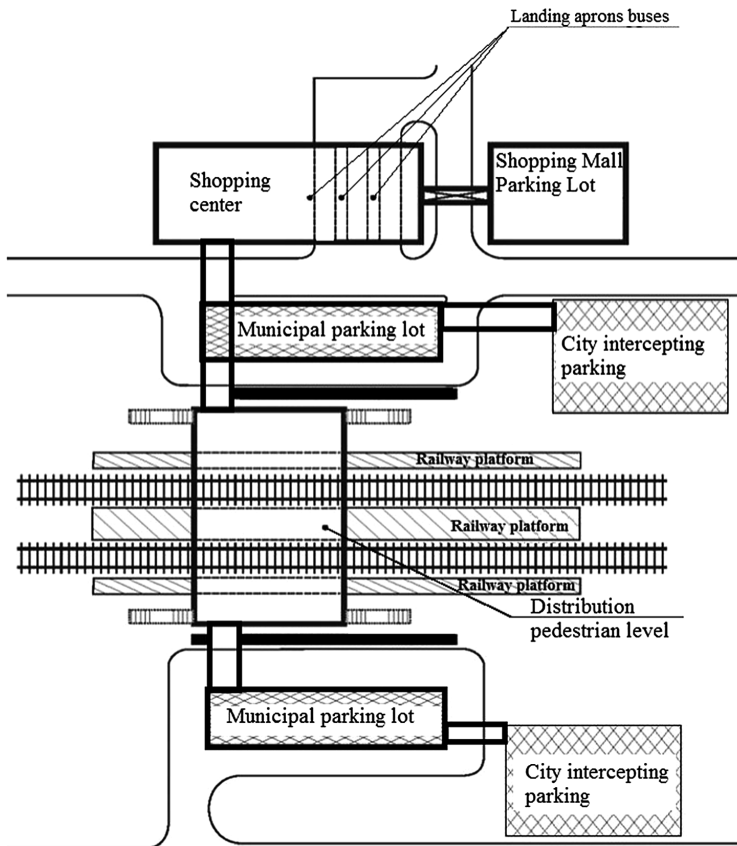


Fig. 1. Composition of the transport hubs in the extreme conditions of the example TIH Matsumoto, Nagano Prefecture (Japan).

5 TIH Concept for the Conditions of the Far North

Existing parameters of transport facilities, developed in spontaneous mode, cannot cope with their designs with loads of influences and harsh climate. Need advancing the formation of engineering and transport communications and associated facilities.

In developing the transport interchange hub provides:

1. “Maximum distinction traffic and pedestrian flows on major and relatively minor issues”, [11];
2. Unobstructed view of entrance with large snow sediment and drifts to the complex of buildings, structures and sites TIH public, special (mail, baggage) and individual transport;
3. Pedestrian accessibility to all installations and facilities TIH to meet the requirements of citizens with limited mobility;
4. The savings, energy efficiency and compactness;
5. Accompanying social and commercial and social facilities, underground and above-ground car park with portable ramps;
6. Closed boarding trains and light rail platforms bilateral directions to the nearest regional center or marina Seaport;
7. Closed recreational areas with greenery and its own temperature and humidity conditions;

In the lower tier of public and utilities sector should be closed is a bus station with the landing terminals.

To determine the parameters necessary to obtain designs TIH drag coefficients and surface pressure distribution of the building from wind and air mass flow perturbed by a moving train. On the structure will act a strong wind, low temperatures, humidity, icing and snow deposition. “Calculation of structural elements should work out according to paragraphs” SP 20.13330.2011 Loads and effects “introducing amendments to the local climatic conditions on the basis of settlement and experimental studies of architectural and construction aerodynamics,” [12].

6 TIH Energy Efficiency and Renewable Energy Technologies in the Harsh Climate of the North

When considering the TIH in the harsh climatic conditions of the following main factors determining the reduction of specific use and growth of energy:

- Modern energy system taking into account the difficult climatic and landscape-geographical conditions;
- Advanced technologies and new types of electrical equipment for transmission, distribution and consumption of electricity in transport and consumption of TIH;
- Installation of energy use, operating on renewable energy sources;
- Range of cogeneration plants of modular type;
- A new generation of systems walling to ensure a significant reduction in energy losses.

It should be noted the special role of energy efficiency for the northern and Arctic regions due to the use of renewable energy technologies RES. First of all, we are talking about the development of solar and wind energy. Subsidiary of “RAO ES Vostoka” holding “Sakhaenergo” is working on the introduction of renewable energy technologies in the Far East, and in some northern regions. “Set in the remote areas of renewable energy facilities leads to cost reduction, making the implementation of renewable energy projects economically viable,” [13]. The program of energy conservation and energy efficiency of the railway industry includes the introduction of LED technology and infrastructure improvements of heating systems of JSC “Russian Railways”.

The theoretical model building TIH provides orientation of its main facade to the east. This is the most successful option based on the urban situation and taking into account the application of technology of photovoltaic cells (PV), as “... a large area of stained glass can be provided on the eastern and southern fronts,” [14]. In connection with the orientation to the cardinal points and recommendations on the FE technology, it was decided to establish in the stained-glass panel photovoltaic arrays of FSM-300 (300 W). Most of them are built in the panoramic windows on 2 levels, TIH and continuous vertical glazing tape on the corners towers. The total area of panels is 1145 m². Accordingly, on the facades may be about 600 cells FSM-300 (300 W). According to the manufacturer, the peak power will be 120 kW and the average annual output - 87 to 400 kW•h. “The average daily amount of solar radiation - no more than 2.5–2.7 kW•h/m² (NASA inform), but it is less than in Novosibirsk, or, for example, in Yakutsk, where the figure is 2.96 kW•h/m²” [15]. For self-powered underground areas TIH need to collect a set of basic components: the FE, battery, charge controller, inverter. Total area of parking spaces on the 472 parking lots is 11 800 m². For illumination of parking from LED lights 24 h a day will need to 126.0 kW. When using fluorescent lamps require 151.2 kW. In this case, the light output of fluorescent lamps is almost 1.5 times higher, respectively, for the illumination of the same area will require more LED lamps than fluorescent. The life of a fluorescent lamp more than 11%, and the cost is 60% lower than that of the LED. Such an objective calculation helps debunk myths about the greater energy efficiency of new technology, which is extremely important in the Far North to the increased responsibility objects, such as TIH.

7 Conclusion

For example, calculating the lighting of parking TIH became clear that the room will be fully available from the PV technology, and renewable energy in general can meet 10% of demand for electricity TIH. By all accounts, including durability, energy efficiency, as well as the cost of maintenance and replacement of fluorescent lamps is superior to LED lamps and incandescent lamps of course. The area of photovoltaic cells to achieve economic efficiency indexes may be from 20 to 55% of the facade area, excluding the area of the FE roof. The area of the building’s roof, this is an additional resource for the FE modules position,” [16].


It should be noted that at low temperatures the work FE will be more effective because of the increase in the conductivity of the system elements, but in the form of

atmospheric icing weather factors are not predictable, and the correction for better conditions for the use of technology can only be done by the results of the pilot operation. However, when any expected adjustment indicators using FE on the facades of the building can greatly save costs TIH electricity, in addition, use of such panel does not spoil the view of construction, and the power generated by them in the summer, may be sufficient to ensure not only the parking space, but also possibly for the common areas in a building or area lighting TIH.

References

1. Energy Strategy of Russia for the period up to 2030
2. Makarov, A.: North and the energy strategy of Russia. North as an object of complex regional studies. Komi Publishing House Scientific Center of UB RAS, Syktyvkar (2007)
3. The development strategy of the Russian Arctic and national security for the period up to 2020 (2013)
4. Kotelnikova, A.: Energy Strategy of Russian Railways. ZHDM (2005)
5. Fadeyev, A.: Improving Economic Approaches to Managing Development of Offshore Hydrocarbon Fields in the Arctic. Russian Academy of Sciences, Apatity (2012)
6. Konovalov, A.: Transport Infrastructure in the Russian Arctic: Problems and Ways of Their Solution. IMEMO RAN, Moscow (2011). (Ed. by, A. Zagorskiy)
7. Konyukhov, D.: Concept of transport and hubs developed in the diploma project, students MSUCE. *Civ. Eng.* **2**(4), 49–56 (2014)
8. Ilvitskaya, S., Polyakov, I.: Stages of development of architecture and nature as a single system. *Nat. Tech. Sci.* **11–12**(78), 443–444 (2014)
9. Plotnikov, A., Stratiy, P.: Numerical-analytical method of calculation of the deflections of the glass panes sealed climate (internal) load. *Bull. MSUCE* **12**, 70–76 (2014)
10. Semenikhin, Y., Novoseltsev, Y.: Features of Transport Development in the Arctic Zone. The Russian Academy of Sciences, Moscow (2015)
11. Dunichkin, I., Kruglikov, E.: Analysis pedestrian multifunctional complexes. *Ind. Civ. Build.* **9**, 46–48 (2011)
12. Vlasov, D., Danilina, N.: Scientific and methodological basis of development of the park-and-ride facilities in the intermodal transport hubs of Moscow agglomeration. *Adv. Mater. Res.* **869–870**, 201–204 (2014)
13. Dunichkin, I.: Territorial planning based on renewable energy sources. *Archit. Build. Russia* **8**, 12–19 (2013)
14. Polyakov, I., Ilvitskaya, S.: Thesaurus architectural mentality of the XXI century. *Archit. Build.* **1–2**, 166–167 (2016)
15. Rafikova, Y., Kiseleva, S., Nefedova, L., Frid, S.: The use of geoinformation technologies for renewable energy and regional aspects of developing renewable energy in Russia. In: *EPJ Web of Conferences*, vol. 3, p. 04005 (2014)
16. Frontini, F., Frizen, T.: FE modules integrated into the building envelope. *Mag. "Building High-Tech"* **1**, 86–91 (2013)

Adjustment of Energy Strategy of Russia to Specific Nature of Far North: Analytic Hierarchy Process

Irina Zaychenko  , Svetlana Gutman , and Olga Kalinina 

Graduate School of Business Technologies,
Peter the Great Saint Petersburg Polytechnic University,
195251 Polytechnicheskaya str. 29, Saint Petersburg, Russia
imz.fem.spbpu@mail.ru

Abstract. The paper describes how the analytic hierarchy process can be used to select a strategic priority for energy development of the Far North regions. The paper also suggests the ways of the Energy Strategy of Russia adjustment to the specific nature of the Far North. There is a list of regional factors which have an impact on the selection of the energy development priority for the region. Preferred development trends for the Far North are presented in the framework of the Energy Strategy of Russia in respect of each group of regional factors. The paper sets forth measures to be taken to implement the energy strategy of the Far North regions selected using the analytic hierarchy process.

Keywords: Energy management · Energy Strategy · Transport infrastructure

1 Introduction

The government has developed and adopted quite a big number of various documents which provide for energy efficiency improvement. Implementation of these documents to a large extent depends on political and socio-economic factors and scientific development. The Federal Law on Energy Saving adopted in 2009 [1] and the Energy Strategy of Russia up to 2035 [2] are the principal applicable regulations. There is also a government-sponsored scheme in Russia titled “Energy Saving and Energy Efficiency Improvement for the Period up to 2020” [3]. If measures prescribed by this scheme are taken, by 2020 Russia will be able to save 1,124 million tonnes of oil equivalent of primary energy, 330 billion cubic metres of natural gas, 630 billion kilowatt hours of electrical energy, 1,550 million Gcal of heat energy and 17 million tonnes of oil products.

However, regulations adopted at the government level cannot improve efficiency of energy systems in all regions of Russia. The main reason is that “due to the uniquely vast territory of Russia with various climatic and economic environment, the energy policy needs to respond to the specific nature of different regions in addition to meeting strategic country-wide targets of rational distribution of productive forces and energy security promotion” [4]. The Far North is one of such regions. The energy system of the Far North is characterized by a big number of isolated electric generation systems,

scattered energy consumers and the problem of organic fuel delivery to northern regions which is crucial for citizens and administration of such regions. In spite of the fact that the Far North is named a priority region in the Energy Strategy of Russia, the specific nature of the energy system in the Far North and insufficient coordination between federal and regional strategies of energy and industrial development of the Far North may slow down socio-economic development of the region. Therefore, it is necessary to adjust the Energy Strategy of Russia up to 2035 in order to work out a unique energy strategy of the Far North.

2 Methods

There are scientific works about development and implementation of energy security models in Russia [5–13] and those specialized in various aspects of energy efficiency in northern regions [14–20]. For example, [17] considers a possibility to use minor streams (brooks, creeks) with different energy potential in order to arrange energy supply in the Murmansk region. [18] is dedicated to increasing significance of northern regions in fuel and energy complex development and energy security of Russia in the long-term perspective. [19] gives insight into economic and energy development of arctic regions, presents the main problems of the arctic energy sector which hinder sustainable socio-economic development of the region and suggests the ways to resolve them by development of small-scale electric power industry. [20] considers a strategic role of energy efficiency increase in the country's economy. Special attention is paid to factor analysis of arctic regions which are characterized by significant energy intensity of the gross regional product.

Therefore, none of the above works describe an overarching development strategy suitable for energy systems in the Far North regions. Consequently, it is necessary to adjust the general Energy Strategy of Russia up to 2035 to the specific nature of the Far North.

The analytic hierarchy process (AHP) [21] widely used to solve various economic problems related to alternative choice may be applied to adjust the general Energy Strategy of Russia up to 2035 to the unique northern environment and to select priority energy development trends for the Far North. The AHP is used to manage strategies in [22], to assess potential of growth options for Russian automobile companies in [23], to select the best supplier in [24], to select the way of power transmission line tower installation in order to decrease general costs of construction works in [25] and to find IT security solutions in [26].

The analytic hierarchy process developed by Thomas L. Saaty is thus a technique widely applied to solve socio-economic problems related to selection of preferred options.

The AHP provides for hierarchical representation of the simulated system elements. The detailed algorithm of the AHP management decision making is described in [27–29] and consists of three stages:

1. Assessment of the regional factors impact on energy development priority selection. The AHP starts with creation of a pairwise comparison matrix in order to compare

pairs of factors and determination of their impact on the ranking of priorities described in the Energy Strategy of Russia. The pairwise comparison of factors against each other is made based on the scale of relative importances.

Assessment results are expressed in a matrix which dimensions depend on the number of factors. If impact assessment of a factor A_1 is W_1 and impact assessment of a factor A_2 is W_2 , the pairwise comparison of A_1 to A_2 results in a ratio of W_1/W_2 and the pairwise comparison of A_2 to A_1 results in a ratio of W_2/W_1 . Therefore, the pairwise comparison matrix for factors $A_1, A_2, A_3, \dots, A_n$ with the elements on the main diagonal equal to 1 will be as follows:

$$M_f = \begin{pmatrix} W_1/W_1 & W_1/W_2 & W_1/W_3 & \dots & W_1/W_n \\ W_2/W_1 & W_2/W_2 & W_2/W_3 & \dots & W_2/W_n \\ W_3/W_1 & W_3/W_2 & W_3/W_3 & \dots & W_3/W_n \\ \dots & \dots & \dots & \dots & \dots \\ W_m/W_1 & W_m/W_2 & W_m/W_3 & \dots & W_m/W_n \end{pmatrix} \quad (1)$$

Then the principal eigenvector is calculated as follows:

$$V_{own} = \sum_{f=1}^m W_f, \text{ where } f = 1, \dots, m; W_f \neq 0 \quad (2)$$

The initial matrix is divided by the vector of priorities in order to calculate the comparison matrix:

$$M_{compar} = M_f \begin{pmatrix} W_1/W_1 & W_1/W_2 & W_1/W_3 & \dots & W_1/W_n \\ W_2/W_1 & W_2/W_2 & W_2/W_3 & \dots & W_2/W_n \\ W_3/W_1 & W_3/W_2 & W_3/W_3 & \dots & W_3/W_n \\ \dots & \dots & \dots & \dots & \dots \\ W_m/W_1 & W_m/W_2 & W_m/W_3 & \dots & W_m/W_n \end{pmatrix} \div V_{own} \quad (3)$$

The column vector is calculated based on the comparison matrix:

$$V_{column} = \sum_{g=1}^n W_g, \text{ where } g = 1, \dots, n; W_f \neq 0 \quad (4)$$

The column vector of priorities is calculated by dividing the column vector by vector dimension n :

$$V_{column}^{prior} = V_{column} \div n \quad (5)$$

The column vector of priorities may become the vector of priorities when normalized:

$$V^{prior} = \sum_{g=1}^m W_g = 1, \text{ where } g = 1, \dots, m; W_g \neq 0 \tag{6}$$

In order to check if the vector of priorities is correct, it is necessary to assess consistency. Another column vector should be calculated as follows:

$$V_{column}^{coord} = M_{compar} \times V^{prior} \tag{7}$$

Then vector V_λ is calculated. The sum of its components amounts to λ_{max} :

$$V_\lambda = V_{column}^{coord} \div V^{prior} \tag{8}$$

$$\lambda_{max} = \sum_{\lambda=1}^m V_\lambda \tag{9}$$

where $\lambda = 1, \dots, m; \lambda_{max} \geq m$; number of compared elements.

The final stage of the AHP is calculation of the index of consistency (IC) and consistency ratio (CR), the latter is acceptable at a ratio lower or equal to 10%. The lower the consistency ratio, the more correct the result is.

$$IC = \frac{\lambda_{max} - m}{m - 1} \tag{10}$$

where m is the number of compared elements

$$CR = \frac{IC}{RI} \tag{11}$$

where RI is random index.

Random indices randomly generated at a scale from 1 to 9 of the reciprocal matrix with the respective values are shown in Table 1.

Table 1. Random index

<i>RI</i>									
Matrix dimension									
1	2	3	4	5	6	7	8	9	10
0.00	0.00	0.58	0.9	1.12	1.24	1.32	1.41	1.45	1.49

2. Determination of priorities among energy development trends in respect of each group of regional factors. This is a stage of pairwise comparison of Russian energy strategy trends and determination of priorities in each group of regional factors.

Priorities are calculated based on matrices depending on the number of groups of factors with the dimension depending on the number of priorities. Calculations are similar to those described above. At this stage it is possible to obtain the vector of priorities in respect of the impact of each group of regional factors on selection of energy development trends and to draft respective recommendations.

3. Calculation of global priorities of energy development trend selection for the Far North regions in the framework of the Energy Strategy of Russia. In order to obtain a generalized assessment of each group of energy priorities, it is necessary to synthesize priorities from the second level down. In such a way it is possible to calculate the global vector of priorities in order to select a preferred option of the development strategy.

The final procedure of the analytic hierarchy process is the economic interpretation of mathematical results and a decision-making on priority energy development trend for the Far North regions.

3 Results and Discussion

Therefore, in order to improve efficiency of the energy system in the Far North it is necessary to divide this process into two stages, namely the stage of selection and the stage of implementation of the energy strategy. Using the AHP a strategic priority of the energy strategy of the Far North will be selected at the first stage based on the factors of socio-economic development of this region.

The energy sector will be developed taking into account the following priorities of the state energy policy [2]:

- Guaranteed energy security of the country and its regions, including prevention of fuel and energy resources deficit in any circumstances, availability of strategic fuel supply, required emergency capacity and ancillary equipment, sustainable operation of energy and heating systems;
- Encouragement and support of innovative activities in the fuel and energy sector companies and related industries in order to ensure more efficient use of fuel and energy resources and improvement of the fuel and energy sector potential;
- Minimization of adverse effects of energy production, transportation and consumption on environment, climate and human health;
- Promotion of competition, including provision of equal competitive conditions on domestic energy markets for all Russian companies, transparent and non-discriminatory pricing and government control over naturally monopolistic activities;
- Efficiency improvement in regulated activities and management of state organizations and joint-stock companies with state participation, including cutting of operating and capital expenses;
- Diversification of Russian energy export and optimization of its commodity pattern;

- Development of energy infrastructure of the Eastern Siberia and the Far East in order to boost economic growth in Russia and to increase energy export to the Asia-Pacific Region.

The following geopolitical and socio-economic development factors were selected for the Far North:

- Significant, diverse and not fully explored reserves of natural resources. Arctic territory has up to 25% of unused world reserves of hydrocarbons, there are also fish resources and precious metals [29, 30];
- Special geopolitical significance, the centre of strategic interests of many countries. Apart from the five countries which surround the North Pole (the United States, Canada, Russia, Norway, Denmark and Greenland), the European Union has also indicated its interest in the Arctic Region. Furthermore, such countries as China and Japan are willing to participate in exploration of arctic resources [31];
- Extreme climate. The climate is characterized by negative average annual temperature, low radiation balance, permafrost zone environment and prevailing tundra vegetation and arctic wilderness, which also provides for low temperatures of ocean waters. In the area of drifting ice, surface water temperature (100–200 m in thickness) is about 2 °C the whole year. Where there is no ice in the summer, water warms up to several degrees above zero [32];
- Multi-ethnic population of the Arctic Region, including indigenous minorities. Arctic population includes northern indigenous minorities who have been able to accumulate knowledge about arctic environment, behavioural and survival patterns and to develop traditional values and unique culture. The population of the Arctic Region of the Russian Federation numbers about 68,000 indigenous people (4.8% of population of the Arctic Region of Russia) [33];
- Environmental issues related to industrial development due to unstable natural balance. Global warming in the Arctic Region may significantly affect human safety on a regional and global scale. Loss of arctic ice has an impact on local ecosystems and leads to catastrophic rise in the ocean level, which threatens small island countries and traditional way of life of indigenous population. By 2020 loss of ice in northern regions may open new opportunities such as access to fish resources, easier exploration of natural resources, new navigable waterways which can make the route from Europe to Eastern Asia shorter by 40% and, therefore, cut transportation expenses [34];
- Specific sectoral structure of industry, namely mining industry, metallurgy, timber industry, wood processing industry, pulp and paper industry, oil and gas extraction, fishing, fish-processing industry, electric power industry, production of construction materials, shipbuilding industry and transportation systems (Arkhangelsk and Murmansk ports rank among the biggest ports in Russia) [35].

The strategic priority selection in respect of the energy system efficiency improvement in the Far North regions is decomposed to a goal hierarchy for future AHP application in Fig. 1.

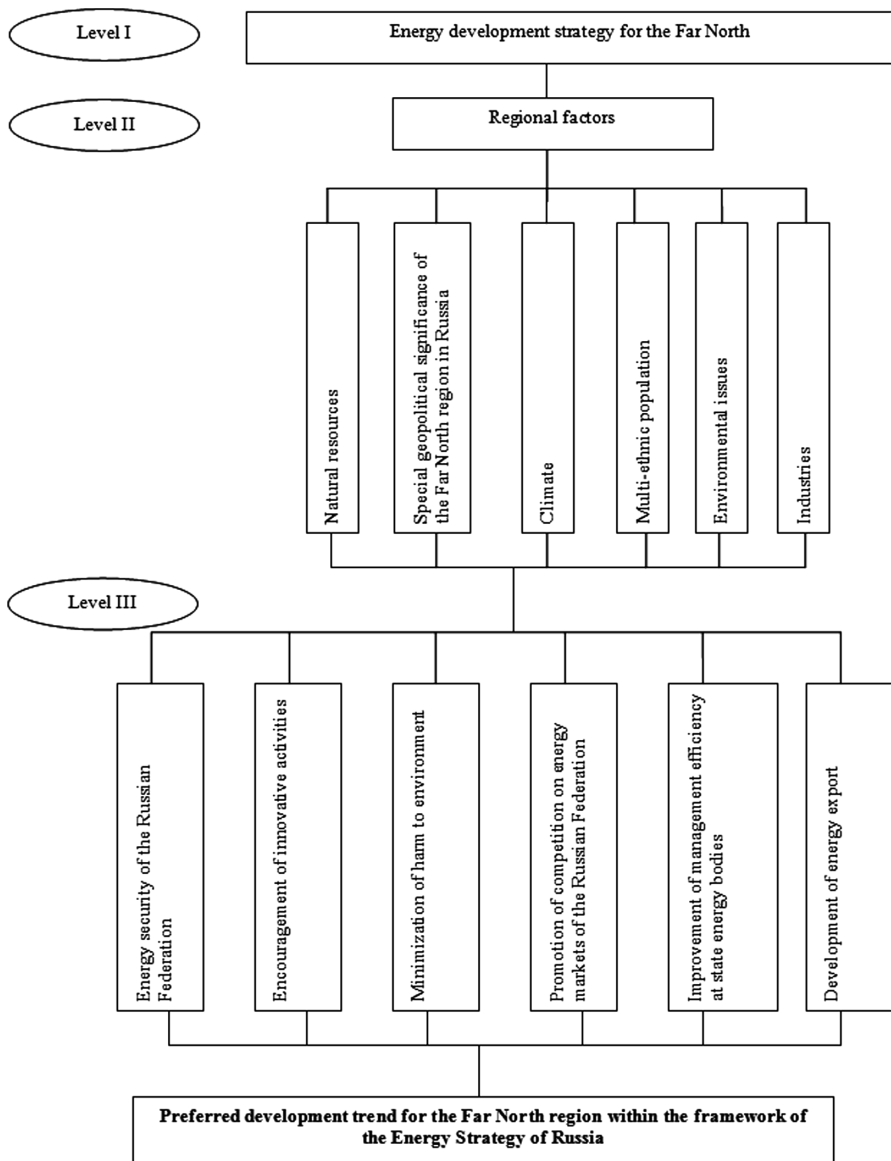


Fig. 1. The process of regional energy development priority selection decomposed into the goal hierarchy

At the second stage of energy efficiency improvement in the Far North, it is necessary to work out a set of measures to be taken to implement the energy strategy selected using the AHP.

The main measures to be taken to improve energy efficiency in the Far North may be divided into four groups:

- Information and methodological support, propaganda and personnel training;
- Financial support, financial incentives and tax benefits;
- Tariff regulation;
- Organizational and administrative support.

Therefore, using the AHP it is possible to select a preferred strategy for the energy system efficiency improvement in the Far North which will be connected with the Energy Strategy of Russia and regional socio-economic development programs taking into account their socio-economic and climatic peculiarities [36–39].

4 Conclusion

The AHP used to calculate preference of a certain strategic alternative when making management decisions on the elaboration of the energy development strategy for the Far North regions allows transformation of the decision-making from a subjective process to a rigorous calculation.

Therefore, the proposed approach to quantitative assessment of parameters used to select an energy efficiency improvement strategy for the Far North regions provides for rather comprehensive analysis of the selected strategic alternative in the long-term perspective.

Acknowledgment. This paper is elaborated in framework of scientific project №16-32-00040 supported by Russian Foundation for Humanities.

References

1. Federal law “About energy saving and increasing energy efficiency”, from 23.11.2009. 261, FZ. http://www.consultant.ru/document/cons_doc_LAW_93978/. Accessed 20 Jan 2017
2. Draft of energy strategy of the Russian Federation for the period up to 2035 (revised from 01.02.2017). <http://minenergo.gov.ru/node/1920>. Accessed 22 Feb 2017
3. The state program “Energy saving and energy efficiency for the period till 2020”. <https://rg.ru/2011/01/25/energoberejenie-site-dok.html/>. Accessed 18 Feb 2017
4. Official Site of the International Energy Agency. <https://www.iea.org/russian/>. Accessed 12 Feb 2017
5. Kurichev, N.K.: Model of energy development in Russia: challenges and opportunities. *Contours Glob. Transform.: Polit. Econ. Law* **3**(4), 130–136 (2011)
6. Pobedonostseva, V.V.: About the influence of market energy in the process of increasing regional energy efficiency in the Arctic zone of the Russian Federation. In: *Proceedings of Kola Science Centre of RAS*, vol. 3, no. 22, pp. 77–86 (2014)
7. Petrov, N.: Past and present of energy of the North with the height of the goals of the future. *Energy of Russia in XXI century. Innovative development and control*. In: *Proceedings of Conference “Energy of Russia in XXI Century. Innovative Development and Administration”*, 1–3 September 2015. Russia, Irkutsk, pp. 449–456 (2015)
8. Bushuev, V.V., Voropai, N.I., Senderov, S.M., Saenko, V.V.: The energy security doctrine of Russia. *Reg. Econ.* **2**, 40–50 (2012)

9. Tuinova, S.S.: Alternative energy policy priorities and economic security. *Natl. Interests: Prior. Secur.* **32**, 62–66 (2010)
10. Fredholm, M.: *The Russian Energy Strategy & Energy Policy: Pipeline Diplomacy or Mutual Dependence?* Defence Academy of the United Kingdom Conflict Studies. Research Centre (2005)
11. Aalto, P. (ed.): *The EU-Russian Energy Dialogue: Europe's Future Energy Security.* Routledge, Abingdon (2016)
12. Dmitriev, M.: Russia's "Energy Key" strategy. *Russia Glob. Aff.* **4**(4), 120–123 (2006)
13. Lang, Y.H., Wang, L.M.: Russian energy geopolitic strategy and the prospects of Sino-Russia energy cooperation. *Resour. Sci.* **29**(5), 201–206 (2007)
14. Øverland, I.: Russia's Arctic energy policy. *Int. J.* **65**(4), 865–878 (2010)
15. Johnston, P.F.: Arctic energy resources and global energy security. *J. Mil. Strateg. Stud.* **12** (2), 1–20 (2010)
16. Piskarev, A., Shkatov, M.: *Energy Potential of the Russian Arctic Seas: Choice of Development Strategy.* vol. 58 (2012)
17. Lagunov, E.N., Khokkanen, V.N.: Prospects for small hydropower development in the conditions of Murmansk and the Kola North. *Bull. Murmansk State Tech. Univ.* **9**(3), 498–501 (2006)
18. Kotomin, A.B.: Role of Northern regions in ensuring the energy security of the Russian Federation. *Natl. Interests: Prior. Secur.* **32**(89), 75–84 (2010)
19. Smolentsev, D.O.: Energy development in the Arctic: challenges and opportunities for small generation. *Arctic: Ecol. Econ.* **3**(7), 22–29 (2012)
20. Selin, V.S.: Possibility of improving the efficiency of the Northern regions economy. In: *Territorial Development Issues*, vol. 8, no. 18 (2014). <http://vtr.vscc.ac.ru/article/1434>. Accessed 19 Feb 2017
21. Saaty, T.: How to make a decision: the analytic hierarchy process. *Int. J. Serv. Sci.* **1**(1), 83–98 (2008)
22. Gradov, A.P. (ed.): *Cyclical Development of Economy and Competitive Advantages Management*, p. 1150. Saint-Petersburg, Poltorak (2011)
23. Efremov, V.S., Dubinskij, A.A.: Assessment of Russian automotive companies development. *Manag. Russia Abroad* **5**, 66–75 (2004)
24. Chulanova, G.U., Mazur, E.P.: Using of method of hierarchical processes for supplier selection. *Innovations* **2**, 122–126 (2013)
25. Gorokhov, E.V., Yugov, A.M., Ignatenko, R.I., Krupenchenko, A.V.: Application of analytic hierarchy process in the development of a rational variant of the organizational and technological process of assembly of complex metal lattice tower transmission towers. Release of the Donbas National Academy of Civil Engineering and Architecture, vol. 6, no. 116, pp. 43–52 (2015)
26. Presnakov, S.A.: Selection and justification of complex decisions on the basis analysis of hierarchies method. *Nauka-rastudent.ru*, vol. 12 (2015). <http://nauka-rastudent.ru/24/3085/>. Accessed 24 Feb 2017
27. Saaty, T.L.: *Fundamentals of the Analytic Hierarchy Process*, 478 p. RWS Publications, Pittsburgh (2000)
28. Ilin, I.V., Iliashenko, O.Yu., Levina, A.I.: Application of service-oriented approach to business process reengineering. In: *Proceedings of 28th International Business Information Management Association Conference. Vision 2020: Innovation Management, Development Sustainability, and Competitive Economic Growth*, 9–10 November 2016, Spain, Seville, pp. 768–781 (2016)
29. Lukin, Y.F.: *Russian Arctic in a changing world.* Arkhangelsk (2012). http://narfu.ru/aan/Russian_Arctic_Lukin/Russian_Arctic_Lukin.pdf. Accessed 21 Jan 2017

30. Fedoseev, S.V., Cherepovitsyn, A.E., Tsvetkov, P.S.: Statement and mathematical characterization of the task of assessing the strategic potential of fuel and energy industry of Russia. *Int. J. Appl. Eng. Res.* **11**(16), 9002–9006 (2016)
31. Konyshchev, V.N., Sergunin, A.A.: National interests of Russia in the Arctic: myths and reality. *Natl. Interests: Prior. Secur.* **29**, 2–11 (2011)
32. Bushuev, V.V., Morgunova, M.O.: Energy in the Arctic. *Partnersh. Civiliz.* **4**, 174–184 (2012)
33. Korczak, E.A.: Indigenous peoples of the North in the state Arctic strategies. <https://www.science-education.ru/pdf/2014/5/103.pdf>. Accessed 26 Jan 2017
34. Bochkarev, D.: Expanding the EU's institutional capacities in the Arctic Region. *External Relations*: <https://eu.boell.org/en/2013/12/03/expanding-eus-institutional-capacities-arctic-region-external-relations/>. Accessed 14 Jan 2017
35. Dorogovtseva, A.A.: Regional policy in Russia and problems of the regions of the European North. *Vestnik of Northern Arctic Federal University. Series: Humanities and Social Sciences*. vol. 1, pp. 92–100 (2005)
36. Gumba, Kh., Uvarova, S., Belyaeva, S., Revunova, S.: MATEC Web of Conferences, vol. 106, p. 08023 (2017). <https://doi.org/10.1051/mateconf/201710608023>
37. Kankhva, V., Uvarova, S., Belyaeva, S.: *Procedia Eng.* **165**, 046–1051 (2016). <https://doi.org/10.1016/j.proeng.2016.11.818>
38. Uvarova, S., Belyaeva, S., Kankhva, V., Vlasenko V.: *Procedia Eng.* **165**, 1317–1322 (2016). <https://doi.org/10.1016/j.proeng.2016.11.857>
39. Kankhva, V.: MATEC Web of Conferences, vol. 106, p. 08027. <https://doi.org/10.1051/mateconf/201710608027>

Energy-Efficient Lighting Systems Design in Industrial Premises of Motor Transport Enterprise

Irina Romanova¹ and Petr Romanov²

¹ Moscow State University of Civil Engineering,
Yaroslavskoye Sh. 26, 129337 Moscow, Russia
romanov_p_s@mail.ru

² State Educational Institution of Higher Education,
Moscow Region State University of Humanities and Social Studies,
Zelyonaya street, 30, 140410 Kolomna, Russia

Abstract. The article deals with the approach to lighting systems design on the basis of energy-saving technologies. Switching to energy-efficient lighting is one of the fastest ways to decrease cost of lighting. Properly designed and executed industrial lighting increases productivity and improves product quality, increases safety and reduces injuries. During the construction of a new or modernization and expansion of the old industrial premises of motor transport enterprise it is necessary to consider the trend of the transition to LED lighting. The paper proposes a new approach to LED lighting design. In order to confirm the advantages of this approach to energy savings in industrial premises were undertaken the calculations of technical and economic efficiency of different options of the lighting systems. The article presents the results of the selection of the most appropriate lighting system for industrial premises of the motor transportation enterprises using the method of spectral analysis.

Keywords: Lighting systems · Light-emitting diodes
Compact fluorescent lamp · Lighting of industrial premises
Energy-efficient lighting · The method of spectral analysis
Quantitative characteristics

1 Introduction

One of the most important tasks in industrial premises design is the occupational safety and health of the personnel. Based on this the organization of rational lighting of industrial premises and workplaces acquires a great importance.

Properly designed and executed industrial lighting increases productivity and improves product quality, helps to reduce visual fatigue and improves the functional state of the organism, increases safety and reduces injuries. Lighting can be natural or artificial. Industrial premises are usually equipped with general and local artificial light. However, regardless of the type of lighting, it should ensure an adequate level of illumination and even distribution of light in the workplace, protect the eyes from the glare of the light sources and the too high brightness, finally, the most favorable for the eyes and body range of light sources [1].

The three main categories of electric lights are incandescent lamps, gas-discharge lamps and light-emitting diodes lamps (LEDs) [2].

Incandescent lamps are sources of light-thermal radiation, in which a filament is heated to a temperature at which a fraction of the radiation falls in the visible spectrum. They are the most common because of its usability, but they have some disadvantages: low luminous efficacy of about 7 lumens/watt and small lifetime (about 2000 h) [3].

Gas-discharge lamps generate light by sending an electrical discharge through an ionized gas (noble gas or metal vapor). There are three basic categories of lamps that operate under this principle: high pressure discharge lamps, low pressure discharge lamps and high-intensity discharge lamps [4].

High pressure discharge lamps have gas with higher than the atmospheric pressure inside the tube (the metal halide lamps, the high pressure sodium lamps and the high pressure mercury-vapor lamps). Low pressure discharge lamps have gas with lower than the atmospheric pressure inside the tube (fluorescent lamps, neon lamps). High-intensity discharge lamps produce light by means of an electric arc between the tungsten electrodes (metal halide lamps, the sodium vapor lamps, the mercury-vapor lamps, the ceramic discharge metal halide lamps, the xenon arc lamps and the ultra-high performance (UHP) lamps) [5, 6].

The most common are fluorescent lamps having the shape of a cylindrical pipe. The inner surface of its phosphor, which converts ultraviolet radiation into visible light. Depending on the distribution of the spectral components of the light bulbs are daylight (DV), fluorescent light with improved light output (LDTS), cold white (LIB) [7].

One of the options of gas-discharge lamps is a compact fluorescent lamp (CFL), which is designed to replace an incandescent light bulb. CFLs are simply miniature versions of full-sized fluorescents. They screw into standard lamp sockets, and give off light that looks similar to the common incandescent bulbs. Compared to general-service incandescent lamps giving the same amount of visible light, CFLs use one-fifth to one-third the electric power, and last eight to fifteen times longer [8].

The main advantages of the gas-discharge lamps are the high luminous efficacy (100 lumens/watt), long lifetime (up to 12,000 h) and a wide range of colors. But they are more complicated to manufacture and require auxiliary electronic equipment such as ballasts to control current flow through the gas. Some gas-discharge lamps also have a perceivable start-up time to achieve their full light output (about 15 min). Another disadvantage of gas-discharge lamps is stroboscopic effect or intermittent light – flickers (flicker is the constant fluctuation of light output from on to off). Flickers make it difficult to work with the moving and rotating objects [9].

LEDs produce light when voltage is applied to negatively charged semiconductors, causing electrons to combine and create a unit of light (photon). The emitted light may be in the infrared, visible, or near-ultraviolet region of the spectrum, depending on the composition and condition of the semiconducting material used. A mix of red, green, and blue LEDs is typically used to make white light. In simpler terms, an LED is a chemical chip embedded in a plastic capsule. Because they are small, several LEDs are sometimes combined to produce a single light bulb [10].

LEDs emit light in a specific direction, reducing the need for reflectors and diffusers that can trap light. This feature makes LEDs more efficient for many uses such as recessed downlights and task lighting. With other types of lighting, the light must be reflected to

the desired direction and more than half of the light may never leave the fixture. Furthermore LEDs emit very little heat. In comparison, incandescent bulbs release 90% of their energy as heat and CFLs release about 80% of their energy as heat [11].

Thus, the main advantages of LEDs are:

- high energy efficiency (the typical LED requires only 30–60 milliwatts to operate, LED light source with the same lighting intensity consumes up to ten times less energy than an incandescent lamp, the luminous flux directivity allows to improve the lighting fixture efficiency up to 100%);
- durable, shockproof and corrosion-resistant unlike glass bulb lamp types;
- long lifetime (about 100 000 h);
- absence of mercury in the lighting fixture elements makes disposal simple and environmentally safe;
- the lighting fixture instant switching and attainment of projected power;
- high lighting intensity values;
- closeness of the lighting to the natural light;
- lower dazzling effect;
- luminous intensity without changes in any supply voltage range;
- high color rendering index, providing better visibility and contrast;
- absence of stroboscopic effect (flicker) make the lighting fixtures irreplaceable in industry.

The main disadvantage of LEDs is sensitivity to great variations in summer/winter temperatures [12].

LED lighting in general is more efficient and longer lasting than any other type of light source, and it is being developed for more and more applications within the home. LEDs are currently popular in under-cabinet strips and some types of downlights.

LEDs are designed to run on low voltage (12–24 V), direct current electricity. However, most places supply higher voltage (120–277 V), alternating current electricity. The LED driver rectifies higher voltage, alternating current to low voltage, direct current and protect LEDs from voltage or current fluctuations, because too much or too little current can cause light output to vary or degrade faster due to higher temperatures within the LED [13].

That's why every LED light source requires a driver, which can be internal (integrated) or external (separated). Household bulbs usually include an internal driver because it makes replacing old incandescent or CFL bulbs easier. LEDs that typically require an external driver include cove lights, downlights, and tape lights, as well as certain fixtures, panels, and outdoor-rated lights. They typically require a separate driver because it's simpler and cheaper to replace the driver than the LEDs [14].

During the construction of a new or modernization and expansion of the old industrial premises of motor transport enterprise it is necessary to consider the trend of the transition to LED lighting. But at the same time to reduce their cost it is necessary to move an existing technology of LED lighting to a new, as follows: to install a rectifier device to a group of LED panels in 220 V alternating current electrical shield instead of LED driver in each lamp.

In order to confirm the advantages of this approach to energy savings in industrial premises were undertaken the calculations of technical and economic efficiency of different options of the lighting systems.

Lighting of industrial premises can be natural, artificial (carried out by the bulbs) and combined. Natural lighting of workplaces is provided by the presence of light holes located in different parts of the building: in the walls or in the roof of the building. The last option gives more favorable distribution of the luminous flux and the higher light levels - top lighting, but isolated upper light is rare. Often along with the upper light is applied and side light, provide light-openings (windows), located within the walls of the building (combined lighting). Artificial lighting can be of three kinds: local, general (uniform without regard to the location of the object and localized based on the location of workplaces) and combined [15].

General lighting is used in administrative and warehouse premises. Combined lighting is used in production site. The use of only local lighting inside the industrial premises is not allowed [16].

The main purpose of lighting in industrial premises is to create the best conditions for the object overview. This problem can be solved by using the lighting system meeting the following requirements [16]:

1. the illumination should match the visual work, which is defined by the following parameters: the smallest object to be discern, its individual parts and defects; brightness difference between the object and its surrounding background; glare of the object.
2. the amount of light must be constant in time.
3. the directivity of a light flux and spectral composition of light should be optimal.
4. all the elements of lighting installations must be durable, electro, explosion and fireproof.

The following attributes should be studied when choosing the light source: light output (lumens), total input wattage, efficacy (lumens per Watt), lifetime, physical size, surface brightness/glare, colour characteristics, electrical characteristics, luminaire efficiency (% lamp light output transmitted out of the fixture), price.

The rational lighting device plays an important role in maintenance and repair of vehicles. It should provide sufficient illumination of the working area, allowing to monitor the object and the operation of the equipment.

In modern conditions it is necessary to use energy-efficient lighting design in industrial premises of motor transport enterprise. In the legal documents on energy efficiency (federal laws, presidential and government decrees of the Russian Federation) is reflected the transition plan from the use of incandescent lamps to the use of gas-discharge lamps, and subsequently LEDs. Furthermore, they noted that LEDs are the lighting tool of the future.

2 Experimental Section

To compare light sources it is necessary to take into account electrical (voltage, current rating and wattage), lighting (light colour appearance, light output and maximum luminous intensity), performance (luminous efficacy, lifetime) and constructive (bulb shape, body shape filament) characteristics.

The first stage is to calculate according to known methods [17] technical and economic efficiency of different options of the lighting systems for industrial premises.

The second stage is to select the most appropriate lighting system for industrial premises of the motor transportation enterprises using the method of spectral analysis.

Stage 1. The calculation of the lighting systems for maintenance and repair area of motor vehicles electrical equipment according to known methods [18]. The size of the industrial premise, type of the work done in the premise, wall and ceiling covering are known.

1. To determine the category of the visual work for this type of premises and type of the work done in the premise [16].
2. To determine the type of lighting (general or combined) and the desired illumination of workplaces [16].
3. To choose the placement of lamp for general and local lighting (if necessary).
4. To calculate the necessary luminous flux of the lamp in lighting installation by means of utilization factors (the ratio of the total flux received by a particular surface to the total lamp flux of the installation).
5. To select a typical lamp based on luminous flux obtained in the previous step. The deviation of the luminous flux of the selected lamp from the calculated range should be from -10% to $+20\%$.
6. To choose the number and type of lamps required to achieve a specific average illuminance. The number of lamps depends on the size of the illuminated area: the number of lamps should be such that the lamps are spaced less than the maximum spacing to mounting height ratio nominated in the coefficient of utilisation tables [16].
7. To calculate the electrical wattage of the general lighting system.
8. To calculate the necessary luminous flux of the lamps for local lighting (point method).
9. To select a typical lamp based on luminous flux obtained in the previous step. The deviation of the luminous flux of the selected lamp from the calculated range should be from -10% to $+20\%$.
10. To calculate the electrical wattage of the combined lighting system.

Stage 2. The selecting the most appropriate lighting system for industrial premises.

If only quantitative characteristics of the technological equipment are known, the most simple and effective method of solving the problem of rational selecting is the method of spectral analysis. The essence of the method is as follows [19].

There are n compare options of lighting system (LS) ($LS_i, i = \overline{1, n}$), which can be assigned to a number of technical characteristics $X_j, j = \overline{1, m}$, that determine the preference of a lighting system. The preference of the lighting system LS from the standpoint of one of the characteristics X_j can be defined by indicator x_{ij} , has a certain physical meaning. It is considered that all characteristics initially are equivalent: $W_i^{(0)} = 1, V_j^{(0)} = 1$, where $W_i^{(0)}, V_j^{(0)}$ – weight values at zero iteration for the lighting system and their characteristics, respectively.

It is necessary to build the array lighting systems from the available set of different models, manufactured in different countries, by preference, taking into account the set

quality indicators x_{ij} , $i = \overline{1, n}$, $j = \overline{1, m}$. Then, make a choice of the most preferred lighting system.

The problem is solved by implementation of spectral analysis iterative procedure:

$$W_i^{(k)} = \left(\sum_{j=1}^m V_j^{(k-1)} \tilde{x}_{ij} \right) / \left(\max_i \sum_{j=1}^m V_j^{(k-1)} \tilde{x}_{ij} \right) \tag{1}$$

$$V_j^{(k)} = \left(\sum_{i=1}^n W_i^{(k-1)} \tilde{x}_{ij} \right) / \left(\max_j \sum_{i=1}^n W_i^{(k-1)} \tilde{x}_{ij} \right) \tag{2}$$

where n is the number of lighting systems; m – the number of technical characteristics; $k = \overline{1, K}$ – the iteration number in the iterative process (if $k \rightarrow \infty$, then $W_i, V_j \rightarrow const$); $W_i^{(k)}, V_j^{(k)}$ – weight values at k -iteration for the lighting systems and their characteristics, respectively;

$$\tilde{x}_{ij} = \begin{cases} \frac{x_{ij}}{\max\{x_{ij}\}}, & \text{if the increase } x_{ij} \text{ leads the enhancement of properties LS;} \\ \frac{\min\{x_{ij}\}}{x_{ij}}, & \text{if the decrease } x_{ij} \text{ leads the enhancement of properties LS.} \end{cases}$$

It is suggested the following algorithm for solving the problem of selecting the most appropriate lighting system:

1. To build a calculated table in the form of Table 1 (the direction of the calculations is shown by arrows).
2. To calculate the normalized matrix x_{ij} , $i = \overline{1, n}$, $j = \overline{1, m}$. Enter all the values \tilde{x}_{ij} in Table 2.
3. For $k = 1$ to calculate by the Eq. (1) values $W_i^{(1)}$, assuming $V_j^{(0)} = 1$ and taking values of \tilde{x}_{ij} , $i = \overline{1, n}$, $j = \overline{1, m}$ obtained in the previous step of the algorithm. Enter all the values $W_i^{(1)}$ in the Table 2.
4. For $k = 2$ to calculate $V_j^{(2)}$ by the Eq. (2) based on the data obtained in the previous step of the algorithm. Enter all the values $V_j^{(2)}$ in the Table 2.
5. To continue the calculation of the values of $W_i^{(k)}$ for odd iterations and $V_j^{(k)}$ for even iterations as indicated in steps 3 and 4 of the algorithm. The calculation was carried out as long as the value of $W_i^{(k)}$ and $V_j^{(k)}$ will not accept the weight values obtained at the previous iteration. A replay of the weight values usually starts at $k \geq 7$.
6. Further filling of the Table 2 is carried out after settlement $W_i^{(k)}$ and $V_j^{(k)}$ by the Eq. (1) and (2), but the calculation starts with finding the values $V_j^{(1)}$ assuming $W_i^{(0)} = 1$, and further by the algorithm.
7. Based on the obtained values of $W_i^{(K)}$ to build the array of lighting systems LS_i , $i = \overline{1, n}$.
8. To determine the best lighting system LS_i . The best option is the one which have the highest value weight $W_i^{(k)}$.

Table 1. Intermediate calculations form.

	V_1	...	V_j	...	V_m	$W_i^{(0)}$	$W_i^{(1)}$	$W_i^{(2)}$	$W_i^{(3)}$
W_1	\tilde{x}_{11}	...	\tilde{x}_{1j}	...	\tilde{x}_{1m}	1	$W_1^{(1)}$...	$W_1^{(3)}$
...
W_i	\tilde{x}_{i1}	...	\tilde{x}_{ij}	...	\tilde{x}_{im}	1	$W_i^{(1)}$...	$W_i^{(3)}$
...
W_n	\tilde{x}_{n1}	...	\tilde{x}_{nj}	...	\tilde{x}_{nm}	1	$W_n^{(1)}$...	$W_n^{(3)}$
$V_j^{(0)}$	1	...	1	...	1				
$V_j^{(1)}$				
$V_j^{(2)}$	$V_1^{(2)}$...	$V_j^{(2)}$...	$V_m^{(2)}$				
$V_j^{(3)}$				
$V_j^{(4)}$	$V_1^{(4)}$...	$V_j^{(4)}$...	$V_m^{(4)}$				

Table 2. Subject of calculations and initial data.

Option	Voltage, V	Electric energy consumption, kWh	Lifetime, h	Cost, RUB
1	220	1.604	2000	7900
2	220	0.736	12000	11800
3	220	0.561	100000	36200
4	12	0.557	100000	22700

According to [20], it is no need to use all the quantitative technical characteristics of this equipment to select the best option of technological equipment, it is enough to select only the main ones that have an impact on the process operation and results of this work. In addition, it is advisable not to use correlated features, if it is possible to allocate them. This does not change the result of selecting the best equipment, but reduces the dimensionality of the task.

3 Results Section

The first stage is to calculate according to known methods [16] technical and economic efficiency of four options of the lighting systems for industrial premises:

1. conventional, on the basis of energy-efficient CFL bulbs for general lighting and incandescent lamps for local lighting;

2. on the basis of energy-efficient CFL bulbs lighting for general lighting and LED lamps for local lighting (energy-efficient CFL bulbs can't be applied for local lighting because of the luminous flux oscillations);
3. on the basis of LED panels for general lighting and LED lamps for local lighting without the installation of rectifier device to a group of LED panels in 220 V alternating current electrical shield instead of LED driver in each lamp;
4. on the basis of LED panels for general lighting and LED lamps for local lighting with the installation of rectifier device to a group of LED panels in 220 V alternating current electrical shield instead of LED driver in each lamp.

Subject of calculations and initial data: room dimensions: $h = 2.1$ m – maximum spacing to mounting height of the lamp above the working surface, $a = 12$ m – the length of the room, $b = 6.1$ m – the width of the room; background wall and ceiling are light.

The calculations has been carried out according to the technique is described previously. The results are presented in Table 2. The length of the wires, wire diameter and circle cross-sectional area, wire type, thermal energy losses in the wires are taken into account. The Table 2 is compiled taking into account calculations for the same illumination of the working surface. The cost of the lighting system includes the costs of: lamps, luminaires, wires, rectifier device and disposal costs for compact fluorescent lamps. The lamp lifetime is taken for a less reliable item.

The thermal energy losses for typical aluminum wire (diameter 4 mm) are about 4 watts per hour, but for thin copper wires (diameter 1 mm) used for energizing the LEDs they are insignificant (200 times less) – about only 0.02 watts per hour. In addition the typical aluminum wire is much thicker and thus more than 6 times expensive (for the specified premise size) than thin copper wire (4-th option of the lighting system).

The second stage is to select the most appropriate lighting system for industrial premises of the four options proposed in Table 1. For calculations has been used a program previously written in Delphi 7 [20]. The number of iterations was taken equal to ten ($k = 10$).

Calculations are made for four lighting systems and four characteristics (including the cost). As a result of calculations was obtained the array of options (the values of assessment are given in the brackets):

- 4 - (1);
- 3 - (0.7869);
- 2 - (0.5014);
- 1 - (0.3748);

and the array of characteristics:

- Electric energy consumption, kWh (1);
- Lifetime, h (0.9208);
- Cost, RUB (0.8981);
- Voltage, V (0.8510);

4 Discussion Section

Thus, the most important characteristic is «Electric energy consumption, kWh», and the best option is 4 (on the basis of LED panels for overall lighting and LED lamps for local lighting with the installation of rectifier device to a group of LED panels in 220 V alternating current electrical shield instead of LED driver in each lamp).

This will allow to apply a secondary wiring system running on the LED panels at 12 V direct current electricity. The size of wire used for a circuit is determined by how much current the wire has to carry, therefore the 220 V wire is much thicker and thus cheaper than the 12 V wire. In addition, applying of 12 V wire will lower the energy lost and increase the safety of operation of such lighting, especially in areas with high fire risk and explosiveness (e.g. in rooms for charging batteries).

5 Conclusions

Thus, during the construction of a new or modernization and expansion of the old industrial premises of motor transport enterprise it is necessary to consider the trend of the transition to LED lighting. LED lighting should be both general and local. It is necessary to install a rectifier device to a group of LED panels in 220 V alternating current electrical shield instead of LED driver in each lamp. A secondary wiring system running on the LED panels should be at 12 V direct current electricity.






In addition to this, it is necessary to take into account that the most important lighting characteristics are electric energy consumption and lifetime.

References

1. Mills, B., Schleich, J.: Household transitions to energy efficient lighting. *Energy Econ.* **46**, 151–160 (2014)
2. Azcarate, I., Gutierrez, J., Lazkano, A., Saiz, P., Leturiondo, L.: Towards limiting the sensitivity of energy-efficient lighting to voltage fluctuations. *Renew. Sustain. Energy Rev.* **59**, 1384–1395 (2016)
3. Ivanco, M., Karney, B., Waher, K.: To switch, or not to switch: a critical analysis of Canada's ban on incandescent light bulbs. In: *IEEE Electrical Power Conference*, pp. 550–555 (2007)
4. Balzani, V., Bergamini, G., Ceroni, P.: Light: a very peculiar reactant and product. *Ang. Chem. Int.* **39**, 11320–11337 (2015)
5. Bergesen, J., Tähkämö, L., Gibon, T., Suh, S.: Potential long-term global environmental implications of efficient light-source technologies. *J. Ind. Ecol.* **20**, 263–265 (2016)
6. Armaroli, N., Balzani, V.: Towards an electricity-powered world. *Energ. Environ. Sci.* **4**, 3193–3222 (2011)
7. Soori, P., Vishwas, M.: Lighting control strategy for energy efficient office lighting system design. *Energ. Build.* **66**, 329–337 (2013)
8. Mironava, T., Hadjiargyrou, M., Simon, M., Rafailovich, M.: The effects of UV emission from compact fluorescent light exposure on human dermal fibroblasts and keratinocytes in vitro. *Photochem. Photobiol.* **88**, 1497–1506 (2012)

9. Lehman, B., Wilkins, A.: Lighting designing to mitigate the effects of flicker in LED. *IEEE Power Electron. Mag.* 18–26 (2014)
10. Narendran, N., Deng, L.: Color rendering properties of LED light sources. In: *Proceeding of SPIE. (Sol. St. Ligh.)*, vol. 61, pp. 4776–4778 (2012)
11. Moreno, I., Avendaño-Alejo, M., Tzonchev, R.: Designing light-emitting diode arrays for uniform near-field irradiance. *Appl. Opt.* **45**, 2265–2272 (2006)
12. Singh, D., Basu, C., Meinhardt-Wollweber, M., Roth, B.: LEDs for energy efficient greenhouse lighting. *Renew. Sustain. Energ. Rev.* **49**, 139–147 (2015)
13. Ryckaert, W., Lootens, C., Geldof, J., Hanselaer, P.: Criteria for energy efficient lighting in buildings. *Energ. Build.* **42**(3), 341–347 (2010)
14. Salata, F., de Lieto Vollaro, A., Ferraro, A.: An economic perspective on the reliability of lighting systems in building with highly efficient energy: a case study. *Energ. Convers. Manag.* **84**, 623–632 (2014)
15. Li, D., Cheung, K., Wong, S., Lam, T.: An analysis of energy-efficient light fittings and lighting controls. *Appl. Energ.* **87**(2), 558–567 (2010)
16. Russian Standart SP 52.13330.2011: *Daylighting and Artificial Lighting* (2011)
17. Kafiev, I., Romanov, P.: Choice of rational option of the device of illumination of workshops on repair of agricultural cars. *Bull. Bashkir Univ.* **2**(26), 83–86 (2013)
18. Kafiev, I., Romanov, P., Romanova, I.: Comparative assessment of decision-making techniques for choosing a lighting system project of farm. *Bull. Bashkir Univ.* **3**(35), 48–52 (2015)
19. Kafiev, I., Romanov, P., Romanova, I.: Decision-making methods to select lighting systems for farm repair shops under uncertainty. *Bull. Bashkir Univ.* **1**(33), 82–90 (2015)
20. Romanov, P., Kirjakov, I.: Assessment of the impact of part characteristics on the choice of metal-cutting machines. In: *3rd International Scientific-Practice Conference on Technology, Politics and Economics*, pp. 86–94 (2016)

Thermal Resistance and Accumulation of Heat by the Wall Construction

Daria Zaborova¹ , Tatiana Musorina¹ , Anna Selezneva¹  ,
and Andrey Butyrin² 

¹ Peter the Great St. Petersburg Polytechnic University,
29 Politechnicheskaya St., St. Petersburg 195251, Russia
anna.selezneva31@gmail.com

² Moscow State University of Civil Engineering,
Yaroslavskoe shosse, 26, Moscow 129337, Russia

Abstract. Nowadays the energy efficiency is one of the main topics in the construction industry and transport infrastructure. Therefore, structural and technological activities are aimed mainly at increasing the wall's thermal resistance. The object of the study is a multilayer enclosing structure (wall). The goal of the article is the selection of the optimal enclosing structures to increase the thermal stability and energy efficiency of the building. The article shows that the heat accumulation in the wall and its thermal resistance are opposite factors. Results of the study show that the thermal resistance of the wall does not depend on the layers alternation. Stationary and periodic temperature, humidity regimes of the walls depend substantially on the layers alternation. Sufficient thickness of the walls helps to reduce energy consumption for heating of building and structures. Consequently, the savings on energy consumption. The studies were conducted by the methods of thermal engineering.

Keywords: Energy management · Transport buildings and structures
Energy efficiency

1 Introduction

The accumulative capacity of wall structures determines the amount of heat absorbed and passed by the structure and used to maintain a required temperature level of the room and enclosing wall when the temperature of the external heat source changes. The better the thermal insulation, the less heat loss. The capacitive resistance of the wall (the storage capacity of the structure) determines the possibility of heat reclaim during the heating season and the thermal stability of the structure. It is evaluated by the rate of change in temperature of wall structure [1, 2]. “The ideal” wall structure should have at the same time real and imaginary part of impedance. It is necessary to determine at what extent “the ideal” is achieved. In general case it comes out a problem about conditional extremum formulated as exact equalities or inequalities in the form of linear programming problem, e.g. thermal resistance, $r \geq [r]$, $[r]$ – characteristic value of resistance, $\beta \rightarrow \max$, or an adjoint problem with limiting in β and an extremum (maximum) in r .

Firstly, there are large amounts of ways to thermal insulation buildings using different materials that have their technological parameters and price. In connection with it, it is arisen the question about the rational use – from the energy and economic point of view – of various materials for the insulation of structures.

Secondly, one of the main parameter that characterizes the features of enclosing structure is their capacity to storage relative stability of the room temperature with a periodical change in heat influence by external and internal environment. The greatest thermal capacity of the enclosure provides not only energy efficiency of building, but also improving room microclimate. It is necessary to set up the possibility of simultaneous accomplishment the requirement that is lodged to wall construction. Due to Federal Act No. 261 of 23.11.2009 on energy saving [3] to residential building it is presented more serious requirement to energy consumption. It means that accumulative capacity of enclosing structure is one of the priority task.

The Russian requirements to heat insulation of building are presented in the Code of Regulations [4, 5]. But in the article [6] it is appeared that regulatory requirements to heat insulation although slightly but were below the requirement of 2003 standards (Set of rules and regulations 23-02-2003). Accordingly, the buildings that would completely satisfy the requirement of current standards would not provide necessary heat insulation. Moreover, lots of building companies do not always fulfill even those standards. Thus, in various researches it is given evidence of unfair compliance the requirements. For example, unheated slab made with defects under the insulated technical floor and so on. Similarly, authors of the articles [7–11] explored wall construction consisting of facing brick and expanded concrete blockwork and they deduced total insolvency such construction. In the articles [12–14] it is given an accurate analysis of energy efficiency and financial viability of hinged ventilated facade (plaster + calcium-silicate brick + slag wool) and multilayers facade (plaster + calcium-silicate brick + slag wool + solid brick). The result is dissatisfaction the requirements to protecting from over moistening but good energy efficiency of hinged ventilated façade [15–19].

The goal of this article is identification of dependence between thermal capacity of wall construction and its heat resistivity. In this connection it should be solved following problem:

To find out connection between thermal resistivity wall construction and the rate of temperature variation at the wall edge;

To set the depth of penetration of temperature wave in wall construction;

The influence of external heat source to the intensity of heat transfer and thermal resistance to the depth of penetration of temperature wave.

Active (thermal) wall resistance r ,

$$r := \delta/\lambda \quad (1)$$

where:

δ – thickness of the layer, mm;

λ – coefficient of thermal conductivity, W/[m·°C].

Accumulative capacity of wall structures β ,

$$\beta := \sqrt{\lambda C_V} \quad (2)$$

where: C_V – specific heat capacity, $J/[kg \cdot ^\circ C]$.

Satisfy the condition:

$$\beta\sqrt{r} := \sqrt{C_V\delta} \quad (3)$$

For each wall construction, the quantity (3) is constant. Consequently, the greater the thermal resistance of the wall, the lower its thermal stability.

As a subject of study various multilayer wall constructions made from aerated concrete (300 mm thick) and bricks (120 mm thick) were taken. As a heat-insulating layer (thickness 100 mm), brands of different manufacturers were chosen. For the facing layer, a brick 120 mm thick was chosen. This relationship (formula 3) is shown in Fig. 1.

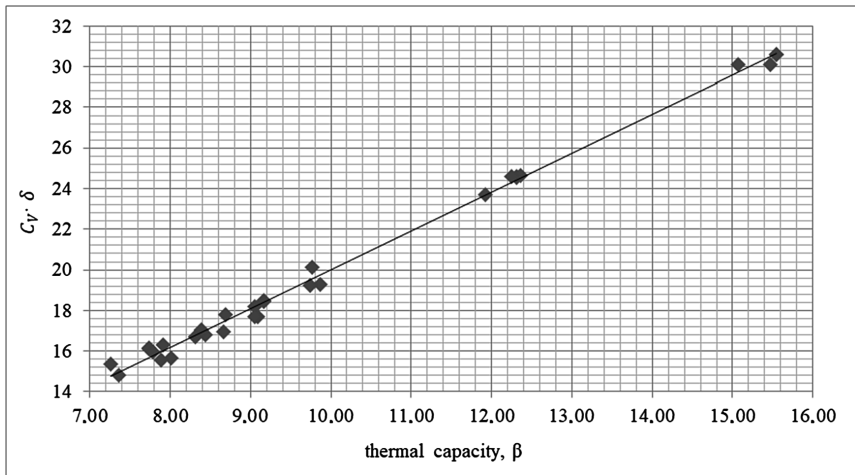


Fig. 1. Attribution of dependence between $\sqrt{C_V\delta}$ and β

The graph shows that with increasing thickness of the thermal insulation material increases, its thermal conductivity increases. Therefore, it is required to select a combination of thermo-technical parameters that ensure $\max\sqrt{C_V\delta}$ under the constraint $r \geq [r]$. Parametric analysis is sufficient for estimating the quality of a wall structure. This analysis is connected with the search of permissible various materials (resistance coefficients, heat-resistance coefficients) in various combinations of layers of the bearing material (concrete, aerated concrete, reinforced concrete, brick) and heat-insulating material (mineral wool, stone and soft, expanded polystyrene, etc.). As an example, confirming the above assumptions, it is presented (Fig. 2) dependence between thermal stability and thermal conductivity.

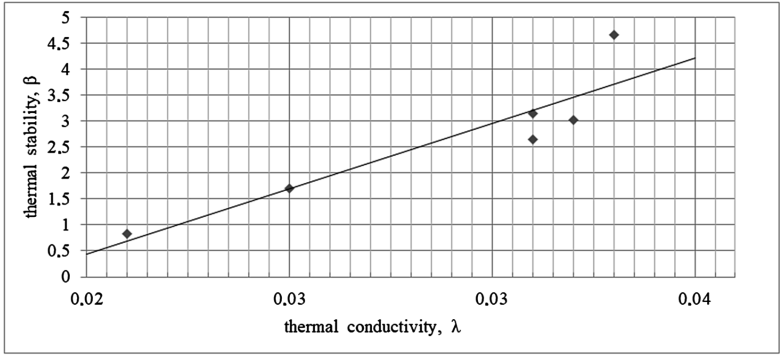


Fig. 2. Thermal stability dependence on the thermal conductivity

It follows from Fig. 2 that for wall structures (approximately 30 types) an increase in the thermal resistance (decrease of λ) leads to a proportional decrease in the coefficient of thermal stability β .

2 Materials and Methods

The elementary (one-dimensional) mathematical model of heat transfer in the enclosing structure is based on the limiting (initial-boundary) Fourier problem for the linear heat equation. This problem is formulated as follows:

$$\frac{\partial T}{\partial \tau} = a_m \frac{\partial}{\partial \xi} \left(f(\xi) \frac{\partial T}{\partial \xi} \right), \xi := x / \sqrt{a_m t_0}, \tau := t / t_0, \mathcal{D}(T) = (\tau > 0, \xi > 0),$$

$$\left(\frac{\partial T}{\partial \xi} \right)_{\xi=0} + h_0 (T_f - T_0) = T(0, \xi) = 0, T_0 := T(\tau, 0),$$
(4)

where: τ – dimensionless time; a_m – scale value of temperature diffusivity of the wall structure; t_0 – time scale; h_0 – Biot number:

$$h_0 = \frac{\alpha \sqrt{t_0}}{\sqrt{C_V \lambda m}},$$
(5)

where: C_V – volumetric heat capacity of the material of the structure, α – heat emission coefficient at the point $x: x = 0$ ($\xi = 0$), T_f – the temperature of the external source exchanging heat with enclosure, $f(\xi)$ – nondimensional coefficient of the temperature diffusivity:

$$f(\xi) := \frac{a}{a_m}. \tag{6}$$

For a layered construction, this is the partially-constant (within the layer) distribution $T_f(\tau)$ is the temperature of the external source. For the problems of building heat engineering it is sufficient to consider that the distribution $T_f(\tau)$ locally summable at the whole time interval $\tau \in (0, \infty)$, $T_f(\tau) \in L^{loc}(0, \infty)$.

Further, it is assumed that the wall construction has an unlimited length $0 < x < \infty$ ($0 < \xi < \infty$). In fact as it will be shown time inhomogeneity of the temperature distribution $T(\tau, \xi)$ is significant for $0 < x < \sqrt{a_m t_0}$, and outside this interval the temperature distribution is particularly permanent.

It already follows from the formulation of the limiting problem (4) that an increase the heat absorption coefficient β is equivalent to adiabaticizing the wall construction; on the contrary if $\beta \rightarrow 0$, i.e., the thermal resistivity increases, then the measure of the external heat transfer also enlarge proportional to $h_0 : h_0 \rightarrow \infty$ [20, 21]. This relationship is shown in Fig. 3.

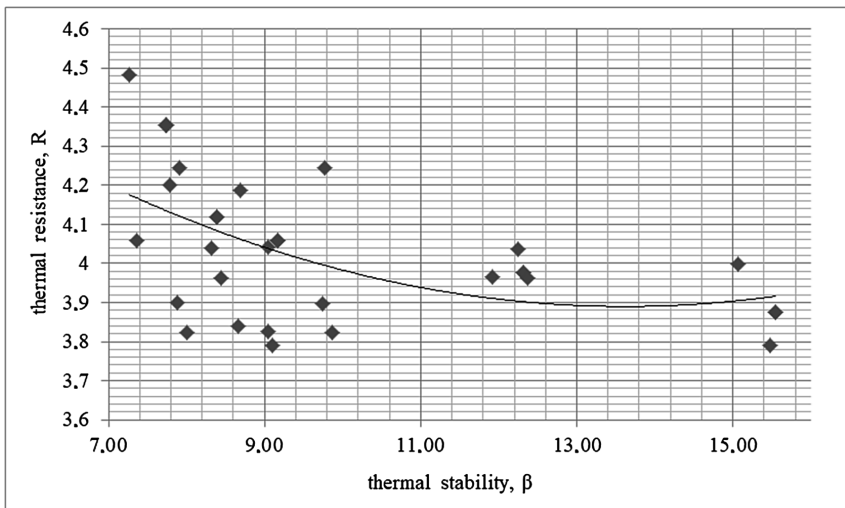


Fig. 3. Thermal resistivity dependence on the thermal stability

To estimate the thermal stability of a wall structure, it is convenient to use the algorithm for solving the limiting problem (4) described in [3, 22, 23]. The basis of this algorithm is the replacement of the Fourier differential equation by an integral identity:

$$\frac{d}{d\tau} \int_0^\infty T(\tau, \xi) d\xi = -f(0)(\partial T / \partial \xi)_{\xi=0} = H_0(T_f(\tau) - T_0(\tau)), \tag{7}$$

where: $H_0 := f(0)h_0$ – modified Biot number. It is usually accepted that h_0 – permanent parameter. Therefore H_0 is also constant. Not excluding the generality it could be considered: $f(0) = 1$, i.e., $a_0 = a_m$, $H_0 = h_0$, and as a scale it is used the temperature diffusivity of the external ($x = 0, \xi = 0$) surface. The temperature distribution in the wall construction is defined in the form:

$$T(\tau, \xi) = T_0(\tau) \exp(-m(\tau)\xi). \tag{8}$$

where: $m(\tau)\xi$ – a function of the dimensionless coefficient of thermal conductivity and time.

Using equality (8), the thickness of the temperature boundary layer of the wall structure Δ (the depth of penetration of the temperature of the external source into the wall structure) can be formally input defining it as follows:

$$T_f(\tau)\Delta = \int_0^\infty T(\tau, \xi)d\xi, \Delta = T_0(\tau)/(m(\tau)T_f(\tau)). \tag{9}$$

Thus, as shown in the article [23] the depth of penetration of the temperature of the external source Δ is equal to:

$$\Delta = h_0 \sqrt{\frac{\int_0^\tau T_f(\omega)d\omega}{T(\tau)}}. \tag{10}$$

where: $(\omega)d\omega$ – a dimensionless variable of integration.

Hence, the temperature distribution has the form:

$$T(\tau, \xi) = h_0 \sqrt{T_f(\tau) \int_0^\tau T_f(\omega)d\omega} \exp\left(-\xi \sqrt{\frac{T_f(\tau)}{\int_0^\tau T_f(\omega)d\omega}}\right). \tag{11}$$

The rate of variation in the temperature of the wall construction on average on the interval $0 < \xi < \infty$, is proportional to $v = \frac{d}{d\tau} \left(\frac{T_0}{m}\right)$.

3 Results

Comparing the measures of the rate of change in the temperature of the wall structure it is obtained: $v_{h_0 \ll 1} \ll v_{h_0 \gg 1}$, i.e., a wall construction with a large accumulative capacity is more stable than a construction with a large thermal resistivity but with a low coefficient of the heat absorption.

Further, the inhomogeneity of the temperature in the wall construction is determined by the magnitude of the exponent $m(\tau)$. From these equalities it follows (using the Cauchy inequality):

$$\frac{m_{h_0 \ll 1}}{m_{h_0 \gg 1}} = \frac{\sqrt{\frac{T_f(\tau)}{\int_0^\tau T_f(\omega) d\omega}}}{\sqrt{\frac{T_f(\tau)}{2 \int_0^\tau T_f^2(\omega) d\omega}}} = \frac{\sqrt{2 \int_0^\tau T_f^2(\omega) d\omega}}{\sqrt{T_f(\tau) \int_0^\tau T_f(\omega) d\omega}} \geq \frac{\sqrt{2 \int_0^\tau T_f(\omega) d\omega}}{\sqrt{\tau T_f(\tau)}}. \tag{12}$$

If $T_f(\tau)$ is an integral rational function (for example, a polynomial), then $\frac{m_{h_0 \ll 1}}{m_{h_0 \gg 1}} = O(1)$ the temperature variation along the thickness of the wall construction does not depend on modified Biot number H_0 . If the temperature of the external source unlimited than the inhomogeneity of the temperature distribution along the thickness of the wall construction does not depend on the heat absorption coefficient.

This assumption remains valid for trigonometric polynomials, i.e., limited changes in the temperature of the external source.

$$T_f(\tau) = 1 + \theta \sin 2\pi\tau, \quad \theta \ll 1$$

(periodical, with period t_0 , the temperature distribution of the external source of heat flow). By the inequality (13):

$$\frac{m_{h_0 \ll 1}}{m_{h_0 \gg 1}} \geq \sqrt{\frac{2\tau + \theta/\pi(1 - \cos 2\pi\tau)}{\tau(1 + \theta \sin 2\pi\tau)}} \xrightarrow{\tau \rightarrow \infty} \sqrt{\frac{2}{1 \pm \theta}}. \tag{13}$$

4 Discussion

According to the Federal Act No. 261 energy efficiency of enclosure structure is regulated by the thermal resistance of the wall. Wherein, it does not take into account such a characteristic of the structure as its thermal stability. The analysis of the requirement of the Federal Act No. 261 shows that not only thermal resistance of enclosure should be taken into account but also its thermal stability. The maximum condition of the thermal stability contradicts to the Federal Act No. 261.

Therefore, it is necessary to find such an (optimal, acceptable) solution in order to simultaneously satisfy the requirements of the Federal Act No. 261 for thermal resistance and thermal stability of the structure. It is necessary that the rate of change of temperature be uniformly limited for all points of the construction [3]. The results of a computational experiment showing the relationship between thermal stability and thermal resistance for a real enclosure are given in the article.

It comes out the model of the temperature field. Each point in the material in given construction reacts differently [9]. In the article each layer is considered a construction

with only one average temperature. The temperature changes only on the verge. The average temperature depends on the alternation of the layers.

In article [23] only mathematical model for inhomogeneous wall was considered. In the current study mathematical model is applied to the certain structures with known parameters. The authors input the notion of a temperature field in order to objectively judge the rate of change in temperature in each structure.

5 Conclusions

In this way, estimates based on an approximate solution of the limiting Cauchy problem (4) allow to affirm that:



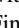
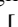
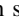
1. The temperature distribution decreases exponentially with distance from the contact surface $x = 0$ ($\xi = 0$) and outside the interval $0 < \xi < 1$ particularly stationary;
2. The temperature of the construction at the contact surface, $T_0(\tau)$, grows with rising thermal resistance of the surface and $T_0(\tau) \xrightarrow{\beta \rightarrow 0} T_f - 0$, steadily by $\tau > 0$. Accordingly, an increase in the heat absorption coefficient β contributes to a kind of “adiabatic” construction, “tuning” the change in the temperature of the surface $T_0(\tau)$ from the temperature change of the source $T_f(\tau)$;
3. A wall construction with a large accumulative capacity is more stable than a construction with a large thermal resistivity but with a low coefficient of the heat absorption β : $\nu_{h_0 \ll 1} \ll \nu_{h_0 \gg 1}$;
4. This ratio of the rate of change in the temperature of the wall structure is due to the fact that the thickness of the temperature boundary layer at $H_0 \ll 1$ is small: the wall structure does not react to a change in the temperature of the source; at large Biot numbers, on the contrary, the wall reacts to a change in the source temperature by increasing Δ .

References

1. Knat'ko, M.V., Efimenko, M.N., Gorshkov, A.S.: *Mag. Civ. Eng.* **2**, 50–53 (2008)
2. Vatin, N.I., Gorshkov, A.S., Korniyenko, S.V., Pestryakov, I.I.: *Constr. Unique Build. Struct.* **1**, 78–101 (2016)
3. Petrichenko, M., Vatin, N., Nemova, D., Kharkov, N., Korsun, A.: *Appl. Mech. Mater.* **672–674**, 1903–1908 (2014)
4. Petrichenko, M., Ostrovaia, A., Statsenko, E.: *Appl. Mech. Mater.* **725–726**, 87–92 (2015)
5. Petrichenko, M., Rakova, X., Vyatkin, M., Musorina, T., Kuznetsova, D.: *Appl. Mech. Mater.* **725–726**, 1101–1106 (2015)
6. Perlova, E., Platonova, M., Pankova, A., Nemova, D., Petrichenko, M., Rakova, X.: *Cep “Proceedings of 26th DAAAM International Symposium*, pp. 795–802 (2015)
7. Vatin, N., Petrichenko, M., Nemova, D.: *Appl. Mech. Mater.* **633–634**, 1007–1012 (2014)
8. Korniyenko, S.V.: *Academia. Archit. Constr.* **5**, 389–394 (2009)
9. Korniyenko, S.V.: *Mag. Civ. Eng.* **8**, 25–37 (2014)

10. Gorshkov, A., Vatin, N., Nemova, D., Tarasova, D.: *Appl. Mech. Mater.* **725–726**, 3–8 (2015)
11. Vatin, N., Gorshkov, A., Nemova, D., Tarasova, D.: *Appl. Mech. Mater.* **633–634**, 991–996 (2014)
12. Vatin, N., Gamayunova, O.: *Adv. Mater. Res.* **1065–1069**, 2159–2162 (2015)
13. Zemitis, J., Borodinecs, A., Frolova, M.: *Energy Build.* **127**, 884–891 (2016)
14. Gorshkov, A.S., Rymkevich, P.P., Vatin, N.I.: *Mag. Civ. Eng.* **8**, 38–48 (2014)
15. Petrochenko, M.V., Strelets, K.I., Petrichenko, M.R., Yavtushenko, E.B.: *Appl. Mech. Mater.* **672–674**, 567–570 (2014)
16. Pukhkal, V., Vatin, N., Murgul, V.: *Appl. Mech. Mater.* **633–634**, 1077–1081 (2014)
17. Musorina, T., Olshevskiy, V., Ostrovaia, A., Statsenko, E.: *MATEC Web of Conferences, TPACEE 2016*, vol. 15, p. 02002 (2016)
18. Pukhkal, V.: Humidity conditions for exterior walls insulation (case study of residential housing development in Saint-Petersburg). *Procedia Eng.* **117**, 616–623 (2015). <https://doi.org/10.1016/j.proeng.2015.08.222>
19. Petrichenko, M.R., Petrochenko, M.V., Yavtushenko, Y.B.: *Mag. Civ. Eng.* **2(37)**, 35–40 (2013)
20. Zaborova, D., Petrochenko, M., Chernenkaya, L.: *MATEC Web of Conferences*, vol. 73, pp. 2–7 (2016)
21. Petrichenko, M.R., Petrochenko, M.V.: *Nauchno-tekhnicheskiye vedomosti SPbGPU.* **147** (2), 276–282 (2012)
22. Petrichenko, M.R.: *XXV Mezhdunarodnaya nauchno-prakticheskaya konferentsiya*, pp. 31–35 (2016)
23. Zaborova, D.D., Kukolev, M.I., Musorina, T.A., Petrichenko, M.R.: *St. Petersburg State Polytech. Univ. J.* **4**, 28–33 (2016)

Experimental Study of Thermal Stability of Building Materials

Daria Zaborova¹ , Gabriel Vieira¹  , Tatiana Musorina¹ ,
and Andrey Butyrin² 

¹ Peter the Great St. Petersburg Polytechnic University,
Politechnicheskaya St., 29, St. Petersburg 195251, Russia
gabriel.vieira@poli.ufrj.br

² Moscow State University of Civil Engineering,
Yaroslavskoe shosse, 26, Moscow 129337, Russia

Abstract. As of today, the energy issues remain relevant not only in civil construction but also in transport infrastructure. Nowadays, as the concern of sustainability and energy efficiency increases, it is important to evaluate a great number of resources and their behavior while exposed to diverse climate conditions. Therefore, the aim of this paper is to analyse the relation between the thermostability of the materials with its properties as density and specific heat, through experiments with various structural materials. The experiments were carried out in a thermal chamber with the temperature ranging from zero to 20 °C (periodic and non-periodic) without thermal insulation materials and with sensors installed all over the structure checking the temperature. Subsequently, graphics were drawn overlapped in order to compare the results obtained; showing how heterogeneous is the heat transfer in different parts of the structure within clay brick (full-bodied), lightweight concrete and reinforced concrete. Finally, the results show that clay brick is more thermally stable, in comparison with samples shown in this article.

Keywords: Energy management · Transport buildings and structures
Energy efficiency

1 Introduction

From the majority of construction materials for building envelopes, used in low-rise construction, it is possible to highlight the most popular: reinforced concrete, brick and lightweight concrete. There are many criteria when choosing a material for a construction [1–5].

The most easy and cheap materials are porous materials. One block of the lightweight concrete replaces 17 bricks, so the construction is accelerated several times and additional reinforcement of the foundation is not required. Moreover, lightweight blocks can be built only on the girder foundation or slab foundation. Insufficient strength of the material causes damage and cracks of blocks during installation. In addition, some disadvantages include the thermal bridges that appear in the joints of the blocks; during the heating period, the building gets warm instantly, but also cools down

very quickly. In consequence of the fact that the material is porous, cracks is appeared because of the temperature differences [6–11].

If the property is located on movable water-saturated soil it is necessary to make a choice for a brick or reinforced concrete. Such houses differ in solidity and durability.

Brick perfectly “breathes”, but it has low thermal insulation properties - low thermal conductivity and a limited frost resistance.

Concrete has a long life cycle with proper usage, and reinforced concrete structures can serve without reducing the strength characteristics for more than 100 years. Furthermore, the concrete is characterized by such advantages as fire resistance and high resistance to dynamic and static loads.

The main disadvantage of this material is its heavy weight. Moreover, concrete has a high level of heat and sound conductivity that require the use of additional materials during the construction.

Finally, when working with concrete there is a need for special equipment and skilled workers [12–15].

Comparing the adaptability of these three materials, it should be noted that it is much easier to drill and cut a lightweight concrete. However, its sensitivity to mechanical stress requires a special approach for installation of windows, doors, hanging furniture, etc. In comparison, brick is a more reliable material. In addition, there are much more options for facade finish of a brick house [16–19].

Ceramic brick, as a building material, exist about 500 years; lightweight concrete is used in the construction no more than 80 years. It is well known, how brick building, which were built 100–200 years ago, is remained. However, the behavior of lightweight concrete buildings through the same time, still unpredictable.

Although the thermal conductivity of lightweight concrete is much higher than reinforced concrete and brick, its heat capacity is much smaller. The simple adoption of insulated brick/reinforced concrete in the structure will conserve heat longer [20–23].

According to [3], thermal stability is one of the most important topics in the building design, as it measures how quickly a material gains or loses heat to the environment. The thermal stability is property of the thermal conductivity coefficient, density of the material, specific heat and heat transfer resistance [24].

The thermal stability determines by the formula

$$b = \rho \cdot c \cdot \lambda, \quad (1)$$

where b – thermal stability, $[\frac{J}{m^2 \cdot K \cdot s}]$, ρ – material density, $[\frac{kg}{m^3}]$, c – specific heat, $[\frac{J}{kg}]$, λ – thermal conductivity, $[\frac{W}{mK}]$.

However, some other parameters can be analyzed based on the results obtained from the experiments, such as humidity and the occurrence of thermal bridges, for example.

As long as this experiment was carried just with temperature sensors, the aim of this paper is to consider the behavior of these materials according to the temperature changing. Therefore, the objective of the article is:

To analyze thermal stability of the most common construction materials: reinforced concrete, lightweight concrete and brick;

Compare experimental data for periodic regime;
 Compare experimental data for non-periodic regime.

2 Materials and Methods

The object of the research is the bearing layer of the enclosing wall. As a bearing layer, it was used as materials: reinforced concrete sample, lightweight concrete sample, clay brick sample.

The experiment has been conducted in an isothermal chamber “CHALLENGE 250” with an approximated volume of 20 L and dimensions of $0.60 \times 0.75 \times 0.52$ m (W \times H \times L) at an initial temperature of 20 °C. The initial average design temperature was approximately 19 °C.

The standard sensors «Dallas DS18B20» carried the measurement of instantaneous temperature. This sensor is also designed to measure the temperature of liquids, and temperature measurement in a humid environment. The sensor is enclosed in a metal flask measuring 6×50 mm. It is equipped with a sealed lead cable 1 m length. The cable consists of 3 wires: red (VCC), blue (DATA), black (GND) (Fig. 1).



Fig. 1. Thermal Chamber used during the experiments

For reading the temperature inside the materials, holes were cautiously made with a drilling machine in order to fit the sensors inside it. Thus, the cables were connected to a computer which, with a software support provided the exactly temperature of each sensor with one (1) decimal place of precision. The experiments were held in the Strength of Materials’ Laboratory of Saint Petersburg Polytechnic University between 20th of April and 2nd of June of 2017.

2.1 Materials Used in the Experiments

The experimental model of the walls:

- Clay brick (full bodied);
- Aerated concrete block (lightweight concrete);
- Reinforced concrete block (Cement B20, steel diameter: 14 mm).

All the samples have the same dimensions: 120 × 195 × 250 mm.

2.2 Procedures

The temperature of the sensor were collected every 3 min, both for periodic and non-periodic regime. It was placed sensors inside the material and one outside, in the outer surface, in order to double check the temperature of the chamber and the precision of the sensor, avoiding potential mistakes during the measurements. As an example of the arrangement of the sensors in the materials during the trial, the Fig. 2 is showed below.

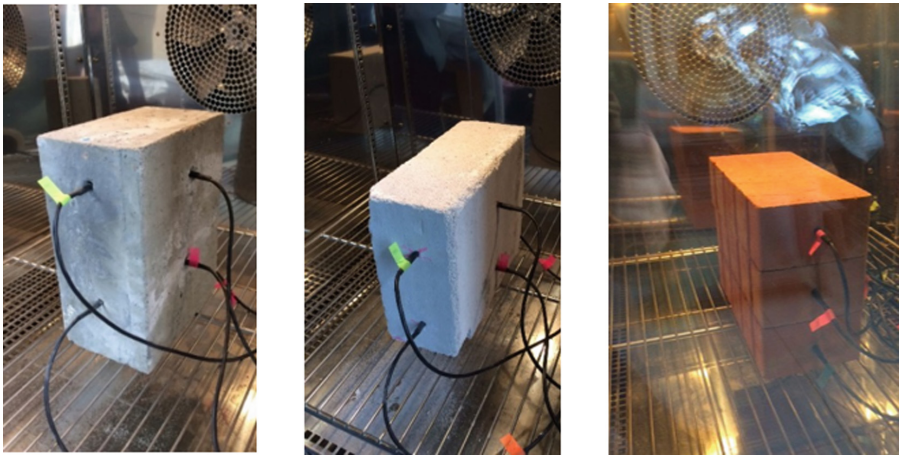


Fig. 2. (a) Reinforced concrete sample, (b) lightweight concrete sample, (c) clay brick sample.

The temperature of the chamber was set for twenty (20) degrees Celsius during the heating period and for zero (0) degrees Celsius during the cooling period.

For non-periodic regime, the measurements for cooling and heating were determined as thirty minutes each. In other words, the trial followed the subsequent order: cooling (30 min.) - heating (30 min.) – cooling (30 min.).

The Fig. 3 shows the dependence of the time on cooling temperature. During the first 3 min, camera has cooled down from 20 °C to 0 °C and, then, the chamber remains with a constant temperature of zero degrees Celsius.

As a result, it can be seemed that the clay brick cools down much slower, than other materials. The main reason behind this explanation is the fact that reinforced concrete

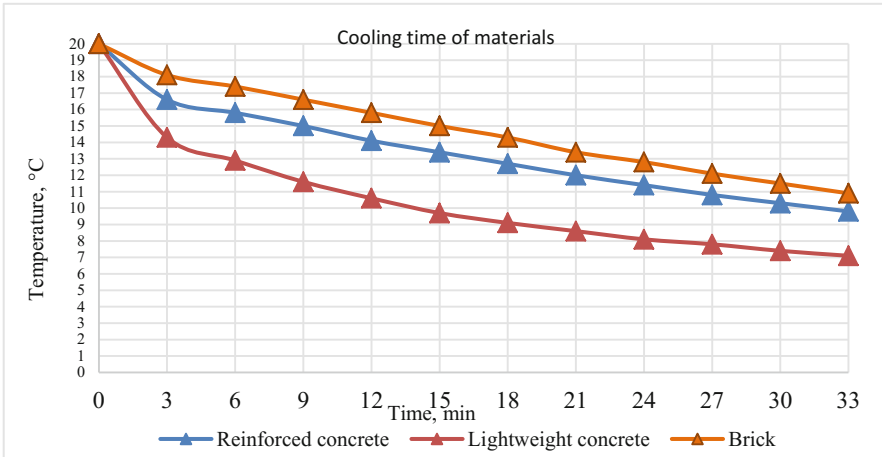


Fig. 3. Cooling time: periodic regime

has the thermal bridges – as result of the presence of the reinforcement bars. In addition, lightweight concrete, despite being a good insulator material, is a bad heat accumulator, which explains the great steepness of it in the graphic.

The Fig. 4 shows the heating period in the matter of time, during 30 min of measurement. The first 3 min of the graphic are related to the chamber heating to 20 °C.

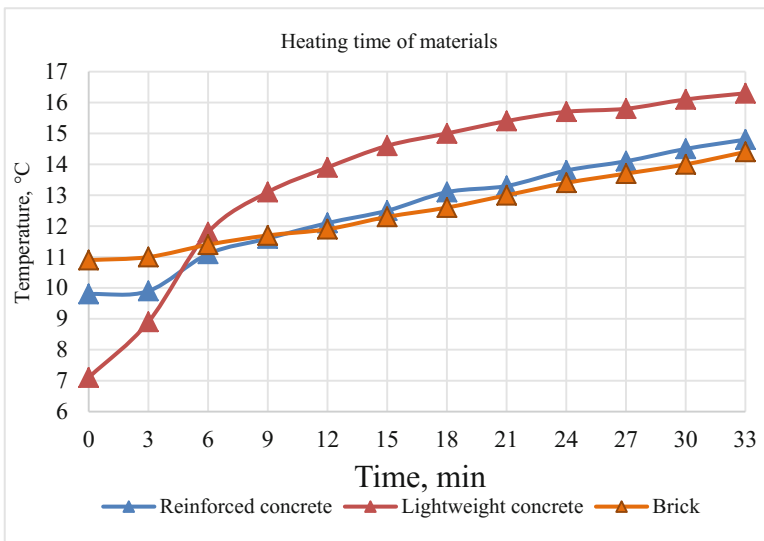


Fig. 4. Heating time: periodic regime

The graph also confirms the dependence that lightweight concrete has with the air in its composition; As long as the specific heat of the air is much higher than the materials rehearsed, it gets warm faster than other samples. The results obtained for brick and reinforced concrete were similar for this experiment.

3 Results

The Fig. 5, presented below, shows the behavior of the materials in a non-periodic regime.

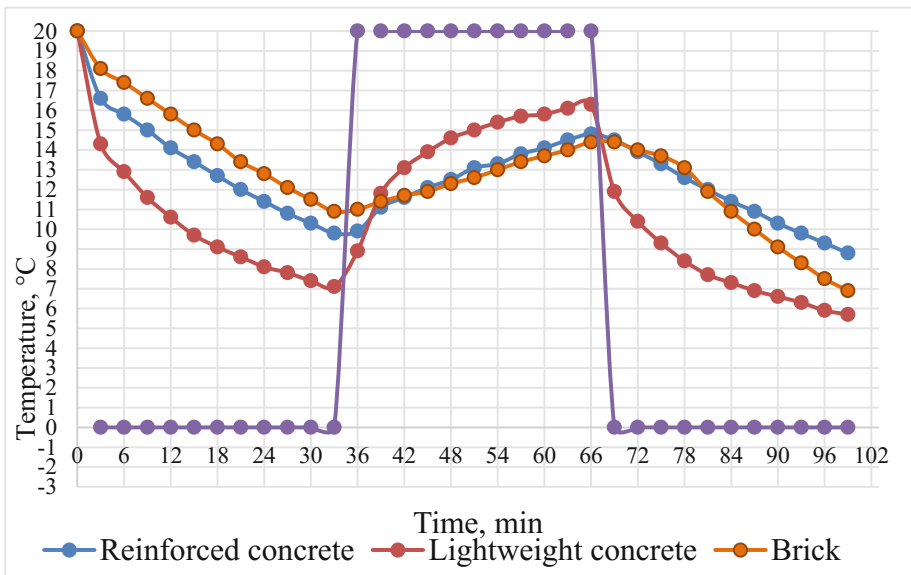


Fig. 5. Non-periodic regime (cooling and heating, the purple line shows the temperature of the air change into the chamber)

As a result, because clay brick is a homogeneous material it gains temperature gradually, with an almost constant tangent in the graphic.

As expected, the lightweight concrete presented a great deviation during this experiment due to its low capacity of storing heat. The reinforced concrete and the brick, as in the figure number 4, presented a similar comportment, being the brick showing a more predictable behavior.

Table 1 presents the theoretical calculations thermostability. Thermal stability is calculated by the formula 1.

Comparison theoretical and practical $\beta = \sqrt{(\rho\lambda c)}$ values is different. Since reinforced concrete is an heterogeneity material, the accumulative capacity will differ from the experimental data, as the steel is considered a “bridge of cold”. As long as aerated concrete is a porous material, it contains a great amount of air on it, which is a good insulator, but it is a bad heat accumulator.

Table 1. Comparison of the physical characteristics of load-bearing materials

Name of material	Density, $[\frac{kg}{m^3}]$	Thermal conductivity, $[\frac{W}{mK}]$	Specific heat, $[\frac{kJ}{kg}]$	Thermal stability, $[\frac{J}{m^2 * K * c^{0.5}}]$
Reinforced concrete 2500	2500	1.69	0.84	59.57
Aerated concrete 800	800	0.17	0.84	10.69
Clay brick	1800	0.56	0.88	29.78

4 Discussion

Most of Russian and Foreign papers consider energy efficiency of the building envelopes from the point of view of the thermal resistance of the structure. This article demonstrates that thermal stability of material also has to be considered at determining energy efficiency of high-rise and low buildings.

In articles [3, 4] importance of accumulative ability of the wall has been theoretically proved, this research confirms these conclusions using a practical experiment.

Authors of the article also considered thermal inertia of the materials [5, 9]. However, the article compares only the surface temperature. In this paper work, the temperature inside the material is also considered.

Thus, the results show that this characteristic must be considered when choosing construction materials. In previous works [1, 2], the mathematical models of the temperature for building envelope were calculated and authors introduced the concept of temperature field. It has allowed to evaluate objectively about the temperature variation rate in each design. In this work, the above-stated characteristics have experimentally been proved.

This experimental study can be applicable in modern construction, for the selection of building materials and constructions. Temperature range of the laboratory chamber (from -70 up to $+150$) allows to conduct experiments under different climatic conditions, which clearly show the temperature changes of the materials.

In further studies, it is planned to connect the moisture sensors and to perform heat and humidity conditions of enclosing structures and materials.

5 Conclusions

As result for this paper work, the following conclusions were made:

1. As a result of all experiences, it has been come to conclusion that the most thermal stability material is brick.
2. Temperature gradient of the brick is insignificant in comparison with lightweight concrete.
3. Despite the reinforced concrete has good thermal properties, the steel on it contributes for the existence of thermal bridges which makes it more properly to loose or gain heat to the air.

References

1. Petrichenko, M.R.: Examples of fundamental and applied research. In: XXV International Scientific and Practical Conference, pp. 31–35 (2016)
2. Zaborova, D.D., Kukolev, M.I., Musorina, T.A., Petrichenko, M.R.: St. Petersburg State Polytech. Univ. J. **4**, 28–33 (2016)
3. Zaborova, D.D., Musorina, T.A., Petrichenko, M.R.: St. Petersburg State Polytech. Univ. J. **23**(1), 18–26 (2017)
4. Zaborova, D., Petrochenko, M., Chernenkaya, L.: MATEC Web of Conferences, vol. 73, pp. 2–7 (2016)
5. Korniyenko, S.: Procedia Engineering. **117**, 191–196 (2015)
6. Zemitis, J., Borodinets, A., Frolova, M.: Energy Build. **127**, 884–891 (2016)
7. Petrichenko, M., Vatin, N., Nemova, D., Kharkov, N., Korsun, A.: Appl. Mech. Mater. **672–674**, 1903–1908 (2014)
8. Petrochenko, M.V., Strelets, K.I., Petrichenko, M.R., Yavtushenko, E.B.: Appl. Mech. Mater. **672–674**, 567–570 (2014)
9. Petrichenko, M., Vatin, N., Nemova, D., Kharkov, N., Staritsyna, A.: Appl. Mech. Mater. **627**, 297–303 (2014)
10. Petrichenko, M., Ostrovaia, A., Statsenko, E.: Appl. Mech. Mater. **725–726**, 87–92 (2015)
11. Vatin, N., Petrichenko, M., Nemova, D.: Appl. Mech. Mater. **633–634**, 1007–1012 (2014)
12. Gumba, Kh., Uvarova, S., Belyaeva, S., Revunova, S.: MATEC Web of Conferences, vol. 106, p. 08023 (2017). <https://doi.org/10.1051/mateconf/201710608023>
13. Vatin, N., Gamayunova, O.: Adv. Mater. Res. **1065–1069**, 2159–2162 (2015)
14. Vatin, N., Gorshkov, A., Nemova, D., Gamayunova, O., Tarasova, D.: Appl. Mech. Mater. **670–671**, 349–354 (2014)
15. Kostenko, V.A., Gafiyatullina, N.M., Semchuk, A.A., Kukolev, M.I.: Mag. Civ. Eng. **68**(8), 18–25 (2016)
16. Jakšić, Ž., Trivunić, M., Adamtsevich, A.: Flexibility and adaptability - key elements of end-user participation in living space designing. In: MATEC Web of Conferences, vol. 106, p. 01001 (2017) <http://doi.org/10.1051/mateconf/201710601001>
17. Barabanshchikov, Y., Muratova, A., Bieliatynskiy, A., Belkina, T.: Mater. Sci. Forum **871**, 9–15 (2016)
18. Vatin, N., Gamayunova, O.: Appl. Mech. Mater. **672–674**, 550–553 (2014)
19. Vatin, N., Gamayunova, O.: Appl. Mech. Mater. **725**, 1493 (2015)
20. Barabanshchikov, Yu., Gutskalov, I.: Adv. Civ. Eng. p. 6562526 (2016)
21. Alihodzic, R., Murgul, V., Vatin, N., Aronova, E., Nikolić, V., Tanić, M., Stanković, D.: Appl. Mech. Mater. **624**, 604–612 (2014)
22. Avdeeva, A., Shlykova, I., Antonova, M., Barabanshchikov, Yu., Belyaeva, S.: MATEC Web of Conferences, vol. 53, p. 01006 (2016)
23. Musorina, T., Olshevskiy, V., Ostrovaia, A., Statsenko, E.: MATEC Web of Conferences, TPACEE, vol. 15, p. 02002 (2016)
24. Barabanshchikov, Yu., Belyaeva, S., Antonova, M., Vasyutina, S.V.: Procedia Eng. **123**, 41–49 (2015)

Measures of Improving the Accuracy of the Calculation of Energy Efficiency and Energy Saving of Construction Transport Infrastructure

Olga Poddaeva¹  , Alexander Kubenin^{1,2} ,
and Dmitry Gribach¹ 

¹ Moscow State University of Civil Engineering,
Yaroslavskoye Sh., 26, 129337 Moscow, Russia
poddaevaoui@gmail.com

² Institute of Mechanics, Moscow State University,
Michurinsky prospect, 1, 119192 Moscow, Russia

Abstract. The paper describes the main approaches to the definition of domestic seepage losses of the building and shown weaknesses in past approaches. On the basis of a comparative analysis of the results of calculations of total infiltration of air through the airport terminal Volgograd known engineering approaches and by using methods of calculating air regime of the building was made a quantitative assessment of how many times the result of engineering approaches overstate.

Keywords: Energy management · Air infiltration · Airy mode of building Construction · Energy efficiency · Infiltration losses

1 Introduction

Energy efficiency - characteristic reflecting the beneficial effects of the ratio of energy use to the cost of energy resources produced in order to obtain such an effect in relation to products, processes, legal entity, individual entrepreneur “as discussed by Malyavina” [1].

Efficient use of energy is one of the main challenges of the XXI century “as discussed elsewhere [2, 3]”. Proper exploitation of resources and the devices that consume energy, new technologies and developments in the energy, technology, energy accounting, construction - all of which are key aspects of energy efficiency. State regulation in the field of rational use of energy resources is one of the priority items leadership of the majority of developed countries. In connection with the annual increase in energy consumption in developing countries there is large-scale energy-saving technologies in order to solve global problems related to the economy, energy and the environment.

Modern apartment building, interacting with the environment, is an energy system which is dependent on the nature of the physical processes occurring in all its elements.

In turn, any physical processes depend on the external climatic factors, the effects of which entails a variety of consequences “as discussed elsewhere [4–6]”.

Thus, it is important to note that the issue of energy saving and energy efficiency must be addressed comprehensively, including interaction with the surrounding environment. It is necessary to carry out a full analysis of thermal engineering and air mode of buildings in different climatic conditions depending on the task. It is important to understand the principle of normalization of heat loss, and therefore lost most of the energy in buildings.

It is important to note the problem of the accuracy of the calculation of energy efficiency and building energy efficiency “as discussed elsewhere [7–9]”. Every year, not only improving the regulatory framework and the documents governing the energy efficiency and energy saving, but also the methodology for calculating energy consumption of the building.

The team of authors engaged in the problems of calculating the air regime of the building, so under the critical eye in an article accepted in national regulations determining the method of seepage losses in the building: are the main disadvantages of this method and the proposed alternatives and calculate infiltration losses.

2 Results

A common approach is the definition of seepage losses in the building:

Calculation of seepage losses reduced to the determination of infiltration air flow entering the premises of the building through leaks building envelope. Immediately it should be noted that air infiltration losses are considered for buildings where indoor acting balanced mechanical ventilation system. In other cases, losses are considered by an imbalance of ventilation flow in each of the rooms of the building “as discussed elsewhere [1, 3]”.

2.1 The Estimated Pressure Difference ΔP

The estimated pressure difference ΔP , Pa, is generally determined by gravity and wind pressure and ventilation work:

$$\Delta p_i = (H - h_i) g (\rho_{out} - \rho_{in}) + 0.5 \rho_{out} v_{out}^2 (c_w - c_l) K_{dyn} - p_{in} \quad (1)$$

Where H - the height of the building from the ground to the top of the cornice or exhaust vents mines (lantern), m; h - the distance from the ground to the top of the windows, doors and openings, or to the middle of the joints of panels, m; $g = 9.81 \text{ m/s}^2$ - acceleration due to gravity; ρ_{out} , ρ_{in} - density of the internal and external air, respectively, kg/m^3 , determined according to the tables or as a function of temperature t by the formula $\rho = 353/(273 + t)$; v - the design wind speed, m/s; K_{dyn} - coefficient taking into account the speed of pressure change in the wind at the height of the building, taken on a set of rules 20.13330.2011 “Loads and effects”;

C_w , C_l - aerodynamic coefficients, respectively, leeward and windward side of the building (accepted $C_w = 0.8$ and $C_l = 0.6$);

p_{in} - nominal pressure in the room, Pa, which is reckoned from the level of the first and second terms of the formula.

2.2 The Overpressure Inside the Building

The value of p_{in} internal pressure may be different for the same oriented rooms one floor due to the fact that the heat loss for each room of the building creates its own value of the internal pressure. Determination of internal pressure in the premises requires payment in full air regime of the building, which is a very time consuming task, so there are simplified methods of appointment of the internal pressure in the premises. The most common approach is that of the internal pressure in the building p_{in} (Pa) taken half the amount of wind and gravity pressure:

$$p_{in} = 0.5H(\rho_{out} - \rho_{in})g + 0.5\frac{\rho_{out}v^2}{2}K_{dyn}(c_w - c_l) \quad (2)$$

Less common approach designed to take into account the uneven arrangement of breathable elements on the facades of the building:

$$p_{in} = 0.5H(\rho_{out} - \rho_{in})g + 0.5\rho_{out}v^2K_{dyn}\frac{(c_w - c_l)A_w + (c_s - c_l)A_s}{A_w + A_s + A_l} \quad (3)$$

where c_s - aerodynamic coefficient on the side facade (accepted $c_s = -0.4$); A_w , A_s , A_l - area of windows and stained-glass windows, respectively, on the windward, leeward and side facades, m^2 . Note that the p_{in} value taken by this method, it turns out different for each facade, considered windward. The difference more pronounced, the greater the differences in density of the stained glass windows and on various fronts. For buildings with a uniform distribution of windows on the facade, this value is close to that obtained by equating the wind pressure to half of the total difference in wind pressure on windward and leeward facades.

To date, the methods presented above there are a number of drawbacks. In this connection, experts of this area are constantly improving it, changing and supplementing regulations, developing new methods for calculating the air mode of buildings.

2.3 Determination of the Total Infiltration Rate ΣG

In determining the cost of heating the outdoor air heating by air infiltration calculation mode buildings can be simplified. The task of engineering calculation is reduced primarily to the determination of the total flow of infiltrating ΣG_i air, kg/h, through individual design reflecting the premises, which depends on the type and nature of the leaks in the outer fence and is determined by the Equation:

$$\Sigma G_i = 0.21\frac{\Sigma p_1^{2/3}}{R_{inf,1}}A_1 + 0.316\frac{\Sigma p_2^{1/2}}{R_{inf,2}}A_2 + \frac{\Sigma p_3^{1/2}}{R_{inf,3}}l_3 \quad (4)$$

Where the designation of index “1” refers to the windows, balcony doors and lamps; index “2” - to the door and open the gate openings; index “3” - to the joints of wall panels (this component is considered only for residential buildings); A- fence area, m²; l₃ - the length of the joints of panels, m; R_{inf} - resistance to air permeability corresponding protections, m² · h/kg for R_{inf,1} and R_{inf,2} or m · h/kg for R_{inf,3}; Δp - pressure drop across the surface of the respective fences on location at the air-permeable element, Pa;

Actual resistance to air permeability r and outer fences are determined by the current SNIP or according to the manufacturer’s organization.

2.4 Consumption of Heat for Heating of Air Infiltration

Consumption of heat for heating infiltrating air Q_{inf}, W is determined by the Equation:

$$Q_{inf} = 0.28 \sum G_i c (t_{in} - t_{out}) \beta \quad (5)$$

where c - mass heat capacity of the outdoor air is equal to 1 kJ/(kg·°C); t_{in}, t_{out} - design temperature of indoor and outdoor air, respectively (t_{out} = t_{out,5}); β - coefficient taking into account the heating of air infiltration in the fence counter heat flow equal to: 0.7 - for the joints of the panels and windows with triple bindings, 0.8 - for windows and balcony doors with separate bindings and 1.0 - for single and windows paired binders; 0.28 - numerical coefficient, resulting in compliance with accepted air flow dimension kg/h, and the heat flow, W (0.28 = 1000/3600).

Methods of determining the rate of infiltration ΣG by formulas 1, 2 and 4 (the procedure number 1), and the subsequent determination of Q_{inf} is a classic in the framework of domestic science (SNIP 41-01-1991 “ Heating, ventilation and air conditioning” and educational publications [1–3]). Determination ΣG by formulas 1, 2 and 4 reflected as well in the SP 50.13330.2012 “SNIP 23-02-2003 Thermal protection of buildings”. Equation [3] does not have experience with in the regulations, but noted in well-known textbooks [1–3]. A major shortcoming of the use of the expression [1] is that the pressure difference ΔP is presented to the windward windows of the facade, however, it is applied simultaneously to all the building facades. Therefore, the assumption that all the facades of the building at the same time accepted windward, and leads to the fact that the infiltration losses through the building obtained overestimated, both on separate premises, and on the whole building.

This deficiency in the definition infiltration building using the expression [1] for the purpose of external pressure will be shown on the example of determination of the terminal building of the airport total infiltration technique operate № 1, method № 2 (using the formulas 1, 3 and 4) and by means of techniques calculate air building mode with a balanced mechanical ventilation implemented as a program on a computer. The technique described in [10–12].

3 Calculations of the Total Air Infiltration Rate for the Airport Terminal Volgograd

3.1 Description of the Object of Study

The airport, located in the city of Volgograd (Fig. 1), relating to the territory of the climatic zone II according to the classification of joint venture “Loads and effects” is “the span structures” [13]. The building is designed and constructed as a rectangular volume terms, the size of which in the axes make 50.0×70.0 m. “The minimum altitude is 13.745 m” [14]. Opposite corner sections of buildings are arranged protruding volumes stairwells. The highest point of the roof in places vertical linkages have a height of 19 m.



Fig. 1. The new airport terminal in Volgograd.

A distinctive feature of the airport is a constructive solution of fronts: the building has glazed facades to 59% of the total area. At the same time the main facade is almost entirely equipped with translucent structures: windows occupied 93% of the total facade area equal to 1158 m^2 . The opposite facade is 86.2% of the glass enclosures (with $S = 1172 \text{ m}^2$). A translucent construction outfitting side facades produced by 57.5 and 0.9% of their areas.

Figure 2 shows a view from the roof of the terminal, the percentage of each of the glass facade and the wind direction, which is given in the calculations. Figure 3 shows a distribution of coefficient of aerodynamic C_p - on the facades of the airport terminal complex.

Total 8 discussed settlement options (see Table 1), all calculations on the above methods are made under the assumptions that the doors of all the terminal buildings are accepted permanently open, that is. $R_{\text{inf},2} = 0$, and no filtration expenses through Non transparent elements of the building envelope. Transparent elements of the building

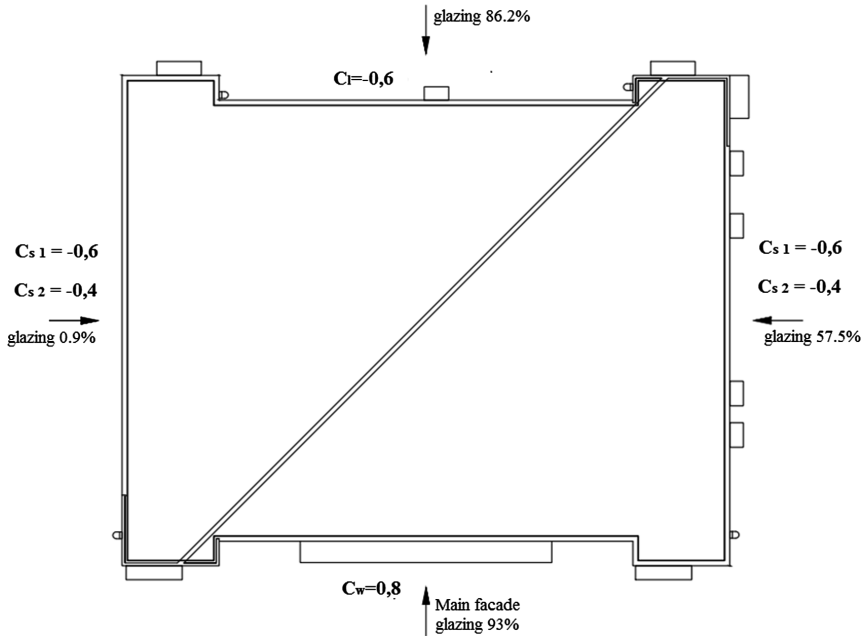


Fig. 2. Top view of the airport of Volgograd.

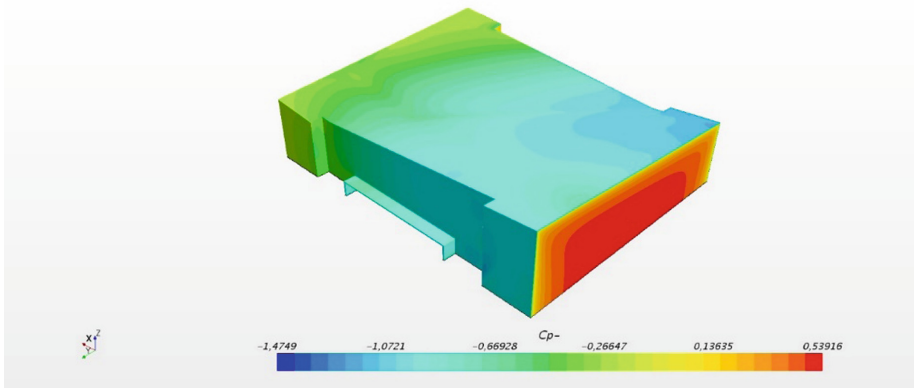


Fig. 3. Distribution of coefficient of aerodynamic C_p - on the facades of the airport terminal complex (90°).

envelope are characterized by the magnitude of the volume of air permeability $L_w = 0.5 \text{ m}^3/(\text{m}^2 \cdot \text{h})$. It uses two wind pressure job scheme by appointing wind pressure coefficient for building facades: the scheme number 1 - $+0.8$ on the windward facade, -0.6 to all others who accepted lee; scheme № 2- $+0.8$ on the windward facade, -0.6 and -0.4 on the leeward side on the facades.

Table 1. Results of the total filtration calculations.

	Option 1	Option 2	Option 3	Option 4	Option 5	Option 6	Option 7	Option 8
V(m/s)	2	10	10	2	2	10	10	2
t _{out} (°C)	-10	-25	-10	-25	-10	-25	-10	-25
Scheme Cp	1	1	1	1	2	2	2	2
ΣG (kg/h)								
Program	-237	-2021	-260	-2229	-228	-1949	-251	-2149
Technique №1	-492	-4210	-543	-4643	-492	-4210	-543	-4643
Technique №2	-549	-4700	-606	-5183	-530	-4539	-586	-5006

4 Conclusions

The predicted results clearly show that the infiltration of the calculations according to the procedures № 1, № 2 give inflated results due to the aforementioned lack of appointment of ΔP on the facades of the building. Oversize results of calculation methods for № 1, № 2 on the entire series of calculations in more than 2 times as compared with the calculation results of the program on a computer. It should be added that this difference would be even greater if the account was made of having the doors to the rooms inside the airport terminal complex. Studies on a simple example reveals flaw in the method of determining the seepage losses common regulatory process. In the light of increasing energy efficiency requirements for buildings and energy saving it is very important to rise and demand for precision engineering approach to the calculation of the loss of the building, including infiltration.

These results reflect the initial stage of research on the subject of seepage losses in building. “As discussed by Parmarth [15]” a global aim is to develop a more accurate method for calculating seepage losses of the building premises and the building as a whole on the basis of a series of air regime building software calculations for the different classifications of buildings and a wide variation of parameters of the outside air breathable environment and elements of the building.

References

1. Malyavina, E.: Heat Loss of the Building: A Handbook. Avoca PRESS (2007)
2. Skanavi, A., Makhov, L.: Heating: Textbook. ASV (2008)
3. Recommendations AVOK: Tool to Calculate the Heat Loss of Premises and Heat Load on the Heating System of Residential and Public Buildings. Avoca PRESS (2012)
4. Herring, H., Sorrel, S., Macmillan, P.: Energy efficiency and sustainable consumption. the rebound effect (2009)
5. Takahashi, L., Noguchi, T.: A new quick response and high efficiency strategy of induction motor. LAS (1985)

6. Hibiki, N., Sueyoshi, T.: DEA sensitive analysis by changing a reference set: regional contribution to Japanese industrial development, *Omega*. *Int. J. Manag. Sci.* **27**, 139–153 (1999)
7. Post, T., Spronk, J.: Performance benchmarking using interactive data envelopment analysis. *Eur. J. Oper. Res.* **115**, 472–487 (1999)
8. Lothgren, M., Tambour, M.: Alternative approaches to estimate returns to scale in DEA-models. In: Working Paper, vol. 90. Stockholm School of Economics (1996)
9. Athanassopoulos, A., Lambroukos, N., Seiford, L.: Data envelopment scenario analysis for setting targets to electricity generation plants. *Eur. J. Oper. Res.* **115**, 413–428 (1999)
10. Kubenin, A.: Study the impact of wind direction on air infiltration through the windows of the building process. *Internet Mag. Naukovedenie* **7**(4), 1–19 (2015)
11. Kubenin, A.: Method for determining the maximum heat consumption for heating infiltrating air through the windows of the building for the entire heating season. *Internet Mag. Naukovedenie* **7**(5), 1–14 (2015)
12. Gagarin, V., Guvernyuk, S., Kubenin, A.: By the method of calculating the effect of the wind effects on the air mode of buildings. In: Proceedings of Higher Educational Institutions, The Technology of the Textile Industry, vol. 4, pp. 234–240 (2016)
13. Fedosova, A., Gribach, Y., Gribach, D.: Numerical simulation of extended structures aerodynamic with high level of responsibility. In: MATEC Web of Conference, vol. 86, p. 05010 (2016)
14. Churin, P., Gribach, Y.: Pilot study of wind and snow impact on the designed airport complex. *Ind. Civ. Eng.* **11**, 24–27 (2016)
15. Gupta, P., Anand, S., Gupta, H.: Developing a roadmap to overcome barriers to energy efficiency in buildings using best-worst multi-criteria decision making methodology. *Sustain. Cities Soc.* **31**, 244–259 (2017)

Choice of Thermal Protection of an Office Building of the Transport Infrastructure by Economic Reasons

Elena Malyavina  and Anastasya Frolova ^(✉) 

Moscow State University of Civil Engineering,
Yaroslavskoye Sh. 26, 129337 Moscow, Russia
privalova-a@mail.ru

Abstract. Administration and office buildings make an important part of the facilities and utilities of airports, river and marine ports, road terminals. Lowering the expenses for their construction and operation is related to a right choice of the building heat protection despite of other factors. Cumulated Discount Expenses (CDE) have been chosen to provide economic estimation of the building heating. The CDE values have been taken for a 10-year limit. The CDE dependence on some factors has been investigated, and their range has been considerably enlarged by comparison with the traditional one. It has been shown, that it is not enough to take into account the capital investments only for the building thermal protection and the heating system operation. The results of the investigation permitted to determine combinations of the heated building geometrical parameters and the cost characteristics of several components of capital and operation expenses, which are reasonable for different types of thermal protection of an office building.

Keywords: Energy management · Price of the heating agent · Heating system Room cooling system · Micro-climate systems · Power medium price Heat price · Electrical power price

1 Introduction

A great interest to the required level of the building thermal protection is manifested all over the world [1–12], especially because of the power consumption for heating and cooling of the buildings, which depends of the heat protection, on the one hand, and the norms and rules of the most countries require the cover of expenditures for a greater thermal protection of the buildings, on the other hand.

By the rule [13, 14], the economic analysis of different types of the building thermal protection is provided by comparison of the expenses required for the heat protection and the heating power to heat the buildings with different thermal protection. The below given investigation provides the economic analysis by comparison of cumulated discount expenses (CDE) in rubles for an all-year-round maintenance of the required micro-climate in the premises at different variants of the building thermal protection.

The given economic comparison of three options of the thermal protection has been made from the point of view of an investor, who is financing the building construction and takes into account the range of the valid market prices for the building heat saving materials, equipments and systems which serve the all-year- round maintenance of a micro-climate in office premises.

2 Initial Data for Calculations

The building dimensions varied from each other by the length and the number of stories. In all cases the building width has been taken equal to 20.2 m by the exterior measuring. All the building end walls have been taken as dead ones (with no windows). Investigation has been made for 3-story (options 1–3) and 12-story (options 4–6) buildings. Glazing of longitudinal walls is given in two options: 0.25; 0.55. The windows are sealed enough to ignore infiltration.

Some characteristics of the building are given in the Table 1.

Table 1. Main geometrical characteristics of the building.

Denomination of the value	The building option					
	1	2	3	4	5	6
Building length, m	20.4	40.8	61.2	20.4	40.8	61.2
Building total area, A , m^2	1 236	2 472	3 709	4 945	9 890	14 835
Area of exterior enclosing structures, B , m^2	1 362	2 252	3 141	4 212	6 533	8 855
Building volume, m^3	4 821	9 643	14 464	19 285	38 571	57 856
Area B to Area A ratio	1.102	0.909	0.847	0.852	0.6605	0.597
Building compactness coefficient	0.283	0.233	0.217	0.218	0.169	0.153

The buildings have office rooms of the same equal dimensions $6.8 \times 10.1 \times 3.9$ (h) m. Four types of premises have been examined: the linear ones on the intermediate floors, the linear ones on the upper floor, the corner ones on the intermediate floors, the corner ones on the upper floor.

The premises have a big deepness (10.1 m), which leads to a considerable variation of heat emissions, which affect the outdoor enclosing structures. For example, the exterior enclosing structures have the total area of 26.5 m in the linear premises on a central floor, and 134.6 m in the corner ones on the upper floor.

Three options of the building thermal protection have been examined being different from each other by the resistance to heat transfer of an outdoor wall and the roof covering. The option 1 provides the resistance to heat transfer of the outdoor walls and the covering near to the normative values required by the sanitary rules according to the formula (5.4) of SP 50.13330.2012 “Heat protection of the buildings”. The option 3 of the heat protection corresponds to the normative rules according to the power consumption (see the Table 3 of the above SP). For the option 2 the resistance to heat transfer of the outdoor walls and coverings has been calculated according to the

formula (5.1) of the above mentioned SP providing a 0.63 reducing coefficient for the walls and 0.8 for the covering as compared with the option 3.

There are the following values of the resistance to heat transfer, $\text{m}^2 \cdot ^\circ\text{C}/\text{W}$, for outdoor enclosing structures, which correspond to the options 1, 2 and 3 of the Moscow normative requirements:

- for walls: 1.254; 1.754; 2.629;
- for coverings: 1.3709; 2.871; 3.621.

The resistance to heat transfer of the windows has been taken equal to $0.54 \text{ m}^2 \cdot ^\circ\text{C}/\text{W}$ for all options.

The heat input to the office rooms has been taken for three levels: 30, 50 and $70 \text{ W}/\text{m}^2$. These values include as well the solar radiation coming through the windows.

A building with a low thermal stability has been taken for the present investigation. All the interior surfaces have a “light” finishing: an AKMIGRAN suspended ceiling, thin plastering of walls and partitions, a kind of carpet on the floor. At the result, the interior thermal resistance is minimal and a slow cooling of a room in the winter season has not been overestimated. The exterior walls have a relatively low through oscillation attenuation of thermal waves because they are made of cellular concrete blocks of $600 \text{ kg}/\text{cu.m}$ density and 200 mm thickness with the thermal protection by mineral wool plates. The covering has been provided on a reinforced concrete slab.

Notwithstanding a permanent temperature of the outdoor air, which has been taken in every individual analysis, the through thermal resistance somehow influences the changes of the indoor temperature during the passage through the enclosing structures.

The analysis has been performed at seven different temperature values of the outdoor air during the year: from the design one for heating needs to the design one for the air conditioning in the warm period of the year. So, all the year was divided into 7 intervals < where the analysis chosen temperatures were the average ones. Duration of the temperature measuring in each interval has been determined according to [15].

To use the existing thermal input more completely in a room in the heating period, it has been decided to maintain the resulting temperature during all working hours from 18 to $24 \text{ }^\circ\text{C}$ (permitted terms according to GOST 30494-2011 Residential and public buildings. Microclimate parameters for indoor enclosures), as well as within $22\text{--}24 \text{ }^\circ\text{C}$ during the working hours in the warm period of the year.

Thermal flows have been chosen in such a way, that to the beginning of the working day it may be possible to enable the room (resulting) temperature equal or slowly higher than the bottom limit of the permitted temperature.

The heating capacity is subject to two restrictions at any temperature of the outdoor air. First, it shall not be more than the heating capacity, which enables the $20 \text{ }^\circ\text{C}$ room temperature during 24 h. Second, the room temperature shall not be lower than $18 \text{ }^\circ\text{C}$ at the beginning of the working day and not higher than $24 \text{ }^\circ\text{C}$ at the end of the working hours.

The cooling flows have been searched for each calculation option individually, and the room temperature within all the day did not exceed $24 \text{ }^\circ\text{C}$.

It is considered, that a central air conditioning system supplies the inflow air with the consumption according to the minimal norm of the outdoor one at the temperature,

which is equal to the required one for the room air. All heat excesses are equalized by fan heat exchangers (fan coils). The room cooling due to an insufficient heating of the inflowing air in the office buildings is excluded.

At first, they are multi-room buildings having premises with different thermal excess all at the same time, and secondly, heat emissions of the office rooms are too high to enable supply the outdoor air in these rooms by commonly used air distribution systems at the minimum adopted norms of the outdoor air consumption. Application of special diffusing devices, which show their effectiveness during a short part of the year, is not reasonable from the financial point of view.

There is a common point of view, that a cooling machine condensers shall be cooled by the 40% solution of ethylene glycol, which circulates by a dry cooler installed in the yard of the building or on its roof. In separate periods of the year the cooling is provided by a machine or free cooling. With all this, the free cooling is understood as application of water in the fan coils after its cooling in a dry cooler.

Attention is called to the fact, that the analysis took into account only the building needs in heating or cooling to enable the design thermal microclimate in premises. Any losses resulting of ineffective operation as well as supplementary power expenses for preparation of the required heat media in heating and cooling systems were not studied. The analysis adopted the free cooling at the outdoor air temperature not more than +5 °C.

3 Investigation Methods

The CDE for T years have been calculated [16, 17] according to the Equation:

$$CDE = C \cdot \left(1 + \frac{p}{100}\right)^T + E \cdot \left[\left(1 + \frac{p}{100}\right)^T - 1\right] \cdot \left(\frac{100}{p}\right), \quad (1)$$

where

- p – the discount norm, %;
- C – capital expenses, rubles, for the appropriate option;
- T – years;
- E – the year operation expenses by options.

The discount norm in this work has been taken according to the refinancing tax of the RF Central Bank $p = 10\%$. Waiting for lowering of this tax, provision has also been made of a 5% discount normative option. In this case the CDE values have been taken within $T = 10$ years, because the cooling equipment durability period is nearly equal to this limit of time. Besides, if the invested money is not recovered within 10 years, the option shall not be considered as a profitable one.

The lump capital expenses C in rubles for each option of the building thermal protection are composed of the price of a supplementary (as compared to the option 1) heat insulation of the exterior enclosing structures C_{ins} in rubles; the price of a heating system C_h , in rubles, as well as free C_{fr} , in rubles, and machine C_m , in rubles, cooling of the rooms, plus the price of connection of the heating and cooling systems to the heat

supplying lines $C_{con,h}$, in rubles, and to the power lines $C_{con,p}$, in rubles, of the Moscow city:

$$C = C_{ins} + (C_h + C_{fr} + C_m) + (C_{con,h} + C_{con,p}) \quad (2)$$

As it follows from (2), the capital expenses come in (1) as an undefined money mass, which does not put any attention to which of the expenses part is dominating: for the building heat insulation C_{ins} , for systems enabling the design microclimate in the building rooms $C_h + C_{fr} + C_m$ for connection to the lines of the power supply companies $C_{con,h} + C_{con,p}$. However, we shall find a link between them beforehand. The power expenses analysis [18] showed, that more is the building heat insulation, less are the heating systems and the price of connection to heating lines. But the price of the cooling systems does not correspond to the above mention. On the contrary, a bigger heat protection, requires the more powerful cooling systems. That's why, to determine the limits of capital expenses K we need to refer every expenses component to the system power unit, which shall be found out during calculation of heating and cooling expenses of each room of the building during the year.

The operation expenses E , in rubles/year, to maintain the building microclimate, are made of the annual heating expenses E_h in rubles/year and the electrical power E_{el} in rubles/year, which has been consumed by heating circulation pumps and the compressor and the pump groups of the cooling system, as well as the depreciation payments to the equipment operation E_{dep} in rubles/year:

$$E = E_h + E_{el,p} + E_{dep} \quad (3)$$

The depreciation payments E_{dep} in rubles/year have been calculated by the Equation [10]:

$$E_{dep} = \frac{1.5 \cdot C}{T_{dep}}, \quad (4)$$

where

- C – capital expenses, rubles, for the appropriate option;
- T_{dep} – the number of the years during which the capital expenses shall be refunded, is taken equal to 10 years.

It is clear, that the potential increase of the additional heat insulation goes up from the option 1 to the option 3, and the price of the equipment and the connection terms to power lines goes down.

However, the prices for each component of the Eq. (2) are taken in some ranges, which make the problem not so easy.

Supplementary expenses for the building heat insulation have been determined by comparison with the heat insulation option 1.

Provision has been made of the most popular heat insulation material with the heat transfer capacity of $0.045 \text{ W}/(\text{m} \cdot ^\circ\text{C})$.

Taking into account the fastening elements, which penetrate through the heat insulation material layer, the analysis has also considered the equivalent heat transfer capacity $0.052 \text{ W}/(\text{m}\cdot^{\circ}\text{C})$.

According to the room location provision shall be made of the following volume, m^3 , of mineral wool plates: in the building with 0.25 glazing – for the rooms of a linear intermediate floor 0.551/1.532; a linear upper floor 6.320/10.186; a corner intermediate floor 1.654/4.565; a corner upper floor 7.423/13.219; in a building with 0.55 glazing – for the room of a linear intermediate floor 0.333/0.926; a linear upper floor 6.102/9.580; a corner intermediate floor 1.436/3.959; a corner upper floor 7.205/12.613 (above the line there is shown the volume of the heat insulation material, m^3 , for the option 2 of the building heat protection, under the line – for the option 3).

The Table 2 gives the volumes of the mineral wool plates, which provide an additional heat protection.

Table 2. Additional volume, m^3 , of mineral wool plates.

Heat protection option	The building option											
	At 0.25 elevation glazing						At 0.55 elevation glazing					
	1	2	3	4	5	6	1	2	3	4	5	6
2	57.8	102.3	146.8	127.2	201.5	275.8	53.8	94.5	135.1	111.5	170.1	228.7
3	115.9	194.9	274.9	307.8	470.0	632.2	105.0	173.6	242.1	264.1	382.7	501.3

The relation between the price of the building heat insulation and the heat transfer capacity of the insulating material has not been taken into account later on, since it depends on many factors. Moreover, the analysis of the heat insulation prices has been made, we have not taken into account the dependence of the heat insulation material thickness on necessary reinforcement of its fixation on the building façade, which leads to the increase of the thermal protection price. After getting the results of an economic comparison, there occurs a possible choice of the price for an exact case.

The price of the thermal insulation of a building has been examined from 9 000 to 22 000 rubles/cu. m. These prices include the price of the heat insulation material, fixtures and the mounting works. The price of the heating system equipment has been taken according to the design cost estimates of really performed civil buildings [19]. The price of the system includes the expenses for all its components: heating devices, stop and regulation valves, pipes, circulation pumps, a screen filter, a heat exchanger, automation facilities. It is referred to the heating capacity of the heating system and is taken within the range from 15 000 to 100 000 rubles/kW. The price of the cooling equipment has also been taken according to cost estimates [20]. It includes the prices of fan coils, pipes, stop and regulation fixtures, a pump group for water circulation by pipes and fan coils through the cooling machine evaporator in case of the machinery cooling, as well as through the heat exchanger in case of the free cooling, a pump group of ethylene glycol circulation through a dry cooler and the cooling machine condenser in case of the machinery cooling, as well as through the heat exchanger in case of the free cooling, a cooling machine, a dry cooler, a heat exchanger, the automation devices. The price of the cooling system has also been reported to the cooling system capacity.

The range of the considered prices goes from 40 000 to 80 000 rubles/kW. The higher price of the cooling equipment is less than the top price of the heating system, because the cooling capacity of a cooling system is more than the heating capacity of a heating system in the office buildings with the design thermal excess. The price of the construction object connection to the heating and power lines has been taken into account. The electrical power for operation of heating circulation pumps, the cooling system pumps and the cooling machine compressor have been also taken into account. In Moscow the price of connection to a heating line makes from 550 to 50 000 rubles/kW, to electrical power lines – from 550 to 100 000 rubles/kW. Such a diversity of prices is explained by the minimal prices and additional expenses, which have been declared by the appropriate legal power companies for connecting facilities and utilities according to the distance to the source and the complexity of the pipeline laying to the construction object.

4 Calculation Results

It is clear, that the higher capital or operation expenses for the building servicing are, the bigger CDE are. But, since all the components of these expenses are subject to changes within different ranges and influence the capital or operation expenses through the power capacity and the annual power consumption, so the influence of the price changes per the resource have a different output to the final CDE value of the building under the same price for the same resource.

To find out the influence of several components of the prices, which are included in the capital and operation expenses, provision has been made for Tables for different buildings, by analogy to the Tables 3 and 4. For data of the Table 3 see [18].

Table 3. Power indices of the building.

Thermal protection option	The system power, kW			Annual power consumption, MW·h				Insulation mineral wool volume, cu. m
	Heating	Machine cooling	Free cooling	Heat	Electrical power	Machine cold	Free cold	
At 30 W/m ² heat emissions								
1	58.0	50.0	2.1	95.7	0.177	21.7	1.4	0
2	47.0	46.0	2.3	58.6	0.143	25.3	1.5	53.8
3	39.0	44.0	3.5	36.0	0.116	28.2	2.1	105.0
At 50 W/m ² heat emissions								
1	58.0	75.0	15.0	62.5	0.177	50.8	17.5	0
2	47.0	71.0	19.0	29.1	0.143	54.4	15.3	53.8
3	39.0	69.0	25.0	12.9	0.116	57.4	27.7	105.0
At 70 W/m ² heat emissions								
1	58.0	98.0	39.0	51.5	0.177	80.2	58.1	0
2	47.0	95.0	43.0	23.4	0.143	83.8	67.2	53.8
3	39.0	94.0	50.0	10.9	0.116	86.8	79.2	105.0

Table 4. Contents of capital and operation expenses of the building.

Thermal protection option	Capital expenses, thous. Rubles per year, for				Operation expenses, thous.rubles per year, for				
	Connection to a heat supply line	Connection to power supply line	The system equipment	The building thermal protection	Heat	Electrical power	Machine cold	Free cold	Depreciation
At 30 W/m ² heat emissions									
1	290 0.0	166 6.7	9814. 8	0	335.1	1.0	42.2	1.1	1472.2
2	235 0.0	153 3.3	8396. 4	1184. 6	205.1	0.8	49.3	1.1	1437.1
3	195 0.0	146 6.7	7444. 3	2310. 0	126.1	0.7	55.0	1.6	14631
At 50 W/m ² heat emissions									
1	290 0.0	250 0.0	11905 .0	0	218.8	1.0	99.1	13.3	1785.8
2	235 0.0	236 6.7	10513 .0	1184. 6	101.8	0.8	106.2	11.6	1754.6
3	195 0.0	230 0.0	9595. 0	2310. 0	45.2	0.7	111.9	210	1785.8
At 70 W/m ² heat emissions									
1	290 0.0	326 6.7	13913 .0	0	180.1	1.0	156.4	44.2	2087.0
2	235 0.0	316 6.7	12601 .0	1184. 6	81.9	0.8	163.5	51.1	2067.8
3	195 0.0	313 3.3	11770 .0	2310. 0	38.2	0.7	169.2	60.2	2112.0

The above Tables show capacities of some systems and the annual power consumption by each of them for a 3-storey building, 20.4 × 20.4 m, with 0.55 glazing. In this case the prices gave been taken very closely to the maximums of the adopted ranges. The price of the insulation material makes 22 000 rubles/cu. m; connection to a heat supply line 50 000 rubles/kW; connection to a power supply line 100 000 rubles/kW; heating systems 100 000 rubles/kW; machine cooling systems 80 000 rubles/kW; free cooling systems 7 000 rubles/kW; heat power 3.5 rubles/kW·h; electrical power 5.68 rubles/kW·h; machinery cold 1.95 rubles/kW·h; free cold 0.76 rubles/kW·h. It shall be mentioned, that the electrical power consumption has been given only for operation of the heating system circulation pumps, and operation of pump groups and the cooling system compressor have been estimated by the cold rate which price results from the appropriate price of the electrical power.

The Table 5 for the same building shows the cumulated discount expenses (CDE), as well as the capital and operation expenses, which have been received according to Tables 3 and 4, the data of which permitted to calculate the CDE. The Table 5 shows that in a 20.4 × 20.4 m 3-storey building with 0.55 glazing of the façade it is reasonable to provide a thermal protection according to the option 3, i.e. according to the Rules SP 50.13330.2012. In 40.8 × 20.4 m and 61.2 × 20.4 m it is reasonable to provide a thermal protection according to the option 2. Such a ranging of capital and operation expenses has been got due to the change of some expense components because of the heat insulation bigness. When the operation expenses are subject to bigger thermal protection, the price of the heating and electrical power go down, and the machine and free cold, as well as the depreciation expenses grow up.

Table 5. Cost estimates of the building thermal protection options.

Thermal protection option	Length of the building 20.4 m			Length of the building 40.8 m			Length of the building 61.2 m		
	<i>C</i> <i>DE</i> ml n. rub les	<i>C</i> , thous. rubles	<i>E</i> , thous.rub les/year	<i>CDE</i> mln.r ubles	<i>C</i> , thous. rubles	<i>E</i> , thous.rub les/year	<i>CDE</i> mln.r ubles	<i>C</i> , thous. rubles	<i>E</i> , thous.rub les/year
At 30 W/m ² heat emissions									
1	66.8	14 381.5	1 851.6	115.2	24 984.4	3 160.3	163.3	35 520.1	4 462.6
2	61.9	13 464.3	1 693.5	109.77	24 080.4	2 967.4	157.4	34 648.4	4 238.5
3	60.4	13 171.0	1 646.4	109.81	24 102.4	2 968.3	159.1	35 010.4	4 285.3
At 50 W/m ² heat emissions									
1	78.6	17 305.0	2 117.9	139.8	30 773.6	3 761.9	200.8	44 224.5	5 404.8
2	74.1	16 414.3	1 975.0	135.1	29 915.3	3 606.6	196.0	43 244.2	5 334.9
3	73.2	16 155.0	1 964.5	136.1	29 989.9	3 656.7	199.0	43 848.2	5 349.8
At 70 W/m ² heat emissions									
1	91.4	20 079.7	2 468.6	166.8	36 572.1	4 516.4	242.0	53 000.0	6 558.2
2	87.8	19 302.3	2 365.1	163.4	35 868.1	4 415.0	238.7	52 349.8	6 456.4
3	87.6	19 163.3	2 380.2	164.7	35 941.7	4 484.6	242.0	52 777.0	65 95.0

A bigger thermal protection leads to the increase of the capital expenses due to connections to heating and electrical power lines, the price of heating and cooling systems goes down and the price of the heat insulation goes up.

The analysis showed, that in a 12-storey building with 0.55 glazing and under the same conditions, the profitable thermal protection options coincide with the thermal protection options of a 3 storey building with 0.55 glazing. For the buildings of the same shape but with 0.25 facade glazing it is reasonable to provide the thermal protection according to the option 3.

It shall be mentioned, that calculations with the traditional account only of the price of the heating material and the thermal power for all options showed the expediency of the thermal protection according to the option 1. However, the Rules SP 50.13.330.2012 prescribes the options 3 and 2 for most of the buildings.

For CDE change plot of a 20.4×20.4 m 3-storey building with 0.25 glazing of the façade see Fig. 1 where the data have been got by calculations according to the above given methods. The maximal and the minimal prices of each resource have been taken into account.

The plots show, that at the maximum prices for everything the price change for the most part of the resources does not avoid the advisability of the thermal protection according to the option 3 (the basic thermal insulation according to the Rules SP 50.13330.2012). However, there are some exceptions. When the prices of the given range for the heating and machinery and here cooling are minimum, the option 1 of the thermal protection becomes the most profitable one. (according to sanitary norms). If the price of the heating system makes 30 000 rubles/kW, the system of machine cooling is 50 000 rubles/kW, the system of free cooling makes 2 500 rubles/kW, the thermal protection according to the option 2 reveals to be the most profitable of all (a smaller thermal protection by comparison to the option 3). When the price of the systems is high, it is reasonable to provide the thermal protection according to the option 3. At the maximum prices for everything and any cost of the building thermal protection, as well as at any cost of the electrical and heating power, any price of connection to power and heat supply lines, the most reasonable is the option 3 of heat insulation.

At the minimal prices for everything, the option 1 is profitable at any costs of the building thermal protection. Besides, it is profitable at any price of the electrical power for the buildings with the heat excess of 50 and 70 W/m². The option 2 of the thermal protection is profitable at the price of the electrical power for a building with 30 W/m² heat excess.

At any price of connection to electrical power lines the option 1 is profitable for a building with 70 W/m² heat gain and the option 2 is profitable at 30 and 50 W/m². At the minimal price of connection to the heat supply lines the option 2 is profitable for a building with 30 W/m² heat emissions and the option 1 is profitable at the emissions of 50 and 70 W/m². When the price of connection to the heat supply lines is higher than 20 000 rubles/kW, the option 3 is profitable at any heat input. In all other cases of the price of the thermal power and the heat emissions in the buildings, the thermal protection shall be provided according to the option 2. The option 1 of the thermal protection is profitable at the minimal cost of the heating systems, machine and free cooling. If the price of the heating systems makes 30 000 rubles/kW, of the machine cooling 50 000 rubles/kW and of the free cooling 2 500 rubles/kW and higher, it is reasonable to provide a thermal protection according to the option 3.

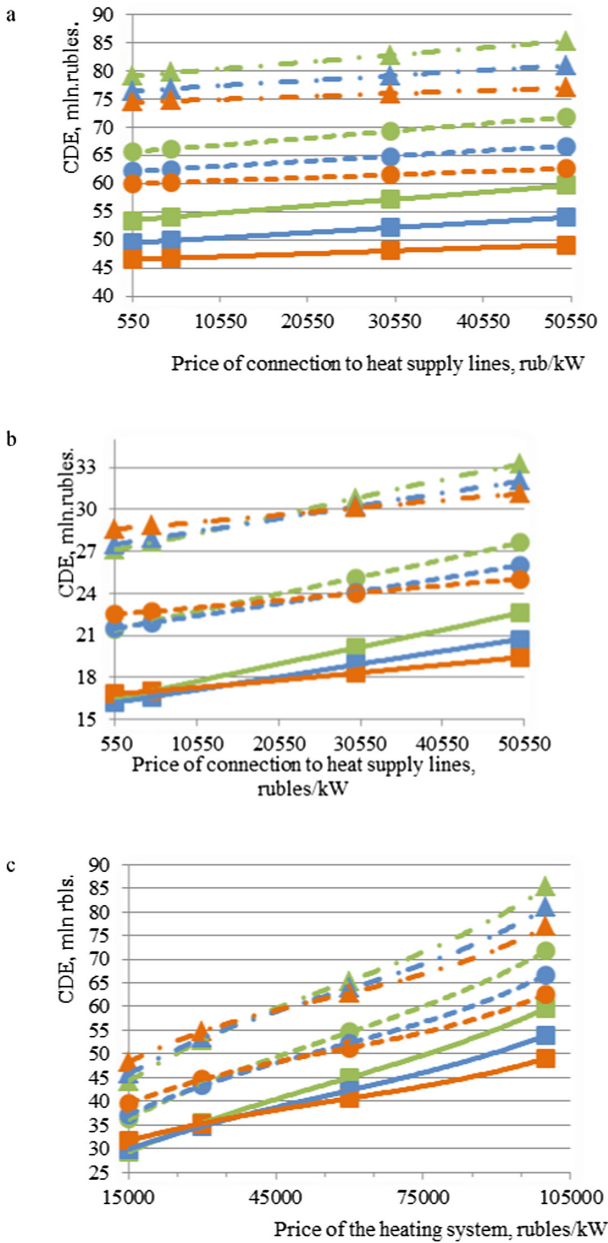


Fig. 1. CDE change at $p = 10\%$ for a 20.4×20.4 m 3-storey building with 0.25 glazing of the façade in dependence of (a) the price of connection to heat supply lines if the cost of each resource is maximal; (b) the same at the minimal price of each resource; (c) the price of the heating system, if the price of each resource is maximal; (d) ditto, if the price of each resource is minimal; (e) the thermal protection price, if the price of each resource is maximal; (f) ditto, if the price of each resource is minimal.

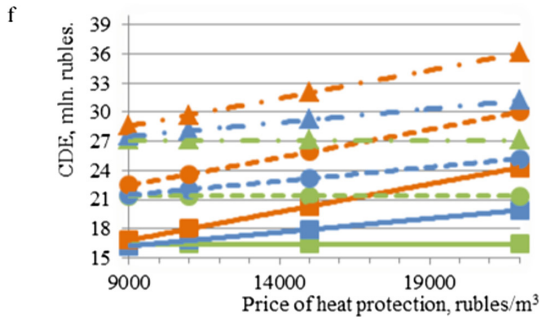
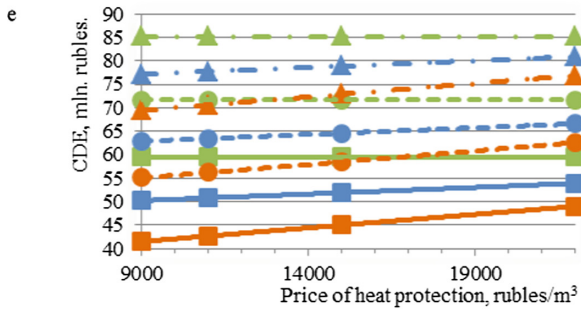
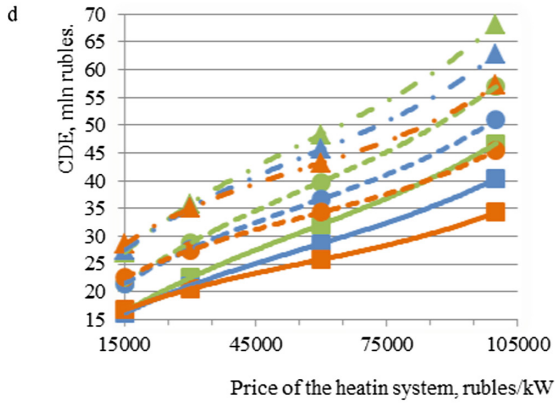




















Fig. 1. (continued)

Symbols:

-  ,  - option 1 of thermal protection, heat gain in the room is 30 W/m²;
-  ,  - option 2 of thermal protection, heat gain in the room is 30 W/m²;
-  ,  - option 3 of thermal protection, heat gain in the room is 30 W/m²;
-  ,  - option 1 of thermal protection, heat gain in the room is 50 W/m²;
-  ,  - option 2 of thermal protection, heat gain in the room is 50 W/m²;
-  ,  - option 3 of thermal protection, heat gain in the room is 50 W/m²;
-  ,  - option 1 of thermal protection, heat gain in the room is 70 W/m²;

-  ,  - option 2 of thermal protection, heat gain in the room is 70 W/m²;
-  ,  - option 3 of thermal protection, heat gain in the room is 70 W/m².

5 Conclusions

The above said makes it clear, that it is not, at least, correct to find out an economically profitable option of the thermal protection for the buildings where the required microclimate parameters are maintained all over the year. All components of capital and operation expenses shall be taken into account.

The analysis of cumulated discount expenses for maintenance of the design microclimate in office premises with the heat gain of 30, 50, 70 W/m² showed, that any increase of the thermal input into the rooms is aimed at reducing the thermal protection. First of all, because in the heating season the inner heat input covers a part of the heat losses, so the major part of the year requires an expensive cooling. Secondly, since the cooling is needed when the outdoor air temperature is lower than the interior one, the higher thermal protection leads to the increased cooling load. That is why, in the buildings with a greater glazing the windows help “to reject” a part of the heating load to cooling.

Since small dimensions of the building by length and by width, notwithstanding the number of floors, leads to the increase of the enclosing structure area per 1 m² of the building total area, and then to a bigger power consumption to maintain the microclimate in summer and in winter, these buildings require a thermal protection according to the option 3 (following the basic requirements of the Rules SP 50.13 330.2012).

When capital and operation expenses approach the top limit of the examined price rates by separate components, the most part of the office buildings shall be provided with the thermal protection according to the sanitary norms for economic reasons, since correlation of the prices of the equipment and power media in RF is such, that the cheap power media cannot be profitable, if insulating materials, equipments and connections to the power lines remain expensive.

References

1. Hong, T., Yang, L., Hill, D.: Data and analytics to inform energy retrofit of high performance buildings. *Appl. Energy* **126**, 90–106 (2014)
2. Orr, H., Wang, J., Fetsch, D., Dumont, R.: Technical note: air tightness of older-generation energy-efficient houses in Saskatoon. *J. Build. Phys.* **36**, 294–307 (2013)
3. D’Orazio, M., Perna, C., Giuseppe, E., Morodo, M.: Thermal performance of an insulated roof with reflective insulation: field tests under hot climatic conditions. *J. Build. Phys.* **36**, 229–246 (2013)
4. Asadi, S., Hassan, M., Beheshti, A.: Performance evaluation of an attic radiant barrier system using three-dimensional transient finite element method. *J. Build. Phys.* **36**, 247–264 (2013)
5. Cheng, Y., Nin, J., Gao, N.: Thermal comfort models: a review and numerical investigation. *Build. Environ.* **47**, 13–22 (2012)
6. Fokaides, P., Kalogirou, S.: Application of infrared thermography for the determination of the overall heat transfer coefficient (U-Value) in building envelopes. *Appl. Energy* **88**, 4358–4365 (2011)
7. Dall’O’, L., Galante, A., Pasetti, G.: Comparison between predicted and actual energy performance for winter heating in high-performance residential buildings in the Lombardy region (Italy). *Energy Build.* **47**, 247–253 (2012)
8. Simões, I., Simões, N., Tadeu, A.: Laboratory assessment of thermal transmittance of homogeneous building elements using infrared thermography (2016). <http://dx.doi.org/10.21611/qirt.2014.081>
9. Alajmi, A.: Energy audit of an educational building in a hot summer climate. *Energy Build.* **47**, 122–130 (2012)
10. Saelens, D., Parys, W., Baetens, R.: Energy and comfort performance of thermally activated building systems including occupant behavior. *Build. Environ.* **46**, 835–848 (2011)
11. Tenpieric, M., Van der Spoel, W., Cauberg, H.: An analytical model for calculating thermal bridge effects in high performance building enclosure. *J. Build. Phys.* **31**, 361–387 (2008)
12. Hoes, P., Hensen, J., Loomans, M.: User behavior in whole building simulation. *Energy Build.* **41**, 295–302 (2009)
13. Petrov, P., Sherstobitov, M., Rezanov, E., Vedruchenko, V.: Methods of effective calculations of the thermal protection of the outdoor enclosing structures of the building walls during the capital repair works. *Sci. Bull. Omsk* **6**(150), 109–113 (2016)
14. Psarov, S., Shumilin, E., Zaretskaya, M.: Cover of expenditures of power saving measures in the heat consuming systems of the buildings. *TOGU Inst. Notes* **4**, 1628–1633 (2013)
15. Construction Climatology: Reference Book to SnIP 23-01-99*/red. In: Savin, V.Sc. (ed.) Research Institute of the Construction Physics of RAASN, Moscow (2006)
16. Samarin, O.: Questions of Economics for the Microclimate of the Buildings. Edition of Association of construction High Schools, Moscow (2011)
17. Osipova, N., Zakharina, K.: To determination of the refunding measures to increase the thermal protection of the exterior walls of the buildings. *Pow. Eff. Resour. Technol. Reg. Constr. Complex* **1**, 128–129 (2011)
18. Malyavina, E., Frolova, A.: Analysis of the year power consumption for heating and cooling of an office building. *AVOK* **1**, 18–23 (2017)
19. Frolova, A., Savina, A., Astanina, O., Barbarova, A.: Analysis of average cost parameters of a heating system. *Success Mod. Sci. Educ.* **12**(5), 62–64 (2016)
20. Malyavina, E., Frolova, A.: Economic comparison of the variants of the transfer to free cooling of the rooms with air conditioning. *High Sch. Bull. Constr.* **4**, 78–83 (2013)

The Study of Flat Convective Stream Formed by Use of Recessed Floor Convection Heaters with Natural Air Circulation in High Height Rooms with Continuous Glassing

Viktor Pukhkal^(✉) 

Saint Petersburg State University of Architecture and Civil Engineering,
Vtoraja Krasnoarmejskaja str., 4, St. Petersburg 190005, Russia
pvalllll@rambler.ru

Abstract. Convection heaters built into a floor prevent descending cold airflow from vertical translucent structures from entering serviced room zone. The study assumes a convection heater with natural air circulation installed near a glassing. Convection heater's length is equal to glassing's length. The height of a room is assumed to be typical for public buildings and is equal to 6 m. Convection heater's heat flow is equal to heat loss through glassing. The computational model is developed and recessed floor convection heater's operation simulation in "ANSYS Fluent 14.5" software package with different distances from a glassing to a convection heater is produced. Studies are carried out for "long" heat source given that convection heater's finned section length is equal to glassing's length. Temperature and velocity fields in the room are calculated. Room's natural convective streams (descending cold airflow near the glassing and ascending warm airflow from the convection heater) are described. The conditions for use of recessed floor convection heaters with natural air circulation are determined. It is recommended that the convection heater should be installed no further than 300 mm from the glassing (distance of 200 mm is optimal). Under such conditions warm airflow adheres to the glassing and uniform temperature field in room's volume is established.

Keywords: Heating · Recessed floor convection heater · Natural convection

1 Introduction

Descending cold air streams entering serviced room zone are produced near glass light apertures. One of the solutions preventing cold air influx is an installation of heat appliance under light aperture — convection heater with natural air circulation build into the floor (recessed floor convection heater) [1–7].

In [2] the simulation of airflows and temperature fields in a room's volume was performed when convection heater with natural convection is installed. The convection heater installed could be deemed as "short" heat source — finned section of convection heater length was related to room's length per each convection heater (heat source)

l_{rel} — as 0.5. Additionally glassing's length was related to room's length also as 0.5 and room's height was 2.6 m. However public buildings frequently use glassing that fill continuously whole width of the room and room's height could be up to 6 m (high height). In that case convection heaters are placed throughout the width of the room (glassing). When exiting from convection heater air is heated and a flat convective stream is formed which adheres on a barrier.

The study's goal is to obtain qualitative characteristics of convective airflows development near the glassing that fill continuously whole width and height of the room in relation to a distance between the glassing and natural air circulation convection heater [8–10].

2 Methods

The simulation of convection heater's operation is performed in “ANSYS Fluent 14.5” software package to study distribution of velocity and temperature fields in the room.

A model room is specified to have following dimensions: width — 6 m; depth — 6 m; height — 6 m (see **Ошибка! Источник ссылки не найден.**1). Glassing's dimensions are 6×6 m. The convection heater is installed at a distance l , mm, from the glassing. That distance varies from 0 to 2000 mm (Fig. 1).

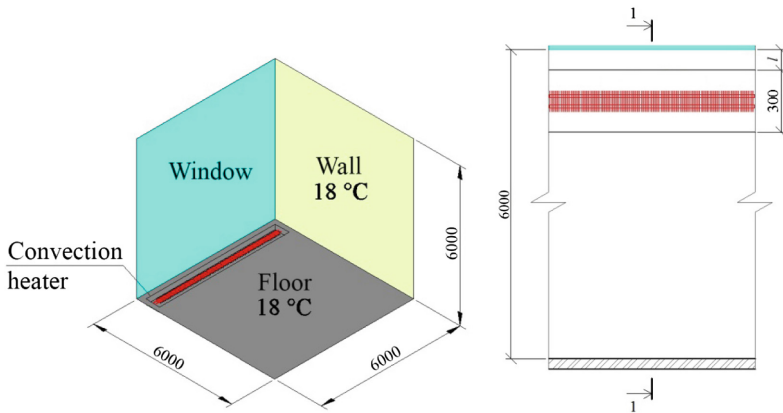


Fig. 1. Room's computational diagram.

The following conditions were specified during simulation:

- inside surfaces temperature (side walls, floor, ceiling) - plus 18 °C;
- outside air temperature - minus 24 °C;
- glassing's outside surface heat-transfer coefficient - 23 W/(m²·K);

- glassing's inside surface heat-transfer coefficient - $8 \text{ W}/(\text{m}^2 \cdot \text{K})$;
- glassing's average heat-transfer resistance - $0.685 \text{ (m}^2 \cdot \text{K)/W}$;
- heating element's surface temperature - $64.5 \text{ }^\circ\text{C}$;
- convection heater's heating element position - in the middle of a casing.

Convection heater's heat flow is equal to heat loss through room's glassing.

3 Results

Heated convective stream exiting recessed floor convection heater, installed near the glassing, diverges from a vertical line and reaching the glassing adheres to it and develops as half-restricted stream.

Stream's deviation is determined by pressure difference between air on both sides of the stream. Ejecting air the stream produces less pressure in the part of the room with smaller volume, i.e. near the glassing (see **Ошибка! Источник ссылки не найден.2**) (Fig. 2).

After the simulation velocity (see **Ошибка! Источник ссылки не найден.2**) and temperature fields in the room were obtained under variable distance between the glassing and the convection heater (l , mm). These calculations allow estimating a nature of an interaction of descending airflow near the glassing and ascending airflow from the convection heater under assumed equality of convection heater's heat flow to heat loss through the glassing.

At a distance $l \leq 300 \text{ mm}$ warm airflow adheres to the glassing. At a distance $l \geq 400$ convective stream over heat source at first adheres to a barrier, then the stream separates and one or multiple cold air closed circulation zones are produced near the glassing. When the convection heater is placed at a distance of 2000 mm from the glassing, descending airflow near a glassing is produced which adheres on floor's surface and enters serviced room zone (see **Ошибка! Источник ссылки не найден.3-4**) (Figs. 3 and 4).

At a distance between the glassing and the convection heater of 200 mm the uniform temperature distribution in room's volume is established (see **Ошибка! Источник ссылки не найден.5**) (Fig. 5).

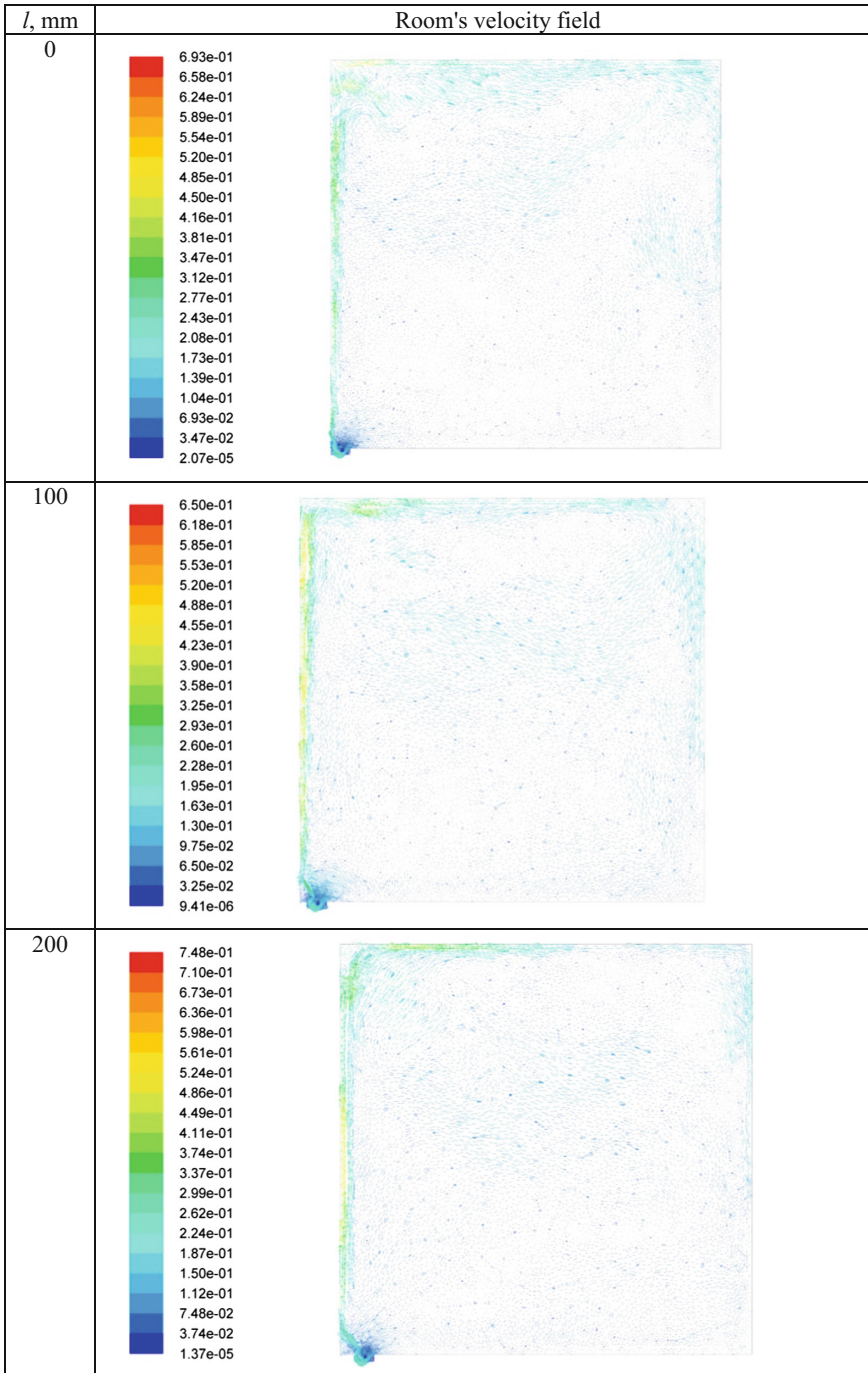


Fig. 2. Room's velocity field simulation result.

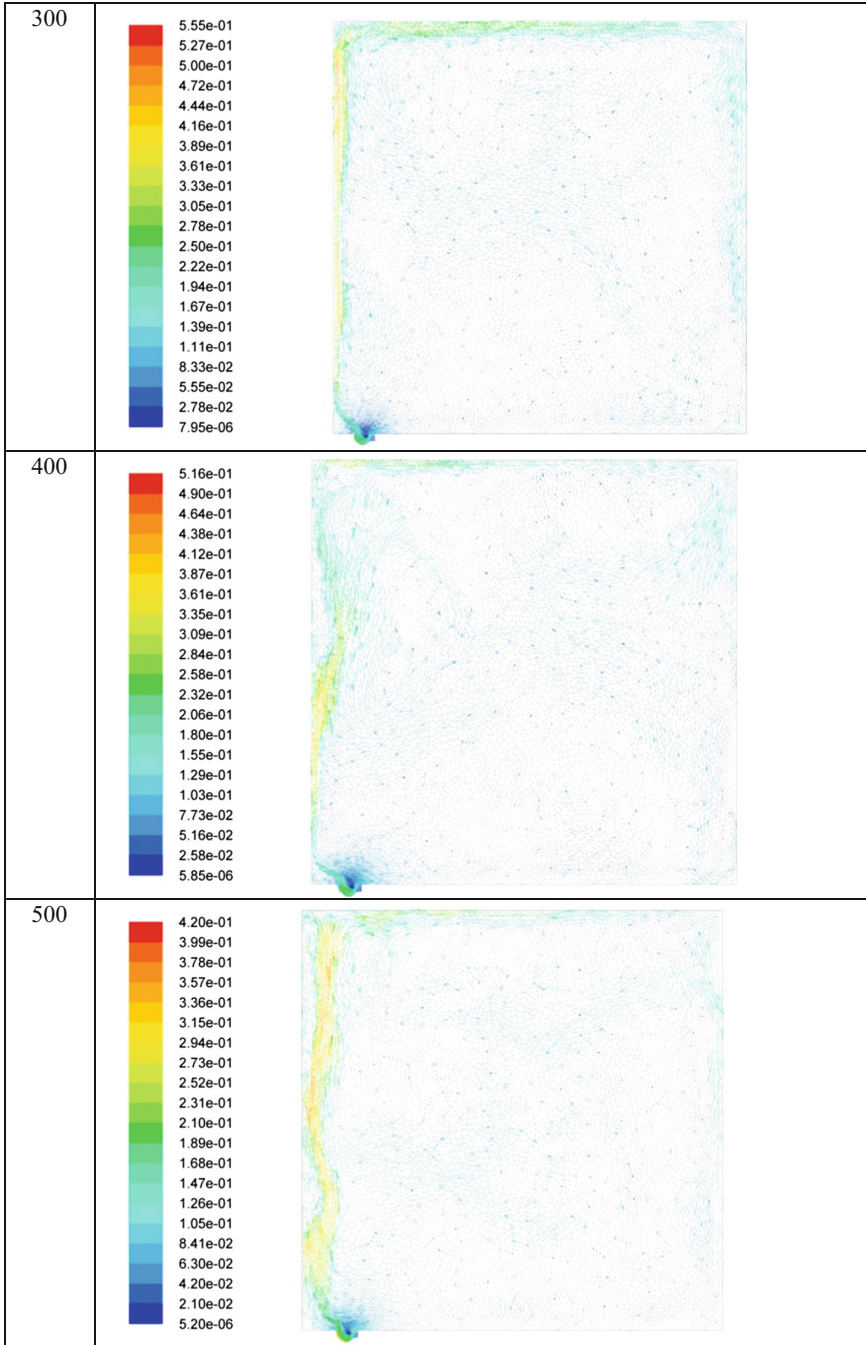


Fig. 2. (continued)

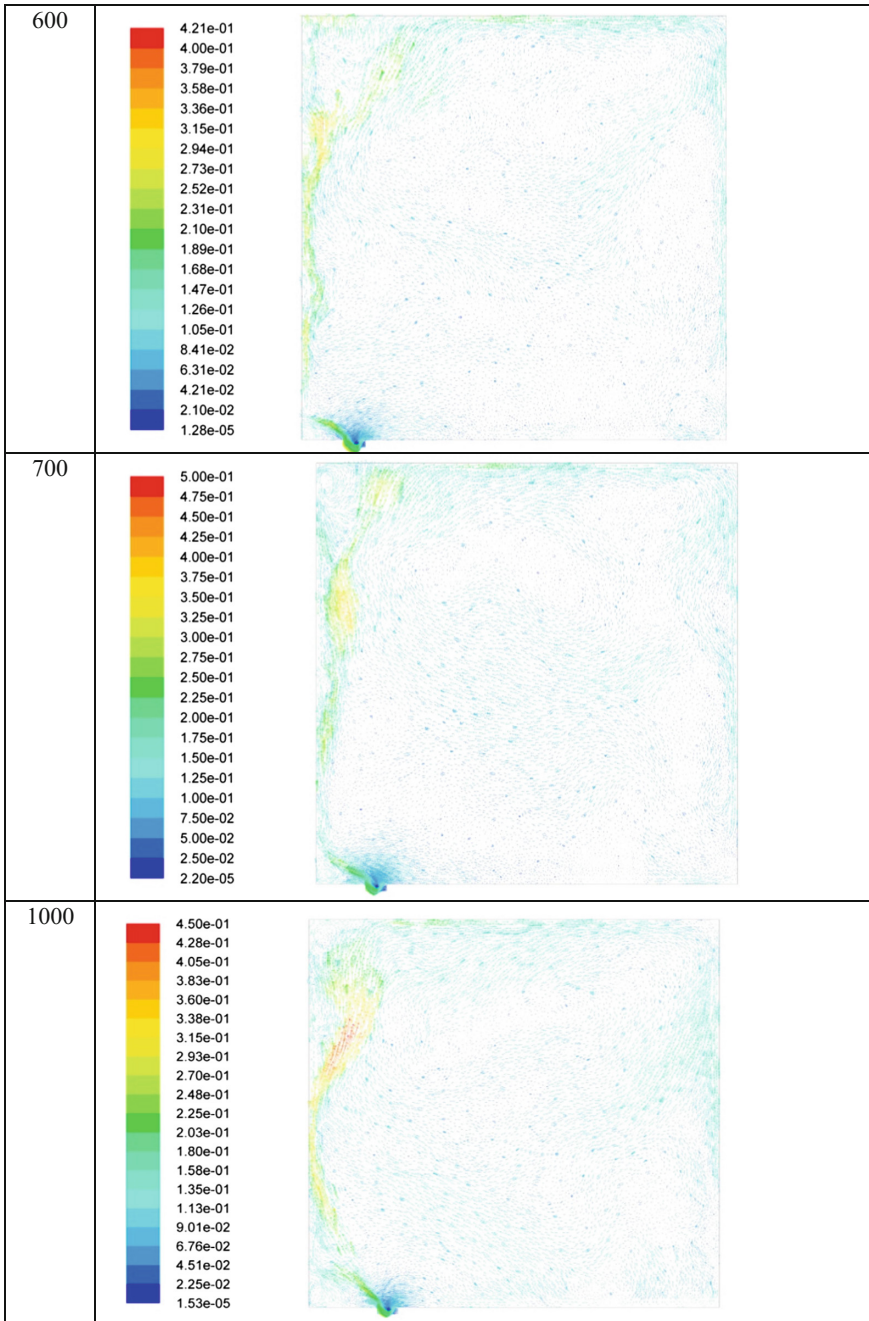


Fig. 2. (continued)

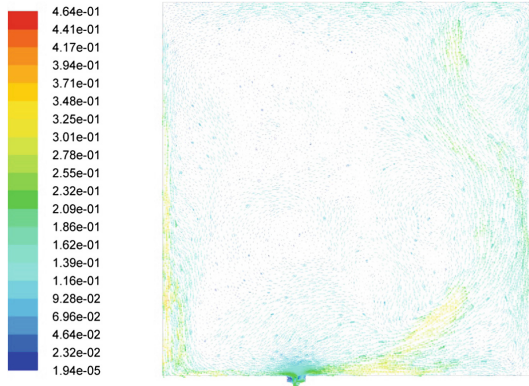


Fig. 3. Room's velocity field simulation results (distance $l = 2000$ mm). For the whole of premise

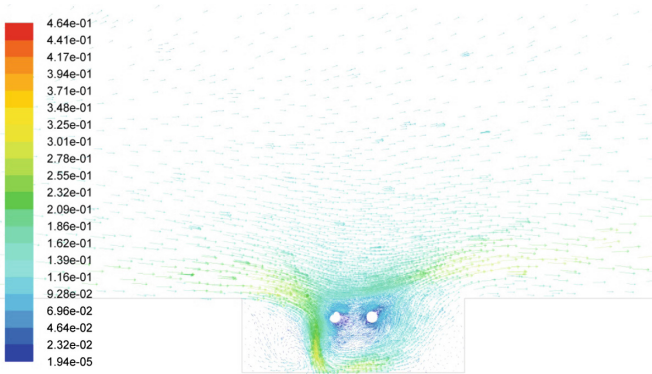


Fig. 4. Room's velocity field simulation results (distance $l = 2000$ mm).

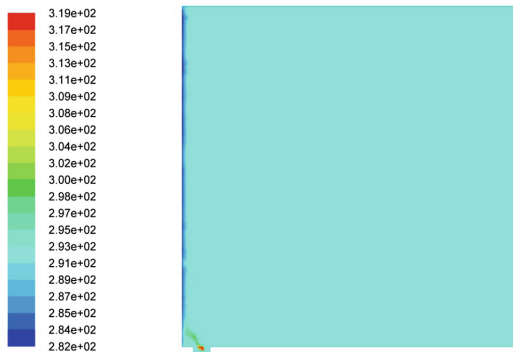


Fig. 5. Room's temperature field simulation results (distance $l = 200$ mm).

4 Conclusions

The recessed floor convection heaters with natural air circulation installed throughout the glassing's length could be used to prevent descending cold airflow from vertical translucent structures from entering serviced room zone in rooms with continuous glassing of a façade (usually in public buildings).





Recessed floor convection heaters which have heat flow equal to heat loss through the glassing and installed no further than 300 mm from the glassing create convective stream adhering to the glassing and protecting the room from descending cold airflow.

Unified temperature field in room's volume is established when the convection heater is installed at 200 mm distance from glassing's surface.

References

1. Babiak, J., Olesen Bjarne, W., Petráš, D.: Low temperature heating and high temperature cooling embedded. In: Water Based Surface Heating and Cooling Systems. REHVA (2013)
2. Bašta, J., Legner, T.: Analýza podlahového otopného tělesa. ČVUT v Praze (2017). <http://elvl.cz/onas/pdf/clanek-16.pdf>. Accessed 08 Sept 2017
3. Boriskina, I.: Zdaniya i sooruzheniya so svetoprozrachnymi fasadami i krovlyami. Teoreticheskie osnovy proektirovaniya svetoprozrachnykh konstruksii [Buildings and structures with translucent facades and roofings. Theoretical basis of translucent structures design]. Inzhenerno-informatsionnyi Tsentr Okonnykh Sistem, Saint Petersburg, RF (2012). (in Russian)
4. Krupnov, B., Krupnov, D.: Otopitel'nye pribory, proizvodimye v Rossii i blizhnem zarubezh'e [Heating devices made in Russia and CIS countries] Izdatel'stvo Assotsiatsii stroitel'nykh vuzov, Moscow (2010). (in Russian)
5. Mayorov, V.: Peredacha teploty cherez okna [Heat transfer through windows]. Izdatel'stvo ASV, Moscow (2014). (in Russia)
6. Makhov, L.: Otoplenie [Heating]. Izdatel'stvo Assotsiatsii stroitel'nykh vuzov, Moscow (2014). (in Russia)
7. Muller, M., Frana, K., Kotek, M., Dancova, P.: The influence of the wall temperature on the flow from the floor convector (experimental results). In: EPJ Web of Conferences, vol. 45 (2013). <https://doi.org/10.1051/epjconf/20134501130>, https://www.epj-conferences.org/articles/epjconf/pdf/2013/06/epjconf_efm2013_01130.pdf. Accessed 08 Sept 2017
8. Zakharevich, A.: Peculiar features of microclimate formation in heated rooms. In: ENERGETIKA, Proceedings of CIS Higher Education Institutions and Power Engineering Associations, vol. 5, pp. 73–85 (2009)
9. Zakharevich, A.: The influence of height of continuous glazing in external walling on indoor climate parameters formation. In: 5th International Scientific and Technical Forum, Theoretical Foundations of Heat and Gas Supply and Ventilation, pp. 95–101. MGSU (2013)
10. Jakšić, Ž., Trivunić, M., Adamtsevich, A.: Flexibility and adaptability - key elements of end-user participation in living space designing. In: MATEC Web of Conferences, vol. 106, p. 01001 (2017). <https://doi.org/10.1051/mateconf/201710601001>

Problems of Energy Efficiency When Design of Construction Objects for Transport Infrastructure

Ekaterina Fomina¹ , Natalia Kozhukhova¹ , Alexander Fomin¹ ,
and Elena Voitovich² 

¹ Belgorod State Technological University named after V.G. Shoukhov,
Kostukova Street, 46, Belgorod 308012, Russia
fomina.katerina@mail.ru

² Moscow State University of Civil Engineering,
Yaroslavskoye Sh., 26, Moscow 129337, Russia
e.voitovich@mail.ru

Abstract. The main task of this work is focused on providing of energy efficiency by correction of requirements to heat- and sound-insulation of autoclave cellular concrete and development of special purpose materials. The high-effective technological solution is proposed. It is based on application of high-reactive aluminosilicate components in cellular concrete to improve porous structure. Using a scanning electron microscopy (SEM), gas adsorption method (BET) the analysis of cellular material microstructure at macro- and micro-level is accomplished; criteria of optimal porosity formation taking into account amount, size and shape of pores as well as density of interpore partition are determined. According to refined parameters and experimental data the relationship between the concrete structure and its resistance to sorption capacity and vapor permeability when surround humidity variation in range of 80–97% are determined. Also reducing of heat-conductivity coefficient for the concrete is observed. It allows construction of stored buildings such as garages as well as light maintenance of vehicle without additional winterization. Generally, on the base of the data obtained in this work the developed autoclave cellular concrete is energy-effective and rational material when design, modernization and service of construction objects of transport infrastructure.

Keywords: Transport buildings and structures · Autoclave cellular concrete
Energy efficiency · Heat conductivity · Sound insulation · Ecology

1 Introduction

One of the priority areas of update development of global economy is enhancement of energy efficiency of construction materials that is very important for construction objects oriented on technical and management activity. When design, development, modernization and service of objects from transport infrastructure the main factor is improving of performance characteristics of buildings by its weight and material consumption reducing as well as providing the required heat and sound insulating

properties to formation the optimal microclimate for a human and provides a good health and working efficiency [1–5].

Taking into account hard requirements to energy saving and building heat insulation as well as severization of requirements to microclimate quality in operational building, the optimal solution for construction of transport infrastructure objects is production of autoclave cellular concrete [6]. At present time autoclave cellular concrete approve oneself as polyfunctional construction material, produced with environmentally friendly technology and is associated to material for «green» construction [7–9]. Significant technical and economical advantages of autoclave cellular concrete application when construction of objects for transport field can be associated with unique combination of sound-insulating properties of its constituents. Controlled variation of sound insulating properties of cellular concrete is possible by optimizing of the following structure parameters: homogeneous pore distribution in bulk of material, thickness and density of interpore partition, inner surface morphology and shape of pore [10, 11].

Also, genetic features of raw materials consisting of the cellular composite are significant [12]. According to earlier studies the growing number of small pores (up to 1 μm) as well homogeneous distribution of differently-sized pores by the composite volume allows enhancement acoustic characteristics [13, 14]. However, current commercial materials don't meet requirements of present standards. For example, when autoclave cellular concrete production it is difficult to provide required porosity and strength characteristics. In this connection, taking into account service conditions in transport infrastructure the introduction of new projects oriented on quality enhancement of sound insulating characteristics is actual.

In earlier studies the application efficiency of aluminosilicate rocks in autoclave cellular concrete is established. Commercially competitive product was obtained due to density reducing by 20% and structure strength improving by 35% [15–17].

In this work the assessment of efficiency of proposed cellular concrete concerning heat and sound insulating parameters is accomplished. This parameter is important when design, reconstruction and repairing of transport infrastructure objects and expanding the application area for innovative construction materials.

2 Methods

The samples of cellular concrete are moulded in form of cubes of $100 \times 100 \times 100$ mm. Autoclave curing is realized at 183 °C by following regime: autoclave blowdown – 40 min; buildup of vapor pressure up to 10 atm – 1 h; holding at 10 atm – 5 h; bulddown of vapor pressure – 2 h. The sample microstructure is studied with high-resolution scanning electron microscope Hitachi-800. Porosity of cellular concrete at micro-level is measured with gas adsorbtion method by SoftSorbi-II ver.1.0.

Heat conductivity is realized with equipment ITP-MG4 «Zond» (Stroypribor) by cylindrical probe method [18]. Vapor permeability and sorption humidity of epy material are determined according to standard procedures [19, 20]. Frequency of sound insulation measurement with interference spectroscopy is accomplished [21].

3 Results

As reference composition the cellular concrete D500 with compressive strength up to grade of B2.5 (AAC) is used [22].

As experimental composition the cellular concrete containing 15% of aluminosilicate (perlite) instead of quartz sand (AACAl) is applied [17]. That allows reducing the final composite density by 22.5% and increasing of compressive strength by 31%.

Microstructure analysis presented in Fig. 1, demonstrates the differences between the developed concrete (AACAl) and traditional one (AAC) as well as formation a lot of close and homogeneously distributed differently-sized pores. The sample structure consists of expanded pores as well as dominant content of micropores with size of 0.3–0.9 mm (Fig. 1b).

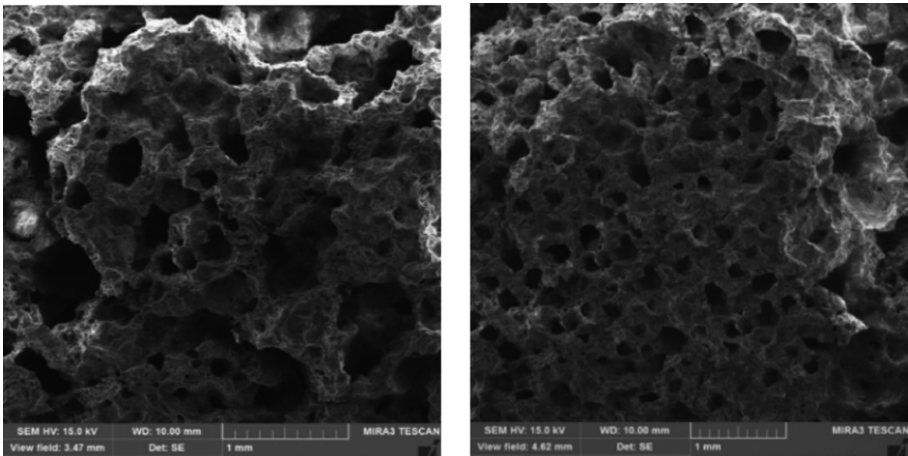


Fig. 1. Microstructure of cellular composites: a – AAC, b – AACAl.

According to a pore distribution analysis carried out at micro-level the increasing of total porosity of composite shifted into nano-sized range (Fig. 2b) is observed. For example, volume of pore with radius less of 94.6 nm is varied from 0.007 to 0.015 cm³/g in AACAl depending of differently-sized pore distribution (Fig. 3).

It is should be noted, the AACAl microstructure of interpore partition and pore surface is covered by compact layer from acicular crystalline new formations, reinforcing the cellular structure into stronger massive that allows reducing a shrinkage (Fig. 2b). Shrinkage reducing in binder system, increasing of interpore partition density and minimization in structure imperfection allows increasing the close spherical pore amount.

Construction objects of transport infrastructure have a different purpose and are differed in service conditions providing a required microclimate (for a health and good man's performance capability) [23]. In garages when the transport storage the low humidity and fixed temperature is required. That is necessary to prevent accelerated

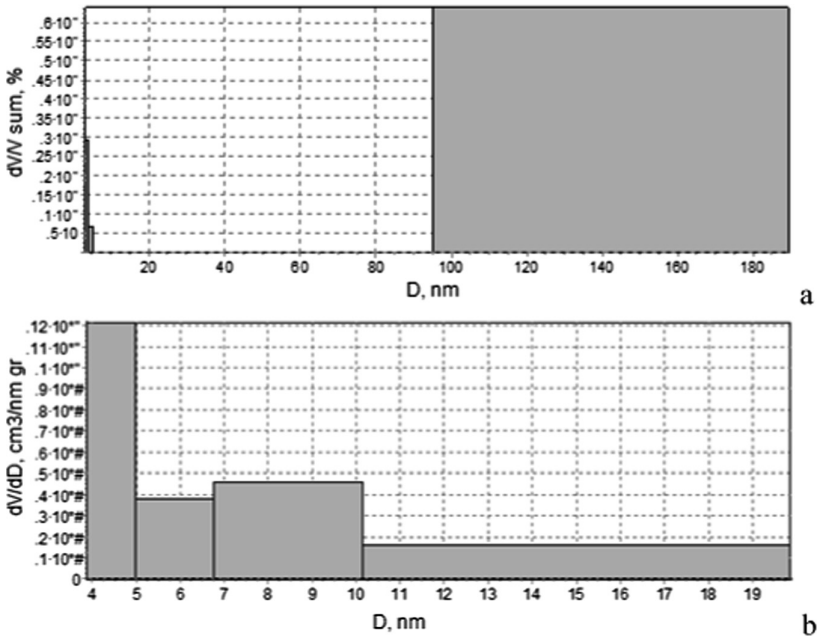


Fig. 2. Nanoporosity distribution in: a – AAC, b – AACAI.

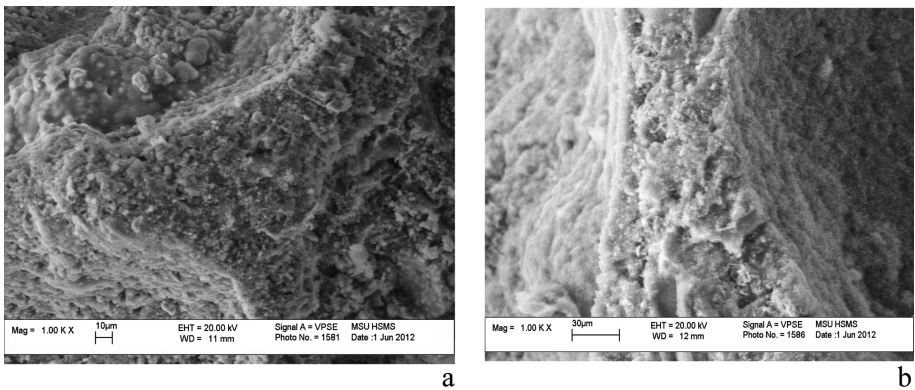


Fig. 3. Microstructure of interpore partition in cellular concrete: a – AAC, b – AACAI.

absorption and metal corrosion. In repairing and management buildings is need to development a required microclimate (for a health and good man’s performance capability).

According to assigned tasks and taking into account typical service conditions for construction objects of transport infrastructure the calculation of thermal and physical characteristics of the developed concrete vs. ordinary concrete analogue is accomplished. Air humidity is determined according to the SNiP [24] depending of climate

and season time conditions for a zone A – 80%, for a zone B – 97%. Calculation of sorption humidity of a material in service conditions for construction objects is realized on the base of sorption isotherm at average temperature of $(19 \pm 1) \text{ }^\circ\text{C}$ [25].

According to calculation results of sorption humidity for AACAI is less vs. AAC. It can be associated with formation of pore structure mainly containing of close pores as well as due to more compact pore surface (Figs. 1b, 2b). It leads to reducing of external active centers, adsorbing water and, as a consequence (Table 1).

Table 1. Performance characteristics of the developed concrete.

Concrete	Density, kg/m^3	Compressive strength, MPa	Heat conductivity of concrete, $\lambda \text{ W/m }^\circ\text{C}$			Vapor permeability coefficient μ , $\text{mg}/(\text{m}\cdot\text{h}\cdot\text{Pa})$	Sorption humidity, %	
			Dry, λ_0	Calculated coefficients			At air humidity A	At air humidity B
				Wet, λ_A	Wet, λ_B			
AAC	562.7	2.72	0.135	0.150	0.163	0.205	1.25	4.20
AACAI	435.7	3.57	0.109	0.110	0.111	0.210	1.12	3.98
Standard 31359-2007	500	Up to 2,5	0.120	–	–	0.200 at least		

In compliance with the application of cellular concrete is planned for external application (envelopes) in framework of normal regimes of climate deviations for calculation of heat conductivity coefficient the average values of working humidity for a zone A – 1%; for a zone B – 4%. Calculation of heat conductivity coefficient is accomplished with the Standard [26].

According to a standard requirements the vapor permeability coefficient μ for AAC is should be $0.2 \text{ mg}/(\text{m}\cdot\text{h}\cdot\text{Pa})$, no more [21]. This parameter for ordinary cellular concrete is $0.205 \text{ mg}/(\text{m}\cdot\text{h}\cdot\text{Pa})$; for the developed material a μ parameter is slightly higher – $0.21 \text{ mg}/(\text{m}\cdot\text{h}\cdot\text{Pa})$, that provide a good heat insulating characteristics and reduced heat conductivity values (experimental and calculated) (Table 1).

For construction of transport buildings (railway yards, depot, control room, as well as bus, trolleybus and tramway parks etc.) the sound absorbing constructions are necessary to meet requirements of sanitary-hygienic zones [27]. The World Health Organization manifests the permanent noise effect with volume higher of 50 dB on a human that initiates the problem with vascular system and increases the risk of infarcts. Daily average noise level in surround zones of transport enterprises is 50–90 dB. At the same time noise level from bus parks is 85–92 dB, from tramway traffic – 70–80 dB.

Analysis of acoustic characteristics of the construction based on the developed concrete is accomplished with using of reference calculated insulation index of airborne noise provided by envelope buildings with solid cross-section [28] according to the following equation:

$$R_w = 37 \cdot \lg(m) + 55\lg(K) - 43, \text{ dB} \quad (1)$$

where

- R_w – insulation index of airborne noise;
 $m = p_{\text{bond}} \cdot h$ – surface well density, kg/m²;
 p_{bond} – bond density;
 h – bond depth;
 K – coefficient, taking into account the sound insulation improvement due to increasing of flexural stiffness and internal friction of envelope based on gas concrete vs. contraction for a heavy concrete with the same surface density $k = 1,75$ (calculated by interpolation technique).

Calculation is realized for a blocks with thickness of 200 mm, introduced into the bond with adhesive component with and without finishing by sand-cement bonding plaster.

Required sound insulation for envelopes defending from airborne noise and rooms containing a noise sources is 54 dB and 52 dB to provide a comfortable noise level [28]. According to calculated data, presented in Table 2, insulation index of airborne noise for the developed concrete meets the Standard requirements. To enhance of wall sound insulation and providing a comfortable conditions for a human in the developed concrete based buildings the additional finishing with sand-cement bonding plaster is required.

On the base of experimental data the frequency characteristics of sound insulation are plotted to determine the sound absorption in frequency range of 125–4000 Hz.

Table 2. Calculated values of sound insulation.

Blocks with depth of 200 mm	Insulation index of airborne noise R_w , dB	
	Without sand-cement bonding plaster	With sand-cement bonding plaster (double faced, depth is 20 mm)
AAC	43	54
AACAI	48	57
SP 23-103-2003	Maximum allowable for a human – 48	

According to Fig. 4 the growing of sound absorption coefficient for AACAI in octave frequency band is observed. Structural feature of the developed concrete consists of a lot of differently-sized pores (dominantly, small ones). Conducting sound wave though a material initiates a pore air to vibration and small pore provide a stronger resistance vs. large ones resulting prevention and transmission of air. This effect initiates a transformation of mechanical energy to heat one [14]. Totally, it provides a high sound insulating characteristics of the developed material.

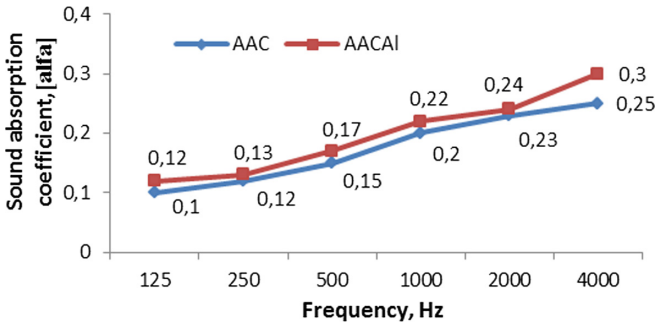


Fig. 4. Sound absorption characteristics for: AACAI and AAC.

4 Conclusion

Directed monitoring of heat and sound insulating properties of AAC is possible keeping base criteria of porous structure such as homogeneous pore distribution in bulk, thickness and density of interpore partition, shape and size of pores. It can be achieved by development of polycomponent binder with aluminosilicate raw materials. The higher amount of close pores, homogeneously distributed in bulk of material allows reduction a concrete density from 562.7 to 435.7 kg/m³, as well as good air exchange and providing comfortable indoor microclimate.

Reinforcement by crystal new formations, dominantly, with acicular morphology leads to increasing of interpore partition density and maximal reducing of structure imperfection as well as strength improvement by 31%, reducing sorption humidity by 10% and increasing of water vapor permeability resistance.

Formation of differently-sized pores and increasing of its amount at macro level allows reducing of heat conductivity coefficient when variation of air humidity in range of 80–97%. So, the developed concrete can be recommended for construction of industrial and stored buildings as well as garages of different purpose without of additional winterization. Feature of formed cellular structure allows enhancement of acoustic characteristics, insulation index of airborne noise and sound absorption in frequency range of 125–4000 Hz. So, the developed cellular concrete is prospective as sound insulating material for buildings in transport infrastructure. Also it is energy saving material with some improved properties that is suitable when design, development, modernization and service of buildings of transport infrastructure and meet all requirements of standards, in particular, for building heat insulation to energy saving and optimization of a building microclimate.

Acknowledgment. The work is realized in the framework of the Program of flagship university development on the base of the Belgorod State Technological University named after V.G. Shoukhov, using equipment of High Technology Center at BSTU named after V.G. Shoukhov.

References

1. Lesovik, V.: Implementation Examples in Construction Material Science: Monography. BSTU, Belgorod (2016)
2. Lesovik, V.: Architectural geonics, looking into the future. *Bull. Volgograd State Univ. Archit. Civ. Eng. Ser.: Build. Architect.* **31-1**(50), 131–136 (2013)
3. Lesovik, V., Vorontsov, V., Frolova, M., Degtev, Y., Fironov, R.: Peculiarities of composition materials for architectural geonics. *Res. J. Appl. Sci.* **12**(9), 1149–1152 (2014)
4. Suleymanova, L., Lesovik, V., Kondrashev, K., Suleymanov, K., Lukutsova, N.: Energy efficient technologies of production and use non-autoclaved aerated concrete. *Int. J. Appl. Eng. Res.* **5**(10), 12399–12406 (2015)
5. Lesovik, V.: The New Paradigm of Creating Composites for Building Industry. Federal State Educational Institution of Higher Professional Education, Grozny, Russia (2015)
6. Rathi, O., Khandve, P.V.: Cost effectiveness of using AAC blocks for building construction in residential building and public buildings. *Int. J. Res. Eng. Technol.* **05**(05), 517–520 (2016)
7. Suleymanova, L., Lesovik, V., Kara, K., Malyukova, M., Suleymanov, K.: Energy-efficient concretes for green construction. *Res. J. Appl. Sci.* **12**(9), 1087–1090 (2014)
8. Rathil, S., Khandve, P.: AAC block - a new eco-friendly material for construction. *Int. J. Adv. Eng. Res. Dev.* **2**, 4 (2015)
9. Lesovik, R., Degtev, Y., Shakarna, M., Levchenko, A.: Green composites in architecture and building material science. *Mod. Appl. Sci.* **9**(1), 45–50 (2015)
10. Zhukov, A., Chugunkov, A., Gudkov, P.: Modeling and optimization of the aeroconcrete technology. *Vestnik MGSU* **4**, 155–159 (2012)
11. Shmitko, E., Rezanov, A., Bedarev, A.: Multiparameter structure optimization of the cellular silicate concrete. *Civ. Eng. J.* **3**, 15 (2013)
12. Lesovik, V.: Enhancement of efficiency of construction materials production taking into account genesis of applied rocks. *ACB, Moscow* (2016)
13. Laukaitis, A.: Acoustical properties of aerated autoclaved concrete. *Appl. Acoust.* **67**(3), 284–296 (2006). <https://doi.org/10.1016/j.apacoust.2005.07.003>
14. Vaisera, S., Puchka, O., Lesovik, V., Bessonov, I., Sergeev, S.: Efficient acoustic glass composites. *Constr. Mater.* **6**, 28–31 (2016)
15. Fomina, E., Strokova, V., Kozhukhova, N.: Application of Natural Aluminosilicates in Autoclave Cellular Concrete. *World Appl. Sci. J.* **1**(25), 48–54 (2013)
16. Fomina, E., Kozhukhova, M., Kozhukhova, N.: Estimation of efficiency of alumina-silicate raw materials application in composite binders. *Bull. Belgorod State Technol. Univ. Named After V.G. Shoukhov* **4**, 31–35 (2013)
17. Fomina, E., Zhernovsky, I., Strokova, V.: Some properties of autoclave silicate aerated construction materials on an aluminosilicate base and character of phase formation in their structure. *Constr. Mater.* **9**, 38–40 (2012)
18. Russian standard 30256–94 Building materials and products. Method of thermal conductivity determination by cylindrical probe
19. Russian standard 25898–83: Building materials and products. Methods of steam-tightness determination
20. Russian standard 24816–81: Building materials. Method of hygroscopic moisture determination
21. Radoutsky, V., Vetrova, Y.: Theoretical and experimental studies resources sound-insulating of abilities of heat-insulated plates on the basis of foamed glass. *Bull. Belgorod State Technol. Univ. Named After V.G. Shoukhov* **5**, 45–49 (2015)

22. Russian standard 31359–2007: Concretes cellular autoclaved hardening. Technical conditions
23. Russian standard SNiP 23-02-2003: Thermal performance of the buildings
24. Russian standard SNiPII-3-79: Construction heat engineering
25. Russian standard 24816–2014: Building materials. Method of equilibrium hygroscopic moisture determination
26. Russian standard 54855–2011: Building materials and products. Determination of design thermal value
27. Russian standard SP 51.13330.2011: Sound protection
28. Russian standard SP 23-103-2003: Projection of sound insulation of separating constructions in domestic and public buildings

The Issues of Energy-Efficiency Increase of Three-Layer Reinforced Concrete Plate Constructions

Alexey Belyaev¹ , Grigory Nesvetaev² ,
and Dmitry Mailyan² 

¹ Scientific Research Institute of Concrete and Reinforced Concrete
after A.A. Gvozdev, 2nd Institutskaya st., 6, 109428 Moscow, Russia
dmailyan868@rambler.ru

² Academy of Civil Engineering and Architecture Don State Technical
University, Sotsialisticheskaya 162, 344022 Rostov-on-Don, Russia

Abstract. The article is about functioning of three-layer concrete plate constructions under load. The load bearing capacity, crack resistance and deformation of these elements were analyzed at different percentages of reinforcement, grade of concrete and etc. One of concrete drawbacks is that the weight of constructions is high compared to the payload which it can carry; so even a small reduction in weight of the construction can lead to significant technical and economic effect and significant increase of their energy-efficiency.

Keywords: Transport buildings and structures · Energy efficiency
Road construction

1 Introduction

The demand for aggregates of all types (heavy and light) in most countries increases significantly outstripping the average growth rate of the construction industry. On the one hand, it is explained by the increase in volumes of road construction, where the aggregates are used both as a bulk material, and on the other hand, - wide use of concrete in many other areas.

Porous aggregates are often made from industrial wastes (such as slags, coal shale, slate waste, ash, etc.). In industrial areas, the use of these materials for the production of aggregates helps to solve the protection problem of environmental pollution. Some of these types of wastes contain a significant amount of fuel required for the manufacturing process.

Quite energy-efficient constructions are three-layer reinforced concrete plates with the upper and lower layers of heavy concrete and the middle of the lightweight concrete [1–10]. It is more effective to use a self-sealing expanded clay concrete as a middle layer.

The compositions of highly mobile and self-compacting lightweight aggregate concrete mixes are developed with a diameter of 38 face breaking cone (DC = 22 cm) to 67 cm, with different particle size aggregates. The compositions were made on two

cements: TS1 and C2 differing normal density, respectively, 24.5% and 28.5. The superplasticizer Sika Viscocrete 5–600 was used. In the cement-TS1 the air-entraining additive formulations Sika Aer 200 S was used. Air-entraining additive with cement U2 proved ineffective, so in the compositions of cement-C2 it has not been applied. Consumption of cement in the compositions ranged from 417 to 515 kg/m³ of concrete grade V12.5 - At 20, grade of concrete for medium density D1400. Design of concrete macrostructure was carried out taking into account the specific of porous aggregates.

Structural properties of investigated self-compacting expanded clay concrete are presented in Table 1.

Table 1. Structural properties self-sealing expanded clay concrete.

№	The average density of the mixture/concrete 1 kg/m ³	Tensile strength, MPa			Chart settings				
		R ²	R ³ _{pr}	R ⁴ _t	E ⁵ ₀ , MPa	ε ⁶ _R , 10 ⁵	ε ⁷ _{bu} 10 ⁵	λ ⁸ _R	k ⁹
1	1445/1300	21.3	18.1	1.59	10810	196	318	0.846	1.18
2	1440/1295	19.2	18.2	1.74	11980	201	440	0.803	1.25
3	1475/1320	21.2	19.3	1.62	11510	264	304	0.634	1.58
4	1495/1340	21.2	17.8	1.81	11140	251	432	0.638	1.57
5	1460/1310	22.3	18.8	1.82	10600	295	310	0.599	1.67
6	1445/1230	24.5	20.2	1.72	10430	242	317	0.8	1.25
7	1540/1290	17.6	14.1	1.38	9370	233	413	0.665	1.5
8	1515/1350	25.1	19.4	1.94	10060	256	352	0.751	1.33

The actual grade of concrete of monolithic constructions is assumed equal: $B_f = 0.8 \cdot R_m$.

The minimum value of limit cube strength amounts to 17.6 MPa, which corresponds to the grade $B_f = 14$, and the maximum value of 25.1 MPa, which corresponds to the grade $B_f = 20.1$. According to the joint venture 63.13330, for lightweight concrete with the brand at an average density of installed D1400 grades on the compressive strength of V3.5 to B30. Thus, the self-sealing expanded clay concretes correspond V12.5 grades; B15 and B20.

Note: 1 - in the dry state; 2 - cube; 3 - prism; 4 - tension; 5 - initial modulus of elasticity; 6 - relative deformation corresponding to the limit of short-term strength of the short-term axial loading; 7 - relative limiting strain on the descending branch of the diagram with short-term axial loading; 8 - elasticity coefficient corresponding to the limit of short-term strength; 9 - coefficient in the formula Sarzhin.

Designed self-sealing expanded clay concrete of grades on compressive strength V12.5 - B20 with the brand at an average density of D1400 will reduce the weight of the concrete plates layered up to 30%.

To study the characteristics of resistance to external influences three-layer concrete plate-like constructions, and also the results of their strength, fracture toughness and deformability special experiments were made. The experimental program included the test 16 three-layer concrete plate elements. 12 samples were manufactured with

conventional (unstrained) and 4 valves - with pre-stressed reinforcement (Fig. 1.). Prototypes have the following dimensions: section – 24 h 20 cm, length $\ell = 300$ cm.

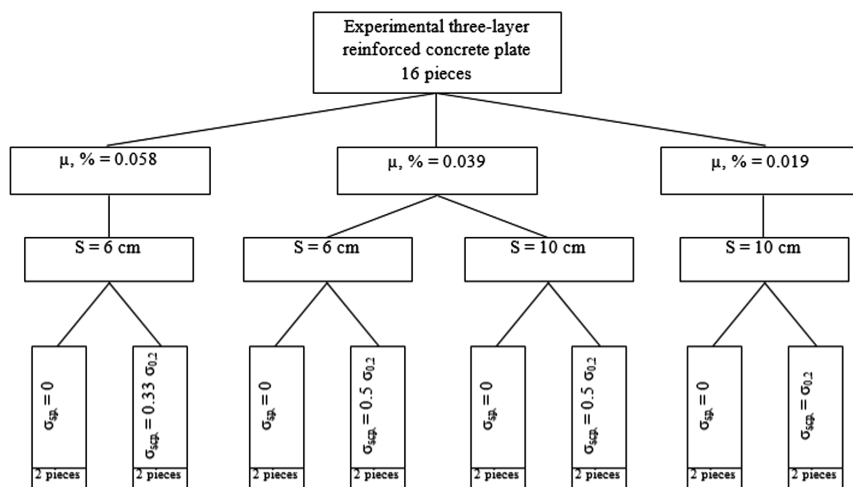


Fig. 1. The program of experimental research.

Varied factors in the experiment were as follows:

percentage of reinforcement $\mu = 0.58\%$; 0.39% ; 0.19%

transverse reinforcement step $s = 6$; 10 cm.

Samples were divided into groups depending on varied factors, each of which consisted of two elements-twins (Table 2).

Note: Code of prototypes adopted the following: the first letter «U» or «P» - unstressed and pre-stressed plate; “1”, “2” or “3” – $\mu = 0$, respectively, 19% , 39% or 58% , numeral “6” or “10” - a step of transverse reinforcement in cm.

In the experimental three-layer concrete plates of the outer layers were made of heavy concrete grade B40 and the average layer - self compacting grade B15 expanded clay concrete [11–14].

The thickness of the layers of heavy and light concretes was taken for the following reasons. Heavy concrete thickness ($h_n = H_b = 4$ cm) was administered the minimum required for anchoring and protection against corrosion of high strength pre-stressed reinforcement. Average layer height ($h_c = 12$ cm) was adopted from considerations of conservation ratio of layer thicknesses in actual designs with light-weight concrete density up to 1300 kg/m^3 (Fig. 2).

For reinforcement of prototypes hot-rod fittings periodic profile of A800 diameter of 10 mm was used. It was placed in the lower concrete layer (h_n). On the top layer (HB) from the ends of the elements to load application sites were located two rods 5 mm diameter steel grade B500. The end sections of plates were reinforced with welded wire mesh. All experimental elements as pre-stressed or unstressed have transverse reinforcement in the form of collars welded in steps 6 and 10 cm.

Grids and collars were made of 5 mm diameter rods grade B-500.

Table 2. Characteristics of advanced three-layer concrete plates.

Code of the prototype	Age of concrete in days when		Concrete strength, MPa				The module of elasticity of concrete, MPa			
	Crimp	Test	Heavy		Expanded clay concrete		Heavy		Expanded clay concrete	
			R^t	R^t	R_b^t	R_b^t	$E_b^t \cdot 10^{-3}$	$E_b^t \cdot 10^{-3}$	$E_{b,1}^t \cdot 10^{-3}$	$E_{b,1}^t \cdot 10^{-3}$
1	2	3	4	5	6	7	8	9	10	11
U1-3-6	–	34	–	43.3	–	13.8	–	25.6	–	10.3
U2-3-6	–	36	–	44.4	–	13.9	–	26.8	–	10.4
P1-3-6	20	28	41.15	43.9	12.3	13.8	25.7	27.8	9.7	10.4
P2-3-6	20	29	41.15	44.6	12.2	13.9	25.6	28.1	9.7	10.4
U1-2-6	–	30	–	45.4	–	11.6	–	25.4	–	11.3
U2-2-6	–	32	–	44.5	–	11.6	–	26.1	–	11.4
P1-2-6	21	34	43.0	48.6	13.4	15.7	23.1	26.1	10.3	10.7
P2-2-6	21	35	43.0	48.9	13.6	15.9	23.1	26.2	10.3	10.8
U1-2-10	–	31	–	45.2	–	13.4	–	25.4	–	11.0
U2-2-10	–	32	–	45.5	–	13.5	–	25.6	–	11.1
P1-2-10	21	28	43.5	44.0	12.6	13.2	22.7	24.7	10.5	10.8
P2-2-10	20	30	41.9	44.4	12.4	13.3	23.5	24.9	10.6	10.9
U1-1-10	–	29	–	45.9	–	3.6	–	25.5	–	10.2
U2-1-10	–	30	–	46.3	–	3.7	–	25.8	–	10.3
P1-1-10	21	31	42.6	47.1	13.0	13.8	23.7	26.2	9.8	10.3
P2-1-10	21	32	42.6	47.5	12.8	13.8	23.7	26.4	9.9	10.4

All prototypes were made in a metal formwork on the bench in a laboratory room at 20 ± 2 °C and a relative humidity of $80 \pm 5\%$. Armature is stretched on the stand stops using a hydraulic jack. Controlled pre-stressing was determined by the pressure gauge jack and an indicator deformometer installed on free stretches tendons. The concrete was laid in layers. The first layer of heavy concrete 4 cm thick and the middle layer thickness 12 cm expanded clay concrete were formed using vibrators. The upper layer 4 cm thick was laid using a screed. Cubes and prisms with the dimensions and 15 h 15 h 15 cm 15 h 15 h 60 cm were manufactured simultaneously with basic patterns of the two types of concrete. The composition of the expanded clay concrete is described above. The composition of the heavy concrete upper and lower layers – in Table 3.

Heavy concrete is made from 5–20 mm gravel bulk density of 1440 kg/m^3 . Brand rubble strength - Dr.-1000. Quarz sand served as fine aggregate, in its grain structure belonging to the small (fineness modulus $M_k = 1.5$). Its bulk density is 1255 kg/m^3 .

As a binder for both types of concrete was used Portland cement 500 Novorossiysk “Proletariat” plant.

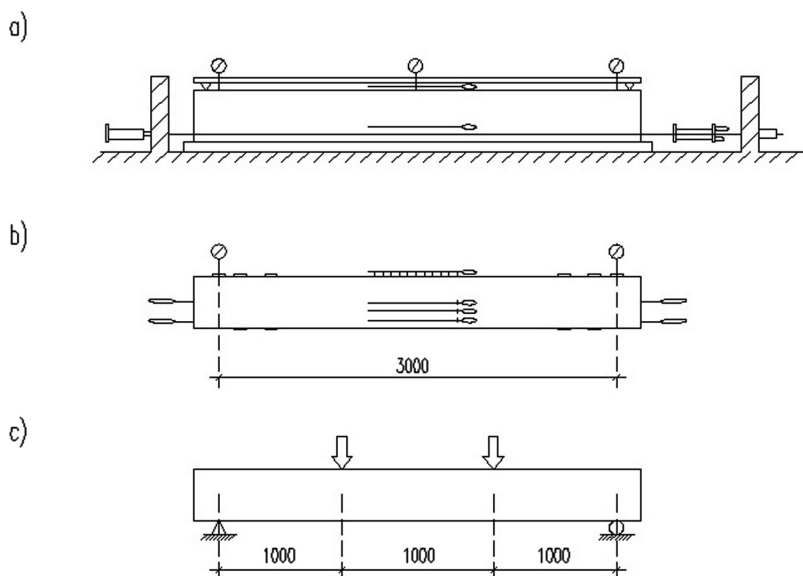


Fig. 2. Driving of prototypes tested at pre-stressing leave (a) the location of the measuring instruments (b) test the external load.

Table 3. Concrete mixture of prototypes.

Type of concrete	Cube strength, MPa	Material consumption, kg/m ³				Density of dry concrete, kg/m ³
		Crushed stone	Sand	Cement	Water	
Heavy	40	1210	570	405	190	2375

Test samples were kept in a room with the air temperature and relative humidity 18–22oS 80–85% after production and before the short-term tests. A few hours after the concreting, the surface was covered with wet sawdust.

Hot rod thermally hardened steel of periodic profile A800 10 mm was unstressed and pre-stressed reinforcement in the experimental three-layer concrete samples. The tests carried out in accordance with GOST 1204-81, showed the following results: tensile strength $\sigma_u = 1283.6$ MPa, proof stress $\sigma_{0.2} = 880.2$ MPa, elastic modulus $E_s = 2.0 \times 10^5$ MPa, elongation at break $\sigma = 8\%$. According to the results of the test fixture complies with the requirements GOST 7348-81.

Pre-stressed rebar passed on concrete on 20–21-th day from the day of concreting under heavy concrete cube strength of 41–43 MPa. During holiday of pre-stressing bend and longitudinal deformation of the concrete and rebar at the ends and in the middle of the element with the help of a data base of indicators 40 cm were measured. The measurement of deformation continues after stress release and before the test of the external load.

Prototypes were tested by short-term load through 27–35 days after concreting. Testing of the samples was carried out at the booth. Load was supplied by 25-ton hydraulic jack.

Three-layer samples were loaded in steps of 10% of the theoretical breaking load delayed by 15 min. The external force is controlled by the pressure gauge jack and cylindrical dynamometer, which strain using strain gauges recorded on the waveform.

At each step of uploading using a deflectometer vertical displacements (deflections) were determined at three points at the poles and in the middle of samples. For removing of samples of fracture point special tools were used in the form of flexible membrane, sensing the vertical displacement of the sample (for measuring the deflection and deformation of the rebar). At these membranes strain gauges were glued connected to an oscilloscope. Longitudinal deformation of concrete were measured on two opposite faces of the sample and on the side surfaces of heavy concrete at different points sectional height pickoff chain. Limiting deformation in the average sectional was recorded using the strain gauges connected to an oscilloscope (see Fig. 6). Deformation of rebar and lightweight concrete were measured using the 40 cm on the basis of indicators. Shear strain were determined by dividing indicators with value of division 0.001 mm, installed at the ends of the elements in the middle of a light layer of concrete and level of work rebar.

During the test the time of formation of cracks and the width of the disclosure were recorded and measured with an electron microscope. Indications of all instruments were recorded twice: once after the load flow and after exposure in step.

Test procedure of all samples was similar. All of them were loaded to the full carrying capacity exhaustion.

As a result of the test obtained new experimental data about the load-bearing capacity, crack resistance, deformability of bent three-layer concrete plate elements have established two typical kinds of destruction: the loss of the bearing capacity of the horizontal cross-section due to the shift of light-weight concrete of the middle layer of self compacting expanded clay and normal - when the in fitting stress over the yield point.

It is found that the largest shearing stresses occur in areas without cracks at the neutral line. If the shear stress exceeds the shear strength of the middle layer of concrete, there is a shift, i.e. a loss carrying capacity in the horizontal section.

Variation step of transverse reinforcement ($s = 6\text{--}10$ cm) has not impact on the value of the external load, causing a shift.

It has been established that the greatest deflection of the transverse forces are pre-stressed three-layer elements, because the length of their sections operating without cracking, and hence the relative height of the compressed zone is greater than of unstrained.

Analysis of the impact of various factors on the bearing capacity and deformation three-layer reinforced concrete bending elements made according to the results of physical experiments showed that the growth of heavy concrete class increases the bearing capacity of the horizontal cross-section slightly. There is more significant influence of the lightweight concrete grade of the middle layer. Increasing the growth twice raises the bearing capacity of the horizontal section three times.

The levels of compression and reinforcing ratio have almost no effect on the bearing capacity of the horizontal section.

References

1. Mailyan, D.: New effective constructive solutions of compressed reinforced concrete elements. *Izvestiya RSUCE* **4**, 27 (2009)
2. Mailyan, D., Medinsky, V., Azizov, A.: Increasing the efficiency of the use of high-strength bar reinforcement in compressed reinforced concrete elements. New types of fittings and welding, pp. 279–282 (2012)
3. Osipov, V.: *Effective Reinforced Concrete for Agricultural Construction*. Rostov University Publishing House, Rostov-on-Don (2012)
4. Chubarov, V., Osipov, V.: *Guidance on the computer calculation of reinforced concrete columns with mixed reinforcement*. SevKavNIPIagroprom, Rostov-on-Don (2007)
5. Osipov, V., Mailyan, D.: *Recommendations for the design of eccentrically compressed reinforced concrete three-layer structures with high reinforcement*, Rostov-on-Don (2013)
6. Osipov, V., Zalessky, V.: Three-layer bearing panels. *Rural construction* **4**, 14 (2015)
7. Khunagov, R.: Double-layer prestressed reinforced concrete columns. In: *Proceedings of the International Scientific - Practical Conference*, p. 17 (2011)
8. Khunagov, R.: Flexible double-layer non-uniformly compressed reinforced concrete panels. In: *Proceedings of the International Scientific - Practical Conference*, p. 34 (2012)
9. Khunagov, R.: Influence of uneven pre-stress sections of reinforced concrete elements. *Vestnik MSTU* **4**, 29 (2011)
10. Khunagov, R.: Calculation of double-layer prestressed reinforced concrete panels. *Vestnik MSTU* **4**, 33 (2011)
11. Khunagov, R., Blyagoz, A.: Double-layer reinforced concrete panels with unevenly compressed sections. *Vestnik MSTU* **4**, 37 (2011)
12. Mailyan, D., Medinsky, V., Azizov, A.: Strength of reinforced concrete columns with high-strength pre-compressed reinforcement. *Questions of calculation of reinforced concrete*, pp. 37–46 (2012)
13. Aksenov, N., Kubasov, A., Nikolaenko, A.: Flexible double-layer non-uniformly compressed reinforced concrete panels. *New research in the field of construction*, pp. 96–101 (2009)
14. Nesvetaev, G., Timonov, S., Kardumyan, G.: Improvement of reinforced concrete constructions, assessment of their condition, strengthening, pp. 123–127 (2001)

Energy-Efficient Reinforced Concrete Columns Made of Concrete, Grade B90...B140

Dmitry Mailyan , Vladimir Aksenov , and Nikolay Aksenov 

Academy of Civil Engineering and Architecture Don State Technical University,
Sotsialisticheskaya, 162, 344022 Rostov-on-Don, Russia
dmailyan868@rambler.ru

Abstract. The article deals with functioning of the concrete columns made of high-strength concrete. The changing factors were flexibility of construction, eccentricity of the external force, reinforcement. The use of the given data will allow to design such constructions efficiently and safely. The increase of energy efficiency of compressed concrete elements can be achieved by using the high-strength concrete. Heavy or fine-grained concrete of compressive strength B60 grade and higher, prepared by using a binder based on Portland cement clinker (GOST 31914-2012), refer to the high-strength concrete. In the existing regulations on calculation and design of reinforced concrete constructions, the concrete of compressive strength B100 grade, inclusive, is provided, but there are not enough real samples of test data in the scientific literature [1–6].

Keywords: High-strength concrete · Concrete grade
Compressed concrete elements · Flexibility · Eccentricity

1 Introduction

To obtain the data on the work of compressed concrete elements of high-strength concrete authors have performed the experimental research work of 27 concrete columns of concrete B87 ... V140 [7].

Different types of concrete mixes and their components were used to make the examined columns (Table 1) [8].

To prepare the concrete mix type-1 of columns (K1-K9) as a coarse aggregate the crushed granite Chelyabinsk deposit with grain size of 5...20 mm was used. For columns of 2 and type 3 (K10–K27) the basalt gravel deposits Yerevan fraction 5–20 mm was used. As a fine aggregate the silica sand, with 2.5 fineness modulus, was used. Large and small aggregate before use were washed and dried.

Columns of type 1 were manufactured on a conventional Portland cement M500 production of “Oskolcement”. For the columns of the 2nd and 3rd type of cement Mika Cement was used, corresponding to the brand M500 D-0.

Regulation of rheological properties and reducing the water requirement of the concrete of columns K1–K9 was achieved by introducing a mixture of superplasticizer Melment F10 (Germany) in an amount of 0.8% by weight of binder. Melment F10 - powdered sulfonated polycondensation product on the basis of melamine. To reduce the water demand of concrete mix and produce high-strength concrete of columns

Table 1. Composition of concrete mixes of prototypes columns.

The components of the concrete mix	Unit	Types of concrete compositions		
		Type 1 (K1–K9)	Type 2 (K10–K18)	Type 3 (K19–K27)
Cement kg	Crushed stone 5–10 mm kg	650	830	860
Gravel 10–20 mm kg	Sand kg	1120	443	443
l Water	Superplasticizer l		824	824
/C b/p	The resulting actual concrete grade	520	240	240
Cement kg	Crushed stone 5–10 mm kg	165	166	165
Gravel 10–20 mm kg	Sand kg	5.2 (kg)	6.64	8.3
l Water	Superplasticizer l	0.254	0.2	0.19
/C b/p		The resulting actual concrete grade	B87	B109

K10–K27, the superplasticizer Mapefluid N200 manufactured by Mapei was used. It is a 40% solution of active polymers based on melamine. This superplasticizer conforms to the international standard GOST 24211-2008 [79.10].

All columns are conditionally divided into three groups. Columns of type 1 had a length of 960 mm, 1680 mm and 2400 mm, which corresponds to the flexibilities $\lambda h = 10/h = 8$, $\lambda h = 14$ and $\lambda h = 20$. The relative eccentricity, $\delta e = e_0/h$, is equal to 0.03; 0.1 and 0.2. All samples had a cross section of 250×120 (h) mm and reinforced with high-strength reinforcement 4Ø12 A800. Four samples are made without reinforcement stress, five - with pre-stress. Columns of type 2 had sectional 120×250 mm and were made of concrete, the composition of which is given in the Table 1. Columns of type 3 - cross section 100×200 mm concrete (Table 1). Detailed specifications of columns are shown in Table 2.

All columns were tested for compression eccentric upright.

Data on columns bearing capacity resulting from the conducted experiment are shown in Table 3. For the possibility further comparison of the experimental data on the columns of different cross-section and made of different concrete grades, there is “relative carrying capacity” in the last column, which is equal to $\frac{N}{R_b b h}$.

The analysis of the test results was carried out in columns according to the varying factors.

Thus, the most significant impact on the carrying capacity of racks provides pre-stressing reinforcement. The work of shorter ($\lambda h = 8$) eccentrically compressed samples must be evaluated by the relative bearing capacity, excluding the effect of varying the prism strength of concrete on the comparison result. Thus, the strength of the rack at the K-8 $\sigma_{sp} = 740$ MPa, is 10% higher strength relaxed racks K-1. Short

Table 2. Characteristics of the studied columns of high-strength concrete.

Number in order	Code	The geometric characteristics of the cross section, m			Materials		The parameters for calculating			
		b	h	l	armature	concrete	$\lambda_h = l/h$	e_0/h	σ_{sp} , MPa	μ
<i>The first group of columns</i>										
1	K-1	0.25	0.12	0.96	A-800 4Ø12	B140	8	0.2	0	1.51%
2	K-2	0.25	0.12	0.96		B97	8	0.033	0	1.51%
3	K-3	0.25	0.12	2.4		B92	20	0.033	0	1.51%
4	K-4	0.25	0.12	2.4		B100	20	0.2	0	1.1%
5	K-5	0.25	0.12	2.4		B99	20	0.033	740	1.51%
6	K-6	0.25	0.12	2.4		B115	20	0.2	740	1.51%
7	K-7	0.25	0.12	1.68		B101	14	0.1	500	1.51%
8	K-8	0.25	0.12	0.96		B117	8	0.2	740	1.51%
9	K-9	0.25	0.12	0.96		B91	8	0.033	740	1.51%
<i>The second group of columns</i>										
10	K-10	0.25	0.12	1	A500C 4Ø12	B87	8	0.033	0	1.51%
11	K-11	0.25	0.12	2		B87	17	0.033	0	1.51%
12	K-12	0.25	0.12	3		B87	25	0.033	0	1.51%
13	K-13	0.25	0.12	1		B87	8	0.2	0	1.51%
14	K-14	0.25	0.12	2		B87	17	0.2	0	1.51%
15	K-15	0.25	0.12	3		B87	25	0.2	0	1.51%
16	K-16	0.25	0.12	1		B87	8	0.5	0	1.51%
17	K-17	0.25	0.12	2		B87	17	0.5	0	1.51%
18	K-18	0.25	0.12	3		B87	25	0.5	0	1.51%
<i>The third group of columns</i>										
19	K-19	0.2	0.1	3	A500C 6Ø12	B109	30	0.033	0	3.39%
20	K-20	0.2	0.1	3		B109	30	0.2	0	3.39%
21	K-21	0.2	0.1	3		B109	30	0.5	0	3.39%
22	K-22	0.2	0.1	3	A500C 4Ø12	B109	30	0.033	0	2.26%
23	K-23	0.2	0.1	3		B109	30	0.2	0	2.26%
24	K-24	0.2	0.1	3		B109	30	0.5	0	2.26%
25	K-25	0.2	0.1	2		B109	20	0.033	0	2.26%
26	K-26	0.2	0.1	2		B109	20	0.2	0	2.26%
27	K-27	0.2	0.1	2		B109	20	0.5	0	2.26%

“centrally” compressed columns show inverse dependence of strength by the presence of pre-stressed reinforcement. Unstrained sample K-2 sustained load at 12% greater than the pre-tensed K-9.

The bearing capacity of pre-stressed column K-5 was only 5% higher than that of the column K-3 without voltage. Character of fracture of the samples showed that the

Table 3. Data on the bearing capacity of the columns of samples.

Number in order	Code	Experimental results		The parameters for calculating				Relativeload bearing capacity, $\frac{N}{R_b b h}$
		Nexp, kN	presence of cracks	λ_h	e_0/h	σ_{sr} , MPa	μ	
1	K-1	2060	+	8	0.2	0	1.51%	0.701
2	K-2	2720	-	8	0.0333	0	1.51%	1.330
3	K-3	2000	-	20	0.0333	0	1.51%	1.037
4	K-4	950	+	20	0.2	0	1.51%	0.454
5	K-5	2100	-	20	0.0333	740	1.51%	1.011
6	K-6	1200	+	20	0.2	740	1.51%	0.489
7	K-7	2100	-	14	0.1	500	1.51%	0.870
8	K-8	1920	-	8	0.2	740	1.51%	0.780
9	K-9	2400	-	8	0.0333	740	1.51%	1.273
10	K-10	2190	-	8.333	0.0333	0	1.51%	1.137
11	K-11	2080	-	16.67	0.0333	0	1.51%	1.080
12	K-12	1850	-	25	0.0333	0	1.51%	0.961
13	K-13	1500	+	8.333	0.2	0	1.51%	0.779
14	K-14	1320	+	16.67	0.2	0	1.51%	0.685
15	K-15	1050	+	25	0.2	0	1.51%	0.545
16	K-16	610	+	8.333	0.5	0	1.51%	0.317
17	K-17	500	+	16.67	0.5	0	1.1%	0.260
18	K-18	380	+	25	0.5	0	1.51%	0.197
19	K-19	1600	-	30	0.0333	0	3.39%	0.921
20	K-20	780	+	30	0.2	0	3.39%	0.449
Number in order	Code	Experimental results		Parameters of counting				Relativeload bearing capacity, $\frac{N}{R_b b h}$
		Nexp, kN	presence of cracks	λ_h	e_0/h	σ_{sr} , MPa	μ	
21	K-21	330	+	30	0.5	0	3.39%	0.190
22	K-22	1220	-	30	0.0333	0	2.26%	0.702
23	K-23	720	+	30	0.2	0	2.26%	0.414
24	K-24	280	+	30	0.5	0	2.26%	0.161
25	K-25	1640	-	20	0.0333	0	2.26%	0.944
26	K-26	1000	+	20	0.2	0	2.26%	0.575
27	K-27	380	+	20	0.5	0	2.26%	0.219

voltage drop on the height of the section near the K-5 was significantly less than that of K-3, since sample K pre-stressed 5-collapsed compressed sectional area throughout the adjustment.

The strength of eccentrically compressed flexible rack K-6 reinforced with pre-stretched reinforcement, is 7% higher than of strength the unstressed sample K-4 (Fig. 1).

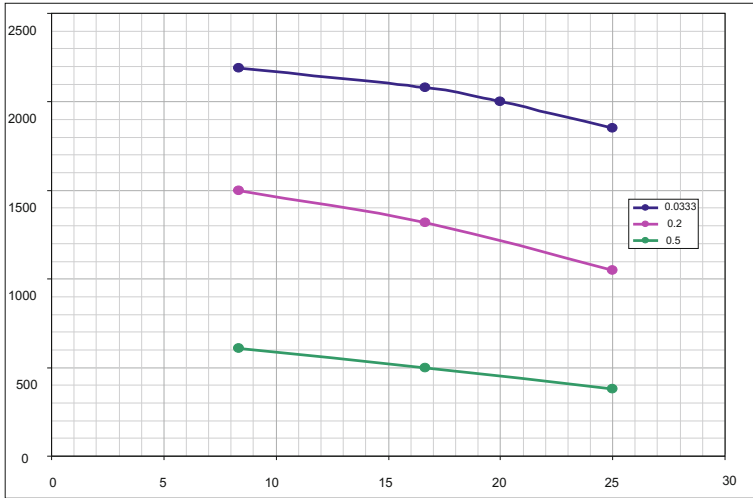


Fig. 1. The dependence of the bearing capacity of columns on the flexibility for different values of the axial eccentricity.

Let us analyze the impact of flexibility on the work of columns. For this we consider the column with the dimensions section 120 h 250 mm, the reinforcement ratio ($\mu = 1.5\%$) and relative $e_0/h = 0.033$. With the growth of eccentricity falling bearing capacity depending on the flexibility is faster. Thus, when the relative eccentricities $e_0/h = 0.2$, reduction of the bearing capacity of racks with flexible $\lambda_h = 8$, $\lambda_h = 8.33$, $\lambda_h = 16.67$, $\lambda_h = 20$ and $\lambda_h = 25$ in relation to the short is 47%, 31.5%, 37%, 56% and 43%, and with $e_0/h = 0.5$ reduction of the bearing capacity of racks with flexible $\lambda_h = 8.33$, $\lambda_h = 16.67$, $\lambda_h = 25$ in relation to the short is 72%, 76%, 80% accordingly.

The obtained results suggest that, all other constant factors with increasing eccentricity increase flexibility, $\lambda_h = 10/h$, in the range of 8 to 25 starts strongly influence the reduction in load-carrying capacity. This is due to the fact that growth increases the flexibility of the longitudinal bending of the column, which in turn added to the value of the axial eccentricity, contributing further reduce the ability of the sample carrier.

We note here that, the increase in flexibility with 20 to 30 reduces the bearing capacity of more than a quarter, while the degree of reduction uniquely depending on the magnitude of the eccentricity is not observed.

Assessing the impact of the relative eccentricity on the bearing capacity of short columns ($\lambda_h = 8$) at $\mu = 1.5\%$ shows that increasing e_0/h from 0.03 to 0.2 reduces of strength by 47%. For columns with flexibility $\lambda_h = 8.33$ at $\mu = 1.5\%$ increasing e_0/h from 0.03 to 0.2 leads to a reduction in strength of 31%, from 0.2 to 0.5–59%. For flexibility of column $\lambda_h = 16.67$ increasing e_0/h of 0.03 to 0.2 leads to decrease in of strength by 37% from 0.2 to 0.5–62%. The total reduction of strength with the eccentricity changes from 0 to 0.5 with the flexibility to column $\lambda_h = 16.67$ was 76% (Fig. 2).

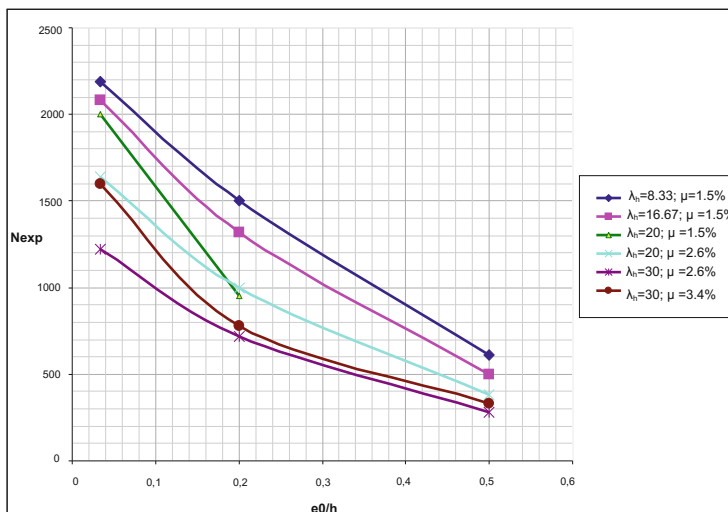


Fig. 2. The dependence of the bearing capacity of columns on the relative eccentricity for different values of flexibility and reinforcement ratio.

For flexible struts ($\lambda_h = 20$): increasing e_0/h of 0.03 to 0.2 leads to decrease in strength at 56%. For flexible struts ($\lambda_h = 25$): increasing e_0/h of 0.03 to 0.2 leads to decrease in strength by 43% from 0.2 to 0.5–64%. The total reduction of strength changes from 0 to 0.5 with the flexibility of the strut $\lambda_h = 25$ was 79.5%.

The increase of the eccentricity and of short flexible columns in any case leads to a decrease in the carrying capacity, but with the pre-stressed reinforcement struts is observed minimal reduction of bearing capacity compared with racks not pre-stressed 8% ($\lambda_h = 8$) and 4% ($\lambda_h = 20$).

Increasing the percentage of reinforcement columns of 50% (up $\mu = 2.26\%$ to $\mu = 3.4\%$) increases the bearing capacity of flexible struts ($\lambda_h = 30$) up 24% under central compression of up to 15% $e_0/h = 0.5$. This may indicate that the degree of influence of percentage content of reinforcement in the cross section on the bearing capacity of flexible columns decreases with increasing eccentricity.

From these figures we conclude that the increase in of strength flexible columns, caused by an increase in the amount of longitudinal reinforcement is slower than the increase in the percentage of reinforcement section. This is due to the fact that a greater contribution to the carrying capacity of columns provides compressed concrete work.

Therefore, to increase the carrying capacity of compressed elements of greater flexibility (λ_h up 20 to 30) from high-strength concrete in the study area relative eccentricity (E_0/h from 0.033 to 0.5) due to the strengthening reinforcement is not effective.

By analyzing the relationship between the relative carrying capacity of columns by their flexibility $\mu = 1.5\%$ and 2.26%, Note that in the case of compression eccentric $e_0/h = 0.5$ can be said that a reinforced pillar in the range of flexibilities $\lambda_h = (20 \dots 30)$ They work as a continuation of the first group of reinforcement struts (with $\mu = 1.5\%$), having flexibility from 8.33 to 25.





Gain relative of strength columns, caused by an increase in the reinforcement, is not revealed in the processing of the results. In the columns, working with fewer eccentricities - $e_0/h = (0.033...0.2)$, in general, is fixed the declining relative of bearing capacity while increasing the reinforcement ratio from 1.5% to 2.26%. For example, if flexibility and $\lambda_h = 25 e_0/h = 0.2$ ratio $N/(R_b b h)$ is reduced by 8%, and at 25 and $\lambda_h = e_0/h = 0.033 - 15\%$. This is due to the influence of the scale factor, as the columns $\mu = 1.5\%$ have cross-sectional dimensions of 250×120 (h) mm and are made of concrete grade B87–B94, reinforcement columns $\mu = 2.26\%$ and 3.4% – sectional dimensions of 200×100 (h) mm and concrete V109. The assumption that the influence of the scale factor by the fact that, as noted above, within one group columns increase in the percentage of reinforcement leads to increased bearing capacity.

The received data of concrete columns functioning, made of high-strength concrete allow to design such constructions more safely and economically.

References

1. Nesvetaev, G.: The perspectives of new technologies development in the construction and training of the new staff in Belorussia **7**, 313–318 (2001)
2. Nesvetaev, G., Timonov, S., Kardumyan, G.: Improvement of reinforced concrete constructions, assessment of their condition, strengthening, pp. 123–127 (2001)
3. El-mahadi, A.: Rheological Properties, Loss of Workability and Strength Development of High-Strength Concrete. University of London, London (2002)
4. Mkrtychyan, A., Mailyan, D., Aksenov, V.: European Applied Sciences; modern approaches in scientific researches **5**, 81–83 (2013)
5. Osipov, V., Mailyan, D.: Recommendations for the design of eccentrically compressed reinforced concrete three-layer structures with high reinforcement, Rostov-on-Don (2013)
6. Mailyan, D.: New effective constructive solutions of compressed reinforced concrete elements. *Izvestiya RSUCE* **4**, 27 (2009)
7. Mailyan, D., Medinsky, V., Azizov, A.: Increasing the efficiency of the use of high-strength bar reinforcement in compressed reinforced concrete elements. New types of fittings and welding, pp. 279–282 (2012)
8. Osipov, V.: Effective Reinforced Concrete for Agricultural Construction. Rostov University Publishing House, Rostov-on-Don (2012)
9. Osipov, V., Zalessky, V.: Three-layer bearing panels. *Rural construction* **4**, 14 (2015)
10. Khunagov, R.: Flexible double-layer non-uniformly compressed reinforced concrete panels. In: Proceedings of the International Scientific-Practical Conference, p. 34 (2012)
11. Mailyan, D., Medinsky, V., Azizov, A.: Strength of reinforced concrete columns with high-strength pre-compressed reinforcement. Questions of calculation of reinforced concrete, pp. 37–46 (2012)
12. Aksenov, N., Kubasov, A., Nikolaenko, A.: Flexible double-layer non-uniformly compressed reinforced concrete panels. New research in the field of construction, pp. 96–101 (2009)

Review of Heat Pumps Application Potential in Cold Climate

Raimonds Bogdanovičs^(✉) , Anatolijs Borodinecs ,
Aleksandrs Zajacs , and Kristīne Šteinerte 

Riga Technical University, Kipsalas str., 6A, Riga, Latvia
raimonds.bogdanovics@rtu.lv

Abstract. Nowadays heat pumps become very popular in the Latvian construction market. The most actual types are air to air and air to water heat pumps. The main reason is low initial investments. The overall season efficiency of heat pump is not widely addressed in existing researches. This paper aims to analyze already existing experience of heat pump application in cold climate. The most appropriate simulation tools were defined and simulation modules were developed. In addition, paper provides deep analysis of Latvian climate in order to get objective data on outdoor air and soil temperature fluctuation. Obtained results allow to reach European Regional Development Fund project “NEARLY ZERO ENERGY SOLUTIONS FOR UNCLASSIFIED BUILDINGS” Nr. 1.1.1.116A048 main targets and provides collection and analyses of information for development of optimal mobile energy source.

Keywords: Energy management · Heat pump · Energy efficiency
Cold climate

1 Introduction

According to “Directive 2010/31/EU of the European parliament and of the council of 19 May 2010 on the energy performance of buildings”: ‘heat pump’ means a machine, a device or installation that transfers heat from natural surroundings such as air, water or ground to buildings or industrial applications by reversing the natural flow of heat such that it flows from a lower to a higher temperature. For reversible heat pumps, it may also move heat from the building to the natural surroundings. Besides the European Union buildings, energy efficiency as well as application of renewable energy became the important issues in Russia and other countries even with relatively low energy costs [15–18].

Heat Pumps (HPs) are a part of the environmentally friendly technologies using renewable energy and do not produce exhaust gases while heating any space, especially if the compressor of HP is driven by green electricity. HPs can provide both space heating and cooling as well as hot water producing by transforming low potential energy from air, ground and water to high potential energy. HP works on the basis of refrigerant cycle, so it consists of 4 main components:

1. evaporator (uses the thermal energy from the outdoor source to boil the refrigerant (the liquid in the Heat Pump) and turns it into a gaseous state),
2. compressor (compresses the refrigerant, which is in gaseous state, to a high pressure, that by consequence increases its temperature),
3. condenser (the refrigerant moves from gaseous into liquid state by releasing the heat into the heating system for the house),
4. expansion valve (pressure lowering device).

Additional valves, thermostats, measurement tools, pumps, fans, or extra heaters can be used too [1, 2]. There are both air and water-based systems that can be used such as the indoor outlet. Air system represents the air conditioner units, while water-based HP is connected to a radiators or floor-heating system [1]. Studies and experience of using show that the floor-heating system is preferable to radiators because it requires low temperature and, thus, has better effectiveness. HPs require good house heat insulation too. The most popular heat sources are air, water and ground, so the comparison between them is the necessity.

One of the most important HPs parameters is COP (coefficient of performance), that shows up the efficiency of the device: a higher number shows better efficiency:

$$\text{COP} = \Delta Q / P \quad (1)$$

where: P is the rated input power of unit, kW (to drive the compressor); ΔQ is rated heating/cooling capacity, kW

$$\Delta Q = \Delta h \cdot m \quad (2)$$

where m denotes the flow rate of refrigerant through the system, Δh denotes the enthalpy difference between the inlet refrigerant and outlet refrigerant through the condenser. The inlet and outlet enthalpy values of refrigerant at different temperatures can be obtained by referring to the pressure-enthalpy diagram [3].

COP may change during the year depending on operating conditions (indoor and outdoor temperature) [4], so that is why there are so big attention to COP analyses in the literature review [19–21].

2 Materials and Methods

The research is based on deep climate analysis and evaluation. This will provide objective data for future evaluation of heat pump efficiency in Latvian climatic conditions. The preliminary COMSOL physics modules adaptation for calculation of heat pump seasonal efficiency was developed. Table 1 combines the air temperature data for Riga (Latvia) from different sources with the aim to compare them with observed data in result section and use in study. Tables 2 and 3 provide the data about soil freezing.

Table 1. Average air temperature (°C) in Riga from different sources.

	I	II	III	IV	V	VI	VII	VIII	IX	X	XI	XII
IDA_iw2	-0.10	-3.00	1.50	6.50	12.30	15.60	17.40	17.80	12.20	7.70	1.80	-1.60
PHPP V9.3	-2.10	-2.70	0.70	7.00	12.30	15.40	19.00	17.80	12.90	7.40	2.80	-0.60
LBN003-15	-4.70	-4.30	-0.60	5.10	11.40	15.40	16.90	16.20	11.90	7.20	2.10	-2.30
CHiP 2.01.01-82	-4.50	-4.20	-1.10	5.20	11.50	15.40	18.00	16.50	12.20	6.70	1.60	-2.30
CHiP II-A.6-72	-5.00	-4.80	-2.00	4.60	10.70	14.30	17.10	15.70	11.70	6.20	1.50	-2.60

Table 2. Frost depth (data from LBN 003-15 [14]) for Riga

Place	Average frost depth						Maximum frost depth		
	X	XI	XII	I	II	III	IV	Average	Maximum
Riga	*	*	7	15	18	13		24	47

* In specific month soil freezing observed less than 50% of years.

Table 3. Average and maximum 0 °C temperature soil depth (data from LBN 003-15 [14]) for Riga.

Depth (cm)	Month					
	XI	XII	I	II	III	IV
Average	*	*	11	14	19	*
Maximum	20	38	48	63	80	80

* In specific month soil temperature decrease 0 °C less than 50% of years.

2.1 Literature Review

Ground Source Heat Pump GSHP technology has been extensively investigated over recent years in view of the fact that it is the most competitive Heating, Ventilation and Air Conditioning (HVAC) system compared to the more widely used Air Source Heat Pump (ASHP) system [5]. By the way, GSHP is widely used in cold climate too, e.g. in Sweden there are 230,000 installed HPs with total capacity 2300 MWt or 9200 GW h/year, but in Canada 36,000 units with 435 MWt and 600 GW h/year [6].

As know, the ground has a stable temperature of around 10–12 °C throughout the year [1] and it increases with depth reaching a gradient of about 0.03 °C/m [5]. This temperature is enough to heat the refrigerant because it has a very low boiling point [1]. The ground heat exchanger (GHE) could be soil or groundwater. For soil GSHP, the orientation of GHE can be either horizontal or vertical. Vertical GHEs occupy less area and can accommodate large air temperature fluctuation [7], because the ground temperature is affected only by air temperature fluctuations at the first meters below the surface [5], while horizontal GHEs experience seasonal temperature cycles due to solar gains and transmission losses to ambient air at ground level [7]. The COP (in average) for GSHP can be in borders from 3 to 5 depending on specific climatic, installation and working conditions [6].

GSHP systems work efficiently when heating and cooling loads are nearly balanced. If the cooling load of a building in summer could not balance the heating load in winter, that usually happens in cold regions, then the HPs long-term efficiency is reduced [5]. The reason is the soil thermal imbalance (or “thermal drift” [5]) – the accumulated heat extracted from the soil is far higher or lower than injected into the soil, leading to serious cold accumulation or heat accumulation. It happens because of the low thermal conductivity of soil, the natural heat dissipation at the boundary of the soil heat retainer around the borehole is very slow [6]. Consequently, the outlet temperature of ground heat exchanger (GHE) will decrease year by year, leading to deterioration in the heating performance and decreasing COP of the GSHP unit.

Existing researches show that the average soil temperature may decrease by 3.0–12.0 °C, COP may decrease by about 0.5–2.2 [6]. To see how dramatically ground temperature decline, there were some simulations with vertical GHE in China:

1. Beijing (−3.1 °C January; 26.7 °C July), the average soil temperature dropped by 3.2 °C during a 20-year operation for a single GCHP system [8] Fig. 1;

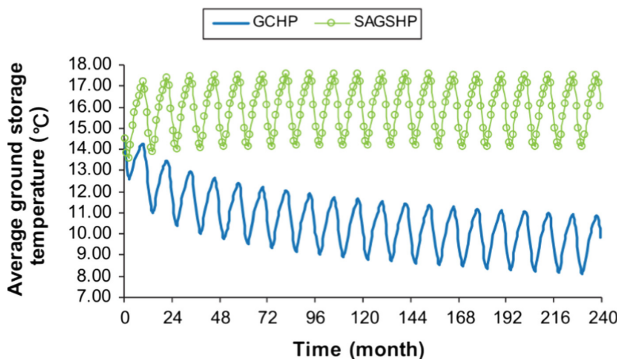


Fig. 1. Comparison of average soil temperature around GHE [8].

2. Nanjing (3 °C January; 29 °C July), with constant heating load of 50 kW in winter and no cooling load, the soil temperature decreased from 17.5 °C to 6.9 °C after 10 years, but after adding constant cooling load of 40 kW in summer, soil temperature fluctuated around the initial soil temperature [7] Fig. 2;
3. Harbin (−17.4 °C January; 23.1 °C July), only used for space heating, the soil temperature decrease from 6.1 °C to −5.6 °C. Used for both space heating and cooling, the soil temperature decrease to −2.2 °C after 10 years [9].

Results show that the GSHP is suitable for buildings with balanced cooling and heating loads and good house heat insulation, which can keep the soil temperature relatively constant for a long operation period [7]. In some cases, despite the unbalanced thermal load of the building, the effect of the thermal drift could be reduced by groundwater flow that reinstates the thermal conditions of the surrounding area [5].

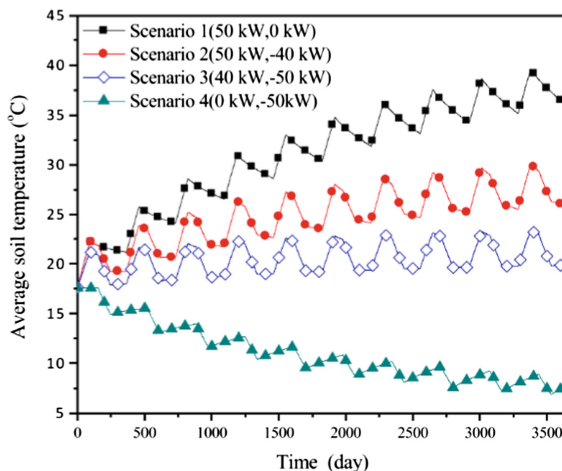


Fig. 2. The temporal variation of soil temperatures over the course of ten years with four different heat flux ratios [7].

One more possible solution how to balance ground loads over a yearly cycle is using the solar assisted ground coupled heat pump (SAGCHP) – a technology to couple solar energy collecting system with the GCHP (Fig. 1). Furthermore, additional solar energy could be utilized for DHW (domestic hot water) supply during non-heating seasons. The average COP of the SGSHP system is 2.78. The COP_{hp} (heating coefficient of heat pump) was found to be about 2.00 in a cloudy day compared with 3.13 in a sunny day [8]. Similar data is shown in research [10] for single U-shaped vertical tube buried 100 meters deep with 5 meters far from each other in Beijing climatic condition. As shown in Fig. 3, adding the solar collector to the GSHP increase the COP for 7%,

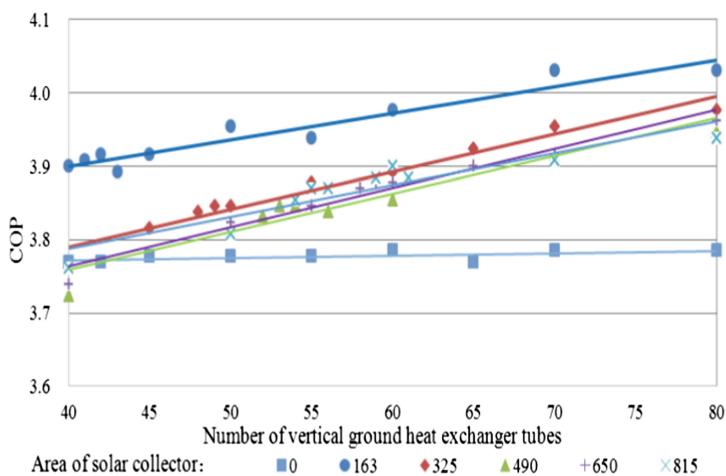


Fig. 3. Accumulated system operation COP [10]

but the soil temperature ($^{\circ}\text{C}$) after 20 years (Fig. 4) become bigger in 2–3 times comparing with situation without solar collector (according to the study, initial average soil temperature of Beijing is 13.1°C).

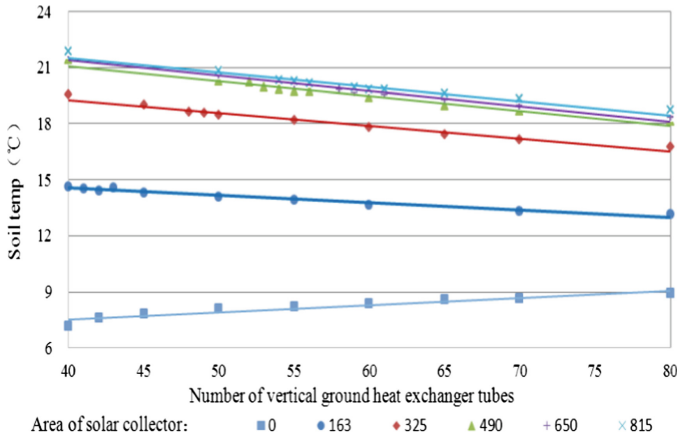


Fig. 4. Soil temperature after 20 year operating [10]

Water source heat pump WSHP can be classified into ground-water source heat pump and surface-water source heat pump (river-water, sea-water, lake-water, etc.) [4]. This system provides more constant input temperature than an air source heat pump because even in winter temperature doesn't fall below 4°C , but moving flow not allow to thermal drift affect appear.

Additionally, it is worthwhile to consider waste (sewage) water source heat pumps (WWSHPs). WW (wastewater) is seen as a renewable heat source for HPs. The heat loss from the urban WW indicates a large potential. Water has a high heat capacity and density, and, therefore, WW provides a concentrated source of heat. In all kinds of low-grade heat sources, urban WW is gradually widely used due to its advantages such as huge quantities, small variation of temperature, being warm in winter and cold in summer. The COP values of the reviewed studies in [11] ranged from 1.77 to 10.63 for heating and 2.23 to 5.35 for cooling based on the experimental and simulated values.

The problem is that if treated WW is used as the heat source, the WWSHP needs to be located near the wastewater treatment plant. Therefore, the pipeline for heating/cooling may become longer, which results in higher costs [11].

To compare different combinations for heat source and sink, four different heat pump systems with the same parameters and experimental setup were studied in [2] research. The difference was only heat source/sink modes: air to air, air to water, water to air and water to water. According to this research data (Fig. 5), the heat pump unit which has the maximum COP value is water to air type (3.94), second one is water to water type (3.73), and third one is air to air type (3.54). The heat pump that has the lowest COP value is air to water type heat pump system (3.40) [2].

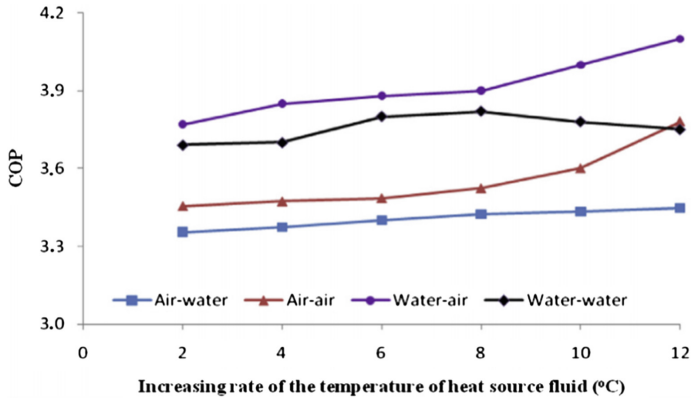


Fig. 5. COP change of heat pumps versus increasing of the evaporator fluid temperature [2].

Air source heat pump (ASHP) Widely used due to the following advantages: no pollution, simple operation, easy heat source, high energy efficiency, low maintenance cost, etc. [3].

The disadvantage of ASHP is that the thermodynamic performance of air source heat pump systems decreases depending on a decrease in the air temperature during the heating seasons and increase in the air temperature in cooling seasons [2]. Another problem is frost formation, that would occur on the outdoor heat exchanger coil surfaces (evaporator) in cold climates, thereby reducing airflow area due to the blockage caused by frost layer and reducing the ability to absorb heat from the outdoor environment and as a result can cause performance degradation. In ASHP applications, the frost should therefore be removed to improve the operation performance and protect the ASHP system [3, 5].

Many researchers offer a lot of different defrosting methods, but most widely used is reversed cycle defrosting, which can protect the ASHP system and improve the operation performance, but may degrade the indoor thermal comfort of occupants and also ask for much more energy, time, and cost to create the necessary conditions [3].

According to the [3] research (Fig. 6), in conditions of Harbin, China, the ASHP system COPs showed low values (1.04–2.44) for the three days with high indoor temperatures (19.8–24.2 °C) and low outdoor temperatures (from –20.9 to –10.4 °C). The ASHP showed no obvious frost due to the low relative humidity (27–37%) for the outdoor air, so it can therefore be applied in building heating for people in cold regions [3].

The cost of the proposed ASHP or AWHP (air to water heat pump) systems was found to be lower compared to an equivalent ground source heat pump. Investment costs for air-to-air heat pump system are 1000–3500, for air-to-water 3000–12000, for ground source 5500–20000 Euro, including VAT [12]. The COP range reported by the manufacturers for AWHP systems (Fig. 7) is 2.0–2.9 for 2 °C and 1.5–2.4 for –15 °C [13].

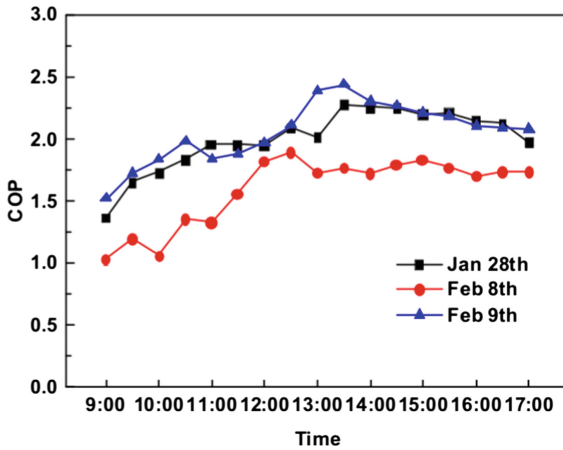


Fig. 6. ASHP System COPs at different times [3].

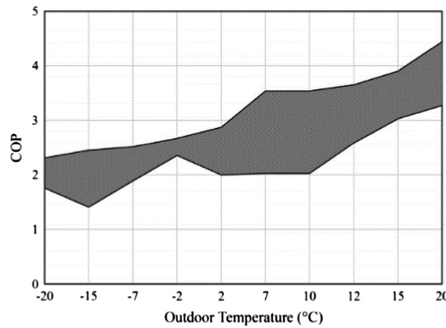


Fig. 7. COP range of various commercially available AHP systems [13].

3 Results

As it can be seen from review of existing studies, climatic condition plays significant role in selection of proper heat pump and its efficient operation. Figure 8 provides analysis of outdoor air temperature fluctuation during the year. While Fig. 9 presents data on soil temperature distribution.

According to the Fig. 8, there are 1742 h (72.6 full days) when the dry-bulb temperature is below or equal to 0 °C, so there is big risk for frost formation in the ASHP. There are 210 h (8.8 full days) when the temperature is below or equal to -10 °C, that may result in low COP value in the ASHP. Maximal temperature 28.7 °C, minimal -21.0 °C.

According to Fig. 9, minimum soil temperature for all depths is reached in the beginning of February, so for the future researches can be used following soil temperature dependence from depth (Table 4).

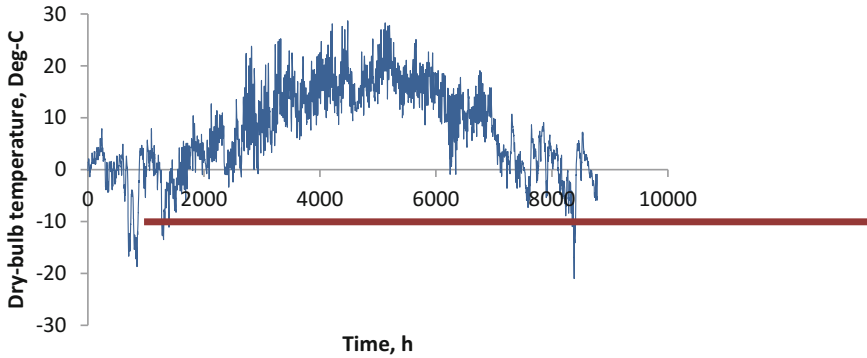


Fig. 8. Dry-bulb temperature during the year in Riga

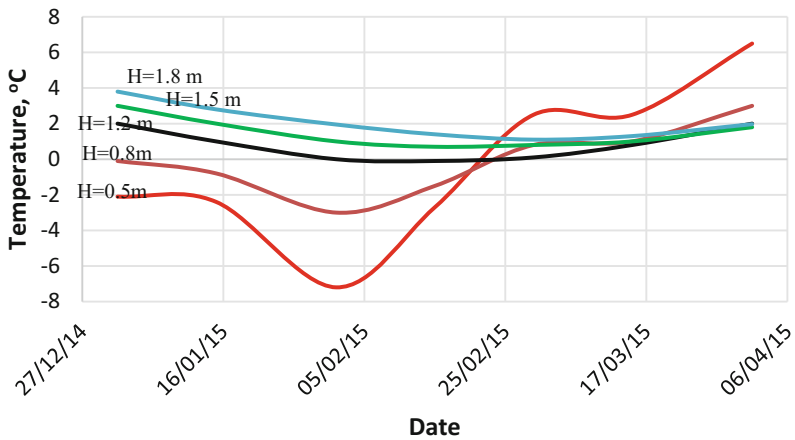


Fig. 9. Soil temperature distribution during the cold period for different depths in Riga. Soil thermal conductivity 2.0 W/(m·K), groundwater depth 5 m.

Table 4. Soil temperature dependence on depth in the beginning of February in Riga.

Depth, m	Temperature, °C
0.0	Outdoor temperature
0.5	-7
0.8	-3
1.2	0
1.5	1
1.8	2

4 Discussion

Literature review shows that heat pump is the great alternative house heating and cooling system that allows to decrease the impact on the environment due to the ecological compatibility of the system, save money in long period comparing with other systems, escape dependence on natural gas, oil, coal etc. prices, be safe, because heat pump is as dangerous as any household appliance.

Thanks to mentioned advantages, the popularity of using heat pumps in Baltic region increase, but, unfortunately, there are lack of studies about the system efficiency after 10–20 years for Latvia and Baltic region. Speaking about ground source heat pumps, the most common ground heat exchanger in Baltic region is horizontal due to lower price and easier installation, so the soil temperature fluctuation near the earth surface is important. It is important to take into account outdoor air fluctuation for the air source heat pumps too.

It might be good to get experimental data from already installed heat pumps and compare theoretical data with real situation.

5 Conclusions

There are different types of heat pumps according to the heat sources. The most popular are GSHP (Ground source heat pump) and ASHP (Air source heat pump). The COP (coefficient of performance) of GSHP usually is bigger (3–5) than of ASHP (1–3) in cold climate but GSHP requires bigger initial costs (5500–20000 Euro comparing to 1000–12000 Euro for ASHP) and area for installation. WSHP (Water source heat pump) has got an advantage over both above mentioned systems because of absence of thermal imbalance comparing with GSHP and more constant temperature comparing with ASHP, but WSHP requires a water reservoir (lake, river, groundwater etc.), so cannot be used everywhere.

The main problem of GSHP is the soil thermal imbalance which results in soil temperature drop for 3–12 °C during a 20-year operation. This problem can be solved by using solar collectors. As we can see from this paper results, the soil temperature in February rapidly decrease moving near the earth surface and the maximum frost depth is almost 0.5 m that can reduce the COP of Ground Source Heat Pump, especially if it take more heat from the soil than soil can accumulate during summer period.

All types of heat pumps may have problems in cold regions, such as the COP decrease during the long exploitation time and depending on outdoor temperature, but possible solutions for each problem exist, so it is possible to use heat pump systems in cold regions.

Acknowledgments. This study was supported by European Regional Development Fund project Nr. 1.1.1.1/16/A/048.

“NEARLY ZERO ENERGY SOLUTIONS FOR UNCLASSIFIED BUILDINGS” Nr. 1.1.1.116A048.

NATIONAL
DEVELOPMENT
PLAN 2020



EUROPEAN UNION
European Regional
Development Fund

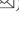




INVESTING IN YOUR FUTURE

References

1. Gaigalish, V., Skema, R., Marcinauskas, K., Korsakiene, I.: A review on heat pumps implementation in Lithuania in compliance with the national energy strategy and EU policy. *Renew. Sustain. Energy Rev.* **53**, 841–858 (2016)
2. Çakır, U., Çomaklı, K., Çomaklı, Ö., Karlı, S.: An experimental exergetic comparison of four different heat pump systems working at same conditions: as air to air, air to water, water to water and water to air. *Energy* **58**, 210–219 (2013)
3. Zhang, Y., Ma, Q., Li, B., Fan, X., Fu, Z.: Application of an air source heat pump (ASHP) for heating in Harbin, the coldest provincial capital of China. *Energy Build.* **138**, 96–103 (2017)
4. Zou, S., Xie, X.: Simplified model for coefficient of performance calculation of surface water source heat pump. *Appl. Therm. Eng.* **112**, 201–207 (2017)
5. Emmi, G., Zarrella, A., De Carli, M., Galgaro, A.: An analysis of solar assisted ground source heat pumps in cold climates. *Energy Convers. Manag.* **106**, 660–675 (2015)
6. You, T., Wu, W., Shi, W., Wang, X., Li, X.: An overview of the problems and solutions of soil thermal imbalance of ground-coupled heat pumps in cold regions. *Appl. Energy* **177**, 515–536 (2016)
7. Qian, H., Wang, Y.: Modeling the interactions between the performance of ground source heat pumps and soil temperature variations. *Energy. Sustain. Dev.* **23**, 115–121 (2014)
8. Xi, C., Lin, L., Hongxing, Y.: Long term operation of a solar assisted ground coupled heat pump system for space heating and domestic hot water. *Energy Build.* **43**, 1835–1844 (2011)
9. You, T., Wu, W., Wang, B., Shi, W., Li, X.: Dynamic soil temperature of ground-coupled heat pump system in cold region In: *Proceedings of 8th International Symposium on Heating, Ventilation and Air Conditioning*, vol. 2, pp. 439–448 (2013)
10. Xie, H., He, S., Fu, Y.: Optimization design and compare of different solar-ground source heat pump system of office building in cold regions. Paper Presented at IOP Conference Series: Earth and Environmental Science, vol. 40, no. 1 (2016). <https://doi.org/10.1088/1755-1315/40/1/012023>
11. Repbaslı, A., Biyik, E., Ekren, O., Gunerhan, H., Araz, M.: A key review of wastewater source heat pump (WWSHP) systems. *Energy Convers. Manag.* **88**, 700–722 (2014)
12. Brēmere, D., Indrikšone, D., Aleksejeva, I.: Energy efficient and ecological housing in Finland, Estonia and Latvia: current experiences and future perspective (2013)
13. Asaee, S., Ugursal, V., Beausoleil-Morrison, I.: Techno-economic feasibility evaluation of air to water heat pump retrofit in the Canadian housing stock. *Appl. Therm. Eng.* **111**, 936–949 (2017)
14. Regulations Regarding Latvian Building Code LBN 003-15 “Construction climatology”. (in Latvian)

15. Aronova, E., Vatin, N., Murgul, V.: Design energy-plus-house for the climatic conditions of Macedonia. *Procedia Eng.* **117**(1), 771–779 (2015). <https://doi.org/10.1016/j.proeng.2015.08.231>
16. Harmati, N., Jakšić, Z., Vatin, N.: Energy consumption modelling via heat balance method for energy performance of a building. *Procedia Eng.* **117**(1), 791–799 (2015). <https://doi.org/10.1016/j.proeng.2015.08.238>
17. Korniyenko, S., Vatin, N., Gorshkov, S.: Thermophysical field testing of residential buildings made of autoclaved aerated concrete blocks. *Mag. Civ. Eng.* **64**(4), 10–25 (2016). <https://doi.org/10.5862/MCE.64.2>
18. Murgul, V., Vatin, N., Zayats, I.: The role of the solar light quantity in the architectural forming of buildings. *Procedia Eng.* **117**(1), 824–829 (2015). <https://doi.org/10.1016/j.proeng.2015.08.146>
19. Han, Z., Yang, J., Lin, M., Zhang, Y.: Analysis of the thermal effect about groundwater flowing to the nest of tubes heat transfer (2017). https://doi.org/10.1007/978-3-319-26950-4_26
20. Liu, H., Zhou, Q., Zhao, H.: Experimental study on cooling performance and energy saving of gas engine-driven heat pump system with evaporative condenser. *Energy Convers. Manag.* **123**, 200–208 (2016). <https://doi.org/10.1016/j.enconman.2016.06.044>
21. Yang, W., Cao, X., He, Y., Yan, F.: Theoretical study of a high-temperature heat pump system composed of a CO₂ trans critical heat pump cycle and a R152a subcritical heat pump cycle. *Appl. Therm. Eng.* **120**, 228–238 (2017). <https://doi.org/10.1016/j.applthermaleng.2017.03.098>

Chlorella Microalga Biomass Cultivation for Obtaining Energy in Climatic Conditions of St. Petersburg

Natalia Politaeva¹ , Tatiana Kuznetsova¹ ,
Yulia Smyatskaya¹ , Iryna Atamaniuk² , and Elena Trukhina¹ 

¹ Peter the Great St. Petersburg Polytechnic University,
Polytechnicheskaya str., 29, 195251 Saint-Petersburg, Russia
conata07@list.ru

² Hamburg University of Technology, Hamburg, Germany

Abstract. There is a special approach of modern science, connected with production and use of biofuel, received from the biomass that is widely developing nowadays. In current paper conditions of cultivation of microalgae *Chlorella sorokiniana* for further use as a source of receiving biofuel and biogas are studied. In comparison with other microalgae, types of *Chlorella* have higher efficiency of photosynthesis. Climatic conditions of St. Petersburg are less suitable for cultivation of *Chlorella*, than conditions of warm regions. But it is possible to receive a sufficient gain of biomass with the help of creation of additional factors of cultivation. According to St. Petersburg conditions, June, July and August are optimum for cultivation of microalgae. In this study cultivation of *Chlorella sorokiniana* under natural conditions of St. Petersburg was carried out, at natural lighting, without aeration when hashing once a day. Control experiment was made on populations which were grown up in vitro at a stable temperature in the same conditions of aeration and also on populations grown up with aeration and periodic hashing. The main condition of cultivation influencing growth of number of cells are aeration and hashing; in these conditions number of cells of algae in 16 days increases by 3.5 times. The same process made under natural conditions in St. Petersburg increases number of cells only by two times. The negative impact of environmental factors is shown in increase of part of dead cells in population that is revealed by means of coloring of temporary medicines by methylene blue. Thus, *Chlorella sorokiniana* cultivation is possible in the conditions of St. Petersburg, however it is necessary to correct cultivation conditions with aeration and periodic cultivation. The scheme of receiving valuable components and biofuel from the cultivated biomass of microalgae *C. sorokiniana* has been offered in this work.

Keywords: Cultivation · Microalgae · *Chlorella sorokiniana* · *C. vulgaris*
Biofuel · Biogas · Biomass · Efficiency

1 Introduction

Unrenewable energy sources (oil, gas) are tried to be replaced by renewable energy sources (such as sun, wind, water, geothermal sources, biofuel) in many countries. Nowadays those branches of studying which are connected with production and use of biofuel, including biofuel, produced from biomass, are widely developing. From the report “The condition of biofuel industry in 2016”, it’s shown that electric power, produced from biomass in 2015 has been grown by 8% a year, with especially high gear in China, Japan, Germany and Great Britain. According to forecasts, annual investments into biofuel till 2020 are estimated in \$400–500 billion [1].

It’s known, that some raw materials, divided on three generations depending on the ways of their production, has been used as a source of biofuel.

Raw materials of the first generation are crops with the high contents of fats, starch and sugars. The nonfood remains of the cultivated plants, grass and wood are called the second generation of raw materials. It’s producing is much less expensive than the one of the cultures of first generation. Such raw materials contain cellulose and lignin. They can be burned (as it was traditionally done with firewood), gasified (with production of combustible gases as a result) or they can carry out pyrolysis. The main shortcomings of the second generation of raw materials are: occupied land resources and relatively low return from unit of area.

The third generation of raw materials is an algae. It doesn’t demand land resources, can have high concentration of biomass and high speed of reproduction. Fuel of the third generation is widely used abroad. So The Department of energy of the USA from 1978 to 1996 investigated algae with the high content of oil according to the “Aquatic Species Program” program. Researchers came to a conclusion that California, Hawaii and New Mexico are suitable for industrial production of seaweed in open ponds. During the next 6 years an alga were grown up in ponds of 1000 m². The New Mexico pond showed high efficiency in capture of CO₂. The productivity was more than 50 gr. algae with 1 m² in day. It has turned out that 200 thousand hectares of ponds can produce the fuel sufficient for annual consumption of 5% of cars of the USA and 200 thousand hectares are less than 0.1% of the lands of the USA which are suitable for cultivation of algae. The technology still has set of problems. For example, algae prefers high temperature, the desert climate is suitable for their production, but a certain temperature regulation at night differences of temperatures is required. In the late nineties current technology didn’t get to industrial production because of the low cost of oil.

Except of cultivation of seaweed in open ponds there are technologies of cultivation of seaweed in the small bioreactors located near electric power stations. Waste heat of thermal power station is capable to cover to 77% of needs for heat necessary for cultivation of seaweed. This technology doesn’t demand hot desert climate.

The Spanish scientists found one of species of microalgae which are capable to breed much quicker, than other biological species in case of a certain lighting. Microalgae grow in the plastic cylinder with a diameter of 70 cm and of 3 m. Seaweed breed of fission. They divide each twelve hours, and gradually water in the cylinder turns into green dense material. Once a day contents of the cylinder are exposed to centrifugation. The rest represents almost absolute biofuel. The part of this weight

saturated with fats transforms to the biodiesel, and hydrocarbons — to ethanol. The Spanish firm “Bio-Fuel-Systems” plans not only to produce fuel from algae, but also to reduce the carbon dioxide level which is formed by electricity generation with the use of organic types of fuel [2].

The large energy Japanese company “Tokyo Gas Co” suggested to use the project of building the plant where the energy will be produced from algae. The methane, emitted from small chopped up seaweed will be used as a fuel for the work of gas generators at the station. For a number of the Japanese prefectures, including capital, pollution of the coast by seaweed remains a serious environmental problem. Rotting algae quite often allocates a fetid smell and spoils a landscape. Meanwhile the newest development of the Japanese experts suggests to solve this problem with an economic benefit.

The experimental model of the plant with the gas electric generator which has already worked in laboratory for several years allows to destroy up to 1 ton of seaweed in a day. As a result of the process about 9.8 kW of the electric power are developed. This pilot installation allows to receive about 20–30 m³ of methane per month – this volume is enough to reduce exactly a half of monthly expense on electricity of an average family [3].

“The Shell” and “HR Biopetroleum” companies have presented the project of establishment on the Hawaiian Islands of plant where obtaining vegetable oil from microalgae and his further processing to biofuel will be set.

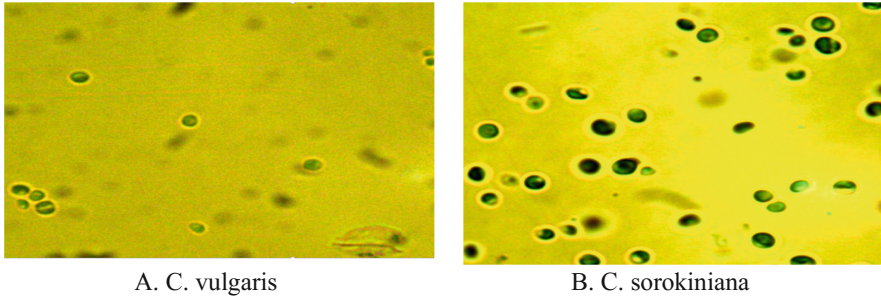
The aviation industry has also declared the beginning of developments of the use of algae as raw materials for production of aviation fuel. The “Boeing” company has reported that production of aviation biofuel can become an alternative to the biodiesel made from seaweed in the future. Specialists of “Boeing” consider that algae from which can be received in 150–300 times more oils, than from soy will become optimum raw materials for production of biofuel. According to these data, biofuel from algae is the future for aircraft. So, if all fleet of airlines of the world as of 2004 used 100% the biofuel received from algae it would be necessary for 322 billion liters of oil. 3.4 million hectares of ground is necessary for cultivation of these algae. As accepted in calculation, 6500 L are annually turned out from one hectare. For these purposes it is possible to use lands which aren’t suitable for cultivation of food agricultural cultures [4].

Despite of wealthy natural energy resources, this direction is also actively developing in Russia. Scientists from Tambov have picked up conditions of cultivation of *Chlorella vulgaris* with high content of lipids for further use as biofuel [5].

In comparison with other microalgae, the types of *Chlorella* have higher efficiency of photosynthesis [6]. According to an experimental data, *Chlorella sorokiniana* is more productive, than *C. vulgaris* [7], which are widely studied in the Russian Federation.

Another purpose of the current work is development of the closed cycle for obtaining energy. Object of our researches are microalgae *Chlorella corokiniana*. It’s species are rarely studied by Russian scientists, but are widely studied in foreign countries.

Chlorella corokiniana cells are authentically larger, a form is the most roundish (the coefficient of oblongness comes nearer to 1) unlike the cells of *C. vulgaris* (Fig. 1).



A. *C. vulgaris*

B. *C. sorokiniana*

Fig. 1. Microscopic picture of populations of *Chlorella* cells.

Cultivation conditions. The main regions for cultivation of microseaweed are situated in rather warm climatic zones. We have investigated a possibility of cultivation of microalgae on the territory of the Northern Capital of Russia, St. Petersburg.

The analysis of the minimum temperatures within a year allows to determine suitable time for natural *Chlorella sorokiniana* cultivation. In June, July and August probable minimum temperatures exceed on average 10 °C (Fig. 2).

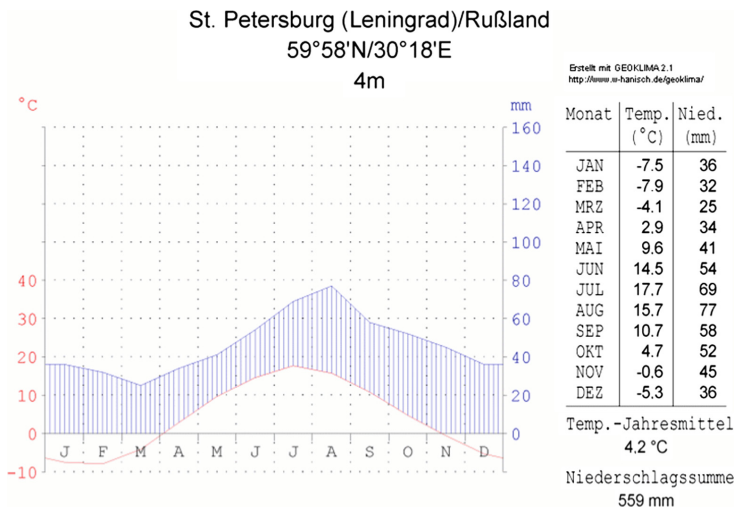


Fig. 2. Dynamics of the maximum and minimum air temperatures within a year in St. Petersburg (Russia).

Cultivation has been carried out from June, 12 to June, 27, 2017 at natural lighting, temperature, without aeration, hashing once a day. Control group: the population of *C. sorokiniana* which is grown up in vitro at a constant optimum temperature of 19–23 °C and lighting by a lamp day light (2600 lux) (Table 1). In vitro cultivation was carried out in two options:

Table 1. Cultivation conditions.

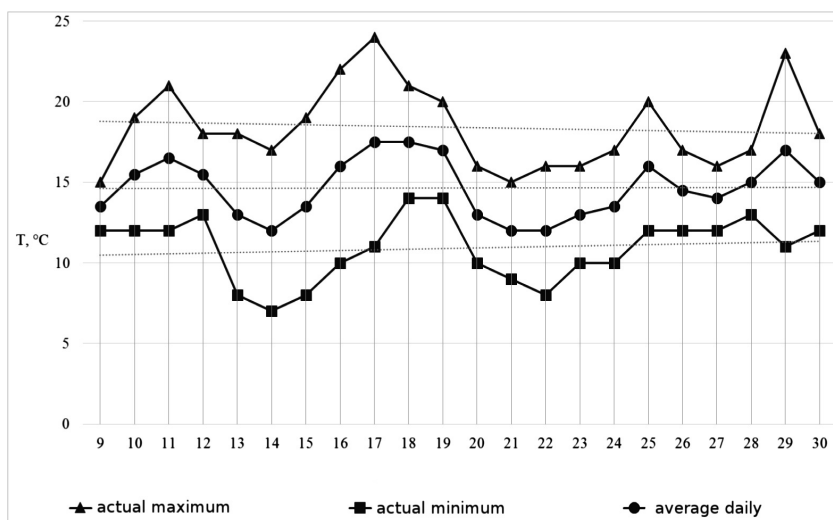
Conditions	№	Lightning, lux	Temperature, °C	Hashing	Aeration
Laboratory (Control)	1	2600	20–23	+	+
	2	2600	20–23	±	–
Experimental	3	2000–4500 (noon hours)	7–25	±	–

1. at periodic hashing by the magnetic MS-20 A mixer (15 min in 2 h) and constant aeration by air by means of the bubbling Xilong AP-003 device (5 W, 2Kh2, 5 l/mines);
2. when hashing 1 times a day, without aeration.

Cultivation was carried out in the mode day/night.

Under natural conditions during cultivation the dispersion of temperatures within a day was on average 7.44 ± 0.65 °C that can be the limiting factor.

The maximum temperatures fluctuated from 15 to 23 °C (Fig. 3). The intensity of lighting reached the 4000 lux in sunny days, in cloudy – 2000. The solar interval was not more than 5 o'clock. Average illumination was 3000–3500 lux in the afternoon. Such combination of environmental factors can become stressful for *C. sorokiniana* population.

**Fig. 3.** The schedule of temperatures in June, 2017, St. Petersburg.

Microalgae grew up on nutrient medium, developed by foreign scientists, so it's mineral structure included macro- and microminerals [8].

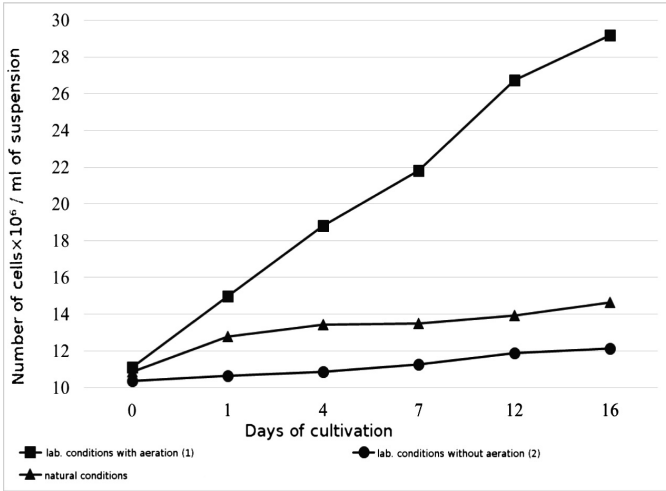


Fig. 4. Dynamics of change of number of *C. sorokiniana* cells at periodic cultivation.

Indicators of growth of population. The initial optical density of seaweed in nutrient medium was 0.30–0.35 ($1.4\text{--}2.4 \times 10^6$ cells/ml). Intensive growth in samples was observed on the 1st days of cultivation (Fig. 4). After 16 days of cultivation under the influence of natural conditions without aeration a twice increase of cells has been fixed, the similar growth rates are observed in vitro (in option without aeration and hashing). The intensive air barbotage of *C. sorokiniana* suspension allows to intensify processes of assimilation of CO_2 that promotes an intensification of exchange processes and reproduction of cells of a *Chlorella* that is reflected in the schedule of cultivation (Fig. 4, option 1).

Table 2. The mathematical description of curves of growth of *C. sorokiniana* population in the conditions of St. Petersburg.

Conditions	The equation of dependence of optical density from cultivation time	Size of reliability of approximation, R^2
Laboratory (Control)	$Y = 0.0525x + 0.4206$	0.9596
	$Y = 0.0054x + 0.3571$	0.9806
Experimental	$Y = 0.0086x + 0.2806$	0.7241

The equations of dependence of number of cells in suspension of seaweed from cultivation time and also the size of reliable approximation (Table 2) are defined for all options.

Thus, an environment of June–July, 2017 in St. Petersburg doesn't make radical negative impact on growth of number of cages in population. However, it is necessary to intensify growth of population due to hashing and aeration. Periodic hashing and aeration have allowed to intensify growth of population in vitro. In 16 days of

cultivation the number of cells in suspension has increased by 3.6 times. Therefore, this technique will provide cheap raw materials for receiving biofuel in the Northern region using its climatic potential. The next flowchart (Fig. 5) has been developed to use the microalgae in the national economy. Economically effective method of extraction of products with high value added, such as lipids and carotinoids (Fig. 5) is developed from the received biomass of microalgae *C. sorokiniana*. Part of residual biomass will be used as adsorbent for purification of industrial sewage of heavy metals. From the other hand, the rest of microalgae after extraction and the fulfilled adsorbents can be used as co-substratum for an anaerobic fermentation for the purpose of receiving biogas. The biogas consisted generally of methane (CH_4) and carbon dioxide (CO_2) has to be divided into components. Methane is recommended to be used for economic needs, as a supply of all process with heat and electricity. Carbon dioxide which is formed in the process of fermentation and after combustion of methane for obtaining energy will be used at a stage of cultivation of microalgae *C. sorokiniana* as a carbon source for photoautotrophic synthesis of biomass.

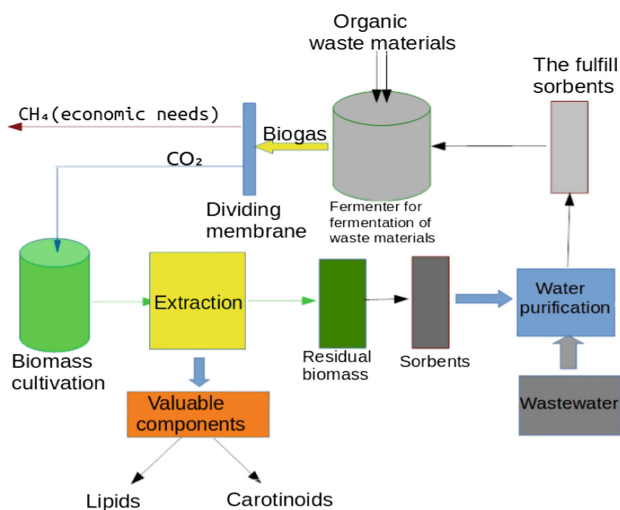


Fig. 5. The scheme of processing of the *C. sorokiniana* biomass received as a result of cultivation in the conditions of St. Petersburg.

2 Conclusions

1. As a result of the literary review it has been shown that use of microalgae as biofuel is very violently developed abroad and is also very relevant for our country. For this purpose it is necessary to study an opportunity of cultivation and to pick up cultivation conditions as in the example made in St. Petersburg.
2. In the conditions of St. Petersburg three months – June, July, August are suitable for cultivating on temperature condition. However, fluctuations of temperatures within a day and the minimum temperatures can become the limiting factor of growth of *C. sorokiniana* population.





3. Within 16 days of cultivation of population of *C. sorokiniana* in June, 2017 in St. Petersburg without aeration and hashing 1 times a day, the number of cells in suspension has increased twice and it's similar to laboratory conditions with the same mode of aeration and hashing.
4. The intensification of growth of population of cells of *C. sorokiniana* cultivation under natural conditions of St. Petersburg is possible with additional aeration and periodic hashing. Cultivation is possible when using additional conditions: aerations, hashing.
5. The scheme of receiving valuable components and biofuel from the cultivated biomass of *C. sorokiniana* microalgae has been offered.

Acknowledgements. This work was performed within the implementation of Federal Targeted Programme for Research and Development in Priority Areas of Development of the Russian Scientific and Technological Complex for 2014–2020, the project «Development and implementation of innovative biotechnologies for treatment of microalgae *Chlorella sorokiniana* and duckweed *Lemna minor*» (Agreement № 14.587.21.0038).

References

1. Derbysheva, J.: The report of biofuel industry condition in 2016. Markets and prospects. Information-analytical brunch, association of participants of the biofuel ENBIO market (2017)
2. <https://hlorella.jimdo.com>. Accessed 27 Aug 2017
3. Sarsekeyeva, F., Ussebaeva, A., Zayadan, B., Mironov, K., Sidorov, R., Kozlova, A., Kupriyanova, E., Sinetova, M., Los, D.: Isolation and characterization of a new cyanobacterial strain with a unique fatty acid composition. *advances. Adv. Microbiol.* **4**, 15 (2014)
4. <http://www.bio-tec.ch/ru/a26-tehnologiya-BIOTEC.html>. Accessed 27 Aug 2017
5. Dvoretzkiy, D., Dvoretzkiy, S., Temnov, M.: The technology of obtaining lipids from microalgae. FSBOU HE “TSTU”, Tambov (2015). ISBN 978-5-8265-1507-5
6. Andrade, C., Andrade, L.: An overview on the application of genus *Chlorella* in biotechnological processes. *J. Adv. Res. Biotechnol.* (2017). www.symbiosisonlinepublishing.com. Accessed 27 Aug 2017
7. Kobayashi, N., Noel, E., Barnes, A., Watson, A., Rosenberg, J., Erickson, G., Oyler, G.: Characterization of three *Chlorella sorokiniana* strains in anaerobic digested effluent from cattle manure. *Bioresour. Technol.* **150**, 377–386 (2013)
8. Richmond, A.: *Handbook of Microalgal Culture: Biotechnology and Applied Phycology*. Blackwell Science, Hoboken (2004)
9. Yao, L., Shi, J., Miao, X.: Mixed wastewater coupled with CO₂ for microalgae culturing and nutrient removal. *PLOS ONE*, pp. 1–16 (2015). <https://doi.org/10.1371/journal.pone.0139117>

Energy Performance Simulation and Evaluation of Various Construction Types for a Residential Building (International ODOO Project)

Norbert Harmathy¹(✉) , Jenő Kontra¹ , Vera Murgul^{2,3} ,
and Zoltán Magyar¹ 

¹ Department of Building Energetics and Building Service Engineering,
Faculty of Architecture, Budapest University of Technology and Economics,
Műgyetemrakpart 3, Budapest 1111, Hungary
harmathy@egt.bme.hu

² Moscow State University of Civil Engineering,
Yaroslavskoe shosse, 26, Moscow 129337, Russia

³ Peter the Great St. Petersburg Polytechnic University,
Politechnicheskaya st., 29, St. Petersburg 195251, Russia

Abstract. The Hungarian ODOO residential building project has achieved an outstanding result on the international Solar Decathlon Competition which is an international innovation competition between the best universities all around the world, organized by the U.S. Department of Energy and the Spanish Government since 2002. The goal of the contest is to popularize the usage of solar energy in architectural solutions and to call into being the social and market support of green technologies. The Hungarian ODOO project according to the total scoring reached the 6th place from 18 participant countries. In the categories of Engineering and construction, and Comfort conditions it won the 2nd place and in energy efficiency category the 3rd place.

The presented research motivation was to investigate the efficient utilization of the existing ODOO building and to assess project quality from the aspect of energy efficiency, building construction characteristics and envelope glazing properties. In order to achieve a detailed understanding of the energy demands and construction-component-operation interaction we utilized multi-zone energy modeling and dynamic energy simulation software. The results presented that the final energy performance can be strategically influenced if a synergetic and deterministic methodological approach is applied.

Keywords: Energy management · Transport buildings and structures
Energy performance simulation

1 Introduction

This research presents and elaborates strategic energy performance planning and selection of adequate building construction and application of energy efficiency measures. The research was conducted with the utilization of dynamic building energy

performance simulation techniques within the international Hungarian ODOO project [1]. Based on the rules of the international Solar Decathlon competition held in Madrid 2012, the Hungarian ODOO building constructed by a team of students and their supervisors of the Budapest University of Technology and Economics has achieved outstanding results in the field of innovative solar buildings where they applied architectural and technical developments. In the competition every team's task was to design and build a solely solar-powered, energy-efficient, cost-effective, light structured house with the collaboration of the market.

The motivation and research scope was to test the ODOO building's annual energy performance if it would be constructed from different construction types (panels or blocks) and explore its annual energy performance with different thermal insulation, glazing ratio and window variations. It total 15 scenarios were simulated and their energy efficiency justified and comparatively analyzed. The purpose of the research was to formulate a preferable solution for the climate conditions of Budapest. In order to define the energy saving potential three building structures (KLH cross laminated timber, WienerbergerPorotherm and Ytong construction) and glazing types were simulated and analyzed. All multi-zone models contain detailed information that influences the heating and cooling requirements, such as internal heat sources, schedules, air temperature adjustment, air change rate, occupants and schedules.

2 Literature Review

Integrated design process and dynamic energy simulation is widespread in the field of energy performance optimization and strategic planning of building energy efficiency. Dynamic simulation is used in determining construction properties, occupant comfort, HVAC system energy demands, energy conservation techniques etc. [2–6] In one of our previous researches we used multi-criteria optimization methodology to determine an optimal energy retrofit solution in case of adequate envelope glazing selection [7]. Optimal design methods for cooling systems considering cooling load analysis using simulation techniques is a topic of interest respectively [8]. Energetic and environmental performance assessment can be parallel analyzed [8, 9]. Extensions on the urban level were made respectively from the aspect of building envelope design for overall energy efficiency [10].

3 Research Methodology

The annual heating and cooling demands of the 15 scenarios were explored through the following ten steps:

1. Geometric modelling of the reference building and development of a simulation base multi-zone 3D model,
2. Assignment of thermal zones, space types to the multi-zone energy model,
3. Multiplying the multi-zone model and designing two different glazing ratios to the building envelope,

4. Exporting the multi-zone energy model and assigning construction set and building material properties,
5. Assigning internal loads and heat gains to the imported energy model,
6. Assigning glazing type and parameters,
7. Defining operation and maintenance, assigning intervals and comfort parameters,
8. Model conversion to numerical IDF data,
9. Performing multiple simulations on annual basis with hourly time-steps for the climate data of Budapest,
10. Evaluating the annual energy performance and determining the adequate building construction and glazing parameters.

4 Building Energy Performance Simulation

4.1 Multi-zone Thermal Model

The first phase included the modelling of the multi-zone thermal model of the building, since the function of the building represents different zone divisions. The ODOO building is shown in Fig. 1. The multi-zone thermal model was divided into five thermal zones depending from its internal gains and position: Zone 1 bedroom, Zone 2 living room, dining room and kitchen, Zone 3 corridor, Zone 4 bathroom and Zone 5 was the second room.



Fig. 1. ODOO building [1]

The thermal zones include the following incorporated data packages: building construction, climate data, solar gains, internal heat sources (people, lighting, electrical equipment), shading surfaces, building operation and schedules.

The multi-zone thermal model was designed with OpenStudio plug-in [11] for Sketchup [12], since the plug-in enables the 3D OPS format conversion into IDF numerical data, which is importable into EnergyPlus [13] dynamic energy simulation engine.

4.2 Climatological Data

The location and climate data were imported from the Swiss global climatology database Meteonorm 7 [14], since the climate data needs to be converted into EPW extension file, importable into EnergyPlus for dynamic energy simulation. The location of the building is Budapest, Latitude = 47.433°, Longitude = 19.183°, Altitude = 140 m and Climatic zone = III, 3. The imported data are the following: Radiation model = Default (hour); Temperature model = Default (hour), Tilt radiation model (Perez) = Default (hour), Radiation: New period = 1986–2005, Temperature: New period = 2000–2009. The climatological data set included more than 20 thousand values downloaded for research purposes from the satellite database. The dataset included parameters such as air temperature, relative humidity, wind direction and speed, air pressure, mean irradiance of global radiation, mean irradiance of diffuse radiation horizontal, global luminance, etc.

4.3 Simulated Construction Types

The research scope was to determine and evaluate the building's energy performance for three different construction types:

- KLH cross laminated timber
- WienerbergerPorotherm brick construction
- Ytong autoclaved aerated concrete (AAC)

The KLH cross-laminated timber is made from spruce slats stacked atop of each other which are bonded using high press force and formaldehyde free adhesives to form large-format building elements. The elements are statically stressed construction elements and are used as wall, ceiling and roof panels in solid timber construction projects. Thanks to the cross-wise structure of the longitudinal and cross-slats, wood expansion and shrinkage in the panel plane is reduced to an insignificant minimum. At the same time, this raises the structural load capacity and dimensional stability in the panel plane [15]. Cross laminated timber panels' thicknesses of 140 mm and 100 mm, were used in the construction including additional layers which are listed in Table 1.

The Wienerberger system solution facilitates brick-laying and permit the creation of homogeneous, high-quality insulating masonry elements [16]. The insulating ability of the Porotherm clay brick construction is 40–50% higher compared to ordinary clay bricks. The energy simulation was performed for three variations of Porotherm wall construction, which are the following:

- Exterior wall 1; PTH block ClimaProfi, 38 cm
- Exterior wall 2; PTH block ClimaProfi, 2 × 38 cm
- Exterior wall 3; PTH block ClimaProfi, 38 cm + Expanded Polystyrene insulation, 14 cm.

The second exterior wall construction was inspired by the Passive Office Building 2226 by BaumschlagerEberle architect. We wanted to explore the efficiency comparing the double brick wall with ordinary EPS insulation. The roof construction was identical in

Table 1. KLH construction properties

KLH cross laminated timber			
	No.	Layer	Material properties
Exterior wall $U = 0.129 \text{ W/m}^2\text{K}$	1 in.	Hardwood panel	$d = 1.8 \text{ cm}$, $\rho = 720 \text{ kg/m}^3$, $\lambda = 0.16 \text{ W/mK}$
	2	Air layer	$d = 3.5 \text{ cm}$
	3	KLH cross lam. timber panel	$d = 10 \text{ cm}$, $\rho = 500 \text{ kg/m}^3$, $\lambda = 0.13 \text{ W/mK}$
	4	Cellulose insulation	$d = 24 \text{ cm}$, $\rho = 30 \text{ kg/m}^3$, $\lambda = 0.039 \text{ W/mK}$
	5	OSB panel	$d = 1.8 \text{ cm}$, $\rho = 650 \text{ kg/m}^3$, $\lambda = 0.13 \text{ W/mK}$
	6	Air layer	$d = 8 \text{ cm}$
	7 ex.	Hardwood panel	$d = 1.9 \text{ cm}$, $\rho = 720 \text{ kg/m}^3$, $\lambda = 0.16 \text{ W/mK}$
Roof $U = 0.127 \text{ W/m}^2\text{K}$	1 in.	Gypsum board	$d = 2 \text{ cm}$, $\rho = 780 \text{ kg/m}^3$, $\lambda = 0.16 \text{ W/mK}$
	2	Air layer	$d = 14 \text{ cm}$
	3	KLH cross lam. timber panel	$d = 14 \text{ cm}$, $\rho = 500 \text{ kg/m}^3$, $\lambda = 0.13 \text{ W/mK}$
	4	Cellulose insulation	$d = 24 \text{ cm}$, $\rho = 30 \text{ kg/m}^3$, $\lambda = 0.039 \text{ W/mK}$
	5	OSB panel	$d = 1.8 \text{ cm}$, $\rho = 650 \text{ kg/m}^3$, $\lambda = 0.13 \text{ W/mK}$
	6	Waterproofing	$d = 0.05 \text{ cm}$, $\rho = 1120 \text{ kg/m}^3$, $\lambda = 0.19 \text{ W/mK}$
	7 ex.	Metal surface	$d = 0.0015 \text{ cm}$, $\rho = 7680 \text{ kg/m}^3$, $\lambda = 45 \text{ W/mK}$
Floor $U = 0.130 \text{ W/m}^2\text{K}$	1 in.	Hardwood panel	$d = 7 \text{ cm}$, $\rho = 720 \text{ kg/m}^3$, $\lambda = 0.16 \text{ W/mK}$
	2	KLH cross lam. timber panel	$d = 14 \text{ cm}$, $\rho = 500 \text{ kg/m}^3$, $\lambda = 0.13 \text{ W/mK}$
	3	Cellulose insulation	$d = 24 \text{ cm}$, $\rho = 30 \text{ kg/m}^3$, $\lambda = 0.039 \text{ W/mK}$
	4	OSB panel	$d = 1.8 \text{ cm}$, $\rho = 650 \text{ kg/m}^3$, $\lambda = 0.13 \text{ W/mK}$
	5 ex.	Waterproofing	$d = 0.05 \text{ cm}$, $\rho = 1120 \text{ kg/m}^3$, $\lambda = 0.19 \text{ W/mK}$

all scenarios, PTH 60/17 + 4 cm C20/25 concrete layer + total 24 cm EPS insulation. The construction with additional layers is presented in Table 2.

Ytong AAC stands for highly efficient thermal insulation, optimal fire protection, and masonry with excellent load-bearing abilities. Lime, sand, cement, and water – mineral and natural raw materials – form the main ingredients of AAC [17]. The simulation was performed for Ytong Thermo block 40 cm exterior wall construction

Table 2. Wienerberger Porotherm construction properties

Wienerberger Porotherm clay block construction			
	No.	Layer	Material properties
Ext. wall 1 $U = 0.264 \text{ W/m}^2\text{K}$	1 in.	Port. cem. malt.	$d = 1 \text{ cm}, \rho = 1858 \text{ kg/m}^3, \lambda = 0.69 \text{ W/mK}$
	2	PTH ClimaProfi	$d = 38 \text{ cm}, \rho = 740 \text{ kg/m}^3, \lambda = 0.106 \text{ W/mK}$
	3 ex.	Port. cem. malt.	$d = 1.5 \text{ cm}, \rho = 1858 \text{ kg/m}^3, \lambda = 0.69 \text{ W/mK}$
Ext. wall 2 $U = 0.136 \text{ W/m}^2\text{K}$	1 in.	Port. cem. malt.	$d = 1 \text{ cm}, \rho = 1858 \text{ kg/m}^3, \lambda = 0.69 \text{ W/mK}$
	2	PTH ClimaProfi	$d = 38 \text{ cm}, \rho = 740 \text{ kg/m}^3, \lambda = 0.106 \text{ W/mK}$
	3	PTH ClimaProfi	$d = 38 \text{ cm}, \rho = 740 \text{ kg/m}^3, \lambda = 0.106 \text{ W/mK}$
	4 ex.	Port. cem. malt.	$d = 1.5 \text{ cm}, \rho = 1858 \text{ kg/m}^3, \lambda = 0.69 \text{ W/mK}$
Ext. wall 3 $U = 0.129 \text{ W/m}^2\text{K}$	1 in.	Port. cem. malt.	$d = 1 \text{ cm}, \rho = 1858 \text{ kg/m}^3, \lambda = 0.69 \text{ W/mK}$
	2	PTH ClimaProfi	$d = 38 \text{ cm}, \rho = 740 \text{ kg/m}^3, \lambda = 0.106 \text{ W/mK}$
	3	EPS board	$d = 14 \text{ cm}, \rho = 24 \text{ kg/m}^3, \lambda = 0.035 \text{ W/mK}$
	4 ex.	Port. cem. malt.	$d = 1.5 \text{ cm}, \rho = 1858 \text{ kg/m}^3, \lambda = 0.69 \text{ W/mK}$
Roof $U = 0.146 \text{ W/m}^2\text{K}$	1 in.	Port. cem. malt.	$d = 1 \text{ cm}, \rho = 1858 \text{ kg/m}^3, \lambda = 0.69 \text{ W/mK}$
	2	PTH Roof	$d = 17 \text{ cm}, \rho = 650 \text{ kg/m}^3, \lambda = 0.60 \text{ W/mK}$
	3	Concrete C20/25	$d = 4 \text{ cm}, \rho = 2250 \text{ kg/m}^3, \lambda = 1.4 \text{ W/mK}$
	4	EPS board	$d = 14 \text{ cm}, \rho = 24 \text{ kg/m}^3, \lambda = 0.035 \text{ W/mK}$
	5	Waterproofing	$d = 0.5 \text{ cm}, \rho = 1120 \text{ kg/m}^3, \lambda = 0.19 \text{ W/mK}$
	6 ex.	Metal surface	$d = 0.15 \text{ cm}, \rho = 7680 \text{ kg/m}^3, \lambda = 45 \text{ W/mK}$
Floor $U = 0.449 \text{ W/m}^2\text{K}$	1 in.	Ceramic tiles	$d = 0.5 \text{ cm}, \rho = 2700 \text{ kg/m}^3, \lambda = 1.6 \text{ W/mK}$
	2	Port. cem. malt.	$d = 4 \text{ cm}, \rho = 1858 \text{ kg/m}^3, \lambda = 0.69 \text{ W/mK}$
	3	Acc.-therm. ins.	$d = 5 \text{ cm}, \rho = 43 \text{ kg/m}^3, \lambda = 0.03 \text{ W/mK}$
	4 ex.	Lightweight c.	$d = 10 \text{ cm}, \rho = 1280 \text{ kg/m}^3, \lambda = 0.53 \text{ W/mK}$

and Ytong roof construction panels' 20 cm + total 24 cm EPS insulation. The Ytong construction with additional layers is presented in Table 3. The applied glazing constructions in the simulation were tri-pane windows with Argon gas insulation and low-E layer. The first window construction had the following parameters:

- Overall thermal conductivity (U-value) $1.0 \text{ W/m}^2 \text{ K}$
- Solar heat gain coefficient (g - value) 0.34
- Visible light transmittance (V_t - value) 0.63.
- The second window construction had the following parameters:
- Overall thermal conductivity (U-value) $0.7 \text{ W/m}^2 \text{ K}$
- Solar heat gain coefficient (g - value) 0.26
- Visible light transmittance (τ - value) 0.52.

In the simulation two window to wall glazing ratios (WWR) were applied (85 and 50%), resulting in a total number of 15 formulated simulation scenarios.

Table 3. Ytong construction properties

Ytong AAC construction			
	No.	Layer	Material properties
Ext. wall $U = 0.201 \text{ W/m}^2\text{K}$	1 in.	Port. cem. malt.	$d = 1 \text{ cm}$, $\rho = 1858 \text{ kg/m}^3$, $\lambda = 0.69 \text{ W/mK}$
	2	Ytong thermo blo.	$d = 40 \text{ cm}$, $\rho = 350 \text{ kg/m}^3$, $\lambda = 0.084 \text{ W/mK}$
	3 ex.	Port. cem. malt.	$d = 1.5 \text{ cm}$, $\rho = 1858 \text{ kg/m}^3$, $\lambda = 0.69 \text{ W/mK}$
Roof $U = 0.128 \text{ W/m}^2\text{K}$	1 in.	Port. cem. malt.	$d = 1 \text{ cm}$, $\rho = 1858 \text{ kg/m}^3$, $\lambda = 0.69 \text{ W/mK}$
	2	Ytong roof	$d = 20 \text{ cm}$, $\rho = 800 \text{ kg/m}^3$, $\lambda = 0.16 \text{ W/mK}$
	3	Concrete C20/25	$d = 4 \text{ cm}$, $\rho = 2250 \text{ kg/m}^3$, $\lambda = 1.4 \text{ W/mK}$
	4	EPS board	$d = 14 \text{ cm}$, $\rho = 24 \text{ kg/m}^3$, $\lambda = 0.035 \text{ W/mK}$
	5	Waterproofing	$d = 0.5 \text{ cm}$, $\rho = 1120 \text{ kg/m}^3$, $\lambda = 0.19 \text{ W/mK}$
	6 ex.	Metal surface	$d = 0.15 \text{ cm}$, $\rho = 7680 \text{ kg/m}^3$, $\lambda = 45 \text{ W/mK}$
Floor $U = 0.449 \text{ W/m}^2\text{K}$	1 in.	Ceramic tiles	$d = 0.5 \text{ cm}$, $\rho = 2700 \text{ kg/m}^3$, $\lambda = 1.6 \text{ W/mK}$
	2	Port. cem. malt.	$d = 4 \text{ cm}$, $\rho = 1858 \text{ kg/m}^3$, $\lambda = 0.69 \text{ W/mK}$
	3	Acc.-therm. ins.	$d = 5 \text{ cm}$, $\rho = 43 \text{ kg/m}^3$, $\lambda = 0.03 \text{ W/mK}$
	4	Lightweight c.	$d = 10 \text{ cm}$, $\rho = 1280 \text{ kg/m}^3$, $\lambda = 0.53 \text{ W/mK}$

4.4 Dynamic Simulation Input Data

Buildings occupancy is the act of occupying spaces during a period of time. In the following energy simulation, the occupancy is defined according to the:

- Occupancy intensity in the function of occupied period, and
- People activity in the function of the occupied period.

The calculations were performed in case of four occupants and the schedules were assigned primarily for the occupancy intensity in the function of occupied period. The “Run Period Profile” was formulated for weekdays according to the ASHRAE 90.1. The default weekday profile is shown in Fig. 2. The heat gains from occupants was estimated as constant 120 W.

The electric lighting schedule was imported from the ASHRAE 90.1 standard as default schedule for the calculation of additional heat gains. The default schedule can be seen in Fig. 3.

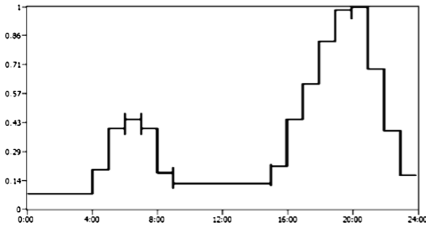


Fig. 2. Default occupancy schedule

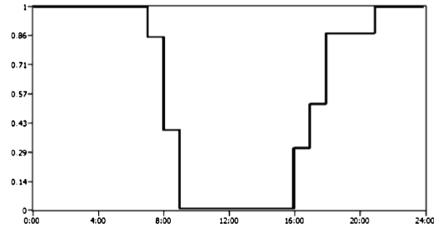


Fig. 3. Default lighting schedule

The air temperature limits in the thermal zones were defined according to occupant comfort requirements. During the spring and summer period from the 15th of April until the 15th of October the air temperature boundaries ranged from 23 °C to 26 °C, specified for a typical average daily interval from 6:00 h to 22:00 h.

During the autumn and winter season from the 16th of October until the 14th of April the minimum allowed mean air temperature was 20 °C and maximum was 25 °C, in accordance with the Hungarian 7/2006 TNM regulation [18] and indoor air temperature requirements.

The air change rate in the energy model was estimated as a constant 0.5 1/h according to the 7/2006 TNM regulation [18], respectively. The simulation was performed with hourly time-steps on an annual basis of 8760 h.

5 Results and Discussion

Energy performance simulation results.

The research included 15 simulations in total and the annual energy performance of all scenarios were compared and evaluated which were the following:

- Scenario 1: KLH cross laminated timber construction, glazing 1, WWR 85%
- Scenario 2: KLH cross laminated timber construction, glazing 2, WWR 85%
- Scenario 3: KLH cross laminated timber construction, glazing 2, WWR 50%
- Scenario 4: WienerbergerPorotherm block construction with 38 cm PTH
- ClimaProfi exterior wall, glazing 1, WWR 85%
- Scenario 5: WienerbergerPorotherm block construction with 38 cm PTH
- ClimaProfi exterior wall, glazing 2, WWR 85%
- Scenario 6: WienerbergerPorotherm block construction with 38 cm PTH
- ClimaProfi exterior wall, glazing 2, WWR 50%
- Scenario 7: WienerbergerPorotherm block construction with 2 * 38 cm PTH
- ClimaProfi exterior wall, glazing 1, WWR 85%
- Scenario 8: WienerbergerPorotherm block construction with 2 * 38 cm PTH
- ClimaProfi exterior wall, glazing 2, WWR 85%
- Scenario 9: WienerbergerPorotherm block construction with 2 * 38 cm PTH
- ClimaProfi exterior wall, glazing 2, WWR 50%
- Scenario 10: WienerbergerPorotherm block construction with 38 cm PTH
- ClimaProfi exterior wall + 14 cm EPS board insulation, glazing 1, WWR 85%

- Scenario 11: WienerbergerPorotherm block construction with 38 cm PTH
- ClimaProfi exterior wall + 14 cm EPS board insulation, glazing 2, WWR 85%
- Scenario 12: WienerbergerPorotherm block construction with 38 cm PTH
- ClimaProfi exterior wall + 14 cm EPS board insulation, glazing 2, WWR 50%
- Scenario 13: Ytong AAC with 40 cm Thermo block exterior wall, glazing 1, WWR 85%
- Scenario 14: Ytong AAC with 40 cm Thermo block exterior wall, glazing 2, WWR 85%
- Scenario 15: Ytong AAC with 40 cm Thermo block exterior wall, glazing 2, WWR 50%.

The annual energy demand of the KLH cross laminated timber construction for the first three scenarios is shown in Fig. 4.

From the comparison of the KLH scenarios it was assessed that the reduction of cooling energy demand in comparison with the heating has a far more saving potential. In scenario 1 the cooling demand is approximately 2.5 times higher according to the heating demand. In conclusion these demands can be equalized if adequate measures are performed, such as WWR reduction of and glazing U-value reduction. Significantly, the visual comfort considering natural day lighting has to be maintained.

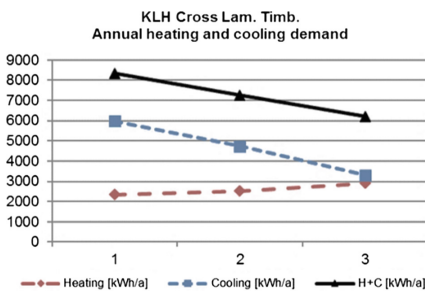


Fig. 4. Energy performance of Scenarios 1–3, KLH cross laminated timber construction

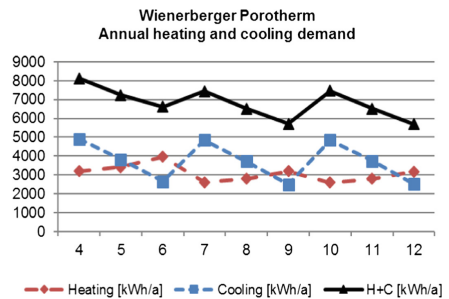


Fig. 5. Energy performance of Scenarios 4–12, WienerbergerPorotherm brick construction

The Wienerberger Porotherm block construction presented even a more significant cooling energy reduction according to the KLH cross laminated timber. The difference between the previous KLH scenario 3 and the Porotherm construction is that the equal heating and cooling demand can be achieved in the second step, scenario 5, as shown in Fig. 5. By improving further, the glazing’s U-value the cooling demand is lower in all Porotherm scenarios 6, 9 and 12.

The annual energy demand of the Ytong ACC construction in case of scenarios 13–15 the results can be seen in Fig. 6. The high thermal characteristics of the Ytong Thermo block positively contributes to the buildings energy performance.

Without additional requirement for thermal insulation the Ytong ACC construction provides closely equal heating and cooling demands as in scenario 14. With the

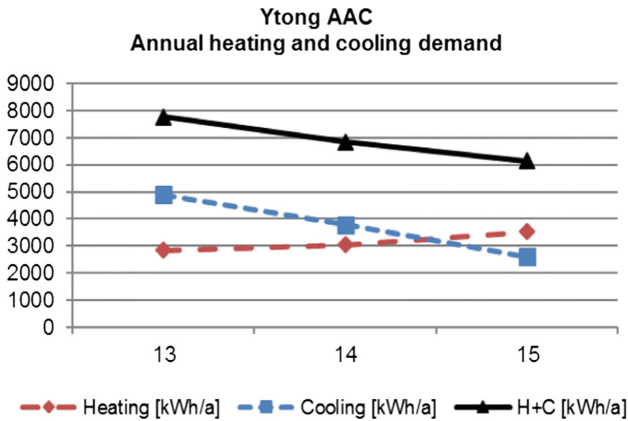


Fig. 6. Energy performance of Scenarios 13–15, WienerbergerPorother brick construction

improvement of the glazing’s thermal characteristics the cooling demand is reduced, resulting in heating demand increment.

The KLH cross laminated constructions advantage is its light weight support structure and high thermal insulation property when combined with 24 cm cellulose insulation. The low heat storage capacity has a negative effect on the heating energy demand. The results demonstrate that if the WWR is reduced from 85% to 50% and the preferred three-layer windows heat transfer coefficient reduced from 1.0 W/m² K to 0.7 W/m² K, then the annual cooling energy demand can be reduced approximately 42% (28 kWh/m²/year). In contrary, the heating energy consumption will be higher by 20% (6 kWh/m²/year), because of reduced internal solar energy gains during the winter period. Thus, the total annual energy reduction equals 22 kWh/m²/year.

The WienerbergerPorotherm block construction’s high thermal insulation characteristics and thermal storage capacity positively influence the buildings heating and cooling energy demand. Three variations of exterior wall construction were simulated and their performance assessed. First of all, the model with 38 cm PTH exterior wall structure had similar annual energy demands compared with the KLH structure. The energy performance of Scenario 3 (KLH, WWR 50%) and Scenario 5 (Porotherm, WWR 85%) is identical, 76 kWh/m²/year. It can be concluded that with higher WWR we can achieve identical energy performance which has further positive effects, such as improvement of visual comfort and reduction of electricity for lighting.

The energy performance of the Porotherm 2 × 38 cm (76 cm) block construction had a slightly lower energy demand according to the single 38 cm thick wall model. However, the lowest energy demand was assessed in scenario 7 it requires only 15% (9 kWh/m²/year) less cooling energy according to the 38 cm PTH structure, while the investment in the exterior walls would double. The results would not be cost effective in this case. Finally, the model with PTH block walls of 38 cm + 14 cm EPS thermal insulation provided the same energy efficiency, as the previous 76 cm thick PTH block wall. The annual heating and cooling energy demands of scenarios 10, 11 and 12 were identical compared to the previous three 7, 8 and 9. However, the investment would be

far more advantageous. The benefits of the YTONG AAC thermo block structure’s thermal insulation is justified by the building’s annual energy demand.

The results showed preferable results if exterior wall are constructed from 40 cm thick thermal block elements, without additional thermal insulation. Significant reduction of the heating load was assessed in scenario 15 compared to scenario 13. It was concluded that if the WWR of 85% is decreased to 50% than the annual cooling energy demand can be reduced by 47% (24 kWh/m²/year). In contrary, the heating energy demand increased by 23% (7 kWh/m²/year) due to decreased solar energy gains during the winter period. High energy efficiency in small residential buildings can be achieved by attempting to balance the annual heating and the cooling loads. Positive solutions usually are avoiding high differences between the annual heating and cooling demands, in order to balancing the energy requirements during the winter and summer period.

The three simulated building construction types annual energy performance divided in heating, cooling and total demands of all 15 scenarios in compared and presented in Figs. 7, 8, 9 and 10. Figure 7 highlights the cooling energy demands which have the highest potential of energy reduction with the application of tri-pane Argon gas filled windows. The cooling energy requirements can furthermore be reduced with the WWR reduction from 85 to 50%. The least cooling energy demand was assessed for the Porotherm 38 cm PTH block + 14 cm EPS 12th scenario (2.5 MWh/year) and the Ytong ACC 15th scenario (2.6 MWh/year).

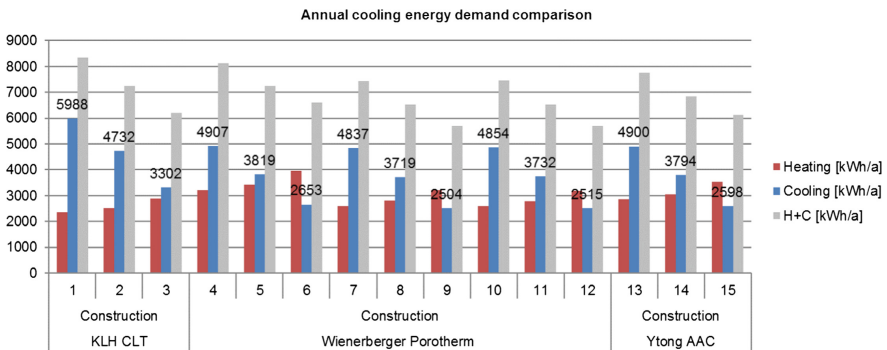


Fig. 7. Annual cooling energy demand comparison

In contrary to the cooling energy demands from Fig. 7, Fig. 8 shown a gradual increase in heating energy. The increase of heating demands can simply be explained be the reduction of the WWR and the improvement of the windows thermal properties. It can be concluded that the WWR and the U-values of windows has the highest influence on the energy demands, even up to 50% in specific cases. Less solar energy gains contribute to higher heating energy needs, whereas the proportional value between heating and cooling is high.

The cooling demand is usually double according to heating for this specific building. As seen in Fig. 8 the lowest heating energy demand was assessed in scenario

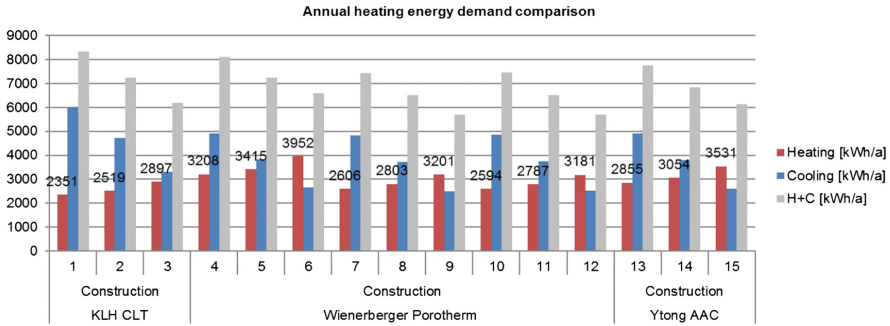


Fig. 8. Annual heating energy demand comparison

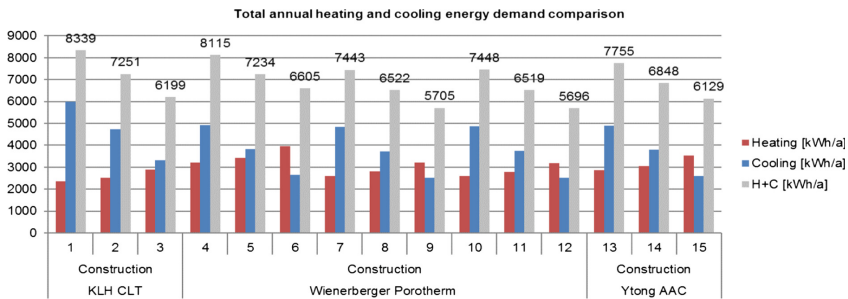


Fig. 9. Total annual heating and cooling energy demand

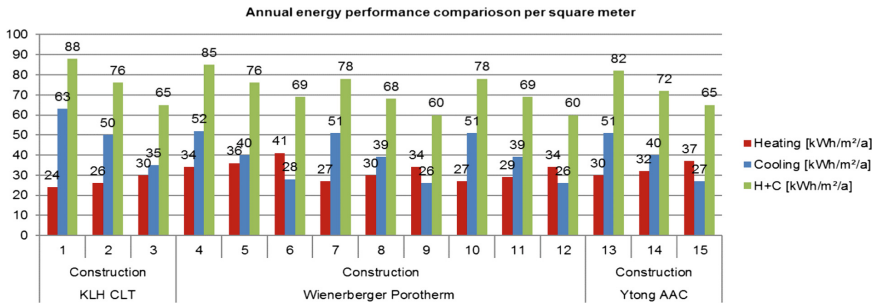


Fig. 10. Annual heating and cooling energy comparison per unit square meter

1 for the KLH structure, scenario 10 for the Porotherm structure and in scenario 13 for the Ytong ACC structure. All three scenarios have equal and highest WWR and identical window types, whereas the solar gains were the highest.

Figure 9 shows the total annual energy demands for heating and cooling where the lowest result is achieved in scenario 12. Scenario 12 and 9 have approximately identical values, yet scenario 9 is not preferable due to higher investment ratio in the double PTH exterior block wall construction.

Figure 10 summarizes the annual heating and cooling energy performance and gives a comparison per unit square meter area. The final decision of the most preferable construction type from the energy efficiency point of view was the Porotherm construction with the following characteristics:

Construction:

- Exterior wall: PTH block 38 cm + 14 cm EPS thermal insulation
- Roof system: PTH 60/17 + 4 cm C20/25 concrete layer + 24 cm thermal insulation plate

Glazing:

Tri-pane insulated glass Argon filled, low-e coating

- heat transfer coefficient, $U = 0.7 \text{ W/m}^2 \text{ K}$
- solar heat gain coefficient, $g = 0.26$
- visible light transmittance factor $\tau = 0.52$
- glazing ratio, 50%.

6 Conclusions

Dynamic building simulation enables strategic planning of building construction in the early design stages. The scope of the research presented that in order to decide which construction and glazing ratio would be the most preferable multiple variations can be analyzed using contemporary techniques in energy performance design.

In conclusion, the energy performance of the analyzed three construction types showed that the block constructions (Porotherm and Ytong) are preferable for the climate of Budapest. According to the simulations the Wienerberger Porotherm with PTH block 38 cm exterior wall with additional EPS insulation had the highest energy efficiency. Nevertheless, if construction technology had been part of the decision process than the KLH cross laminated timber panels would have the advantage. However, the highest influence on the building's energy performance was from the glazing's thermal characteristics, solar heat gain coefficient and glazing ratio. For example, the Ytong ACC constructions annual cooling energy demand can be reduced by 47% if adequate glazing is applied.

Further directions of research will be the analysis of solar gains and illumination dispersion in the interior spaces of the ODOO building model. Solar simulations will include the assessment of illumination quality in the function of the window's light transmission coefficient. Thermal comfort of occupants, comfort parameters such as air temperature and mean radiant temperature oscillation will cover the continuing research objectives.

Acknowledgement. This article is linked to the "Solar Decathlon Competition for investigating efficient utilization of the BME ODOO project's professional objectives". The project is supported by the New Széchenyi Plan ED_13-1-2013-0005 program.

References

1. ODOO. <http://www.odooproject.com/hu/house/>. Accessed 27 Aug 2017
2. ŠijanecZavrl, M., Stegnar, G., Rakušček, A., Gjerkeš, H.: A bottom-up building stock model for tracking regional energy targets – a case study of Kočevlje Sustainability, **8**(10), 1–16 (2016). <https://doi.org/10.3390/su8101063>
3. Kmeková, J., Krajčík, M.: Energy efficient retrofit and life cycle assessment of an apartment building. *Energy Procedia* **78**, 3186–3191 (2015). <https://doi.org/10.1016/j.egypro.11.778>
4. Pukhkal, V., Tanic, M., Vatin, N., Murgul, V.: Studying humidity conditions in the design of building envelopes of passive house (in the case of Serbia). *Procedia Eng.* **117**, 859–864 (2015). <https://doi.org/10.1016/j.proeng.2015.08.152>
5. Szabó, L.: Effect of architectural glazing parameters, shading, thermal mass and night ventilation on public building energy consumption under hungarian climate. *PeriodicaPolytechnica – Civ. Eng.* **59**(2), 209–223 (2015). <https://doi.org/10.3311/PPci.7091>
6. Sacht, H., Braganca, L., Almeida, M., Caram, R.: Glazing daylighting performance and trombe wall thermal performance of a modular facade system in four different Portuguese cities. *Indoor Built Environ.* **24**(4), 544–563 (2015). <https://doi.org/10.1177/1420326X14525976>
7. Harmathy, N., Magyar, Z., Folic, R.: Multi-criterion optimization of building envelope in the function of indoor illumination quality towards overall energy performance improvement. *Energy* **114**, 302–317 (2016). <https://doi.org/10.1016/j.energy.2016.07.162>
8. Gang, W., Wang, S., Xiao, F., Gao, D.: Robust optimal design of building cooling systems considering cooling load uncertainty and equipment reliability. *Appl. Energy* **159**, 265–275 (2015). <https://doi.org/10.1016/j.apenergy.2015.08.070>
9. Krstic-Furundzic, A., Kotic, T.: Assessment of energy and environmental performance of office building models: a case study. *Energy Build.* **115**, 11–22 (2016). <https://doi.org/10.1016/j.enbuild.2015.06.050>
10. Eui-Jong, K., Plessis, G., Jean-Luc, H., Jean-Jacques, R.: Urban energy simulation: simplification and reduction of building envelope models. *Energy Build.* **84**, 193–202 (2014). <https://doi.org/10.1016/j.enbuild.2014.07.066>
11. OpenStudio. <https://www.openstudio.net/>. Accessed 27 Aug 2017
12. SketchUp. <http://www.sketchup.com/>. Accessed 27 Aug 2017
13. EnergyPlus. <http://apps1.eere.energy.gov/buildings/energyplus/>. Accessed 27 Aug 2017
14. Meteonorm. <http://www.meteonorm.com/>. Accessed 27 Aug 2017
15. KLH. <http://www.klh.at/en/product/klh/>. Accessed 27 Aug 2017
16. Wienerbergerporotherm. <http://www.wienerberger.com/products-brands>. Accessed 27 Aug 2017
17. http://www.xella.com/en/contruction_materials.php. Accessed 27 Aug 2017
18. Hungarian TNM 7/2006V. 24 regulation on the energy efficiency of buildings. https://net.jogtar.hu/jr/gen/hjegy_doc.cgi?docid=A0600007.TNM. Accessed 27 Aug 2017

Calculation of Heat Energy Consumption by a Typical Historical Building with a Courtyard

Aleksandr Gorshkov¹  and Vera Murgul^{1,2}  

¹ Peter the Great St. Petersburg Polytechnic University,
29 Politechnicheskaya St., 195251 St. Petersburg, Russia
vera.murgul@mail.ru

² Moscow State University of Civil Engineering,
Yaroslavskoe shosse, 26, Moscow 129337, Russia

Abstract. The article presents the assessment of thermal protective properties for the enclosing structures of the particular historical residential building, considering the overall thermal balance of the building. Actual thermal resistance of the building was estimated taking into account the thermal resistance of all enclosing structures. In order to carry out the research and necessary calculations, external and internal environmental conditions were analyzed. The research exposes the calculations of transmission heat losses, heat losses occurring due to ventilation and air infiltration. Taking into account heat supply, solar heat input and all thermal losses, the annual heat consumption of the building was estimated. Proceeding from the results of the research the authors offer particular measures in order to improve energy efficiency of the building. Proceeding from the results of the research the authors prove the reasonability of creating a glass dome over the courtyard space in order to improve energy efficiency of the whole building.

Keywords: Energy management · Heat consumption · Ventilation · Heating
Energy efficiency

1 Introduction

Apartment buildings located in the historical center of Saint Petersburg comprise a significant part of city's residential areas. Saint Petersburg authorities aim to preserve the historical image of buildings. Therefore, besides passing the construction inspection, any reconstruction works in the center of the city are under control of the Committee for the state preservation of historical and cultural monuments.

Average operation time of such a building lasts over 100 years. Reconstruction of those buildings has involved in most cases only strengthening or renewing bearing structures within major repairs, whereas complex measures for reducing their energy consumption have not been taken. Meanwhile those buildings are exceedingly energy intensive, especially in terms of heating (one building demands over 200 kWh/(m²·year). In this regard, operational heat expenses of such type of buildings are the highest as compared with buildings that are more modern.

Besides, those buildings have become obsolete for the last 100 years, particularly in meeting today thermal shield requirements [1–9].

Therefore, it became necessary to not only reconstruct the buildings, but also modernize their heat protective properties in order to reduce their energy consumption and increase their energy efficiency.

Lack of green spaces is another problem of historical center of the city. “Well courtyards” located closely to each other within a neighborhood are almost out of greenery. Natural pollutions, transport emissions, lack of ventilation in “well courtyards” cause chronic diseases of respiratory system of citizens. Preserving health of population is a national issue; therefore, urban greening is an urgent problem for city’s authorities.

2 Object Description

The object of the study is a for-story residential apartment house. The building designed and built by architect N. Grebenka in 1855 is located in the historical center of Saint Petersburg at the junction of Dekabristov Street and Fonarny Lane. The building has cold pitched roof with sheet-metal covering. Heating pipelines run through the attic. The basement is built-in only in the internal part of the building.

The facades of the building are plastered. The angular facades faced to traffic lanes are decorated with such finishing elements as cornices, rustication, pediments above the windows from 2nd to 4th levels (Fig. 1). Facades oriented to the courtyard are not decorated with any finishing elements (Fig. 2).



Fig. 1. Corner of the building at the junction of Dekabristov Street and Fonarny Lane.

The building has 5 staircases, the number of flats is 27. Premises located on the 1st floor and faced to the traffic lanes of Dekabristov Street and Fonarny Lane are occupied by shops (2 food stores and 1 bakery). All the other premises in the building are residential. The utility spaces of public service are 1806 m² in area, including:

- basement - 146 m²;
- staircases $A_{(st)}$ - 550 m²;
- attic - 1110 m².



Fig. 2. Courtyard.

The total area occupied by owners (individuals and legal entities) is A_p - 3840 m², including:

- the total area of non-residential premises $A_{(n/r)}$ - 580 m²;
- the total area of residential premises A_r - 3260 m².

The total heated area of the building A_h is 4390 m².

The “well courtyard” of the building is provided with the vehicular passage (Fig. 3). The courtyard is rectangular, 11.44 × 20.66 m in plan and has extra passages to the entrances of staircases.



Fig. 3. Vehicular passage to the courtyard.

3 Description of External Enclosing Structures

External walls are laid with solid loam bricks (the thickness of the wall is 640 mm or 2.5 bricks). Thermal resistance of the external walls is $0.95 \text{ m}^2 \cdot ^\circ\text{C}/\text{W}$.

The windows are of various types. Part of them are wooden double-glazed windows of customary glass set in separate sashes, with thermal resistance of $0.44 \text{ m}^2 \cdot ^\circ\text{C}/\text{W}$, according to data from Appendix L of Construction Regulations SP 23-101 [2]. Another part of the windows are one-chamber insulated glass units in single sashes made of customary glass with thermal resistance of $0.35 \text{ m}^2 \cdot ^\circ\text{C}/\text{W}$ according to data from Appendix L of Construction Regulations SP 23-101 [2].

External entrance doors of staircases are metallic and heat-insulated. Thermal resistance of those doors is $0.3 \text{ m}^2 \cdot ^\circ\text{C}/\text{W}$. External entrance doors of commercial premises are single-chambered of metal-filled plastic with thermal resistance of $0.35 \text{ m}^2 \cdot ^\circ\text{C}/\text{W}$.

The attic floor is made of metal truss, on which wooden panels are laid and 200 mm thick slag filling is made. Thermal resistance of the attic floor is $1.2 \text{ m}^2 \cdot ^\circ\text{C}/\text{W}$.

The floor above the basement is concrete and not heat-insulated. Its thermal resistance is $0.24 \text{ m}^2 \cdot ^\circ\text{C}/\text{W}$.

The floor over the vehicular passage is made of wooden beams, the space between which is filled with 250 mm thick slag filling. The thermal resistance of the floor over the vehicular passage is $1.35 \text{ m}^2 \cdot ^\circ\text{C}/\text{W}$.

Areas of external enclosing structures are:

- walls - 2621.6 m^2 ;
- windows - 632.3 m^2 ; of which the area of single-chamber double-glazed windows is 321.5 m^2 , the area of wooden window blocks with separate sashes is 310.8 m^2 ;
- entrance external doors – 46.9 m^2 ; Of which 7 doors are of metal-filled plastic with a total area of 23.4 m^2 , 9 doors are metal with a total area of 23.5 m^2 ;
- attic floors - 1110 m^2 ;
- floors above the basement - 146 m^2 ;
- floors on the ground - 917 m^2 ;
- overlapping above the passages - 47 m^2 .

The total area of external enclosing structures is 5520.8 m^2 .

4 Internal Environmental Conditions

Design conditions of inside air in operated residential buildings are accepted according to National State Standard GOST 30494 [4]. The design temperature of inside air of residential and commercial premises tins, $^\circ\text{C}$, is set to $20 \text{ }^\circ\text{C}$. The design temperature of inside air in staircases is set to $15 \text{ }^\circ\text{C}$.

5 External Environmental Conditions

The design temperature of outside air in cold period of the year t_{out} , °C, which is accepted by Construction Regulations SP 131.13330 [5] as average temperature of the coldest five-day period with probability of 0.92 and average temperature of outside air $t_{h/s}$, °C during the heating season in respect to Saint Petersburg climatic conditions, is presented in Table 1.

Table 1. Design temperatures of outside air in cold season.

Locality name	Design temperatures of outside air, °C	
	Average temperature of the coldest five-day period, t_{out}	Average temperature during the heating season $t_{h/s}$ (for residential buildings)
Saint Petersburg	-24	-1.3

The duration $z_{h/s}$ and degree-day HDD °C·day of the heating season for climatic conditions of Saint Petersburg are set to 213 days and 4537 °C·day respectively. For staircases with the design temperature of air tins = 15 °C. HDD is set to $(15 + 1,3) \cdot 213 = 3472$ °C·day.

6 Calculation Methodology

The calculation is carried out according to the Regional Methodical Documents RMD 23-16-2012 [6, p. 7.4.1, Appendix C].

The annual heating energy consumption during the cold and transition seasons Q_{hv}^a , kW·h/year is calculated according to Equation [6]:

$$Q_{hv}^a = \left[Q_{tr}^a + Q_{vent}^a + Q_{inf}^a - (Q_{hh}^a + Q_{solar}^a) \cdot v_{in} \cdot \zeta \right] \cdot \beta_h \tag{1}$$

where

- Q_{tr}^a – building transmission losses of thermal energy through external enclosing structures for the heating period, kW·h/year;
- Q_{vent}^a – thermal energy losses due to ventilation heat exchange for the heating season, kW·h/year;
- Q_{inf}^a – loss of thermal energy due to infiltration of cold air during the heating season through external enclosing structures, kW·h/year;
- Q_{hh}^a – household heat supply in apartments and public premises for the heating season, kWh/year;
- Q_{solar}^a – heat input through external translucent enclosing structures from solar radiation, taking into account the orientation of the facades in eight bearing angles for the heating period, kWh/year;

- v_{in} – coefficient of reduction of heat input due to thermal inertia of the enclosing structures;
- ζ – coefficient of efficiency of automatic heat control systems for heating;
- β_h – coefficient taking into account the additional heat consumption of the heating system due to the discreteness of the nominal heat flow of the nomenclature series of heating appliances, with their additional heat losses through the radiator sections of the enclosing structures, with heat losses of pipelines passing through unheated rooms.

Transmission losses of thermal energy through external enclosing structures of a building Q_{tr}^y , kW·h are calculated according to the Equation [6]:

$$Q_{tr}^a = 0.024 \cdot \left(\frac{A_{wall}}{R_{wall}^{adj}} + \frac{A_{win}}{R_{win}^{adj}} + \frac{A_l}{R_l^{adj}} + \frac{A_d}{R_d^{adj}} + \frac{A_{cov}}{R_{cov}^{adj}} + \frac{A_{fl}}{R_{fl}^{adj}} + \frac{A_{at,fl}}{R_{at,fl}^{adj}} + \frac{A_{s,fl}}{R_{s,fl}^{adj}} + \frac{A_{d,fl}}{R_{d,fl}^{adj}} \right) \times HDD, \quad (2)$$

where

- A_{wall}, R_{wall}^{adj} – area, m² and the calculated value of the adjusted thermal resistance, m²·°C/W, external walls of the building (excluding openings), respectively;
- A_{win}, R_{win}^{adj} – the same of fillings of light-openings (window blocks and balcony doors, shop windows and fixed glazing);
- A_l, R_l^{adj} – the same of roof lights with vertical glazing
- A_d, R_d^{adj} – the same of the external doors and gates
- A_{cov}, R_{cov}^{adj} – the same of combined coverings (including ones above the bay-windows), attic floors of cold lofts;
- A_{fl}, R_{fl}^{adj} – the same of floors above the passages and under the bay-windows;
- $A_{at,fl}, R_{at,fl}^{adj}$ – the same of attic floors of warm attics;
- $A_{s,fl, floor}, R_{s,fl, floor}^{adj}$ – the same of socle flooring over unheated basements and underground;
- $A_{d,fl}, R_{d,fl}^{adj}$ – the same of the enclosing structures of heated basements contacting with the ground; deck floors on the ground for buildings without a basement (underground floor)
- 0.024 – conversion coefficient of transmission losses of thermal energy from W·day in kW·h (1 day = 24 h, 1 W = 0.001 kW);
- HDD – heating degree-day, °C·day

7 Heating

Taking into account the obtained climatological data, the transmission heat losses of the building are calculated:

$$\begin{aligned}
 Q_{tr}^a &= 0.024 \cdot \left(\frac{2397.0}{0.95} + \frac{310.8}{0.44} + \frac{321.5}{0.35} + \frac{4.0}{0.3} + \frac{23.4}{0.35} + \frac{47.0}{1.35} \right. \\
 &\quad \left. + \frac{1110.0}{1.2} + \frac{146.0}{0.24} \cdot 0.6 + \frac{597.0}{3.95} \right) \cdot 4537 + 0.024 \\
 &\quad \cdot \left(\frac{224.6}{0.95} + \frac{35.4}{0.44} + \frac{19.5}{0.3} + \frac{312.0}{1.2} + \frac{312.0}{3.95} \right) \cdot 3472 \\
 &= 681191.1 \text{ (kW} \cdot \text{h/year)}.
 \end{aligned}
 \tag{3}$$

The distribution scheme of transmission heat losses according to types of external enclosing structures is shown in Fig. 4.

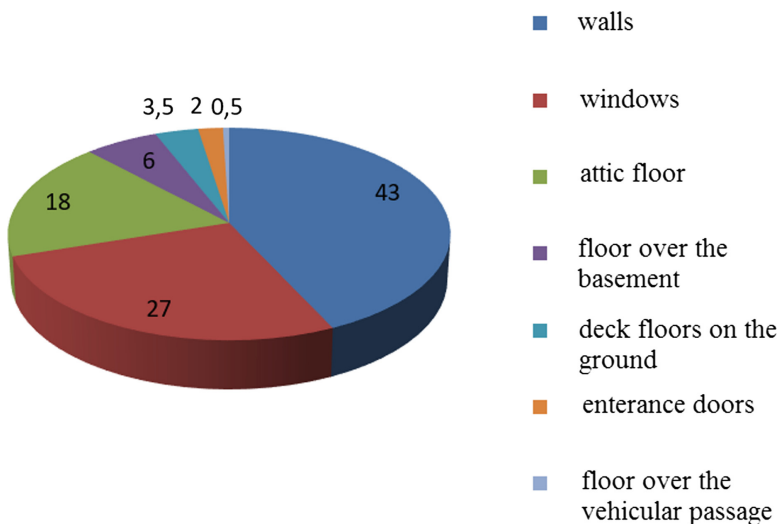


Fig. 4. The distribution scheme of transmission heat losses according to types of external enclosing structures.

The introduced scheme of transmission heat losses shows that the maximum heat consumption during the heating season accrues to walls (43%), windows (27%) and attic floor (18%).

8 Ventilation

For buildings with free ventilation, heat losses occurring due to ventilation heat exchange during heating season Q_{vent}^y , kW · h/year, are calculated according to Equation [6]:

$$Q_{vent}^a = 0,0067 \cdot L_{sup.a} \cdot c_a \cdot \rho_a^{hs} \cdot HDD
 \tag{4}$$

where 0.0067 is the conversion coefficient for the duration of the heating period included in the formula for calculating HDD from days to hours; and for the heat loss due to ventilation heat exchange from kJ to MJ (1 day = 24 h, 1 kJ = 1/3600 kWh: $24/3600 = 0.0067$);

$L_{sup.a}$ – volume of supply air, m³/h;

c_a – specific mass heat capacity of air, is assumed equal to 1.005 kJ/(kg·°C);

ρ_a^{hs} – the average density of air, for the climatic conditions of St. Petersburg is taken equal to 1.3 kg/m³.

The design quantity of supply air for residential premises is assumed [7]:

$$0.35 \cdot A_r \cdot h = 0.35 \cdot 3260 \cdot 3.5 = 3994 \text{ (m}^3/\text{h)},$$

where

A_r – area of residential premises, m²;

h – level height from floor to ceiling, m

The design quantity of supply air for non-residential premises under condition of stores working 7 days a week with 10-h day is accepted according to calculation $4 \cdot A_{n/r}$ – during working hours and air exchange 0.15 h^{-1} – during non-working hours

$$[7]: \frac{4 \cdot A_{n/r} \cdot 10 + 0.2 \cdot A_{n/r} \cdot h \cdot 14}{24} = \frac{4 \cdot 580 \cdot 10 + 0.15 \cdot 580 \cdot 4 \cdot 14}{24} = 1179 \text{ (m}^3/\text{h)}.$$

Substitute the initial values into the Eq. 4 and obtain:
 $Q_{vent}^a = 0.0067 \cdot 5173 \cdot 1.005 \cdot 1.3 \cdot 4537 = 205\,444.9 \text{ (kW} \cdot \text{h/year)}.$

9 Air Infiltration

Losses of the heat energy through the exterior wall envelope Q_{inf}^y , kWh/year, due to the cold air infiltration during the heating season should be calculated using the following Equation [6]:

$$Q_{inf}^y = 0.0067 \cdot G_{inf} \cdot \frac{n_{inf}}{168} \cdot c_a \cdot HDD, \quad (5)$$

where

0.0067 – same as in the Eq. 3;

G_{inf} – the amount of the infiltrated air into the building through the exterior wall envelope, kg/h; for the building under review it is the amount of air, coming through its windows and entrance doors per day during the heating season;

A_i – square area of the windows and entrance doors, m²;

n_{inf} – time period of tracking of the air infiltration within a week, h; for buildings with the free ventilation n_{inf} is 168 h;

c_a – same as in the formula (3), kJ/(kg · °C);

HDD – same as in the formula (2), for staircase areas it is 3472 °C·day.

The amount of the infiltrated air G_{inf} , kg/h, coming into building due to the clearance losses with the known differential pressure of the inside and outdoor air, should be calculated using the following Equation:

$$G_{inf} = \sum \left(\frac{A_w}{R_{inf(w)}^{design}} \right) \cdot \left(\frac{\Delta p_w}{10} \right)^{2/3} + \sum \left(\frac{A_d}{R_{inf(d)}^{design}} \right) \cdot \left(\frac{\Delta p_d}{10} \right)^{1/2}, \quad (6)$$

where

A_w, A_d – total square area of the windows and entrance doors respectively, m^2 ;

$R_{inf(w)}^{design}, R_{inf(d)}^{design}$ – design values of air permeability resistance of the windows and entrance doors respectively, $m^2 \cdot h/kg$;

$\Delta p_w, \Delta p_d$ – design differential pressure of the inside and outdoor air, Pa, for:

– the windows and entrance doors faced to traffic lanes by formula:

$$\Delta p_{w(d)}^{st} = (H - h) \cdot (\rho_{out} - \rho_{in}) \cdot g + 0.28 \cdot \rho_{out} \cdot v^2 \quad (7)$$

– the windows and entrance doors faced to courtyard by Equation:

$$\Delta p_{w(d)}^{c.yard} = (H - h) \cdot (\rho_{out} - \rho_{in}) \cdot g. \quad (8)$$

Equations 7, 8 have the following designations:

H – height of building (from the first floor to the top of the exhaust shaft), it is 19.5 m for the considered building;

h – height of considered element of the building (window, entrance door) from the ground level, m;

ρ_{out} – density of the outdoor air is 1.30 N/m^3 for the climate conditions of Saint-Petersburg;

ρ_{in} – density of the inside air is:

– 1.21 kg/m^3 for premises with the design temperature of the inside are of $t_{in} = 20 \text{ }^\circ\text{C}$;

– 1.23 kg/m^3 for premises with the design temperature of the inside are of $t_{in} = 15 \text{ }^\circ\text{C}$;

g – free fall acceleration, that equals 9.81 m/s^2 ;

v – maximal average wind speed by rhumb lines in January, which frequency is 16% and higher, is 4.2 m/s for the climate conditions of Saint-Petersburg [6]; v should be multiplied by the coefficient of the wind speed change due to height level ζ according to the Table 12 of RMD 23-16 [6].

If air permeability of the plastic sash window units at $\Delta p_o = 10 \text{ Pa}$ is set to $G_{w(pvc)} = 5.0 \text{ kg/(m}^2 \cdot \text{h)}$, air permeability of the wooden window units at $\Delta p_o = 10 \text{ Pa}$ is set to $G_{w(wood)} = 8.0 \text{ kg/(m}^2 \cdot \text{h)}$ with account of their deterioration and for the entrance doors at $\Delta p_o = 10 \text{ Pa}$ it is set to $G_d = 7.0 \text{ kg/(m}^2 \cdot \text{h)}$, then the amount of the infiltrated air will be:

- 2304 kg/h for premises with the design temperature split of 20 °C;
- 385 kg/h for premises with the design temperature split of 15 °C.

Due to the absence of the experimental data, index of the filtration mode n in Eq. (8) is set to 2/3 for windows and 1/2 for entrance doors.

According to the initial values, losses of the heat energy due to cold air infiltration are calculated using the Eq. (4):

$$Q_{inf}^y = 0.0067 \cdot G_{inf} \cdot \frac{n_{inf}}{168} \cdot c_a \cdot HDD = 0.0067 \cdot 2304 \cdot 1 \cdot 1.005 \cdot 4573 + 0.0067 \cdot 385 \cdot 1 \cdot 1.005 \cdot 3472 = 79\,946.3 \text{ (kW} \cdot \text{h)}.$$

Structure of the design heat energy losses in the considering building is shown in Fig. 5.

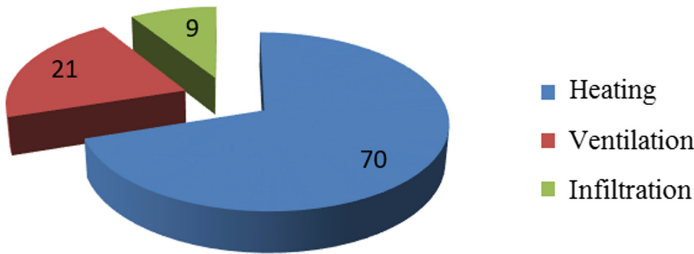


Fig. 5. Structure of heat energy losses in building.

Based on the Fig. 5, the major losses of the heat energy in the building accrue to the restoring of the heat energy leakage through exterior wall envelopes (70%).

10 Household Heat Gain

Household heat gain during the heating season Q_{hh}^y , kW·h/year, should be calculated using the (C.10) RMD 23-16 Equation [6]:

$$Q_{hh}^y = 0,024 \cdot q_{hh} \cdot z_{hs} \cdot A_{design}, \tag{9}$$

where

- 0,024 – same as in the Eq. 2;
- z_{hs} – same as in the formula (3), days (for building at design stage z_{hs} is 213 days);
- A_{design} – design floor space of the building, which is calculated by summing up the total square area of all rooms except corridors, wind porches, passes, staircases, elevator shafts, inside open stairways and ramps as well as rooms for utility equipment and network, m^2 (for the considering building A_{design} is 3840 m^2);

q_{hh} – value of the household heat emissions for 1 m² of the design floor space (A_{design}), W/m² is:

- 10 W/m² for residential premises;
- 25 W/m² for business premises.

Therefore, household heat gain during the heating season is:

$$Q_{hh}^y = 0.024 \cdot q_{hh} \cdot z_{hs} \cdot A_{design} = 0.024 \cdot 10 \cdot 213 \cdot 3260 + 0.024 \cdot 25 \cdot 213 \cdot 580 = 240\,775.2 \text{ (kW} \cdot \text{h/year)}.$$

11 Solar Heat Gain

Heat gain through translucent building envelope from solar radiation taking into account facades orientation in 8 rhumbs during the heating season Q_{solar}^y , kW·h/year, should be calculated using the (C.12) RMD 23-16 Equation [6]:

$$Q_{solar}^y = \tau_w \cdot k_w \cdot \left(\sum_{i=1}^8 A_{w,i} \cdot I_{v,i} \right) + \tau_l \cdot k_l \cdot A_l \cdot I_l, \quad (10)$$

where

- τ_w, τ_l – coefficients, which take into account area light shading of the windows and roof lights with nontransparent web members according to the design values;
- k_w, k_l – coefficients of the relative penetration of solar radiation for translucent web members of the windows and roof lights, which are chosen according to product certificates respectively;
- $A_{w,i}$ – surface area of the facade light openings faced to 8 sides (light openings of the staircase and elevator section are not taken into account), m²;
- A_l – surface area of roof lights as well as dormer windows with an angle of inclination to the horizon of less than 45 °, m²;
- $I_{v,i}$ – average value of the solar radiation at vertical surfaces under actual conditions of cloudiness, respectively, oriented along 8 facades of the building over the heating season, kW·h/m²; the Table 2 is used for Saint-Petersburg climate conditions [6];
- I_l – average value of the solar radiation at horizontal surfaces under actual conditions of cloudiness over the heating season, MJ/m²; it is set to 253.3 kW·h/m² for the climate conditions of Saint-Petersburg [6].

Roof lights and dormer windows are not planned. Area surfaces of the windows with their orientation are presented in the Table 3.

Coefficient for single-chamber glasses, which takes into account shading of the light opening of the windows with non-transparent web members τ_w , is set to 0.8; coefficient of the relative penetration of solar radiation for translucent web members k_w is 0.7.

Table 2. Average value of the total solar radiation at vertical and horizontal surfaces under actual conditions of cloudiness I_t , MJ/m² (kW·h/m²), over the heating season.

Name of the settlement	Horizontal surface	Vertical surfaces with orientation to:				
		North	Northeast/ Northwest	East/ West	Southeast/ Southwest	South
Saint-Petersburg	912 (253.3)	394 (109.4)	455 (126.4)	650 (180.6)	902 (250.6)	1009 (280.3)

Table 3. Area surfaces of the translucent building envelopes.

Facade	Orientation	Surface area of plastic sash windows, m ²	Surface area of wooden windows, m ²
1	South	28.3	37.4
6	South	120.8	68.9
2	North	27.4	49.8
3	West	60.8	17.3
5	West	70.9	77.4
4	East	13.3	60.0

For wooden windows with separate covers from ordinary glass, the coefficient taking into account shading of the light opening of the windows with non-transparent web members τ_{ok} for the adopted design decision is taken equal to 0.65; Coefficient of the relative penetration of solar radiation for translucent web members k_{ok} is 0.62.

Coefficient of the relative penetration of solar radiation for the windows, that are faced to the courtyard, is multiplied by 0.6.

Therefore, solar heat gains through the exterior translucent building envelope with an account of facades orientation in 8 rhumbs over the heating season will be:

$$\begin{aligned}
 Q_{solar}^y &= 0.8 \cdot 0.7 \cdot (120.8 \cdot 280.3 + 70.9 \cdot 180.6) \\
 &\quad + 0.65 \cdot 0.62 \cdot (68.9 \cdot 280.3 + 77.4 \cdot 180.6) \\
 &\quad + 0.8 \cdot 0.7 \cdot (28.3 \cdot 280.3 + 74.1 \cdot 180.6 + 27.4 \cdot 109.4) \cdot 0.6 \\
 &\quad + 0.65 \cdot 0.62 \cdot (37.4 \cdot 280.3 + 77.3 \cdot 180.6 + 49.8 \cdot 109.4) \cdot 0.6 \\
 &= 54945.4 \text{ (kW} \cdot \text{h/year)}.
 \end{aligned}$$

12 Coefficients

The coefficient of heat gain reduction due to the thermal inertia of the building envelopes v_m is assumed equal to 0.8.

The coefficient of efficiency of automatic heat regulation in heating systems ζ is 0.5 (system is without thermostats and automatic regulation at the input since there is central regulation in the boiler room).

The coefficient that takes into account the additional heat consumption by the heating system, connected with the discreteness of the nominal heat flux of the nomenclature row of the heating devices, with their additional heat losses through the radiator sections of the building envelopes, with heat losses of the pipelines passing through the unheated premises β_h for the designed building is set to 1.07.

12.1 Annual Heat Energy Consumption to Warm Building Under Design During the Heating Season

Applying to the Eq. 1 design heat and power parameters, the equation will be the following:

$$\begin{aligned} Q_{hv}^y &= \left[Q_{tr}^y + Q_{vent}^y + Q_{inf}^y - (Q_{hh}^y + Q_{solar}^y) \cdot v_{in} \cdot \zeta \right] \cdot \beta_h == [681191.1 \\ &+ 205444.9 + 79946.3 - (240775.2 + 54945.4) \cdot 0.8 \cdot 0.5] \cdot 1.07 \\ &= 907674.6 \text{ (kW} \cdot \text{h/year)}. \end{aligned}$$

Therefore, the annual consumption of heat energy to warm and ventilate the building under design is 907674.6 kW·h/year or 780 Gcal/year.

Specific design annual consumption of heat energy of the building is:

$$q_{hv}^y = \frac{Q_{hv}^y}{A_h} = \frac{907674.6}{4390} = 206.7 \left(\frac{\text{kW} \cdot \text{h}}{\text{m}^2 \cdot \text{year}} \right).$$

The difference between design and actual parameters of the heat consumption is due to the following reasons:

- the difference between the design (normalized) and actual characteristics of the heating season (HDD);
- the difference between the actual values of the inside air temperature from the appraised one (20 °C) due to the fact that at certain periods of time the actual temperature of the inside air can be either higher or lower than the design temperature;
- an error in determining the geometric characteristics of the building envelopes during the measuring;
- an error in appraising of the design values of thermal resistance of exterior building envelopes (walls, windows, attic floor, etc.);
- an error in the estimation of actual air exchange parameters (volume of supply air) of premises;
- an error in the estimation of the air permeability of the exterior building envelopes;
- an error in the estimation of the numerical values of solar and household heat gain;
- an error in assigning the coefficients v_{in} , ζ , β_h in the heat balance equation of the building;
- other unaccounted factors.

However, the presented above calculation can be taken as a basis planning the refurbishment of the building in order to reduce the heat energy consumption costs, since the difference between design parameters of the building under consideration and its actual ones (according to the heat meter readings) is less.

13 Measures to Improve the Energy Efficiency of the Building

Device of the translucent dome and creation of the closed atrium in the courtyard of the building with maintaining the temperature of 16 °C throughout the heating period are considered as the main recommended measure aimed to improve the energy efficiency of the building. There is also considered an option to construct a green zone with a fountain instead of the asphalt pavement in order to maintain humidity level in the atrium zone. In connection with the fact that the courtyard is planned to be covered with translucent gates with a device in the passage of a warm porch, the fountain may also be a reserve source for fire-fighting water supply.

Due to the fact that at a temperature difference of 4 °C between the design temperature of the inside air in the premises (20 °C) and the air temperature in the atrium (16 °C), there is a significant reduction of transmission losses of heat energy through the exterior building envelopes (walls, windows, floors, entrance doors), that are faced to the yard. In this regard, the heating system in such premises can be left only as a backup in case of disruption of the microclimate parameters in the green atrium.

Solar collectors, being installed on the roof of the building with the panels' orientation to the south and south-west, can be considered as sources of heat supply to warm the atrium. Solar batteries on the roof of the building can be considered as sources of electricity supply of the atrium and common facilities (staircases).

Inside air from the atrium can be used for ventilation of living premises in the building with subsequent disposal of the heat of the exhaust air. For this purpose, it is recommended to install combined extract-and-input system of ventilation with the disposal of heat emission from the vents.

In this case, the main losses of heat energy in the building will be determined by the amount of transmission losses of heat energy through the exterior building envelopes (walls, windows, entrance doors) that overlap the roadway, as well as losses through the attic floor. When replacing the windows with more efficient ones, the insulation of the entrance doors, the internal insulation of the walls and the additional insulation of the attic floor, the transmission losses of thermal energy can also be significantly reduced.

References

1. Gorshkov, A.: Ob okupayemosti investitsiy na utepleniye fasadov sushchestvuyushchikh zdaniy. *Energoberezheniye* **4**, 12–27 (2014)
2. Russian Standard SP 23–101-2004 *Proyektirovaniye teplovoy zashchity zdaniy*
3. Malyavina, Y.: *Teplopoteri Zdaniya: Spravochnoye Posobiye*. AVOK-PRESS, Moscow (2007)
4. Russian Standard GOST 30494-2011 *Zdaniya zhilyye i obshchestvennyye. Parametry mikroklimate v pomeshcheniyakh*
5. Russian Standard SP 131.13330.2012 «*Stroitel'naya klimatologiya*»
6. Russian Standard RMD 23-16-2012 *Rekomendatsii po obespecheniyu energeticheskoy effektivnosti zhilykh i obshchestvennykh zdaniy*

7. Rukovodstvo AVOK-8-2007 «Rukovodstvo po raschetu teplopotrebleniya ekspluatiruyemykh zhilykh zdaniy»
8. Jakšić, Ž., Trivunić, M., Adamtsevich, A.: Flexibility and adaptability - key elements of end-user participation in living space designing. In: MATEC Web of Conferences, vol. 106, p. 01001 (2017). <https://doi.org/10.1051/mateconf/201710601001>
9. Pukhkal, V.: Humidity conditions for exterior walls insulation (case study of residential housing development in Saint-Petersburg). Procedia Eng. **117**, 616–623 (2015). <https://doi.org/10.1016/j.proeng.2015.08.222>

Employment of Skirting Board Heating Water System in Accommodation

Kirill Sukhanov^(✉)  and Anatoly Smirnov 

Saint-Petersburg State University of Architecture and Civil Engineering,
2-nd Krasnoarmeiskaya st. 4, 190005 St. Petersburg, Russia
suhanov.kirill1993@mail.ru

Abstract. The numerical simulation of skirting convector heater operation in accommodation has been substantiated and developed using STAR CCM+ software package. An accommodation with typical for living quarters dimensions and fresh air supply through adjustable window sash was specified. Skirting convector-type heating unit was computer-simulated which is to be mounted on accommodation external wall instead of plinth. Convector heat flow was sufficient to compensate accommodation heat loss underrating 10%. Rate and temperature field distribution was derived for accommodation and on internal faces cladding. Temperature increase of internal face cladding and resulting temperature inside apartment is found. Temperature decrease in the vicinity of external wall horizontal butt joints in flooring support area is excluded. The zone of discomfort in accommodation serving area is derived. The considered model of skirting heating water system was considered as the relations to ensure controlled microclimate parameters in the accommodation.

Keywords: Numerical simulation · Accommodation · Skirting heating system

1 Introduction

Junctions of the main structural parts of buildings (horizontal butt joints in flooring support area, external wall vertical butt joints in partition abutment area etc.) are more heat-conducting than external walls and decrease the value of thermal resistance. Figure 1 shows temperature fields in horizontal butt joints of apartment building exterior wall panels in flooring support area [1] as an example. Calculation results for single-layer panel 300 mm thick made of ceramsite concrete with the density of $\rho = 900 \text{ kg/m}^3$ with thermal resistance $R_0 = 0.986 \text{ m}^2 \cdot \text{°C/W}$ are given.

Based on the data presented, difference between ambient air temperature and the temperature in the butt joint equals 5.6, 6.0 °C which is greater than controlled temperature difference between internal air temperature and that of cladding structure internal face during of Catalogue development [1] (for external walls – $\Delta t' = 6 \text{ °C}$; for flooring over passages, basement and cellars – $\Delta t' = 2 \text{ °C}$ [2]). The standards in force at the time of writing the article [3], provide for still smaller rated temperature difference (for external walls – $\Delta t' = 4 \text{ °C}$).

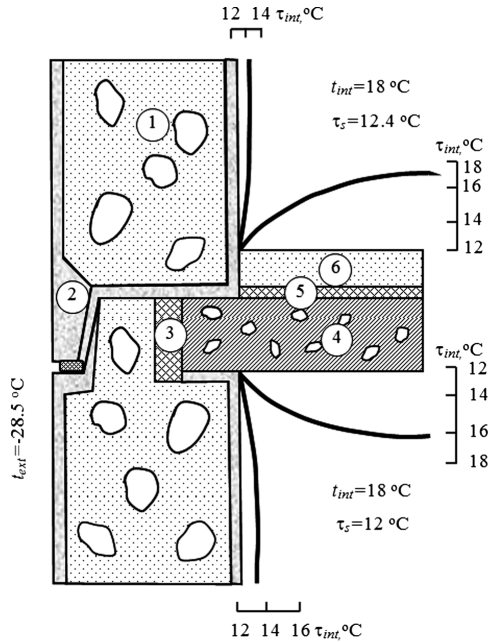


Fig. 1. Temperature fields for horizontal butt joints of external wall panels with flooring with rain barrier with lagged joint. (1 – ceramsite concrete, $\rho = 900 \text{ kg/m}^3$; 2 – cement and sand composition, $\rho = 1800 \text{ kg/m}^3$; 3 – expanded polystyrene foam, $\rho = 40 \text{ kg/m}^3$; 4 – reinforced concrete, $\rho = 2500 \text{ kg/m}^3$; 5 – hard mineral wool board, $\rho = 350 \text{ kg/m}^3$; ceramsite concrete, $\rho = 1200 \text{ kg/m}^3$)

The increase of external wall thermal resistance does not allow excluding heat-conducting insertions in cladding and temperature decrease in external wall horizontal butt joints [4].

One of possible solutions for surface temperature increase in horizontal butt joint and entire cladding area (in order to increase resulting room temperature) is the use of skirting convector-type heater [5]. Convector-type skirting heater is mounted on room external and internal walls around room perimeter instead of plinth.

No investigations of these systems applicability in accommodation were performed.

2 Research Objective and Technique

The problem was set to investigate convector-type skirting heater operation conditions for accommodation in Saint-Petersburg and determine distribution of rate and temperature fields in this accommodation.

Research tool for the present investigation was hydrodynamic computer complex STAR-CCM+ [6–10].

A room with standard accommodation dimensions was taken as a model: width (between centers) – 3 m; depth – 6 m; height (difference between finished floor levels

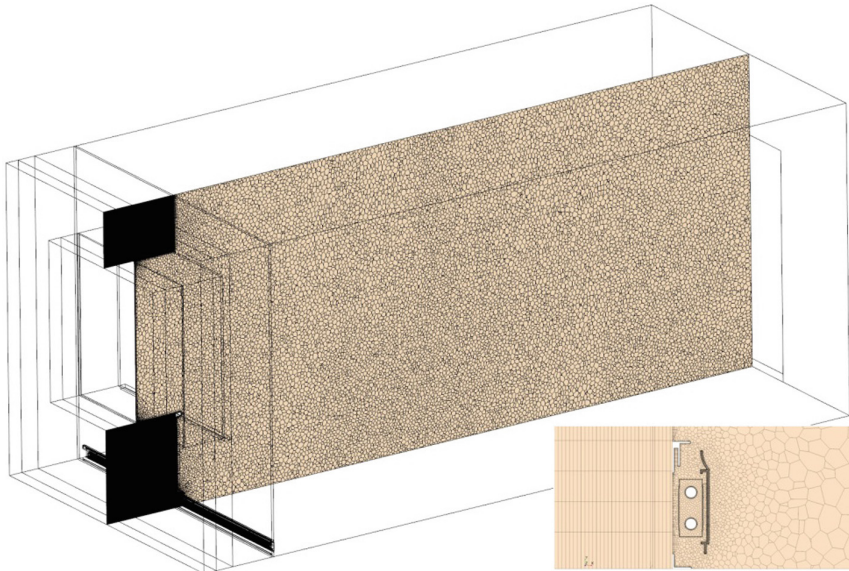


Fig. 2. Room computation mesh.

for two adjacent floors) – 3 m. External wall direction – southward. Window dimensions – 1.4×1.5 m. The design air temperature outside is minus $24\text{ }^{\circ}\text{C}$. The design air temperature Inside is plus $20\text{ }^{\circ}\text{C}$.

External wall structure:

- cement and sand composition – layer thickness - $\delta = 0.02$ m; thermal conductivity - $\lambda = 0.93\text{ W}/(\text{m}\cdot^{\circ}\text{C})$;
- brickwork of common brick on cement and sand composition - $\delta = 0.38$ m; $\lambda = 0.81\text{ W}/(\text{m}\cdot^{\circ}\text{C})$;
- mineral wool panel “CAVITY BUTTS” - $\delta = 0.12$ m; $\lambda = 0.044\text{ W}/(\text{m}\cdot^{\circ}\text{C})$;
- brickwork of ceramic hollow brick with the density of $1400\text{ kg}/\text{m}^3$ (gross) on cement and sand composition - $\delta = 0.12$ m; $\lambda = 0.64\text{ W}/(\text{m}\cdot^{\circ}\text{C})$.

External wall corrected thermal resistance – $R_0 = 2.997\text{ m}^2\cdot^{\circ}\text{C}/\text{W}$.

Window corrected thermal resistance – $R_0 = 0.51\text{ m}^2\cdot^{\circ}\text{C}/\text{W}$.

Room heat loss including household emission of heat (10 W per 1 m^2 of accommodation living space) is equal 898 W incl. 796 W for heat flow to warm up infiltrating outdoor air in the amount of sanitary norm for outdoor air supply ($3\text{ m}^3/\text{h}$ per 1 m^2 of accommodation living space). Outside air supply is provided through adjustable window sashes. Air removal is conducted through a slot of 0.02 m high between floor surface and internal door leaf bottom surface of the door opposite the window along room centre-line.

Convector-type skirting heater 140 mm high and 30 mm wide mounted on external wall only instead of plinth was modeled. Heating element (heat-exchanging module) is fixed on brackets inside aluminum housing. Heating element consists of two copper

tubes OD 13 mm and 1 mm thick and brass plates set on them. Skirting heater specific heat flow is 330 W/m.

Numeric model of skirting heater operation in accommodation areas was developed in STAR CCM+ program (Fig. 1).

3 Investigation Results

Rate and temperature fields' computation results for rooms are given in Figs. 3, 4 and 5.

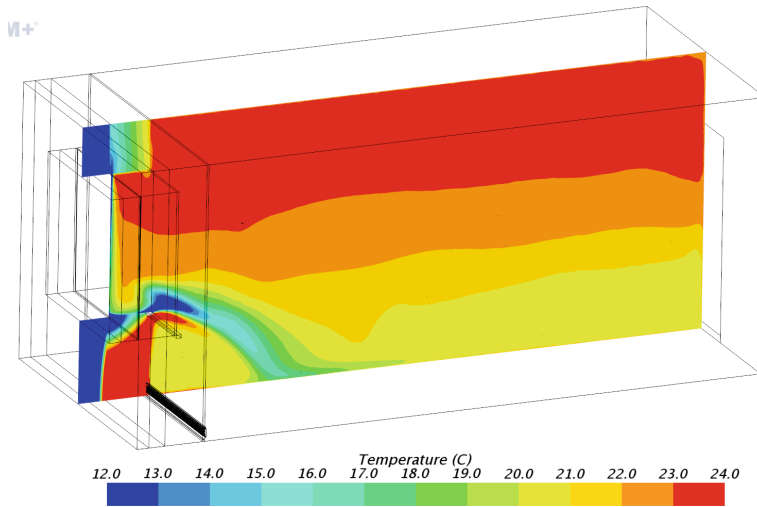


Fig. 3. Temperature field cross-section (room axis).

Microclimate controlled parameters (permissible or optimal) shall be ensured in serving area (habitation zone) [11]. For accommodation, serving area is accepted as the space limited by planes parallel to the floor and walls at the height of 0.1 and 1.5 m above floor level and at a distance of 0.5 m from internal surfaces of external and internal walls, windows and heating units.

The calculations made allow assessing type of interaction between down flow at the glazing and upward flow from the converter. Down flow of the air cooled at the glazing and outdoor air supply is transferred into room serving area at the rate of 0.3 m/s which exceeds permissible value for air flow rate which is equal to 0.2 m/s (Figs. 2 and 4). At the rate of 0.3 m/s the flow goes down to the floor surface at a distance of 1.2 m from external wall. To prevent the air from reaching serving area, measures to deviate down flow air to upper area of the room shall be provided.

Upward flow of air from the heating unit outside the window is transferred to upper area of the room which results in its overheating – air temperature goes as high as 24 °C. Great temperature stratification is observed in the room – from 20 to 24 °C along room height, and in the coverage area of downward flow going to the floor

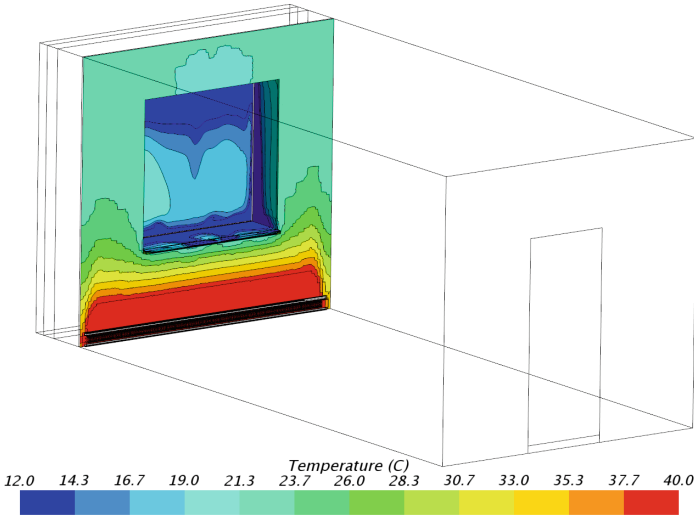


Fig. 4. Temperature field of external wall internal surface and glazing

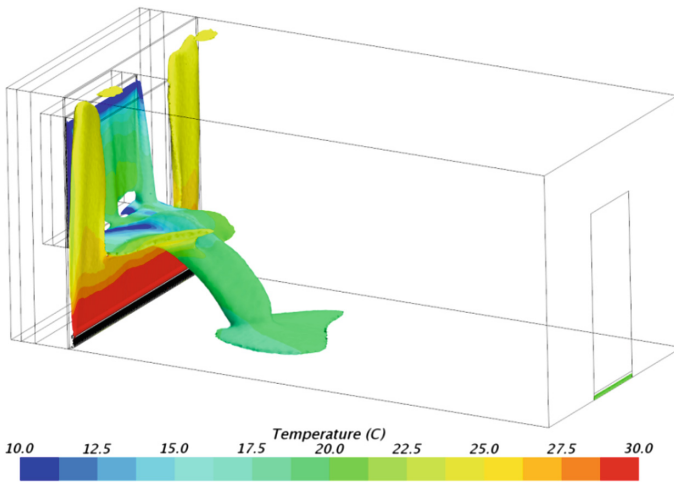


Fig. 5. Heat Pattern of isotaches 0.3 m/s of air flow in compartment

surface – from 17 to 24 °C. For accommodation areas, air temperature difference not exceeding 3 °C is permissible if permissible microclimatic conditions are provided.

External wall horizontal butt joints in flooring support area have the following values: at floor level – plus 24 °C; at the ceiling – plus 20 °C.

External wall surface temperature above the unit reaches 40 °C and goes down to 21 °C at the top of the room. The lowest temperature observed on glazing surface is plus 12 °C.

4 Conclusion




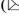

1. With convector-type skirting heater for heat replenishment installed along external wall in accommodation, temperature of external wall on internal surface and resulting room temperature increase. Temperature decrease in the area of external wall horizontal butt joints in flooring support area is prevented.
2. Down flow of lower temperature supply air (as compared to internal air temperature) is supplied to room serving area and creates discomfort area.
3. The version considered of skirting heating system with air supply through adjustable window sashes does not allow ensuring controlled microclimatic parameters (air temperature and flow rate) within serving area or controlled temperature difference in different points of serving area.

References

1. Drozdov, V.A. (eds.): Catalogue of Temperature Fields for Standard Cladding Structure Units. P. 1. Accommodation Buildings. Stroyizdat, Moscow (1980)
2. Construction Heat Engineering. Construction Rules and Regulations II-3-79. Stroyizdat, Moscow (1979)
3. Building Heat Insulation. SP 50.13330.2012. Ministry of Regional Development of Russia. Moscow (2012)
4. Schekin, R.V. (eds.): Reference-Book on Heat Supply and Ventilation. Book 1. Budivelnik, Kiev (1976)
5. Pukhkal, V.A., Sukhanov, K.O.: Numerical study of skirting-type convector. *Novaya Nauka: Idea Result* **6-2**(90), 169–173 (2016)
6. Grititlin, A.M., Datsyuk, T.A., Denisikhina, D.M.: Numerical Simulation in Design of Ventilation and Air Conditioning Systems. AVOK Severo-Zapad, Saint-Petersburg (2013)
7. Denisikhina, D.M.: Features of the numerical simulation of air movement inside concert and theater halls. <https://naukovedenie.ru/PDF/81TVN314.pdf>. Accessed 18 Aug 2017
8. Pukhkal, V.A., Sukhanov, K.O., Grititlin, A.M.: Indoor thermal comfort maintenance by means of water skirting board heating system. *Vestnik Grazhdanskikh Inzhenerov* **6**(59), 156–162 (2016)
9. Chui, E., Raithby, G.: Computation of radiant heat transfer on a non-orthogonal mesh using the finite-volume method. *Numer. Heat Transf.* **23**, 269–288 (1993). Part B
10. Ploskic, A., Holmberg, S.: Heat emission from thermal skirting boards. *Build. Environ.* **45** (5), 1123–1133 (2010)
11. Accommodation Buildings and Public Facilities. In-Door Microclimate Parameters. GOST 30494-2011. Standartinform. Moscow (2011)

Transport Buildings and Structures

Effect of the Structural Characteristics on Frost Resistance of Concrete

Lev Alimov , Victor Voronin , Oksana Larsen  ,
and Vasilij Korovyakov 

Moscow State University of Civil Engineering,
Yaroslavskoye sh. 26, 129337 Moscow, Russia
larsen.oksana@mail.ru

Abstract. Today, in buildings and constructions for transport infrastructure, such as tunnels, elements of the bridges, viaducts, roads, are used concretes with high performance properties. This paper presents the results of the study of frost resistance of concretes for road infrastructure. The results of the study show the influence not only of water-cement ratio and porosity of the concrete for such transport buildings, but also of structural and technological characteristics: true water-cement ratio and volume concentration of cement paste in concrete. Investigation shows that the lowest frost resistance has pure cement paste. Frost resistance increases sharply up to a certain value with the increase of amount of aggregate. The increase of the aggregate content in cement compositions leads to the decrease of expectancy of unimpeded crack distribution. This effect increases the frost resistance of the material.

Keywords: Road infrastructure · Resistance · Concrete · Cement paste

1 Introduction

The next characteristics of concrete, determined by the end of the period of structure formation, were taken into consideration:

- effective water-cement ratio of cement paste in concrete W_e , which has a crucial impact on the scope and nature of pores in cement stone and properties of interfacial transition zone between cement stone and aggregate [1, 2]. True water-cement ratio of the cement paste in concrete W_e forms the initial structure of concrete within range:

$$W_e = (0.876 - 1.65)C_{sc}, \quad (1)$$

C_{sc} - coefficient is equal to w/c ratio of standard consistence of cement paste [3].

- volume concentration of cement paste C_c expressed in fractions of the volume of concrete which quantitatively determines the macrostructure of concrete as the structure of the concrete-like conglomerate:

$$C_c = \frac{\text{Cem}}{1000} \left(\frac{1}{\rho_c} + W_e \right), \quad (2)$$

Cem - consumption of cement, kg;

ρ_c - density of cement, t/m^3 ;

W_e - effective water-cement ratio of cement paste.

Structural characteristics of concrete are based on the amount of water which aggregate consumes during the period of structure formation.

It is possible to calculate the water related to cement W_c basing on cement consumption Cem and the values of the true water-cement ratio W/C_t :

$$W_c = \text{Cem} \cdot W_e \quad (3)$$

The difference between the quantity of mixing water W_m and the water related to cement W_c gives possibility to calculate the water demand of the aggregate W_a :

$$W_a = W_m - W_c \quad (4)$$

The effective water-cement ratio of the cement paste W_e in concrete is:

$$W_e = \frac{W_m - W_a}{\text{Cem}} \quad (5)$$

2 Materials and Methods

The cement used in this study was ordinary Portland Cement type CEM I 32.5 N Holcim Rus in accordance with [4]. Mineral content was: C3A = 7.2%, C3S = 60.8%, C2S = 13.7%, C4AF = 10.0% with specific surface area equal to 3600 cm^2/g . Chemical composition is presented in Table 1.

Table 1. Chemical composition of CEM 32.5 N.

Component	Percentage	Component	Percentage
SiO ₂	18.6	TiO ₂	0.3
Al ₂ O ₃	4.5	P ₂ O ₅	0.1
CaO	63.6	SO ₃	3.1
Fe ₂ O ₃	3.1	Na ₂ O	0.2
MgO	3.2	K ₂ O	0.6

Standard consistence of cement paste was equal to 25%.

Crushed granite with a maximum size of 20 mm according to [5], specific gravity of 2.7 kg/m^3 , water absorption of 0.2% according to [6], packing density of 1480 kg/m^3 and water requirement of 3.43% was used as coarse aggregate.

Quartz sand with specific gravity equal to 2.65 kg/m^3 with the fineness modulus of 2.3 and water requirement of 7% was used as fine aggregate.

The cement system was researched with W_e with the following values:

$W_e = 0.22$, which is equal to $0.867C_{sc}$, $W_e = 0.41$, which is equal to $1.65C_{sc}$ and $W_e = 0.31$ which is equal to a average value between 0.22 and 0.41.

Volume concentration of cement paste C_c was adopted to each water-cement ratio: $C_c = 0.15$; $C_c = 0.2$; $C_c = 0.3$; $C_c = 0.4$; $C_c = 0.5$; $C_c = 1$.

Granulometric content of aggregates was constant.

Such systematization of the compositions gives the possibility to perform the entire range of possible cement compositions from these materials and, consequently, allows you to obtain general order of the investigated parameters of structure and properties of concrete. The cube samples $100 \times 100 \times 100 \text{ mm}$ were cased in accordance with [7–9] from each composition. Demolding of the cubes was carried out 24 h after casting. The cubes were placed in a $20 \text{ }^\circ\text{C}$ water curing tank until tests. All the studied compositions (Table 2) were tested in accordance with [10] after 28 days of curing.

Table 2. Characteristics of the studied concretes.

№	W_e	C_c	W_m	Consumption of materials, kg/m^3			
				Cement	Water	Quartz sand	Crushed granite
1	0.22	0.15	0.563	277	156	676	1354
2	0.31	0.15	0.71	237	168	676	1354
3	0.41	0.15	0.87	205	179	676	1354
4	0.22	0.2	0.46	369	169	637	1274
5	0.31	0.2	0.59	316	186	637	1274
6	0.41	0.2	0.73	273	201	637	1274
7	0.22	0.3	0.36	553	199	557	1114
8	0.31	0.3	0.47	475	224	557	1114
9	0.41	0.3	0.6	410	245	557	1114
10	0.22	0.4	0.3	738	223	478	956
11	0.31	0.4	0.4	633	257	478	956
12	0.41	0.4	0.52	546	284	478	956
13	0.22	0.5	0.28	922	259	398	796
14	0.31	0.5	0.38	791	301	398	796
15	0.41	0.5	0.49	683	336	398	796
16	0.22	1	0.22	1845	406	–	–
17	0.31	1	0.31	1582	490	–	–
18	0.41	1	0.41	1366	560	–	–

Porosity was determined using three-stage water saturation of the concrete samples. It allows to classify the pores into three groups. Concrete samples were dried to constant weight, and then exposed to three-stage saturation with water. The first stage involves the exposure of the samples to constant weight in conditions with relative humidity of 100% and temperature 20 ± 2 °C. In this case saturation is caused by capillary condensation, which occurs due to the ability of the microcapillaries with radius of less than 10–5 cm to absorb moisture from the air. Thus, in the first stage, the capillaries are saturated completely, while microcapillary (a radius of more than 10–5 cm) do not contain condensing water. This is total porosity. The second stage involves water saturation of the samples to constant weight mainly by absorption. Water fills all the interconnected pores, cracks. The third stage involves the saturation of samples with water under vacuum. Such conditions of saturation contribute to fill by water conditionally closed pores, not filled with regular saturation of the pores.

3 Results

The dependence of frost resistance of concrete from its basic structural parameters was investigated. In Table 3 the results of the study of frost resistance of concrete, the total porosity and the second stage porosity are shown. It was failed to establish the dependence of frost resistance neither from water-cement ratio and total porosity nor the second stage porosity. For example, frost resistance of concrete with $W/C = 0.4$ can be at the range of 50 to 240 cycles. Frost resistance of the concrete depends on W/C

Table 3. Properties of the studied concretes.

No.	Frost resistance, cycles	Total porosity, %	Porosity II
1	225	15.5	10.5
2	125	16	11
3	75	17.5	12
4	230	17	11
5	175	17.5	12
6	100	18.0	13
7	300	17.5	12.5
8	200	18.5	13
9	125	21.5	14
10	325	18.5	13
11	225	21.5	14
12	145	23.5	16
13	345	21.5	14
14	175	23.5	16.5
15	155	27.5	18.5
16	200	23	18
17	100	35	23.5
18	55	39	28.5

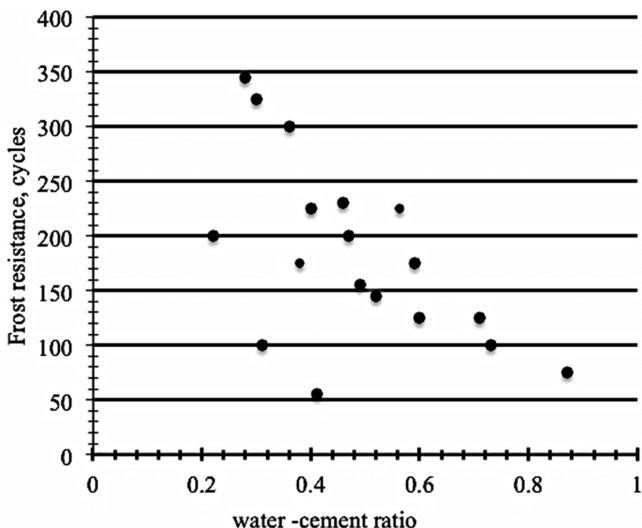


Fig. 1. The dependence of frost resistance of concrete from water-cement ratio.

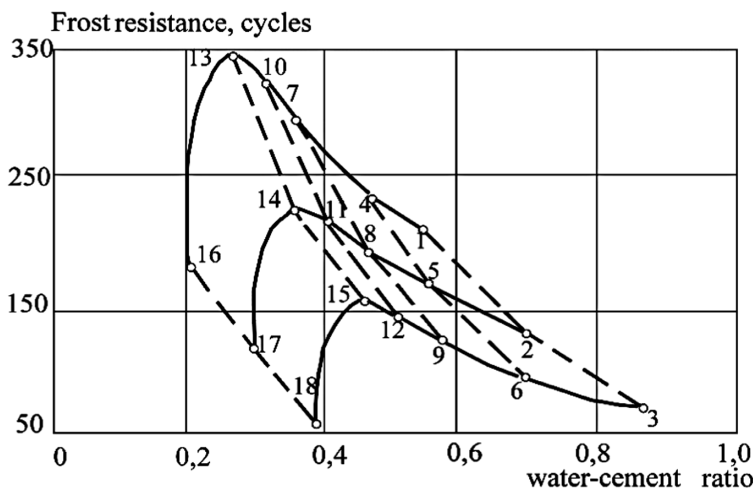


Fig. 2. The dependence of the frost resistance of concrete from of the water-cement ratio.

ratio (W_m) of the mixture [11] and porosity [12, 13] into account of the volume concentration of cement paste C_c in concrete mix and W_c (Figs. 1, 2, 3 and 4). Pure cement paste has the lowest frost resistance. Frost resistance increases sharply up to a certain value with increase of amount of aggregate.

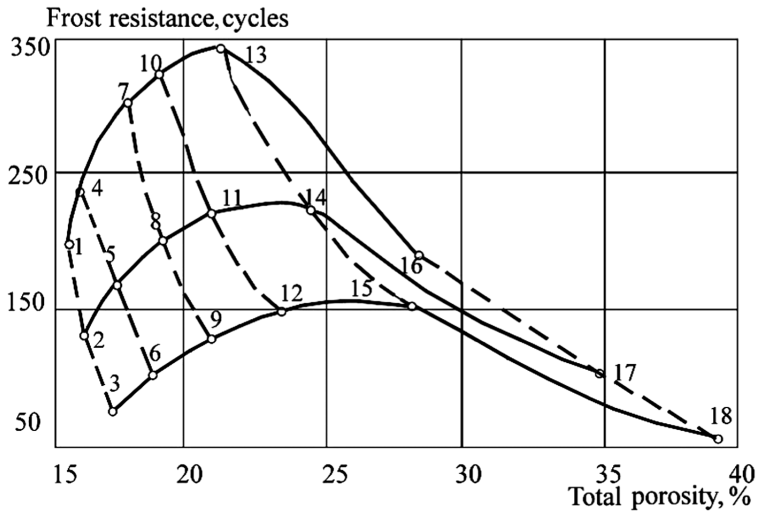


Fig. 3. The dependence of the frost resistance of concrete from the total porosity with the following the structural characteristics: $W_e = 0.22; 0.31; 0.41$ - dotted line; $C_c = 0.15; 0.2; 0.3; 0.4; 0.5$ - continuous line.

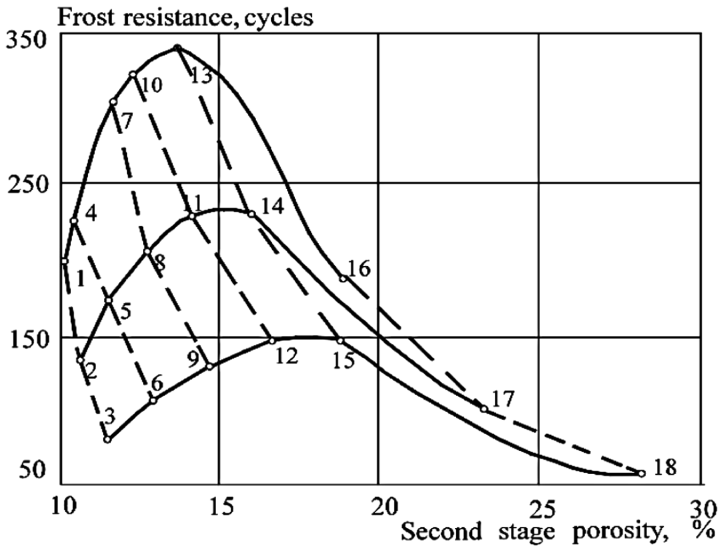


Fig. 4. The dependence of the frost resistance of concrete on the second stage porosity with considering the structural characteristics: $W_e = 0.22; 0.31; 0.41$ - dotted line; $C_c = 0.15; 0.2; 0.3; 0.4; 0.5$ - continuous line.

It should be noted that there is no dependency of frost resistance from both total porosity and second stage porosity. The dependence of frost resistance from porosity exists either at a constant value of C_c or W_e (Fig. 3)

It is connected with the nature of destruction of the samples. The samples containing pure cement paste cracked into several parts in the direction of the major “backbone” cracks while freezing and thawing. The increase of the aggregate content in cement compositions leads the decrease of expectancy of unimpeded crack distribution. This effect increases the frost resistance of the material.

4 Conclusions

The increase of the W_e with $C_c = \text{const}$ leads to degradation of the structure of cement paste in the concrete and, consequently, to a decrease of frost resistance. The increase of porosity (total porosity, second stage porosity) enhances frost resistance with volume concentration of cement paste in concrete up to values of $C_c = 0.5\text{--}0.6$. The increase of C_c reduces the length of the contact area. Porosity is increased due to the growth of own porosity of cement paste [14, 15]. According to dependences of frost resistance on total porosity and frost resistance on second stage porosity while C_c is const (Figs. 3 and 4) leads to a decrease of frost resistance for all values of C_c .

References

1. Bazhenov, Y., Gorchakov, G., Alimov, L., Voronin, V.: Concrete of the Specified Properties. Stroyizdat, Moscow (1974)
2. Sáez del Bosque, I., Zhu, W., Howind, T., Matías, A., Sánchez de Rojas, M., Medina, C.: Properties of interfacial transition zones (ITZs) in concrete containing recycled mixed aggregate. *Cement Concr. Compos.* **81**, 25–34 (2017)
3. EN 197-1 Composition, specifications and conformity criteria for common cements (2000)
4. Russian standard 31108-2016 Common cements. Specifications (2017)
5. Russian standard 8267-93 Crushed stone and gravel of solid rocks for construction works. Specifications (2017)
6. Russian standard 8269.0-97 Mountainous rock road-metal and gravel, industrial waste products for construction works. Methods of physical and mechanical tests (2017)
7. Russian standard 10181-2014 Concrete mixtures. Methods of testing (2017)
8. Russian standard 18105-2010 Concretes. Rules for control and assessment of strength (2017)
9. Russian standard 7473-2010 Fresh concrete. Specifications (2017)
10. Russian standard ГОСТ 10060.3-95 Concretes. Dilatometric rapid method for the determination of frost-resistance (2014)
11. Liu, Z., Hansen, W.: Effect of hydrophobic surface treatment on freeze-thaw durability of concrete. *Cement Concr. Compos.* **69**, 49–60 (2016)
12. Carrara, P., De Lorenzis, L.: Consistent identification of the interfacial transition zone in simulated cement microstructures. *Cement Concr. Compos.* **80**, 224–234 (2017)
13. Cavalline, T., Calamusa, J., Kitts, A., Tempest, B.: Field-observed cracking of paired lightweight and normalweight concrete bridge decks. *Int. J. Concr. Struct. Mater.* **11**(1), 85–97 (2017)
14. Ozbeka, A., Weerheijmb, J., Schlangen, E., Breugel, K.: Dynamic behavior of porous concretes under drop weight impact testing. *Cement Concr. Compos.* **39**, 1–11 (2013)
15. Lee, J., Jang, Y., Park, W., Kim, S.: A study on mechanical properties of porous concrete using cementless binder. *Int. J. Concr. Struct. Mater.* **10**(4), 527–537 (2016)

Concrete Waste Recycling and Re-use of Shielding Wall Materials After Decommissioning of Fusion Reactors

Andrey Pustovgar^(✉) , Aleksey Adamtsevich ,
and Liubov Shilova 

Moscow State University of Civil Engineering,
Yaroslavskoye Sh. 26, 129337 Moscow, Russia
PustovgarAP@mgsu.ru

Abstract. The paper considers possible processing and re-use of waste products obtained in the process of removal from service of pre-fabricated concrete structural elements of biological protection shields at thermonuclear fusion reactors. The experimental concrete compositions have been obtained through the mechanical-and-chemical processing of crushed concrete structures which had worked under neutron radiation with the energy of 14.8 MeV. These concrete compositions have been studied, and some ways of total or partial substitution of the Portland cement by crushed small-grain waste products in the process of erection of concrete or reinforced concrete structures are considered as well.

Keywords: Building materials · Concrete · Transport buildings and structures
Mineral composites · Mechanical-and-chemical treatment · Binding agent

1 Introduction

Nowadays, 31 countries use nuclear power plants (NPP); there operate more than 190 NPP with 449 power units [1]. Some countries curtail their nuclear programmes [2], and the maintenance period of many nuclear power units comes to its end. Thus, the removal of nuclear power units from service becomes more and more urgent.

So, about 40 nuclear power units were removed from service during the last decade.

At the same time, the research works in the field of controlled thermonuclear fusion passed from the stage of scientific experimental works to the stage of engineering project development. The assumed maintenance period for structural elements of thermonuclear fusion plants (TFP) will be only 2 to 3 year long, while the NPP have a 60 year long maintenance period [3]. Therefore, the problem of removal of TFP from service will become urgent very soon. So, it is expedient to develop some technologies of efficient re-use of waste products right now.

The demolition waste products obtained in the process of removal of nuclear engineering plants (NEP) from service are mainly the concrete load-carrying and

fencing structures, the volumes of which may achieve the value of several thousand m^3 depending on the NEP type.

The demolition waste products differ in their composition as well as in the level of their radioactive contamination. Mainly these waste products have only superficial contamination with a low radio-activity level. Such materials may be deactivated and re-used in the construction production without any further radiation monitoring [4].

The solution of the problem of utilization of demolition waste products not only reduces the volume of the burial of radioactive waste but also allows us to insert the aforesaid waste products in a closed cycle for their further re-use in the building industry.

2 World Experience in the Field of Re-use of Waste Products

One of the difficult problems in the nuclear industry is the process of separation of waste products with respect to the nature and the intensity of their contamination.

In this connection, much attention is paid to the development of various robotics platforms with reliable fast-acting visualization systems allowing the automation of the process of nuclear waste classification. Till now, the process of nuclear waste classification has been carrying out by hand [5].

Besides, a large-scale generation of nuclear wastes require the development of cadastres containing the information about the radioactive waste products generated both during the process of maintenance of NPP and the period of its removal from service [6].

In case, when the re-use of waste products is impossible, the recommendations on their burial are developed.

But one of the main purposes of the process of treatment of such wastes is the possible reduction in their amount due to their re-use [7].

Some suggestions on treatment and conditioning of non-standard radioactive wastes and others are described in [8].

However, the known methods of utilization of demolition wastes of the process of removal of NEP from service mainly include only the following: the road building fill, the backfill for underground working rooms and ravines. The suggestions on the use of these waste products as the raw materials for the production of concrete compositions or concrete structural elements are conceptual and are not supported by any developed technologies.

The complication of this problem is the fact that the process of crushing of the aforesaid reinforced concrete structures gives a high amount (up to 40%) of small-grain fractions with the grain size of not more than 6 mm. These fractions cannot be used in practical building as they contain much (up to 60%) of the dust-like fraction with the particle size less than 0.16 mm.

As to the thermonuclear fusion plants, the thermonuclear fusion technologies will be widely applied in the world power industry in the near future. So, there will be a great demand for regular removal of concrete structural elements from service. The elements in question are pre-fabricated concrete elements working in the biological protection shields which have a low induced radioactivity gained through a neutron

radiation with the energy of 14.8 MeV. In this connection, the development of efficient ways of processing and re-use of building materials obtained from the demolished structures becomes very important.

1. Research hypothesis and research purpose.
2. The chemical analysis of crushed small-grain waste products showed that they may contain up to 20% of not-hydrated Portland cement. Therefore, we came to a suggestion on the possible use of these waste products (after an appropriate processing) as a binding agent for building mortars or concrete as well as for the radioactive waste grouting.
3. Materials and methods.
4. The research works resulted in the development of a technology of processing of small-grane concrete waste products through a combined mechanical-and-chemical treatment with active mineral additives in the presence of surface-active substances. This technology uses a continuous drum shock mixer. The waste from the ferrosilicon production (the main components: iron and silicon) was used as on active mineral additive. A super-plasticizer based on sulphate-naphthalene-formaldehyde compositions was used as a surface-active substance. The small-grain waste products included crushed shield concrete structures which worked in the 14.8 MeV neutron fields as well as crushed concrete structures which weren't exposed to radiation. The X-ray patterns and the results of the X-ray phase analysis (Ritwell's method) of the mortar part of some concrete specimens are presented in Figs. 1 and 2, respectively.

After the mechanical-and-chemical processing, the specific area of the surface of small-grain waste products was equal to 6500 cm²/g. The following concrete compositions were produced for the determination of strength characteristics of the binding agent (Table 1).

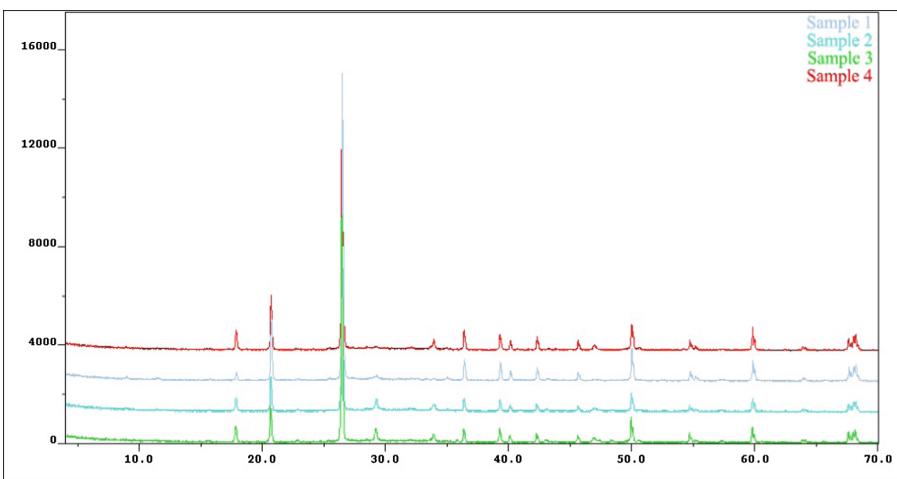


Fig. 1. The X-ray patterns of the mortar part of some concrete specimens.

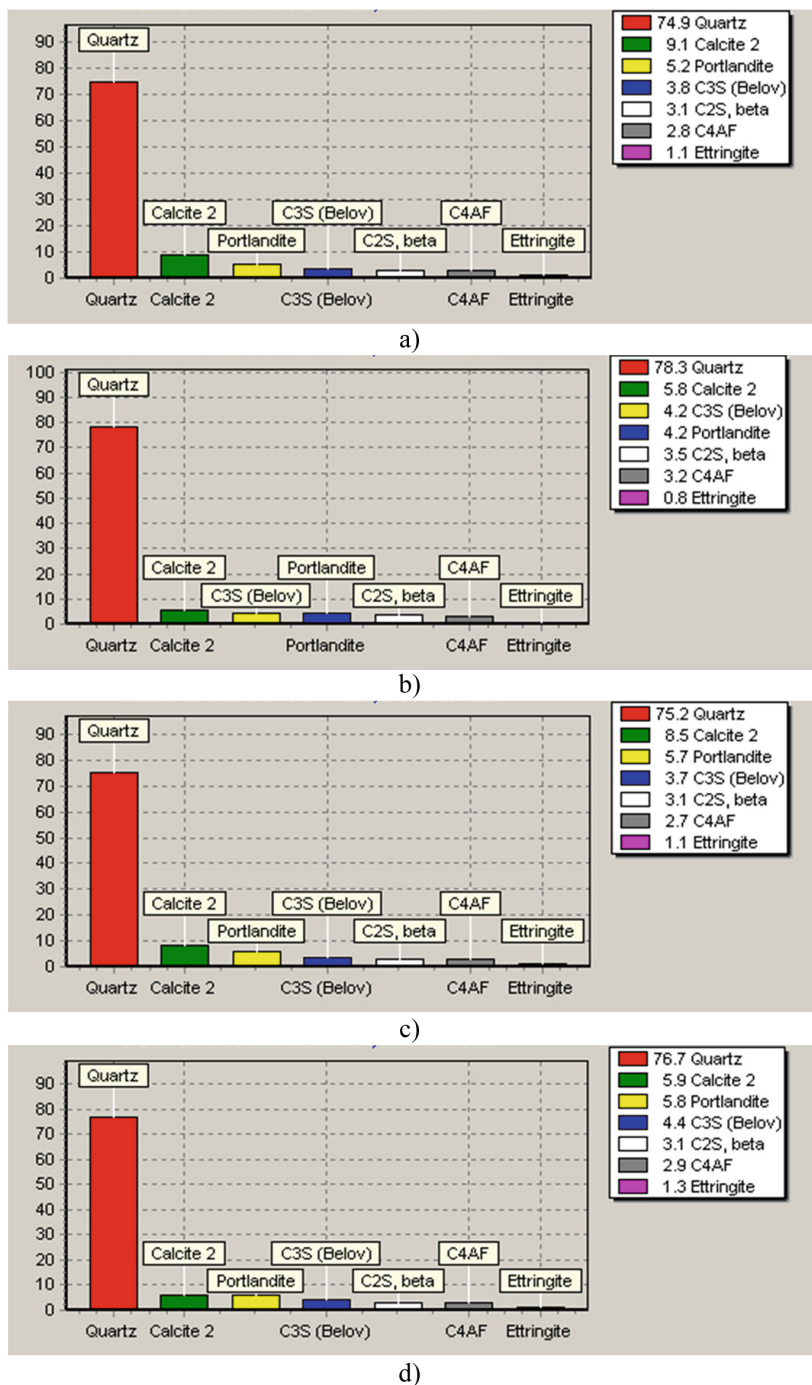


Fig. 2. The results of the X-ray phase analysis (Ritwell's method) of the mortar part of some concrete specimens.

Table 1. Dosage of components in experimental compositions, kg/m³.

	Composition 1	Composition 2	Composition 3	Composition 4
Portland cement CEM 32,5	200	–	–	–
Binding agent from small-grain waste products	–	200	250	300
Small-grain waste products	700	700	700	700
Crushed stone from the reinforced concrete waste	1120	1120	1120	1120

The produced samples were tested in the research laboratories (SRI CM&T MGSU) for the compression strength at the age of 28 days in accordance with Russian Standard «GOST 10180-2012 Concrete. Methods of strength determination through test specimens with the use of the servo-hydraulic press Advantest-9».

3 Results and Discussion

The compressive strength (after 28 day long hardening under wet conditions) of the compositions with a binding agent made from small-grain waste products increases with a higher dosage of the binding agent, Fig. 3.

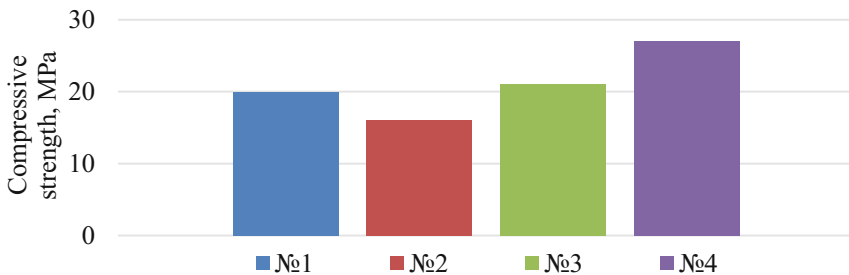


Fig. 3. Compressive strength of the concrete compositions after 28 days of hardening under wet conditions.

With the binding agent dosage of 200 kg/m³ (compositions 1 and 2), the strength of concrete with the binding agent from small-grain waste products is lower than the strength of the standard concrete specimen (based on the Portland cement CEM 32.5). With the increase in the binding agent dosage up to 250 kg/m³ (composition 3), the specimen strength is even higher than the strength of the standard specimen. The further increase in the dosage of the binding agent from small-grain waste products up

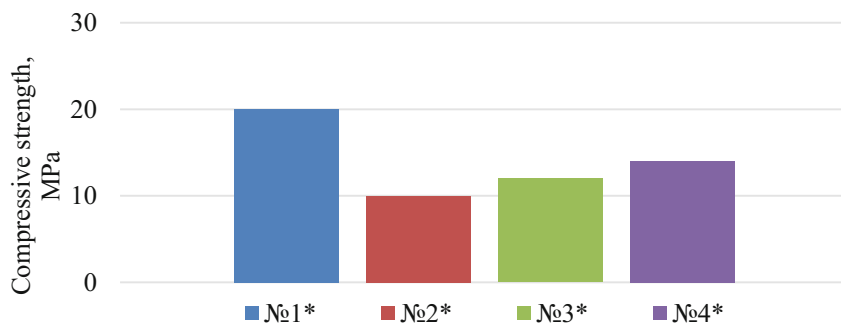


Fig. 4. Compressive strength of the concrete compositions after 28 days of hardening under wet conditions (compositions 1*, 2*, 3*, 4*) (increase in the dosage of the binding agent from small-grain waste products).

to 300 kg/m^3 (composition 4) causes a considerable increase in the strength in comparison with the standard specimen. For a comparative analysis, the similar tests were carried out for the compositions 2*, 3*, 4*, where the small-grain concrete waste products which were not exposed to radiation were used as the binding agents after a mechanical-and-chemical processing, Fig. 4.

The compression strength (after 28 days of hardening under wet conditions) of the compositions with binding agents made of small-grain waste products which were not subject to the radiation tends to greater values with the increase of the dosage, but it does not exceed the strength value for the standard specimen. Obviously, the higher strength values for the specimens are caused by the influence of radiation on the cement stone and the formation of microdefects, which contribute much to the activation of not hydrated cement phases during the mechanical-and-chemical processing.

A considerable difference in the strength characteristics of the specimens is connected with the influence of the radiation on the concrete components with the increase in the dosage of binding agent as it is seen from Fig. 3. The strength values for the compositions 1 and 2 are less than those for the standard specimen (concrete with the CEM 32.5 cement). The strength value for the composition 3* (with the binding agent dosage of 350 kg/m^3) even exceeds that for the standard specimen.

4 Conclusion

The binding agent produced in the process of mechanical-and-chemical treatment of small-grain concrete waste products may be used in the process of erection of concrete and reinforced concrete structures. This research work also includes the study of possible use of the obtained binding agent for the process of cementation of radioactive waste products as well as the study of the influence of different active mineral additives and surface-active substances on physical-and-mechanical properties of binding agents produced from small-grain waste products obtained in the process of removal of NEP from service. The performance of these research works will contribute much to the




existing methods and technologies concerning the utilization of demolition waste products obtained in the process of removal of NEP from service. The given catalogue could include the methods of crushing of different fractions of concrete stone, the methods of production of binding agents through an additional grinding of crushed products and their mechanical-and-chemical processing, the methods of production of concrete stone and binding agent through a low-temperature processing and the further crushing and grinding, and, at last the method of production of the concrete compositions consisting completely (100%) of the processed demolition waste products, the concrete intended for the erection of load-carrying, fencing and shield structures for nuclear engineering plants.

Acknowledgements. This study was performed with the financial support of the RF Ministry of Education and Science, President Grant, agreement #14.Z56.17.3456-MK.

References

1. <https://www.iaea.org/PRIS/WorldStatistics/OperationalReactorsByCountry.aspx>. Accessed 21 Aug 2017
2. Kuznetsov, V.: Removal of Nuclear Power Engineering Projects from Service. NIU MGSU, Moscow (2003)
3. Pustovgar, A.: Problems of Ensuring of Radiation Safety for Thermonuclear Reactors. NIU MGSU, Moscow (2015)
4. Engovatov, I., Mashkovich, V.: Radiation safety in the process of removal of civil and military reactor plants from service. Moscow (1999)
5. Shaukata, A., Gaoa, Y., Kuob, J., Bowenc, B., Mortd, P.: Visual classification of waste material for nuclear decommissioning. *Robot. Auton. Syst.* **75**, 365–378 (2016)
6. Rosanvallon, S., Torcy, D., Chon, J., Dammann, A.: Waste management plans for ITER. *Fusion Eng. Des.* **109–111**, 1442–1446 (2016)
7. Rosanvallon, S.: ITER waste management. *Fusion Eng.* **85**, 1788–1791 (2010)
8. Strážoveca, R., Hrnčířc, T., Lištjaka, M., Nečasa, V.: Selection of optimal treatment procedures for non-standard radioactive waste arising from decommissioning of NPP after accident. *Nucl. Eng. Des.* **301**, 391–401 (2016)

Solving Problems of Distribution Network Tracing: Example of Gas Distribution Using the Search Optimization Methodology

Aleksej Klochko , Victor Zhila , and Asmik Klochko ^(✉) 

Moscow State University of Civil Engineering,
Yaroslavskoye Sh. 26, 129337 Moscow, Russia
klo4ko_aleksey@mail.ru

Abstract. The search optimization methodology was designed to address problems of optimized tracing for distribution networks. Apart from gas pipeline diameters, this methodology is able to vary the installation coordinates of gas-distribution stations and the network and trunk gas pipeline joining points. Such problems share the following features. Compared to similar problems with reinforced concrete structures, where increment of variable parameters must result in higher costs, and decrement in lower cost of the solution, such circumstances may be observed in the field of gas distribution only with the factors of the section's diameter: the larger diameter, the higher the cost of the gas line construction, and the reverse. Meanwhile, changes in the coordinates of characteristic points of the gas distribution network may both increase and decrease total cost of construction.

Keywords: Mathematical method of search optimization
Search point · Movement of search point
Optimization of transportation network configuration

1 Introduction

Considerable resources in questions of financial resources saving at construction of distributive networks are covered in optimization of a transport network configuration. Often it is possible to accept minimization of transport network extent as criterion of optimization. However at design of engineering distributive systems there is an additional parameter - ensuring the required site capacity of network at the set parameters (pressure). The majority of optimizing techniques accept as optimizing parameter the minimization of network extent and are incapable to consider additional criteria.

2 Materials and Methods

Many authors have demonstrated that where the target function and the region of feasibility limits are non-linear and convex, there the optimum point is unambiguous, singular and situated on the boundary of the feasibility region [1–4]. Therefore, as we apply the search methodology we need to consider the change of the target function K

(d), while we also need to unambiguously define the boundary condition for the problem’s solution. In terms of distribution network design, such will be the lowest gas pressure at user entry points.

The initial search point (understood here as a combination of variable parameters) can lie both in the range of legitimate and illegitimate solutions.

Movements of the search point (defined here as changes of the numeric value of at least one of the combination’s variable parameters) is traced by intermediate iterations. An intermediate iteration is a combination of variable parameters that only differs from the original iteration by one variable parameter (see Table 1):

Table 1. Change pattern of variable parameters in intermediate iterations.

Iterations	Variable parameter values			
Initial (r)	$a_{1,r};$	$a_{2,r};$	$\dots;$	$a_{i,r}$
Intermediate iterations	$a_{1,r} + \Delta a$	$a_{2,r}$	\dots	
	$a_{1,r} - \Delta a$		\dots	
	$a_{1,r}$	$a_{2,r} + \Delta a$	\dots	
	$a_{1,r}$	$a_{2,r} - \Delta a$	\dots	
	$-/-$	$-/-$	$-/-$	$-/-$
			\dots	$a_{i,r} + \Delta a$
		\dots	$a_{i,r} - \Delta a$	
Iteration (r + 1)	$a_{1,(r+1)}$	$a_{2,(r+1)}$		$a_{i,(r+1)}$

Movement from iteration (r) to iteration (r + 1) is controlled with the value of target function $K(r)$, generalized non-viscous $H(r)$ and generalized redundancy $R(r)$.

The values of generalized non-viscous $H(r)$ and generalized redundancy $R(r)$ are generated by the restricting condition for the lowest value of the parameter:

$$\varphi_j = \frac{g(\bar{y})}{\{g\}} - 1 \geq 0 \tag{1}$$

where

- j – serial number of the restriction: $j = 1; 2; 3; \dots; n$;
- $g(y)$ – current value of the parameter;
- $\{g\}$ – limiting value of the parameter.

Non-viscous and redundancy values n_j and u_j of parameter j depend on:

$$n_j = 0 \text{ and } u_j = \varphi_j, \text{ if } \varphi_j \geq 0; \tag{2}$$

$$n_j = \varphi_j \text{ and } u_j = 0, \text{ if } \varphi_j \leq 0.$$

By adding up the squared values of n_j and u_j we generate indicators $H(r)$ and $R(r)$ [1, 5, 11]:

$$H_{(r)} = \sqrt{\sum_{j=1}^n u_j^2} \tag{3}$$

$$R_{(r)} = \sqrt{\sum_{j=1}^n u_j^2} \tag{4}$$

A positive value of $H(r) > 0$ means that the search point is in the range of illegitimate solutions. If $H(r) = 0$, the search point is in the legitimate range.

Thus we need to direct the search in a way that would make the value of generalized non-viscous $H(r)$ diminish with each step of iteration, to the ultimate zero. Implementation of this approach is known as «C Procedure».

If $H(r) = 0$, while $R(r) > 0$, then the search point lies in the legitimate range of the problem. If $H(r) = 0$ and $R(r) = 0$, the search point is on the boundary of the legitimate range.

The procedure of selecting the values of variable parameters, by diminishing the generalized redundancy with each iteration step is known as the «F Procedure».

The change of variable parameter $a_{i,(r)}$ to value $a'_{i,(r)} = a_{i,(r)} \pm \Delta a_i$ causes the change of the value of target function $K(r)$, generalized non-viscous $H(r)$ and generalized redundancy, described by increments ΔK_i , ΔH_i and ΔR_i ,

$$\Delta K_i = K_{i,(r)} - K_{(r)}, \quad \Delta H_i = H_{(r)} - H_{i,(r)} \quad \text{и} \quad \Delta R_i = R_{(r)} - R_{i,(r)} \tag{5}$$

In real life, increments ΔH_i and ΔK_i can take on any numeric values, represented as combinations (Table 2):

Table 2. Possible combinations of changing generalized non-viscous and target function.

Scenario 1		Scenario 2		Scenario 3	
	$\Delta H_i < 0$ moving into the illegitimate range of solutions		$\Delta H_i = 0$ fixed position of search		$\Delta H_i > 0$ moving towards the boundary of legal solutions
1.1	$\Delta H_i < 0$ and $\Delta K_i < 0$	2.1	$\Delta H_i = 0$ and $\Delta K_i < 0$	3.1	$\Delta H_i > 0$ and $\Delta K_i < 0$
1.2	$\Delta H_i < 0$ and $\Delta K_i = 0$	2.2	$\Delta H_i = 0$ and $\Delta K_i = 0$	3.2	$\Delta H_i > 0$ and $\Delta K_i = 0$
1.3	$\Delta H_i < 0$ and $\Delta K_i > 0$	2.3	$\Delta H_i = 0$ and $\Delta K_i > 0$	3.3	$\Delta H_i > 0$ and $\Delta K_i > 0$

Indicator $\Delta H_i < 0$ signals that the search point shifts into the illegitimate range of solutions. Therefore, the C-procedure will ignore combinations of generalized non-viscous and redundancy parameters 1.1–1.3.

Indicator $\Delta H_i = 0$ signals that the search point stays put. However, if the target function’s value decreases ($\Delta K_i < 0$), then this movement (combination 2.1) would be effective to seek the optimum. The other combinations (2.2 and 2.3) don’t fit, because the target function either is fixed ($\Delta K_i = 0$) or raises the project costs ($\Delta K_i > 0$).

Indicator $\Delta H_i > 0$ signals that the search point is shifting towards the boundary of the legitimate range. Therefore, combinations 3.1–3.3 are first priorities in search of the optimum.

Thus we can represent the results of condition validation with C-procedure in Table 3:

Table 3. Priority condition validation for shifts with C-procedure.

Procedure of priority-based condition validation	Combination of evaluation parameters	Priority for shift by C-procedure
Condition No. 1 (3.1)	$\Delta H_i > 0$ and $\Delta K_i < 0$	Z_1
Condition No. 2 (3.2)	$\Delta H_i > 0$ and $\Delta K_i = 0$	Z_2
Condition No. 3 (3.3)	$\Delta H_i > 0$ and $\Delta K_i > 0$	Z_3
Condition No. 4 (2.1)	$\Delta H_i = 0$ and $\Delta K_i < 0$	Z_4

If Condition No. 1 is true once during the transition from iteration step (r) to step (r + 1), then search movement proceeds in the direction, and the other conditions described in Table 3 should be ignored. If Condition No. 1 becomes manifest repeatedly, the movement direction is selected based on the condition $Z_{1i} = \max$. The value of search procedure Z_{1i} is found as:

$$Z_{1i} = \Delta H_i \cdot |\Delta K_i|. \tag{6}$$

This is also how we select the direction for the optimum solution with C-procedure as set forth in Table 3 according to the parameter priority. Numeric values of Z_2, Z_3, Z_4 are found with this formula:

$$Z_{2i} = \Delta H_i, \quad Z_{3i} = \frac{\Delta H_i}{\Delta K_i}; \quad Z_{4i} = |\Delta K_i|. \tag{7}$$

The search direction for F-procedure is selected based on condition 2.1 in Table 3. If Condition F is manifest repeatedly in intermediate iterations, the search movement is selected based on direction $F_i = \max$, where:

$$F_i = \frac{\Delta K_i}{\Delta R_i}. \tag{8}$$

When «non-viscous» does not exist, and $F_i = 0$, then the search point lies within the shortest distance from the boundary of legitimate solutions for the problem.

Consequently, C and F procedures as an aggregate transition the search point from a random place in an illegitimate set to the legitimate set, moving it closer to the boundary.

It has to be noted that once-off success of the C and F procedure series does not guarantee the point of optimal solution. So we need to use an I procedure for reverse movement from the boundary of the legitimate set into the illegitimate set, and then repeat the C and F procedure series.

An appropriate sequence of condition check priority for movement into the illegitimate set with procedure I is represented in Table 4:

Table 4. Priority of condition check for movement using the I-procedure.

Procedure of priority-based condition validation	Combination of evaluation parameters	Formula to find value I
condition No. 1 (1.1)	$\Delta H_i < 0$ and $\Delta K_i < 0$	$I_{1i} = \frac{\Delta H_i}{\Delta K_i}$.
condition No. 2 (1.2)	$\Delta H_i < 0$ and $\Delta K_i = 0$	$I_{2i} = \Delta H_i $.
condition No. 3 (1.3)	$\Delta H_i < 0$ and $\Delta K_i > 0$	$I_{3i} = \frac{ \Delta H_i }{\Delta K_i}$.

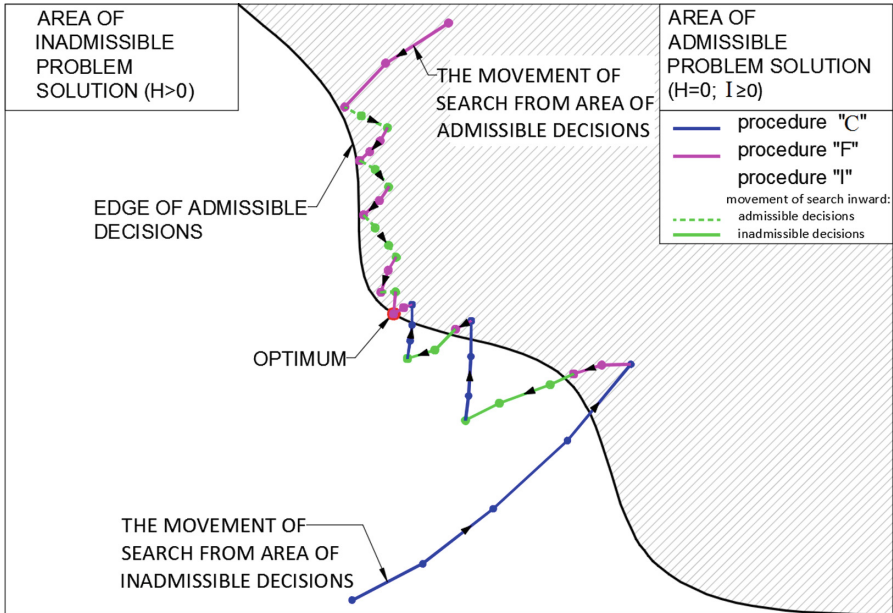


Fig. 1. Diagram of optimum search using the sequence of C-F-I procedures.

Therefore, the sequence of procedures C-F-I- ...C-F-I... is a zigzag path to the point of optimum solution (Fig. 1).

Now let us visually demonstrate the application of search methodology in the solution for gas-distribution network design.

Optimization of the pattern and configuration of gas-distribution networks gives significant economy [4–9].

We need to stake out in plane the position of the gas-regulating station aligned with minimal capital investment in the gas-distribution network.

Given:

- gas pressure (absolute) at the point of joining the trunk line: 0.40 MPa;
- gas pressure (overpressure) downstream of the GDS: 5 kPa;
- trunk connection point in adopted system of coordinates: (800; 200) m;
- methane density at filtering pumps: $\rho = 0.73 \text{ kg/m}^3$;
- absolute equivalent pipe wall roughness (steel) $K_e = 0.1 \text{ mm}$;
- user characteristics are described in Table 5.

Table 5. Characteristics of users in the gas-distribution network.

Parameter	User A	User B
User connection coordinates, (x; y) m	(200; 1.700)	(1.800; 1.000)
Gas flow rate, Q, m ³ /h	900	700
Lowest gas pressure P, Pa	2.000	2.000

To solve the problem, we assume the following random values of variable parameters:

- position of the gas regulating station $(x_4; y_4) = (1,200; 800) \text{ m}$;
- \varnothing of gas line from point 3 to point 4–10.2 cm;
- \varnothing of gas line from point 3 to community A (d_{1-4}) = 14.0 cm;
- \varnothing of gas line from point 3 to community B (d_{2-4}) = 11.4 cm.

The process of seeking the solution is briefly described in Table 6.

In Fig. 2, the first position of search is highlighted in color green.

Now let us verify the solutions to the problem.

For this end, let us solve it again, having changed the search starting position and assigning other numeric values to the parameters.

To solve the problem, we assume the following random values of the variables:

- position of the gas regulating station $(x_4; y_4) = (1000; 1350) \text{ m}$;
- \varnothing of gas line from point 3 to point 4–11.4 cm;
- \varnothing of gas line from point 3 to community A (d_{1-4}) = 32.5 cm;
- \varnothing of gas line from point 3 to community B (d_{2-4}) = 24.5 cm.

The process of seeking the solution is briefly described in Table 7.

In Fig. 2, the second position of search is highlighted in color blue.

Table 6. Search for solution from starting position 1.

(r)	Coordinates		Inner diameter of pipe (cm)			Cost (Rubles)	Non-viscous	Procedures		
	X_4	Y_4	d_{3-4}	d_{1-4}	d_{2-4}	Total	$\sum n$	C	F	I
1	1200.00	800.00	10.20	14.00	11.40	10 689 240	17.329	2.502		
50	1199.00	847.00	10.20	14.00	12.10	10 709 856	15.044	61.538		
100	1167.00	859.00	10.20	15.90	14.00	10 915 233	6.472	1.289		
150	1142.00	878.00	10.20	19.40	15.90	11 323 289	1.303	9.804		
200	1136.00	920.00	10.20	20.30	16.80	11 471 668	0.496	1.880		
220	1136.00	937.00	9.50	21.90	18.00	11 689 929	0.000	0.000	301.930	
250	1110.00	937.00	7.30	21.90	18.00	11 586 790	0.000		22.186	
300	1060.00	937.00	7.30	21.90	18.00	11 550 384	0.000		13.468	
350	1027.00	918.00	7.30	21.90	18.00	11 527 095	0.000		7.634	
400	999.00	894.00	7.30	21.90	18.00	11 513 791	0.000		3.286	
439	979.00	871.00	7.30	21.90	18.00	11 510 198	0.000		0.000	0.125
450	978.00	874.00	6.30	21.90	18.00	11 483 460	3.570	263.158		
500	970.00	834.00	7.00	21.90	18.00	11 507 361	0.064	14.706		
538	988.00	823.00	7.30	21.90	18.00	11 519 074	0.000	0.000	6.153	
550	988.00	833.00	7.30	21.90	18.00	11 515 951	0.000		4.975	
596	979.00	871.00	7.30	21.90	18.00	11 510 198	0.000		0.000	

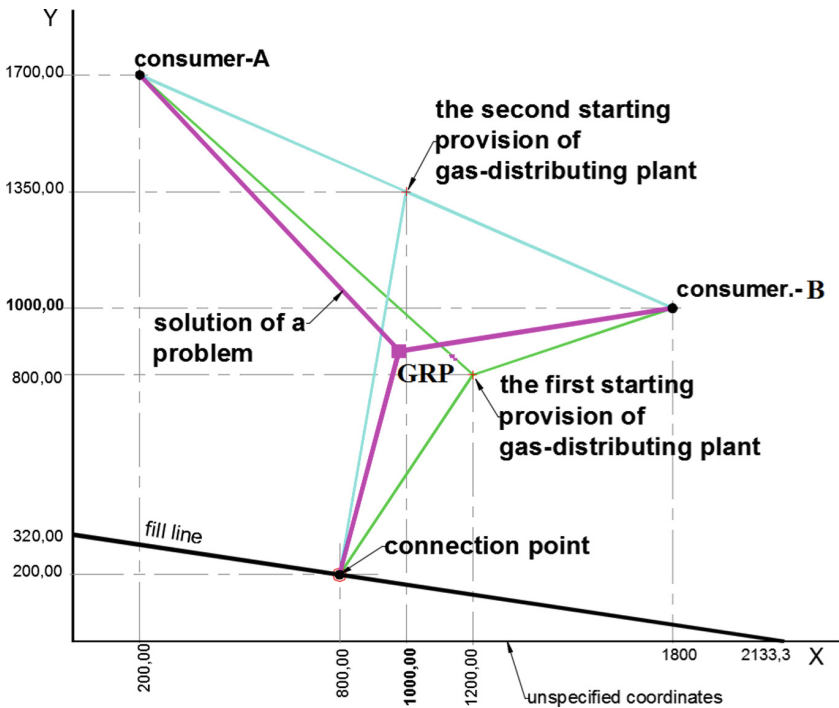


Fig. 2. Gas pipeline tracing option with the search optimization method.

Table 7. Search for solution from starting position 2.

(r)	Coordinates		Inner diameter of pipe (cm)			Cost (Rubles.)	Non-viscous	Procedures		
	X ₄	Y ₄	d ₃₋₄	d ₁₋₄	d ₂₋₄	Total	∑n	C	F	I
1	1000.00	1350.00	11.40	32.50	24.50	14 179 037	0.000		3552.393	
50	1000.00	1312.00	8.30	20.30	19.40	12 301 581	0.000		60.359	
100	1000.00	1262.00	8.30	20.30	19.40	12 125 771	0.000		52.077	
150	1000.00	1213.00	8.30	20.30	18.00	11 879 039	0.000		44.006	
187	990.00	1186.00	8.30	20.30	18.00	11 800 864	0.000		0.000	0.008
189	990.00	1186.00	8.30	20.30	15.90	11 667 775	1.367			0.018
190	990.00	1186.00	8.30	20.30	15.20	11 626 067	2.128	2.559		
200	988.00	1181.00	8.30	20.30	18.00	11 787 207	0.002	0.007		
210	988.00	1173.00	7.60	21.90	18.00	11 873 758	0.000	0.000	60.792	
250	988.00	1133.00	7.60	21.90	18.00	11 784 771	0.000		47.121	
300	988.00	1083.00	7.60	21.90	18.00	11 692 032	0.000		34.084	
350	988.00	1033.00	7.60	21.90	18.00	11 619 565	0.000		23.763	
400	988.00	983.00	7.60	21.90	18.00	11 567 000	0.000		15.225	
450	988.00	934.00	7.30	21.90	18.00	11 525 136	0.000		10.235	
500	988.00	884.00	7.30	21.90	18.00	11 511 203	0.000		1.758	
520	979.00	871.00	7.30	21.90	18.00	11 510 198	0.000		0.000	

Apparently, all variables and the target function value are identical regardless the starting position of the search and do correspond to the data of Table 8. This is evidence of correct solution to the problem of optimum GDS positioning using the search optimization method.

Table 8. Optimal characteristics of the target gas-distribution network.

Solution to problem no. 1	Coordinates (m)				Branch length (m)				Cost (Rubles)
					Pipe diameter (cm)				
	X ₃	Y ₃	X ₄	Y ₄	l ₃₋₄	l ₁₋₄	l ₂₋₄	Total	K _(r)
By search methodology	800.0	200.0	979.0	871.0	694.5	1137.6	831.1	2663.2	11,510,198
					7.3	21.9	18.0		

3 Results

In this article the developed algorithm on optimization of gas-distributing network configuration at the accepted scheme of gas distribution is given. On a present example possibilities of this technique at inter-settlement design gas transmission networks are shown. And also as a result of a settlement experiment ability of a technique to find the optimal solution of a task from different starting provisions of search is confirmed.

The received results can be applied when developing questions on expansion of gas transmission network. In the subsequent adaptation of a technique for the solution of tasks of extensively extensive networks configuration seems possible [10–19].

4 Conclusion




This technique can act as the optimization of transport networks finishing results of various mathematical methods, such as method of the smallest squares, Steiner's method, creation of a Pryma's tree algorithm on the accepted criterion function.

References

1. Arutyunyan, R.: Determination of rational strengthening of the reinforced concrete structures, working in the conditions of seismic impacts, by search optimization method. Ph.D. Thesis, MGSU (2000)
2. Skladnev, N.: About one search algorithm of reinforced concrete structures optimization. Sat. works MISI of V.V. Kuybishev (1981)
3. Tabunshchikov, Yu., Koptev, D., Zhila, V., Klochko, A., Soloveva, E.: Gas distribution systems efficiency preference. *Vestn. MGSU Period.* **8**, 222 (2011)
4. Tamrazyan, A.: Optimum designing of the steel concrete plates working in the conditions of a cross bend and flat tension. Dissertation of Canadian Technology Science, Moscow (1982)
5. Rosen, J.B.: The gradient projection method for nonlinear programming. *J. Soc. Industr. Appl. Math.* **8**, 181–217 (1960)
6. Zhila, V., Klochko, A., Spirina, E.: Cost determination on a construction of gas distribution networks by method of the smallest squares. *Internet Messenger Volg.* **3**(23), 27 (2012)
7. Borovskij, B., Kunsikij, M.: Optimization of gas supply systems of city residential districts. *Constr. Technog. Saf.* **50**, 29–33 (2014)
8. Klochko, A., Arutjunjan, G.: The analysis of the factors influencing an optimum configuration of gas distribution network. *Sci. Rev.* **12**, 239–243 (2013)
9. Zhila, V., Klochko, A., Markevich, J.: Finding of a configuration of gas distribution networks by mathematical methods. *Internet Messenger Volg.* **1**(25), 1 (2013)
10. Tabunshnikov, J., Prohorov, V., Brjuhanov, O., Zhila, V., Klochko, A.: Purposes and tasks of gas networks distribution optimization. *MGSU Bull.* **4**, 73–77 (2012)
11. Zhila, V., Klochko, A., Gusarova, E.: Receipt of a configuration of an inter-settlement gas distribution network with use of a method of the smallest squares. *Internet Messenger Volg.* **3**(23), 28 (2012)
12. Arutjunjan, R.: Strengthening of steel concrete designs by method of search optimization. *Hous. Constr.* **11**, 12–13 (2000)
13. Kuspekov, K.: An algorithm of creation of an optimum gas distribution network configuration on the plane with an orthogonal metrics. *Omsk Sci. Bull.* **1**(107), 14–16 (2012)
14. Kalashnikov, R.: Creation of a Steiner tree by the modified method news of SFU. *Tech. Sci.* **2**(31), 311 (2003)
15. Ejbozhenko, D.: Approximate methods of the Steiner task solution on the oriented columns. St. Petersburg State University, St. Petersburg (2012)
16. Bagov, M., Kudaev, V.: Local solution of a network Steiner task. *Rep. Adyg. (Circassian) Int. Acad. Sci.* **4**, 9–14 (2014)

17. Melkumov, V., Chujkin, S., Papshickij, A., Skljarov, K.: Modeling of structure of engineering networks in case of territorial planning of the city. *Constr. Archit.* **2**(38), 41–48 (2015)
18. Tarasjan, V., Ten, D.: Optimization of transport infrastructure by means of genetic algorithms. *Innov. Transp.* **3**(9), 29–32 (2013)
19. Litvinenko, V., Hovanskov, S., Hovanskova, V., Litvinenko, E.: Application of parametrical adaptation in algorithms of orthogonal Steiner tree creation. *Inform. Comput. Facil. Eng. Educ.* **4**(28), 9–16 (2016)

Stabilization of Low Bearing Soil Using Fly Ash and Chemical Additive Polybond

Mirjana Vukićević^(✉) , Veljko Pujević , and Miloš Marjanović 

Faculty of Civil Engineering, University of Belgrade, Belgrade, Serbia
mirav@grf.bg.ac.rs

Abstract. The results of laboratory research of high plasticity clay stabilization using liquid chemical additive Polybond and the fly ash from Serbian thermal electric power plant Kostolac are presented in this paper. In order to determine the effects of stabilization, extensive laboratory study of physical and mechanical properties of the stabilized soil (unconfined compression strength, shear strength parameters, CBR, deformation parameters, swelling, coefficient of permeability, resistance to freezing) were performed. The results of the research clearly indicate the positive effects of the clay stabilization using Polybond, as well as fly ash, and confirm that these additives can be successfully applied as a clayey soil stabilizers in various practical applications such as: stabilization of low bearing subgrade, construction of embankments and geotechnical structures of low permeability, improvement of mechanical properties of top subgrade layers etc. The use of stabilizers reduces energy consumption, as well as the usage of natural materials such as stone aggregates.

Keywords: Soil stabilization · Polybond · Fly ash · High plasticity clay

1 Introduction

Soil stabilization is a technological process that improves the engineering properties of soil. Main stabilization methods are mechanical and chemical stabilization. Mechanical stabilization is based on the addition of missing grain fractions, so the optimal grain size distribution is achieved. After that soil is compacted at optimum moisture content (OMC). Mechanical stabilization is used on non-coherent, uniformly graduated soil.

Chemical stabilization is based on the addition of a binding agent (most often portland cement or lime) into the soil. Due to the presence of water in the soil, chemical reactions occur, which result in the formation of cement compounds. In the last decades, fly ash is increasingly used for mechanical and chemical soil stabilization. Fly ash produced from burning pulverized coal in power plants is fine grained material that is carried off in the flue gas and collected by means of electrostatic precipitators or mechanical collection devices (cyclones). Two classes of fly ash are defined by ASTM C618: Class F (non self-cementing) fly ash and Class C (self-cementing) fly ash. Fly ashes from Serbian power plants belong have pozzolanic properties and because of low concentrations of calcium compounds (less than 10% CaO), don't have self-cementing characteristics, namely belong Class F. It can be used alone or in combination with traditional additives - cement or lime. In addition to traditional

additives, innovative chemicals are increasingly used for chemical soil stabilization. One of these materials is Polybond, a liquid ionic chemical additive.

Polybond is a dark brown liquid based on sulfuric acid and surfactant, which provide a unique feature of the stabilizer that is reflected in the reduction of inorganic binder consumption in reinforced soil, increased soil strength and resistance to moisture and frost. According to the manufacturers, Polybond effect is based on its ability to perform ionic water substitution on the soil particles' surface using stabilizing molecules. Due to this, soil particles become smaller. The characteristic of the stabilizing molecules that are attached to the soil particles' surface is to repel moisture, thereby reducing the ability of clay particles to attract water. Treated soil becomes harder and waterproof, making it resistant any climatic conditions, with sufficient bearing capacity even after long-term precipitation [1]. Application of Polybond is especially effective in treating fine grained clayey soil. As a result of the soil stabilization using Polybond, the entire thin layer of water on the clay particles' surface becomes free and easily evaporates from the ground. Soil swell potential is significantly reduced. By creating the top anti-frost soil layers strengthened with the Polybond, the penetration of moisture into the lower subgrade is practically interrupted.

The results of the high plasticity clay stabilization using Polybond, as well as fly ash from Serbian thermal power plant (TPP) Kostolac are presented in this paper. The authors of this paper have also carried out a comprehensive study [2] discussing the possibilities of using fly ash from Serbia's thermal power plants for subgrade soil stabilization. Obtained results showed that the ash from TPP Kostolac in Serbia, despite the lack of self-cementing properties, is an effective material for the stabilization of fine-grained materials.

2 Testing Materials

High plasticity clay with expansive properties was sampled at the location Radljevo, municipality of Ub, Serbia. Fly ash was sampled directly from the electro filter of the thermal power plant Kostolac (KOS-FA). It is a dark gray, silty-sanded waste material. Its chemical composition was determined in the laboratory of the Faculty of Physical Chemistry in Belgrade (Table 1).

Table 1. Chemical composition of fly ash.

SiO ₂	Al ₂ O ₃	Fe ₂ O ₃	CaO	MgO	K ₂ O	Na ₂ O	TiO ₂	SO ₃	P ₂ O ₅
56.38	17.57	10.39	7.46	2.13	0.57	0.38	0.52	0.95	0.025

Due to the fact that the SiO₂ + Al₂O₃ + Fe₂O₃ content is above 70%, and the SO₃ content is less than 5%, this fly ash can be categorized into class F (silicate acidic ash), according to ASTM C 618 [3], or class V (alumo-silicate ash) according to EN 14227-4 [4], with pozzolanic properties and without self-cementing properties.

Physical-mechanical properties of used soil and fly ash are displayed in Tables 2 and 3. Grain size distribution of used materials is displayed on Figs. 1 and 2. Displayed

Table 2. Basic physical properties of used materials.

MATERIAL LOCATION	BASIC PHYSICAL PROPERTIES												
	Grain size distribution						Atterberg limits and soil classification						
	G_s	Organic matter %	$CaCO_3$ %	Clay < 0.002 mm	Silt 0.002-0.06 mm	Sand 0.06-2.0 mm	Fines < 0.075 mm	LL %	PL %	PI %	USCS	AASHTO	Group index
High plasticity clay Radljevo	2.67	1.24	0.00	22	72	6	96	50.6	19.1	31.5	CH	A7-6	18
Fly ash Kostolac	2.22			0	75	25	80						

Table 3. Mechanical properties of tested materials.

MATERIAL LOCATION	MECHANICAL PROPERTIES											
	Compaction Proctor test		Compressibility				Strength					
	$\gamma_{d,max}$ kN/m ³	OMC %	M_v kPa			C_c	C_r	Swelling pressure kPa	Direct shear		UCS	CBR %
			50-100	100-200	200-400				ϕ' °	c' kPa		
High plasticity clay Radljevo	16.64	19.07	14330	10380	10800	0.010	0.010	156.0	25.5	26.2	231.4	4.6
Fly ash Kostolac	9.85	37.55	27230	39430	42950	0.083	0.018		30.9	28.5	87.0	57.9

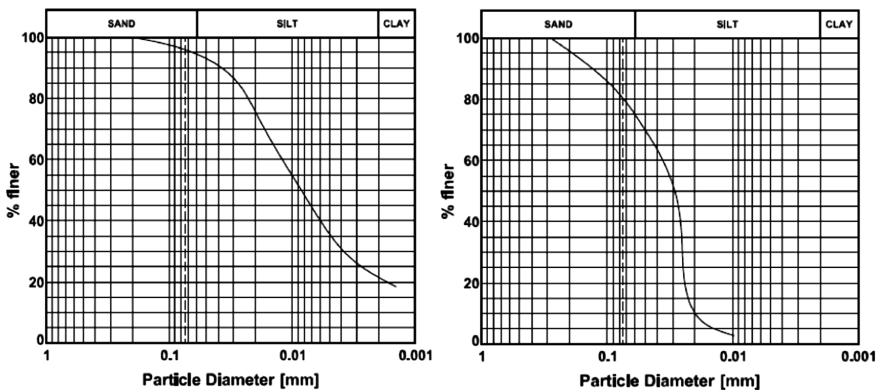


Fig. 1. Grain size distribution of high plasticity clay (left) and fly ash KOS-FA (right).

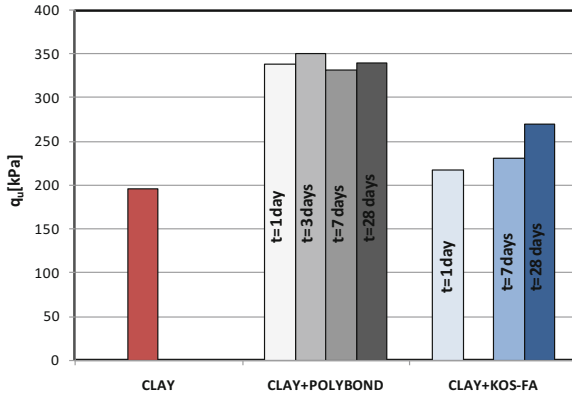


Fig. 2. Unconfined compression strength.

data is taken from previously mentioned study [2]. Displayed values are average values for all tested specimens.

3 Samples Preparation, Program and Testing Methods

3.1 Samples Preparation

Test specimens for laboratory testing were prepared with the minimum recommended Polybond content according to STO 69646750-001-2011 [5]. Used amount of Polybond was 0.175 l/m^3 of compacted material. First the Polybond-water solution (0.08% of the water weight) was formed, and then the corresponding amount of solution was added to the dry mass of the soil (Group 1), or soil and fly ash (Group 2). During preparation of the soil-fly ash mixtures, the previously determined optimum percentage of ash for the tested soil-ash combination (high plasticity clay from Radljevo and fly ash from TPP Kostolac) was used [2]. This amount was 20% of fly ash, compared to the dry soil mass. The basic parameter in choosing the optimal percentage of ash in the case of the applied soil type was the maximum increase in the CBR values after one day from compaction [2].

Test specimens were prepared at the same initial conditions. First the dry homogeneous mixtures of soil and corresponding amount of ash (relative to the dry mass of the soil) were made by careful mixing, and then the compaction was done without delay at the optimum moisture content according to the standard Proctor compaction test. The applied OMC for tested groups of mixtures are displayed in Table 4. Prior to testing, specimens were stored in desiccators at a temperature of 25 °C.

Table 4. Optimum moisture contents of tested mixtures.

Group	Description	OMC %
1	Soil + Polybond	19.07
2	Soil + fly ash	21.59

In order to determine the time dependence of the soil stabilization effects, the basic mechanical properties of the stabilized soil were monitored by performing experiments on test specimens after 1, 3, 7 and 28 days. The obtained results from Groups 1 and 2 were compared with the characteristics of untreated soil (displayed in Tables 2 and 3).

3.2 Testing Methods

In order to determine the physical and mechanical properties of stabilized soil, appropriate laboratory tests were performed. All tests were performed according to Serbian SRPS standards. Unconfined compression strength, California bearing ratio (CBR), effective shear strength, compressibility, permeability and resistance to freezing were tested.

4 Results

4.1 Stabilization of High Plasticity Clay Using Polybond and Fly Ash from TPP Kostolac (KOS-FA)

Unconfined Compression Strength - UCS. The results of the unconfined compression test of the soil treated with Polybond are displayed in Fig. 2. The addition of Polybond at the minimum recommended amount caused a significant increase in short-term strength of 72%. The results of the test after 3, 7 and 28 days indicate the insensitivity of the considered parameter to the elapsed time. The observed trend is in some way expected, since the Polybond stabilization mechanism is based primarily on the reduction of bound water.

On the other hand, mixtures prepared with fly-ash exhibit negligible increase in short-term strength. KOS-FA, despite no self-cementing properties, obviously influences the increase in strength over time for the considered high plasticity clay.

Effective Shear Strength Parameters. Effective shear strength parameters are displayed in Fig. 3. The obtained results show that the addition of the Polybond doesn't

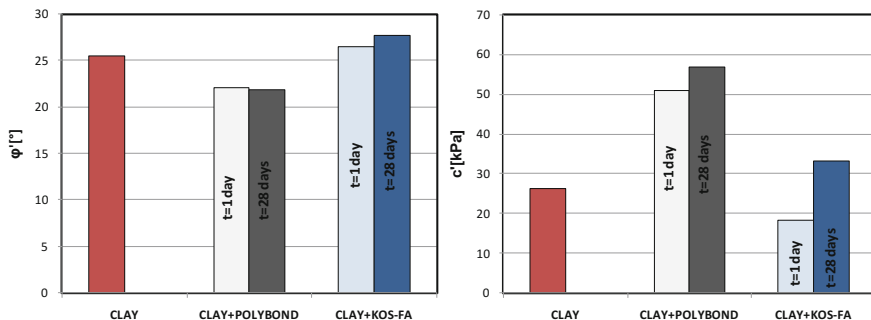


Fig. 3. Effective shear strength parameters.

improve the angle of internal friction ϕ' (it is slightly decreased compared to untreated soil, about 15%). The results obtained after 28 days show the independence of the friction angle to elapsed time. On the other hand, the effects of treating this type of soil with Polybond are particularly expressed in terms of soil cohesion. A significant increase in cohesion (about 95%) was recorded. The results of a direct shear test after 28 days indicate a slight increase in cohesion over time.

Results obtained for mixtures with fly-ash show that the internal friction angle ϕ' was moderately increased, which was somewhat expected due to larger grain size distribution of used fly-ash. Although the long-term cohesion for specimens with fly-ash is slightly increased compared to untreated soil, there is obvious gain in strength with time analogous to UCS.

California Bearing Ratio (CBR). It is known that clays in general have a low CBR value, which makes them unsuitable material for road subgrade. The results of the California bearing ratio for soil treated with Polybond are displayed in Fig. 4. Compared to the CBR value of untreated soil, addition of Polybond increased soil CBR by 110%. This is a very significant improvement, as the stabilized soil becomes usable in road construction.

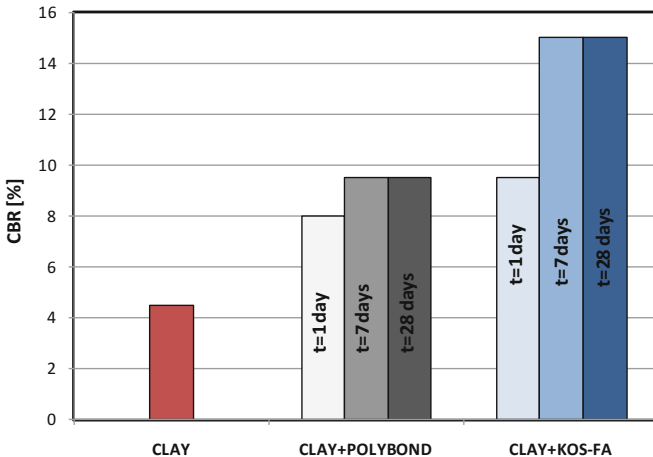


Fig. 4. CBR values.

Results obtained for mixtures with fly-ash show significant increase in both short and especially long-term CBR values. The observed results and trend were expected, considering that fly-ash itself has extremely high CBR value (58%).

Deformation Parameters. Compressibility modulus M_v for vertical stress intervals of 100–200 kPa and 200–400 kPa are displayed in Fig. 5. Obtained results indicate a moderate decrease in the deformability of treated soil. With the addition of Polybond in the minimum recommended amount, the final modules were increased by 43%, and 56%, respectively, compared to the untreated soil.

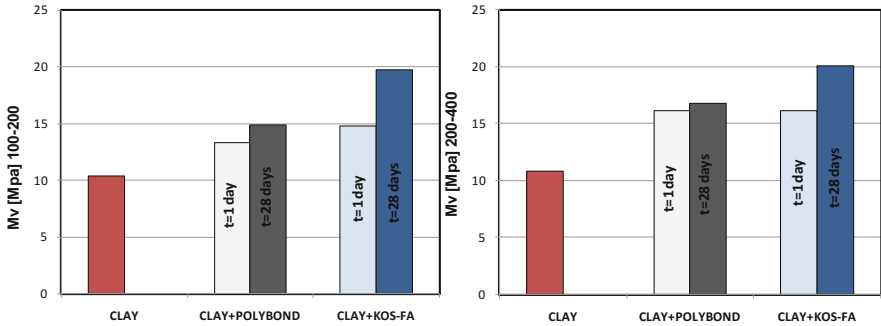


Fig. 5. Compressibility modulus.

Results obtained for mixtures with fly-ash indicate significant increase in both soil moduli in the range of 90–100%. Similar to the case of CBR values, fly ash also has a major impact to the behaviour, which is especially expressed by increase with elapsed time (aging of the samples).

Swelling. Tested soil before addition of Polybond showed a swell potential - the swelling pressure determined in the oedometer test was 156 kPa, and swelling deformation was $\varepsilon = 2.16\%$, which is associated with the presence of montmorillonite. By adding Polybond, the soil swell potential has been significantly reduced. Swell pressure and deformation were reduced 48 kPa and $\varepsilon = 0.92\%$.

On the other hand, results of the previously conducted study [2] showed that the treatment of high plasticity clay (location Radljevo) with KOS-FA fly ash completely eliminates its swelling potential.

Coefficient of Permeability. It is generally known that high plasticity clays have low water permeability. The results of the performed tests show that the addition of Polybond further decreases the coefficient of permeability of treated soil. According to the classification proposed by Terzaghi and Peck [6], mixtures stabilized by Polybond can be considered as practically impermeable ($k_f = 1,97e-10 < e-9$ m/s).

Unlike Polybond, KOS-FA fly ash, due to a coarse grain size distribution, works unfavorably from the permeability point of view. The addition of ash increases the permeability of the high plasticity clay under consideration, and thus makes it less suitable for use in the construction of embankments and hydraulic structures.

Resistance to Freezing. The results of the carried study indicate that the compressive strength of the samples treated with Polybond after 14 cycles of freezing and thawing was slightly reduced, compared with the strength of the samples which were simultaneously immersed in the water. The obtained freeze resistance index is $R = 91\%$, which meets the requirements of standard SRPS U.B1.050 ($R > 80\%$) [7]. That's why we can consider the treated soil resistant to the effects of freezing.

Volumetric Weight and Moisture Content. In order to create the clearer picture of mechanism of stabilization using Polybond, changes in moisture contents and volumetric weight over time were analyzed. Obtained results are displayed in Figs. 6 and 7.

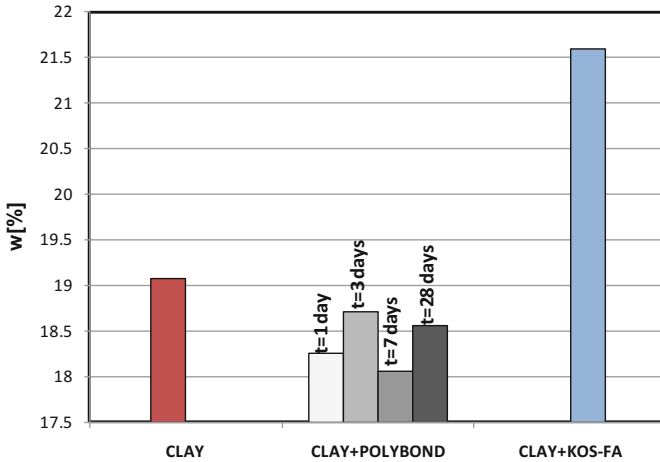


Fig. 6. Moisture contents.

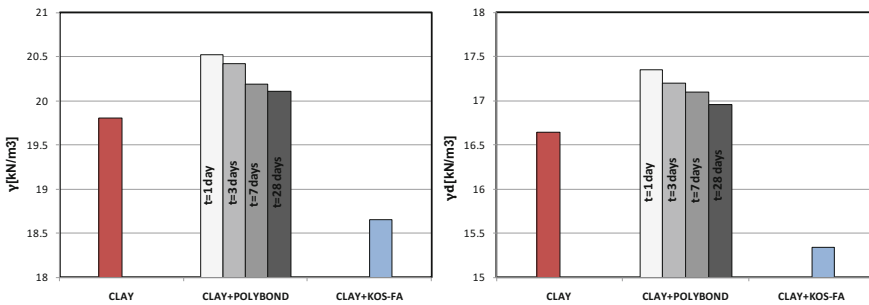


Fig. 7. Volumetric weight.

The immediate decrease in moisture content was recorded, immediately after the addition of Polybond-water solution into the dry soil. This is the result of chemical reactions with clay minerals. The increase in volumetric weight for the Polybond treated specimens (compared to untreated soil) indicates that for the same initial optimal moisture content of the prepared material and the same applied compacting energy, the addition of Polybond in the minimum amount increases the sample compaction. In general, the increase in compaction directly affects the improvement of mechanical properties of soil, by increasing the strength and reduction of deformability, which is in line with the obtained results.

KOS-FA due to its very high OMC forms mixtures with higher moisture and lower dry weight. This lower density reflects on UCS and cohesion values which are lower compared to mixtures with Polybond. We saw that in the case of Polybond, the stabilization is dominantly of a chemical type. On the other hand in the case of KOS-FA fly-ash, the stabilization is more of mechanical type with minor contribution of cementation. Effects of this type of stabilization are more pronounced on CBR, ϕ' and soil moduli values.



5 Conclusions

The stabilization of low bearing soils significantly reduces the need for material replacement and allows the application of soil with low mechanical properties for the construction of the embankment. The results of the performed tests clearly indicate the positive effects of the stabilization of the clay using Polybond, as well as with fly ash, and confirm the attitudes that these additives can be successfully applied as a clayey soil stabilizers in various practical applications such as: stabilization of low bearing capacity soil, construction of embankments and geotechnical structures of low permeability, improvement of mechanical properties of the top layers of road subgrade etc. Use of fly ash and Polybond can reduce the consumption of natural stone material, which is traditionally used as the replacement of low bearing soils and construction of embankments. Energy used for production of stone aggregate is also saved. In the case of ash, there is an additional positive effect for environmental protection, as the quantities of deposited waste are reduced.

References

1. <http://superroads.rs/technology.html>. Accessed 27 Aug 2017
2. The use of fly ash from thermal power plants for soil stabilization, SCC and RCC concrete, with a view to the durability of cementitious mortars and fine-grained concrete. University of Belgrade, Serbia (2014)
3. ASTM C618-15: Standard Specification for Coal Fly Ash and Raw or Calcined Natural Pozzolan for Use in Concrete. ASTM International (2015)
4. EN 14227-4: Hydraulically bound mixtures. Fly ash for hydraulically bound mixtures (2014)
5. STO 69646750-001-2011: Soil and asphalt-granules-concrete mixtures reinforced with soil stabilizer. Polybond for use during automobile road, railroad and airfield constructions. SuperRoadRus (2011)
6. Terzaghi, K., Peck, R., Mesri, G.: Soil Mechanics in Engineering Practice. Wiley, USA (1967)
7. SRPS U.B1.050:1970: Testing of soils, resistance cement stabilized soils to freezing. Institute for standardization of Serbia (1970)

Evaluation of the Effectiveness of the Creation of Antifiltration Curtains in Hydroelectric Power Plant in Syria

Konstantin Mordvintsev¹  and Yaser Abd Alwahab² 

¹ Peoples' Friendship University of Russia,
Miklukho-Maklaya str., 6, Moscow 117198, Russia

² Yerevan State University of Architecture and Construction,
Teryan Street, 0009 Yerevan, Armenia
yasr1985@yahoo.com

Abstract. Meeting demands of water and energy is a vital question for any country, especially for Syria. There is a shortage of water suppliance for people and for most of industries in this country. Syrian authorities should concern more about hydroelectric power in order to increase electricity production at hydroelectric power plants. The article analyzes the efficiency of works on creation of ant filtration grouting curtain in the dam Foundation (Zeta, Homs) in Syria.

Keywords: Hydroelectric power · Energy management
Hydroelectric power · Soil

1 Introduction

Satisfaction of energy and water needs for any state is an important task, especially for Syria, where there is a large deficit in water supply for both the population and various industries.

For the efficient production of electricity at hydroelectric power plants is necessary to pay more attention based of hydroelectric power.

To solve this problem, several reservoirs have been built in Syria (for example, the dam of Zeta, Homs), but the experience of their operation showed that about 29.5% of the water volume is lost each year due to water filtration through the bottom of the reservoir bed base.

Syria characterized by complex geological conditions, the main feature of which is a serious fracturing and water permeability [1, 4].

To reduce water losses from the reservoirs, special measures should be taken to strengthen the base soils and reduce their water permeability. The greatest spread in the ways of strengthening the grounds of the foundations of hydraulic structures was the creation of injection curtains. This method has been widely used in the construction of reservoirs in Syria, but the problem of water loss is still relevant.

Source materials for the research provided by the Ministry of water resources (Syria - HOMS).

To study the effectiveness of impervious grouting curtain in the dam Foundation carried out field studies of soil and statistical analysis of the results of cementation. For research, we have chosen 4 of the veils 19, 3, 7, 15.

In these areas, the injection carried out with cement mortar based on ordinary Portland cement Syrian.

To determine the effectiveness of the grout curtain carried out the injection of water and cement in the control wells.

Hydroproline (test water) for most wells were carried out according to the method of the Packer, the water pressure in the range of 1–6 bar, discharge pressure (P) within 3–9 bar. The density of injection of grout (water-cement ratio) administered, depending on the permeability of soil layer K (Table 1).

Table 1. Water-cement ratio

The coefficient of permeability K, Lu	<10	10–25	25–50	50–100	>100
Water-cement ratio W/Ce	10/1–8/1	8/1–4/1	4/1–2/1	2/1–1/1	1/1–0.8/1

The most common soils in Syria can divided into 4 groups (Fig. 1):

1. Clay sedimentary rocks.
2. Limestone sedimentary rocks.
3. Ruined basalts.
4. Strong basalts.

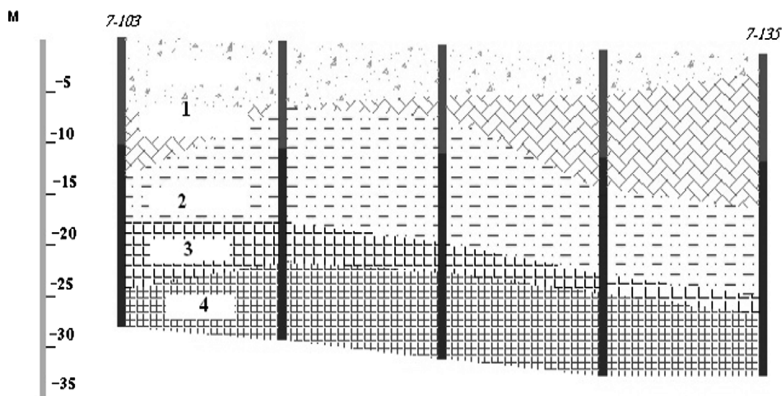


Fig. 1. Geological section on the site 7

Soils of group 1 (clayey deposits) have the following form:

- layers of clay to sand clays, sand-gravel limestone with various proportions of gravel color from yellowish-brown to red, slightly monolithic;
- Layers of clay to sandy, clay with a small percentage of gravel and basalt stones, the color of which varies from red to light brown.

Soils of the second group (limestone sedimentary rocks) consist of layers of clay limestone - marl, limestone with an admixture of clay with inclusions of other rocks (conglomerates). These layers have a strong cracking and karst formations.

The soils of the third groups consist of basaltic rigid monoliths of rather large sizes.

Soils of the fourth group are destroyed basalts, strongly fissured. The size of the cracks can be very significant.

When carrying out injection cementation of soils, it is necessary to carefully select the properties of injected solutions and the technologies for their injection. The effectiveness of the work carried out can only be assessed with the help of experienced tests of the curtain.

During the construction of the carburizing veil on the Zeta dam, pilot tests were carried out, which showed that in clay sedimentary rocks their efficiency was extremely small (Fig. 2).

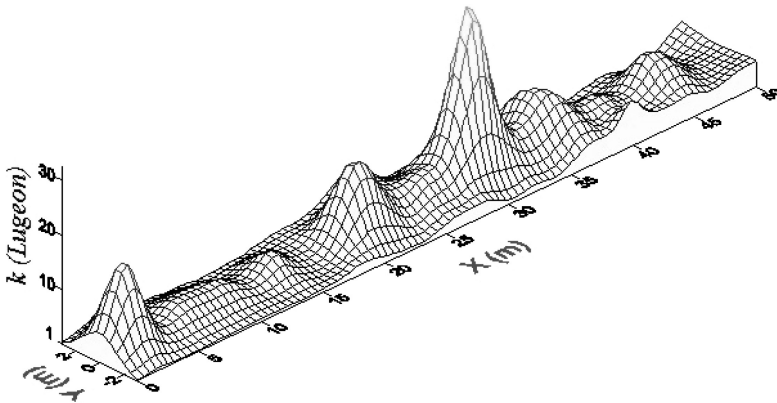


Fig. 2. Dependence of water permeability on depth after cementation

1. The permeability of the soils has remained too high, and the pressure at the injection of solutions is high for soils. These circumstances lead to the conclusion that when the injection pressure increases in the soils around the wells, fracturing zones are formed (Fig. 3), which increase the permeability of the soils (Ministry of water resources in Syria, 2015)

Experimental tests have shown that the voids formed during hydraulic fracturing extend to sufficiently large distances [2].

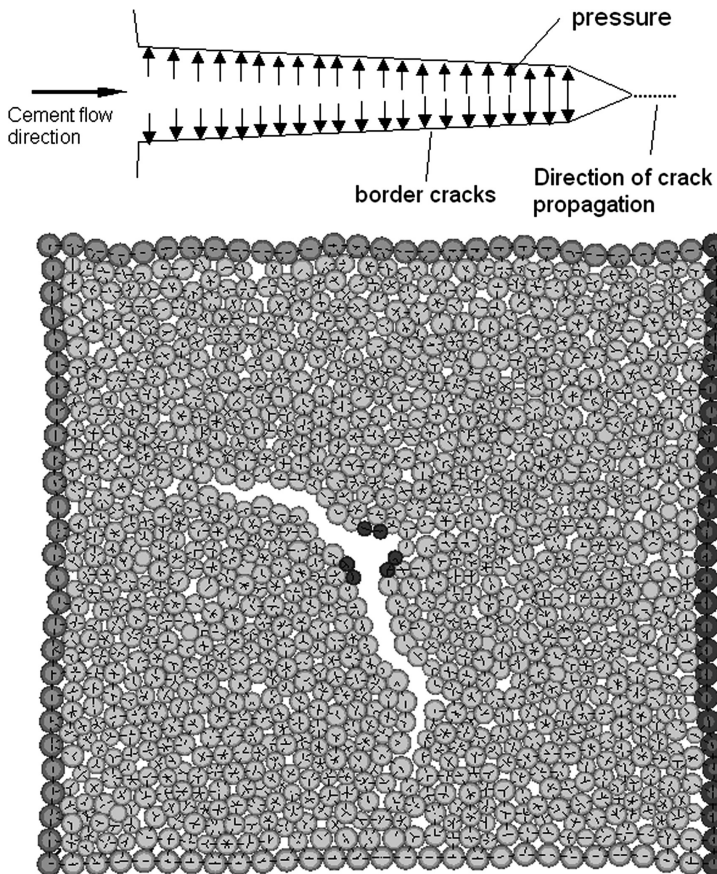


Fig. 3. Formation of a hydraulic explosion at a high injection pressure

As a result, for the conditions of the Zeta dam it was necessary to perform several additional injections using bentonite and sodium silicate. As a result, the creation of an effective anti-filtration curtain in clay soils has become too costly [4].

Result of the study of the effectiveness of the creation of cementation curtains in limestone's, statistical relationships between soil water permeability and cement consumption were obtained (Fig. 4). According to these dependencies, the necessary consumption of cement was determined, for injections into soils.

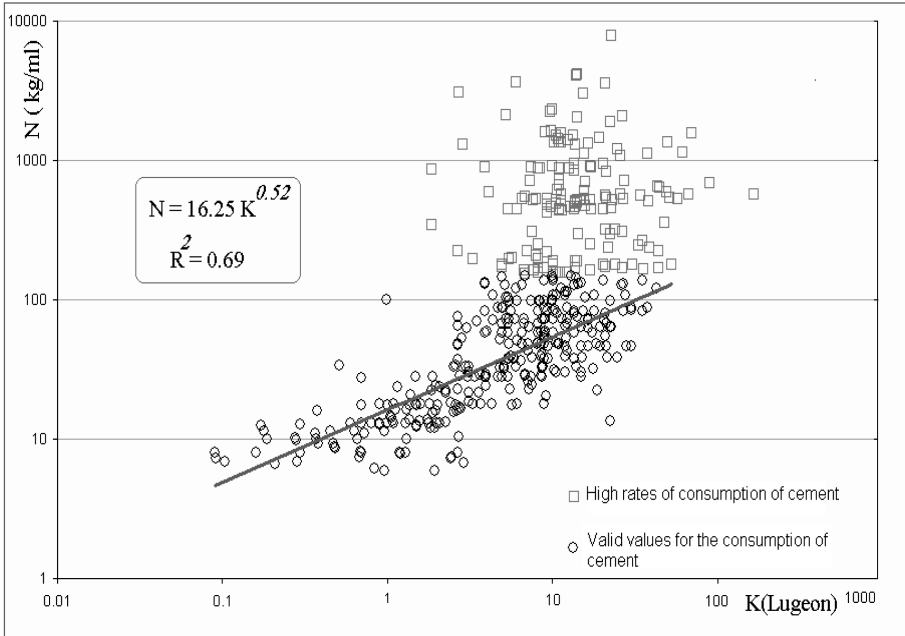


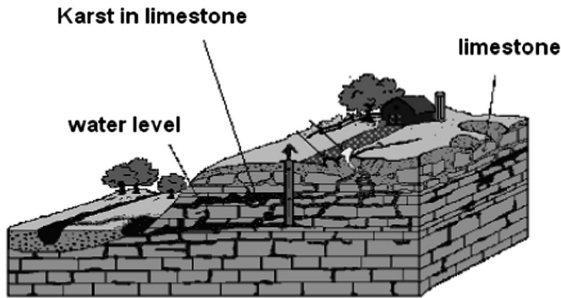
Fig. 4. Dependence between water permeability and discharge pressure for limestone soils

2 Result of These Tests

2.1 Shown that for Limestone Soils

- Boundaries of the permeability region [1–60 Lugeon];
- Borders of the discharge pressure range [5 ± 2 bar].

Tests carried out for limestone soils also showed that karst zones are widely distributed in them, the presence of which sharply increases the consumption of cements during the creation of cementation curtains (Fig. 5).



Source: Hallberg, ET AL

Fig. 5. Karst structures in limestones

2.2 For Destroyed Basalts

- Limits of the permeability region [1–100 Lugeon];
- Borders of the discharge pressure area [6.5 ± 1.5 bar].

For monolithic basalts, experiments have shown that about 45% of basalt has crack sizes not exceeding 100 microns, i.e. 45% of basalt is practically impermeable and does not require special cementation works.

3 The Results of the Ground Tests of the Zeta Dam (Homs, Syria) Found that:

1. When creating cementation processes during the development of underground space in conditions of a swelling ground-rock massif, it can be realized using the developed methods that take into account the specific features of the deformation of swelling clay soils in Syria.
2. These tests should be carried out for each group of soils separately.
3. Careful identification of karst zones is necessary.

References

1. Banfill, P.F.G.: The rheology of fresh cement and concrete – a review. Paper Accepted for Publication in Proceedings of the 11th International Cement Chemistry Congress, Durban, May 2003
2. Grouting Systems – Ground Treatment Systems, Documentations of A KELLER Company © Australia, Hayward Baker.ltd (2003). <http://www.hawardbacker.com>. Accessed 22 Aug 2017
3. Dams Grouting, © Wahlstrom, Ernest Dams, Dam Foundations and Reservoir Sites, UK (2003). <http://www.dur.ac.uk>. Accessed 21 Aug 2017

Research on Long-Term Strength of Glass-Fiber Reinforced Concrete

Antonina Ryabova¹ , Alexey Kharitonov¹ ,
Larisa Matveeva¹ , Nina Shangina² , and Yuri Belentsov² 

¹ Saint Petersburg State University of Architecture and Civil Engineering,
2-ya Krasnoarmeyskaya str., 4, 190005 Saint Petersburg, Russia
peepdv@mail.ru

² Emperor Alexander I St. Petersburg State Transport University,
Moskovsky ave., 9, 190031 Saint Petersburg, Russia

Abstract. The article describes the research results of physical & mechanical properties of glass-fiber reinforced concrete through time, at different dosing of alkaliproof fiber and metakaolin of MKZhL-2. The bending strength data of glass-fiber reinforced concrete, modified by metakaolin, in the age of 28 and 180 days were obtained. The co-effect of metakaolin and microsilica on strength properties of fine glass-fiber reinforced concrete was considered. It was demonstrated that the injection of metakaolin in a quantity of 30% of Portland cement allows retaining the long-term strength of fiber reinforced concrete. The complex usage of MKZhL-2 & MK-85 allows retaining or even increasing the bending strength in the age of 28 and 180 days.

Keywords: Glass-fiber reinforced concrete · Metakaolin
Microsilica · Transport structures

1 Introduction

Last time, the interest for the usage of different mineral concrete modifiers, having pozzolanic activity, increased. Despite that silica pozzolanic additives have been applied during construction already some tens of years, scientists of the whole world continues studying its effects on properties and durability of concretes including dispersion-reinforced concrete.

We have accumulated extensive experience in the application of dispersion-reinforced concrete. Well-studied properties of steel fiber reinforced concrete, as well as concrete, reinforced by basalt, asbestos fiber. However, the use of a particulate reinforcement of glass fiber, although conducted in this area of research, currently in the domestic construction still remains limited. Last but not least this is due to insufficient knowledge of the properties of GFRC, particularly on the question of the persistence of fibers in cement matrix.

Such additives as microsilica, flue ash, blast-furnace granulated slag, being the industry waste, were the most wide-spread [1–3]. Everyone is used to consider that the pozzolanic reaction of ashes and slag in concrete is delayed in time and begins no

earlier than 6–40 days after mortar tempering [4]. Such a delayed reaction is often related to the quality of ash-slag waste.

Microsilica dust is a by-product of the production process of ferrosilicon, ferrochrome, crystal silicon and other ferrous alloys. Nevertheless, high pozzolanic activity of microsilica allows its showing unique properties already at the early stage of concrete curing. Microsilica has a high specific surface (20000–35000 cm²/g) and is the finest dust of gray color with a high content of silicon dioxide (75–95%). The bulk density of microsilica depending on the manufacturer varies within the range of 0.15–0.26 t/m³. Today, this industry waste is widely used in the obtainment process of High Performance Concrete, applied during construction of dams, viaducts, drilling platforms, bridges.

Despite that silica pozzolanic additives have been applied during construction already some tens of years, scientists of the whole world continues studying its effects on properties and durability of concretes.

Highly active metakaolin (HAM), being the dehydration product of kaolin clay (natural hydroalumosilicate) is not less prospective for research. Due to the fact that metakaolin is the prime product with the careful selection of raw material and control of production technology, it has clearer quality parameters than its by-products.

Kaolinite is the main component of white clays (kaolin), formed during destruction (weathering) of granites, gneisses and other rocks, containing feldspars (primary kaolins) [10]. By its appearance, metakaolin is a fine powder of beige, pinky and white color. Metakaolin mainly contains 36–45% of aluminum oxide and 50–57% of silicon oxide in its chemically active formula unit. It stipulates a high pozzolanic metakaolin activity (lime quantity, neutralized by 1 g HAM), which is equal to more than 1000 mg [6]. As a rule, metakaolin particles have a size of 0.5 to 5 micron in diameter that is by a factor of ten lower than the size of cement grain and by a factor of ten higher than the one of microsilica particles [7, 8].

In order to obtain the High Performance Concrete (HPC), last years, complex modifiers, got using hyperplasticizing agents of a new (III–IV) generation and active mineral additives, have been applied on an organo-mineral base.

The cumulative effect of metakaolin and microsilica as active modifiers for glass-fiber reinforced concrete is of interest.

The injection of a plasticizing component is required during the injection of superfine mineral additives to compensate the increase of water demand of fiber-cement compounds. By the data [5, 9], hyperplasticizing agents of polycarboxylate type, e.g. Sika Visco Crete, Melflux, Pantarhit, Glenium, etc., are the most efficient in Portland cement-based composite materials.

Glass fiber, despite all its advantages, also has some demerits. A rather high cost of glass fiber as well as risks related to high alkalinity of cement systems restrict its universal application. The impact of alkali contained in cement during a long time on glass fiber has not been enough studied.

2 Materials and Methods

The work aim is to study the impact of active mineral additives on the retention of strength concrete properties through time. The two-factor experiment model was chosen to study the set task.

Domestic metakaolin MKZhL-2 from the Zhuravlinyi Log deposit and MK-85 microsilica made by the Novolipetskii Iron and Steel Works was applied as modifying additives. The properties of modifiers are described in Table 1.

Table 1. Physical & chemical properties of active mineral additives

Parameter name	Value	
	MKZhL-2	MK-85
Mass fraction of aluminum oxide (AL ₂ O ₃), %	41.2	11–14
Mass fraction of silicon oxide (SiO ₂), %	50.7	86.8
Mass fraction of iron oxide (Fe ₂ O ₃), %	0.49	0.4–1.7
Puzzolanic activity, (mg (CaOH) ₂ /g)	1340	
Bulk density, kg/m ³ within	250–350	150–200
Humidity, %	0.15	0.66
Color	Ecru	Gray

Portland cement CEM I 42.5 was used as a binding substance, sand of 0–2.5 mm fraction was used as a filler, and the role of plasticizing agent was played by the polycarboxylate plasticizing agent of Synergy RC 160 Plv type. The compounds had the same water/cement ratio equal to 0.49. Alkaliproof fiber of Cem Fill trademark with the 10-mm length acts as a reinforcing component of fiber concrete. The fiber thickness is 14 μm.

3 Results and Discussion

Sample beams of fine glass-fiber concrete with the variable fiber content were subjected to bending and compression tests. Tests were done after 28 and 180 storage days in a water medium. The bending strength parameters of reinforced concrete are of the most interest. The summary of compound variation levels is described in Table 2.

Table 2. Planning matrix of two-factor experiment

Name of factors	Codes	Variation levels			Variation step
		-1	0	1	
Metakaolin flow rate, % of PC	X1	0	15	30	15
Fiber flow rate, % w/w	X2	1	2	3	1

By test results, the strength data of glass-fiber concrete were obtained depending on the content of injected glass-fiber and metakaolin.

The 3D diagram clearly shows the positive metakaolin effect on the deformation properties of glass-fiber reinforced concrete. Without metakaolin, at the maximum possible reinforcement (3% w/w), the bending strength is about 14 MPa (Fig. 1). When the fraction of active mineral additive increases, the deformation properties of glass-fiber concrete increase too. So, with the same reinforcement percent, but with the addition of metakaolin in 30% of PC, the compression strength will rise to 24 MPa. The strength gain was 71%.

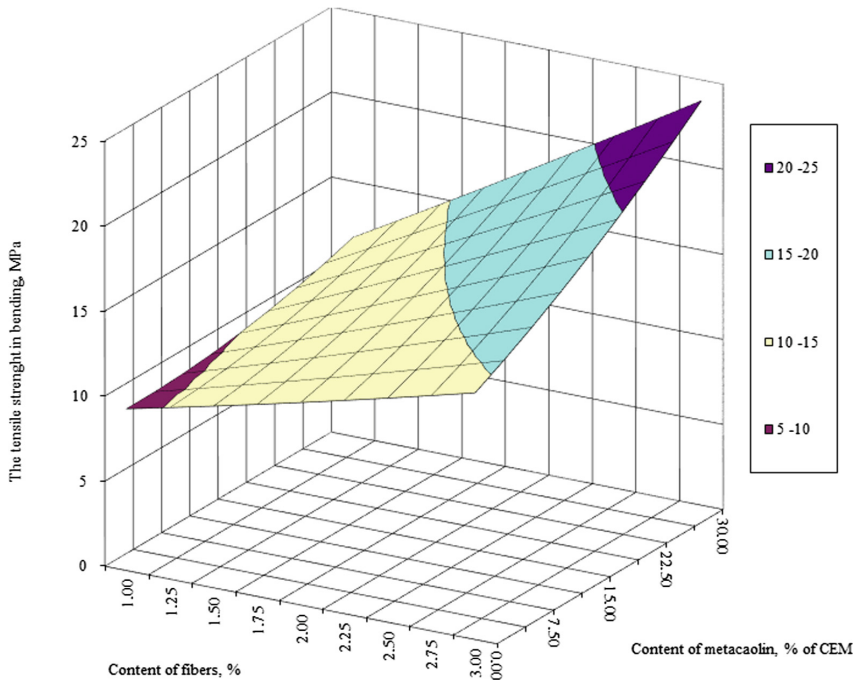


Fig. 1. Effect of fiber and metakaolin flow rate on bending strength of glass-fiber reinforced concrete in age of 28 days

An extremely negligible drop of strength parameters, inherent for compounds with a low metakaolin flow rate (less than 15% of PC) is observed after 180 storage days in a water medium (Fig. 2). It is most likely explained by the insufficient content of a highly-active mineral additive in the glass-fiber concrete that did not allow considerable binding free CaO. For compounds with a high reinforcement degree and metakaolin content of more than 15% of PC, the bending strength drop does not take place that evidences about an important role of pozzolanic additive in the glass-fiber concrete.

Prior researches of physical and mechanical properties of glass-fiber concrete with microsilica addition demonstrate that, in the age of 28 days, such compounds have higher strength parameters than compounds with metakaolin addition. However,

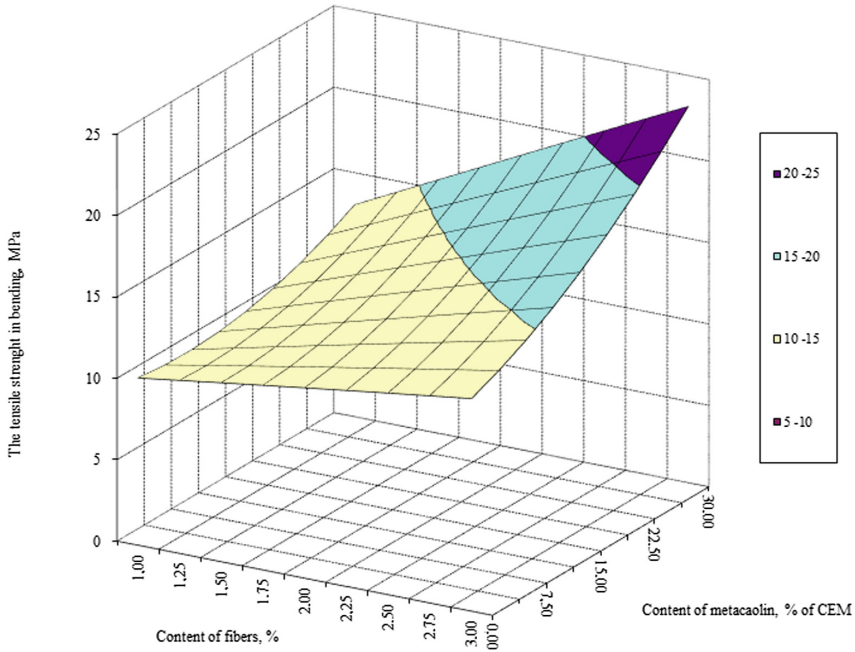


Fig. 2. Effect of fiber and metakaolin flow rate on bending strength of glass-fiber concrete in age of 180 days

already up to 90 days, a bending strength drop is by 15–20%. Probably, the microsilica morphology contributes to the reinforcement of cement stone structure, therefore, the degree of fiber cohesion with cement matrix increases. But a loss of glass-fiber concrete strength occurs due to possible fiber destruction. So, it is required to study the co-effect of microsilica and metakaolin on glass-fiber concrete properties.

Three compounds with different content of MKZhL-2 and MK-85 were studied. The quantitative content of components is described in Table 3.

Table 3. Component content in complex GRC compounds

No.	Component	Compound 1	Compound 2	Compound 3
1	PC 500 D0, %	38.0	38.0	38.0
2	Synergy RC 160 Plv, %	0.1	0.1	0.1
3	10 mm fiber, %	3.0	3.0	3.0
4	Metakaolin, %	2.0	5.0	8.0
5	Microsilica, %	8.0	5.0	2.0
6	Sand of 0–2.5 mm fr., %	48.9	48.9	48.9

The water/cement ratio was equal to 0.5 for all the compounds. The following dependences, specified at Fig. 3, were obtained as a result of long-time tests.

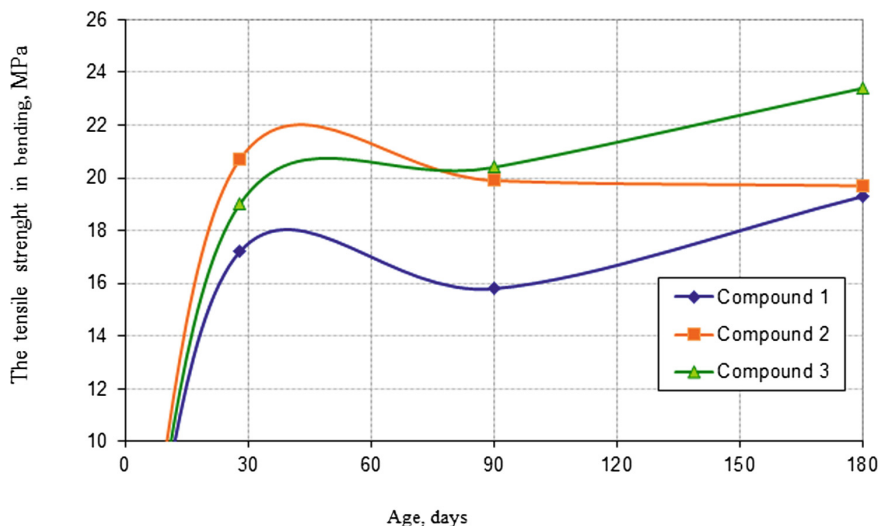


Fig. 3. Co-effect of microsilica and metakaolin on bending strength through time.

The graphical dependences demonstrate the positive effect of the joint usage of metakaolin and microsilica (Fig. 3).

The least parameters of bending strength were observed in compound 1, containing 2% MKZhL-2 and 8% MK-85. The maximum bending strength values in the age of 90 and 180 days were observed in compound 3. Up to 180 days, the bending strength reached 23.5 MPa.

4 Conclusions

By the results of made researches, the following conclusions can be made:

- the injection of MKZhL-2 metakaolin into the glass-fiber concrete mixture causes the increase of deformation properties of glass-fiber concrete;
- the positive effect of injection of highly-active mineral additive becomes noticeable during its dosing of no less than 15% of PC;
- after 180 storage days in water, fine reinforced concrete modified by metakaolin did not lose or lost its strength properties;
- the joint application of two additives of pozzolanic type (microsilica and metakaolin) positively influence the bending strength of glass-fiber concrete;
- the optimal flow rate of microsilica is 2% w/w, metakaolin – 8% w/w.

References

1. Kononova, O.V., Anisimov, S.N., Smirnov, A.O., Leshkanov, A.I.: Mod. High-Technol. **6** (2), 259–263 (2016)

2. Rusina, V.V.: Mineral adhesives on basis of large-tonnage industrial waste, 226 pp. Tutorial, Bratsk (2007)
3. Alekseenko, A.A., Moskvina, E.I., Ptichnikov, V.A.: *Young Sci.* **24**, 80–85 (2015)
4. Egorova, E.V.: Self-compacting concrete with multifunctional modifier on basis of industry waste. DrSc, thesis (2016)
5. Pustovgar, A.P., Burianov, A.F., Vasiliev, E.V.: *Constr. Mater.* **10**, 78–81 (2010)
6. Zakharov, S.A., Kalachik, B.S.: *Constr. Mater.* **5**, 56–57 (2007)
7. Golubeva, O.A., Potapova, E.N.: *Successes Chem. Chem. Technol.* **XXVIII**(8), 28–31 (2014)
8. Krasnikova, N.M., Stepanov, S.V., Iskandarova, A.F.: *Int. Sci. J. “Innovatsionnaya nauka” [Innovative Science]*. **7**, 41–43 (2015)
9. Kirsanova, A.A., Ionov, I.V., Kramar, L.I.: Materials of international workshop conference of students, postgraduates and young scientists, pp. 198–203. SibADI, Omsk (2015)
10. Nizina, T.A., Balbalin, A.V.: *Bulletin of Tomsk state construction & architectural university*, vol. 2, pp. 148–153 TGASU, Tomsk (2012)

Foundation Deformations Modeling in Underworking and Hydroactivated Rocks

Peter Dolzhikov , Albert Prokopov  ^(✉), and Vladimir Akopyan 

Don State Technical University, sq. Gagarina, 1, Rostov-on-Don 344010, Russia
prokopov72@rambler.ru

Abstract. The article investigates the deformation behavior of foundation bases in conditions of underworking and flooding. The vertical dislocations of the foundation and the soil mass in hydroactivation state and under its injection stabilization have been analyzed by the finite element method. The change regularities of the absolute deformations on three types of engineering-geological sections have been established which are peculiar to the conditions of Donbass.

Keywords: Modeling · Soil mass · Deformations of foundation
Finite element method

1 Introduction

The full flooding of coal mines' workings in mining towns and villages has led to the change in physical and mechanical properties of rocks that caused the uneven deformation activation of the foundation bases [1–3]. As a result, building constructions and facilities have been exposed to damages or destructions [4–6].

The various engineering activities are applied to ensure the stabilization of deformation processes in the soil mass and to protect against inadmissible subsidence of foundations, among which the construction of artificial base is rather prospective [7–10]. The finite element method, which is implemented on the engineering program Phase2, is used to study the deformation process in the ground as a result of the formation of an artificial foundation on the underworking and flooded areas. To create models, the authors' experience was used [11–15].

2 Setting the Aims and Objectives

The aim of the given research is to estimate the vertical dislocations of the “foundation-basis” system with the injecting fixing of hydroactivation soil mass, using the finite element method. The following objectives are set to achieve the aim:

- 1 To analyze vertical dislocations of the foundation and the soil mass in the natural state and under its hydroactivation by the method of finite element analysis in the engineering program Phase2, considering geomorphological features of rock mass and the Coulomb-Mohr's strength criterion.

- 2 To determine values of the foundation subsidence obtained by injecting fixing of hydroactivation soil mass from the point of view of three kinds of engineering-geological sections, which are specific to the conditions of Donbass.

3 Result and Discussion

The major factor of critical deformations of building constructions is a soil mass hydroactivation due to three characteristic types of engineering and geological sections (Fig. 1) during the buildings and facilities construction and operation under the conditions of the underworking and flooded areas of Donbass.

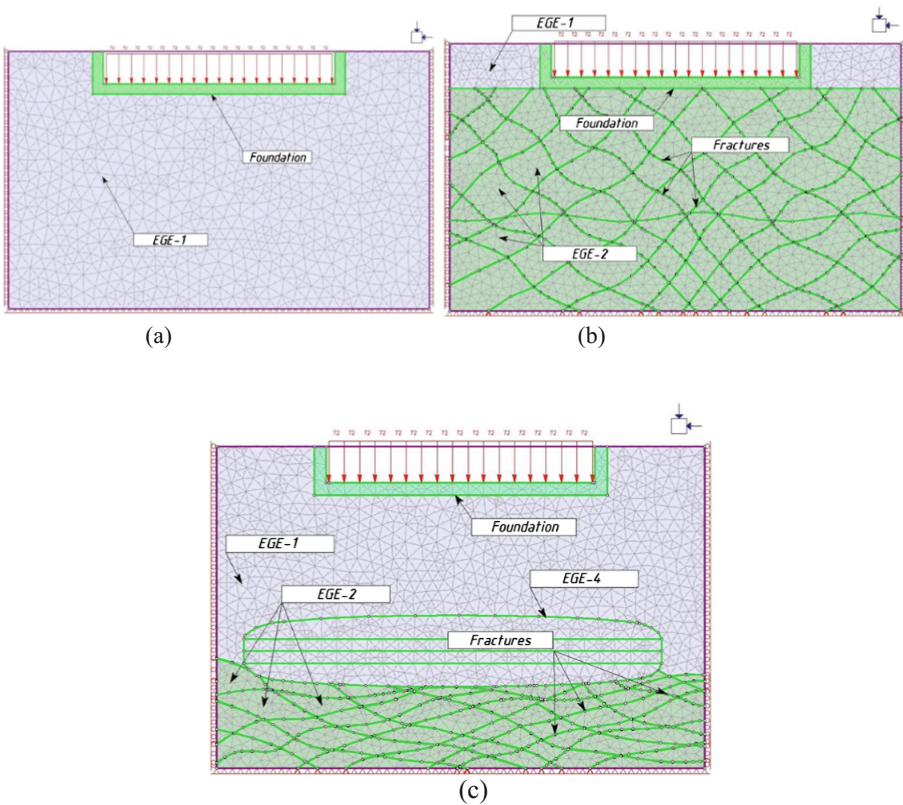


Fig. 1. The characteristic types of engineering and geological sections under the conditions of Donbass: a – decompressed loam; b – fracture-block system; c – contact of cover and bed-rocks

The physical and mechanical characteristics of top engineering and geological elements (EGE) are shown in Table 1.

Table 1. The physical and mechanical characteristics of soil mass

Section type, №	Name of engineering and geological elements	Density γ , kN/m^3	Cohesion C , kPa	Angle of internal friction φ , degree	Strains module E , kPa	The poisson coefficient μ
1	EGE-1 – loam	20.0	14	20	9400	0.35
	EGE-2 – stabilized loam	21.0	16	23	28000	0.32
2	EGE-1 – loam	20.0	14	20	5400/9400	0.35
	EGE-2 – argillite	22.5	16	25	36000/88000	0.30
	EGE-2* – stabilized argillite	23.6	18	38	88000	0.28
	EGE-4 – clay and cement mortar	21.0	34	25	36000	0.27
	EGE-5 – filling	22.6	0	17	1500/36000	0.00
3	EGE-1 – loam	20.0	14	20	9400/25000	0.35
	EGE-2 – argillite	22.5	18	38	88000	0.30
	EGE-4 – clay and cement mortar	21.0	34	25	36000	0.27
	EGE-5 – filling	22.6	0	17	1500/36000	0.00

The values are as a fraction: the numerator is in the water-saturated condition; the denominator – in the natural state

The engineering program of the finite element analysis Phase2 by version 8.0 of Rocscience Inc. (www.rocscience.com) is used to estimate the geomechanical processes and to determine the values of absolute deformations. The initial objective is to determine the values of possible subsidence of the foundation bases of the constructions in the natural state of soil mass for three type models. For this purpose the geometrical parameters of the soil mass investigated type sections are presented, based on the obtained data and engineering - geological surveys.

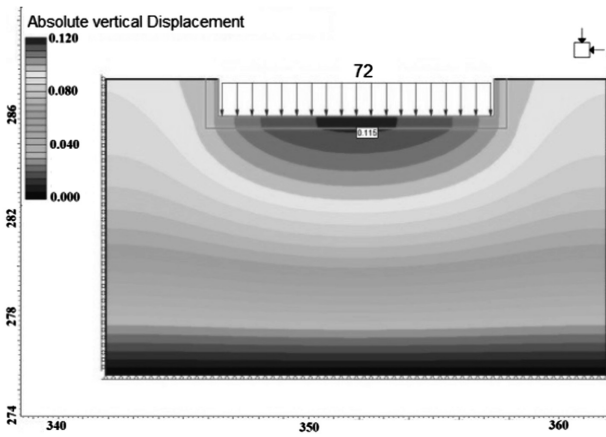
The technogenic load on the model is a five-storey typical apartment building with semi-basement, represented as a cross section. The vertical load, effecting the basis, is equal to 72 kN/m^2 .

The area of the geometric models is divided into finite elements, and the physical and mechanical characteristics of soil mass are given to the engineering geological layers according to the data shown in Table 1. The Coulomb-Mohr criterion is selected as a criterion of strength for modeling of soil mass, which is often used to estimate the strength of soil and soft rocks. The model №1 is characterized by the general spread loam, which is modeled as the continuous isotropic medium. As a result of modeling, the vertical subsidence of foundations construction in natural conditions are determined. The maximum values of vertical subsidence are observed at the base of the foundation in its central part and are $U_{y \text{ abs}} = 0.044 \text{ m}$. The obtained values are within acceptable limits according to the requirements (BN&R (building norms and regulations) 2.01.09-91 1991).

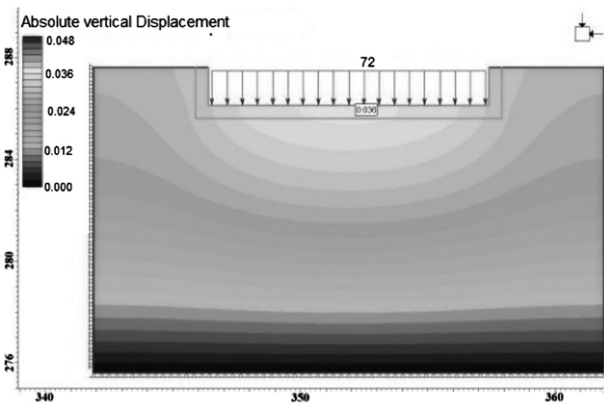
The operational complexity of the constructions in conditions of underworking areas of Donbass is that the soil mass, which is above the workings, experiences the intensive watering due to the rising of groundwater, this leads to the change of its

deformation properties. The loam hydroactivation causes the significant reduction in modulus of deformation and, as a result, increases the subsidences. The modeling of soil mass in full water saturation has been carried out to determine the values of absolute dislocations. The results are shown in Fig. 2a.

As can be seen from the obtained data, the result of loam watering and decrease of its modulus of deformation is an increase of subsidences $U_{y \text{ abs}} = 0.115 \text{ m}$, which is unacceptable for normal operation of the facility. The next geotechnical model type is represented by the model №2, which is characterized by the weak spread EGE-2 and argillite, which is broken with the systems of fractures (EGE-5) with its going out to the surface. The soil mass is modeled as an isotropic medium, broken with the systems of



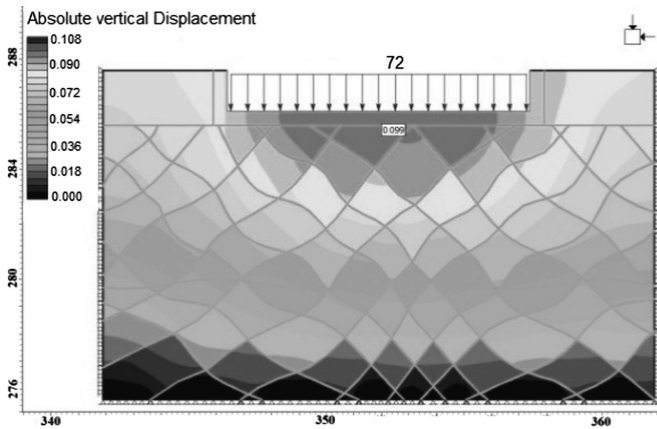
(a)



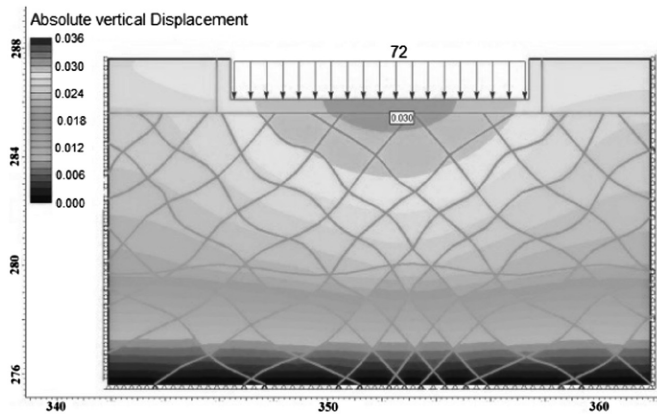
(b)

Fig. 2. The izopols of vertical dislocations of the massif for the model №1: a – at the hydroactivation, b – at the injection stabilization.

transversely isotropic fractures, to which the physical and mechanical characteristics of Table 1 are given. As a result of modeling, the vertical subsidences of foundation constructions in natural conditions are determined, the maximum absolute vertical dislocations are increased to mid of the foundation ($U_{y \text{ abs}} = 0.046 \text{ m}$), but the character of display of izopoles dislocations indicates the uneven subsidences due to the structural weakening through the system of fissures. Also, the reduction of argillite strength occurs due to the watering, which leads to the significant reduction of its deformation properties. The results of the hydroactivation argillite loading modeling are shown in Fig. 3a. The character of the izopole dislocation indicates the absolute value increase in comparison with the natural state of the massif, $U_{y \text{ abs}} = 0.099 \text{ m}$ and shows the increase of uneven values of subsidences.



(a)



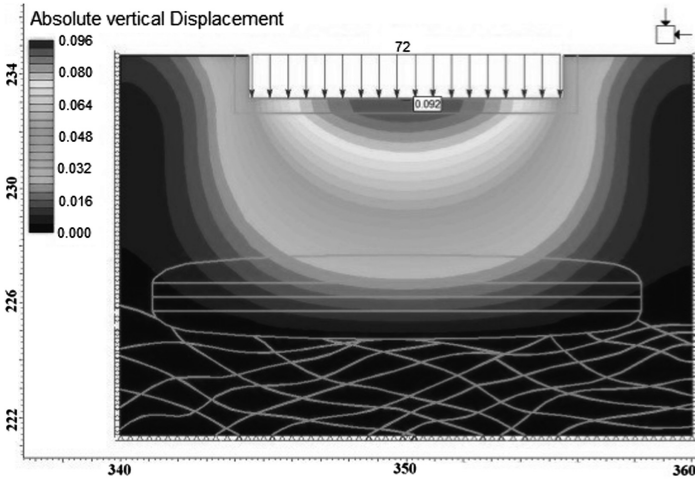
(b)

Fig. 3. The izopols of vertical dislocations of the massif for the model № 2: a – at the hydroactivation, b – at the injection stabilization.

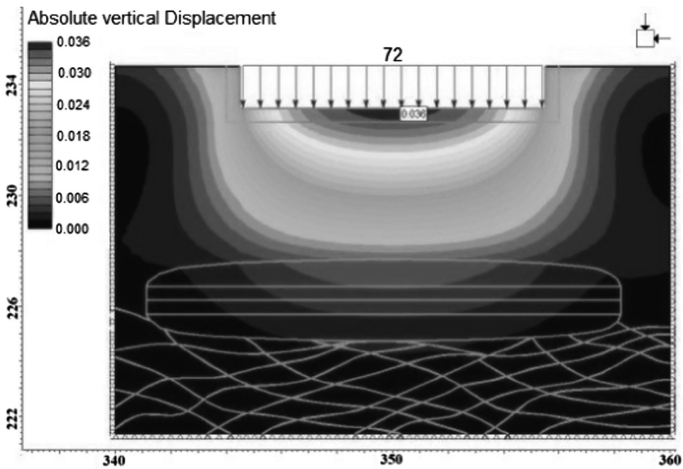
The model №3 is also rather widespread. The soil mass is presented by argillite (EGE-2), which is broken by the system of fissures (EGE-5) and is blocked by the insignificant loam layer on thickness (EGE-1).

As a result of the soil mass modeling in a natural state, the maximum vertical displacements of the foundation are $U_{y \text{ abs}} = 0.038 \text{ m}$.

The hydroactivation mechanism of loam is implemented by the groundwater raising through the systems of fissures occurring at EGE-2, thereby the wetting of EGE-1 happens. The results of the soil mass modeling in the wetting state are presented in Fig. 4a.



(a)



(b)

Fig. 4. The izopols of vertical displacements of the massif for the model № 3: a – at the hydroactivation, b – at the injection stabilization

The maximum vertical dislocation of foundation is $U_{y \text{ abs}} = 0.092$ m, which is unacceptable. The critical values attainment of the vertical dislocations leads to the uncontrolled redistribution of stresses and strains in exploited constructions, causing, thus, the progressive destruction, thereby the building is led to the emergency state and the impossibility of its further use.

The scheme of injecting fixing of the unstable ground structures for each of the standard models is developed to prevent or to stabilize the arising of the uncontrolled subsidence of the foundations base.

On the first model, the scheme is implemented as the hydrofracturing of water-saturated clay loam by the outflow of the liquid phase and formation of consolidation zones and as a result of the density increase of the ground framework. The second model is characterized by the creation of the artificial clay-cement-block system by pumping the mortar through vertical boring wells. The mortar in the first place fills the fracture systems, forming a “monolithic” massif. The feature of the model №3 is the pumping with a clay-cement mortar on a contact of zones EGE-1 and EGE-2 thereby forming an injection stabilizing cushion which prevents the development of strains in the foundations base.

The physic-mechanical and deformation characteristics of the stabilized models are shown in Table 1, and the results of modeling are shown in Figs. 2b, 3b, 4b.

The soil (ground) areas, exposed to the maximum deformation of the values of the absolute dislocations for each model, are obtained as a result of numerical modeling: № 1 – $U_{y \text{ abs}} = 0.036$ m; № 2 – $U_{y \text{ abs}} = 0.030$ m; № 3 – $U_{y \text{ abs}} = 0.036$ m. The subsidence distribution regularities of the system “foundation-base” for the three models are presented in Fig. 5.

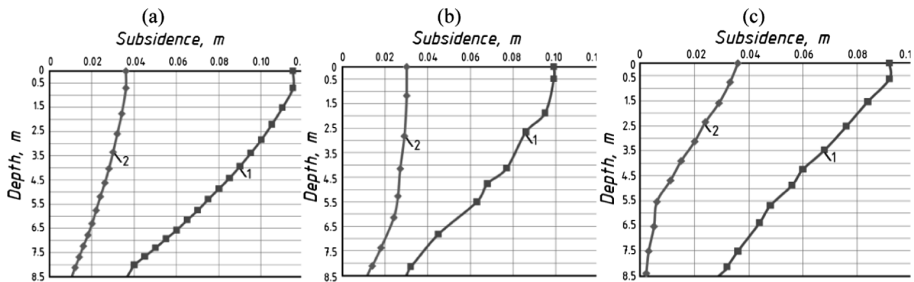


Fig. 5. The distribution regularities of the basis subsidence before (1) and after (2) the formation of an artificial base: a – in a decompressed loam; b – in an argillite broken with the system of fissures; with – on a contact of the cover and bed-rocks.

The analysis of the obtained regularities shows that for the model №1 the distribution of the subsidence is submitted to a hyperbolic function, for the model №2 the piecewise-broken dependence at the hydroactivization and a smooth degree dependence after the grouting are shown, for the model № 3 the dependence is almost linear with a fracture at a depth of stabilization cushion’s setting. These results demonstrate the efficiency of the foundation base grouting.






4 Conclusion

The change regularities of the absolute deformations for each model are determined on the base of the obtained results. So, for the model № 1 the injection stabilization of water-saturated loam reduces the subsidence 3.2 times; the injection fixing of fissuring argillite and the formation of cement-block system in the model № 2 show a decrease in the absolute dislocation 3.3 times; the formation of stabilizing cushion on a contact of the rocks in the implementation of the model № 3 reduces the subsidence 2.6 times.

References

1. Vorobyev, A., Prokopov, A., Lotsev, G.: Experience and prospects of restructuring and development of the coal industry of the countries of the European union and the CIS. Novochoerkassk, p. 394 (2011)
2. Prokopov, A., Zhur, V., Rubtsova, Y.: Problems of security of urban construction on the processed territories of Eastern Donbass. PFUR, pp. 346–351 (2016)
3. Prokopova, M., Lukyanova, G.: On possible changes in soil properties with increasing groundwater level. In: Construction-2011: Mat. Intern. Scientific-prak. Conf., Rostov-on-Don, pp 137–138 (2011)
4. Prokopov, A., Teterin, A., Teterin, E.: Displacement and deformation of foundations in areas of intensive underground mining. Sci. Rev. (12), Part 2, pp. 519–523 (2014)
5. Prokopova, M., Lukyanova, G.: Reducing the impact of the consequences of the elimination of mines on the deformation of buildings and structures. In: Construction-2010: Mat. Intern. Scientific-Prak. Conf, Rostov-on-Don, pp. 142–143 (2010)
6. Prokopov, A., Prokopova, M., Rubtsova, Y.: The experience of strengthening subsidence of the soil under the existing building in the city of Rostov-on-Don. MATEC Web Conf. **106**, 02001 (2017)
7. Ivlieva, E., Furdey, P.: Formation of artificial base of the foundations at undermined areas. In: Proceedings of International Conference on Prospect of building Technologies, pp 34–37 (2013)
8. BN&R 2.01.09-91: Buildings and facilities on undermined areas and subsiding grounds. Stroyizdat, Moscow, 44 (1991)
9. Dolzhikov, P., Ivlieva, E.: Influence of watering and fracturing on the deformation properties of foundation bases collection of scientific works. DonSTU **40**, 168–172 (2013)
10. Kipko, E., Dolzhikov, P., Dudlya, N., Kipko, A.: The complex method of tamping in the mines construction tutorial. Dnepropetrovsk, p. 367 (2004)
11. Akopyan, V., Akopyan, A., Podolko, K., et al.: Simulation of piles in subsidence grounds. Inženernyj vestnik Dona. (Rus), no. 3 (2017)
12. Akopyan, V., Akopyan, A.: Experimental and theoretical investigation of the interaction of the reinforced concrete screw piles with the surrounding soil. Procedia Eng. **150**, 2202–2207 (2016)
13. Prokopova, M., Tkacheva, K., Vaskovtsova, Y.: Modeling of structures taking into account the stages of construction. In: Improving the Technology of Construction of Mines and Underground Structures: Scientific Works, Donetsk, vol. 17, pp. 46–48 (2011)
14. Prokopov, A., Akopyan, V., et al.: Study of the stress-strain state of the soil massif and the mutual influence of underground structures. Inženernyj vestnik Dona, 4 (2013)
15. Popkov, Y., Prokopov, A., Prokopova, M.: Information Technologies in Mining. Novochoerkassk, 201 p. (2007)

Subminiature Eddy-Current Transducers for Conductive Materials and Layered Composites Research

Sergey Dmitriev¹ (✉) , Alexey Ishkov² , Alexander Katasonov¹ ,
Vladimir Malikov¹ , and Anatoly Sagalakov¹ 

¹ Altai State University, Lenina Ave., 61, Barnaul 656038, Russia
osys@me.com

² Altai State Agrarian University,
Krasnoarmeyskiy Ave., 98, Barnaul 656049, Russia

Abstract. The measuring system based on subminiature eddy-current transducers has been developed to carry out local investigations of aluminum-magnesium alloy plates for flaws. The Delianna filter has been modified to allow the significant increase of signal-to-noise ratio. A scheme that uses a computer as a generator and receiver of signals from windings is proposed. It is capable of automatically changing the filtering cutoff frequency and operating frequency of the device. The transducer has been tested on a number of aluminum-magnesium alloy plates with flaws. The article presents data on the relationship of eddy-current transducer response to the presence of flaws in alloys as hidden holes at signal frequencies comprised between 300–700 Hz on an exciting winding.

Keywords: Transport buildings and structures · Eddy current
Titanium alloys · Measuring system

1 Introduction

Non-destructive testing of a number of structures occupies a special place in modern materials science. Layered composite metal-insulator-metal, aluminum alloy (aluminium-magnesium and duraluminium), titanium alloys welds are among these objects. Layered metal-polymer composites of metal - insulator – metal type are widely used as sound and thermal insulation of aircraft, surfaces of equipment and devices reflecting the radiation, materials for manufacturing of printed circuit boards. Such composites contain one, two or more metallic layers separated by dielectric layers. Titanium and its compounds are largely used in aviation equipment, shipbuilding, chemical industry, important units of machines. Technical titanium is used for the production of products intended for the use in aggressive environments. However bad-quality titanium welds can lead to the destruction of the products made from this material. Aluminum-magnesium (AMG) alloys are the main structural materials in aircraft and astronautics, thanks to good combination of strength and lightness. Duralumin is used in the electrical engineering, chemical and food industries. They are

also used in manufacturing of ventilation systems, in radio engineering, in construction. For example, the D16AM alloy brand is used in extreme cold environments. D16T duralumin is flexible and therefore it is used in shipbuilding.

Despite our great experience in using vortex-current transducers (VCT) in the sphere of nondestructive control, several important aspects still need to be studied nowadays. In particular, the most vital problems are: carrying out local contactless measurements combined with controlled object scanning; price reduction in sensor engineering; making the control locality more accurate and the quick allocation of the frequency range, the most proper to scan the controlled object. The worked out conception of the virtualized measuring device enables a researcher to make a great number of measurements in different spheres with the help of one sensor only. To these spheres belong fault detection of conducting materials and stratified compos, thickness measuring, profilometry, tension measuring of permanent and variable magnetic fields and conductivity measuring of un ferromagnetic materials and some others. In the past there were several attempts to use highly sophisticated magnetic field sensors like SQUID and Fluxgate sensors for sensitive low frequency eddy current testing to detect deep defects in metal parts [1–3]. Although very good results could be achieved such testing systems can hardly be used in real industrial applications because of their complexity, prices and insufficient robustness. A very promising sensor performance could be obtained by using highly sensitive inductive coils. The problem is that such sensors have to be produced by skillful specially trained operators; it results in low reproducibility and low productivity [4]. To solve these problems the VCT is often provided with an extra magnetic conductor [5].

One of its terminals has a shape of a truncated cone. This solution of the problem has only one disadvantage. Despite the increased localization of the magnetic flux, the construction of the magnetic conductor has become considerably more complicated. It makes the measuring accuracy worse, because the output signal of the VCT depends to a great extent on the interaction between two magnetic conductors, which can influence the intensification of the vortex-current field in a rather unpredictable way.

There are different well-known constructions of superimposed VCTs, whose working surface has either a plane or hemispherical form. Such kind of a surface provides a satisfactory contact of the VCT with the surface under control, but the tension quantity, sent to the VCT, greatly depends on the curvature of the controlled surface. The edge effect influences the work of the VCT considerably. This effect makes it impossible to control the details of a complicated configuration and of small sizes. If the size of the sample is small, the measurement error is unavoidable. The results show that the relative errors increase with the decrease of the size of the sample [6]. The small size of the cores (starting with 1 mm), used in the virtualized VCT, gives an opportunity to improve the control locality, without applying additional complication of the construction. Due to that the influence of hindrances on the VCT is considerably reduced.

The core, shaped either as a cone or pyramid, supports a high degree of localization of the magnetic field that is why the influence of the edge effects and the surface curvature is practically avoided. The existence and shape of a defect can be recognized by observing the difference in variation of the equivalent impedance. Magnetic systems with various interior deep defects are numerically analyzed by finite element method

and their data are compared with those of the experimental systems. The measured data of the impedance variation are distinguishable enough to be used to estimate the existence and shape of defects in the steel structure [7]. In the laid on VCTs theory the most general objective is the study about the distribution of the electromagnetic field, created by the circular wind with the alternating current, in the multilayer media [8]. Defects in welding joints of the LSMP may significantly reduce the material strength. Eddy Current Testing (ECT) is considered as a powerful NDT tool for the detection and sizing of defects [9].

With the development of computer equipment, numerical methods have become a frequent practice for solving tasks in non-destructive testing based on the interaction of electromagnetic fields with defects.

Rigorous numerical methods were mainly used for solving two-dimensional tasks with the application of integral equations and finite elements.

Shaternikov [10] suggested generalizing theoretical calculation models for complex shapes products. Based on these models, the solutions for the method of quasi-conformal mappings were made and the algorithms for calculating the output parameters of ECP with arbitrary section windings were designed.

Bizyulev and Muzhitskii [11] proposed a three-dimensional mathematical model based on the representation of secondary charges by the surface currents, flowing along the side edges of the defect. The surface current density was linked to the magnitude of the initial magnetic field. Muzhitskiy analyzed the basic interaction laws of the defects under normal magnetization of the controlled objects and under the longitudinal magnetization at an angle to the side edge of the defect [12].

An approximate calculation method of the attachable ECP was suggested by Shkarlet [13] in order to control flat-shaped conductive items (the model is a round coil with alternating current over a flat two-layer conductive object). It allowed to disclose the basic laws of the electromagnetic field distribution of the model under study and to find effective signal processing methods.

The efforts of Russian and foreign scholars led to the development of a large number of other methods for signal processing in addition to the above mentioned amplitude and phase, phase and amplitude, in order to separate the information about the measured parameter and the detuning from confounding factors - autogenous, variable frequency, multifrequency, modulation and etc. [14–16].

The development of eddy-current measuring system used for detecting defects in layered composites, aluminum alloys, able to assess the quality of titanium alloy welds is an urgent task. Since eddy-current testing method is insensitive to non-conductive layers of paint, it can be used to diagnose the details with varnish-and-paint cover.

2 Materials and Methods

One of the well-known drawbacks of eddy-current flaw detection is the ability to control the quality of a relatively thin surface layer of a conductive material. Upgraded design of the measuring system includes two differentially included subminiature transducers. Such a construction allows to detect defects at the depth up to 5 mm due to its small size and the special shape of the cores.

Eddy-current measuring system has been developed on the basis of super small eddy-current transducer [17–21]. Controlled parameter is the value of electrical conductivity of the material and its distribution over the surface and the thickness of the tested object. Eddy-current transducer is connected to a series of bandpass filters and amplifiers, managed using a PC working on the bases of special software. The software controls voltage supply to transducer generator winding, and also reads voltage values from measuring winding in conventional units, which are then converted into electrical conductivity values, given the preliminary calibration.

Exciting subminiature transmitter winding consists of 10 turns, and its diameter is 0.13–0.12 mm. Measuring winding consists of 130 turns and its diameter is 0.05–0.08 mm.

In order to minimize the influence of the exciting windings on the received signal, compensating winding is included into the circuit. The compensating winding is connected to the measuring winding so that the voltage of the exciting windings can be subtracted. The compensating winding consists of 20 turns. Copper wire 5 μm thick is used to the wind the turns. The windings are wound on pyramidal shape core. The core is made of HM3 2000 ferrite with initial magnetic permeability of the value of $\mu_{\text{max}} = 500$. The scheme of the subminiature eddy-current transducer (ECT) is shown in Fig. 1.

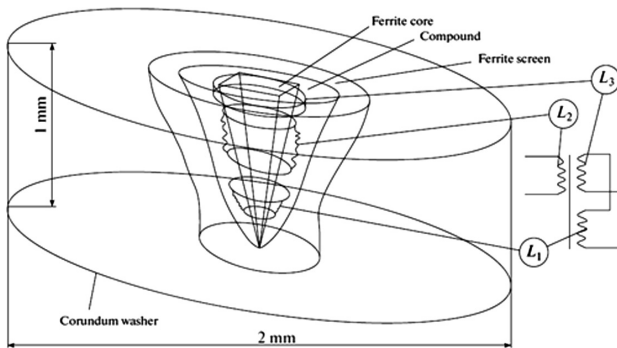


Fig. 1. Scheme of eddy-current transducer. L1 - measuring winding L2 - the exciting winding L3 - compensation winding.

Specifications of developed transducers allow to efficiently localize magnetic field within the limits of $2500 \mu\text{m}^2$ and to provide considerable depth of its penetration into the object under study.

Digital signal from the virtual oscillator is fed to analog-to-digital transducer (ADC) input of sound card, after which the analog signal through the power amplifier is fed to the exciting winding transducers. Passing through the excitation windings, sine wave signal creates electromagnetic field which induces voltage in the measuring windings of eddy-current transducer. The voltage depends on the parameters of the object under control. The transducers are included counter-currently, whereby the resultant signal represents the difference between two values of voltage. This signal is

fed to a series of amplifiers and bandpass filters, and then supplied to the microphone input of the sound card and then through the preamplifier - to the input of an analog-to-digital transducer (ADC) of sound card. The analog signal is converted to the digital one and transferred to software processing and control unit. The processing and control unit records the level of the digital signal in conventional units corresponding to the difference between the voltages on the measuring windings.

This level is assumed to be zero, it corresponds to the signal that takes place when both transducers are situated over the defect-free sections the object under control.

Using computer sound card makes it possible to carry out scanning of electromagnetic field frequency variation which is generated by transducer exciting winding in the range of 20 Hz to 2 kHz. The developed measuring system allows effective investigate the metal-insulator transitions in miniature metal-polymer composite objects. Similar composites may include several metal layers separated by thin dielectric layers of polymer. The typical defects of such materials are, for example, the disturbance of layers continuity and the formation of link between the layers.

3 Results and Discussion

3.1 Layered Composites

To demonstrate the proposed method operability the structure of alternating aluminum foil of 100 μm thick and paper of 100 μm thick has been used. As a defect model between the layers a hollow parallelepiped with a wall of 300 μm thick has been placed. The defect was at a distance of 600 μm from the sensor in the depth of the layered structure. In Fig. 2 there is a spectral picture, observed when the sensor is moved above the layered medium, inside of which there is a defect.

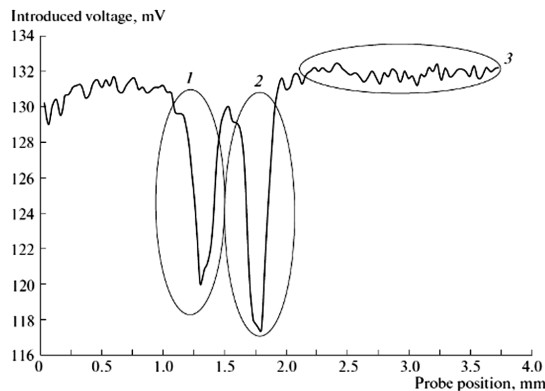


Fig. 2. Picture observed when the probe moves along the layered medium with a defect. The frequency of the transducer is 1000 Hz: (1, 2) walls of the parallelepiped, (3) defect-free part of the sample.

The signal level from the measuring winding characterizes conductivity values on the survey section. For fundamental operating frequency of 1000 Hz the voltage level included in the measuring winding was 130 ± 2 mV. Areas 1 and 2 on the graph where in voltage level drop is up to 115 mV correspond to the walls of the parallelepiped. This change in the signal amplitude is equal to 11% of the signal level, corresponding to the defect-free section of the sample. At the same time the fluctuations of signal amplitude at the defect-free section does not exceed 4 mV, representing 3% of the signal corresponding to the defect-free region of the sample.

When operating frequency of the device is beyond the given limits the results of the measurements will be distorted by amplitude fluctuations caused by microcracks on the surface of the sample or by the decreasing of field localization inside the layered structure. As seen from the graph, the amplitude changes, caused, in this case, by the microcracks on the sample surface, are much higher than the amplitude changes, caused by the defect directly. Right up to the depth of the defect, equal to 1400 μm , there is a clear dependence of the response of transducer, on the position of the transducer over the defect. By fixing change in amplitude response in the converter caused by a defect, it is possible to change the frequency of the current in the exciting winding so that the eddy-currents are concentrated in the layers of composite placed above the defect.

The solution of the inverse problem allows to determine the depth of the defect. After calibration, the Fourier analyzer for typical defects, can use the "IENM-5FA" for the diagnosis of composite laminates with a thickness of 1 to 1400 μm .

3.2 Welds in Titanium Alloys Scanning

In order to demonstrate the performance of the device to determine the quality of titanium alloys welds a series of measurements. The samples were titanium plates, combined by means of welds. The thickness of the plates equaled 5 mm. The weld width equaled 5 mm.

The tested feature is the voltage induced by the eddy-current field developing in the object under control. The sensor calibration was performed before the beginning of measuring operations. It consisted in the detection of the inserted voltage from the defect-free section. In the experiment the calibration section was chosen on the titanium defect-free plate similar to the tested one. The calibration was performed at different frequencies. At the same time the variation of the frequency in the 500–2000 Hz range at the pitch of 100 Hz was performed. The further scanning was conducted by means of the sensor moving through the length or breadth of the weld or crosswise the defective section. During the experiments, it was found out that the optimum frequency range of the induction winding electromagnetic field for titanium study equaled to 1500–1700 Hz.

In the experiment scanning was conducted crosswise the weld. The length of the weld was 150 mm. The seam was divided into 30 sections, 5 mm each, so that the signal from both the weld and directly from the plate could be read. The dependences received were averaged. The results of the experiment are presented in Fig. 3(a), (b) (A1–A2 correspond to the edges of the weld seam).

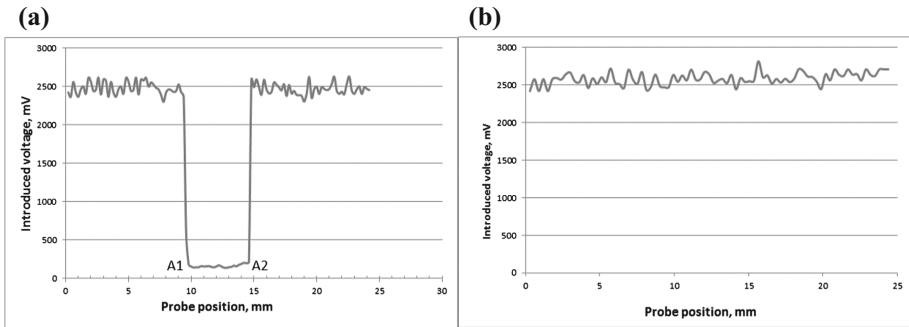


Fig. 3. (a) Results of scanning sample №1. (b) Results of scanning sample №2.

In the given sample the influence of a deficient weld on the inserted voltage is clearly traced by the significant drop in the signal amplitude in the weld area in comparison with the plate area. On the bases of the experiment the conclusion about the low quality of Sample 1 weld was made. The low quality of welding was confirmed directly by the weld cutting. Sample 2 scanning showed the absence of the signal amplitude deflection within the weld seam. The weld of Sample 2 cutting showed the high quality of welding.

3.3 Plates Linking Without Welding

In order to simulate such amplitude drop an additional experiment was conducted. During the experiment, two titanium plates of the same thickness were linked tightly, the area of the junction being scanned afterwards. The results of the experiment are presented in Fig. 4.

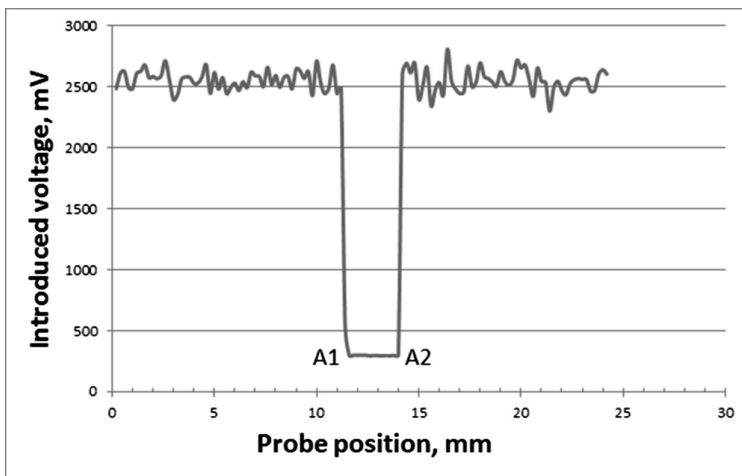


Fig. 4. Voltage value to the measuring winding of the transducer, while scanning in the area of two plates junction. Scanning frequency is 1600 Hz. A1–A2 correspond to the edges of the area where the junction influences the inserted voltage.

The dependence analogous to that observed in Fig. 3b. in the Sample weld section was received in the experiment. The signal amplitude in the area of the junction changed by times in comparison with the signal amplitude from the plates themselves.

3.4 Aluminum-Magnesium Alloy with Model Defects Scanning

Samples with model defects were prepared in order to assess the maximum depth and the linear dimensions of the defects, for the detection of them it is advisable to use the eddy-current inspection method.

The samples were plates of Al-Mg alloy. The thickness of the first plate was 5.5 mm. The plate contained three defect in the form of slits 1 mm thick at the depths of 1, 3 and 4 mm. The thickness of the second plate was 5.5 mm. The plate contained six defects in the form of slits of 0.25 mm thick at the depths of 1, 2, 3, 4, 5 and 5.3 mm.

In order to determine the sensitivity of the sensor to the defects at the depth of the metal, scanning of defect-free side of the sample was performed. During the experiments with the first plate the magnitude of the inserted voltage to the exciting winding of the transducer was 2 V.

The results of the defectoscopy of the first plate, with the defects of 1 mm thick at the frequency of 500 Hz and 2 V signal amplitude allowed to detect all three slits by means of signal amplitude drop Fig. 5.

Signal amplitude drop in the first defect was 0.75 V, in the second one -0.2 V, in the third one -0.1 V.

With increase in amplitude of the signal at the exciting winding, the output signal from the measuring system will be exceeded and the results will be significantly distorted. To improve the localization of the magnetic field, the measuring system must

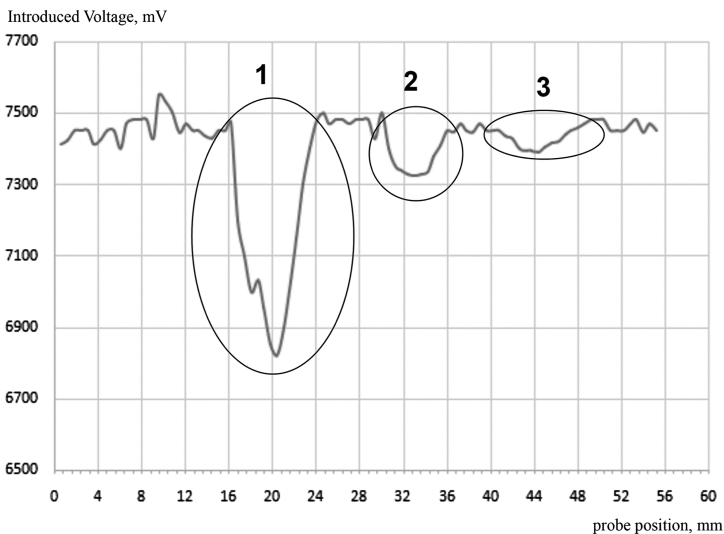


Fig. 5. Results of the plates №1. 1, 2 and 3 scanning - the defects numbers

be significantly modernized. To increase the power of the electromagnetic field by increasing the voltage U_e at the exciting winding from 2 to 3.5 V, a second eddy-current transformer is introduced in the system. The results of defectoscopy at the frequency of 500 Hz and 3 V signal amplitude allowed to reveal five defects Fig. 6.

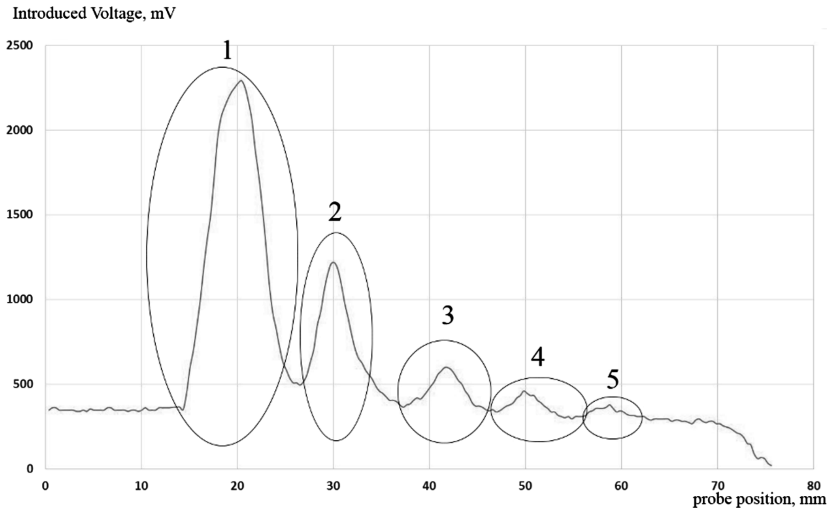


Fig. 6. Results of plate №2 scanning

The signal amplitude drop at the first defect was 2.5 V, at the second defect -1 V, at the third one -0.4 V, at the fourth one -0.2 V, at the fifth defect -0.1 V. The changes in the response signal when passing over the sixth defect were not fixed.

The experimental results show the effectiveness of the developed measuring system to find defects of the thickness from 0.25 mm at the depth of 5 mm.

4 Conclusions

The developed measurement system based on eddy-current subminiature transducers, allows greater localization of electromagnetic field in comparison with previously known similar systems. The pyramidal shape of the core, the system of band pass filters and selective amplification allow to reduce interference and achieve significant penetration depth of eddy currents in the object under study. The developed eddy-current transducers can effectively produce scanning of titanium alloys welds and analyze their quality. Defects scanning in aluminum alloys can detect defects with linear dimensions of the order of 100 microns at the depth of 5 mm. The developed software allows to automate measurements and make rapid changes in the operating frequency of the device.

References

1. Hohmann, R., Lomparski, D., Krause, H.-J., Kreutzbruck, M.V., Becker, W.: Aircraft wheel testing with remote eddy current technique using a HTS SQUID magnetometer. *IEEE Trans. Appl. Supercond.* **11**(1), 1279–1282 (2001)
2. Gabor, V., Antal, G.: Nondestructive material evaluation by novel electromagnetic methods. *Mater. Sci. Forum* **414–415**, 343–352 (2004)
3. Allweins, K., Gierelt, G., Krause, H.-J., Kreutzbruck, M.V.: Defect detection in thick aircraft samples based on HTS SQUID-magnetometry and pattern recognition. *IEEE Trans. Appl. Supercond.* **13**(2), 250–253 (2003)
4. Hesse, O., Pankratyev, S.: Usage of magnetic field sensors for low frequency eddy current testing. *Meas. Sci. Rev.* **5**, 86–93 (2005)
5. Lemeshko, M.A., Adigamov, K.A., Osackiy, S.S.: RU Patent 2200299
6. Wang, J., Fu, Y., Sun, M., Liu, Z., Fan, Z., Shi, K.: Thickness measurement of ferromagnetic material based on pulsed eddy current testing technology. *J. Beijing Jiaotong Univ.* **36**, 133–136 (2012)
7. Lee, K.H., Baek, M.K., Park, I.H.: Estimation of deep defect in ferromagnetic material by low frequency eddy current method. *IEEE Trans. Magn.* **48**, 3965–3968 (2012)
8. Kluev, V.V.: Non-destructive testing, vol. 1 (2008)
9. Zhang, D., Li, H., Chen, Z., Wang, Z.: Applications of multi-frequency inversion algorithm to quantitative NDE of cracks in welding joints of a metallic lattice sandwich plate. *Int. J. Appl. Electromagn. Mach.* **39**, 137–143 (2012)
10. Shaternikov, V.: The interaction of electromagnetic fields with complex shapes converters conductive bodies. *Russ. J. Nondestruct. Test* **2**, 54–63 (1977)
11. Bizyulev, A., Muzhitskii, V.: Eddy current flaw detector WA-12 NFP and processing methods of the measured signal from the defect. *Russ. J. Nondestruct. Test* **5**, 85–91 (2004)
12. Zagidulin, R., Muzhitskii, V.: Determination of geometrical parameters of continuity defect in a ferromagnetic plate by minimizing the smoothing functional. Part 2. The results of evaluating the continuity of the defect parameters. *Russ. J. Nondestruct. Test* **10**, 13–19 (2001)
13. Shkarlet, Y.: Basic theory and models of overhead electromagneto elasticity electromagnetic acoustic transducers. *Russ. J. Nondestruct. Test* **2**, 39–45 (2004)
14. Lunin, V., Zhdanov, A., Lazutkin, D.: A neural-network classifier of flaws for multifrequency eddy-current tests of heat-exchange pipes. *Russ. J. Nondestruct. Test* **3**, 37–45 (2007)
15. Shekhar, H., Polikar, R., Ramuhalli, P., Liu, X., Udpa, L., Udpa, S.: Dynamic thresholding for automated analysis of bobbin probe eddy current data. *Int. J. Appl. Electromagn. Mech.* **15**, 39–46 (2003)
16. Egorov, A., Polyakov, V., Kolubaev, A., Pirogov, A.: Multi-frequency eddy current testing of aluminum alloys. *Izv. Altai State Univ.* **81**, 176–180 (2014)
17. Dmitriev, S., Katasonov, A., Malikov, V., Sagalakov, A.: Flaw detection of alloys using the eddy current method. *Russ. J. Nondestruct. Test* **52**, 32–37 (2016)
18. Dmitriev, S., Ishkov, A., Malikov, V., Sagalakov, A., Katasonov, A.: Non-destructive testing of the metal-insulator-metal using miniature eddy current transducers. *IOP Conf.: Ser. Mater. Sci. Eng.* **71**, 1–6 (2015)
19. Dmitriev, S., Malikov, V., Sagalakov, A., Shevtsova, L., Katasonov, A.: Subminiature eddy current transducers for studying semiconductor material. *J. Phys.: Conf. Ser.* **643**, 1–7 (2015)

20. Malikov, V., Davydchenko, M., Dmitriev, S., Sagalakov, A.: Subminiature eddy-current transducers for conductive materials research. In: International Conference on Mechanical Engineering, Automation and Control Systems, Tomsk, pp. 1–4 (2015)
21. Dmitriev, S., Katasonov, A., Malikov, V., Sagalakov, A.: Eddy-current measuring system for analysis of alloy defects and weld seams. Russ. Eng. Res. **36**, 626–629 (2016)

Influence of the Longitudinal Compressive Force on Parametric Vibrations and Dynamic Stability of Thin-Walled Above-Ground Steel Oil Pipelines with Large Diameter

Vladimir Sokolov¹  and Igor Razov^{1,2} 

¹ Industrial University of Tyumen,
Volodarskogo str. 38, Tyumen 625001, Russia
RazovIO@mail.ru

² Tyumen Higher Military Engineering Command School named
after Marshal of Engineering Troops A.I. Proshlyakova,
L'va Tolstogo str. 1, Tyumen 625001, Russia

Abstract. This article deals with the problem of parametric vibrations of the above-ground main oil pipelines of large diameter subjected to the action of non-stationary internal operating pressure and the parameter of the longitudinal compressive force. The main pipeline is considered as a thin-walled cylindrical shell, because only with the use of this design scheme one can account for the deformation of the cross section and the effect of internal operating pressure on parametric vibrations and dynamic stability. The pipeline is set on an elastic ground base, which corresponds to the Fuss-Winkler model. To solve the problem of parametric vibrations, differential equations of the middle surface of the shell are obtained on the basis of the geometrically nonlinear semi-momentary theory of cylindrical shells of middle bending. After mathematical transformations, we obtain a separating system of homogeneous Mathieu differential equations. The resulting system of Mathieu's equations allows to investigate the dynamic stability of an above-ground thin-walled large-diameter oil pipeline by constructing regions of dynamic instability, such as modified Ains-Strett diagrams, for different values of wave numbers $m, n = 1, 2, \dots$. Dimensions and positions of dynamic instability areas strongly depend on the geometric and mechanical parameters.

Keywords: Parametric vibration · Elastic foundation
Longitudinal compressive force · Natural frequency

1 Introduction

One of the most popular problem in design of thin-walled oil pipelines with elastic foundation is dynamic calculation. As practice shows, during operation oil pipelines are subjected to the effect of non-stationary internal operating pressure, and the pulsating flow of oil fluid, and also as a result of the operation of the pumps of the pumping station, result in the excitation of a longitudinal compressive force.

At present, the Russian Federation is implementing the construction of new and development of existing trunk pipeline networks made of modern thin-walled pipes with diameter up to 1000 mm. Depending on the region, climate and geological conditions there are different types of technological solutions used for laying pipelines such as underwater [1, 2], above-ground [3–6], underground [7–9, 12, 13] and semi-underground [14, 15]. For each type of laying there are the features of calculation and collecting of loads to be considered for exploitation. The layout of the above-ground pipeline looks as in the Fig. 1 [16].

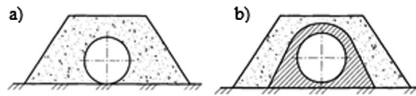


Fig. 1. Above-ground pipeline laying. (1) Mound of mineral ground; (2) mound of ground water-repellent

The problem of parametric vibrations and dynamic stability of thin-walled large-diameter pipelines with a flowing liquid was investigated on the basis of the theory of thin cylindrical shells. One of the first works in this field was published in 1953 in an article by Grigoluk, where the solution of the problem of parametric vibrations of a cylindrical shell loaded with a pulsating axial force is described [17].

The most complete foundations of the general theory of dynamic stability of elastic systems are described in the book by Bolotin [18], where, as a particular case, parametric vibrations of a cylindrical shell loaded with periodically changing forces are considered. Parametric vibrations of a cylindrical shell with a pulsating flow of a liquid are investigated in book by Volmir [19]. Where on the basis of the theory of the potential flow of an ideal fluid, a solution is obtained for determining the hydrodynamic pressure of the liquid flow on the wall of the tube. A system of associated differential equations of Mathieu is obtained and the boundaries of dynamic instability areas are constructed. The most detailed research of parametric vibrations of cylindrical shells with a non-stationary fluid flow, with the construction of upper and lower boundaries of the main and minor areas of dynamic instability, was investigated by Paidussys [20–23]. In these papers, the theory of shells simplified by assumptions was used, and studies of dynamic instability were carried out on the basis of a complex numerical solution of associated systems of Mathieu differential equations.

In all papers related to the estimation of the dynamic stability of thin-walled large diameter pipes with a flowing liquid based on the theory of thin cylindrical shells, systems of non-separating, that is, associated, Mathieu differential equations. This means that solutions of these equations require the application of numerical methods with succeeding construction of dynamic instability areas for each particular case. This difficulty is overcome in the works of Il'in and Sokolov [24], Efimov and Sokolov [2], where problems are solved of parametric vibrations and dynamic stability of part of large-diameter pipelines with a pulsating flow of a fluid on the basis of a geometrically nonlinear version of the semi-moment theory of cylindrical shells and the theory of the potential flow of an ideal fluid. In these papers, a separating system of Mathieu

differential equations was obtained, and the Ains-Strett diagrams modified for practical application were constructed and analyzed.

2 Materials and Methods

Based on the geometrically nonlinear semi-moment theory of cylindrical shells of the average bending and using semi-moment assumptions of the theory, we obtain the equation of motion in displacements [4]:

$$\begin{aligned} \frac{\partial^3 u}{\partial \xi^3} + h_{\tilde{v}}^2 \cdot \frac{\partial^3}{\partial \theta^3} \left(\vartheta_2 + \frac{\partial^2 \vartheta_2}{\partial \theta^2} \right) + 2 \frac{\partial^2}{\partial \theta^2} \left(\frac{\partial^2 w}{\partial \xi^2} \cdot \varepsilon_0 \right) - \frac{R}{Eh} \rho_0 \frac{\partial^3 \vartheta_2}{\partial \theta^3} + \frac{R}{Eh} \frac{\partial^2}{\partial \theta^2} [\Psi(\theta)w(\xi, \theta, t)] - \\ - \frac{R^2 \rho}{E} \left(\frac{\partial^3 u}{\partial \xi \partial t^2} - \frac{\partial^2 v}{\partial \theta \partial t^2} - \frac{\partial^4 w}{\partial \theta^2 \partial t^2} \right) + \rho_0 \Phi_{mn} \frac{R}{Eh} \left(R^2 \frac{\partial^2 w}{\partial \theta^2 \partial t^2} + V^2 \frac{\partial^4 w}{\partial \theta^2 \partial \xi^2} \right) = 0 \end{aligned} \tag{1}$$

were u, v, w – moving components middle surface attributed to the radius R ; ϑ_2 – rotation angle of the tangent to the median cross-sectional surface; E – the elastic modulus of the shell material;

\tilde{v} – Poisson’s ratio; $h_{\tilde{v}} = \frac{h}{R\sqrt{12(1-\tilde{v}^2)}}$ – parameter of the relative thickness of the shell; h – thickness of the shell; $\varepsilon_0 = \frac{F}{EA}$ – original longitudinal deformation caused by the action of the longitudinal compressive force, which is determined on the assumption of non-deformable cross section, ρ – the density of the shell material, $\rho_0^* = \rho_0 \frac{R}{Eh h_{\tilde{v}}}$ – fluid density parameter; ρ_0 – fluid density; $\Phi_{mn} = \frac{I_m(\lambda_0)}{\lambda_0 I_m'(\lambda_0)}$ – parameter of the Bessel function and its derivative; V_0 – velocity of fluid flow; $\rho_0 \Phi_{mn}$ – adjoin mass of liquid;

$$\begin{aligned} \Psi(\theta) = \frac{kR}{\pi} \left[\frac{\varphi_0^3}{3} + \sum_{m=1}^{\infty} \beta_m \cos m\theta \right]; \\ \beta_m = (-1)^m m^{-3} [2\varphi_m \cos \varphi_m - (\varphi_m^2 - 2) \sin \varphi_m]; \quad \varphi_m = m\varphi_0, \end{aligned} \tag{2}$$

where $\Psi(\theta)$ – soil pressure on the radial an external surface of the pipe [21], k - soil ratio in accordance with the model Fuss-Winkler, $\varphi_0 = \sqrt[3]{\frac{3Q_y}{2kR^2}}$, – linear pipe weight, Q_y – foundation reaction, N/m, R – the radius of the middle surface.

The equations of motion in displacements (5) has four unknowns $u, v, w,$ and ϑ_2 . For complete system of equations we add assumptions of semi-moment theory:

$$\frac{\partial v}{\partial \theta} + w = 0; \frac{\partial v}{\partial \xi} + \frac{\partial u}{\partial \theta} = 0; \vartheta_2 = \frac{\partial w}{\partial \theta} - v, \tag{3}$$

As a result, we obtain a complete system of Eqs. (5), (7). Solve the resulting system by separation of variables (Fourier method) represent the function of the radial displacement $w(\xi, \theta, t)$ for the case of an articulated fastening at a [20]:

$$w = \sum_m \sum_n f(t) \sin(\lambda_n \xi) \cos(m\theta) \tag{4}$$

where $\lambda_n = \frac{n\pi R}{L}$; $m, n = 1, 2, \dots$ – wave numbers in the circumferential and longitudinal directions.

The other components of displacement and rotation angle of the tangent are determined from the semi momental assumptions of the theory, which have the form:

$$\begin{aligned} u &= - \sum_m \sum_n \frac{\lambda_n}{m^2} f(t) \cos(\lambda_n \xi) \cos(m\theta), \\ v &= - \sum_m \sum_n \frac{1}{m} f(t) \sin(\lambda_n \xi) \sin(m\theta), \\ \vartheta_2 &= - \sum_m \sum_n \frac{m^2 - 1}{m} f(t) \sin(\lambda_n \xi) \sin(m\theta). \end{aligned} \tag{5}$$

The result of the differentiation of the term $\frac{\partial^2}{\partial \theta^2} [\Psi(\theta)w(t, \xi\theta)]$ represented as a product of the partial sums. First we multiply the ranks, and then calculate the derivative. We introduce two partial sums:

$$\begin{aligned} S_1 &= \sum_m a_m \cos(m\theta); \quad m = 1, 2, 3, \dots \quad a_0 = 0, S_2 = b_0 + \sum_m b_m \cos(m\theta); \quad b_0 \\ &= \frac{\varphi_0^3}{3}; \quad b_m = \beta_m. \end{aligned}$$

Next we have:

$$Z = S_1 S_2 = z_0 + \sum_{k=1}^{\hat{m}} z_k \cos k\theta,$$

Differentiation sums reduces to differentiation of terms:

$$\frac{\partial}{\partial \theta} (Z) = - \sum_{k=1}^{\hat{m}} z_k k \sin k\theta, \quad \frac{\partial^2}{\partial \theta^2} (Z) = - \sum_{k=1}^{\hat{m}} z_k k^2 \cos k\theta.$$

Further will take the notation $k = m$:

$$\frac{R}{Eh} \frac{\partial^2}{\partial \theta^2} (\Psi(\theta)w(\xi, \theta, t)) = \frac{k_s R^2}{\pi Eh} f(t) \sum_{m=1}^{\infty} m^2 z_m \cos m\theta, \tag{6}$$

where k – soil ratio [N/m³], m – circumferential wave number. Calculating z_m with different wave numbers $m = 1, 2, 3, \dots$ represented in the form:

$$\begin{aligned}
 z_1 &= a_0b_1 + a_1b_0 + \frac{1}{2}(a_1b_2 + a_2b_1 + a_2b_3 + a_3b_2 + a_3b_4 + a_4b_3 + a_5b_4 + a_4b_5); \\
 z_2 &= a_0b_2 + a_2b_0 + \frac{1}{2}(a_1b_3 + a_3b_1 + a_2b_4 + a_4b_2 + a_3b_5 + a_5b_3 + a_1b_1) \\
 z_3 &= a_0b_3 + a_3b_0 + \frac{1}{2}(a_1b_4 + a_4b_1 + a_2b_5 + a_5b_2 + a_1b_2 + a_2b_1) \\
 z_4 &= a_0b_4 + a_4b_0 + \frac{1}{2}(a_1b_5 + a_5b_1 + a_1b_3 + a_3b_1 + a_2b_2); \\
 z_5 &= a_0b_5 + a_5b_0 + \frac{1}{2}(a_1b_4 + a_4b_1 + a_2b_3 + a_3b_2);
 \end{aligned}
 \tag{7}$$

$$\begin{aligned}
 a_m &= 1; \quad b_0 = \frac{\varphi_0^3}{3}; \quad b_m = \beta_m, \quad \beta_m = (-1)^m m^{-3} [2\varphi_m \cos \varphi_m - (\varphi_m^2 - 2) \sin \varphi_m]; \quad \varphi_m \\
 &= m\varphi_0.
 \end{aligned}$$

Substituting (8), (9) в (5) and equating coefficients of the same trigonometric functions, we obtain a system of equations of separable:

$$\begin{aligned}
 &[\lambda_n^4 + m^4(m^2 - 1)(m^2 - 1 + p^*) + k * m^4 - \lambda_n^4 m^4 P/n^2]f(t) + \\
 &[\rho * Rh(\lambda_n^4 h_v + m^2 + m^4) + \rho_0^* \Phi_{mn} R^2 m^4]f''(t) = 0,
 \end{aligned}
 \tag{8}$$

where $p^* = p \frac{R}{Ehh_v^2}$, $\rho^* = \rho \frac{R}{Ehh_v^2}$, $\epsilon_0^* = \frac{F}{EAh_v^2}$, $\rho_0^* = \rho_0 \frac{R}{Ehh_v^2}$, $k^* = \frac{kR^2}{Ehh_v^2} z_m$

Considering that the free vibrations are harmonic, represent the function of time $f(t)$ in form:

$$f(t) = \sin \omega_{mn} t, \quad f''(t) = -\omega_{mn}^2 \sin \omega_{mn} t,
 \tag{9}$$

The resulting system is a solution to the problem of free vibrations of a thin-ground large diameter oil pipelines at steady impact. Substituting (13) in (12) transforming an equation for determining the square of the frequency of free vibrations of a ground pipeline:

$$\omega_{mn}^2 = \frac{\tilde{\lambda}_n^4 + m^4(m^2 - 1)(m^2 - 1 + p^*) + k^* m^4 - \tilde{\lambda}_n^4 m^4 P - \tilde{\lambda}_n^2 \rho_0^* \Phi_{mn} V^2 m^4 h_v}{\rho^* R \cdot h(\tilde{\lambda}_n^2 h_v + m^2 + m^4) + \rho_0^* \Phi_{mn} R^2 m^4},
 \tag{10}$$

The expression (14), allows you to define a wide range of frequencies for enveloped forms at wave numbers $m n = 1, 2, 3, \dots$, considering the internal operating pressure parameter of the longitudinal compressive force and elastic soil foundation, at different values of the geometric characteristics.

Dynamic calculation of thin-walled pipes, and now days is an actual problem, which confirms a series of works devoted to this problem [1–31]. Practice shows that the pipelines during operation are subjected to dangerous kind of dynamic effects and vibrations. Long exposure of increased vibration in combination with other factors may cause fatigue destruction of the pipeline elements. So to perform dynamic calculation is necessary to know the dynamic characteristics of the thin-walled main gas pipeline of large diameter, such as the spectrum of its own frequencies.

As practice shows, during operation, oil pipelines are subjected to the action of non-stationary internal operating pressure, and the pulsating oil flow, and also as a result of the pumps of the pumping station, of a stationary longitudinal compressive force to the non-stationary. It is proved that for certain relations of natural frequency ω

and forced frequency γ phenomenon of parametric resonance is begins. Parametric resonance is more dangerous than usual resonance, under parametric resonance conditions, the pipeline construction undergoes a dangerous cyclic action, which can lead to fatigue failure. Therefore, the main task of dynamic calculation in this problem is to determine the boundaries of dynamic instability, to ensure reliable exploitation.

In the process of operation of oil pipelines, pumping stations lead to the excitation of a stationary internal operating pressure according to the formula:

$$p(t) = p_0(1 + \mu \cos \gamma t) \tag{11}$$

longitudinal compressive force:

$$F(t) = F_0(1 + \mu \cos \gamma t) \tag{12}$$

and fluid flow:

$$V(t) = V_0(1 + \mu \cos \gamma t) \tag{13}$$

where γ – frequency of stimulation, determined by the technology of pump stations; μ – stimulation parameter limiting the variable pressure component (according to [18] $\mu \leq 0.5$); p_0 – internal operating pressure; F_0 – longitudinal compressive force; V_0 – fluid flow rate.

Using the method described in [4] on the basis of a geometrically nonlinear version of the semi-momental theory of cylindrical shells, the equation of the oil pipeline motion is obtained with the stationary internal operating pressure, the elastic foundation, the stationary flow of the flowing liquid, and the longitudinal compressive force, for the case of hinged support:

$$\begin{aligned} & [\lambda_n^4 + m^4(m^2 - 1)(m^2 - 1 + p^*) + k^*m^4 - \lambda_n^4m^4P - \lambda_n^2p_0^*\Phi_{mn}V_0^2m^4h_v]f(t) \\ & + [\rho^*R \cdot h(\lambda_n^2h_v + m^2 + m^4) + \rho_0^*\Phi_{mn}R^2m^4]f''(t) = 0 \end{aligned} \tag{14}$$

where $\lambda_n = \frac{n\pi R}{L\sqrt{h_v}}$; $f(t)$ and $f''(t)$ – the time function and its derivative; $p^* = p_0 \frac{R}{Ehh_v^2}$ – internal operating pressure parameter; p_0 – internal operating pressure; $\rho^* = \rho \frac{R}{Ehh_v^2}$ – shell material density parameter; ρ – shell material density; $\rho_0^* = \rho_0 \frac{R}{Ehh_v^2}$ – fluid density parameter; ρ_0 – fluid density; $\Phi_{mn} = \frac{I_m(\lambda_0)}{\lambda_0 I_m'(\lambda_0)}$ – parameter of the Bessel function and its derivative; V_0 – velocity of fluid flow; $\rho_0 \Phi_{mn}$ – adjoin mass of liquid; $k^* = \frac{R^2k}{\pi Ehh_v^2} z_m$ – parameter of elastic foundation (the procedure for determining the coefficient z_m is shown in the article [25]; k – coefficient of elastic foundation in accordance with the model of Fuss-Winkler; R – radius of the middle surface; h – pipe wall thickness; $m, n = 1, 2, 3, \dots$ – wave numbers in circumferential and longitudinal directions; $P = F_0/F_e$ – parameter of longitudinal compressive force; F_e – Euler’s force; h_v – parameter of the relative thickness of the shell $h_v = \frac{h}{R\sqrt{12(1-\nu^2)}}$ where ν – Poisson’s ratio.

As a result of the transformation (18), taking into account (15), (16) and (17), we obtain the equation of motion of the pipeline section subjected to non-stationary action:

$$\begin{aligned} & \{ \lambda_n^4 + m^4(m^2 - 1)(m^2 - 1 + p^*) + k * m^4 - \lambda_n^4 m^4 P - \lambda_n^2 \rho_0^* \Phi_{mn} V^2 m^4 h_v \\ & - m^4 \lambda_n^4 \mu \cos \gamma t \cdot [P - (p^* (m^2 - 1) + 2\rho_0^* \Phi_{mn} V^2 \lambda_n^2 h_v) / \lambda_n^4] \} f(t) \\ & + [\rho * Rh(\lambda_n^4 h_v + m^2 + m^4) + \rho_0^* \Phi_{mn} R^2 m^4] f''(t) = 0. \end{aligned} \tag{15}$$

After the transformation (5), we get:

$$\begin{aligned} f''(t) + & \frac{\lambda_n^4 + m^4(m^2 - 1)(m^2 - 1 + p^*) + k * m^4 - \lambda_n^4 m^4 P - \lambda_n^2 \rho_0^* \Phi_{mn} V^2 m^4 h_v}{\rho * Rh(\lambda_n^2 h_v + m^2 + m^4) + \rho_0^* \Phi_{mn} R^2 m^4} \\ & \frac{\lambda_n^4 m^4 [P - (p^* (m^2 - 1) + 2\rho_0^* \Phi_{mn} V^2 \lambda_n^2 h_v) / \lambda_n^4]}{\lambda_n^4 + m^4(m^2 - 1)(m^2 - 1 + p^*) + k * m^4 - \lambda_n^4 m^4 P - \lambda_n^2 \rho_0^* \Phi_{mn} V^2 m^4 h_v} \cos \gamma t) f(t) \end{aligned} \tag{16}$$

or the system of separating Mathieu equations:

$$f''(t) + \omega_{mn}^2 (1 - \delta_{mn} \cos \gamma t) f(t) = 0, \tag{17}$$

where the square of the free vibration frequency of the oil pipeline has the form:

$$\omega_{mn}^2 = \frac{\lambda_n^4 + m^4(m^2 - 1)(m^2 - 1 + p^*) + k * m^4 - \lambda_n^4 m^4 P / n^2 - \lambda_n^2 \rho_0^* \Phi_{mn} V^2 m^4 h_v}{\rho * R \cdot h(\lambda_n^2 h_v + m^2 + m^4) + \rho_0^* \Phi_{mn} R^2 m^4} \tag{18}$$

The excitation coefficient:

$$\delta_{mn} = \frac{\lambda_n^4 m^4 [P - (p^* (m^2 - 1) + 2\rho_0^* \Phi_{mn} V^2 \lambda_n^2 h_v) / \lambda_n^4]}{\lambda_n^4 + m^4(m^2 - 1)(m^2 - 1 + p^*) + k * m^4 - \lambda_n^4 m^4 P - \lambda_n^2 \rho_0^* \Phi_{mn} V^2 m^4 h_v} \tag{19}$$

The obtained system of Mathieu’s equations (17) makes it possible to investigate the dynamic stability of the hinge-supported section of the ground oil pipeline under

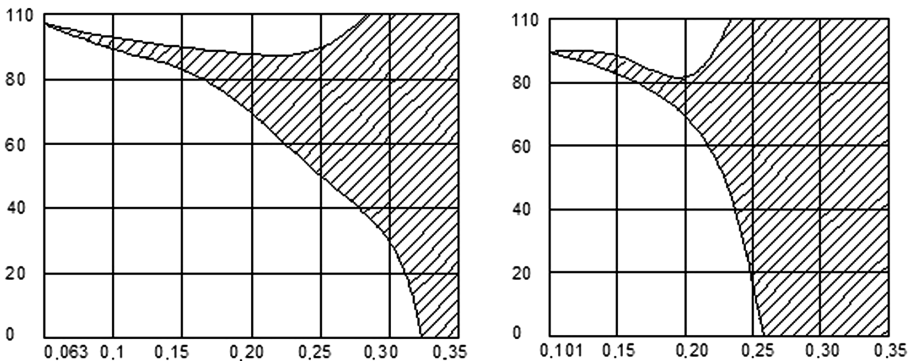


Fig. 2. Areas of dynamic instability for an oil pipeline with an above-ground laying at different ratios h/R and P .

condition $P > (p * (m^2 - 1) + 2\rho_0^* \Phi_{mn} V^2 \lambda_n^2 h_v) / \lambda_n^4$ for different values of wave numbers $m, n = 1, 2, \dots$

With constructing instability areas of the Ains-Strett type, which are determined by the following relations between the frequencies of free vibrations ω_{mn} and the excitation frequencies γ : $\omega_{mn} = \frac{\gamma}{2}k, k = 1, 2, 3 \dots$. The main, widest areas, called the main areas of dynamic instability, is realized at a coefficient $k = 1$, that is, when $\omega_{mn} = \frac{\gamma}{2}$. The secondary instability regions for $k > 1$ have a much smaller width and are usually overlapped by the main areas. The solution obtained for the main areas of dynamic instability is the inequality:

$$1 - \frac{\delta_{mn}}{2} < \left(\frac{2\omega_{mn}}{\gamma}\right)^2 < 1 + \frac{\delta_{mn}}{2} \tag{20}$$

Table 1. Determination of excitation frequencies $\gamma.Gz$

		<i>P</i>						
<i>h/R</i>		0.063	0.1	0.15	0.2	0.25	0.3	0.35
1020x25	1/20	107.97	$\frac{102.63}{98.83}$	$\frac{95.33}{85.28}$	$\frac{88.68}{69.86}$	$\frac{87.77}{51.69}$	$\frac{-}{28.99}$	$\frac{-}{-}$
<i>P</i>								
Tube. mm	<i>h/R</i>	0.101	0.15	0.20	0.25	0.30	0.35	-
720x11	1/33	102.66	$\frac{90.96}{81.71}$	$\frac{82.17}{55.01}$	$\frac{-}{16.70}$	$\frac{-}{-}$	$\frac{-}{-}$	$\frac{-}{-}$
<i>P</i>								
Tube. mm	<i>h/R</i>	0.126	0.15	0.20	0.25	0.30	0.35	-
1420x18	1/40	54.54	$\frac{51.26}{118.84}$	$\frac{44.77}{35.04}$	$\frac{-}{-}$	$\frac{-}{-}$	$\frac{-}{-}$	$\frac{-}{-}$
<i>P</i>								
Tube. mm	<i>h/R</i>	0.157	0.20	0.25	0.30	0.35	-	-
1420x14	1/50	42.95	$\frac{38.19}{34.39}$	$\frac{34.56}{-}$	$\frac{-}{-}$	$\frac{-}{-}$	$\frac{-}{-}$	$\frac{-}{-}$

Note: The numerators give the frequencies of the excitation value γ the upper boundary of the area of dynamic instability. and in the denominator. the excitation frequency corresponding to the lower boundary of the area of dynamic instability.

3 Results

To analyze the solutions obtained, consider a steel pipeline with a modulus of Yung, $E = 2 \cdot 10^5 \text{ MPa}$, a Poisson's ratio of $\nu = 0.3$, a pipe material density $\rho = 78.5 \text{ kN/m}^3$, pipe sizes taken: 1020x25, 720x11, 1420x18, 1420x14.

Consider the oil pipeline section with $L = 10R$, $p = 2 \text{ MPa}$, $k = 1.0 \text{ MN/m}^3$, $V = 3 \text{ m/sec}$, were the effect of the parameter of the longitudinal compressive force P and the parameter of thin-walled tube h/R was investigated. According to the proposed method, the obtained results are tabulated 1 and the results are presented in the form of modified Ains-Strett diagrams in Figs. 1, 2. An analysis of the values obtained showed that with an increase the parameter of the longitudinal compressive force P , and reducing the thin-walledness parameter of the pipe h/R the areas of dynamic instability are expanding, for example, when we use parameter $h/R = 1/50$, $L = 10R$,

Table 2. Determination of excitation frequencies $\gamma \cdot Gz$

		$p_0=2\text{MPa}; L/R=10; V=3\text{m/sec}; h/R=1/33$					
Tube	MN/m^3	P					
		0.101	0.15	0.20	0.25	0.30	0.35
1220x20	$k=4$	99.05	$\frac{86.98}{77.22}$	$\frac{80.07}{48.67}$	$\frac{-}{4.83}$	$\frac{-}{-}$	$\frac{-}{-}$
		P					
Tube	h/R	0.101	0.15	0.20	0.25	0.30	0.35
1220x20	$k=30$	110.72	$\frac{99.87}{91.55}$	$\frac{89.89}{68.16}$	$\frac{-}{37.69}$	$\frac{-}{-}$	$\frac{-}{-}$
		$p_0=2\text{MPa}; L/R=10; V=3 \text{ m/sec}; h/R=1/40$					
		P					
Tube	h/R	0.126	0.15	0.20	0.25	0.30	0.35
1220x15	$k=4$	51.03	$\frac{47.58}{44.95}$	$\frac{41.13}{29.65}$	$\frac{-}{-}$	$\frac{-}{-}$	$\frac{-}{-}$
		P					
Tube	h/R	0.126	0.15	0.20	0.25	0.30	0.35
1220x15	$k=30$	61.95	$\frac{59.11}{57.03}$	$\frac{53.13}{45.53}$	$\frac{49.87}{31.40}$	$\frac{-}{-}$	$\frac{-}{-}$

Note: The numerators give the frequencies of the excitation value γ the upper boundary of the area of dynamic instability. and in the denominator. the excitation frequency corresponding to the lower boundary of the area of dynamic instability.

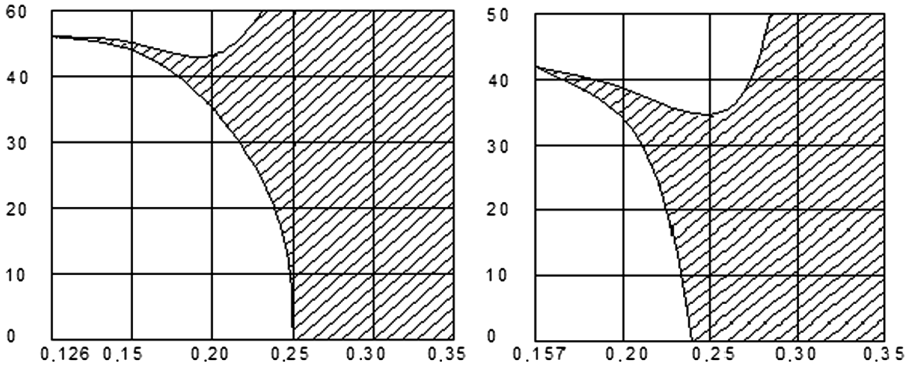


Fig. 3. Areas of dynamic instability for an oil pipeline with an above-ground laying at different ratios h/R and P .

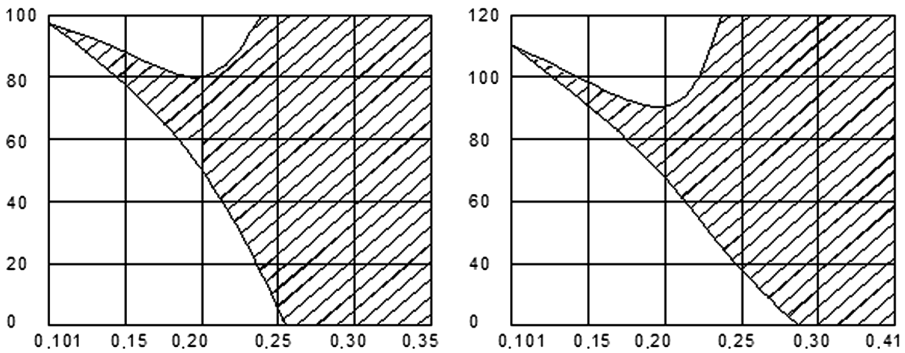


Fig. 4. Areas of dynamic instability of an above-ground oil pipeline with different parameter values P with $p_0 = 2 \text{ MPa}$; $h/R = 1/33$ and $k = 4 \text{ MN/m}^3$

Fig. 5. Areas of dynamic instability of an above-ground oil pipeline with different parameter values P with $p_0 = 2 \text{ MPa}$; $h/R = 1/33$ and $k = 30 \text{ MN/m}^3$

$p = 2 \text{ MPa}$, $k = 1.0 \text{ MN/m}^3$, $V = 3 \text{ m/sec}$ the areas of dynamic instability take almost the entire flat.

« $\gamma - P$ ». This means that the chance of loss of dynamic stability of the oil pipeline is much higher. Then was investigated influence of coefficient of soil on size and position of areas of dynamic instability (Tables 1, 2, Figs. (3, 4, 5, 6 and 7)).

An analysis of the values obtained for the above-ground oil pipeline showed that with increasing values of the soil coefficient the areas of dynamic instability narrows and shifts in the direction of increasing values γ .

The method for determining dynamic stability as in the case of an above-ground oil pipeline reduces to determining the position of a point on the plane of the parameters (γ, P) on Figs. 3, 4, 5 and 6. If the point is in a non-tinted area then the stability of the oil pipeline is ensured. Otherwise it is necessary to change the main parameters of the oil pipeline or the pumping station.

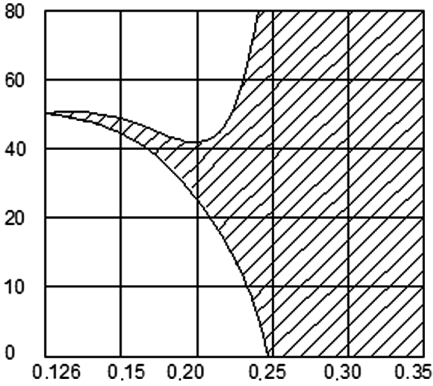


Fig. 6. Areas of dynamic instability of an above-ground oil pipeline with different parameter values P with $p_0 = 2 \text{ MPa}$; $h/R = 1/33$ and $k = 4 \text{ MN/m}^3$

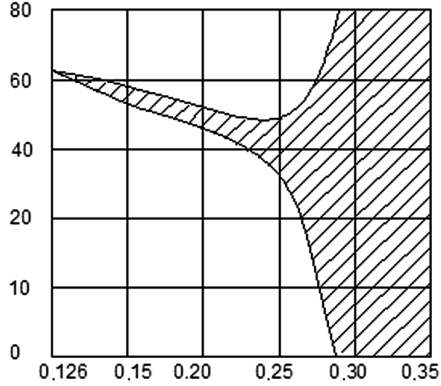


Fig. 7. Areas of dynamic instability of an above-ground oil pipeline with different parameter values P with $p_0 = 2 \text{ MPa}$; $h/R = 1/33$ and $k = 30 \text{ MN/m}^3$

4 Conclusion

As a result of the analysis of the obtained solutions and the results of the calculation the following conclusions were made:

1. The problem of parametric vibrations of about-ground oil pipelines with different ratios h/R was solved with non-stationary action of internal operating pressure the parameter of the longitudinal compressive force and the flow of the flowing liquid. Was obtained a separating system of Mathieu differential equations. This system of equations allows us to evaluate the dynamic stability of the pipeline by constructing areas of dynamic instability in the form of modified Ains-Strett diagrams with the joint influence of the pipe thin-wall parameter, the soil coefficient, the internal operating pressure, the longitudinal compressive force parameter and the flowing fluid velocity (for the oil pipeline).
2. The dynamic stability of above-ground straight-line sections of large-diameter oil pipelines is studied at various geometric and mechanical characteristics. The analysis of the obtained results showed:
 - with an increase in the parameter of the longitudinal compressive force the dynamic instability area expands;
 - pipes with the ratio $h/R = 1/40 - 1/50$ are more dangerous from the position of dynamic stability than the pipes $h/R = 1/20$ and $1/30$. The chance of parametric resonance in such pipes increases due to the expansion of the area of dynamic instability and its shift down in the direction of decreasing values γ ;
 - with an increase in the soil coefficient k the area of dynamic instability narrows and shifts in the direction of increasing values γ ;

- the area of dynamic instability with fixed geometric and mechanical characteristics for oil pipelines is much wider than for gas pipelines, which means a higher chance of loss of dynamic stability for oil pipelines.

The proposed method of investigating dynamic stability will allow us to evaluate the effect of each parameter of the system on the dimensions and position of the regions of dynamic instability. In the one case where the value of the « $\gamma - P$ » falls within the shaded area. the system is dynamically unstable. it is necessary to change the characteristics of the transfer unit or the geometric characteristics of the pipeline section. The presented solutions will matching for designers who does dynamic calculations at the design stage, as well as to experts performing inspect of the pipeline section with technical expertise.

The corresponding results in this article were obtained during the execution of the state task of the Ministry of Education and Science of Russia 7.4794.2017/8.9.

References

1. Sokolov, V.G.: Svobodnye kolebanija magistral'nyh glubokovodnyh gazoprovodov s uchedom uprugogo osnovanija. Promyshlennoe I grazhdanskoe stroitel'stvo **8**, 46–47 (2010). (in Russian)
2. Efimov, A.A., Sokolov, V.G.: Dinamicheskaja ustojchivost' stal'nyh gazoprovodov pri podvodnoj prokladke. Izv. vuzov Nefti gaz **4**, 47–51 (2007). (in Russian)
3. Sokolov, V.G., Razov, I.O.: Svobodnye kolebanija nazemnykh gazoprovodov. Obzhatykh prodol'noy siloy. s uchedom uprugogo osnovaniya grunta. Vestnik grazhdanskikh inzhenerov **1**(36), 29–32 (2013). (in Russian)
4. Razov, I.O., Sokolov, V.G.: Svobodnye kolebanija I staticheskaja ustojchivost' nefteprovoda bol'shogo diametra s uchedom potoka zhidkosti. Vestnik grazhdanskikh inzhenerov **1**, 49–53 (2014)
5. Razov, I.O., Sokolov, V.G., Ogorodnova, Y.V.: Effect of internal pressure on parametric vibrations and dynamic stability of thin-walled ground pipeline larger diameter connect with elastic foundation. In: MATEC Web Conference on XV International Conference “Topical Problems of Architecture. Civil Engineering. Energy Efficiency and Ecology”, vol. 73, pp. 1–11 (2016)
6. Lilkova-Markova, S.V., Lolov, D.S.: Vibration of a pipe on elastic foundation. Sadhana **29**(3), 259–262 (2004)
7. Denisov, G.V.: Opredelenie pervoy chastity sobstvennykh prodol'nykh kolebaniy sterzhnya na kusochno-odnorodnom uprugom osnovanii. obrazovannom dvumya uchastkami razlichnoy zhestkosti. Nauchnyy vestnik Voronezhskogo gosudarstvennogo arkhitekturno-stroitel'nogo universiteta Stroitel'stvo i arkhitektura **1**(41), 101–108 (2016). (in Russian)
8. Lalin, V.V., Denisov, G.V.: The dynamic behavior of infinite rod elements on the visco-elastic foundation under point source of disturbance. Sci. Her. Voronezh State Univ. Archit. Civil Eng. Constr. Archit. **3**(23), 100–111 (2014)
9. Lalin, V., Rybakov, V., Sergey, A.: The finite elements for design of frame of thin-walled beams. Appl. Mech. Mater. **578–579**, 858–863 (2014)
10. Yavarov, A.V., Kolosova, G.S., Kuroedov, V.V.: Napryazhenno-deformirovannoe sostoyanie podzemnykh truboprovodov. Stroitel'stvo unikal'nykh zdaniy i sooruzheniy **1**(6), 1–10 (2013). (in Russian)

11. Yavarov, A.V.: Chislennoe modelirovanie soprotivleniya massiva grunta peremeshcheniyam podzemnogo truboprovoda. *Elektronnyy nauchnyy zhurnal. Neftegazovoe del.* **3**, 360–374 (2012). (in Russian)
12. Malekzadeh, P., Faridb, M., Zahedinejad, P., Karami, G.: Three-dimensional free vibration analysis of thick cylindrical shells resting on two-parameter elastic supports. *J. Sound Vib.* **313**(3–5), 655–675 (2008)
13. Aragh, B.S., Zeighami, A., Rafiee, M., Yasc, M.H., Wahab, M.A.: 3-D thermo-elastic solution for continuously graded isotropic and fiber-reinforced cylindrical shells resting on two-parameter elastic foundations. *Appl. Math. Model.* **37**(9), 6556–6576 (2013)
14. Sokolov, V.G., Razov, I.O.: Svobodnye kolebaniya tonkostennykh gazoprovodov bol'shogo diametra pri polupodzemnoy prokladke. *Vestnik grazhdanskikh inzhenerov* **6**(59), 114–120 (2016). (in Russian)
15. Gunawan, H., Mikami, T., Kanie, S., Sato, M.: Finite element analysis of cylindrical shells partially buried in elastic foundations. *Comput. Struct.* **83**(21), 1730–1741 (2005)
16. Mustafin, F.M.: Sposoby prokladki truboprovodov s primeneniem obspyki spetsial'no obrabotanny migruntami. *Neftegazovoe delo* **1**, 1–5 (2003). (in Russian)
17. Grigolyuk, E.I., Kabanov, V.V.: *Ustoychivost' obolochek*. Nauka, Moscow (1978). 360 p.
18. Bolotin, V.V.: *Dinamicheskaya ustoychivost uprugih system*. Gos. Izd. teh. Lit., Moscow (1956). 600 p.
19. Volmir, A.S.: *Obolochki v potoke zhidkosti i gaza Zadachi gidrouprugosti*. Nauka, Moscow (1979). 320 p.
20. Paidoussis, M.P.: Dynamic stability of pipes conveying fluid. *J. Sound Vib.* **33**(3), 264–294 (1974)
21. Paidoussis, M.P.: Experiments on parametric resonance of pipes containing pulsate flow. *J. Appl. Mech.* **43**(2), 198–202 (1976)
22. Paidoussis, M.P.: Flutter of thin cylindrical shells conveying fluid. *J. Sound Vib.* **20**(1), 9–26 (1972)
23. Paidoussis, M.P.: Flow-induced instabilities of cylindrical structures. *Appl. Mech. Rev.* **40**, 163–175 (1987)
24. Il'in, V.P., Sokolov, V.G.: *Voprosy mehaniki stroitel'nykh konstrukcij I materialov. Mezhvuzovskij tematicheskij sbornik L* (1987)
25. Aksel'rad, E.L., Il'in, V.P.: *Raschet truboprovodov L. Mashinostroenie* (1972)
26. Razov, I.O.: Naprjzheniya I peremeshheniya na kontaktnoj poverhnosti nazemnogo truboprovoda bol'shogo diametra. *Vestnik grazhdanskikh inzhenerov* **3**, 58–62 (2015)
27. Vedeld, K., Sollund, H., Hellesland, J.: Free vibrations of free spanning offshore pipelines. *Eng. Struct.* **56**, 68–82 (2013)
28. Popov, A.A.: Parametric resonance in cylindrical shells: a case study in the nonlinear vibration of structural shells. *Eng. Struct.* **25**(6), 789–799 (2003)
29. Sollund, H.A., Vedeld, K., Hellesland, J., Fyrileiv, O.: Dynamic response of multi-span offshore pipelines. *Mar. Struct.* **39**, 174–197 (2014)
30. Luan, Y., Liang, D., Rana, R.: Scour depth beneath a pipeline undergoing forced vibration. *Theor. Appl. Mech. Lett.* **5**(2), 97–100 (2015)
31. Carkovs, J., Matvejevs, A., Pavlenko, O.: Stochastic stability of a pipeline affected by pulsate fluid flow. *Procedia Comput. Sci.* **104**, 12–19 (2017)

Methodology of Monitoring of Hydrocarbon Transportation Hydraulic Reliability

Maria Zemenkova  

Industrial University of Tyumen, Volodarskogo st., 38, Tyumen 625000, Russia
muzemenkova@mail.ru

Abstract. The author developed a complex of indicators to assess the functional reliability of hydrocarbon transportation facilities. The results of modeling of the hydraulic reliability indicator in petroleum and petroleum product transportation are presented as an example. It is proved that the proposed indicator allows performing the reliability monitoring of the facility, as well as monitoring its technical and economic efficiency. Using a registered block of dispatching data in online mode, the suggested method of reliability assessment and the indicator model allow tracking the development of the technical system state and obtaining different stable expert assessments of reliability, which provides constant control of the petroleum pipeline efficiency.

Keywords: Hydrocarbon transportation facilities · Intellectual control Reliability · Pipeline · Safety · Oil · Gas · Hydrocarbon

1 Introduction

Modern conditions of operating pipeline systems as hazardous production facilities require solutions to improve their safety and reliability. Russian safety requirements necessitate special monitoring of the service life of the linear section and oil pumping stations (OPS). Deviation of the operating parameters of the system from the planned ones during operation requires appropriate control and regulation. There is a need for advancements that increase efficiency and, in general, improve management of operated hazardous production facilities, which raises the problems of systematization, analysis, control and management of the reliability indicators of a hazardous production facility. At present, in a number of cases regulation is carried out without taking into account the impact on the safety and reliability indicators of the facility, considering mainly the economic factor, with a significant time lag [1].

Domestic and foreign experience in the use of various means of monitoring the technical state during operation of the pipeline system shows that applying software complexes or decision support systems for this purpose is effective. Of particular importance is not only assessment of the actual state, but also of forecast indicators.

Toughening international environmental requirements for production facilities necessitates the development of methods and technologies for processes monitoring for conducting expert assessments of the technological state of facilities by various federal supervision services and independent public organizations. In times of crisis, operating

organizations are interested in technologies for promptly making effective decisions on maintenance and improving the functional reliability of pipeline transport systems [2].

2 Problem

When oil is pumped through main pipelines, under certain conditions paraffin deposits accumulate on the inner walls of pipes. Accumulation of deposits leads to a sharp decrease in the pipeline throughput and an increase in the cost of pumping. It is estimated that 2 mm thick deposits in an oil pipeline 500 mm in diameter lead to a reduction in throughput by 2.5% with approximately the same increase in the cost of pumping.

The main factors influencing the deposition of paraffin are physicochemical properties of the pumped oil, the change in the temperature regime (cooling) of oil during its pumping through the pipeline, the change in the content of dissolved gases, the nature of the pumping mode (change in pressure, stops, etc.). The physicochemical properties of deposits on the walls of pipes are determined by the temperature of the oil flow at which they were formed [3].

The wall material has a great influence on the rate of paraffin accumulation on pipeline walls. Other things being equal, the intensity of paraffinization of the surface of various materials depends on the degree of their polarity. Materials with high polarity have a weak adhesion to paraffins. High quality surface treatment of steel pipes is not an obstacle to their paraffinning. The influence of the steel surface treatment quality is exerted only at the initial stage of paraffinization.

When studying the role of high-molecular components of oil in the process of deposits formation, it was established that resins do not play an independent role [4]. Asphaltenes are able to drop out of the solution and independently participate in the formation of dense deposition. In the presence of resins, this process increases. The presence of asphaltic-resinous oil components contributes to the formation of dense and solid deposits. The condition for the formation of a large number of dense deposits is the presence of the main components of high-molecular oil.

In pipelines, there is a differentiated deposition of paraffin on the walls of pipes in accordance with the change in the temperature of the oil flow. The nature of the deposits distribution along the length of the pipeline, and most importantly the regularity of the change in their quantity, composition and properties indicate the greatest probability of paraffin deposits formation due to the emergence and growth of crystals.

Paraffin is released from oil in the form of crystals, which, connecting with each other, form a paraffinic mass. It is a porous skeleton, the pores of which are filled with oil and water. The melting point of such a mass depends on its composition and ranges from 40 to 50 °C. Viscosity and pour point of paraffinic oil depend on the amount of paraffin in it and the temperature. The higher the paraffin content and the lower the oil temperature, the more its viscosity increases and the less its fluidity.

The process of deposits formation on the walls can be represented as follows. When moving, the oil cools down and, at a certain temperature, solid hydrocarbons begin to drop out of it. At this temperature (or close to it) deposits appear on the walls of the pipes. As the temperature decreases, the amount of paraffin coming out of the oil

increases, and accordingly the amount of paraffin deposited on the walls increases. Paraffin crystals arise and grow both in the volume of oil and on the surface of the walls. The crystals that arise and grow on the walls basically form deposits in the oil pipeline. Crystals that arise and grow in the flow have a poor ability to stick to the walls of the pipes and, obviously, only a very small part of them participate in the formation of deposits to some extent. Their bulk is stabilized, loses its adhesive ability and is transported in the flow of oil [5].

Deposits are unevenly distributed along the pipeline. In the initial section of the pipeline where the temperature is higher than the temperature at which paraffin begins to separate its deposits are insignificant. Further, where the temperature is lower, paraffin is intensively released and its deposits are significant. Then, the thickness of paraffin deposits along the length of the pipeline decreases, since oil is already moving at an almost constant temperature equal to the soil temperature, and the bulk of the paraffin that drops out at this temperature has already deposited in the previous section. A particularly intensive deposition of paraffin occurs during the stoppage of pumping when oil in the pipeline begins to solidify. The solidifying process begins at the walls of the pipe and gradually spreads to the center, the rate of formation of the solidified layer being greater at the upper generatrix of the tube, i.e., the coolest part. During the pumping period, the solidified paraffin layer is not washed away by the flow of oil [6, 7].

The presence of the zone of maximum deposits is primarily associated with a certain fractional composition of paraffins by the crystallization temperature and transition to a solid state. The nature of deposits distribution along the length of the pipeline also indicates that the dependence of the amount of drop-out paraffin on temperature is not linear.

To maintain the pipeline throughput at a level close to the designed one, it is necessary to clean it of paraffin deposits. The most effective way of cleaning the inner surface of the oil pipeline is currently mechanical cleaning with scrapers. Many designs of metal scrapers have been developed in which the cleaning element is disks, knives and wire brushes. Scrapers of different designs are different in efficiency of deposits removal from the walls of pipes, in terms of wear resistance and patency. The latter is very important for pipelines with at least slight obstacles in the internal cavity.

The optimal frequency of passing pigs through the pipeline is determined by minimizing the total cost of pumping and pipeline cleaning. Paraffin clogging of the pipeline causes a decrease in its throughput capacity and corresponding losses, and the greater the interval between the pig passes, the greater the losses. On the other hand, the shorter the interval between the pig passes, the greater the cost of pigs (as well as the losses due to station stops when pigs pass past them, if such stops are required by the cleaning technology used) [8].

The main oil pipeline is cleaned in order to maintain its throughput and reduce the cost of pumping. The scheduled cleaning of the pipeline is performed with a reduction in its throughput by no more than 3%. The quality of cleaning is determined by comparing the effective diameter with the equivalent one. The difference in diameters above 1% requires the use of a more efficient cleaning device and re-cleaning. If the effective diameter is differentiated before and after cleaning by more than 1%, the inter-cleaning period should be reduced. The equivalent diameter is the internal

diameter of a simple single-line pipeline equivalent in terms of the hydraulic characteristic to the complex oil pipeline under consideration without sedimentation (determined from the actual layout of the pipes).

$$D_{ekv} = \left(\frac{L}{\sum l_i / D_i^{4.75}} \right)^{1/4.75} \quad (1)$$

For a multi-line section (looped section):

$$D_{ekv} = \left(\sum D_{ej}^{4.75/1.75} \right)$$

The effective diameter is the value of the internal diameter of the pipeline which corresponds to the actual head loss and takes into account the effect of various deposits on its hydraulic characteristics.

$$D_{eff} = \left(\frac{0.0251 * Q^{1.75} * v^{0.25} L}{H - h - \Delta z} \right)^{\frac{1}{4.75}} \quad (2)$$

The efficiency of the oil pipeline E is the ratio of theoretical head losses to actual ones. The approximation of E to unity makes it clear whether to clean or not. With a decrease in D_{eff} compared to D_{ekv} by more than 1%, i.e. at:

$$\Delta D = (1 - D_{eff}/D_{ekv}) * 100\% \leq 1\% \quad (3)$$

pipeline cleaning is required.

The degree of pipeline throughput decrease is calculated by:

$$\Delta Q = \left(1 - (D_{eff}/D_{ekv})^{4.75/1.75} \right) * 100\% \quad (4)$$

The degree of the increase in the throughput capacity of an oil pipeline as a result of cleaning is determined by the formula, where D_{eff1} – before cleaning, D_{eff2} – after cleaning.

$$\Delta Q = \left((D_{eff2}/D_{eff1})^{4.75/1.75} - 1 \right) * 100\% \quad (5)$$

Let us consider, as an example, the dynamics of the change in hydraulic reliability and efficiency and estimate how informative each of the indicators is.

It can be seen from Figs. 1, 2, 3, 4, 5 and 6 that abrupt changes in performance and efficiency of operation are not interconnected or are directly proportional. This can be caused by an incorrect procedure of taking instrument readings or accuracy of the instruments themselves, as well as factors such as changes in oil composition (oil flow through the pipeline with a high water content, mechanical impurities, paraffin).

Thus, it can be concluded that there is no clear correlation between the performance and efficiency of the pipeline, but at the same time there is. This means that one should

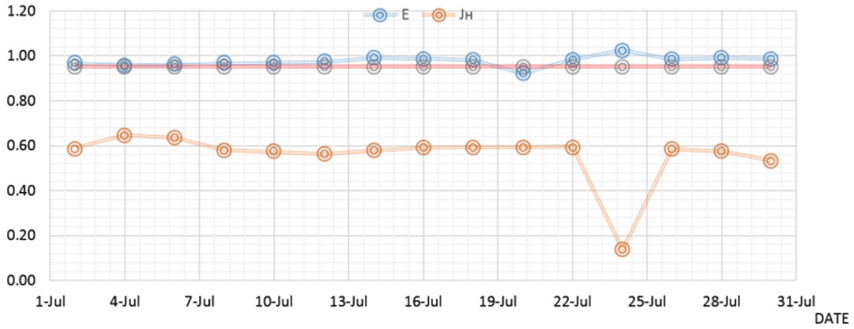


Fig. 1. Graph of changes in hydraulic reliability and efficiency at the oil pipeline section in July

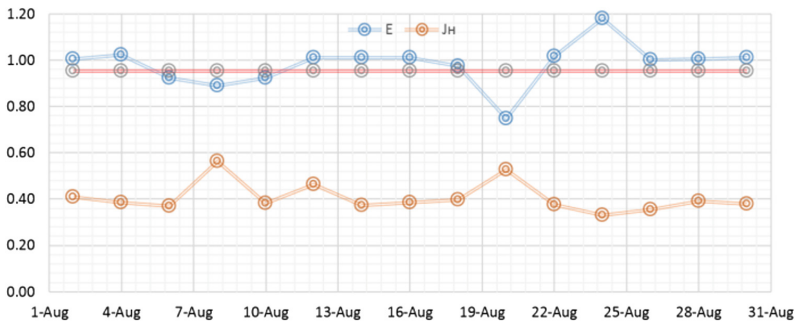


Fig. 2. Graph of changes in hydraulic reliability and efficiency at the oil pipeline section in August

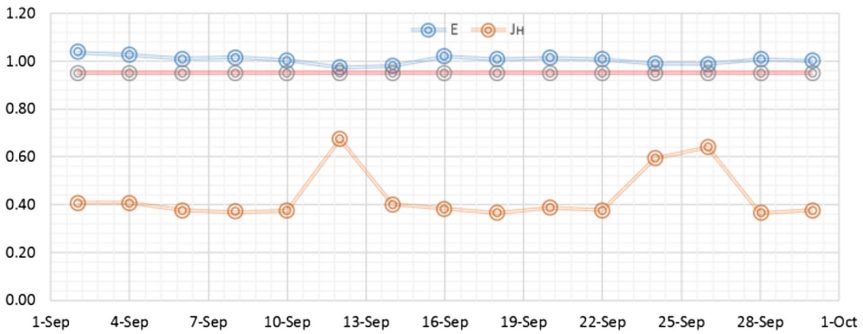


Fig. 3. Graph of changes in hydraulic reliability and efficiency at the oil pipeline section in September

pay special attention to the operation of the pipeline with a sharp increase in performance, since in practice this change often leads to a corresponding decrease in its operation efficiency [9].

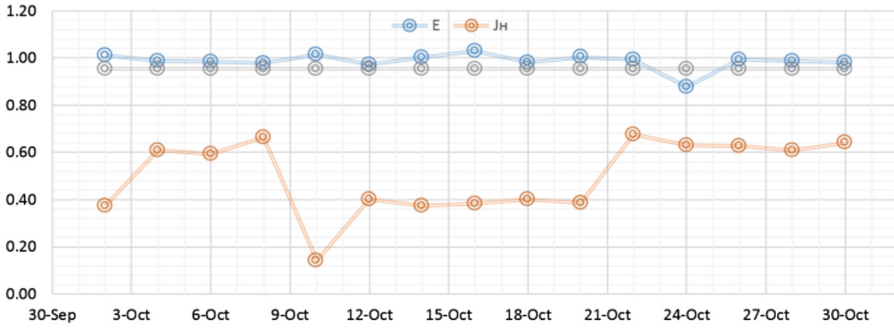


Fig. 4. Graph of changes in hydraulic reliability and efficiency at the oil pipeline section in September

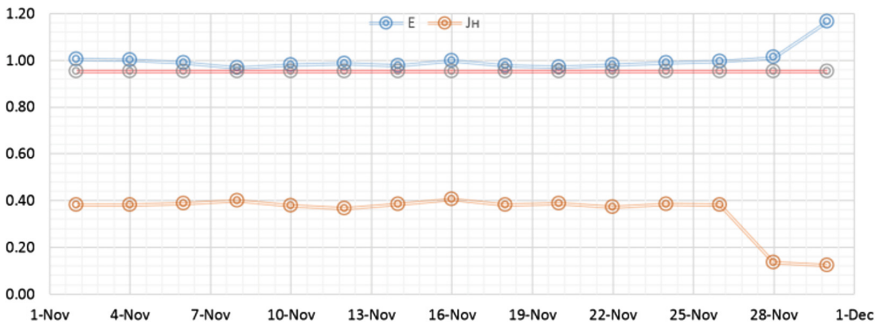


Fig. 5. Graph of changes in hydraulic reliability and efficiency at the oil pipeline section in November

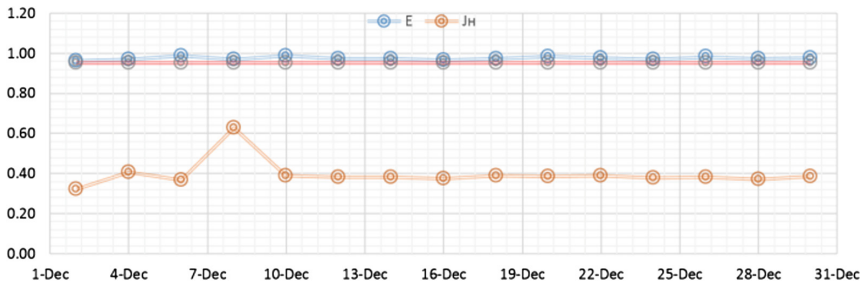


Fig. 6. Graph of changes in hydraulic reliability and efficiency at the oil pipeline section in December

Analysis of the graphs of the change in hydraulic reliability allows us to state that the existing system for estimating the change in hydraulic indicators only with the aid of the hydraulic efficiency coefficient does not allow us to make a correct estimate of the retentivity of the hydraulic indicators of the system.

Analysis of changes in the values of the coefficient of hydraulic efficiency in combination with the change in hydraulic reliability indicates that the known coefficient of hydraulic efficiency E allows only to assess the change in the state of the internal cavity of the pipeline without taking into account changes in the overall hydraulic mode of the pipeline (which manifests itself in a significant decrease in hydraulic indicators). In addition, when using the hydraulic efficiency coefficient to analyze the retentivity of the hydraulic indicators of the system, a careful analysis of all factors affecting the system is required, as well as checking for errors in the instruments, errors in the dispatching services [10–13].

Thus, it was found that hydrodynamic indicators E and J_H may be used in evaluating the system retentivity. However, it is necessary to use a comprehensive approach that allows the most correct estimate.

3 Methods and Results

The methodology developed by the author for assessing the retentivity of hydraulic parameters of pipeline transport systems is based on the evaluation of hydraulic parameters and characteristics. Thus, as an indicator characterizing the reliability of supply of products and allowing assessment of the functional reliability and retentivity of the system, a dimensionless coefficient of hydraulic reliability may be used.

In accordance with the goal, the main tasks at the stage of mathematical modeling of the coefficient of hydraulic reliability are:

- (1) Modeling of the technological process of transport (hydraulic calculation);
- (2) Modeling of the retentivity indicator of the hydraulic characteristics of the system;
- (3) Approbation of the developed model.

One of the indicators characterizing the reliability of supply of products and allowing assessment of the functional reliability and retentivity of the system, a dimensionless coefficient of hydraulic reliability may be used:

$$J_{Hi} = \frac{N_i}{N_0} = \frac{\rho_i \cdot g \cdot Q_i \cdot \Delta H_i}{\rho_0 \cdot g \cdot Q_0 \cdot \Delta H_0} = \left(\frac{\rho_i}{\rho_0} \right) \cdot \left(\frac{Q_i}{Q_0} \right) \cdot \left(\frac{H_i}{H_0} \right), \quad (6)$$

where N_i - the net power value in the i -th time period, $N_i = \rho g H_i Q_i$; N_0 - the net power value in the initial (basic) period of operation, $N_0 = \rho g H_0 Q_0$; Q_i - the performance of the pipeline in the i -th period; Q_0 - the design performance of the pipeline in the i -th period; ΔH_i - head losses at the section at the pipeline performance Q_i ; ΔH_0 - design head losses at the section at the pipeline performance Q_0 .

The technique has many uses, depending on the purpose of monitoring and type of facility.

It should be noted that the coefficient of hydraulic efficiency E , widely used in practice, is a particular solution of the coefficient of hydraulic reliability. Calculation of ΔH_i by the set points will give an overestimated result in terms of hydraulic losses; however, in calculations sufficient for the analysis of operational conditions, one can take $\Delta H_i = \Delta H_p$, determined from the actual performance of the pipeline.

The developed methodology can be used not only to assess the facility operation reliability, but also to assess the economic losses to the enterprise operating under modes other than design, when calculating the J_H coefficient for the power consumption.

The reliability assessment system has been tested in the prediction of the ability of the existing oil pipeline to maintain efficiency within the limits established by the technical documentation. When analyzing the experimental data of various oil pipelines, for instance, it was found that the effect of cleaning is observed in 65% of cases and is performed with a decrease in the effective diameter by less than 1% or with a decrease in efficiency to less than $E = 0.952$. This fact contradicts the rules of technical operation of oil pipelines and increases the cost of pumping. Only in 35% of cleanings we observed the effect expressed in increasing the effective diameter and consequently the efficiency of the oil pipeline. Based on the results of the experiment, it was also found that the use of standard equipment and information on one experiment does not give grounds for using the data obtained for statistical processing and revealing the dependence of the coefficient E on time due to a low correlation coefficient.

Taking into account the field development prospects, the conditions for the passage of the route and the properties of liquids, pipelines of Western Siberia are designed for different performance with the same diameters. Based on the results of processing numerous experimental data, the author obtained dependencies for the rapid estimation of the values of the hydraulic reliability coefficient. For example, for oil pipelines with a diameter of 1220 mm designed for different capacities, the curves for the variation of J_H (Fig. 7), the dependency has the form:

$$J_H = 1.016 \cdot Q_{pr}^{-2.7634} \cdot Q_{act}^{2.745} \tag{7}$$

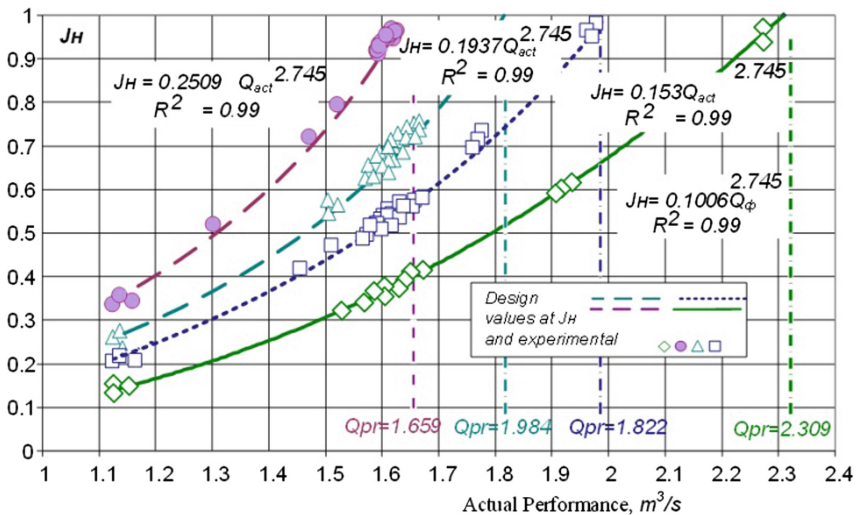


Fig. 7. Coefficient of hydraulic reliability at different pumping modes ($Q, m^3/s$)

$$J_H = 1.016 \cdot Q_{pr}^{-2.7634} \cdot Q_{act}^{2.745} \quad (8)$$

where Q_{pr} , Q_{act} – the design and actual mass flow rates, respectively, m^3/s .

Analysis of the values of the hydraulic reliability coefficient allows us to conclude that it is advisable to increase the inter-cleaning period at the oil pipeline under study, and the number of cleanings should be reduced. On average, the efficiency of the pipeline is reduced by 0.01 for 1.5 months or 0.08 per year. Thus, the efficiency of the pipeline, according to forecasts, will reach the value of 0.952 7 months after the next cleaning. On the basis of this, it is proposed to increase the inter-cleaning period for the specified period.

4 Conclusion

The obtained results make it possible to determine not only the quantitative characteristics of the reliability level of the pipeline for subsequent expert and operational assessments, but also allow making operative decisions on the next cleaning of the oil pipeline not according to a pre-drawn up schedule, but on the basis of a virtual reduction in the functional reliability of the pipeline.

We should note the importance of constant monitoring of the efficiency and reliability of the pipeline, and a timely response to unpredictable changes in operating efficiency associated with changes in the properties of oil, the receipt of a lot of off-spec oil with increased water and impurities, and other factors.

The control can be carried out automatically. This requires only the creation of a software environment that will take data from the remote controller and process them.

The telemechanics system is now set up so that the remote controller receives instantaneous performance, density and viscosity values from the oil metering station. There, from the same pressure sensor along the route, the value of the pressure at the points along the pipeline.

In order to accomplish the task, it is required to remove these data and make the necessary calculation: for this mode the value of the theoretical and actual head loss and, accordingly, the efficiency of its operation. It is also necessary to put this value in the database and give out the graphs of the change in efficiency, as well as additionally signal when there is a sudden abrupt change in the efficiency of operation and approaching its value to the critical one, when oil pipeline cleaning is required.

It is possible to set a task when large deviations (sudden, abrupt changes) appear, to perform an additional calculation. It is also important to analyze the change in operation performance in conjunction with changes in other parameters, such as temperature and composition of oil, in order to obtain a more complete and accurate picture of the process of pipeline paraffinization.

In this mode, there is constant monitoring of the efficiency of the pipeline and there is the possibility of carrying out regular cleanup of the pipeline not according to a pre-drawn up schedule, but on the basis of a real reduction in the effective diameter of the oil pipeline.

Thus, the developed reliability monitoring model built into the automated reliability management system allows using the registered block of dispatcher data to scan the development of reliability indicators of pipeline systems in real-time and obtain various stable expert assessments of the functional reliability, which provides constant control of the petroleum pipeline efficiency.

References

1. Antip'ev, Y.N., Nevolin, A.P., Zemenkov, Y.D.: Operation of intermediate pumping stations on transport of gas saturated oils. *NEFT KHOZ* **10**, 46 (1981)
2. Vlasenko, V.S., Slesarenko, V.V., Gulkov, A.N., Lapshin, V.D.: Preparation of arctic oil and gas condensate deposit formation fluid for storage and transport in the form of hydrocarbon hydrate-containing dispersed system. In: *Proceedings of the International Offshore and Polar Engineering Conference 1863* (2015)
3. Kurushina, V., Zemenkov, Y.: Innovative cyclical development of the Russian pipeline system. *WIT Trans. Ecol. Environ.* **190**(2), 881–888 (2014). <https://doi.org/10.2495/EQ140822>
4. Zemenkov, Yu.D., Shalay, V.V., Zemenkova, M.Yu.: Immediate analyses and calculation of saturated steam pressure of gas condensates for transportation conditions. *Procedia Eng.* **113**, 254–258 (2015)
5. Zemenkov, Yu.D., Shalay, V.V., Zemenkova, M.Yu.: Expert systems of multivariable predictive control of oil and gas facilities reliability. *Procedia Eng.* **113**, 312–315 (2015)
6. Kurushina, E.V., Kurushina, V.A.: Evolution of economic development aims assessment of the smart growth. *Life Sci. J.* **11**(11), 517–521 (2014). Article no. 88
7. Kurushina, E.V.: On regularities of economic dynamics in times of crisis. *Can. J. Sci. Educ. Cult.* **2**(6), 378–384 (2014)
8. Zemenkov, Y., Zemenkova, M., Gladenko, A., Zakirov, N.: Monitoring of phase distribution when controlling safety of transport processes and hydrocarbon storage. In: *MATEC Web of Conferences*, vol. 86. <https://doi.org/10.1051/matecconf/20168604054>
9. Gorelik, J.B., Shabarov, A.B., Sysoyev, Y.S.: The dynamics of frozen ground melting in the influence zone of two wells. *Earth's Cryosphere* **12**(1), 59
10. Dudin, S.M., Zemenkov, Y.D., Shabarov, A.B.: Modeling the phase composition of gas condensate in pipelines. *IOP Conf. Ser.: Mater. Sci. Eng.* **154**(1) (2016). <https://doi.org/10.1088/1757-899X/154/1/012010>
11. Dudin, S.M., Zemenkov, Y.D., Maier, A.V., Shabarov, A.B.: Research and design of thermophysical gas-liquid mixture parameters in product pipelines. *IOP Conf. Ser.: Mater. Sci. Eng.* **154**(1). <https://doi.org/10.1088/1757-899X/154/1/012021>
12. Filippov, A.I., Shabarov, A.B., Akhmetova, O.V.: Temperature field of turbulent flow in a well with account for the dependence of thermal conductivity coefficient on temperature. *J. Eng. Phys. Thermophys.* **1** (2017). <https://doi.org/10.1007/s10891-017-1533-x>
13. Gulkov, A.N., Lapshin, V.D., Slesarenko, V.V., Morozov, A.A., Solomennik, S.F.: January adiabatic conversion method for the development of marine hydrate deposits. In: *Proceedings of the International Offshore and Polar Engineering Conference*, p. 73 (2015)

Trenchless Technology Application of Protective Coatings That Provide Energy Savings Associated with Transport of Water via Pipelines

Vladimir Orlov^(✉)  and Sergey Zotkin 

Moscow State University of Civil Engineering,
Yaroslavskoye Sh. 26, 129337 Moscow, Russia
orlov950@yandex.ru

Abstract. The article presents the analysis of trenchless technologies and different types of inner protective coatings of the pipelines, which may be used as the repairing materials to enable the power saving effect during the water transport. As the protective coatings the article examines round and deformed profile pipes, sprayed coatings on the base of non-organic and organic materials. The notion of a power saving potential has been formulated, when the protective coatings are used for trenchless repairing works of water supply pressure pipelines, as well as the methods of its calculation per running meter of a pipeline length per year. The Swagelining power effective technology was subject to a complex examination on the basis of the created automated software. There is presentation of the algorithm for calculation of some geometrical and power parameters, in particular, the wall thickness of a polyethylene pipe to be pulled after its compressing and straightening into the old pipeline, as well as the dynamical changes of the pressure losses before and after the renovation works in the pipeline by the Swagelining technology, when SDR are taken within a wide range of limits determining the ratio of the pipe diameter to its wall thickness. The data, which have been got at the result of the automated calculation, show that during renovation of old pipelines by the Swagelining technology the required effect may be got both from the technical point of view (complete restoration of the old pipeline part by elimination of damaged points) and the economical one due to a great power saving effect.

Keywords: Pipelines · Renovation · Trenchless technologies
Protective coatings · Power saving potential · Hydraulic characteristics

1 Introduction

The repairing and renovation of the pipelines for transport of liquids and gas use a wide range of operational trenchless methods based on application of the inside protective coatings (coverings) such as pipes and thin wall hoses made of different materials [1].

The widely used composite materials are an effective mean of localization of the pipeline defects in the pipelines of water supply, water deviation and gas supply, i.e. cracks, blowholes, joint ruptures, etc. [2].

The progressive development of trenchless technologies of the engineering pipeline renovation suggests some effective methods, which provide not only restoration of the strength characteristics of an old pipeline, but also a power saving effect. In this case the final task is to make a right choice of a protective coating to be found out by research and design engineers [3].

The Fig. 1 shows the coatings, which are the most widely used in practice in research investigations.

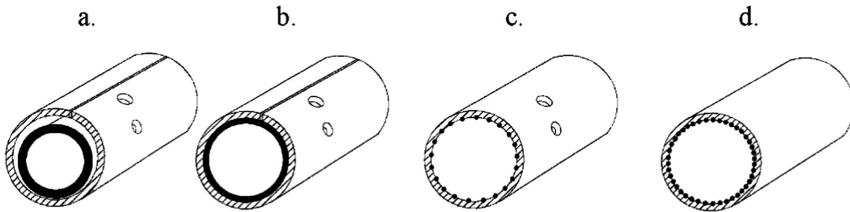


Fig. 1. Examples of protective coverings for renovation of old pipelines by different trenchless methods.

- a - covering by a round pipe of a smaller diameter, than the old pipeline;
- b - ditto, a polymer hose or pipe, which lays closely to the old pipeline;
- c - sprayed coating on the base of non-organic materials;
- d - ditto, on the base of organic materials.

The performed investigation has been aimed at estimating the power saving effect of the pipelines, which are operating or are under the trenchless renovation. Analytical and theoretical findings have been used as the methods of calculation of the power saving effect.

The round profile pipe, which is used as the protective covering (Fig. 1a), is pulled into the old pipeline. It is widely used for renovation of old water supply pipelines made of different materials (steel, cast iron, reinforced concrete, chrysotile cement) at nearly all the diameters of the operating pipelines. The pipes to be pulled through, most of all, are polymer, corrugated and non-corrugated, but the pipes made of any other materials are not excluded. In particular, in case of use of non-corrugated pipes of a small diameter, they may be successfully delivered to the place under renovation through the pit hole without dismantling its construction. After being turned to 90°, the pipe is shaped in an oval form with no structural folds and at the low friction force. Restoration of the round shape before pulling into the old pipeline is performed by a special equipment, which represents a frame with a guiding rolling system to be located in the pit and above its entrance [4].

This method shall be used for detection of the pipe defects, such as creaks (longitudinal, transversal, screw-shaped), joint dilatations, blowholes. It enables the strength characteristics of the pipeline under renovation, which are required by the design.

However, there are some shortcomings of the method of pulling a round-shaped pipe, i.e. necessary filling of the space between the new and the old pipe, as well as application of big pulling forces [5]. Moreover, a considerable throwing of the living

pipeline diameter may lead to worse operational hydraulic parameters of the renovated pipeline, so then, the power saving effect can not be achieved.

To avoid the above problem provision shall be made of the technology, which enables pulling of such a pipe, that will lay closely to the interior surface in the old pipeline (Fig. 1b). In practice it shall be made by pulling shaped (deformed) U or C-type polymer pipes into the pipeline to be renovated with their posterior straightening by steam at the required pressure. The pipes may be shaped both at the factory (rolled on the spools) and at the trench edge. This method of pulling enables lower pulling forces and permits to save practically the existing diameter of the pipeline, which will provide necessary conditions for the required hydraulic parameters [6].

The same effect of the close pressing of the protection coatings against the inner side of the pipeline under renovation may be attained, when the pulling has been performed by the hoses (the sleeves), which represent single- or multi-lay “soft hoses”, as well as when provision is made of tape coatings. The hydraulic and strength parameters of the repaired pipeline do not really change due to the hose strength and the smooth interior surface of the new pipe. Application of a tape technology to cover the inner surface of the old pipelines permits to form a new pipe within the old body without any local resistances, since there are no welding joints [7]. The winding of a tape coating is provided by different types of spiral winding machines. With all this, the thickness of the protective coating, which forms the pipe, is so minor, that it does not affect the hydraulic characteristics of the pipeline system, because the new polymer pipe lays very closely to the interior surface of the old pipeline [8].

The coating on the Fig. 1c is referred to the centrifugal spraying method with the use of the ends, which spray a special construction mortar [9]. A typical representative of such coating is a cement-sand one, which enables location of defective points, i.e. cracks, blowholes and other damages. The thickness of the protective coating varies from 4 to 16 mm respectively for the diameters from 70 to 2000 mm. It shall be noted, that this thickness of the layer does not permit to restore the bearing capacity of the pipeline, but meets the required design hydraulic characteristics of the flow.

A serious alternative of the cement-sand coating is the Scotchkote 169HB coating, which is made by centrifugal spraying method and is composed by mixing two organic components [10]. The thickness of the layer is not big (3–8 mm), but it enables the following items: injection into the blowholes of a big diameter (up to 5 mm) without working out of the plane of the pipeline exterior cylinder surface; a higher durability of the restored pipeline; a smooth surface and capability to stand to increasing hydraulic pressures in the pipelines. After application of the protective coating it is nearly splicing to the old piping at the molecular level, see the Fig. 1d.

Notwithstanding the type of the used protective coatings, provision shall be made of the pipeline renovation all along its whole length [11]. The quality control of the performed pipeline renovation works shall be provided by the modern tele-diagnostic means [12].

The above trenchless renovation methods are referred to the nondestructive ones, because their application saves the skeleton of the old pipeline [13].

When the old pipeline can not be renovated, it shall be dismantled and new pipes shall be pulled in simultaneously all along the piping route. This way is applied, for example, for renovation of the crysotile cement pipes [14].

2 Results and Discussions

Nowadays, notwithstanding the strength and the hydraulic properties of the above mentioned coatings, it is extremely important to estimate the power efficiency of the alternative protective coatings to be performed. To estimate the renovation power efficiency, provision shall be made of the notation of the energy power saving potential, which depends (under other equal conditions of the old and renovated pipeline) on the thickness of the coating layer, the pipeline geometrical size (the inner diameter) and the hydraulic coefficients.

The comparison of the above mentioned options (Fig. 1) of the protective coatings and their types leads us to a nearly unique statement, that the option on the Fig. 1a will not give a positive effect as far as the power saving is concerned [15]. The other options, in some way, are similar and shall be estimated by calculation of the power saving potential.

If we look at a pipeline system under renovation, the relative power saving potential may be considered as the difference between the real annual power consumption (i.e. during operation of the existing part of the pipeline) and the consumption after termination of the repairing and renovation works by the appropriate protective coatings. It shall be noted, that the trenchless renovation works of the pipelines using protective coatings, are very economical (of manpower and materials) by comparison to the traditional replacement of the pipeline parts performed by the open site means [16].

So, it may be concluded here, that relatively small expenses for the pipeline renovation and the choice of the appropriate renovation technologies and the repairing materials (protective coatings) with low specific resistances, permit to gain a considerable economic effect.

The Swagelining trenchless technology is one of such technologies of the pipeline renovation, that may provide the resource and the power saving effect. It concerns in pulling round shape polyethylene pipes, which have been preliminary compressed by their section, through the old pipelines [17]. It shall be noted, that a temporary thermo-mechanical compression of a pipe does not affect the exclusive property of a thermoplastic pipe to save the initial form memory effect. Within a short period of time the preliminary compressed pipes straighten out and join closely the interior side of the old pipeline without any voids between the pipes' walls.

The Swagelining method makes possible renovation of the pipelines of 100 to 1200 mm diameter at a long site of renovation works. Renovation of old pipelines may be provided by some plots up to 300 m long using the start and the finish pits. The Swagelining technology means pulling of a polymer pipeline to be compressed (for example, a 100 dia polyethylene pipe) through the furnace, where it is heated to 70–80 °C (Fig. 2).

The pipes to be compressed are joined by the butt welding before the furnace and are formed as a bundle of some pipes. At the end of the furnace the pulled pipeline passes through a special device - the constriction matrix. At the result, the diameter of the pipe becomes smaller, but the pipe itself does not extend. After the furnace the compressed polymer pipe is pulled by a winch or a mechanism with the hydraulic tensioning control into the pipeline to be renovated. The rate of deformation and

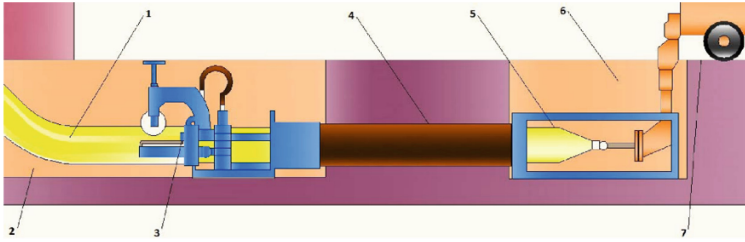


Fig. 2. General scheme of the pulling technology by the Swagelining method. 1 - polymer pipe to be compressed thermo-mechanically, 2 - the start pit, 3 - the equipment for pulling the pipeline with the furnace and the constriction matrix, 4 - the part of the pipeline to be renovated, 5 - deformed polymer pipeline, 6 - finish pit, 7 - place of the equipment location to perform the works.

pulling of the pipes of approximately 1000 mm diameter makes from 40 to 80 m/h, so the distance of 300 to 800 m may be passed in 24 h. When the pulled bundle gets the finish pit, the process of the diameter enlargement begins till the polymer pipe lays tightly to the inner surface of the existing pipeline.

The use of polyethylene pipes of different SDRs (diameter to wall thickness ratio) with the above described Swagelining technology has the advantage to get a wide range of the inner diameters at the renovated part of the pipeline. The degree of the polymer pipe thermo-mechanical compression shall be determined by the selection of the constriction matrix diameter. It needs the optimal variant of choice of the SDR and the compression degree.

Theoretical investigations and mathematic calculations included determination of a number of renovation parameters and their analysis to find an optimal solution of the old pipeline renovation by the Swagelining method. A standard polyethylene pipe of the exterior diameter $d_n = 315$ mm (with SDR values: 11, 17, 21, 26, 33, 41 и 50), which has been subject to the thermo-mechanical compression, was examined as the research object. According to the task conditions a polymer pipe has been pulled into an old steel pipeline with the $d_{vs} = 300$ mm inner diameter.

The following parameters have been analyzed:

- geometrical parameters of the pipeline system (the interior diameter of the new pipeline after renovation, the thickness of the wall after compression-straightening of the pipe);
- hydraulic parameters (pressure losses in the old and the new pipe after renovation);
- average annual savings of electrical power (per running meter of the pipeline and along the whole piping), what has been a real characteristic of relatively potential electrical power savings.

To solve the given task, an algorithm has been used, which provided, at first, calculation of the “x” wall thickness after the thermo-mechanical compression and straightening of a polyethylene pipe in the old pipeline taking into account the conservation of mass of the polyethylene pipe material. Under the conditions of the pipe compression without its tension, the areas of its ending part, which represent circling rings, are identical before and after the thermo-mechanical compression (Fig. 3).

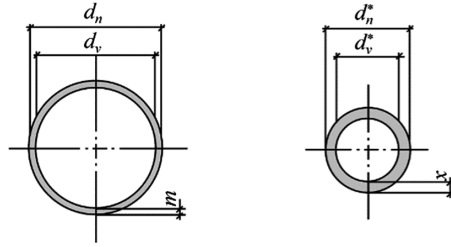


Fig. 3. Fragments of end parts (profiles) of the pipeline as the circling rings before (at the left) and after (at the right) compression.

- d_n – standard exterior diameter of a polymer pipeline before compression, which corresponds to an exact SDR_i , mm;
- m – the wall thickness of the corresponding SDR , mm;
- d_v – the inner diameter of the polymer pipeline before compression, which is determined as $d_n - 2m$, mm;
- d_n^* – the exterior diameter of the polymer pipeline after compression, mm;
- d_v^* – the inner diameter of the polymer pipeline after compression, mm;
- x – the thickness of the pipe wall to be determined after compression, mm

The area of the circling ring S_1 before compression shall be determined by the Eq. (1):

$$S_1 = \pi \left[\frac{d_n^2}{4} - \frac{(d_n - 2m)^2}{4} \right] = \pi(d_n m - m^2) \tag{1}$$

Making the similar mathematical operations, the area of the circling ring after compression S_2 may be presented as the Eq. (2):

$$S_2 = \pi(d_n^* x - x^2) \tag{2}$$

The condition, that the areas remain constant before and after the thermo-mechanical compression, permits to equalize the circling ring areas before and after compression, i.e. $S_1 = S_2$ (3):

$$d_n m - m^2 = d_n^* x - x^2 \tag{3}$$

After reduction of the above dependence to the standard form of a quadratic equation we get the resulting Eq. (4):

$$x^2 - d_n^* x + d_n m - m^2 = 0 \tag{4}$$

It shall be noted, that according to the task of pulling into the old pipeline and its straightening after the thermo-mechanical compression, the value of d_n^* diameter is the inner diameter of the old steel pipeline d_{vs} , i.e. $d_n^* = d_{vs}$.

Then, if we introduce the new symbols in (4), the final quadratic equation will be as follows (5):

$$x^2 - d_{vs} \cdot x + d_n m - m^2 = 0 \tag{5}$$

After that, taking the standard diameters d_n and the wall thickness m of the polymer pipelines for the corresponding SDR, calculations shall be made for the design values of the inner diameters and the wall thickness after the thermo-mechanical compression and straightening of the polymer pipes. Got design values serve the basic material for a designer, who will look for a final decision of renovation of an old pipeline by the choice of the corresponding SDR for the pipeline linear plot, where there is the highest power saving potential. Creation of hydraulic models and automated software programs for the result processing with the use of modern PC complexes may be the most effective variant of calculations and the data analysis in designing of renovation works. The task of the further investigations was to develop an automated software for calculation of operation parameters of the pressure pipelines made of different materials, which shall be restored by preliminary compressed polymer pipes [18]. For the first software dialogue window see the Fig. 4, and for the output information see Fig. 5.

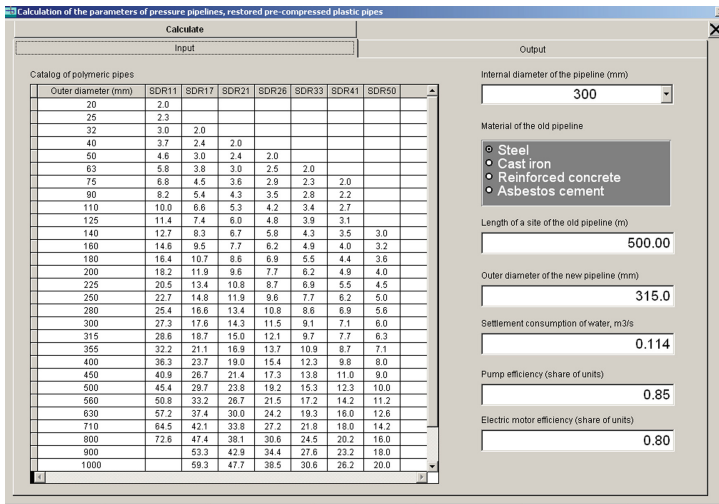


Fig. 4. Dialogue window of the automated software.

Besides the information on geometrical parameters, hydraulic and economic parameters, the output form of the automated software program (Fig. 5) contains the commands for drawing in Microsoft Excel the graphics of dependence of the average annual electrical power savings $\Delta E_{1m,i} = f(SDR_i)$ and the measurement of the polymer pipe inner diameter after the procedure of its straightening in the old pipeline $D_i = f(SDR_i)$.

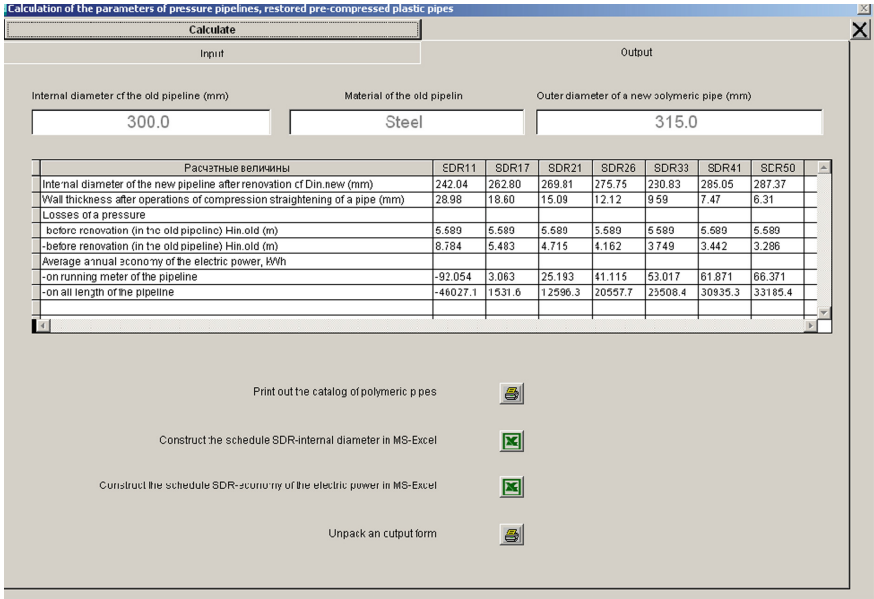


Fig. 5. The output form of the automated software.

The annual electrical power economy ΔE (kWh) shall be computed according to the following basic Eq. (6):

$$\Delta E = [\rho g Q \Delta H / 1000 \eta_p \eta_m] 24 \cdot 365 \tag{6}$$

where ρ is the liquid density, kg/m^3 ; g – free fall acceleration, m/s^2 ; Q – consumption of water supplied by the pipeline, m^3/s ; η_p и η_m – efficiency of the pump and the electrical motor respectively; 24- number of the pump operation hours per 24 h, h; 365 – the number of days in the year; 1000 – conversion factor from W to kW; ΔH – reduction of the pressure losses along the pipeline length, m of water column.

The Table 1 doubles the results of the automated calculations, which are given on the printed page at the Fig. 4, if the water rate makes $0.114 \text{ m}^3/\text{s}$, that provides the most economical water flow rate (about 1 m/s).

The automated software complex permits to determine the power saving potential for a wide range of the transported water rates, for example, from 0.2 to 2.5 m/s, which are the most typical for water supply pipelines.

For the above mentioned example the Table 2 shows the summarized data, which illustrate changes of the power saving potential for the whole range of the examined SDR values at a variable rate (consumption).

The analysis of the got design data given in the Table 1 permits to state the following items:

when a polyethylene pipe with SDR 11 is chosen as the renovation material to be used according to the Swagelining technology, the pressure losses increase at the liquid

Table 1. Summarized table of design data at the inner diameter of the old steel pipeline $d_{vs} = 300$ mm and the exterior diameter of the new polymer pipe $d_n = 315$ mm.

Design values	SDR values						
	11	17	21	26	33	41	50
1. Interior diameter of the new pipeline after renovation $D_{in, new}$, mm	242.04	262.8	269.81	275.75	280.83	285.05	287.37
2. The wall thickness after the pipe compression-straightening procedures x , mm	28.98	18.60	15.09	12.12	9.59	7.47	6.31
3. Pressure losses:							
-Before renovation, m of the water column	5.589	5.589	5.589	5.589	5.589	5.589	5.589
-After renovation, m of the water column	8.784	5.483	4.715	4.162	3.749	3.442	3.286
4. Average annual power savings, kWh:							
-Per running meter of the pipeline ΔE_{1m}	-92.054	3.063	25.193	41.115	53.017	61.871	66.371
-Along the whole length of the pipeline E_L	-46027.1	1531.6	12596.3	20557.7	26508.4	30935.3	33185.4

Table 2. Design values of the power saving potential in dependence of the Q rate of the transported water and SDR values.

SDR values							
Q rate of water, m^3/s (the inner diameter of the old steel pipe is 300 mm, the exterior diameter of the polymer pipe is 315 mm)	11	17	21	26	33	41	50
Design values of the power saving potential E , kWh, per year, per 1 m of the pipeline							
0.016	-	0.008	0.07	0.114	0.147	0.171	0.183
0.038	-	0.113	0.933	1.523	1.964	2.292	2.458
0.061	-	0.469	3.86	6.299	8.122	9.479	10.168
0.076	-	0.908	7.464	12.182	15.709	18.332	19.665
0.091	-	1.558	12.814	20.913	26.966	31.471	33.759
0.106	-	2.463	20.252	33.053	42.621	49.738	53.356
0.126	-	4.136	34.015	55.514	71.583	83.537	89.614
0.144	-	6.174	50.774	82.866	106.85	124.69	133.77
0.162	-	8.469	69.649	113.67	146.57	171.05	183.49
0.171	-	10.339	85.025	138.76	178.93	208.81	224.01
0.191	-	14.182	116.63	190.34	245.45	286.44	307.27

flowing at the pipeline part, and consequently, there are negative values of the power savings (-92.054 kWh), i.e. there is no power saving potential; in this case the pipeline renovation by the Swagelining methods is not reasonable;

when a pipe with SDR 17 is used for renovation works, there is no the power potential increase, i.e. the pressure losses after renovation (5.483 m of water column) remain nearly the same as in the old pipeline (5.589 m of water column);

when the pipes with SDR 21 and SDR 26 are used, we note the power saving potential increase; in this case it makes 25.193 kWh per 1 running meter of the pipeline per year for SDR 21 and 41.115 kWh for SDR 26;

beginning from SDR 33 the power saving is increasing up to 86.371 kWh for SDR 50 per 1 running meter of the pipeline, i.e. it becomes $66.371/3.063 = 21.67$ times bigger from the moment of the first manifestation at SDR 21.

Using the automated design complex, by analogy to the results given in the Table 2, it is possible to get information on the design values of the annual power saving potential kWh per 1 m of the pipeline for any other (others) pair(s) of diameters of the renovated and new pipelines taking into account the pipe material, as well as the efficiency of pumps and electrical motors.

It shall be noted here, that the higher is the pump and the electrical motor efficiency, the less is the power saving potential increase within all the SDR range.

The information of the Table 2 may be considered as an auxiliary tool for a designing specialist, which will help to make the final choice of the option of a pipeline renovation by the trenchless method [19, 20].

At the conclusion it shall be noted, that the received data show the possibility to get the required effect from the technical point of view (total reconstruction of the structure of the old part of pipelines), as well as form the economic one by obtaining a considerable power saving effect, if the renovation works have been performed by the Swagelining technology.

3 Conclusion

1. The choice of the interior protective coating and the trenchless method of the old pipeline renovation shall be guided by the requirements, which enable the appropriate strength and hydraulic parameters of the pipeline system to be renovated, and which ensure the power saving effect.
2. The complex of the performed investigations shows, that during renovation of the old pipelines by the Swagelining technology, if SDR values are subject to any variations, it is possible to get not only the power saving effect due to the pipeline damage liquidation, but also a considerable reduction of the electrical power consumption of the water transport.
3. The developed automated analysis software program of calculation of the operation parameters of pressure pipelines, which are renovated by preliminary compressed polymer pipes, makes possible for the designers to take decisions quickly by modeling the situation and to use a wide range of polymer pipes with the appropriate diameters and *SDR* values.

References

1. Rabmer-Koller, U.: No-dig technologies – innovative solution for efficient and fast pipe rehabilitation. In: 29 NO-DIG International Conference and Exhibition, NO-DIG, vol. 2C-1, pp. 1–10 (2011)
2. Janssen, A.: Importance of lateral structural repair of lateral lines simultaneously with main line CIPP rehabilitation. In: 31 NO-DIG International Conference and Exhibition, vol. 012287, pp. 1–10 (2012)

3. Kuliczkowski, A.: *Rury kanalizacyjne*. Wydawnictwo Politechniki Swietokrzyskiej (2004)
4. Freimuth, B.: Long pipe lining of sewage pipes «Tigt-in-Pipe» in the city of Salzgitter. In: 29 NO-DIG International Conference and Exhibition, NO-DIG, vol. 4B-3, pp. 1–7 (2011)
5. Rameil, M.: *Handbook of pipe bursting practice*. Vulkan verlag, Essen (2007)
6. Kuliczkowski, A., Kuliczowska, E., Zwierzchowska, A.: *Technologie beswykopowe w inzynierii srodowiska*. Wydawnictwo Seidel-Przywecki Sp (2010)
7. Ishmuratov, R., Orlov, V., Andrianov, A.: The spiral wound pipeline rehabilitation technique for pipe networks: an application and experience in Moscow City. In: 31 NO-DIG International Conference and Exhibition, NO-DIG, pp. 1–7 (2013)
8. Schmager, K.: Overblew of spiral-wound pipe lining technologies. In: 29 NO-DIG International Conference and Exhibition, NO-DIG, vol. 2B-4, pp. 1–10 (2011)
9. Cruz, C., Emerson, M.: Spray applied coatings for the rehabilitation of drinking water pipelines. In: 31st NO-DIG International Conference and Exhibition, vol. 011521, pp. 1–7 (2012)
10. Dulcy, M., Abraham, A., Gillani, S.: Innovations in materials for sewer system rehabilitation. *Trenchless Technol. Res.* **14**(1), 43–56 (1990)
11. Wei, G., Xu, R., Huang, B.: Analysis of stability failure for pipeline during long distance pipejacking. *Chin. J. Rock Mech. Eng.* **24**(8), 1427–1432 (2005)
12. Santiago, A., Durango, M.: Most advanced technology for pipeline inspection in the world: see, measure and navigate in 3D through pipes and manholes. In: 31 NO-DIG International Conference and Exhibition, vol. 011595, pp. 1–7 (2012)
13. Ahern, E.: Non-invasive rehabilitation technologies. In: 30 NO-DIG International Conference and Exhibition, vol. 2–20, pp. 1–9 (2013)
14. Freimuth, B.: Trenchless renewal of asbestos pipes in the Brazilian city of Campinas. In: 29 NO-DIG International Conference and Exhibition, NO-DIG, vol. 3A-2, pp. 1–7 (2011)
15. Orlov, V., Hantai, I., Orlov, E.: *Trenchless technology*. ASV (2016)
16. Ariaratnam, S., Sihabuddin, S.: Comparison of emitted emissions between trenchless pipe replacement and open cut utility construction. *J. Green Build.* **4**(2), 126–140 (2009)
17. Zwierzchowska, A.: *Technologie bezwykopowej budowy sieci gazowych, wodociagowych i kanalizacyjnych*. Politechnika swietokrzyska (2006)
18. Orlov, V., Zotkin, S., Zotkina, I., Khrenov, K.: Calculation of operation parameters of the pressure pipelines to be renovated by preliminary compressed polymer pipes. Certificate of the PC software State Registration no. 2014612753 (2014)
19. Khrenov, K., Averkeev, I., Orlov, V., Nechitaeva, V.: Strength investigations of organic protective coatings to be used in the trenchless renovation of pipelines. *Nat. Tech. Sci.* **2**, 158–159 (2015)
20. Orlov, V., Mikhaylin, A., Khrenov, K.: Reduction of power consumption at renovation of circular water supply pipelines by trenchless methods. *Sci. Rev.* **4**, 155–158 (2015)

The Neural Modeling for the Assessment of Hazardous Hydro Meteorological Phenomena Including the Case of the Providing a Sustainable Work (Reliability) on Transport

Larisa Haritonova^(✉) 

Volgograd State Technical University,
Lenin Avenue, 28, Volgograd 400005, Russia
haritonova410@yandex.ru

Abstract. The article presents a comprehensive analysis of using artificial neural networks and neural modeling to assess hazardous hydro-meteorological phenomena. The techniques of the undertaken studies are the elements of the mathematic modeling, neural modeling based on the integrated environment MATLAB R2017a, the regression analysis. According to the survey, the conclusion has been made on the expedience of applying the neural modeling to analyze big bulks of data for the assessment of hazardous hydro-meteorological phenomena (hydrological and agro-meteorological inclusive); the geometry of the neural model was selected; the regression analysis of the predicted results and the target outputs was carried out, the regression lines equations and the correlation coefficients were obtained to assess the forecast the neural model utilization under the obtained architecture of the neural network, various training functions, and transfer functions. According to the performed calculations, it was revealed that using the neural network for neural models to assess hazardous hydro-meteorological phenomena (hydrological and agro-meteorological ones included) in the given range of sizes, the normalization of an input, target results in the lesser value of the MSE. In this case, it is appropriate to use the Levenberg-Marquardt algorithm and the transfer function – hyperbolic tangent.

Keywords: Neural modeling · Neural networks · Transport infrastructure

1 Introduction

This issue is urgent and perspective to avoid emergency situations and blackouts for transportation reliability and safety, to preserve road and bridges, industrial and residential buildings, their infrastructure, to forecast and manage the national economy correctly, as well as to meet the demands of the population and their comfortable living conditions under hazardous hydro-meteorological phenomena.

The Report on the climatic characteristics in the Russian Federation (which is an official publication of the Federal Service for Hydrometeorology and the Environmental Monitoring (Roshydromet)) says that in 1998 the dangerous hydro-meteorological phenomena were observed 206 times; the year 2015 saw 75 more hazardous hydro-meteorological phenomena on the RF territory than in 2014 (973 and 898 correspondingly). According to the monitoring data, there is a considerable increase in the total number of such hazardous phenomena yearly [1]. These phenomena lead to great harm in the bulk of branches of economy including the power management for urban transportation and its sustainable functioning, construction sector, its infrastructure, impede the economic activities, aggravate human life and activities. The harm amounts to billions of rubles. By way of illustration, the traffic on the newly erected bridge over the Volga River in Volgograd had been stopped on the 20th of May 2010 due to the intense vibration of the structure. The vibration amplitude had come up to about 1 m. Because of the considerable wind loading, the bridge went into resonance with the vibration amplitude vertically approximately by 0.5–0.6 m. The vibrations of such amplitude are hardly possible without some weakening of structural strengths. The bridge was dubbed a “dancing” one.

The following hydro-meteorological phenomena can be called hazardous: strong wind, whirlwind, subnormal temperatures, untimely frost, heavy frost, snowstorm, heavy rainfall, fog, hail shower, snow slush build-up, icing, dust storms.

They result in a great number of power line imperfections (the blackouts at the critical infrastructures, industrial facilities, medical institutions etc.), damages to house roofs, fallen trees, destruction of small structures, incl. public transport stops, etc. The continuous heavy rain leads to under-flooding of considerable areas and small holdings. The extreme fire risks result in the increase of fire areas. A considerable damage is done to the soil and atmospheric draughts (that is agro-meteorological phenomena). There are inflammations of residential houses and even human losses. The lists of such phenomena present the mass data hard to analyze and to forecast by the common mathematical methods [2–6].

By the Russian Federation Government Decree of October 31, 2015, № 2217-p adopted a number of improvements for the fundamental research program for the years 2013–2020. The most promising ones are the development of methods for knowledge extraction out of the big mass data, the assessment of the situation and management decision making, neural network systems for adaptive control for the complicated ... systems.

A great amount of factors impacting the hazardous phenomena are unknown. The character of their interrelations is also unknown. However, the solution of this problem is possible if neural networks are used – the innovative technologies which enable to approach the solution of forecasting for various phenomena since they provide the backtracking of dependences both explicit and hidden among the initial data [7–21].

2 Materials and Methods

The last version of the package MATLAB R2017a with the Neural Network was used (the extension package MATLAB containing the tools for designing, modeling, development and visualization of neural networks).

The training sample is a set of values for the input and output variables characterizing the state of an object. To train a neural network, some initial data were used: the statistic data from the Report on the climatic characteristics in the Russian Federation as of 2015 taken from the Federal Service for Hydrometeorology and the Environmental Monitoring with 14 indices. By way of the input indicators were applied x_1 – the year (years 1998 through 2015), and x_2 – the months (January through December). That is a 2×216 matrix was introduced. A series of experiments was carried out, some results of which are presented in Figs. 1, 2, 3, 4, 5, 6 and 7. As a network type, a one-way network (feed - forward back prop NN) was used. The studies were performed to reveal the impact of the following adaption learning functions:

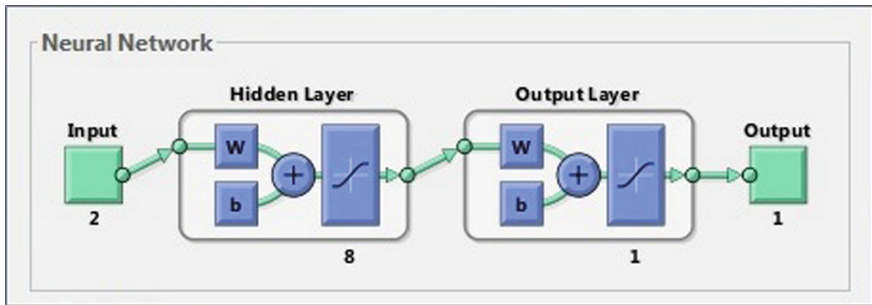


Fig. 1. The example of the network structure 2-8-1-1.

- training gradient descent function,
- training gradient descent function with momentum.

Also was done the analysis of changing of the following transfer activation functions:

- sigmoid (logistic) function;
- transfer function hyperbolic tangent;
- linear transfer function.

The best values were acquired when using the adaption teaching gradient descent function with momentum and the transfer function -the hyperbolic tangent.

With the best training function and the activation function, the influence of changing the following training functions was studied:

- Bayesian regularization;
- the method of bound gradients (Powell - Beale);
- the method of bound gradients (Fletcher-Powell);

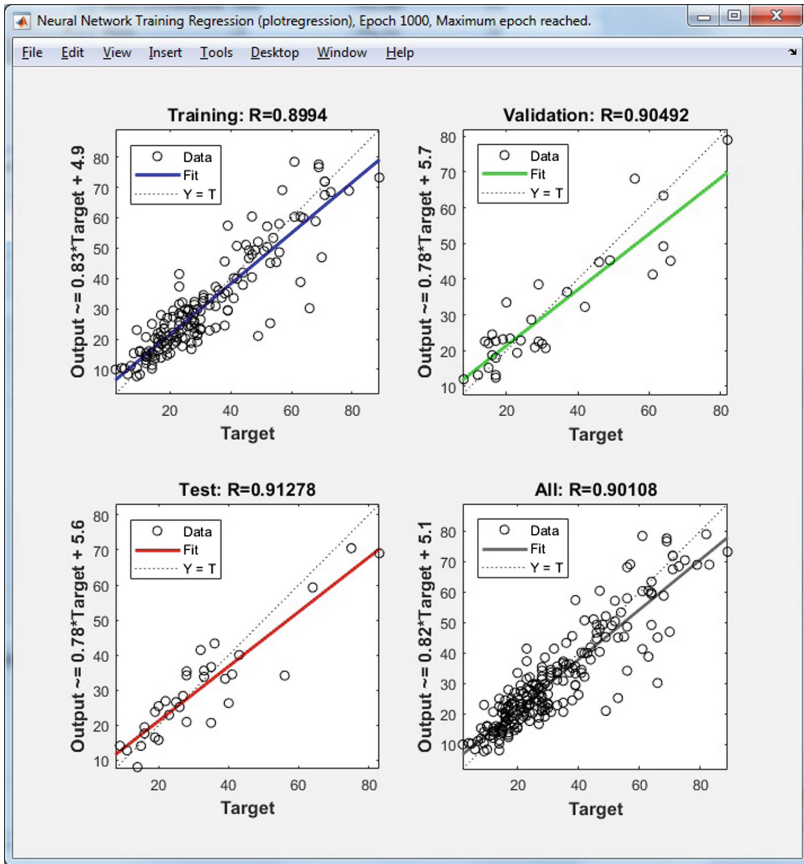


Fig. 2. Equations for the target outputs and correlation coefficients in training, validation, testing, and the total for the network structure 2-8-1-1 without normalization.

- the method of bound gradients (Polar-Ribiere);
- the gradient descent method;
- gradient Descent with Momentum;
- gradient Descent with Momentum & Adaptive LR;
- the method of random increments;
- the algorithm of the elastic back propagation;
- the technique of the scale bound gradients;
- the method of Levenberg-Marquardt.

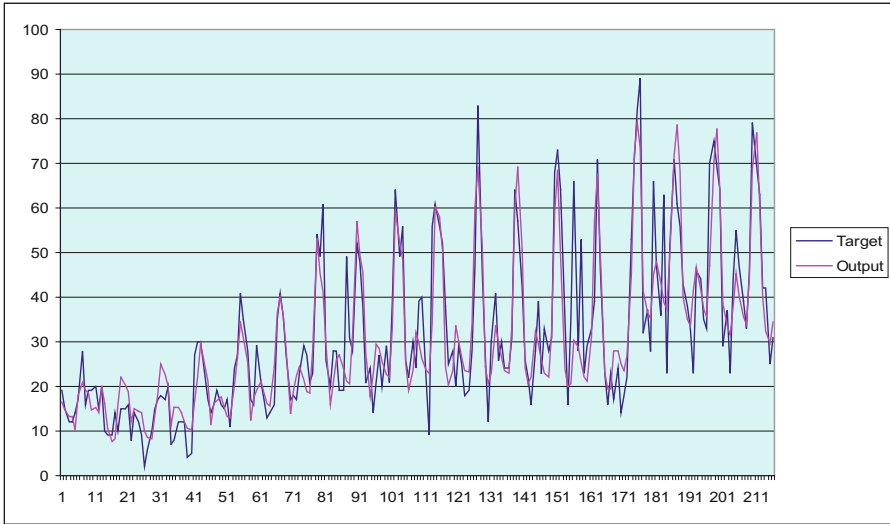


Fig. 3. The graph of the comparison for the target data of the hazardous phenomena from the publication [1]) with the output values (calculated with the help of neural network) for the network structure 2-8-1-1 without normalization.

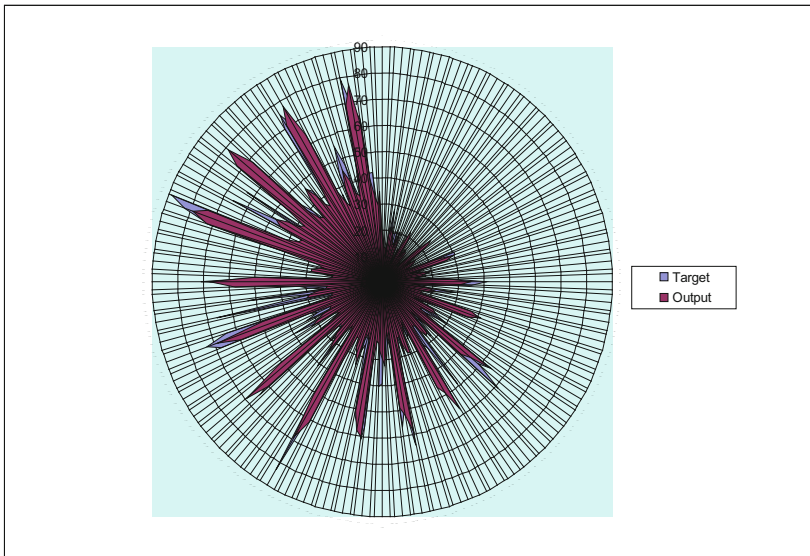


Fig. 4. The radar plot of comparison for the target data of hazardous phenomena from publication [1]) with the output values (calculated with the help of neural network) for the network structure 2-8-1-1 without normalization.

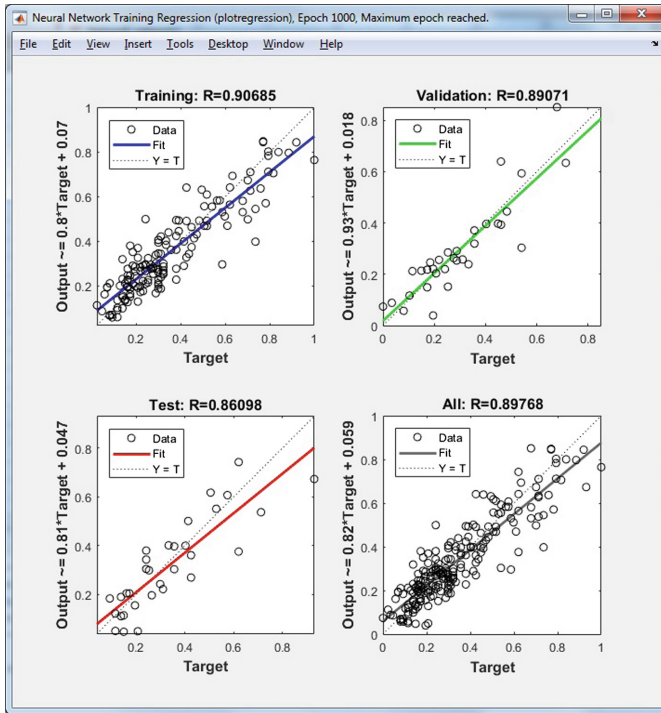


Fig. 5. Equations for the target outputs and correlation coefficients in training, validation, testing, and the total for the network structure 2-8-1-1 with normalization by the formula (1).

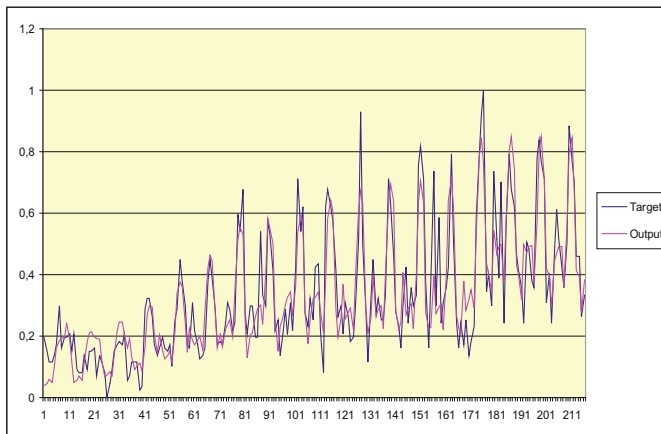


Fig. 6. The graph of comparison for the target data of the hazardous phenomena from publication [1]) with the output values (calculated with the help of neural network) for the network structure 2-8-1-1 with normalization by formula (1).

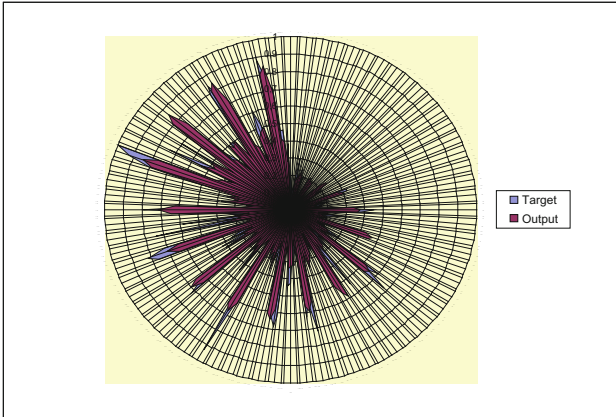


Fig. 7. The radar plot of comparison for the target data of the hazardous phenomena from publication [1] with the output values (calculated with the help of neural network) for the network structure 2-8-1-1 with normalization by formula (1).

3 Results and Discussions

After the analysis of the obtained results, the following algorithms were used: as the training function - the method of Levenberg-Marquardt, as the adaption learning function - the training function of the gradient descent with momentum, as the Performance function - MSE (Mean Squared Error); as the transfer function - the hyperbolic tangent.

We studied the impact of the number of the inner neurons on the obtained models. As a result, the number of neurons in the hidden layer was taken as 8 (herewith, the most high values for the correlation coefficients were observed), and in the output layer - as 1.

The neural model geometry is shown in Fig. 1.

The important issue is the problem of the need for normalization of the input and the anti-normalization of the output data. For instance, the source [17] mentions that when the absolute values of the input variables are exceeding the definite level, the output values will vary insignificantly and the efficiency of the network training becomes very low resulting in some troubles with the convergence. That is to avoid the mentioned circumstances, the input data should be limited by some definite range, to this end, the input sample data need to be normalized.

There exist many methods to normalize the input data, by way of illustration some are given in [20, 21]. The proposed approaches to normalize the data, as in [17], are rather complicated for the data processing.

In the study [16], the data were normalized by the formula:

$$R_n = \frac{R_A - R_{min}}{R_{max} - R_{min}} \quad (1)$$

where R_A - the actual value;
 R_{\min} - the minimum value out of R_i under examination;
 R_{\max} - the maximum value out of R_i under examination;
 R_N - the normalized value of R_i .

Here with, R_N will be located within the range from 0 to 1.

In the course of investigations, the calculations have been made with the regard to the geometry of the neural model given in Fig. 1: experiment 1 – without the normalization (Figs. 2, 3 and 4), experiment 2 (Figs. 5, 6 and 7) – with the normalization by the formula (1).

MSE (Mean Squared Error) was determined by the formula:

$$MSE = \frac{\sum_{i=1}^n (Y_i - \bar{Y}_i)^2}{n},$$

where Y_i - i -th sample element;
 \bar{Y}_i - arithmetic average of the sample;
 n - amount of sampling.

Figures 3 and 6 (graphs) and Figs. 4 and 7 (radar plots) show the comparison of the Target (hazardous phenomena data from the publication [1]) with the Output values (calculated with the help of Neural Network). It follows from these graphs that the obtained results describe the examined phenomena quite satisfactorily.

4 Conclusions

The application of artificial neural networks and neural network modeling has been analyzed in various fields of human activities based on which the conclusion was drawn on the necessity for the use of neural modeling to analyze big data bulks to assess the hazardous hydro-meteorological phenomena (including hydrological and agro-meteorological ones):

- the neural model geometry has been chosen;
- based on the performed calculations, it was obtained that applying the Neural Network to get the neural models for the assessment of hazardous hydro-meteorological (the hydrological and agro-meteorological ones included) in the given range of values, the normalization of Input, Target by the formula (1) results in a considerably lesser value of MSE;
- the regression analysis was performed of the predicted results and the target outputs and obtained the equations of the regression lines and the correlation coefficients (to assess the prediction of using the neural network model): in training, validation, testing, and the total with the various geometry of the neural network (the number

of the inner neurons), the calculation algorithms and activation functions. The formulas are presented in Fig. 2 (without the normalization), Fig. 5 (with the normalization by the formula (1));






- when using the Neural Network to obtain the neural models for the evaluation of hazardous hydro-meteorological phenomena (including hydrological and agro-meteorological) in the given range of values it is reasonable to apply: as the training functions – the method of Levenberg – Marquardt, as the adaption learning function – the training function of the gradient descent with momentum and the transfer functions – the hyperbolic tangent.

References

1. The Report on the climatic features in the Russian Federation for the year 2015, p. 68. Roshydromet, Moscow (2016)
2. Haritonova, L.P.: MATEC Web Conf. **106**, 06006 (2017)
3. Haritonova, L.P., Azarov, V.N.: Bulletin of Volgograd State University of Architecture and Civil Engineering (VSUACE) Series: Civil Engineering and Architecture, vol. 44-2, no. 63, pp. 178–188 (2016)
4. Haritonova, L.P.: Bulletin of Volgograd State University of Architecture and Civil Engineering (VSUACE). Series: Yestestvennie nauki, vol. 6, no. 23, pp. 98–104 (2007)
5. Haritonova, L.P.: Bulletin of Volgograd State University of Architecture and Civil Engineering (VSUACE) Series: Civil Engineering and Architecture, vol. 39, no. 58, pp. 224–232 (2015)
6. Okladnikov, I.G., Gordov, E.P., Titov, A.G.: IOP Conf. Ser.: Earth Environ Sci. **48**, 012030 (2016)
7. Haritonova, L.P.: International Research Journal **8–3**(50), 155–158 (2016)
8. Haritonova, L.P.: Proceedings of the Second International Scientific and Practical Conferences “The Top Actual Researches in Modern Science (28–29 July 2016 Ajman UAE)” International Periodical Scientific Edition: International Scientific and Practical Conferences “World science”, 2 August, vol. 8, no. 12, pp. 47–55 (2016)
9. Hush, D.R., Horne, B.G.: IEEE Signal Process. Mag. **10**(1), 8–39 (1993)
10. Kondratyev, A., Tyumentsev, Yu.V.: Izv Vuz Av Tekhnika [Russian Aeronautics (Engl. Trans.)], vol. 56, no. 2, pp. 23–30 (2013)
11. Emaletdinova, L.Y., Tsaregorodtseva, E.D.: Izv Vuz Av Tekhnika [Russian Aeronautics (Engl. Trans.)], vol. 56, no. 3, pp. 247–256 (2013)
12. Novikova, S.V.: Neural network simulation for solving the monitoring problems under conditions of incomplete fuzzy information (by an example of ecological monitoring) (DrSc thesis) (2013)
13. Rutkovska, D., Pilinski, M., Rutkovski, L.: Neural networks, genetic algorithms, and fuzzy systems, p. 452. Hotline – Telecom, Moscow (2006)
14. Novikova, S.V., Yu, A., Tunakova, Yu.A., Shagidullin, A.R., Kuznetsova, O.N.: Herald Technol. Univ. **18**(23), 131–134 (2015)
15. Novikova, S.V.: Russian Aeronautics (Izv VUZ), vol. 59, no. 2, pp. 263–270, April 2016
16. Oduroa, S.D., Metiaa, S., Duch, H., Ha, Q.P.: Predicting Carbon Monoxide emissions with multivariate adaptive regression splines (MARS) and artificial neural networks (ANNs) FFACE-ISARC15-3023378 (2015)
17. Wu, Z., Cao, Y.: Int. J. Latest Res. Eng. Technol. (IJLRET) **2**(4), 75–87 (2016)

18. Haritonova, L.P.: *Int. Sci. J. (ISJ) Theor. Appl. Sci.* **34**(2), 164–171 (2016)
19. Haritonova, L.P.: *International Research Journal* **3–2**(45), 91–93 (2016)
20. Ezugwu, E.O., Fadare, D.A., Bonneya, J., Silva, R.B.D., Sales, W.F.: *Int. J. Mach. Tools Manuf.* **45**, 1375–1385 (2005)
21. Sanjay, C., Jyothi, C.: *Int. J. Adv. Manuf. Technol.* **29**, 846–852 (2006)

The Principles of the Layout and Evaluation of Systems for Protection from Dust Pollution of the Air

Natalia Sergina¹ , Tatyana Kondratenko²  ,
Maxim Nikolenko¹ , and Sergey Pushenko¹ 

¹ Volgograd State Technical University,
st. Akademicheskaja, 1, Volgograd 400074, Russia

² Don State Technical University,
pl. Gagarina, 1, Rostov-on-Don 344010, Russia
tatkondr@rambler.ru

Abstract. The technical condition of vehicles directly depends on the condition of highways. Maintaining the quality of the pavement will ensure the reduction of overhauls. The use of dust collection systems in the technological process for laying the asphalt concrete pavement and other layers of the pavement construction will provide protection against dust pollution of atmospheric air. A significant part of modern technological processes are associated with the manufacture, processing, transportation and use of powdered materials, and is accompanied by intensive release into the atmospheric air of significant amounts of dust. In the current environmental situation, even at relatively low initial concentrations, it increases the technogenic impact on the surrounding environment, and also entails the loss of valuable components and the increased costs of air treatment in ventilation and air conditioning systems. In the prevailing practice of design and operation, multistage plants for cleaning industrial emissions from suspended solids have become the most widespread. The article provides a systematization of the basic principles of the layout of such systems, as well as a calculation for a preliminary evaluation of their effectiveness using the example of a dust collection system proposed for the production of aerated concrete.

Keywords: Dust pollution · Dust collection systems
Asphalt concrete pavement · Road construction

1 Introduction

With the purpose of increasing the efficiency of the systems for localization of dust pollution, as well as saving energy, material and operational resources, inertial dust collection systems is used in most construction industry enterprises [1–22]. The experience of design and operation of such systems in Russia and abroad allows us to identify the main principles of their rational layout.

It is accepted to divide the basic principles of the assembly of dust collection systems into the following: the sequence of installation of dust collecting devices in the

system (parallel, sequential, combined); Placing the fan in relation to the dust collectors (to the apparatus, after the apparatus, between the apparatus) [1, 2, 5, 6, 8, 11].

Sequential connection of devices, for example, can be used in production, where cleaning of highly dusty stream is required, i.e. when capturing particles whose diameter is in the range of 3 μm to 100 μm . In this case, the devices of the next stage catch that part of the dust, which, because of the high dust content, was removed from the apparatus of the previous stage. The successive connection of the apparatus is characterized by a fine-dispersed purification of the dust-gas flow. Often, a serial connection is used in the design of low-capacity systems up to 30 m^3/h .

Parallel connection of devices, for example, can be used in production, where it is required to clean large volumes of purified gas. Such systems usually have average capacity, capable of cleaning from 30 m^3/h to 150,000 m^3/h of air and higher productivity. Parallel connection is also used in systems where low hydrodynamic resistance is required or when coarse dispersion is carried out, i.e. at capture of the particles which diameter exceeds 20 μm .

2 Experimental Section

At the same time, the development of dust collection technology has widened the variable boundaries of the layout schemes for dust removal systems. For example, at present, such a principle is widely practiced, such as the arrangement of systems for the organization of the movement of gas-air flows, through which it is possible to isolate systems that are open and partially closed, that is, without recirculation and recirculation of purified air (gas). In an open dedusting system, air aspirated from the process equipment passes successively through the dust collecting apparatus of all stages, and after purification it is discharged into the atmosphere. At a sufficiently high overall efficiency of the system, uncontaminated dust enters the atmospheric air, which, on the one hand, leads to an increase in the technogenic impact on the natural environment. On the other hand, the removal of dust from the airflow from the engineering and ecological system causes an increase in the cost of processing the air supplied to the premises, and for a number of industries, the loss of valuable components. In partially closed systems, part of the exhaust air after dedusting is returned either to the process or to one of the purification stages.

In addition, another realizable principle is the absence or organization of recycling of the captured powdered product with its return either to process equipment or to the system entrance, or to one of the dust collectors [3, 4, 9, 10, 12–22].

Also in the systems of dust pollution localization it is possible to allocate additional constructive elements involved in the organization of air movement, such as swirlers, unwinders, suction from the bunker zone, blowing elements, separators-concentrators, etc. The rational arrangement of these auxiliary devices depends on the efficiency of the systems as a whole.

A generalized diagram of principles of the layout of inertial dust collection systems is shown in Fig. 1.

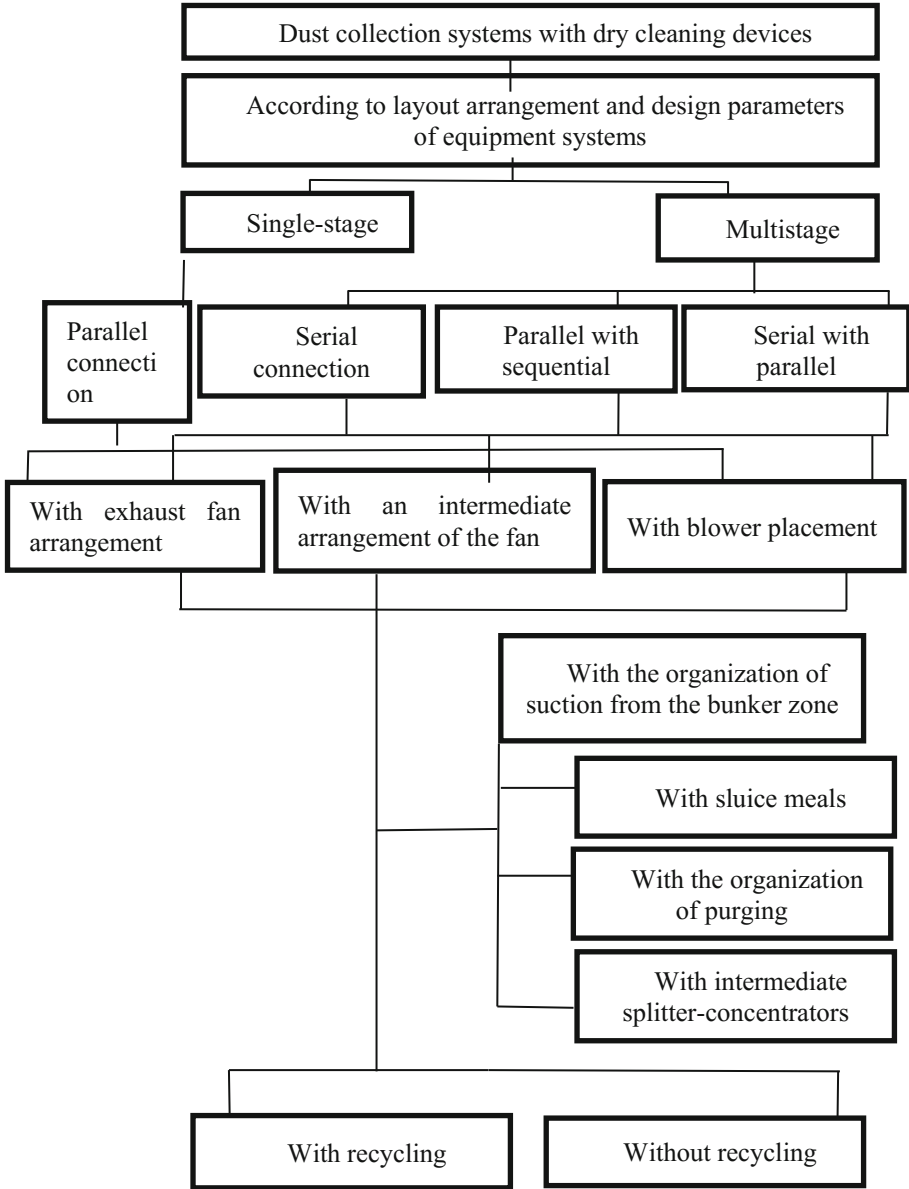


Fig. 1. Diagram of generalization of the layout principles of inertial dust collection systems for the organization of gas-air flows, placement and design parameters of dust collecting devices

3 Discussion Section

When using any option of the layout solution for evaluating the effectiveness of the system, the balance method can be used at the design stage of the facility [12, 19, 20, 22]. Let us consider its application with the example of a system for reducing the intake of dust into the air of the working area and into the atmospheric air proposed for the production of aerated concrete [21]. The scheme of the system is shown in Fig. 2.

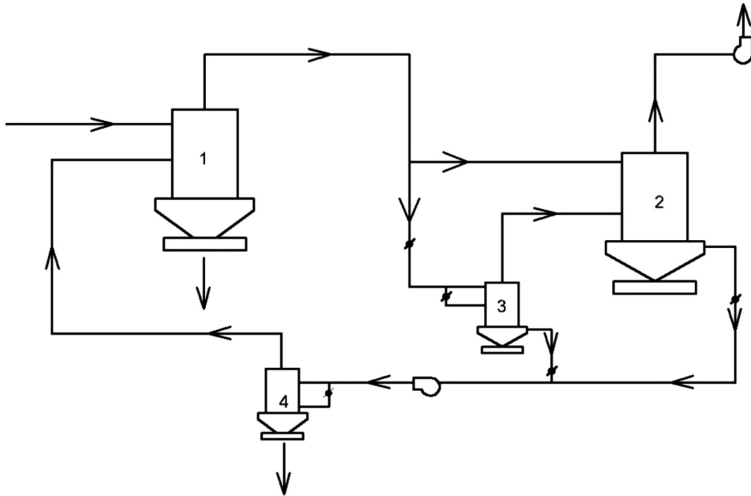


Fig. 2. Diagram of the dust collection system for the production of expanded clay. 1, 2 - the main dust collectors on opposite swirling flows; 3, 4 - additional dust collectors in counter-swirling flows with a smaller diameter

Let us compose a system of balance equations for air flows in the system (1). To do this, we take the following notation and indices: L - air flow, m^3/h ; G - dust weight, kg/h ; C - concentration of dust in the stream, mg/m^3 ; as - aspiration system; en - entrance to the dust collector; Out - exit from the dust collector (system); $caut$ - captured dust; suc - suction from the hopper; U - the upper input of the dust collector; L - the lower input of the dust collector.

$$\begin{cases} L_{as} + L_4 = L_{en3} + L_{en2}^u; \\ L_{en2}^u + L_{en2}^l = L_{out} + L_{suc2}; \\ L_{en3} = L_{en2}^l + L_{suc3}; \\ L_4 = L_{suc2} + L_{suc3}. \end{cases} \quad (1)$$

Now we will compose a system of balance equations for dust flows

$$\left\{ \begin{array}{l} G_{as} + G_4 = G_{out1} + G_{cau1}; \\ G_{out1} = \varepsilon_1(G_{as} + G_4); \\ G_{en2}^u = \frac{L_2^u}{L_{as} + L_4} G_{out1}; \\ \frac{L_2^u}{L_{as} + L_4} G_{out1} = G_{22} + G_{34}; \\ G_{en2}^u + G_{en2}^l = G_{out} + G_{suc2}; \\ G_{en2}^l = \varepsilon_3 G_{en3}; \\ G_{out} = \varepsilon_2(G_{en2}^u + G_{en2}^l); \\ G_{en4} = G_{out4} + G_{cau4}; \\ G_{en4} = G_{suc2} + G_{suc3}; \\ G_{out4} = \varepsilon_4 G_{en4}. \end{array} \right. \quad (2)$$

At the same time, dust perforation for each of the devices will be.

$$\begin{aligned} \varepsilon_1 &= \varepsilon_1(L_{as}; L_4/L_{as}; G_4/G_{as}); \\ \varepsilon_2 &= \varepsilon_2(L_{en2}^l/L_{en2}^u; L_{suc2}; G_{en2}^l/G_{en2}^u) \\ \varepsilon_3 &= \varepsilon_3(L_{en3}^l/L_{en3}^u; L_{suc3}) \\ \varepsilon_4 &= \varepsilon_4(L_{en4}^l/L_{en4}^u). \end{aligned} \quad (3)$$

We use the results of experimental studies [12] and represent the slip function ε_i in the form

$$\varepsilon_i = \varepsilon_{io} + a_1(\bar{L}_i - \bar{L}_{io})^2 + a_2(\bar{L}_{il} - \bar{L}_{ilo}) + a_3(\bar{L}_{isuci} - \bar{L}_{isuco})^2 + a_4(c_i - c_{io})^2 \quad (4)$$

Thus, we rewrite constants and parameters in the following form

$$\varepsilon_i = \varepsilon_{io} + \sum_{i=1}^4 a_i(x_i - x_{io})^2 \quad (5)$$

where the indices $i = 1, 2, 3, 4$ respectively denote the total flow rate, the fraction of the flow entering the lower inlet, the fraction of the flow entering the suction, the concentration.

We designate the CDW apparatus in the diagram (Fig. 2) by the indices $j = 1 \div 4$, where: $j = 1$ corresponds to the basic apparatus of the CDW of the first stage; $J = 2$ corresponds to the basic apparatus of the CDW of the second stage; $J = 3$ corresponds to the auxiliary apparatus at the lower input to the main unit of the second stage CDW; $J = 4$ corresponds to the auxiliary apparatus for air purification, sucked it from the bins of apparatus 2 and 3 (the purified gases after it are returned to the input of the apparatus 1). Let the indices characterizing the input or output for each device have the form: $k = 1$ - upper input; $K = 2$ - lower input; $K = 3$ - suction; $K = 4$ - trapping; $K = 5$ is the output.

We divide all the equations of system (2) by and take the notation: $\bar{G}_4 = G_4/G_{as}$; $\bar{G}_{out1} = G_{out1}/G_{as}$; $\bar{G}_4 = G_4/G_{as}$; $\bar{G}_{en2}^u = G_{en2}^u/G_{as}$; $\bar{G}_{22} = G_{22}/G_{as}$; $\bar{G}_{34} = G_{34}/G_{as}$; $\bar{G}_{en2}^l = G_{en2}^l/G_{as}$; $\bar{G}_{out} = G_{out}/G_{as}$; $\bar{G}_{suc2} = G_{suc2}/G_{as}$; $\bar{G}_{en4} = G_{en4}/G_{as}$; $\bar{G}_{out4} = G_{out4}/G_{as}$; $\bar{G}_{cau4} = G_{cau4}/G_{as}$; $\bar{G}_{suc3} = G_{suc3}/G_{as}$.

Then we obtain

$$\left\{ \begin{array}{l} 1 + \bar{G}_4 = \bar{G}_{out1} + \bar{G}_{cau1}; \\ \bar{G}_{out1} = \varepsilon_1 (1 + \bar{G}_4); \\ \bar{G}_{en2}^u = \frac{L_2^u}{L_{as} + L_4} \bar{G}_{out1}; \\ \frac{L_2^u}{L_{as} + L_4} \bar{G}_{out1} = \bar{G}_{22} + \bar{G}_{34}; \\ \bar{G}_{en2}^u + \bar{G}_{en2}^l = \bar{G}_{out} + \bar{G}_{suc2}; \\ \bar{G}_{en2}^l = \varepsilon_3 \bar{G}_{en3}; \\ \bar{G}_{out} = \varepsilon_2 (\bar{G}_{en2}^u + \bar{G}_{en2}^l); \\ \bar{G}_{en4} = \bar{G}_{out4} + \bar{G}_{cau4}; \\ \bar{G}_{en4} = \bar{G}_{suc2} + \bar{G}_{suc3}; \\ \bar{G}_{out4} = \varepsilon_4 \bar{G}_{en4}. \end{array} \right. \quad (6)$$

Now we use the above notation to describe this system.

For the universality of the proposed approach of the estimated evaluation of the effectiveness of the proposed technical solutions, we systematize all the equations in three groups:

Group I - continuity equations

$$y_{j1} + y_{j2} = y_{j3} + y_{j4}, j = 1, 2, 3, 4; \quad (7)$$

II group - the equations of efficiency (breakthrough)

$$y_{j4} = \varepsilon_j (y_{j1} + y_{j2}), j = 1, 2, 3, 4; \quad (8)$$

III group - equations characterizing the features of the layout of the system

$$\begin{aligned} y_{11} &= 1; \\ y_{12} &= y_{44}; \\ y_{21} &= k_{12} y_{14}; \\ y_{31} + y_{32} &= (1 - k_{12}) y_{14}; \\ y_{32} &= k_{33} (y_{31} + y_{32}); \\ y_{22} &= y_{34}; \\ y_{44} &= y_{23} + y_{33}; \\ y_{42} &= k_{44} (y_{23} + y_{33}). \end{aligned}$$

With respect to y_{ji} ($i = 1 \div 4, j = 1 \div 4$), this system is nonlinear, because Function ε_i depends on the dust concentration and, respectively, on the quantities y_{j1} and y_{j2} .

Denote as vector Y the characteristic vector of the dust collector, of dimension 16, and as the vector B, the vector of the original data, which is composed of the free terms of the system of equations of dimension 16.

Then the system of equations can be written in the following form

$$SY = B$$

If the determinant of the matrix is not “zero” ($\|S\| \neq 0$), then the vector Y is uniquely determined as follows

$$Y = BS^{-1},$$

where S^{-1} is the matrix inverse to the matrix S .

The values of the experimentally obtained coefficients k_{12}, k_{33}, k_{44} depend on the ratio of costs and are chosen from the requirements of optimality for dust in the production of aerated concrete. Wherein $k_{12} = 0.7; k_{33} = k_{44} = 0.28$.

We rewrite the system in a form convenient for solving it by the method of successive approximations

$$SY = B \rightarrow Y = BS^{-1} \tag{9}$$

$$Y = \begin{pmatrix} y_{11} \\ y_{12} \\ y_{13} \\ y_{14} \\ y_{21} \\ y_{22} \\ y_{23} \\ y_{24} \\ y_{31} \\ y_{32} \\ y_{33} \\ y_{34} \\ y_{41} \\ y_{42} \\ y_{43} \\ y_{44} \end{pmatrix} \quad B = \begin{pmatrix} 0 \\ 0 \\ 0 \\ 0 \\ 0 \\ 0 \\ 0 \\ 0 \\ 1 \\ 0 \\ 0 \\ 0 \\ 0 \\ 0 \\ 0 \\ 0 \end{pmatrix}$$

$$S = \begin{pmatrix} 1 & 1 & -1 & -1 & 0 & 0 & 0 & 0 & 0 & 0 & 0 & 0 & 0 & 0 & 0 & 0 \\ 0 & 0 & 0 & 0 & 1 & 1 & -1 & -1 & 0 & 0 & 0 & 0 & 0 & 0 & 0 & 0 \\ 0 & 0 & 0 & 0 & 0 & 0 & 0 & 0 & 0 & 1 & 1 & -1 & -1 & 0 & 0 & 0 \\ 0 & 0 & 0 & 0 & 0 & 0 & 0 & 0 & 0 & 0 & 0 & 0 & 1 & 1 & -1 & -1 \\ -\varepsilon_1 & -\varepsilon_1 & 0 & 1 & 0 & 0 & 0 & 0 & 0 & 0 & 0 & 0 & 0 & 0 & 0 & 0 \\ 0 & 0 & 0 & 0 & -\varepsilon_2 & -\varepsilon_2 & 0 & 1 & 0 & 0 & 0 & 0 & 0 & 0 & 0 & 0 \\ 0 & 0 & 0 & 0 & 0 & 0 & 0 & 0 & -\varepsilon_3 & -\varepsilon_3 & 0 & 1 & 0 & 0 & 0 & 0 \\ 0 & 0 & 0 & 0 & 0 & 0 & 0 & 0 & 0 & 0 & 0 & 0 & -\varepsilon_4 & -\varepsilon_4 & 0 & 1 \\ 1 & 0 & 0 & 0 & 0 & 0 & 0 & 0 & 0 & 0 & 0 & 0 & 0 & 0 & 0 & 0 \\ 0 & 1 & 0 & 0 & 0 & 0 & 0 & 0 & 0 & 0 & 0 & 0 & 0 & 0 & 0 & -1 \\ 0 & 0 & 0 & -k_{12} & 1 & 0 & 0 & 0 & 0 & 0 & 0 & 0 & 0 & 0 & 0 & 0 \\ 0 & 0 & 0 & -(1-k_{12}) & 0 & 0 & 0 & 0 & 1 & 1 & 0 & 0 & 0 & 0 & 0 & 0 \\ 0 & 0 & 0 & 0 & 0 & 0 & 0 & 0 & -k_{33} & (1-k_{33}) & 0 & 0 & 0 & 0 & 0 & 0 \\ 0 & 0 & 0 & 0 & 0 & 1 & 0 & 0 & 0 & 0 & 0 & -1 & 0 & 0 & 0 & 0 \\ 0 & 0 & 0 & 0 & 0 & 0 & -1 & 0 & 0 & 0 & -1 & 0 & 0 & 0 & 0 & 1 \\ 0 & 0 & 0 & 0 & 0 & 0 & -k_{33} & 0 & 0 & 0 & -k_{44} & 0 & 0 & 1 & 0 & 0 \end{pmatrix}$$

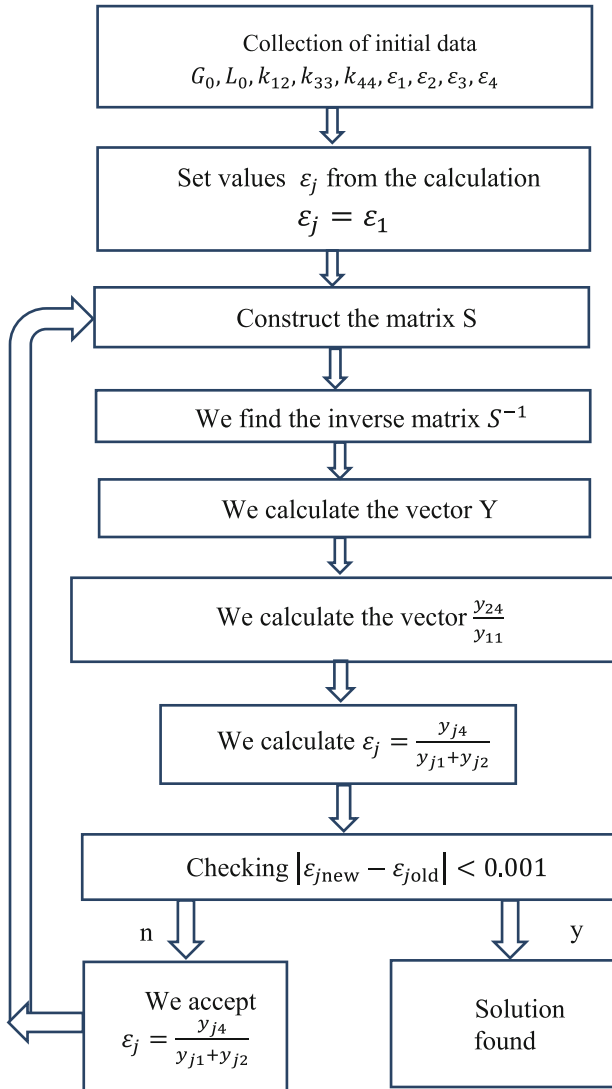


Fig. 3. Block diagram of the solution of the problem

The solution of the problem is carried out in the following sequence (Fig. 3). Initially select the values $G_{as}, L_{as}, k_{12}, k_{33}, k_{44}$. Then we set the value of ε_i , from the calculation that the input concentration in the apparatus $c_{j1} = c_0$ and $c_{j2} = c_0$. Then we construct the matrix S . We find the inverse matrix S^{-1} . We calculate the vector Y . From the equation we find the efficiency of the entire system as $\frac{y_{24}}{y_{11}}$.

For all $j = 1 \div 4$ calculate values $\varepsilon_j = \frac{y_{j4}}{y_{j1} + y_{j2}}$.

If for all j the condition

$$|\varepsilon_{j\text{new}} - \varepsilon_{j\text{old}}| < 0.001, \quad (10)$$

then a solution is found, and the efficiency of the system ε is defined. If the condition does not hold, then we calculate the new values y_i , go up and again perform the calculations, until the condition (3.9) is satisfied.

For the convergence of the solution, it is important to choose the first approximation, that is, the set ε_j where $j = 1 \div 4$. As a first approximation, we choose for all values j .

Thus, the value obtained ε System allows to calculate the efficiency of the whole system for given flow ratios within the system. The value depends essentially on the flow rate L_0 , cost ratios L_4/L_{as} , concentration ratio c_4/c_0 , size d_{50} at the entrance to the first dust collector. Similarly ε_j depends on the parameters at the entrance to this dust collector and the amount of suction from the dust collectors (this applies to the 3 and 4 dust collector).

4 Conclusions

The proposed systematization of the principles of the layout of inertial dust collection systems allows unifying the balance equations for the estimated estimation of the degree of reduction of dust emissions into the air of the working area and into the atmospheric air of the city using different schemes for assembling the dedusting units, as is shown in the example of the system proposed for the production of aerated concrete.

References

1. Buick, K.: *Verfahrenstechnik* **11**, 51 (1970)
2. Ciliberti, D.F., Lancaster, B.W.: *AIChE* **2**, 499 (1976)
3. Azarov, V.N.: *Constr. Mater.* **11**, 20 (2002)
4. Azarov, V.N., Sergina, N.M.: *Constr. Mater.* **8**, 14 (2003)
5. Strauss, W.: *Industrial Gas Cleaning*. Pergamon Press, London (2006)
6. Cortelis, C., Gil, A.: *Prog. Energy Combust. Sci.* **5**, 409–452 (2007)
7. Samarskaya, Yu.G.: *Bul. VolgGASU* **1**(5), 4 (2008)
8. Kharoua, N., Khezzer, L., Nemouchi, Z.: *AIChE* **111** (2011)
9. Sergina, N.M., Borovkov, D.P., Semjonova, E.A.: *Eng. Bul. Don.* **4**, 1191 (2012)
10. Sergina, N.M., Azarov, D.V., Semjonova, E.A.: *Sci. Probl. Humanit. Stud.* **7**, 229 (2012)
11. Hong, C.-H., Han, Ji.-W., Kim, B.-S., Park, Ch.-S., Kwon, Oh.K.: *Int. J. Mech. Aerosp. Eng.* **6**, 37 (2012)
12. Sergina, N.M., Kisenko, T.A., Semjonova, E.A.: *Eng. Bul. Don.* **4**, 1498 (2013)
13. Sergina, N.M., Semjonova, E.A., Kondratenko, T.O.: *Altern. Energy Ecol.* **112**, 43 (2013)
14. Sergina, N.M., Azarov, D.V., Gladkov, E.V.: *Constr. Mater.* **2**, 86 (2013)
15. Kondratenko, T.O., Semjonova, E.A., Solomachina, L.Ya.: *Eng. Bul. Don.* **3**, 1388 (2013)
16. Kondratenko, T.O.: *Sci. Rev.* **11**, 518 (2014)
17. Azarov, V.N., Borovkov, D.P., Redhwan, A.M.: *Int. Rev. Mech. Eng.* **4**, 750 (2014)
18. Sergina, N.M., Nikolenko, M.A., Kondratenko, T.O.: *Eng. Bul. Don.* **1**, 2751 (2015)

19. Sergina, N.M., Abduljalil, M.S.A.: *Bul. VolgGASU* **42**(61), 108 (2015)
20. Sergina, N.M., Druzhinina, D.S., Evseeva, V.A., Orlov, S.A.: *Eng. Bul. Don.* **4**, 3071 (2016)
21. Bogomolov, A.N., Sergina, N.M., Kondratenko, T.O.: *Procedia Eng.* **150**, 2036 (2016)
22. Bogomolov, A.N., Sergina, N.M., Druzhinina, D.S., Evseeva, V.A., Orlov, S.A.: *Bul. VolgGASU* **46**(65), 128 (2016)

Blasting Operations in Conditions of Buildings and Facilities Reconstruction

Denis Synitsyn  

Moscow State University of Civil Engineering,
Yaroslavskoe shosse, 26, Moscow 129337, Russia
SlavinaAY@mgsu.ru

Abstract. Drilling and blasting work carried out in transport construction, is considered in the article. They are quite common. Different ways of performing these operations is proposed. The various methods of blasting operations execution are described for such purpose. The operations technological order is given herein. The application of various methods and ways for the blasting operations execution in conditions of buildings and facilities reconstruction permits to speed significantly the construction process and to improve its efficiency.

Keywords: Blasting operations · Transport construction
Drilling and blasting work carried

1 Introduction

Specific blasting operations relating to concrete, reinforced concrete and steel structures demolition as well as to old buildings and facilities demolition are carried out during industrial facilities reconstruction. Such operations are executed on special projects. Blasting operations on foundations demolition are executed at open construction and plant sites as well as indoors. Foundations blasting in buildings is executed “for loosening” only.

2 Practical Application

Blasting charges for foundations demolition are placed into blastholes or channels. In case of foundations demolition straight to full height by blasthole method, then blastholes depth is set equal to 0.9 of foundation height (v. the Fig. 1 below). If the foundation demolition is executed by separate plies, then the blastholes depth shall be equal to a thickness of each ply except the last ply of foundation. To prevent foundations bases damage the blastholes depth in the last ply shall be equal to 0.9 of excavated ply thickness.

If foundation demolition is executed by means of horizontal blastholes, then the protective ply equal to 0.2...0.4 m in thickness shall be between the foundation base and these blastholes. During the foundations demolition the blastholes diameter is equal to 35...60 mm, calculated resistance line – 0.5...0.7 of blasthole depth.

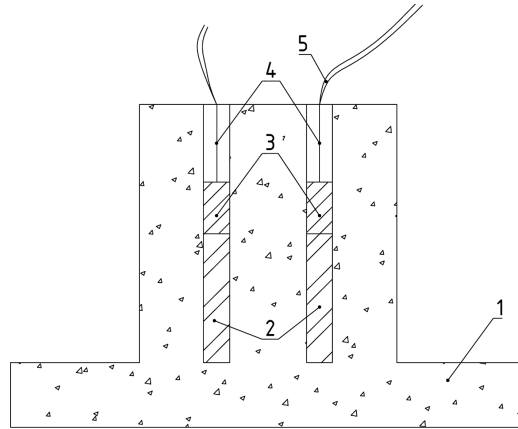


Fig. 1. Blasthole charges layout while foundation grinding: 1 – foundation; 2 – blasting charge; 3 – electric detonator; 4 – stemming; 5 – wires.

The distance between blastholes in series is equal to $1/0.1 \dots 1.3/W$, and between blastholes ranges as well as from the foundation edge – equal to W . Foundations blasting material ratio /ammonite No.6/ is equal from 0.3–0.45 to 0.5–0.7 kg/m^3 .

While putting the blasting charges in channels, their sections are equal to $0.1 \times 0.1 \dots 0.2 \times 0.2$ m. The channels are placed in such a way as to the charge center should be in the midpoint of foundation width. The channels length is not more than 1,5 m. The distance between the channels series and from the foundation edge is equal to their length, and the distance between the charges centers – 1.0...1.5 of channel length. The foundation is preliminary dug around at a depth of blasting area for purposes of seismic effect decrease.

In order to avoid fragment dispersion while blasting, the foundation is covered with sandbag, metal mesh or is fenced around with special shields equal to 50 mm in thickness, placed at a distance of about 60 cm from foundation. Surrounding packaged units and other building parts located nearby the blasted foundation are covered with wooden shields.

In order to decrease fragment dispersion applied is the hydro-blasting method of foundations, brick work, concrete and reinforced concrete demolition. 9–12 fibers of detonating cord /DC/ are used as a charge. DC fibers length is equal to 0.65...0.75 of blasthole depth. To decrease the quantity of DC fibers, the small water-resistant blasting charge /50...100 g/ may be placed at the lower part of blasthole. To avoid the side fragment dispersion, the blasthole empty space is filled with water, upper level of which is by 10 cm lower than the blasthole collar. Clay mortar is used instead of water at fissured foundations demolition. Therewith a charge weight tends to be increased in 1.3–1.5 times. Hydro-blasting method is ineffective for demolition of reinforced concrete with high reinforcement ratio.

As general, reinforced concrete blasting leads to concrete knockout from steel reinforcement. Then handheld power cutter or autogenous welder are used for steel reinforcement cutting. Thus, reinforced concrete mass is divided into transportable

blocks. Then high-order blasting material charge is placed at their edges and blasted. In case of plate or wall demolition with thickness less than 40 cm, the blastholes are made in the direction of cutting. Such blastholes depth is equal to 2/3 of wall thickness.

Depending on the reinforced concrete density, the distance between blastholes is equal to $10-15/d$, where d – blasthole diameter.

Surface concrete facilities demolition is executed by means of blastholes or borehole charges, depending on their force. The blastholes depth is equal to 0.9 of blasted facility thickness if operations are executed by blasthole method. Blastholes are checkerboarded, blasting material ratio for concrete is equal to $0.4...0.5 \text{ kg/m}^3$.

Blastholes are made at upper or side facility surface. As general, applied are electric, delay-action blasting operations. In order to avoid fragment dispersion the facility is covered with metal mesh /Fig. 2/.

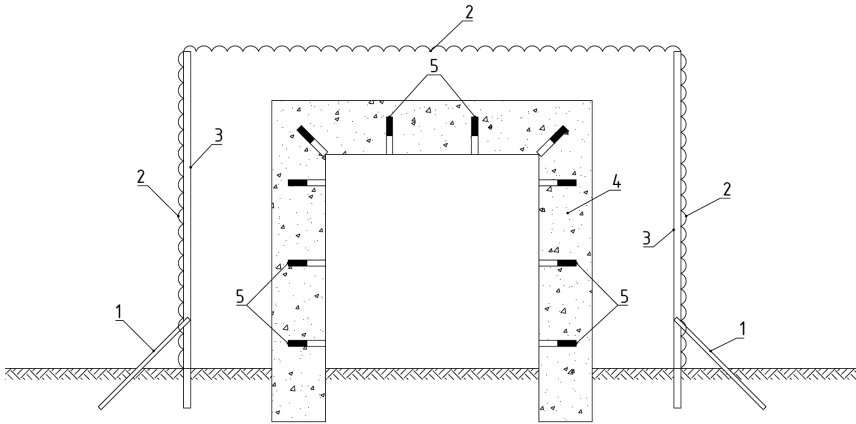


Fig. 2. Layout of concrete tunnel cover by metal mesh to prevent the fragment dispersion: 1 – braces; 2 – mesh; 3 – supporting poles; 4 – concrete tunnel; 5 – blasthole charges.

If a concrete block has high force, then the borehole charges method will be applied. The boreholes of d in diameter are placed on square mesh $a=b=25...27/d$ in single or several lines, depending on the block dimensions.

Blasting method is also used during steel structures demolition to smaller parts, which are appropriate for moving. Blasting operations for large steel blocks and structures demolition are executed if any special project, providing the operations safety. It is preferable to use for blasting operations the external and blasthole charges with high-order blasting material.

Pressure /external/ charges are used for breaking of figured or built-up frames and structures, metal sheets and plates of $t \leq 15$ cm in thickness. These charges quantity is calculated by the following formula, kg:

$$Q = q t^2 a_1,$$

where q – calculated specific ratio of ammonite No.6, kg/cm^3 / for earth $q = 0.005$, for steel – $q = 0.007$; al – sheet width /cutting length/, cm.

Mass of charge used for breaking of figured or built-up structures is calculated separately for each component. Stick powder or cartridge-type charges are used. External charges are covered all-around with slightly compacted stemming material / 25–30 cm in thickness, made of sand, clay, etc.

Blasthole charges of 30...35 mm in diameter are used for structures breaking of $t > 15$ cm in thickness. Such blasthole charges are burnt by oxygen or drilled out. Blastholes location lines /cutting lines/ are identified depending on dimensions of separate pieces, which shall arise as a result of demolition. Blastholes are made on cutting length at a distance 1.0...1.5 of blasthole depth, but not further than 30–40 cm from one another. Blastholes depth shall be not less than $2/3$ / for steel $3/4$ / and not less than $1/3$ of a facility demolished thickness.

Buildings and facilities demolition is executed to their footing or in the intended direction /intended demolition/. As general, high-rise buildings and facilities /chimney stacks, towers, etc./ are demolished in the intended direction.

The method of buildings and facilities demolition to their footing involves the formation of through breaking-in hole around the building or facility perimeter. As the result of blasting, a facility is demolished falling on its footing. As general, breakdown (building failure) height does not exceed $1/3$ of building height, and breakdown width sideways other than building perimeter – $1/2$ of walls height. As general, all interior partitions and furnaces, floors, roof timbers, roof, door and window frames are taken down and cleared away prior to blasting.

Buildings and facilities demolition is executed by charges in blastholes and channels. During the buildings demolition to their footing, the blastholes are placed inside the building. Blastholes diameter is equal to 40...60 mm, and their depth – $2/3$ of wall thickness. As general, blastholes are placed in two series checkerwise. Distance between blastholes is equal to 0.8–1.4 at length, and between series – 0.75...1.0 of blasthole depth /Fig. 3/.

Charges in the walls corners are put in blastholes made one above the other and directed on the angle bisector.

In case of falling in intended direction, the horizontal blastholes are placed in the form of wedge. Wedge narrow side sets the falling directions /v. Figure 4/. Upper blastholes series is set at the angle 10° , and lower one – at the angle 20° to the wedge top. Blastholes depth is equal to $3/4$ of wall thickness, the distance between blastholes is about 30 cm as a rule.

Building or facility intended demolition is executed for protective purposes of other buildings and shops located nearby. As general, the bisector of allowable demolition sector is such a direction /demolition axis/. Buildings and facilities, which height exceeds the horizontal section dimension /at the kerf level/ in 4 times and more, are appropriate to the intended demolition. The horizontal section dimension is calculated in the direction of demolition axis. To demolish a tower or stack in intended direction, it is required to execute the walls blind breaking-in hole from the demolition direction, equal to $2/3$ – $3/4$ of perimeter, and to execute the footing on the remained wall perimeter, above the breaking-in hole level for 0.7...1.5 m /Fig. 4/. Kerf is made by

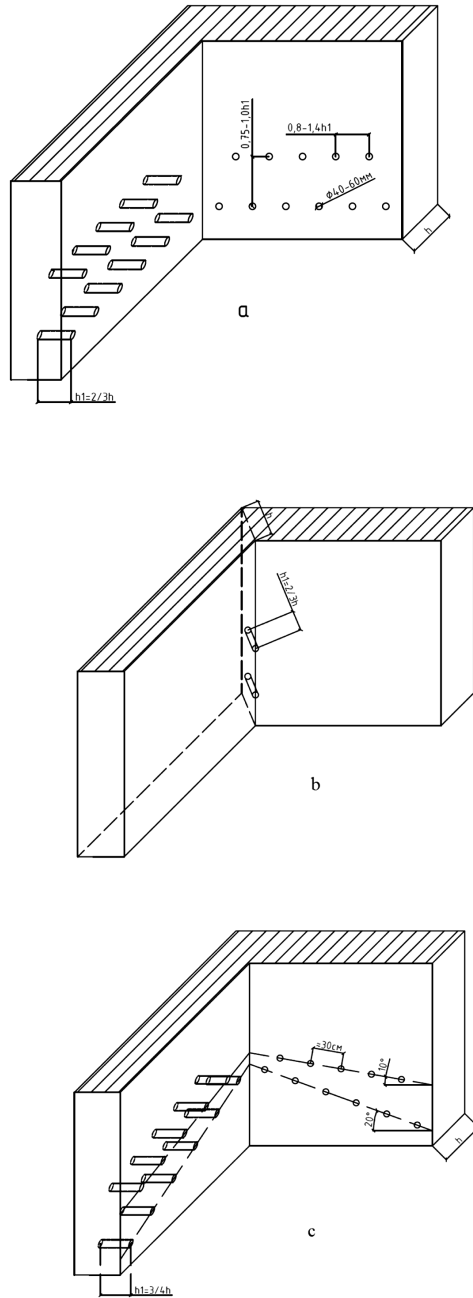


Fig. 3. Blastholes layout at buildings demolition to footing within a wall at a corner in case of intended demolition

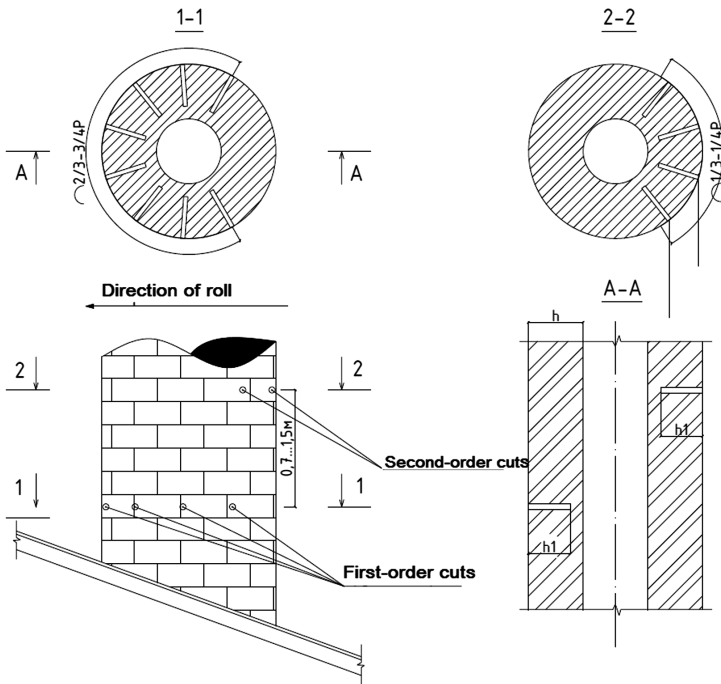


Fig. 4. Blastholes layout at a wall demolition in the intended direction.

two charges series and more. 2–3 lower series has the same lengths, other series is shorter, in accordance with the kerf angle adopted /Fig. 5/.

Place of stack/tower/ breaking-in hole is selected at a level, where are no openings/gas flues, doors, etc./. If it is impossible, the openings are sealed off carefully to make a core equally in strength.

Blasting by means of detonating cord or using electrical method is used for building, facility and stalks demolition. If the demolished building is located nearby the facilities, which are to be protected from wrecking or chattering, it is necessary to take special measures for their protection /cover with wooden shields, cushion layer packing at the falling place, etc./

During the reconstruction of a winery shops it was required to take down the reinforced concrete container, which was used for wine storage. It was like a rectangular structure, consisting of 20 tanks. Square tanks with sides dimensions equal to 2.8 m and with height equal to 1.8 m were located in two series, with the distance equal to 1.5 m between them. The walls, deck and bottom thickness was the same for all tanks – 0.25 m. Rolled sections (U-sections, H-beams, etc.) as well as reinforcing rods were used for reinforcing. The container was located at the distance 10–20 m of operating shops. Glass wine pipe, consisting of 3 lines, was located on both sides of tanks at the distance of 10 m from that tanks.

Usage of demolition hammers and excavator equipped with demolition ball for the said container was ineffective due to reinforced concrete high strength. It was proposed

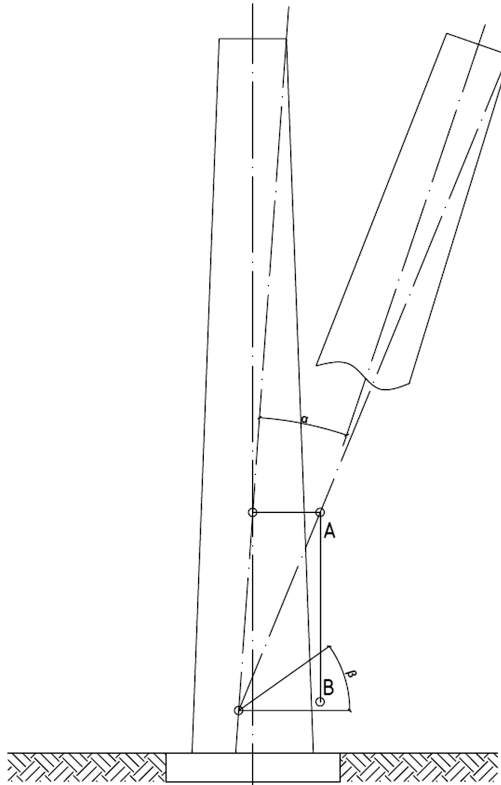


Fig. 5. Condition of stack tipping in the intended direction.

to use blasting method. Since the operations were executed in conditions of operating enterprise and nearby the existing utilities and facilities, it was decided to use the hydro-blasting method. The tanks were filled with water to the top, then all hatches were well-closed. In the tanks decks drilled were the holes with dimensions of 10×10 cm, through which the blasting material charges were moved down. Blasting operations execution diagram is given in Fig. 6.

Charges mass value was calculated by the following formula:

$$Q = 2.6 c^2 [\delta_{ck} + (h/a)\delta_p]^2 : 10\sqrt{HR}$$

where c – tank walls thickness (0.25 m);

δ_{ck} – reinforced concrete ultimate shearing strength (950000 N/cm²);

δ_p – reinforced concrete ultimate tensile strength (240000 N/cm²);

h – blasted ring height (1.4 m);

a – distance between working steel reinforcement (0.4 m);

H – charge depth (1.4 m);

R – distance from the tank center to the wall, m.

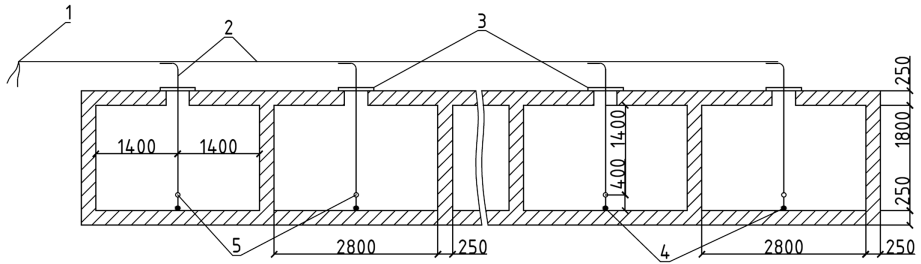


Fig. 6. Layout of hydro-blasting operations during the reinforced concrete container demolition 1 – electric detonator; 2 – detonating cord; 3 – fixing rods for DC hanging; 4 – load; 5 – blasting material charge.

The charge mass per one tank was calculated by the formula given, equal to 0.7 kg.

Water-resistant ammonite No. 6GV was used as blasting material. The charge was put into a plastic bag, as well as the detonating cord. The whole detonating system was mounted from the latter. Injection was executed by instantaneous electric detonators connected to the end sections of detonating cord main lines. Machine KPM-1 was used as the current source.

Blasting was executed without the concrete pieces dispersion. Therewith the maximum value of the latter did not exceed 0.7 m in diameter. 14 kg of ammonite, 170 m of detonating cord, 4 electric detonators, 20 plastic bags were used for operations execution. Therewith the work labor input given in the following table is significantly lower than other possible methods for in-situ reinforced concrete structures demolition [1–9].

3 Results

See Table 1.

Table 1. Work labor input for in-situ structures demolition by various methods

Type of in-situ structure	Demolition method	Work labor input, pers.-h, per demolition for 1 m ³ of structure
Mass concrete	Manual (depending on concrete grade)	58–84
	By means of pneumatic tool (depending on concrete grade)	29–42
	Drill-and-blast method	5.6
	By means of electrohydraulic effect plant	0.37


4 Conclusion

The various methods of blasting operations execution are used in the construction practice. Their selection is determined by the type and purpose of construction structures of buildings and facilities, and by the construction and installation work conditions. Therefore, the application of various methods and ways for the blasting operations execution in conditions of buildings and facilities reconstruction permits to speed significantly the construction process and to improve its efficiency.

References

1. Prokhorkin, S.F.: Construction –and-installation works technology and organization during the industrial enterprises reconstruction, Stroyizdat (1976)
2. Gevorkyan, G.A.: Specific Works in Industrial Construction. CBNTN, Moscow (1973)
3. Kushnarev, D.M.: Blasting energy usage in construction, Stroyizdat (1973)
4. Unified safety regulations for blasting operations
5. STO NOSTROY 2.6.54-2011: In situ concrete and reinforced concrete constructions. Technical requirements, regulations and methods of control
6. Russian Standard SP 70.13330.2012 SNiP 3.03.01-87: Load-bearing and separating constructions (Revised edition)
7. Russian Standards SP 48.13330.2016 SNiP 12.01-2016: Construction organization (Revised edition)
8. Ershov, M.N., Lapidus, A.A.: Modern Technologies of Civil Buildings Reconstruction. ACB, Moscow (2014)
9. Zhadanovskiy, B.V., Sinenko, S.A., Kuzhin, M.F.: Practical organizational and process diagrams of construction and installation works execution in conditions of operating enterprise reconstruction. *Tekhnologiya i organizatsiya stroitel'nogo proizvodstva* [Construction organization and technology], Moscow, 1 (2014)

Methodology of Comprehensive Slope Stability Evaluation Based on Engineering Geodesy and Soil Mechanics Methods for the Road Engineering Application

Vladimir Simonyan^(✉) 

Moscow State University of Civil Engineering,
Yaroslavskoye Sh. 26, 129337 Moscow, Russia
simonyan.vladimir55@gmail.com

Abstract. Issues related to the road engineering in the slope areas are the critical and topical ones. The article in point offers the packaged slope stability analysis under the geodesic monitoring and soil mechanics data. The geodesic data allow to adjust the design characteristics of soils, and the further soil deformation analysis subject to the joint techniques allows to forecast the time deformations of soil bodies with the utmost accuracy. Ignoring the geodesic data, the forecast error is equal to 12%.

Keywords: Landslide · Strain-Stress State · Evaluation · Deformation Simulation · Creep · Flow · Consolidation · Analysis · Risk

1 Introduction

Mountainous area characterized by the terrain complexity and slope steepness. The complexity of the terrain is accompanied by the complexity of the geological structure and alternating layers of rocks of different durability, protruded out of the surface of the slope at different angles, which causes different stability of the roadway platform. The landslide slopes are, as a rule, characterized with the complex Strain-Stress State (SSS), which requires additional explorations on the road engineering subject to the quantitative assessment of stresses and deformations. The stability degree evaluation and the reasoning of procedures to ensure the necessary stability of the slope of subgrade and natural slopes, within which the structures in design stage are located, are the main objectives of road engineering in difficult geological engineering conditions [1]. The cases when slopes demonstrate the soil creep properties [2, 13], require additional packaged engineering-geologic, engineering-geodesic and geotechnical surveys. The given article offers the packaged slope stability evaluation technique, using the engineering geodesics and soil mechanics techniques.

2 Materials and Methods

The recent techniques predominantly used to solve the soil mechanics applications include the numerical base and foundation SSS design techniques subject to the Finite Element Method (FEM), the Finite-Difference Technique (FDT), and the Boundary-Element Method (BEM) [3].

It is known [4, 5, 12, 16] that on solving the FEM problems the continuous area is viewed as a totality of the finite elements number. The given Paper includes use of triangular elements with fifteen nodes allowing to regard the SSS in the two-dimensional and three-dimensional statements subject to the sufficient level of accuracy.

The mathematical (numerical) simulation of the base soil SSS inside the envelope and outside its limits requires the following [5, 7, 11]:

- geomechanical model of the soil body accommodating the analyzed system of structures;
- mechanical model of the soils forming the soil body in point;
- design parameters of the engineering-geologic elements (EGE) soils;
- initial and boundary conditions of the model;
- the Software Package to be used for the efficient numerical simulation.

The present Paper stipulates use of Plaxis 3D 2012 Software Package [6].

Success in the quantitative SSS forecast for the soil bodies, which serve as a base or medium of various structures [10], is largely based on selection of the mechanical base soils model. The widely spread models currently include the following ones:

- More-Coulomb elasto-plastic model;
- Elasto-plastic model of the hardening soil;
- Cam-Clay elasto-plastic model;
- Loose water-saturated soil model subject to the Soft Soil Creep.

All of them allow to describe the elastic and plastic constituents of the soil deformations based on the Drucker-Prager Elasto-Plastic Theory (associated option) for the FEM systems.

The key principle of the elasto-plastic theory concludes in splitting deformations and incremental deformations into the elastic and plastic parts:

$$\varepsilon = \varepsilon^e + \varepsilon^p, \quad (1)$$

where ε – total deformation; ε^e – elastic deformation; ε^p – plastic (irreversible) deformation.

Hooke's law is used to fix the incremental elastic deformation, i.e.:

$$\Delta \varepsilon^e = \frac{\Delta \sigma}{E}, \quad (2)$$

where $\Delta \sigma$ – incremental stresses, E – Elasticity Module.

The incremental plastic deformations are described with the following relationship:

$$d\varepsilon_{ij}^p = \lambda \frac{\partial g}{\partial \sigma_{ij}}, \tag{3}$$

where λ – constant, g – plastic potential, which depends on the soil strength condition. For the elastic environment: $\lambda = 0$.

All models above use More-Coulomb strength criterion. More-Coulomb yield condition is a generalization of Coulomb Law for the complex (three-dimensional) stressed condition of soil. The given condition actually warrants compliance with Coulomb Law in any plane within the material element. More-Coulomb yield condition can be entirely fixed with use of the three yield functions subject to their presentation as the main stresses functions:

$$\begin{aligned} f_1 &= \frac{1}{2} |\sigma'_2 - \sigma'_3| + \frac{1}{2} |\sigma'_2 + \sigma'_3| \sin \varphi - c \cos \varphi \leq 0; \\ f_2 &= \frac{1}{2} |\sigma'_3 - \sigma'_1| + \frac{1}{2} |\sigma'_3 + \sigma'_1| \sin \varphi - c \cos \varphi \leq 0; \\ f_3 &= \frac{1}{2} |\sigma'_1 - \sigma'_2| + \frac{1}{2} |\sigma'_1 + \sigma'_2| \sin \varphi - c \cos \varphi \leq 0. \end{aligned} \tag{4}$$

The slope stability was evaluated subject to the soil creep parameters by the three-dimensional geomechanical model $390 \times 320 \times 62$ m composed of 55,269 finite elements. The design model diagram is shown in Fig. 1.

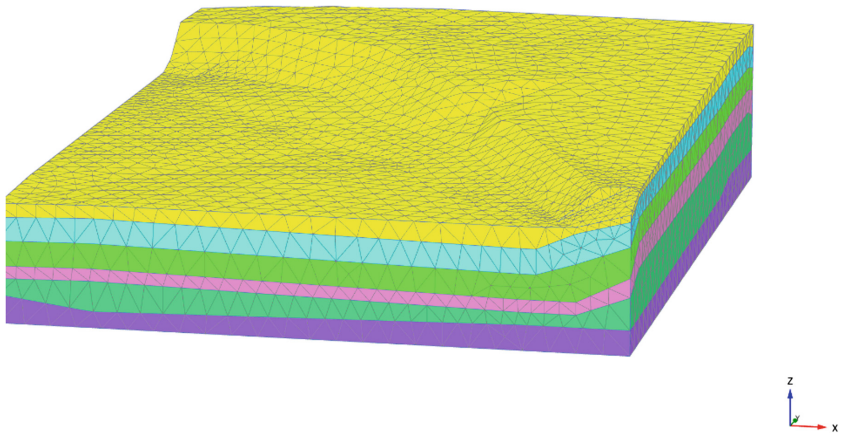


Fig. 1. Design diagram of the three-dimensional geomechanical model in X0Z plane.

The algorithm drawn up for the packaged evaluation of the slope SSS is the as follows:

1. Creation of the three-dimensional geomechanical slope model subject to the engineering-geologic surveys.

2. The slope time deformation design for the period of the engineering geodesic surveys.
3. Comparison of the geomechanical slope model design results with the geodesic monitoring results.
4. Updating the design data of the soils forming the soil body to calculate the slopes stability subject to the geodesic monitoring results.
5. Time slope deformations design subject to the updated soil parameters;
6. Calculation of the secondary consolidation end time for the slope-forming soils subject to the initial and updated soil parameters;
7. Packaged quantitative time analysis of slope deformations subject to and ignoring the geodesic monitoring results.

The packaged evaluation of the slope SSS using the engineering geodesics and soil mechanics techniques was run with a number of calculations using the Finite Element Method in PLAXIS 3D PC. The calculations were aimed at the packaged slope deformation analysis subject to the geodesic monitoring results. The geomechanical model subject to the engineering-geologic surveys was designed to this end. The given design allows to provide preliminary quantitative evaluation of the slope deformation over the time [14, 15]. It should be noted that its results are of the preliminary nature, and they may differ from the actual deformations of the slope surface, which can be explained with a number of reasons, for instance:

- the engineering-geologic surveys and the subsequent laboratory soil tests are run subject to the averaged values within one engineering-geologic element and may differ in various areas of the researched project site;
- the engineering-geologic surveys succeeded to identify the geologic processes taking place at the researched project site;
- the SSS calculation using the Finite Element Method does not include impact of the fertile layer on the slopes stability – it may be increased by the bushes and the tree roots.

The preliminary SSS calculation was run subject to the following stages:

1. Generation of the initial soil stresses (Gravity Loading Procedure).
2. Calculation of the filtration (primary) soil consolidation up to the minimum excessive porous pressure.
3. The staged secondary consolidation design over the time in the run geodesics monitoring interval.

Below are presented results of the preliminary slope SSS design subject to the soils creep and to the engineering-geologic surveys. Figure 2 shows that the slope surface deformations isofields are at the secondary consolidation stage. As shown in Fig. 2, the slope deformations are of irregular nature. To provide more objective evaluation, the calculation results were processed with the statistical probability techniques. The 46 points used in the geodesics monitoring process were taken as the measurements points. Figure 3 shows the average deformations of slope with reference to the geodesic monitoring cycles and the geodesic monitoring data (the space displacements were obtained over the mean-square shift ellipsoids [8, 9]).

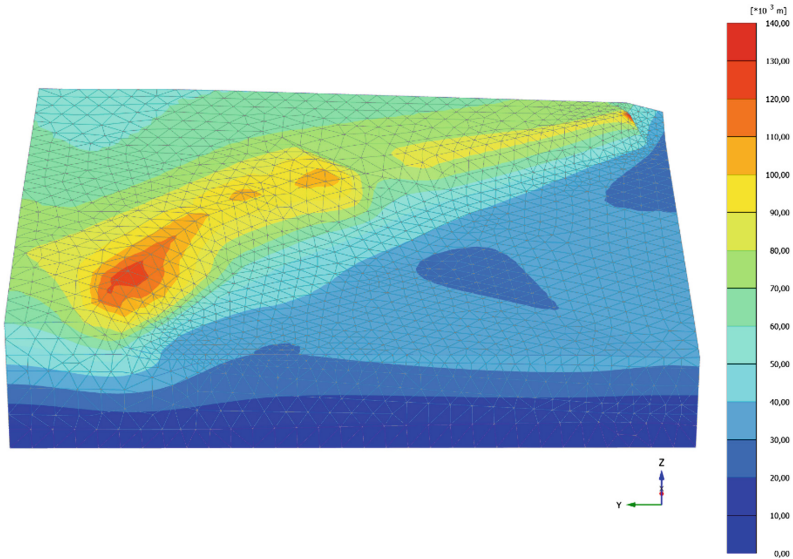


Fig. 2. The slope deformations isofields at the secondary consolidation stage on termination of the geodesic monitoring process.

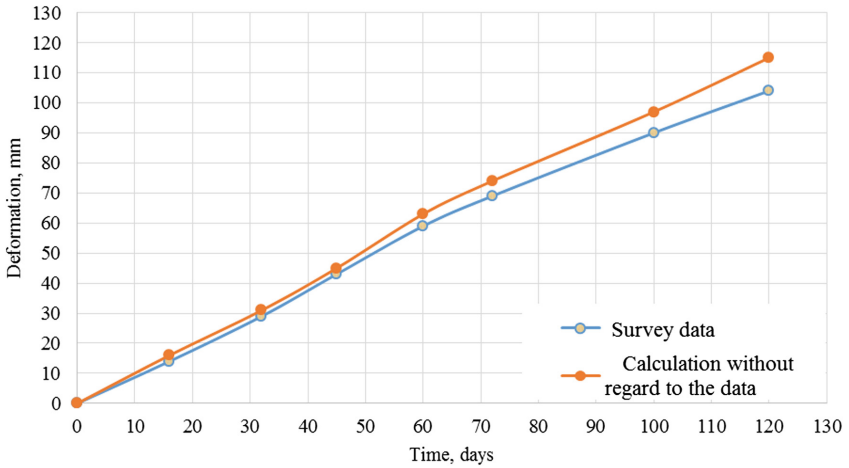


Fig. 3. Deformations of the slope surface under the design results and the geodesic monitoring data.

As is clear from Table 1, deformations under the design results are on the average higher for 12.2%, than shifts of the slope surface under the geodesic monitoring data. Probable reasons of such error are described above.

The secondary consolidation end time is one of important factors on road engineering next to the slopes or on their surface. The given factor allows to consider

Table 1. Comparison of the preliminary design results with the geodesic monitoring results.

Cycles	1	2	3	4
Geodesic monitoring results	14	29	43	59
Initial design results	16.1	33.2	48.5	66.2

development of road engineering and to envisage the engineering protection techniques subject to the minimum finance and labor costs. The secondary consolidation time in such case shall be calculated with the utmost accuracy. That is why road engineering on the slopes requires all-inclusive studies of the project site conditions with use of the engineering geodesics and soil mechanics techniques.

Let’s run the calculation repeatedly and use the soil characteristics values increased for 12.2%, i.e., for the difference between the preliminary calculations results and the geodesic monitoring data. Table 2 summarizes the changed soils deformability parameters subject to the joint analysis of the initial design results and the geodesic monitoring data.

Table 2. Updating the soils deformability parameters.

# of the engineering geological element	Parameters	Initial ones, unit fractions	Correction factor	Corrected parameters, unit fractions
H1 and H2	C_c	0.00015	1.122	0.00017
	C_s	0.00006		0.00007
	C_α	0.0002		0.0002
1	C_c	0.00009		0.00010
	C_s	0.000032		0.000036
	C_α	0.00015		0.00017
2	C_c	0.00025		0.00028
	C_s	0.00009		0.00010
	C_α	0.00035		0.00039
3	C_c	0.00018		0.00020
	C_s	0.00005		0.00006
	C_α	0.00023		0.00026
4	C_c	0.00022		0.00025
	C_s	0.00008		0.00009
	C_α	0.00031		0.00035
5	C_c	0.00013		0.00015
	C_s	0.00005		0.00006
	C_α	0.00022		0.00025

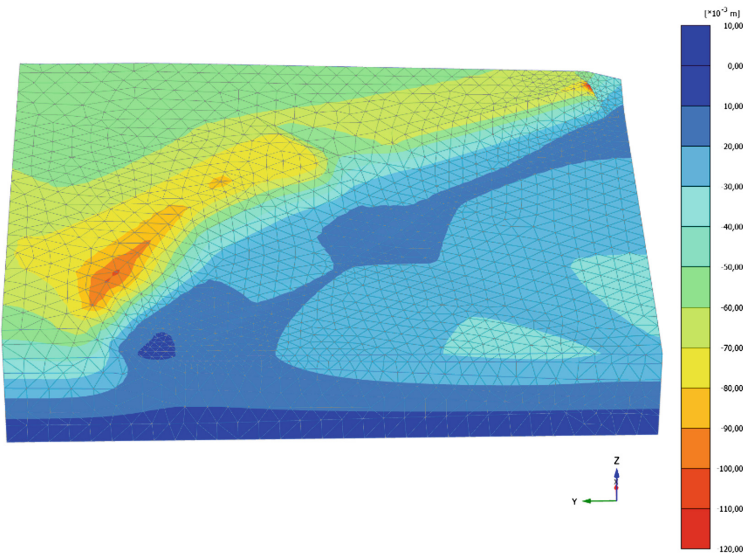
Results of such calculation can be compared with results of all geodesic monitoring cycles (Table 3).

Table 3. Comparison of the updated calculation results with the geodesic monitoring results.

# of cycle	1	2	3	4	5	6	7
Geodesic monitoring data	14	29	43	59	69	90	104
Updated calculation results	13.2	28.1	40.6	55.2	65.4	87.1	103.2

Subject to the good reproducibility of the design results with the geodesic monitoring data of the slope surface one can say that the methodology proposed in this Paper allows to forecast time deformations of the slopes surface. Accurate forecast of the slope surface time deformations will allow to provide road engineering on its surface with the maximum economic gain.

Calculation results with the updated base soil characteristics are summarized below. Figure 4 demonstrates the slope surface deformations isofields showing that deformations of the slope surface are, on the average, for 10% less, and, thus, saying that the geomechanical model is closer to the real slope behavior. To provide more objective assessment, the calculation results were processed with use of the statistical probability techniques. 46 points used in the engineering geodesic process were also taken as the measurements points. Figure 5 shows the average slope deformations with reference to the engineering geodesic stages under the preliminary calculation and under the calculation with the updated base soil characteristics and the engineering geodesic data. As it is clear from the plot, the geomechanical model with the updated soil characteristics behaves more closely in relation to the real slope versus the initial one.

**Fig. 4.** Slope deformations isofields at the secondary consolidation stage with the updated base soils characteristics on termination of the geodesic monitoring process.

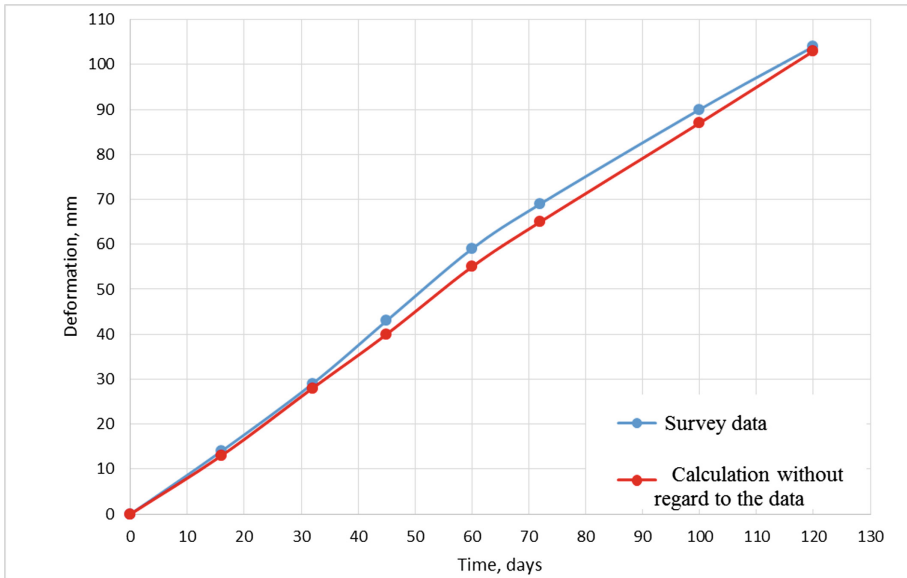


Fig. 5. Deformations of the slope surface acc. to the calculation results and the geodesic monitoring data.

The above packaged evaluation techniques and calculation of the slopes SSS subject to the base soil creep allow to build the geomechanical model being the closest one to the natural slope. It should be noted that such approximation is wrapped up in the geodesic monitoring cycles' number. The above calculations demonstrate the geodesic monitoring data sufficient to provide reproducibility of the calculation results with the updated soil characteristics up to 2%, which says on the general good reproducibility of the given methodology.

The geomechanical slope model obtained under the packaged data analysis allows to assess the slope deformations in the long term. The deformations values and the secondary consolidation end time are the main two parameters of the slope analysis allowing to evaluate the need for the engineering slope protection measures.

The slope surface deformations were designed subject to and ignoring the geodesic monitoring results to evaluate deformations after the secondary base soils consolidation and its end time. Both calculations were run subject to the following stages:

1. Generation of the initial soil stresses (Gravity Loading Procedure);
2. Calculation of the filtration (primary) soil consolidation up to the minimum excessive porous pressure;
3. Time calculation of the secondary consolidation up to its termination.

The results of such calculations are presented below. To provide more objective evaluation, the calculation results were processed with the statistical probability techniques. The 46 points used in the engineering geodesic surveys process were also taken as the

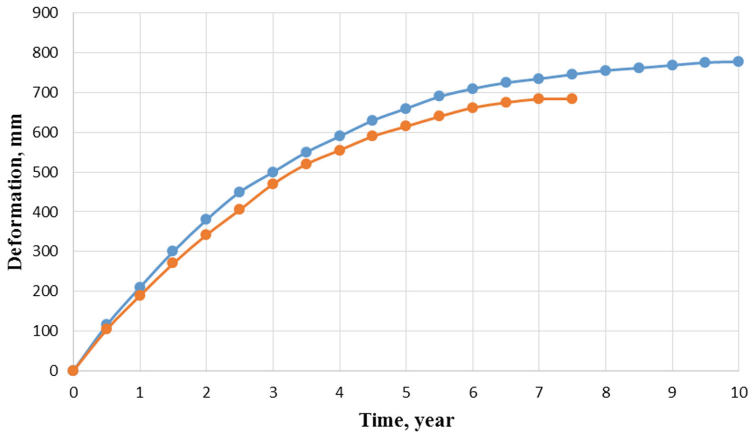


Fig. 6. Crossplot of the average slope surface deformation versus time ignoring (blue line) and subject to the (red line) geodesic monitoring results.

measurements points. Figure 6 shows the crossplot of the average slope surface deformation versus time ignoring and subject to the geodesic monitoring results, accordingly.

According to the run designs, the secondary consolidation end time ignoring the geodesic monitoring data is equal to 9.7 years, and the one subject to the data is 7.2 years; the average deformations of the slope surface differ for 12% - 778 and 684 mm, accordingly.

3 Conclusions




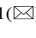

Results of all designs above demonstrate that the packaged soil deformation analysis with the engineering geodesics and soil mechanics techniques application allows to forecast time deformations of soil bodies with the utmost accuracy, and thus will allow to cut risks while making road engineering for the slide-hazardous slopes and provide safety of roads and highways in mountainous areas.

References

1. Recommendations for the subgrade design of roads in difficult geotechnical conditions, Moscow (1974)
2. Ukhov, S., Semenov, V., Znamensky, V.: The mechanics of soils, bases and foundations. Tutorial for Building Specialized Colleges, Higher School, Moscow (2007)
3. Ter-Martirosyan, Z.: Soil Mechanics. Association Building Universities (2009)
4. Golovanov, A., Berezhnaya, D.: The Finite Element Method in the Mechanics of Deformable Solids. DAS, Kazan (2001)
5. Fadeev, A.: The Finite Element Method in Geomechanics. Nedra, Moscow (1987)

6. Zamensky, V., Ruzaev, A., Polinkov, I.: Comparison of the results of field experiments with calculations using finite element program PLAXIS 3D foundation for driven piles in clay soils. *Vestnik MGSU* **2**, 18–23 (2008)
7. Vlasov, A., Volkov-Bogorodskij, D., Znamenskij, V., Mnushkin, M.: Finite element modeling of problems of geomechanics and geophysics. In: *Proceedings of Moscow State University of Civil Engineering*, vol. 2, pp. 52–65 (2012)
8. Simonyan, V., Tamrazyan, A., Kochiev, A.: Theoretical substantiation of construction of the generalized mean-square displacements of ellipsoids landslides. *Geodesy Cartogr.* **12**, 10–14 (2015)
9. Simonyan, V.: *The Study of Landslide Processes Geodetic Methods: A Monograph*. MGSU, Moscow (2015)
10. Brinkgreve, R.: Selection of soil models and parameters for geotechnical engineering application. In: *Soil Constitutive Models: Evaluation, Selection, and Calibration*, vol. 128, pp. 69–98. American Society of Civil Engineers (2005)
11. Barla, M., Barla, G.: Torino subsoil characterization by combining site investigations and numerical modelling. *Geomech. Tunelling* **3**, 214–232 (2012)
12. Benz, T., Schwab, R., Vermeer, P.: On the practical use of advanced constitutive laws in finite element foundation analysis. In: *FONDSUP 2003 International Symposium*, pp. 8–16 (2013)
13. Vermeer, P., Stolle, D., Bonnier, P.: From the classical theory of secondary compression to modern creep analysis. In: *9th International Conference on Computer Methods and Advances in Geomechanics*, vol. 4, pp. 2469–2478 (1998)
14. Augustesen, A., Liingaard, M., Lade, P.: Evaluation of time-dependent behavior of soils. *Int. J. Geomech.* **3**(137), 137–156 (2004)
15. Yin, Z., Karstunen, M., Chang, C., Koskinen, M., Lojander, M.: Modeling time-dependent behavior of soft sensitive clay. *J. Geotech. Geoenviron.* **137**, 1103–1113 (2011)
16. Petalas, A., Galavi, V.: *PLAXIS Liquefaction Model UBC3D-PLM* (2013). <http://kb.plaxis.nl/models/udsmubcsand3d-model>. Accessed 27 Aug 2017

Fire Resistance of Prefabricated Monolithic Reinforced Concrete Slabs of “Marko” Technology

Ekaterina Nedviga¹ , Natalia Beresneva¹ , Marina Gravit¹  ,
and Angelina Blagodatskaya² 

¹ Peter the Great St. Petersburg Polytechnic University,
Politechnicheskaya St., 29, Saint-Petersburg 195251, Russia

marina.gravit@mail.ru

² Moscow State University of Civil Engineering,
Yaroslavskoe shosse, 26, Moscow 129337, Russia

Abstract. Prefabricated monolithic slabs represent a construction structure that effectively combines the positive properties of precast reinforced concrete structures and monolithic concrete with additional reinforcement. Systems of the prefabricated monolithic constructions correspond to the modern trends, but require special attention and scrutiny. There are results of prefabricated monolithic slab fire test in the article. The prototype of the reinforced concrete slab was installed on the fire chamber of the test installation with an applied static load in accordance with the design scheme. There are results of prefabricated monolithic slab fire test on the temperature effect in the article. Signs of construction limit states and collapse of the structure were not registered after 125-min fire testing, and also there are no through cracks and holes on the unheated side of the samples. Visual inspection of prototypes of prefabricated monolithic reinforced concrete slab was carried out after their removal from the test installation, according to the results of which it was established that there was no deformation (kink), a slight damage to the heated surface and no destruction of the metal and concrete of beams. To create a methodology for calculating the prefabricated monolithic slab on the flame impingement, it is necessary to carry out further tests for fire resistance taking into account the span of the structure, as well as the type of filling blocks.

Keywords: Transport buildings and structures
Prefabricated monolithic slabs · Fire resistance

1 Introduction

Prefabricated monolithic reinforced concrete slabs (PMS) are a new, technologically and economically advantageous type of structures [1–4]. Prefabricated monolithic slabs can significantly reduce the weight of the structure while maintaining the required carrying force and increase the heat insulating properties [5–12]. Use of PMS let to reduce construction time and costs with no loss of performance durability, reliability

and quality [13], and does not require a complicated construction equipment and therefore eliminates the cost of their maintenance and operation [14, 15].

In European countries the design of buildings and civil structures made of reinforced concrete, as well as calculations for fire resistance of structures are carried out in accordance with EN 1992 EUROCODE 2. In the territory of the Russian Federation, calculations of reinforced concrete structures in the fire conditions are carried out in accordance with STO 36554501-006-2006, in which prefabricated monolithic ceilings are not included [16].

The authors analyze the fire resistance test for the structures of prefabricated monolithic slabs of the Russian manufacturer of PMS systems «PMS MARKO», made in the testing laboratory of the scientific and testing center of fire safety of the FGU VNIPO of EMERCOM of Russia.

2 Materials and Methods

The objects of the test are samples of prefabricated monolithic reinforced concrete slab consisting of four beams «MARKO-universal» with filling blocks of dimensions $200 \times 250 \times 600$ mm and density D400 and monolithic concrete BST B25 P4 GOST 7473-2010 reinforced steel mat (technology – «PMS MARKO») (Fig. 1).

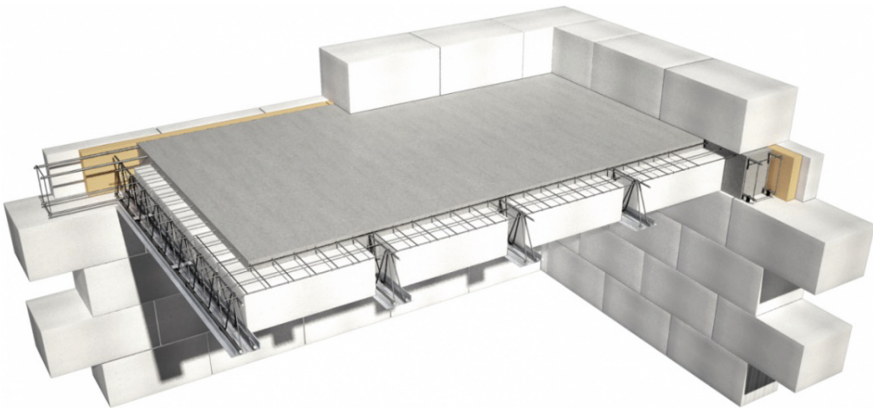


Fig. 1. Structures of PMS «MARKO-aeroc» with beams «MARKO-universal».

The methodology of testing of building structures for fire resistance is described in the international standard ISO 834-75 «Fire resistance tests. Elements of building constructions» (in the updated version – ISO 834-1:1999). The Russian standards on fire resistance are based on the provisions of the following international standards: ISO 834-75, ST COMECON 1000-88 and part of the provisions of national standards BS 476-10, CSN 730-85, DIN 4102-2 etc. [17, 18].

Tests of samples of prefabricated monolithic reinforced concrete slab in order to determine the fire resistance limit in the territory of the Russian Federation are carried out in accordance with GOST 30247.0-94 «Elements of building constructions. Fire resistance tests methods. General requirements» и GOST 30247.1-94 «Elements of building constructions. Fire-resistance tests methods. Load-bearing and separating constructions».

2.1 Description of the Test Object

Two prototypes of prefabricated monolithic reinforced concrete slabs with dimensions of $6300 \times 2296 \times 250$ mm each were presented for the tests.

The main structural elements of the PMS, carried out according to the technology «PMS MARKO», are welded reinforcing beams, which form the bearing ribs in the design position, along which the aerocrete blocks were laid, after which the concrete was poured.

In the upper zone the monolithic reinforced concrete slab is reinforced with steel mat with a cell size of 100×100 mm, made of wire with a diameter of 4 mm.

At the time of the tests, the age of the monolithic concrete of the prototypes of the overhead structure was more than 28 days (Table 1).

Table 1. Test conditions.

	Experiment No. 1	Experiment No. 2
Date of the event	20.03.2017	23.03.2017
Ambient temperature, °C	14	15
Relative air humidity, %	48	50
Speed of air movement, m/s	≤ 0.5	≤ 0.5

In Fig. 2 shows a sample prepared for testing of a reinforced concrete slab with an applied static load in accordance with design scheme.

2.2 Test Procedure

Experimental samples of prefabricated monolithic reinforced concrete slab are installed on the fire chamber of the test installation and subjected to unilateral thermal action according to the standard temperature regime in accordance with GOST 30247.0-94.

Fire tests are carried out under the influence of a static load transmitted through the system of its distribution to four points of the working span of the slab in accordance with the design and calculation scheme shown in Fig. 3. Load transfer is carried out using a loading system that includes a hydraulic jack with a capacity of 200 tons, a device for applying the load, as well as a steel frame for sensing the loading force (Figs. 2 and 3). The load value is 56.41 kN (5.75 tons) per sample slab, which



Fig. 2. An experimental sample of a reinforced concrete slab of a ceiling installed on the fire chamber of a test installation with an applied static load in accordance with the design scheme.

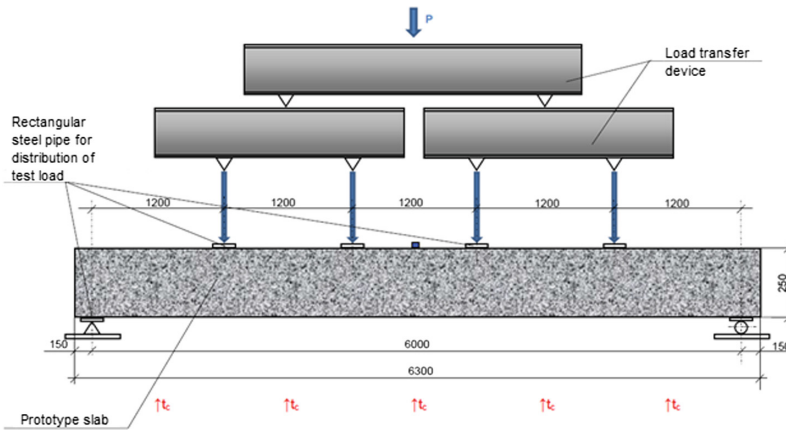


Fig. 3. The scheme of support and loading of a prototype of a reinforced concrete slab.

corresponds to 4.9 kPa (500 kg/m²). The test load on the test specimens is established 60 min before the start of the tests and is maintained constant (with an accuracy of at least $\pm 5\%$) during the entire time of their conduct. Samples of reinforced concrete slab have a 2-sided support on the hinge-fixed and hinge-mobile supports. The distance from the ends of the slab to the hinged supports is 150 mm. Thus, the working span of a reinforced concrete slab is 6000 mm. Kinks in the middle of the span, during loading and during the testing are measured by flexometer MP-3. At the time of the start of flame impingement, the kink of the reinforced concrete slab No. 1 is 3.0 mm, sample No. 2 is 3.2 mm. The temperature in the fire chamber is measured by furnace

thermoelectric converters uniformly distributed along the length of the sample in seven places, and on the experimental samples the temperature is measured by thermoelectric converters THA set in an amount of 5 pieces in accordance with the requirements set out in clause 7.3.1 of GOST 30247.1-94.

- $\uparrow t_c$ — direction of thermal impact on the prototype;
- $\downarrow P$ — direction of impact and load distribution;
- — kink measuring point.

3 Results

During the tests, the following characteristic features of the behavior of the prototypes of the PMS: 35 min - there is a slight evaporation of moisture on the unheated surface, which lasted 25–30 min (Fig. 4).

- t_B, t - standard temperature curve;
- - - upper and lower permissible limits of deviation from t_B, t ;
- average temperature in the furnace fire chamber, experiment No. 1 (sample No. 1);
- average temperature in the furnace fire chamber, experiment No. 2 (sample No. 2);
- average temperature on the unexposed surface of the slab, sample No. 1;
- average temperature on the unexposed surface of the slab, sample No. 2;
- × — kink in the middle of span of the slab, sample No. 1;
- — kink in the middle of span of the slab, sample No. 2

Further visible changes, with the exception of the growth of kink, were not recorded in the state of the samples (Fig. 5).

At the time of the end of the fire impact (125 min), no collapse of the test samples of the prefabricated monolithic slab occurred. The kink value reached 264 and 262 mm for the first and second samples, respectively.

The average temperature on the unheated surface was 36 and 38 °C for the first and second samples, respectively. The temperature rise on the unheated surface at one of the monitored points in comparison with the temperature before the test by more than 180 °C during the testing was not recorded.

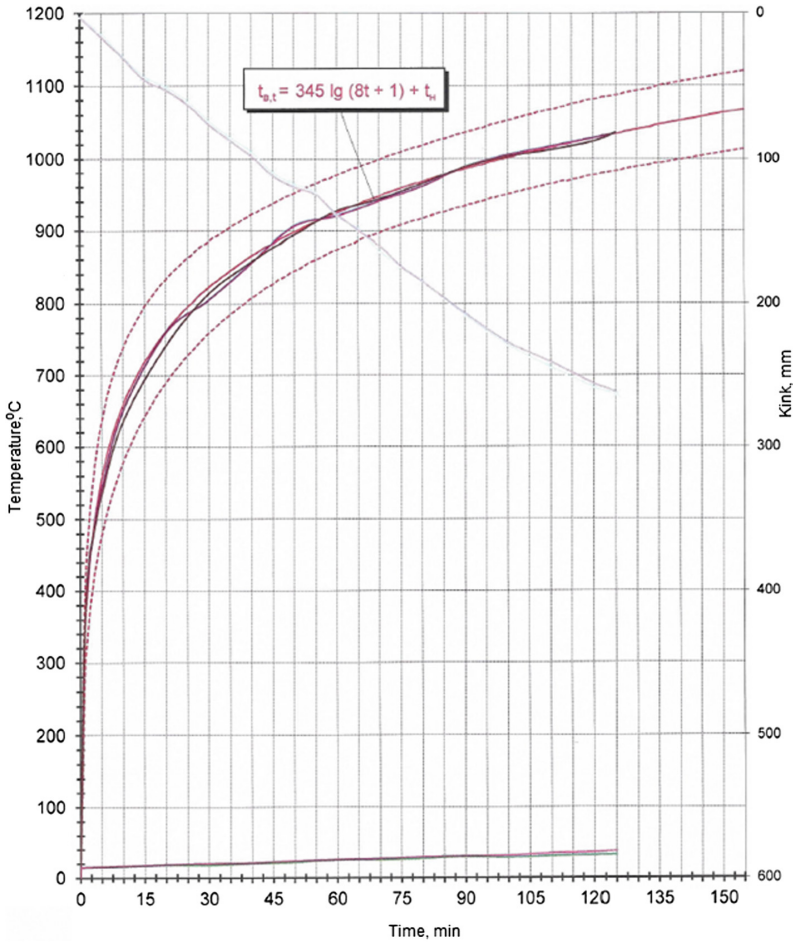


Fig. 4. Curves of changes in temperatures and growth of kinks, prototypes of prefabricated monolithic reinforced concrete slabs.

The average temperatures in the fire chamber did not exceed the permissible deviations in accordance with GOST 30247.0-94. The curves for the temperature and kink of the experimental PMS samples are shown in Fig. 4.

During the tests on the unheated side, no through cracks or holes are also fixed. Thus, none of the limiting states during the time of fire tests was achieved.

After the removal of the test load and the cooling of the prototypes, a partial restoration of the structures was observed, characterized by a decrease in the deformation (kink) of reinforced concrete slabs.



Fig. 5. 95-min test, prototype No. 1.



Fig. 6. Prototype No. 2 after the test, view of the lower (heated) side of the slab.

4 Discussion

The building or structure must be designed and constructed in such a way that in case of a fire it maintains stability [19] and the strength of the load-bearing structures during the time necessary for the evacuation of people and actions aimed at reducing the

damage from the fire, and also limited the formation and spread of dangerous factors within the fire area. Therefore, when designing load-bearing structures, special attention should be given to their fire resistance. The fire resistance index of a structure is the fire resistance limit [20–22].

You can achieve the required fire resistance of reinforced concrete structures in several ways:

- the designation of the optimum section of the structure, the limiting state of which does not come within the required fire resistance limit [23, 24];
- application of fire protection means for building structures, including those with heat-insulating properties [25–27].

The second method is expensive in most cases and requires additional time. Also, some fire retardant coatings and materials have a certain shelf life, after which it is necessary to reuse them or it is required to provide free access to the structure for monitoring the state of fire protection [28]. Therefore, the most economical option is the proof that PMS provide the resistance of load-bearing elements to the flame impingement without constructive fire protection.

The fire resistance limit of the reinforced concrete structure comes when the working reinforcement in the construction is heated to the critical temperature, and also when the concrete is heated in the calculated section above its critical temperature [29–31].

Limit of fire resistance of building structures is established in minutes before the onset of one or several successive signs of limiting states [32].

For interstitial ceilings, the limiting states in the fire resistance test, in accordance with GOST 30247.1-94, are the loss of carrying force (R) due to collapse of the structure or occurrence of ultimate deformations (the maximum kink in the middle of the span for a given slab is 300 mm, the rate of increase of deformation is more than 1.6 cm/min); loss of integrity (E); loss of thermal insulation capacity (I).

According to Federal Law No. 123-FZ dated 22.07.2008 “Technical regulations on fire safety requirements”, multi-storey and residential buildings in the RF, predominantly related to the I and II degrees of fire resistance, shall provide the fire resistance limit of load-bearing structures of the interstitial floors (including attic and above the basement), respectively, equal to REI 60 and REI 45 and beams - R 30 and R 15. If the structure is involved in providing stability and spatial rigidity - R 120 and R 90 (Table 21, No. 123-FZ).

In accordance with the European standard EN 1992-1-2:2004 Eurocode 2: Design of concrete structures – Part 1-2: General rules – Structural fire design requirements for the minimum limit of fire resistance of load-bearing structures [33].

Since beams of «MARKO-universal» have a section of 125 × 250 mm with a wall thickness of 50 mm, according to Table 5.6 of EN 1992-1-2 the fire resistance limit is R 60. For flat reinforced concrete slabs (including prestressed ones) of 250 mm thickness according to Table 5.9 of EN 1992-1-2, the fire resistance limit is not less than REI 90.

For the widespread introduction of PMS in the practice of building multi-storey public and residential buildings, it is necessary to test such slabs for fire impact to

determine the fire resistance of structures and the subsequent creation of regulatory documents.

According to the tests carried out, the fire resistance limit of the type of prefabricated monolithic reinforced concrete slab, consisting of beams «MARKO-universal» with filling concrete blocks and monolithic concrete reinforced with steel mat, according to «PMS MARKO» technology, tested under the action of a constant static load equal to 56.41 kN (5.75 tons), which corresponds to 4.9 kPa (500 kg/m²), distributed over the four points of the working span, without taking into account the own weight of the slab, on the loss of carrying force (R), loss of integrity (E) and loss of thermal insulation capacity (I) – Not less than 125 min, which corresponds to the classification of REI 120 in accordance with GOST 30247.0-94.

5 Conclusions

The results of experimental studies showed positive results of the design of the prefabricated monolithic slab. After 125 min of testing were not recorded:

- collapse of prototypes;
- through cracks or openings on the unheated side of the samples;

Visual inspection of prototypes of prefabricated monolithic reinforced concrete slab after their removal from the test facility showed:

- slight deformation (kink) of prototypes of the PMS;
- slight damage to the lower (heated) surface of the samples;
- absence of destruction of metal and protective layer of concrete bearing beams (Fig. 6).

To create a methodology for calculating PMS for fire impact, it is necessary to conduct a series of tests on fire resistance, which will take into account changes in the size of the span of the structure, as well as the effect of various types of hollow and solid lightweight aggregates.



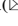
References

1. Teplova, Z., Vinogradova, N.: Combined and monolithic overlappings of “MARKO” system. *Constr. Unique Build. Struct.* **8**(35), 48–59 (2015)
2. Mel’nik, I., Sorokhtey, V., Pristavskiy, T.: Pilot studies of deformation fragments of monolithic flat reinforced concrete overlapping with polystyrene foam inserts. *Bull. Belarus-Russ. Univ.* **4**(49), 103–112 (2015)
3. Selyaev, V., Tsyganov, V., Utkin, Yu.: The combined combined and monolithic overlappings on the basis of previously strained reinforced concrete beams of bezopalubochny formation. *Reg. Archit. Eng.* **3**, 5–11 (2012)
4. Shipulya, A.: Refinement of deformative characteristics in determining of deflections in flat plate floor. *Her. Ural State Univ. Railw. Transp.* **1**(13), 81–86 (2012)
5. Nedviga, E., Vinogradova, N.: Systems of prefabricated monolithic slabs. *Constr. Unique Build. Struct.* **4**(43), 87–102 (2016)

6. Parashchenko, N., Gorshkov, A., Vatin, N.: Partly ribbed combined and monolithic overlappings with cellular concrete blocks. *Mag. Civ. Eng.* **6**, 50–68 (2011)
7. Kaveh, A., Behnam, A.: Cost optimization of a composite floor system, one-way waffle slab, and concrete slab formwork using a charged system search algorithm. *Scientia Iranica* **19**, 410–416 (2012)
8. Al-Bayati Ahmed, F., Lau Teck, L., Clark, L.: Concentric punching shear of waffle slab. *Struct. J.* **112**, 533–542 (2015)
9. Abdolreza, A., Bradford Mark, A., Liu, X.: Experimental study of composite beams having a precast geopolymer concrete slab and deconstructable bolted shear connectors. *Eng. Struct.* **114**, 1–13 (2016)
10. Fernandez-Cenceros, J., Fernandez-Martinez, R., Fraile-Garcia, E., Martinez-de-Pison, F.: Decision support model for one-way floor slab design: a sustainable approach. *Autom. Constr.* **35**, 460–470 (2013)
11. Ibrahim, A., Salim, H., El-Din, H.: Moment coefficients for design of waffle slabs with and without openings. *Eng. Struct.* **33**, 2644–2652 (2011)
12. Pushkarev, B., Koren'kov, P.: Combined and monolithic reinforced concrete designs, scopes of application and features of calculation. *Constr. Technog. Saf.* **46**, 30–35 (2013)
13. Pettisold, T., Tura, V.: *Reinforced Concrete Structures: Basic Theory, Analysis and Design*. BGTU, Brest (2003)
14. Sagadeev, R.: *Modern methods of construction of monolithic and combined and monolithic overlappings*. GOU DPOGASIS, Moscow (2008)
15. Babkov, V., Samofeev, N., Hajrullin, V., Klyavlina, Y., Knyazeva, O.: Feasibility study for the introduction of solutions precast and precast-monolithic expanded-clay concrete versions of coverings and overlappings in the housing projects of the Republic of Bashkortostan. *Naukovedenie* 7(1) (2015)
16. Gravit, M., Nedviga, E., Vinogradova, N., Teplova, Z.: Fireproof of prefabricated monolithic multiribbed plate with rolled steel beam. *Constr. Unique Build. Struct.* **12**(51), 73–83 (2016)
17. Gravit, M.: Fire resistance of building constructions in the European and Russian standards. *Stan. Qual.* **2**(919), 36–37 (2014)
18. Gravit, M.: The new standard regulating distribution results of fire resistance tests for the translucent non-bearing enclosure structures. In: *Materials of a Scientific and Practical Conference* (2015)
19. Baran Eray, A.: Effects of cast-in-place concrete topping on flexural response of precast concrete hollow-core slabs. *Eng. Struct.* **98**, 109–117 (2015)
20. Heinisuo, M., Laasonen, M., Outinen, J., Hietaniemi, J.: Systematisation of design fire loads in an integrated fire design system. In: *Application of Structural Fire Design*, Prague (2015)
21. Milovanov, A.: *Durability of Reinforced Concrete Structures in Case of Fire*. Stroyizdat, Moscow (1998)
22. Epshtein, S.A., Adamtsevich, A.O., Gavrilova, D.I., Kossovich, E.L.: Thermal methods exploitation for coals propensity to oxidation and self-ignition study. *Gornyi Zhurnal* **7**, 100–104 (2016). <https://doi.org/10.17580/gzh.2016.07.22>
23. Kolomiitsev, D.: Fire endurance of inserted floor in terms of C section. *Mag. Civ. Eng.* **8** (18), 32–37 (2010)
24. Venanzi, I., Breccolotti, M., D'Alessandro, A., Materazzi, A.: Fire performance assessment of HPLWC hollow core slabs through full-scale furnace testing. *Fire Saf. J.* **69**, 12–22 (2014)
25. Arshad, A., Siti Ayesah, H., Adnan, R., Mohamad, W., Saharudin, H.: A risk-based method for determining passive fire protection adequacy. *Fire Saf. J.* **58**, 160–169 (2013)
26. Gravit, M., Gumenyuk, V., Nedryshkin, O.: Fire resistance parameters for glazed non-load-bearing curtain walling structures. *Procedia Eng.* **117**, 114–118 (2015)

27. Gravit, M., Gumenyuk, V., Sychoy, M., Nedryshkin, O.: Estimation of the pores dimensions of intumescent coatings for increase the fire resistance of building structures. *Procedia Eng.* **117**, 119–125 (2015)
28. Nedviga, E., Solov'yeva, K., Kiselev, S.: Ways of fire protection of metal and reinforced concrete building constructions. *Young Sci.* **24**(104), 160–163 (2015)
29. Pustovgar, A., Tanasoglo, A., Garanzha, I., Shilova, L., Adamtsevich, A.: Optimal design of lattice metal constructions of overhead power transmission lines. In: *MATEC Web of Conferences*, vol. 86, article no. 04003 (2016). <https://doi.org/10.1051/mateconf/20168604003>
30. Bonić, Z., Čurčić, G.T., Trivunić, M., Davidović, N., Vatin, N.: Some methods of protection of concrete and reinforcement of reinforced-concrete foundations exposed to environmental impacts. *Procedia Eng.* **117**, 419–430 (2015)
31. Pashkevich, S., Pustovgar, A., Adamtsevich, A., Eremin, A.: Pore structure formation of modified cement systems, hardening over the temperature range from +22 °C to –10 °C. *Appl. Mech. Mater.* **584–586**, 1659–1664 (2014). <https://doi.org/10.4028/www.scientific.net/AMM.584-586.1659>
32. Belov, V., Semenov, K., Renev, I.: About the directions of development of methods of assessment of fire resistance of reinforced concrete designs. *Mag. Civ. Eng.* **6**(16), 58–61 (2010)
33. Pashkevich, S., Pustovgar, A., Eremin, A., Adamtsevich, A., Nefedov, S.: PEG molecular weight effects on physical and mechanical properties of ETICS plaster, hardening at lowered positive and small negative temperatures. *Adv. Mater. Res.* **1004–1005**, 1482–1485 (2014). <https://doi.org/10.4028/www.scientific.net/AMR.1004-1005.1482>

Mechanization of Technological Processes Assembly of Threaded Joints

Anatoly Drozdov  and Vitaliy Stepanov  

Moscow State University of Civil Engineering,
Yaroslavskoye Sh. 26, 129337 Moscow, Russia
mms@mgsu.ru

Abstract. The paper proposes a methodology to calculate indicators of the process of tightening threaded joints using impact wrenches. Such indicators include the “moment – number impacts” diagram, and the limiting tightening torque. Calculations consider the elastic-friction properties of the joint itself and the energy of single impact by the wrench. Having no data on wrench energy, we provide a method to measure it indirectly in production conditions based on the proposed methodology. The computing algorithm has produced accuracy level sufficient for engineering calculations (at least 10%) in the course of tests. The resulting methodology reduces bolt driver calibration time and improves accuracy of assembly manipulations; it also identifies the area of rational use of available assembly tools. The above aspects are particularly relevant when critical joints are assembled.

Keywords: Impact wrench · Power tools · Threaded joints
Mechanization of construction

1 Introduction

Mechanized assembly of threaded joints in the threading diameter range of M8...M24 uses manual impact wrenches. Currently, their manufacturers quote as their technical characteristics such indicators as the maximum torque, threading diameter range, and impact frequency. It is known that the torque of a wrench depends a lot on rigidity of the bolt and the pack of parts bolted together. In fact, the maximum torque stated in the certificate is the force the wrench can overcome in the releasing mode. Thus, this information is insufficient for assembly processes. Energy of single impact is a more versatile indicator for impacting machines. This paper proposes an engineering methodology that can be used to measure energy of single impact wrenches during production, and for mechanization of production processes for assembly of threaded joints.

Examination of available literature [1–15] identified a lot of interest to the issues of threaded joints and related tightening methods. In [1], the authors address the issue of raising the efficiency and accuracy of a mathematical model of an electric impact wrench for further optimization of its design. General issues with design strength of threaded joints are covered in [2]. Simulation of impact tightening of threaded joints is discussed in [3, 6]. The studies worked out a new model that considers dynamic yield

of the impact mechanism, spindle shaft and the components of the striker’s kinematic pairs. Nonlinear occurrences of contact interactions were considered and examined. Parametric identification is based on the approach of multi-criteria optimization (MCO). The results of calculations correlate with experimental studies of the process of threaded joint tightening in a satisfactory manner. In other studies, the numeric method of finite elements is used to research threaded joints rigidity and contact interactions. Analysis of the studies related to the subject hereof identified absence of reliable means to mechanize the processes of threaded joint assembly.

2 Problem Statement

Presenting a threaded joint as an elastic-friction dynamic model with self-braking as shown in Fig. 1, we can find the analytic formula to find the coordinate of the wrench spindle and the bolt head depending on the energy and number of impacts [2].

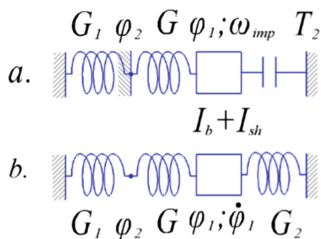


Fig. 1. Dynamic model of threaded joint during impact tightening: a – in tightening mode with fixed thread; b – in traction mode, G_1 – torsional rigidity of spring emulating yield of parts; G – torsional rigidity of bolt; φ_1 – angular coordinate of bolt; φ_2 – angular coordinate of self-braking element (threading); I_{sh} – inertia moment of spindle; I_b – inertia moment of bolt; T_2 – moment of friction under bolt head; ω_{imp} – post-impact velocity of wrench spindle.

3 Results of Mathematical Model Analysis

Mathematical model of the impact tightening process for the dynamic diameter (Fig. 1) is described with a piecewise-linear equation of type:

- in tightening mode with a fixed thread

$$(I_{sh} + I_b)\ddot{\varphi}_1 + T_2 + G(\varphi_1 - \varphi_2) = 0 \tag{1}$$

$$\varphi_2 = \text{const}$$

- in traction mode

$$(I_{sh} + I_b)\ddot{\varphi}_1 + T_2(\varphi_1) + C_1\varphi_1 = 0 \tag{2}$$

$$\varphi_2 = \frac{G}{G_1 + G} \varphi_1$$

The mathematical model uses the following notation for dynamic parameters:

$$C1 = \frac{GKr^2 \text{tg} \alpha \text{tg}(\rho' + \alpha)}{G + Kr^2 \text{tg} \alpha \text{tg}(\rho' + \alpha)} - \text{reduced rigidity of joint in traction mode};$$

$$G1 = Kr^2 \text{tg} \alpha \text{tg}(\rho' + \alpha) - \text{torsional rigidity of spring emulating yield of parts};$$

$$T_2 = -PRf \text{sign} \varphi_1 - \text{moment of friction under bolt head};$$

$$P = \frac{GKrtg\alpha}{G + Kr^2 \text{tg} \alpha \text{tg}(\rho' + \alpha)} \varphi_1 - \text{tightening force};$$

G – torsional rigidity of bolta; p – threading step; α – lead angle of threading; r – average radius of threading; $\rho' = \arctg \frac{f}{\cos \frac{\beta}{2}}$ – reduced friction angle in thread; f – friction coefficient of friction pair; β – angle of threading profile; R – reduced radius friction on support surface of bolt head; φ_1 – angular coordinate of bolt; φ_2 – angular coordinate of self-breaking element (threading); I_{sh} – inertia moment of spindle; I_b – inertia moment of bolt; $\text{prest}' = \arctg \frac{f_{\text{rest}}}{\cos \frac{\beta}{2}}$ – reduced angle of friction at rest in thread; K – equivalent longitudinal rigidity of bolt and body; $f_{\text{rest}} = kf$ – coefficient of friction at rest.

Analysis of the energy balance equation of the mathematical model produced a recurrent dependency:

$$\varphi_k = \sqrt{E\omega_{\text{imp}}^2 + (E^{\text{rest}} - E\sigma^{\text{rest}})\varphi_{k-1}^2}, \tag{3}$$

where φ_k – coordinate of bolt head, reached after the next impact; φ_{k-1} – coordinate of bolt head after previous impact; E, E^{rest} , σ^{rest} – parameters of specific threaded joint (from Table 1); $\omega_{\text{imp}} = \sqrt{\frac{2E_{\text{imp}}}{I_{sh} + I_b}}$ – post-impact velocity of wrench spindle; E_{imp} – energy of single wrench impact.

Table 1. Numeric values of parameters $E[\text{c}^2]$, E^{rest} , σ^{rest} [c^{-2}] (for spindles $\frac{1}{2}$ ").

E	Stacking distance, mm							
	8	10	12	14	16	20	25	30
M6	1.752e-7	2.04e-7	2.323e-7	2.603e-7	2.881e-7	3.431e-7	4.113e-7	4.791e-7
M8	6.576e-8	7.564e-8	8.535e-8	9.493e-8	1.044e-7	1.231e-7	1.463e-7	1.693e-7
M10	3.096e-8	3.528e-8	3.952e-8	4.369e-8	4.782e-8	5.598e-8	6.604e-8	7.601e-8
M12	1.766e-8	1.996e-8	2.222e-8	2.444e-8	2.663e-8	3.095e-8	3.628e-8	4.157e-8
M16	7.36e-9	8.246e-9	9.117e-9	9.977e-9	1.083e-8	1.252e-8	1.463e-8	1.674e-8
M20	3.502e-9	3.913e-9	4.321e-9	4.73e-9	5.139e-9	5.963e-9	7.01e-9	8.081e-9
M24	1.971e-9	2.209e-9	2.45e-9	2.694e-9	2.943e-9	3.455e-9	4.122e-9	4.823e-9
E	Stacking distance, mm							
	35	40	45	50	55	60	65	70
M6	5.466e-7	6.139e-7	6.811e-7	7.482e-7	8.152e-7	8.822e-7	9.492e-7	1.016e-6

(continued)

Table 1. (continued)

E	Stacking distance, mm							
	35	40	45	50	55	60	65	70
M8	1.921e-7	2.149e-7	2.376e-7	2.603e-7	2.83e-7	3.056e-7	3.283e-7	3.51e-7
M10	8.594e-8	9.584e-8	1.057e-7	1.156e-7	1.255e-7	1.354e-7	1.453e-7	1.553e-7
M12	4.683e-8	5.209e-8	5.735e-8	6.263e-8	6.792e-8	7.323e-8	7.857e-8	8.393e-8
M16	1.886e-8	2.1e-8	2.317e-8	2.537e-8	2.759e-8	2.985e-8	3.214e-8	3.446e-8
M20	9.181e-9	1.031e-8	1.147e-8	1.267e-8	1.391e-8	1.517e-8	1.648e-8	1.782e-8
M24	5.559e-9	6.331e-9	7.14e-9	7.986e-9	8.87e-9	9.793e-9	1.075e-8	1.175e-8
E ^{rest}	Stacking distance, mm							
	8	10	12	14	16	20	25	30
M6	1.01458	1.01566	1.01651	1.01719	1.01775	1.01863	1.01943	1.02002
M8	1.01205	1.01309	1.01393	1.01462	1.01519	1.01611	1.01696	1.01761
M10	1.01037	1.01138	1.01221	1.01289	1.01347	1.0144	1.01529	1.01597
M12	1.00927	1.01026	1.01108	1.01177	1.01236	1.01333	1.01427	1.015
M16	1.00646	1.00725	1.0079	1.00846	1.00895	1.00977	1.01057	1.01121
M20	1.00571	1.00646	1.0071	1.00765	1.00813	1.00895	1.00976	1.01042
M24	1.00513	1.00585	1.00647	1.007	1.00748	1.00828	1.0091	1.00977
E ^{rest}	Stacking distance, mm							
	35	40	45	50	55	60	65	70
M6	1.02048	1.02084	1.02114	1.02139	1.0216	1.02178	1.02193	1.02207
M8	1.01811	1.01852	1.01886	1.01914	1.01938	1.01959	1.01977	1.01993
M10	1.0165	1.01694	1.01731	1.01762	1.01789	1.01812	1.01832	1.0185
M12	1.01559	1.01608	1.01649	1.01684	1.01714	1.01741	1.01764	1.01785
M16	1.01173	1.01217	1.01255	1.01287	1.01316	1.01341	1.01363	1.01383
M20	1.01097	1.01143	1.01183	1.01217	1.01248	1.01275	1.01299	1.01321
M24	1.01032	1.0108	1.01121	1.01157	1.01189	1.01217	1.01243	1.01266
σ^{rest}	Stacking distance, mm							
	8	10	12	14	16	20	25	30
M6	1.867e5	1.723e5	1.594e5	1.481e5	1.382e5	1.218e5	1.06e5	9.377e4
M8	4.06e5	3.837e5	3.618e5	3.413e5	3.225e5	2.9e5	2.57e5	2.306e5
M10	7.372e5	7.101e5	6.797e5	6.491e5	6.197e5	5.661e5	5.094e5	4.622e5
M12	1.116e6	1.093e6	1.06e6	1.024e6	9.871e5	9.161e5	8.366e5	7.677e5
M16	1.875e6	1.876e6	1.85e6	1.811e6	1.764e6	1.665e6	1.542e6	1.43e6
M20	3.483e6	3.527e6	3.508e6	3.454e6	3.379e6	3.204e6	2.974e6	2.753e6
M24	5.557e6	5.654e6	5.635e6	5.549e6	5.424e6	5.12e6	4.713e6	4.323e6
σ^{rest}	Stacking distance, mm							
	35	40	45	50	55	60	65	70
M6	8.407e4	7.618e4	6.964e4	6.414e4	5.944e4	5.538e4	5.184e4	4.872e4
M8	2.09e5	1.911e5	1.759e5	1.63e5	1.518e5	1.421e5	1.335e5	1.259e5
M10	4.226e5	3.891e5	3.603e5	3.354e5	3.136e5	2.945e5	2.774e5	2.622e5
M12	7.082e5	6.566e5	6.116e5	5.72e5	5.369e5	5.056e5	4.776e5	4.523e5
M16	1.328e6	1.237e6	1.156e6	1.084e6	1.018e6	9.59e5	9.054e5	8.567e5
M20	2.55e6	2.366e6	2.2e6	2.051e6	1.916e6	1.794e6	1.683e6	1.582e6
M24	3.964e6	3.641e6	3.351e6	3.093e6	2.861e6	2.654e6	2.468e6	2.3e6

e = 10.

4 Engineering Methodology to Calculate Energy of Wrench Impact

Calculation algorithm of the proposed methodology understands:

1. Finding the bolt coordinate as the wrench switches to the impact mode $\varphi_0 = \frac{T_{st}}{C_1}$, where T_{st} – maximum torque in static mode of the wrench (typically not above 5...8 Hm).
2. Finding post-impact velocity ω_{imp} by preset energy of wrench impact (assuming spindle inertia moment $2.107 \cdot 10^{-5}$ and $9.057 \cdot 10^{-5}$ kg/m² for spindles fitting heads $\frac{1}{2}$ and $\frac{3}{4}$ respectively).
3. Iteration calculation of coordinate with Eq. 3 for a given impact quantity (here k – number of impact) and the respective torque:
4. $T(k) = C_1 \varphi_k$.
5. Finding maximum torque for tightening of the given threaded joint with the given wrench using the formula

$$\varphi_{lim} = \sqrt{\frac{E}{1 - (E^{rest} - E\sigma^{rest})}} \omega_{imp}, T_{lim} = C_1 \varphi_{lim}. \quad (4)$$

6. Finding the energy of wrench impact, by measuring the limiting torque on production site (at representative threaded joint) to compare the measured value and your results from par. 4.

5 Calculation Example

The illustration below quotes the calculated results for a serially manufactured wrench with the following characteristics:

- impact frequency 0...2700 strikes per minute;
- spindle rotation 0...2400 rpm;
- maximum torque 180 Nm;
- spindle with square head $\frac{1}{2}$ " ($I_{sh} = 2.107 \cdot 10^{-5}$ kg/m²);
- bolt diameter up to M12.

Step one calculated tightening indicators using the above algorithm for a number of representative threaded joints:

- joint No. 1. M12 * 8 mm;
- joint No. 2. M12 * 20 mm;
- joint No. 3. M12 * 45 mm.

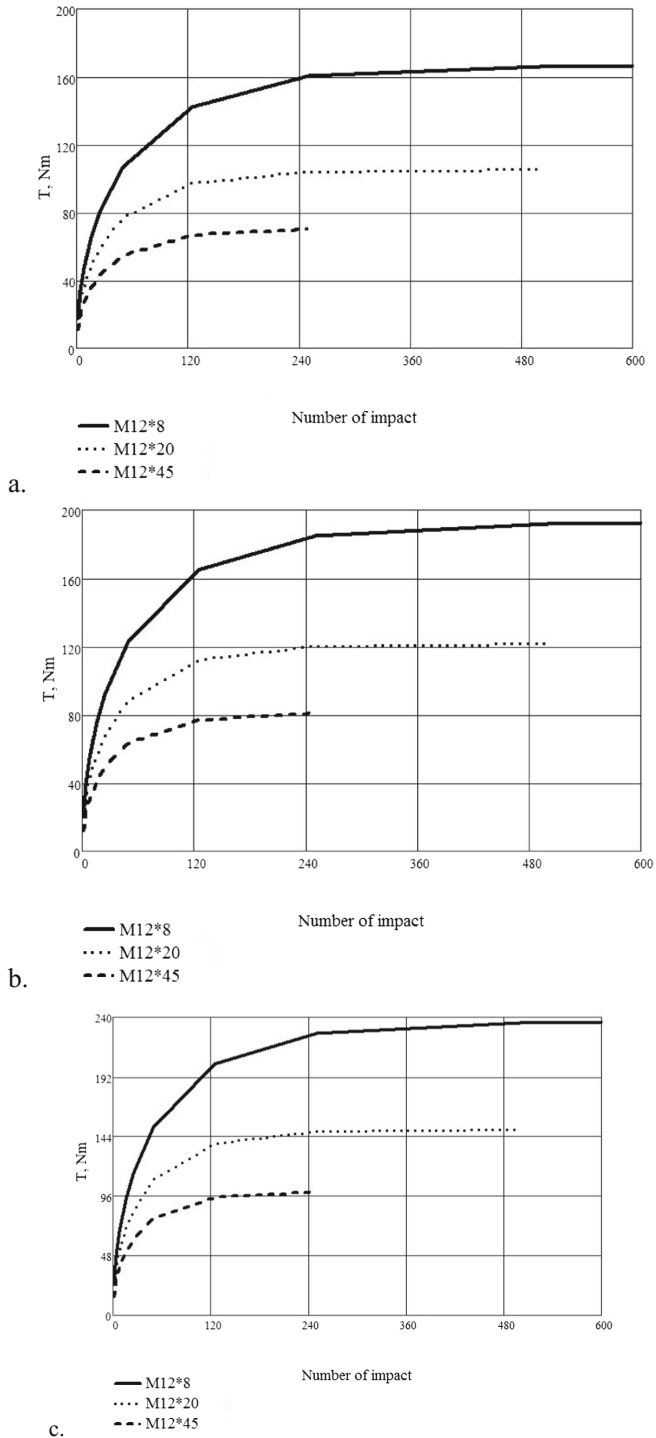


Fig. 2. Theoretical diagrams for tightening of representative threaded joints for different impact energy: (a) $E_{\text{imp}} = 0.6 \text{ J}$; (b) $E_{\text{imp}} = 0.8 \text{ J}$; (c) $E_{\text{imp}} = 1.2 \text{ J}$.

Results of calculation

Reduced rigidity of the threaded joint in traction mode is:

- joint No. 1. $C_1 = 538.895 \text{ N/m}$;
- joint No. 2. $C_1 = 310.175 \text{ N/m}$;
- joint No. 3. $C_1 = 170.514 \text{ N/m}$.

1. Finding the coordinate of the bolt as wrench switches to the impact mode

- joint No. 1. $\varphi_0 = 0.009278 \text{ rad}$;
- joint No. 2. $\varphi_0 = 0.01612 \text{ rad}$;
- joint No. 3. $\varphi_0 = 0.02932 \text{ rad}$.

For $T_{st} = 5 \text{ Nm}$.

2. Finding post-impact velocity ω_{imp} by preset energy of wrench impact

for $E_{imp} = 0.6 \text{ J}$

joint No. 1. $\omega_{imp} = 238 \text{ rad/sec}$;

joint No. 2. $\omega_{imp} = 237 \text{ rad/sec}$;

joint No. 3. $\omega_{imp} = 234 \text{ rad/sec}$

for $E_{imp} = 0.8 \text{ J}$

joint No. 1. $\omega_{imp} = 275 \text{ rad/sec}$;

joint No. 2. $\omega_{imp} = 274 \text{ rad/sec}$;

joint No. 3. $\omega_{imp} = 271 \text{ rad/sec}$

for $E_{imp} = 1.2 \text{ J}$

joint No. 1. $\omega_{imp} = 336 \text{ rad/sec}$;

joint No. 2. $\omega_{imp} = 335 \text{ rad/sec}$;

joint No. 3. $\omega_{imp} = 332 \text{ rad/sec}$

3. Results of iterating calculation of torque depending on number of impacts k are shown in Fig. 2 as curves.

Finding maximum torque for tightening of given threaded joint with given wrench by Eq. (4):

for $E_{imp} = 0.6 \text{ J}$

joint No. 1. $M_{lim} = 167 \text{ Nm}$;

joint No. 2. $M_{lim} = 105 \text{ Nm}$;

joint No. 3. $M_{lim} = 70 \text{ Nm}$

Table 2. Results of wrench tests (mean values for a series of 8 tests).

T, Nm	Control points									
	Tightening time/number of impacts									
	1	2	3	4	5	6	7	8	9	10
	1.3/60	2.6/120	3.9/180	5.2/240	6.5/300	7.7/360	8.9/420	10.1/480	11.4/540	12.7/600
M12 * 8	13	122	149	160	167	170	174	172	173	175
M12 * 20	13	89	103	109	114	112	116	111	113	113
M12 * 45	10	55	70	73	78	80	80	76	77	73

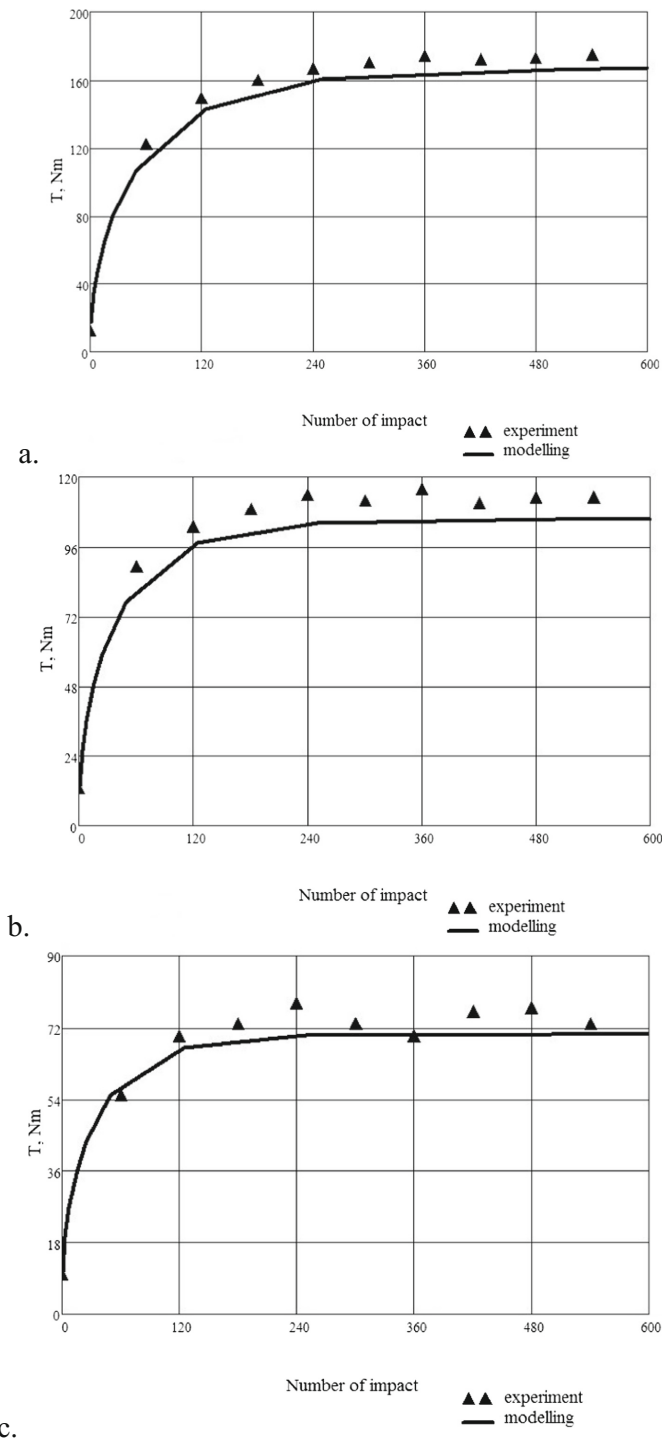


Fig. 3. Comparing estimates and test diagrams for tightening of representative threaded joints for impact energy 0.6 J: (a) M12 * 8 mm; (b) M12 * 20 mm; (c) M12 * 45 mm.

for $E_{imp} = 0.8 \text{ J}$
 joint No. 1. $M_{lim} = 192 \text{ Nm}$;
 joint No. 2. $M_{lim} = 122 \text{ Nm}$;
 joint No. 3. $M_{lim} = 81 \text{ Nm}$
 for $E_{imp} = 1.2 \text{ J}$
 joint No. 1. $M_{lim} = 236 \text{ Nm}$;
 joint No. 2. $M_{lim} = 149 \text{ Nm}$;
 joint No. 3. $M_{lim} = 99 \text{ Nm}$

4. Finding energy of wrench impact and measuring the limiting torque.

Step two of our activities realized par. 5 of the methodology. Tightening torque was measured at 10 control points on the diagram, over equal time intervals of 1.33 s (45 impacts). The wrench was activated and deactivated by an electronic trigger as part of the machine’s electric motor circuit. Torque was measured by a digital dynamometer. Each test was duplicated as a series of 8 tests.

The results of measurements are represented in Table 2 and in Fig. 3. The least departure of values was observed compared to the impact energy curves of 0.6 J.

Table 3. Limiting torques T_{lim} [Nm] for given wrench with $E_{imp} = 0.6 \text{ J}$.

T_{lim}	Stacking distance, mm															
	8	10	12	14	16	20	25	30	35	40	45	50	55	60	65	70
M6	38	34	31	29	27	24	21	20	18	17	16	15	14	14	13	13
M8	70	62	57	53	49	44	39	36	33	31	29	28	27	25	24	24
M10	111	99	91	84	79	70	63	57	53	50	47	44	42	41	39	38
M12	167	149	136	126	118	105	94	86	80	75	70	67	64	61	58	56

Table 3 illustrates limiting torques found with formula (4) for the given wrench used with different bolt sizes. Values above respective standards for strength class 8.8 are highlighted; such joints can be regarded as the reasonable ranges to use the machine under consideration.

6 Conclusions

The main performance indicator for the handheld impact wrench is the single impact energy, but certificates quote its maximum torque and the range of threading diameters of bolts.

On the one hand, this approach simplifies the procedure to select a wrench for any specific production task with non-critical threaded joints. On the other hand, rigidity of threaded joints is overlooked, though for critical structures the tightening torque should be test-selected (calibrated) depending on the time for each specific case.

Single impact energy of the wrench defies accurate analytical measurement or immediate estimation, since it depends on multiple factors.

This paper offers a methodology, the core of which is a mathematical model emulating the process of threaded joint tightening with preset energy and number of impacts. The methodology provides calculation diagrams to describe tightening of several (1 to 5) representative threaded joint designs for different impact energy levels.

Step two puts the wrench through a hot test, after which the estimate diagrams and measured results are compared to find the value of energy impact for the equipment model.

Thus, as we know the impact energy, we can chart a tightening diagram and find the limiting torque for the wrench used with any threaded joint.



Our tests experimentally proved calculation accuracy of the method to be under 10%.

The proposed methodology reduces the time costs for calibration of the bolt driver and improves accuracy of assembly.

References

1. Zhang, Sh., Tang, J.: System-level modeling and parametric identification of electric impact wrench. *J. Manuf. Sci. Eng.* **138**(11) (2016)
2. Braginskij, V.: Dynamics of the screwing of screwed connections with periodic impacts. *Mach. Sci.* **5**, 28–31 (1979)
3. Birger, I., Iosilevich, G.: Threaded links designer library. *Mach. Sci.* (1973)
4. Vodolazskaya, N., Vodolazskaya, E., Iskrickij, V.: Problems and prospects of improving the technology of assembling threaded connections. *Vestnik SevNTU* **128**, 22–26 (2012)
5. Vodolozskaya, N., Vodolazskaya, E., Iskrickij, V.: Thread-tightening assembly tool with tightening torque control according to the number of strokes. *Vestnik SevNTU* **117**, 32–37 (2011)
6. Vodolozskaya, N., Vodolazskaya, E., Iskrickij, V.: Energy analysis of the tightening process of threaded joints with a rare impact wrench. In: *Proceedings of the International Conference RaDMI*, pp. 464–469 (2012)
7. Koteneva, N., Maksimenko, A.: Investigation of the contact stiffness of threaded joints. *Bull. Altai Sci.* **2–2**, 213–216 (2013)
8. Lanshchikov, A.: Technological methods for ensuring the quality of automated assembly of threaded connections. The dissertation of a Cand. Tech. Sci. Penza (2004)
9. Vodolozskaya, N., Vodolazskaya, E., Iskrickij, V.: *Assembling Large Threaded Joints with Impact Wrenches*. LAP Lambert Academic Publishing, Saarbrücken (2014)
10. Nassar, S., Abboud, A.: An improved stiffness model for bolted joints. *J. Mech. Des.* **131** (12), 121001 (2009)
11. Stepanov, V., Drozdov, A.: Process of an inhaling of a carving connection by a shock nuttor. *Mech. Constr.* **08**, 15–18 (2011)
12. Stepanov, V., Drozdov, A.: *Electric Impact Wrenches Dynamics*. MGSU, Moscow (2013)
13. Drozdov, A.: *Manual Machines for Construction and Installation Works*. MGSU, Moscow (1999)
14. Ushakov, L.: *The World's Experience in Calculation and Design*. Germany Publishing House Palmarium Academic Publishing, Saarbrücken (2013)
15. Nikitin, Y.: *Hydraulics and Hydropneumatic Drive*. Bauman MSTU, Moscow (2010)

Modeling of Movement the Flowable Building Load in the Operating Vessel of Vehicle

Evgeny Plavelsky  and Rashid Sharapov  

Moscow State University of Civil Engineering,
Yaroslavskoye Sh. 26, 129337 Moscow, Russia
eplavelsky@gmail.com, ptm_zavkaf@mail.ru

Abstract. The result of metering movement of the flowable building load in the working vessel is installed, the excitation of stable oscillations of the free surface of the load transported in a particular plane of the first form of oscillations. Established ideas about the rheology of the building mixes associated with the study of the movement of the last positive coordinate of shear stress and velocity gradient. Elaborated rheometer of type “ring – ring” rheograms transported the mortar and fine concrete mixtures are hysteresis shape. The revealed hysteresis of the viscous flowable building load under alternating deformation mode is similar to the elastic hysteresis and can be represented in complex form with the coefficient of resistance determined by the area of the hysteresis loop. It is shown that for deriving the equations of motion flowable building load can be used the equations of fluid mechanics in terms of stresses based on the above modified formula of Newton. Determined rheodynamic characteristics of partially filled working vessels: amplitude, frequency and decrement of oscillations of the free surface of the flowable building load, the interaction forces it with a vessel, geometry of the masses. The system of equations consisting of three equations of the second order describing the motion of the system “working vessel – flowable building load “ by coordinates of lateral displacement, the roll angle of the working of the vessel relative to the longitudinal axis and wave motion of the free surface of the flowable building load.

Keywords: Odelling · Flowable construction materials · Working vessel
Non-Newtonian Fluid · Free surface · Equations of motion · Angles of roll

1 Introduction

The quality movement of wheeled vehicles with flowable load (petroleum products, diesel fuel, gasoline, bitumen, various mortar and concrete mixtures, etc.) is determined by the structural peculiarities, road irregularities, control actions and characteristics of the transported load. In the general case the flowable load is non-Newtonian fluid, i.e., the dependence between stress and strain rate is nonlinear. Experience of experimental studies and tests of the fluctuations of the working vessels of wheeled vehicles with flowable load, by definition, modes of deformation in operating and stand conditions, and the conditions of the special roads of the testing ground as the result of measurements allowed to reveal the nature of the angular oscillation of the sprung masses

in the transverse and longitudinal planes. These low-frequency vibrational motion are the cause of the generation of oscillations of the free surface of the flowable load in a working vessel, is rigidly fixed to the sprung mass (chassis). Defining the energy contribution to the movement of the whole dynamic system of the machine is the first mode shape of the free surface. The modes of deformation of flowable load, thus, are alternating in nature.

The period of low-frequency angular oscillations of the working vessels of the most common wheeled vehicles of medium size with a flowable load is in the range of 1.5 s (in transverse plane) and 3.0 s (in longitudinal plane). The frequency range of vertical oscillations caused by irregularities in the road surface, is in the range of 2...3 Hz and 7...8 Hz.

2 Methods

The most typical representative of flowable load with the non-Newtonian characteristics, is a movable concrete (mortar) mixture. The prevailing ideas about the rheology of concrete mixtures related to the study of the flow of a composition of the mobile concrete mixtures in a positive coordinate shear stress τ and the velocity gradient $\dot{\gamma}$. Further expansion of these views related to the consideration of the conduct of concrete mixtures at the same time in all coordinate regions τ - $\dot{\gamma}$, which corresponds to the alternating modes of deformation of the concrete mixtures in the working vessels of wheeled vehicles.

Obtained the rheograms on our developed ring-ring type rheometer of transported the mortar fine-grained concrete mixtures have a loop-like form and are placed symmetrically about the origin in the first and third coordinate fields. Loop-like form obtained rheograms characterizes the viscous hysteretic properties of concrete under alternating deformation mode. With an increase normal load on the test mixture, there has been increasing non-linearity the hysteresis loop, due to a more vivid expression tribometric properties of the concrete mix. In contrast to elastic hysteresis, which is observed in structural materials with elastic imperfections, viscous hysteresis is associated in this case with the viscous imperfections of the concrete mix [1]. Loop-like form obtained rheograms characterizes the viscous hysteretic properties of concrete under alternating deformation mode. With an increase normal load on the test mixture increased nonlinearity hysteresis loop, due to a more vivid expression tribometric properties of the concrete mix. In contrast to elastic hysteresis, which is observed in structural materials with elastic imperfections, viscous hysteresis is associated in this case with the viscous imperfections of the concrete mix [2].

Identified viscous hysteresis of a concrete mix with alternating deformation mode may be similar to the elastic hysteresis is represented by a complex index K of the consistency the concrete mix with a coefficient ε of the resistance determined by the area of the hysteresis loop. Then, passing from the exponential curve to the hysteresis components of the stress tensor T_{ij} in the concrete mix in accordance with a generalized Newton formula for power law fluid will take the form of

$$T_{ij} = p\delta_{ij} + 2K(1 + j\varepsilon)\sqrt{J_2^{n-1}}\dot{\gamma}_{ij} = -p\delta_{ij} + 2K^*Q\dot{\gamma}_{ij} \tag{1}$$

where n is the index of non-Newtonian behavior of the concrete mix; J_2 is second invariant of the tensor of rate of deformation $\dot{\gamma}_{ij}$; p is the isotropic pressure in the mixture; δ_{ij} is the symbol of Kronecker.

For derivation of equations of the dynamics of transported concrete mixture used equations of fluid mechanics in terms of stresses, which are valid for all liquids.

$$\rho \frac{dV_i}{dt} = \frac{dT_{ij}}{dX_i} + \rho F_i \tag{2}$$

where V_i is the speed of fluid flow in the i -th dimensional basis; F_i - stress vector of mass forces; ρ is the fluid density.

Substituting (1) into (2) and having made the conversion, got the equations of motion of the transported concrete mixture in the working vessel

$$\begin{aligned} \frac{dV_i}{dt} + (V_i\Lambda)V_j = F_i - \frac{1}{\rho} \frac{\partial p}{\partial X_i} + \frac{K^*}{\rho} [Q\Delta V_i + 2 \frac{\partial V_i}{\partial X_i} \frac{\partial Q}{\partial X_i} + \left(\frac{\partial V_i}{\partial X_j} + \frac{\partial V_j}{\partial X_i} \right) \frac{\partial Q}{\partial X_j} \\ + \left(\frac{\partial V_i}{\partial X_k} + \frac{\partial V_k}{\partial X_i} \right) \frac{\partial Q}{\partial X_k}] \end{aligned} \tag{3}$$

where Λ , Δ are the differential operators, respectively of Hamilton and Laplace.

The equations of motion (3) are supplemented with the equation of continuity of flow of the concrete mix.

Linearization of the skeletal curve of the rheogram of the concrete mix and the transition to the ellipsoidal hysteretic loop, which corresponds to $n = 1$, not dilutes from the energy point of view, the rheological properties of the transported concrete. And assuming $Q = 1$ the system of Eq. (2) transforms into the well-known Navier-Stokes system for Newtonian fluids. In this case the value of K degenerates into stanovskoy coefficient of viscosity η .

The Equations of motion (3) are supplemented with the equation of continuity of flow of the concrete mix.

$$\text{div}V_i = 0. \tag{4}$$

The boundary conditions reflect the consequences of the conservation laws of energy and mass continuity changes of flow parameters of the concrete mix when passing through the media interface. In this case the boundary conditions on the wetted internal surface S of the working of the vessel from the condition of continuity of the stress vector for the case of small oscillations have the form

$$V_i|_S = 0. \tag{5}$$

For the case of considerable fluctuations of the concrete mix, which is characteristic of longitudinal-angular fluctuations of the working of the vessel, more feasible is the

proposed Bogoryad [3] conditions for the tangential components of the velocity vector in the form

$$\eta \frac{\partial V_i}{\partial n} = f_{in} V_i, \tag{6}$$

where f_{in} is a coefficient of friction of the concrete mix with the wet cement paste of the inner surface S of the working vessel.

When $f_{in}/\eta \rightarrow \infty$ the boundary conditions (6) asymptotically move into the known conditions of adhesion (5).

The boundary conditions on the free surface Σ of concrete mix obtained from the condition of absence at the media boundary shear stresses

$$\left(\frac{\partial V_i}{\partial X_j} + \frac{\partial V_j}{\partial X_i} \right) \Big|_{\Sigma} = 0, \tag{7}$$

and equal to the atmospheric pressure p_a normal stress

$$\left[-p + 2K(1 + j\varepsilon) \frac{\partial V_i}{\partial X_i} \right] \Big|_{\Sigma} = p_a. \tag{8}$$

In addition to dynamic conditions (7) and (8) on the free surface of the concrete mixture adopted by the kinematic conditions are of the form

$$\frac{\partial \xi}{\partial t} = V_i + V_j \frac{\partial \xi}{\partial X_i} \text{ or } \frac{\partial \xi}{\partial t} \approx V_i, \tag{9}$$

where $\xi = f(X_i, t)$ the equation of the free surface of the concrete mix.

To solve the above problem of determining the motion parameters of mobile concrete mixture in the working vessel wheeled vehicles using finite-difference calculation scheme. In this case the development of programs for numerical calculation of the fluctuations of the concrete mixture in the working vessel are considered two-dimensional problem in the transverse and longitudinal planes. The validity of this decomposition is confirmed experimentally and is determined by the significant difference of the frequency characteristics in the transverse and longitudinal planes. The studied cross-section was approximated depending on the required accuracy of the calculation of the corresponding finite-difference grid. Compiled by the technical task of the authors of the program of calculation allow to determine such rheodynamic characteristics of partially filled working vessels of wheel-vehicles like the amplitude, frequency, and decrement of oscillations of free surface of the concrete mix, the strength of the interaction of concrete mix with a vessel, geometry of the masses.

Calculations of oscillations of free surface of the concrete mixture in the working vessels wheeled vehicles of small, medium and large sizes, the numerical methods offer the perturbation of the free surface by setting her initial form or horizontal acceleration. The calculated profiles of the perturbed free surface of the concrete mixture in the working vessels coincide with an accuracy of up to 10% with experimentally obtained

values of the parameters of the oscillations of points on the free surface of the transported concrete mix. Study of the effect of the decrement δ of the vibrations of the free surface averaged rheological properties η and τ_0 (threshold stress shift) of the transported concrete mixtures shows that in the first case the relationship is linear and the second quadratic, i.e.

$$\delta = \delta_0 + K_1 \tau_0; \delta_0 = K_2 \eta^{\frac{1}{2}}, \quad (10)$$

where δ_0 is the initial value of the decrement of oscillations of free surface of the concrete mix in the proposal $\tau_0 = 0$; K_1, K_2 – coefficients of proportionality.

Analysis of plots of velocities of the concrete mix in vertical section of the working vessel with free vibrations shows that in the middle part of the section is formed of non-deforming vibrating - concrete mix that with increase in stiffness of the concrete mix increases and in the limit oscillates “hardened” concrete mixture in the working vessel at the thin edge of the mortar layer. Next, the features of the modeling system “working vessel – flowable load” seen.

3 Results Section

As settlement is considered a vessel with perfectly rigid walls, partially filled with the flowable load. Thus, there is always a free surface of the flowable load, which in the perturbed state are prone to wave generation. As a relaxed condition of the free surface, we consider the translational motion of the work vessel with flowable cargo along the longitudinal axis. We introduce a coordinate system $O'x'y'z'$, axis $O'z'$ which are opposite in direction to the vector of gravitational acceleration \bar{g} , and the coordinate system $Oxyz$, rigidly connected with a vessel. At the beginning of the movement, these coordinate systems coincide.

The forces acting from the support elements of the working vessel classified as external forces F_{ex}, M_{ex} . On the basis of the theorem on change of momentum and angular momentum, and potential theory of displacement [4, 5] taking into account wave motion of the free surface of the flowable load and the effects of dissipation the system of equations consisting of three equations of the second order, and characterize the motion of the system “working vessel-flowable load” by coordinates of lateral displacement y_c , of the roll angle of the working of the vessel relative to the longitudinal (transverse) axis y_c and wave motion of the free surface of the flowable load s

$$\begin{aligned} (m^0 + m)\ddot{y}_c + (m^0 + m)z_{cm}\ddot{y}_c - \lambda_1 \dot{s}_1 &= F_{ex}; \\ (I^0 + I)\ddot{\gamma}_c + \beta(1 + j\varepsilon)\dot{\gamma}_c - (m^0 + m)gz_{cm}\gamma_c + (m^0 + m)z_{cm}\ddot{\gamma}_c - [\lambda_{01}\dot{s}_1 + \beta(1 + j\varepsilon)\dot{s}_1] &= M_{ex}; \\ \mu_1 [\ddot{s}_1 + \beta_1(1 + j\varepsilon)\dot{s}_1 + \omega^2 s_1] - \lambda_{01}\ddot{y}_c - \lambda_{01}\ddot{\gamma}_c - \beta_{01}(1 + j\varepsilon)\dot{\gamma}_c &= 0. \end{aligned} \quad (11)$$

Here m^0, I^0 is the mass and moment of inertia of the empty vessel; m, I is the mass and moment of inertia of a flowable load; z_{cm} – coordinate of the center of mass of the working vessel with flowable load; s_1 is the generalized coordinate of the wave motion

flowable load; y_c, γ_c – generalized coordinates of motion of the working vessel with flowable load, respectively, in the direction of the axis $O'y'$ axis $O'x'$, λ_1, λ_{01} – respectively, the coefficients of hydrodynamic force and hydrodynamic moment

$$\lambda_1 = \frac{F_{l\max}}{\omega_1^2 A_1}; \lambda_{01} = \frac{M_{l\max}}{\omega_1^2 A_1}, \tag{12}$$

acting from the flowable load, respectively, in the direction of the axis $O'y'$ and relative to the axis $O'x'$; β, ε – factors, taking into account respectively the dissipative properties of systems and their nonlinearities:

$$\mu_1 = \frac{2P_{\max}}{\omega_1^2 A_1^2}, \tag{13}$$

μ_1 is the coefficient of the generalized mass for the 1st mode shape of the free surface of the flowable load; P_{\max} – the maximum value of the potential energy oscillation flowable load in the working vessel; A_1 – the amplitude of the first vibration modes of the non-viscous load corresponding to P_{\max} .

The coefficients $m_1, \lambda_1, \lambda_{01}$ are determined by the numerical method [6, 7].

Invariant properties of a system “working vessel – flowable load” are the characteristics remodeling presentation of the specified business of the vessel with flowable load, which have a clear physical meaning, i.e. the pendulum analogy. In this case, the circuit parameters remodeling representation of a work vessel with flowable load is determined by the following equations:

$$m_1 = \frac{\lambda_1^2}{\mu_1}; c_1 = \frac{\lambda_{01}}{\lambda_1}; l_1 = \frac{g}{\omega_1^2}; m_0 = m^0 + m - m_1; I_0 = I^0 + I - m_1 c_1^2. \tag{14}$$

Here m_1, l_1, c_1 are respectively the mass, length and coordinate of the point of suspension of the pendulum is equivalent to the determined first mode shape of the free surface of the flowable load.

The dissipative coefficients of the equivalent pendulum is formed by two dampers. The first damper produces a torque proportional to the angular velocity of the pendulum relative to the movable ($Oxyz$) and the second relatively stationary ($O'x'y'z'$) coordinate system. The coefficients have the following form

$$\beta_1^* = m_1 l_1^2 \beta_1; \beta_1^* = \frac{m_1 l_1}{\lambda_1} \beta_{01}. \tag{15}$$

Described remodeling representation system, “working vessel – flowable load” is a characteristic of the transverse and longitudinal plane of the working vessel wheeled vehicle [8, 9].

Then, based on the Lagrange equations of II-nd kind equation system (11) has the form:

$$\begin{aligned}
 &(m^0 + m_1)\ddot{y}_c + (m_0z_c + m_1c_1)\dot{\gamma}_c - m_1l_1\dot{\xi}_1 = F_{ex}; \\
 &(I^0 + m_1c_1^2)\ddot{\gamma}_c - g(m_0 + m_1c_1)\gamma_c + (m_0z_c + m_1c_1)\ddot{y}_c - m_1c_1l_1\ddot{\xi}_1 - \beta_{01}^*(1 + j\varepsilon)\dot{\xi}_1 = M_{ex}; \quad (16) \\
 &m_1l_1^2\ddot{\xi}_1 + \beta_{11}^*(1 + j\varepsilon)\dot{\xi}_1 + m_1gl_1\xi_1 - m_1l_1\ddot{y}_c - m_1c_1l_1\dot{\gamma}_c - \beta_{01}^*(1 + j\varepsilon)\gamma_c = 0.
 \end{aligned}$$

Where $z_c = \frac{1}{m_0} \left[\left(z_{c0} + \frac{\rho I_y}{m^0 + m} \right) (m^0 + m) - m_1c_1 \right]$ – coordinate of the center of masses of an equivalent solid body; z_{c0} – coordinate of the center of mass of the system “working vessel flowable load” for “hardened” in a calm (unperturbed) state and the flowable load; I_y – equivalent moment of inertia of area of the free surface of the flowable load relative to the transverse axis of the working vessel.

The coordinates s_1 and ξ_1 interrelated by the following relationship:

$$\xi_1 = \frac{\mu \omega_1^2}{\lambda_1 g} s_1. \quad (17)$$

Physical modelling of wave disturbance flowable load working vessel wheel of the vehicle to determine rheodynamic these characteristics are basic similarity criteria of Reynolds Re and Froude Fr . Moving from a system of “working vessel – flowable load” to the system “road – chassis (sprung mass) with a vessel – flowable load” note that the coordinate system $Oxyz$ is rigidly connected with the chassis. The axis Ox coincides with the roll axis of the sprung mass (chassis with a receptacle, the flowable load) to the movement of wheeled vehicles. The axis Oz directed vertically upward through the center of mass of the wheeled vehicle. The axis Oy is directed to the left in the direction of motion of the vehicle.

4 Discussion Section

In practice of research of lateral stability of wheeled vehicles there are three main types of stability: the roll stability (stability against overturning), lateral stability (resistance to lateral displacement), directional stability (stability against changes of direction). The roll stability of wheeled vehicles with flowable load [10–13].

$$\Omega = \frac{v^2}{r} \cdot \frac{ad + ch(M + m)}{ab - c^2}; \quad (18)$$

$$\gamma = \frac{v^2}{r} \cdot \frac{cd + bh(M + m)}{ab - c^2}, \quad (19)$$

where $a = c + c_t + gh(M + m)$; $b = c + Mg(l_0 + l') + mgl_0$; $c = c_{cs} + c_{cp}$; $d = M(l_0 + l')ml_0$.

Here c_s, c_t, c_p – given the angular stiffness of the springs of the suspension, the tyres, the chassis frame; h, l_0, l, l' – the distance respectively from the reference surface to the roll axis, from roll axis to the center of sprung mass, from the point of suspension to the center of mass of the pendulum, from the point of suspension to center of suspension of the masses (Fig. 1).

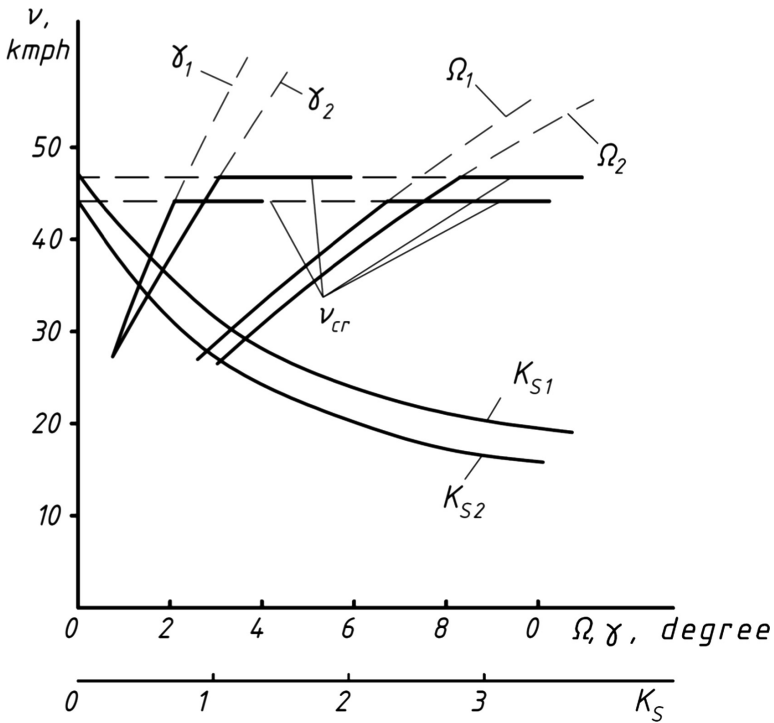


Fig. 1. Dependences of the coefficients of the safety the stability (K_s) and transverse roll angles of the unsprung (γ) and suspension (Ω) mass with partially filled working vessels mass mixers, respectively, on the chassis of KrAZ-6505 (1) and KAMAZ-5511 (2) the vehicle speed when a turning radius of 35 m.

5 Conclusion



The figure shows the obtained according to Eqs. (18) and (19) dependence of roll angles γ and γ' of the speed of motion of the wheeled vehicle (1-mixer truck on chassis KAMAZ-5511, 2-concrete mixer on chassis KrAZ-6505). Horizontal lines mark the maximum speed of rotation specified wheeled vehicles with flowable building load (movable concrete mixture).

Developed above, the estimated models are a good base to use mathematical models of wheeled vehicles with fixed load that will minimize the number of expensive tests of full-scale models of wheeled vehicles with flowable building load.

References

1. Potakhov, D., Potakhov, E., Vatulin, C.: Simulation of the dynamics of lifting machines. In: *Transport: Problems, Ideas, Perspectives Proceedings of the LXXVI All-Russian Scientific-Technical Conference of Students, Postgraduates and Young Scientists*, pp. 273–277 (2016)
2. Mamiti, G.: The new equation and the traction and braking dynamics of a wheeled vehicle. In: *Design of Special Machines for the Development of Mountain Territories, Materials of International Scientific-Practical Conference* (2016)
3. Bogoryad, I.: *Dynamics of a Viscous Fluid with a Free Surface*. Izd-vo Tomsk. University Press, Tomsk (1980)
4. Sharapov, R., Agarkov, A., Sharapov, R.: Matrix modeling of technological systems grinding with closed circuit ball mill. *World Appl. Sci. J.* **24**(10), 1399–1403 (2013)
5. Franchuk, V.: Application of generalized functions in solving problems of dynamics of nonlinear systems vibration of technological machines. *Vibration Technology, Mechatronics and Machine-Driven* (2014)
6. Lagerev, I.: Modification the Runge-Kutta's method to study the dynamics of lifting machines. In: *Materials of Scientific Conference of the Council of MNTO the Ministry of Education and Science of the Russian Federation, Bryansk State Technical University*, pp. 32–34 (2012)
7. Kotiev, G., Gorelov, V., Zakharov, A.: Study of the dynamics of wheeled vehicles on the dynamometer. *Automot. Ind.* **7**, 9–12 (2014)
8. Shrubchenko, I., Hurtasenko, A., Sharapov, R., Duyun, T., Shchetinin, N.: Investigation of characteristics of contact bandages and support rollers of rotating technological drums. *Mod. Appl. Sci.* **9**, 195–203 (2015)
9. Artemov, N., Lebedev, A., Alekseev, O., Volkov, V., Podrigalo, M., Polyansky, A.: Method of partial accelerations and its application to study the dynamics of mobile machines. *Sci. Notes Crime. Eng. Pedagog. Univ.* **24**, 33–36 (2010)
10. Sidorov, N.: Modelling of dynamics of transport-technological machines with a cargo portal. *Achiev. Sci.* **9**, 118–121 (2014)
11. Switachev, A., Razuvaev, A., Chekeev, A.: Modeling the dynamics of traction-transport vehicles with structural elements of variable mass. *Mod. Technol. Syst. Anal. Model.* **1**, 91–92 (2012)
12. Sharapov, R., Mamedov, A., Agarkov, A.: Comparative characteristics of passability on soft soils walking crawler cranes. *Bulletin of BSTU named after Shukhov, V.G.*, vol. 5, pp. 198–200 (2015)
13. Plavelsky, E., Nikul'nikov, E., Plavelsky, A.: The decision of problems of investigation and proof of compliance of wheeled vehicles with a high center of mass and moving load. *Automot. Ind.* **7**, 9–11 (2009)

The Interaction of Piles in Double-Row Pile Retaining Walls in the Stabilization of the Subgrade

Anatoly Buslov¹  and Vladimir Margolin² 

¹ NIIOSP them. Gersevanov JSC “SIC” Construction, Moscow, Russia

² Moscow State University of Civil Engineering,

Yaroslavskoye Sh. 26, 129337 Moscow, Russia

MargolinVM@mgsu.ru

Abstract. In the practice of designing anti-landslide structures for stabilization of the subgrade along with the single row pile walls find use two-row wall. The second row of piles contributes to the bearing capacity of retaining structure. However, the conditions in the most efficient capacity utilization of the second row to be studied. The article presents the results of analytical studies frame construction flexible piles, the combined grillage hard, perceiving landslide pressure. Effective capacity utilization of the second row of piles was assessed using the utilization of the bearing capacity of piles second through 4.000 different designs double row of walls made of piles of various cross-sections, length, their reinforcement, the depth of application of landslide pressure, as well as with different variants of soil conditions.

Keywords: Anti-slide structures · Pile rows · The interaction of piles
Bearing capacity

1 Introduction

The theory and practice of strengthening of landslides piles have been numerous studies both in our country and abroad [1–20]. Mostly they dealt with the issues of calculation of stability and load-carrying ability of anti-piles under the action of landslide pressure. The effective application of anti-landslide constructions are particularly relevant for regions with complex geographical terrain and abundant precipitation.

One such area is the far Eastern region, having currently the economic and strategic value of particular importance to our state. Oil and gas fields of Sakhalin, for example, determine the economic development of the Far East for decades to come. However, this region is characterized as extremely landslide-prone, especially in places of passage of roads and Railways [1].

Domestic researches in the field of application of anti-piling retaining walls have a fairly long history. These include, for example, include long-term studies of the conditions of opolznevoye and experience of the successful consolidation of the slopes of the subgrade on the number of landslides of the far Eastern railway [1–5].

In the practice of designing anti-landslide pile structures along with the single-row walls find use in General multi-row two-row and retaining walls [6–12]. This assumes

that the second row of piles will greatly enhance the bearing capacity of retaining structure. The joint work of the piles in the rows and methods of their calculation are presented in a number of works of domestic and foreign researchers [5–12, 15, 16, 18–20]. At the same time conditions the most effective use of the second row in the double row pile retaining walls remain to be studied.

2 The Purpose of the Research

Since double-row pile retaining wall, the combined grillage represents a frame of flexible piles on an elastic Foundation, the load distribution between the piles from the existing on the wall of landslide pressure will depend on the flexibility of the piles, the ordinates of the load from the landslide pressure on the first row, the soil properties of landslide slope.

To determine the valid picture of the work of anti-slide pile structures was tasked to establish the role of the second row in the work of double-row pile retaining walls.

The study was conducted on the basis of 4,000 options calculations and analysis of the results of piles of various cross-sections, length, their reinforcement, the depth of application of the horizontal load is below the surface of the soil, and also by different types of soil conditions. Due to the significant complexity of the implementation many variants of the analytical calculations were carried out with the use of computers.

3 The Results of the Research

The design scheme is shown in Fig. 1. Piles first and second row arranged one against the other, and United by a grid-type frame construction. Load R (total resultant landslide pressure) acts on the first row of piles. The point of application of this load is at a depth “ a ” from the surface of the soil and depends on the type of landslide plots of pressure acting on a retaining structure.

With the aim of establishing General laws was considered theoretically possible a wide range of options changes to this ordinate.

The load from the first row of piles is passed through the grid in the second row. The redistribution of the total load between the piles of both series occurs with regard to their flexibility. Piles are seen as long flexible conditional pinching below the surface of the slide in place of the maximum bending moment at a depth of L . Its presence is in most theoretical methods for calculation of piles for horizontal load, for example, in [14].

The effect of the second row is evaluated by the reaction of R , perceived the second row and the coefficient of capacity utilization η of the second pile. The reaction is determined in fractions A (Eq. 1) from the total load on the recessed P_{ul} construction.

Calculation Equation:

$$R = \frac{Sh\lambda l \cdot \cos \lambda a Ch\lambda b - \sin \lambda l Ch\lambda a \cdot \cos \lambda b}{2(Sh\lambda l \cdot Ch\lambda l - \sin \lambda l \cdot \cos \lambda l)} \cdot P = AP. \quad (1)$$

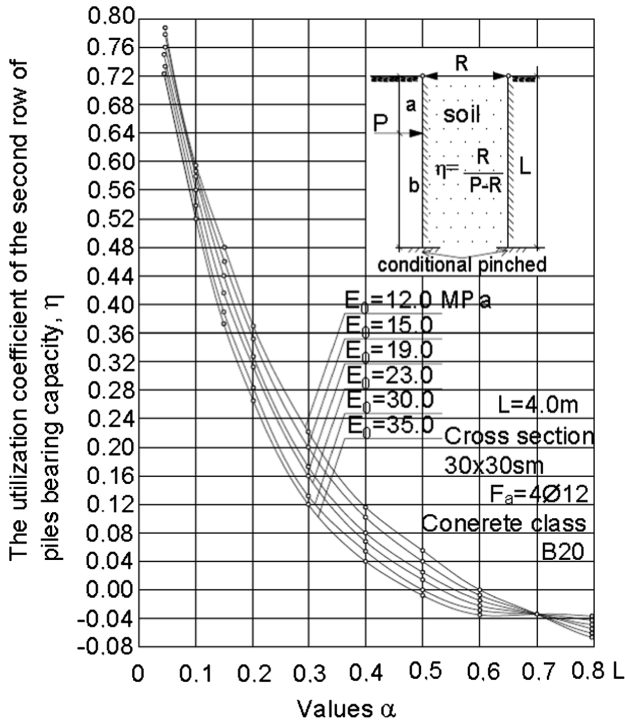


Fig. 1. A graph of the ratio η of use of the bearing capacity of the second row, a – the depth and application of the horizontal load P (landslide pressure), and total module of deformation of soil E_o . R – reactive resistance of the second pile.

$$\eta = \frac{R}{P - R} \tag{2}$$

Here:

- P – load (landslide pressure) acting on the double row retaining wall;
- R – response, perceived second row of piles;
- A – proportion of the total load P , per second number of retaining walls;
- H – the coefficient of use of the bearing capacity of piles second.

The indicator of flexibility of the piles

$$\lambda = 0.635^4 \sqrt{\frac{E_o}{(1 - \mu_o^2)EI_{pr}}} \tag{3}$$

- where: E_o – the module of total deformation of the soil;
- μ_o – is the Poisson’s ratio of soil;
- EI – given the stiffness of the reinforced concrete cross-section;
- L – is the length of the pile;

a – ordinate the application of the resulting landslide pressure P;
 b = L - a [14].

In Fig. 1 shows the results of calculations of changes of the coefficient η depending on the depth of application of the horizontal load P (landslide pressure). Its values fall rapidly with the depth of the point of application of force. Uniform load distribution between the piles of both series is observed at $a = 0.1 L$.

With the increase of the ordinate “a” the effectiveness of the second row of piles is reduced, as in the first row accounts for a large part of the load from the landslide pressure.

For the purpose of uniform redistribution of the load between the rows in this case, it is advisable to increase the spacing between piles in series and piles in the second row to install the extension against the piles of the first row [7, 16]. Then the part of soil, not kept in the first row and forced between the piles of the first row, it will be perceived the second row.

The analysis shows that the efficacy of the second row of piles is higher in weaker soil of the landslide massif (Fig. 1). This fact is confirmed by studies of the effect of the thinned row of piles on the velocity of landslides-flows [15, 17, 18].

From Figs. 2 and 3 shows that most efficiently used the bearing capacity of the second row of piles in soft soils and greater rigidity of the cross section.

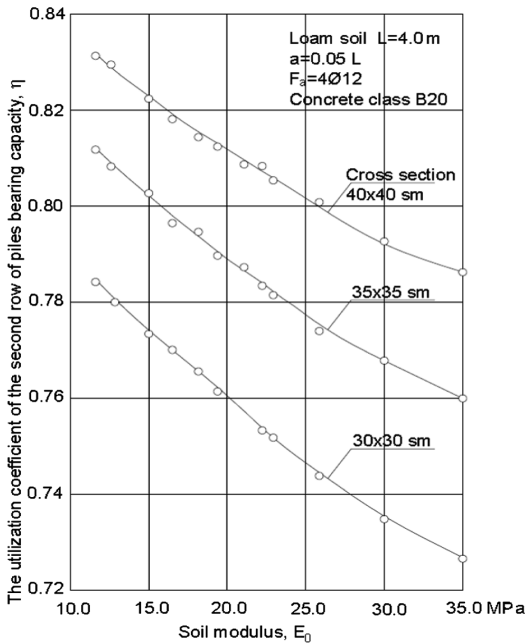


Fig. 2. Graph of the ratio η of the deformation properties of the soil E_0 and geometric dimensions of the cross-section piles.

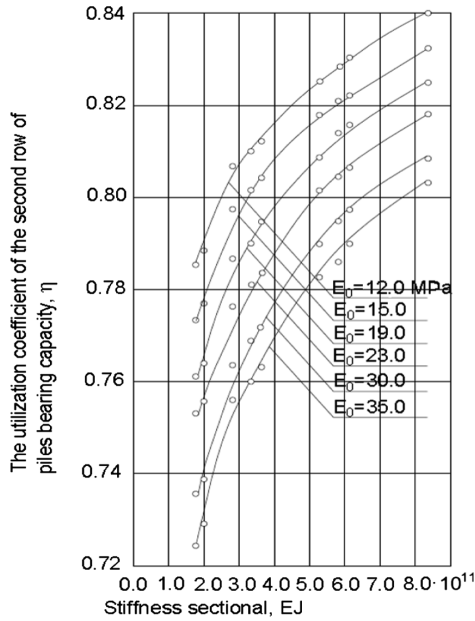


Fig. 3. A plot of the ratio η of the stiffness of the cross-section piles EI and deformation properties of the soil E_0 .

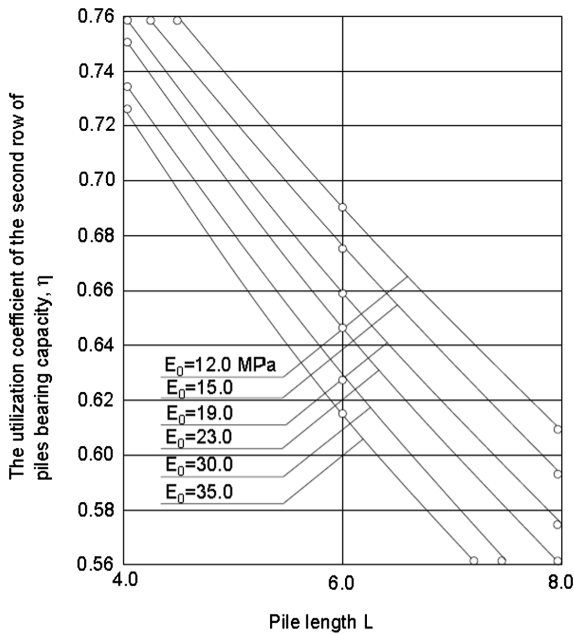


Fig. 4. Graph of ratio η – use the bearing capacity of the second row of piles of length L and deformation properties of the soil E_0 .

Besides reduction of the length of the piles (Fig. 4) that directly show on the feasibility of double-row pile wall on the landslides of small capacity (small thickness slide layer).

4 Conclusion

Thus, the analysis of piles in landslides allows to draw the following conclusions:

1. The second row of piles with a stable array below the pressure of the wall on the slope of the landslide is advisable to apply at the location of the point of application of the resulting landslide pressure from the bottom of the pile cap on the value of $0.2...0.3 L$, where L is the length of the pile. At a deeper location of the point of application of landslide pressure the efficacy of the second row of piles reduces.
2. It is recommended to use double-row pile wall on the landslides, the body of which is composed of relatively weak soils.
3. Composed of double row of walls with great effect work short piles with a greater transverse rigidity.
4. The first row of piles, it is advisable to design more durable in comparison with piles of the second row.

References

1. Polevichenko, A., Buslov, A., Solodovnikov, B.: Analysis of the work and evaluation of the effectiveness of various types of anti-landslide structures. *HabIIGT* (1998)
2. Polevichenko, A., Bogdanov, G., Samsonov, B., Kirillov, V., Buslov, A.: Investigation of the work of the anti-landslide pile retaining wall. In: *Proceedings of HabIIGt*. Transport, Moscow (1997)
3. Polevichenko, A., Bogdanov, G., Buslov, A.: Generalization of the results of the study of the work of piles on the landslide section of the FECD. In: *Material of the XXIst Scientific and Technical Conference*. HabIIGT, Habarovsk (1968)
4. Polevichenko, A., Gdanova, S.: *Anti-deformation structures for the stabilization of the roadbed: a textbook*. DVGUPS, Habarovsk (2005)
5. Polevichenko, A.: *Calculation of the pile retaining wall for strengthening unsteady slopes and slopes*. DVGUPS, Habarovsk (2006)
6. Derevenets, F., Matsii, S.: Investigation of the interaction of a landslide ground with piles of a two-row retaining structure by the finite element method. In: *Urban Agglomerations on Landslide Territories: Materials 3 International Scientific Conference Dedicated to the 75th Anniversary of Building Education in Volgograd*, vol. 1, pp. 114–119 (2005)
7. Gotman, A.: Calculation of the influence of the mutual action of vertical and lateral loads on the variable section piles with finite element method. *Bases Found. soil Mech.* **1**, 6–12 (2000)
8. Otori, K., Takahashi, K., Kawai, V., Shiota, K.: Static analysis model for double sheet-pile wall structures. *Geotech. Eng.* **114**(7), 810–825 (1988)
9. Lee, C., Chen, H., Wei, Y., Lin, Y., Huang, W., Chiang, K.: Centrifuge modeling of a self-supported double solder-piled wall in sandy soil. *J. Geoenviron. Eng.* **2**(3), 97–109 (2007)

10. Bo, Z., Yong-Chao, Z.: Influence of space of double row piles on soil arching effect. *Int. J. Eng. Res. Appl.* **5**(2), 19–21 (2015)
11. Ashour, M., Pilling, P., Norris, G.: Lateral behavior of pile groups in layered soils. *J. Geotech. Geoenvironmental Eng.* **130**(6), 580–592 (2004)
12. Won, J., You, K., Jeong, S., Kim, S.: Coupled effects in stability analysis of soil-pile Systems. *Comput. Geotech.* **32**(4), 304–315 (2005)
13. Pataleev, A., Buslov, A.: To calculate the pile on a horizontal load. In: *Proceeding of Conference on summarizing the experience of design, construction and implementation of the completed research in the field of pile foundations on the construction sites of the far east, Habarovsk* (1998)
14. Buslov, A.: *The work of piling on a horizontal load beyond the elasticity in cohesive soils. Monograph, Tashkent* (1979)
15. Buslov, A., Kalacheva, E.: Speed of movement of landslides of a viscous current at the device of a pile series and a continuous retaining wall. *MSUCE.* **3**, 16–25 (2012)
16. Buslov, A.: Recommendations for the calculation of piles on landslides in cohesive soils. *HabIIGT, Habarovsk* (1970)
17. Rasulev, A., Kogevnikov, N., Ovchinnikov, A.: The railway way. In: *Ovchinnikov, A. (ed.) TashIIT, Tashkent* (2006)
18. Bakulina, A., Buslov, A.: FEM analysis of the laterally loaded pile with rigid plate. In: *Proceedings of 14th International Conference on Computing in Civil and Building Engineering* (2012)
19. Kalacheva, E., Buslov, A.: Features of interaction of viscous landslips with anti-landslide structures. *New Technol.* **4**, 52–56 (2012)
20. Kalacheva, E.: Solutions of engineering problems viscous and viscoplastic flow of landslides in interaction with buttresses. In: *International Conference on Engineering Sciences: Modern Problems and Development Prospects. Privolzhsky Research and Development Center, Yoshkar-Ola* (2013)

Reasonability of Application of Slags from Metallurgy Industry in Road Construction

Natalia Kozhukhova¹ , Nikolay Kadyshev¹ ,
Alla Cherevatova¹ , Elena Voitovich² , and Kirill Lushin² 

¹ Belgorod State Technological University named after Shoukhov, V.G.,
308012 Belgorod, Russia

kozuhovanata@yandex.ru

² Moscow State University of Civil Engineering,
Yaroslavskoye Sh. 26, 129337 Moscow, Russia

Abstract. In this paper the analytical studies of metallurgical slag properties from three plants are carried out. The obtained results demonstrate low values of radioactivity, comparable with widely used construction materials. The possibility of high-performance construction composite (including road construction) is confirmed. The results of study allow recommendation of metallurgy slag as effective low-radioactive raw materials in construction composites.

Keywords: Metallurgical slag · Radiation safety · Construction composites

1 Introduction

Generally, ionizing radiation background at the Earth is formed under influence of the basic constituents such as:

- radiation initiated by cosmic processes;
- radiation initiated by scattering natural radionuclides in lithosphere, including soil layer, atmosphere, hydrosphere and others objects consisting of biosphere;
- radiation initiated by artificial radionuclides produced as a results of nuclear weapon exploitation in form of local atmospheric condensation (Fig. 1).

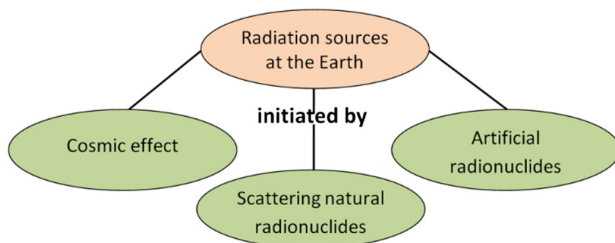


Fig. 1. Radiation types at the Earth.

Associated with comprehensive radiation effect, the Earth population as well as all bioorganisms is under radiation influence in non-stop regime that leads to inconvertible negative ecological consequences [1].

One of the basic potential resources of radiation pollution is metallurgical and power plants those are «suppliers» of by-products, consisting of, primary, mineral components containing radioactive elements [2–4]. The most popular types of metallurgical wastes are slag, required in utilization (Fig. 1).

Metallurgical, phosphoric, steelmaking and others industrial slag are quite good raw components for construction materials production. At the same time a wide distribution of these wastes (but not uniformly for all the territory of country) makes its application very effective and prospective due to the transportation distance to construction objects is reduced. The most interest is focused on slag from ferrous metal industry, in particular, blast-furnace slag [5–9]. More than 50% of blast-furnace slag is transformed to granulated ones.

In others industrialized countries also steelmaking slag are used. In field of road construction the aggregates based on steelmaking slag are more effective to apply when asphalt-concrete pavements development [10]. It is connected with the fact, the steelmaking slag based aggregates and containing asphalt-concrete pavement have a high wear-resistance as well as good friction performance, providing to the pavement a required adhesion characteristics.

Gravel and fine aggregate from steelmaking slag are used in asphalt- and cement concrete, as well as in sub grades, additional layers of road pavements and roadbeds.

Granulated slag from reactive blast-furnace resource can be applied as individual binder when construction of road bases, soil pavements and composites containing rock materials (Fig. 2).

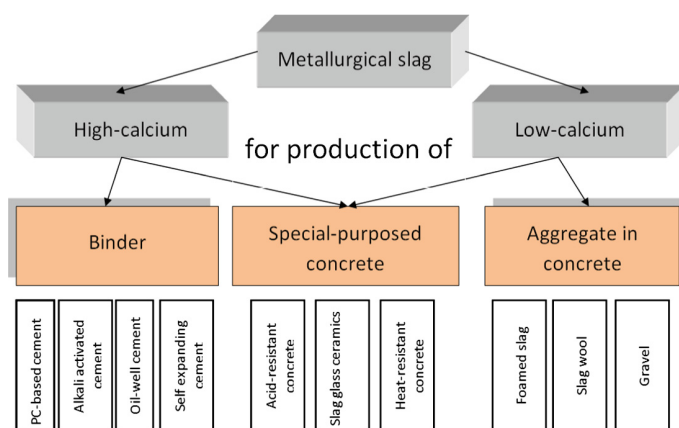


Fig. 2. Application areas of metallurgical slag.

According to statistic information, annually on Russian ironworks the more than 20 million tons of slag are formed that is equivalent to radioactivity of $3,0 \cdot 10^{12}$ Bq.

Ferrous slag are applied for production of road gravel, lightweight aggregate in concrete as well as heat and sound-proof composites [2, 5–9].

Earlier, the studies, oriented to radioactive properties of these slag were realized but quite slightly [3, 10].

2 Experimental Section

Goal of this investigation is study of radioactive and acid-base background of metallurgical slag as main factors of its potential negative effect when application as raw components of construction area as well as its reactivity as pozzolanic material and as individual binder component.

In the paper the metallurgical slag from three Russian companies are used.

Chemical composition of the studied slags is presented in Table 1.

Table 1. Chemical composition of the studied slag.

Chemical composition, % by wt.												
Slag producer*	LOI	SiO ₂	Al ₂ O ₃	Fe ₂ O ₃	CaO	TiO ₂	K ₂ O	Na ₂ O	MgO	MnO	SrO	Σ
S1	1.6	38.6	6.1	0.6	43.4	0.1	0.7	0.6	0.9	0.2	0.01	92.81
S2	0.15	38.1	5.6	0.5	41.6	0.2	0.5	0.56	12	0.05	0.07	101.6
S3	0.8	24.5	4.2	15	40.7	0.2	0.1	0.5	12.5	0.9	0.1	100.4

3 Results Section

3.1 Radioactive Analysis

For realization of procedure of effective specific activity of natural radioactive nuclides (ESANRN) determination for the studied slag and estimation of its safety degree the gamma- spectrometric analysis is carried out in this study (Table 2), realized with scintillation gamma-ray spectrometer « PROGRESS » according to a Standard procedure [11, 12].

According to data of ESANRN (A_{eff}) from Table 2, the studied types of slag are associated to the class I in radiation hazard, where A_{eff} is up to 370 Bq/kg.

Table 2. Values of A_{eff} for the studied slags.

Slag producer	Parameter, Bq/kg				
	Specific ¹³⁷ Cs activity	Specific ²²⁶ Ra activity	Specific ²³² Th activity	Specific ⁴⁰ K activity	ESANRN A_{eff}
S1	<3	40.2924 ± 7.6119	33.7577 ± 7.2538	223 ± 63	103.4699 ± 12.2544
S2	<3	42.2112 ± 81117	27.6249 ± 6.9718	251 ± 70.7	99.7773 ± 12.3259
S3	<3	39.1684 ± 7.6883	24.8989 ± 6.5987	<40	71.7859 ± 11.5383
According to Russian Standard 30108-94					up to 370

So, these materials can be applied in different types of construction materials [12].

To realize a comparative and estimative analysis of data from Table 2 the values of ESANRN for the most popular and widely applied construction materials are shown in Table 3.

Table 3. Values of A_{eff} for mineral raw resource and construction materials.

Type of material	Plastic wood filler	Inorganic adhesive cement	Marble	Glazed tile	Ceramic tile	Gypsum	Self-smoothing compound
ESANRN A_{eff} , Bq/kg	40.2	90.2	137.2	324	273.4	168	136.7

According to data in Table 3 we can see, the studied slag materials are fully in the framework of values of ESANRN for construction composites, even as raw component, where potential radioactive components are in disconnected state. This fact allows conclusion the safety of the slag application in materials for construction purpose. Also, one of the most important factors, characterizing metallurgical slag as waste products collected and stored in open landfills is pH-value of its water extract as indicator of connectivity degree of chemical component in its structure, including potential radioactive elements as pollutants of soil landscape and underground water. So, within of this study the evolution of pH-value of slag water extracts in time is realized (Table 4).

Table 4. pH-values of the slag water extracts depending of exposure duration of slag samples.

Slag producer	Duration of exposure in water environment, hours						
	1	2	3	4	5	24	30
S1	9.42	9.49	9.54	9.63	9.97	9.75	9.43
S2	8.7	8.76	8.81	8.85	9	8.65	8.53
S3	10.1	10.25	10.3	10.33	10.4	10.03	9.95

According to data of pH-values of slag water extracts for three types of slag the slow grow of environment alkalinity during the first five hours when the experiment realization is observed. That can be associated with leaching of alkali-bearing components from sample and its dissociation in water environment.

However, we can observe a followed reducing of pH-values of water extracts after 24 and 30 h of experimental process presented in Fig. 3.

Generally, the negligible alkality of the studied slag is observed with minimal value for slag S1 and maximum value – for slag S3.

It can be associated with binding of cations of alkaline metals into chemical formation when air carbonatization during reaction with carbon dioxide CO_2 .

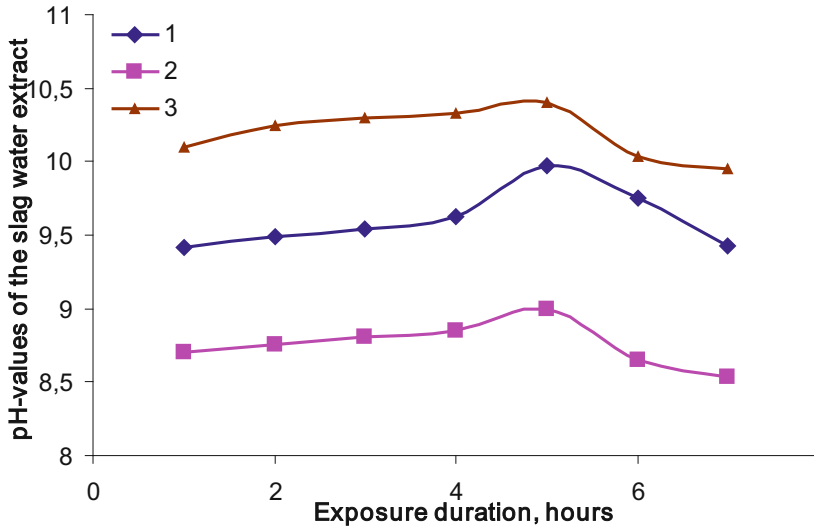


Fig. 3. Variation of pH-values of the slag water extracts depending of exposure duration of slag samples.

Thus, this experimental part confirms effect of migration of free chemical elements including radioactive ones. That describes efficiency of its application/utilization to conserve dangerous components and so, prevent its migration from composite to environment in-service time.

3.2 Compressive Strength Characteristics

As it was mentioned above, metallurgical slag are widely used in road and civil engineering as aggregates of different purpose.

However, earlier studies demonstrate the high-reactive metallurgical slag can be effectively used for high-performance concrete production with tensile strength 5.2–6.4 MPa and compressive strength 30–45 MPa [4, 5, 7].

For approbation and conformation of the information about potential reactivity of metallurgical slag in this work the four compositions with different «Portland cement – slag» ration were prepared and molded.

Results of compressive characteristics of the experimental samples after 28 days of hardening period are presented in Table 5.

According to the data obtained for strength characteristics of slag-containing binders a quite high hydraulic reactivity of the studied slag samples jointly cement component as well as individual binding material should be noted. So, the studied metallurgical slag can be used as potential effective raw resource for construction composite production.

The current problems of limited utilization of metallurgical slag taking account its potential radioactive effect on environment, analyzed in this work and the investigation data obtained for three types of metallurgical slag demonstrate its ecological safety as

Table 5. Strength characteristics of slag-containing binders with different composition.

Parameter	Strength characteristics of slag-containing binders with different Portland cement content, %									
	0			20			50			100
	1	2	3	1	2	3	1	2	3	
R _{comp} , MPa	46	43	32	54	50	45	63	58	50	64
R _{tens} , MPa	5.3	5.1	4.4	5.9	5.9	4.7	5.4	5.3	4.2	5.7

well as good chemical activity and mechanical performance and, thus, its application efficiency as raw materials when production of construction/road construction objects.

4 Conclusion

On the base of this study the experimental metallurgical slag, annually produced in great numbers are fully ecologically save (presence of free dangerous/radioactive components). Results of strength characteristic of slag-bearing binder based on three studied types of metallurgical slag demonstrate values those are comparable with cement binder. At the same time, «cement – slag» composite is characterized by high tensile strain resistance that is very important for road construction composite.

The realized analytical and experimental studies concerning to mineral wastes of metallurgical industry from a point of view of its ecological safety, reactivity in water medium and strength performance in mineral concrete allows application these materials as environmentally friendly and energy-effective road construction composites.

Acknowledgements. The article was prepared within a development program of the Base University on the basis of BSTU named after V.G. Shukhov, using equipment of High Technology Center at BSTU named after V.G. Shoukhov.

References

1. Kozhukhova, N., Lebedev, M., Vasilenko, M., Goncharova, E.: Ecology-toxicology study of low-calcium solid wastes from power plants. *Int. J. Pharm. Technol.* **8**(3), 15349–15360 (2016)
2. Hobotova, E., Ukhneva, M., Baumer, V., Kalmyikova, Y.: Investigation of radioactive properties of blast-furnace slag. *DonNTU. Chem. Chem. Technol.* **13**, 118–127 (2009)
3. Fomina, E., Voitovich, E., Fomin, A., Lebedev, M., Kozhukhova, N.: Analysis of radiation degree of OEMK slag for its application in construction composites. *Bulletin of Belgorod State Technological University named after V.G. Shoukhov* **6**, 130–133 (2015)
4. Kozhukhova, N., Kalashnikova, V., Zernovsky, I.: Ecological aspect of mineral industrial waste utilization into construction area. In: *Proceeding of 3rd International Conference in «Ecology and Rational Environmental Management of Agroindustrial Regions»*, Belgorod (2015)

5. Kadyshev, N., Kozhukhova, N.: Application aspects of blast-furnace granulated slag when production of effective non-cement binders. In: Proceedings of the International Conference in «Modern Construction Materials, Technologies and Structures», Grozny (2015)
6. Kozhukhova, N., Zhernovsky, I., Kadyshev, N.: The question of metallurgical slag application when production of energy-effective alkali-activated binders. In: 2nd All-Russian Research and Technical Conference «Innovative materials and technologies in design», St. Petersburg (2016)
7. Lesovik, V., Ageeva, M., Ivanov, A.: Granulated slag in composite binder production. Bulletin of Belgorod State Technological University named after V.G. Shoukhov **3**, 29–32 (2011)
8. Fomina, E., Kudayarova, N., Tukavkina, V.: Activation of hydration process in composite binder based on technogenic raw materials. Constr. Mater. **12**, 61–64 (2015)
9. Goncharova, M., Komarichev, A., Krokhotkin, V.: Dry building mixtures with wastes of metallurgical industry. Constr. Mater. **5**, 66–67 (2013)
10. Goncharova, M.: Application of slag from ferrous metal industry in asphalt concrete. In: Proceeding of International Conference in «Modernisation and Researches in Transport System», Perm (2014)
11. Russian Standard 30108-94, Building materials and elements. Determination of specific activity of natural radioactive nuclei (1995)
12. Russian Standard NRB-99/2009, Moscow (2009)

Problems of Fire Extinguishing in Buildings of the Transport Transit Hubs Using Carbon Dioxide and Gaseous Chladones

Dmitry Korolchenko^(✉)  and Andrey Pigurin 

Moscow State University of Civil Engineering,
Yaroslavskoye Sh., 26, Moscow 129337, Russia
ICA_kbs@mgsu.ru

Abstract. Emergence of the fire inside the transport transit hub (TTH) leads not only to injury and death of passengers and transport workers, but also to destruction of transport facilities. Therefore, solving of such problems as localization and extinguishing fires in TTH buildings is actually. As a result of conducted analysis of the indoor flame suppression process we have received quantitative ratios for calculation of the time and the specific consumption depending on flow rate of extinguishing agent. It is shown that in case of application of gaseous compounds, as well as other extinguishing agents, dependence of the specific consumption on the flow rate passes through the minimum point that allows defining optimum flow rate during extinguishing of combustible materials of different nature.

Keywords: Transport transit hub · Transport lines · Extinguishing agents
Fire extinguishing · Gaseous extinguishing compounds
Phlegmatizing concentration · Specific consumption

1 Introduction

The transport transit hubs are connecting elements of the city transport system including all types of urban and mainline transport. They are formed depending on the interaction of two and more types of urban mass transport during the transfer of passengers. One of the main problems of TTH is a fire safety. With the growing pace of urban development the special attention is paid to transport system. Traffic streams provide mass transportation of people and goods (including fire hazardous substances).

Emergence of the fire in buildings of TTH leads to destruction of transport facilities, injury and death of passengers and transport workers, and causes an irreparable damage to goods. Therefore, solving of such problems as localization and extinguishing fires in TTH is actually.

Unlike water, which is widely used to extinguish fires in buildings, application of gaseous agents allows to extinguish objects under the voltage and objects which could lose the initial form and practical value under the influence of water [1–5]. Gaseous extinguishing agent is a substance which boiling point is lower than room temperature.

Such substances are the freons, hydrocarbon-based compounds, and carbon dioxide both in pure form and in a mixture with argon and nitrogen [5–8].

Among the chladones, having liquid form under the normal conditions, we want to select the chladone 114B2 and the perfluoroketone 3M Novec 1230 OSK GROUP-Fire Protection Systems [9–12]. Due to the special attention which is paid to environment protection it is necessary to specify that perfluoroketone - 3M Novec 1230 is ecologically safe and has zero ozone depletion potential. Compared with other common gaseous fire extinguishing agents, it has a low global warming potential and short life time in the atmosphere. Gaseous suppression of a flame requires low concentration of extinguishing agent, therefore level of oxygen in the air does not decrease [13–17].

2 Materials and Methods

The suppression mechanism of gaseous extinguishing agents is approximately identical. In this paper we have considered the process of indoor fire extinguishing; as combustible load we have used materials with increased burning rate. To estimate the critical flow rate of extinguishing agent it should be determined the value of minimum phlegmatizing concentration of phlegmatizer and fire extinguishing agent, in relation to a gas-air mixture formed during thermal decomposition of the burning solid material. To determine the minimum phlegmatizing concentration of phlegmatizer it could be used the method described below.

According to the theory of burn termination suppression of a flame becomes possible when its temperature in a burning zone reduces to 1000 °C that is equivalent to absorption of 50% of heat generated per unit of time during combustion process. Although the gaseous fire extinguishing is based on this theory, but ways to reduce the flame temperature and the heat generation rate in the single volume are different and depend on the chemical structure and physical properties of gas molecules. If the concentration of phlegmatizer is high, then the dilution effect of combustible mixture becomes appreciable [18–21]. The molar heat capacity of argon and nitrogen molecules is lower than that of gas-air mixture, so their main action in the process of phlegmatization is dilution of mixture. Irrespective of suppression mechanism of gaseous extinguishing agents, the result of phlegmatization should realize in decreasing of combustible mixture temperature to a temperature of extinction $T_e = 1050$ K.

Carbon dioxide is the most commonly used extinguishing agent. In order to determine the time for extinguishing of fire in the closed space, in conditions of limited gas exchange with external environment (only through the vertical aperture), it have been researched a zone model of extinguishing process. This model clearly identifies zone of smoke blanketing which is characterized by presence of the equal pressure and zero pressure (in relation to atmospheric) planes.

Extinguishing of fire in closed room, using carbon dioxide, is actual in following conditions:

- Formation of carbon dioxide, which concentration in a gas-air environment is equal to minimum phlegmatizing concentration;

- Combined accumulation of combustion products and carbon dioxide supplied from external source. As condition for flame extinction, in this case, should be lowering of the equal pressure plane (EPP) to the level of burning material.

Zone model, presented in Fig. 1, implies division of the room into separate areas numbered consequently: 1 - fire load; 2 - rising column of combustion products; 3 - ceiling layer of combustion products and carbon dioxide mixture; 4 - extended vertical aperture. The movement directions of combustion products and fresh air are indicated by arrows.

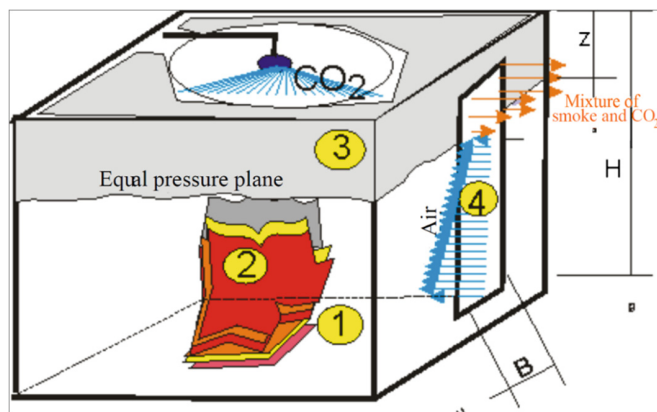


Fig. 1. Scheme of the room with zonal model of internal fire. 1. Fire load (wood products). 2. Column of rising combustion products. 3. Zone of smoke blanketing above the plane of zero pressure. 4. Extended aperture.

The distinctive feature of zone model is the presence of zero pressure plane (ZPP), where the pressure of gas medium is equal to the atmospheric pressure. Therefore there is no movement of air masses neither into, nor out of the room. Position of EPP is the main characteristic of zone model illustrating development of fire in the room. Practical importance of this parameter is connected with possibility of the safe evacuation of people. The ambient temperature, below the plane of equal pressure, is rather low to provide comfortable movement of fire brigade.

To determine position of EPP, at any time from beginning of supply of carbon dioxide, we should consider material balance of carbon dioxide in conditions when the balance between combustion products and the flow of mixed gases is already established through the vertical aperture. In such case it should be analyzed the change of EPP level caused only by supply of carbon dioxide.

3 Results

The analysis of extinguishing process have been conducted on the basis of material balance of fire extinguishing agent, according to the scheme which was applied earlier in works [13–15]. The material balance equation of combustion products, coming into closed space and then partially lost through the vertical aperture, can be presented by following equation:

$$G d\tau = \rho S dz + \rho U F_z d\tau \quad (1)$$

where: g - flow rate of carbon dioxide, kg/s; ρ - density of carbon dioxide and combustion products mixture, m^3/kg ; z - distance from ceiling to EPP; S - ceiling area, m^2 ; U - average rate of movement of carbon dioxide and combustion products mixture through the aperture; F_z - aperture area. The volumetric flow of gases is proportional to aperture area and could be determined by value of aperture area - F_z , participating in gas exchange. The volumetric flow is equal to result of multiplication of the layer thickness, placed over EPP - z , and aperture width - b , i.e. $Q = \rho U z b$.

Taking into account this formula, we can find the material balance equation, which allow detecting EPP position per unit time and extinguishing time, when EPP position will fall till the surface of the burning load.

$$G d\tau = \rho S_0 dz + \rho U z b d\tau \quad (2)$$

We should lead the formula (7) in a form suitable for integration.

$$d\tau = \rho S_0 \frac{dz}{G - \rho U b z} \quad (3)$$

If $z = H$; $\tau = \tau_T$, then we can obtain the formula for determination of extinguishing time, in conditions when flame is suppressed by carbon dioxide in closed room with extended aperture for gas exchange.

$$\tau_T = -\frac{\rho \cdot S_0}{bU} \text{Ln} \left(1 - \frac{\rho \cdot UbH}{G} \right) \quad (4)$$

The formula (4) allows analyzing dependence of extinguishing time on instantaneous consumption of carbon dioxide. As in case of application of other extinguishing agents, extinguishing time for carbon dioxide decreases together with growth of its consumption. If the value of carbon dioxide consumption in denominator of the formula (4) will decrease till a value in numerator, which is equal to $\rho U b H$, the situation could become critical, when $\rho U b H = G = J_k$.

The density of CO_2 and combustion products mixture could vary depending on the flow rate of carbon dioxide. It is accepted that the minimum density of gas mixture should not be lower than appropriate phlegmatizing concentration of carbon dioxide in a steam - air mixture, which is equal to $\phi_f = 25\text{--}30\%$. Suppression of flame by supplying of the carbon dioxide is accompanied by such concomitant effect as partial

compression of gas medium. Therefore density of gas mixture in a zone of smoke blanketing will exceed the minimum value, appropriate to phlegmatized mixture. The higher the gas flow rate, the greater the value of gas density inside the room.

Such conditions provide the optimum mode of fire extinguishing process. The higher the flow rate, the greater the content of carbon dioxide in the flow of smoke, lost through the aperture. If the value of flow rate is such that condition of gaseous extinguishing mixture is closer to phlegmatizing, then the amount of carbon dioxide for fire extinguishing will decrease.

Dependence of gaseous mixture density on its composition, by analogy with the methods used in works [13–17], can be expressed by a simple empirical ratio:

$$\rho = \beta J^n, \quad (5)$$

where: n - coefficient for account the rate of change of gaseous mixture density; β - coefficient of proportionality, J - gas flow rate.

If $J = J_k$; $p = p_f$, so it become relevant to the minimum phlegmatizing concentration of CO_2 . By substituting the expression $p = p_f$, if $J = J_k$, we have received:

$$\beta = \rho_f / J_k^n. \quad (6)$$

In order to calculate the value of extinguishing time, the formula (4) should be transformed, considering expression for β and p .

$$\tau_T = -\frac{\pi_f S_0}{bU} \left(\frac{J}{J_k}\right)^n \text{Ln} \left(1 - \left(\frac{J_k}{J}\right)^{1-n}\right) \quad (7)$$

To calculate specific consumption of carbon dioxide, used for fire extinguishing, we should multiply extinguishing time – Q by relevant flow rate of carbon dioxide, and specific consumption can be related both to extinguishing area in room - Q_S and to volume of room - Q_V ., In calculated ratios, giving below, $Q = Q_S$.

$$Q = -\frac{\rho_f S_0 J}{bU} \cdot \left(\frac{J}{J_k}\right)^n \text{Ln} \left(1 - \left(\frac{J_k}{J}\right)^{1-n}\right) \quad (8)$$

In Eqs. (7) and (8) $J_k = -\frac{\rho_f b U H}{S_0}$.

Density of phlegmatizing gaseous mixture is determined by the Equation:

$$\rho = \varphi_F \rho_{\text{CO}_2} + (1 - \varphi_F) \rho_V, \quad (9)$$

where: φ_F - minimum phlegmatizing concentration of CO_2 ;

ρ_{CO_2} - carbon dioxide density, kg/m^3 ;

ρ_V - air density, kg/m^3 .

4 Discussion

Analysis of the formula (9) shows that dependence of specific consumption of carbon dioxide on its flow rate passes through a minimum point, which position corresponds to the value of optimum flow rate.

The experimental results of extinguishing of various materials, from plastics to rubber products with different values of critical flow rate, were obtained using formulas (7) and (8). The graphic analysis of results is presented in Fig. 2.

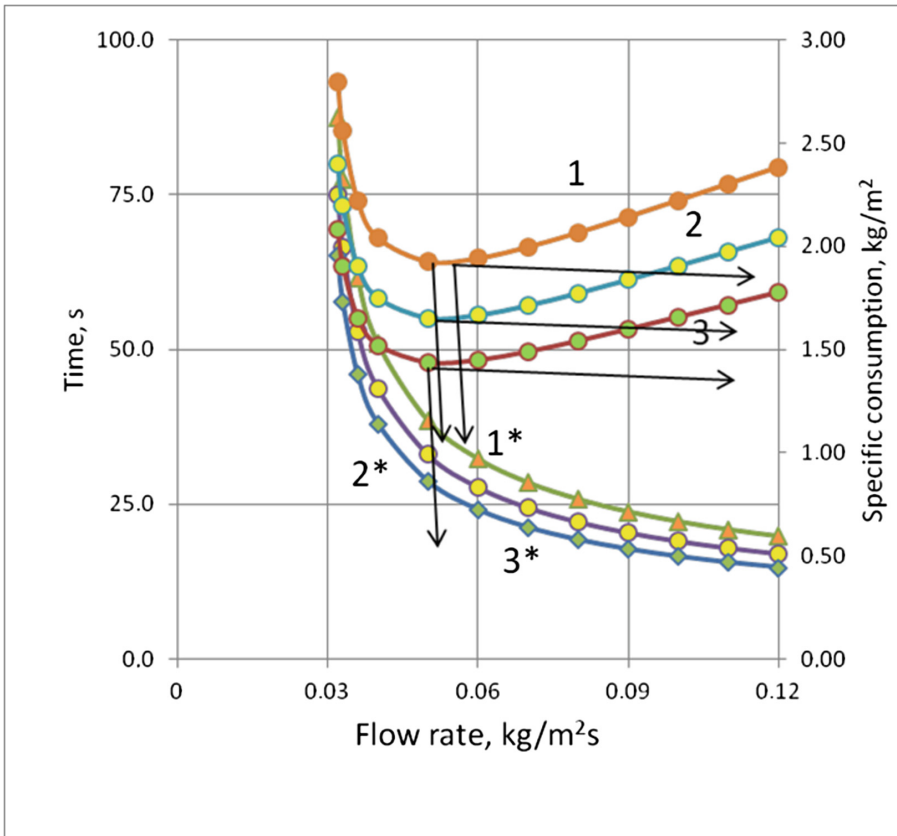


Fig. 2. Dependence of extinguishing time (1–3) and specific consumption of carbon dioxide (1*–3*), in conditions of closed space and varying value of critical flow rate: 1–0.03 kg/m²s; 2–0.05 kg/m²s; 3–0.08 kg/m²s. The minimum specific consumption and the optimum flow rate are indicated by arrows.

The higher the burning rate of fire load, the more the specific consumption, increased from 1.4 kg/m² to 2.8 kg/m² due to the growth of critical flow rate from 0.03 kg/m²s до 0.8 kg/m²s.

The value of optimum flow rate, determined by position of the minimum point on curve, has also increased during extinguishing of material with the higher burning rate.

5 Conclusion

The analysis of indoor fire extinguishing process allowed us to obtain quantitative ratios for calculation of extinguishing time and specific consumption depending on the flow rate of extinguishing agent.

It has been revealed that gaseous agents are suitable for extinguishing of various combustible materials, as it is possible to define optimum flow rate of the agents. It is graphically presented in Fig. 2.

References

1. Krupenin, S.: Development of the system and management providing fire safety of the railway transport. *Sci. Technol. Transp.* 16–29 (2004)
2. Korzeniowski, S., Cortina, T.: Firefighting foams – Reebok reduxl. *Ind. Fire J.* 18–20 (2008)
3. Cortina, T.: The safety & benefits of AFFF agents. Special analysis: Foam. *Ind. Fire J.* 70–75 (2007)
4. Pabon, M., Corpart, J.: Fluorinated surfactants: synthesis, properties, effluent treatment. *J. Fluorine Chem.* **114**(2), 149–156 (2002)
5. Korolchenko, D., Voevoda, S.: Influence of spreading structure in an aqueous solution-hydrocarbon system on extinguishing of the flame of oil products. In: *MATEC Web of Conferences*, vol. 86 (2016). <https://doi.org/10.1051/mateconf/20168604038>
6. Shaefer, T., Dlugogorski, B., Kennedy, E.: Sealability Properties of Fluorine-Free Fire Fighting Foams. University of Newcastle (2007)
7. Korolchenko, D., Tusnin, A., Trushin, S., Korolchenko, A.: Physical parameters of high expansion foam used for fire suppression in high-rise buildings. *Int. J. Appl. Eng. Res.* **10** (21), 42541–42548 (2015)
8. Kokorin, V., Romanova, I., Khafizov, F.: The problems of effective fire suppression of vertical steel storage tanks in the fuel layer. *Electron. Sci. J. Oil Gas Bus.* **3**, 255–260 (2012)
9. Patent us 6732809. Kidde-Fenwal apparatus for distributing granular material (2004)
10. Patent us 7155347. Fike corporation pre-inerting method and apparatus for preventing large volume contained flammable fuels from exploding (2006)
11. Patent us 20040226301. Airwars Defense Lp, A Colorado Limited Partnership Liquid nitrogen enabler (2004)
12. Patent us 20050001065 Nozzle apparatus and method for atomizing fluids (2005)
13. Sharovarnikov, A., Korol'chenko, D.: Fighting fires of carbon dioxide in the closed buildings. *Appl. Mech. Mater.* **475–476**, 1344–1350 (2004)
14. Korolchenko, D., Degaev, E., Sharovarnikov, A.: Dependence of fire extinguishing efficacy of low expansion foams solutions homology sodium sulfate on the molecular weight of the surface-active substances. In: *2015 2nd International Conference on Material Engineering and Application* (2015)
15. Korolchenko, D., Degaev, E., Sharovarnikov, A.: Determination of the effectiveness of extinguishing foaming agents in the laboratory. In: *2015 2nd International Conference on Material Engineering and Application* (2015)

16. Volkov, R., Kuznetsov, G., Strizhak, P.: Influence of the initial parameters of liquid droplets on their evaporation process in a region of high-temperature gas. *J. Appl. Mech. Tech. Phys.* **2**, 248–256 (2015)
17. Eliseev, V., Lutsenko, V.: Static hysteresis phenomena in ka-pillar. *Geotech. Mech.* **66**, 157–163 (2006)
18. White, D.: Make room for safety. *Ind. Fire World* **21**(1), 8–10 (2006)
19. Westwood, K.: Dark skies over England. *Ind. Fire World* **21**(1), 4–7 (2006)
20. Zhang, Q., Wang, L., Bi, Y., Zhi, H., Qiu, P.: Experimental investigation of foam spread and extinguishment of the large-scale methanol pool fire. *J. Hazard. Mater.* **287**, 87–92 (2015). <https://doi.org/10.1016/j.jhazmat.2015.01.017>
21. Ranjbar, H., Shahraki, B.: Effect of aqueous film-forming foams on the evaporation rate of hydrocarbon fuels. *Chem. Eng. Technol.* **36**, 295–299 (2013). <https://doi.org/10.1002/ceat.201200401>

Railway/Road Level Crossing Design – Aspect of Safety and Environment

Milica Vilotijević , Luka Lazarević , and Zdenka Popović  

Faculty of Civil Engineering, University of Belgrade,
Bulevar Kralja Aleksandra, 73, 11000 Belgrade, Serbia
zdenka@grf.bg.ac.rs

Abstract. At the railway/road level crossings, two essentially different modes of transport intersect, both with a variety of vehicle performance parameters and traffic organization rules. Level crossing presents a collision zone for both transport modes from the aspect of traffic safety. Unfortunately, the probability of accidents at level crossings is still high. Railway Infrastructure Manager controls only one part of the problem (traffic management and ensuring the safety of level crossings using technical equipment and signalization). Level crossings are not always avoidable on the existing railway lines, although the preferred solution is overpass crossing. On the European railway network, level crossings occur even on the reconstructed railway lines for speeds up to 200 km/h, with the appropriate design principles and safety measures for both transport modes. This paper describes the basic design principles for the level crossings where rail vehicles reach speeds up to 200 km/h, as well as the review of the necessary measures to increase safety level.

Keywords: Railway · Infrastructure · Level crossing · Design · Safety

1 Introduction

From the aspect of environmental protection, the best railway routing solution is the infrastructure below ground surface in the urban area (tunnel or deep cut) [12]. Otherwise, “above ground” position of railway infrastructure in the urban environment is the worst solution that requires the railway/road level crossing.

Crossing of railway and road could be designed either as a level crossing or as an overpass crossing. The preferable design of crossing depends mainly on safety of both modes of transportation.

According to current European agreement, high-speed railways, as well as new and reconstructed railways should not have level crossings due to the reasons related to traffic safety. Increase in the speed of railway traffic leads to decrease in the safety of level crossings. UIC leaflet [16] specifies speed of 200 km/h as the upper limit for the design of level crossing. In addition, speed of 120 km/h is the upper limit for application of particular safety measures on level crossings [16], since there is a risk of derailment in the case of collision of rail and road vehicle. Recommendations specified in [16] could be applied for railway reconstruction when it is not possible to design all crossings as overpass. In such case, some crossings would be designed at first as level

crossings with additional safety measures, and these would be reconstructed to overpass crossings when necessary conditions are fulfilled.

Level crossing of railway and road should be secured using automatic signaling devices, full or half barriers with appropriate lights, audio and visual signals, as well as providing necessary site distance. Infrastructure Manager should carry all costs for design, construction and securing of level crossing.

When considering an operating program for train speeds above 120 km/h, it is desirable, in tackling the problem of level crossings, to examine the practical possibilities of eliminating all those points where rail and road cross at the same level [16]. The following criteria should be used as a basis for prioritizing level crossing for:

- elimination of dangerous crossings with heavy and/or slow-moving road traffic, and crossings where the passage of heavy vehicles and exceptional loads occurs with statistical frequency,
- elimination of level crossings in cases where even a small profit emerges in terms of annual savings comparing attendance and maintenance costs with the investment required for the construction of bridge or road deviations,
- elimination of private or rarely used level crossings, and as far as possible, of level crossings reserved for pedestrians.

Therefore, overpass crossing should be applied whenever it is possible and financially viable. In addition, each case demands the analysis of construction costs for both crossing types and comparison with risk of potential incident (as shown in **Ошибка! Источник ссылки не найден.**) and traffic delay costs (Fig. 1).



Fig. 1. The example of incident on level crossing - freight train crashes into charter bus in Biloxi, Mississippi on February 8th, 2017 [7].

Nevertheless, the existing technical regulations do not include specificities of level crossings of railway and road in the vicinity of road intersection. Practical experience so far has shown that design of level crossing does not consider the influence of near-by road intersection, which could lead to accidents due to inability of road vehicle to move off track before train arrival (**Ошибка! Источник ссылки не найден.**) (Fig. 2).

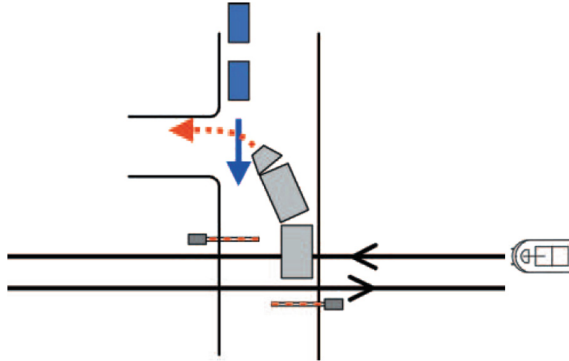


Fig. 2. Inability of clearing the level crossing due to the busy traffic on near-by road intersection [3].

2 Alignment Design of Railway/Road Level Crossing

The ideal level crossing implies that both railway and road are straight and that intersection angle is 90° . Since the design parameters for roads are more flexible comparing to those for railways, the one should first design alignment of railway whenever it is possible. Afterwards, alignment of road should be adjusted to the design of railway. If railway is straight in the area of level crossing, railway grade should coincide with road cross level. In addition, railway grade in level crossing depends on the level of rails in cross section. Therefore, if railway is straight in the area of level crossing, it means that road grade is 0%.

If it is not possible to avoid level crossing in the area of railway curve, it is necessary to adjust road grade to designed railway cant in curve. The previous statement applies only to single track railway. If railway has two or more tracks, it should be straight in the area of level crossing, or it could be in curve without designed cant (very large radius).

2.1 Horizontal Alignment Elements

Intersection angle at level crossing that is less than 90° is inadequate from the aspect of sight distance. According to [14], level crossing should be designed with intersection angle of 90° (preferable) or less, but not less than 60° (**Ошибка! Источник ссылки не найден.**). In addition, technical regulations do not specify upper speed limit [14], although several statements clearly defines cases for speed greater than 100 km/h. On the other hand, passenger trains with speed up to 120 km/h and freight trains with speed up to 75 km/h demand shorter area of conflict on the level crossing [5]. Minimum intersection angle is 70° according to [5] (Fig. 3).

Road curve in the area of level crossing negatively influences sight distance. In addition, it could move focus of the driver from level crossing to curve negotiation.

If single track railway is curved in the area of level crossing, road vehicles that arrive from the outer side of the curve have better sight distance than those arriving

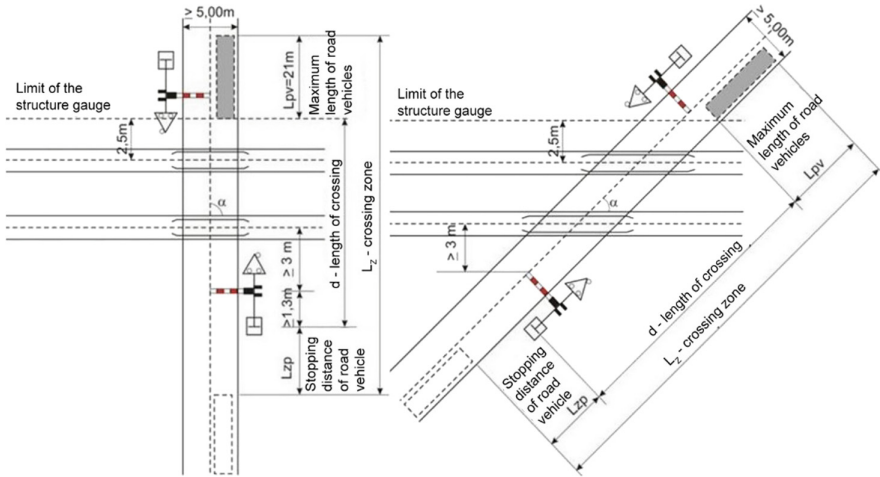


Fig. 3. Level crossing with intersection angle: $\alpha = 90^\circ$ (left) and $\alpha < 90^\circ$ (right) [14].

from the inner side of the curve. Minimum radius of curve in the area of level crossing on single track railway is not specified by national technical regulations. If it is considered that upper limit for cant is 150 mm, it implies that maximum cross level equals 10%. Therefore, one should put effort to design level crossing on straight section of railway. Nevertheless, if level crossing in curved section could not be avoided, curve radius should be large enough so that there is no need to design cant. For example, speed 120 km/h demands curve radius $R > 10224$ m according to Eq. (1), and speed 160 km/h demands curve radius $R > 16640$ m according to Eq. (2) [10, 13].

$$R > 7.1 \frac{V_{\max}^2}{10}, \text{ for } V_{\max} \leq 120 \frac{\text{km}}{\text{h}} \tag{1}$$

$$R > 6.5 \frac{V_{\max}^2}{10}, \text{ for } V_{\max} > 120 \frac{\text{km}}{\text{h}} \tag{2}$$

2.2 Vertical Alignment Elements

Road pavement should have the same level as track running surface along 3 m distance measured from track axis to both sides (single track), or from last track axis to left or right side (two or more tracks) [14]. In addition, road grade should be up to 3% on the distance of at least 20 m before and after level crossing (**Ошибка! Источник ссылки не найден.**) (Fig. 4).

It should be mentioned that “Policy on Geometric Design of Highways and Streets” by AASHTO (American Association of State Highway and Transportation Officials) specifies recommendations that differ from state to state. **Ошибка! Источник ссылки не найден** shows longitudinal profile of the road in the area of level crossing according to [1] (Fig. 5).

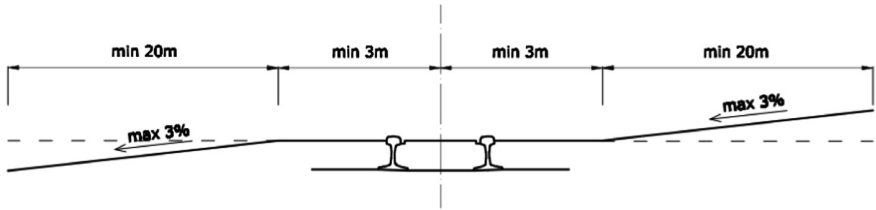


Fig. 4. Longitudinal profile of road in the area of level crossing [14].

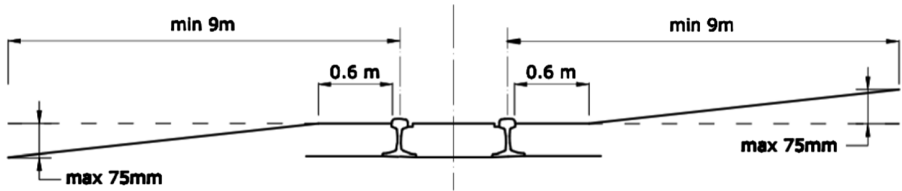


Fig. 5. Longitudinal profile of road in the area of level crossing according to recommendations by AASHTO [1].

Radius of convex vertical curve of road on both sides of level crossing should meet the requirements of the vehicle with largest axle distance, in order to avoid vehicles getting stuck and damaging of both vehicle and road pavement during vertical curve negotiation (**Ошибка! Источник ссылки не найден.**). There are many examples of stuck vehicles due to the inadequate radius of road vertical curve on level crossing, as it is shown in **Ошибка! Источник ссылки не найден.** and **Ошибка! Источник ссылки не найден.** For example, if $R_{v,\min} = 50$ m and largest axle distance of the road vehicle is $a = 7$ m, maximum length of focus f equals 13 cm according to Eq. 3 [9] (Figs. 6, 7 and 8).



Fig. 6. Example of road pavement damage due to the inadequate radius of vertical curve [9].



Fig. 7. Bus with large axle distance that was stuck at the level crossing in Biloxi, Mississippi on February 8th 2017 [7].

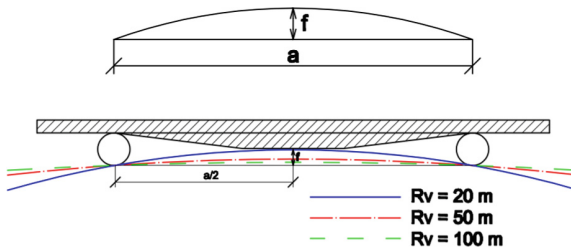


Fig. 8. Influence of radius of convex vertical curve ($R_v = 20\text{-}100\text{ m}$) on curve negotiation of the road vehicle with 7 m axle distance.

$$f = \frac{\left(\frac{a}{2}\right)^2}{2R_{v,\min}} = \frac{3.5^2}{100} = 12.25\text{ cm} \approx 13\text{ cm} \tag{3}$$

According to **Ошибка! Источник ссылки не найден.** and recommendations in [14], it is possible to apply large vertical curve radius which would correspond to the vehicles with large axle distance.

3 Road Structure on the Level Crossing

Road structure on the level crossing should provide safe passage of road (**Ошибка! Источник ссылки не найден.** and **Ошибка! Источник ссылки не найден.**) and railway vehicles (**Ошибка! Источник ссылки не найден.**), as well as quick and simple access for track inspection and maintenance. In some cases, it is necessary to provide safe crossing of pedestrians. Selection of road structure on the level crossing depends on:

- traffic load,
- resistance of the road pavement to the acceleration and breaking forces,
- resistance of the road pavement to the wheel slippage,
- gap width for passage of rail wheel flange between road pavement and rail head,

- adjustment of road pavement and track (**Ошибка! Источник ссылки не найден.**),
- resistance to the intentional damage (vandalism).

Considering the shape of rail wheel and expected vertical wear of rail head (maximum allowed vertical wear is 14 mm for rail profile 60 E1), the upper surface of rail head should be laid above the upper surface of road pavement on the outer side of track. Furthermore, there should be enough gap width on the inner side of track for passage of rail wheel flange (**Ошибка! Источник ссылки не найден.**) (Fig. 9).

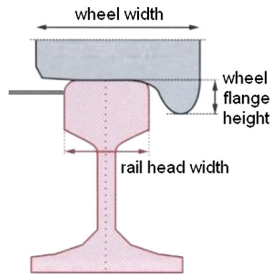


Fig. 9. Position of the road pavement and the wheel flange relative to the rail profile 60 E1.

Asphalt pavement is the most common on the level crossings. The main disadvantage of asphalt pavement is the inability of simple access to the elements of railway superstructure (correction of track longitudinal level and alignment, rail replacement etc.). In addition, the contact between two materials with different properties (asphalt and steel) leads to breakage of asphalt (**Ошибка! Источник ссылки не найден.**) and crack development over time. Therefore, level crossing demands intense maintenance in order to avoid development of impact spots for road vehicles. On modern

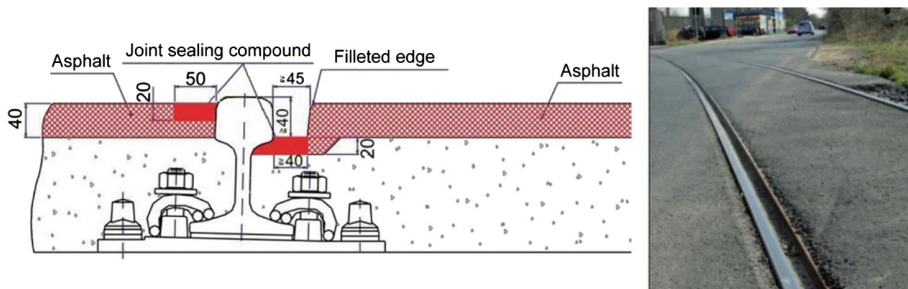


Fig. 10. Asphalt pavement on the level crossing (left) and the example of its breakage (right) [2, 15].

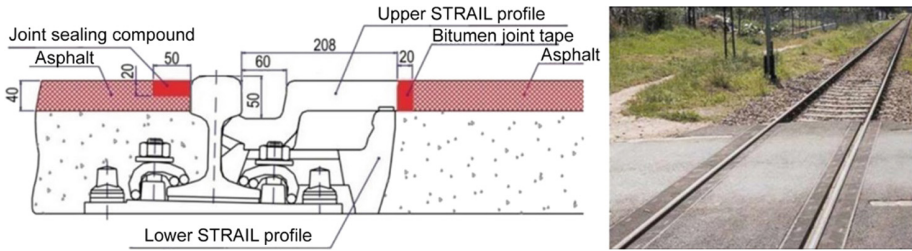


Fig. 11. The example of STRAIL solution for level crossing (rubber element between rail and asphalt pavement): cross section (left) and installed crossing (right) [2].

level crossings, gap for passage of rail wheel flange could be provided by placing rubber elements between rail and asphalt pavement (**Ошибка! Источник ссылки не найден.**) (Figs. 10 and 11).

Special assembling rubber panels that are used for the level crossings are classified as flexible pavements (**Ошибка! Источник ссылки не найден.**). These rubber panels are installed right next to the rail web, and they are designed to fit any type of fastening system (either elastic or rigid fastening system). The advantages of rubber panels are:

- application on each road category,
- simple transport and simple and fast installation,
- simple removal and easy access to elements of railway superstructure,
- electric insulation of rails,
- reduction of noise and vibration emission, which is the most important aspect in the urban area [11],
- design of the upper surface of panels increase slip resistance of the wheels,
- long service life.

Reinforced concrete slabs on level crossings are classified as rigid pavements. These slabs could be poured on-site or they could be made of precast concrete (**Ошибка! Источник ссылки не найден.**). Dimensions of concrete slabs depend on traffic load. Special attention should be drawn to maintenance of these slabs in order to avoid different types of damage e.g. cracks, damage of joints and top surface, occurrence of ballast voids under sleepers [8] and others. Longitudinal and transverse joints enable slab displacements due to the temperature changes and transfer of forces from one slab to another. Therefore, it is of great importance that joints are regularly constructed and maintained. Regular joint sealing should have water proofing property and it should prevent filling of joint with dirt and gravel. Sealing of joint could be performed using bitumen compound or synthetic rubber (Figs. 12 and 13).



Fig. 12. Installation of rubber panels on railway line Belgrade - Pančevo in 2015.



Fig. 13. Reinforced concrete slabs made of precast concrete [4, 6].

4 Conclusion

From the aspect of railway and road traffic safety, level crossing presents collision area for both modes of transportation. Increasing the speed of trains reduce the safety of both railway and road traffic on the level crossings. The paper specifies speed of 120 km/h as the limit speed that demands application of special safety measures on the level crossings due to the high risk of train derailment in the case of collision with road vehicle. In addition, speed of 200 km/h was designated as the upper limit for the design of level crossings. Level crossings on the railways with maximum train speed over than 200 km/h could only be designed using particular safety measures, but only when designing the overpass crossing is not possible [16]. These level crossings should be in service until it is feasible to replace it with overpass crossings.

Paper presents review of different road and railway horizontal and vertical alignment in the area of level crossing. In addition, paper considers sight distance requirements and specific requirements for road vehicles with large axle distance.





In the last part of the paper, there are presented modern designs of level crossings. Level crossings with installed rubber panels were assessed as the favorable solution, which provides comfort for road vehicles and easy access to the elements of railway superstructure during maintenance activities, especially in the case of track geometry correction.

Acknowledgement. This work was supported by the Ministry of Education and Science of the Republic of Serbia through the research project No. 36012: “Research of technical-technological, staff and organization capacity of Serbian Railway, from the viewpoint of current and future European Union requirements”.

References

1. American Association of State Highway and Transportation Officials. A Policy on Geometric Design of Highways and Streets (2011)
2. Elberg, R.: Der Bahnübergang als Teil der Fahrbahn von Schiene und Straße. *EI-Eisenbahningenieur* **51**(3), 5–10 (2000)
3. Freystein, H., Menge, J., Ruhs, W.: Sicherheit an Bahnübergängen Stand und aktuelle Initiativen in Deutschland und Europa. *ETR– Eisenbahn technische Rundschau* **52**(12), 771–782 (2003)
4. <http://max-boegl.de/en/downloads-en/106-bueb-level-crossing-boegl/file.html> (2017)
5. <http://www.fhwa.dot.gov/publications/research/safety/86215/86215.pdf> (2017)
6. <http://www.rtands.com/index.php/safety-training/crossing-with-the-utmost-care.html> (2017)
7. <http://www.youtube.com/watch?v=anOW7ET-oPk> (2017)
8. Lazarević, L., Vučković, D., Popović, Z.: Assessment of sleeper support conditions using micro-tremor analysis. *Proc. Inst. Mech. Eng. Part F: J. Rail Rapid Transit* **230**(8), 1828–1841 (2016)
9. Lorenz, A.: Linienführung und Gradienten am Bahnübergang. *EI-Eisenbahningenieur* **58**(10), 20–21 (2007)
10. Popović, Z.: Osnove projektovanja železničkih pruga. Građevinski fakultet, Beograd (2004)
11. Popović, Z., Lazarević, L., Brajović, L., Vilotijević, M.: The importance of rail inspections in the urban area-aspect of head checking rail defects. *Procedia Eng.* **117**, 596–608 (2015)
12. Popović, Z., Lazarević, L., Vukićević, M., Vilotijević, M., Mirković, N.: The modal shift to sustainable railway transport in Serbia. In: *MATEC Web of Conferences*, vol. 106, p. 05001 (2017)
13. Pravilnik o tehničkim uslovima i održavanju gornjeg stroja železnickih pruga, “Službeni glasnik RS” vol. 39, p. 74 (2016)
14. Pravilnik o načinu ukrštanja železničke pruge i puta, pešačke ili biciklističke staze, mestu na kojem se može izvesti ukrštanje i merama za osiguranje bezbednog saobraćaja, “Službeni glasnik RS” vol. 89, p. 2 (2016)
15. Seehafer, W.: Bahnübergang mit geschlossener Spurrille. *EI –Eisenbahningenieur* **58**(6), 50–51 (2007)
16. UIC code 762., Safety measures to be taken at level crossings on lines operated from 120 to 200 km/h (2005)

Building Platforms of Polymer Matrix Based Composite Construction Materials for Transportation Facilities

Andrey Glasunov¹ , Victor Bobryashov¹ , Victor Bobryashov¹ ,
and Nikolay Bushuev² 

¹ TSNIISK Named After Koucherenko, V.A. Research Center of Construction
Joint Stock Company, 2nd Institutskaya St., 6, Moscow 109428, Russia

² Moscow State University of Civil Engineering,
Yaroslavskoye Sh. 26, Moscow 129337, Russia
bush_ni@mail.ru

Abstract. The paper proposes that full-pack platforms of composite structures based on single-direction pultrusion fiberglass reinforced plastic based on polyether matrixes be built for transportation facilities. The test results of some fragments of real-life platforms are presented. Engineering solutions are developed to build railroad platforms with structures of polymer composite materials. Static field tests have been conducted, including continuous load tests.

Keywords: Polymer composite materials · Railroad platforms

1 Introduction

Platforms of pultruded fiberglass reinforced plastic have found use in the railroad transportation sector. They contain H-bar steel, U-bar steel, angle steel, box-section steel, etc. The platform components were bolted together. Pultrusion composite profiles of fiberglass-reinforced plastic were the main platform element that called for a special study [1–6]. Therefore, research was done to examine the physical and mechanical properties of the profile material, complete with tests of fragments of real-life railroad platforms.

2 Researching the Physical and Mechanical Properties of Profile Material

To know the physical and mechanical properties of the fiberglass composite materials used to manufacture the platform fragment, we cut samples out of H-bar 200 × 200 10 mm, U-bar 200 × 80 × 8 mm, box-section steel 60 × 60 × 4.5 mm, and angle bar 76.2 × 76.2 × 9.53 mm. We had cut five samples of each type, both along and across the fiber.

Tests were done with testing machine FP 100/1 (Germany) that ensured load measurement accuracy of 1%; the ‘load-deformation’ diagram was recorded automatically.

Before the test, the samples were subject to 16-h conditioning to meet GOST 12423-66* “Plastics. Terms of Sample Specimen Conditioning and Testing under temperature $(296 \pm 2) \text{ }^\circ\text{K}$ ($23 \pm 2) \text{ }^\circ\text{C}$ and relative humidity level of $(50 \pm 5)\%$ ” [7]. The quoted experimental results and probability estimates suggest that all of the above theoretical distributions match well the results of the tests [8–10]. The best fitting probability distribution will be Type B according to Graham-Chaliers.

3 Testing Platform Fragments

A fragment of the platform (Figs. 1, 2 and 3) sized in plane $4.0 \times 4.0 \text{ m}$ included two main cross-beams (1 and 2), and six stringers (spans) (3, 4, 5, 3*, 4*, 5*) with the deck (6) on them, all made of H-bar $200 \times 200 \times 10 \text{ mm}$ except the barrier beam that was made of two paired U-bars $200 \times 80 \times 8 \text{ mm}$. The crossbeams were bolted with galvanized bolts $M12 \times 45$ (GOST 7798-70) and 3 mm thick washers of diameter 37 mm (DIN 9021). The deck was made of strips with antislip coating of Plank type fiberglass composite. Deck stripes had a Z-lock type connection between them. The deck laid across the stringers was clamped to them with composite plates sized $60 \times 40 \times 8 \text{ mm}$ with round-head bolts $M8 \times 50$.

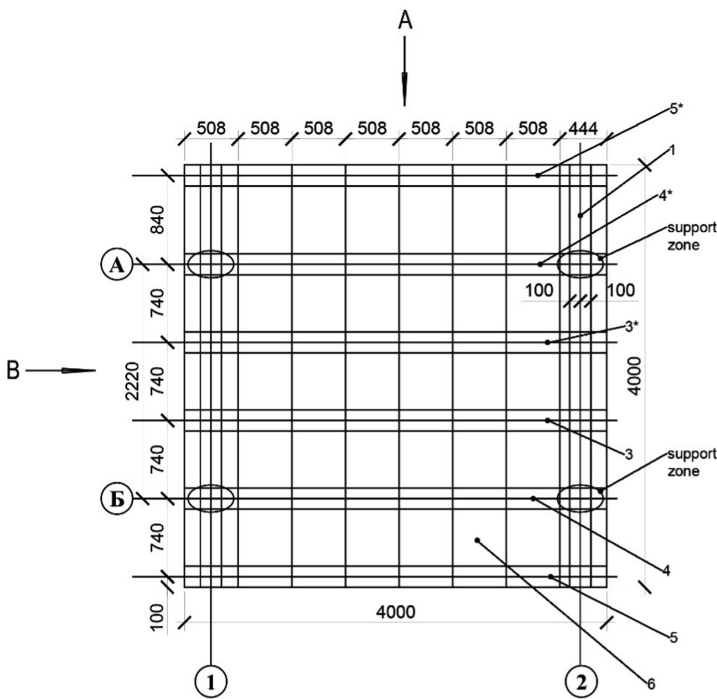


Fig. 1. Fragment of platform made of fiberglass reinforced plastic. 1, 2, 3, 4, 5, 3*, 4*, 5* - beams, 6 - deck.

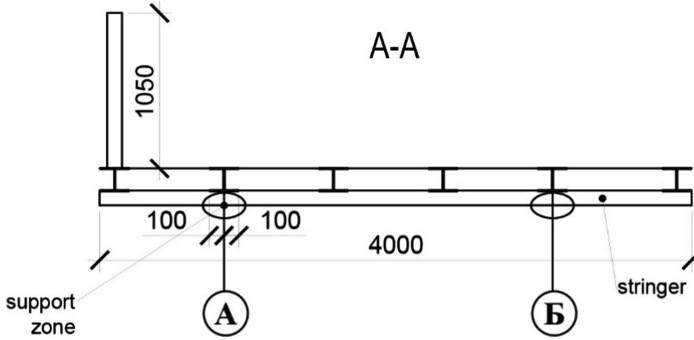


Fig. 2. Fragment of platform made of fiberglass reinforced plastic (incision A-A)

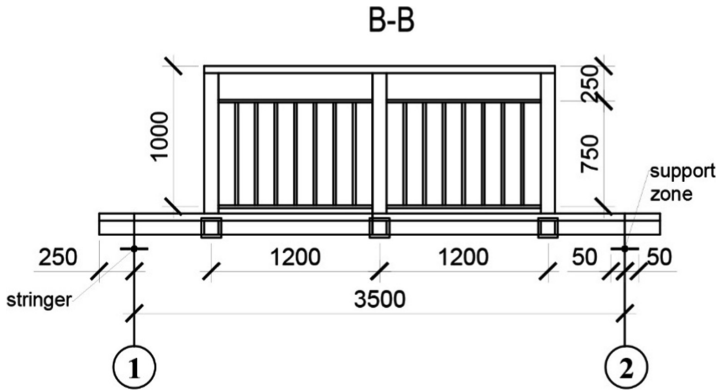


Fig. 3. Fragment of platform made of fiberglass reinforced plastic (incision B-B)

The fragment was tested under a brief load on a test bench, supported on a plate $200 \times 100 \times 10$ mm to simulate transfer of the load on the actual structure's base foundation.

The fragment was tested to withstand the designed load of own weight, snow, and standard loads under SP 20.13330.2011 "Loads and Impacts" [11].

The fragment was put under load in five 1,860 kgf stages, using foundation blocks FBS 6-4-6 ($600 \times 400 \times 600$ mm) each weighing 310 kg. Each foundation block was set on two roller bearings (one fixed, one mobile), to create the required freedom of cross motion over the platform width, simulating the equivalent of the load regularly distributed over the deck. The greatest combined load on the fragment, including its own weight, was 10,370 kgf (737 kgf/m^2). The value of each loading stage was 1,860 kgf (133 kgf/m^2).

See Fig. 4 for general view of the fragment structure prior to the 737 kgf/m^2 load test.

To calculate the structure's mode of deformation at each loading stage, we measured the sag and relative longitudinal strains [12–21]. We used the Maksimov



Fig. 4. The fragment before the test under load of 737 kgf/m².

deflectometer with scale interval 0.1 mm and the Mokin deflectometer with scale interval 0.01 mm; we measured relative deformation by the readings on wire-strain gages with 50 mm base, using an AID semi-automatic measuring instrument. The values of relative deformations and the elasticity modulus were then used to compute the normal strain in the fragment’s structure.

Following a brief test of the platform fragment, we then conducted continuous tests of the creep that featured sag increment in time relative to the initial sag value.

4 Results of Research

Under low load of 297 kgf/m², relative sag in stringers 3, 4, and 5 was: $(1/340) \times 0.40 = 1/850, 1/750, \text{ and } 1/1,270$, respectively.

SP 20.13330.2011 regulates the greatest sag value of 1/160 for the above beams, depending on the span. Deformation safety factor for stringers 3, 4 and 5 withstanding a low load (297 kgf/m²) will be $(1/160)/(1/850) = 5.3, 4.7 \text{ and } 7.9$, respectively.

The values of the extreme longitudinal stress (kgf/cm²) at the middle span of stringers 3, 3*, 4, 4*, 5 and 5* in the (vertically) extreme fibers of the beams, calculated with approximating formulas for the diagrams (assuming the designed load at 737 kgf/m²) are shown in Table 1.

The first marginal state of the fragment’s structures was determined by longitudinal normal stress in the ledges of the most stressed beam 4. For brief designed load of

Table 1. Extreme longitudinal stress in beams, kgf/cm².

Stress condition type	Beam no.					
	3	3*	4	4*	5	5*
Compression	128	115	152	114	91	92
Stretching	105	103	99	114	64	34

737 kgf/m², compression stress will be ≈ 150 kgf/cm², or less than the brief bending resistance of the beam's material, specifically 1,200 kgf/cm².

Obtained experimentally, the values of the fragment structure's relative sage for regulated values of permanent continuous loads 297 kgf/m², which, as stated above, for stringers 3, 4, and 5 are respectively 1/850, 1/740, and 1/1270, will grow in time under the effect of continuous load (297 kgf/m²) due to the creep of the structure's elements.

Tests have been conducted under permanent and continuous designed load (737 kgf/m²) indoors with ambient temperature of 16 °C. The tests, compared to the mandatory tests under continuous standard load that is lower (297 kgf/m²) help to rapidly identify the nature of the structure's deformation by creep, and to measure the creep rate, creep yield and core.

The results of the fragment structure test to withstand permanent and continuous designed load (737 kgf/m²) have demonstrated that creep is a fading process, and therefore, the same type will have the same process under a lower load (297 kgf/m²). Table 2 shows values of sag and related increments found during the test under load of 664 kgf/m².

Table 2. Beam sag and increment thereof for beams withstanding the load of 664 kgf/s, mm.

Item	Main beam No. (span 2,280 mm)		Stringer No. (span 3.500 mm)		
	1	2	3	4	5
Initial sag, mm (relative sag)	2.33 (1/1,500)	1.29 (1/2,710)	9.56 (1/370)	10.47 (1/335)	5.6 (1/625)
Sag after 7 days test (relative sag)	2.415 (1/945)	1.37 (1/1.665)	9.565 (1/365)	10.675 (1/330)	5.8 (1/600)
Sag increment after 7 days test	0.085	0.08	0.005	0.205	0.2
Sag increment after 7 days test, %	3.65	6.20	0.05	1.96	3.57

5 Conclusion

We have found that the second marginal state (deformation propensity) of a fragment's structure is determined by the greatest relative sage of the structure's beam. Under the regulated permanent continuous loads of 297 kgf/m² this beam sag is 1/750 of the beam's span (3,500 mm). This is below the sag limit of 1/160 regulated in SP 20.13330.2011 "Loads and Impacts", and also less than the admissible sag of 1/200 accepted for the structure by its designer Roszheldor OAO.

The first marginal state (strength) of the fragment's structure is determined by the greatest allowed normal longitudinal stress in the ledges of the structure's beam. Under a brief designed load of 737 kgf/m², the stress is 150 kgf/cm², which is below the brief bending resistance of the beam's material, which was 1,200 kgf/cm² as tested by Rishon Inter OOO.

A 22-day long creep test of a structural fragment under permanent continuous designed load of (737 kgf/m²) proved the creep to be a fading process. This is due to a low level of stress in the structure's material, the maximum for normal longitudinal stress being $150/2,260 = 0.066$ of the destructive stress (2,260 kgf/cm², or bending stress limit according to Rishon Inter OOO). Maximum increment of the initial sag in the beam was 0.08 mm or 6.2%.

The test of the fragment proved the design of the elements to meet the requirements of SP 20.13330.2011 for marginal state group 1 and group 2.




Examination of Russian and national studies, long-term tests conducted previously by V.A. Kucherenko TSNIISK on other projects and its tests currently in progress, has demonstrated the estimated service life of a railroad platform made of fiber-glass composite profile (fragment manufactured by NAFTAROS ZAO) to be up to fifty (50) years. Every ten years the structure needs to pass inspection by experts of V.A. Kucherenko TSNIISK.

References

1. Vasilev, V., Protasov, V., Bolotin, V.: Kompozicionnie materialy. Mashinostroenie, Moscow (1990)
2. Brautmano, L., Kroka, R.: v 8 t. Mir, Moscow (1978)
3. Weaver, C., Williams, J.: Mater. Sci. 10, 1323 (1975)
4. Ferri, D.: Vyazkoprugie svoistva polimerov, Moscow (1963)
5. Bagenov, S., Berlin, A., Kulkov, A., Oshmian, V.: Polimernie kompozicionnie materialy: Nautnoe izdanie. Intellect, Dolgoprudnii (2010)
6. Grunenfelder, L., Suksangpanya, N., Salinas, C., Milliron, G., Yaraghi, N., Herrera, S.: Bio-inspired impact-resistant composites. Acta Biomater. **10**(9), 3997–4008 (2014)
7. Russian standard GOST 12423-66*. Plastmassy. Usloviya kondizionirovaniya I ispitaniya obraztsov (prob) pri temperature (296 ± 2) OK (23 ± 2) °C i odnositelnoi vlagnosti $(50 \pm 5)\%$
8. Bobryashov, V., Bobryashov, V.: Ocenka chastnykh koeffitsientov nadezhnosti po nagruzke I materialam na osnove veroyatnostnykh modelei i urovne bezotkaznosri stroitelnykh konstruktsii po Evrokodam. Moscow (2009)
9. Ventcel, E.: Teoriya veroyatnostei. Vishskaya shkola, Moscow (2001)
10. Mitropovskii, L.: Tehnika staticheskikh vychislenii. Nauka, Moscow (2001)
11. SP20.13330.2011. Nagruzki i vozdeistviya
12. Fudzii, T., Dzako, M.: Mehanika Razrusheniya Kompozitsionnykh Materialov. Mir, Moscow (1982)
13. Bobryashov, V., Vulfov, C., K teorii glitelnoi prochnosti nasledstvennykh sped. Issledovaniya po stroitelnoi mehanike. TSNIISK, Moscow (1985)
14. Batrak, V., Bobryashov, V., Bobryashov, V.: Metod ostenki dolgovechnosti konstruktsii s primeneniem plastmass pri deistvii dlinelnykh nagruzok. Aktualnye problemi issledovaniya po teorii sooruzhenii. Sbornik nauchnykh statei v dvukh chastyakh. Chast 1. TSNIISK, Moscow (2009)
15. Chamis, K.: Mikromekhanicheskie teorii prochnosti. V kn. Razrushenie i ustalost. In: Brautmana L. Mir, Moscow (1978)
16. Tarnopolskii, U., Skudra, A.: Konstruktsionnaya prochnost i deformativnost stekloplastikov. Sinatne, Riga (1996)

17. Bagenov, S.: Mehanizmi razrusheniya armirovannih plastikov pri sgatii i rastyagenii. Diss. na soiskanie stepeni d-ra f. UHF RAN, Moscow (1996)
18. Roginskiy, S., Kanovuch, Koltunov, M.: Visokoprochnie stekloplastiki. Himiya, Moscow (1979)
19. Narisava.: Prochnost polimernih materialov. Himiya, Moscow (1987)
20. Malmaister, A., Tamush, V., Geters, G.: Soprotivlenie zestkih polimernih materialov. Zinatne, Riga (1967)
21. Svistkov, A., Ugegova, N.: Mehanika kompozitsionnih materialov i konstrukzii. Mehanika kompozitsionnih materialov i konstrukzii 22 (3), 3215–323 (2016)

Finite Element Modeling of the Creep of Shells of Revolution Under Axisymmetric Loading

Anton Chepurnenko^(✉) , Natalia Neumerzhitskaya ,
and Michael Turko 

Don State Technical University,
Sotcialisticheskaya st., 162, Rostov-on-Don 344022, Russia
anton_chepurnenk@mail.ru

Abstract. The article is devoted to the development of a method for calculating the shells of revolution under conditions of axisymmetric loading, taking into account the viscoelastic properties of the material. When solving the problem, finite element modeling is used. The derivation of the resolving equations for one-dimensional axially symmetric finite elements in the form of truncated cones with allowance for creep is presented. The solution is performed in a quasi-static setting: the calculation is performed step-by-step, the creep strains are assumed to be constant at each step, and a linear approximation of the deformation growth rate is used to determine their values at the next step. Calculations were made in the package Matlab.

Keywords: Shells of revolution · Finite element modeling
Axisymmetric loading

1 Introduction

Axisymmetric problems are quite often encountered in the practice of calculating building structures. For rotational shells, the axisymmetric loads include the self-weight, the uniform snow loading, the fluid pressure in the reservoir, etc. In engineering calculations, in most cases, many authors are limited to membrane theory, neglecting the influence of bending moments and transverse forces on the stress-strain state of the structure. The membraneless theory gives satisfactory results if the boundary conditions provide the edges of the shell with free displacements along the normal to the surface. If this condition is violated, an edge effect is observed in the support zone. The methods for calculating the boundary effect in elastic shells are well developed and are given in the classical papers [1, 2].

As for the shells of viscoelastic material, this question remains poorly studied, there are only some particular solutions. The boundary effect in a polymeric cylindrical shell loaded with hydrostatic pressure is investigated in [3]. In this paper it is established that, due to creep, hoop stresses increase, which can lead to the destruction of the structure during operation. In [4], general equations for the creep of reinforced concrete shells in curvilinear coordinates are given, taking into account the temperature effects, however, methods for solving these equations are not proposed. Some problems of

calculating thick-walled axisymmetrically loaded shells with allowance for creep are given in [5, 6], but the shells in them are modeled as a three-dimensional body.

We consider a reinforced concrete tank, the middle surface of which is a single-sheet hyperboloid of rotation (Fig. 1). The meridian equation for this surface is written as:

$$r = \frac{a}{b} \sqrt{b^2 + z^2} \tag{1}$$

where a and b – parameters of hyperbola.

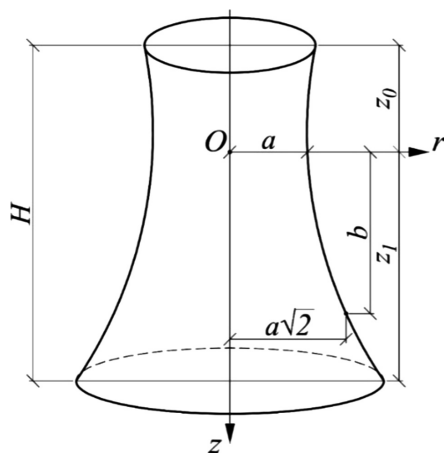


Fig. 1. The one-sheeted hyperboloid of rotation

As the law of creep we will use the equations of the viscoelastic model of hereditary aging [7], according to which the relationship between stresses and deformations for the case of a plane stress state has the form:

$$\begin{aligned} \varepsilon_s(t) &= \frac{1}{E(t)} (\sigma_s(t) - \nu\sigma_\theta(t)) - \int_{\tau_0}^t \{ \sigma_s(\tau) - \nu\sigma_\theta(\tau) \} \frac{\partial C(t, \tau)}{\partial \tau} d\tau; \\ \varepsilon_\theta(t) &= \frac{1}{E(t)} (\sigma_\theta(t) - \nu\sigma_\phi(t)) - \int_{\tau_0}^t \{ \sigma_\theta(\tau) - \nu\sigma_\phi(\tau) \} \frac{\partial C(t, \tau)}{\partial \tau} d\tau, \end{aligned} \tag{2}$$

where $C(t, \tau)$ – a measure of creep, defined as follows:

$$C(t, \tau) = C \frac{e^{\alpha t} - e^{\alpha \tau}}{e^{\alpha t} - 1} + B(e^{-\gamma \tau} - e^{-\gamma t}), \tag{3}$$

where B, C, α, γ – rheological constants.

Relations (2) can be rewritten as:

$$\begin{aligned} \varepsilon_\theta &= \frac{1}{E} (\sigma_\theta - \nu\sigma_s) + \varepsilon_\theta^*; \\ \varepsilon_s &= \frac{1}{E} (\sigma_s - \nu\sigma_\theta) + \varepsilon_s^*, \end{aligned} \tag{4}$$

where $\varepsilon_\theta^*, \varepsilon_s^*$ – creep strains.

The index s in formulas 2–4 corresponds to the meridional direction, and θ - to the hoop one.

The transition from the integral form of the creep equations to the differential form using the creep measure (3) is given in [8]:

$$\begin{aligned} \frac{\partial \varepsilon_{1s}^*}{\partial t} &= \frac{\alpha e^{\alpha t}}{e^{\alpha t} - 1} [C(\sigma_s - \nu\sigma_\theta) - \varepsilon_{1s}^*]; \\ \frac{\partial \varepsilon_{2s}^*}{\partial t} &= B\gamma e^{-\gamma t} (\sigma_s - \nu\sigma_\theta); \\ \varepsilon_s^* &= \varepsilon_{1s}^* + \varepsilon_{2s}^*. \end{aligned} \tag{5}$$

To obtain expressions for the growth rates of the deformation ε_θ^* components, it suffices to interchange the subscripts s and θ in the right-hand part of the formulas given above. The differential form of the creep equations allows us to introduce a time grid for the calculation, creep strains at each step are considered constant, and to determine their values at a time, we use the linear approximation:

$$\varepsilon_{t+\Delta t}^* = \varepsilon_t^* + \frac{\partial \varepsilon^*}{\partial t} \Delta t. \tag{6}$$

The following system of integro-differential equations in a spherical coordinate system was obtained in [9] for the case of axisymmetric loading of shells of revolution:

$$\begin{aligned} \frac{R_2}{R_1} \frac{d^2 \alpha}{d\phi^2} + \frac{d\alpha}{d\phi} \left[\frac{d}{d\phi} \left(\frac{R_2}{R_1} \right) + \frac{R_2}{R_1} ctg\phi \right] + \alpha \left(-ctg^2\phi \frac{R_1}{R_2} - \nu \right) + \frac{R_1 V}{D} \\ = \frac{1}{D \sin\phi} \left[M_\theta^* R_1 \cos\phi - \frac{d}{d\phi} \left(M_\phi^* r \right) \right]; \\ \frac{R_2}{R_1} \frac{d^2 V}{d\phi^2} + \frac{dV}{d\phi} \left[\frac{d}{d\phi} \left(\frac{R_2}{R_1} \right) + \frac{R_2}{R_1} ctg\phi \right] + V \left(\nu - \frac{R_1}{R_2} ctg^2\phi \right) = Eh\alpha R_1 + \Phi(\phi) + \Phi^*(\phi), \end{aligned} \tag{7}$$

where $\Phi(\phi) = -\frac{d}{d\phi} (pR_2^2) + tR_2(R_2 + \nu R_1) - \frac{F(\phi)}{\sin^2\phi} \left[\left(\frac{R_1}{R_2} - \frac{R_2}{R_1} \right) ctg\phi + \frac{d}{d\phi} \left(\frac{R_2}{R_1} \right) \right];$

$$F(\phi) = - \int_{\phi_0}^{\phi} p_z R_1 r d\phi; \Phi^*(\phi) = R_2 \frac{d}{d\phi} \left(N_\theta^* - \nu N_\phi^* \right) - ctg\phi R_1 (1 + \nu) \left(N_\phi^* - N_\theta^* \right);$$

$$M_\theta^* = \frac{E}{1 - \nu^2} \int_{-h/2}^{h/2} (\varepsilon_\theta^* + \nu \varepsilon_\phi^*) y dy; N_\theta^* = \frac{E}{1 - \nu^2} \int_{-h/2}^{h/2} (\varepsilon_\theta^* + \nu \varepsilon_\phi^*) dy; M_\phi^* = \frac{E}{1 - \nu^2} \int_{-h/2}^{h/2} (\varepsilon_\phi^* + \nu \varepsilon_\theta^*) y dy;$$

$N_\phi^* = \frac{E}{1-\nu^2} \int_{-h/2}^{h/2} (\epsilon_\phi^* + \nu\epsilon_\theta^*)ydy$; p_z – vertical component of the surface load; p and t are the normal and tangential components of the load, respectively; R_1, R_2 are the principal radii of curvature; α is the angle of rotation of the normal; $V = R_2Q$; Q – meridional lateral force; $D = \frac{Eh^3}{12(1-\nu^2)}$ – cylindrical rigidity.

The index ϕ in Eq. (7) corresponds to the meridional direction. By y in the formulas for $M_{\theta(\phi)}^*$ and $N_{\theta(\phi)}^*$ we mean the local axis directed along the normal to the middle surface of the shell. The y coordinates are measured from the middle surface. The solution of system (7) can be performed only numerically, in [9] the finite difference method is applied for this.

2 Materials and Methods

The finite element used is shown in Fig. 2. At each nodal point, 3 degrees of freedom are given: displacements v_i and w_i in the direction of the tangent and the normal to the surface of the shell, and also the angle of rotation ϕ_i . For the displacement v , we take a linear approximation:

$$v(s) = \alpha_0 + \alpha_1 s. \tag{8}$$

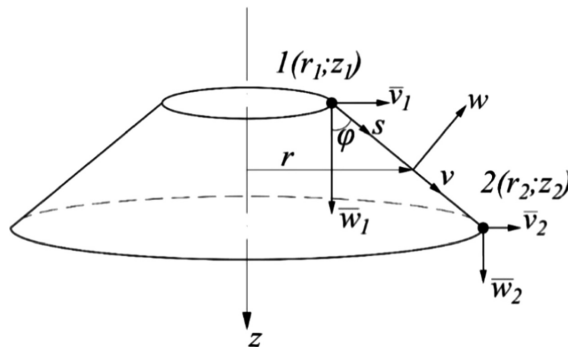


Fig. 2. Finite element of the axisymmetric shell

The displacement w in the direction of the normal is approximated by a polynomial of the third degree with 4 indeterminate coefficients:

$$w(s) = \alpha_2 + \alpha_3 s + \alpha_4 s^2 + \alpha_5 s^3. \tag{9}$$

The coefficients α_i can be determined from the following conditions:

$$\begin{aligned}
 v(0) = v_1; w(0) = w_1; \phi(0) = \left. \frac{dw}{ds} \right|_{s=0} = \phi_1; \\
 v(l) = v_2; w(l) = w_2; \phi(l) = \left. \frac{dw}{ds} \right|_{s=l} = \phi_2,
 \end{aligned}
 \tag{10}$$

where l - length of the generatrix of the conical finite element.

The matrix representation of relations (7) has the form:

$$\{U\} = \begin{Bmatrix} v_1 \\ w_1 \\ \phi_1 \\ v_2 \\ w_2 \\ \phi_2 \end{Bmatrix} = \begin{bmatrix} 1 & 0 & 0 & 0 & 0 & 0 \\ 0 & 0 & 1 & 0 & 0 & 0 \\ 0 & 0 & 0 & 1 & 0 & 0 \\ 1 & l & 0 & 0 & 0 & 0 \\ 0 & 0 & 1 & l & l^2 & l^3 \\ 0 & 0 & 0 & 1 & 2l & 3l^2 \end{bmatrix} \cdot \begin{Bmatrix} \alpha_0 \\ \alpha_1 \\ \alpha_2 \\ \alpha_3 \\ \alpha_4 \\ \alpha_5 \end{Bmatrix} = [C]\{\alpha\}.
 \tag{11}$$

From (11): $\{\alpha\} = [C]^{-1}\{U\} = [\Phi]\{U\}$.

The deformations of each point of the shell are completely determined by deformations of the middle surface ε_s^0 and ε_θ^0 , as well as curvatures χ_s and χ_θ . The values ε_s^0 , ε_θ^0 , χ_s , χ_θ are called generalized strains [10]. For the adopted in Fig. 2 positive directions of displacement, the generalized strain vector is written as:

$$\{\varepsilon\} = \begin{Bmatrix} \varepsilon_s^0 \\ \varepsilon_\theta^0 \\ \chi_s \\ \chi_\theta \end{Bmatrix} = \begin{Bmatrix} \frac{dv}{ds} \\ \frac{w \cos\phi + v \sin\phi}{r} \\ -\frac{d^2w}{ds^2} \\ -\frac{\sin\phi}{r} \frac{dw}{ds} \end{Bmatrix}
 \tag{12}$$

Substituting (8) and (9) in (12), we obtain:

$$\{\varepsilon\} = \begin{bmatrix} 0 & 1 & 0 & 0 & 0 & 0 \\ \frac{\sin\phi}{r} & \frac{s\sin\phi}{r} & \frac{\cos\phi}{r} & \frac{s\cos\phi}{r} & \frac{s^2\cos\phi}{r} & \frac{s^3\cos\phi}{r} \\ 0 & 0 & 0 & 0 & -2 & -6s \\ 0 & 0 & 0 & -\frac{\sin\phi}{r} & -\frac{2s\sin\phi}{r} & -\frac{3s^2\sin\phi}{r} \end{bmatrix} \cdot \begin{Bmatrix} \alpha_0 \\ \alpha_1 \\ \alpha_2 \\ \alpha_3 \\ \alpha_4 \\ \alpha_5 \end{Bmatrix} = [\lambda]\{\alpha\} = [B]\{U\},
 \tag{13}$$

where $[B] = [\lambda][\Phi]$.

In [9] the following relation was obtained between internal forces and generalized deformations:

$$\begin{aligned}
 M_\theta &= D(\chi_\theta + v\chi_s) - M_\theta^*; \\
 M_s &= D(\chi_s + v\chi_\theta) - M_s^*; \\
 N_\theta &= \frac{Eh}{1 - \nu^2} (\varepsilon_\theta^0 + v\varepsilon_s^0) - N_\theta^*; \\
 N_s &= \frac{Eh}{1 - \nu^2} (\varepsilon_s^0 + v\varepsilon_\theta^0) - N_s^*,
 \end{aligned}
 \tag{14}$$

We rewrite relations (14) in the matrix form:

$$\{N\} = \begin{Bmatrix} N_s \\ N_\theta \\ M_s \\ M_\theta \end{Bmatrix} = [D]\{\varepsilon\} - \{N^*\}, \tag{15}$$

where $[D] = \frac{Eh}{1-\nu^2} \begin{bmatrix} 1 & \nu & 0 & 0 \\ \nu & 1 & 0 & 0 \\ 0 & 0 & \frac{h^2}{12} & \frac{\nu h^2}{12} \\ 0 & 0 & \frac{\nu h^2}{12} & \frac{h^2}{12} \end{bmatrix}, \{N^*\} = \{N_s^* \quad N_\theta^* \quad M_s^* \quad M_\theta^*\}^T.$

The potential strain energy is defined as follows:

$$\Pi = \frac{1}{2} \int_V \{\sigma_s \sigma_\theta\} \begin{Bmatrix} \varepsilon_s^{el} \\ \varepsilon_\theta^{el} \end{Bmatrix} dV, \tag{16}$$

where $\varepsilon_s^{el}, \varepsilon_\theta^{el}$ – elastic deformations representing the difference between total deformations and creep strains.

$$\begin{Bmatrix} \varepsilon_s^{el} \\ \varepsilon_\theta^{el} \end{Bmatrix} = \begin{Bmatrix} \varepsilon_s \\ \varepsilon_\theta \end{Bmatrix} - \begin{Bmatrix} \varepsilon_s^* \\ \varepsilon_\theta^* \end{Bmatrix} \tag{17}$$

Complete deformations are represented as a sum of deformations of the middle surface and deformations caused by a change in the curvature:

$$\begin{Bmatrix} \varepsilon_s \\ \varepsilon_\theta \end{Bmatrix} = \begin{Bmatrix} \varepsilon_s^0 \\ \varepsilon_\theta^0 \end{Bmatrix} + y \begin{Bmatrix} \chi_s \\ \chi_\theta \end{Bmatrix} = \{\varepsilon_0\} + y\{\chi\}. \tag{18}$$

Stresses are expressed through deformations as follows:

$$\begin{Bmatrix} \sigma_s \\ \sigma_\theta \end{Bmatrix} = [\tilde{D}] \left(\begin{Bmatrix} \varepsilon_s \\ \varepsilon_\theta \end{Bmatrix} - \begin{Bmatrix} \varepsilon_s^* \\ \varepsilon_\theta^* \end{Bmatrix} \right) = [\tilde{D}] (\{\varepsilon_0\} + y\{\chi\} - \{\varepsilon^*\}), \tag{19}$$

where $[\tilde{D}] = \frac{E}{1-\nu^2} \begin{bmatrix} 1 & \nu \\ \nu & 1 \end{bmatrix}, \{\varepsilon^*\} = \begin{Bmatrix} \varepsilon_s^* \\ \varepsilon_\theta^* \end{Bmatrix}.$

Finally, the expression for the potential strain energy takes the form:

$$\Pi = \frac{1}{2} \left[\int_A (\{N\}^T - \{N^*\}^T) \{\varepsilon\} dA - \int_V \{\varepsilon^*\}^T [\tilde{D}] \{\varepsilon^*\} dV \right]. \tag{20}$$

Taking into account relations (10) and (12), formula (16) can be rewritten as:

$$\Pi = \frac{1}{2} \{U\}^T 2\pi \int_0^l [B]^T [D] [B] r ds \{U\} - \{U\}^T 2\pi \int_0^l [B]^T r ds \{N^*\} - \frac{1}{2} \int_V \{\varepsilon^*\}^T [\tilde{D}] \{\varepsilon^*\} dV. \tag{21}$$

Minimizing the total energy representing the difference between the potential deformation energy and the work of external forces, along the vector of nodal displacements, we obtain:

$$\frac{\partial W}{\partial \{U\}} = \frac{\partial \Pi}{\partial \{U\}} - \frac{\partial A}{\partial \{U\}} = [K]\{U\} - \{F^*\} - \{F^e\} = 0, \tag{22}$$

where $[K]$ - the stiffness matrix, $\{F^*\}$ - the contribution of creep to the load vector, $\{F^e\}$ - the vector of external nodal forces.

$$[K] = 2\pi \int_0^l [B]^T [D] [B] r ds; \{F^*\} = 2\pi \int_0^l [B]^T r ds \{N^*\}. \tag{23}$$

The matrix $[K]$ contains elements that are functions of s , so numerical integration using the trapezoidal formula is used for calculation.

The matrix $[K]$ and the vector $\{F^*\}$ in (23) are written in the local coordinate system associated with the element. In order to compile the system of FEM equations, it is necessary to perform a transition to the global coordinate system, which is carried out according to the formulas:

$$[\bar{K}] = [L]^T [K] [L]; \{\bar{F}\} = [L]\{F\}, \tag{24}$$

where $[L] = \begin{bmatrix} \sin\phi & \cos\phi & 0 & 0 & 0 & 0 \\ \cos\phi & -\sin\phi & 0 & 0 & 0 & 0 \\ 0 & 0 & 1 & 0 & 0 & 0 \\ 0 & 0 & 0 & \sin\phi & \cos\phi & 0 \\ 0 & 0 & 0 & \cos\phi & -\sin\phi & 0 \\ 0 & 0 & 0 & 0 & 0 & 1 \end{bmatrix}$

3 Results

The concrete shell was calculated for its own weight and water pressure at the following initial data: $a = 13$ m, $b = 28.16$ m, $z_0 = -7.8$ m, $z_1 = 45.5$ m, $E = 2 \cdot 10^7$ kPa, $\nu = 0.17$, $h = 0.25$ m, specific weight of material $\gamma_m = 24 \frac{\text{kN}}{\text{m}^3}$. Rheological constants of concrete: $\gamma = 0.062 \text{ days}^{-1}$, $C = 3.77 \cdot 10^{-8} \text{ kPa}^{-1}$, $B = 5.68 \cdot 10^{-8} \text{ kPa}^{-1}$, $\alpha = 0.032 \text{ days}^{-1}$. At the base of the shell, a hinged support was adopted.

The growth graph of the largest value of the deflection w for the case of the action of the self-weight on the shell is shown in Fig. 3. The dashed line corresponds to the solution of Eq. (7) by the method of finite differences.

In the calculation it is established that the internal forces and stresses in the shell do not change. Figure 4 is a graph of the variation in the shell height of the meridional bending moments at the end of the creep process. The dashed line corresponds to the

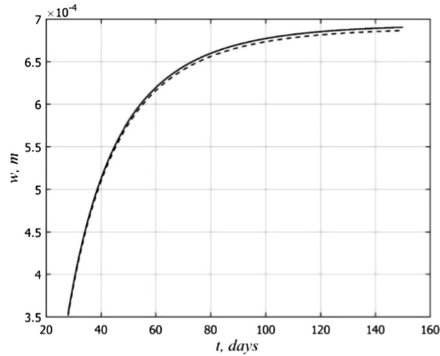


Fig. 3. Graph of growth of deflection when acting on a shell of its own weight

result obtained using the method of finite differences (FDM), continuous line – using the finite element method.

Figure 4 shows that in the finite element analysis, the peak value is smoothed at $z = 0$. A similar picture is observed for the hoop bending moment. This can be explained by the fact that in finite element method the solution is performed in displacements, and the forces are determined by double differentiation.

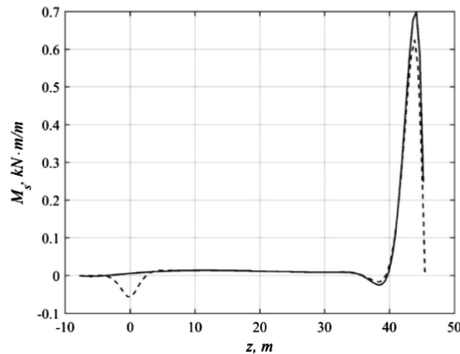


Fig. 4. Change in the height of the shell of meridional bending moments as $t \rightarrow \infty$: dashed line – finite differences method, solid line – FEM

The distribution of the meridional bending moment with respect to the height of the shell when hydrostatic pressure acts on it is shown in Fig. 5. The notation is the same as in Fig. 4. The maximum value of the bending moment was overestimated by 13% in comparison with the results obtained with the help of FDM.

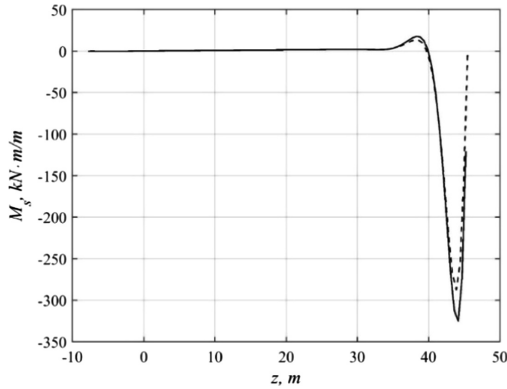


Fig. 5. The distribution of the meridional bending moment over the height of the shell when hydrostatic pressure acts on it

4 Discussion

It can be seen from the calculation that creep causes a significant increase in displacements. In case of self-weight, the deflection increased in 1.95 times. Despite the fact that the shell at the base is hingedly supported, an edge effect is observed. This is because the points at the base of the shell can not move freely in the direction of the normal to the surface. Outside the support zone, the solution is well described by the membrane theory. The absence of redistribution of forces is probably due to the fact that in the theory of creep of concrete the Poisson's ratio for elastic deformations is taken equal to the Poisson's ratio for creep strains. For shells of polymeric materials, in which the Poisson's ratio for inelastic deformations is taken equal to 0.5, an increase in the hoop bending moments was observed in [3].

5 Conclusions






The obtained equations and the technique developed on the basis of the finite element method simplify considerably the calculation taking into account the creep of the axisymmetrically loaded shells. The law of viscoelastic deformation does not impose any restrictions, it can be arbitrary.

Also, finite element method allows to calculate shells of variable thickness. Comparison of the results with the solution obtained on the basis of the method of finite differences indicates their reliability. When using FEM, the effect of smoothing the peak values of the bending moments in the cross section of the shell with a minimum radius is revealed, but this cross section is not the most dangerous.

References

1. Samul, V.: Fundamentals of the Theory of Elasticity and Plasticity. Higher School, Moscow, 265 p. (1982)
2. Ogibalov, P.: Shells and plates. Publishing House of Moscow University, Moscow, 695 p. (1969)
3. Andreev, V., et al.: *Procedia Eng.* **165**, 1141–1146 (2016)
4. Tamrazyan, A., Kozhanova, A.: *Ind. Civil Constr.* **10**, 15–20 (2015)
5. Yazyev, B.: Some Problems and Methods of Mechanics of a Macro-Inhomogeneous Viscoelastic Medium. Rostov-on-Don, 208 p. (2009)
6. Andreev, V.: Some Problems and Methods of Mechanics of Inhomogeneous Bodies. ASV Publishing House, Moscow, 288 p. (2002)
7. Tamrazyan, A., Yesayan, S.: *Mechanics of Creep of Concrete: Monograph.* MGSU, Moscow, 492 p. (2013)
8. Mailyan, L., et al.: *Procedia Eng.* **165**, 1853–1857 (2016)
9. Chepurnenko, A., et al.: *MATEC* **106**, 04011 (2017)
10. Zienkiewicz, O.: *The Finite Element Method.* McGraw-Hill, London, p. 787 (1977)

Increase of Fire Resistance Limits of Building Structures of Oil-and-Gas Complex Under Hydrocarbon Fire

Marina Gravit¹ , Eliza Gumerova¹  , Alexey Bardin¹ ,
and Vitaly Lukinov² 

¹ Peter the Great St. Petersburg Polytechnic University, Politekhnikeskaya str.,
29, 195251 St. Petersburg, Russia

eliza_gumerova@mail.ru

² Moscow State University of Civil Engineering, Yaroslavskoe shosse, 26,
129337 Moscow, Russia

Abstract. The article deals with the technical documentation in design of building constructions of oil-and-gas complex under special load – fire in case of hydrocarbon fire. It gives the detailed review of international, European and American standards for determine of the fire resistance limits in the modeling of hydrocarbon combustion. Much attention is given to analysis of technical regulations in fire protection designing of ships and sea platforms. It should be stressed that requirements for the fire resistance limits in conditions of hydrocarbon fire for some buildings and structures are absent. Therefore the building structures testing without appropriate calculations is superfluous and economically inadvisable. It is necessary to evaluate the time variation in the area of oil or oil products under various spreading conditions and to justify the need for the structure protection from the hydrocarbon fire. The development of industry standards for Russian oil and gas enterprises with a list of indicators for fire-proofing and flame-retardant coating for building structures in the conditions of a hydrocarbon fire is proposed.

Keywords: Building structures of oil-and-gas complex
Marine transport and offshore structures · Fire resistance limits
Passive fire protection

1 Introduction

The standards for the fire resistance testing define standard (cellulosic) and alternative hydrocarbon, slow heating and external heating regimes. Steel structures of reservoirs, equipment, buildings, constructions of sea-going vessels, fire and explosion hazards are exposed to high temperatures due to the type and intensity of fire load. Average surface flame temperature of majority of oil products rises above the 1000 °C mark. That is why the above structures should have a superior resistance to special load in case of hydrocarbon fire. Best practice of hydrocarbon offshore productions in Russia, Great Britain, the USA, Norway, Australia and France involves carrying out a fire risk analysis and an assessment of consequences in order to determine the degree of protection required for the duration of the hazard. The risk-based approach enables the development of more safe and economical design solutions.

In Russian scientific sources there are regulations according to the standard heating regime for hydrocarbon processing industry. International, European and American standards determine the fire resistance limits in the modeling of hydrocarbon combustion in oil-and-gas complex from the end of last century [1].

The purpose of this article is to give a review of technical documents in using of modern means of fire protection of building structures and vessels in case of hydrocarbon fire.

2 Test Methods for Fire Resistance of Structures

ISO Technical Committee 92 «Fire safety» is particularly relevant to standards for the fire resistance testing. ISO TC 92 developed the standard ISO 834 with real-scale tests for fire resistance of building construction elements. It is considered to be basis for testing methods in various countries, including Russia.

The aim of Russia National Standard EN 1363-2-2014 “Fire resistance tests. Alternative and additional procedures” is to harmonize the approaches to the choice of heating regimes for petroleum and chemical industries and it shall be read in conjunction with EN 1363-1:2012 “Fire resistance tests. General requirements”. The standard specifies alternative heating conditions and other procedures that may need to be adopted under special circumstances and involves the details of external, slow heating and hydrocarbon heating regimes which relate to those occurring in real fires (Fig. 1). A hydrocarbon-fire temperature-time curve has a rapid flame temperature rise after ignition. The typical temperature value 7.5 min after ignition is more than 1000 °C and 30 min after reaches 1100 °C mark and is constant until 120 min.

European, Russian and American normative documents which establish methods for fire resistance testing are in Tables 1 and 2.

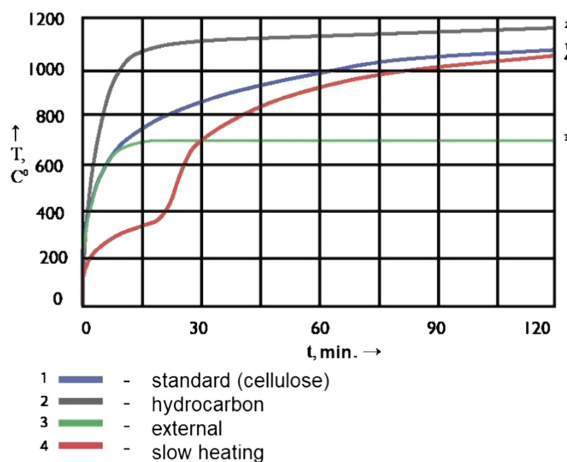


Fig. 1. Temperature/time curves according to EN 1363-2:1999 Fire resistance tests. Part 2: Alternative and additional procedures (Russian National Standard EN 1363-2-2014).

Table 1. European, international and Russian normative documents, establishing test methods for fire resistance of structures.

European/International normative document	Russian normative document	The content of the document, the difference and similarity	Degree of compliance with ND/Reference to standards-test methods for fire resistance
ISO 834-75 Fire resistance tests. Elements of building constructions. EN 1363-1:2012. Fire resistance tests. General requirements. EN 1363-2:1999 Fire resistance tests - Part 2: Alternative and additional procedures. ENV 1363-3. Fire resistance tests - Part 3: verification of furnace performance	Russian National Standard 30247.0-94 Building constructions. Fire resistance tests. General requirements	Standard heating conditions (difference in 20 °C – initial temperature), samples for testing of structures are the same. Excess pressure 10 ± 2 Pa (Russia), the European - not more than 20 Pa. European standard introduces the concept of “principle of extended application”	Sections 6, 7, 9 have an authentic text to ISO 834-75. In conjunction with ENV 1363-3. Fire resistance tests - Part 3: verification of furnace performance
EN 1363-2:1999 Fire resistance tests - Part 2: Alternative and additional procedures	Russian National Standard EN 1363-2	Details of the alternative hydrocarbon, slow heating and external fire exposure heating curves and the additional impact test and measurement of radiation procedures are included within this standard	Russian National Standard EN 1363-2 is the Russian language version of EN 1363-2:1999 Fire resistance tests - Part 2: Alternative and additional procedures
ISO 834-1-1999 EN 1363-1:1999 EN 1363-2:1999	Modifications in Russian National Standard 30247.0-94 (in process of inclusion)	Differences in initial temperatures of tests, allowances in heating conditions. Additional procedures are as in EN 1363-2:1999	Not equaled to ISO 834-1-1999, EN 1363-1:1999, EN 1363-2:1999. Sections 6, 7, 9 - an authentic text to ISO 834-1-1999
IEC 60721-2-8:1994. Classification of environmental conditions - Part 2: Environmental conditions appearing in nature - Fire exposure	Russian National Standard 54081-2010 Influence of environmental conditions appearing in nature on the technical products. Overall performance. Fire	Standard fire and external fire exposure, determination of slow heating conditions, processes which regard to fire in constructions	Modification of Russian National Standard 60721-2-8:1994

(continued)

Table 1. (continued)

European/International normative document	Russian normative document	The content of the document, the difference and similarity	Degree of compliance with ND/Reference to standards-test methods for fire resistance
EN 13381-8:2013 “Test methods for determining the contribution to the fire resistance of structural members. Part 8: Applied reactive protection to steel members”	Russian National Standard 53295-2009 Fire retardant compositions for steel constructions. General requirement. Method for determining fire retardant efficiency	Standard and slow heating regimes are described without requirements for the hydrocarbon conditions	Not harmonized EN 1363-1:1999 EN 1363-2:1999
DIN 4102-2:1977 Fire tests on building materials and structures. Methods for determination of the fire resistance of load bearing elements of construction	–	Methods for determination of the fire resistance of load bearing elements of construction for the hydrocarbon conditions	Equaled to UL 1709 Standard for Safety for Rapid Rise Fire Tests of Protection Materials for Structural Steel
BS 476-20:1987. Fire tests on building materials and structures. Method for determination of the fire resistance of elements of construction (general principles)	–	Series of Britain Standards for the standard heating conditions. Appendix D contains Method for determination of the fire resistance of elements of construction for the hydrocarbon conditions	BS 476-21, BS 476-22, BS 476-23, BS 476-24, BS 4422, BS 4937-4, BS 4937-5, <u>ISO 834</u>
ISO 22899-1:2007 Determination of the resistance to jet fires of passive fire protection materials - Part 1: General requirements	–	Determination of the resistance to jet fires of passive fire protection materials. Dimensions of sample smaller than in real situation	ISO/TR 834-3, ISO 13702:2015 Petroleum and natural gas industries – Control and mitigation of fires and explosions on offshore production installations — Requirements and guidelines

(continued)

Table 1. (continued)

European/International normative document	Russian normative document	The content of the document, the difference and similarity	Degree of compliance with ND/Reference to standards-test methods for fire resistance
ISO/TR 22899-2:2013 Determination of the resistance to jet fires of passive fire protection - Part2: Guidance on classification and implementation methods	–	Determination of the resistance to jet fires of passive fire protection; guidance on implementation methods (large-scale tests)	ISO/TR 834-3 and EN 1363-2:1999
ISO 13702 Petroleum and natural gas industries — Control and mitigation of fires and explosions on offshore production installations — Requirements and guidelines	ISO 13702:2015 Petroleum and natural gas industries – Control and mitigation of fires and explosions on offshore production installations – Requirements and guidelines	ISO 13702 describes the objectives and functional requirements for the control and mitigation of fires and explosions on offshore installations used for the development of hydrocarbon resources	ISO 22899-1, API RP 2FB, API RP 14 J, API RP 14G, API RP 75, API RP 500, API RP 505, API RP 2003, API 2030, ASTM E119, EN 1834, EN 13463, IMO resolution A.1021 (26), UL 1709

Table 2. The normative documents of the United States, containing test methods with different temperature conditions.

Name of standard	Definition area	Links to standards-methods
UL 1709 standard for safety for rapid rise fire tests of protection materials for structural steel	UL 1709 remains a leading standard in the evaluation by testing of PFP materials used to protect structural steel from the effects of hydrocarbon fires. The test method includes a supplementary test method for beams, intended to evaluate the ability of protective materials to perform when subject to significant deflections, for use in conjunction with the full-scale exposure test and applicable for beams and other sections subject to bending	NFPA 1H, API RP 14FZ, API RP 2218, API STD 2510, API RP 14G, NFPA 30H, NFPA 850, NFPA 556, CEN EN ISO 13702, ASTM C1094, NFPA 502

(continued)

Table 2. (continued)

Name of standard	Definition area	Links to standards-methods
ASTM E119 Fire tests of building construction and materials	Prescription of standard exposing fire of controlled extent and severity. Performance is defined as the period of resistance to standard exposure elapsing before the first critical point in behavior is observed. For the masonry and combined constructions	ISO 834-1 Fire Resistance Tests - Elements of Building Construction - Part 1: General Requirements
ASTM E 1529-14A Standard test methods for determining effects of large hydrocarbon pool fires on structural members and assemblies	Contains requirements for hydrocarbon fire	IMO A754, ISO 834-1 Fire Resistance Tests - Elements of Building Construction - Part 1: General Requirements
NFPA 290 standard for fire testing of passive protection materials for use on LP-Gas containers. Current Ed. 2013	This standard provides a test method to determine the fire resistance of passive fire protection (PFP) materials applied to the exterior of LP-Gas containers. It is intended to identify insulation systems that retard or prevent the release of the container's contents in a fire environment	UL 1709, ISO 22899-1, ISO 13702

Disadvantage of Russian National Standard EN 1363-2 is an absence of conjunction with EN 1363-1:1999 and ISO/TR 834-3. ISO 13702:2015 contents requirements to hydrocarbon regime and is in conjunction with American Standards ASTM E119 and UL 1709, however, ISO/TR 22899-2:2013 is equaled to European Standards.

It should be stressed that the values of the consumption of means of fire protection according to ASTM E119 and UL 1709 require correlation due to Global Asset Protection Services LLC (GAPS) [2].

3 Guidance Documents for the Design of Fire-Resistant Structures for Marine Transport and Offshore Structures

The International Code for application of fire test procedures, 2010 (FTP Code), adopted by Resolution MSC.307 (88) [3] are the parts of International Convention for the Safety of Life at Sea (SOLAS) [4].

International Code for the Construction and Equipment of Ships Carrying Dangerous Chemicals in Bulk (IBC Code) [5] and International Code for Construction

and Equipment of Ships Carrying Liquefied Gases in Bulk (IGC Code) [6] are taking into account in the case of transportation of liquids and make additional calculations for risk of hazards.

Bulkheads and decks of ships are divided into main vertical zones and horizontal zones by structural elements with thermal insulation and without it in order to achieve the objectives of fire safety; there is a restricted use of combustible materials to meet the fire safety requirements [4].

The Convention provides only with the definition of “standard resistance test”, in which samples of the relevant bulkheads or decks are exposed to heating in furnace at temperatures due to Cellulosic-Fire (standard fire) temperature/time curve in accordance with the method that meets the requirements of FTP Code [3].

The main guidance documents for the design of fire-resistant structures for marine transport and offshore structures, which refer to ISO 834-1:

- International Convention for the Safety of Life at Sea (SOLAS) [4];
- FTP Code [3];
- IBC Code [5];
- IGC Code [6];
- Technical regulation on the safety of sea transport, Government Decree No 620 of August 12, 2010 [7];
- IMO Resolution A 754 (18) Recommendation for fire resistance tests for structural floor “A”, “B” and “F” [8];
- Rules for the classification and construction of sea-going ships [9];
- Rules for the classification, construction and equipment of mobile offshore drilling units and fixed offshore platforms [10];

All the documents above, except for [10], describe the requirements to constructions for classes “A”, “B”, “F” and “C”. Only structures of class “C” are testing without using standard heating regime. Method in [10] contains only standard fire resistance test. This regime is described in FTP code, adopted by Resolution MSC.307 (88) [3].

«Type «H» constructions» [10] - structures formed by bulkheads and decks that must be constructed in such a way as to prevent smoke and flame from passing through them within 120 min of a standard fire resistance test; are insulated with non-combustible materials or equivalent fire retardants so that cf. and max. the temperature on the side opposite to the fire effect did not increase compared to the original temperature by more than 140 °C and 180 °C.

Designations are assigned in the process of standard test designations: H-120; H-60; H-0.

The structures are tested for fire resistance according to the procedure described in Resolution A.754 (18) [14], taking into account that «the temperature curve as a function of time should correspond to the temperature curve versus time in the case of carbon combustion».

For instance, the definition of “H” Class Divisions in Rules for building and classing facilities on offshore installations [11] is not equal to determination in [4, 10]: instead of the standard fire regime there hydrocarbon fire conditions are pointed out. This document makes more correctly demands regarding “H” Class Divisions. According to [11], intumescent coating can be applied for increasing the value of

H-parameter, but it must have low flame-spread, smoke generation and heat dissipation. It is also necessary to assess the toxicity of emitted products of combustion. In Table 3 there is a fire integrity of desks separating adjacent spaces/areas according to [11].

Table 3. Fire integrity of desks separating adjacent spaces/areas.

Space below ↓ Space above →	(1)	(2)	(3)	(4)	(5)	(6)	(7)	(8)	(9)	(10)	(11)	(12)	
Control stations including central process control rooms	(1)	A-0	A-0	A-0	A-0	A-0	A-60	A-0	H-60 (d)	A-0	A-0	*	A-0
Corridors	(2)	A-0	*	*	A-0	*	A-60	A-0	H-60 (d)	A-0	A-0	*	*
Accommodation Spaces	(3)	A-60	A-0	*	A-0	*	A-60	A-0	×	A-0	A-0	*	*
Stairways	(4)	A-0	A-0	A-0	*	A-0	A-60	A-0	H-60 (d)	A-0	A-0	*	A-0
Service spaces (low risk)	(5)	A-15	A-0	A-0	A-0	*	A-60	A-0	H-60 (d)	A-0	A-0	*	A-0
Machinery spaces of category A	(6)	A-60	A-60	A-60	A-60	A-60	* (a)	A-60	H-60 (d)	A-60	A-60	*	A-0
Other machinery spaces	(7)	A-15	A-0	A-0	A-0	A-0	A-0 (a)	* (a)	H-0 (d)	A-0	A-0	*	A-0
Process areas, storage tank areas, wellhead/manifold areas	(8)	H-60 (d)	H-60 (d)	×	H-60 (d)	H-60 (d)	H-60 (d)	H-60 (d)	–	–	H-60 (d)	–	H-60 (d)
Hazardous areas	(9)	A-60	A-0	A-0	A-0	A-0	A-60	A-0	–	–	A-0	–	A-0
Service spaces (high risk)	(10)	A-60	A-0	A-0	A-0	A-0	A-0	A-0	H-60 (d)	A-0	A-0 (c)	*	A-0
Open decks	(11)	*	*	*	*	*	*	*	–	–	*	–	*
Sanitary and similar spaces	(12)	A-0	A-0	*	A-0	*	A-0	A-0	H-60 (c)	A-0	*		*

“H” Class Divisions [11] – divisions formed by bulkheads and decks that are constructed of steel or other equivalent material, suitably stiffened, and are designed to withstand and prevent the passage of smoke and flame for the 120-min duration of a hydrocarbon fire test. “H” class divisions are to be insulated so that the average temperature of the unexposed face will not increase by more than 139 °C any time during the two-hour hydrocarbon fire test, nor will the temperature, at any point on the face, including any joint, rise more than 180 °C above the initial temperature, within the time listed below: Class “H-120”: 120 min Class “H-60”: 60 min Class “H-0”: 0 min This division is to remain intact with the main structure of the vessel, and is to maintain its structural integrity after two (2) hours”.

Hydrocarbon Fire Test – A test in which specimens of the relevant bulkheads or decks are exposed, in a test furnace, to temperatures corresponding to the hydrocarbon fire time-temperature curve as defined by the U.K. Department of Energy/Norwegian Petroleum Directorate Interim Hydrocarbon Fire Resistance Test for Elements of Construction for Offshore Installations.

4 Means of Fire Protection Under Conditions of a Hydrocarbon Fire Regime

In Table 3 there are data based on certificates of bulkheads and decks “H”- class from the official site of Russian Maritime Register of Shipping (RMRS) 2015–2017. Structures meet the requirements of Part VI (I.2.2, 2.1) due to conducted tests [10]. There are extra mentions about compliance to in some certificates. Materials from the official site RMRS are shown in Table 4 (6 of 16).

RMRS for standard products uses various documents and testing normatives. In Table 3 there are data for the class A for comparison some decks and partitions. There is no difference between consumption of means of passive fire protection for classes A-60 and H-60 for materials Sherwin-Williams, but for Russian materials for A-60 value of consumption is lower (30%).

5 Normative Documents for Fire Protection of Steel Structures in Industry of Oil-and-Gas Complex

The anti-corrosion protection standards are developed in Russian PJSC “LUKOIL”, Open Joint Stock Company “Gazprom” and Public Joint Stock Company “Transneft”, but not for passive fire protection: fireproofing and flame-retardant coating for building structures (hydrocarbon fire), only the standard regime is described in Construction Rules. “Fire protection. Requirements to fireproofing coverings of buildings and constructions” is the project of standard, which Gasprom is developing, where testing methods in hydrocarbon fire are described.

French oil and gas corporation Total S.A. has its own standard for means of fire protection. “General specification safety. GS EP SAF 337. Passive fire protection: Basis of design” [12] defines the requirements to design, choice and using of passive fire protection for marine transport and offshore structures. This document also classifies the means of passive fire protection.

The standard NORSOK M-501 “Surface preparation and protective coating” [13] can be used also for the marine platforms. Document contains a list of various methods and values of technical characteristics of coverings for different types of constructions and conditions. Most of noted systems are in conjunction with ISO 20340:2003(E) “Paints and varnishes. Technical requirements for the system of protective paint coatings for marine and similar structures”. There are 8 systems, which differ in functions, preparing the surface, thickness of dry outer skin, etc. The fifth system is used for sprayed systems of passive fire protection, which contains of epoxy and concrete fire protections. Optimal consumption is recommended [14–17].

In Table 4 there are data from official sites of some companies, who give the information about means of passive fire protection, which were tested in hydrocarbon heating regime, and the certificates UL 1709 in Database of Underwriters Laboratory. The thickness of the layer of fire retardant coating according to UL 1709 is equaled approximately 6 mm (column W10 × 49). The process of applying of epoxy intumescent coatings (YAMAL LNG) are displayed on Fig. 2 (Table 5).

Table 4. Type “H” constructions. RMRS 2015–2017.

Name of material, manufacturer	Fire and technical characteristics	Laboratory, documents on the basis of which the tests were carried out
*Deck «H»-class (H-0, H-60, H-120). Jotachar JF750. Jotun paints (Europe) Ltd.	Decks with minimal thickness 4.5 mm, which isolated from the reinforcing rib by epoxy covering with thickness from 5.5 mm for decks H-0; 11.9 mm for decks H-60 and 17.9 mm for decks H-120	«BRE Global», UK. Part 3 of FTP Code. Resolution IMO A.754 (18)
*Bulkhead «H» (H-0, H-60, H-120). Jotachar JF750	Bulkhead with thickness from 4.5 mm, which isolated from the other side by epoxy covering Jotachar JF750. Its minimal value of thickness 5.6 mm for bulkhead H-0, 12.9 mm for bulkhead H-60 and 17.6 mm (H-120)	«BRE Global», UK. Part 3 of FTP Code. Resolution IMO A.754 (18)
Steel bulkhead, type H-0 (400). Rockwool International	Bulkhead with thickness from 4.5 mm, which isolated by 2 layers of mineral wool SeaRox SL 660 ($\rho = 150 \text{ kg/m}^3$) $2 \times 30 \text{ mm}$. Isolation is fastened by wire screen and steel pins. Covering is foil or fiberglass with density 200–400 g/m^2 by glue 3PVDC Latex	Danish Institute of Fire and Security Technology (DIFT). Part 3 of FTP Code. Resolution IMO A.754 (18). Hydrocarbon curve (EN 1363-2)
*PITT-CHAR XP. PPG Protective @ Marin Coating, Poland. Steel deck “H-120”, “H-60”, “H-0” (“H-30”)	Steel deck: inner layer is epoxy covering Piltt-Char XP with thickness 4.9–8.0 mm, which is reinforced with fiberglass or screen Piltt-Char XP; external layer is epoxy covering Piltt-Char XP. Nominative value of dry outer skin of 2-layer covering: 8.2 mm for floor H-0, (H-30); 11.9 mm, for floor H-60; 16.3 mm, for floor H-120	Exova Warringtonfire, UK. Application can be in case of prepared steel or soil with coat
*PPG Coatings SPRL/BVBA. Belgi Bulkhead “H-120”, “H-60”, “H-0” (“H-30”)	Bulkhead: inner layer is epoxy covering Piltt-Char XP 4.9–10.8 mm, which is reinforced by fiberglass Piltt-Char XP; external layer is epoxy covering Piltt-Char XP. Nominative value of dry outer skin of 2-layer covering: 7.6 mm H-0, (H-30); 10.5 mm H-60 (without reinforcement); 14.4 mm for bulkhead H-120 (without reinforcement)	Part 3 of FTP Code. Resolution IMO A.307 (88). Exova Warringtonfire, UK
*Decks «H»-class (H-0, H-60, H-120). Sherwin-Williams Protective & Marine Coatings. United Kingdom	Steel deck with thickness from 4.5 mm, which isolated by epoxy coating FIRETEX M90. Minimal thickness 6 mm for H-0; 11.0 mm - H-60 and 15.4 - H-120. The screen «Firetex J220» can also be used	«Warrington Fire Research Center», UK due to requirements in Part 3 of FTP Code (Resolution IMO A.307 (88), BS 476, part 20, app.D)

Annotation. *Covering is flammable and can be applied only to external surfaces and in spaces which are not intended for people attendance. Isolated side should be from fire influence and from the other side of reinforcing rib.



Fig. 2. Application of fire-retardant coating Firetex® M93/02 (left) and Firetex M90, Sherwin-Williams® 11 mm. Modules for YAMAL LNG. Photos were provided by Muehlhan Morflot LLC and LLC Osoran.

Table 5. Indicators of means of fire protection under conditions of a hydrocarbon fire regime.

The name of mean	Binder	Reinforcement	Duration of maintenance	R(HC) 45	R(HC) 60	R(HC) 90	R(HC) 120	R(HC) 150	R(HC)180/240
OGRAKS-SKE	ES	+	40	5.0/6.0	5.0/6.0	8.0/9.6	11.5/13.8	15/18	–
Chartek 1709	ES	+	25	3.76/3.76	5.12/5.12	7.85/7.85	10.57/10.57	13.3/13.3	–
Chartek 7	ES	+	25	–	8.38/8.38	10.16/10.16	15.24/15.24	20.32/20.32	23.93/23.9331.14/31.14
FIRETEX M90	ES	+	25	5.61/5.61	7.45/7.45	10.79/10.79	13.66/13.66	16.07/16.07	18.02/18.0220.54/20.54
FENDOLITE MII	Portland cement	–	50	17.5/11.3	20.7/13.4	27.0/17.4	33.4/21.5	39.7/25.6	46.0/29.758.8/37.9
Pyrocrete 241	Portland cement	+	35	15.9/11.0	17.4/12.0	23.8/16.4	28.6/19.7	33.3/23	35.0/24.239.7/27.4

Note. ES - epoxy resin; reinforcement “+” - is present; numerator - the thickness of the layer of fire retardant coating, denominator - theoretical consumption per sq.m.

6 Conclusion

Hydrocarbon-Fire has a rapid flame temperature rise after ignition. The standard HF-curve shall be taken from UL 1709, EN 1363-2:1999, ISO 834-1:1999, ASTM E 1529, DIN 4102-2, BS 476-20.

Definitive requirements to the limits of fire resistance of structures to the effects of the hydrocarbon fire regime are present only for the designs of drilling platforms and offshore installations in some industry documents of oil-and-gas complex.

The normalization of the fire resistance limits for the hydrocarbon fire regime is absent; the testing process goes haphazardly and leads to additional costs for manufacturers of fire protection means.

It is necessary to differentiate the protection objects against a possible fire regime, justify the calculation and confirm the experimental data with the limits of fire resistance of structures. Assessment of fire risk and consequences should be carried out before using means of passive fire protection in order to define the degree of required protection.

References

1. Dennis, P., Nolan, P.: Fire & Explosion Protection Engineering Principles for Oil, Gas, Chemical, and Related Facilities. Noyes Publications, Westwood (1996)
2. Fireproofing for hydrocarbon fire exposures. GAPS Guidelines. Publication of Global Asset Protection Services LLC
3. The International Code for application of fire test procedures. Resolution MSC 307(88) (2010)
4. The International Convention for the Safety of Life at Sea (SOLAS)
5. International Code for the Construction and Equipment of Ships Carrying Dangerous Chemicals in Bulk (IBC Code)
6. The International Code for Construction and Equipment of Ships Carrying Liquefied Gases in Bulk adopted by IMO by resolution MSC 5(48)
7. Technical regulation on the safety of sea transport. Government Decree No 620 (2010)
8. IMO Resolution A754(18). Recommendation for fire resistance tests for structural floor “A”, “B” and “F”
9. Rules for the classification and construction of sea-going ships
10. Rules for the classification, construction and equipment of mobile offshore drilling units and fixed offshore platforms
11. Rules for building and classing facilities on offshore installations. American Bureau of Shipping (2014)
12. General Specification Safety GS EP SAF 337. Passive fire protection. Basis of design (2009)
13. NORSOK Standard M-501. Surface preparation and protective coating (2012)
14. Adamtsevich, A., Pustovgar, A., Pashkevich, S., Eremin, A., Zhuravlev, A.: Appl. Mech. Mater. **670–671**, 339–343 (2014). <https://doi.org/10.4028/www.scientific.net/AMM.670-671.339>
15. Pashkevich, S., Pustovgar, A., Eremin, A., Adamtsevich, A., Nefedov, S.: Adv. Mater. Res. **1004–1005**, 1482–1485 (2014). <https://doi.org/10.4028/www.scientific.net/AMR.1004-1005.1482>
16. Adamtsevich, A., Eremin, A., Pustovgar, A., Pashkevich, S., Nefedov, S.: Appl. Mech. Mater. **670–671**, 376–381 (2014). <https://doi.org/10.4028/www.scientific.net/AMM.670-671.376>
17. Pashkevich, S., Pustovgar, A., Adamtsevich, A., Eremin, A.: Appl. Mech. Mater. **584–586**, 1659–1664 (2014). <https://doi.org/10.4028/www.scientific.net/AMM.584-586.1659>

Experimental Determination of Permeability Coefficient

Gulnara Gabitova¹ , Daria Zaborova¹ , and Sergey Barinov² 

¹ Hydraulics and Strength of Materials, Institute of Civil Engineering,
Peter the Great St. Petersburg University, Polytechnicheskaya st., 29,
Saint-Petersburg 195251, Russia
gabitovaga@gmail.com

² Moscow State University of Civil Engineering,
Yaroslavskoe shosse, 26, Moscow 129337, Russia

Abstract. The article exposes a new concept of structural (partition, construction pit, the road network, etc.) permeability coefficient which is different from the concept of the material permeability coefficient. Substantiation of the differences of those concepts is given. Permeability coefficient is essential for solving the most of foundation engineering problems and transport infrastructure. The permeability coefficient of a structure (partition) is determined according to the value of seepage through the partition in case of a variable water-level in the backwater. The study proves that permeability coefficient value for the partition depends on the water pressure, which allows to reconsider the Boussinesq's hydraulic filtration theory. Soil permeability characteristic depends not only on head pressure in the backwater and initial ground water level, but first of all depends on mechanical and physical properties of soil.

Keywords: Permeability coefficient · Transport infrastructure · Foundation

1 Introduction

All buildings and structures are exposed to humidity. Structures of the building envelope moisten due to the water infiltration by rain precipitations or ground waters. This leads to the premature destruction of structures, decrease of it's insulating properties and irregularities in the microclimate of rooms [1, 2].

Most of the constructional materials have porous structure allowing to infiltrate water, which is a significant drawback.

Such type of a problem is common for the Saint-Petersburg with its moderate and humid climate, which is transitional between the continental and oceanic one. The problems of preventing the city areas from flooding and saturation as well as the overland and base flow disposal are the breach issues of the modern urban development of Saint-Petersburg.

As noticed by Startsev [3], the main danger is the presence of water in the basements, particularly the longtime basement dewatering. This may cause the foundation washout and eventually lead to the building failure.

Besides the filtrating properties of underlying soils, the dewatering technical equipment such as bore-hole pumps, partitions and wellpoint systems play an important role not only in basement dewatering, but also in the building construction technology at large. It is important to select economically efficient dewatering methods and equipment.

Dewatering and drainage of construction pits are problems which compose the filtration theory. Girgidov [4], Tolpaev [5] and other researchers performed calculations of filtration parameters.

The paper [6] exposes the solution of the limit problem for the Boussinesq's equation without the limitations for the value of permeability coefficient $k = k(h)$. It was proven that in the conditions of non-stationary filtration the maximal value of unit filtration discharge will be achieved in the tailwater.

Basic filtration law for liquids and gases in the porous environment is the Darcy's law:

$$\vec{u} = -k \cdot \vec{I}, \quad (1)$$

where \vec{u} is the infiltration rate, cm/s;

k – constant permeability coefficient, cm/s;

\vec{I} – head gradient

The hydraulic version of laminar filtering theory in the form of Dupuit's differential formula:

$$v = -k \frac{\partial h}{\partial x}, \quad (2)$$

where v is the average infiltration rate, h – otherwise the piezometric height or the depth of a free filtration flow.

Permeability coefficient is the main characteristic of a soil permeability. Its value depends on the soil type, particularly on its porous space, and on the physical properties of liquid (viscosity and density). According to this, it is obvious that the permeability coefficient is traditionally given the natural characteristics [7].

According to the research, the new concept of a structural (partition, construction pit) permeability coefficient is introduced, which is different from the concept of the material permeability coefficient [7]. The fact is that the structural permeability coefficient is determined not only by the properties of a natural material, but also by the technological aspects such as the structure erecting method, the way of soil laying and consolidation and etc., as well as by size and geometry of a structure.

2 Materials and Methods

In order to determine the numerical value of permeability coefficient the Darcy's mechanism is used. Besides, this method has a number of drawbacks. For example, the soil can significantly change its texture, porosity and finally the filtration properties [8].

As a part of the study, the measuring method for the structural permeability coefficient was introduced, which is different from the method with the Darcy’s mechanism.

The experimental facility allows to conduct the researches devoted to water conductivity and suffusion stability of soil samples. The study allows to determine not only the critical values of infiltration flow, but also to study the objective laws of the interaction between soil and infiltration flow, which is rarely could be achieved during the natural experiments [9].

Experimental laboratory facility is presented on the Fig. 1a, installation diagram is presented on Fig. 1b.

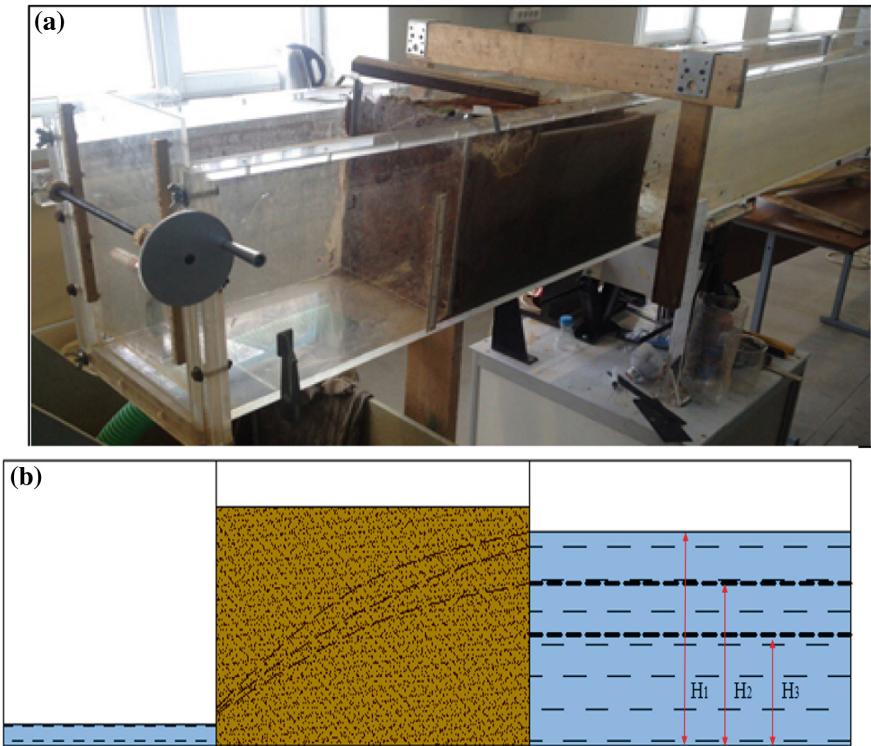


Fig. 1. (a) Experimental installation; (b) experimental installation diary

The benefit of such installation is that it was made of transparent material (plexi-glass), which allowed to visualize the filtrating process be the means of water coloring in the backwater and to register the configuration of a depression curve to the accuracy of the “capillary fringe.

According to the installation on the Fig. 1a, it consists of the horizontal rectangular-sectioned container with a solid bottom. The container is separated to the backwater and tailwater by the partition made of fine-grained sand with a known type (M15 sand was used for the experiment) [9].

In order to sustain the constant water level in the facility, the upper part of the column provides the water supply. The water is filtered through the sand during the constant head differentials. Head differential is various in different experiments. Filtered water goes to the graduated vessel by the tube.

2.1 Conduction of Laboratory Researches

Similar series of experiments are conducted to determine the permeability coefficient of a sandy soil.

From the water facility the flow is pumped to the backwater till the specific pressure head is achieved. Then the slider in the tailwater is opened, and after the water level in piezometers is stabilized, the water flow rate is determined with the volumetric method during the infiltration through the soil by the means of graduated vessel and a stop-watch. Several various pressure head values in the backwater are gradually set with the adjusting valve, then all measurements are repeated [10, 11].

Soil partition (barrier) is made of the M15 type sand, 45 cm length and 28 cm width. The mass of the partition is 100 kg.

3 Results

Measurements were performed four times for the volume of 100 mm with the pressure heads $H_1 = 21$ cm, $H_2 = 16$ cm, $H_3 = 11$ cm.

For the volume V in the graduated vessel, time t and a partition width b , seepage discharge q , cm^3/s is determined:

$$q = \frac{V}{b \cdot t}. \quad (3)$$

According to the Darcy's formula, the structural permeability coefficient value is calculated:

$$k = \frac{2 \cdot q \cdot L}{H^2} \quad (4)$$

where L is the partition length, in our case it is similar for all experiments and equals 45 cm;

H – pressure head value which equals 21, 16, 11 cm.

Calculation results are presented in Table 1:

As a part of the study, the permeability coefficient was determined considering the backwater level values: $H_1 = 21$ cm, $H_2 = 16$ cm, $H_3 = 11$ cm. Permeability coefficient values differ from each other and are decreasing accordingly to the pressure head decrease.

The relationship between flow rate Q and graduated volume, which is in fact time, is presented on the Fig. 2. According to the diagram, the biggest water flow rate is reached with the highest backwater level. Decreasing the pressure head H leads to the decrease of the flow rate.

Table 1. Calculation results

Pressure head, H, cm	Volume V, cm ³	Partition width b, cm	Time t, s	Partition length L, cm	Flow rate Q, cm ² /s	Permeability coefficient k, cm/s	$\tau = \frac{k \cdot t}{H}$
21	100	28	289	45	0.012	0.0009	0.0124
	100	28	604	45	0.006		0.0259
	100	28	624	45	0.005		0.0267
	100	28	778	45	0.003		0.0333
16	100	28	1373	45	0.0026	0.0008	0.0687
	100	28	1422	45	0.0025		0.0711
	100	28	1575	45	0.0022		0.0788
	100	28	1645	45	0.0021		0.0823
11	100	28	3456	45	0.001	0.0006	0.1885
	100	28	3897	45	0.0009		0.2126
	100	28	4345	45	0.0008		0.2370
	100	28	4799	45	0.0007		0.2618

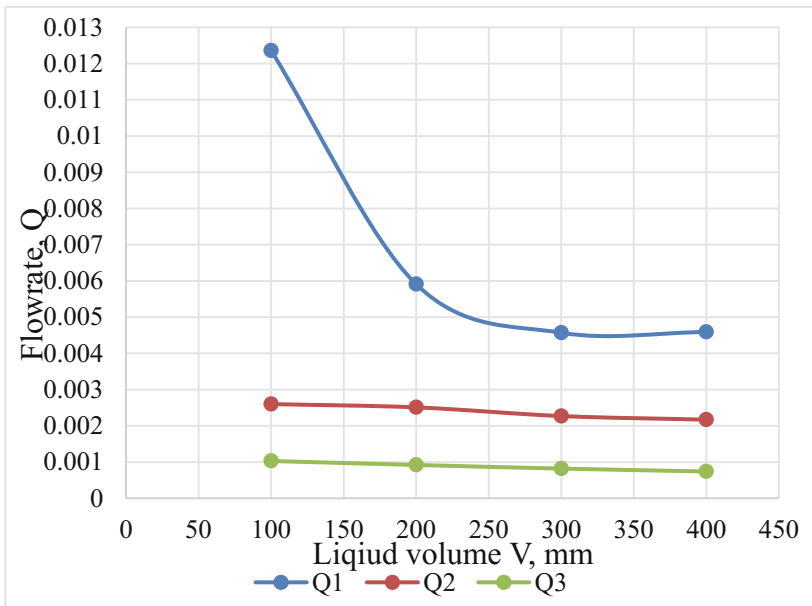


Fig. 2. Relationship between the flow rate and the volume

The Fig. 3 clearly shows that the flow rate is decreasing with time.

Obtained results indicate that the same sand type with the same compaction has various permeability coefficient, therefore the introduction of a concept of structural permeability coefficient which differs from the material permeability coefficient is

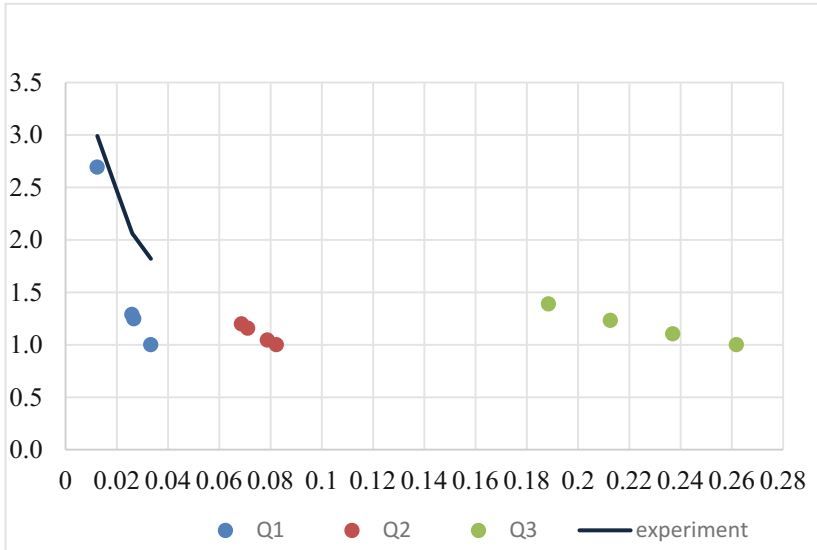


Fig. 3. Relationship between the flow rate and the time

reasonable. According to this, the «permeability coefficient» of M15 type sand is order accurately sized and is about $10^{-3} \dots 5 \cdot 10^{-4}$ cm/s.

The structural permeability coefficient itself is to be used for the calculations applicable in construction technology during the first steps of construction, and also for selecting the equipment for basement and construction pit dewatering [12].

4 Discussion

Nowadays, the main method of determining the soil permeability coefficient is the use of Darcy's mechanism. The problem is, the soil can significantly change its properties while being carried to the device cylinder from the natural conditions.

The paper [13] exposes the modernization of Darcy's experimental installation for the confined filtration, but in this case the structure type and pressure heads in it are not considered during the experiment conducted with the Darcy's device. Therefore, Darcy's mechanism and methodology allow to determine the material permeability coefficient only in the case of a stationary confined filtration.

But at the same time it is experimentally proven that there is a relationship between the permeability coefficient and the pressure head for the free filtration flow on the vertical plane [14, 15].

In the near term it is also planned to experimentally determine the height of the water seepage interval from the backwater to the tailwater, considering various soil types.

5 Conclusions


According to the obtained results the following conclusions are made:

1. Permeability coefficient of the M15 type sand partition depends on the backwater water level and varies from 0.0006 to 0.0009 cm/s, increasing monotonically with the head pressure increase;
2. After decreasing the liquid level by 5 cm, the specific flow ratio of the filtration water is decreased by one order less;
3. Soil permeability characteristics directly depend on the pressure head in the backwater and on the initial ground water level, not only they depend on mechanical and physical properties of soil.

References

1. Teleshev, V.I., Vatin, N.I., Marchuk, A.N., Churakov, A.I.: *Proizvodstvo gidrotekhnicheskikh rabot*, 430 p. ACB, Moscow (2008)
2. Elhakim, A.: *Alexandria Eng. J.* **55**, 2631–2638 (2016)
3. Startsev, S.A.: *Mag. Civil Eng.* **2**, 36–42 (2009)
4. Girgidov, A.D.: *Mag. Civil Eng.* **4**, 52–57 (2012)
5. Tolpayev, V.A.: *Izv VNIIG im B E Vedeneyeva* **293**, 98–109 (2001)
6. Polubarinova-Kochina, P.Y.: *Teoriya dvizheniya gruntovykh vod*, 664 p. Nauka, Moscow (1997)
7. Tingfeng, H., Ding, Q.: *Soil Tillage Res.* **166**, 179–184 (2017)
8. Bukhartsev, V.N., Petrichenko, M.R., Golovkova, N.V.: *Mag. Civil Eng.* **1**, 22–25 (2009)
9. Bukhartsev, V.N., Petrichenko, M.R.: *Gidrotekhnicheskoye stroitlstvo* **3**, 29–35 (2012)
10. Petrichenko, M.R.: *Nauchnoe obozrenie fiziko-matematicheskikh i tekhnicheskikh nauk v XXI veke*, pp. 3–7 (2012)
11. Zaytsev, O.I., Orlov, V.T.: *Gidravlika: metodicheskoye ukazaniye po razdelu «Filtratsiya»*, 48 p. *Izd-vo Politekhni, Saint-Petersburg. un-ta* (2009)
12. Girgidov, A.D.: *Mekhanika zhidkosti i gaza*, 545 p. *Izd-vo Politekhni, Saint-Petersburg. un-ta* (2007)
13. Kasperov, G.I., Levkevich, G.E.: *Vestnik Komandno-inzhenernogo instituta MCHS Respubliki Belarus* **22**, 68–72 (2015)
14. Priyank, G., Alam, J.: *Perspect. Sci.* **8**, 757–759 (2016)
15. Petrichenko, M.R., Khar'kov, N.S.: *Vestnik MANEHB.* **2**, 129–133 (2008)

Photoelasticity-Based Study of Stress-Strain State in the Area of the Plain Domain Boundary Cut-Out Area Vertex

Lyudmila Frishter^(✉) 

Moscow State University of Civil Engineering, Yaroslavskoye Shosse, 26,
Moscow 129337, Russian Federation
lfrishter@mail.ru

Abstract. In the article, the local stress-strain state of structures and constructions is investigated, various variants for the design of the boundary are taken into account: special lines, points. The acting forced deformations don't satisfy the compatibility conditions. They have a finite discontinuity along the contact line (surface) of the domains, including the irregular point of the boundary, causing stresses. The subject of article is stress concentrators - the singularity of the stress-strain state of structures and constructions exhibiting "constructive heterogeneity" and discontinuous forced deformations determined on polymer models of photoelasticity and defrosting of deformations. A complex theoretical-numerical-experimental approach, for obtaining and analyzing the stress state in the neighborhood of the irregular point of the plane domain boundary, is proposed to extrapolate reliable experimental data to a domain where the fringe contour is not readable.

Keywords: Stress concentrators · Stress-Strain state
Transport Buildings and Structures

1 Introduction

The stress-strain state (SSS) of structures and constructions in the domain of significant constructive heterogeneity (incoming angles, special lines, points) is characterized by the emergence of stress concentration. Acting forced deformations, that don't satisfy the compatibility conditions, have a finite discontinuity along the contact line (surface) of the domains, entering the irregular point of the boundary, and cause stresses. The shape of the boundary and the final discontinuity of the given forced deformations determine the appearance of a singularity of the stress-strain state of the structures.

The relevance of the of investigation of stress from the action of incompatible deformations arises when investigating the SSS of structural elements under the action of temperature gradients, the temperature changes in joints of dissimilar materials with different coefficients of thermal expansion, abrupt changes in distortions having a finite discontinuity in joints of domains with different mechanical properties, as well as the stresses from the installation and the sequence of fabrication of structures, force fit, etc.

The main objective of the study - to obtain with the strict certainty a local stress-strain state in the vertex domain of the angular cut-out of the domain boundary into which the forced deformations gap leaves. The singularities of the SSS of structures and constructions with “constructive heterogeneity” and discontinuous forced deformations are determined as stress concentrators on polymer models of photoelasticity and defrosting of free temperature deformations [1–7]. Fundamentals of the method of photoelasticity are given in fundamental works [1–5].

2 Materials and Methods

We consider a plane problem of the theory of elasticity in the neighbourhood of an irregular boundary point [8–19], into which the contact line of the domains with the jump in the values of the forced deformations comes out. A homogeneous or piecewise-homogeneous body, being in a plane stress state, has an angular point at the boundary. Along the contact boundary $\gamma = \gamma_1 \cup \gamma_2$ of Ω_1 and Ω_2 domains, components of the elastic body, forced deformation and volume forces have a jump (finite discontinuity) as follows:

$$\Delta \varepsilon_{ij}^b = \varepsilon_{ij}^b|_{\gamma_2} - \varepsilon_{ij}^b|_{\gamma_1}; \quad \Delta F_i = F_i|_{\gamma_2} - F_i|_{\gamma_1}; \quad i, j = x, y$$

Young’s modulus, Poisson’s coefficients, coefficients of linear expansion of Ω_1 and Ω_2 domains are constant and different: $E_1, \nu_1, \alpha_1, i, j \in \Omega_1$ and $E_2, \nu_2, \alpha_2, i, j \in \Omega_2$, respectively.

Boundary conditions in the neighborhood of an irregular point $O(0, 0)$ on boundary L_0 are homogeneous. We consider a small neighborhood of an irregular point $O(0, 0)$ of the part B of an elastic body: $x^2 + y^2 < \varepsilon_1^2; z < \varepsilon_0, \varepsilon_1, \varepsilon_0 -$ are positive small numbers. We use the following similarity group:

$$\begin{aligned} x_1 &= tx; & y_1 &= ty; & z_1 &= z \\ \sigma_{ij} &= t\bar{\sigma}_{ij}; & \varepsilon_{ij} &= t\bar{\varepsilon}_{ij}; & U_i &= \bar{U}_i \end{aligned}$$

The resolving system of equations of the plane problem of the theory of elasticity in new variables in this neighborhood will be rewritten as follows:

$$\sum_{j1} \frac{\partial \bar{\sigma}_{ij}}{\partial j1} + \frac{1}{t^2} F_j = 0 \quad \bar{\varepsilon}_{ij} = \frac{\partial \bar{U}_i}{\partial j1} + \frac{\partial \bar{U}_j}{\partial i1}, \quad i, j \in \Omega_1, \Omega_2 \tag{1a}$$

$$\sum_{j1} \bar{\sigma}_{ij} n_{j1}|_{L_0} = 0; \quad \sum_{j1} \bar{\sigma}_{ij} n_{j1}|_{\gamma_B} = \frac{1}{t} \sigma_{in}^b|_{\gamma_B} \tag{1b}$$

$$\bar{\sigma}_{in}|_{\gamma_1} = \bar{\sigma}_{in}|_{\gamma_2}; \quad \bar{U}_i|_{\gamma_1} = \bar{U}_i|_{\gamma_2} \tag{1c}$$

$$\bar{\varepsilon}_{ij} = \frac{1}{E_k} [(1 + \nu_k)\bar{\sigma}_{ij} - \nu_k\bar{S}\delta_{ij}] + \frac{1}{t}\varepsilon_{ij}^b + \frac{1}{t}\alpha_k T\delta_{ij} \tag{1d}$$

when $k = 1, (x_1, y_1) \in \Omega_1$; $k = 2, (x_1, y_1) \in \Omega_2$, $j1, i1 = x_1, y_1$, $n_{j1} = n_j$ - is a normal to the contact line of the domains $\gamma = \gamma_1 \cup \gamma_2$, γB - is a domain boundary, containing a neighbourhood $O_\delta(0)$ of an irregular boundary point.

Depending on move away or moving closer to the irregular boundary point, which is determined by the change in the geometric parameter t , the form of the resolving system of Eqs. (1) in $O_\delta(0)$ varies as follows:

- (a) With an unlimited increase in the geometric parameter $t = \frac{\varepsilon_1}{\varepsilon_2} \rightarrow \infty$, $\varepsilon_1 \ll \varepsilon_2$ the plane problem of the theory of elasticity of a piecewise homogeneous body ($E_k, \nu_k, \alpha_k, k = 1, 2$) with given loads (forced deformations, temperature deformations, volumetric forces, in the neighborhood of an irregular point $O(0, 0)$ of a boundary) is reduced to a homogeneous boundary value problem $\bar{\xi}^E = (\bar{\sigma}_{ij}^E, \bar{\varepsilon}_{ij}^E, \bar{U}_i^E)$ for a piecewise-homogeneous body with homogeneous boundary conditions (canonical, singular).

The solution of the obtained homogeneous boundary-value problem with homogeneous boundary conditions characterizes the singularity of the SSS at an irregular point $O(0, 0)$ and its neighborhood, depends on the given form of the boundary, type of homogeneous boundary conditions and the values of the mechanical characteristics of the material ($E_k, \nu_k, k = 1, 2$). A nontrivial solution of the obtained homogeneous problem is defined as a eigensolution.

- (b) When $t \rightarrow 1$, the system of Eqs. (1) coincides with the initial one taken under the action of given loads. When $t \rightarrow 1$, SSS $\xi^S = (\sigma_{ij}^S, \varepsilon_{ij}^S, U_i^S)$ is conditioned by given loads and boundary conditions.
- (c) In the intermediate range of variation of the parameter values $t \in (1 + \alpha, N)$, where $N > 0$ - is sufficiently large, $\alpha > 0$ - is quite small, it operates both like own SSS $\bar{\xi}^E$ and SSS given from the loads $\bar{\xi}^S$ of the system (1).

According to the considered cases of change in the parameter t , the solution of the plane problem of a piecewise homogeneous body in a neighborhood of an irregular boundary point can be represented in the following form:

$$\bar{\sigma}_{ij} = \bar{\sigma}_{ij}^E + \bar{\sigma}_{ij}^S, \bar{\varepsilon}_{ij} = \bar{\varepsilon}_{ij}^E + \bar{\varepsilon}_{ij}^S, U_i = \bar{U}_i = \bar{U}_i^E + \bar{U}_i^S, \text{ or } \bar{\xi} = \bar{\xi}^E + \bar{\xi}^S$$

when $\bar{\xi}^E = (\bar{\sigma}_{ij}^E, \bar{\varepsilon}_{ij}^E, \bar{U}_i^E)$ - is a singular (eigen) solution of a homogeneous boundary value problem that characterizes the singularity of the SSS in the neighbourhood of an irregular boundary point; $\bar{\xi}^S = (\bar{\sigma}_{ij}^S, \bar{\varepsilon}_{ij}^S, \bar{U}_i^S)$ - is solution of system (1), caused by the effect of the action of given loads of the following form:

$$F_i^a = \frac{1}{t^2} F_i; \quad \sigma_{in}^b \Big|_{\gamma_B} = \frac{1}{t} \sigma_{in}^b \Big|_{\gamma_B}, \quad \varepsilon_{ij}^a = \frac{1}{t} \varepsilon_{ij}^b + \frac{1}{t} \alpha_k T \delta_{ij}$$

and also the influence of the action of the jump of the forced deformations and the volume forces along the line of contact $\gamma = \gamma_1 \cup \gamma_2$ of Ω_1 and Ω_2 domains:

$$\Delta F_i^a = \frac{1}{t^2} \left(F_i \Big|_{\gamma_2} - F_i \Big|_{\gamma_1} \right) = \frac{1}{t^2} \Delta F_i,$$

$$\Delta \varepsilon_{ij}^a = \frac{1}{t} \left(\varepsilon_{ij}^b \Big|_{\gamma_2} - \varepsilon_{ij}^b \Big|_{\gamma_1} \right) = \frac{1}{t} \Delta \varepsilon_{ij}^b,$$

$$\Delta \varepsilon_{ij}^{a1} = \frac{1}{t} \left(\alpha_2 T \Big|_{\gamma_2} - \alpha_1 T \Big|_{\gamma_1} \right) \delta_{ij} = \frac{1}{t} \Delta \alpha \Delta T \delta_{ij}.$$

Considering the relationship between the terms in the SSS representation: $\xi = \xi^E + \xi^S$ in the neighbourhood of the irregular point of the boundary, we can distinguish the following specific areas of SSS action:

- (a) There exists a neighborhood of the irregular point of the boundary of a plane domain in which the singular solution of the homogeneous boundary value problem is true, characterizes that $\sigma_{ij} \rightarrow \sigma_{ij}^E, \sigma_{ij}^S \rightarrow 0$. The singularity of inner stresses σ_{ij}^E (deformation ε_{ij}^E) has a power-law form $r^{\text{Re } \lambda - 1}, \lambda \in [0, 0.5]$. The fringe order in the domain of the stress concentrator on the model (the domain of the singular solution) are not readable for any increase in the neighbourhood of the irregular point.
- (b) There exists a neighborhood of an irregular point of the boundary of the domain in which $\sigma_{ij} \approx \sigma_{ij}^E, \sigma_{ij}^S \approx 0$ and the nonsingular homogeneous elastic problem with the same “eigenvalue” value $\min \text{Re } \lambda$ is valid as is in the singular problem. The domain of a nonsingular solution does not contain a neighbourhood of the singular solution and the irregular point itself, but adjoins it. When approaching from the outside to the boundary of the domain of a singular solution, the stress and the deformations change continuously, their values are large, but finite. The fringe order on the model corresponding to the nonsingular domain of the solution are readable with some possible exceptions.
- (c) If there is a sufficient distance from the irregular point of the boundary, there exists a domain in which $\sigma_{ij} = \sigma_{ij}^S, \sigma_{ij}^E = 0$ and stresses are caused by the given loads (common stress field).

It is possible to give estimates in the domain of a nonsingular solution of a homogeneous planar elastic problem. While using them, it is possible to extrapolate the data to sections close to the irregular point of the boundary, taking into account the experimental data and the practical accuracy of the data measurement by the photoelasticity.

Analyzing the stress state at the vertex of a rectangular wedge by the example of the known [2] experimental solution of Frocht (Fig. 1), choosing the domain of the

nonsingular solution ($m = 7$), which adjoins the domain of the singular solution, the load value is restored. On the basis of this, it is concluded that it is possible to restore the fringe order in a small neighborhood of the wedge vertex according to the practical possibility of the experimental solution and the accuracy of photoelasticity within the limits of linear elastic statement.

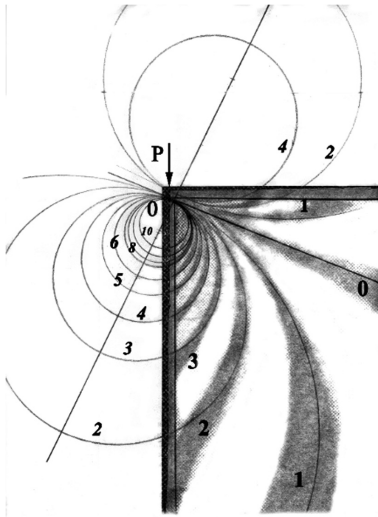


Fig. 1. Diagrams of the fringe orders according to the experimental data. The fringe orders for the right angle was obtained in [2].

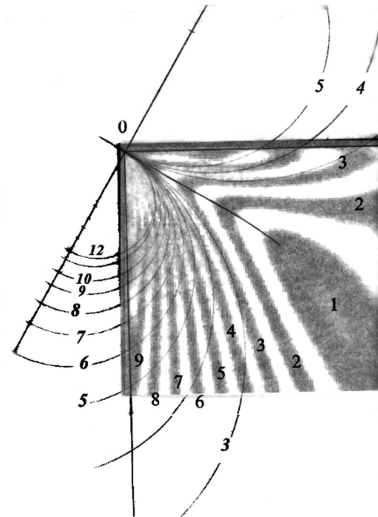


Fig. 2. A comparison of the theoretical and experimental fringe contour for the domain of the straight end of the beam

The experimental solution of the thermoelastic problem is considered for a beam model in one of the domains with created free temperature deformations $\alpha T \delta_{ij}$, and the other domain is free of loads. The jump of forced deformations $\Delta \varepsilon_{ij} = \alpha T \delta_{ij}$ on the contact line of the domains making up the model, goes to an irregular point $O(0, 0)$ of the boundaries of the straight end of the beam. The fringe contour obtained by the “defrosting” method for one of the beam domains is shown in Fig. 2. The inner stresses in the neighborhood of the irregular point of the boundary of the straight end of the beam have the following form:

$$\sigma_r = \frac{\alpha ET}{r} (c_1 \cos \theta + c_2 \sin \theta); \quad \sigma_\theta = \tau_{r\theta} = 0$$

The singularity of the inner radial stresses in the domain of the straight end of the beam (Fig. 2) is the same as the singularity of radial stresses for a rectangular wedge (Fig. 1) under the action of force in problem of Frocht, when. Therefore, the isochrome contour of Fig. 1, corresponding to the radial stresses in the experimental solution of Frocht [2], is a picture of the inner radial stresses in the neighbourhood of the irregular boundary of the straight end of the beam of Fig. 2.

The diagrams of fringe order (isochrom) for several radial sections, plotted in the domain of the straight end of the beam, are shown in Fig. 3. The similarity is established for the fringe order [20, 21]. From the experimental data, the calculated cross section in the domain of the nonsingular solution of the homogeneous problem (d-d) is chosen. Taking into account the continuity and similarity of the changes in fringe order in the cross section (k-k), isochrome order diagrams of (Fig. 3) are constructed, as well as made on their basis radial stresses diagrams (Fig. 4). The section (k-k) is located in the domain of the singular solution, where fringe contour is not readable or is “badly” readable.

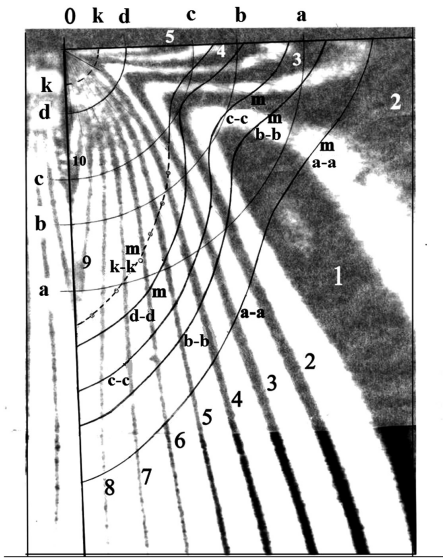


Fig. 3. Diagrams of fringe order according to the experimental data. The section d-d is the calculated section.

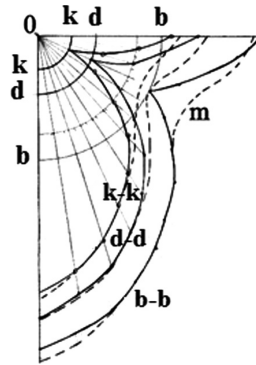


Fig. 4. Diagrams of fringe order and radial stresses (dashed lines) in the domain of the straight end of the beam.

3 Results

According to the theoretical-experimental analysis, the stress state in the neighborhood of the irregular point of the boundary of the plane domain into which the jump of the forced deformations comes out, the following formula is proposed for extrapolating the experimental data:

$$m_{i+1} = \left(\frac{r_i}{r_{i+1}} \right)^{1-\lambda_0} m_i \tag{2}$$

when m_i - is a fringe order from the experimental data in the calculated cross section r_i in a neighbourhood of a nonsingular solution of a homogeneous boundary value

problem, m_{i+1} - is a fringe order in the cross section of smaller radius $r_{i+1} < r_i$, located in a domain with not readable or “badly” readable isochrome contour of the model, $\lambda_0 = \min \operatorname{Re} \lambda$ - the minimal value of the real part of the complex root of the characteristic equation of a homogeneous boundary value problem for a model wedge.

4 Discussion

The article presents a solution to the problem of obtaining the local stress-strain state with the greatest certainty in the domain of the vertex of the corner cut-out of the boundary of the domain into which the rupture of forced deformations occurs.

The considered singularities of the stressed state are relevant for structural elements working with temperature changes in the joints of dissimilar materials with different coefficients of thermal expansion, during the installation, the sequence of fabrication of structures, force fit.

The presented complex investigations of the stress state in the neighborhood of the irregular point of the domain boundary allows us to compare the data of numerical, analytical and experimental methods and to reveal the advantages and disadvantages of each of them.

The singularity of stresses and deformations due to the corner cut-out of the boundary of the domain is determined by the idealization of the statement of the linear problem of the theory of elasticity in the neighborhood of the irregular point of the boundary.

5 Conclusions


The theoretical-numerical-experimental analysis of the stress state in the neighborhood of the irregular point of the boundary of a plane domain, in which a finite discontinuity (jump) of the forced deformations occurs, and the extrapolation formula of the experimental data (2) proposed on its basis, allow us to restore the fringe order in the domain of the singular solution of the elastic problem, in which isochromes on the model are not readable or “badly” readable. The nearness of the cross section to the irregular point of the boundary is due to the linear-elastic statement of the problem, the accuracy of measuring the experimental data and the practical accuracy of photoelasticity method.

References

1. Hesin, G.L., et al.: The photoelasticity method, vol. 3, p. 311. Stroyizdat, Moscow (1975)
2. Frocht, M.M.: Photoelasticity, edited by N.I. Prigorovskiy, vol. 2, p. 432. GITTL, Moscow – Leningrad (1948)
3. Durelli, A., Riley, W.: Introduction to photoelasticity, edited by N.I. Prigorovskiy. Mir, Moscow (1970)

4. Aleksandrov, A.Ja., Ahmetzjanov, M.H.: Polarization-optical methods for deformable solid mechanics, p. 576. Nauka, Moscow (1974)
5. Kobayashi, A.: Experimental Mexhanics, vol. 1, p. 615. Mir, Moscow; vol. 2, p. 551. Mir, Moscow (1990)
6. Koshelenko, A.S., Poznjak, G.G.: Theoretical foundations and practice of photomechanics in mechanical engineering, p. 296. Granica, Moscow (2004)
7. Razumovskij, I.A.: Interference-optical methods of deformable solid mechanics, p. 240. Publisher MGTU named after N Je Bauman, Moscow (2007)
8. Kuliev, V.D.: Singular boundary value problems, p. 719. Nauka, Moscow (2005)
9. Netrebko, V.P.: Photoelasticity method-based study of stress intensity factors near inclined cracks in orthotropic plates, pp. 69–77. Mechanical Engineering Research Institute of the Russian Academy of Sciences, Moscow (2003)
10. Ahmetzjanov, M.H., Tihomirov, V.M., Surovin, P.G.: News of higher educational institutions. Construction **1**, 19–25 (2003)
11. Zadojan, M.A.: Bulletin of the Russian Academy of Science. Mechanics of Rigid Body, vol. 1, pp. 111–122 (2003)
12. Xu, L.R., Kuai, H., Sengupta, S.: Exp. Mech. **44**, 608–615 (2004)
13. Xu, L.R., Kuai, H., Sengupta, S.: Exp. Mech. **44**, 616–621 (2004)
14. Yavari, A., Sarkani, S., Moyer, E.T.: J. Appl. Mech. **69**, 65–72 (2002)
15. Yao, X.F., Yeh, H.Y., Xu, W.: Int. J. Solid. Struct. **43**, 1189–1200 (2006)
16. Frishter, L.Ju., Vatskij, V.A.: Vestnik MGSU **8**, 51–58 (2013)
17. Pestrenin, V.M., Pestrenina, I.V., Landik, L.V.: Vestnik TGU. Math. Mech. **4**, 80–87 (2013)
18. Matveenکو, V.P., Nakarjakova, T.O., Sevodina, N.V., Shardakov, I.N.: Stress singularity at the top of homogeneous and composite cones with different boundary conditions. J. Math. Mech. **72**, 477–484 (2008)
19. Albaut, G.N., Kharinova, N.V., Sadovnichij, V.P., Semenova, J.I., Fedin, S.A.: Nonlinear problems of mechanics of destruction. Vestnik of Lobachevsky University of Nizhni Novgorod, vol. 4, pp. 1344–1348 (2011)
20. Vardanjan, G.S., Frishter, L.Ju.: Int. J. Comput. Civil struct. Eng. **3**, 75–81 (2007)
21. Frishter, L.Ju.: Vestnik MGSU **1**, 169–174 (2008)

Simulation of Blast Load on a Reinforced Concrete Slab in the Time Domain

Galina Kravchenko^(✉) , Dmitry Kostenko ,
and Sergey Tsurikov 

Don State Technical University,
Gagarin Square, 1, Rostov-on-Don 344000, Russia
galina.907@mail.ru

Abstract. The article aims at simulation and analyses of reinforced concrete slabs under blast load by finite element method in LS-DYNA. Properties of rebar and composite materials have been changing. The study of efficiency has been performed. The problem of estimation of bearing structures of buildings is extremely urgent due to the increasing incidence of domestic gas explosion in emergency actions, hitting vehicles on the construction of buildings and structures, man-made disasters, acts of terrorism. At present, when calculating the frame of a building for progressive collapse, the technique of removing the heaviest column of the first floor is applied. However, existing methods for calculation of buildings on the progressive collapse caused many disputes. The paper considers simulation of emergency response using the finite element method in the calculation of reinforced concrete frame elements of a building.

Keywords: Blast load · Finite element method
Simulation of emergency response

1 Introduction

The purpose of this work is to investigate the load-bearing capacity of a reinforced concrete slab with various design solutions for emergency response.

Explosive effect was modeled by the Euler-Lagrange method involves the formation of a spatial domain from the finite elements (domain) in which the investigated elements are located. In this method, the behavior of air and explosive is described by the Euler method, and the behavior of the reinforced concrete slab is described by the Lagrange method. Explosive generally can has any geometric shape. In this example, the explosive has been modeled by spherical shape.

To simulate the connection between the materials in the LS-DYNA keyword is used `CONSTRAINED_LAGRANGE_IN_SOLID`.

The pressure released by blast wave energy during the explosion is simulated using JWL EOS. In using methods pressure models as a function of time, described by the Eq. (1):

$$p = A \left(1 - \frac{\omega\eta}{R_1} \right) e^{-R_1/\eta} + B \left(1 - \frac{\omega\eta}{R_2} \right) e^{-R_2/\eta} + \omega\eta\rho_0 E \tag{1}$$

where A, B – linear explosion coefficients, ω, R_1, R_2 – nonlinear explosion coefficients, $\eta = \rho/\rho_0$, ρ_0 – initial density of the material, E – internal energy of a unit of mass.

When the blasting powders are TNT, according to the explosives equivalent mass, the aforesaid parameters are respectively: $A = 3.712 \cdot 10^{11} \text{Pa}$, $B = 3.231 \cdot 10^9 \text{Pa}$, $\omega = 0.3$, $R_1 = 4.15$, $R_2 = 0.95$, $\rho_0 = 1630 \text{kg/m}^3$, $E = 4.29 \cdot 10^6 \text{J/kg}$.

In this problem for simulation of blast load effect are used keyword LINEAR_POLYNOMIAL, which model air:

$$P = C_0 + C_1\mu + C_2\mu^2 + C_3\mu^3 + (C_4 + C_5\mu + C_6\mu^2)E_0 \tag{2}$$

where E_0 is the initial energy density, $\mu = \rho/\rho_0 - 1$, $C_i (i = 0 - 6)$ – coefficients. For ideal gases $C_0 = C_1 = C_2 = C_3 = C_6 = 0$ и $C_4 = C_5 = \gamma - 1$. Thus, Eq. (2) may be shown as:

$$P = (\gamma - 1) \frac{\rho}{\rho_0} E_0 \tag{3}$$

where ρ/ρ_0 – relative density, γ – rate of change to the specific heat of air, ρ_0 – initial air density value, ρ – current air density.

The design scheme is a reinforced concrete slab. Figure 1 demonstrates the finite element model of the reinforced concrete slab.

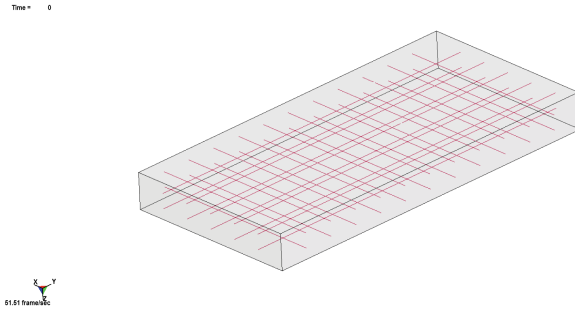


Fig. 1. Finite element model of reinforced concrete slab

The finite element model of the slab was generated by LS-PrePost. The concrete and the steel were represented by solid and bar finite elements. The concrete and steel material types were selected for the model with regard to their actual behavior in explosion. The concrete has been modeled by 8-node finite elements with 24 degrees of freedom in the preprocessor LS-PrePost [2]. Concrete have been modeled by type material 159 CSCM_CONCRETE [3], Table 1.

Table 1. Parameters of the material model CSCM_CONCRETE

Parameter	Value	Unit
Mass density	2400	kg/m ³
ERODE	1.05	–
Pre-existing damage	14.5	MPa

For rebar MAT_PLASTIC_KINEMATIC_TITLE material model is used [4]. The model describes a material whose strain chart is represented as a bilinear with a given density, elastic modulus, Poisson's ratio, the yield stress.

The characteristics of the longitudinal and transverse reinforcement of the slab were modeled with a material of type 3 PLASTIC_KINAMATIC (Table 2).

Table 2. Parameters of the material model PLASTIC_KINAMATIC

Parameter	Value	Unit
Mass density	7850	kg/m ³
Modulus of elasticity	210 000	MPa
Poissons ratio	0.3	–
Yield stress	390	MPa
Failure strain	0.12	–

In this example, an empirical method is used to model the blast load effect. The blast load is modeled by the keyword LOAD_BLAST_ENHANCED. Table 3 shows the parameters of the blast load.

Table 3. Parameters of the keyword LOAD_BLAST_ENHANCED

Parameter	LS-DYNA symbol	Unit
Equivalent mass of TNT	M	kg
X-coordinate of point of explosion	XBO	m
Y-coordinates of point of explosion	YBO	m
Z-coordinates of point of explosion	ZBO	m
Detonation time	TOB	ms

The problem is modeled explosive effect equivalent to 10 kg of TNT. The coordinate of the epicenter of the explosion is located at a distance of 1 m from the surface of the investigated structural element. Three versions of the reinforced concrete slab model with different finite element mesh variants have been developed: with the dimensions of the volume finite elements with a side of 10, 20 and 40 mm [5]. Graphs of the dependence of the pressure values on the surface of the structure on time are obtained for different variants of the finite element model (Fig. 2).

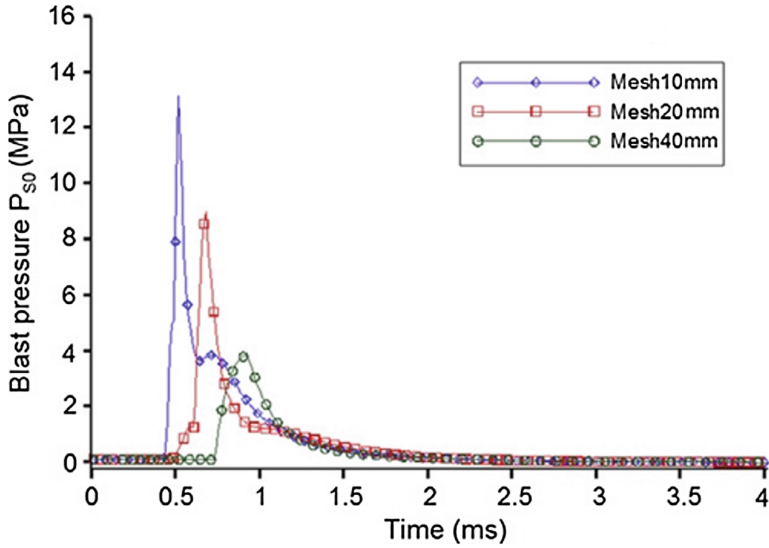


Fig. 2. Blast wave pressure on reinforced concrete slab

The finite element model is designed for the action of an explosive load. The pressure caused by the explosion, when reaching the surface of the plate, was 97 MPa, the stress-strain state of the plate is shown in Fig. 3.

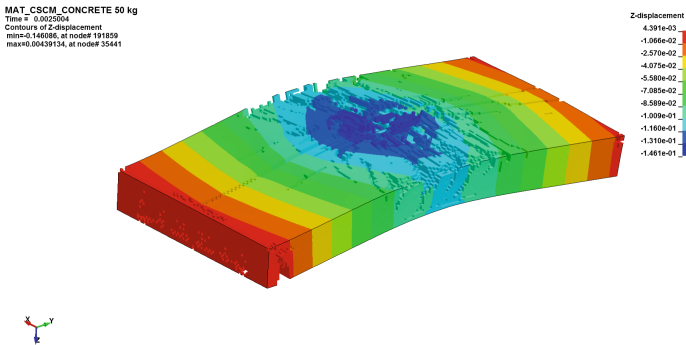


Fig. 3. Slab members displacement

In Fig. 4 shows the process of destruction of the overlap plate in the time domain under the action of an explosive load equal to 10 kg in TNT equivalent. For clarity, the results of the plate are visualised with a turn of 180°.

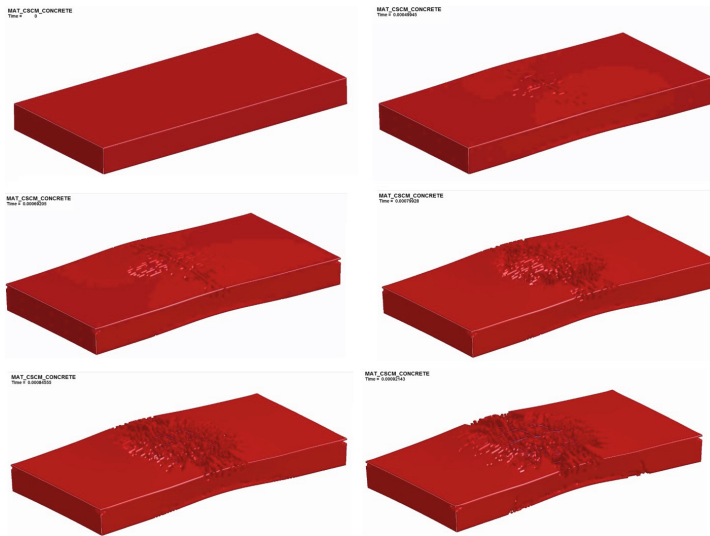


Fig. 4. Destruction concrete process in the time domain

In a series of numerical experiments, the boundary conditions varied, the physical and mechanical characteristics of the materials, the percentage of plate reinforcement, the reinforcement options for composite materials [6].

In the first series of numerical experiments, the percentage of reinforcement varied. In the second series, the reinforcement options for composite materials were changed: a continuous patch on the lower edge, tape sticking along the working direction of the reinforced concrete slab. The `CONSTRAINED_LAGRANGE_IN_SOLID` command was used to provide for collaboration of steel and concrete. This command sets the coupling of the Lagrangian (subordinate) grid of solid elements to the material points at the nodes of the Eulerian (main) grid. The criteria of explosion resistance are the possibility of failure of the reinforcement system due to loss of adhesion of the carbon fiber liner to the plate surface under the action of the blast wave, as well as a change in the bearing capacity.

In the series of numerical experiments, the mass of the explosive and the distance from the explosion cent to the surface of the structure under study are chosen such that, after the action of the special load, the coefficient of bearing capacity is reduced by 20–40%. This allows us to assess the effectiveness of the measures taken to increase sustainability. The effectiveness of the measures was evaluated by the percentage reduction in the load-bearing capacity of the plate after the action of the explosive load.

2 Conclusions

In accordance with the selected types of materials, the elements of the model operate in the plastic stage. This causes deformation of the volumetric elements of the design scheme. When the stresses in the final elements exceed the ultimate strength, their destruction occurs. From the finite-element model, such elements disappear.

Within 0.15 ms, the blast wave propagates throughout the volume of the reinforced concrete slab. In Fig. 5 shows the movements of the elements simulating the reinforcing bars under the action of an explosion of 10 kg in TNT at the time $t = 2.5$ ms.

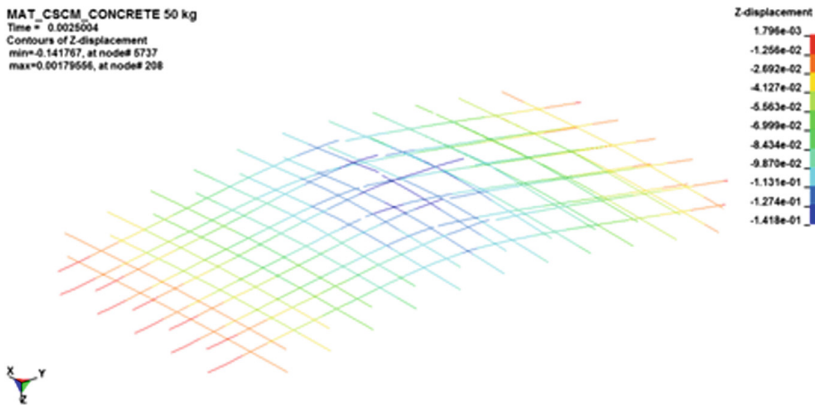


Fig. 5. Fringe level of displacement along z-axis

Analysis of the results of numerical experiments showed that the most effective measures to improve the stability of concrete floor slabs are resistant to the explosive increase in the percentage of reinforcement and applying the external reinforcement composite. Figure 6 shows the changes in the coefficient of bearing capacity of the slab in the event of an explosion, depending on the percentage of reinforcement of the structure and the number of layers of the external composite reinforcement.

Comparison of economic efficiency makes it possible to give recommendations on increasing the stability of the building frame elements by increasing the percentage of reinforcement, which is the most economical.

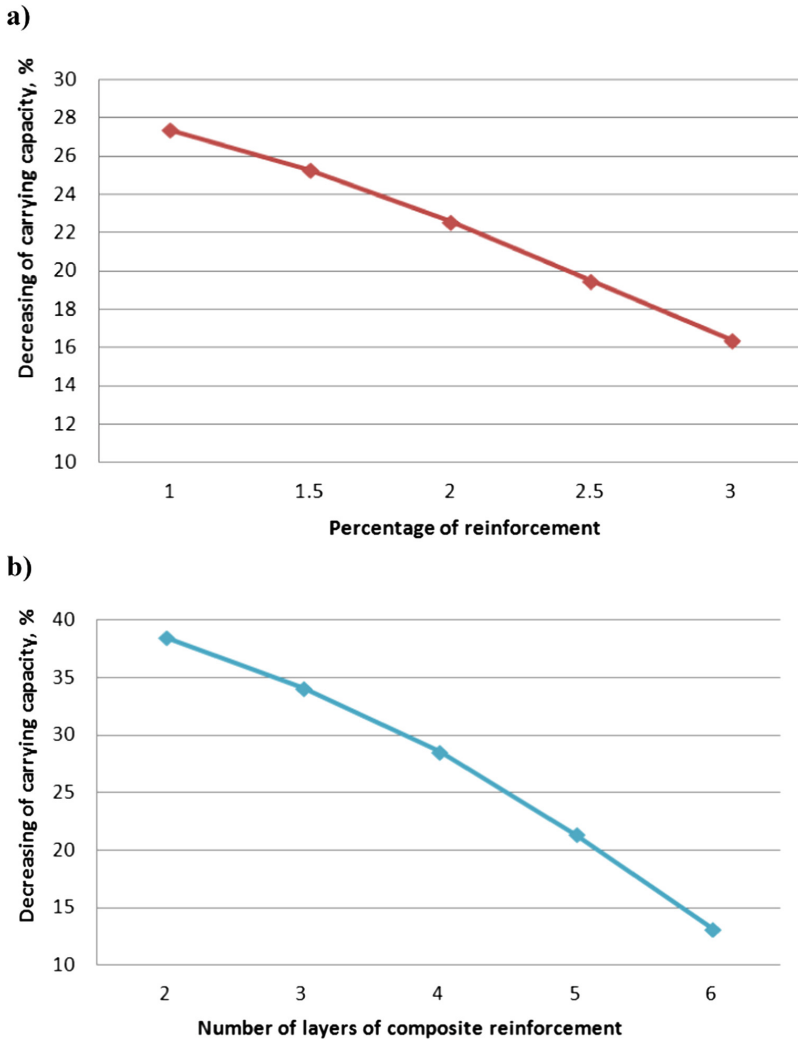



Fig. 6. Decrease of the bearing capacity coefficient, depending on (a) the percentage of reinforcement; (b) the number of layers of composite reinforcement

References

1. Kravchenko, G., et al.: *Inzhenernyj vestnik Dona* **2**, 2886 (2015)
2. Saatci, S., Vecchio, F.: *ACI Struct. J.* **106**, 717–725 (2009)
3. Murray, Y.: *User's Manual for LS-DYNA Concrete Material Model 159*, 77 p. Federal Highway Administration, McLean (2007)
4. *LS-DYNA Keyword User's Manual Volume II Material Models*, 1256 p. Livermore Software Technology Corporation, Livermore (2014)
5. Cervera, F., et al.: *Numer. Methods* **87**, 962–987 (2011)
6. Mailjan, D., et al.: *Inzhenernyj vestnik Dona*. **2**, 1673 (2013)

The Modified Fiber Cement Panels for Civil Construction

Rustem Mukhametrakhimov^(✉)  and Liliya Lukmanova 

Kazan State University of Architecture and Engineering,
Zelenaya str., 1, Kazan 420043, Russia
muhametrahimov@mail.ru

Abstract. At present for decoration facades of buildings are used ventilated facade systems, that allow restoring the old facades by giving them a more modern look. As a covering material, these systems use different materials, among them fiber cement board (FCB). However, they have high cost and they cannot always be used for building in harsh weather conditions like in Russia.

The most widespread and available facing material on the domestic Russian market is fiber cement panels, based on the asbestos fibers. Due to the meanwhile proven carcinogenicity of asbestos, the demand for these products is decreasing year by year to almost zero.

Therefore, it becomes urgent to develop a new effective facing material made from environmentally safe and pure raw materials of low cost, capable of ensuring the reliability, durability and energy efficiency of buildings. One of these materials are FCB on the basis of cellulose fibers.

Existing FCB based on the cellulosic fibers have following disadvantages: low strength, high water absorption and low resistance to frost. These problems require urgent work to develop issues of quality and durability of FCB, based on cellulose fibers.

Based on the realization of three-factor plan of the second-order, the influence of modifying agents on physico-mechanical properties and durability of fiber cement boards, based on cellulose fibers was investigated.

Keywords: Modifying agents · Fiber cement panels · Durability

1 Introduction

At present a large proportion of buildings, that have long life, do not meet modern thermo-technical and aesthetic requirements. For decoration facades of the newly constructed and renovated buildings for heat insulation are used ventilated facade systems, that allow restoring the old facades by giving them a more modern look. As a covering material, these systems use different materials such as granite, aluminum panels, polymeric materials, fiber cement board (FCB), etc. However, most of them are imported from other countries. In addition they have high cost and they cannot always be used for building in harsh weather conditions like in Russia.

The most widespread and available facing material on the domestic Russian market is fiber cement panels, based on the asbestos fibers. Due to the meanwhile proven

carcinogenicity of asbestos, the demand for these products is decreasing year by year to almost zero.

The numerous studies were aimed to improve the performance properties and durability of the fiber-cement plates [1–9], to develop the new test methods [10], to study the use of a secondary waste [11] to show the relevance and prospects of application of these materials in construction. Therefore, it becomes urgent to develop a new effective facing material made from environmentally safe and pure raw materials of low cost, capable of ensuring the reliability, durability and energy efficiency of buildings. In addition, this raw material has to offer the possibility to be processed on the production lines of asbestos-cement boards making maximum use of the existing equipment. One of these materials are FCB on the basis of cellulose fibers. The process of their production is similar to asbestos-cement boards. In fact, asbestos-cement boards are fiber cement, but on the Russian market FCB refers to the asbestos-free boards.

The disadvantages of the existing FCB based on the cellulosic fibers are low strength, high water absorption and low resistance to frost. These problems require urgent work to develop issues of quality and durability of FCB, based on cellulose fibers. In our previous research [12, 13] we investigated the effect of the matrix (cement: sand) with varying degrees of dispersion of silica sand, the coefficient of fiber reinforcement, the grinding of cellulose fibers on the physico-mechanical characteristics of the FCB. Besides, the effect of a number of active mineral admixtures (AMA), characterized by their mineralogical composition and hydraulic activity [14], organosilicon compounds and additives of polyacrylamide on the kinetics of hydration mixed binder and physical and mechanical properties of the FCB were investigated. [15].

2 Materials and Methods

The results of experiments to improve the hydraulic activity of kaolin and improving physical and mechanical properties and durability of fiber cement boards, based on cellulose fibers produced with the wet method are presented. The materials that were used were AMA (activated kaolin, organosilicon compound (OSC) - “FES-50” manufactured by Khimprom, Novocheboksarsk and polyacrylamide (PCA) «Besfloc K4046» from «KOLON LIFE SCIENCE, INC.», South Korea.

The hydraulic activity of kaolin is increased by heating up and subsequent acid activation. It was found that the thermal treatment of kaolin increases its hydraulic activity with 693–1238 mg/g, while the optimum temperature of heat treatment lies around 600 °C with the processing time 30 min (Fig. 1).

The subsequent activation of metakaolin with a formic acid solution of 3% doubles the hydraulic activity compared with the original kaolin (Fig. 2).

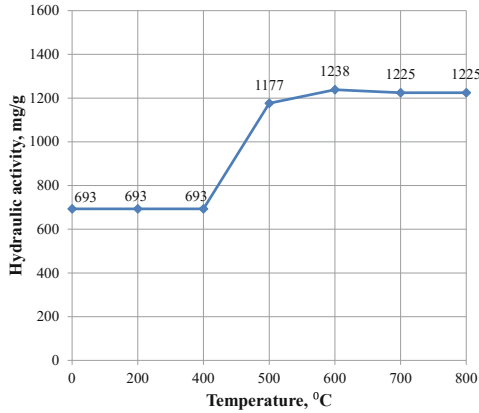


Fig. 1. The effect of heating up temperature of kaolin on its hydraulic activity

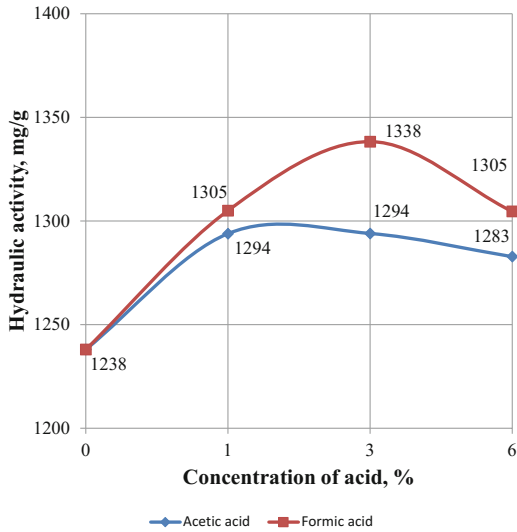


Fig. 2. The effect of acid activation on the hydraulic activity of metakaolin

3 Results and Discussion

Features on the effect of thermal and acid treatment of kaolin to change its phase composition were examined by IR spectroscopy. Investigations on metakaolin activated by a formic acid solution of 3% (hereinafter referred to as metakaolin-A) showed a sharp intensity increase of the wave numbers $3600\text{--}2900\text{ cm}^{-1}$, corresponding to the stretching vibrations of associated OH-groups, and in the $1651\text{--}1644\text{ cm}^{-1}$ wave area.

On the other hand, the relative intensity of the peaks in the frequency ranges $913\text{--}912$ and $1032\text{--}1029\text{ cm}^{-1}$, which are responsible for the perturbation of oxygen-containing

groups Si-O and the bond in the octahedral layers of Al_{3+} , O_{2-} and OH_{-} , decreases with the factor 1.6 to 2.3. Of particular interest is the IR spectra appearance of metakaolin-A peak in the region $2146\text{--}2144\text{ cm}^{-1}$, which is quite possibly related to formation in the communication system Si-H. Characteristically, with increasing concentration of formic acid in the system with 1 to 3 wt%. The intensity of this absorption band is doubled, which is probably caused by the partial destruction of the aluminosilicate under the action of formic acid. Presumably, the formation of the salvation shell on the surface of the solid phase increases significantly the number of bound OH-groups, as well as the possible formation of Si-H-connections.

Thus, treatment of metakaolin formic acid enables increase of the number of associated OH-connections. From our point of view, it enables the formation of Si-H-connection.

Optimization of the FCB compound on the basis of the modified mixed binder with high durability through a three-factor of the second-order plan was achieved on the next step of research. The initial independent variables are defined by factors such as content: PCA (X_1), AMA-metakaolin-A (X_2), OSC (X_3) in percent by weight of cement as a response of selected flexural strength of FCB (R), water absorption (W) and frost resistance (F).

Processing of the results of mathematical planning as provided the following mathematical relationship:

$$R = -43.135 + 326.4X_1 + 3.13X_2 + 162.53X_3 + 0.35X_1X_2 - 2252.9X_1^2 - 0.053X_2^2 - 550.86X_3^2; \quad (1)$$

$$W = 37.44 - 171.98X_1 - 1.82X_2 - 60.73X_3 + 0.095X_1X_2 - 28.57X_1X_3 - 0.0476X_2X_3 + 1180.21X_1^2 + 0.0369X_2^2 + 174.1X_3^2; \quad (2)$$

$$F = -1757.5 + 13485.9X_1 + 97.58X_2 + 3476.64X_3 - 91506X_1^2 - 1.952X_2^2 - 9436.4X_3^2; \quad (3)$$

It was assessed their statistical significance with the tabulated value (Fisher test) to determine the adequacy of the obtained regression equations. Figures 3, 4 and 5 show a graphical interpretation of the results of mathematical model's processing.

As follows from the regression Eq. (1) and the data shown in Fig. 3, with increasing costs of AMA and PAA in the fiber-cement mixtures, the strength of the FCB increases. Joint increasing doses of PCA with AMA, and AMA with OSC leads to a gradual increase of strength, and afterwards to a reduction. The decrease of strength of FCB with increasing doses of PCA and OSC is apparently caused by blocking action on the particles of Portland cement additive molecules, which is especially clearly manifested in their joint introduction.

The water absorption (mathematical dependence 2 and Fig. 4) of FCB decreases with increasing doses of OSC and increases within creasing doses of co-PCA and AMA.

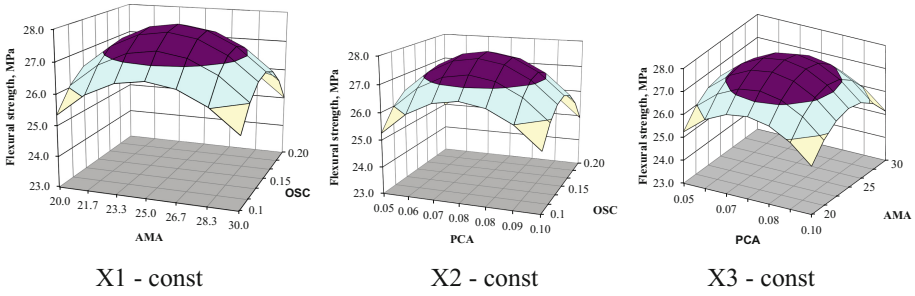


Fig. 3. The effect of the form and content of the modifying additives on the flexural strength of FCB.

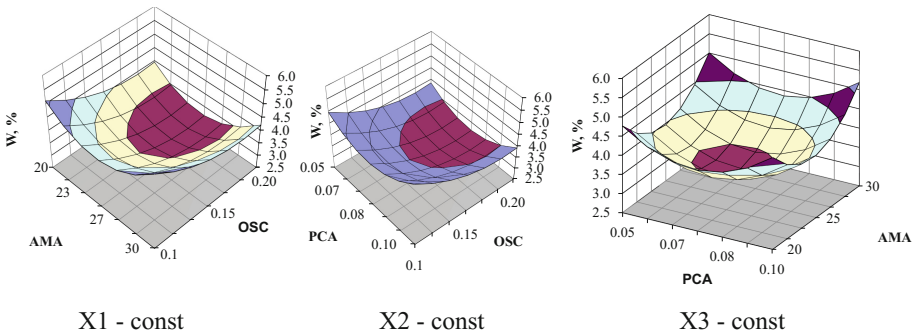


Fig. 4. The effect of the form and content of the modifying additives on the water absorption of FCB.

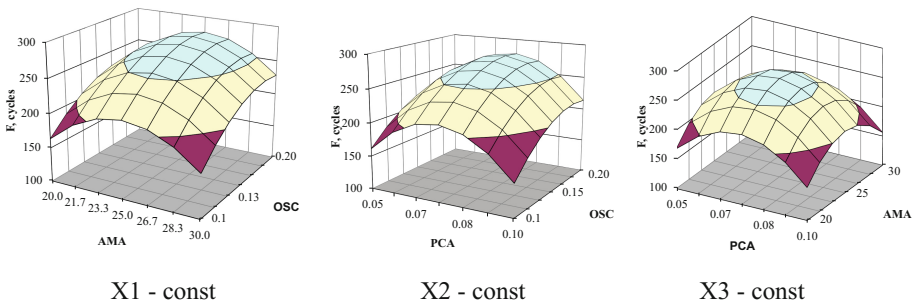


Fig. 5. The effect of the form and content of the modifying additives on the hardness of FCB.

The increase in frost resistance (mathematical dependence 3 and Fig. 5) occurs at higher doses of AMA, as well as the combined action of increased additives AMA and OSC.

Figure 3 shows the optimum content of modifying agents markedly affects the strength of the FCB.

Thus, on the basis of mathematical experiment planning the optimal dosage of the active mineral and chemical additives in the fiber-cement mixtures: PCA - 0.075%, AMA - 25%, OSC - 0.15% respectively to the cement weight. Further research was carried out taking into account the optimal content of modifying additives in the fiber-cement mixture.

The optimum content of the mixed components of the modified binder for FCB with high durability was determined on the basis of mathematical experiment planning.

Results of the study phase of fiber-cement matrix based on modified mixed binder showed that in general there is a substantial increase in the number of hydro C_2SH (C) with an inter planar distance of 2.77 Å, lowly basic hydro-type calcium CSH (A) (2.74 Å) and tobermorit (2.97 Å) as well as lower peak values of $Ca(OH)_2$ and the highly basic types of hydro C_2SH_2 (2.18 Å). Reducing the peak of calcium hydroxide due to its binding to the AMA means low basic hydrosilicates type calcium CSH.

Samples of the fiber-cement matrix using differential thermal analysis showed that on the basis of the mixed modified binder there are able to form a deeper hydration of the silicate phase, as evidenced by an increase in endo effect at 160–170 °C.

IR spectroscopy of cement confirms the results RPA and DTA.

Samples FCB of increased durability were tested for shrinkage deformation/swelling resistance of the air and thermal conductivity.

The obtained FCB had the following specific characteristics: flexural strength - 27.5 MPa, thermal conductivity - 0.22 W/m °C, shrinkage - 0.2 mm/m, frost - 250 cycles, resistance of the air - 300 cycles, impact strength 2.5 kJ/m².

4 Conclusions

- It has been established that the increase of hydraulic activity kaolin 693 to 1338 mg/g ensured by thermochemical activation consisting in the preliminary heat treatment at a temperature of 600 °C and the subsequent activation of the acid in a solution of formic acid.
- On the basis of mathematical planning of the experiment, the optimal dosage of modifying additives composed fiber cement mixture of high durability is the following: PAA - 0.075%, AMA - 25%, OSC - 0.15% by weight of cement.
- It has been shown that the increase of physical and mechanical properties and durability of fiber cement matrix caused by the formation of an optimal microstructure of the cement stone with a high contain of calcium hydro amounts, mainly lowly basic type.




Acknowledgements. This research is carried out under the Russian Government Program of Competitive Growth of Kazan Federal University.

References

1. Mohr, B.J., Nanko, H., Kurtis, K.E.: Cem. Concr. Compos. **2**, 435–448 (2005)
2. Silva, F., Filho, R., Filho, J., Fairbairn, E.: Constr. Build. Mater. **24**, 777–785 (2010)

3. Pehanich, J., Blankenhorn, P., Silsbee, M.: *Cem. Concr. Res.* **34**, 59–65 (2004)
4. Cristelo, N., Cunha, V., Gomes, A., Araújo, N., Miranda, T., Lopes, M.: *Constr. Build. Mater.* **138**, 163–173 (2017)
5. Akhavan, A., Catchmark, J., Rajabipour, F.: *Constr. Build. Mater.* **135**, 251–259 (2017)
6. Abiola, O.S.: *Advanced High Strength Natural Fibre Composites in Construction*, pp. 205–214. Woodhead Publishing, Cambridge (2017)
7. Onuaguluchi, O., Banthia, N.: *Cem. Concr. Compos.* **68**, 96–108 (2016)
8. Krasnikova, N.M., Morozov, N.M., Borovskikh, I.V., Khozin, V.G.: *Mag. Civ. Eng.* **51**, 46 (2014)
9. Fernández-Carrasco, L., Claramunt, J., Ardanuy, M.: *Constr. Build. Mater.* **66**, 138–145 (2014)
10. Schabowicz, K., Gorzelańczyk, T.: *Constr. Build. Mater.* **102**, 200–207 (2016)
11. Ashori, A., Tabarsa, T., Valizadeh, I.: *Mater. Sci. Eng.* **528**, 7801–7804 (2011)
12. Izotov, V.S., Mukhametrakhimov, R.Kh., Sabitov, L.S.: *Stroitel'nye Materialy* **5**, 20–21 (2011)
13. Mukhametrakhimov, R.Kh., Izotov, V.S.: *Izvestiya KGASU* **2**, 213–217 (2011)
14. Izotov, V.S., Mukhametrakhimov, R.Kh., Galautdinov, A.R.: *Stroitel'nye Materialy* **725**, 20 (2015)
15. Mukhametrakhimov, R.Kh., Izotov, V.S.: *Stroitel'nye Materialy* **710**, 116 (2014)

Designs from Innovative Materials in Transport Construction

Alexandr Kvitko  and Viktor Shendrik  

Saint Petersburg State University of Architecture and Civil Engineering,
2-ya Krasnoarmeiskaya st., 4, 190005 Saint-Petersburg, Russia
vicinshendrik@yandex.ru

Abstract. The main purpose of testing dealt with determining the bearing capacity of a bored composite pile in respect to vertical static and cyclic loads. Both field and laboratory tests were carried out. Tests were performed using composite bored piles made of fiberglass having 100 mm diameter with a single-screw blade of 450 mm diameter. The testing technique is explained. The results of settlement of bored composite piles using various metal tips are reported, and cyclograms of static and cyclic loads are plotted. Based on the results obtained, recommendations are given to use composite fiberglass bored piles to develop structures for transport facilities. The main areas to proceed with further studies are discussed to obtain performance indicators of composite fiberglass piles in real structures of transport facilities.

Keywords: Bored pile · Composite materials · 3D modeling · Fiberglass Testing · Static load · Deflection gauge · Settlement

1 Introduction

Novel technologies, innovative approaches to construction, and new promising materials have been widely implemented in the construction industry (including transport construction) over the last decade [1].

A distinctive trend in applying new materials in construction deals with using composite materials combining properties of various components into a single structure [2].

In fact, fiberglass is a composite material as it is composed of glass fibers and cured resin. Fiberglass is characterized by high strength, relatively small specific weight, and a multitude of shapes. Its radio-frequency transmissivity, low electrical conductivity, and decorative properties play an important role in some applications [3].

Another important feature is that production of fiberglass can be initiated without much efforts and expense [16]. Operating production lines will reduce the cost of construction work and improve the project economics.

Application of fiberglass has vast potential in the development of transport facilities that allow replacing numerous standard metal products reducing thereby construction expenses and optimizing metal consumption in the areas where it cannot be replaced. According to webzine BUILD SIMPLY, when metal is replaced with fiberglass, the

total specific weight of the purchase is reduced by 9 times, with its cost and delivery effort getting lower.

One of the trends in fiberglass application in developing transport facilities is associated with production of bored composite piles based on pultrusion fiberglass pipes [3].

Application of composite piles is advantageous as they have high corrosion resistance, they are immune to earth currents; the piles have high specific strength and low weight, they are also easy to operate, and they do not require painting or priming [14, 15]. Furthermore, no high qualifications of working personnel, special equipment and machinery are required to drive piles or arrange pile heads at design elevation. This makes the piles high in demand and competitive as compared to metal analogs.

2 Study Description

A composite pile manufactured for tests is made of a pultrusion fiberglass pipe 100 mm in diameter where the glass material has a special patented laying pattern and a metal screwed welded or cast tip 40 cm in diameter. It can be screwed using the same technology as for metal ones or by using the rod specially welded into the tip. To level the screwed piles in horizontal plane, they are cut using a conventional disc grinder; a metal cap can be placed on top of the pile, on which the structural channel is secured using bolts in the same manner as for metal piles.

A bored composite pile based on pultrusion fiberglass pipes is shown in Fig. 1.

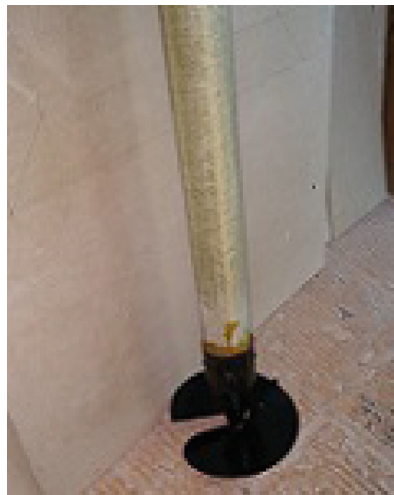


Fig. 1. Bored composite pile based on pultrusion fiberglass pipes (Source: Author's research).

Within a joint research and development program, R&D company Rantes manufactured and delivered seven bored composite piles based on pultrusion fiberglass pipes

for testing to the department of motor roads, bridges and tunnels in the Saint Petersburg State University of Architecture and Civil Engineering.

The tests were intended to determine the bearing capacity of the bored composite piles. The character of changes in soil deformation as a response to increasing the load in a step-like manner was also of interest.

The bored composite piles were tested at the working site of SpetsStroy construction company in the settlement of Ryzhiki, Leningrad Region.

A pilot site was selected for tests featuring clay deposits.

The laboratory studies of soil samples revealed that at the depth up to 5.0 m, the earth is made of grey continuous fluid-plastic clay loam [6–9]. Table 1 lists the rated and design values of the earth foundation.

Table 1. Rated and design values of the earth foundation.

Geological index	Nomenclature type of soil	EGE No.	Parameter	Plasticity index I_p	Natural water content W	Soil density ρ , t/m^3	Porosity coefficient e	Consistency index		Strength index		Deformation modulus E , kg/cm^2	
								I_L	C_B	φ , degrees	c , kg/cm^2		
1	2	3	4	5	6	7	8	9	10	11	12	13	
lg III	Continuous fluid-plastic clay loams		P_r	0.04	0.38	1.91	1.017	1.00		7	0.07	70	
			P_I								1.91 ± 0.10		0.05
			P_{II}								1.91		0.07

C_B — consistency index for undisturbed soils, P_r — rated value of soil parameter accounting for the soil safety factor.

Physical and mechanical properties of the soil were determined using the results of laboratory studies according to effective GOST national standards [7, 9]. Control of density and deformation modulus values was carried out according to the manual for laboratory and field practice in engineering geology and soil science [1]. In order to ensure the credibility of results for the studied rated and design soil parameters, at least six measurement values of the parameter analyzed were taken [4, 10, 12].

The confidential probability of design values of soil characteristics was taken equal to 0.95 [12]. The design soil characteristics of the model installation (internal friction angle, cohesion coefficient, and deformation modulus) were obtained accounting for the rated values and the soil safety factor f_s [5, 11]. The soil safety factor was determined depending on the number of measurements and the confidential probability value [11].

3 Experimental Investigation

For testing, four piles (two piles with bored welded metal tips connected with a pultrusion fiberglass pipe using an adhesive solution and two piles having bored case metal tips connected with a pultrusion fiberglass pipe using self-tapping screws) were driven in the soil. The piles were driven by screwing using a drilling machine having the maximum driving torque of 5,200 kgf/m^2 . The piles were driven into the soil until stop (until the pultrusion pipe collapsed). The process of driving bored composite piles with a pultrusion fiberglass pipe is represented in Fig. 2.

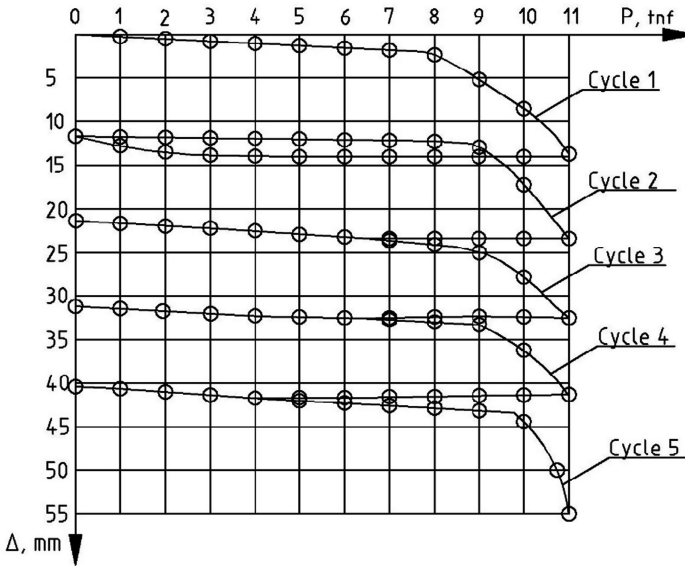


Fig. 2. Single-screw piles with metal welded tip 100 mm in diameter, blade diameter equals to 400 mm. (Source: Author’s research).

The distance between the pile axes was 2.0 m. The piles were driven at the depth of 1.7 m into the soil. During driving, one pile having a bored welded metal tip had the pultrusion fiberglass pipe sheered from the tip connected using an adhesive solution at the end of driving.

For comparison, two metal bored piles having the same diameter were driven into the soil 2.5 m off the bored composite pile using a drilling machine. The driving for metal piles stopped at the same depth of 1.7 m from the ground surface.

For testing of bored composite piles, an installation having prefabricated design was used consisting of a double-T metal beam No. 30 welded to the metal bored piles. To ensure obtaining of the desired weight, the double-T beam was additionally loaded with a 1.0 ton weight.

The testing installation layout is given in Fig. 3.

The piles were tested using vertically applied static and cyclic compression loads [1, 13]. The loading was applied by a 100-ton hydraulic jack. The pressure was constantly applied by pumping oil into the jack using a manual pump on as-needed basis. The hydraulic pressure transferred to the pile was recorded by a pressure gauge. The loading was converted into tons depending on hydraulic pressure using the hydraulic jack conversion table.

The vertical deformation of soil during pile tests was monitored using PAO-6 Aistov deflection gauges installed on reference units.

To ensure load application to the center, the piles tested were screwed in a strictly vertical position. Furthermore, the required axial alignment between piles and the jack

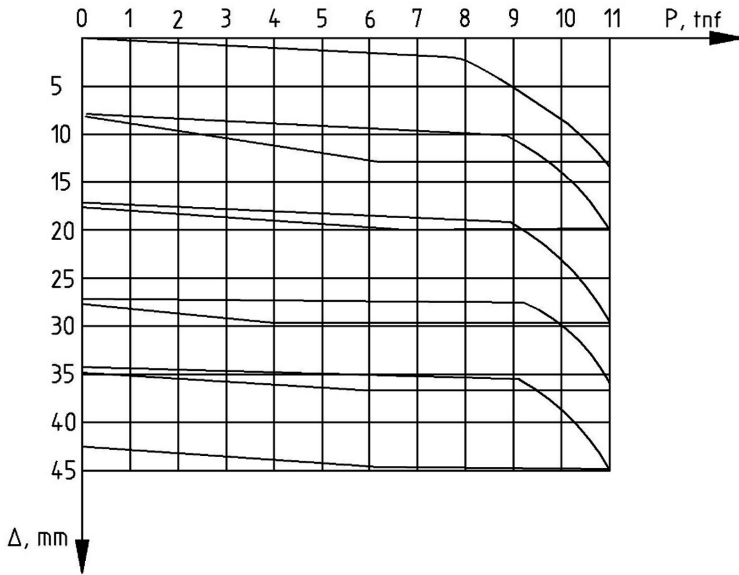


Fig. 3. Single-screw piles with cast metal tip 100 mm in diameter, blade diameter equals to 400 mm. (Source: Author's research)

was monitored using a metal plate at the pile head. All instruments applied and equipment used underwent respective gauging inspections with issuing of proper certificates.

The tests were carried out from August 12, 2015 to August 16, 2015. After assembly of the installation and inspection of the measurement instruments, the piles were loaded with weight.

At a relatively small loading at the initial stage, the anchor piles were pulled out of soil. The pile loading was around 2.0–3.0 tons.

To prevent this, auger flights were put on and welded to the metal anchor piles after which the piles were driven by 1.3 m into the soil.

The real experiment was carried out in two stages [12]. The stages and the scope of experimental studies are listed in Table 2. The required number of tests in each experiment was determined based on the required accuracy and reliability of measurements using respective methodological recommendations to process the test results. The calculations were made through instrumental measurements after the pilot test soil deformation was stabilized. The criterion of “damping” of the soil deformation at the pilot test dealt with the measured values showing no increase during 15 min of testing. This was followed by taking instrument readings and entering them into the field test log [1].

The bored composite pile settlement was determined as an arithmetic mean of the readings. The statistical data were processed using software SPSS v9.0 for Windows.

The physical and mechanical properties of the soil at the pilot site were determined at the initial stage following which the test installation was assembled.

Table 2. Stages and scope of experimental studies.

Experiment	No. of tests in a series	Stages and scope
Field single-factor	5	Preparation stage
		Studies of psychical and mechanical properties of soil at the pilot site
		Assembly of the test installation and inspection of measuring equipment
		Primary stage
		1st series of experiments
	5	Determining the bearing capacity of a bored composite pile against static load
	5	Determining pilot site settlement against static load 2nd series of experiments
	11	Determining residual deformations of soil at the pilot site against static load
	11	Determining the bearing capacity of a bored composite pile against cyclic load
	11	Determining pilot site settlement against cyclic load
Determining residual deformations of soil at the pilot site against cyclic load		

The first stage comprised two series of experiments. In the first series, the pile loading was changed with 1000 kg increment. Under each loading, the pile was kept for 5 min. The maximum load reached for a bored composite pile was 11,000 kg. After it, anchor piles were pulled out from the soil. In this manner, it was impossible to test the bored composite pile for the limiting loading. The theoretical calculations indicate that a bored pile having 100 mm diameter with a single-screw blade of 400 mm in diameter in clay loams can take a 30 ton load.

Figures 2 and 3 show the graphs of testing single-screw composite piles 100 mm in diameter with metal welded or cast tips and a blade of 400 mm in diameter. As the charts show, the maximum displacement of the piles was 52 and 44 mm, respectively. The test results of the piles subject to compression load show that the function of pile settlement against the load in the charts shows no pronounced breaks, complicates determining the limiting loads. In similar cases, it is recommended to determine the loaded state according to the loading that corresponds to the double settlement value permitted for the structure when the constant loading caused by the structure weight prevails. Therefore, cyclic loading tests were carried out in addition to static loading tests.

In the second series, the pile was immediately loaded with 10,500 kg and then fully unloaded in order to reveal the nature of residual deformations. Loading and unloading to zero was sufficiently quick as each loading/unloading cycle took no longer than 2–3 min. During the last loading cycles, the settlement increment was less than 0.1 mm, the total additional settlement during cyclic pile loading was 18 mm and 15 mm, respectively, or 34% (Figs. 4 and 5).



Fig. 4. Drilling of bored composite piles with a pultrusion fiberglass pipe (Source: Author’s research).

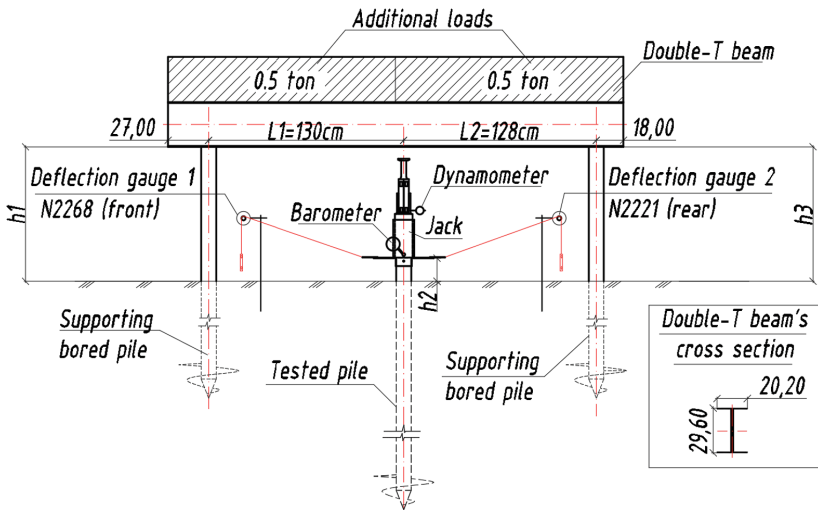


Fig. 5. Testing installtion layout (Source: Author’s research).

4 Experimental Results

After 7–8 fold loading of piles, the settlement stopped almost completely. The results of testing piles against cyclic loading are shown in Figs. 6 and 7.

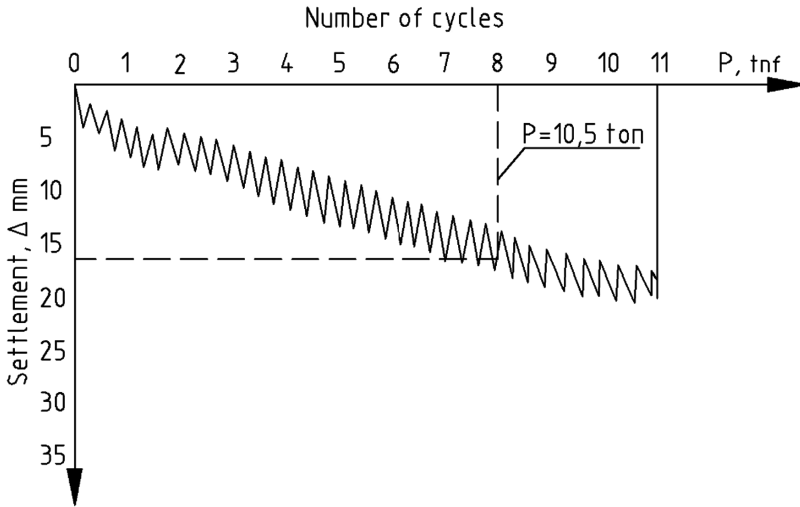


Fig. 6. Single-screw piles with metal welded tip 100 mm in diameter, blade diameter equals to 400 mm. (Source: Author’s research).

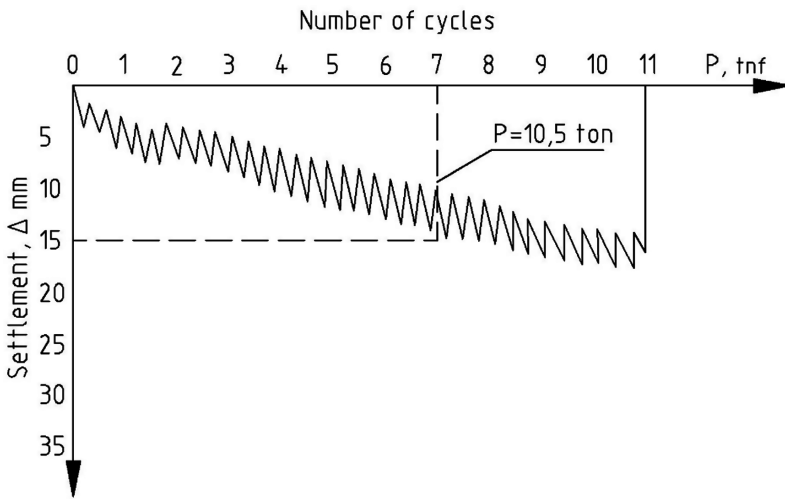


Fig. 7. Single-screw piles with cast metal tip 100 mm in diameter, blade diameter equals to 400 mm. (Source: Author’s research).

At the end of the field experiment, the piles were dug out and inspected for deformations. The inspection revealed that the piles having a connection between the pultrusion fiberglass pipe and a metal tip using an adhesive solution showed cracks at the interface. Furthermore, the deformation of the welded blades of metal tips developed (the blades were bent upwards) by 9–13°.

Cast metal tips and connections of the pultrusion fiberglass pipe with a metal tip using a screwed connection sustained no deformations.

5 Findings and Conclusions

The experimental results allowed making the following conclusions:

1. The bored composite piles proved reliable to withstand tests against the static and cyclic compression load. Carrying a load of 11 tons by a pile 100 mm in diameter with a blade having 400 mm diameter is more than sufficient to recommend using these piles in the construction industry, including the development of transport facilities.
2. During tests, the bored composite piles proved the following advantages: they are easy to install, they have high bearing capacity, corrosion resistance, low weight, etc.
3. According to the field tests, a cast metal tip connected to a pultrusion fiberglass pipe using screws can be recommended as a metal tip.

The field experiment made it possible to develop a program of future studies to obtain the following experimental results:

- to estimate the maximum permitted torque when composite piles are subject to torsion strain;
- to estimate the maximum permitted force in pull-out and horizontal loading of composite piles;
- to carry out experiments on engaging the side surface of a bored composite pile in work to specify the factor accounting for increase in the bearing capacity of bored composite piles.






These piles can be recommended to develop foundations in various transport facilities. They can also be used to reinforce the soil foundation under transport facilities through developing geo-anthropogenic massifs capable of improving the quality of construction and increasing the structural bearing capacity.

References

1. Zhelezkov, V.: Application of Bored Piles in Power-Generating and Other Industries. Pragma Publishing House, Saint Petersburg (2004)
2. Kvitko, A.: Opportunities of using composite materials in developing transport facilities. Road Nation 56 (2014)
3. Kvitko, A.: Specificity of using composite materials in developing transport facilities. Roads. Innovations in construction 42 (2014)
4. Rumshinskiy, L.: Mathematic Processing of Results. Nauka Publishing House, Moscow (1971)
5. Goldstein, M., Tsarkov, A., Cherkasov, I.: Mechanics of Soils and Foundations. Transport, Moscow (1981)
6. Russian Standard GOST 25100-2011 Soils. Classification (2013)

7. Russian Standard GOST 20276-2012 Soils. Methods for field determination of deformability characteristics (2013)
8. Russian Standard GOST 12536-2014 Soils. Methods for laboratory determination of granulometric and microaggregate composition (2015)
9. Russian Standard GOST 12071-2014. Soils. Sampling for laboratory studies (2015)
10. Dolidze, D.: Testing of Buildings and Structures. Vysshaya Shkola, Moscow (1975)
11. Ryzhkov, A.: Determination of Strength and Deformability of Soils in the Construction Industry. Budivelnik, Kiev (1976)
12. Turner, J.: Probability, Statistics, Operational Research. Statistika, Moscow (1976)
13. Harr, M.: Mechanics of particulate media: a probabilistic approach. New York (1997)
14. El Gawady, M.: Seismic behavior of self-centering precast segmental bridge bents. *J. Bridge Eng.* **16**(3), 328–339 (2011). State University, Washington
15. Dawood, M.: Performance-based seismic design of unbonded precast post-tensioned concrete filled GFRP tube piers. Virginia Polytechnic University (2012)
16. Lubin, G.: Handbook of Composites. Mashinostroyeniye Publishing House, Moscow (1988)

Task for a Prestressed Reinforced Concrete Cylinder with External Reinforcement and Cylinder Optimization by Varying the Modulus of Elasticity

Serdar Yazyev¹  , Mukhtar Bekkiev² , Evgeniy Peresypkin³ ,
and Mikhail Turko¹ 

¹ Don State Technical University, Sotcialisticheskaya,
162, 344022 Rostov-on-Don, Russia
ps62@yandex. ru

² Mountain Geophysical Institute, Republic of Kabardino-Balkaria,
pr. Lenina, 2, 360030 Nalchik, Russia

³ Sochi State University, Krasnodar Territory, Sovetskaya st., 26 A,
354000 Sochi, Russia

Abstract. We consider the calculation of the shell in the case when the stressing reinforcement is located on the outer surface. The solution is carried out numerically by the finite element method. A distribution of the modulus of elasticity is determined for which the maximum stresses are zero throughout the entire cylinder.

Keywords: Modulus of elasticity · Prestressed reinforced concrete · Optimization

1 Introduction

We know that if we reduce in any area of the body the modulus of elasticity, in this same area there will be a reduction of stress [1–6]. This leads to the fact that when solving optimization problems you can resort to the consideration of inverse problems of elasticity theory, i.e. tasks in which is found the law of distribution of the characteristics of the material in which the stress state is given. Solving an inverse problem, specifying a certain strength criterion, according to which find the laws of change of the mechanical characteristics from the coordinates.

However, using iterative algorithms for optimization, it is possible not to resort to the solution of inverse problems of the theory of elasticity, and instead solve the direct problem at each step. Finite element method opens wide opportunities for solving this problem.

2 Materials and Methods

Let us consider the calculation of the shell in the case when the prestressing reinforcement is located on the outer surface. The action of the prestressed reinforcement on a concrete cylinder can be replaced by contact pressure p_b (Fig. 1).

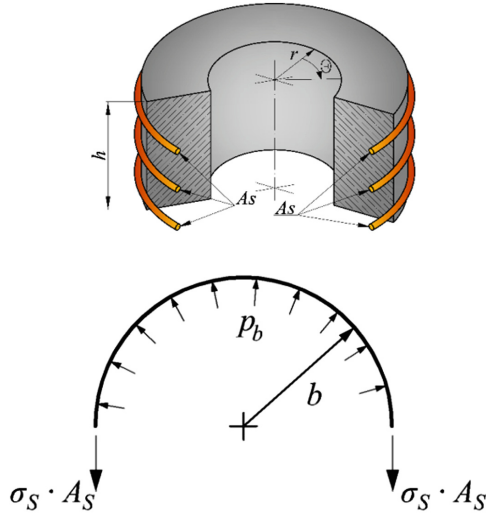


Fig. 1. To determining the contact pressure p_b .

We assume that the shell is under conditions of plane deformation. The value can be determined from the equilibrium condition of its half

$$2\sigma_S A_S = h \int_{-\pi/2}^{\pi/2} p_b b \cos \varphi d\varphi = 2p_b b h \Rightarrow \sigma_S = \frac{p_b b h}{A_S} \tag{1}$$

The stresses in the annular reinforcement are given by:

$$\sigma_S = E_S \varepsilon_{\theta}|_{r=b} + \sigma_{sp} \tag{2}$$

Where σ_{sp} - the initial stresses in the ring reinforcement (until the moment of transfer of forces to the concrete).

Let the modulus of elasticity of concrete be constant. Then this problem can be solved analytically.

From the solution of the Lamé problem for the case of PDS, a formula for displacements [7, 8], $u(r)$:

$$u = \frac{(p_a a^2 - p_b b^2)(1 - \nu_1)}{(b^2 - a^2)E_{b1}} r - \frac{(p_b - p_a)a^2 b^2(1 + \nu_1)}{(b^2 - a^2)E_{b1}} \frac{1}{r}, \tag{3}$$

where $E_{b1} = \frac{E_b}{1-\nu^2}$, $\nu_1 = \frac{\nu}{1-\nu}$.

Then the expression for the circumferential deformation can be written in the form:

$$\varepsilon_{\theta}|_{r=b} = \frac{u|_{r=b}}{b} = \frac{(p_a a^2 - p_b b^2)(1 - \nu_1)}{(b^2 - a^2)E_{b1}} - \frac{(p_b - p_a)a^2(1 + \nu_1)}{(b^2 - a^2)E_{b1}}, \quad (4)$$

Substituting expressions (1) and (4) into (2), after some transformations we obtain the formula for the contact pressure:

$$p_b = \frac{\frac{2p_a a^2}{(b^2 - a^2)E_{b1}} + \frac{\sigma_{sp}}{E_s}}{\frac{bh}{A_s E_s} + \frac{1}{E_{b1}(b^2 - a^2)}(b^2(1 - \nu_1) + a^2(1 + \nu_1))}. \quad (5)$$

Further, in order to determine the stresses $\sigma_{b\theta}$ and σ_r in concrete, it is necessary to substitute the value p_b in the well-known formulas for the Lamé problem.

Let us find, at what value A_s in the thickness of the cylinder there are no tensile stresses. Stresses $\sigma_{b\theta}$ can be determined by the following formula [1, 9]:

$$\sigma_{b\theta} = -\frac{(p_b - p_a)a^2 b^2}{(b^2 - a^2) \cdot r^2} + \frac{p_a a^2 - p_b b^2}{b^2 - a^2} \quad (6)$$

Since the greatest tensile stresses arise on the inner surface, we put in (6) $\sigma_{b\theta}(a) = 0$. Then we obtain the following relation between p_a u p_b :

$$p_b = p_a \frac{a^2 + b^2}{2b^2} \quad (7)$$

Expressing from (1) A_s , we obtain:

$$A_s = \frac{p_b bh}{\sigma_s} = \frac{p_b bh}{\sigma_{sp} + E_s \varepsilon_{\theta}|_{r=b}} \quad (8)$$

To find A_s , using formula (7), we p_b , then using formula (4) calculate $\varepsilon_{\theta}|_{r=b}$ and substitute the values obtained in (8).

In Fig. 2 shows the stress distribution diagram for $\sigma_{b\theta}$. Calculations were carried out with the following initial data [10–13]:

$$\begin{aligned} p_a &= 10 \text{ MPa, } a = 1 \text{ m, } b = 2 \text{ m, } \nu = 0.2, E_b = 2.16 \cdot 10^4, \\ E_s &= 2 \cdot 10^5, \sigma_{sp} = 500 \text{ MPa.} \end{aligned}$$

In order to avoid tensile stresses, 2285 kg of reinforcement per 1 m of pipe length were required for the example in question. As can be seen from the graph, $\sigma_{b\theta}$ only for $r = a$, that is the limiting state in this case occurs only at the inner surface.

In the case when the elastic modulus in the thickness is not constant, it is not possible to obtain an analytical solution. Solve the problem numerically, for example, using the finite element method.

We consider the solution of the problem with the help of FEM. We divide the cylinder n along the thickness by one-dimensional finite elements (Fig. 3). The displacements of the nodes of the i -th finite element are denoted by u_i, u_{i+1} .

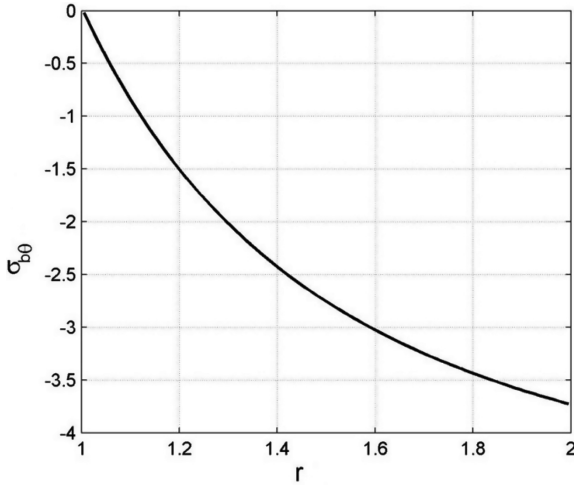


Fig. 2. Graph of stress distribution σ_{b0} .

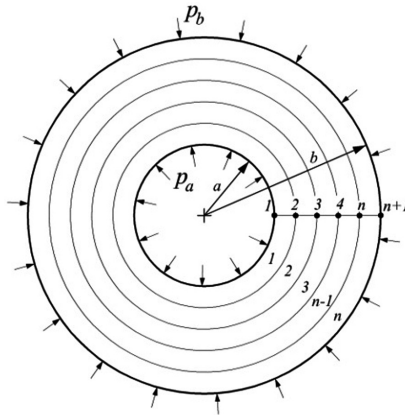


Fig. 3. The scheme of partitioning the cylinder into finite elements.

For the stresses in the valve, taking into account the fact that $\epsilon_\theta = \frac{u}{r}$, we can write:

$$\sigma_S = E_S \epsilon_\theta|_{r=b} + \sigma_{sp} = E_S \frac{u_{n+1}}{b} + \sigma_{sp}.$$

Then $p_b = \frac{\sigma_s A_s}{bh} = \frac{E_s A_s}{b^2 h} u_{n+1} + \frac{\sigma_{sp} A_s}{bh}$. The work of external forces is defined as follows:

$$A = p_a \cdot 2\pi a \cdot u_1 - p_b \cdot 2\pi b \cdot u_{n+1} = 2\pi \left(p_a \cdot a \cdot u_1 - \frac{E_s A_s}{bh} \cdot u_{n+1}^2 - \frac{\sigma_{sp} A_s}{h} \cdot u_{n+1} \right)$$

After differentiating the work of external forces with respect to nodal displacements, we get:

$$\frac{\partial A}{\partial u_1} = 2\pi a p_a, \frac{\partial A}{\partial u_i} = 0, \text{ if } i \neq 1 \text{ и } i \neq n+1, \frac{\partial A}{\partial u_{n+1}} = 2\pi \left(-2 \frac{E_s A_s}{bh} \cdot u_{n+1} - \frac{\sigma_{sp} A_s}{h} \right),$$

Or in the matrix form:

$$\frac{\partial A}{\partial \{U\}} = 2\pi \left\{ \begin{matrix} p_a \cdot a \\ 0 \\ \dots \\ 0 \\ -\frac{\sigma_{sp} A_s}{h} \end{matrix} \right\} + \left[\begin{matrix} 0 & 0 & \dots & 0 & 0 \\ 0 & 0 & \dots & 0 & 0 \\ \dots & \dots & \dots & \dots & \dots \\ 0 & 0 & \dots & 0 & 0 \\ 0 & 0 & \dots & 0 & -\frac{4\pi E_s A_s}{bh} \end{matrix} \right] \cdot \{U\} \quad (9)$$

Thus, in the stiffness matrix obtained when solving a problem for a cylinder loaded with internal and external pressure, the element $K(n+1, n+1)$ must be added to the element $-(4\pi E_s A_s)/(bh)$, and the load vector will be determined by the first term of expression (9).

3 Results

Let us find a distribution of the modulus of elasticity for which $\sigma_{\theta} = 0$ the entire thickness of the cylinder. Consider the equilibrium of its half:

$$2\sigma_s A_s = h \int_{-\pi/2}^{\pi/2} p_a b \cos \varphi d\varphi = 2p_a b h$$

But from (1):

$$2\sigma_s A_s = 2p_b b h$$

Then $p_b = \frac{p_a \cdot a}{b}$.

The dependence of the modulus of elasticity, in which $\sigma_{\theta} = const$ in the entire thickness of the cylinder, loaded with p_a internal pressure and external p_b pressure, has the form [14]:

$$E(r) = E_0 \left(\frac{r}{a} \cdot \frac{A(1-m) - ma\sigma_0}{A(1-m) - mr\sigma_0} \right)^{\frac{1}{1-m}}, \quad (10)$$

Where $E_0 = E(a)$, $A = \frac{(p_b - p_a)ab}{b-a}$, $m = \frac{1-2\nu}{1-\nu}$.

Substituting $p_b = \frac{p_a \cdot a}{b}$ in (4.19), we obtain: $E(r) = E_0 \left(\frac{r}{a} \right)^{\frac{1}{1-m}}$.

It remains to determine the required area of the reinforcement, in which $\sigma_{\theta} = 0$.

$$p_a a h = \sigma_S A_S = (\sigma_{SP} + E_S \varepsilon_{\theta}|_{r=b}) A_S \tag{11}$$

The circumferential deformation of the concrete on the outer surface can be found as follows:

$$\varepsilon_{\theta}|_{r=b} = \frac{1}{E_b|_{r=b}} (\sigma_{\theta} - \nu(\sigma_r + \sigma_z)) = \frac{1}{E_b|_{r=b}} \{ \sigma_{\theta} - \nu[\sigma_r + \nu(\sigma_r + \sigma_{\theta})] \}.$$

Given that $\sigma_{b\theta} = 0$ and $\sigma_r|_{r=b} = -p_b$ we get:

$$\varepsilon_{\theta}|_{r=b} = \frac{p_b}{E_b|_{r=b}} (\nu + \nu^2) = \frac{p_a \cdot a}{b \cdot E_b|_{r=b}} (\nu + \nu^2) \tag{12}$$

Substituting (12) into (11), after the transformations, we obtain the required area of the reinforcement:

$$A_S = \frac{p_a \cdot a \cdot h}{\sigma_{sp} + \frac{E_S}{E_b|_{r=b}} \cdot \frac{p_a a}{b} (\nu + \nu^2)} \tag{13}$$

We note that in formula (13) it depends on the magnitude of the elastic modulus at the outer surface ($E_b|_{r=b}$). The smaller $E_b|_{r=b}$, the smaller the required reinforcement.

In Fig. 4 the curve $E(r)$ obtained at is presented $p_a = 10$ MPa, $a = 1$ m, $b = 1.5$ m, $\nu = 0.2$, $E_0 = 3.10 \cdot 10^4$, $E_s = 2 \cdot 10^5$, $\sigma_{sp} = 500$ MPa.

In Fig. 5 the stress graph $\sigma_{b\theta}$ is obtained using the finite element method. The deviation $\sigma_{b\theta}$ from zero can be explained by the fact that in calculations the matrix $[B]$, in which the coefficients depend on the radius, was replaced by a matrix $[B]$ in which all values were calculated in the middle of the element to simplify integration.

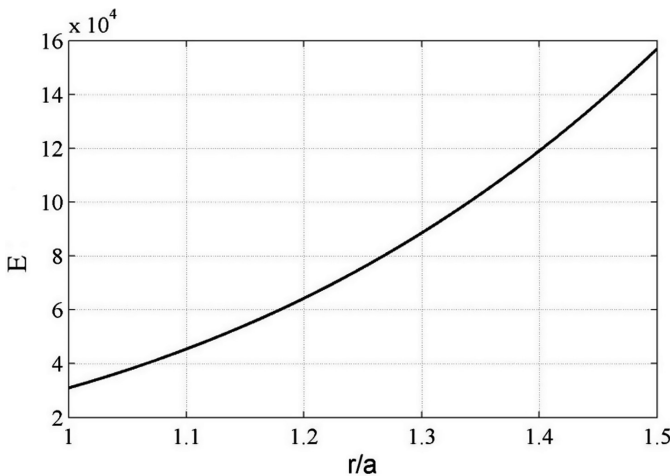


Fig. 4. Dependency graph $E(r)$ for the optimal cylinder.

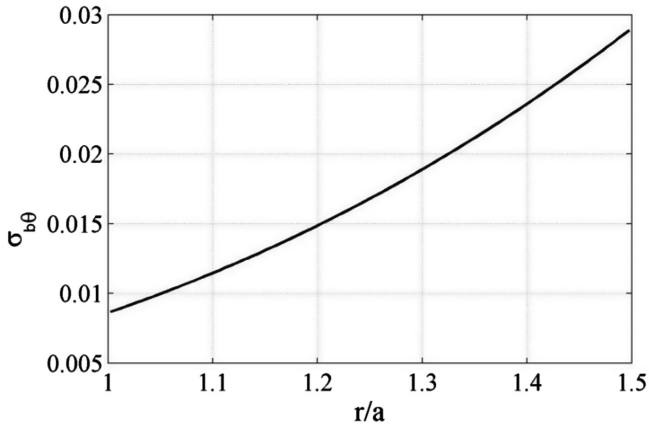


Fig. 5. Dependency graph σ_{b0} for the optimal cylinder.

It should be noted that the decrease in the flow rate of reinforcement for a non-uniform cylinder will be the greater, the larger its thickness, but the modulus of elasticity will also vary over a wider range.

4 Conclusions





The solution of the problem of determining the stress-strain state for a reinforced concrete cylinder with unstressed reinforcement and a prestressed cylinder with the location of the stressed reinforcement on the external surface and in the thickness is obtained. By varying the modulus of elasticity, the problem of optimizing the cylinder with external reinforcement was solved, while a reduction in the flow rate of the reinforcement by 10% was achieved. As the thickness of the shell increases, the effect of creating an inhomogeneity increases, but the range of variation of the modulus of elasticity also increases.

References

1. Yazyev, B.: Nonlinear creep of continuously inhomogeneous cylinders (1990)
2. Andreev, V., Chepurmenko, A., Yazyev, B.: *Adv. Mater. Res.* 869–872 (2014)
3. Yazyev, B., Chepurmenko, A., Andreev, V.: The construction of the model of an equally stressed cylinder on the basis of the Mor theory of strength. *Vestnik MGSU* 5, 56–61 (2013)
4. Yazyev, B., Chepurmenko, A., Muhanov, A.: *Inzhenernyj vestnik Dona* 3(26), 141 (2013)
5. Isaev, S.A., Vatin, N.I., Baranov, P.A., Sudakov, A.G., Usachov, A.Y., Yegorov, V.V.: *Mag. Civil Eng.* 36(1), 103–109 (2013). <https://doi.org/10.5862/MCE.36.13>
6. Usanova, K., Rechinsky, A., Vatin, N.: *Appl. Mech. Mater.* 635–637, 2090–2094 (2014). <https://doi.org/10.4028/www.scientific.net/AMM.635-637.2090>
7. Andreev, V.: *Some problems and methods of mechanics of heterogeneous solids: monograph.* Publishing House ASV (2002)

8. Andreev, V., Bulushev, S.: Optimization of an inhomogeneous thick-walled spherical shell in a temperature field. *Vestnik MGSU* **12**, 40–46 (2012)
9. Yazyev, B., Chepurnenko, A., Andreev, V.: *Vestnik MGSU, Proceedings of Moscow State University of Civil Engineering*, pp. 56–61 (2013)
10. Andreev, V., Potekhin, I.: About equally strong and equally stressed structures. *Collection of works of Voronezh State University of Architecture and Civil Engineering*, pp. 84–90 (2007)
11. Andreev, V., Potekhin, I.: On the method of creating optimal building structures on the basis of solving inverse problems in the theory of elasticity of inhomogeneous bodies. *Bull. Build. Sci. Kursk* **11**, 48–52 (2007)
12. Andreev, V., Potekhin, I.: *Optimization of the Strength of Thick-Walled Shells*. MGSU, Moscow (2011)
13. Andreev, V., Potekhin, I.: Construction of a model of an equally stressed cylinder on the basis of the second and fourth strength theory. In: *Works of XVI Slovakia-Russia-Poland Seminar, Theory of the Bases of Construction*, pp. 29–34 (2007)
14. Litvinov, S., Yazyev, S., Yazyeva, S.: Flat deformation of inhomogeneous multilayer cylinders with allowance for nonlinear creep. *Vestnik MGSU* **1**, 128–132 (2010)

Cracking in Reinforced Concrete Structures of Buildings at Seismic Exposure

Mukhtar Bekkiev¹(✉) , Sergey Skuratov² ,
Evgeniy Peresyarkin³ , and Dmitry Vysokovsky⁴ 

¹ High-Mountain Geophysical Institute, pr. Lenina, 2, 360030 Nalchik, Russia
ps62@yandex.ru

² Sochi State University, Sovetskaya str., 26-A, 354000 Sochi, Russia

³ Kuban State Agrarian University, Kalinin str., 13, 350004 Krasnodar, Russia

⁴ Don State Technical University,

pl. Gagarina, 1, 344002 Rostov-on-Don, Russia

Abstract. Considered numerical experiment model considering simplified-tion, and approximation on the basis of resonance-oscillatory scheme. The idea is based on the cross-shear diagrams of structural failure. Reduce their thickness or increase the possible load. The local nature of the action of the traveling wave leads to the fact that the main phenomena in the wave process are concentrated on the wave front, where the features in the distribution of deformations and forces are concentrated. When the transverse wave propagates, local shifts arise, generating transverse forces of large magnitude. The impact of a wave can significantly exceed the ability of a structure to absorb energy by forming fracture surfaces (cracks).

Keywords: Reinforced concrete · Building · Seismic exposure

1 Introduction

Often, the implementation of complex calculations of structures for seismic impacts is perceived as an enhanced guarantee of reliability. But the actual behavior of the structure in a strong earthquake depends on a large number of factors that are difficult to formalize in the form of mathematical models [1, 3–7]. The forecast of seismic loading characteristics, the reaction of the structure under alternating intensive dynamic impact are uncertain. Besides, there are no universal calculation models. In order to establish the limits of the applicability of a particular model, it is necessary to evaluate the accepted simplifications and approximations on the final result, as well as neglect of small quantities, which were considered as unimportant. For a complex system, it is rarely possible to establish an estimate of this kind, and not all hypotheses and simplifications have an experimental justification or are verifiable on a physical object, physical model. In this case, numerical experiments are necessary, in which certain parameters vary and the results obtained are estimated. Calculations are also needed for fundamentally different models, and not for different software complexes built on essentially one finite element model.

Such fundamentally different are the model based on the resonance-vibrational scheme, and the model based on the shear-shear scheme of structural destruction. The last one is realized when propagating along the construction of a traveling transverse wave.

2 Materials and Methods

Consider the conditions under which the formation of cracks in the path of a wave has a single or multiple character. We assume equation of a plane wave in the form of

$$u(x, t) = A_u \cos(\omega t - kx + \varphi) \quad (1)$$

where A_u - amplitude of oscillation; ω - circular frequency; c - wave front speed; φ - initial phase; t - time; x - coordinate along which the wave propagates; $k = \omega/c = 2\pi/\lambda$ - wave number (- wavelength). His total energy of the wave (W), equal to the sum of the kinetic (K) and potential (P) energies at each instant of time, is, if the viscous resistance of the medium is neglected, a constant value:

$$W = K + P = m\omega^2 A_u^2 / 2, \quad (2)$$

m - mass of oscillating particles.

In the process of particle vibrations, only the conversion of potential energy to kinetic energy occurs and vice versa, while maintaining their total value. The average value of the kinetic energy (\bar{K}) равно is equal to the average value of the potential energy (P) and is equal to half the total energy

$$K = P = W/2 = m\omega^2 A_u^2 / 4. \quad (3)$$

Dividing the total energy by the volume $V = m/\rho$, where ρ is the density of the medium material, we obtain the wave energy density

$$w = W/V = (m\omega^2 A_u^2 / 2) / (m/\rho) = \rho \omega^2 A_u^2 / 2 \quad (4)$$

The quantity equal to the energy transferred by the wave through unit area S per unit time is called the wave intensity (or energy flux density)

$$I = \Delta W / (S\Delta t) = P/S, \quad (5)$$

where $P = \Delta W / (S\Delta t)$ - wave power.

By the time $\Delta t \gg T$ (T - Period of fluctuation) through the surface S will be contained in the volume $\Delta V = S \cdot c \cdot \Delta t$ energy $\Delta W = w\Delta V = w \cdot S \cdot c \cdot \Delta t$, where c - wave speed. Substitution of the obtained ΔW , and also w from (4) into (5) yields:

$$I = \Delta W / (S\Delta t) = wSc\Delta t / (S\Delta t) = wc = c\rho\omega^2 A_u^2 / 2 \quad (6)$$

$$P = \Delta W / \Delta t = w \cdot S \cdot c \cdot \Delta t / \Delta t = w \cdot S \cdot c = c \cdot \rho \cdot \omega^2 \cdot A_u^2 \cdot S / 2 \quad (7)$$

Thus, the intensity of the wave is proportional to the seismic rigidity ($c \cdot \rho$), the square of the circular frequency and the square of the amplitude. If instead of the circular frequency substitute its expression in a period $\omega = 2\pi/T$, obtain

$$I = 2\pi^2 c \cdot \rho \cdot A_u^2 / T^2 \quad (8)$$

When a crack is formed at each point on the line of its development, energy is released $R^2/(2E)$, where R - Resistance of the material to separation, E - modulus of elasticity.

The release of energy due to crack opening occurs not only on its path, but also in the adjacent areas up to l_{crc} on both sides of the crack, that is, on the square $0.5 \cdot l_{crc} \cdot 2l_{crc} = l_{crc}^2$ or in volume $b \cdot l_{crc}^2$, where b - Section width, l_{crc} - crack length. The intensity of the released energy upon opening the crack is obtained by dividing the energy of the volume by the cross-sectional area and by the time Δt_{crc} , during which the crack passed the path l_{crc} : $\Delta t_{crc} = l_{crc}/c_{crc}$, where c_{crc} - Crack propagation velocity.

Thus, the intensity of the energy released when the crack opens:

$$\begin{aligned} I_{crc} &= [R^2/(2E)] \cdot b \cdot l_{crc}^2 / (bh \cdot \Delta t_{crc}) \\ &= [R^2/(2E)] \cdot b \cdot l_{crc}^2 / (bh \cdot l_{crc}/c_{crc}) = [R^2/(2E)] \cdot \zeta \cdot c_{crc}, \end{aligned} \quad (9)$$

here $\zeta = l_{crc}/h$ - the relative length of the crack in comparison with the size of the sectional height, in the direction of which the crack extends.

3 Results and Discussion

We make approximate estimates of the quantities determined by formulas (8) and (9).

Let the seismic rigidity of the building be $1.05 \cdot 10^6 \text{ kg} \cdot \text{m}^{-2} \cdot \text{s}^{-1}$ (Taken from the book [1] with an effective (averaged) density $\rho_e = 700 \text{ kg/m}^3$ and effective speed of propagation of shear waves $c_{es} = 1500 \text{ m/s}$, the oscillation period will be an amplitude of 0.1 m. The intensity of the seismic wave according to the formula (8) will be equal to:

$$I = \frac{2\pi^2}{T^2} \cdot c \rho \cdot A_u^2 = 2 \cdot \frac{3.14^2}{0.4^2} \cdot 1.05 \cdot 10^6 \cdot 0.1^2 = 1.295 \cdot 10^6 \text{ N} \cdot \text{m} / (\text{m}^2 \cdot \text{s})$$

For calculations using formula (9), we take a material (for example, concrete) with the following characteristics:

$$R = 2 \text{ MPa} = 2 \cdot 10^6 \text{ N/m}^2, E = 20000 \text{ MPa} = 2 \cdot 10^{10} \text{ N/m}^2, c_{crc} = 200 \text{ m/s}, \zeta = 0.6.$$

With these data, the intensity of energy release during the propagation of a crack will be:

$$I_{crc} = [R^2/(2E)] \cdot \zeta \cdot c_{crc} = \left[(2 \cdot 10^6)^2 / (2 \cdot 2 \cdot 10^{10}) \right] \cdot 0.6 \cdot 200 = 0.012 \cdot 10^6$$

As it is seen, the velocity of wave propagation also significantly exceeds the speed of propagation of a crack ($c_{es} = 1500 \text{ m/s} > c_{crc} = 200 \text{ m/s}$). Under these conditions, the development of cracks will be of a multiple nature, since the energy of the wave is too great to form a single crack and, due to a much higher velocity, the wave “runs away” from it, carrying its energy to form new and new cracks. In order to form no more than one crack, the following condition must be fulfilled:

$$I/I_{crc} = (2\pi^2/T^2 \cdot c\rho \cdot A_u^2) / \{ [R^2/(2E)] \cdot \zeta \cdot c_{crc} \} < 2, \quad (10)$$

From which the relation

$$c/c_{crc} < 2 \cdot R^2 \zeta \cdot T^2 / [(2\pi^2 \cdot 2E) \cdot \rho \cdot A_u^2]. \quad (11)$$

We substitute in (11) the data values used above:

$$c/c_{crc} < 2 \cdot (2 \cdot 10^6)^2 \cdot 0.6 \cdot 0.4^2 \cdot / (2 \cdot 3.14^2 \cdot 2 \cdot 2 \cdot 10^{10} \cdot 700 \cdot 0.1^2) = 0.139.$$

The value obtained has no physical meaning, since the wave velocity cannot be less than the crack speed. This is because the speed of the wave depends on the modulus of elasticity, density, and, in general, on the coefficient of transverse deformation. Its dependence on the structure of the material is mediated, since both the modulus of elasticity and density are related to the structure. The speed of crack propagation directly depends on the structure: the larger the total contact surface between the heterogeneous components of the material, the smaller the average (or effective) crack propagation velocity, since the cracks propagate predominantly over the contact surfaces between the matrix and the filler. This happens often (though not always) even when the strength of the filler is lower than the strength of the matrix, since the boundaries of dissimilar materials localize the features of the stress and strain fields. In a perfectly homogeneous material, the propagation velocity of the wave and the propagation speed of the crack coincide. In an inhomogeneous material, the propagation velocity of the crack will be less than the velocity of propagation of the wave, and the smaller, the larger the inhomogeneity index.

Therefore, only the multiple formation of cracks corresponds to the chosen values of the parameters. But if the amplitude is half that of the oscillation period, and the period of the oscillations is one and a half times higher than the above, the numerator of the ratio (11) will increase by 2.25 times, the denominator will decrease by 4 times, and the ratio (11) will be greater than unity, which is physically possible and corresponds to the case Formation of a single crack.

We perform simple transformations for the ratio of the intensity of the wave (8) and the intensity of energy release when the crack is opened (9):

$$I/I_{crc} = (2\pi^2/T^2 \cdot c\rho \cdot A_u^2) / \{ [R^2/(2E)] \cdot \zeta \cdot c_{crc} \} = 4\pi \cdot c\rho \cdot A_u^2 \cdot E / (T^2 \cdot R^2 \cdot \zeta \cdot c_{crc}).$$

Bearing in mind the expression of the wave velocity through the modulus of elasticity and density $c = \sqrt{(E/\rho)}$, wherefrom $E = c^2\rho$, expression of the amplitude of the wave period A_u and the acceleration of gravity (g):

$T = 2\pi(A_u/g)^{1/2}$, - where from $T^2 = 4\pi^2 A_u/g$, and also by introducing designation $k_c = c/c_{crc}$, we obtain:

$$I/I_{crc} = 4\pi^2 \cdot (k_c/\zeta) \cdot (c\rho)^2 \cdot A_u^2 / (4\pi^2 A_u/g \cdot R^2) = (k_c/\zeta) \cdot (c\rho)^2 \cdot A_u \cdot g/R^2. \quad (12)$$

If in the process of wave propagation no cracks are formed, inequality

$$(k_c/\zeta) \cdot (c\rho)^2 \cdot A_u \cdot g/R^2 < 1 \quad (13)$$

Or the inequality resulting from it

$$A_u < \zeta / (k_c g) \cdot [R / (c\rho)]^2 \quad (14)$$

In the last expression, we can get rid of the speed of the wave (c), using the substitution $c = \sqrt{(E/\rho)}$. Then (14) takes the form

$$A_u < \zeta / (k_c g) \cdot [R / (c\rho)]^2 = \zeta / (k_c g) \cdot R^2 / (E \cdot \rho), \quad (15)$$

More convenient in the sense that instead of the speed of the wave, the value of the elasticity modulus more often encountered and experimentally simpler is used.

With the relative depth of the crack in the reinforced concrete structure (in comparison with the height of the cross section) $\zeta = 0.6$, acceleration of gravity $g = 10 \text{ m/s}^2$, tensile strength of concrete $R = 2 \cdot 10^6 \text{ Pa}$, elastic modulus $25 \cdot 10^9 \text{ Pa}$ and the density of concrete 2400 kg/m^3 the relation between the amplitude of the wave and the parameter k_c , which is the ratio of the velocity of propagation of the wave to the propagation velocity of the crack, appears in the form

$$A_u < (\zeta/g) \cdot [R^2 / (E \cdot \rho)] / k_c = (0,6/10) \cdot [(2 \cdot 10^6)^2 / (2 \cdot 10^9 \cdot 2400)] / k_c = 0.004/k_c$$

The restriction imposed on the amplitude of the wave to avoid the appearance of cracks is proportional to the square of the tensile strength of the material and inversely proportional to the square of the seismic rigidity ($E \cdot \rho = (c \cdot \rho)^2$) and inversely proportional to the ratio of the propagation velocities of the wave and crack k_c .

The joint action of tangential stresses on shear forces and normal stresses caused by longitudinal and flexural forces leads to the formation of inclined cracks. It should be noted a very important feature of the development of inclined cracks, due to the presence of two mechanisms of destruction - detachment (o) and shear (c).

Flexural normal cracks near the compressed zone, the size of which is determined by the reinforcement factor, are braked, the detachment mechanism ceases to function

(the stretching region before the tip of the crack contracts to the point), and the concrete of the compressed zone is destroyed by the crushing mechanism, crushing. The presence of cracks in the stretched zone has no effect on the course of failure in the final stage, the leveling “plastic” deformations make the stress diagram in the compressed zone close to rectangular, as a result of which the calculated and experimental destructive forces are well coordinated without considering the process of crack development.

A different picture takes place when an inclined crack develops. In the final (or “terminal”) stage, the destruction of concrete in front of a crack occurs as a result of a “cut”, that is, of the type (c), while the region of the stress and strain field before the tip of the crack does not contract to a point, as in the case of peeled cracks. As a result, disregard for the efforts that are being made in this area can lead to significant errors. That is, with the destruction of the element from the action of transverse force, the entire process, beginning from the stage of cracking and ending with the exhaustion of the bearing capacity, proceeds as a process of development of a crack.

The account of shear deformations under transverse action is accompanied by a decrease in the propagation velocity of forces, which is close to the velocity of transverse waves. Without this account, this velocity is close to the velocity of longitudinal waves. The wave nature of the seismic action reflected in the calculation model causes a slight change in the bending moments in comparison with the results of the calculation without taking into account the wave effects, but shows a significant increase in the transverse forces. This is an important circumstance that prompts a serious adjustment of the resonance vibrational computational model.

Seismic action creates transverse forces of large magnitude in the vertical bearing structures of structures. Tangent and compressive normal stresses along horizontal platforms cause the appearance of the main tensile stresses along the areas oriented at an angle to the initial ones:

$$\alpha = 0.5 \cdot \arctg(2\tau/\sigma_0).$$

In the case when the tangential stresses τ caused by the seismic load significantly exceed the normal stress σ_0 from the intrinsic weight, the angle α is close to $\pi/4$.

Main tensile stresses $\sigma = \sqrt{(\sigma_0^2/4 + \tau^2)} - \sigma_0/2$ lead to the formation of inclined crack, the conditions of which are substantially different from those of dipping fractures in such constructions fairly well studied as a beam under static loading.

The criterion for the development of inclined cracks in beams has the form [2, 8, 9]:

$$K_I^2 + K_{II}^2 = K_{Ic}^2 + K_{IIc}^2,$$

where K_I , K_{Ic} - the stress intensity factor at the tip of the crack, growing under the influence of the detachment mechanism, and its critical value;

K_{II} , K_{IIc} - The stress intensity factor at the tip of a crack that grows under the influence of a shear-shear mechanism, and its critical value.

In vertical structural elements under the action of a seismic load, due to a short but significant excess of K_{II} over K_I , the first term in the above criterion can be neglected; In addition, the direction of the development of the crack is more specific in

comparison with the beam, instead of the curvilinear trajectory of cracks in the beams, we obtain a nearly rectilinear along the lines. In vertical structural elements under the action of a seismic load, due to a short but significant excess of K_{II} over K_I , the first term in the above criterion can be neglected; In addition, the direction of the development of the crack is more specific in comparison with the beam, instead of the curvilinear trajectory of cracks in the beams, we obtain a nearly rectilinear along the lines $\alpha + \pi/2$.

The dynamic nature of the load imposes additional restrictions on the process of development of cracks. The short duration of the pulse and a significant decrease in the propagation velocity of cracks in the concrete as compared to the speed of sound propagation due to lengthening of the path when traversing large aggregate particles can lead to the fact that the crack does not have time to dissect the cross section during the time of the pulse. In addition, the impulse effect generates multiple micro-fractures that grow simultaneously and mutually hamper development. For the critical density of microfractures, apparently, one can take the size of the plastic region in front of the crack tip in the Irvine model [10].

4 Conclusions






In this concept, many problems have been little investigated, in particular, the speed of crack propagation in materials, the critical values of stress intensity coefficients at the tops of cracks developing by shear and mixed mechanisms, and a number of others. However, the study of the consequences of strong earthquakes leads us to conclude that a new view is needed on the causes of seismic destruction, which could improve the theory of seismic resistance and improve the reliability of building calculations for seismic loading. At the same time, the transverse-shift concept should not be considered as an alternative to the resonant-vibrational concept. Each of them has its own fields of application, it is important to determine these area.

References

1. Krivev, V.: Wave Processes in Structures of Buildings Under Seismic Influences. Nauka, Moscow (1987)
2. Peresykin, E.: Calculation of Core Reinforced Concrete Elements. Stroizdat, Moscow (1988)
3. Peresykin, E., Peresykin, S.: Criterion for the development of cracks in the transverse shear in reinforced concrete structures under seismic actions. In: Abstracts of the reports of the 1st National Conference on Earthquake-Resistant Construction and Seismic Zoning with International Participation. Poltex, Moscow (2001)
4. Peresykin, E.: Critical stress intensity factor K_{IIc} of heavy concrete on a fine aggregate. Trud-KubGTU XII, Scientific Journal, Krasnodar, Publishing House of Kuban State Technical University, pp. 167–174 (2002)
5. Yazyev, B.: Vestnik MGSU, Proceedings of Moscow State University of Civil Engineering, pp. 56–61 (2013)
6. Yazyev, B., Chepurmenko, A.: Nauchnoe obozrenie 202–204 (2012)

7. Grinfeldi, G.I., Gorshkov, A.S., Vatin, N.I.: Adv. Mater. Res. **941–944**, 786–799 (2014). <https://doi.org/10.4028/www.scientific.net/AMR.941-944.786>
8. Litvinov, S.: Flat deformation of inhomogeneous multilayer cylinders with allowance for nonlinear creep. Vestnik MGSU **1**, 128–132 (2010)
9. Potekhin, I.: On modeling of an equally stressed cylinder on the basis of the energy theory of strength. Collection of works, KGSHA, Kostroma, vol. 2, pp. 72–74 (2009)
10. Potekhin, I.: The method of optimizing designs on the basis of solving inverse problems in the theory of elasticity of inhomogeneous bodies. DrSc thesis, Moscow (2009)

Optimization of the Solution of a Plane Stress Problem of a Polymeric Cylindrical Object in Thermoviscoelastic Statement

Lyubov Trush¹ , Stepan Litvinov¹  , Nadezhda Zakieva¹ ,
and Salis Bayramukov² 

¹ Don State Technical University,
Gagarin square, 1, 344000 Rostov-on-Don, Russia
litvstep@gmail.com

² North-Caucasus State Humanitarian-Technological Academy,
Stavropol str., 36, 369001 Cherkessk, Russia

Abstract. The article deals with the problem of calculation of a hollow polymeric object in axisymmetric statement under the influence of temperature load taking into account temperature-dependent physical and mechanical parameters (elastic and rheological) of the material. The results of problem solution are given, received with application of two methods: finite difference method and finite element method. To increase the accuracy and improve the convergence of results a number of optimizations is carried out that is urgent when using step-by-step methods.

Keywords: Optimization · Solution · Thermoviscoelastic · Polymeric

1 Introduction

Nowadays it is hard to imagine modern technologies and most people's life without structures, their elements, various products made from polymeric materials. For example, in the field of construction polymeric details and structures are light, strong and resistant to the impact of aggressive environment that considerably facilitates the process of transporting the material to the site, constructing and maintaining a structure. To determine the deflected mode of objects in axisymmetric statement there is a set of numeral, numeral analytical and analytical methods. Analytical and numeral analytical methods can be used under rather significant simplifications in the tasks (considering of work of an object only in elastic statement, a single-layer task, etc.), but provide more accurate results. On the other hand, the most universal methods are numerical ones — a finite difference method (FDM) and a finite element method (FEM), allowing to solve the tasks in any statement taking into account a set of the factors which are modeling the operation of a structure as close as possible to the work under realistic operating conditions. However, numeral methods provide less accurate results, and it is necessary to use a set of optimizations which allow getting the most exact solution of the tasks.

Initially the issue of definition of the deflected mode of objects in axisymmetric statement was explored by such scientists as member of Russian Academy of Architecture and Construction Sciences Andreyev [1, 2], professor Turusov [3], later — by professor Yazyev [4–7], associate professor Litvinov [8]. The solution of the specified authors was made by means of FDM that placed considerable restrictions on the initial problem definition. Further, solutions were made by means of FEM [9–12]. While solving plane elastic problems the following types of the deflected mode are explored:

- Plane strain condition. It is supposed that axial deformations along axis z are equal to zero, and strain along this axis has some value. It is considered that plane strain condition takes place if cylinder length considerably exceeds its external radius
- Plane stress condition. It is supposed that axial stress at end faces is equal to zero due to existence of axial deformations along an axis z . It is considered that Plane stress condition takes place if length of the cylinder is much less than its external radius.

Practical examples of plane strain condition are pipes for different purposes; Plane stress condition rarely occurs as is. Thus, further calculations are the ones for plain strain condition.

2 Materials and Methods

To develop the main solution equations of a finite difference method differential balance equation in cylindrical coordinates and the Saint-Venant’s compatibility condition are used taking into account that for plane strain condition in axisymmetric statement: $\frac{\partial}{\partial \theta} = 0$:

$$\frac{\partial \sigma_r}{\partial r} + \frac{\sigma_r - \sigma_\theta}{r} = 0; \quad \frac{\partial \varepsilon_\theta}{\partial r} + \frac{\varepsilon_\theta - \varepsilon_r}{r} = 0. \tag{1}$$

Also the first three expressions of Hooke’s law in a direct form are necessary:

$$\begin{aligned} \varepsilon_r &= \frac{1}{E} [\sigma_r - \nu(\sigma_\theta + \sigma_z)] + \varepsilon_T + \varepsilon_{cr,r}; \\ \varepsilon_\theta &= \frac{1}{E} [\sigma_\theta - \nu(\sigma_r + \sigma_z)] + \varepsilon_T + \varepsilon_{cr,\theta}; \\ \varepsilon_z &= \frac{1}{E} [\sigma_z - \nu(\sigma_r + \sigma_\theta)] + \varepsilon_T + \varepsilon_{cr,z} = 0. \end{aligned} \tag{2}$$

Having performed a number of mathematical operations, we receive the differential second order equation:

$$\frac{\partial^2 \sigma_r}{\partial r^2} + \varphi(r) \frac{\partial \sigma_r}{\partial r} + \gamma(r) \sigma_r = f(r), \tag{3}$$

We express a stress vector from the expression (7) and having performed matrix inversion, we receive the following dependence:

$$\begin{aligned} \begin{Bmatrix} \sigma_r \\ \sigma_\theta \end{Bmatrix} &= \frac{E}{(1+\nu)(1-2\nu)} \begin{bmatrix} 1-\nu & \nu \\ \nu & 1-\nu \end{bmatrix} \begin{Bmatrix} \varepsilon_r \\ \varepsilon_\theta \end{Bmatrix} \\ &- \frac{E}{1-2\nu} \begin{Bmatrix} 1 \\ 1 \end{Bmatrix} \varepsilon_T - \frac{E}{(1+\nu)(1-2\nu)} \begin{bmatrix} 1-\nu & \nu & \nu \\ \nu & 1-\nu & \nu \end{bmatrix} \begin{Bmatrix} \varepsilon_{cr,r} \\ \varepsilon_{cr,\theta} \\ \varepsilon_{cr,z} \end{Bmatrix}. \end{aligned} \tag{8}$$

We perform a substituting

$$[D] = \frac{E}{(1+\nu)(1-2\nu)} \begin{bmatrix} 1-\nu & \nu \\ \nu & 1-\nu \end{bmatrix}. \tag{9}$$

Further, the expression (7) needs to be transformed to:

$$\{\sigma\} = [D] \cdot (\{\varepsilon\} - \{\varepsilon_T\} - \{\varepsilon_{cr}\}). \tag{10}$$

Further calculations will depend on the theory describing creep deformations:

- If full creep deformation isn't equal to zero, i.e. $\theta_{cr} = \varepsilon_{cr,r} + \varepsilon_{cr,\theta} + \varepsilon_{cr,z} \neq 0$, then the expression (8) is the following:

$$\begin{Bmatrix} \sigma_r \\ \sigma_\theta \end{Bmatrix} = [D] \cdot \left(\begin{Bmatrix} \varepsilon_r \\ \varepsilon_\theta \end{Bmatrix} - (1+\nu) \begin{Bmatrix} 1 \\ 1 \end{Bmatrix} \varepsilon_T - \begin{bmatrix} 1 & 0 & \nu \\ 0 & 1 & \nu \end{bmatrix} \begin{Bmatrix} \varepsilon_{cr,r} \\ \varepsilon_{cr,\theta} \\ \varepsilon_{cr,z} \end{Bmatrix} \right). \tag{11}$$

- If full creep deformation is equal to zero, i.e. $\theta_{cr} = \varepsilon_{cr,r} + \varepsilon_{cr,\theta} + \varepsilon_{cr,z} = 0$, then the expression (8) is the following:

$$\begin{Bmatrix} \sigma_r \\ \sigma_\theta \end{Bmatrix} = [D] \cdot \left(\begin{Bmatrix} \varepsilon_r \\ \varepsilon_\theta \end{Bmatrix} - (1+\nu) \begin{Bmatrix} 1 \\ 1 \end{Bmatrix} \varepsilon_T - \begin{bmatrix} 1-\nu & -\nu \\ -\nu & 1-\nu \end{bmatrix} \begin{Bmatrix} \varepsilon_{cr,r} \\ \varepsilon_{cr,\theta} \end{Bmatrix} \right). \tag{12}$$

2.2 Total Energy of System

Total energy of system E represents a difference between elastic deformation energy of an object P and work of external forces A where in case of plane strain condition of elastic deformation energy of an object is as follows:

$$P = \frac{1}{2} \int_V (\sigma_r \varepsilon_{el,r} + \sigma_\theta \varepsilon_{el,\theta}) dV = \frac{1}{2} \int_V \{\sigma\}^T \cdot \{\varepsilon_{el}\} dV, \tag{13}$$

with

$$\{\sigma\} = [D] \cdot (\{\varepsilon\} - \{\varepsilon_T\} - \{\varepsilon_{cr}\}); \quad \{\varepsilon_{el}\} = \{\varepsilon\} - \{\varepsilon_T\} - \{\varepsilon_{cr}\}.$$

Full deformation $\{\varepsilon\}$ is defined by Cauchy's expression. Using FEM above-mentioned expression can be presented in the following form:

$$\{\varepsilon\} = \begin{bmatrix} -\frac{1}{R_j - R_i} & \frac{1}{R_j - R_i} \\ N_i/r & N_j/r \end{bmatrix} \begin{Bmatrix} u_i \\ u_j \end{Bmatrix} = [B]\{U\}. \quad (14)$$

The stress vector in the expression (13) should be transposed. So, the stress vector will be transformed:

$$\{\sigma\}^T = [[D] \cdot (\{\varepsilon\} - \{\varepsilon_T\} - \{\varepsilon_{cr}\})]^T = (\{U\}^T \cdot \{B\}^T - \{\varepsilon_T\}^T - \{\varepsilon_{cr}\}^T) \cdot [D]. \quad (15)$$

After substitution of expressions (14) and (15) in (13), expression for energy of elastic deformation will be transformed in:

$$\begin{aligned} P &= \frac{1}{2} \int_V (\{U\}^T \{B\}^T [D] - \{\varepsilon_T\}^T [D] - \{\varepsilon_{cr}\}^T [D]) \times (\{B\}\{U\} - \{\varepsilon_T\} - \{\varepsilon_{cr}\}) dV \\ &= \frac{1}{2} \int_V (\{U\}^T \{B\}^T [D] \{B\}\{U\} - \{U\}^T \{B\}^T [D] \{\varepsilon_T\} - \{U\}^T \{B\}^T [D] \{\varepsilon_{cr}\} \\ &\quad - \{\varepsilon_T\}^T [D] \{B\}\{U\} + \{\varepsilon_T\}^T [D] \{\varepsilon_T\} + \{\varepsilon_T\}^T [D] \{\varepsilon_{cr}\} \\ &\quad - \{\varepsilon_{cr}\}^T [D] \{B\}\{U\} + \{\varepsilon_{cr}\}^T [D] \{\varepsilon_T\} + \{\varepsilon_{cr}\}^T [D] \{\varepsilon_{cr}\}) dV. \end{aligned} \quad (16)$$

2.3 Deriving the Rigidity Matrix and Load Vector of a Finite Element

According to the Lagrange variation principle, from all kinetically possible deflected modes of a deformable solid body, total energy of deformations reaches the minimal value in case of the actual deformed state. Thus, in the following operation is necessary to find the displacement energy minimum.

$$\begin{aligned} \frac{\partial E}{\partial \{U\}} &= \frac{1}{2} \int_V (2\{B\}^T [D] \{B\}\{U\} - \{B\}^T [D] \{\varepsilon_T\} \\ &\quad - \{B\}^T [D] \{\varepsilon_{cr}\} - \{B\}^T [D] \{\varepsilon_T\} - \{B\}^T [D] \{\varepsilon_{cr}\}) dV \\ &= \int_V (\{B\}^T [D] \{B\}\{U\} - \{B\}^T [D] \{\varepsilon_T\} - \{B\}^T [D] \{\varepsilon_{cr}\}) dV. \end{aligned} \quad (17)$$

The volume of a finite element which is given in the expression (17) can be determined approximately according to a formula:

$$dV \approx r dr \approx r(R_j - R_i), \tag{18}$$

with r — distance to the gravity center of a finite element section. In calculations which are given in this article this distance is defined by two methods: $r = \frac{R_i + R_j}{2}$ or $r = \sqrt{\frac{R_i^2 + R_j^2}{2}}$. In the first case a commonly used approach is used when a required accepted point is in the arithmetic center of an element, in the second it is situated in the gravity center of the element. Further, the expression, (17) taking into account (18) must to be as follows:

$$[K] \cdot \{U\} = \{F\}, \tag{19}$$

with $[K] = \sum_{e=1}^E [k^{(e)}]$ — a global rigidity matrix; $\{F\} = \sum_{e=1}^E \{f^{(e)}\}$ — global load vector. Elements of this matrix and vector are defined by ratios:

$$\begin{aligned} [k^{(e)}] &= \{B\}^T \cdot [D] \cdot \{B\} \cdot \{U\} \cdot r \cdot (R_j - R_i); \\ \{f^{(e)}\} &= (\{B\}^T \cdot [D] \cdot \{\varepsilon_T\} + \{B\}^T \cdot [D] \cdot \{\varepsilon_{cr}\}) \cdot r \cdot (R_j - R_i), \end{aligned} \tag{20}$$

with $\{\varepsilon_T\}$ and $\{\varepsilon_{cr}\}$ defined according to the accepted creep theories in expressions (11) and (12). The solution of the problem is made by means of MATLAB computer programs. There are several ways of inputting the matrixes $[k^{(e)}]$ and $\{f^{(e)}\}$ into the program code. The first way is a numerical solution. I.e. the matrix $[K]$ and a vector $\{F\}$ are set by expressions (20). The second way is the analytical solution. It means that elements of a matrix $[K]$ and a vector $\{F\}$ are defined separately by direct integration.

2.4 Boundary Conditions of the Problem

Boundary conditions for plane strain condition are as follows:

$$\sigma_r(r_a) = -P_a; \quad \sigma_r(r_b) = -P_b, \tag{21}$$

with P_a and P_b — pressure on the internal and external surfaces of the cylinder respectively. However the problem is solved by means of the finite elements displacement method. Then to compare the pressure on the surfaces of the cylinder and movement of the corresponding construction units we can use the first expression of Hooke’s law in the reciprocal form:

$$\sigma_r = \lambda\theta + 2\mu\varepsilon_r - 3K\varepsilon_T - 2\mu\varepsilon_{cr,r} - \lambda\theta_{cr}. \tag{22}$$

Deformations ε_r и ε_θ are also approximated on a finite element by means of the expression (14). Final boundary condition for extreme finite elements is as follows:

$$u_i \left(\frac{-1 + v \frac{R_i}{r}}{R_j - R_i} \right) + u_j \left(\frac{1 - v \frac{R_i}{r}}{R_j - R_i} \right) = \frac{\sigma_r}{E} (1 + v)(1 - 2v) + (1 + v)\varepsilon_T + (1 - 2v)\varepsilon_{cr,r} + v\theta_{cr}. \quad (23)$$

In the expression (23) instead of σ_r stresses on the internal and external cylinder surfaces for internal and external final elements respectively are used.

3 Results

We consider a hollow epoxide cylinder. The material is chosen in order to compare our results with other authors' ones. Geometrical parameters and boundary conditions are the following: $R_a = 8$ mm, $R_b = 28$ mm — internal and external radiuses of the cylinder respectively; $P_a = 0$ MPa, $P_b = 0$ MPa — pressure at internal and external end faces of the cylinder respectively. Stress-strain and rheological characteristics of polymeric material: $\nu = 0,3$ — Poisson's ratio; $E(T) = -17,5T + 3525$ MPa — coefficient of elasticity accordingly; $E_{\infty 1}(T) = -30T + 3150$ MPa — modulus of high elasticity; $\eta_1^*(T) = 104430e^{-0,0275T}$ MPa · h — modulus of relaxation viscosity; $m_1^*(T) = -0,011T + 4,75$ MPa — modulus of speed. Temperature on the external surface of the cylinder is 28°C. Initial temperature on the internal surface of the cylinder is 28°C; final temperature on the internal surface of the cylinder is 100°C. Time during which the deflected mode is calculated, 3.6 h, time of temperature rise on the internal surface of the cylinder from the initial to the final value 1.2 h.

The solution has been made at different radial approach. Quantity of intervals of radial partition (FDM) or quantity of finite elements (FEM): 9 pieces, 99 pieces and 999 pieces; quantity of points of time division (linear interpolation) 101 pieces.

Five ways of calculation have been performed. The first — solution by means of FDM; the second — solution by means of numerical FEM, the distance to the gravity center of the finite element section is determined by the formula $r = \frac{R_i + R_j}{2}$; the third — solution by means of numerical FEM, the distance to the gravity center of the finite element section is determined by the formula $r = \sqrt{\frac{R_i^2 + R_j^2}{2}}$; the fourth — solution by means of analytical FEM, the distance to the gravity center of the finite element section is determined by the formula $r = \frac{R_i + R_j}{2}$; the fifth — solution by means of analytical FEM, the distance to the gravity center of the finite element section is determined by the formula $r = \sqrt{\frac{R_i^2 + R_j^2}{2}}$.

Calculation results are presented in the form of tangential stress σ_θ in Table 1.

In Table 1: $N_{el,r}$ — quantity of elements of radial partition; $N_{pts,t}$ — quantity of time division points; R — radius in a certain point; $\sigma_{\theta,FDM}$ — the values of stress we have arrived at by means of FDM; $\sigma_{\theta,FEM1}$ — values of stress we have arrived at by means of numerical FEM under the assumption that the distance to the gravity center of the finite element section is determined by the formula $r = \frac{R_i + R_j}{2}$; $\sigma_{\theta,FEM2}$ — the values of stress we have arrived at by means of numerical FEM under the assumption that the distance

Table 1. Calculation results of problem solution by means of FDM and FEM.

$N_{el,r}$	$N_{pts,t}$	R, mm	$\sigma_{\theta,FDM}$	$\sigma_{\theta,FEM1}$	$\sigma_{\theta,FEM2}$	$\sigma_{\theta,FEM3}$	$\sigma_{\theta,FEM4}$
9	101	8	-4.3199	-4.4119	-4.3753	-4.5256	-4.3856
		18	0.1245	0.1176	0.1361	0.0359	0.1080
		28	4.9185	4.9834	4.9823	4.9304	4.9689
99	101	8	-3.9119	-3.8762	-3.8764	-3.8772	-3.8763
		18	0.0668	0.1352	0.1353	0.1344	0.1351
		28	5.3688	5.3771	5.3771	5.3766	5.3770
999	101	8	-3.7948	-3.7904	-3.7904	-3.7904	-3.7904
		18	0.1274	0.1342	0.1342	0.1342	0.1342
		28	5.4108	5.4116	5.4116	5.4116	5.4116

to the gravity center of the finite element section is determined by the formula $r = \sqrt{\frac{R_i^2 + R_j^2}{2}}$; $\sigma_{\theta,FEM3}$ — the values of stress we have arrived at by means of analytical FEM under the assumption that the distance to the gravity center of the finite element section is determined by the formula $r = \frac{R_i + R_j}{2}$; $\sigma_{\theta,FEM4}$ — the values of stress we have arrived at by means of analytical FEM under the assumption that the distance to the gravity center of the finite element section is determined by the formula $r = \sqrt{\frac{R_i^2 + R_j^2}{2}}$.

4 Conclusions





As far as determining of polymeric bodies deflected mode is connected with a material rheology, it is necessary to carry out maximal optimizations to increase the accuracy of the solution even if at first sight this increase seems very insignificant. The results given in Table 1 show that to achieve the best accuracy, several optimizing actions are necessary: to do numerical multiplication of matrixes and $[D]$ replace them with analytical integration, and also to accept not the arithmetic center of a finite element, but the gravity center of the whole element.

References

1. Andreev, V.: Elastic and elastoplastic equilibrium of thick-walled cylindrical and spherical continuously inhomogeneous bodies (2006)
2. Andreev, V.: Some Problems and Methods of Mechanics of Heterogeneous Solids: Monograph. Publishing House ASV (2002)
3. Turusov, R.: Mechanical phenomena in polymers and composites (in the process of formation) (1983)
4. Yazyev, B.: Nonlinear creep of continuously inhomogeneous cylinders (1990)
5. Yazyev, B., Litvinov, S.: Materialy IV Mezhdunarodnoy nauchno-prakticheskoy konferentsii KBGU, pp. 337–342 (2008)

6. Yazyev, B.: Features of the relaxation properties of mesh and linear polymers and composites based on them (2009)
7. Yazyev, B., Chepurnenko, A., Litvinov, S., Avakov, A.: *Nauchnoe obozrenie* **9**, 863–866 (2014)
8. Litvinov, S.: *Materialy III International Conference KBGU*, pp. 27–32 (2007)
9. Dudnik, A., Chepurnenko, A., Litvinov, S.: *Nauchno-tekhnicheskij vestnik Povolzh'ya* **6**, 49–51 (2015)
10. Dudnik, A., Chepurnenko, A., Litvinov, S.: *Plast. Massy* **1–2**, 30–33 (2016)
11. Dudnik, A., Chepurnenko, A., Litvinov, S., Denego, A.: *Inzhenernyj vestnik Dona*, vol. 2 (2015)
12. Chechevichkin, V.N., Vatin, N.I.: *Mag. Civil Eng.* **50**(6), 67–74 (2014). <https://doi.org/10.5862/MCE.50.7>

Optimization of the Thick-Walled Sphere by the Energy Method on the Basis of the Strength Criterion of P. Balandin

Serdar Yazyev^(✉) , Sergey Skuratov , Valery Bondarenko ,
and Svetlana Yazyeva 

Don State Technical University,
Sotcialisticheskaya str., 162, 344022 Rostov-on-Don, Russia
ps62@yandex.ru

Abstract. A centrally symmetric problem of the theory of elasticity of inhomogeneous bodies for a thick-walled sphere loaded with external pressure and located in a stationary temperature field is considered. The essence of the problem is to determine such a dependence of the modulus of elasticity on the radius at which the stress state of the sphere will be given. The third theory of strength is considered - the theory of maximal tangential stresses and the theory of Balandin P. Thus, the introduction of artificial heterogeneity leads to optimization of the shells, which makes it possible to reduce their thickness or increase the possible load.

Keywords: Optimization · Sphere · Energy · Strength criterion

1 Introduction

The idea of an optimization method for thick-walled cylindrical and spherical shells due to a change in the modulus of elasticity of the material belongs to the academician RAASN Andreev [1] and analytically the derivation for various strength theories was obtained in [2]. The essence of the inverse problem is to find such dependences of the mechanical characteristics of the construction material on the coordinates at which the state of the construction will be specified [3–6]. As a result of the solution of inverse problems, models of inhomogeneous thick-walled shells are created [7–10]. Here, the equivalent stress, corresponding to a particular theory of strength, is constant throughout the volume of the structure.

However, we should note that the authors above restrict themselves to the consideration of a stationary temperature field and the solution of an analytically stressed-deformed state can be obtained only for the first and third strength theory. In reality, the law of distribution of temperature, as well as strength criterion may be completely arbitrary. Add to the above problem of optimizing the thick shell when the temperature load is possible only under the simultaneous action of power loads (internal, external pressure) [6].

2 Materials and Methods

The algorithm presented in this article is also suitable for problems with allowance for temperature effects. Only the equations for determining the stress-strain state of the structure are changing. The design scheme for a thick-walled sphere is shown in Fig. 1.

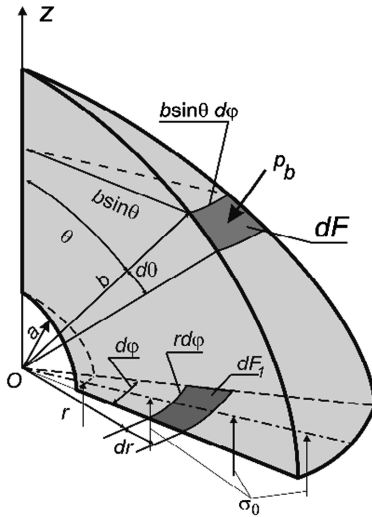


Fig. 1. The design scheme of the thick-walled sphere.

For a centrally symmetric problem the resolving equation takes the form [6, 12, 13]:

$$\frac{\partial^2 \sigma_r}{\partial r^2} + \left(\frac{4}{r} - \frac{\partial E}{\partial r} \right) \cdot \frac{\partial \sigma_r}{\partial r} - \frac{1}{r} \cdot \frac{2(1-2\nu)}{1-\nu} \cdot \frac{1}{E} \frac{\partial E}{\partial r} \sigma_r = - \frac{2E\alpha_T}{r(1-\nu)} \frac{\partial T}{\partial r}. \quad (1)$$

The finite element method with the influence of the temperature dependence of the stress-strain can be written as [11]:

$$\varepsilon = \begin{Bmatrix} \varepsilon_r \\ \varepsilon_\theta \\ \varepsilon_\varphi \end{Bmatrix} = \begin{Bmatrix} \frac{du}{dr} \\ \frac{u}{r} \\ \frac{u}{r} \end{Bmatrix} = [B] \cdot \{U\}, \text{ where } [B] = \begin{bmatrix} -\frac{1}{r_j-r_i} & \frac{1}{r_j-r_i} \\ \frac{N_i(\bar{r})}{\bar{r}} & \frac{N_j(\bar{r})}{\bar{r}} \\ \frac{N_i(\bar{r})}{\bar{r}} & \frac{N_j(\bar{r})}{\bar{r}} \end{bmatrix} \quad (2)$$

$$\{\sigma\} = \begin{Bmatrix} \sigma_r \\ \sigma_\theta \\ \sigma_\varphi \end{Bmatrix} = [D] \cdot (\{\varepsilon\} - \{\varepsilon_T\}) = [D] \cdot ([B] \cdot \{U\} - \{\varepsilon_T\}) \quad (3)$$

Where $\{\varepsilon_T\} = \alpha_T \cdot T \cdot \begin{Bmatrix} 1 \\ 1 \\ 1 \end{Bmatrix}$ - for a centrally symmetric problem, $[D]$ - matrix of elastic constants.

$$[D] = \frac{E(1 - \nu)}{(1 + \nu)(1 - 2\nu)} \begin{bmatrix} 1 & \nu/(1 - \nu) & \nu/(1 - \nu) \\ \nu/(1 - \nu) & 1 & \nu/(1 - \nu) \\ \nu/(1 - \nu) & \nu/(1 - \nu) & 1 \end{bmatrix}. \tag{4}$$

The standard formula for the local stiffness matrix is of the form:

$$[K^{(e)}] = [\bar{B}]^T \cdot [D] \cdot [\bar{B}] \int_{V^{(e)}} dV = [\bar{B}]^T \cdot [D] \cdot [\bar{B}] \cdot \frac{4}{3} \pi (r_j^3 - r_i^3). \tag{5}$$

The contribution of temperature deformations to the load vector will be determined by expression:

$$\{P\}_T^{(e)} = \int_{V^{(e)}} [\bar{B}]^T [D] \{\varepsilon_T\} dV = [\bar{B}]^T [D] \{\varepsilon_T\} \cdot \frac{4}{3} \pi (r_j^3 - r_i^3). \tag{6}$$

For the numerical solution of the optimization problem, the solution has been implemented using Matlab software package. To verify it, the initial data and temperature distribution were taken to be the same as in [6, 14].

To determine the elastic modulus distribution law, in which the structure will be uniformly stressed, the method of successive approximations was used. The essence of it is as follows:

At the first stage, we calculate a homogeneous structure ($E = \text{const.}$) and calculate the maximum equivalent stresses at each point.

At the second stage, the modulus of elasticity at each point is inversely proportional to the stresses:

$$E^*(r) = E(r) \cdot \frac{\sigma_0}{\sigma_{calc}(r)},$$

where $\sigma_{calc}(r)$ - The calculated stress for any theory of strength at a given point, σ_0 - calculated stress at $r = a$.

The process is repeated until the elastic modulus at the outer surface $E(b)$ in the previous and subsequent approximation differs by more than 1%. The stresses in each approximation can be determined by the method of finite differences, If the modulus of elasticity is a continuous function of the radius and the finite element method, if function $E(r)$ piecewise continuous.

But in addition to a number of advantages, the numerical algorithm has one essential drawback. Equivalent stresses at each point in each approximation must be of the same sign, otherwise there is a point at which $\sigma_{eq} = 0$ and the corrected modulus of elasticity $E^*(r)$ at this point it tends to infinity.

3 Results

To verify the correctness of the algorithm, calculations were performed for the third theory of strength at the following values: $p_a = 0$, $p_b = 100$ MPa, $a = 1$ m, $b = 2$ m, $T_a = 100$ °C, $\alpha_T = 10^{-5}$ 1/°C. At Fig. 2 curves of equivalent stresses are shown σ_{eq} . The solid line shows the solution for an inhomogeneous cylinder, the dashed line for a homogeneous cylinder.

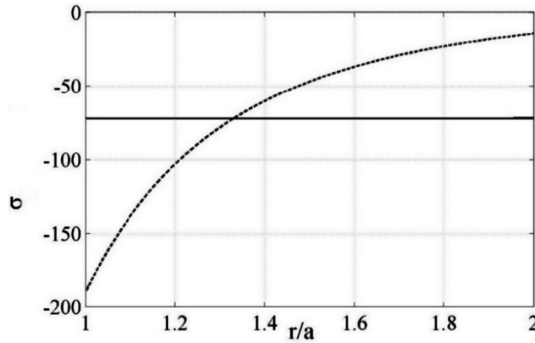


Fig. 2. Graphs of variation of equivalent stresses.

The results completely coincide with the decision of Academician Andreev and Bulushev [6]. To achieve the specified accuracy, 9 approximations were required. The maximum design stresses for a non-uniform cylinder were $\sigma_{max}^{eq} = -72.08$ MPa (in [6] $\sigma_{max}^{eq} = 2\tau_{max} - 72.14$ MPa), and for homogeneous cylinder $\sigma_{max}^{eq} = -189.18$ MPa (in [6] $\sigma_{max}^{eq} = 2\tau_{max} - 180$ MPa).

Bearing capacity for a non-uniform sphere has increased in 2.62 times in comparison with homogeneous at the same thickness. But, as mentioned earlier, this sphere is only equally strained. The algorithm presented in this article makes it possible to construct an equivalent-shell model.

Consider the solution of the problem of optimizing a thick-walled sphere in a temperature field, based on another criterion – Theory of strength of Balandin [15, 16].

In the case when an external pressure acts on the sphere, the main stresses are determined as follows: $\sigma_1 = \sigma_r$, $\sigma_2 = \sigma_3 = \sigma_\theta = \sigma_\varphi$.

Equivalent stress in this case takes the form:

$$\sigma_{eq} = \frac{(\sigma_r - \sigma_\theta)^2}{\sigma_r + 2\sigma_\theta}$$

For the calculation, the following initial data were taken: $p_a = 0$, $p_b = 100$ MPa, $a = 1$ m, $b = 1.2$ m, $T_a = 100$ °C, $\alpha_T = 10^{-5}$ 1/°C, $T_b = 0$ °C, $\nu = 0.2$.

The temperature distribution was determined by the formula (6) from [6]. The dependence of the strength on the modulus of elasticity in solving the problem for an

equiresistant sphere was assumed to be the same as in the previous problem. Figures 3 and 4 show respectively the plots of the modulus of elasticity and equivalent stresses by the criterion of the strength of Balandin for a homogeneous (black dashed line), non-uniform, equally strong (solid blue line), and an inhomogeneous uniformly stressed sphere (solid red line). The ratio of equivalent stresses to the design resistance $\frac{\sigma_{eq}}{R}$ for equiresistant sphere was 0.77. For a homogeneous sphere with $E = 3.1 \cdot 10^4$ MPa the maximum value of this ratio is 1.34.

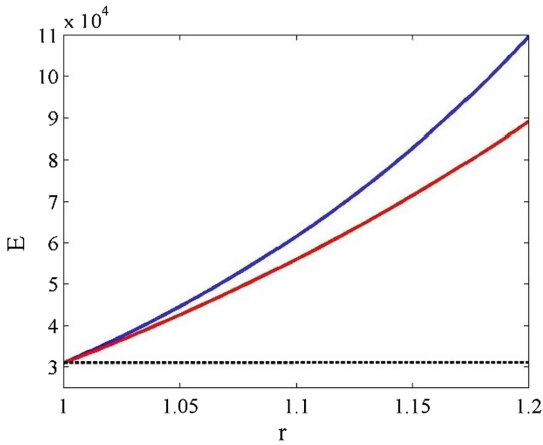


Fig. 3. Graphs of the modulus of elasticity.

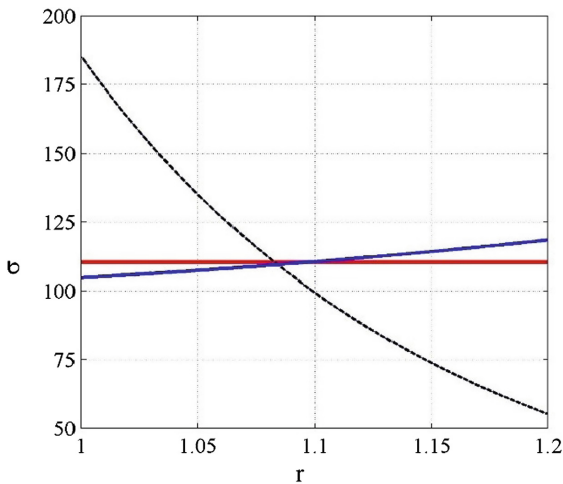


Fig. 4. Graphs of the modulus of elasticity.

Thus, the carrying capacity of the sphere in creating heterogeneity increased 1.74 times.

At Figs. 5, 6 and 7 graphs of stress changes σ_r and σ_θ respectively, for a homogeneous, equally stressed and equiresistant sphere. The black line shows the stresses σ_r , and purple - σ_θ .

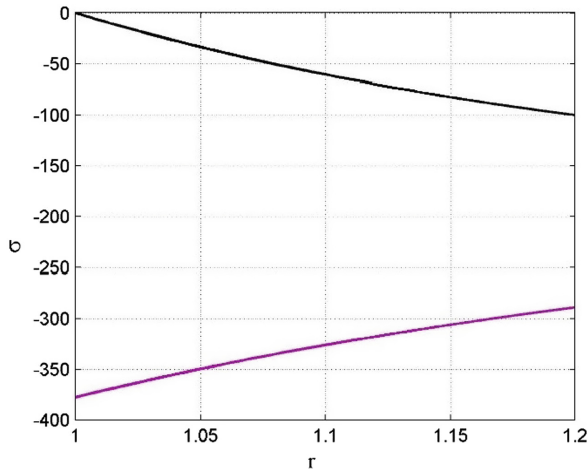


Fig. 5. Stress variation σ_r (black line) and σ_θ (purple line) for a homogeneous sphere.

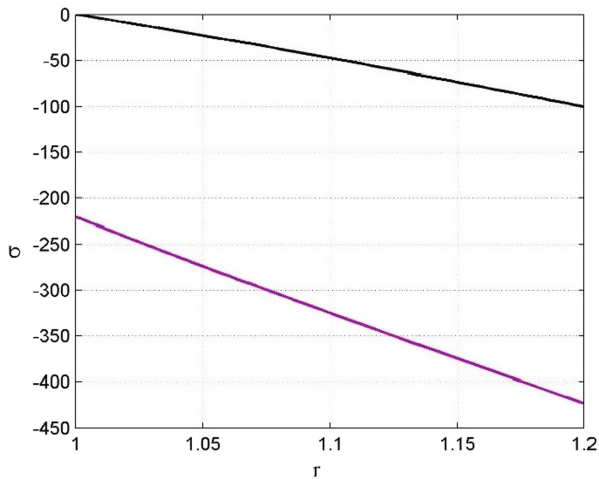


Fig. 6. Stress variation σ_r and σ_θ for an equally stressed sphere.

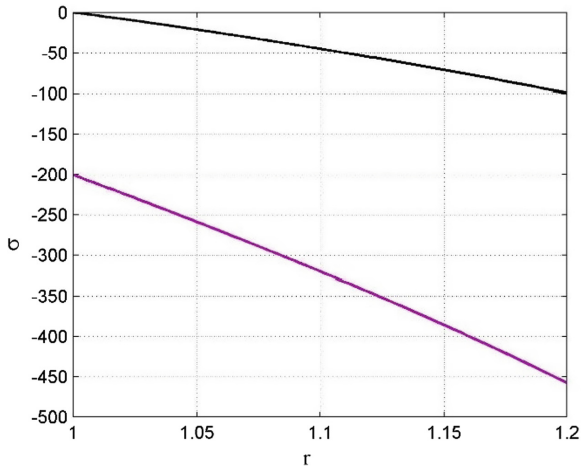


Fig. 7. Stress variation σ_r and σ_θ for equiresistant sphere.

4 Conclusions

A numerical algorithm for constructing equal strength and equal stress models is developed and compiled a program for a computer, suitable for any strength criteria. The problem is solved for equally strong thick-walled shells on the basis of the Balandins strength criteria. With the same shell thickness, and the same load value, the results based on different criteria are significantly different. Thus, in the solution of optimization problems, the correct choice of the theory of strength is very important.





By comparing the results with the solutions of other authors, it is shown that the proposed algorithm can work for problems with a temperature effect. The advantage of the numerical method is the possibility of applying it under any laws of temperature distribution in the thickness and also arbitrary theories of strength. The problem is solved for the first time for an equally strong sphere located in a temperature field on the basis of the Balandins P.P. theory.

References

1. Andreev, V.: Adv. Mater. Res. 869–872 (2014)
2. Yazyev, B.: Nonlinear creep of continuously inhomogeneous cylinders. DrSc thesis (1990)
3. Yazyev, B.: Vestnik MGSU **5**, 56–61 (2013)
4. Chechevichkin, V.N., Vatin, N.I.: Mag. Civil Eng. **50**(6), 67–74 (2014). <https://doi.org/10.5862/MCE.50.7>
5. Andreev, V.: Some problems and methods of mechanics of heterogeneous solids: monograph. Publishing House ASV (2002)
6. Andreev, V., Bulushev, S.: Vestnik MGSU **12**, 40–46 (2012)
7. Andreev, V., Potekhin, I.: Collection of works Voronezh State University of Architecture and Civil Engineering, pp. 84–90 (2007)

8. Andreev, V., Potekhin, I.: *Bull. Build. Sci.* **11**, 48–52 (2007)
9. Potekhin, I.: *Collect. Works* **2**, 72–74 (2009)
10. Potekhin, I.: The method of optimizing designs on the basis of solving inverse problems in the theory of elasticity of inhomogeneous bodies. DrSc thesis (2009)
11. Yazyev, B.: *Vestnik MGSU* **12**, 56–61 (2012)
12. Yazyev, B., Chepurmenko, A.: *Nauchnoe obozrenie*, pp. 202–204 (2014)
13. Arseniev, D.G., Rechinskiy, A.V., Shvetsov, K.V., Vatin, N.I., Gamayunova, O.S.: *Appl. Mech. Mater.* **635–637**, 2076–2080 (2014). <https://doi.org/10.4028/www.scientific.net/AMM.635-637.2076>
14. Litvinov, S.: *Vestnik MGSU* **1**, 128–132 (2010)
15. Andreev, V., Potekhin, I.: *Vestnik MGSU* **86** (2011)
16. Andreev, V., Potekhin, I.: *Works of XVI Slovakia-Russia-Poland seminar Theory of the Bases of Construction*, pp. 29–34 (2007)

Forecasting the Strength of an Adhesive Bond Over a Long Period of Time

Stepan Litvinov¹ , Alexander Zhuravlev¹ ,
Salis Bajramukov² , and Serdar Yazyev¹ 

¹ Don State Technical University, Rostov-on-Don,
Socialisticheskaya str., 162, 344022 Rostov-on-Don, Russia
litvstep@gmail.com

² North-Caucasus State Humanitarian-Technological Academy,
Stavropol str., 36, 369001 Cherkessk, Russia

Abstract. We consider the problem of the adhesion compound of calculation by finite element method in axisymmetric along two axes: the axial z and radial r . To improve the accuracy of the solution to the problem posed, a number of optimizations are introduced: obtaining an exact solution of the stiffness matrix and the load vector for a given interpolation polynomial, using a nonconstant approximating time interval, thickening of the finite element grid to the edges of a cylindrical body, etc. At the end, predicting the strength of the adhesive compound in question. At the end, an analysis of the result obtained and a prediction of the strength of the adhesive compound under consideration are given.

Keywords: Strength · Adhesive bond · Time

1 Introduction

The question of the calculation of the adhesion compound has been considered by many scientists, among them Professor Turusov [1–8] and Professor Yazyev [5, 6, 9]. To calculate the adhesion compound, the authors used the boundary-layer method, based on two hypotheses:

In the adhesion state, the polymer is a thin layer and, therefore, the properties of the measured samples of the thin polymer films are assumed to be adequate for the properties of the polymer from the adhesive compound.

A possible difference in the properties of the polymer in the composition of an adhesive compound is the chemical and/or physical interaction of the polymer with the substrate.

The calculation by the boundary layer method leads to a homogeneous differential equation of the second order with respect to tangential stresses (not given in this article) arising between the adhesive and the substrate in the boundary layer [1, 2, 7].

However, this approach is weakly applicable to the solution in modern computational complexes oriented to be used in modern numerical methods, and in this connection an attempt was made to calculate the adhesion by the finite element method.

Physic-mechanical properties of the adhesive are highly dependent on temperature. Solution axisymmetric problems with the dependence of the elastic material and the rheological parameters of the temperature is considered in [10–16].

2 Materials and Methods

It is necessary to calculate the strength of the adhesive bonding of epoxy resin of two continuous steel disks under normal separation (Fig. 1). Substrates (steel disks) are stretched along their axes with some constant tension q . In connection with the fact that the problem is symmetric, it is sufficient to consider only one half (Fig. 2).

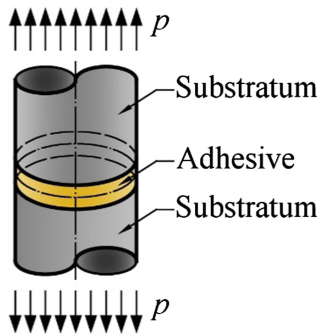


Fig. 1. Statement of the original problem.

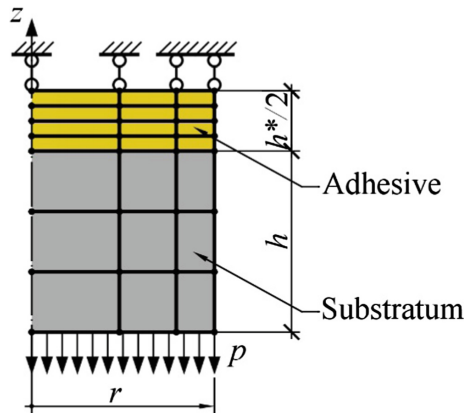


Fig. 2. The calculated scheme by the finite element method of the problem.

Since the tangential stresses between the substate and the adhesive will reach the maximum values with the adhesive in the elements contacting the substrate and located at the outermost face, it is rational to divide the elements along the radius not by a

constant but rather from the cylinder axis to the outer surface of the cylinder. Thus, in the problem under consideration, the element located at the outer surface is 10 times smaller than the element located at the axis of the cylinder.

Under the action of the applied load, creep deformations occur in the adhesive, described by the nonlinear generalized Maxwell-Gurevich equation

$$\frac{\partial(\varepsilon_{ij}^*)_s}{\partial t} = \frac{\frac{3}{2}(\sigma_{ij} - p\delta_{ij}) - E_{\infty S}(\varepsilon_{ij}^*)_s}{\eta_s^*} \quad (i, j = r, \theta, z); \tag{1}$$

$$\delta_{ij} = \begin{cases} 1 & \text{at } i = j \\ 0 & \text{at } i \neq j \end{cases} \quad 3p = \sum_1^3 \sigma_{pp}.$$

Here η_s^* —the coefficient of the initial relaxation viscosity, in the calculations has the form

$$\eta_s^* = \eta_{0S} \exp \left[- \frac{\left| \frac{3}{2}(\sigma_{pp} - p) - E_{\infty S}(\varepsilon_{pp}^*)_s \right|_{\max}}{m_s^*} \right]. \tag{2}$$

In the expressions (1) and (2): σ_{pp} и ε_{pp}^* —accordingly, the stresses and high-elastic deformations in the principal stresses; $E_{\infty S}$ —high-elastic deformation module; η_{0S} —coefficient of initial relaxation viscosity s-th component of the spectrum of high-elastic deformation; m_s^* —a velocity module that reflects the effect of the strain rate on the stress at a given constant deformation.

In this problem, only two time-strain spectrums were considered: first $(\varepsilon_{ij}^*)_I$, senior, predominant on small time intervals and second $(\varepsilon_{ij}^*)_II$, junior, prevailing over long time intervals (generally at a time greater than 100 h). The total deformation of creep at an arbitrary instant of time is the sum of the components:

$$\varepsilon_{ij}^* = (\varepsilon_{ij}^*)_I + (\varepsilon_{ij}^*)_II.$$

To calculate the creep of the polymer, a step-by-step method was used, in which, by using expression (1), the deformation rate at the current time, determined by the strain values at the next time point

$$(\varepsilon_{ij}^*(t+1))_s = (\varepsilon_{ij}^*(t))_s + \frac{\partial(\varepsilon_{ij}^*)_s}{\partial t} \cdot \Delta t,$$

where Δt —the time interval between the two calculation steps.

The “breakdown” of the time during which the calculation took place was applied to the intervals not uniformly, but according to the power law, as well as the breaking of the radius. The ratio of the extreme time interval to the first is, which allows us to use

the interval measured in seconds and minutes at the very beginning of the calculation, and by the end of the calculation - the intervals measured in days. To solve the problem directly, we use the system of equations of the finite element method, obtained by minimizing the potential energy of elastic deformation P and the work of external forces A

$$\frac{\partial P}{\partial \{U\}} = \int_V ([B]^T [D] [B] \{U\} - [B]^T [D] \{\varepsilon_T\} - [B]^T [D] \{\varepsilon^*\}) dV, \quad (3)$$

where $\{\varepsilon_T\}$ and $\{\varepsilon^*\}$ —respectively, the vector of temperature deformations and the vector of high-elastic deformations (creep).

When using the finite element method, expression (3) is usually determined numerically (Fig. 3), replacing the element volume by the approximate formula $V \approx r dr \approx r(R_j - R_i)$.

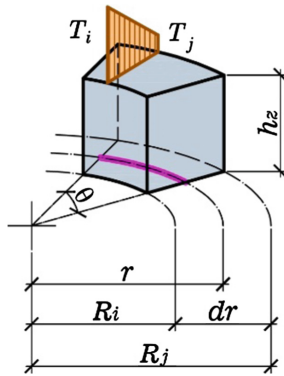


Fig. 3. Approximation of the volume of the finite element.

In determining the initial deformed state of a polymer material, more precision is required over time, and therefore the coefficients of expression (3) were determined analytically by an exactly direct integration for a given interpolation polynomial. Finally, the coefficients of the finite element take the form

$$[K] \cdot \{U\} = \{F\},$$

where $[K] = \sum_{e=1}^E [k^{(e)}]$ —global stiffness matrix; $\{F\} = \sum_{e=1}^E \{f^{(e)}\}$ —global load vector.

Here

$$[k^{(e)}] = \begin{bmatrix} k_{11} & k_{12} & k_{13} & k_{14} & k_{15} & k_{16} & k_{17} & k_{18} \\ & k_{22} & k_{23} & k_{24} & k_{25} & k_{26} & k_{27} & k_{28} \\ & & k_{33} & k_{34} & k_{34} & k_{36} & k_{37} & k_{38} \\ & & & k_{44} & k_{45} & k_{46} & k_{47} & k_{48} \\ & & & & k_{55} & k_{56} & k_{57} & k_{58} \\ & & & & & k_{66} & k_{67} & k_{68} \\ & & & & & & k_{77} & k_{78} \\ & & & & & & & k_{88} \end{bmatrix}; \quad \{f^{(e)}\} = \begin{Bmatrix} f_1 \\ f_2 \\ f_3 \\ f_4 \\ f_5 \\ f_6 \\ f_7 \\ f_8 \end{Bmatrix}.$$

Coefficients of matrices $[k^{(e)}]$ and $\{f^{(e)}\}$ are very cumbersome and are not given in this article.

The initial data of the problem: $r = 12 \text{ mm}$, $h = 1.2 \text{ mm}$, $h^* / 2 = 0.09 \text{ mm}$, $T = 30 \text{ }^\circ\text{C}$. Elastic and rheological parameters of the adhesive have the following temperature dependences:

$$\begin{aligned} E &= -18.2(T + 273) + 8200 \text{ MPa}; \nu = 0.37; \\ E_{\infty,I} &= 2.4 \cdot 10^6 / (T + 273) - 6400 \text{ MPa}; E_{\infty,II} = 0.1E_{\infty,I}; \\ m_I^* &= m_{II}^* = -0.0155(T + 273) + 7.73 \text{ MPa}; \\ \eta_{0,I} &= 10 \exp[9500 / (T + 273) - 20] \text{ MPa} \cdot \text{h}; \\ \eta_{0,II} &= 10 \exp[35400 / (T + 273) - 90] \text{ MPa} \cdot \text{h}. \end{aligned}$$

Figure 4 shows the results of the calculation of the problem.

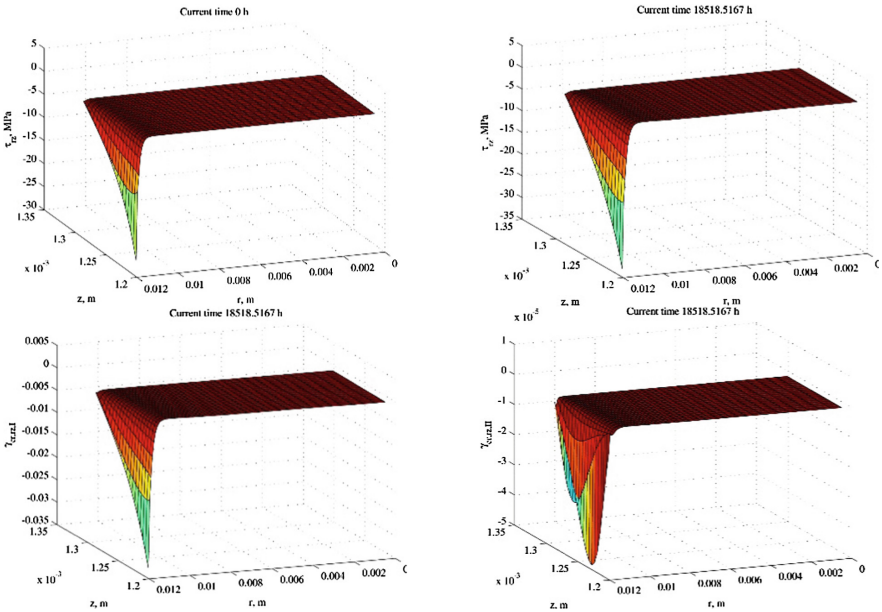


Fig. 4. Changing the shear stresses over time.

3 Results

Comparing the obtained graphs of tangential stresses growth (Fig. 2a, b) with the graphs obtained by Professor R.A. Turusov in [1, 2] one can find a number of similarities and differences: At the first calculation step, when there are no high-elastic deformations, the maximum stresses coincide and make up $\tau_{rz} = 26.5770$ MPa at $t = 0$ h. The maximum stresses at all time steps obtained with the help of the FEM are $\tau_{rz} = 33.9366$ MPa at $t = 100.5705$ h. Which also agrees with the decision received by Professor R.A. Turusov. However, with a further increase in time, the nature of the change in stress is different: at the time $t = 1.9518 \cdot 10^4$ h. The graph obtained by Professor R.A. Turusov reaches the value of $\tau_{rz} = 50$ MPa. The result of the solution with the help of the FEM gives the value $\tau_{rz} = 33.1713$ MPa. Thus, some relaxation of stresses is observed, which agrees better with the standard solutions of axisymmetric problems obtained by Professor B.M. Yazyev. At the same time it is observed (Fig. 2b, c) and some growth of high-elastic deformations of the second, minor, spectrum.

In addition, modeling with FEM makes it possible to take into account the joint work of the substrate and adhesive as much as possible, which makes it impossible to make the boundary layer method.






4 Conclusions

To evaluate the strength of adhesion compounds lasting up to several months, finite element analysis can be used, which in this case gives good agreement with specialized methods designed specifically for these tasks.

References

1. Turusov, R., Manevich, L.: Glues. Sealants. Technol. **5**, 2–8 (2009)
2. Turusov, R., Manevich, L.: Glues. Sealants. Technol. **6**, 2–11 (2009)
3. Turusov, R., Manevich, L.: Polymer Sci. Ser. D **4**(2), 209–213 (2009)
4. Turusov, R., Manevich, L.: Glues. Sealants. Technol. **1**, 6–17 (2009)
5. Turusov, R.: Glues. Sealants Technol. **7**, 14 (2011)
6. Turusov, R.: Glues. Sealants. Technol. **7**, 17–25 (2011)
7. Turusov, R., Berlin, A.: From the collection: adhesive materials a collection of reports of the scientific and technical conference 2 (2016)
8. Turusov, R., Berlin, A.: Mater. Sci. News. Sci. Technol. **2**(20), 2 (2016)
9. Yazyev, B.: Features of the relaxation properties of mesh and linear polymers and composites based on them. DrSc thesis (2009)
10. Yazyev, B.: Polymers, Polymer Blends, Polymer Composites and Filled Polymers: Synthesis. Properties and Applications, pp. 155–158. Nova Publishers, Hauppauge (2006)
11. Yazyev, B.: Surv. Appl. Ind. Math. **2**(15), 380–381 (2008)
12. Yazyev, B.: Some problems and methods of mechanics of a macro-inhomogeneous viscoelastic environment. RSBU, Rostov-on-Don (2009)
13. Yazyev, B., Yazyev, S.: Mater. Sci. **2**, 10–13 (2009)
14. Dudnik, A.: Plast. Masses **1–2**, 30–33 (2016)
15. Litvinov, S.: Inženernyj vestnik Dona **2**(41), 29 (2016)
16. Litvinov, S.: Procedia Eng. **150**, 1686–1693 (2016)

MSW Landfills Reclamation Based on Monitoring of Biogas Emissions

Vladimir Maslikov¹ , Alexander Chusov¹  ,
Viacheslav Zhazhkov¹ , and Olga Vasilyeva² 

¹ Peter the Great St. Petersburg Polytechnic University, Polytechnicheskaya str.,
29, 195251 St. Petersburg, Russia
chusov17@mail.ru

² National Research Moscow State University of Civil Engineering,
Yaroslavskoe sh., 26, 129337 Moscow, Russia

Abstract. In the paper the problem of reclamation of solid waste landfills is considered. The way of reclamation is defined by a condition of the ground and its sites. Data on emission of biogas and its component structure can give information on this process. Results of actual-service tests are given in a number of the Russian solid waste landfills. The essential zonal distribution of methane emissions from waste landfill body reflecting processes of decomposition of the buried waste is revealed. Experience of waste management biodegradation are analyzed and on the example of the operating ground options of reclamation the sites with a possibility of an intensification the biochemical processes are considered.

Keywords: Landfills · Biogas emissions · Reclamation

1 Introduction

The problem of neutralization and utilization of the municipal solid waste (MSW) in Russia continues to remain rather sharp. Annually formed about 50 million t. In Russian Federation more than 90% are buried on landfills and dumps, the condition most of which doesn't answer with the requirement of environmental protection [1, 2]. Considerable scales of necessary works operation and their high cost defines relevance of a problem the development of solid waste landfills reclamation effective technologies. For example, if waste have completely decayed and represents inert weight, rather cheap way – creation of a superficial soil covering of a body of the ground can be used. In case the landfill is in the active phase operation which is followed by considerable emission of biogas with the high content of methane (about 50% and more), then the creation of collecting biogas system is expedient. Wherein its ecological safety is ensured, and also the possibility of obtaining the additional income at power use of biogas for needs of local energetics appears, etc. Such system represents an expensive engineering construction, includes the top and lower multilayered isolating coverings; gas wells; drainage and collector networks for collecting and removal of biogas and a filtrate; clearing equipment, power station [3], etc. Thus the type of reclamation will be defined in many respects by intensity and structure of the gas issues characterizing

processes of waste decomposition on concrete sites and their state for the settlement period of time [4–7].

2 Experimental Studies

Efficiency of solid waste landfill energy potential use will be defined in many respects by reliable estimates of biogas emission, that represents a complex scientific and technical challenge. Different volumes and morphological structure of waste, time and some ways of their burial, climatic conditions, temperature condition, etc. cause variability of structure, patchiness of gas distribution issues to landfill body surfaces, seasonal and annual fluctuations of biogas emissions. This complicates the creation of the universal mathematical models which are adequately reflecting specifics functioning of concrete landfills. Application of the known mathematical models considering limited quantity of factors leads to big errors in determination of biogas potential. As a result, real energy output of expensive systems of collecting and use of biogas is much lower than forecasted, economic indicators worsen [8]. There is a need for development and approbation of the methods of an assessment and the forecast of biogas emission from the landfills allowing to obtain with use of rather inexpensive equipment reliable data about their energy potential. It demands the organization of carrying out actual-service tests and laboratory researches for obtaining necessary information on biogas composition, the size of the current issue, dynamics of change in situ and volumes. At the first stage the gas-geochemical shooting of a waste landfill body allowing to define composition of biogas and to allocate sites of the landfill with high content methane components [9] is carried out. In Fig. 1 presents distribution of methane and carbon dioxide waste landfill body the northern region of Russia [10].

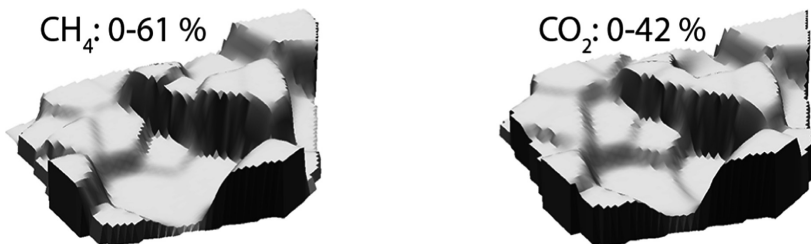


Fig. 1. Three-dimensional (3D) maps of methane and carbon dioxide content at a depth of 50 cm in the surface layer of the MSW landfill.

Zonal distribution of biogas component composition on landfill body surface has been revealed. It is established that there are extensive sites of the landfill where the content of methane a blanket of waste makes 50–60% about.

The following stage of researches – determination the specific volumes of biogas emission on these sites. The following methods can be for this purpose used: “analytical”, “borehole”, “by means of boxing gas trap”, etc. [11].

Is possible to recommend to make an assessment of intensity the biogas emission on the studied sites with use of a gas trap in the form of the flux box for conditions for Russian landfills.

It should be noted that actual-service researches allow to define issue for the current time, but don't allow to predict it on the near-term outlook therefore the following stage is laboratory experiment in which the studied waste is placed in the bioreactor, where is created anaerobic and temperature moisture conditions, corresponding to landfill conditions.

Creating optimum conditions in bioreactors, it is possible to accelerate decomposition of waste in tens and more time, and for several months of operation the laboratory installation to obtain information on the processes happening under natural conditions within many decades. Laboratory data can be used at the choice of mathematical models and specifications of their parameters for the concrete landfill for the purpose of the forecast for resource biogas dynamics [12].

As it has been noted, the type of reclamation will be defined by a condition of the landfills and its sites in many respects depends on a possibility of biogas potential usage.

As an example we will consider one of large solid waste landfills located in the territory of St. Petersburg, assumed to closing due to an exhaustion of specified volume. The landfill is operated since the beginning of the 70th of the last century and is one of the largest in the northwest region of the country.

On the landfill there are sites with various terms of operation (operating sites; the relatively recently closed sites; the long time ago closed landfill sites) differing in quantity of the buried waste, morphological structure, intensity of biodegradation processes, degree of landfill masses mineralization, etc., and, therefore, the level and nature of impact on environment [13]. Recently the quantity of hazard components as a part of MSW increases that exerts impact on biochemical processes and structure of gas and water issues [14].

Clear need for the differentiated approach at the choice of the reclamation technologies on the landfill providing reliable environment protection taking into account conditions of concrete sites is obvious.

3 Results and Discussion

Field investigations were performed by the authors on a number of Russian landfills showed significant zonality of biogas emissions. Biodegradation processes are in the active phase in operated sites, also there will be intensive biogas emissions, containing up to about 50–60% methane by volume, for a relatively long period (over 10 years) after landfills closing. It is advisable to create a biogas collection and utilization system on such sites. A significant reduction of biogas emissions will be in the following period (about 25 years), which makes it impractical to use energy potential. At the same time there will be permanent air pollution, risk of fire, as well as the possible migration of biogas in the thick soil of lands located in the vicinity of landfills.

The residual emission of biogas with methane low concentration (less than 15 vol.%) will be observed on the long time ago closed landfill sites for an extended period so far the

waste biodegradation processes won't stop. Obviously, it's necessary to accelerate mineralization of waste in such sites.

A relatively small emission of biogas with a high methane concentration (less than 30 vol.%) is observed on the relatively recently closed sites, which makes them unpromising for biogas usage. It is reasonable to create passive degassing system on these areas for removing the biogas.

The task of zonal management of waste decomposition processes in the landfill arises for better use of biogas potential from sites with active emissions, as well as for conversion as soon as possible sites with residual biogas emissions to environmentally safe inert state. The intensification of waste decomposition processes payed much attention in the developed countries, because the main task is to reuse large areas of expensive lands (in urban areas), that previously were allocated for waste disposal [15, 16].

The intensification of the processes of municipal solid waste decomposition in landfills is carried out by aeration of landfill body in sites with residual gas emission [17–20] and by irrigation of waste with water or treated leachate in sites with active biogas emissions [21–28].

In the case of waste aeration (Fig. 2(1)) the acceleration of the decomposition processes (of organic carbon) is increased by 6–8 times, methane emissions practically decrease as a result of its oxidation, drastically reduced the content of organic substances in the leachate. The duration of landfill aeration polygon defined by residual content of organic carbon and can proceed for several years. Disadvantages of the aeration technology are the high costs associated with air entering the landfill body, as well as removing and cleaning landfill gas with high carbon dioxide content, also the energy potential of the waste is not used.

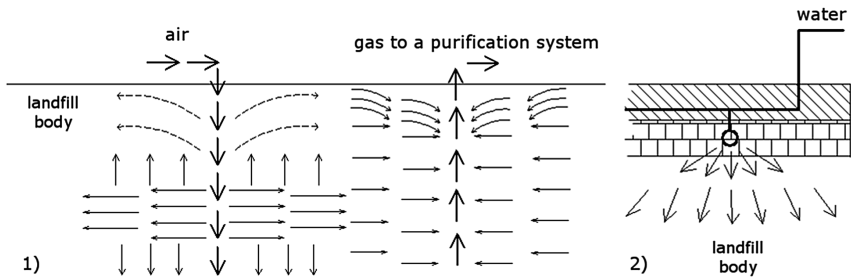


Fig. 2. 1- The scheme of landfill aeration. 2- The irrigation system of wastes [17–25].

Waste decomposition process is accelerated (time of waste decomposition with 80–100 years could be reduced to 10–15 years) by supply of water or treated leachate in the landfill body (Fig. 2(2)). In this case, the bulk of biogas is formed in a short time, which increases the efficiency of its use [22].

To determine the required amount of air for aeration of the sites with a residual emission of biogas is reasonable to use the research results presented in [17], which showed that the decomposition of residual organic matter in the 25–30-year-old landfill

deposits require from 10 to 25 mgO₂/g (of waste). Aeration of the sites is continued usually about nearly one year.

It's necessary to create an insulated coating, preventing biogas leakage to the atmosphere on sites where it is supposed to collecting it. But in this case atmosphere precipitations practically stop penetrate into landfill body, the moisture content of the waste will decrease rapidly as it is used in the process of biodegradation, and hence this will reduce the biogas emission. When the moisture content of the waste in the range of 30–50% its increase of 1% will increase the biogas emission by about 3.5%. Therefore, it's necessary to ensure irrigation with treated leachate followed by the withdrawal of contaminated water to maintain optimal humidity of waste [18].

It's recommended to feed water in an amount not less than 0.15–0.2 l/m³ waste per day, which corresponds approximately to the natural flow of water from rainfall. This volume should be increased in about three times to accelerate the decomposition of waste.

The cumulative forecasting graphs of biogas emission from operated landfill sites for natural and managed modes are presented in the Fig. 3.

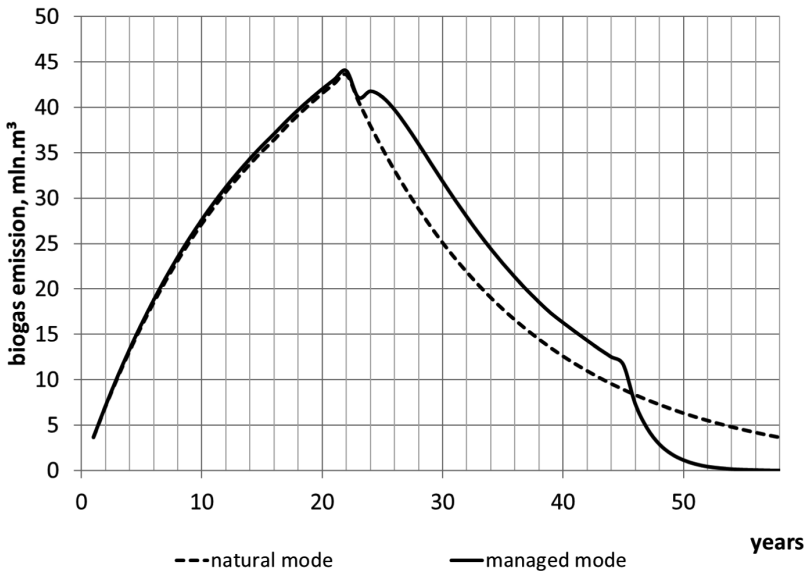


Fig. 3. Biogas emission from the landfill (theoretical potential).

The average annual biogas emission will be increased by 20–25% in the case of the managed mode (with irrigation of waste) in the first ~20 years after the landfill closing, which allows more intensive use of the biogas potential. After that, the emission of biogas will practically stop and the sites will be transferred to the aeration mode for a short period and after that they can be used for economic needs.

The energy use of biogas will not only meet the needs of a landfill, but also to get additional income from the supply the excess of electricity for the local consumers

needs. It is also possible to obtain additional income from the sale of quotas for greenhouse gas emissions reductions that will offset some of the costs of the reclamation of the landfill.

4 Conclusion

The consideration of biogas emissions zonality allows to create a rational scheme of using landfill sites, as well as to substantiate a possible managed mode of waste decomposition with the aim of taking full advantage of the landfill biogas potential and of reducing the impact on the environment.





The implementing of managed mode on a landfill allows to put into circulation its considerable areas for the economic use. It is reasonable for the period of works on the degassing to use landfill sites for industrial purposes (growing seedlings for urban landscape management, placement of warehouses, parking facilities, developing industrial zones, etc.). The recreational use of the territory is also possibly after the completion of the degassing.

References

1. On the state and Environmental Protection of the Russian Federation in 2013 (2017). <https://www.mnr.gov.ru/upload/iblock/6c7/gosdokladeco.pdf>
2. Wastes in Russia: Rubbish or a valuable resource? Development scenarios for the sector of municipal solid waste (2017). <http://tpprf.ru/download.php?GET=6LPAY%2F81BmxXbFDr7vGx5g%3D%3D>
3. Recommendations for design, construction and reclamation of MSW landfills. Academy of Municipal Economy named after K.D. Pamfilova, Moscow (2009)
4. Fedorov, M., Korablev, V., Maslikov, V., Ioksha, E.: *Ecol. Life* **4**(77), 16–22 (2008)
5. Fedorov, M., Zinchenko, A., Korablev, V., Maslikov, V., Chusov, A., Ioksha, E.: *St. Petersburg State Polytech. Univ. J.* **6**(70), 135–142 (2008)
6. Vaysman, Ya., Korotaev, V., Petrov, V.: *Waste Management. MSW Landfills: Study Guide.* Perm State Technical University Publishing House (2007)
7. Vasilov, R., Ovchinnikov, Y.: *Biotechnol. Phys. Chem. Biol. Bull.* **3**(3), 54–61 (2007)
8. Neumann, H.: *Top Agrar* **10**, 103–105 (2007)
9. Chusov, A., Maslikov, V., Molodtsov, D.: *Saf. Technosphere* **6**, 24–28 (2013)
10. Chusov, A., Maslikov, V., Molodtsov, D., Zhazhkov, V., Riabuokhin, O.: *Mag. Civil Eng.* **6**, 44–55 (2015)
11. Di Trapani, D., Di Bella, G., Viviani, G.: *Waste Manag.* **33**(10), 2108–2115 (2013)
12. Maslikov, V., Chusov, A., Negulyaeva, E., Cheremisin, A., Molodtsov, D.: *St. Petersburg State Polytech. Uni. J.* **2–2**(147), 229–235 (2012)
13. Maslikov, V., Chusov, A., Molodtsov, D., Ryzhakova, M.: *St. Petersburg State Polytech. Uni. J.* **2–1**(147), 260–265 (2012)
14. Ryzhakova, M., Maslikov, V., Chusov, A., Korablev, V.: *Appl. Mech. Mater.* **675–677**, 761–769 (2014)
15. Tolaymat, T., Green, R., Hater, G., Barlaz, M., Black, P., Bronson, D., Powell, J.: *J. Air Waste Manag. Assoc.* **60**(1), 91–97 (2010)
16. Alam, P., Alam, M.: *Int. J. Appl. Sci. Eng. Res.* **3**(1), 187–193 (2014)

17. Rettenberger, G.: Stabilisierung einer Altlast durch Einblasen von Luft am Beispiel der Altablagerung Lorenkamp (2017). http://www.ruk-online.com/Service/Downloads/LORE_GAS.pdf
18. Rettenberger, G.: Brandenburgische Umwelt-Berichte **6**, 127–148 (2000)
19. Ritzkowski, M., Stegmann, R.: Waste Manag. **32**(7), 1411–1419 (2012)
20. Cossu, R., Raga, R., Cannas, M., Demontis, S., Fraghi, A., Zanella, M.: Crete Proceedings (2008)
21. Hupe, K., Heyer, K., Stegmann, R.: Deponietechnik, vol. 18, pp. 237–264. Verlag Abfall aktuell, Stuttgart (2002)
22. Henken-Mellies, U., Schwab, P.: Nürnberger Deponieseminar **19**, 117–128 (2008)
23. Beaven, R., Knox, K., Powrie, W.: A technical assessment of leachate recirculation. Report: SC030144/R6. Environment Agency (2009)
24. Rastogi, M., Hooda, R., Nandal, M.: Int. J. Plant Anim. Environ. Sci. **4**(4), 110–117 (2014)
25. Hossain, S., Kemler, V., Dugger, D., Manzur, S., Penmethsa, K.: Sustain. Environ. Res. **21** (4), 253–258 (2011)
26. Adamtsevich, A., Pustovgar, A., Pashkevich, S., Eremin, A., Zhuravlev, A.: Evaluation the strength of cement systems, modified by accelerators. In: Applied Mechanics and Materials, vol. 670–671, pp. 339–343 (2014). <https://doi.org/10.4028/www.scientific.net/AMM.670-671.339>
27. Pashkevich, S., Pustovgar, A., Eremin, A., Adamtsevich, A., Nefedov, S.: PEG molecular weight effects on physical and mechanical properties of ETICS plaster, hardening at lowered positive and small negative temperatures. In: Advanced Materials Research, vol. 1004–1005, pp. 1482–1485 (2014). <https://doi.org/10.4028/www.scientific.net/AMR.1004-1005.1482>
28. Adamtsevich, A., Eremin, A., Pustovgar, A., Pashkevich, S., Nefedov, S.: Research on the effect of prehydration of Portland cement stored in normal conditions. In: Applied Mechanics and Materials, vol. 670–671, pp. 376–381 (2014). <https://doi.org/10.4028/www.scientific.net/AMM.670-671.376>

Mathematical Simulation of Flood Management by Hydro Systems with Temporarily Flooded Reservoirs

Roman Davydov¹ , Valery Antonov¹ , Dmitry Molodtsov¹ ,
and Anatoliy Trebukhin² 

¹ Peter the Great St. Petersburg Polytechnic University,
Polytechnicheskaya str., 29, 195251 St. Petersburg, Russia

² Moscow State University of Civil Engineering,
Yaroslavskoe shosse, 26, Moscow 129337, Russia
licence05@list.ru

Abstract. The mathematical model for calculating the parameters of a hydro system to control flood waterflows is proposed. This model is implemented in the mathematical software Octave and allows to specify the parameters of several types of anti-flood hydro systems, considering the design of the hydro system and data from the GIS systems, and can be used to calculate the maximum flow rates for specific rivers, as well as for joint management of floods in the river basin with the river water reservoirs of the hydroelectric power station.

Keywords: Simulation · Management · Hydro systems · Flood · Reservoirs

1 Introduction

Nowadays, in many countries one of the main problem is the protection against floods, which has always been considered a significant natural hazard in terms of economic losses. The observed climate change has led in various regions of the world to a sharp increase in the frequency of major floods, which are accompanied by significant economic damage and many casualties. About one fifth of European cities (with a population of more than 100 thousand in each) is vulnerable to sudden floods caused by extreme precipitation [1–4].

Protection of the territory from floods is currently carried out by both engineering and other (economic and administrative, etc.) methods [5], which are focused on the current situation and do not consider its development in the future - urbanization, climate change and land use patterns, etc. [6, 7]. As a result, these costly methods are ineffective.

In view of these circumstances, the concept of flood control is changing - from local protection methods in a particular place to managing the risk of flooding the entire river basin [8–10].

The problem of floods also exists in Russia, and due to climatic changes, it is expected to grow [11]. Considering the size of economic losses, the problem of floods is most acute in the Far Eastern region. For example, the flood of 2013, which

happened because of intensive rains lasting about two months, flooded the vast territories of the Far East and Northeast China [12]. An effective method to combat floods is the regulation of floodwater in the hydro systems. In Russia, as in other countries, a common and effective way of dealing with the flood is to regulate the maximum waterflow of complex hydro systems with large flood-control capacity [13]. Constructed on the main river, they protect the land located downstream. In addition, hydro systems with temporarily flooded reservoir are placed on the lateral tributaries. To increase the protected zone in the river basin, it is advisable to place anti-flood hydro systems on the lateral tributaries, which are very helpful in case of increasing river water content under climate changes [14–21].

2 Materials and Methods

The most reliable and safe in operation flood control hydro systems are hydro systems with uncontrolled bottom culverts and uncontrolled surface spillways. The construction of such a system is presented in Fig. 1.

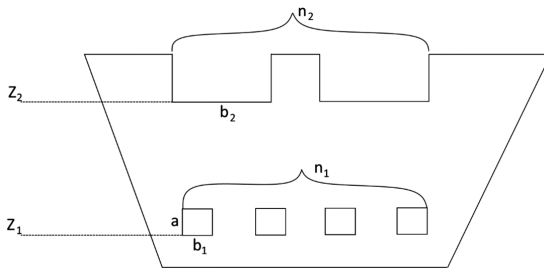


Fig. 1. Scheme for locating culverts in a flood control hydro system.

For the computer simulation of the operation of a flood control hydro system with temporarily flooded reservoir, a mathematical model is proposed, considering various design and operating modes for system:

Calculation of the volume of flood waters accumulating in the reservoir at time t is made by the balance method

$$V_{stor}(t) = V_{stor}(t - \Delta t) + (Q_{in}(t) - Q_{reg}(t) - Q_{evap}(t) - Q_{filt}(t))\Delta t, \quad (1)$$

where:

- $Q_{in}(t)$ – waterflow, which comes into the reservoir;
- $Q_{evap}(t)$ – losses of water by evaporation from the surface of the reservoir;
- $Q_{reg}(t)$ – waterflow in the downstream;
- $Q_{filt}(t)$ – waterflow for filtration purposes;
- t – current time.

The time step Δt can be set manually based on the initial waterflow data.

The following requirements are imposed on flood management at the lateral tributaries:

- maintenance of waterflows in the downstream as part of environmental protection requirements:

$$Q_{reg}(t) \geq Q_{env} \tag{2}$$

where Q_{env} – waterflow in the river, providing its environmental flood-floodplain regime.

- not to exceed the maximum permissible waterflow in the upstream for the purpose of minimizing land flooding to preserve the natural environment:

$$Z(t) \leq Z_{max} \tag{3}$$

where $Z(t)$ – water level in the reservoir.

The waterflow in the downstream is calculated depending on the mode of operation of the system:

- in unflooded mode, the hydro system provides free, near-natural flow of water through the bottom openings. To calculate the waterflow a formula for a spillway with a wide threshold is used (support from the downstream is not considered) [15]:

$$Q_{reg}(t) = n_1 m b_1 \varepsilon \sqrt{2g(Z(t) - Z_1)^{3/2}} \tag{4}$$

where m – coefficient of flow, b_1 – width of bottom culverts, ε – coefficient of lateral compression, Z_1 – bottom mark of bottom culverts, n_1 – number of bottom culverts.

- in flood period bottom culverts operates as flooded holes with variable pressure. Considering the possibility of clogging them (partially or completely), additional surface spillways are provided. When $Z(t) \leq Z_2$, where Z_2 – bottom mark of surface spillways, waterflow in the downstream is calculated according to the following formula [16]:

$$Q_{reg}(t) = n_1 \mu \omega \sqrt{2g(Z(t) - Z_1 - a/2)} \tag{5}$$

where μ – coefficient of flow for bottom culvert, ω – cross-sectional area of bottom culvert, a – height of bottom culvert. When $Z(t) > Z_2$, waterflow in the downstream is calculated as:

$$Q_{reg}(t) = n_1 \mu \omega \sqrt{2g(Z(t) - Z_1 - a/2)} + n_2 m b_2 \varepsilon \sqrt{2g(Z(t) - Z_2)^{3/2}} \tag{6}$$

when n_2 – number of surface spillways, b_2 – width of surface spillways.

The dependence $Z(V)$ is given in tabular form, therefore for computer calculations the method of approximation is needed. Since this dependence is a monotone or piecewise monotone function, interpolation by piecewise cubic Hermite polynomials can be used to obtain a smooth continuous function $Z(V)$ [17].

The proposed model is implemented in the mathematical package Octave [18]. It is possible to specify the design of the hydro system and use various initial data.

3 Results and Discussion

To verify the capabilities of the mathematical model, waterflow data is used from the anti-flood hydro system on the lateral tributary of a river in the Far Eastern region of Russia with high levels of water upwelling caused by rainfall.

For hydro systems on lateral tributaries, the main environmental requirements are to be met: conservation of flood-floodplain processes - regulated waterflows in the downstream must correspond to the flood with 10% of provision, flooding of ecosystems - the maximum water level in the upstream must not exceed the permissible level. As an example (Figs. 2 and 3) the variants of waterflow regulation are shown depending on the parameters of the anti-flood hydro system. The user can choose one that ensures effective regulation of the maximum waterflow, considering environmental requirements. Several suitable sets of parameters are found for the hydro system, when maximum waterflow of flood is reduced from 4450 m³/s to 2990–3030 m³/s, which is

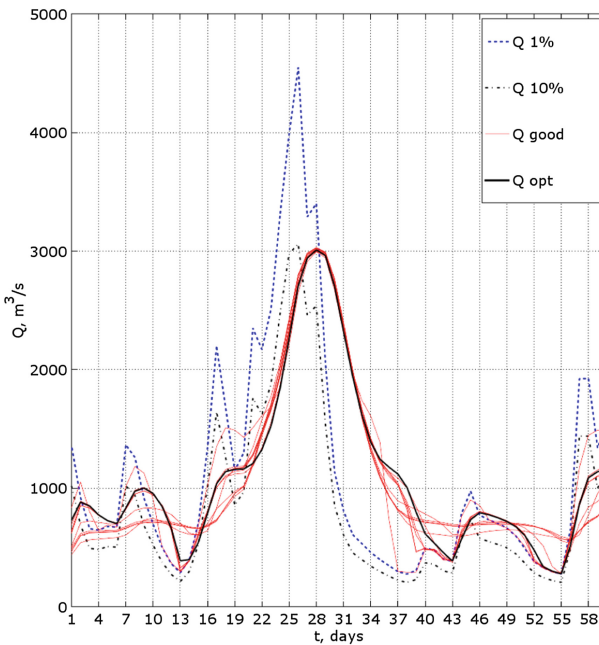


Fig. 2. The change in waterflow for various parameters in the downstream of the hydro system.

near the maximum waterflow for flood with 10% of provision. It is acceptable for preservation of natural flood-floodplain processes. In addition, the design of the hydro system (corresponding to the bold black line in Fig. 2 and Fig. 3) is found, which during the flood several times passes from the pressure regime to the non-pressure regime, which ensures free passage for fish to the spawning sites.

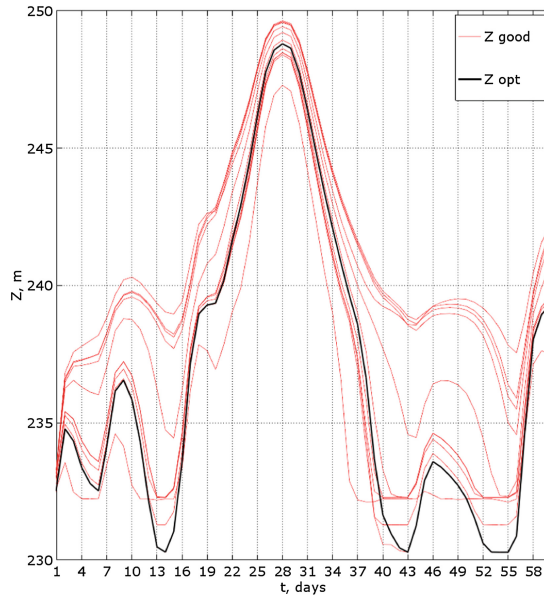


Fig. 3. The change in water level in the reservoir for various parameters in the upstream of the hydro system.

4 Conclusion





The developed mathematical model for flood management by hydro systems with a temporarily flooded reservoir has been successfully used to select suitable parameters of the hydro system. It is possible to study specific designs of anti-flood hydro systems or search optimal parameters for them based on waterflow data. Using this model in conjunction with the model of the reservoir with hydro power plant will significantly reduce the risk of flooding the entire river basin with minimal impact on the natural environment.

Acknowledgment. The research was supported by Russian Science Foundation (grant №16-17-00050).

References

1. United Nations Office for Disaster Risk Reduction. The human cost of weather-related disasters 1995–2015 (2015)
2. Climate Service Centre Report No. 12. The European Floods Directive and Opportunities offered by Land Use Planning (2016)
3. Alfieri, L., Feyen, L., Salamon, P., Thielen, J., Bianchi, A., Dottori, F., Burek, P.: *Nat. Hazards Earth Syst. Sci.* **16**, 1401–1411 (2016)
4. Jha, A., Bloch, R., Lamond, J.: *Cities and Flooding: A Guide to Integrated Urban Flood Risk Management for the 21st Century*. World Bank Publications, Washington (2012)
5. Avakyan, A., Istomina, M.: *Bull. Russ. Acad. Sci.* **72**(12), 1059–1068 (2002)
6. Badenko, V., Badenko, N., Nikonorov, A., Molodtsov, D., Terleev, V., Lednova, Ju., Maslikov, V.: *MATEC Web of Conferences*, vol. 73, p. 03003 (2016)
7. Fedorov, M., Badenko, V., Maslikov, V., Chusov, A.: *Procedia Eng.* **165**, 1629–1636 (2016)
8. Fedorov, M., Maslikov, V.: *Bull. Russ. Acad. Sci. Energetics* **4**, 47–52 (2013)
9. Thieken, A., Kreibich, H., Müller, M., Merz, B.: *Hydrol. Sci. J.* **52**, 1016–1037 (2007)
10. Guan, M., Sillanpää, N., Koivusalo, H.: *Hydrol. Process.* **29**, 2880–2894 (2015)
11. The second assessment report of Roshydromet on climate change and its consequences on the territory of the Russian Federation as part of the main volume, a technical summary and a general summary (2014)
12. On the state of protection of the population and territories of the Russian Federation from emergency situations of natural and man-made nature in 2013 (2014)
13. *Rivers and lakes of the world: Encyclopedia*, Encyclopedia, Moscow (2012)
14. Fedorov, M., Badenko, V., Maslikov, V., Chusov, A.: *MATEC Web of Conferences*, vol. 73, p. 01002 (2016)
15. Chugaev, R.: *Hydraulics*. Energoizdat, Leningrad (1982)
16. Kiselev, P.: *Handbook of Hydraulic Calculations*. Energiya, Moscow (1974)
17. Teukolsky, S., Vetterling, W., Flannery, B.: *Numerical Recipes: The Art of Scientific Computing*. Cambridge University Press, London (2007)
18. Svein, L., Petter, L.: *Programming for Computations - MATLAB/Octave: A Gentle Introduction to Numerical Simulations with MATLAB/Octave*. Springer (2016)
19. Artiukh, V., Mazur, V., Adamtsevich, A.: Priority influence of horizontal forces at rolling on operation of main sheet rolling equipment. *MATEC Web of Conferences*, vol. 106, Article no. 04001 (2017). <https://doi.org/10.1051/mateconf/201710604001>
20. Pustovgar, A., Tanasoglo, A., Garanzha, I., Shilova, L., Adamtsevich, A.: Optimal design of lattice metal constructions of overhead power transmission lines. *MATEC Web of Conferences*, vol. 86, Article no. 04003 (2016). <https://doi.org/10.1051/mateconf/20168604003>
21. Shilova, L., Soloviev, D., Timatkov, V., Adamtsevich, A.: About the Territorial Potential of the Construction of Battery-Charging Stations for Autonomous Electric Motor Vehicles in the Regions. *MATEC Web of Conferences*, vol. 73, Article no. 02017 (2016). <https://doi.org/10.1051/mateconf/20167302017>

Functional Model That Evaluates the Impact of Hydrotechnical Works and Facilities on a Water Object

Alexander Shishkin¹(✉) , Alexander Chusov¹ ,
Marina Epifanova² , and Dmitriy Silka³ 

¹ Peter the Great St. Petersburg Polytechnic University,
Polytechnicheskaya str., 29, 195251 St. Petersburg, Russia
vskanhva@mail.ru

² Saint Petersburg State University of Industrial Technologies and Design,
Bolshaya Morskaya str., 18, 191186 St. Petersburg, Russia

³ Moscow State University of Civil Engineering,
Yaroslavskoe sh., 26, 129337 Moscow, Russia

Abstract. The article contains a functional model to evaluate the impact of hydrotechnical works and structures on water areas. There are classified main types of hydrotechnical works which lead to the pollution of water areas. The choice and methods of the hydrological non-stationary model of wind and effluent currents of the water object are explained. Furthermore, some standard models of convection-diffusion transfer and transformation of pollutants are mentioned. There is proposed the structure of the initial database and the results of calculations based on a geo-informational foundation.

Keywords: Hydrotechnical construction · Impact on water areas
Mathematical modeling · Convection-diffusion transfer

1 Introduction

During the production of various hydrotechnical works in rivers, lakes, reservoirs and the coastal zone of seas, the formation of large clouds of fine suspended solids is one of the main types of environmental damage. Afterwards, these solids tend to subside slowly, spread in the aquatic environment, and travel a significant distance (tens of kilometers). Some calculations must be carried out during the drafting of this work, namely time evolution of the volumes of such clouds of contaminated water with minimum concentrations of suspended solids, their area, and the thickness of the layer of sediment deposited on the bottom. This is a rather complex objective of mathematical geoinformation modeling. This model takes into account the flow fields, which are basically non-stationary, as well as sedimentation rates of soil, depending on the ratio of soil and water densities, sizes, and shapes of particles. There is required the solution of current tasks in a three-dimensional setting and with a sufficient grid resolution inside large water areas. There is introduced a special specificity of significance according to the mass of the yield of fine particles into the suspension using different

techniques of work. The damage to the environment is estimated according to the results of geoinformation modeling, for various types and technologies of production of hydrotechnical engineering works.

2 Materials and Methods

The developed functional model for assessing the level of impact of hydrotechnical works and structures on the water area includes the following stages [1] (Fig. 1).

1. Description of the object and works of hydrotechnical construction with further identification of activities leading to the pollution of water area and a second output of pollutants.
2. Determination of the location of works and sources of pollution of water areas, determination of the path of movement of the source of pollution and the regime of discharge of pollutants.
3. Construction of a mathematical model of convective-diffusion transport of pollutants, taking into account determining factors for the standardized impact on the water object.
4. Assessment of exposure parameters (duration of exposure, volumes of contaminated water with different concentrations of pollutants, maximum concentrations of pollutants, bottom sludge areas, etc.).
5. Explanation of water protection measures which are based on planning, operational and optimal management of indicators of water composition and properties.

Basic water-protection complex (BWC) is being developed to provide the protection of the water object from pollution by sewage from industry, municipal services, agricultural production, as well as surface effluents of built-up areas and industrial sites. In addition, some technical means of water protection which are included further are designated as U_m - management. Water protection measures are required to compensate the impact of hydrotechnical works and structures, the totality of them is a compensatory water-protection complex (CWC). It was concluded considering the design and technological parameters of hydrotechnical objects (N_p) including inside water-protection measures, i.e. N_p -controls [2].

Integral natural and technical complex (INTC) is the totality of the types of various activities at water objects related to hydrotechnical, basic and compensatory construction [3, 4]. The costs for the implementation of BWC relate to industry enterprises and industries operating in various basins where hydrotechnical construction is carried out. The cost of CWC should be included in the estimated cost of hydraulic engineering, the cost of INTC is the entire expenditure spent on water protection in the framework of hydrotechnical engineering construction within the NTC.

It is a natural approach when

$$I_{INTC} = [I_{BWC}(U_m) + I_{CWC}(U_m, H_n)] \rightarrow \min, \quad (1)$$

where I is the total value functional.

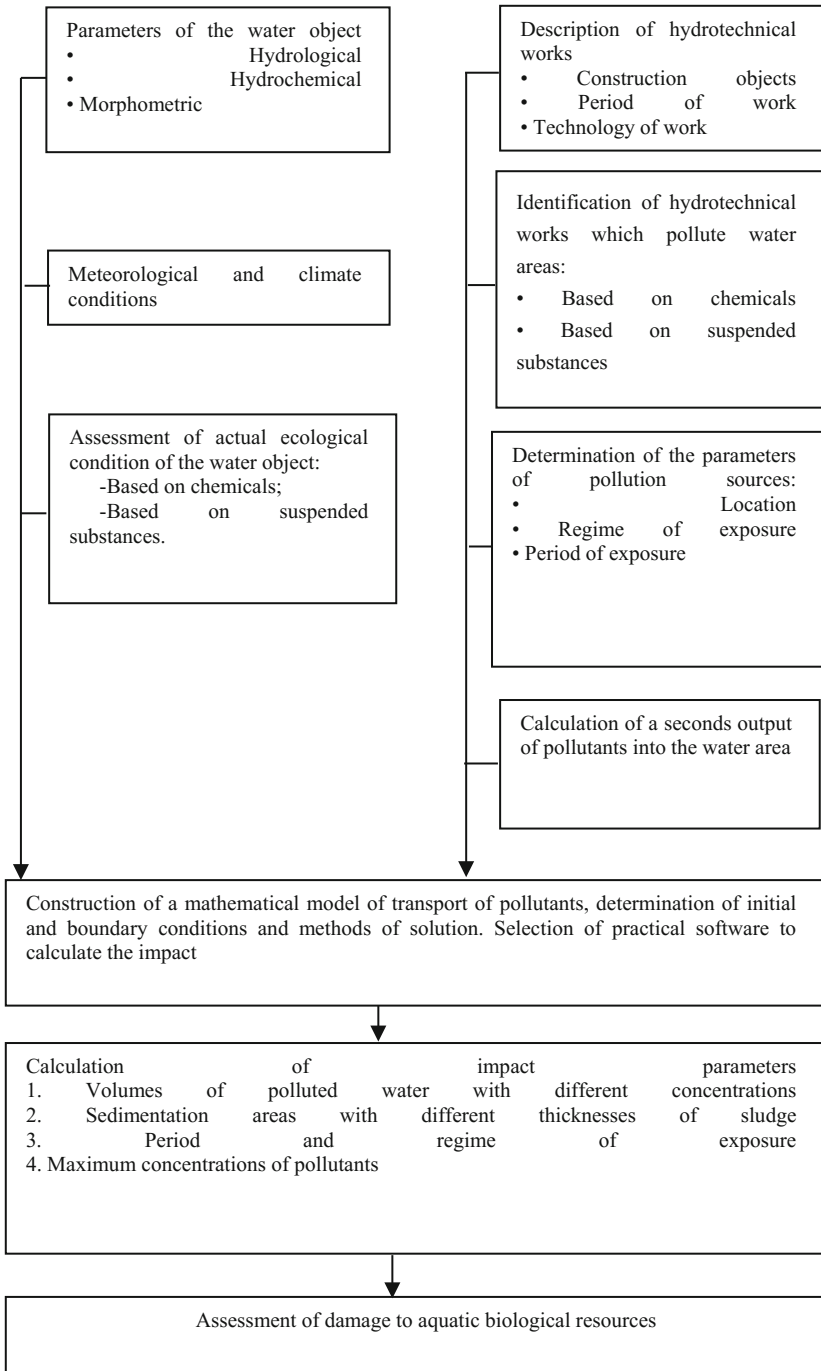


Fig. 1. Functional model for assessing the impact of hydrotechnical works and structures on aquatic biological resources.

The methodology to develop water-protection measures in hydrotechnical construction presupposes a complex approach towards the formation of technical means to manage water quality. In other words, these means are aimed to limit the input of pollutants into the water object from the catchment area (Um-allochthones), and aimed on limiting the in-water production of contaminants, as well as intensification of self-purification processes (Hn-autochthonous). Standards of permissible effluents (SPE) are provided by means of Um-managements, within the limits of basin standards of permissible impacts (SPI).

Morphometric and hydrodynamic characteristics of the being created or reconstructed water object are included into the composition of Hn-controls includes, as well as structural and technological parameters of hydrotechnical structures on it, which influence the formation processes of water quality, as well as special water protection structures.

The system of constraints of the optimization objective includes the requirements towards water quality in the calculation areas. The target functional usually determines the correspondence between water security departments and the cost of their implementation. It is minimized according to provided specified restrictions. It allows finding the required set of technological parameters of water protection measures that would provide the achievement of the best water quality indicators possible with the available allocations. In general, an optimization-imitation simulation model which is based on GIS for calculating a water security complex with a minimum cost can be written as:

$$I = [I1 (Hn) + I2 (Um) +] + I3 (Hn)] \rightarrow \min \tag{2}$$

$$\frac{dC_i}{dx} = f_i (Hn, Um, C_j, \dots) \tag{3}$$

$$C_j(0) = C_{j0}, C_j(1) = C_{j1} \tag{4}$$

$$Hn, Um \in V \tag{5}$$

In this case, the functional I includes the cost of water protection departments (Np), which takes into account the specifics of hydrotechnical engineering construction. The vector equation which describes the state of the system (3) should be written in the form of models allowing to establish the dependence of water quality formation in water objects considering the dependence between j-impurities and Um and Np-controls.

This allows us to connect the abiotic parameters of aquatic ecosystems that are changed under the influence of hydrotechnical engineering construction with the biotic structural and functional characteristics responsible for the formation of water quality.

The constraint system of the optimization task (5) reflects permissible control levels that determine the range of changes Um and Hn by the technical capabilities of the corresponding control.

Expression of C_j indicates initial conditions for each of the water object sections under consideration for j-indicators of water quality. The condition C_j (1) describes the water quality requirements in the water users' pads of the NTC, which are adopted taking into account basin SPI and individual SPE for water users.

The ecological-mathematical model (2)–(5) allows to solve main tasks of development of water protection measures for hydrotechnical construction. Based on the solution of Eq. (3), the water quality vector is predicted in the water use points, depending on the technical solutions for NTC- C_j (N_p). Planning of water quality at the design and management stage of construction and operation of hydrotechnical structures can be carried out with the help of appropriate U_m and N_p -controls. Their collection can also be determined by solving Eq. (3) with respect to U_m and N_p , provided that the vector of normative requirements for water quality is in the right part of its solution in the form of vector control. Let's consider some kinds of influences in the developed system of models.

In practice, H_n -control systems are associated with technological solutions aimed to reduce the chemical impact on water objects, or reducing turbidity fields. Concentrations of pollutants and particles with a hydraulic size of less than or equal to 0.05 mm are taken as the magnitude of the impact. Larger particles precipitate directly in the work area or at insignificant distances from the work site. These impacts are determined for each type of hydrotechnical engineering works. Typical works are considered as: installation and dismantling of sheet piling; installation and dismantling of piles; alluvial work; seizure of soil; work on bank protection, etc. Each negative impact is characterized by the level of exposure and duration. The duration of the impact is determined, as a rule, by the duration of the hydrotechnical works.

The level of impact depends on the types of impact and can be determined by the following typical approaches:

1. During the aggradation of the territory there can be extracted contaminants and fine particles from the ground. They lead to increased turbidity. In general, a seconds output of finely dispersed suspended particles during washing of territories can be calculated according to the formula:

$$G = V * q * \gamma * 1000000 * k / (T * td * 3600), \quad (6)$$

where V is the volume of the laid soil, m^3 ; q is the density of the soil, g/cm^3 ; T - number of days of work; td - the number of hours of work per day; γ - fraction of dust particles with a particle diameter of less than 0.05 mm; K - fraction of leachable fine particles [5].

Information about the proportion of dust particles depending on the type of soil can be obtained from the results of granulometric and chemical analysis or passport data.

2. When sandblasting works, a stream of abrasive particles is directed to the surface at high speed. Particles, colliding with the surface, destroy foreign layers of contaminants, thereby purifying the material. The most common abrasive material is sand. After cleaning, sand enters the water area.

Knowing the area of the site of work and the specific consumption of sand per $1 m^2$ of the granite embankment, the necessary mass of sand is calculated

$$M_{sand} = S * q, \quad (7)$$

where: S area of the surface to be cleaned, m²; Q - sand consumption per 1 m² of surface, kg/m².

Then a seconds output of the fine particles into the suspended state is calculated.

3. When dredging works, the mass yield of suspended solids during the production of dredging and burial of soil can be calculated in accordance with the methodology for calculating the payment for pollution of the seas and surface water bodies [6]. When removing the bottom soil by a milling dredger, the transition of the fine material to the suspended state occurs mainly during loading with overflow of technological water over the side of the chalet.

The mass of the particles of soil discharged into suspension during loading with overflow (Mpm) is determined by the formula:

$$M_p = \delta g \times \gamma \times V_{gr}, \quad (8)$$

where delta is the coefficient determined in accordance with the methodology for calculating pollution charges for the seas and surface water objects, taking into account types of soil under development and the numerical value of the ratio gv/V; delta g fraction of fine particles; gamma- density of dry soil, t/cubic m; Vgr - volume of the developed soil, cubic m.; gv - hourly productivity of the dredge on the ground, cubic m/h; V - capacity of the hold (bunker) of the ship, cubic m.

4. During the burial of soil which is developed by a hydro-mechanized method, the mass of particles causing primary water contamination with suspended substances (mpg) is:

$$M_{pg} = n \gamma g \times \gamma \times V_{gr}, \quad (9)$$

where n is the auxiliary coefficient; gamma is the density of dry soil, t/cubic m.; Vgr - volume of the developed soil, cubic m.

5. Dismantling of temporary metal structures can be carried out either by cutting or pulling out. A clamshell dredger helps to cut off the bottom of dismantled metal structures. Then a trench is developed along a sheet pile wall 1 m deep and 1 m wide. Afterwards the diver performs cutting at the level of the trench bottom with a welding machine. In the case of dismantling of a metal pipe, a bucket is developed around the dismantled pipe with a depth of 1 m and a width of 1 m with the help of a clamshell dredger. Then the cut metal structures are removed from the water using a floating crane (g.p.100t).

Accordingly, to calculate a seconds output of fine particles into a suspended state, the volume of the extracted soil must be calculated according to geometrical parameters of the dowel or pipe. You can calculate a seconds output to the suspended state considering the value of the content of fine particles. When dismantling piles, it is assumed that, in a suspended state, the volume of the soil is equal to the volume of the piles.

After determining the duration and level of exposure, the degree of impact to aquatic biological products can be easily determined. The degree of impact on aquatic biological resources depends on the following parameters: volumes of contaminated water, bottom silting areas, maximum concentrations, etc. Mathematical models are used to calculate these parameters. The initial data are the parameters of the water object, information about the hydrological and hydrochemical regimes, the morphology of the banks and the bottom, the presence of inflows and in-and-out flowing water objects, meteorological conditions [8, 9].

In practical terms, the most well-known among the typical mathematical models describing the processes of pollutant transport is the adapted three-dimensional thermo-hydrodynamic model and its modifications of Princeton University, USA [11].

In the domestic practice there is widely known software package (PC) CARDINAL [http://cardinal-hydrosoft.com] which was developed by KA. In this work, the three-dimensional mathematical model of the following form is implemented [12]:

$$\begin{aligned} \frac{\partial u}{\partial t} + u \frac{\partial u}{\partial x} + v \frac{\partial u}{\partial y} + w \frac{\partial u}{\partial z} = & -g \frac{\partial \zeta}{\partial x} - \frac{g}{\rho_o} \int_z^{\zeta} \frac{\partial \rho}{\partial x} dz - \frac{1}{\rho_o} \frac{\partial P_a}{\partial x} + f_c v \\ & + K \left(\frac{\partial^2 u}{\partial x^2} + \frac{\partial^2 u}{\partial y^2} \right) + \frac{\partial}{\partial z} \left(v_T \frac{\partial u}{\partial z} \right) \end{aligned} \quad (10)$$

$$\begin{aligned} \frac{\partial v}{\partial t} + u \frac{\partial v}{\partial x} + v \frac{\partial v}{\partial y} + w \frac{\partial v}{\partial z} = & -g \frac{\partial \zeta}{\partial y} - \frac{g}{\rho_o} \int_z^{\zeta} \frac{\partial \rho}{\partial y} dz - \frac{1}{\rho_o} \frac{\partial P_a}{\partial y} + f_c u \\ & + K \left(\frac{\partial^2 v}{\partial x^2} + \frac{\partial^2 v}{\partial y^2} \right) + \frac{\partial}{\partial z} \left(v_T \frac{\partial v}{\partial z} \right) \end{aligned} \quad (11)$$

$$\frac{\partial u}{\partial x} + \frac{\partial v}{\partial y} + \frac{\partial w}{\partial z} = \omega_s \quad (12)$$

$$\frac{\partial \zeta}{\partial t} + \frac{\partial U}{\partial x} + \frac{\partial V}{\partial y} = \varpi_s \quad (13)$$

$$\frac{\partial c}{\partial t} + u \frac{\partial c}{\partial x} + v \frac{\partial c}{\partial y} + (w - \omega_0) \frac{\partial c}{\partial z} = \omega_s c_s - \lambda c + K_c \left(\frac{\partial^2 c}{\partial x^2} + \frac{\partial^2 c}{\partial y^2} \right) + \frac{\partial}{\partial z} \left(v_c \frac{\partial c}{\partial z} \right) \quad (14)$$

where g is the acceleration of gravity, ρ (T, S) is the water density determined by the UNESCO [7] dependence, ρ_o is the average value of the water density, P_a is the atmospheric ϕ pressure, $f_c = 2\omega \sin\phi$ - coriolis parameter, is the latitude, ω is the angular velocity of rotation of the Earth, K and k - coefficient of horizontal turbulent exchange and vertical turbulent exchange, U and V - specific consumption:

$$U = \int_{-h}^{\zeta} u dz, \quad V = \int_{-h}^{\zeta} v dz, \quad (15)$$

where h is the undisturbed water depth, ω_0 is the sedimentation rate (hydraulic size) of the suspended impurities, λ is the nonconservativity coefficient of the impurity, K_c is the coefficient of horizontal turbulent diffusion, v_c is the vertical turbulent diffusion coefficient, ω_s is the consumption of discharge water from sources per unit volume, ω_{Σ} is the consumption of waste water from sources per unit surface area, c_s is the concentration of impurities in waste water sources. The ‘z’ coordinate is directed vertically upwards.

This system of equations is solved by finite-difference methods [13]. In the solution, the transition to curvilinear boundary-dependent coordinates is used, which makes it possible to improve the accuracy of solving problems in areas of complex shape and with abrupt changes in the bottom relief.

If there is insufficient initial data for shallow water objects, there is used a simplified two-dimensional model developed by Felzembraum-Lineikin for calculating wind currents [14] as well as a two-dimensional nonstationary model of transport of pollutants proposed by Karushev,

$$\frac{\partial C}{\partial t} + V_x \cdot \frac{\partial C}{\partial x} + V_y \cdot \frac{\partial C}{\partial y} = D \cdot \left(\frac{\partial^2 C}{\partial x^2} + \frac{\partial^2 C}{\partial y^2} \right) \tag{16}$$

$$r_s = v_n \cdot C - D \cdot \frac{\partial C}{\partial n}; \tag{17}$$

$$q_{ija}^k - q_{ijb}^k + q_{ijc}^k - q_{ijd}^k = \left(H \cdot \frac{\partial C}{\partial t} \right) \cdot \Delta x \cdot \Delta z, \tag{12}$$

where v_n is the value of the averaged flow speed, m/s; C is the concentration of matter at the point of intersection of the normal n with the reference surface, g/m^3 ; D is the coefficient of turbulent diffusion at the same point, m^2/s .

For shallow watercourses with a lack of morphometric data and field observations, a two-dimensional mathematical stationary model can be used. The coefficient of longitudinal diffusion can be neglected, since the water speed in the river is significant and the convective component of the transport of suspended substances in the direction of the main flow is much higher than the diffusion transfer.

Based on the schematization, a two-dimensional stationary mathematical model of the water quality forecast for non-conservative impurities is used in the form of:

$$V_x \frac{\partial C}{\partial x} = D_y \frac{\partial^2 C}{\partial y^2} - K_1 C \tag{19}$$

This equation is approximated as a finite difference expression

$$C_{(m+1,n)} = \frac{2D_y \Delta x}{V_{cp} \Delta y^2} (C_{(m,n+1)} - 2C_{(m,n)} + C_{(m,n-1)}) + C_{(m-1,n)} - \frac{2K_1 C \Delta x}{V_{cp}} \tag{20}$$

and is realized by an explicit calculation scheme.

3 Approbation of a Functional Model to Assess the Impact of Hydrotechnical Engineering Work on a Water Object

One of the examples is the reconstruction of the Sinopskaya Embankment along the territory of Moiseenko Street to Kherson Passage.

This reconstruction provided for the following works in the water area of the Neva river: construction of a new embankment in granite facing and repair of the existing embankment. Scheme of the location of the site of work is shown in Fig. 2.

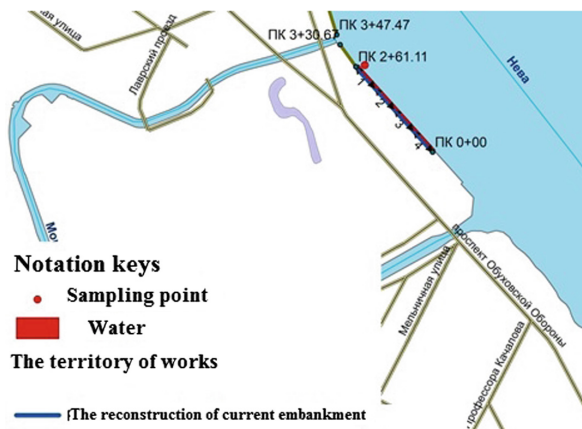


Fig. 2. Scheme of the site for repair of the Sinopskaya embankment.

During the conduction of works, the existing concrete wall of the embankment is partially disassembled, and in front of it a new embankment is constructed from pre-fabricated reinforced concrete blocks with a height of 3.0 m. Two blocks of granite facing are fixed to the prefabricated blocks, a granite cornice and a parapet are installed at the top.

The carried-out analysis of the technology of works has shown that the following technological operations will have the main negative impact on water quality:

- Vibration with a high-frequency vibrator pile Larsen V (fencing pit in the water area).
- Arrangement of the fencing of the trench to the existing embankment, and then to the sections of the new wall, by means of temporary bridges from the paved dowl.
- Development of a foundation pit between the embankment wall and sheet piling at the temporary road with the side exit device.
- Immersion of the front row of vertical piles by means of a pile installation from the shore.
- Filling of stone and crushed stone.

The total area of the water area of the Neva River, occupied during the production period is 2081 m². The total area of the water area of the Neva River irretrievably rejected under the new wall of the embankment will be 1085 m², along the wall of the embankment in the areas of strengthening the bottom - 3640 m².

The results of the analysis of works on the reconstruction of the embankment showed that hydrotechnical construction will lead to some permanent and temporary damage. Permanent damage will be caused due to the irretrievable rejection of sections of the Neva river bed under the wall of the embankment under construction, and temporary damage due to damage to the bottom and formation of a zone of increased turbidity during the conduction of works.

Main types of the impact on the water area is the formation of turbidity fields. When repairing the Sinopskaya embankment, the bulk of the suspended matter will pass to the river Neva when the rubble is filled with a volume of 4130 m³ and the stone is poured into the water area of the river Neva with the volume of 9880 m³. According to these data, the level of impact was determined based on the following calculations. The content of fine particles in the stone, depending on the composition and size, is 2–3 orders of magnitude smaller than in the gravel and varies from 0.01% to 0.1%. Therefore, when modeling the transport of fine particles, particles that pass into the water during the deposition of the stone can be neglected. In accordance with ISO, the content of pulverized and clay particles (less than 0.05 mm in size) in crushed stone and gravel intended for construction work should not exceed two percent. According to the calculation results, the second output of fine dispersed suspended solids will be 15.8 g/s.

Assessment of the degree of negative impact was carried out with the help of the software product “GIMS-river”, which allows carrying out modeling of the transport of pollutants in water bodies on a geoinformation basis [15, 16].

A two-dimensional model of convection-diffusion transport and transformation of substances for a non-conservative impurity is implemented in the software product [17].

Based on the results of calculations it was shown that the maximum permissible concentration limit for suspended substances will be exceeded only at a distance of 63 m, the width of this zone of influence will not exceed 5 m. The maximum concentration will be 0.63 mg/lit. At the time of production, fine particles will precipitate to the bottom. The length of the sediment layer with a thickness of more than 5 mm is 27 m, and the area of the silted bottom is 135 m². What is completely included in the area of the water area torn off for the construction of the embankment. The bottom area with a thickness of more than 1 mm will be 20 655 m² with a length of 1089 m. Sediment with a given thickness does not precipitate further than 25 m from the current embankment. The maximum layer of the precipitate of fine particles is 7.3 mm (Figs. 3 and 4).

The following engineering solutions (Hn) were developed to minimize the negative impact:

- application of sandblasting for dust-free cleaning with an abrasive accumulator, a dust collector and a vacuum cleaner;
- engineering activities that exclude the possibility of falling of thawed and rainwater from the construction site to the ground and aquifers: washing, repair, maintenance and refueling of construction machines and equipment are carried out outside the zone of hydrotechnical engineering works;
- conducting systematic monitoring of the state of the environment;
- exclusion of effluents of any types of untreated sewage, industrial and domestic waste and garbage into the water area of water bodies;
- exclusion of soil placement in the coastal protection zone of the water body;

- a ban on work in the water area of the river during their spawning period - from April 15 to June 15 including night time during the spawning migration of the Neva salmon in the period from September 1 to November 15.



Fig. 3. Calculated field of concentrations (mg/lit) for the reconstruction of the Sinopskaya embankment.

Fig. 4. Calculated field of thickness of the layer of suspended solids during the reconstruction of the Sinopskaya embankment.

The second example of approbation of a functional model is the assessment of the impact of dredging in the bucket of Turukhtnaya harbor.

The main factor of influence in these works is an increase in the content of suspended matter in the water area and siltation of the bottom. The degree of impact was determined on the basis of mathematical modeling of the calculation of the fields of concentrations of pollutants in the water object and the areas of increased turbidity with the definition of the optimal production performance parameters ensuring the permissible impact on aquatic biological resources (Fig. 5).

As a basis for the calculation, the results of engineering-geological, hydrological and hydrochemical investigations were taken. Based on the information on the technological parameters of the dredging, a seconds output of the fine particles into a suspended state was calculated. For mathematical calculations of flow fields, the prevailing wind directions were taken at a speed of 2.5 m/s. When solving the boundary conditions on the outer boundary, the prevailing directions and speeds of the currents were established in the Neva Bay of the Gulf of Finland.

Calculation of the transport of pollutants was carried out on the basis of the constructed conformal grid (see Fig. 6). The grid spacing was 10 m. Direction and flow



Fig. 5. Dredging zone in navigation 2015 year.



Fig. 6. Calculation grid for modeling the transport of suspended solids.

speed values were obtained according to hydrological calculations, the depth value according to the results was taken according to bathymetric studies. Estimated time step of 16 min.

Non-stationary work performance mode (eight hours per day) causes the abrupt change in the concentration of pollutants in the waters of Big Ruff harbor. Within 8 h of operation the maximum concentration is continuously increasing, but during 16 h of downtime reduced.

The field of suspended solids concentrations after the conduction of the work is shown in Fig. 7. The maximum concentration of suspended solids in the production of dredging operations for the counting of fine particles is 20.3 mg/lit. In the production of dredging, the amount of contaminated water is: $C > 0.25 - 4.464$ million m^3 ; $C > 1 - 1.344$ million m^3 ; $C > 10 - 0.192$ million m^3 .

The bottom silting area with a thickness of more than 5 mm did not exceed 1 ha.

The change in the volume of contaminated water over time is shown in Fig. 8. It follows from the figure that the concentration field leaves the stationary state 9 days

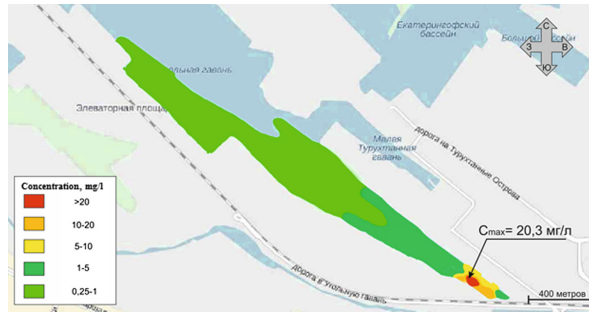


Fig. 7. Field of pollutant concentrations after completion of dredging.

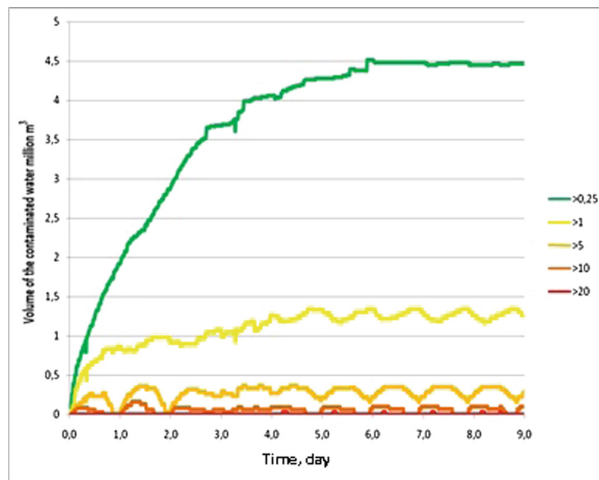


Fig. 8. Time course of the volume of water space (million m^3), in which the concentrations of suspended particles exceeded the specified values.

after the start of the work. The volumes of contaminated water with insignificant concentrations ($C > 0.25$ mg/lit) after 6 h of operation do not actually change. It happens because in the work of the incoming new suspended particles, the dispersion of particles to smaller concentrations is compensated, and in the case of technological interruptions, condensation is due to the dilution of high concentrations. For high concentrations ($C > 0.25$ mg/lit), the course of contaminated water corresponds to periods of work and idle time, during the work volume reaches the maximum values, and in the period of work tends to zero.

4 Results and Discussion

Developed functional model for assessing the impact of typical hydrotechnical works on a water object has been developed. The formation of the model is based on approaches to identify the main processes of pollution of the water area and the calculation of a seconds output of pollutants. The key step in the assessment of the impact is the justification and construction of adequate mathematical models for the calculation of the transport of pollutants using appropriate software to solve them. The proposed functional model has been tested for several hydrotechnical works in water areas based on the created geodatabase.

References

1. Antonov, I., Shishkin, A., Epifanov, A.: Geoinformation technologies in the technospheric security: educational-methodological manual. VSTEP SPbGUPTD, SPb (2017)
2. Alexandrova, N., Chusov, V.: Application of integral equations of hereditary theories to calculate the change in measures of damage theory under the effect of repeated loads. *Eng. Constr. J.* **2**(62), 69–82 (2016)
3. Zhilnikova, N., Shishkin, A., Epifanov, A., Epifanova, M.: Algorithm for managing the redistribution of anthropogenic load for territorial natural-technical complexes based on geoinformation systems. *Inf.-Control Syst.* **1**, 93–101 (2017)
4. Chusov, A.: Ecological and economic substantiation of natural-technical systems in hydropower engineering. *Reg. Ecol.* (1-2), 54–62 (2004)
5. ISO 8267-93 Crushed and gravel from dense rocks for construction works
6. Method for calculating payment for pollution of the seas and surface water bodies, Moscow (1999)
7. Chusov, A., Shilin, M., Ryabchuk, D., Sergeev, A., Timoshina, A.: Use of the washed coastal territory in the Neva Bay for the construction of the Lakhta Center. *Sci. Mem. Russ. State Hydrometeorol. Univ.* **35**, 156–164 (2014)
8. Fedorov, M., Chusov, A., Yakovlev, V.: Models of safety management of natural-technical systems. Publishing House Polytechnic. University, S.-Petersburg (2014)
9. Blumberg, A.: A description of a three-dimensional coastal ocean circulation model. In: Heaps, N. (ed.) American Geophysical Union, Washington, D.C. (1987)
10. Klevanny, K., Smirnova, E., Shavykin, A., Vaschenko, P.: Distribution of suspended matter and its impact on biota during dredging in the Kola Bay (Barents Sea). *Prot. Environ. Oil Gas Complex* **3**, 18–24 (2013)
11. Klevaniy, K.: Modeling of long-wave processes in geophysical hydrodynamics. Thesis, Russian State Hydrometeorological University (1999)
12. Felsenbaum, A.: Theoretical Foundations and Methods of Calculating Steady Sea Flows. Publishing House of the USSR Academy of Sciences, Moscow (1960)
13. Shishkin, A., Epifanov, A., Antonov, I., Alekseev, V., Kuraki, N., Zheltov, E.: No. 2009615259 (2009)
14. Serebryakov, A., Epifanov, A., Shishkin, A., Antonov, I., Epifanov, M.: VAT of the river - certificate of state registration of the computer program №2016662535 (2016)
15. Druzhinin, H., Shishkin, A.: Mathematical modeling and forecasting of surface water pollution of land. Leningrad: Gidrometeoizdat (1989)

16. Zhilnikova, N., Antonov, I., Shishkin, I.: Management of industrial-territorial complex of radio-electronic industry according to eco-technological indicators. *Quest. Radio Electron.* **5** (6), 47–51 (2010)
17. Zhilnikova, N., Alekseev, V., Shishkin, I.: Information-measuring system for monitoring the protection of the territory of the fuel and energy complex against flooding on the basis of geoinformation technology. *Inf. Control Syst.* **6**, 93–97 (2015). <https://doi.org/10.15217/issn1684-8853.2015.6.93>

Assessment of the Subsurface Fire-Fighting System Pipeline Impact on the Tank Stress State During the Foundation Settlement

Alexander Tarasenko¹ , Petr Chepur¹ ,
and Alesya Gruchenkova² 

¹ Industrial University of Tyumen,

Volodarskogo str., 38, Tyumen 625001, Russia

² Surgut Oil and Gas Institute, Entuziastov str., 38, Surgut 628404, Russia
alesya2010-11@yandex.ru

Abstract. The paper objective is to conduct a numerical study of the subsurface fire-fighting system pipeline impact on the structure stress-strain state during the tank settlement. The numerical simulation of the subsurface fire-fighting system pipeline was performed on the basis of the previously designed vertical steel tank model. The PC ANSYS finite element software complex was used to calculate the deformation of the tank structures during the foundation settlement. The values of the obtained stress results indicate that when the vertical steel tank settlement is 20 cm, the equivalent stresses in the wall do not exceed 30 MPa. The paper presents the proposals for possible use of compensating devices for small-diameter technological pipelines in order to minimize the risks of destruction in case of the tank foundation settlement.

Keywords: Tank · Vertical steel tank · Stress-strain state · Base · Foundation
Finite-element method · Subsurface fire-fighting system

1 Introduction

During the operation of the large-sized vertical steel tanks (VST), one often has to face the problem of the foundation settlement. According to [1–3], the differential settlement causes the change in the VST structure stress-strain state (SSS) at various assemblies: the wall and the corner weld joint [4, 5], base setting ring [6], the steel covering elements. However, even the gradual settlement can cause dangerous overpressure in the tank metal structures if there are additional stiffening braces with the wall – pipelines, pipe nozzles, etc. The existing analytical techniques do not allow to accurately assess the tank SSS level due to the non-axisymmetric loading of the additional stiffening elements during the settlement.

Thus, the authors' work [7] presents how numerical methods performed in ANSYS program allowed to assess the impact of the inlet-dispensing nozzle on the stress state of the VST-20000 tank during the settlement. It is known that the tank connections include fire-fighting pipelines, emergency spray pipelines, etc. Generally, they are welded to the wall by means of connecting beams of various profiles (angle, channel (C-beam), pipe, etc.).

Outside the tank, these pipelines have pillars (foundations) that are separate from the VST or even pass underground and go out to the daylight surface directly in front of the object. Usually, the diameter of these pipelines does not exceed 159 mm [8–10]. These facts indicate that these elements cannot displace together with the VST shell during the tank settlement. Consequently, it leads to the various elements deformations and a non-axisymmetric change in the SSS of the metal structures.

The paper objective is to conduct a numerical study of the subsurface fire-fighting system (SSFFS) pipeline impact on the structure stress-strain state (SSS) during the tank settlement. Figure 1 displays the VST-20000 tank and the examined SSFFS connection.



Fig. 1. Overall view of the fire-fighting pipeline and VST-20000 connecting assembly: 1 – pipeline connections with the VST wall, 2 – examined assembly.

2 Methods

In [11], the finite element model (FEM) of the VST-20000 was created and verified using the ANSYS physical analysis complex. On its basis, it is proposed to simulate the deformation process of the SSFFS pipeline during the tank settlement. Geometric and structural parameters of the model are set in accordance with the actually operated tank and its technological connections at the “Torgili” line pumping & control station.

The design scheme represents a tank resting on a circular foundation. The SSFFS pipeline is rigidly connected to the tank wall by means of spot welding. This type of contact makes it possible to simulate the fastening of the shell thin-walled pipeline to the wall by using the beam rod elements, which correspond to the given metal profile – the $100 \times 100 \times 7$ equal-leg angle [12]. The VST settlement is simulated with the displacement command. The target geometry is the bottom edge of the foundation ring and the lower plane of the tank bottom central part. The displacement is set by the tabular data command with the settlement limit values of 10–200 mm.

The free end of the SSFFS pipeline with DN100 diameter is rigidly fixed with a complete disable of displacements and rotations within the axes of the global coordinate system. Figure 2 displays the VST-20000 design scheme with the results of the decomposition into the finite element grid. The grid is created in automatic mode with zones of increased sampling in the contact assemblies of the elements of the simulated tank metal structures.

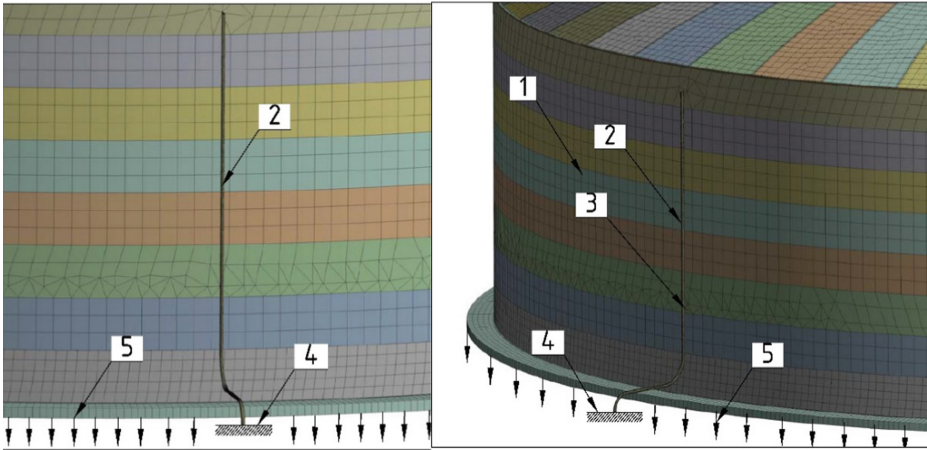


Fig. 2. Design scheme of the VST-20000 with the gas-equalizing system (GES) during the foundation settlement: 1 – VST-20000 wall, 2 – fire-fighting pipeline, 3 – point of attachment to the wall, 4 – rigid fixing, 5 – tank settlement direction.

After the preprocessing preparation of the model (compiling the elemental matrix of stiffness and external loads, taking into account the boundary conditions with the specified zero and nonzero displacement of joints), the iterative solver ANSYS is started. As a result, the FEM equations systems are solved [13, 14]. Upon completion of the automated decomposition of the coefficient matrix and the system solution, the internal forces in the VST elements are determined: finite elements displacement vectors are constructed with necessary transformations of the local coordinate systems, stress and strain matrixes are constructed separately for each finite element. Results are processed within the ANSYS interface for further post-processing.

3 Results

Thus, Figs. 3 and 4 show the stress and strain diagrams for VST-20000 structure and the SSFFS elements. The diagrams were obtained as a result of simulation according to the design scheme proposed by the authors.

The results of post-processing made it possible to determine the relationship of the VST-20000 settlement extent and the actual equivalent stresses in the metal structures of the wall and the SSFFS pipeline. Figure 5 shows the diagrams of the determined functional dependencies.

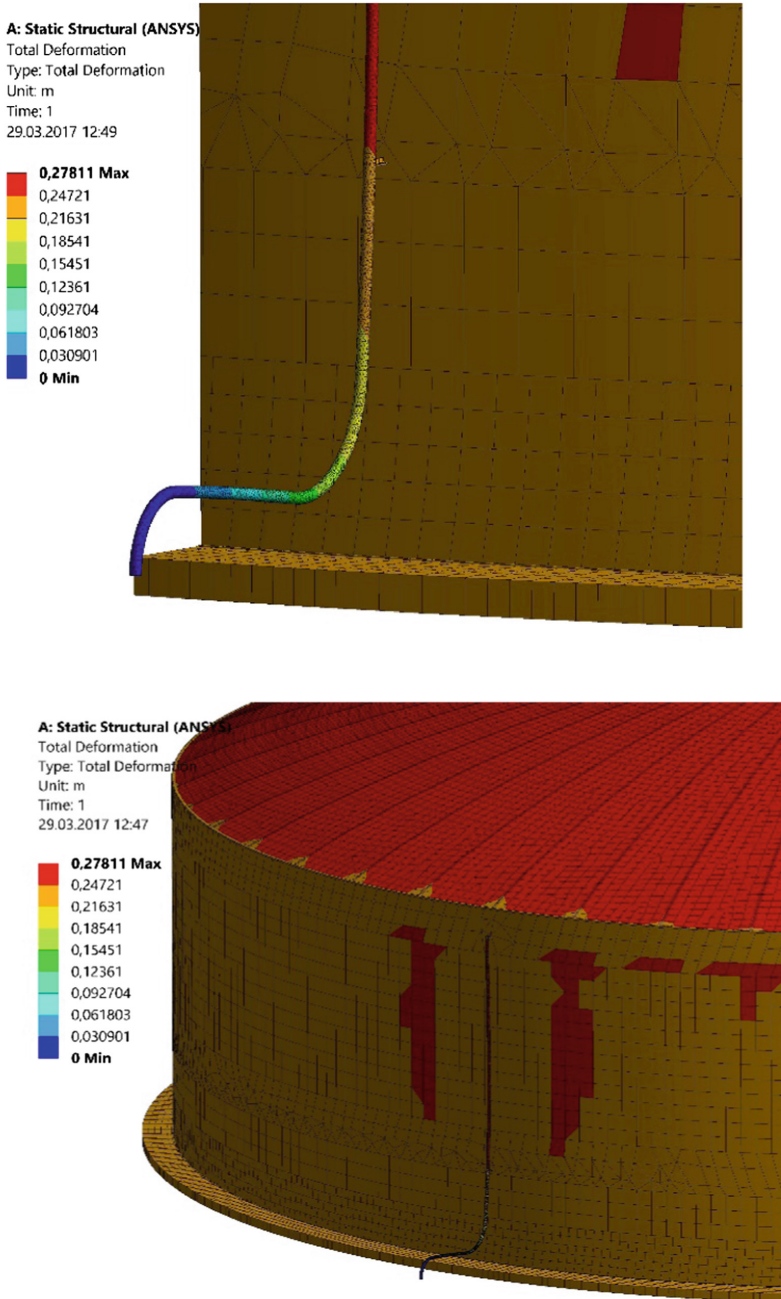


Fig. 3. Deformations of the VST-20000 metal structures in the points of connection with the fire-fighting pipeline.

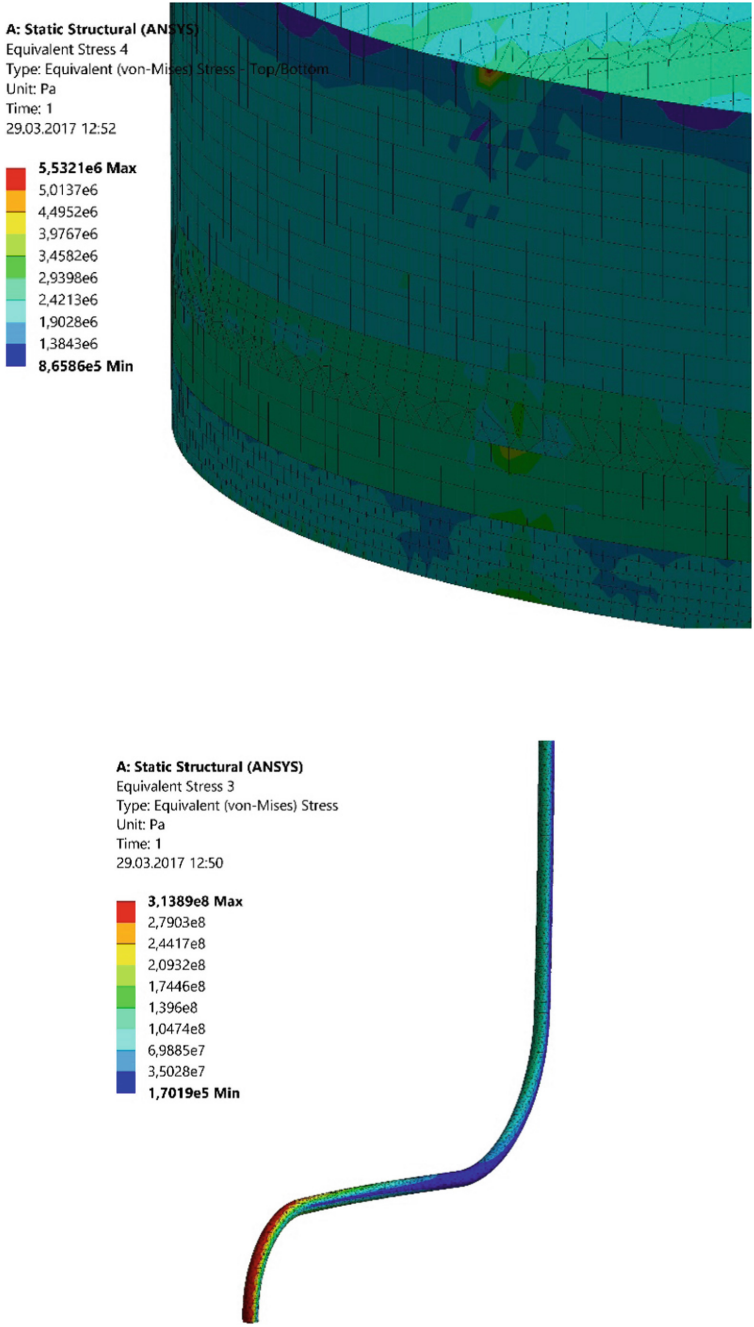


Fig. 4. Actual equivalent stresses in the VST-20000 metal structures: (a) in the wall, (b) in the fire-fighting pipeline.

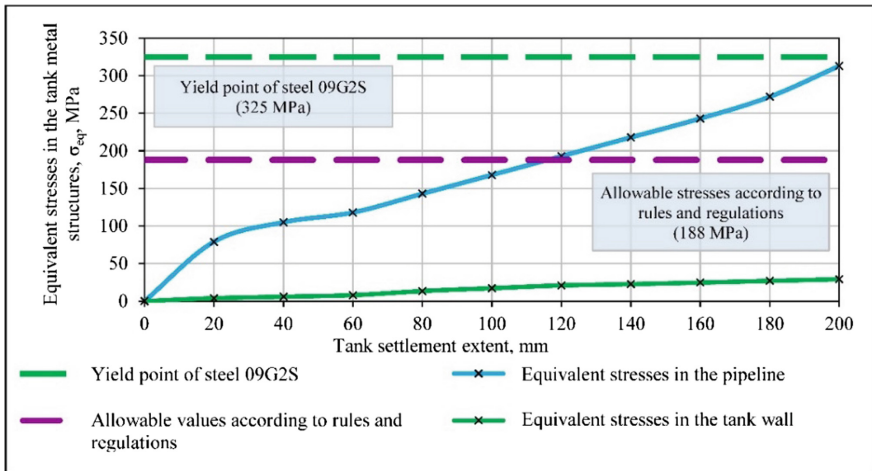


Fig. 5. Dependence of the actual equivalent stresses in the metal structures of the wall and the SSFFS pipeline on the extent of the VST-20000 settlement.

4 Discussion

The diagram of the Figure 5 also shows the zones of the limit states in metal structures. The first horizontal intercept corresponds to the level of allowable stresses according to rules and regulations –188 MPa [15]. The second one corresponds to the limit state in the tank steel σ_{yld} 09G2S = 325 MPa. At this stress magnitude, dangerous plastic deformations occur in the metal, leading to a disruption in the operational suitability of the structure or even to the emergency destruction of the assembly or element.

The obtained dependencies make it possible to assert that during the settlement, the rigid joint of the SSFFS pipeline does not cause any dangerous stresses in the VST-20000 wall even if the tank settlement is 200 mm. However, the excessive stresses occur in the DN100 pipeline itself, reaching the yield point during the 20 cm settlement.

5 Conclusions

The paper presents the numerical simulation of the SSFFS pipeline DN100 performed on the basis of the previously designed VST-20000 tank model [11]. The ANSYS finite element software complex was used to calculate the deformation of the tank structures during the foundation settlement. At geometric modeling, the actually operated VST-20000 tank at the “Torgili” line pumping & control station was used to set the basic design features. The problem of the elements contact interaction was solved: the SSFFS pipeline – the rod connection – the VST wall. The spot welding technique was chosen to calculate the changes in the metal SSS in the zones of the additional stiffening elements impact during the VST foundation settlement. The obtained stress

results indicate that the equivalent stresses in the wall do not exceed 30 MPa when the VST settlement is 20 cm. However, the stresses in the SSFFS pipeline itself reach the critical values of 325 MPa at the same settlement extent. This corresponds with the yield point of the 09G2S steel and the deformation curve passing into the zone of the metal plastic deformations. The allowable stresses of 188 MPa (as in rules and regulations) in the DN100 pipeline are exceeded already at the 115 mm settlement, whereas the stress in the wall is 25 MPa. Proceeding from the fact that the settlement of the tank foundation with the connected SSFFS pipelines can cause extreme stresses in the additional stiffening elements themselves without endangering the elements of the VST shell, it is proposed to consider and justify the possible use of displacement compensation devices for small-diameter technological pipelines, such as SSFFS with the nominal diameter of 100 mm.



Acknowledgement. The paper was prepared within the implementation of the basic part of the government task for the project № 7.7858.2017/BP: “Development of the scientific principles of the techniques for determining the stress-strain state of the large-sized storage tanks during the differential settlement of the substructures and foundations”.

References

1. Slepnev, I.V.: Stress-strain elastic-plastic state of steel vertical cylindrical tanks with inhomogeneous base settlement. Moscow Engineering and Building Institute, Moscow (1988)
2. Kononov, P.A., Mangushev, R.A., Sotnikov, S.N., Zemlyansky, A.A.: Foundations steel tanks and deformation of it's bases, 336 p. The Association of construction universities, Moscow (2009)
3. Zemlyansky, A.A.: The design principles and experimental and theoretical studies of large tanks, Balakovo, 416 p. (2006)
4. Vasilev, G.G., Salnikov, A.P.: Analysis of causes of accidents with vertical steel tanks. *J. Oil Ind.* **2**, 106–108 (2015)
5. Nekhaev, G.A.: Design and calculation of steel cylindrical tanks and tanks low pressure, 216 p. The Association of Construction Universities, Moscow (2005)
6. Yasin, E.M., Rasshchepkin, K.E.: The upper zones stability of vertical cylindrical tanks for oil-products storage. *J. Oil Ind.* **3**, 57–59 (2008)
7. Guan, Y., Huang, S., Zhang, R., Tarsenko, A.A., Chepur, P.V.: Influence of laminated rubber bearings parameters on the seismic response of large LNG storage tanks. *J. World Inf. Earthq. Eng.* **1**, 219–227 (2016)
8. Russian Standard GOST 31385-2008, The vertical cylindrical steel tanks for oil and oil-products. General technical conditions, Standartinform, Moscow (2010)
9. Russian Standard RD-23.020.00-KTN-283-09. The rules of the repair and reconstruction of tanks for oil storage capacity of 1000-50000 cubic meters, OAO AK “Transneft”, Moscow (2009)
10. Russian Standard GOST 52910-2008, The vertical cylindrical steel tanks for oil and oil-products. General technical conditions, Standartinform, Moscow (2008)
11. Tarasenko, A., Gruchenkova, A., Chepur, P.: Joint deformation of metal structures in the tank and gas equalizing system while base settlement progressing. *J. Procedia Eng.* **165**, 1125–1131 (2016)

12. Russian Standard RD-23.020.00-KTN-170-13, Requirements for the installation of metal structures vertical cylindrical tanks for oil and oil-products storage at new building facilities, technical re-equipment and reconstruction, OAO AK "Transneft", Moscow (2013)
13. Bruyaka, V.A., Fokin, V.G., Soldusova, E.A., Glazunova, N.A., Adeyanov, I.E.: Engineering analysis in ANSYS Workbench, Samara State Technical University, Samara (2010)
14. Beloborodov, A.V.: Evaluation of the finite element model construction quality in ANSYS. Ural State Technical University, Ekaterinburg (2005)
15. Russian Standard RD-23.020.00-KTN-018-14, Main pipeline transport of oil and oil products. Vertical steel tanks for oil storage capacity of 1000-50000 cubic meters. The design standards, OAO AK "Transneft", Moscow (2014)

Justification of the Most Rational Jack Method in the Corroded Tank

Mikhail Tarasenko^(✉)  and Alexander Tarasenko 

Industrial University of Tyumen, Volodarskogo str., 38, Tyumen 625001, Russia
tma72@rambler.ru

Abstract. The article considers the problem of carrier reconstruction capacity of tanks with intolerable corrosion flaws. The authors propose a method for the temporary carrier reconstruction until the next overhaul repair. Analytical dependences of binding band ring parameters for tanks with the capacity of 20.000 m³ are obtained. The installation process of the banding ring is developed. The proposed method was tested on OPS “Grushovaya” to strengthen the shells in VST-20000.

Keywords: Inherent rigidity · VST · Tank · ANSYS · Differential settlement

1 Introduction

A large number of the tanks in service have been used for more than 20 years. Available tanks are characterized by high corrosion deterioration [1, 2]. Vertical steel tanks (VST) continue to operate, despite the excess of the service time [3–7]. When carrying out partial technical diagnosis, unacceptable corrosion flaws of the tank shells are often identified, which discredits the further facility operation due to strength condition disregard. According to the current normative-technical documentation, the subject must be removed from service and repaired [8–11]. As a result, the owner incurs considerable losses due to the reduction of commodity-transport operations. To increase the lifetime of the object with corrosion damage until the next overhaul, the level of oil loading is reduced, while economic losses are also quite substantial.

The authors analyzed technical diagnostics reports of 25 tanks VST-20000, operating on the territory of Western Siberia for more than 20 years. All tested tanks were manufactured by a rolling method of steel 09G2S, thickness of the first zone of the shell is 12.8 mm. While analyzing the results of technical diagnostics, it is established that a large number of the corrosion defects are located at the bottom, T-butt weld and the first zone of the tank shell, owing to the following reasons: the presence of produced water near the bottom, the presence of fields of static electricity, the biological activity of sulfate-deoxidizing microorganisms etc. A constructed histogram of the corrosion defects distribution on the height of the 1 zone in tanks (Figure-1) shows that the greatest number of them is concentrated near the T-butt weld and it almost does not occur at a distance of 20 cm from it.

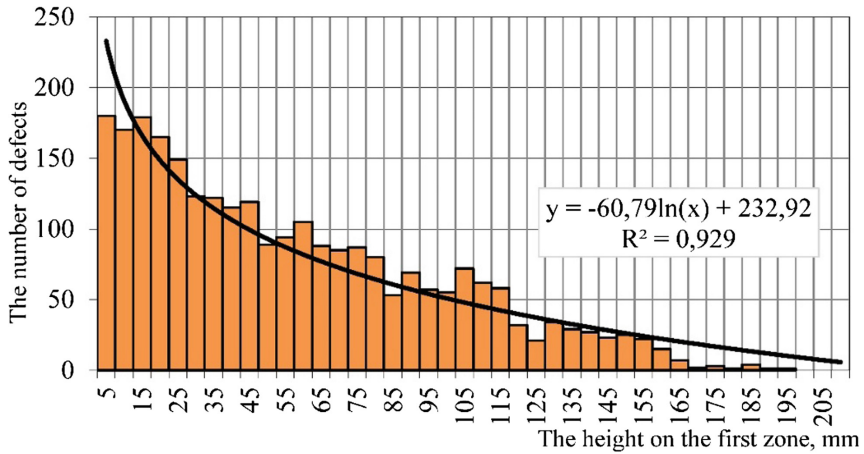


Fig. 1. Histogram of the corrosion flaws distribution on the height of the 1 zone in a tank.

To describe trends in the data and be able to analyze the problem of prediction, the histogram is characterized with a function. Coefficient of determination is specified (R^2) for the function, which reflects the closeness of the trend line values to the actual data and can take values from 0 to 1. A trendline is most true when the value of R^2 is close to 1. In Fig. 1 the trend line has a value of $R^2 = 0,929$, which indicates a good agreement between a pitch line and the data.

Analyzing the nature of corrosion damage, as well as types of defects, along with a continuous corrosion, it is pitting corrosion that is most often found, characterized by the appearance of single or multiple damages on the surface of the metal, the depth and lateral dimensions of which are comparable among themselves and range from a fraction of a millimeter to several millimeters (Figs. 2 and 3).



Fig. 2. Ulcerative individual corrosion defect of the first zone in the vertical steel tank.



Fig. 3. Multiple ulcerative corrosion damage of the T-butt weld in the vertical steel tank.

So before solving the main task – the restoration of the bearing capacity of the tank, you should ensure yourself that the stress concentration in the vicinity of single defect points in the tank shell does not change the overall picture of the stress-strain state of the tank during operation.

2 Methods

Exploring the influence of such defects, the tank shell has to be demonstrated in the form of a metal plate. Given the small curvature of the shell, this assumption will not affect the accuracy of calculations. Let’s consider the most unfavorable case of the through-shell damage in the tank shell. Considering that the tank shell is subject to biaxial tension, the task is formulated as the calculation of stresses near a hole in the tank shell exposed to vertical and horizontal loads that are continuously distributed on its outer contour (Fig. 4). Analyzing the data obtained, we should conclude that the

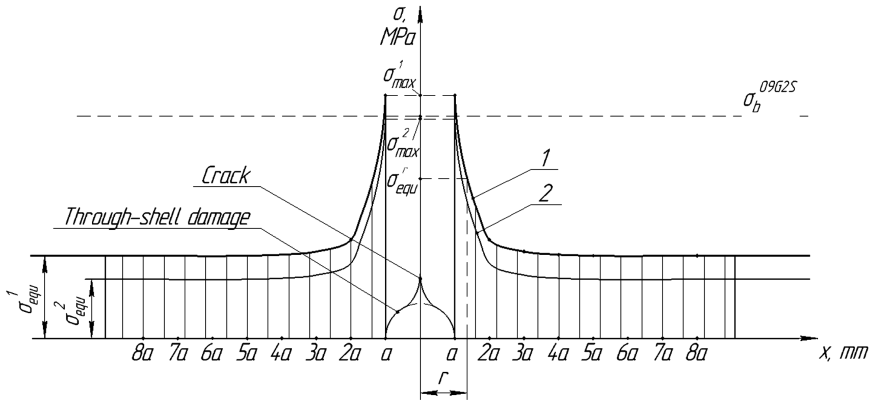


Fig. 4. Distribution diagram σ_{equ} near a hole with radius a : 1 – decay curve of equivalent stresses for the filled VST with level of the oil filling 11.5 m; 2 – decay curve of equivalent stresses for the filled VST with level of the oil filling 10.5 m; $\sigma_{Eq. 1}$ – maximum equivalent stress for filled VST level of the oil filling 11.5 m; $\sigma_{Eq. 2}$ – maximum equivalent stress for filled VST level of the oil filling 10.5 m; σ_{b09G2S} – ultimate resistance for steel 09G2S; σ_{equ}^r – the value of the equivalent stresses at a distance r from the center of the hole.

border of the defect is characterized by tension that exceeds the ultimate resistance for steel 09G2S. However, the tension is fading fast, and at a distance of 30 mm from the border of the defect it is only 7% higher than the overall equivalent stress σ_{equ} . Thus, stress spikes are local in nature and do not affect the total SDS of the tank.

To restore the bearing capacity of a corroded tank, the authors propose to strengthen the tank shell with binding band rings. While using this method, you can achieve a temporary increase of strength and stability of the tank shell up to standard values, stated differently, to restore the carrying capacity of the tank. The method of stiffening the shells with the tires is recommended in the normative-technical documentation [11] for tanks with relatively small storage capacity, up to 5.000 m³. The authors have considered butting-up tanks with a pot of 20.000 m³ capacity. Binding band ring strengthening is basically split steel rings installed on the outer side of the tank shell, tightened by threaded joints. 10–20 rings at a height of 4 belts can be installed on a tank, depending on the corrosive wear of the metal and geometrical cross-section of the strip. The number of such rings and strengthening of their tension is determined through the calculations [12, 13]. While tightening the binding band rings, it is necessary to prevent the loss of lateral stability of a cylindrical shell. Studies have shown that to solve the assigned tasks, it is possible to be limited to a single retaining ring. Selection of the binding band ring parameters is conducted by varying the cross sectional area as the construction works only in tension. Thus, you can use various metal structures as binding band rings, for example, steel bands or cables. If you need to replace one design of the binding band ring to another, you should respect the equality of the areas of their cross sections, while steel type is irrelevant (for the case of corrosion under consideration).

So as to select the best way to reinforce the tank shell, the authors have developed and verified a finite-element model of the tank given the large displacements of the shell and plastic material properties that allows taking into account the contact interaction of base-bottom and side-binding band ring, giving the possibility to evaluate the influence of corrosion of the lower belt on SDS construction in VST with stiffener.

Assessment of SDS structures obtained using the finite element method [14, 15] is traditionally conducted by comparing the calculated equivalent stress of the fourth strength theory (von Mises) in the tank model with yield strength in the steel, out of which the actual construction is made of, and also evaluation of deviation from the vertical forming shell of the tank. When installing a binding band ring, a significant impact on SDS of VST has a height of installation (H) and the geometrical dimensions of the ring (the width “h” and thickness “b”). Basic combinations of parameters are presented in Table 1.

Table 1. Options for the location and geometric parameters of the retaining ring.

	H = 20; 100; 200; 300; 400; 500; 600; 700; 800; 900; 1000 mm			
h, mm	100	200	300	400
b, mm	10; 20; 30	10; 20; 30	10; 20; 30	10; 20; 30

3 Results

The calculations were carried out for all parameter combinations given in Table 1. As a result, the gradients of stresses and displacements of the tank shell are obtained (Fig. 5).

Setting the binding band ring at the level of $H = 100$ mm from T-butt weld with some combinations of width (h) and thickness (b) of the ring, led to satisfactory results. Thus, peak stress is set with the linear dimensions of retaining ring ($h \cdot b$). It is similar with other ratios ($h \cdot b$). The result is a surface plot (Fig. 6), allowing to estimate the dependence of maximum equivalent stresses on the geometric dimensions of the binding band ring at the level of 100 mm from T-butt weld.

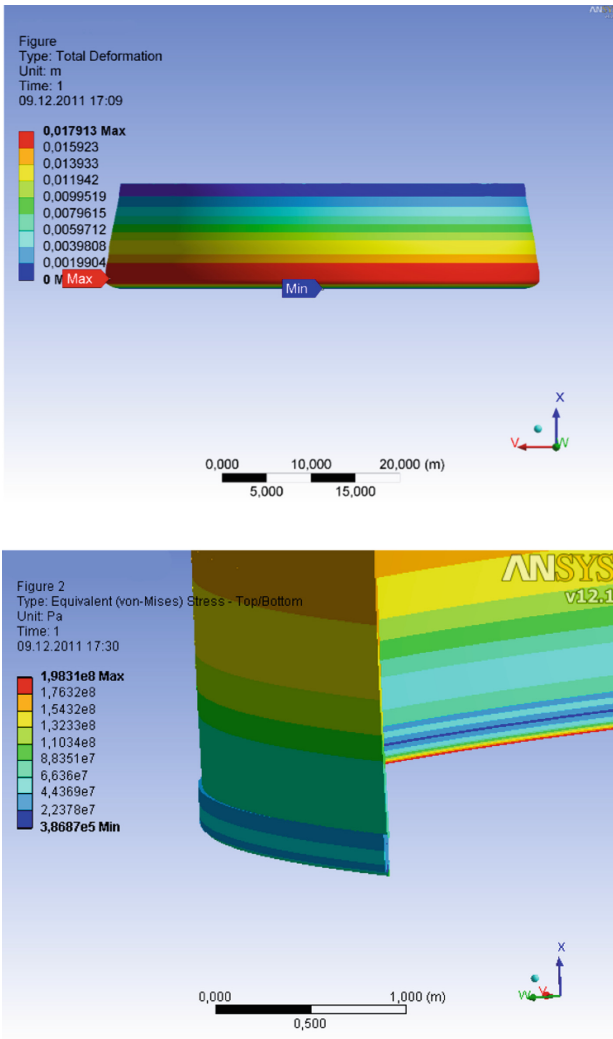


Fig. 5. The gradients of stresses and displacements in the FE model of the tank.

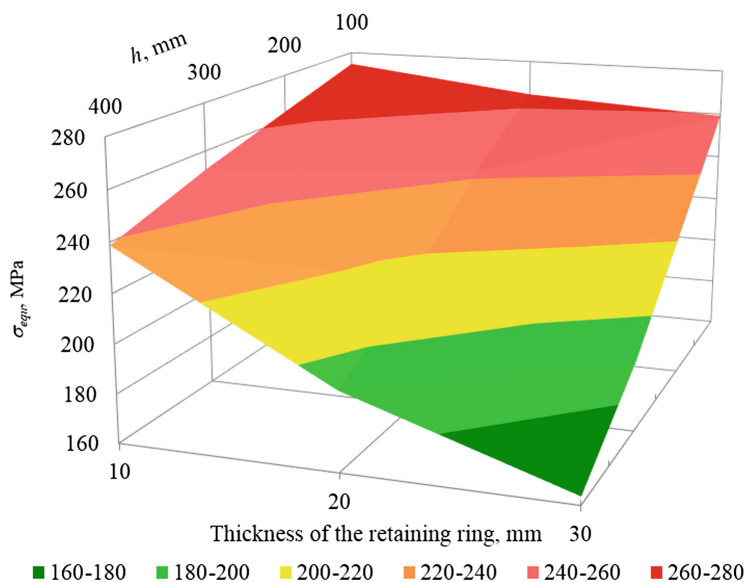


Fig. 6. Surface plot of the maximum stresses distribution in the tank shell at the level of 100 mm from T-butt weld depending on the width (h) and the thickness of the retaining ring.

Diagrams of the surface are similarly constructed when $H = 20, 200, 300$ mm (Fig. 7).

It should be noted that strength assessment of the retaining ring was conducted for all combinations of numerical experiments (Fig. 8) by analogy with the assessment of the tank shell strength. It was found that for all combinations of experiment parameters at which the maximum equivalent stress in the tank shell does not exceed the allowable values, the strength condition of the stiffening ring is also observed.

4 Discussion

Analyzing the dependencies of surface diagrams, the most rational dimensions of a retaining ring and places of its setting are determined (Table 2).

Thus, the most common VST-20000 in Western Siberia, applied for the storage of crude oil, is assigned for the most rational jack method for the corrosion damage from 1 to 8 mm, that involves the setting of the retaining ring 200×10 mm at the height of 20 mm from the T-butt weld.

The process of retaining ring setting is recommended to perform in the following way. Set temporary supports on a base ring. After the construction, the ring is tightened by means of screw connections (measuring the torque), so that the tank does not lose stability in a drained condition. The proposed method was tested on OPS “Grushovaya” to strengthen the tank shell.

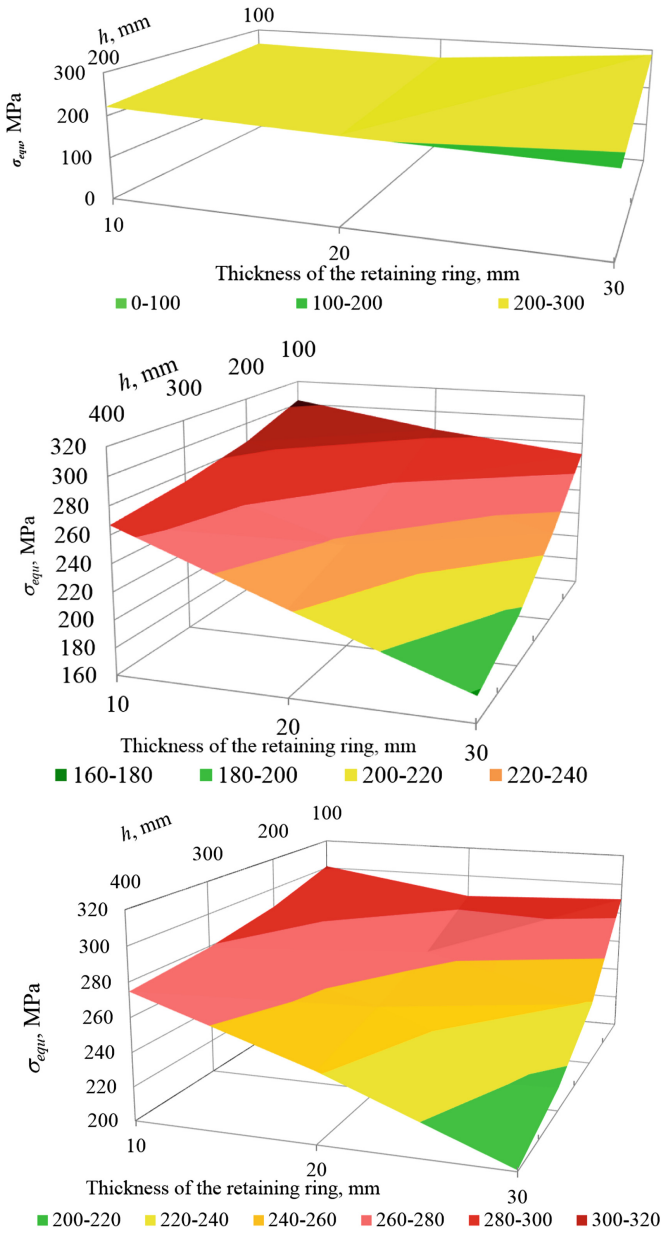


Fig. 7. Surface plot of the maximum stresses distribution in the tank shell at the level of 20, 200 and 300 mm from T-butt weld depending on the width (h) and the thickness of the retaining ring.

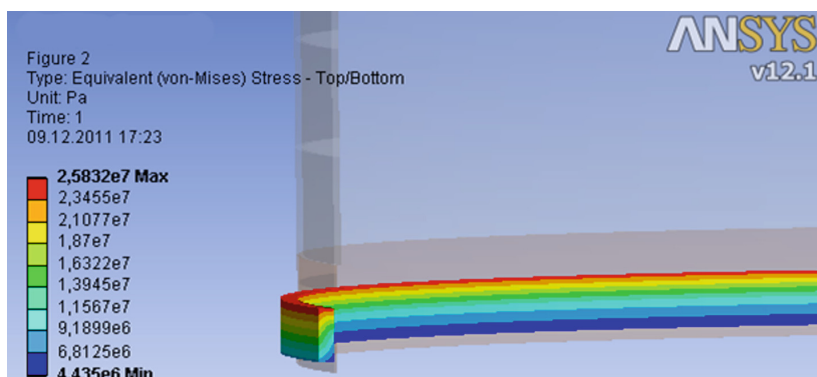


Fig. 8. Gradient stress of the retaining ring with the size of 100×30 , set at the height of 20 mm from the T-butt weld.

Table 2. The most rational dimensions of a retaining ring and places of its setting.

Machine height H, mm	Geometrical dimensions of the binding band ring			Maximum active stresses in the shell σ_{equ} , MPa
	Width (h), mm	Thickness (b), mm	Cross-section, sm^2	
20	200	10	20	221.1
100	200	30	60	223.6
100	300	20	60	213.9
200	300	30	90	188.7
200	400	20	80	221.3
300	300	30	90	214

5 Conclusions

A finite element model of the tank is constructed, taking into account large shell displacements and non-linear material properties, which allows taking into account the contact interaction of the bottom with the base and shell with a retaining ring. This model allows us to estimate the effect of corrosion of the lower zone to the SDS construction in VST with stiffener.

The values of maximum equivalent stresses in steel structures of VST, depending on the geometric dimensions of the retaining ring at different heights from T-butt weld, are obtained. The most rational jack method in the corroded tank in VST-20000 is justified, that involves the setting of a retaining ring 200×10 mm at the height of 20 mm from the T-butt weld. This technique has been successfully tested at the production facility.

Acknowledgement. The paper was prepared within the implementation of the basic part of the government task for the project № 7.7858.2017/BP: “Development of the scientific principles of the techniques for determining the stress-strain state of the large-sized storage tanks during the differential settlement of the substructures and foundations”.

References

1. Korshak, A.A.: Diagnostics of oil pumping stations objects, Ufa, 176 p. (2008)
2. Alifanov, L.A.: Normalization shape defects and resource vertical cylindrical tanks, Krasnoyarsk, 224 p. (2003)
3. Salnikov, A.P.: Evaluation of stress-strain state of the tank according to the results of terrestrial laser scanning, Russian state University of oil and gas named Gubkin I. M., Moscow (2016)
4. Gorelov, A.S.: Inhomogeneous soil bases and their impact on vertical steel tanks. Nedra, Saint Petersburg (2009)
5. Konovalov, P.A., Mangushev, R.A., Sotnikov, S.N., Zemlyansky, A.A.: Foundations steel tanks and deformation of it's bases, 336 p. The Association of Construction Universities, Moscow (2009)
6. Tarasenko, A., Chepur, P., Chirkov, S.: Justification of a method for complete lifting of a tank to repair its base and foundation. In: AIP Conference Proceedings, vol. 1772, p. 060010 (2016)
7. Gruchenkova, A., Tarasenko, A., Chepur, P., Tarasenko, D.: Justification of the necessity to harmonize Russian and international standards concerning the determination of allowable VST immersion. In: AIP Conference Proceedings, vol. 1800, p. 040019 (2017)
8. Russian Standard RD-23.020.00-KTN-271-10, Rules of technical diagnostics of tanks. OAO AK “Transneft”, Moscow (2010)
9. Russian Standard RD-08-95-95, Regulations on the system of welded vertical cylindrical tanks for petroleum and petroleum products technical diagnostics. Industrial Safety, Moscow (2002)
10. Russian Standard RD-23.020.00-KTN-283-09, The rules of the repair and reconstruction of tanks for oil storage capacity of 1000-50000 cubic meters. OAO AK “Transneft”, Moscow (2009)
11. Russian Standard RD-34.23.601-96, Recommendations for the repair and safe operation of metal and reinforced concrete tanks, Moscow (1998)
12. Recommendations for restoring the bearing capacity of cylindrical tanks by the method of reinforcing the wall with steel ring bandages, Astrakhan (1984)
13. Recommendations for the operation of tanks reinforced by the method of substitution of ring bandages, Astrakhan (1984)
14. Bruyaka, V.A., Fokin, V.G., Soldusova, E.A., Glazunova, N.A., Adeyanov, I.E.: Engineering analysis in ANSYS Workbench. Samara state technical University, Samara (2010)
15. Beloborodov, A.V.: Evaluation of the finite element model construction quality in ANSYS. Ural state technical University, Ekaterinburg (2005)

The Investigation of Freezing and Thawing Processes of Metal Foundations Ground of Pipelines

Sergey Kudryavtsev , Vyacheslav Kovshun ^(✉) ,
and Aleksandra Mut 

Far Eastern State Transport University,
47 Seryshev St., 680021 Khabarovsk, Russia
prn@festu.khv.ru

Abstract. The paper considers the definition of the freezing and thawing indices of soils in settlements along the route of the oil pipeline “Kuyumba-Taishet-Kozmino”, estimated geocryological conditions, determine the depth of soil freezing and frost heaving force with the help of numerical simulation and developed measures for their elimination. In areas with seasonally freezing soils accepted measures to eliminate frost heaving forces and in areas with permafrost are used seasonally cooling devices.

Keywords: Metal Foundations · Numerical simulation
Freezing and Thawing Indexes

1 Introduction

During the construction of the pipelines located in the permafrost zone, the main danger is the formation around the metal pile foundations thawing soil. Major inclusion of ground ice thaw causes thermokarst failures and subsidence of the foundation soil.

Thermopiles are used to prevent thawing of soil around the basement. Thermopiles designed to maintain the soil in a frozen state, which ensures the stability of structures on piles, keep frozen ground around the pile. At the same time it is the foundation of the pipeline. The technology of seasonally active cooling device is the heat transfer device (thermosyphon), which in winter extracts heat from the ground and transfers it to the environment. An important feature of this technology is the natural action, it does not need an external power source. In winter convection circulation of coolant in the liquid device allows lowering the temperature of frozen soil foundation.

With the onset of summer, when the temperature of the upper located on the outside air, the cone (capacitor) device is higher than the temperature of the coolant circulation is stopped and the process is suspended with partial thawing of the active layer of soil in the summer.

There are concepts of freezing index \bar{F} and thawing index \bar{U} in engineering practice. Comparing the indices \bar{F} and \bar{U} we can estimate the geocryological conditions of a particular locality. If $\bar{F} > \bar{U}$, the frozen soil grows year after year, as a result, higher layer of permafrost is formed [1–3].

We conducted a research of the freezing and thawing processes along the Kuyumba-Taishet-Kozmino oil pipeline route (Fig. 1), and with help of the freezing and thawing indices we determined regions with permafrost soils and seasonally freezing.



Fig. 1. Oil pipeline route.

2 Methods of Numerical Modeling

Investigation of the processes of freezing and thawing of the soil base of the thermopiles foundation is expedient to carry out the methods of numerical simulation [2, 4].

Numerical simulation of the thermopile foundation in permafrost performed in the software package «FEM-models», developed by Geotechnics St. Petersburg under Professor V.M.Ulitskogo. Integral part of «FEM-models» is a program «Termoground», which allows you to explore with the help of numerical simulation in the spatial setting processes of freezing, frost heaving and thawing in the annual cycle of the finite element method [7].

General equation describing the freezing and thawing processes for a transient thermal regime in a three dimensional soil space can be expressed as following:

$$C_{th(f)}\rho \frac{\partial T}{\partial t} = \lambda_{th(f)} \left(\frac{\partial^2 T}{\partial x^2} + \frac{\partial^2 T}{\partial y^2} + \frac{\partial^2 T}{\partial z^2} \right) + q_v \tag{1}$$

where $C_{th(f)}$ - specific heat of soils (frozen or thawed), J/kgK; ρ - soil consistency, kg/m³; T - temperature, K; t - time, s; $\lambda_{th(f)}$ - thermal conductivity of soil (frozen and thawed), W/mK; x, y, z - coordinates, m; q_v - internal heat source capacity, W/m³ [3].

The core of a mathematical modeling of thermophysical processes in “Termoground” program is the model of high ice, thawed and frozen soils offered by Tsytovich, Kronik and Kiselev [7].

The major factors determining the defined surface temperatures on the embankment elements and the adjacent territory are the atmospheric air temperature and the heat exchange conditions between the air and the structure surface that depend on the wind conditions, solar radiation, vaporation, and others [1-3].

The calculation value of the defined average monthly air temperature is determined from the formula:

$$T_c = T_{av} + \Delta t_r - \Delta t_e \quad (2)$$

where T_{av} is average monthly air temperature, °C; Δt_r and Δt_e are corrections to average monthly air temperatures due to solar radiation and evaporation, °C.

The correction to air temperature due to solar radiation (Δt) is calculated according to formula:

$$t_r = \frac{R}{0.073\alpha} \quad (3)$$

where R is monthly sum of radiation balance for the considered element of the surface, kkal/sm² · months; α is surface heat exchange coefficient, kkal/M² · h · °C, and its empirical-formula dependence is:

$$\alpha = 10\sqrt{V} \quad (4)$$

where V is wind velocity.

The monthly sums of radiation balance for horizontal surfaces are determined from the formula:

$$R_o = Q_o \times k - 0.42 \quad (5)$$

where Q_o is average monthly sum of total solar radiation striking the horizontal surface, kkal/sm² · months; k – empirical coefficient in terms of the surface reflecting capacity (albedo).

The monthly sums of radiation balance for bevel faces (subgrade embankments) are determined from the formula:

$$R_\beta = (m_\beta I_o + P_\beta D_o) \times k - 0.42 \quad (6)$$

where I_o and D_o – average monthly sums of direct and diffuse radiations striking the horizontal surface, kkal/sm² · months, the values being taken from the climatological guide; m_β – nondimensional coefficient in terms of the bevel face angle to horizon and spatialization of the face for beam radiation intake.

P_β – coefficient in terms of the bevel face angle to the horizon and spatialization of the face for a sky radiation intake that is determined from the formula:

$$P_\beta = \cos^2 \frac{\beta}{2} \quad (7)$$

where β – angle of the bevel face to the horizon, degrees.

The thermophysical characteristics of the roadway and roadbed soils in thawed and frozen states are taken in accordance with the SR 25.13330.2012 – Permafrost Foundation Engineering Standards. The relative thawing strains of permafrost are determined according to the results of the standard laboratory tests. In this case the relative stresses are calculated according to the formula:

$$\varepsilon_{th} = A_{th} + \delta_{ith} \tag{8}$$

where A_{th} is the relative strain of thaw thermal subsidence; δ_{ith} is the relative strain of thaw loading subsidence.

$$\delta_{ith} = m_{0th} \cdot p_i \tag{9}$$

where m_{0th} is the coefficient of compressibility of thaw soil (MPa-1); p_i is the compacting vertical stress (MPa) [3].

3 Determination of Freezing and Thawing Indices

There is the concept of freezing index F in engineering practice. It is calculated as the sum of the products of the absolute values of the negative temperature (T_i) by the time (Δt_i):

$$\bar{F} = \sum (|T_i| \cdot \Delta t_i) (\text{°C} \cdot \text{hour}) (\text{°C} \cdot \text{Day}) \tag{10}$$

The annual freezing index F is usually found using the monthly mean values of the negative air temperature of the year.

The annual thawing index U can be found by using the monthly averages of the positive air temperatures of the year [1–3].

The values of freezing and thawing indices are given in the chart 1 (Table 1).

Table 1. Freezing and thawing indices.

Area	Freezing index \bar{F}	Thawing index \bar{U}
Kuyumba	3844.5	1615.2
Taishet	2256.6	2113.4
Bratsk	2417	1865.8
Skovorodino	3576.9	1936.9
Komsomolsk-on-Amur	2678.1	2444.3
Khabarovsk	2252.9	2881.1
Partizansk	1197.6	2851.3

Average values of annual freezing indices and thawing for several settlements located along the way of the Kuyumba-Taishet-Kozmino oil pipeline are shown in Fig. 2.

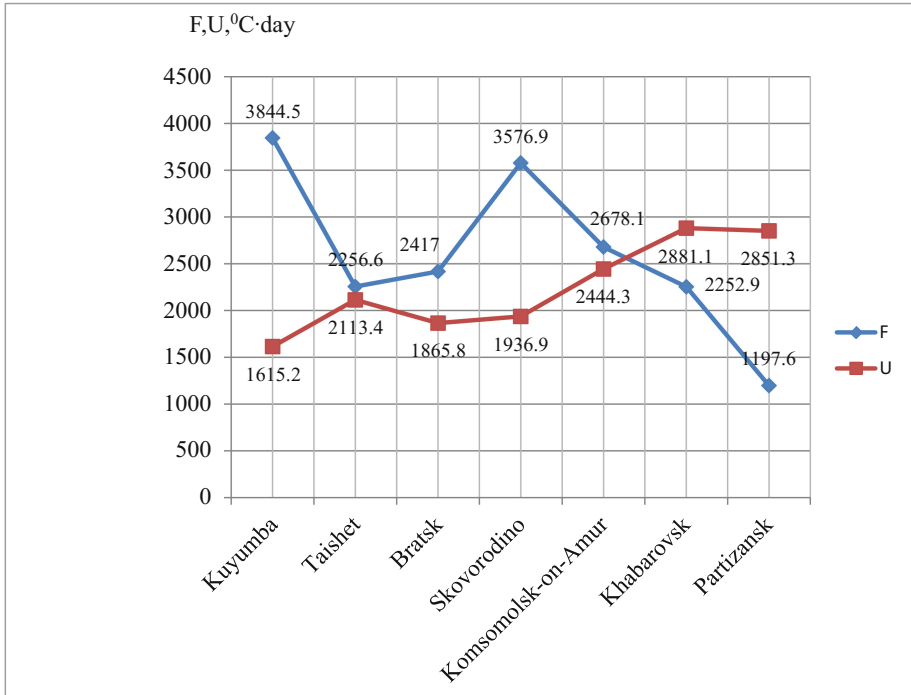


Fig. 2. Changing of the lines of freezing indexes (F) and thawing (U) from Kuyumba to Partizansk.

Analyzing the values of the freezing index (F) and thawing (U), we can note the following. For example, there are twofold excess of freezing index over the thawing index in Skovorodino, so the permafrost capacity reaches a considerable value. In Bratsk, where the excess of F over U is only 22%, permafrost occurs in the form of islands and lenses.

In the cities up to Komsomolsk-on-Amur ($F > U$), frozen ground capacity reaches a considerable value, as a result frozen upper layers of the soil dominate in this area, and after Komsomolsk-on-Amur ($F < U$) there are seasonal freezing upper layers of the soil, since a warm time of the year all the winter frozen ground has time to thaw.

To prevent thawing of soil around the foundation use seasonal-cooling devices named thermopiles.

4 Numerical Simulation

Numerical simulation of the work of the thermopiles for creating a frozen ground condition of the base was made in the software package «FEM-models», developed by Geotechnics St. Petersburg under Professor V.M. Ulitskogo. Integral part of «FEM-models» is a program «Termoground», which allows you to explore with the help of numerical simulation in the spatial setting processes of freezing, frost heaving and thawing in the annual cycle of the finite element method [7].

For installation above-ground pipeline on permafrost used seasonally-cooling device - thermosiphons that reduce the depth of thawing of the soil and prevent buckling foundations during the freezing of the active layer base pipeline (Fig. 3).

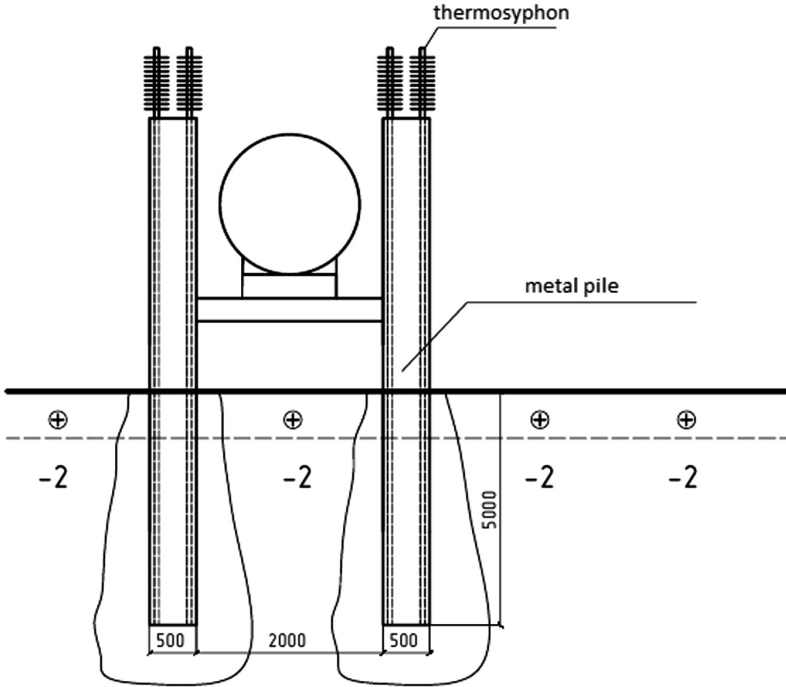


Fig. 3. The settlement scheme.

Thermopiles designed to maintain the soil in a frozen state, which ensures the stability of structures on piles, keeps frozen ground around the pile and at the same time is the foundation of the pipeline. The technology seasonally active cooling device is the heat transfer device (thermosyphon), which in winter extracts heat from the ground and transfers it to the environment. An important feature of this technology is the natural action, it does not need an external power source. In winter convection circulation of coolant in the liquid device allows lowering the temperature of frozen soil foundation. With the onset of summer, when the temperature of the upper located on the outside air, the cone (capacitor) device is higher than the temperature of the coolant circulation is stopped and the process is suspended with partial thawing of the active layer of soil in the summer.

We investigated the metal thermopile foundations with a diameter of 0.5 m and a length of 5 m. The power of the active layer is about 1 m. Ground foundation - permafrost loam soil with a temperature of minus 20 °C. Investigated thermophysical state of soil base in the annual cycle of temperatures without work thermosiphon and integrated into the metal pile thermosiphons (Fig. 4).

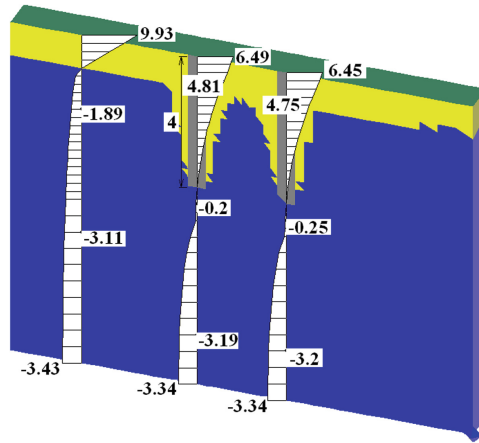


Fig. 4. Zone thawing soil around thermopiles and diagrams of soil temperature with depth of the September, without thermosiphons.

As a result of the research using the thermopiles decrease the depth of thawing from 4 m to 2. The device operates without negative consequences for environmental conditions.

Using the seasonally-cooling devices significantly reduces the depth of thawing of the soil around the base of thermopiles with integrated thermosyphon. The depth of thawing around the pile can be reduced depending on the power and the amount used thermosiphons. Using thermosiphons prevent thawing and buckling foundation during the freezing of the active layer of the thermopile foundation of pipeline.

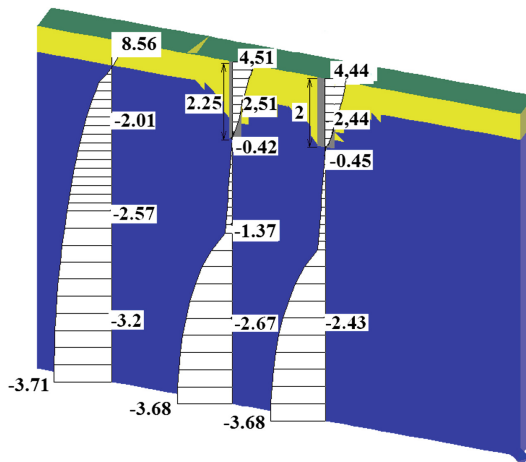


Fig. 5. A figure caption is always placed below the illustration. Short captions are centered, while long ones are justified. The macro button chooses the correct format automatically.

5 Conclusions

1. The aim of this investigation is to prove the possibility of using seasonal cooling devices to reduce the depth of thawing of the base and prevent buckling foundations during the freezing of the active layer base oil pipeline on permafrost.
2. With the help of freezing and thawing indices was determined that frozen soils predominate up to Komsomolsk-on-Amur, but starting from Khabarovsk there are seasonally-freezing soils (Fig. 2).
3. Pipelines in the permafrost advisable to lay above-ground to prevent deformation and buckling and the preservation of permafrost in natural conditions using seasonally-cooling devices.
4. Without seasonal cooling devices the soil thaws without action of pile up to 1 m, and around piles thaws to a depth of 4 m. The temperature of the soil is positive and ranges from 0 to 6.5. Under the edge of the pile soil temperature is -0.2° , which corresponds to the plastic-frozen state.
5. With seasonal cooling devices the soil thaws without action of pile up to 0.5 m, and around piles thaws to a depth of 2.25 m. The temperature of the soil is positive and ranges from 0 to 4.51. Under the edge of the pile soil temperature is -0.45° , which corresponds to the plastic-frozen state.
6. As a result Fig. 5 shows a reduction of the depth of thawing soil using seasonal cooling devices. The depth of thawing depends on the capacity and number of units of the thermosyphons.
7. The Economic effect of using thermopiles based on a reduction up to 50% of maintenance foundations of pipeline system.

References

1. Ulitsky, V.M., Paramonov, V.N., Kudryavtsev, S.A., Shashkin, A.G., Shashkin, K.G.: Frost heave soil. In: 2nd Canadian Specialty Conference on Computer Applications in Geotechnique, Winnipeg, Canada, pp. 167–171 (2002)
2. Ulitsky, V.M., Paramonov, V.N., Kudryavtsev, S.A., Shashkin, K.G., Lisyuk, M.B.: Contemporary geotechnologies providing safe operation of railway embankments in permafrost conditions. In: 8th International Conference on Permafrost. Extended Abstracts, Reporting Current Research and New Informational, Zurich, Switzerland, 20–25 July 2003, pp. 167–168 (2003)
3. Kudryavtsev, S.A., Berestyanyy, Y.B., Goncharova, E.D.: Engineering and construction of geotechnical structures with geotechnical materials in coastal arctic zone of Russia. In: The 23rd International Offshore (Ocean) and Polar Engineering Conference Anchorage, Alaska, USA, 30 June–5 July, pp. 562–566 (2013)
4. Kudryavtsev, S.A., Berestiani, Y.B., Valtseva, T.Y., Kazharskyi, A.V., Goncharova, E.D.: Predictive numerical modeling of a permafrost thermal regime in the subgrade support of a railroad section in Russia. In: The 1st International Symposium on Transportation Soil Engineering in Cold Regions. Sciences in Cold and Arid Regions, Xinin, China, vol. 5, no. 4, pp. 404–407, August 2013

5. Kudryavtsev, S., Kazharskiy, A.: Numerical modeling of moisture migration process depending on velocity of soil freezing. In: The 5th International Geotechnical Symposium-Incheon, Geotechnical Engineering for Disaster Preventional and Reduction, pp. 176–180 (2013)
6. Kudryavtsev, S., Paramonov, V., Sakharov, I.: The freezing and thawing of ground (practical examples and finite-element calculations), 248 p. (2014)
7. Kudryavtsev, S., Berestianiy, Y., Valtseva, T., Mikhailin, R., Goncharova, E.: Motorway structures reinforced with geosynthetic materials in polar regions of Russia. In: The 24rd International Offshore (Ocean) and Polar Engineering Conference, pp. 502–506 (2014)
8. Kudryavtsev, S., Berestianiy, Y., Kazharskiy, A., Goncharova, E.: Study of moisture migration in clay soils considering rate of freezing. In: The 10th International Symposium on Permafrost Engineering in Cold Regions. Sciences in Cold and Arid Regions, pp. 474–478 (2014)
9. Kudryavtsev, S., Valtseva, T., Mikhailin, R., Goncharova, E.: Using designs of variable rigidity on weak soils roads in the Russian Far. In: East 6th International Geotechnical Symposium on Disasters Mitigation in Special Geoenvironmental Conditions, pp. 409–412 (2015)
10. Ulitskii, V., Paramonov, V., Sakharov, I., Kudryavtsev, S.: Bed – structure system analysis for soil freezing and thawing using the termoground program. In: Soil Mechanics and Foundation Engineering: 2015, pp. 1–7. Springer, New York, Consultants Bureau (2015). ISSN 0038-0741
11. Paramonov, V., Sakharov, I., Kudryavtsev, S.: Strengthening thawed permafrost base railway embankments cutting berms. In: MATEC Web of Conferences 15. Cep. “15th International Conference “Topical Problems of Architecture, Civil Engineering, Energy Efficiency and Ecology - 2016”, TPACEE 2016”, p. 05002 (2016)
12. Sakharov, I., Paramonov, V., Kudryavtsev, S.: Forecast the processes of thawing of permafrost soils under the building with the large heat emission. In: MATEC Web of Conferences 15. Cep. “15th International Conference “Topical Problems of Architecture, Civil Engineering, Energy Efficiency and Ecology - 2016”, TPACEE 2016”, p. 05007 (2016)
13. Kudryavtsev, S., Kazharskiy, A., Goncharova, E., Valtseva, T., Kotenko, Zh.: Thermo-physical feasibility of railway embankment design on permafrost when projecting side tracks. In: 15th International Scientific Conference “Underground Urbanisation as a Prerequisite for Sustainable Development”, St. Petersburg, Russia, 12–15 September 2016. *Procedia Eng.* **165**, 1080–1086 (2016)
14. Kudryavtsev, S., Maleev, D., Tsvigunov, D., Goncharova, D.: Disalgnment of railroad poles as dynamic effect of rolling stock. In: 15th International Scientific Conference “Underground Urbanisation as a Prerequisite for Sustainable Development”. *Procedia Eng.* **165**, 1858–1865 (2016)

Sizing the Residual Deformation of Metal Structures in the Tank After Shell Replacement

Alexander Tarasenko¹ , Petr Chepur¹ ,
and Alesya Gruchenkova² 

¹ Industrial University of Tyumen,

Volodarskogo str., 38, Tyumen 625001, Russia

² Surgut Oil and Gas Institute, Entuziastov str., 38, Surgut 628404, Russia
alesya2010-11@yandex.ru

Abstract. The work focuses on numerical simulation of the deformation process in a metal tank after shell replacement of the first ring taking into account thermal effects during the welding process. SYSWELD 2016.5 was implemented so as to determine the welding deformation of T-joint area of the shell and annular plate. The average value of the vertical displacement for the entire part has made up to 0.86 mm, this value is adopted as the base for further calculations in ANSYS. The calculations showed that the neglect of thermal deformation caused by welding process impairs the accuracy of the final values of stress and strain by 4.4% and 5.9%, respectively.

Keywords: Tank · SYSWELD · Weld · Finite-element model · ANSYS
Stress-strain state

1 Introduction

Vertical steel tanks are essential structures that ensure a continuous cycle of commodity-transport operations in the logistic system of oil transportation from production sites to storage sites and finally to the consumer. It is essential to regularly conduct technical diagnostics and, if necessary, to carry out repair work to maintain the tanks in an operating condition so as to carry out reliable operation of such facilities. One type of repair is the replacement of the shell with new makeup steel plates. The shell of the tank, according to the results of many well-known works [1–5] is one of the most load-bearing elements receiving the load from the weight of the product as well as from the environment (wind, precipitation, seismic action, the vacuum pressure and the pressure oil vapor, etc.). Therefore the replacement of the shell by cutting out an old one and installing a new shell by welding is a fairly common phenomenon. Current regulations [6, 7] define the limiting quantity of deviations of shell plates from a vertical forming element. In accordance with the requirements of these regulations the repair work of the facility is assigned, wherein the thickness of the shell plates is calculated on the basis of mechanical strength, methodological approach of which is applied in [8].

However, there is a problem concerning the fact that the strength calculation does not take into account the real geometry of the shell at the time of bringing VST for

repair, as well as possible welding deformations and residual stresses acquired in the process of construction and installation works. Therefore, the authors attempt to address the welding deformations in the strength calculations of the tank shell after replacement of the shell plate. It is suggested to consider the widely accepted cases of a shell plate replacement of 1 ring, having the size of $6 \times 1.5 \times 0.013$ m, the radius of curvature - 22.8 m. The first step is to determine the value of welding deformation for the area of the welding seal. For this purpose it is decided to apply a software package SYSWELD 2016.5. During the next step, knowing the values of deformations for the base section, and implementing finite element method ANSYS, it is possible to obtain the distribution of strains and stresses for the whole model VST-20000, including the area outside the shell plate that is being replaced. In conclusion we compare the obtained values of stress and deformation of steel structures of VTS – including and excluding the effects of welding.

2 Methods

To implement the first stage of the assigned task, we have developed a model of welding T-joint section of the shell and the annular plate applying software SYSWELD 2016.5 [9–11]. To obtain adequate finite element grid and the successful calibration of the heat source, the following model parameters were accepted – Table 1.

Table 1. The model parameters of T-joint.

Parameter	Amount	Unit of measure
The length of the simulated area	300	mm
The height of the simulated shell section	120	mm
The height of the simulated annular plate area	200	mm
Thickness of the shell, 1 ring	14	mm
Thickness of the annular plate	9	mm
Discretization value of finite element grid	0.5–20	mm
Steel grade	09G2S	–
The number of passes in welding (each side)	4	–
The application rate of the weld	24	mm/s
The size of the penetration	7	mm
Environment temperature	20	°C

In accordance with the model parameters listed in Table 1, calibration of heat source while welding was carried out. Parameters of the welding current were selected in such a way that during the distributions of the thermal field the fusion zone with a temperature of 1500 °C goes beyond the welded side.

Figure 1 illustrates the model of the welded joint after calibration.

Next, using the module “Weld Advisor” the calculation of welding deformations was carried out; as a result it was found that the maximum value of displacement of the butt end of the shell was 1.18 mm in the vertical direction.

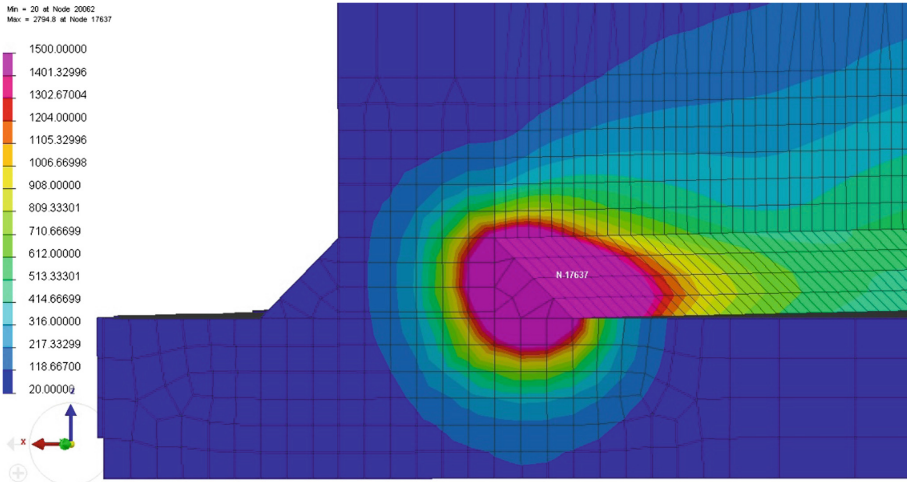


Fig. 1. The distribution of temperature fields due to the results of heat source calibration.

The average value of the vertical displacement for the entire part was 0.86 mm, this value is adopted as the base for further multidisciplinary calculation in PC ANSYS in order to determine the deformations of the whole structure of VST when replacing the shell plate [12–14].

Figure 2 illustrates the image of joint weld with the distribution of the displacement element due to the thermal influence of the heat source.

Finite element model VST-20000 is established and verified with the help of complex physical analysis ANSYS in [1, 15]. Geometrical and structural parameters of the model are taken in accordance with the standard project 704-1-60. A design scheme for a tank is a structure, resting on a circular footing, which in turn, is rigidly secured across the lower edge. Model VST-20000 takes into account the following elements: 8 rings of shell, frame and plate roof construction, annular plate and central part of the bottom, base setting ring, etc. The following types of finite elements are applied: SHELL181 (shell), SOLID186 (solid element), SURF156 (load application element), TARGE170 and CONTA175 (contact elements). The following loads are taken into account: oil loading height of 10.88 m, oil density of 865 kg/m^3 , snow load - 2400 Pa, wind load - 300 Pa.

The values of welding deformations obtained in the program SYSWELD are listed in the design scheme of the static calculation ANSYS in the following way.

The function “displacement” helped to obtain the average value of the welding displacement - 0.86 mm that is applied in downward direction to each edge of the maintenance opening (“frame” of the zone of shell plate alter of the 1 ring). 60 points of a given move were generated. Figure 3 presents a schematic diagram of an interdisciplinary calculation.

The final phase of static structural analysis is the generation of finite element grid of the macro model VST. The grid is generated directly on the geometry model and is the basis for the automatic generation of matrix equations.

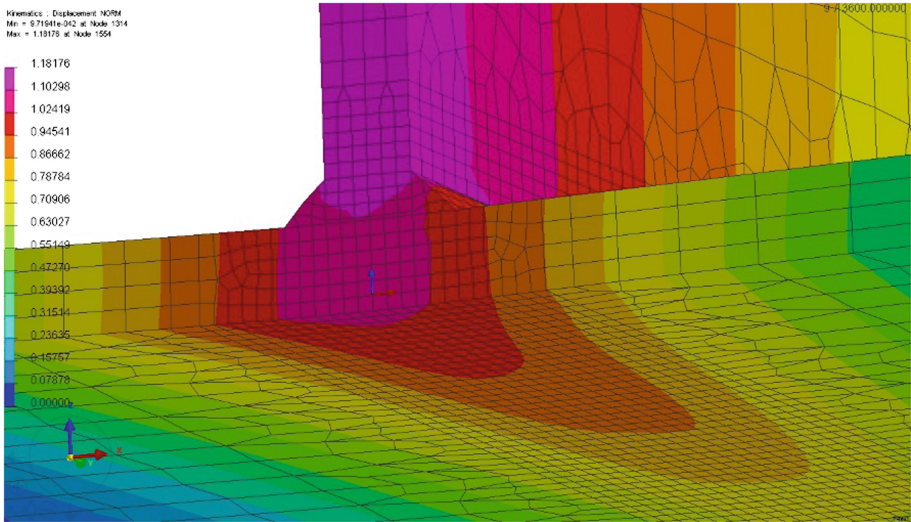


Fig. 2. The distribution of elements displacements in welded joints caused by thermal influence of a heat source.

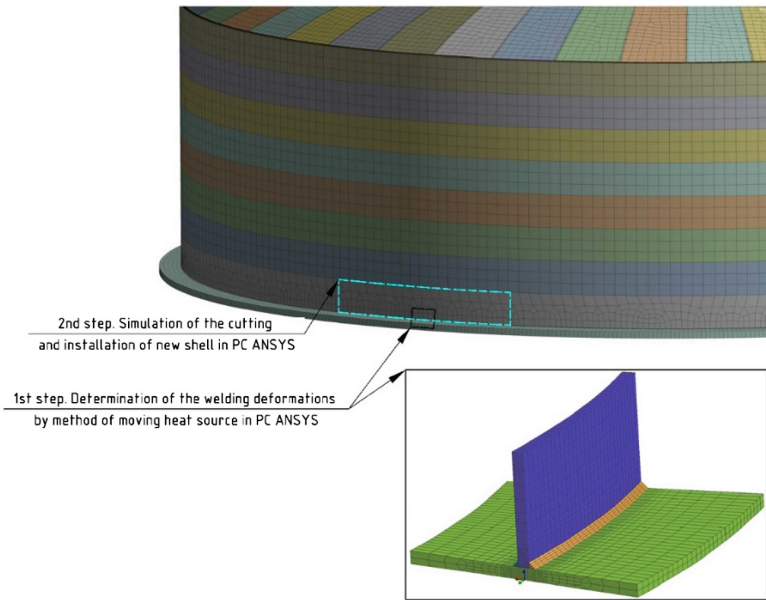


Fig. 3. Design model.

Each structural element of the tank has the determined shape function and is assigned to a finite element. The parameters of the finite element grid are shown in Table 2.

Table 2. The basic parameters of the finite element grid of the macro model VST-20000.

Parameter	Amount	Unit of measure
Factor of the grid density (measured from -100 up to +100)	10	-
Average length of the beam (sizing) for:		
- shell	0.5	m
- annular plate and ring foundation	0.5	m
- central part of the bottom	0.6	m
- roof boards	0.4	m
- plate of stiffening ring	0.03-0.1	m
Test the elements form	Aggressive	-
The smoothing factor	Average	-
The minimum beam length for automatic partitioning of frame elements	0.242	m
Node capacity of the model	123906	pcs
The number of elementary model elements	102562	pcs

3 Results

According to the calculation results, diagrams of the distribution of the current equivalent stress and deformation of steel structures of VST-20000 are obtained.

In the area of the shell plate being changed, there is a jump voltage and an increase in the local deformation at the level of the 1st – 2nd rings.

The results of numerical simulations on the macro model are shown in Figs. 4 and 5.

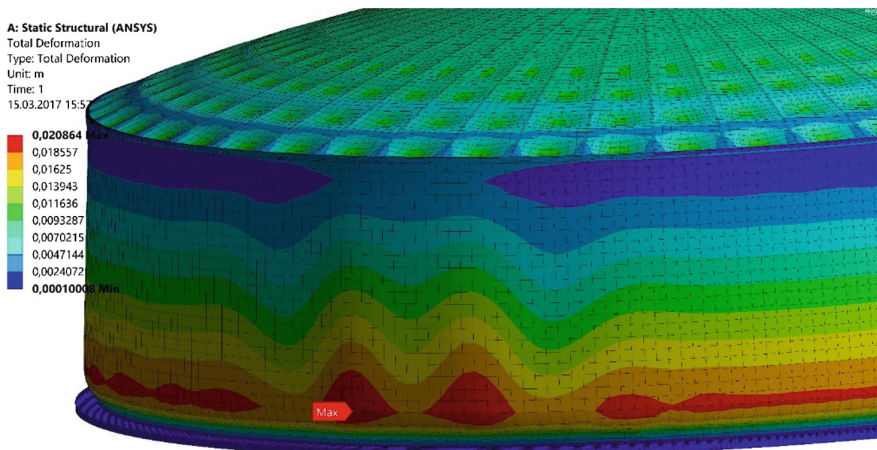


Fig. 4. Deformation of steel structures of VST-20000 after mounting 1 ring shell plate.

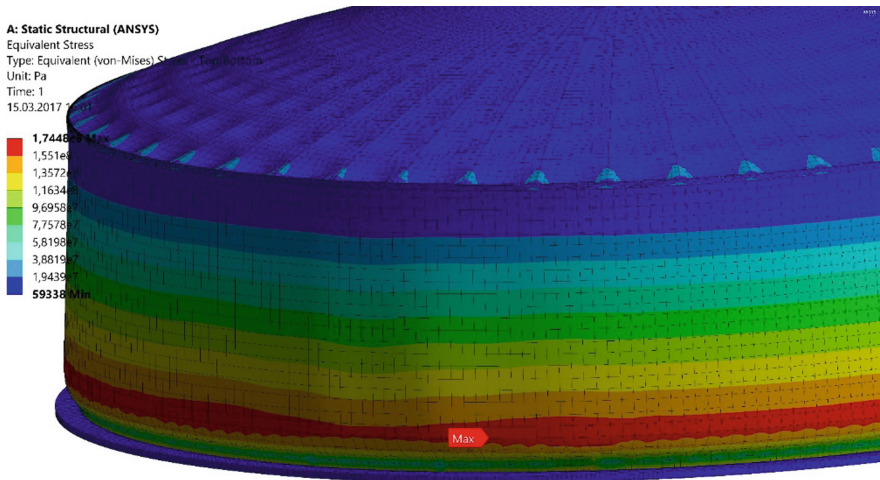


Fig. 5. Equivalent stress in metal constructions VST-20000 after mounting 1 ring shell plate.

4 Discussion

We have conducted the comparison of two cases of simulation results in stressed-strain state (SSS) construction VST-20000 at replacement of a fragment of the 1 ring shell: with and without regard to the thermal effects of the welding arc. The results of numerical simulation are presented in Table 3.

Table 3. Results of numerical simulation.

Parameters SSS	Inclusive of the welding thermal effect	Excluding the welding thermal effect
The maximum equivalent stress, MPa	174.5	168.7
The maximum deformation, mm	20.86	19.64

The maximum equivalent stress in the shell makes up to 174.5 and 168.7 MPa, respectively, the difference in calculation results is 4.4%, the maximum deformation of the shell makes up to 20.86 and 19.64 mm respectively, the difference in calculation results is 5.9%.

5 Conclusions

The authors of the article conducted numerical modeling of the deformation process of metal constructions VST-20000 at the substitute of the 1 ring shell plate taking into account thermal effects during the welding process. During the simulation geometry the basic design and structural features of the tank, built on a standard project TP 704-1-60 were taken into account. Let us refer to the research findings.

The calculations showed that the neglect of thermal deformation caused by the welding process reduces the accuracy of the resulting values of stress and strain by 4.4 and 5.9%, respectively.

Introduction of the thermal effects while welding increases the total SSS of the construction, which is obvious. Preliminary modeling of welding of T-joint connections of the shell and the annular plate through the moving heat source in the PC SYSWELD allowed determining the offset edges of the plates.

These data were used for the static calculation of the stresses and strains of the whole structure of VST-20000 applying FEM package ANSYS.

Thus, the results obtained by the authors suggest that when carrying out the strength calculations of the tank constructions (in various stages of VST repair), welding deformation can improve the accuracy of results of determination of the SSS by up to 6%, which undoubtedly affects the subsequent design decisions.

Acknowledgement. The paper was prepared within the implementation of the basic part of the government task for the project № 7.7858.2017/BP: “Development of the scientific principles of the techniques for determining the stress-strain state of the large-sized storage tanks during the differential settlement of the substructures and foundations”.

References

1. Tarasenko, A., Chepur, P., Gruchenkova, A.: Using linear spectral method when calculating seismic resistance of large-capacity vertical steel tanks. In: MATEC Web of Conferences, vol. 73, p. 01018 (2016)
2. Konovalov, P.A., Mangushev, R.A., Sotnikov, S.N., Zemlyansky, A.A.: Foundations steel tanks and deformation of it's bases, 336 p. The Association of Construction Universities, Moscow (2009)
3. Zemlyansky, A.A.: The design principles and experimental and theoretical studies of large tanks, Balakovo, 416 p. (2006)
4. Vasilev, G.G., Salnikov, A.P.: Analysis of causes of accidents with vertical steel tanks. *J. Oil Ind.* **2**, 106–108 (2015)
5. Slepnev, I.V.: Stress-strain elastic-plastic state of steel vertical cylindrical tanks with inhomogeneous base settlement. Moscow Engineering and Building Institute, Moscow (1988)
6. GOST 31385-2008. The vertical cylindrical steel tanks for oil and oil-products. General technical conditions. Standartinform, Moscow (2010)
7. RD-23.020.00-KTN-283-09. The rules of the repair and reconstruction of tanks for oil storage capacity of 1000–50000 cubic meters, OAO AK “Transneft”, Moscow (2009)
8. RD-23.020.00-KTN-018-14, Main pipeline transport of oil and oil products. Vertical steel tanks for oil storage capacity of 1000–50000 cubic meters. The design standards, OAO AK “Transneft”, Moscow (2014)
9. Bilenko, G.A.: The use of SYSWELD to study welding deformation. *J. CAD Graph.* **1**, 28–32 (2011)
10. Efemenkov, I.V.: Modelling and optimization of the welding metallurgical process technological parameters software SYSWELD. *J. Success Modern Sci.* **9**, 108–111 (2016)
11. Bilenko, G.A.: Analysis of structures residual stresses and deformations after welding working under pressure in the program SYSWELD. *J. Metall.* **8**, 32–34 (2012)

12. Tarasenko, A., Chepur, P., Gruchenkova, A.: Determining deformations of the central part of a vertical steel tank in the presence of the subsoil base inhomogeneity zones. In: AIP Conference Proceedings, vol. 1772, p. 060011 (2016)
13. Korobkov, G.E., Zarirov, R.M., Shammazov, I.A.: Numerical modeling of the stress-strain state and stability of pipelines and tanks in complicated operating conditions, Nedra, St. Petersburg (2009)
14. Bruyaka, V.A., Fokin, V.G., Soldusova, E.A., Glazunova, N.A., Adeyanov, I.E.: Engineering analysis in ANSYS Workbench, Samara State Technical University, Samara (2010)
15. Beloborodov, A.V.: Evaluation of the finite element model construction quality in ANSYS, Ural State Technical University, Ekaterinburg (2005)

Numerical-and-Analytical Method of Estimation Insulated Glass Unit Deformations Caused by Climate Loads

Pavel Stratiy^(✉) 

Moscow State University of Civil Engineering,
Yaroslavskoye shosse, 26, Moscow 129337, Russia
limited@list.ru

Abstract. The numerical-and-analytical method of estimation of sags of glasses of the insulated glass units deformations, developed in Moscow State University of Civil Engineering taking into account the internal (climate) loading allowing to predict the level of “lensing” of insulated glass units and mutilating the curvature of glasses is offered in this article. Two physical models of insulated glass units as hermetic gas are offered. In the first model the glasses have high rigidness, and their deformation is close to zero. The difference of pressure is perceived at the expense of tension in glasses, which works as plates. In the second model the glasses are flexible and easily deformed. The difference of pressure is perceived according to the estimation of changes of the chamber. The theory of flexible plates is used in the analytical decision. The numerical algorithm consists of iterative loop of computation. The pilot studies of a insulated glass unit under loading are completed. The offered method was realized in the form of the computer programme “Calculation of Insulated Glass Unit under Climate Loading”.

Keywords: Sags of glasses · Transport buildings and structures
Estimation insulated glass

1 Introduction

In modern architecture of buildings the continuous glazed facades with filling from double-glazed windows Insulated Glass Units (IGU) are widely applied in the world [1, 2]. One of the shortcomings of double-glazed windows is the effect of a lens (a flexure of glasses) [3, 4]. Glasses are partially reflecting (mirror) and under certain weather conditions and solar publicizing of deformation of glasses lead to distortions of the reflected image on facades. In certain cases it leads to distortion of all image of the building (Fig. 1). Lensing of double-glazed windows influences not only esthetic qualities of facades of buildings, but also their tightness (respectively and durability of a structure) and durability [5]. The size of distortion depends on the deformation (deflection) of external glass [6].

Nowadays the methods of calculation of deflections of glasses of double-glazed windows are insufficiently studied in the world. The numerical-and-analytical method of estimation of the deflections of glasses of single-chamber double-glazed windows



Fig. 1. IGU pane deformation on a translucent façade

developed in Moscow State University of Civil Engineering taking account the internal (climate) loading is offered in the article. The estimation of deflections of glasses because of internal (climate) loading allows to predict the degree of lensing of double-glazed windows and the distorting curvature of glasses.

2 Materials and Methods

The reason of glasses deformations is the tightness of double-glazed windows [7]. The double-glazed window are the glasses, which are hermetically connected among themselves with the air layer, in which the pressure can differ from atmospheric pressure. There is a loading deforming glasses because of the difference of pressure outside and from the double-glazed window, that is accepted to be called internal loading in double-glazed windows or climate loading in double-glazed windows [8–10] (Fig. 2). The degree of the climate loading ΔP depends on the difference of atmospheric pressure, air temperature in the double-glazed window and geodetic heights. The loading and can make up about 5–15 kPa.

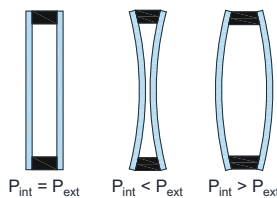


Fig. 2. Effect of climatic loads (the internal pressure of a double-glazed window P_{int} , external (atmospheric) P_{ext})

In case of emergence of internal pressure, glass are deformed and perceive such a loading [11]. However it is incorrect to design double-glazed windows only by classical methods of materials resistance [12]. Since the internal volume changes because of deformations of glasses, that thanks to tightness of a double-glazed window, reduces

loading. I.e. the double-glazed window works partially as a pneumo-structure. It is obvious that the method considering the both ways of perception of internal loading a double-glazed window is necessary for the estimation of glasses deflections of double-glazed windows.

In case of deformations of glasses there is a change of internal volume without change of mass of gas. The change of internal volume is connected with the internal pressure and is described by the law of ideal gas:

$$\frac{P_1 \cdot V_1}{T_1} = \frac{P_2 \cdot V_2}{T_2} = \text{const} \quad (1)$$

where:

P_1 and P_2 – the starting and ending gas pressure;

V_1 and V_2 – the initial and final volume of gas;

T_1 and T_2 – the initial and final temperature of gas;

At change of volume and pressure in a double-glazed window temperature changes slightly therefore it is possible to use Boyle-Mariotta's law in the form of a formula:

$$\frac{P_2 \cdot V_2}{P_1 \cdot V_1} = \text{const} \quad (2)$$

It is necessary to define the absolute value of climate loading. It can be estimated as the difference between the atmospheric pressure and isochoric pressure (at the invariable volume of gas) in a double-glazed window taking into account cumulative change of temperature of gas and atmospheric pressure (at climatic differences and change of height) as ΔP_{\max} .

$$\frac{P_2}{P_1} = \frac{P_1 + \Delta P_{\max}}{P_1} = \frac{P_{\max}}{P_1} + 1 \quad (3)$$

Relatively the size of climatic loading can be also presented as the isochoric pressure and as the greatest possible relative change of internal volume:

$$\frac{V_2}{V_1} = \frac{V_1 + \Delta V_{\max}}{V_1} = \frac{V_{\max}}{V_1} + 1 \quad (4)$$

To calculate deflections of glasses, it is necessary to define which part of the internal loading [20] will be compensated by the change of internal volume (law by Mendeleyev-Klapeyron) and which part will be perceived due to the efforts in glasses.

The author of the article offered to consider two models during the consideration of a chamber.

Within the first model glasses possess high rigidity, and their deformations are close to zero. The difference of pressure is perceived at the expense of tension in glasses which work as flat plates under uniform loading.

Within the second model the flew down flexible and are easily deformed. The difference of pressure is perceived due to change of volume of a chamber. The double-glazed window works as a pneumo-structure. Glasses are bent and work as a spatial structure.

It is established by the means of pilot studies, that usual double-glazed windows are in the intermediate position close to system to flexible walls. But in process of increase in climate loading and rigidity of glasses the state changes not linearly. The glasses begin to work as a spatial cover, while the increase in deflections appears nonlinearity.

Both physical models are presented in Fig. 3. For ideally rigid glasses internal loading will be perceived completely due to work of glasses (Fig. 3b). For ideally flexible glasses internal loading will be compensated completely at change of the volume (Fig. 3c). In the valid work of a double-glazed window it is necessary to consider both models (Fig. 3a).

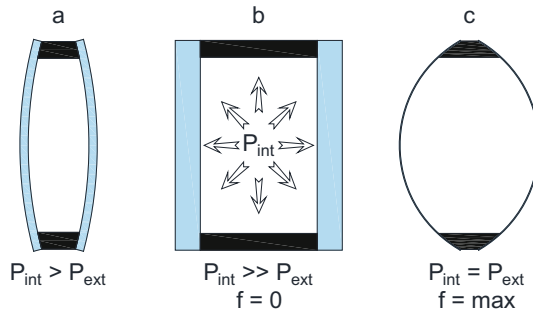


Fig. 3. (a) - regular double-glazed window; (b) - the first model with a perfectly rigid walls; (c) - the second model with a perfectly flexible walls. f-deflections of glasses

According to the first model, we can assume, that there is some internal loading of q operating from within on package glasses. Considering that double-glazed window volume in this case is invariable, the internal loading of q will correspond to climatic loading ΔP_{max} . That can be expressed as follows:

$$\frac{q}{\Delta P_{max}} = 1 \tag{5}$$

According to the second model, the internal pressure of q cannot be supported in a double-glazed window by flexible walls and through deformations of walls will be at once transformed to change of internal volume ΔV . This change of volume ΔV will be equally maximum ΔV_{max} . That can be expressed as follows:

$$\frac{\Delta V}{\Delta V_{max}} = 1 \tag{6}$$

In fact both ways of perception of internal loading are involved, mathematically it can be expressed as follows:

$$\frac{q}{\Delta P_{max}} + \frac{\Delta V}{\Delta V_{max}} = 1 \quad (7)$$

The use in a method and an analytical-and-numerical component is caused by the fact that with the known internal pressure it is possible to receive the exact solution of a deflection of glasses analytically. But as the deflection of glasses internal volume changes, there is a geometrical nonlinearity that results in the need of the numerical decision [13–15].

At deformation of glasses from internal loading, the size of deflections can be comparable to thickness of glasses. There is an effect of spatial work of glasses as membranes and it is necessary to consider geometrical nonlinearity. Glass needs to be counted as a flexible plate in which there is some membrane tension in the median surface. The approximate method, recommended by A. Feopl (Föppl A.), the solution of a flexible plate is submitted as a combination of the famous solutions of theories of small deflections and the theory of membranes [16–18].

Let us assume, that the internal load of glass q can be spread out to two components of q_1 and q_2 in such a way that q_1 will be perceived at the expense of a bend and shift of a plate, calculated according to the theory of small deflections, and q_2 will be perceived due to work of a membrane on stretching.

For estimation it is necessary to use the analytical decision: either supported on hinge of glasses, or rigidly fixed. Actually, as the experiments prove, glasses are fastened with semi-hard sealant. The exact decision will be intermediate (semifixed), therefore the solution of both types of fixing is necessary.

The deflection in the center of rectangular freely supported the plate with the parties of $a \cdot b$ calculated according to the theory of small deflections is the folloeing:

$$f^{chinge} = \frac{k_{hng} \cdot q_1 \cdot b^4 \cdot 12 \cdot (1 - \mu^2)}{E \cdot t^3} \quad (8)$$

where:

k_{hng} - the known tabular coefficient [22] depending on a ratio of the parties;

q_1 - loading, kPa;

b - length of the smaller party, m;

E - module of elasticity, kPa;

t - thickness of a plate flew down, m;

μ - Poisson's coefficient.

Considering a plate as a membrane, we will calculate its deflection:

$$f^{flex} = k_{flex} \cdot \sqrt[3]{\frac{q_2 \cdot b^4}{16 \cdot E \cdot t}} \quad (9)$$

where:

k_{flex} - the known tabular coefficient [22] depending on a ratio of the parties.

The combination of solutions of a plate according the theory of small deflections and the theory of membranes gives the decision for a flexible plate:

$$f_{flex}^{hinge} = f^{hinge} + f^{flex} = \frac{k_{hng} \cdot q_1 \cdot b^4 \cdot 12 \cdot (1 - \mu^2)}{E \cdot t^3} + k_{flex} \cdot \sqrt[3]{\frac{q_2 \cdot b^4}{16 \cdot E \cdot t}} \quad (10)$$

Similar to the deflection the rigid fixing of plates is estimated.

For calculation of volumes of deflections (Fig. 4), we will integrate the equations of surfaces for hinged (hinge) and for rigid (hard) of conditions of fixing of plates twice:

$$\Delta V_{hinge} = f_{hinge} \int_{-\frac{a}{2}}^{\frac{a}{2}} \int_{-\frac{b}{2}}^{\frac{b}{2}} \cos\left(\frac{\pi x}{a}\right) \cdot \cos\left(\frac{\pi y}{b}\right) dydx = \frac{4ab}{\pi^2} f_{hinge} \approx 0.41abf_{hinge} \quad (11)$$

$$\Delta V_{hard} = f_{hard} \int_{-\frac{a}{2}}^{\frac{a}{2}} \int_{-\frac{b}{2}}^{\frac{b}{2}} \left(1 + \cos\left(\frac{2\pi x}{a}\right)\right) \cdot \left(1 + \cos\left(\frac{2\pi y}{b}\right)\right) / 4 dydx = \frac{ab}{4} f_{hard} = 0.25abf_{hard} \quad (12)$$

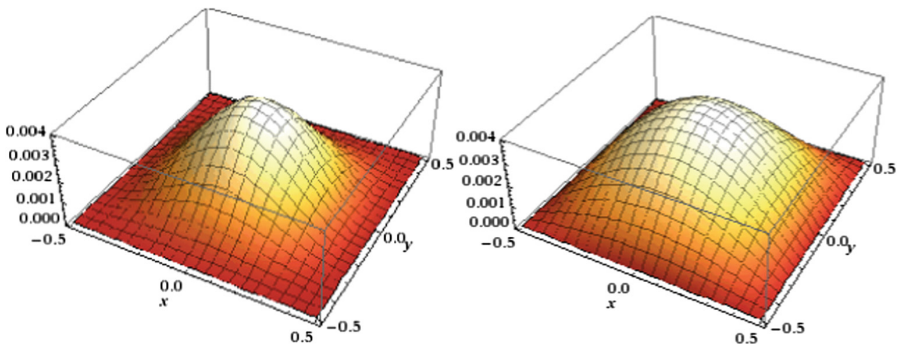


Fig. 4. Form bending square plates 1 × 1 m: (a) freely supported; (b) rigid fixing

The change of internal volume ΔV is the function from deflections of glasses ΔV (f), and deflections of glasses f are function from loading of f(q). The geometry of a double-glazed window changes and, respectively, $q = q_1 + q_2$ changes ratio at every stage of the estimation. The condition of the iteration procedure is checked on each step proceeding with the help of the formula (8):

$$\frac{q}{\Delta P_{max}} + \frac{\Delta V}{\Delta V_{max}} = 1 \quad (13)$$

Algorithm of the estimation of deflections of glasses of a single-chamber double-glazed window is the following:

- to set the initial size of internal loading of q;
- to calculate the maximum internal load ΔP_{max} (as isochoric pressure);

- to calculate the maximum change of internal volume ΔV_{max} under the influence of this loading from a condition that the double-glazed window works as a pneumodesign;
- to calculate glass f deflections from q loading analytically;
- to calculate the volume of deformations of a double-glazed window ΔV at the known deflections of glasses f ;
- to check the iteration procedure condition.

After stay with the set accuracy of the volume of internal pressure of q it is possible to determine deflections of glasses and internal tension.

3 Results and Discussion

Test methodology include: an IGU, brand 4M1-24-4M1, size 1000×1000 mm, was inserted into a frame made of profiled PVC. Guide bars with the deflection sensors were set and fixed on glass surfaces (see Fig. 5). Overpressure was created inside the IGU with air injected through an air valve (see Fig. 5a). Zond-10 digital micro pressure gage was used to control internal pressure. Deflection of the top pane was measured with digital deflection meters of linear type, DPL-10 and DPL-20, with readings taken automatically by Terem 4.1 recording set.



Fig. 5. (a) pneumatic valve for creating internal pressure in the pane; (b) measuring devices – digital deflection meters of linear type and digital micro pressure gage

Results are presented in Fig. 6. The geometrical nonlinearity in work of glasses is demonstrated At loadings about 0.5–1 kPa. Experimentally received curve lies between a curve of hinged and rigid fixing of flexible plates. At introduction of intermediate coefficient of rigidity of fixing of glasses with sealant, we will receive a curve of approximate calculation (see Fig. 6b). This curve has high convergence with experimental results in the field of loads of glass approximately to 1 kPa.

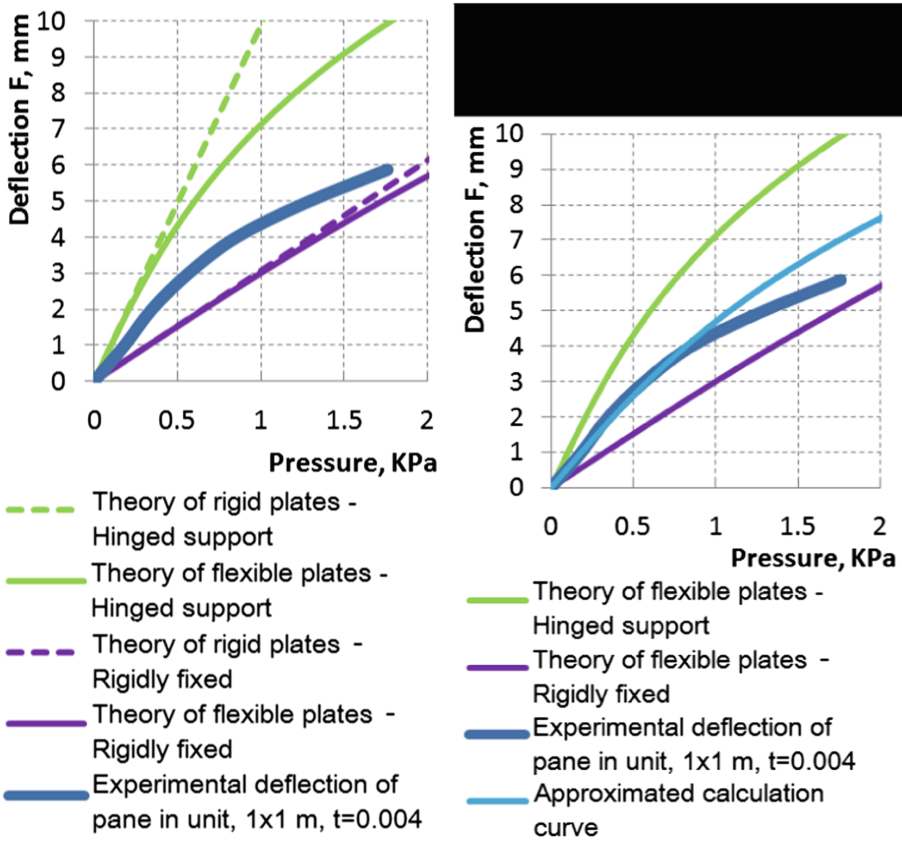


Fig. 6. Comparing experimental and theoretical deflection of glass panes

The results of theoretical calculations prove that the actual work of a double-glazed window generally corresponds to the model with flexible walls (depending on rigidity of the applied sealants, the sizes of a double-glazed window, ratio of the parties and other factors). Climatic load of 93–97% is compensated by change of internal volume due to deformation of glasses, and only 3–7% of loading are perceived by efforts in glass plates. Pilot studies prove the operability of the offered numerical and analytical method.

This method was realized in the form of the computer programme “Calculation of Single-chamber Double-glazed Windows on Climatic Loading” (Fig. 7). The programme allowed to conduct theoretical researches of various parameters of double-glazed windows for its work under climatic loading.

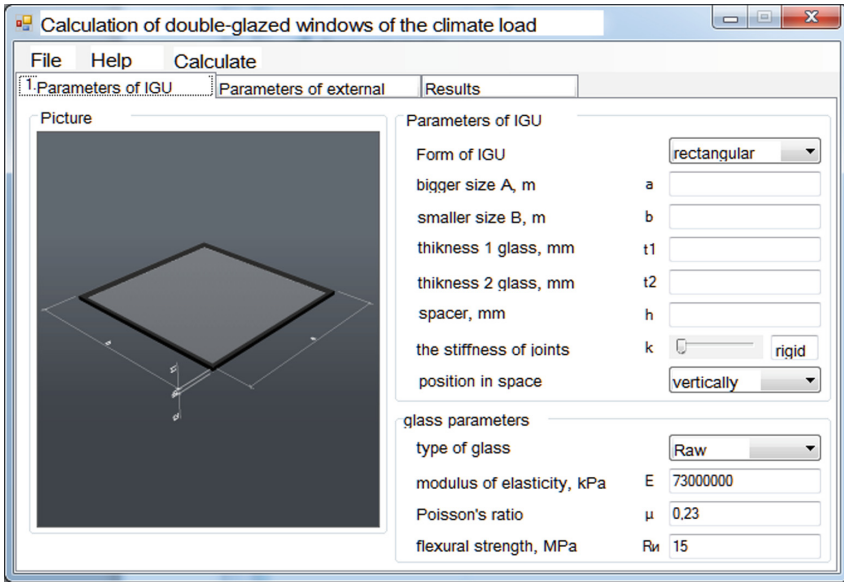


Fig. 7. Source data worksheet program “Calculation of double-glazed windows of the climate load”

4 Conclusions

The double-glazed window owing to the tightness is the subject to difference of temperatures and pressure, and that leads to some deformations of glasses and distortion of any architectural form. This internal loading is perceived at the same time and at the expense of resistance of glasses to deformations, and due to the compensation of internal pressure with change of internal volume. Since the change of internal volume is interconnected with deflections of glasses, the equation with two unknown turns out.

The numerical-and-analytical method is developed for the sake of estimation of the glasses deflections in Moscow State University of Civil Engineering. The analytical part of the method consists in the use of analytical dependences of a deflection on loading for the estimation of flexible plates, and the numerical part of the method consists in iterative calculation of the equation with two unknown with a necessary accuracy.




The pilot studies proved that the valid glass deflections are within the results which are theoretically obtained by this method for hinged and rigid fixing of glasses. This method can be used for the estimation of deflections of glasses at the loading of about 1 kPa with introduction of coefficient of rigidity of fixing (sealant) of glasses.

Acknowledgement. My heart-felt respect and gratitude go to my Research Supervisor, Mr. Aleksander Plotnikov.

References

1. Derbina, S., Boriskina, P., Plotnikov, A.: Bull. of MGSU **2**(2), 26–30 (2011)
2. Magay, A., Dubynin, N.: Bull. MGSU **2**, 14–20 (2010)
3. Boriskina, I., Plotnikov, A., Zakharov, A., Schurov, A., Konstantinov, A., Stratiy, P., Derbina, S., Kiseleva, I.: Buildings and structures with translucent facades and roofs. St. Petersburg: ed. “Lubavitch”, 396 p. (2012)
4. Plotnikov, A.: Bull. MGSU **11**, 7–15 (2015)
5. Buddenberg, S., Beyer, J., Oechsner, M.: Proceedings of the Challenging Glass 4 and Cost Action TU0905 Final Conference, pp. 297–304 (2014)
6. Wörner, J.-D., Pfeiffer, R., Schneider, J., Shen, X.: Bautechnik **75**, 280–293 (1998)
7. Huvener, E., Van Herwijnen, F., Soetens, F.: Heron **48**, 99–122 (2003)
8. Feldmeier, F.: Stahlbau **75**, 467–478 (2006)
9. Feldmeier, F.: Stahlbau **65**, 285–290 (1996)
10. Penkova, N., Iliev, V., Neugebauer, J.: Proceedings of COST Action TU0905 Mid-Term Conference on Structural Glass, pp. 295–303 (2013)
11. Respondek, Z., Rajczyk, M.: Adv. Mater. Res. **583**, 191–194 (2012)
12. Plotnikov, A., Boriskina, I., Stratiy, P.: Housing Constr. **4**, 33–36 (2011)
13. Saari, J., Sermiyagina, E., Kaikko, J., Vakkilainen, E., Sergeev, V.: Energy **113**, 574–585 (2016). <https://doi.org/10.1016/j.energy.2016.06.102>
14. Velchev, D., Ivanov, I.: Proceedings of the Challenging Glass 4 and Cost Action TU0905 Final Conference, pp. 311–318 (2014)
15. Von Grabe, J., Winter, S.: Bautechnik **88**, 425–432 (2011)
16. Plotnikov, A., Stratiy, P.: Sci. Rev. **9**, 190–194 (2013)
17. Saari, J., Sermiyagina, E., Kaikko, J., Vakkilainen, E., Sergeev, V.: Energy **113**, 574–585 (2016). <https://doi.org/10.1016/j.energy.2016.06.102>
18. Sergeev, V.V., Aleshina, A.S.: Thermal Eng. **58**(3), 268–270 (2011). <https://doi.org/10.1134/S0040601511030116>

Statistical Test Data Evaluation of Track Rutting in Stone Mastic Asphaltic Concrete

Dmitry Yastremsky^(✉) , Tatiana Abaidullina , and Petr Chepur 

Industrial University of Tyumen, Volodarskogo str., 38, Tyumen 625001, Russia
yaster.dmitry@yandex.ru

Abstract. The paper presents results of the test conducted to determine the durability of stone mastic asphalt concrete with stabilizing additives “Viatop 66” (Germany) and “Armidon” (authors’ development) to rutting. Durability to rutting was determined using the asphalt pavement analyzer APA, Pavement Technology Inc. It was established experimentally that SMA-20, containing SA “Armidon”, has increased performance properties. Due to a large number of obtained results, errors assessment in measurements was performed using the standard deviation values. The authors specified the rate of rutting v at the time of the N -th pass of the wheel, it was established that the rate of rutting decreased by 17% due to the introduction of the developed additives. The stages of rutting were determined in the course of the research.

Keywords: Stone mastic · Asphalt concrete · Road infrastructure

1 Introduction

The task to increase the durability of asphalt coatings is particularly relevant nowadays in Russia as well as abroad. Due to the development of the road network, the importance of this problem increases every year. In modern conditions there is a steady increase in the number of vehicles and their weight, while standard documents for the design of road surfaces remains unchanged [1]. Existing asphalt concrete testing methods stipulated by the Russian Federation state standards do not allow to fully assess the durability of the material in service and to reliably predict the pavement service life [2, 3]. National regulations define asphalt concrete durability basing on maximum loads at failure, while the surfacing material is subjected to cyclic loads of much less critical values. Therefore, to evaluate the ability of asphalt to resist exploitation impacts, a set of tests was conducted so as to determine durability to rut formation at high positive temperatures [4], applying the asphalt pavement analyzer APA, Pavement Technology Inc. Tests were carried out in accordance with the method AASHTO TP 63 (APA method) [5].

2 Methods

APA method involves determining the rut depth caused by the force moving along the air hose of metal wheel (Fig. 1a). Predetermined pressure was maintained in the hose. Thus, real operating conditions for the surface material are simulated [6].

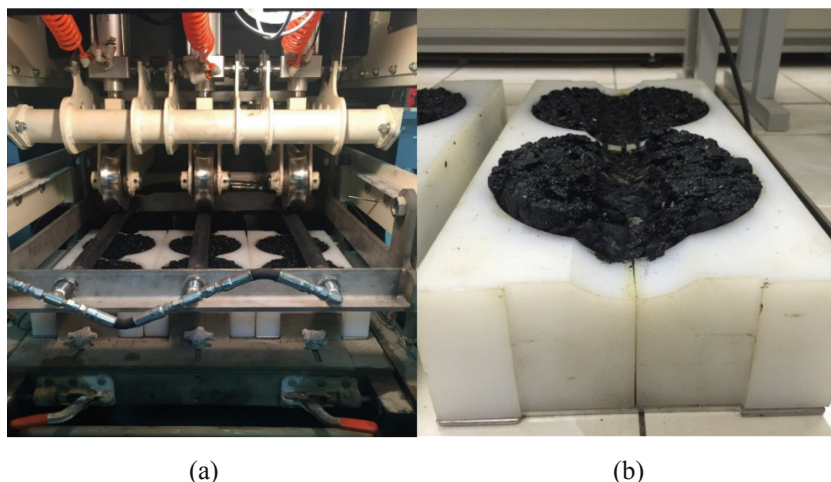


Fig. 1. The scheme of loading on the sample while conducting a test according to the method of APA (a), Sample of SMA after the test (b)

So as to determine the rut according to the method AASHTO TP 63, a series of samples of SMA-20 with stabilizing additives (DM) “Viatop 66” (Germany, composition No. 1) and “Armidon” (Russia – developed by the authors, composition No. 2) was prepared. The samples were compacted using the vibropress AVCII and had the following dimensions: height – 70 mm, diameter – 150 mm. Selection of raw materials and their optimum quantity in asphalt concrete mixture was determined in the previous work of the authors [7, 8]. The composition of the prepared mixes is given in Table 1.

Table 1. The compositions of the stone mastic asphalt mixes.

Name of the material	Composition of the material, %	
	Composition №1	Composition №2
Crushed rock graded 20–15 mm	45	45
Crushed rock graded 15–10 mm	18	18
Crushed rock graded 10–5 mm	10	10
Grind screenings	16	16
Mineral dust	11	11
Native asphalt	5.5	5.5
Stabilizer	0.4	0.4

The test duration was limited to 12.000 cycles of the wheel-run with applied wheel load of 0.69 MPa. The pressure in air hoses was set to 700 ± 35 kPa. The rut depth was automatically recorded throughout the entire test period. The temperature of samples and test chamber was 50 °C.

Assigned accuracy δ_i in the measurements was determined using the standard deviation σ_x , the value of which was calculated with the formula:

$$\sigma_x = \sqrt{\frac{\sum_{i=1}^N (x_i - \bar{x})^2}{N - 1}} \tag{1}$$

where \bar{x} – average value in m parallel measurements; x_i – parameter value in i -th test; N – the total number of tests.

Analysis of the test data was conducted applying the Chauvenet criterion according to the method described in [8].

3 Results

Thus, Fig. 2. shows the results of rutting due to the number of passes of the metal wheel along a pneumatic hose.

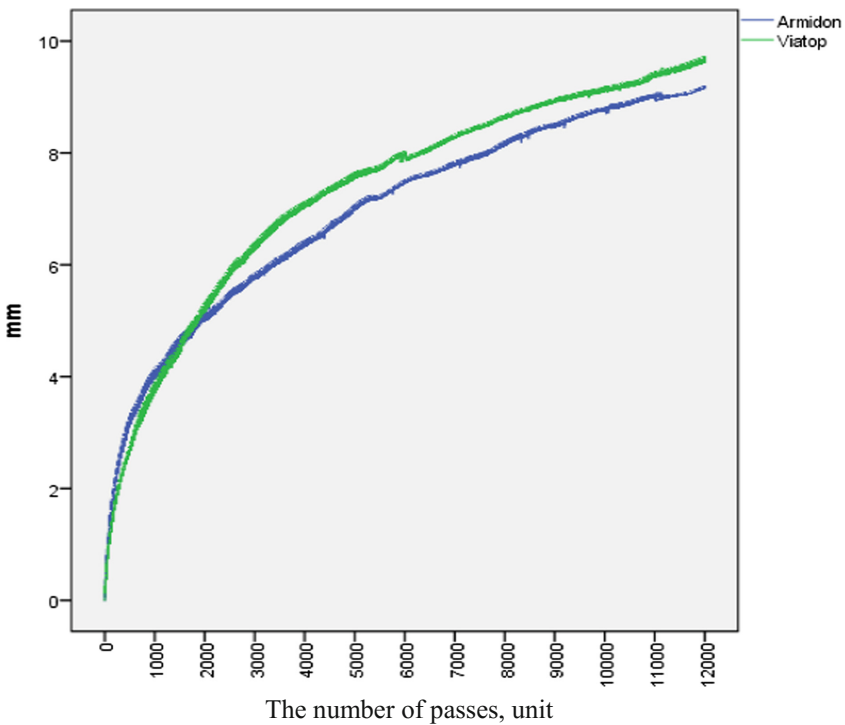


Fig. 2. The dependence of the rut depth on the number of wheel passes and additive type.

While conducting a test of averages congruence for two samples, it was found that on average, the second tracking rut is deeper than the first one by 0.37, whereby, the test statistics, equaling $t = 140.4$, the significance of which is less than 0.0001, proves that this difference is statistically significant (Tables 2 and 3).

Table 2. Paired samples statistics

	Mean	N	Std. deviation	Std. error mean
Armidon	6.955	12001	1.856	0.017
Viatop	7.324	12001	2.055	0.019

Table 3. Paired samples test

	Paired differences				t	df	Sig. (2-tailed)	
	Mean	Std. deviation	Std. error mean	95% confidence interval of the difference				
				Lower				Upper
Differences between Armidon and Viatop	-0.369	0.288	0.002	-0.374	-0.363	140.4	12000	<0.0001

In particular, these conditions comply with the three-parameter dependence:

$$H(N) = a \left(\frac{2}{1 + e^{-bN}} - 1 \right) + cN \tag{2}$$

where H(N) – the tracking rut depth after N-th wheel pass; a, b, c – empirical coefficients, determined on the basis of the experiment - model parameters (Table 4).

Table 4. Values of the model parameters H(N).

Additive	Value of empirical coefficients		
	a	b	c
Armidon	4.6429	0.002470	0.000418
Viatop	5.7425	0.001267	0.000502

Differentiating (2), we obtain the dependence of the rutting rate v at the time of the N-th wheel pass:

$$v(N) = H'(N) = \frac{2abe^{-bN}}{(1 + e^{-bN})^2} + c \tag{3}$$

The dependence of the rutting rate on the number of wheel passes and different additives is shown in Fig. 3.

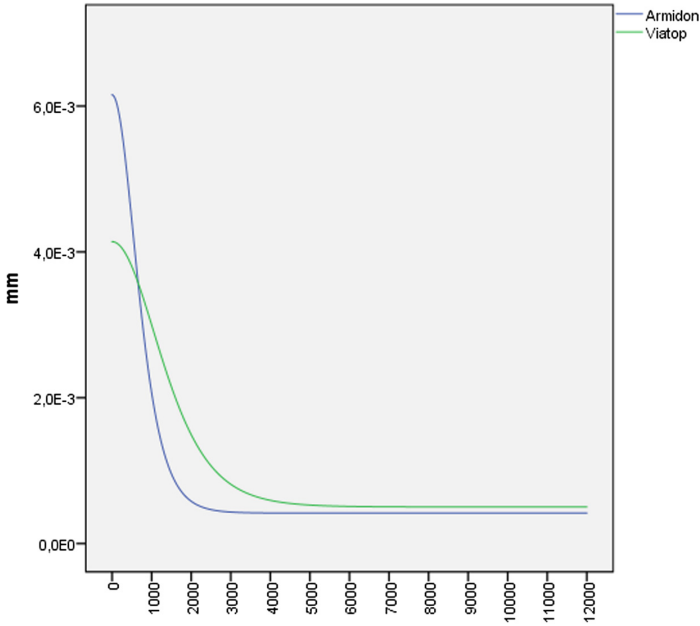


Fig. 3. The dependence of the rutting rate on the number of wheel passes and type of the stabilising additives.

4 Discussion

It follows from Fig. 2 that the rutting rate is high only on the first cycles at the time of the N-th wheel pass on the model with a developed additive, and then it is less everywhere.

Analysis of Table 4 and Eq. 3 shows that the coefficient C is indicative of the rutting rate in samples. Comparison of the coefficient values (Table 4) shows that the introduction of the developed additive decreases the rutting rate by 17% ($0.418/0.502 = 0.83$).

The process of rutting is marked by two characteristic stages: postcompaction and creeping [9, 10]. Characteristic points (number of wheel passes), marked by a change of rutting phases, were determined based on the conditions that the radius of curvature of the curve (given by Eq. 2) and the curve matching with the radius of the osculating circle at a given point should be minimal. The reciprocal of the curvature radius ($k = 1/r$) is the curvature of a curve calculated according to formula [11, 12]:

$$k(N) = \frac{H''(N)}{\sqrt{1 + H'(N)^2}^3} = \frac{H''(N)}{(1 + H'(N)^2)^{3/2}} \tag{4}$$

where H' and H'' - derivatives of first and second order in the function (2).

The analysis of Fig. 4 allows defining boundaries of distinctive rutting stages: the initial stage – stage of postcompaction when the tracking rut is formed by the compaction of asphalt concrete and subsequent creeping stage when the tracking rut increases due to the accumulation of plastic flow. As it can be seen from Fig. 4, postcompaction SMA with the use of stabilizing additives “Armidon” occurs within the first 550 wheel passes, and with the addition of “Viatop 66” – within up to 1050 passes, respectively, while the rut depth of the developed composition at this stage is 1.2–1.3 times higher than that of the composition with the addition of “Viatop”. Shorter duration of postsompcation phase of the developed composition is due to high rate of rigidity and elasticity modulus at elevated temperatures, whereby there is no significant compaction and reduction of residual porosity.

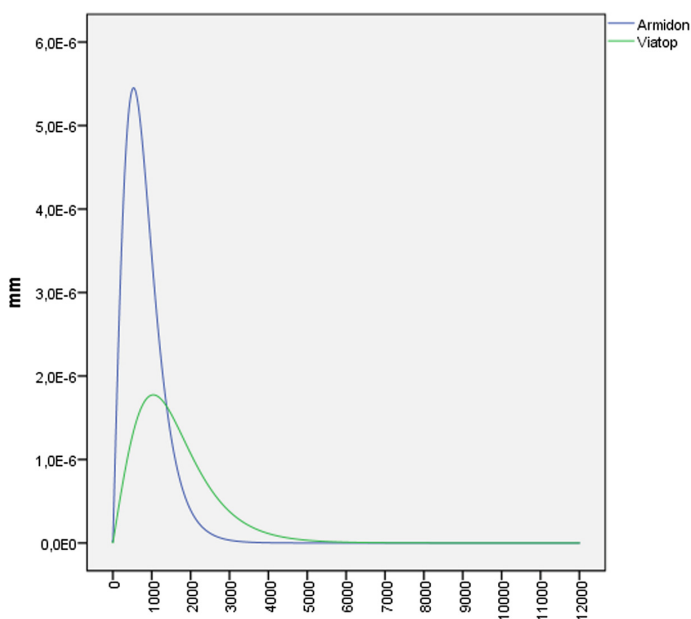


Fig. 4. The dependence of the curvature of the rutting curve from the number of passes of the wheel and type of stabilizing additives.

It should be noted that method AASHTO TP 63 regulates the maximum permissible rut depth of 12 mm after 8000 cycles. During the experiment, the tracking rut of any of the compounds has not reached the maximum value, even after 12.000 cycles of the wheel pass (the maximum rut depth for compositions with the addition of “Armidon” made – 9,16 mm, and with the addition of “Viatop 66” – 9.7 mm) (Fig. 2).






5 Conclusions

The paper presents results of the test conducted to determine the durability of stone mastic asphalt concrete with additives “Viatop 66” and “Armidon” to the formation of ruts applying the asphalt pavement analyzer APA, Pavement Technology Inc. It has been established that after 12,000 cycles of wheel passes the max rut depth for compositions with the addition of “Armidon” amounts to – 9.16 mm, and with the addition of “Viatop 66” amounts to 9.7 mm. Thus, it is determined that SMA-20, containing SA “Armidon”, resists to plastic deformation by repeated application of wheel loads better than SMA-20 with the use of SA “Viatop 66” by 6%. When conducting the test on congruence of average values, it was obtained that on average the second track is deeper than the first by 0.37, and test statistics, equaling $t = 140.4$, is statistically significant. Comparison of the coefficient values (Table 4) shows that the introduction of the developed additive “Armidon” decreases the rutting rate by 17%. Analysis of the diagrams has allowed establishing the stages of rutting: initial stage - postcompaction when the track is formed by the compaction of asphalt concrete and subsequent creeping stage when the tracking rut increases due to the accumulation of plastic deformations.

References

1. Yastremsky, D.A., Chepur, P.V., Abaidullina, T.N.: *Sovremennyye naukojomye tehnologii* 3–2, 307–310 (2016)
2. *Dorogi avtomobil'nye obshhego pol'zovanija. Normativnye nagruzki, raschjotnye shemy nagruzhenija i gabarity priblizhenija, GOST R 52748-2007 (Highways. Normative load, the calculated load circuit and approach dimensions)* Moscow, Standartinform, 17 p. (2008)
3. *Proektirovanie nezhestkih dorozhnyh odezhd, ODN 218.046-01 (Design of non-rigid pavements)*. Moscow: Standartinform, 92 p. (2001)
4. Kostin, V.I.: *Highways and aerodromes and listeners of system of additional professional education*. N. Novgorod, NNGASU, 65 S (2009)
5. <http://www.nocnt.ru/oborudovanie/laboratoriya-dorognih-materialov/195-analizator-asfaltovogo-pokrytiya>. Accessed 15 Mar 2017
6. Gladkikh, V.A., Korolev, E.B., Husid, D.L.: *Vestnik MGSU* 2, 70–78 (2016)
7. Yastremsky, D.A., Abaidullina, T.N.: *International Research-to-Practice Conference*. Tyumen, pp. 268–273 (2016)
8. Yastremsky, D.A., Chepur, P.V., Abaidullina, T.N.: *Microstructure of the pulp and paper additives for stone-mastic asphalt concrete*. In: *AIP Conference Proceedings*, vol. 1800, article number, 020002 (2017). <https://doi.org/10.1063/1.4973018>
9. Tarasenko, A.A., Chepur, P.V., Tarasenko, D.A.: *Neftyanoe khozyaystvo - Oil Ind.* 4, 88–91 (2015)
10. Mozgovoy, V.V., Onischenko, A.N.: *Experimental evaluation of the asphalt-concrete coating stability to the formation of rutting, Road machinery and technology: directory, «Slavutich»*. Saint-Petersburg, pp. 114–128 (2010)
11. Kostelov, M.P., Perevalov, V.P., Paharenko, D.V.: *The practice of combating the rutness of asphalt concrete pavements can be successful, Road-building machinery* (2011). http://www.slavutichmedia.ru/catalog/dorozhnaya_tehnika/0/praktika_borbi.html
12. Pogorelov, A.V.: *Differential Geometry*, 6th edn. Moscow, Science (1974)
13. Rashevsky, P.K.: *Course of Differential Geometry*, 3rd edn. GITLL, Moscow (1950)

Mathematical Models of the Output of Major Pollutants in the Process of Burning Water Fuel Oil Emulsions in Boiler Plants

Viktor Katin¹ , Vladimir Kosygin²  , Midkhat Akhtiamov¹ ,
and Igor Vol'khin¹ 

¹ Far Eastern State Transport University,
Serysheva str., 47, 680000 Khabarovsk, Russia

² Computer Center, Far Eastern Branch of the Russian Academy of Sciences,
Kim Yu Chen str., 65, 680000 Khabarovsk, Russia
kosyginv@inbox.ru

Abstract. We have studied the influence of the parameters of the combustion process in the existing low capacity boiler plants on the level of formation of nitrogen oxides, carbon monoxide and soot. This study resulted in regression equations that describe the emission of these substances. The developed mathematical models of the ecological characteristics of boilers can be used for selecting rational regimes of burning water fuel oil emulsions from the point of view of minimal emissions of harmful substances and improved operation of boiler plants.

Keywords: Boiler plant · Water fuel oil emulsion (WFOE)
Regression equation · Harmful emissions · Excess air ratio
Nitrogen oxides · Carbon monoxide · Soot particles

1 Introduction

The major measures, which can reduce harmful emissions during the operation of boiler plants, are improved design characteristics and the regulation of operational modes. From the point of view of economy and ecological compatibility of fuel use the combustion regimes should be of maximum efficiency. The complexity of the burning processes and the impossibility of obtaining analytical solutions based on combustion theory without corresponding simplifications that distort the results obtained, determine the use of experimental research as a basic method of studying these processes as applied to boilers. Analysis of literature [1–6] showed that the most influential factors that affect the pollutant concentration level in emitted gases are the moisture content of the water fuel-oil emulsion W and the excess air ratio α . In this connection, with reference to boilers of the DE (reference designation letters assigned by the manufacturer) type [3] that were used for conducting research the following controlled factors were chosen: excess air ratio with the range 1.05–1.20 and water fuel oil emulsion moisture content – from 4 to 20%. In the course of the experiment we measured the concentration values of three groups of harmful agents: soot particles,

nitrogen oxides and carbon monoxide that depend upon on the mentioned factors. Based on the experimental data obtained we need to select an analytical model that adequately describes the dependency of the concentration of harmful substances in the emission gases on the above mentioned controlled factors. It is practically impossible to derive the dependencies of the boiler operation parameters analytically. Conducting experiments according to conventional methodology with all the influencing parameters kept invariable, requires a considerable number of long-term and costly experiments. Although the parameters obtained are particular, they can serve as a source of “optimal” values for parameters of operation of boilers. Experiments aimed at optimization of operating parameters are conducted without the use of any particular methods.

2 Research Technique

At present, the method of mathematical experiment planning has become wide spread [7, 8]. The major goal of the experiment is to study the impact of operating parameters in the combustion process on the generation of harmful substances. It is expedient to apply mathematical planning in the course of the experiment to resolve the issue of pollutant reduction. The most topical method is the selection of the target function, analysis of the factor selection and the establishment of their neutral levels and variability intervals. A boiler plant is considered to be an object affected by measurable and regulated input factors x_1 , x_2 ; output parameters Y_{soot} , Y_{NO_x} , Y_{CO} are determined from the emissions. Here: x_1 is the percentage of water fuel-oil emulsion moisture content, %; x_2 is the excess air ratio; Y_{soot} is the concentration of soot particles, mg/m³; Y_{NO_x} is the concentration of nitrogen oxides in mg/m³; and is the carbon monoxide concentration, mg/m³. Defining several output parameters at the same values of variable factors is based on the assumption that these parameters are not correlated.

When a boiler plant is considered as a source of harmful emissions we need to determine the input and output parameters which define the possible ways of affecting the objective and its properties. In our case, the object property (target function) is the concentration of harmful substances in combustion products. When considering input parameters, they are divided into controlling, controllable and disturbed. We will consider the excess air ratio and the water fuel oil emulsion moisture content, i.e. x_1 и x_2 as controlling factors. The type of boiler and the duration of retention of combustion products in the furnace are referred to as controllable parameters. The disturbed parameters are unregulated and their values vary in the course of time in a random way.

At the first stage of studying the impact of operating parameters of the burning process on the generation of harmful emissions, we calculate the basic statistic parameters of data samplings for each pollutant agent and establish the distribution principles for these data samplings.

Tables 1 and 2 display average values of concentration of substances at different levels of air excess under combustion (factor x_2) and water fuel-oil emulsion moisture content (factor x_1).

Table 1. Average values of concentration of substances at different levels of factor x_2 .

Level	x_2	Soot particles	Nitrogen oxides	Carbon monoxide
1	1	211.188	39.417	163.679
2	1.05	185.313	54.756	195.129
3	1.1	174.376	64.305	204.230
4	1.15	161.370	88.992	215.365
5	1.2	144.507	121.331	236.865

Table 2. Average values of concentration of substances at different values of factor x_1 .

Water content in fuel oil, %																			
5	6	7	8	9	10	11	12	13	14	15	16	17	18	19	20				
Soot particles																			
259.796	247.383	231.131	197.322	151.386	116.007	112.524	74.065	68.858	104.136	134.502	191.367	202.934	228.256	235.867	250.0768				
Nitrogen oxide																			
199.423	194.678	179.821	138.079	109.472	78.149	68.019	50.529	41.111	20.334	20.542	16.159	14.6002	13.821	11.912	13.0022				
Carbon monoxide																			
273.865	272.514	249.232	223.365	215.253	190.425	177.818	161.442	155.346	162.418	161.085	179.812	182.645	194.984	223.886	224.769				

Tables 3 and 4 display the values of estimated variance for the concentration of pollutant agents at different levels of air excess ratio under combustion (factor x_2) and water fuel-oil emulsion moisture content (factor x_1).

Table 3. Values of estimated variance for concentration of substances at different levels of factor x_2 .

Level	x_2	Soot particles	Nitrogen oxides	Carbon oxide
1	1	6056.489	2510.347906	2586.365846
2	1.05	4647.317983	4365.493232	1825.282675
3	1.1	3931.880433	4656.097305	1712.507844
4	1.15	4022.834406	5376.235907	1308.220052
5	1.2	4246.147736	9572.917586	1273.680436

Table 4. Values of estimated variance for concentration of substances at different levels of factor x1.

Water content in fuel-oil, %															
5	6	7	8	9	10	11	12	13	14	15	16	17	18	19	20
Soot particles															
1966.74	532.68	1226.6	351.561	150.77	311.77	1607.92	621.925	329.528	1346.99	499.222	2776.536	929.417	626.702	580.57	1414.167
Nitrogen oxides															
864.5281	4350.227	7010.391	2472.832	1590.625	1847.386	1484.795	1801.438	1515.07	453.2493	447.2976	339.0987	138.6226	65.7336	109.5635	99.57251
Carbon monoxide															
304.865	87.57065	337.8193	231.763	392.8943	212.3491	773.449	490.5966	979.0367	650.4141	1629.984	1049.502	2125.581	1566.709	2099.127	2203.892

We determined the distribution principles using the Kolmogorov-Smirnov fit criterion and on the basis of the analysis of the relative frequency histograms [9]. The use of the Kolmogorov-Smirnov fit criterion was accompanied by the analysis of hypothesis H to ascertain that samplings are of normal distribution law.

We used the distance between distribution functions defined within uniform metrics to express the similarity of these functions [9]. This allows us to evaluate the distance D_n between empirical F_n and theoretical F distribution according to the following formula:

$$D_n = \sup_{-\infty < x < \infty} |F_n(x) - F(x)|$$

Obviously, the distance D_n is a random variable as its value depends on the random variable F_n . In case hypothesis H is true, $F_n(x) \rightarrow F(x)$ at $n \rightarrow \infty$ under any value of x . Therefore, $D_n \rightarrow 0$. In case hypothesis H is incorrect, $F_n \rightarrow G$ where $G \neq F$, therefore

$$\sup_{-\infty < x < \infty} |F_n(x) - F(x)| \rightarrow \sup_x |G(x) - F(x)|$$

This latter value is positive as G fuel-oil emulsions do not coincide with F. This discrepancy in behavior of D_n , depending on the validity of hypothesis H (whether the hypothesis is right or wrong) allows for the use of D_n as statistics for verification of H.

The value of statistics D_n were calculated to check the normality of the distribution of the source sampling. The value D_n obtained was then compared with the critical

value extracted from the tables. Hypothesis H had to be rejected (at the chosen significance level), if the value Dn obtained in the course of the experiment exceeded a chosen critical value that corresponded to this significance level.

As a result of the research conducted we found out that all samplings of experimental data were distributed following normal law at the significance level 0.05.

The method of mathematical data processing employing the principles of regression and correlation analysis gives an opportunity to obtain the relationships among the variable input factors and output parameters in the form of a mathematical model. It is a response function, which is convenient for comprehensive analysis and is capable of assessing the accuracy of the developed mathematical model. The mathematical planning procedure of the experiment widely employs second-order polynomials to describe non-linear response functions with extreme points [10]. Obtaining such response functions is only possible with the use of second-order experiment planning. The specific feature of such plans is conducting experiments within the range close to the hypothesized extremum. The limits of the domain boundaries are determined by the range of controlled factors.

On the basis of the above, let us suppose the quadric polynomial model with arguments x_1 and x_2 to be a stochastic dependency among the concentrations of any of the mentioned pollutants Y and controlled factors x_1 and x_2 . It is defined by the following expression:

$$Y = b_0 + b_1x_1 + b_2x_2 + b_3x_1^2 + b_4x_1x_2 + b_5x_2^2 + \varepsilon \tag{1}$$

where b_k are unknown numerical coefficients subject to definition; and ε is a normally distributed random variable, called the remainder, with a mathematical expectation value $M(\varepsilon) = 0$ and variance $D(\varepsilon) = D(Y) = \sigma^2$.

This model of stochastic dependency is a special case of a general linear model with five arguments which is easy to check if we assign

$$x_1 = x_1, x_2 = x_2, x_3 = x_1^2, x_4 = x_1x_2, x_5 = x_2^2 \tag{2}$$

If we substitute (2) into (1) we will obtain a linear model with five arguments x_1, x_2, x_3, x_4, x_5 , where x_j is defined by the correlations (2):

$$Y = b_0 + b_1x_1 + b_2x_2 + b_3x_3 + b_4x_4 + b_5x_5 + \varepsilon \tag{3}$$

to which the theory of the general linear model is applicable.

In order to make use of this model we have conducted n $(5 + 1)$ -measured observations. Each i -observation of the conducted consists of one value Y_i and five values $x_{i1}, x_{i2}, x_{i3}, x_{i4}, x_{i5}$, where x_{ij} is the value of j -argument, obtained in i -observation. Using expression (3), we can record the following system of equations:

$$Y_i = b_0 + \sum_{j=1}^5 b_jx_{ij} + \varepsilon_i, i = 1, 2, \dots, n \tag{4}$$

where ε_i is an independent normally distributed random value that has average values equal to zero and variance σ_i^2 equal to D (Y).

Having introduced dummy argument $x_{i0} \equiv 1$ at all $i = 1, 2, \dots, n$, the system of Eqs. (4) can be presented as follows:

$$Y_i = \sum_{j=0}^5 b_j x_{ij} + \varepsilon_i \quad i = 1, 2, \dots, n \tag{5}$$

The system of Eqs. (5) can be presented in matrix form. For that we will introduce consideration matrices X, Y, ε , B and will define them in the following way:

$$X_{n,6} = \begin{pmatrix} x_{10} & x_{11} & x_{12} & x_{13} & x_{14} & x_{15} \\ x_{20} & x_{21} & x_{22} & x_{23} & x_{24} & x_{25} \\ \cdot & \cdot & \cdot & \cdot & \cdot & \cdot \\ x_{n0} & x_{n1} & x_{n2} & x_{n3} & x_{n4} & x_{n5} \end{pmatrix}, Y_{n,1} = \begin{pmatrix} Y_1 \\ Y_2 \\ \vdots \\ Y_n \end{pmatrix}, \varepsilon_{n,1} = \begin{pmatrix} \varepsilon_1 \\ \varepsilon_2 \\ \vdots \\ \varepsilon_n \end{pmatrix}, B_{6,1} = \begin{pmatrix} b_0 \\ b_1 \\ b_2 \\ b_3 \\ b_4 \\ b_5 \end{pmatrix} \tag{6}$$

where the bottom indices of the first members of equations indicate the order of matrix.

Taking into consideration matrix indices (6) the system of Eqs. (5) can be recorded by way of a matrix in the following way:

$$Y_{n,1} = X_{n,6} \cdot B_{6,1} + \varepsilon_{n,1}$$

We used the least square method to obtain the assessments of unknown parameters b_k . According to this method we find the minimum sum of squared remainders

$$L = \sum_{i=1}^n \varepsilon_i^2 = \sum_{i=1}^n (Y_i - \sum_{j=0}^5 b_j x_{ij})^2$$

Value set \bar{b}_k , corresponding to minimum L, is called an evaluation of coefficients b_k , obtained by the least square method.

In order to obtain coefficients \bar{b}_k , corresponding to the minimum L, the partial derivative $\partial L / \partial b_k$ should be equated to zero and the resulting system of equations should be resolved relative to \bar{b}_k , i.e. the following system of equations should be solved:

$$\frac{\partial L}{\partial b_k} = -2 \sum_{i=1}^n \left(Y_i - \sum_{j=0}^5 \bar{b}_j x_{ij} \right) \cdot x_{ik} = 0, \quad k = 0, 1, 2, 3, 4, 5 \tag{7}$$

Let us convert the system of Eqs. (7) into the following equivalent:

$$\sum_{j=0}^5 \bar{b}_j \sum_{i=1}^n x_{ik} x_{ij} = \sum_{i=1}^n x_{ik} Y_i \tag{8}$$

The system (8) consists of 6 linear equations and contains 6 unknown evaluations \bar{b}_k of the coefficients b_k , obtained by the least square method.

We have marked the column of unknown evaluations \bar{b}_k of coefficients b_k as $\bar{B}_{6,1}$ and will record the system of Eqs. (8) in matrix form taking into consideration the table of symbols (6):

$$\left(X_{6,n}^T \cdot X_{n,6} \right) \cdot \bar{B}_{6,1} = X_{6,n}^T \cdot Y_{n,1} \tag{9}$$

In consequence of the linear independence of the function system $1, x_1, x_2, x_3, x_4, x_5,$ that consists of regulated parameters and an identity, matrix X and, consequently, X^T have the maximum possible dimensionality equal to 6. From this it follows that the sextic quadratic symmetric matrix $(X_{6,n}^T \cdot X_{n,6})$ has as well a rank equal to 6 and, therefore is nonsingular. The quadratic system of Eqs. (8) and its matrix analogue (9) with a nonsingular matrix $(X_{6,n}^T \cdot X_{n,6})$ always possesses a solution and this solution is unique and is presented as the following matrix formula that results immediately from the correlation (9):

$$\bar{B}_{6,1} = \left(X_{6,n}^T \cdot X_{n,6} \right)^{-1} \cdot \left(X_{6,n}^T \cdot Y_{n,1} \right)$$

If the random variables ε_i (remainders) are independent and normally distributed with mathematical expectations (average values) equal to zero and with constant dispersion $\sigma^2 = D(Y)$. that depends neither on b_k nor on x_{ij} , solutions $\bar{b}_0, \bar{b}_1, \bar{b}_2, \bar{b}_3, \bar{b}_4, \bar{b}_5$ of the system of Eqs. (8) will be the maximum probable evaluations for coefficients $b_0, b_1, b_2, b_3, b_4, b_5$. The maximum likelihood of evaluations \bar{b}_k is understood in the sense that under given evaluations the results of the observations conducted will be the most probable.

Having taken mathematical expectation from both parts of Eq. (3) and taking into consideration that $M(Y) \approx \bar{Y}$ and $M(\varepsilon) = 0$, as well as found values \bar{b}_k for the coefficients b_k , we will deduce the so called equation of multiple regression.

$$\bar{Y} = \bar{b}_0 + \bar{b}_1 x_1 + \bar{b}_2 x_2 + \bar{b}_3 x_3 + \bar{b}_4 x_4 + \bar{b}_5 x_5 \tag{10}$$

that expresses the functional relationship between the manipulative variable x_j and the average value \bar{Y} of the concentration of some of the listed pollutants in the emissions from boilers.

3 Results

The calculations resulted in the following values of the coefficients of the model for different pollutants (Table 5).

Using the calculated coefficients of the multiple regression model, as well as the notation system (2), we obtained regression Eq. (10) for each pollutant agent:

Table 5. Assessment of the coefficients of the mathematical model.

Coefficient	Soot particles	Nitrogen oxides	Carbon monoxide
\bar{b}_0	383.582	169.687	300.401
\bar{b}_1	-52.223	-28.204	-36.723
\bar{b}_2	-20.981	10.325	12.151
\bar{b}_3	3.110	1.204	1.667
\bar{b}_4	-0.186	-1.831	1.431
\bar{b}_5	1.139	4.377	-1.276

1. Soot particles

$$\bar{Y}_{soot} = 383.583 - 52.223x_1 - 20.981x_2 + 3.110x_1^2 - 0.186x_1x_2 + 1.139x_2^2;$$

2. Nitrogen oxides

$$\bar{Y}_{NOx} = 169.687 - 28.204x_1 + 10.325x_2 + 1.204x_1^2 - 1.831x_1x_2 + 4.377x_2^2;$$

3. Carbon monoxide

$$\bar{Y}_{CO} = 300.401 - 36.723x_1 + 12.151x_2 + 1.667x_1^2 + 1.431x_1x_2 - 1.276x_2^2.$$

The validity of the coefficients of regression equations was estimated by the Student criterion and the appropriateness of the adopted mathematical model was checked by the Fisher variance ratio test.

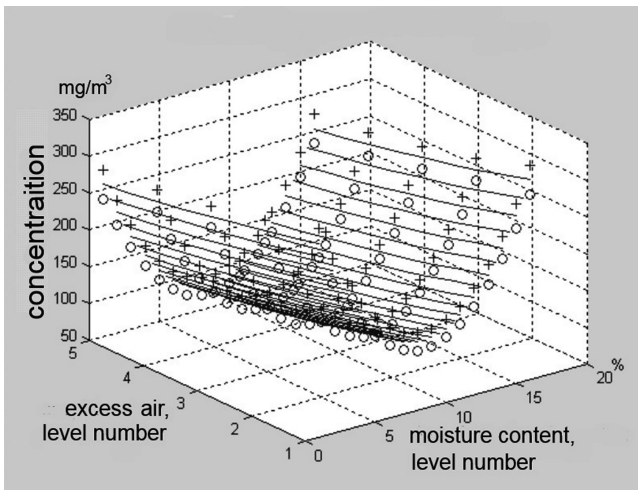


Fig. 1. The dependency of multiple regression of the concentration of soot particles on the moisture content in water fuel oil emulsion and the excess air ratio.

We have shown the coincidence of calculated characteristics obtained with the help of modeling and from experimental data.

Graphic illustration of the results of calculations of the values of the mathematical model for different pollutants is presented in Figs. 1, 2 and 3.

All figures use the following keys: + – upper limit of confidence interval; 0 – lower limit of confidence interval; — – value of multiple regression.

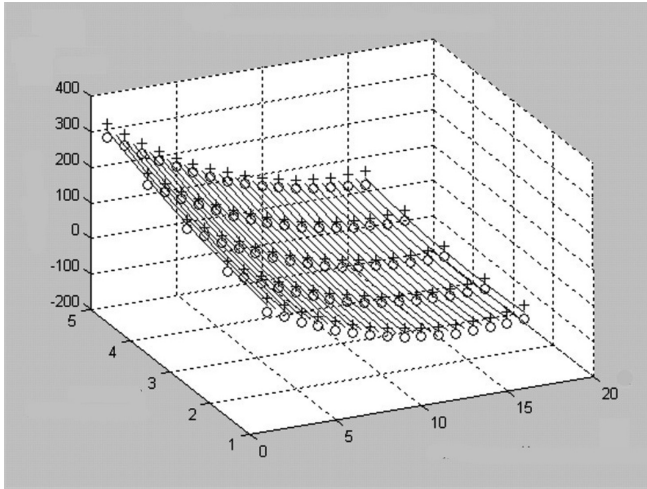


Fig. 2. The dependency of multiple regression of the concentration of nitrogen oxides on the moisture content in the water fuel oil emulsion and excess air ratio (notations for coordinate axis is the same as for Fig. 1).

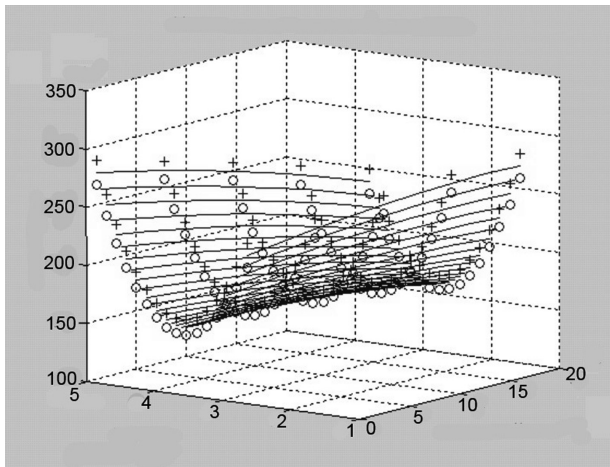


Fig. 3. The dependency of multiple regression of the concentration of carbon monoxide on the moisture content in water fuel oil emulsion and excess air ratio.

4 Conclusions

Analysis of the calculations and Figs. 1, 2 and 3 shows that the amount of harmful combustion products decreases when burning water fuel oil emulsion. The physical effect consists in the explosive evaporation of dispersed water droplets and follow-up micro explosion of water fuel oil emulsion droplets. Micro explosions result in additional fuel spraying and its mixture with air which reduces soot formation (Fig. 1). Water and water vapour influences the chemical mechanism of the reactions first and foremost by the formation of additional amounts of active H, OH and O due to the dissociation of H₂O. When soot particles burn-out, water vapor serves as a homogeneous catalyst and reacts with incandescent particles (in temperature exceeding 1000 °C) to form carbon monoxide (Fig. 3). The decrease in the output of nitrogen oxides when burning WFOE is first explained by the reduction of flame temperature and by ballasting the aerofuel mixture with water vapour (Fig. 2). Simultaneously, when the coefficient of air excess α increases from 1.05 to 1.2, the formation of soot particles and carbon monoxide decreases as a result of the chemical completeness of their combustion. However, when α equals 1.1 or exceeds it, the amount of nitrogen oxides increases which can be explained by the formation of “aerial” NO. Nevertheless, if compared with the quantitative formation of nitrogen oxides, we can make a conclusion that the significance level of WFOE moisture content (W) will prevail over its combustion duty parameter (α).

This condition objectively reflects the physical and chemical processes of formation of nitrogen oxides that take place in the course of fuel burning and conform to the thermal mechanism suggested by Academician Zel'dovich [11].

Table 6 presents the consolidated analysis of the recommended values W and α that will minimize emissions of the harmful substances under study from the most common boilers of DE type.

Table 6. Recommended values W and α for DE boilers.

Factor	Range of factors for harmful substances		
	Nitrogen oxides	Carbon monoxide	Soot
1. Moisture content WFOE, W, %	14–15	12–14	11–13
2. Excess air ratio, α	1.05–1.1	1.15–1.2	1.15–1.2

References

1. Avduevskiy, V.: Snizhenie vybosov okislov azota ot energeticheskikh ustanovok putem vvoda vody v zonu goreniya fakela. Ohrana okruzhaushchey sredy ot vybrosov energeticheskikh ustanovok, 3–19 (1999)
2. Butovskiy, M.: Vodotoplivnye emulsii iz nefesoderzhashchih othodov. Zheleznodorozhniy transport, 22–25 (1998)
3. Volikov, A.: Szhiganie gazovogo i zhidkogo topliva v kotlah maloy moshchnosti. Nedra 160, Leningrad (1999)

4. Gavrilov, A.: Vliyanie vlagi, vvodimoy v goryachiy vozduh, na sodержanie okislov azota v produktah sgoraniya mazuta. *Heat-and-power Engineering*, 13–15 (1998)
5. Gorbarenko, A.: Vliyanie vvoda vlagi v topku kotla BKZ-320-140 GM na vybrosy okislov azota. *Electric Power Stations*, 22–23 (1999)
6. Grishkova, A.: Umen'shenie vybrosov oksidov azota ot vodogreinyh kotlov. *Industrial Heat-and-Power Engineering*, 32–33 (2004)
7. Grachev, Y.: *Matematicheskie metody planirovaniya eksperimentov*. DeLi, Moscow (2005)
8. Johnson, N.: *Statistika i planirovanie eksperimenta v tehnikе i nauke. Metody obrabotki*. Mir, Moscow (1980)
9. Kobzar', A.: *Prikladnaya matematicheskaya statistika. Dlya inzhenerov i nauchnyh rabotnikov*. Fizmatlit, Moscow (2006)
10. Draper, N.: *Prikladnoi regressivniy analiz. Finansy i statistika*, Moscow (1986)
11. Zel'dovich, Y.: *Okislenie azota pri gorenii*. USSR Academy of Sciences Publications, Moscow (1946)

Method of Evaluation of Ground Frost Heaving Pressure on Ice-Ground Barrier of an Underground Construction and Well Strengthening Walls

Vyacheslav Kim^(✉)  and Marina Kim 

Voronezh State Technical University,
20 years of October st., 84, Voronezh 394006, Russia
vyachhkim@yandex. ru

Abstract. This article describes experimental and theoretical investigations of heaving pressure formation regularities in freezing grounds, as well as the application of the investigations in practice of building of underground constructions in frost hazard grounds. The experimental and theoretical investigations demonstrated that it is necessary to make a distinction between a pressure arising at the expense of free (gravitational) water crystallization and the pressure ensuing arising at the expense of bound (film) water crystallization freezing ground systems. The implementation of the obtained regularities together with the elaborated analytical methods has permitted to carry out the practical realization of research results. The comparison of a design pressure with actual magnitudes of pressure of rocks (grounds) on shafts strengthening walls (tubings) of Jakovlevskiy mine (Kursk Magnetic Anomaly) obtained on the base of experimental researches of the institute WIOGEM shows sufficiently high convergence of design and actual magnitudes. This fact attests that the application of the proposed method would be appropriate.

Keywords: Freezing of grounds · Intensity of heaving · Heaving pressure
Artificial freezing · Ice-rock barrier · Freezing front

1 Introduction

During constructing underground constructions in complex hydrogeological conditions with us-age of artificial freezing of ground, the frost heaving processes can develop resulting in an additional pressure on the underground structures. This pressure is especially high at the time of ground thawing in the zone of the contact with concrete well (shaft) strengthening walls under the action of the exothermic warm, releasing while the concrete is hardening and after the ground is freezing in the contact zone.

If the ground frost heaving is underestimated, additional forces arise in bearing underground structures. These forces disturb normal work of technical constructions and not infrequently lead to damages.

For example in Russia during tunneling of shaft N2 of Yakovlevskiy mine (Kursk magnetic anomaly) by Kasikaev et al. and in German Federal Republic during erecting

mine shaft Lohberg by Kratzschunderthe defense of ice-ground barrier the frost heaving processes brought the bearing structures to emergency conditions. A frost heaving influence on ice-ground barrier and concrete support wasn't investigated before [1–3].

2 Theoretical Exploration

Experimental and theoretical researches of authors permitted to establish next fact: it is necessary to distinguish the pressure, arising at the expense of free water crystallization, and the pressure, arising in the process of frozen ground cooling at the expense of non-frozen film (loosely bound) water [4, 5].

The pressure, which arises during a freezing of the water, not having an opportunity to enlarge its volume, can be calculated by Tammann-Bridgmen formula

$$p_{i,w}^{\infty} = 1 + 127 \cdot T - 1.519 \cdot T^2, \quad (1)$$

where $p_{i,w}^{\infty}$ – pressure, 10^{-1} MPa; T – ice melting temperature, °C.

Enlarging of the ground volume in a freezing zone is conditioned not only by crystallization of free water, being before a freezing, but also by a presence of film water in heaving grounds and its migration in liquid phase towards a freezing front.

In freezing ground the pressure from growing in pores ice crystals [6] will be perceived both by mineral part of the ground and firmly bound water, the last has characteristics analogous to characteristics of solid body. The loosely bound (film) water doesn't perceive the pressure, since in contact places of mineral particles hydrostatic pressure doesn't exist, this fact is proved by Lebedev. So we can suppose that in time of increasing of frost heaving pressure p_i mineral ground particles in freezing zone together with firmly bound water make stiff lattice skeleton, which perceives the pressure and lets the film water- freely to flow through holes in the lattice towards the ice crystals growing in the pores.

Design schematic model of development of P_i can be obtained by this way (Fig. 1): resistance of structural bonds of thawed ground skeleton can be conditionally replaced by springs 7 which are placed inside of a closed cylinder, the springs take (absorb) external loads and heaving pressure arising in freezing area. In this case in open system this load is completely taken (absorbed) by ground skeleton 7, and in closed system the load is partly transferred to free water 8. A skeleton from mineral ground particles in freezing area can be presented as two cylinders with free supports, the cylinders take (absorb) a pressure from a spring being inside them, the spring simulates of ice crystals, arising in a freezing area at the expense of bound (film) water-freezing. In this case non-frozen bound (film) water doesn't take (absorb) external pressure.

The proposed scheme permits to obtain an evaluation of P_i in the ground pores, the evaluation is made from positions of equilibrium thermodynamics.

Let's write in differential form the thermodynamic equilibrium condition [7, 8], taking into account the Gibbs-Duhem equation:

$$V_i \cdot dp_i - s_i \cdot dT_i = V_{bw} \cdot dp_{bw} - s_{bw} \cdot dT_{bw}, \tag{2}$$

where V_i and V_{bw} – specific volumes of the ice and bound water, m^3/kg ; p_i and p_{bw} – specific pressures on the ice and bound water, MPa; s_i and s_{bw} – specific entropies of the ice and bound water; T_i and T_{bw} – temperatures of the ice and bound water, °K.

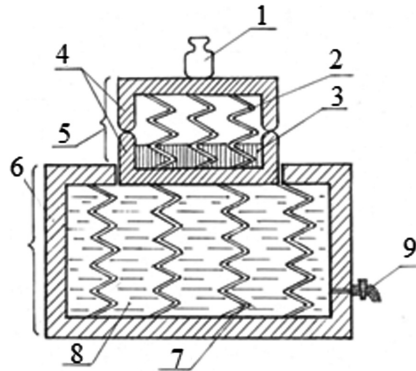


Fig. 1. A schematic model of a process of a frost heaving pressure developing during icing in ground pores: 1 – external load; 2 – formation (arising) of ice at the expense of bound (film) water freezing; 3 – bound (film) water, $p_{bw} = 0$; 4 – rigid frame of ground skeleton in freezing area; 5 – freezing area; 6 – thawing area; 7 – skeleton of thawed ground; 8 – free (gravitational) water; 9 – cock (tap, valve), which simulates of closed $p_w > 0$ and opened $p_w = 0$ system.

As a hydrostatic pressure of mineral ground particles in film water isn't transferred, and an intensity of film fields of force doesn't depend on external pressure, but mainly due to capillary-porous structure and nature of dispersed grounds mineral part, we can write in the Eq. (2)

$$p_{bw} = 0. \tag{3}$$

In order to solve the Eq. (2) we express a difference s_i and s_{bw} in terms of latent heat $L(T)$ of phase transition of the bound water into ice:

$$L(T) = T(s_i - s_{bw}). \tag{4}$$

The temperature dependence of latent heat phase transition of film water into ice may be expressed, according to the procedure, as

$$L(T) = L^\infty(T) + \Delta\mu(h), \tag{5}$$

where $L(T)$ – a temperature dependence of a crystallization latent heat of free (gravitational) water, J/kg; $\Delta\mu(h)$ – deviation of a chemical potential of the film unfrozen water from its value for free water.

Let' assume that

$$\Delta\mu(h) = \frac{[L_0^\infty(T - T_0)]}{T_0}, \tag{6}$$

where L_0^∞ – specific heat of a phase transition for free water; T_0 – temperature of ice melting or water freezing °C, water must be under the pressure of 1 atm; $T_0 = 273$ °K; T – temperature of bound water, °K.

Table 1. Comparison of pressure values during freezing of free water (formula 1) and bound or film water (formula 7) in ground.

Formulas for calculating p_i	Pressure (MPa) at temperature (°C)				
	-2	-5	-10	-15	-20
(1)	24.89	61.25	111.91	156.42	193.34
(7)	2.27	6.63	11.98	16.98	21.83

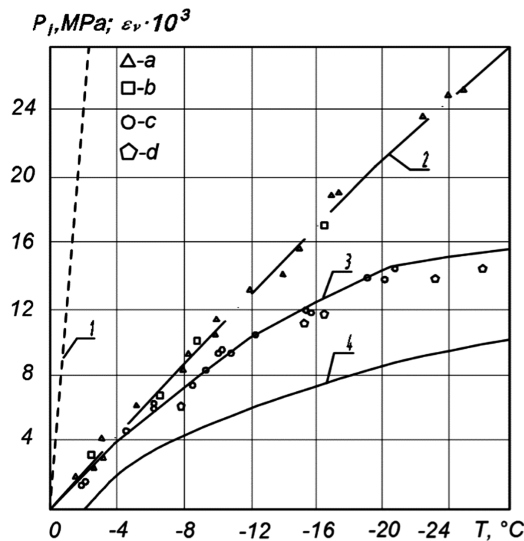


Fig. 2. Experimental and calculated data, obtained for one side ground freezing in a closed volume: 1 – temperature dependence of $p_{i,w}^\infty$ to formula (1); 2 – temperature dependence of heaving, the dependence was determined according to formula (7), MPa; 3 – the same, but according to formula (9), MPa; 4 – calculated dependance for allowed relative volume deformation, $\varepsilon_v \times 10^3$; a – experimental data, obtained by Takachi [9] for water-saturated clayish grounds; b – data by F.J/Radd and D.H. Ortle [11]; c – water-saturated clay with the parameters $w = 0.246$ and $\rho = 2.19$ g/cm³; d – water-saturated clay with the parameters $w = 0.193$ and $\rho = 2.15$ g/cm³

A solution of the equation of thermodynamic (2) with the conditions (4)–(6) permits to get a design formula for the determination of p_i (MPa), the pressure p_i develops in freezing ground at a temperature T as a result of film water freezing:

$$p_i = 3176.2 - 1881.88 \ln \left| \frac{273}{T} \right| - 16.395T + 2.161 \cdot 10^{-2}T^2 - 1.528 \cdot 10^{-5}T^3. \quad (7)$$

A calculation by the formula (7) shows us (see the Table 1) that p_i obtained by this formula, practically is less on one order of magnitudes than the value of $p_{i,w}^\infty$, obtained by the formula (1).

The value of p_i , determined by the formula (7), is well correlated with the experimental results, obtained by Japanese scientist [9], who studied the development of the pressure p_i , when an one-sided freezing of heave ground in closed volume exist (Fig. 2).

3 Experimental Exploration

An experimental investigation of a dependence of P_i from temperature under one-sided freezing of ground in a closed volume was conducted on the equipment, which can make a one-dimensional refrigerating in opened and closed system [10]. The equipment consisted from

1. a working steel cylinder for placing a specimen of ground, a thickness of cylinder wall was $h = 7.5$ mm, the cylinder had a welded bottom and a cover with thickness 23.8 mm;
2. a device for temperature regulation;
3. a magnetoelastic pressure sensor, placed under the cylinder cover;
4. a set of registering devices.

The equipment can work with pressures up to 16 MPa.

The modeling of the one-sided ground freezing was executed by thermoisolating of walls and bottom of the cylinder with cotton wool, flexible polyurethane foam (porolon) and rigid cellular plastic. The bottom must be kept out of freezing, this was fulfilled by warming of the bottom with a transportable copper heat exchanger, connected by rubber tubes with a liquid thermostat.

In the course of the experiment there were measured pressure, temperatures (by V. V. Paladko thermoresistors) and vertical displacements of the cylinder cover by clock type indicators

Ground specimens of clay, taken from districts near Moscow, had diameter 205 mm and height 300 mm- The specimens were completely frozen in the closed system, the temperature was decreased by step up to -32 °C.

On the Fig. 2 it was shown the function $p_i(T)$ for water-saturated clay. From this illustration can be seen that- experimental values of p_i are a little lower that values calculated by formula (7).

In conditions of complete ground freezing in a closed volume the possibility of volume deformation together with temperature compression of frozen ground causes in the ground a variation of interphasic equilibrium state, and as a consequence it will be a decreasing of unfrozen water content because this water partially became ice. It results in decreasing of p_i calculated by formula (7). In this case the decreasing of p_i is taken into consideration by introduction of lowering coefficient k_u :

$$k_u = 1 - \frac{\rho_w(\varepsilon_v + 3\alpha_m T)}{0,09\rho_d w_{mmw}} \quad (8)$$

where ρ_d and ρ_w – densities of ground skeleton and water respectively, kg/m^3 ; ε_v – relative deformation causing the bound water to freeze; α_m – a temperature coefficient of frozen ground linear contraction $^{\circ}\text{C}^{-1}$; w_{mmw} – maximum molecular moisture-holding capacity.

Then, taking into account the above mentioned assumption, the expression for the pressure p_i may be written in such form

$$p_{iu} = k_u p_i. \quad (9)$$

A calculation by formula (9) gives us the results which well agree with experimental results, obtained in the case of one-sided freezing of clay in a closed volume, the clay was taken from districts hear Moscow (Fig. 2).

4 Practical Using

With the help of formulas (7), (9) one can make a quantity evaluation of heave pressure on the well (shaft), made by artificial freezing of ground.

In this case the pressure grows at the expense of secondary freezing of the ground, defrosted before under the action of exothermic heat, emanated in the course of hardening (setting) of concrete in a limited volume (the volume is limited by concrete strengthening walls and frozen ground of ice-ground barrier).

An influence of the heave pressure on well strengthening walls (tubings) may be represented as a result of an interaction between two thick wall cylinder placed one into another. These cylinders (tubings and ice-ground barrier) are under the action of thawed ground pressure p_1 on the ice-ground barrier (the pressure p_1 is put to the external surface of the outer cylinder), and heave pressure p_2 , arising on interface of the two cylinders.

A description of stressed and strained state of a thick-wall cylinder under the action of external and internal pressures can be fulfilled with the help of elasticity theory formulas. In such a case the displacement in a radial direction of the ice ground barriers u_1 and the external surface of tubings u_2 can be determined from next formulas:

$$u_1 = \frac{p_2 b^3 [(1 - \nu_f) + (1 + \nu_f)c^2/b^2] - 2p_1 b c^2}{E_f(c^2 - b^2)}, \quad (10)$$

$$u_2 = \frac{p_2 b^3 [(1 - \nu_k) + (1 + \nu_k) a^2 / b^2]}{E_k (a^2 - b^2)}, \tag{11}$$

where a and b – internal and external radius of tubings, m ; c – external radius of the cylinder of ice-ground barrier; E_f, ν_f – modulus of deformation and Poisson coefficient for frozen ground; E_k, ν_k – modulus of deformation and Poisson coefficient for material, from which the tubings are made.

During a freezing of thawed ground having a thickness of a layer d_f a some radial ground deformation u_3 is possible, the reasons of the deformation are heave forces, the tubings and ice-ground cylinder yield under the action of the forces, the displacement of the tubings is u_2 , the displacement of the ice ground cylinder is u_1 .

According to the above mentioned formulas we can write such a system of equations:

$$\begin{aligned} u_3 &= u_1 + u_2; & p_2 &= p_i (k_a - k_b u_3); \\ u_1 &= p_2 k_c - p_1 k_d; & u_2 &= p_2 k_e. \end{aligned} \tag{12}$$

The coefficients k_a, k_e in the system of Eq. (12) we shall find from next expressions:

$$\begin{aligned} k_a &= 1 - \frac{3 \rho_w \alpha_f T}{0.09 \rho_d w_{mmw}}; \\ k_b &= \frac{\rho_w}{0.09 \rho_d w_{mmw} d_f} \text{ (m}^{-1}\text{)}; \\ k_c &= \frac{b^3 [(1 - \nu_f) + (1 + \nu_f) c^2 / b^2]}{E_f (c^2 - b^2)} \text{ (m} \cdot \text{MPa}^{-1}\text{)}; \\ k_d &= \frac{2bc^2}{E_f (c^2 - b^2)} \text{ (m} \cdot \text{MPa}^{-1}\text{)}; \\ k_e &= \frac{b^3 [(1 - \nu_k) + (1 + \nu_k) a^2 / b^2]}{E_k (a^2 - b^2)} \text{ (m} \cdot \text{MPa}^{-1}\text{)}. \end{aligned} \tag{13}$$

A solution of system (12) for p_2 (MPa) is:

$$p_2 = \frac{p_i (p_1 k_d k_b + k_a)}{1 + p_i (k_c k_b - k_e k_b)}; \tag{14}$$

The expression (14) gives us a possibility to evaluate the pressure, which is generated in course of thawing-freezing of the ground in zone of interface between ice-around barrier and tubings.

Let’s appreciate the pressure on the tubings in a period of ice-ground barrier formation. Our appreciating will arise from a next preconditions: the tubings are so stiff that no heave deformations arise, and therefore a heaving ground, freezing in a radial direction, will compress the thawed ground, and the value of the compression is equal to the so called “internal” heaving (according to Morarescu).

In this case a resistance of structural links of a ground, taking into account an historical factor of loading, is assumed to be equal to p_{zq} – an earth pressure at rest.

Neglecting by creepage of ground (a creep deformation of a ground is very little in comparison with a plastic one) we can obtain a heave pressure p_f , acting on a freezing a thawed ground, from such an expressions: $p_f = p_{zq} + p_q$, where p_q is a pressure, which consolidates a thawed ground on a value of “internal” heave, MPa.

For an evaluating of p_q we can use the formula from the elasticity theory [12], which was proposed by Lamé for a description of a stressed deformed state of a plane, having a circular- hole, when a uniform pressure is applied to the outline of the hole. This formula was used for- a determination of pressure of the ground, freezing around a cylindrical vessel with a cooling agent; it was registered a good argument of calculated and experimental values.

For our case we have next formula:

$$p_q = \frac{E_0 h_f}{(1 + \nu_0)(R + z)}, \tag{15}$$

where E_0 and ν_0 – modulus of deformation and Poisson coefficient for- thawed ground; h_f – displacement deformation (“internal” heave) when the ground is frozen on the distance z ; R – external radius of ice-ground barrier- after a placing of tubings; z – thickness of a frozen ground.

In formula (15) a part $(R + z)$ represents a radius of a conditional hole, and h_f is an elongation of the radius, corresponding with a heave deformation, this deformation is determined by a heave intensity. Since an increase of a frozen ground cylinder thickness d_z is equal to an increase of an ice-ground barrier radius d_r (see Fig. 3), heave intensity f_i may be expressed as $f_i = dh/dr$.

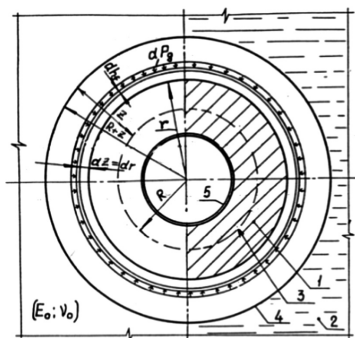


Fig. 3. Picture of the pressure, acting on the ice-ground barrier: 1 – frozen ground (ice-ground cylinder); 2 – thawed ground; 3 – contour of ice-ground barrier after the installation of tubings; 4 – design contour of ice-ground cylinder; 5 – tubing; dp_q – additional pressure (increment of the pressure), arising when a radius of the frozen cylinder increases on dr and accordingly a heaving increases on dh_f ; R - external radius of ice-ground barrier after an installation of tubings; z - thickness of a frozen ground layer.

Let's write the formula (15) for an increase of pressure dp_q , which arises when a heave deformation increases by dh_f :

$$dp_q = \frac{E_0 dh_f}{(1 + \nu_0)r} \tag{16}$$

provided that $r + dr \approx r$, taking into consideration the value f_i .

$$dp_q = \frac{E_0 f_i dr}{(1 + \nu_0)r}. \tag{17}$$

Expressing rectangular and triangular epures of heave intensity by

$$h_f(1) = f_i(1)z; \quad h_f(2) = \frac{f_i(2)z^2}{2(r - R)} \tag{18}$$

we obtain after an integration the expression (17), taking into consideration the expressions (18) in limits of frozen ground radius variation, from R to $R + z$, pressures $p_{q(1)}$ and $p_{q(2)}$ for above mentioned epures:

– for a rectangular epure

$$p_{q(1)} = \frac{E_0 h_f(1)}{(1 + \nu_0)z} \ln\left(1 + \frac{z}{R}\right); \tag{19}$$

– for a triangular epure

$$p_{q(2)} = \frac{2E_0 h_f(2)}{(1 + \nu_0)z^2} \left[z - R \ln\left(1 + \frac{z}{R}\right) \right] \tag{20}$$

The corresponding expression for a trapezoidal epure of heave intensity has such a formula:

$$p_{q(3)} = p_{q(1)} \mp p_{q(2)}. \tag{21}$$

The formulas (19)–(21) represent, taking into account an earth pressure at rest, the value of the pressure p_f , acting on external surface of the ice-ground barrier, the pressure p_f mustn't exceed the value p_p , which appears on an elastoplastic deformation stage. In the work [13] there is a solution of a plane problem from soil mechanics. The problem concerns a determination of a displacement u in a well with a radius r_o , the displacement is determined as a function of a pressure p , arising in conditions of elastoplastic deformation developing.

In our case one can assume that $u = h_f$ and $r_o = R + z$ and then for $p = p_p$ we can write

$$p_p = (1 + \sin\varphi)(p_b + c \cdot \text{ctg}\varphi) \left[\frac{E_0 h_f}{(1 + \nu_0)(p_b + c \cdot \text{ctg}\varphi)(R + z)\sin\varphi} \right]^{\frac{\sin\varphi}{1 + \sin\varphi}} - c \cdot \text{ctg}\varphi \tag{22}$$

where φ – angle of internal friction; c – specific adhesion of thawed ground.

Taking into account the formulas (7), (19)–(21) we write the conditions for the pressure p_f acting on external surface of ice-ground barriers: $p_f \leq p_p$, $p_f \leq p_i$. A determination of p_f from these conditions permits us to calculate the frozen ground pressure of ice-ground barrier p_3 on underground tubings.

The action of the pressure p_3 one can represent as result, at compression of an internal hollow cylinder (tubing) by an external cylinder (ice-ground barrier), to an external surface of the second cylinder the pressure p_f is applied, and to an internal surface of this cylinder the reaction pressure p_3 is applied.

Using the formulas (10) and (11) and expressing the condition of deformations compatibility in the form $u_1 = u_2$, we obtain

$$p_3 = p_f \frac{2E_0(b^2 - a^2)c^2}{E_k(b^2 - a^2)[(1 - \nu_f)b^2 + (1 + \nu_f)c^2] + E_f(c^2 - b^2)[(1 - \nu_k)b^2 + (1 + \nu_k)a^2]} \tag{23}$$

The fulfilled research permit us to determine a frost heaving pressure on an underground construction elements when heave grounds are artificially frozen.

Table 2. Comparison of calculated frost heaving pressure with real rock pressure on well strengthening wails (tubings)

WIOGEM data			Design heaving frost pressure of	Design error	
Componets of ground layers	Depths of ground layers, m	Pressure of ground layers on tubings, MPa			
		Calculated values	Actual (measured) values		
Cambridge-Oxford clay	406	3.75	5.76	4.9	17
Bath-Bayeux clay	471	5.78	8.48	8.1	5
	496	6.14	8.15	8.2	1

5 Conclusion

As can be seen from Table 2, the comparison of calculated pressure, determined with the help of proposed method, with actual values of pressure, which ground (rock) exerted upon tubings of a shaft № 2 of Yakovlevskiy mine (Kursk magnetic anomaly),

obtained on the of experimental researches of WIGEM institute, shows sufficiently high coincidence of calculated values with actual ones. This testifies, that an utilization of the proposed formulas in practice is reasonable.

References

1. Russo, G., Corbo, A., Cavuoto, F., Autuori, S.: Measurements and back analysis. *Tunnel Ling Underground Space Technol.* **50**, 226–238 (2015)
2. Marwan, A., Zhou, M.-M., Zaki Abdelrehim, M., Meschke, G.: *Comput. Geotech.* **75**, 112–125 (2016)
3. Xiangdong, H., Shengjun, D.: *Procedia Eng.* **165**, 633–640 (2016)
4. Azmatch, T.F., David, C., Sego, L.U., Arenson, K., Biggar, W.: *Cold Regions Sci. Technol.* **82**, 8–13 (2012)
5. Jiazuo, Z., Changfu, W., Houzhen, W., Long, T.: *Cold Regions Sci. Technol.* **104–105**, 76–87 (2014)
6. Hao, Z., Shunji, K., Fujun, N., Anyuan, L.: *Cold Regions Sci. Technol.* **118**, 30–37 (2015)
7. Bejan, A.: *Advanced Engineering Thermodynamics*, 4th edn., p. 782. Wiley, Hoboken (2016)
8. Borgnakke, C., Sonntag, R.E.: *Fundamentals of Thermodynamics*, 8th edn., p. 916. Wiley, Hoboken (2013)
9. Takashi, T.: Upper limit of heaving pressure derived by pore water pressure measurements of partially frozen soil. In: *Proceedings of 2nd International Symposium Ground Freezing Trondheim*, pp. 713–724 (1980)
10. Orlov, V., Kim, V.: *Soil Mech. Found. Eng.* **25**, 129–135 (1988)
11. Radd, F.J., Ortle, D.H.: *Permafrost Second International Conference National Asad. Washington DC*, pp. 377–384 (1973)
12. Boresi, A., Chong, K., Lee, J.: *Elasticity in Engineering Mechanics*, 3rd edn., p. 654. Wiley, Hoboken (2010)
13. Budhu, M.: *Soil Mechanics and Foundations*, 3rd edn., p. 780. Wiley, Hoboken (2010)

Comparative Analysis of the Simplest Finite Elements of Plates in Bending

Vladimir Agapov^(✉)  and Roman Golovanov 

Moscow State University of Civil Engineering,
Yaroslavskoe shosse, 26, Moscow 129337, Russia
agapovpb@mail.ru

Abstract. The triangular finite element with nine nodal degrees of freedom built up using displacement function as a complete cubic polynomial in Cartesian axes is described. The element is formed by averaging the characteristics of the three sub triangles; the function of the displacements for each sub triangle is given in the form of incomplete cubic polynomial in the local coordinate system, rotated with respect to the general system for the entire triangle. After adduction of all of the sub triangle characteristics to the total coordinate system for the whole triangle and averaging them, the final displacement function contains all ten terms of the complete cubic polynomial. The quadrilateral element, which is obtained by averaging the four basic triangle characteristics, is also described. The results of the test analysis of the developed elements are presented.

Keywords: Triangular finite element · Simplest finite element
Quadrilateral element

1 Introduction

The theory of bending thin plates, which was developed on the basis of the Kirchhoff hypotheses in the XIX century and received final form in the beginning of the XX century (historical review on this subject can be found in [1]), helped to solve many practical problems in different areas of technics. At the same time, a lot of problems related to the calculation of plates with a complex-shaped contour and loaded in a complex manner, remained unresolved. Only with the appearance of the finite element method in 1956 [2] an opportunity to solve these problems emerged. The first results on the plate in bending analysis by finite element method were obtained in [3]. The triangular bending element with 9 degrees of freedom has been described in this work, where the displacement function was approximated by incomplete cubic polynomial in Cartesian coordinates with the “xy” term omitted. Later it was found that of all the variants of incomplete cubic polynomials, the one with the term “ x^2y ” omitted gives the best results. This option provides the consistency of deflections and normal slope along the side of the triangle, which coincides with the local axis “x”, while along of the other sides only consistency of deflection is provided. These elements are called inconsistent.

It should be noted that the element proposed in [3] is the simplest implementation, since all the terms of the stiffness matrix can be easily found in the analytical form. At the same time, it does not provide the desired accuracy. These circumstances led to further efforts to improve the element proposed in [3]. Improvements came down to the construction of the composite triangles. One of these elements which is widely used, was described by Clough and Tocher in [4]. Element is formed by division of the whole triangle into three subtriangles having one common apex at the internal point. The compatibility of lateral displacements and normal slopes on the external borders of the triangle is provided by appropriate choice of the local coordinate systems for subtriangles. Internal degrees of freedom are eliminated at the stage of the element characteristics evaluation and this complicates all the formulations.

In [9] it was shown that the stiffness matrix of the triangular element with the function of the lateral displacements in the form of full cubic polynomial may be obtained by using so-called L-coordinates (coordinates associated with the area). To obtain the analytical expressions for the coefficients of the stiffness matrix in this case is problematic and this forced to perform numerical integration.

At that time a large number of finite elements of varying degrees of accuracy, and therefore, different complexity for analysis of plate bending are developed [6–10]. Description of the various approaches to the designing of such elements can be found in [6]. The element choice in the structural analysis is determined by the specific type of problem to be solved. For example, in the nonlinear analysis it is desirable to use such elements for which the stiffness matrix would be calculated in the simplest way because in such analysis these matrices have to be repeatedly recalculated. In transient dynamic analysis the finite element sizes have to be taken quite small, so the use of complex precision elements in such analysis is inappropriate.

Therefore, it's desired to have the simple triangular and quadrilateral finite elements of plate in bending in the finite element method programs. Such elements are implemented in the program PRINS developed by the authors. The description of these elements is provided below.

2 Materials and Methods

2.1 The Triangular Finite Element of Plate in Bending

Let's impose the function of lateral displacements of the middle surface of the triangular element shown in Fig. 1, in the form of:

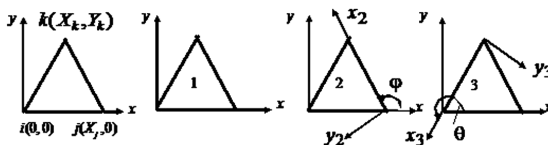


Fig. 1. Triangle element as the sum of three sub triangles: given triangle and sub triangles

$$w = \frac{1}{3} (\widehat{w}_1 + \widehat{w}_2 + \widehat{w}_3), \tag{1}$$

where $\widehat{w}_1, \widehat{w}_2, \widehat{w}_3$ - the lateral displacements functions defined on subtriangles 1, 2, 3 (see Fig. 1) as:

$$\begin{aligned} \widehat{w}_1 &= a_1 + a_2x_1 + a_3y_1 + a_4x_1^2 + a_5x_1y_1 + a_6y_1^2 + a_7x_1^3 + a_8x_1y_1^2 + a_9y_1^3; \\ \widehat{w}_2 &= b_1 + b_2x_2 + b_3y_2 + b_4x_2^2 + b_5xy_2 + b_6y_2^2 + b_7x_2^3 + b_8x_2y_2^2 + b_9y_2^3; \\ \widehat{w}_3 &= c_1 + c_2x_3 + c_3y_3 + c_4x_3^2 + c_5x_3y_3 + c_6y_3^2 + c_7x_3^3 + c_8x_3y_3^2 + c_9y_3^3. \end{aligned} \tag{2}$$

The polynomials coefficients in the formula (2) can be expressed through the nodal displacements $\{q_1\}, \{q_2\}, \{q_3\}$:

$$\{a\} = [A_1^{-1}]\{q_1\}; \{b\} = [A_2^{-1}]\{q_2\}; \{c\} = [A_3^{-1}]\{q_3\}, \tag{3}$$

where

$$\begin{aligned} \{a\} &= [a_1 \ a_2 \ \dots \ a_9]^T; \{b\} = [b_1 \ b_2 \ \dots \ b_9]^T; \\ \{c\} &= [c_1 \ c_2 \ \dots \ c_9]^T; \\ \{q_1\} &= [w_i\alpha_i\beta_i w_j\alpha_j\beta_j w_k\alpha_k\beta_k]_{(x_1,y_1)}^T; \{q_2\} = [w_j\alpha_j\beta_j w_k\alpha_k\beta_k w_i\alpha_i\beta_i]_{(x_2,y_2)}^T; \\ \{q_3\} &= [w_k\alpha_k\beta_k w_i\alpha_i\beta_i w_j\alpha_j\beta_j]_{(x_3,y_3)}^T. \end{aligned}$$

Matrices $[A_1^{-1}], [A_2^{-1}], [A_3^{-1}]$ are defined in dependence from the coordinates of nodal points of subtriangles in their local axis.

With account of (2) and (3) we obtain:

$$\begin{aligned} \widehat{w}_1 &= [1 \ x_1 \ y_1 \ x_1^2 \ x_1y_1 \ y_1^2 \ x_1^3 \ x_1y_1^2 \ y_1^3] [A_1^{-1}]\{q_1\}; \\ \widehat{w}_2 &= [1 \ x_2 \ y_2 \ x_2^2 \ x_2y_2 \ y_2^2 \ x_2^3 \ x_2y_2^2 \ y_2^3] [A_2^{-1}]\{q_2\}; \\ \widehat{w}_3 &= [1 \ x_3 \ y_3 \ x_3^2 \ x_3y_3 \ y_3^2 \ x_3^3 \ x_3y_3^2 \ y_3^3] [A_3^{-1}]\{q_3\}. \end{aligned} \tag{4}$$

Let's express the vectors $\{q_3\}$ and $\{q_2\}$ through the vector $\{q_1\}$, and coordinates x_2, y_2, x_3, y_3 through $x_1 \equiv x$ and $y_1 \equiv y$. We shall obtain:

$$\{q_2\} = [P_2][T_2]\{q_1\}; \{q_3\} = [P_3][T_3]\{q_1\}. \tag{5}$$

$$x_2 = (x - X_j) \cos \varphi + y \sin \varphi; y_2 = -(x - X_j) \sin \varphi + y \cos \varphi. \tag{6}$$

$$x_3 = (x - X_k) \cos \theta + (y - Y_k) \sin \theta; y_3 = -(x - X_k) \sin \theta + (y - Y_k) \cos \theta. \tag{7}$$

In formulae (5) $[T_2]$ and $[T_3]$ - the matrices of direction cosines of axis x_2y_2 and x_3y_3 in the axis xy , respectively, $[P_2]$ and $[P_3]$ - permutation matrices. At that:

$$\left. \begin{aligned} [T_2] &= \begin{bmatrix} \bar{T}_2 & 0 & 0 \\ 0 & \bar{T}_2 & 0 \\ 0 & 0 & \bar{T}_2 \end{bmatrix}; & [T_3] &= \begin{bmatrix} \bar{T}_3 & 0 & 0 \\ 0 & \bar{T}_3 & 0 \\ 0 & 0 & \bar{T}_3 \end{bmatrix}; \\ [\bar{T}_2] &= \begin{bmatrix} 1 & 0 & 0 \\ 0 & \cos \varphi & \sin \varphi \\ 0 & -\sin \varphi & \cos \varphi \end{bmatrix}; & [\bar{T}_3] &= \begin{bmatrix} 1 & 0 & 0 \\ 0 & \cos \theta & \sin \theta \\ 0 & -\sin \theta & \cos \theta \end{bmatrix}; \\ [P_2] &= \begin{bmatrix} 0 & E_1 & 0 \\ 0 & 0 & E_1 \\ E_1 & 0 & 0 \end{bmatrix}; & [P_3] &= \begin{bmatrix} 0 & 0 & E_1 \\ E_1 & 0 & 0 \\ 0 & E_1 & 0 \end{bmatrix}; & [E_1] &= \begin{bmatrix} 1 & 0 & 0 \\ 0 & 1 & 0 \\ 0 & 0 & 1 \end{bmatrix}. \end{aligned} \right\} \quad (8)$$

Substituting relations (5)–(7) in the formula (4), we obtain (intermediate conversion omitted):

$$\left. \begin{aligned} w_1 &= [1 \ x \ y \ x^2 \ xy \ y^2 \ x^3 \ xy^2 \ y^3] [A_1^{-1}] \{q_1\}; \\ w_2 &= [1 \ x \ y \ x^2 \ xy \ y^2 \ x^3 \ x^2y \ xy^2 \ y^3] [C_2] [A_2^{-1}] [P_2] [T_2] \{q_1\}; \\ w_3 &= [1 \ x \ y \ x^2 \ xy \ y^2 \ x^3 \ x^2y \ xy^2 \ y^3] [C_3] [A_3^{-1}] [P_3] [T_3] \{q_1\}. \end{aligned} \right\} \quad (9)$$

Matrix $[C_2]$ and $[C_3]$ have the order of 10×9 and are determined depending on the coordinates of the nodal points of a given triangle and angles φ and θ (Fig. 1).

We represent the first line of the formula (2) in the form of:

$$w_1 = [1 \ x \ y \ x^2 \ xy \ y^2 \ x^3 \ x^2y \ xy^2 \ y^3] [\bar{A}_1^{-1}] \{q_1\}, \quad (10)$$

where $[\bar{A}_1^{-1}]$ - the augmented $[A_1^{-1}]$ matrix, and the expansion is carried out by adding the zero line between the seventh and eighth rows of the matrix, i.e.

$$[\bar{A}_1^{-1}] = \begin{bmatrix} 1 \text{ - st row of matrix } A_1^{-1} \\ 2 \text{ - nd row of matrix } A_1^{-1} \\ \vdots \\ 7 \text{ - th row of matrix } A_1^{-1} \\ 0 \ 0 \ 0 \ 0 \ 0 \ 0 \ 0 \ 0 \ 0 \\ 8 \text{ - th row of matrix } A_1^{-1} \\ 9 \text{ - th row of matrix } A_1^{-1} \end{bmatrix}$$

With account of formulas (1), (9) and (10) we obtain:

$$w = [1 \ x \ y \ x^2 \ xy \ y^2 \ x^3 \ x^2y \ xy^2 \ y^3] [A] \{q_1\}, \quad (11)$$

where

$$[A] = \frac{1}{3} \left[[\bar{A}_1^{-1}] + [C_2][A_2^{-1}][P_2][T_2] + [C_3][A_3^{-1}][P_3][T_3] \right]$$

The function of lateral displacements (11) is a complete cubic polynomial whose coefficients are expressed over nine nodal displacements of finite element.

Such a function in Cartesian coordinates obtained by the authors and apparently for the first time was described in [11]. Thus, all transformations used to calculate the coefficients of the polynomial are nonsingular and have a place for a triangular finite element of any kind. The stiffness matrix and load vector for the triangular finite element with lateral displacement function (11) are calculated by the standard procedure described repeatedly in the literature (see, for example, [8]).

Triangular element described above identified in the program PRINS as Elem34.

2.2 Quadrilateral Finite Element of Plate in Bending

To construct a quadrilateral element in the program PRINS an idea accepted which was first suggested in [6, 7]. At that quadrilateral (not necessarily square) finite element is divided into triangles, as shown in Fig. 2. However, described above basic triangles are used as the components, and no additional degrees of freedom are introduced, which considerably simplifies all formulations. Local axis x_m for subtriangles coincide with the diagonals of the quadrilateral, which ensures compatibility of displacements and normal slope all around the element.

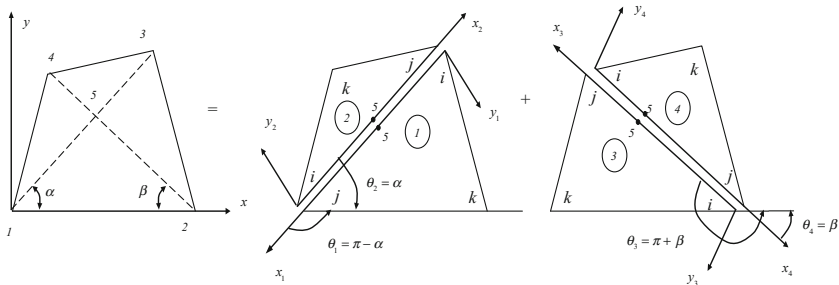


Fig. 2. Quadrilateral element

The stiffness matrix of quadrangular element in its local axes xy is found by the averaging of the subtriangles 1–4 stiffness matrices reduced to this axis according to the formula:

$$[K]_{xy} = \frac{1}{2} \left([K_1]_{xy} + [K_2]_{xy} + [K_3]_{xy} + [K_4]_{xy} \right)$$

Stiffness matrices of triangles in their local axis are calculated by standard method, and the transition to the local axes of the quadrilateral is made by standard transformations:

$$[K_m]_{xy} = [L_m]^T [K_m]_{x_m y_m} [L_m], \quad m = 1, 2, 3, 4$$

where $[K_m]_{xy}$ - stiffness matrix of m -th subtriangle in local axes of quadrilateral, $[K_m]_{x_m y_m}$ - stiffness matrix of m -th subtriangle in his own local axes, $[L_m]$ - matrix of the direction cosines of the local axes of the m -th sub triangle in the local axes of the quadrilateral. Thus obtained element was identified in the program PRINS as Elem26.

3 Results

To assess the accuracy and precision of the proposed elements the square plate with simply supported and clamped edge subjected to uniform loading was calculated at different values of the grid parameter ‘n’. The results as a function of the error of central point displacement from the grid parameters are shown in Figs. 3, 4, 5 and 6. These same figures show the results obtained by well known finite elements of Clough-Tocher for the triangular and Clough-Felippa for the rectangular grid.

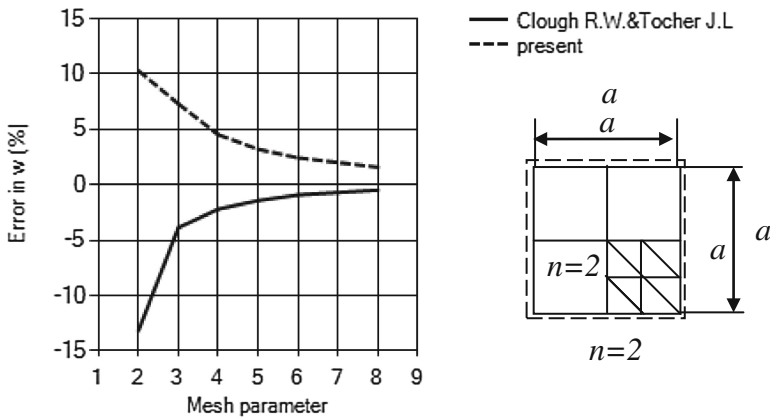


Fig. 3. Simply supported uniformly loaded square plate - triangles

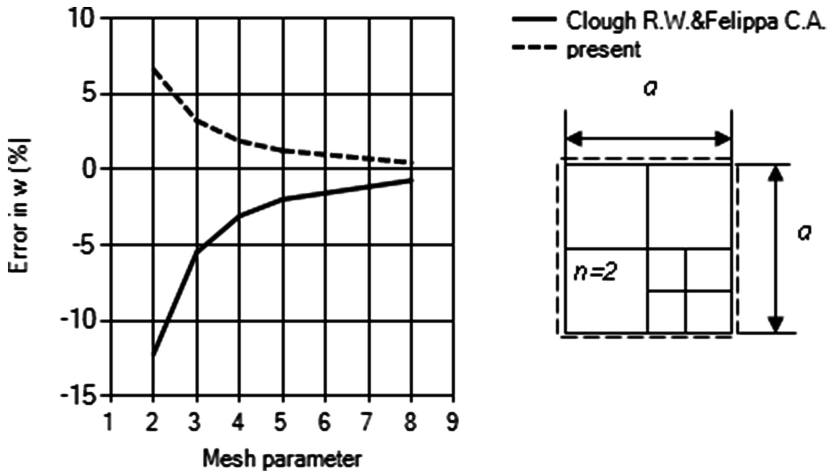


Fig. 4. Simply supported uniformly loaded square plate – quadrilaterals

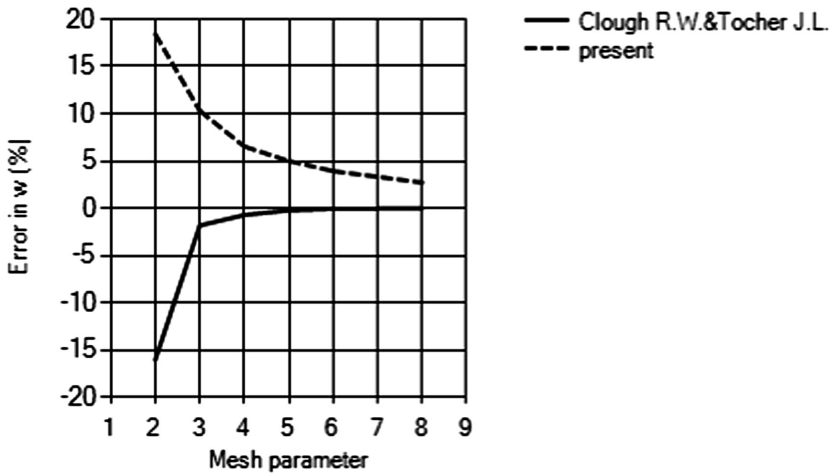


Fig. 5. Clamped uniformly loaded square plate – triangles

4 Discussion

Developed by the authors elements ensure accuracy and precision of the same order as the known elements widely applicable in practice. Because of the simplicity of the formulations these elements are suitable for use in cases when it's necessary repeatedly recalculate characteristics of the elements in the problem solutions process.

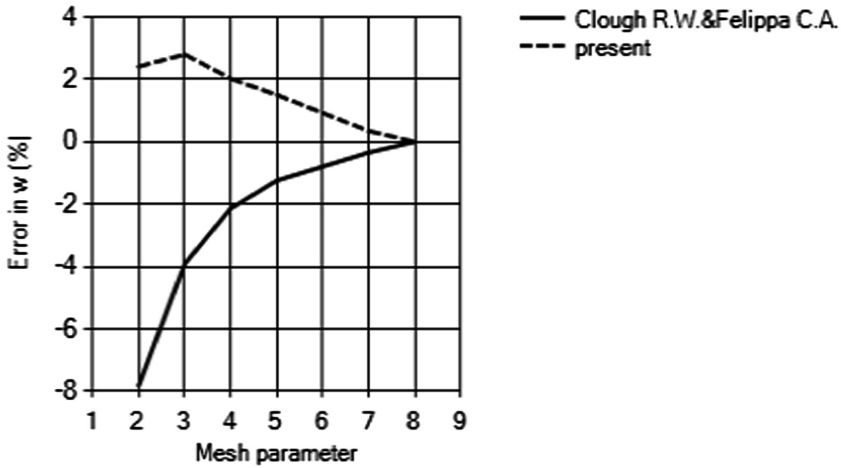


Fig. 6. Clamped uniformly loaded square plate – quadrilaterals






5 Conclusions

The finite elements described in this article can be useful in the implementation of both linear and nonlinear calculations of structures, as well as in performing of dynamic calculations in the time domain.

References

1. Timoshenko, S.P., Woinowski-Krieger, S.: Theory of Plates and Shells, 2nd edn, p. 635. McGraw Hill, New York (1959)
2. Turner, M.J., Clough, R.W., Martin, H.C., Topp, L.J.: Aero. Sci. **23**, 805 (1955)
3. Adini, A., Clough, R.W.: Technical Report G-7337 Report to National Science Foundation, USA (1961)
4. Clough, R.W., Tocher, J.L.: Proceedings of 1st Conference on Matrix Methods in Structural Mechanics: AFFDL-TR-68-80, Ohio, pp. 515–545 (1956)
5. Clough, R.W., Felippa, C.A.: Proceedings of 2nd Conference on Matrix Methods in Structural Mechanics: AFFDL-TR-68-150, Ohio, pp. 399–440 (1968)
6. Sander, G.: Bull. Soc. R. des Sci. de Liege. **33**, 456 (1974)
7. De Veubeke, B.F.: Int. J. Solids Struct. **4**(1), 95 (1968)
8. Zienkiewicz, O.C., Taylor, R.L.: The Finite Element Method for Solid and Structural Mechanics, 6th edn., p. 631. Elsevier Butterworth-Heinemann (2005)
9. Bazeley, G.P., Cheung, Y.K., Irons, B.M., Zienkiewicz, O.C.: Proceedings of 1st Conference on Matrix Methods in Structural Mechanics: AFFDL-TR-68-80, Ohio, pp. 547–576 (1965)
10. Agapov, V.P.: Metod konechnykh elementov v ststike, dinamike i ustoychivosti konstrukcii (Finite Element Method in Static, Dynamic and Buckling Analysis of Structures). ASV, Moscow, p. 247 (2005)
11. Agapov, V.P.: Usovshenstvovannyiy ploskiy mnogosloynnyiy treugolnyiy konechnyy element kombinirovannogo tipa (Advanced flat multilayer triangular finite element of combined type) News of Higher Educational Institutions. Construction and Architecture. Novosibirsk **10**, 31–34 (1985)

The Influence of Cement Plant on the Atmospheric Pollution with Microscale Particulate Matter in Spassk-Dalny Town (Primorsky Region, Russia) – Particle Size Analysis

Aleksei Kholodov^(✉) , Sergey Ugay , Vladimir Drozd ,
Svetlana Gulkova , and Kirill Golokhvast 

Far Eastern Federal University, 8, Sukhanova St., Vladivostok 690090, Russia
alex.holodov@gmail.com

Abstract. The paper is focused on the research of the influence of a large cement plant on the atmospheric particulate matter of Spassk-Dalny town by laser granulometry methods. Atmospheric particulates were studied in the snow cover collected during snowfall in January 2015. The sampling points were located near plants, along major streets, as well as in the residential area. It is shown that the atmosphere of this town is notably polluted with particles under $10\ \mu\text{m}$ (PM_{10}). In 8 sample points out of 12 we found hazardous to health microscale particles in significant quantities – from 16.8 to 27.8%. Large particles sized above $400\ \mu\text{m}$ prevail in residential areas of the town amounting to 69.7%. We can conclude that the atmosphere of Spassk-Dalny suffers from the negative influence of a large source of microscale pollution. It is evidenced by the presence in almost all areas of particles under $10\ \mu\text{m}$ in size which may be hazardous for human health and the environment.

Keywords: Atmospheric suspension · Ecology · Spassk-Dalny
Microparticles

1 Introduction

It is a common belief that air pollution is higher in large cities than in small towns, and that people in mega cities are more susceptible to environmental-related diseases. Major cities in Russia have operating environment monitoring systems with dozens of controlled parameters, while environmental studies in small and medium-sized towns are often not systematic and do not provide consistent data [1, 2]. Earlier we have studied the environment of major cities of Russia's Primorsky Region: Vladivostok, Ussuriysk and Nakhodka with populations of 100 to 700 thousand people [3, 4].

It is worth noting that small and medium-sized towns are often the territories where town-forming enterprises are located [1]. In certain cases these enterprises heavily pollute the atmosphere, emitting hazardous and potentially hazardous substances in

such quantities that make these towns equal to large cities in terms of the environmental damage.

The current research is dedicated to the study of microscale air pollution of Spassk-Dalny – a small town in Primorsky Region by means of the laser diffraction analysis of snow water. The snow sampling is considered to be highly informative, since the host medium contains the particles as they are present in the atmosphere [5]. Moreover, there is little need for sample preparation: the samples don't need to be filtered or concentrated.

Spassk-Dalny town is the administrative center of Spassky district of Primorsky Region. The town is located in an open area in the basin of the Kuleshovka and Spasovka rivers, 243 km north of Vladivostok. The climate is moderate monsoon, the prevailing wind direction is the southwestern (northwestern in the winter), the average annual wind speed is 2.5–3 mps. The weather during the winter is dry, frosty and clear [6]. The population in 2015 was 42,020 people.

The major town-forming enterprise of Spassk-Dalny is AO Spasskement – the company producing portland cement and other construction products and the main cement producer in the region. This cement plant was formed by the merger of the Spassky and Novospassky plants, both operating within the city limits. Spassky plant was founded in 1907 during the period when Trans-Siberian railway was under construction. To date, the plant production capacity is 3.127 thousand tons of portland cement per year.

According to the previous studies Spassk-Dalny is heavily polluted with dust and particulate matter (among other types of pollution), and the cement plants are its primary sources. The studies have shown direct correlation between the amount of airborne particulate matter and health issues in the population [7, 8]. Airborne PM is known to be a complex heterogeneous mixture of solid and liquid particles varying in size and chemical composition [9]; certain particles may cause various health issues due to their ability to adsorb large quantities of toxic materials and easily penetrate human body. Cement production is an industry that generates dust and particulate matter, which causes lung illnesses and other diseases in humans and poses a threat to the environment [10–15].

Other major stationary pollutants of the environment in the town include the Spassk plant of asbestos and cement and a railway station.

2 Materials and Methods

The particles size analysis was conducted using the snow water. Snow sampling points were chosen alongside the territories of the above mentioned enterprises, along the roads and in the residential areas. The schematic map with the locations of snow sampling points is presented in Fig. 1. In this figure only the old cement plant is pictured. The new cement plant is located further the southwest.

The atmospheric particulate matter was studied in the snow collected during snowfalls in January 2015. In order to exclude the secondary pollution of anthropogenic aerosols, only the top layer (5–10 cm) of freshly fallen snow was collected. It was placed in sterile 3 L plastic containers and transported to the laboratory. After

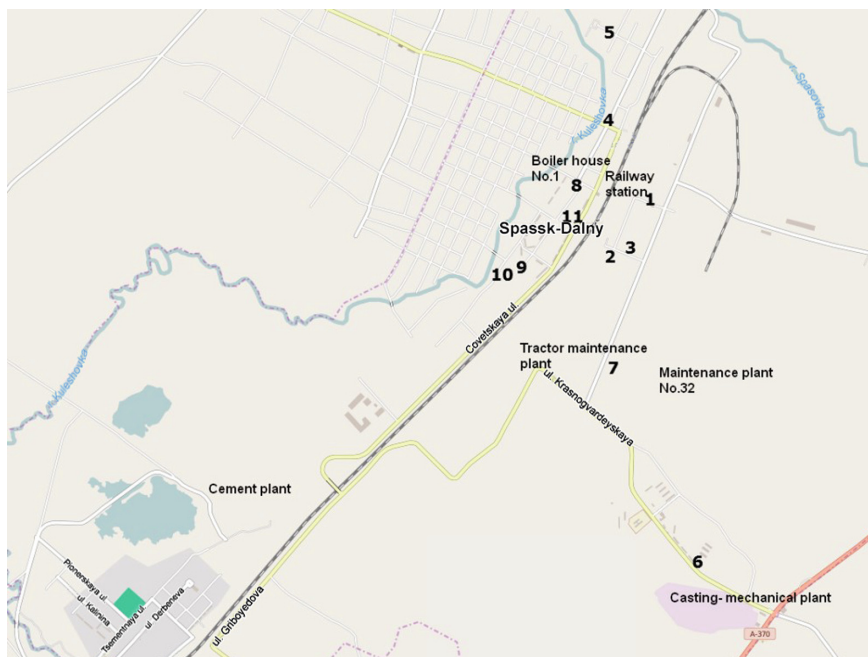


Fig. 1. Snow sampling points in Spassk-Dalny town: (1) - 22 Ofiterskiy per.; (2) - 10 Suvorovskaya Str.; (3) - 8a Borisova Str.; (4) - 8 Vokzalnaya Str.; (5) - 14 Kommunalnaya Str.; (6) - 91 Krasnogvardeyskaya Str.; (7) - 27 Krasnoznamenennaya Str.; (8) - 5 Kustovinovskaya Str.; (9) - 42 Leninskaya Str.; (10) - 31 Parkovaya Str.; (11) - 86 Sovetskaya Str.; (12) - Central Square. OpenStreetMap contributors

several hours when the snow melted in the container, the liquid was stirred and 60 ml portion was taken from each sample and analyzed on the laser particle analyzer Analysette 22 NanoTech plus (Fritsch GmbH, Germany). The measurement was carried with the settings of the measured system “quartz/water 20 °C”, the measurement range was 0.008–2000 μm .

3 Results and Discussion

The percentage of fractions in particulate matter samples in all sampling points is presented in Table 1; physical parameters of the particle are given in Table 2. Comparing the particle sizes of PM in different areas of Spassk-Dalny town, several conclusions can be made.

First, according to the sampling, the atmosphere of the town is polluted with particulate matter under 10 μm (PM_{10}). The particles of this size were found in significant proportions (from 16.8 to 27.8%) in almost all areas of Spassk-Dalny (8 out of 12 sampling points, see Fig. 2). There are several residential areas that are dominated with large particles over 400 μm in diameter, which is natural (Fig. 3).

Table 1. Distribution of particle fractions in the snow samples in Spassk-Dalny, %

Sampling points	Fraction, μm						
	under 1	1–10	10–50	50–100	100–400	400–700	Over 700
	Quantity, %						
1	2.2	31.5	11.5	-	-	2.2	52.6
2	2.6	16.8	20.7	-	22.4	34.3	3.2
3	0.3	1.9	5.2	2.4	23.4	43.7	23.1
4	1.9	20.1	7	-	-	4.8	66.1
5	1	24.5	9.5	-	-	11.1	53.9
6	2.3	20.5	15.4	-	-	5.9	55.9
7	0.3	1.5	3.4	1.4	26.6	38.9	29.1
8	3	27.8	18.7	-	-	3.1	47.4
9	0.4	7.2	11.9	0.2	1	11.5	67.8
10	0.2	0.9	2.8	0.7	25.7	46.7	23
11	2.7	20.1	14.6	-	-	5.5	57.1
12	3.2	18.2	18.7	-	25.4	32.1	2.4

Table 2. Physical properties of particles in the snow samples in Spassk-Dalny, μm

Sampling points	Mean diameter, μm	Mode, μm
1	531.57	941.69
2	278.83	460.85
3	509.04	597.61
4	664.28	911.59
5	566.6	854.25
6	566.23	882.46
7	545.97	726.2
8	480.38	911.59
9	701.32	882.46
10	530.19	542.12
11	579.22	882.46
12	266.88	446.13

Spassk-Dalny is among the most polluted towns in Primorsky Region, comparable to Ussuriysk and Artem [2, 7]. The car traffic in the town is not as intensive as in mega cities and the only large-scale production in the town is its town-forming enterprise.

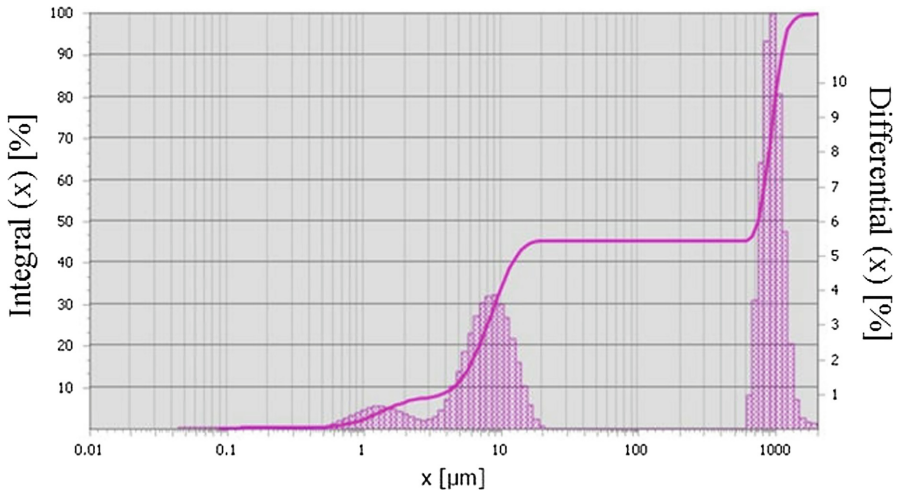


Fig. 2. The correlation of particulates of different size fractions in snow water sample from Ofitserskiy per. (sampling point 1). The number of PM_{10} particles is 33.7%

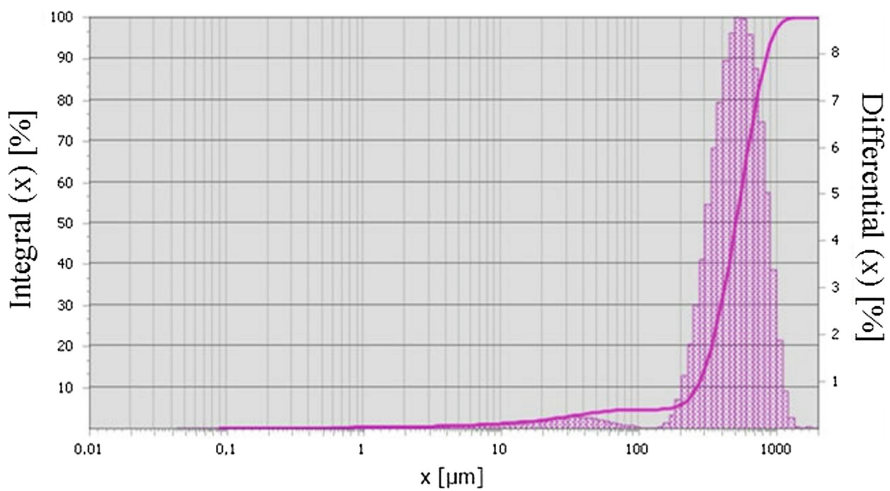


Fig. 3. The correlation of particulates of different size fractions in snow water sample from Parkovaya Str. (sampling point 10). The number of particles over $400 \mu m$ is 69.7%

Since the major pollutant in the town is the cement production plant (consisting of two facilities), it is evident that this production has a marked effect on the microscale atmosphere pollution of the town and may be among the reasons of the degradation of health of the population. Due to the winds prevailing in the area the cement dust and particulate matter are transported by air over the whole territory of the town.

4 Conclusion

We can conclude that, judging from the results of our study, Spassk-Dalny can be considered a problem town from the standpoint of location of particles sized under 10 μm in the atmosphere. Particles under than 10 μm were found in most areas of the town. The pollution with microscale particulate matter is possibly due to the influence of the cement plant, because this type of production is associated with fine dust. The distance from the old cement plant to the center of the town is only 3.5 km, which is not a serious obstacle for fine dust and particulate matter.

The consequences of this type of air pollution are potentially very dangerous. The medical literature describes cementoses – lung diseases associated with inhalation of cement dust. Dust induces huskiness, irritation of the respiratory tract, pain, cough, and as a result, there is proliferation of the connective tissue, lungs loose elasticity, and ventilation suffers.

Also, the influence of other air pollutants is likely in other areas: boiler houses, the railway station and the casting-mechanical plant, and road traffic.

As a practical conclusion of this work, it should be noted that there is a necessity to control the composition of the atmospheric suspension in Spassk-Dalny town and emissions of a number of enterprises.

Acknowledgements. The research was conducted using the equipment of the Interdepartmental Center of Analytical Control of the State of Environment FEFU and Nanocenter FEFU.






This work was supported by Grant of the President of the Russian Federation for young doctor of sciences (MD-7737.2016.5).

References

1. Golokhvast, K.S.: *Atmosfernye Vzvesi Gorodov Dalnego Vostoka*. FEFU, Vladivostok (2013)
2. Khristoforova, N.K.: *Ekologicheskie Problemy Regiona: Dalny Vostok – Primorye*. Khabarovsk Publication, Khabarovsk (2005)
3. Drozd, V.A., Kholodov, A.S., Agoshkov, A.I., et al.: Potential toxic risk from the nano- and microparticles in the atmospheric suspension of Russky Island (Vladivostok). *Der Pharma Chemica* **8**(11), 231–235 (2016)
4. Golokhvast, K.S., Soboleva, E.V., Borisovsky, A.O., Khristoforova, N.K.: Composition of atmospheric suspensions of Ussuriisk city according to snow pollution. In: 20th International Symposium on Atmospheric and Ocean Optics: Atmospheric Physics, vol. 9292, p. 929242. SPIE (2014)
5. Golokhvast, K.S., Khristoforova, N.K., Kiku, P.F., Gulkov, A.N.: Granulometricheskii i Mineralogicheskii Analiz Vzveshennykh Chastits v Atmosfernom Vozdukh. *Bull. Physiol. Pathol. Respir.* **40**, 94–100 (2011)
6. Baklanov, P.Ya., Zonov, Yu.B., Romanov, M.T., et al.: *Geografiya Primorskogo Kraja*, 2nd edn. DalPress, Vladivostok (2000)
7. Kolomeytseva, O.L., Khristoforova, N.K.: Comparative assessment of air pollution of the two industrial cities of Primorsky krai—Ussuriysk and Spassk-Dalny. *RUDN J. Ecol. Life Saf.* **4**, 76–81 (2012)

8. Senotrusova, S.V.: Vliyanie Zagryazneniya Okruzhayushchey Sredy na Zabolevaemost Naseleniya Promyshlennykh Gorodov. Doctor of Biology thesis, Vladivostok (2005)
9. Brook, R.D., Franklin, B., Cascio, W., et al.: Air pollution and cardiovascular disease. *Circulation* **109**, 2655–2671 (2004)
10. Merenu, I.A., Mojiminiyi, F.B.O., Njoku, C.H., Ibrahim, M.T.O.: The effect of chronic cement dust exposure on lung function of cement factory workers in Sokoto, Nigeria. *Afr. J. Biomed. Res.* **10**, 139–143 (2007)
11. Jones, L.C., Hungerford, D.S.: Cement disease. *Clin. Orthop. Relat. Res.* **225**, 192–206 (1987)
12. Vasilyeva, O.S.: Pnevmoniozy. *Russ. Med. J.* **24**, 1441 (2010)
13. Falaleeva, N.A., Falaleev, A.G.: *Ekologiya Shlakovikh Tsementov i Betonov*. Publishing house of DVGU, Vladivostok (2010)
14. Dzyuba, O.V., Paramonova, O.N.: Analysis of the impact of cement plants on air quality across the Russian Federation. *Int. Res. J.* **5–2(36)**, 47–49 (2015)
15. Gorchakova, A.Yu.: O Vliyanii Tsementnogo Proizvodstva na Rasteniya. In: *Proceedings of the Samara Scientific Center of the Russian Academy of Sciences*, vol. 16, no. 1, pp. 120–126 (2014)

Estimation of Practical Significance for Application of Composite Pipes in Comparison with Metal and Polymer Materials

Konstantin Strogonov¹  , Alexander Fedyukhin¹ ,
Tatiana Stepanova¹ , and Oleg Derevianko² 

¹ National Research University “Moscow Power Engineering Institute”,
Krasnokazarmennaya 14, Moscow 111250, Russia
StrogonovKV@yandex.ru

² Peter the Great St. Petersburg Polytechnic University, Polytechnicheskaya 29,
Saint Petersburg 195251, Russia

Abstract. In recent years, highly efficient pre-insulated pipes, made of heat-resistant polymer (usually polyethylene) materials are used during the reconstruction and repair of heat networks. Their advantage is the convenience and ease of installation, long service life, corrosion protection. This material is often used for internal heating circuits when water temperature is up to 95 °C and pressure is up to 1.6 MPa due to limitations of the physico-chemical properties of the material. At the same time for manufacturing of modern, highly efficient and durable pipe system, depending on destination, location and method of installation various composite materials: basalt, glass or carbon fiber; synthetic fiber; rubber, fluoropolymers and others can be used. High specific strength and stiffness of fibrous composite materials, along with chemical stability, relatively low weight and other properties make these materials attractive for the manufacture of pipes for various purposes. The advantages of using pipelines made of composite materials is to increase the estimated service life of heat networks in two times in comparison with metal pipes, reducing the hydraulic and thermal losses due to the physico-chemical properties of the material, and also lower labor and financial costs for the construction of heating mains.

Keywords: District Heating System · Composite pipes · Fiberglass
Thermal insulation · Foam rubber · Polyurethane foam

1 Introduction

Nowadays in Russian Federation metal pipes with mineral wool and fiberglass insulation are the most common materials for district heating providing. At this, service period of the majority of heat networks has exceeded the 25-years designed period. Now wear degree of communal infrastructure is about 70–80% and it is increasing every year for 1–2%. Nowadays metal and polymeric pipes with foamed polyurethane

(FPU) insulation are widely used for repairing of old heat pipelines and for laying of new ones. Various composite materials (steel, fiberglass composite, polymer) are used for manufacturing of modern highly efficient and long-term operating pipes depending on their purpose, location and method of installation.

2 Materials and Methods

This paper considers efficiency of application of pipelines made from composite materials for heat supply system designing. The calculations are performed for model heat supply system of Technological Park located at Far Eastern Federal District. The calculations were performed using ZuluGIS software, the initial data are put into Tables 1, 2 and 3 (Fig. 1).

Table 1. Initial data for the electronic model (1).

Characteristics	Value
Design temperature at supply pipeline, °C	95
Design temperature of cold water, °C	5
Design temperature of ambient air, °C	-29
Current temperature at supply/return pipeline, °C	95/70
Current temperature of ambient air, °C	-29
Pressure at supply pipeline, m	40
Pressure at return pipeline, m	20
Annual average temperature at supply pipeline, °C	65
Annual average temperature at return pipeline, °C	50
Annual average soil temperature, °C	1
Annual average temperature of ambient air, °C	-9.5
Annual average temperature of air at basement level, °C	5
Current soil temperature, °C	1
Current temperature of air at basement level, °C	5
Heat network tracing type	Underground channelless
Soil type (dry)	Sand, sandy loam
Thermoinsulation material of the supply pipeline	Foamed polyurethane (FPU)/foam rubber (FR)
Thermoinsulation material of the return pipeline	FPU/FR
Design temperature of indoor air, °C	20

Table 4 presents calculation data of thermal and hydraulic losses at Technological Park units based on initial data from Table 1.

According to the obtained data (Table 4), composite pipeline has the lowest specific thermal losses (82.84 W/m).

Table 2. Initial data for the electronic model (2).

Consumer	Design load for heating, kW	Design load for heating, Gcal/h
Section 3	1128.11	0.97
Section 4	1314.19	1.13
Section 5	1407.23	1.21
Section 6	744.32	0.64
Section 7	1081.60	0.93
Section 8	1081.60	0.93
Section 9	2023.62	1.74
Section 10	2407.41	2.07

Table 3. Initial data for the electronic model (3).

No.	Section beginning	Section end	Section length, m	Inner diameter of the supply pipeline, m	Inner diameter of the return pipeline, m
1	Power park	TU1	64	0.309	0.309
2	TU1	TU2	120	0.259	0.259
3	TU2	TU3	63	0.259	0.259
4	TU3	TU4	54	0.259	0.259
5	TU4	TU5	50	0.207	0.207
6	TU5	TU6	54	0.207	0.207
7	TU1	TU7	140	0.259	0.259
8	TU2	Section 8	20	0.150	0.150
9	TU3	Section 3	20	0.150	0.150
10	TU4	Section 7	20	0.150	0.150
11	TU5	Section 4	20	0.150	0.150
12	TU6	Section 5	29	0.150	0.150
13	TU6	Section 6	20	0.125	0.125
14	TU7	Section 9	20	0.207	0.207
15	TU7	Section 10	80	0.207	0.207

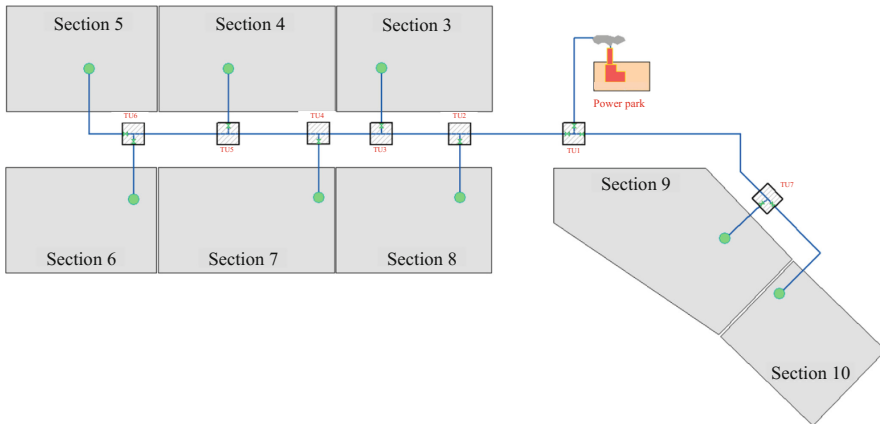


Fig. 1. Appearance of Technological Park heat supply system

These values will be further used for estimation of cost savings by means of thermal losses reduction. Table 5 presents calculation of thermal losses for composite pipeline with various insulations. The estimation shows that using of FR reduces thermal losses for 13.85 W/m. Table 6 presents calculation data of hydraulic losses for the Technological Park taking into account incrustation of metal pipes for 25 mm. Incrustation depends on water quality, water treatment technology, pipeline service conditions and other factors. So, incrustation value for one exploitation period varies a lot and can be forecasted basing on experience or statistical data. This approach is applicable for characteristics analysis of heat networks with service period more than 13 years.

During exploitation steel pipes usually break down due to corrosion processes and incrustation of the inner dimensions by corrosion products and carbonate deposits. According to various estimates, inner surface roughness of steel galvanized pipes increases by 30–35 times after 5 years service period and by more than 100 times after 15 years service period. For example, equivalent roughness coefficient K_e of a new steel pipe is generally equal to 0.5 mm, in 5 years' service period it is equal to 5 mm and after 10 years it is 15–20 mm. In particular, this coefficient for steel galvanized pipes of $D = 25$ mm which were used at hot water system for 15 years is equal to be 22 mm [1].

Calculation data from Table 6 show that metal pipe incrustation of 25 mm impairs its hydraulic characteristics for more than 2 times as compared to new material. For new pipeline Delivery head losses are about 3.5 m H₂O; with incrustation it is about 9.6 m H₂O. Quantitative analysis of these values will be performed further for estimation of cost savings by means of hydraulic losses reduction. Thus, exploitation of thermoinsulation from foam rubber with polyethylene housing is heat exchange optimized for pipes of all diameters.

According to the performed analysis, the following conclusions can be made:

1. Outer surface temperature of non-insulated pipe and heat flow (heat loss) through insulated surface is less for composite pipes than for metal ones for all pipe diameters.
2. Calculation data (according to SO 153-34.20.523-2003) show that the optimum thickness of the thermal insulation for composite pipes is 4–5 mm less than for metal ones. So, we recommend to use composite pipes with insulation length which is 7–10% less than that one for metal pipes (according to Russian State Standard 30732-2006) for all nominal pipe diameters.
3. Exploitation of foam rubber thermoinsulation is heat exchange optimized.
4. It is recommended to use composite pipes with FPF/FR insulation and polyethylene/composite housing for underground channelless heat networks tracing. In view of low heat conductivity of polyethylene and composite as well as small housing thickness, the question of optimum material choice is not crucial for heat exchange processes. So it is manufacturer who chooses polyethylene or composite housing. At a first approximation optimum housing thicknesses can be chosen according to [2, 3].

The calculations of capital expenses for various diameter pipeline tracing were performed for heat networks sections according to costing standards [4].

Table 4. Calculation data of thermal and hydraulic losses for various pipeline materials at Technological Park.

Temperature chart	95/70		
Pipeline material	Metal	Polymer	Composite
Thermoinsulation material of the pipeline	FPU		
Input center	Section 3		
Delivery head at consumer input, m	16.564	18.293	17.716
Delivery head losses, m	3.436	1.707	2.284
Input center	Section 4		
Delivery head at consumer input, m	15.565	17.776	17.044
Delivery head losses, m	4.435	2.224	2.956
Input center	Section 5		
Delivery head at consumer input, m	15.565	17.044	16.785
Delivery head losses, m	4.813	2.431	3.215
Input center	Section 6		
Delivery head at consumer input, m	15.343	17.648	16.889
Delivery head losses, m	4.657	2.352	3.111
Input center	Section 7		
Delivery head at consumer input, m	16.228	18.115	17.489
Delivery head losses, m	3.772	1.885	2.511
Input center	Section 8		
Delivery head at consumer input, m	17.202	18.618	18.143
Delivery head losses, m	2.798	1.382	1.857
Input center	Section 9		
Delivery head at consumer input, m	18.086	19.027	18.719
Delivery head losses, m	1.914	0.973	1.281
Input center	Section 10		
Delivery head at consumer input, m	17.489	18.818	18.456
Delivery head losses, m	2.299	1.182	1.544
Thermal losses at heat networks, Gcal/h	0.07455	0.07234	0.07123
Thermal losses at heat networks, W	86701.65	84131.42	82840.49
Specific thermal losses at heat networks, W/m	86.70	84.13	82.84

Table 5. Calculation data of thermal losses for various thermoinsulation materials at Technological Park

Temperature chart	95/70	
Pipeline material	Composite	
Thermoinsulation material of the pipeline	FPU	FR
Thermal losses at heat networks, Gcal/h	0.07123	0.05932
Thermal losses at heat networks, W	82840.49	68989.16
Specific thermal losses at heat networks, W/m	82.84	68.99

Table 6. Calculation of hydraulic losses for metal pipeline with 25 mm incrustation for Technological Park

Temperature chart	95/70
Pipeline material	Metal
Thermoinsulation material of the pipeline	FPU
Pipeline incrustation	25
Input center	Section 3
Delivery head at consumer input, m	10.833
Delivery head losses, m	9.167
Input center	Section 4
Delivery head at consumer input, m	8.170
Delivery head losses, m	11.830
Input center	Section 5
Delivery head at consumer input, m	6.939
Delivery head losses, m	13.061
Input center	Section 6
Delivery head at consumer input, m	7.129
Delivery head losses, m	12.871
Input center	Section 7
Delivery head at consumer input, m	10.175
Delivery head losses, m	9.825
Input center	Section 8
Delivery head at consumer input, m	12.326
Delivery head losses, m	7.674
Input center	Section 9
Delivery head at consumer input, m	14.428
Delivery head losses, m	5.572
Input center	Section 10
Delivery head at consumer input, m	12.777
Delivery head losses, m	7.223

The adjustment factors (deflators) [5] were chosen for new construction in the year 2017 and for reconstruction in 2044. The results of the calculations are given in Table 7.

Construction costs shall comprise the following elements: costs of construction materials, labour and construction machinery exploitation costs, overhead costs and profit, temporary building construction costs and addition costs for winter building, as well as expenses involved in obtaining of initial data, technical specification by customer and engineering company, expenses for building risks insurance, expenses for design, survey and project inspection, expenses for customer service and construction supervision services, unexpected expenses reserve.

The economic effect is derived from different costs of non-insulated pipes, construction and installation works for metal and composite pipes, as well as metal pipeline reconstruction necessity in 25 years' time.

Table 7. Comparison of capital expenses for metal and composite pipes application for 25-years service period.

No.	Nominal pipe diameter, mm	Total cost for 25-years' service period, thousands roubles				
		Metal			Composite	Economic effect
		New construction	Reconstruction	Total sum	New construction	
1	80	15861.49	39105.83	54967.31	16353.72	38613.59
2	100	16526.98	40746.58	57273.55	16862.91	40410.64
3	150	20160.81	49705.63	69866.43	19964.74	49901.69
4	200	24245.22	59775.58	84020.80	23145.53	60875.26
5	250	28184.41	69487.49	97671.91	26964.62	70707.29
6	300	31426.56	77480.88	108907.44	29981.10	78926.33
7	400	42222.66	104098.20	146320.85	40770.06	105550.80
8	500	55627.39	137147.01	192774.41	54350.54	138423.86

Figure 2 presents graphical representation of data from Table 7. The curves present total capital expenses taking into account general conditions for metal and composite pipelines depending on nominal diameter. Price for running meter of pre-insulated metal pipes for small diameters is less than for metal ones, so capital expenses for new metal construction will be less for nominal diameters up to 150 mm.

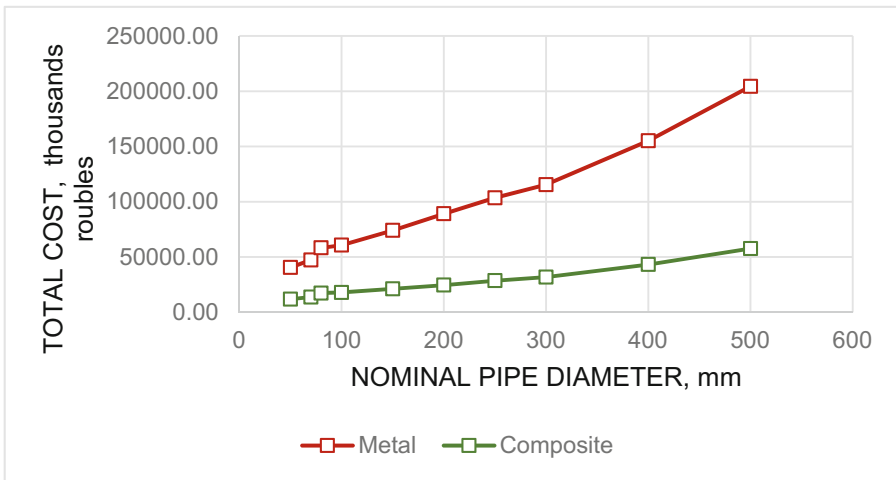


Fig. 2. Comparison of capital expenses for metal and composite pipes application for 25-years service period

It is seen from Fig. 2 that taking into account declared service period of metal pipeline (25 years) and composite pipeline (50 years), capital expenses with deflator for composite pipeline will be 3–4 times less than for metal one for all nominal diameters.

In Table 7 economic effect was calculated basing on capital investment to composite pipeline for 25 years (new construction) and to metal pipeline for 25 years (new construction + reconstruction). This approach is ruled by design service period of metal pipeline (25 years [6, 7]) and composite pipeline (50 years [8]).

Table 8 and Fig. 3 present capital expenses for the discussed pipeline variants for 25 years service period taking into account metal pipeline reconstruction.

Table 8 shows that calculated capital expenses for heat pipeline tracing are the following: for metal pipeline about 20 mln.roubles and for composite pipeline about 19.5 mln.roubles, which makes project with composite materials more attractive. Additional expenses for metal pipeline reconstruction with account of deflator will be about 50 mln.roubles in 25 years' time. In this case the total cost of the composite pipeline tracing for the Technological Park will be 3 times less and the absolute difference of capital expenses will be about 50.5 mln.roubles.

Table 8. Comparison of capital expenses for metal and composite pipes application for 25-years service period (Technological Park)

No.	Nominal pipe diameter, mm	Total section length, m	Total cost for 25 years service period, thousands rubles					Economic effect
			Metal			Composite		
			New construction	Reconstruction	Total sum	New construction		
1	125	20	367.64	906.40	1274.03	355.53	918.51	
2	150	109	2197.53	5417.91	7615.44	2176.16	5439.28	
3	200	204	4946.02	12194.22	17140.24	4721.69	12418.55	
4	250	377	10625.52	26196.78	36822.31	10165.66	26656.65	
5	300	64	2011.30	4958.78	6970.08	1918.79	5051.29	
Total sum			20148.01	49674.09	69822.10	19337.82	50484.28	

Figure 3 presents calculation data from Table 8 in graphic form. Metal pipeline histogram includes both new construction and reconstruction costs, which are marked by different colours. It should be noted that positive economic effect of composite material application is observed even at initial investment.

3 Results

Tables 9 and 10 present calculated cost saving due to hydraulic and heat losses for Technological Park. Hydraulic losses reduction allows one to create lower pressure of pumping group at heat supply source.

This reduces power costs for motor drive of line and feed pumps. Besides this, at relative power decrease (more than 30% for Table 9) it is recommended to use pumps of lower installed capacity which leads to capital expenses reduction. In this case the installed capacity of the pumping group can be reduced up to 13.5 kW for composite pipeline and up to 19.92 kW for polymer pipeline.

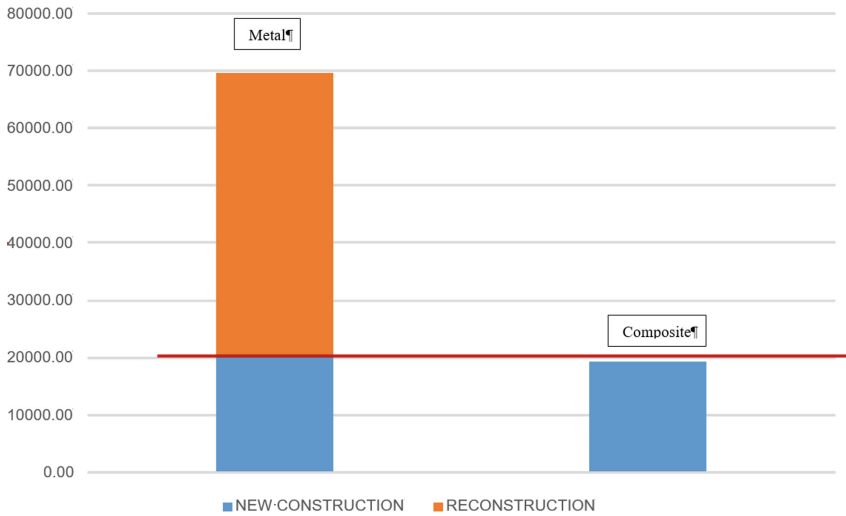


Fig. 3. Comparison of capital expenses for metal and composite pipes application for 25-years’ service period (Technological Park)

According to the calculation results from Table 9, polymer pipeline has the best hydraulic characteristics (relative drop of hydraulic losses) (2.382 m relatively to metal). However, there are no heat supply polyethylene pipes with diameter more than 200 mm, so this variant could not be considered as priority.

Table 9. Calculated cost savings due to pipeline hydraulic losses

Characteristics	Metal	Polymer	Composite
Operating hours, h		8000	
Electricity rate, roubles/kW·h		2	
Nominal power of pumping group, kW		115	
New pipeline characteristics			
Delivery head losses, m	4.813	2.431	3.215
Relative hydraulic loss drop, m		2.382	1.598
Relative power, %		82.68	88.26
Absolute power drop, kW		19.92	13.50
Annual cost saving, roubles		318.720	216.000
Monetary value of energy saving at the source for 25 years service period		13.912.128	9.428.400
Characteristics taking into account 25 mm incrustation of metal pipeline			
Delivery head losses, m	13.061		
Relative hydraulic loss drop, m		10.630	9.846
Relative power, %		32.07	36.18
Absolute power drop, kW		78.12	73.39
Annual cost saving, roubles		1.249.920	1.174.240

Besides this, in case of source temperature rising (more than 95 °C at supply pipeline) polymer materials application becomes impossible because of maximum operating temperature limits.

It should be noted that annual money savings for heating agent transportation through composite pipeline with respect to metal one will be 1,174,240 roubles. The total heat network length for Technological Park is 774 m, the diameter range is from 125 to 300 mm.

Total money savings due to thermal and hydraulic losses for 25 years' service period taking into account deflator for fuel and electricity (Tables 9 and 10) at composite pipeline application will exceed 10 mln.roubles.

Table 10. Calculated cost savings due to pipeline thermal losses

Characteristics	Metal	Polymer	Composite
Thermal losses at heat network, Gcal/h	0.07455	0.07234	0.07123
Hours of maximum power usage, h	2000		
Annual thermal losses, Gcal	149.1	144.7	142.5
Annual economy in volume terms, Gcal		4.4	6.6
Annual economy in monetary terms, Gcal		11.000	16.500
Monetary value of fuel saving at the source for 25 years' service period		611.358	917.037

Table 11. Calculated money savings due to hydraulic and thermal losses for 25 years' service period

No.	Characteristics	Variant 1 (D 200, L 1000)	Variant 2 (Technological Park)
		Thousands roubles	
1	Calculated cost saving due to hydraulic losses (for 25 years' service period with deflator accounting)	1508.54	9428.40
2	Calculated cost saving due to thermal losses (for 25 years' service period with deflator accounting)	536.33	917.04
3	Total economic effect	2044.87	10345.44

Table 12. Calculated cost savings due to hydraulic and thermal losses for 50 years' service period

No.	Characteristics	Variant 1 (D 200, L 1000)	Variant 2 (Technological Park)
		Thousands roubles	
1	Calculated cost saving due to hydraulic losses (for 50 years' service period with deflator accounting)	3818.02	23862.60
2	Calculated cost saving due to thermal losses (for 50 years' service period with deflator accounting)	1516.53	2593.02
3	Total economic effect	5334.54	26455.62

Calculated money savings due to hydraulic and thermal losses for application of composite pipeline with respect to metal one are presented in Table 11 (for 25 years), Table 12 (for 50 years).

4 Discussion

Basing on the performed calculations, the following conclusions can be made:

1. Hydraulic losses at polymer pipelines are less for $\sim 43\%$ than that one for metal; hydraulic losses at composite pipeline are less for $\sim 30\%$ than that one for metal.
2. Economic effect of composite pipeline application with respect to metal one show Table 13.

Table 13. Economic effect of composite pipeline application with respect to metal

No.	Characteristics	Technological Park
		Thousands roubles
1	Calculated capital expenses savings for construction of heat network with composite pipeline with respect to metal one	810.19
2	Capital expenses for metal pipeline reconstruction (in 25 years' service period with deflator accounting)	49674.09
3	Calculated cost saving due to hydraulic losses (for 25 years' service period with deflator accounting)	9428.40
4	Calculated cost saving due to thermal losses (for 25 years' service period with deflator accounting)	917.04
5	<i>Total calculated economic effect (for 25 years' service period)</i>	<i>60829.72</i>
6	Calculated cost saving due to hydraulic losses (for 50 years' service period with deflator accounting)	23862.60
7	Calculated cost saving due to thermal losses (for 50 years' service period with deflator accounting)	2593.02
8	<i>Total calculated economic effect (for 50 years' service period)</i>	<i>76939.90</i>

3. Nowadays composite pipe production is weakly developed in Russian Federation. A number of factors are responsible for weak development of this branch of industry. Among them are the following: absence of sufficient regulatory documents, providing quality and usage features for composite pipelines; lack in technology of Russian composite pipe manufacturers; high development degree of manufacturing base and lobbying of traditional materials for pipelines.

5 Conclusions

The presented conclusions state that composite pipes implementation for heat supply system is perspective both from economical and technical points of view and it is recommended for practical realization.

References

1. Dobromyslov, A.Ya.: About the pipe role in housing and communal services reform. *Plumb. Syst.* **5**, 2–4 (2004)
2. Russian State Standard GOST 10704-91. Steel electric-welded longitudinal pipes
3. Russian State Standard GOST 30732-2006. Steel pipes and shaped objects with foamed polyurethane thermal insulation with protective housing
4. Russian State Costing Standards. Enlarged Standards for Construction Cost (SCC). SCC 81-02-13-2014. Part 13 Outdoor heat networks. (Appendix 12 to Act № 506/pr of Ministry of Construction, Housing and Utilities of the Russian Federation from 28.08.2014)
5. Act № 698 of Ministry of Economic Development of the Russian Federation from 3.11.2016: Deflator coefficients for the year 2017
6. Russian State Standard SP 131.13330.2012. Construction climatology
7. Russian State Standard SP 60.13330.2012. SNiP 41-01-2003. Heating, ventilation and air conditioning
8. Petrakov, G.P.: The service life of plastic pipe in the polyurethane foam insulation, used for heating systems. *Mag. Civil Eng.* **3**, 54–62 (2012)

Autodesk Revit and Robot Structural Analysis in Design of Framed Buildings

Rustam Gilemkanov¹, Ruslan Bagautdinov¹,
and Vadim Kankhva²

¹ Peter the Great St. Petersburg Polytechnic University,
Polytechnicheskaya st., 29, St. Petersburg 195251, Russia
asf-rust@ya.ru

² Moscow State University of Civil Engineering,
Yaroslavskoe Shosse, 26, Moscow 129337, Russia

Abstract. The Russian state began the gradual introduction of building information modelling (BIM) technologies in construction in December 2014. BIM is difficult to implement in a short time, as it requires a complete re-equipment of the company, retraining of the employees and accumulation of experience and knowledge. The main difficulties in collision with new technologies are the degree of correspondence and adequacy of the obtained results to reality. The solution is the comparison of the calculation methods by new technologies and the traditional approach application for the building and structure analysis. This is the fundamental method of solving the problem in this article. The real project of autocenter has been analyzed. The analysis of individual load-bearing structures of the object is performed: manually, using SCAD Office and Robot Structural Analysis software. The difference between three methods of not more than 4% was obtained. It is good for BIM implementation.

Keywords: BIM technologies · Transportation sector · Design of framed buildings

1 Introduction

Building Information Modeling (hereinafter called BIM) – design concept that provide complex data collection, processing and analysis from each stage in the design process (architecture, construction and etc.) and the use of that information throughout the entire lifecycle of the object. Moreover, the information from the model is interrelated, so, the design collisions can be avoided.

BIM has three main advantages over CAD:

1. The objects of BIM is not just 3D models. The information provides the ability to create drawings automatically, perform analysis of project, etc. It helps to find the best design decisions.
2. BIM supports collaborative design. Different specialists can use all the information during each phase of design and construction, eliminating the loss of data during the sharing process.
3. Reduced costs and design errors (collisions).

In a typical design approach (here in after called CAD approach) information is collected separately from each other, leading to collisions. And often it's the collision that appears directly in the construction, resulting in a subsequent design change and rise in price of construction (Fig. 1).

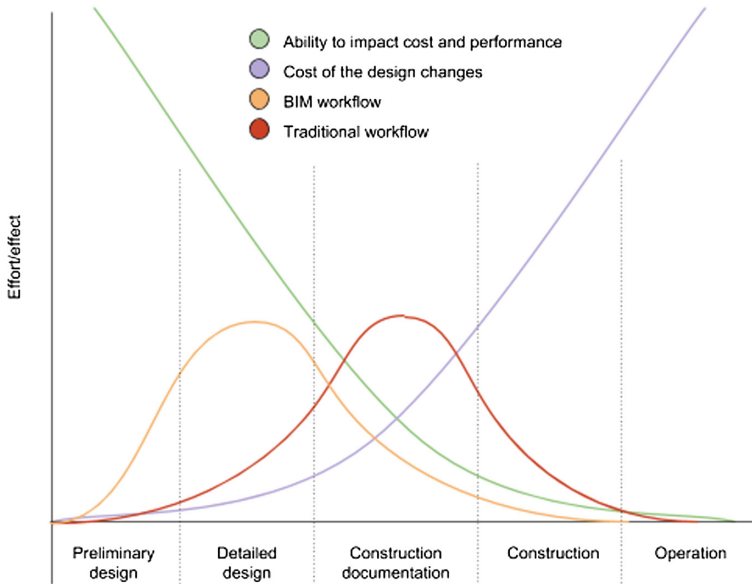


Fig. 1. BIM productivity curve.

Of course, in all these arguments lies the drawback. There is no program that will be able to give unbiased results if we do not have objective theoretical knowledge. Design techniques are merely tools. And the results depend on how the engineers use this tools. Any errors in the way of thinking over a task will bring errors in the program and inevitably provide errors in reality.

In the Russian market many platforms, working with BIM (Tekla Structures, Autodesk Revit, Allplan etc.). Each product has its pros and cons. Autodesk products wide spread in Russia. This company has a wide range of products for implementing the concept of BIM (Autodesk Revit, Autodesk Robot Structural Analysis Professional, Autodesk Navisworks, Autodesk Ecotect, etc.). Obviously, it is wrong to introduce all the products. We decided to focus on Autodesk Revit and Autodesk Robot Structural Analysis Professional [24], as this will allow you to produce project documentation, not applying the remaining products.

BIM is difficult to implement in a short time. The main difficulty is the degree of correspondence and adequacy of the obtained results. The logical solution is to compare the results of calculating new technologies and the traditional approach to the calculation of buildings and structures. This is the fundamental method of solving the problem. Thus, if the calculations result of Robot Structural Analysis (software for

BIM) is not inconsistent with the manual calculation and calculation in SCAD Office [25] (popular software for CAD approach in Russia), the BIM works right.

The scientific literature on this subject has been studied [1–22]. The comparison analysis of the structural analysis software was discussed in article [22], where the comparison of structural analysis results was studied from software Lira SAPR and SCAD. The analysis of the results from SCAD and Robot software was discussed in [11]. The aim of the paper was to compare the results of settlement computations by SNIP (building code in Russia) usage. The authors obtained the deviation of 20–25%. As the soils modeling process can be treated as rather complicated one the results was assessed as acceptable. The BIM technologies are widely discussed [1–22], but the topic of current research was not developed enough. Therefore, we decided to produce such a study. The real project of autocenter has been selected to solve the problem. The calculation and analysis of individual load-bearing structures of the object will be calculated: manually, by using professional software the SCAD and Robot. The results of calculations of different methods are compared.

2 Methods and Results

2.1 Initial Data

The input data for the load summary:

- The construction area is the city of Ufa, Shaksha district, Republic of Bashkortostan.
- Climatic area - 1B;
- Characteristic value of wind load for the area II is 0.3 kPa;
- Design value of snow load for the area V – 3.2 kPa;
- The average wind speed in winter 4 km/h;
- The average monthly temperature in January: –15 °C;
- The average temperature in July – 20 °C;

Loads summary for the beams and columns is presented in Tables 1 and 2.

Table 1. Loads summary for the beam coating

Position	The name of the load	The magnitude of the load				
		The standard value	Safety factor for load, γ_f	Load	The load on the beam	Units
Constant loads						
1	Each weight	0.861	1.05	0.904	0.904	kN/m
2	Roof	0.205	1.13	0.232	0.920	kN/m
Short-term load						
3	Snow load	2.29	1.4	3.20	12.67	kN/m

Table 2. Loads summary for the supporting columns

Position	The name of the load	The magnitude of the load			
		The standard value	Safety factor for load, γ_f	Load, kN	Moment, kN * m
1	3	4	5	6	7
Dead loads					
1	Each weight	7.54	1.05	7.92	–
2	Roof	17.8	1.13	20.1	–
3	Beam coating	8.9	1.05	9.4	–
4	The crane beam (in the console)	4.61	1.05	4.84	1.94
Short-term load					
5	Snow load	197.9	1.4	277.10	–
6	The maximum support reaction (Fmax)	63.46	1.2	76.15	30.46
	The horizontal support reaction (Qk)	2.8	1.2	3.4	23.8 (at the base)
Total				398.0	56.2

The columns height is 8 m. At a height of 7 m columns have the console for the crane structures installation.

Columns have the rigid joint at the bottom level in the perpendicular plane to the main frame of the building and pinned joint along the main building frame (Fig. 3). The crane transmit loads to the column through the console. The distance from the face of the column to the crane girder – not less than 160 mm (according to the instructions from the manufacturer of the crane). In order to provide the calculations of the design stage on the safety side 200 mm should be added. Thus, the total eccentricity from the crane loads on the column – 400 mm.

The I-beam cross section of the column was chosen (Fig. 2).

Load summary was made for the most loaded column (Fig. 3a). The load area for the column 86.4 square meters:

$$\left(\frac{18}{2} + \frac{6}{2}\right) \cdot \left(\frac{8.4}{2} + \frac{6}{2}\right) = 86.4 \text{ m}^2$$

2.2 Calculation of Structural Column

The result of calculation structural column according to SP 16.13330.2011 [24] shown in Table 3.

The software tool Kristall (SCAD) was used (Fig. 3). The results of the calculations executed in SCAD office software are shown in Fig. 7.

The calculation scheme of Robot is presented in Fig. 4. The results of the Robot calculation are presented in Fig. 7.

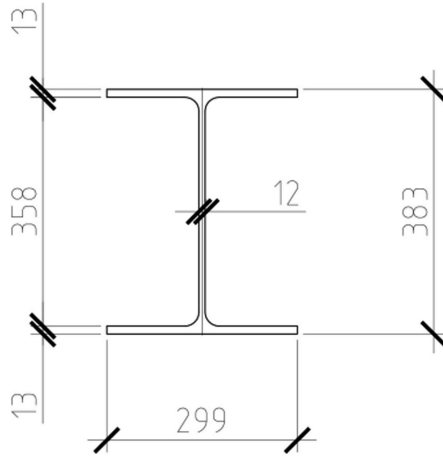


Fig. 2. I-beam cross section (in mm)

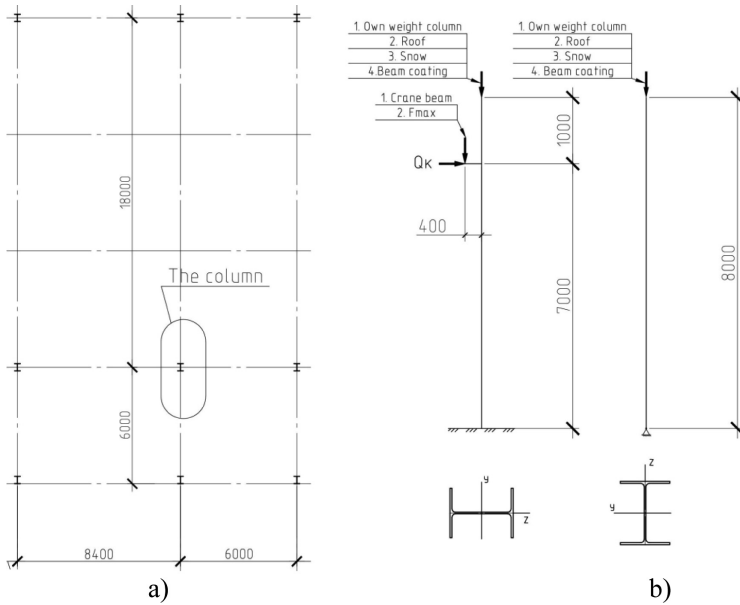


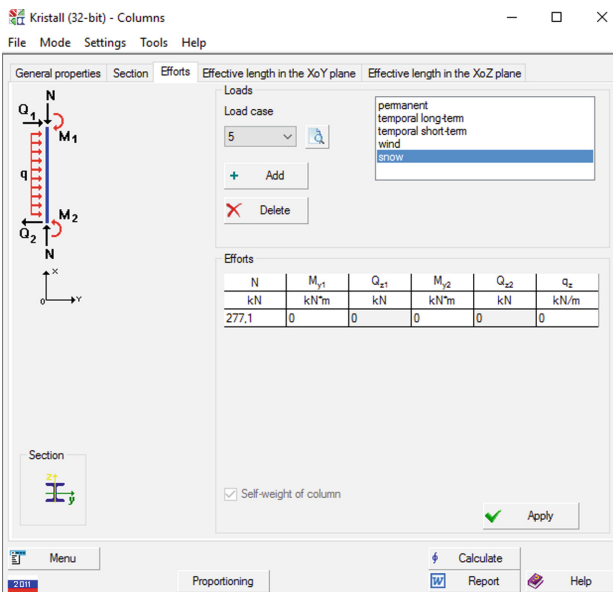
Fig. 3. The scheme of load-bearing: (a) columns location (b) design scheme (in mm).

2.3 Calculation Spatial Scheme

In the next phase, the analysis of the whole building frame in the SCAD (Fig. 5) and Robot (Fig. 6) was made.

Table 3. Calculation of a structural column according to SP 16.13330.2011

	Result	Criterion
Strength under the action of bending moment M_x (paragraph 8.2.1 [13])	0.146	1
Member stability subjected to axial compression in the plane XOY (paragraph 7.1.3 [13])	0.3	1
Member stability subjected to axial compression in the XOZ plane (paragraph 7.1.3 [13])	0.25	1
In plane buckling resistance from the bending moment M_y for the non-centrally compressed element (paragraph 9.2.2 [13])	0.43	1
Out of plane buckling resistance from the bending moment M_y for the non-centrally compressed element (paragraph 9.2.4 [13])	0.47	1
Ultimate flexibility in the plane XOZ (Table 32 [13])	0.43	0.5

**Fig. 4.** The software tool “Kristall” (SCAD)

In case of Robot Structural Analysis software usage it is not necessary to execute sections dimensioning and geometrical modeling for the finite element division. It is done automatically and it is transmitted from the Revit Structure BIM model with all sections and geometry. As a result, we get a design scheme much easier.

The Revit and Robot two-way model sharing is available. So, if we modify a cross-section for any element the drawings in Revit for current model will be updated automatically without any actions of an engineer.

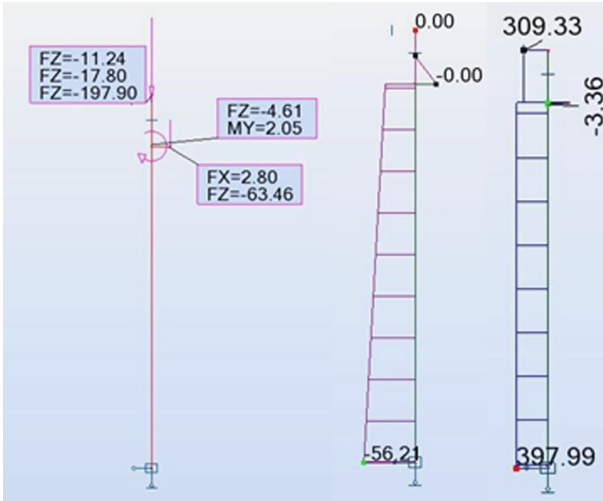


Fig. 5. The calculation scheme in Robot

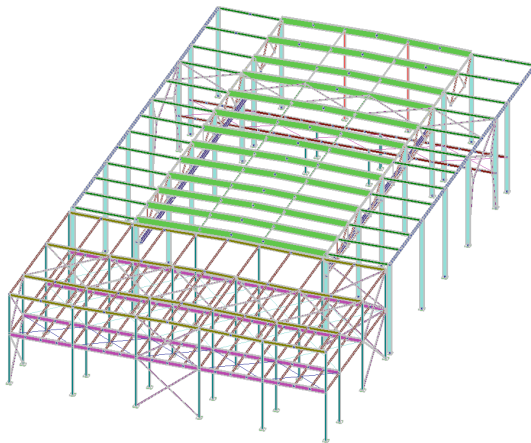


Fig. 6. The design scheme in SCAD.

3 Discussion

The discrepancy of results does not exceed 4% (Figs. 7 and 8). It is associated with a small difference in the considered software and the adequacy of the results. This discrepancy is valid and allows you to proceed the calculation of the frame by any of described method whether it provide any benefits.

The discrepancy of results within tolerance (Fig. 8). Moreover, as the unit of measurement very small and the divergence of the program Robot Structural Analysis calculation results it was stated that the principle of the design stress combinations

assignment is different from the principle in SCAD Office. Zero divergence for the manual calculation and SCAD Office is because the manual calculation have the same principles that the SCAD Office software use (Fig. 9).

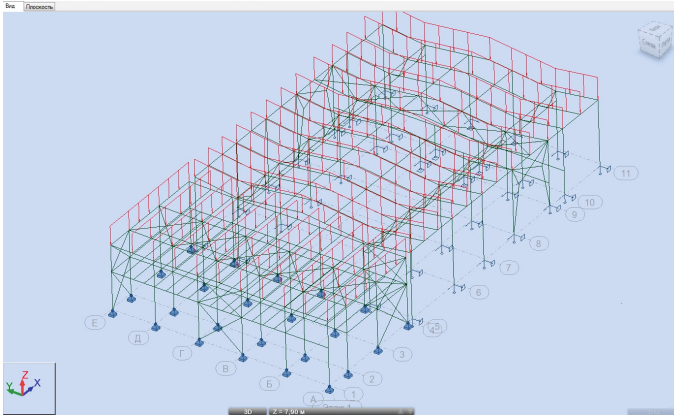


Fig. 7. The design scheme in Robot

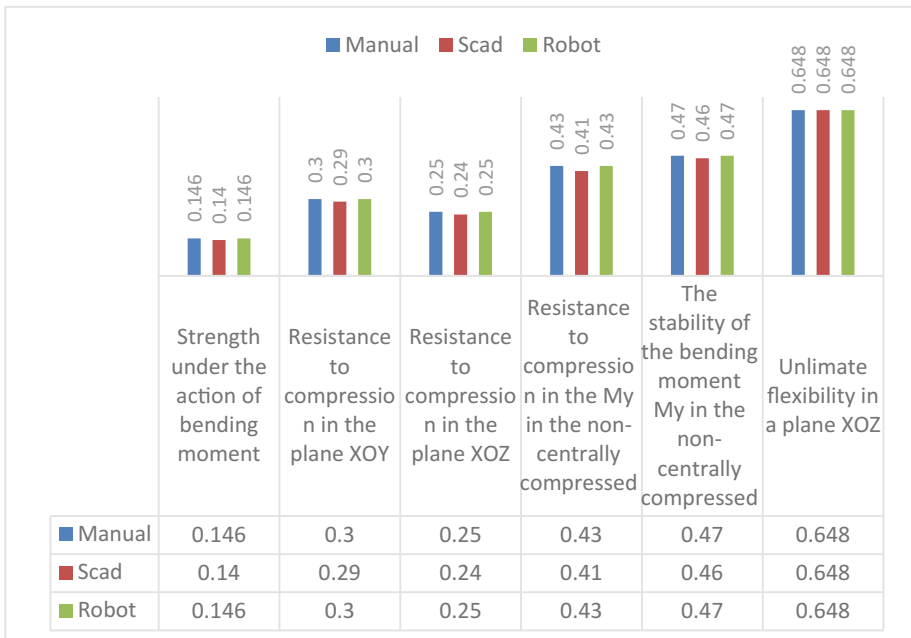


Fig. 8. The histogram of the divergence of calculation results

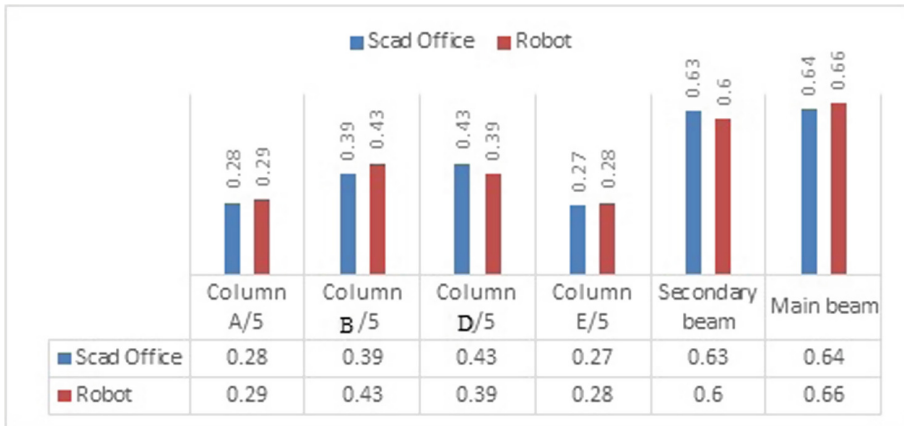


Fig. 9. The histogram of the spatial scheme result.

4 Discussion

The reason for the discrepancy: the design stress combinations. The matching algorithm presented in the [12] for the design stress combination in different programs for crane loads. More reliable we assume the result issued by the “SCAD Office”, as it has a module for the calculation of the crane loads by “Loads and actions” (Russian’s building code). Thus, if the same FEM models are used, it is possible to obtain identical results. Since the finite element method in both cases is the same.

5 Conclusions

1. The design of simple elements was performed by the modern approach;
2. The discrepancy of not more than 4% was obtained, for the studied frame.





A lot of work about quick and adequate approaches development is needed for the compliance with the domestic standards, for instance, in case of designing stress combinations according to SP “Loads and actions”, etc. But it was important to take the first step towards the development of BIM approach. The development process of BIM technology is possible only step by step by the accumulation of experience and knowledge.

References

1. Lee, G., et al.: Specifying parametric building object behavior (BOB) for a building information modeling system. *Autom. Constr.* **15**, 758–776 (2006)
2. Azhar, S., et al.: Building information modeling (BIM): now and beyond, *Austral. J. Constr. Econ. Build.* **12**, 15–28 (2012)

3. Sacks, R., Barak, R.: Impact of three-dimensional parametric modelling of building on productivity in structural engineering practice. *Autom. Constr.* **17**, 439 (2007)
4. Lee, M.S.: Analysis and design of reinforced concrete bridge column based on BIM. *CAD Graph.* **7**, 126–130 (2008)
5. Sacks, R., et al.: Parametric 3D modeling in building construction with examples from precast concrete. *Autom. Constr.* **13**, 291–312 (2004)
6. Gu, N., London, K.: Understanding and facilitating BIM adoption in the AEC industry. *Autom. Constr.* **19**, 988–999 (2010)
7. Chen, N., et al.: A BIM-based construction quality management model and its applications. *Autom. Constr.* **46**, 64–73 (2014)
8. Zuppa, D., et al.: BIM's impact on the success measures of construction projects. *Comput. Civ. Eng.* **24**, 503–512 (2009)
9. Porwal, A., et al.: Building Information Modeling (BIM) partnering framework for public construction projects. *Autom. Constr.* **31**, 204–214 (2013)
10. Motawa, I., et al.: A knowledge-based BIM system for building maintenance. *Autom. Constr.* **29**, 173–182 (2013)
11. Cerovsek, T., et al.: A review and outlook for a 'Building Information Model' (BIM): a multi-standpoint framework for technological development. *Adv. Eng. Inform.* **25**, 224–244 (2011)
12. Volk, R., et al.: Building Information Modeling (BIM) for existing buildings — literature review and future needs. *Autom. Constr.* **38**, 109–127 (2014)
13. Arayici, Y.: Towards building information modelling for existing structures. *Struct. Surv.* **26**, 210–222 (2008)
14. Cerovsek, T.: A review and outlook for a Building Information Model (BIM): a multi-standpoint framework for technological development. *Adv. Eng. Inform.* **25**, 224–244 (2011)
15. Zavadskas, E.K., et al.: Risk assessment of construction projects. *J. Civil Eng. Manag.* **16**, 33–46 (2010)
16. Tomek, A.: The impact of BIM on risk management as an argument for its implementation in a construction company. *Procedia Eng.* **85**, 501–509 (2014)
17. Wang, J., et al.: Geotechnical and safety protective equipment planning using range point cloud data and rule checking in building information modeling. *Autom. Constr.* **49**, 250–261 (2015)
18. Tran, V., et al.: Impact of supply chain management practices on sustainability. *Int. J. Constr. Supply Chain Manag.* **2**, 66–79 (2012)
19. Ioskevich, A., et al.: Comparison of SCAD office and LIRA-SAPR on the example of calculation of communications tower. *Constr. Unique Build. Struct.* **10**, 7–21 (2014)
20. Stepanov, A., et al.: Comparison of calculations using SNiP 2.02.01-87 and using special software. *Constr. Unique Build. Struct.* **22**, 9–23 (2014)
21. Ministry of Regional Development of Russia (RUS) 2011 SP 16.13330.2011 Steel structures (SP 16.13330.2011) Moscow
22. Autodesk Robot Structural Analysis Professional 2010 Training Manual, Autodesk (2010)
23. SCAD Office. Electronic Reference Manuals, SCAD Soft (2014)

Determination of Environmental Impact Factors of Flood Control Hydrosystems with Temporarily Filled Self-regulating Reservoirs

Alexander Chusov¹(✉) , Vladimir Maslikov¹ ,
Dmitry Molodtsov¹ , and Olga Manukhina² 

¹ Peter the Great St. Petersburg Polytechnic University,
Polytechnicheskaya str., 29, 195251 St. Petersburg, Russia
chusov17@mail.ru

² Moscow State University of Civil Engineering,
Yaroslavskoe sh., 26, 129337 Moscow, Russia

Abstract. In the paper, the way of lands protection from torrential floods is considered by control of flood discharge in a river basin using the system of reservoirs distributed on the catchment-basin as part of a hydrosystem with a hydroelectric power plant of a complex purpose on the main river, as well as flood control hydrosystems in the upper reaches of the river and on lateral streams with temporarily filled self-regulating reservoirs. The task of determining the main impact factors on the environment of flood control hydrosystems and their quantitative assessment is considered. The most frequently encountered impact factors on the natural environment during the creation and operation of flood control hydrosystems are determined and considered. For specific hydrosystems, the choice of priority impact factors on the natural environment is proposed to be carried out using expert analysis. It's recommended at the stage of choice of the location for flood control hydrosystems and the substantiation of their parameters, use the express-assessment of the impact on the natural environment. The article considers the impact of inundation caused by temporarily filled self-regulating reservoirs of flood control hydrosystems on forests, bogs, water quality and ecosystem diversity. The final parameters and operation modes of flood control hydrosystems are proposed to be determined for the minimum of permissible areas of short-term inundation of the upper pool, calculated for each priority environmental impact factor.

Keywords: Floods · Flood-control hydrosystems
Environmental impact assessment

1 Introduction

Among the most dangerous natural hazards showery flooding takes the first place by the total annual damage [1]. In the last decades, catastrophic floods were happened on repeated occasions in the Russia, the USA, Italy, Great Britain, China, Vietnam, etc.

In Russia, as in other countries, a control of high runoff by the multipurpose hydrosystems with large detention basins is widespread and powerful tool for flood mitigation. Installed in a main river, they protect lands located downstream.

Recently, to reduce inundation, there is a trend to construct a low-pressure multipurpose hydrosystem on the main river, with minimum water-surface elevation and comparable low detention basin. At the same time, the possibility to control an extreme water flow is decreased, which leads to search for new more efficient approaches for flood protection, using hydropower plants.

Reduction of flood hazards is rational to carry out by control of flood discharge in the river basin, distributed on the catch area via system of basins with minimum impact on the environment. It is including a multipurpose hydrosystem (energy generation, flood protection) with hydro power plant (hydroelectric power chain) on the main river with lowest water surface elevation and regulation capacity of high runoff, as well as detention basins on the river head and on the lateral inflows with temporary filling self-regulating basins [2]. In them additional required volume is created to accumulation flood discharge in the river basin.

A characteristic property of flood-control hydrosystems is existence of temporary filling self-regulated reservoirs, which is used solely for cutting down extremely flow rate. During accumulation period of overflow waters, the reservoir floor is short-term flooded (from some hours to some dozen of days) and after self-emptying in all the other time (up to the next flooding) remains dry in its natural state. In rainless period, the hydrosystem does not back up on the river and does not interfere with the free passage of fish.

In case of flooding of the reservoir floor even in a short-term period, the flood control hydrosystem has an impact on the environment, being a part of natural-technical system. Such type of hydrosystem requires developing specific methods to their environmental impact assessment. In comparison with permanent filled reservoirs, the processes occurring in temporary filling hydrosystem have short-term frame, characterized by a rapid velocity of changes in the accumulation parameters of flood flow rate, instability and poorly predicted. Russian regulatory documents do not consider the specifics of the functioning of temporary filling reservoirs of flood control hydrosystems. The use of foreign methods is difficult due to the lack of available practical information on its application during environmental impact assessment for such type of hydrosystems. The task is to determine the main factors of flood-control systems, which have an impact on the environment, and its quantitative assessment.

2 The Main Environmental Factors

Despite of variety of natural and climatic conditions of flood control hydrosystem functioning, it is possible to determine a group of impact factors, that appears the most frequently during their construction and operation, which is necessary to development corresponding assessment approaches. Due to river upstream and its lateral inflows, as a rule, covered by forest or boggy, and it is a breeding site for valuable fish species, the environmental impact assessment priority of short-term flooding of reservoir floor

should take into account damaging of stand trees and peat on flooded bogs, water quality changes due to income of nutrients from flooded areas, a rate of the offence of fishery conditions, etc. [3] In the Fig. 1 the main impact on the environment of flood-control hydrosystem during construction and operation is shown.

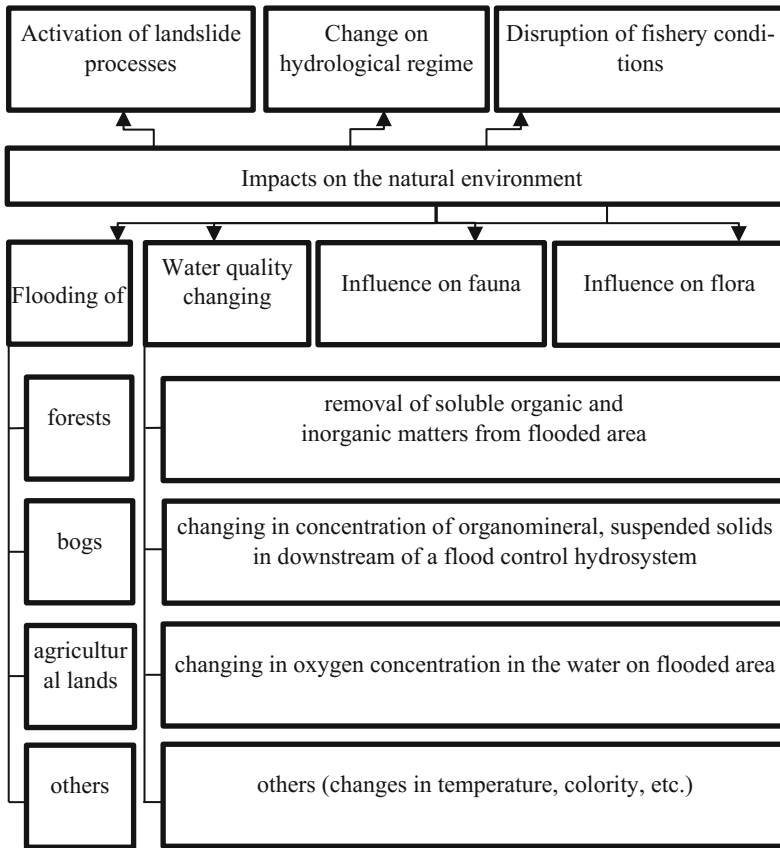


Fig. 1. Impact on the natural environment of flood control hydrosystems.

For specific objects, the choice of the most significant impact factors of flood-control hydrosystems is carried out in accordance with the expert analysis procedure [4]. The algorithm of its implementation is shown in Fig. 2.

In relation to the lack of necessary information of the natural and climatic conditions, the state of natural systems, environmental conditions in river basins, at the stages of selecting cross sections for flood-control hydrosystems and verification their parameters, it is rational to use rapid environmental impact assessments, considered below for the most frequently encountered factors.

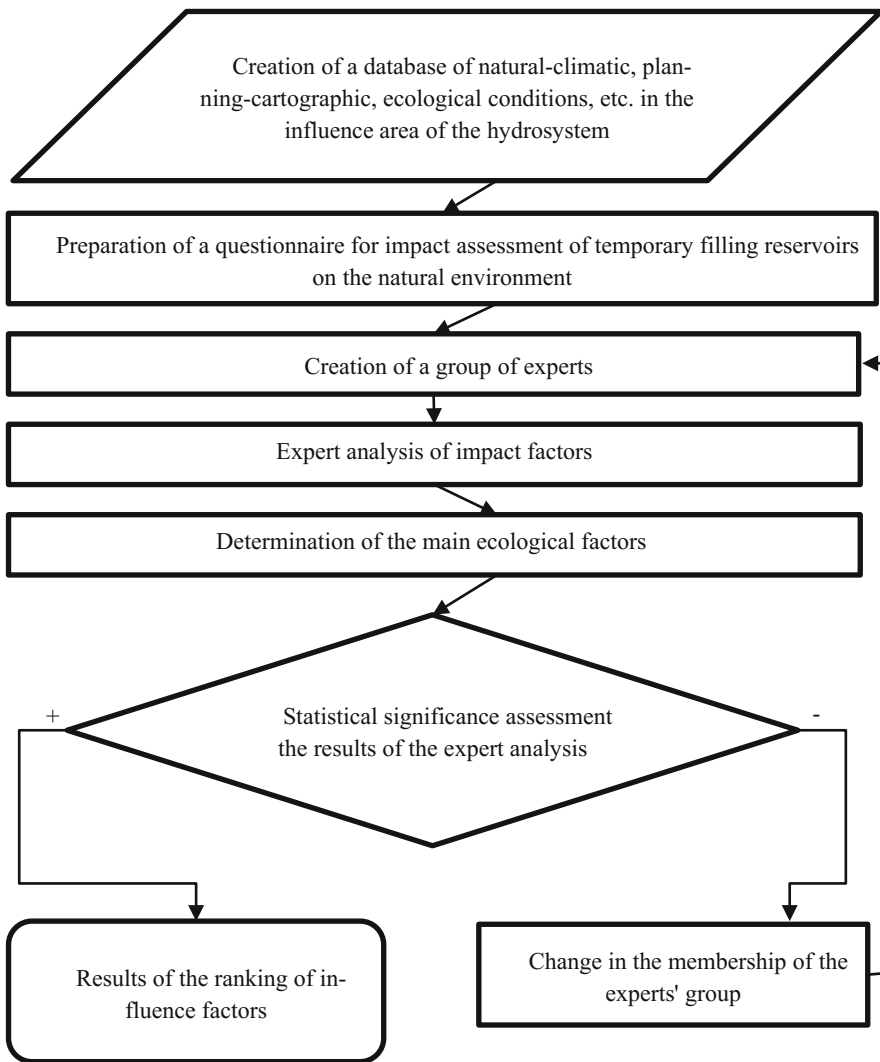


Fig. 2. Determination of priority factors of impact on the environment during operation of flood control hydrosystems.

3 Assessment of Plant Community Sustainability (Forest Stand)

Among all types of terrestrial ecosystems and categories of natural resources of our planet, the most widespread and most valuable is forest. Forest ecosystems regulate the intensity of snowmelt, rainwater runoff and water level in rivers, stabilize the parameters of the atmosphere and thus are in themselves a natural counteraction to flooding by cloudburst flood. Therefore, during construction of a flood-control hydrosystem

with temporary filling reservoirs it is necessary to consider that forest protection (short-term flooded) by flooding control will allow to reduce the volume of accumulation, as well as costs of flood control hydrosystems.

Specific factors, affecting on forest stability during flooding, are the height of the standing water, the duration of flooding, the time of year, the quality and thermal regime of the flood waters, and the degree of their flow [5–7], which are poorly predictable. Many plant species can be damaged at a relatively shallow depth of flooding, which is several dozen centimeters.

The main influence on the safety of temporarily flooded forests is not so much the duration of flooding, as the lack or complete absence of oxygen in the water. It is important to prevent a decrease the oxygen content in the water below the threshold at which the inhibition of physiological processes and the dying off of the roots come. The influence of various concentrations of carbon dioxide in water on the development of trees has been less studied. In the period of rest or retardation of physiological activity, the roots of tree species are more resistant to soil flooding. They are less sensitive to soil flooding in a cooler period of vegetation. Literature review on the stability of stands was shown that empirical data are characterized by poor comparability, which makes it difficult to develop a sustainability assessment, as well as modeling processes. In such conditions, it is justified to apply the method of “aggregating” forest cenoses by types based on the use of geobotanical maps or forest management plans [8], which was used in stability assessing of various types of forests for short-term flooding.

In case of flooding of alluvial and valley-growing forests during period of water stand up to 10 days significant changes is not occur. In case of the period 10–20 days the forest stand is partially survive. In case of the period more than 20 days the forest stand is significant disturb or failure. It should be noted, that for upland forests a temporary flooding up to 10 days are dangerous and longer flooding can lead to forest failure.

The knowledge of flooded area, forest types and flood’s duration gives a possibility to forecast the survival rate of forests during short-term flood.

4 Peat Floating-Up Assessment

Wetlands are one of the most important ecosystems on the planet. They accumulate significant water reserves, actively participate in the water cycle, and in many respects, determine the local climate. Wetlands enriched with biogens are extremely productive ecosystems in which rare plant species grow, valuable species of aquatic fauna inhabit. Conservation of wetlands is an indispensable condition for maintaining the biological diversity of natural species of organisms, which is of great importance for nature and society [9]. In addition, forests, as well as wetlands, counteract to overflow floods. Therefore, when designing hydrosystems in boggy zones, the same conditions are fulfilled as for forest zones, such as maximum conservation of bogs during short-term flooding. The main criterion for the conservation of bogs can be the state of the peat deposit.

For many years, the emergence of peat from flooded bogs in the creation of reservoirs was considered only as a significant obstacle to the normal operation of hydroelectric power stations, shipping, fishing, etc.

Literature review, based on papers [10–14] allows to analyze results of accumulated observations by this issue. It can be stated that the relationship between the emersion of peat and its composition, the physical and mechanical properties, the degree of decomposition, the depth of flooding, as well as the meteorological conditions (air temperature, time of beginning and end of flooding of bogs, etc.) is revealed. This, in turn, allowed to solve practical issues in forecasting the emergence of peat and to develop protection action to quaking mat.

Using the data on peat surfacing obtained during long floods of bogs (a year or more) when creating reservoirs, it is possible to make a preliminary prediction on possibility to preserve the marshes during short-term flooding (several hours, days). For example, in case of flooding time of up to 2 years with a water column the following results was observed: 25–50% of the peat bog, up to 3 m, 3–5% – 10–25%, more than 5 m – 5–10% [11].

It can be assumed that during a short-term flooding (up to several dozen days) the proportion of floating peat will not exceed 5–25%, depending on the depth of flooding. However, the emergence of peat does not mean its complete separation, and, consequently, the actual area of the bog, which has not undergone unfavorable changes during short-term flooding, will be greater.

5 Water Quality Assessment

One of the most important indicators of the environmental friendly works of flood-control hydrosystem is water quality. The upper water of reservoir is characterized by water absorption of water soluble nutrients and organic materials, contained into the green plants, soils of inundation valleys, forests, bogs, etc.

As this water will be discharged into the lower tail, it is important to know the compliance of its composition with regulatory requirements. As noted early, for the safety of flooded forests, the oxygen content in the water of the reservoir should not fall below threshold.

It is possible to identify the main sources of water-soluble nutrients from the flooded territory: wood and litter; soil; bogs.

There are corresponding works on water quality assessment in case of vegetation, soil, and marshes, which are applicable to long-term flooding periods [13, 15–17]. However, there are no recommendations for cases of short-term flooding in these publications. Based on analysis of the data presented, some relationships were observed, which are the same for short-term floods and can be used for an approximate prediction of the entry mood of water-soluble nutrients and organic matters. In particular, the equations and coefficients for calculating the content of nutrients and organic substances were obtained in [16] in the vegetation decomposition and from flooded soils and marshes for the following basic ingredients: organic carbon, organic nitrogen, NH_4^+ , PO_4^{3-} . Using these data for calculation short-term flooding, it is possible to obtain somewhat higher values of the concentration of these substances

contained in water. However, from the point of view of ecological safety of the water environment, this is quite justified.

During construction flood control hydrosystems in the wetland area, forest devastation is unlikely. As a result of short-term flooding of woody vegetation, primarily the water quality will be affected by its coniferous-foliated part containing relatively many water-soluble substances, the washing out of which begins already from the first days of flooding [18]. Therefore, it is extremely important to predict the dynamics of the oxygen content in water when it interacts with the coniferous-leafy part of the phytomass.

It should be noted the methodology of Saint Petersburg State Forest Technical University [19] for prediction of oxygen regime of the reservoir of the antiflood facility, which allows to simulate the process of leaching of water-soluble substances from wood and litter. This methodology can be used to estimate the oxygen content during short-term flooding of woody vegetation.

6 Ecosystem Biodiversity Conservation

One of the main environmental factors for creating flood control hydrosystems is alienation and land conversion, which leads to change in the species diversity of ecosystems. This can adversely affect the stability of the natural environment. It should be noted that if the species diversity of ecosystems is preserved in the formation of a natural-technical system with minimal losses, then they have greater stability under conditions of insufficient anthropogenic loads and their predictable dynamics [20, 21].

To estimate the diversity of ecosystems during short-term flooding, it is proposed to use the Shannon index, which allows taking into account the level of structuring of the system [20]:

$$H = - \sum_{i=1}^N P_i \log_2 P_i, \quad (1)$$

where P_i - probability of any (i) sign (state) of an element from N possible signs (states): i.e. $i = 1, 2, 3, \dots, N$.

Estimation of ecosystem diversity is carried out using GIS technologies for the flooded area of the temporarily filled reservoir of the flood control facility at various design levels of the upstream [22–24].

The diversity of ecosystems H in Eq. (1) is determined by the coefficients $P_i = S_i/S$, which characterize the measure of the distribution of ecosystems within the considered catchment area. Here $S = \sum_{i=1}^N S_i$ is the catchment area in which $i = 1, 2, 3, \dots, N$ types of ecosystems are located, including natural (forest, marsh, lake, etc.) and anthropogenic (agricultural land, industrial buildings, settlements, reservoirs, etc.) each S_i area.

Assessment of the ecosystem biodiversity can be made by following criteria:

- non-decreasing of diversity

$$dH/dt \geq 0 \quad (2)$$

and ratio components of ecosystems both anthropogenic H_a and natural H_n .

$$H_a < k_a H_n, \quad (3)$$

where k_a is a coefficient, which determines allowable part of diversity of anthropogenic H_a ecosystems.

Environmental friendly flood control hydrosystems with temporary filling self-regulating reservoirs can be considered such systems, when during operation the natural biodiversity is preserved.

7 Conclusions

The final parameters and operating modes for flood control hydrosystems are determined for the minimum of permissible areas of short-term inundation in the upper pool, calculated for each priority factor of environmental impact.







Acknowledgements. The research was supported by Russian Science Foundation (grant № 16-17-00050).

References

1. News and information on the latest flood events from around the world (2017). <http://floodlist.com/>
2. Fedorov, M., Maslikov, V., Badenko, V., Chusov, A., Molodtsov, D.: Reducing the risk of flooding using distributed hydroschemes on the drainage basin. *Hydrotech. Constr.* **5**, 2–7 (2017)
3. Vasilevich, V., Maslikov, V., Makarova, M.: Ecological aspects of flood management with a system of reservoirs with distributed functions. *Interuniversity Collected Works: Ecological problems of rational use and protection of water resources* (1996)
4. Makarova, M.: Regulation of floods by the distributed system of reservoirs considering environmental factors. Published summary of a thesis (Candidate of Technical Sciences), St. Petersburg (1996)
5. Rusalenko, A.: Structure and Productivity of Forests During Underflooding and Flooding. *Nauka i Tekhnika Publishing, Minsk* (1983)
6. Istomina, M.: Ecological consequences of floods. *Eng. Ecol.* **4**, 3–19 (2004)
7. Macher, C.: Wenn Bäumen das Wasser bis zum Hals steht. *LWF aktuell* **66**, 26–29 (2008)
8. Vasilevich, V.: Dominant floristic approach to the selection of plant associations. *Bot. J.* **80** (6), 28–34 (1995)
9. State Committee of the Russian Federation for Environmental Protection. Strategy for the Conservation of Wetlands of the Russian Federation. Moscow (1999)
10. Methodological instructions for forecasting the process of peat floating in reservoirs of the temperate climatic zone of the USSR. Moscow (1983)
11. Molkin, G.: On the preliminary prediction of peat floating up and its drift towards the hydroelectric facilities. In: *Proceedings of Lengidroyekt*, vol. 38, pp. 155–167 (1973)

12. Panov, V.: About the role of hydrostatics of peatlands in their development. In: Proceedings of Instorf, vol. 56, pp. 3–11 (2011)
13. Korpachev, V.: Pollution and Clogging of HPP Reservoirs with Tree and Shrub Vegetation, Organic Substances and their Influence on Water Quality. The Russian Academy of Natural History, Moscow (2010)
14. Ryabokon, Yu.: Assessment of peat reserves in the flood zone of the reservoir bed of the projected Motynginskaya HPP on the river Angara. In: Proceedings of the International Scientific and Practical Conference, Moscow, vol. 1, pp. 506–510 (2009)
15. Recommendations for assessing the impact of flooded tree vegetation and soil in the bed of projected reservoirs on water quality. Hydroproject, Moscow (1987)
16. Denisova, A.: Formation of Hydrochemical Regime of the Dnieper Reservoirs and Methods of its Forecasting. Naukova Dumka, Kiev (1979)
17. Poleva, A.: Experimental studies to evaluate the influence of flooded timber on the quality of water reservoir. In: Proceedings of the Saint Petersburg State Forest Technical Academy, vol. 199, pp. 73–80 (2012)
18. Gashkova, M., Nikolaev, S., Tashev, A.: Oxygen regime of water in the presence of wood, bark, needles and leaves of various tree species. Ecology and forest protection, Leningrad (1985)
19. Nikolaev, S.: Decomposition of foliage of woody plants in an aquatic environment and its influence on water quality. Published summary of a thesis (Candidate of Biological Sciences), Leningrad (1988)
20. Fedorov, M.P., Bogolyubov, A.G., Maslikov, V.I.: Environmental safety of power plants using renewable sources of energy. Power Technol. Eng. **29**(6), 353–357 (1995)
21. Dmitriev, V., Frumin, G.: Ecological Regulation and Sustainability of Natural Systems. Nauka Publishing House, St. Peterburg (2004)
22. Fedorov, M., Badenko, V., Maslikov, V., Chusov, A.: Site selection for flood detention basins with minimum environmental impact. Procedia Eng. **165**, 1629–1636 (2016)
23. Solovyev, A., Pustovgar, A., Shilova, L., Adamtsevich, A., Solovev, D.: Simulating power efficiency of heat transfer agent cooling recirculation systems at power plants. Procedia Eng. **165**, 1275–1280 (2016). <https://doi.org/10.1016/j.proeng.2016.11.850>
24. Epshtein, S.A., Adamtsevich, A.O., Gavrilova, D.I., Kossovich, E.L.: Thermal methods exploitation for coals propensity to oxidation and self-ignition study. Gornyi Zhurnal **7**, 100–104 (2016). <https://doi.org/10.17580/gzh.2016.07.22>

Comparative Analysis of Alternative Solutions of Excavation for Section of Hydropower Tunnel HPP “Dabar”

Uroš Mirković¹ , Slobodan Radovanović^{1,2} ,
Ljubo Divac^{2,3} , Nikola Mirković² , Nikola Obradović² ,
and Zdenka Popović² 

¹ Institute for the Development of Water Resources “Jaroslav Černi”,
Jaroslava Černog 80, 11226 Belgrade, Republic of Serbia
uros.mirkovic@jcerni.co.rs

² Faculty of Civil Engineering, University of Belgrade,
Bulevar kralja Aleksandra 73, 11000 Belgrade, Republic of Serbia

³ Stucky DOO, Belgrade, Republic of Serbia

Abstract. The subject of this paper is a comparative analysis of the alternative solutions for the construction of the supply tunnel section of HPP “Dabar” from km 4 + 272.54 to km 12 + 125.0 with the application of TBM technology, milling machines technology and combinations of TBM technology and milling machines. Hydraulic tunnel of the HPP “Dabar” is a tunnel under the pressure with a length of 12125.0 m, which will conduct water from the reservoir Nevesinje to the machine building of the hydropower plant “Dabar” in Dabarsko polje (Republic of Srpska, Bosnia and Herzegovina). Four different construction alternatives of the mentioned tunnel section were analysed: use of milling machines, use of Gripper TBM, use of Double Shield TBM, a combination of Gripper TBM and milling machines.

Keywords: Supply tunnel · Alternative solutions · Excavation
TBM · Analysis

1 Introduction

The supply tunnel of HPP “Dabar” is a hydro-technical tunnel for water supply from the accumulation of Nevesinje to Dabarsko polje where the generators of HPP “Dabar” are located. The entire supply tunnel belongs to the multipurpose system Upper Horizons, which geographically includes karst fields whose altitude is over 500.0 m above sea level, and they are located between the Neretva and Trebišnjica rivers. The most important and largest karst fields are Gatačko, Nevesinjnsko, Dabarsko and Fatničko.

The area of the Upper Horizons is characterized by significant water resources that have as a basic characteristic the abundance of rainfall in the period of inundation (October - May) with long-term floods in the karst fields and a significant surface water deficit in the summer period when the watercourses completely dry up. Due to the

significant karstification process, groundwater levels are very low and unsuitable for exploitation in the summer period [3].

The Upper Horizons system covers the construction of a large number of facilities located in the mentioned karst fields with the main goal of transferring part of the available waters to the existing accumulation of “Bileća”. These additional quantities of water have a significant impact on the Lower Horizons, which results in great energy effects. This system includes the construction of three hydropower plants: HPP “Nevesinje” (capacity of about 60.0 MW), HPP “Dabar” (capacity of 160.0 MW) and HPP “Bileća” (capacity of 32.0 MW) [3].

HPP “Dabar” uses water from the accumulation in the Nevesinjsko polje, which will be formed by the construction of dam “Pošćenje”. The “Dabar” supply tunnel should conduct water from the Nevesinje reservoir to the pipeline under pressure, which further carries water to the machine building of HPP “Dabar” in Dabarsko polje.

The HPP “Dabar” water supply tunnel (Fig. 1) is 12125.0 m in length and according to the Main construction design [3] it should be built using the New Austrian tunnel method. The tunnel has four tunnel faces. One is located at the entry into the tunnel where the entrance building will be located. The second is located at the tunnel exit at the position of future surge tank. The other two faces will be formed by the construction of access tunnel “Straževica”, which is connected with the supply tunnel at the station km 4 + 272.54 of the supply tunnel. In this paper, the designation of tunnel faces will be introduced, which will be used in the text below. The tunnel face at the entrance - TF1, the tunnel face at the connection of access tunnel “Straževica” towards the entrance building - TF2, the tunnel face from connection of the access tunnel “Straževica” towards surge tank - TF3 and the tunnel face from the surge tank to the connection with access tunnel “Straževica” - TF4.

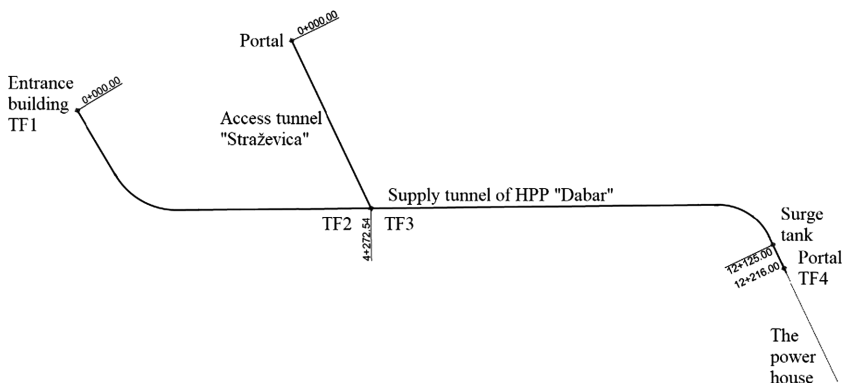


Fig. 1. Site plan of supply tunnel of HPP “Dabar”

From the geotechnical point of view, the tunnel passes through a series of conglomerates and sands at the entrance section, and on the part after km 3 + 700.0 tunnel passes through limestone masses. The overburden of the tunnel ranges from 10.0 m at the entrance section and gradually increases up to 300.0 m in some sections.

The aim of this paper is to present a technical-economic analysis of tunnel construction by analysing different construction alternatives compared to the one presented in the design documentation. The tunnel section from km 4 + 272.54 to km 12 + 125.0 was taken into consideration. The initial section from km 0 + 000.0 to km 4 + 272.54 was not considered due to problems with groundwater flow and flood waves in the period of inundation in Nevesinje field and thus leaving a justified option to apply New Austrian tunnel method using mining for excavation.

2 Description of Alternative Solutions

In this paper, four alternative solutions for the construction of the HPP “Dabar” tunnel were analysed on the section from km 4 + 272.54 to km 12 + 125.0.

2.1 Alternative Solution 1 – Mechanized Excavation with Two Milling Machines

This solution suggests that the supply tunnel will be built using the NATM (New Austrian Tunnel Method). The tunnel construction consists of a primary and secondary lining. The primary lining is designed to accept mountain pressures and groundwater effects. The secondary lining is 30.0 cm thick and designed to accept internal water pressures. The cross-section of the tunnel excavation is circular.

Based on stress-deformation analyses carried out in accordance with methodology presented in [5] different types of primary lining are defined. During stress-deformation analysis and the selection of lining types, properties of the rock mass (composition, cracks, faults and degradation), initial stress state (height of the overburden) etc. were taken into account.

After completing the excavation and securing the complete tunnel with primary lining, a secondary, reinforced concrete lining with a thickness of 30.0 cm, in combination with stress injection [1] is constructed, resulting in final cross-section of the tunnel with an internal diameter of \varnothing 4.60 m.

Entire HPP “Dabar” supply tunnel is supposed to be finished in less than 4 years. The construction period is planned to be from June 2016 to April 2020 or 47.0 months.

In the first year, all preparation works and works on the construction of access tunnel “Straževica” will be carried out and construction of supply tunnel at all four tunnel faces will begin.

In the second year, excavation works from tunnel face “Vodostan” (TF4) and entrance building (TF1) will resume, and excavation works on tunnel face “Straževica” will start.

In the third year, works on excavation of the supply tunnel will be completed and works on secondary concrete tunnel lining will start. Together with tunnel concreting, injection works will begin.

In the fourth year, concrete and injection works will be completed. In addition, works on the entrance building will be carried out during the fourth year.

2.2 Alternative Solution 2 - Gripper TBM

Gripper TBM is predicted to be used as a part of this solution (Fig. 2, left). This machine is suitable for use in rock masses in which the support of excavated cross-section in the area of excavation face and the protection of the machine itself is not required or can be achieved with lesser efforts and elements such as anchors, steel elements and sprayed concrete, which can be applied locally in tunnel calotte. It is applicable in stable rock masses with low groundwater penetration. The most important elements of this machine's construction are:

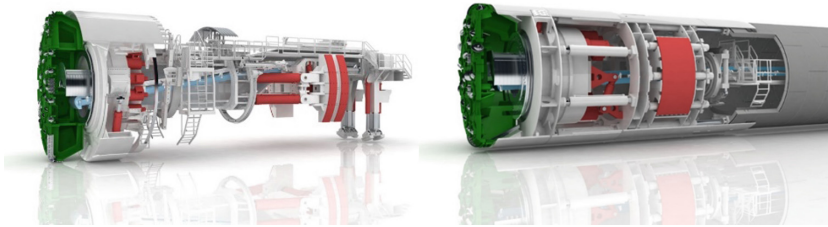


Fig. 2. Gripper TBM (left) and Double shield TBM (right) - longitudinal cross-section [8]

- Main truss,
- Cutter head with built-in cutting discs,
- Main bearing and cutting head drive,
- Gripper plates - convex metal structures attached to TBM machine on both sides, by which the front of the machine is braced against the rock mass during excavation (gripper plates are powered by hydraulics and can be adapted to the shape of excavation surface),
- Part of the machine between the cutterhead and the grippers - in this part, there are devices for tunnel lining construction: anchor drills, devices for installing lattice girders and reinforcement meshes [7].

The rock mass in the karstic conditions can have pronounced karstic characteristics: fractures and pockets filled with water, small dry cavities, fractures and pockets filled with material, as well as large open karst cavities - caverns (Fig. 3, left).

Fractures and pockets filled with water rarely make problems and reduce the progress of the machine. Less opened cavities create limited problems and many of them can be overcome without additional rock support. Larger filled cavities represent a major problem and cause a significant halt in operation of TBM. Entering into these zones causes the cutter head to jam and the TBM to sink. Under these conditions, TBM machines with single or double shields represent a significantly better choice.

There are currently several developed systems for detecting the karst during excavation. The most common are geophysical methods and the conventional drilling method [4]. After detection a section that would potentially cause problems during excavation, it is advised to construct roundabout tunnels of smaller lengths around the work face of TBM. This would allow direct access to the problematic site for its manual and machine repair.

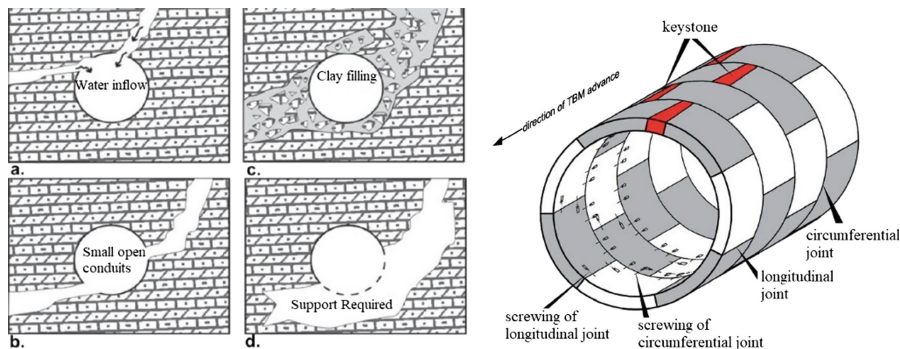


Fig. 3. Different types of karst formations (left); segment lining system (right)

The predicted diameter of TBM is 5.20 m and it was obtained based on analysis of excavation stability in case of construction in weaker rock masses. Secondary tunnel lining of Solution 2 will be the same as the secondary lining of Solution 1 described in the previous section, but will also include elements of the primary lining due to the limited TBM diameter of 5.20. This lining will have a bearing role in the construction phase, but also a role in bearing the loads from hydrostatic pressures in the exploitation phase.

2.3 Alternative Solution 3 – Double Shield TBM

Double Shield TBM (Fig. 2, right) is among the technically most advanced tunnelling machines. It combines TBM machines with grippers and Single Shield TBM.

In stable geological conditions, this machine allows the installation of concrete segments simultaneously with the excavation of the tunnel (Fig. 3, right), while achieving very high performance. This powerful technology is therefore perfect for excavation of long tunnels in hard rock masses.

Double Shield TBM consists of two main components: front shield with cutterhead, main bearing and main drive, and gripping shield with gripper units, auxiliary thrust cylinders and tail part of the machine. The main thrust cylinders connect these two parts. A telescopic shield protects them and therefore a Double Shield TBM is sometimes called a “telescopic shield”.

In a stable rock mass, the machine braces radially using the gripper. This means that the front shield can progress independently of the gripper shield using the main thrust cylinders. Reaction forces during the digging process are transferred to the rock mass through the expanded gripper plates. Simultaneously with the excavation of the tunnel, segments are placed in the tail of the machine. The auxiliary thrust cylinders serve only to secure the position of concrete segments that are mounted. When progress is completed, the grippers loosen and gripper shield is pushed to the front shield by auxiliary thrust cylinders. New gripping takes only a few minutes, which means that the excavation is almost continuous. In an ideal rock mass, a Double Shield TBM machine can also work without mounting the lining segments [7].

2.4 Alternative Solution 4 – a Combination of Gripper TBM and Milling Machines

Excavation Solution 4 of section of HPP “Dabar” supply tunnel represents a combination of Solutions 1 and 2 and in that sense contains their elements discussed in Sects. 2.1 and 2.2.

Excavation according to this solution is carried out with the help of one milling machine at tunnel face TF3 and at tunnel face TF4 excavation is carried out with the help of Gripper TBM.

The primary lining in this case is, based on the previous analysis, the same as the primary lining of Solution 1 on the part where the excavation is performed using a milling machine, or Solution 2 on the part where the excavation is carried out using a Gripper TBM.

The secondary lining is, based on the previous analysis, the same as the secondary lining of Solution 1 on the part where the excavation is performed using a milling machine, or Solution 2 on the part where the excavation is carried out using a Gripper TBM.

3 Technical - Economic Analysis

Price analysis of individual construction positions is based on the current prices of mechanization and equipment, spare parts, construction materials and labour. Calculations were carried out in accordance with construction and mechanical norms, and based on data obtained from the manufacturer of mechanization and equipment.

Based on previous discussion and on the progress speed of TBM machines and the progress speed of milling machine (7.0 m/day), the price for each of the solutions was calculated, whereby the prices were treated as initial or “zero” values for further calculation of possible savings based on achieving higher progression speeds of TBM machines.

For the starting value of tunnel construction price, the following TBM progression speeds were used: Gripper TBM (Solution 2) - 12.91 m/day, Double Shield TBM (Solution 3) - 7.81 m/day, Gripper TBM (Solution 4, for a meeting with a milling machine station km 7 + 077.50) - 8.30 m/day. These speeds were obtained from the conditions of the supply tunnel excavation of known length and completion of works on the entire tunnel in a period of 47.0 months, and in terms of length to excavation ratio. In addition, it was taken into account that Gripper TBM in Solution 2 shows a significant reduction in time required for the excavation, since the segment lining placing and injection works are carried out simultaneously with the excavation, while for the remaining solutions it is necessary to provide additional time for the mentioned operations.

The initial or “zero” price values for each solution, obtained based on calculations and estimated costs, are as follows:

- Solution 1 (Two milling machines): 34 227 726.85 EUR,
- Solution 2 (Gripper TBM): 38 344 720.44 EUR,
- Solution 3 (Double Shield TBM): 39 301 284.11 EUR,
- Solution 4 (Gripper TBM and one milling machine): 40 547 656.34 EUR.

For the last solution, it is important to note that the savings calculation was done for the most likely station meeting of TBM with a milling machine (km 6 + 455.58) and

for the different progression speeds of Gripper TBM. This is possible because the milling machine, according to the dynamic work plan, makes a halt in the work due to the water inflow into the tunnel, which is why its work is disabled in that period.

Savings at higher progression speeds of TBM machines in all solutions include labour costs, mechanisation and energy necessary for their operation.

The total monthly cost of mechanisation is based on the fact that the machines are working 30.0 days a month in three shifts of 8.0 h, with breaks in each shift of 1.0 h for the fuel supply and rest.

The obtained results are shown in the following diagrams (Figs. 4, 5 and 6).

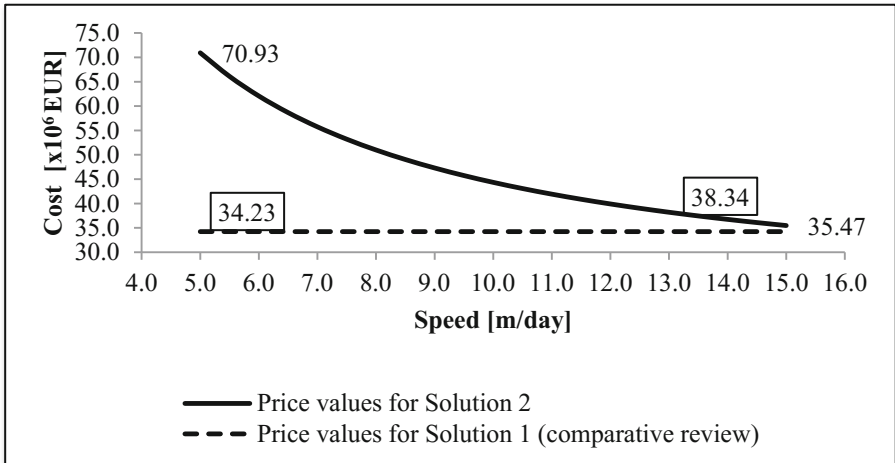


Fig. 4. Dependency of tunnel construction cost on progression speed of Gripper TBM (according to Solution 2)

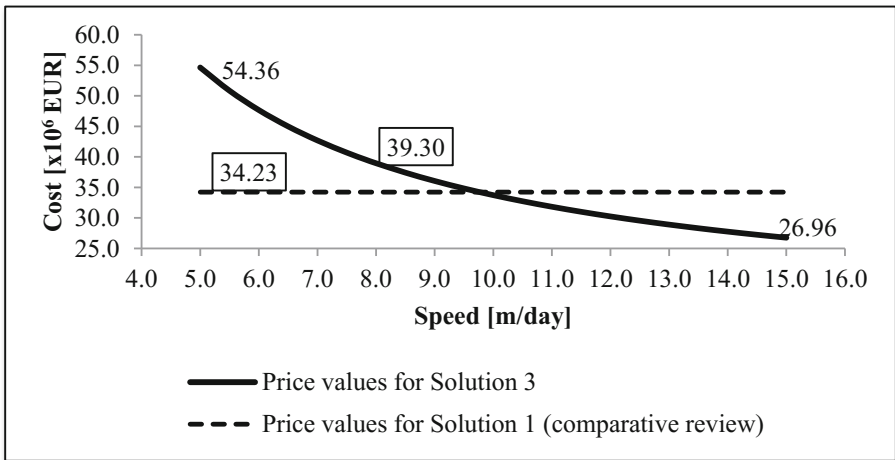


Fig. 5. Dependency of tunnel construction cost on progression speed of Double shield TBM (according to Solution 3)

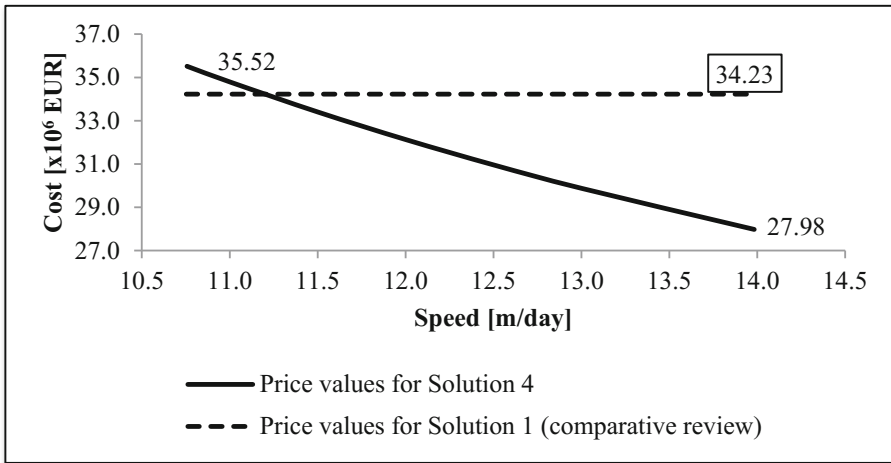


Fig. 6. Dependency of tunnel construction cost on speed of Gripper TBM for meeting station km 6 + 455.88 (according to Solution 4)

On the example of supply tunnel of HPP “Dabar” the cost estimates model for tunnels where the excavation is done mechanically was also applied [2]. When applying this model to a given section of the tunnel, the following values of parameters used in the expressions are used:

- The rate of progress in terms of m^3/day was estimated based on the predicted progression speed of TBM 10.0 m/day and based on the experience acquired during the excavation of Fatničko polje tunnel - the accumulation of “Bileća” in similar geological conditions [6],
- RMR and RQD are obtained on the basis of detailed geological surveys at the place of construction,
- $A = 20000.00$ (as author of the model recommended),
- $M = 1.30$ (the lowest level of finishing works and electro-mechanical works),
- GDP is adopted for Bosnia and Hercegovina in 2016 and its value is 10937.55 USD,
- Ratio USD/EUR is adopted as 0.89 (December 2016),
- Tunnel diameter is 5.20 m.

Based on the calculations that primarily include shorter sections of the tunnel with known RMR values, total cost of construction of the considered section (km 4 + 272.54 – km 12 + 125.0) is 36 391 855.81 EUR.

Based on the previous, a match of 94.91% was obtained with the “zero” price for Solution 2 (excavation with Gripper TBM – 38 344 720.44 EUR), that is, a match of 92.60% with the “zero” price that was obtained for Solution 3 (excavation with Double Shield TBM – 39 301 284.11 EUR) which speaks to the accuracy of the applied model.

4 Conclusion

Based on the calculated values, at first, it can be concluded that the solution given by the Main construction design (Solution 1) of the supply tunnel is the most economical solution that requires the least investment for the construction period of 47.0 months.

However, by analysing the prices depending on the achievement of higher speeds of excavation progress with TBM machines and shortening of the construction period, the following conclusions can be drawn:

- Solution 2 will show a cost reduction in relation to the Solution 1 for TBM progression speed greater than about 13.50 m/day,
- Solution 3 will show a cost reduction in relation to the Solution 1 for TBM progression speed greater than about 8.0 m/day,
- Solution 4 will also show a cost reduction in relation to the Solution 1 for TBM progression speed greater than about 10.50 m/day.

In accordance with the last paragraphs, Solution 3 (excavation with Double Shield TBM) represents the most favorable solution for the construction of the considered tunnel section. This solution has slightly increased initial investment in relation to the other solutions, but due to shortening of construction time caused by installation of segment lining and injection simultaneously to the excavation, it gives the best opportunity to reduce costs based on savings (labour, mechanization, operational energy) in relation to Solution 1. The progress speed leading to the mentioned cost reduction is very realistic. However, this solution may have additional problems regarding the possibility of installing the necessary facilities (above all the concrete factory) on the ground that would lead to cost increase. Such problems are not considered in this paper, but in reality, due to inaccessible terrain, they are very possible.

Solution 4 is a medium-sized solution with realistic progression rates. This excavation, with two tunnel faces, with the use of TBM machine and milling machine, also requires slightly higher initial investment, but very quickly brings, similar to the previous solution, to a reduction in construction costs compared to Solution 1.

Solution 2 asks for the smallest initial investment compared to the previous two, but also provides a reduced (but realistic) probability of cost reduction in relation to the Solution 1, as it requires the highest speeds of progression.

The biggest disadvantage of TBM machines is in terms of geological composition of the terrain. When TBM comes along a fault area or caverns it goes to a complete standstill, and continues to work after solution of these problem in terms of technology and work organization, their repair and creating conditions for further excavation.

In accordance with the previous conclusion, it is necessary to pay attention to the previous geological and hydrogeological researches, in order to obtain the highest quality of engineering-geological profile of the tunnel. Moreover, this is important so that the contractor can be ready for the rapid change in the organization and construction technology or that he has the appropriate equipment for fast repair in unfavourable geological conditions and quick return to work with TBM machines.

References

1. Andjelkovic, V., Lazarevic, Z., Nedovic, V., Stojanovic, Z.: Application of the pressure grouting in the hydraulic tunnels. *Tunn. Underground Space Technol.* **37**, 165–179 (2013)
2. Gumusoglu, C.: A global cost estimation model for mechanized tunnels based on in - situ data. In: *ITA World Tunnel Congress 2015: SEE Tunnel: Promoting Tunnelling in SEE Region*, HUBITG, Dubrovnik, Croatia (2015)
3. Institute “Jaroslav Černi” – “Stucky”: HPP “Dabar”: supply tunnel, entrance building, access tunnel – Main design, Institute “Jaroslav Černi”, Belgrade (2014)
4. Log, S., Ofiara, D., Anderson, T., Wetlesen, T.: Hard rock TBM tunnelling in karst conditions: Developments and lessons learned from the field. In: *ITA World Tunnel Congress 2015: SEE Tunnel: Promoting Tunnelling in SEE Region*, HUBITG, Dubrovnik, Croatia (2015)
5. Radovanović, S., Rakić, D., Divac, D., Živković, M.: Stress-strain analysis and global stability of tunnel excavation. In: Chiorean, C.G. (ed.) *2nd International Conference for PhD students in Civil Engineering and Architecture CE-PhD 2014*, Technical University of Cluj-Napoca, Cluj-Napoca, Romania, pp. 248–255 (2014). ISSN 2392-9715
6. Šćepanović, S.: Analysis of the effects of different methods of the excavation of the tunnel “Fatničko polje - Akumulacija Bileća” in the hydrosystem Trebišnjica. *Tehnika* **68**(4), 617–624 (2013)
7. Wittke, W.: *Rock Mechanics Based on an Anisotropic Jointed Rock Model (AJRM)*. Wiley, Berlin (2014)
8. Herrenknecht AG.: <https://herrenknecht.com/en/home.html>. Accessed 01 Dec 2016

Evaluation of Surface Deformations of Rolling Mills Stands Elements Resulting from Horizontal Forces Acting at Rolling

Victor Artiukh¹ , Vladlen Mazur² , and Elena Nidziy³ 

¹ Peter the Great St. Petersburg Polytechnic University,
Polytechnicheskaya str., 29, Saint-Petersburg 195251, Russia
artiukh@mail.ru

² LLC “Saint-Petersburg Electrotechnical Company”,
Pushkin, Parkovaya, 56, Saint-Petersburg 196603, Russia

³ Moscow State University of Civil Engineering,
Yaroslavskoe Shosse, 26, Moscow 129337, Russia

Abstract. Paper describes theoretical deformation of housing vertical surfaces of hot thick strip rolling stand resulting from a single strike from bottom work roll chock. At multiple horizontal impacts of roll chock against housing residual deformations arise in the corresponding elements of rolling stands which values should be controlled. Detailed diagram is shown indicating wear of flat contact surfaces of rolls chocks, surface panels and stands, also showing their degree of wear in the form of wedges, thus simplifying considerably the analysis of the wear of contact surfaces.

Keywords: Dynamic loads · Horizontal impacts · Deformation
Rolling mill frame · Surface panels · Main line
Contemporary materials for metallurgy

1 Introduction

It is known that for prevention and protection of rolling mills housings and rolls chocks from wear in horizontal direction (direction of rolling) lining straps and facing strips are used. Flat contact surfaces of rolls chocks, facing strips, lining straps and housings are heavily loaded elements of rolling mills [1–5]. Stress calculations of details of 4-hi thick strip rolling stand undergoing horizontal forces during rolling are shown in [6–10] where the main criterion of equipment durability is calculation of von Mises stresses and their comparison with yield limits of particular steel grades.

Prediction of residual deformations values of contact surfaces undergoing horizontal forces during rolling is important for evaluation of necessity to revamp equipment. It is expansive to revamp these surfaces because welding and accurate machining are used.

2 Materials and Methods

Positions of vertical surfaces 1 and 2 of housing (from steel 161 grade 430 according to B.S. 1504 (76)) are shown on Fig. 1. These vertical surfaces deform after above-mentioned horizontal impacts considered at stress calculation done by means of FEM analysis [8] with several assumptions:

- impact of bottom work roll (BWR) chock against housing is done with full flat contact of surfaces designed as per real geometry of elements: housing, hydraulic cylinder (installed in slot with surface 2), lining strap, facing strip and BWR chock;
- contact surface area of housing undergoing impact from BWR chock is equal to sum of areas 1 and 2 (refer to Fig. 1).

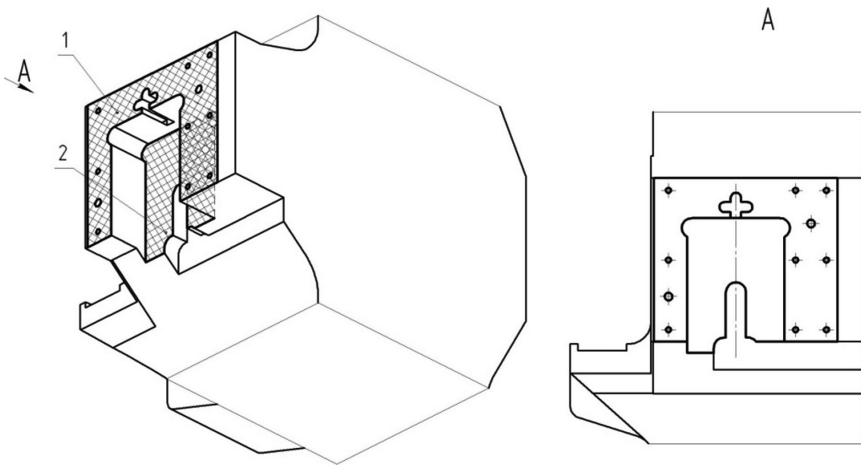


Fig. 1. Positions of vertical surfaces of housing for calculation of their deformations.

Results of theoretical calculation of deformations of housing vertical surfaces by means of FEM during horizontal impact of BWR chock with force $F = 2\text{MN}$ at mathematical model (MM) [8] in which facing strip and lining strap are from steel 080 M 46 according to B.S. 970 are shown on Fig. 2 where value of maximum deformation is equal to $0.00003085\text{ m} = 0.03085 \cdot 10^{-3}\text{ m}$ (refer to Table 1).

In addition, more calculations with another two similar MM were done where:

- facing strip and lining strap are from bimetallic steel (outer surface is from rigid Steel 65G according to CIS state standard 20072–74 and soft inside surface is from soft Steel 3 according to CIS state standard 380–94);
- BWR chock lining strap is from polyurethane grade Adiprene L-167.

Results of housing deformations calculation of vertical surfaces by means of FEM during horizontal impact of BWR chock with force $F = 2\text{MN}$ (single impact with single loading) with facing strip and lining strap from different materials are shown in Table 1.

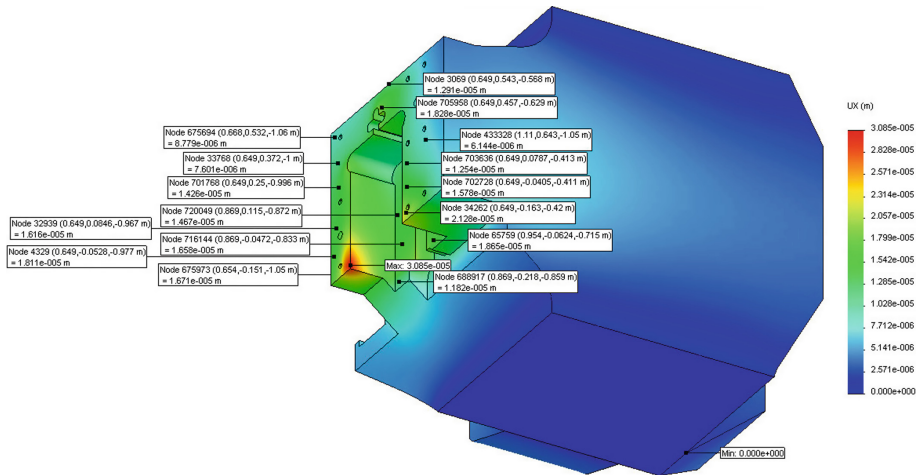


Fig. 2. Results of theoretical calculation of deformations of housing vertical surfaces during horizontal impact of BWR chock (lining strap) against the housing.

Table 1. Values of maximum deformations of housing vertical surfaces of different MM

Material of lining strap	Material of facing strip	Deformation of housing, m
Steel 080 M 46	Steel 080 M 46	$0.03085 \cdot 10^{-3}$
Bimetal	Bimetal	$0.03094 \cdot 10^{-3}$
Polyurethane adiprene L-167	Steel 080 M 46	$0.02117 \cdot 10^{-3}$

Analysis of data in Table 1 shows that it is reasonable to use lining straps from polyurethane grade Adiprene L-167 on chocks of top and bottom work rolls (WRs) because it results in reduction of deformations of vertical contact surfaces by 31% (at single impact). Moreover, at numerous horizontal impacts (ordinary use of rolling stand) residual deformations of particular abovementioned details of rolling stand arise that must be monitored and controlled because increases of gaps between contact surfaces result in increases of impacts of WRs chocks against housings [11].

Turning of WRs in horizontal plane increases axial loads acting from WRs chocks on their clamping devices. Furthermore, increases of described gaps result in misalignment of WRs with chocks in housings that contributes to nonuniform wear of contact surfaces (chocks and lining straps, housings and facing strips) that factually happen.

It is known that during metal bite first impact of chock against housing mostly happens by angle (edge) of chock (lining strap) [12] and especially it happens when total horizontal gap between chock lining strap and housing facing strip is equal to $\Sigma\Delta = 4 \dots 6$ mm. Recommended values of $\Sigma\Delta$ for different rolling stands should be not more than $2 \dots 3$ mm (refer to Fig. 3, where $\Sigma\Delta_{\min P} = 2 \cdot \Delta_{\min P}$ and $\Sigma\Delta_{\max P} = 2 \cdot \Delta_{\max P}$).

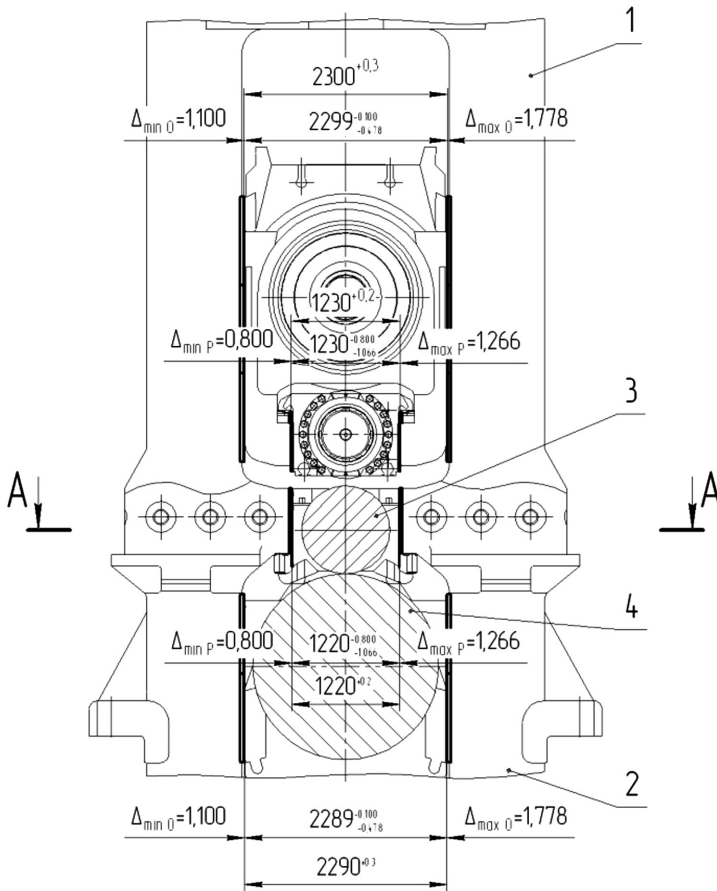


Fig. 3. General view of reversing roughing rolling stand from operator side: 1 is housing from operator side; 2 is housing from drive side; 3 is BWR; 4 is bottom backup roll.

On many rolling mill shops individual systems for measuring and monitoring wear of housings, facing strips, chocks and lining straps are used and operational personal knows that increased wear results in decrease of quality or rolled metal. Unfortunately, these individual systems are not useful enough [13]. Taking into consideration some individual systems and their productivity authors of that paper propose to show wear in a form of wedge where its figures come from maximum and minimum values. Values of wear of flat contact surfaces of hydraulic cylinders and housings are shown in a proposed way on Fig. 4.

Resistance to horizontal impacts loading and wear of contact surfaces depend on material of details [14], roughness of surfaces [15], their thermal and thermo-chemical treatment [16], contact areas [17] and use of lubrication in areas of contact [18]. It is proposed to scrutinize wear of the details on the base of area of BWR installation [8] (section A–A on Fig. 3). Wear is shown for case where:

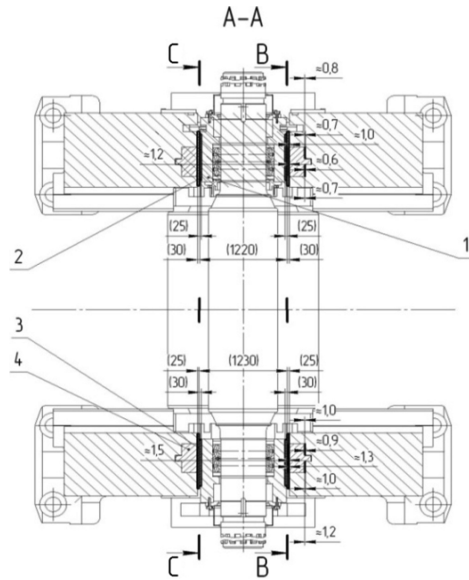


Fig. 4. BWR together with chocks in rolling stand: 1 is BWR chock; 2 is lining strap of BWR chock; 3 is facing strip of housing; 4 is hydraulic cylinder for press of BWR chock to bottom backup roll.

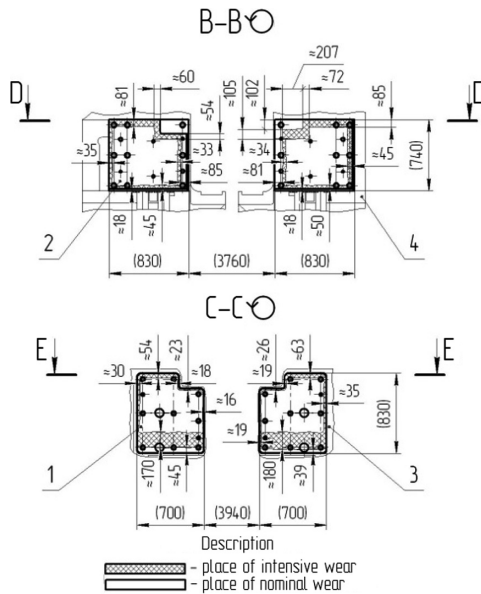


Fig. 5. Maximum wear of contact surfaces of lining straps and facing strips in vertical planes: 1 is lining strap on drive side; 2 is facing strip on drive side; 3 is BWR chock.

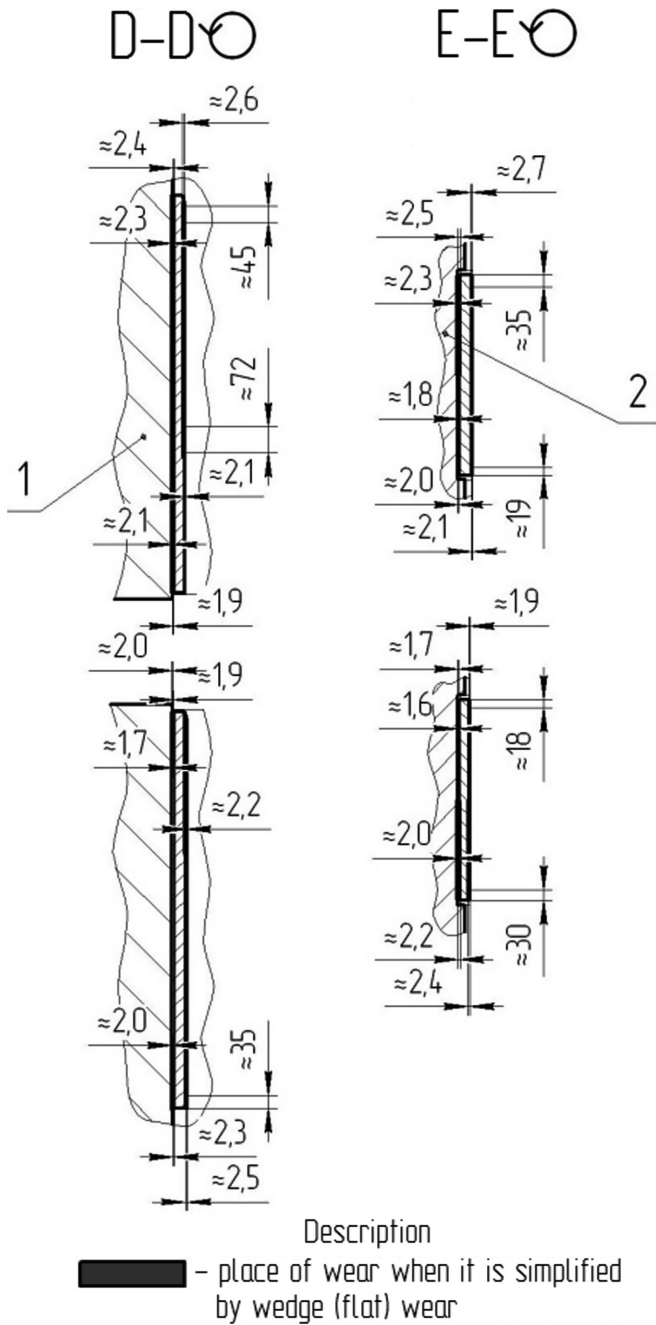


Fig. 6. Maximum wear of flat contact surfaces of lining straps and facing strips of BWR area: 1 is housing on operator side; 2 is BWR chock.

- lining straps and facing strips are from steel 080 M 46;
- lubrication between lining straps and facing strips is used;
- around 600000t of metal were rolled;
- wear is symmetrical in relation to vertical axis of reversing rolling stand.

On Fig. 3 $\Delta_{\min O}$ and $\Delta_{\max O}$ are minimal and maximal project gaps between lining straps of backup roll chocks and corresponding facing strips of housings; $\Delta_{\min P}$ and $\Delta_{\max P}$ are minimal and maximal project gaps between lining straps of WR chocks and corresponding facing strips of housings (lining straps of backup roll chocks). Maximum wear values of flat contact surfaces undergoing horizontal forces during rolling are shown on Figs. 4, 5 and 6.

Places of intensive and nominal wear of flat contact surfaces of lining straps in vertical planes (refer to section C–C on Fig. 5) correspond to places of intensive and nominal wear of flat contact surfaces of BWR chocks in vertical planes.

Places of intensive and nominal wear of flat contact surfaces of facing strips in vertical planes (refer to section B–B on Fig. 5) correspond to places of intensive and nominal wear of flat contact surfaces of housings in vertical planes.

Values of maximum wear of flat contact surfaces of housings under facing strips of thick strip rolling mill 3000 (Ukraine, PJSC Illich Iron and Steel Works) after 11 years of use [15]:

- are 6.0...20.0 mm on roughing rolling stand, area of bottom backup roll chocks installation;
- are 4.0...14.0 mm on finishing rolling stand, area of bottom backup roll chocks installation.

Values of maximum wear of flat contact surfaces of housings under facing strips of thick strip rolling mill 3600 (Ukraine, PJSC Azovstal Iron and Steel Works) in area of installation of bottom backup roll chocks are 0.5...5.6 mm [16].

Analysis of wear of flat contact surfaces undergoing horizontal forces during rolling of hot strip mills 1700 and 2000 (Russia, PJSC Cherepovets Iron and Steel Works) states that rolling in one direction makes negative influence on wear, deformation and durability of rolling stands equipment [19, 20].

3 Conclusions

1. Theoretical deformation of vertical surfaces of housings due to single impact from BWR chock (lining strap) is shown. Residual deformation of the elements arise at real numerous impacts and it should be controlled by operating personal.
2. Necessity to install lining straps on top and bottom WR chocks from polyurethane Adiprene L-167 is proved.
3. Wear of vertical surfaces undergoing horizontal forces is shown in a way as wedge that simplifies its analysis.

Acknowledgments. The reported study was funded by RFBR according to the research project №16-08-00845a «Verification and development of models of inelastic deformation at the passive loading».

Conflict of Interests. The authors declare that there is no conflict of interest regarding the publication of this paper.

References

1. Ishenko, A.: Experimental analysis of impact forces acting on housings of rolling stands of thick sheet rolling mills. *Steel* **5**, 56–58 (2009)
2. Mazur, V., Artyukh, V., Artyukh, G., Takadzi, M.: Current views on the detailed design of heavily loaded components for rolling mills. *Eng. Des.* **37**(1), 26–29 (2012)
3. Kitaeva, D., Rudaev, Y., Subbotina, E.: About the volume forming of aluminium details in superplasticity conditions. In: *METAL 2014 - 23rd International Conference on Metallurgy and Materials, Conference Proceedings* (2014)
4. Kukhar, V., Artiukh, V., Serduik, O., Balalayeva, E.: Form of gradient curve of temperature distribution of lengthwise the billet at differentiated heating before profiling by buckling. *Procedia Eng.* **165**, 1693–1704 (2016)
5. Semenov, A., Melnikov, B., Gorokhov, M.: About the causes of cyclical instability at computations of large elasto-plastic strains. In: *Proceedings of SPIE – the International Society for Optical Engineering*, vol. 5831(25), pp. 167–173 (2005)
6. Sorochan, E., Artiukh, V., Melnikov, B., Raimberdiyev, T.: Mathematical model of plates and strips rolling for calculation of energy power parameters and dynamic loads. In: *MATEC Web of Conferences*, vol. 73, p. 04009 (2016)
7. Gharaibeh, N., Matarneh, M., Artyukh, V.: Loading decrease in metallurgical machines. *Res. J. Appl. Sci. Eng. Technol.* **8**(12), 1461–1464 (2014)
8. Artiukh, V., Raimberdiyev, T., Mazur, V.: Use of CAE-systems at evaluation of shock absorbers for metallurgical equipment. In: *MATEC Web of Conferences*, vol. 53, p. 01039 (2016)
9. Al-Quran, F., Matarneh, M., Artiukh, V.: Choice of elastomeric material for buffer devices of metallurgical equipment. *Res. J. Appl. Sci. Eng. Technol.* **4**(11), 1585–1589 (2012)
10. Artiukh, V., Karlushin, S., Sorochan, E.: Peculiarities of mechanical characteristics of contemporary polyurethane elastomers. *Procedia Eng.* **117**, 938–944 (2015)
11. Mazur, V., Artiukh, V., Matarneh, M.: Horizontal force during rolling as indicator of rolling technology and technical conditions of main rolling equipment. *Procedia Eng.* **165**, 1722–1730 (2016)
12. Artiukh, V., Mazur, V., Shilova, L.: Device for making horizontal wedge thrust of rolling stand. In: *MATEC Web of Conferences*, vol. 106, p. 03002 (2017)
13. Alexandrov, I.: Reconstruction of rolling stands by means of bimetallic lining straps. *Metal Cast. Ukr.* **3**(4), 51–52 (2004)
14. Kiril'chenko, P.: Use of metall-polymer materials for revamp of rolling mills equipment. *Steel* **1**, 67–68 (2007)
15. Ishenko, A.: Repair of housings of work stands of rolling mill 3000. *Steel* **5**, 63–65 (2003)
16. Ishenko, A.: New technology for revamp of rolling mills housings. *Metall. Min. Ind.* **2**, 71–73 (2002)
17. Lipukhin, Y.: Increase of durability of roll bearings of wide strip mills. *Steel* **1**, 56–61 (1987)

18. Komarov, A.: Influence of wear of rolling stands elements on accuracy of hot rolling strip. *Rolling Met.* **60**, 117–121 (1980)
19. Artiukh, V., Mazur, V., Prakash, R.: Increasing hot rolling mass of steel sheet products. *Solid State Phenom.* **871**, 3–8 (2016)
20. Artiukh, V., Mazur, V., Adamtsevich, A.: Priority influence of horizontal forces at rolling on operation of main sheet rolling equipment. In: *MATEC Web of Conferences*, vol. 106, p. 04001 (2017)

Low-Temperature Swirl Burning as Technological Method of Simultaneous Decrease in Emissions of Nitrogen and Sulfur Oxides (Part 1. Principles, Organization and Mathematical Model of Furnace Process)

Aleksey Trinchenko^(✉)  and Aleksandr Paramonov 

Peter the Great St. Petersburg Polytechnic University,
Polytechnicheskaya, 29, St. Petersburg 195251, Russia
trinchenko@spbstu.ru

Abstract. The work is devoted to the solution of the problem of increasing ecological indicators of power boilers. The technology of simultaneous decrease in content of nitrogen and sulfur oxides in combustion products by the organization of low-temperature vortex burning is considered. The model of burning process of solid fuel considering generation and transformation of gaseous pollutants in the furnace camera is developed. Results of modeling and numerical researches of generation and decomposition of nitrogen oxides on surface of carbon particles are given, decrease in concentration of sulfur oxides due to their binding with components of mineral part at combustion of organic fuel is shown.

Keywords: Boiler plant · Emissions of pollutants · Nitrogen oxide

1 Introduction

High ecological standards show the demand of further improvement of processes of using hydrocarbon fuels. The increased concentration of gaseous pollutants of combustion products of power boilers, nitrogen oxides (NO_x) and sulfur oxides (SO_x), very often are unacceptable for developing the infrastructure of the cities and industrial centers [1] that defines need in search of new ecologically safe technologies of fuel combustion for producing heat and electrical energy [2].

It is possible to organize decrease in content of harmful dopant gases in combustion gases of boilers at three stages: (1) at stage of preparation of fuel for burning; (2) at stage of its burning; (3) by cleaning of products of combustion [3–8]. And economically reasonable constructive and regime (technological) actions which without demanding considerable financial expenses admit the most perspective now, allow to achieve acceptable concentration of pollutants in the leaving combustion gases. The essence of these actions consists in creation of special designs of fire chambers and impact on furnace process so that at preservation of economic indicators of process of burning to

provide decrease in content of harmful impurity in combustion products to acceptable level [9].

Combustion of fuel widely now in use in the direct-flow coal-dust torch (DFCDT) [10], along with advantages, has a number of shortcomings. To one of the main shortcomings inherent in direct-flow torch, existence of the high-temperature kernel of the burning which is zone of intensive generation of nitrogen oxides and increasing danger of slagging of surfaces of heating of boiler installation belongs. The known ways of impact on high-temperature zones of coal-dust torch (recirculation of products of combustion, injection of moisture in zone of active burning and so forth) not always result in desirable results, and in some cases reduce economic indicators of process. Burning according to the scheme PPF of low-calorie and low-grade fuels as a rule requires torch illumination by gas or fuel oil that in turn considerably increases temperature in torch kernel zone. Difficulties of impact on the formed sulfur oxides for the purpose of decrease in their content in furnace gases are caused by small time of stay of products of combustion in fire chamber that defines the increased concentration of SO_x to exit from boiler.

Perspective technological way of simultaneous decrease in emissions of gaseous nitrogen oxides and sulfur oxides is the low-temperature swirl (LTS) technology of combustion of organic fuel offered by professor V.V. Pomerantsev [11], researches on to which improvement, are successfully conducted at the St. Petersburg polytechnic university of Peter the Great [12–16] now.

The furnace camera of prismatic design in which three pronounced aerodynamic zones of the movement of fuel-air flows will be organized forms basis of the LTS organization of technology: The I – flow of fuel-air mix coming to fire chamber through the torches established on front aerodynamic ledge, the II – flow of hot air coming to fire chamber through the system of the lower blasting (SLB), the III – lower swirl zone of fire chamber formed at interaction of flows of I and II [17–19]. In the lower swirl zone repeated forced circulation of the burning particles is organized that allows to coarsen fuel grind, and in some cases completely to exclude system of dust preparation and to pass to combustion of shredded fuel [20]. Continuation of burner flow is the zone of direct-flow torch in which the fine particles of fuel which have left swirl zone burn down. Such organization of aerodynamics allows to level considerably the temperature field in furnace volume, on 100–150 K to reduce maximum of temperatures [21], to exclude illumination of torch and slagging of surfaces of heating.

In the lower swirl zone on surface of the burning coke particles there is intensive decomposition of the generated nitrogen oxides to education ecologically safe carbonic acid and molecular nitrogen [22], and repeated circulation of ash particles leads to the binding of sulfur oxides with CaO (and MgO) components of mineral part of fuel [23].

Advantages of LTS of technology remain in case of power use low-calorie (high-wet and high-ash) fuels which treat, including brown coals. Need of effective combustion of brown coal situated near Moscow has arisen on the Novomoskovsk state district power plant (NGRES) for what on LTS technology it has been decided to reconstruct boiler of BKZ-220-9,8 of the Art. No. 15. The planned reconstruction has

defined the purpose of work -to develop technique and mathematical model of LTS-furnace process in BKZ-220 boiler fire chamber with which use to conduct researches of generation and transformation of gaseous nitrogen oxides and sulfur oxides during the work on brown coal situated near Moscow for increase in ecological indicators of boiler, to carry out their quantitative assessment for successful implementation of the project.

2 Materials and Methods

The LTS organization of furnace process in boiler of BKZ-220-9,8 (the Art. No. 15) is carried out by NGRES (Fig. 1a) by reconstruction of the furnace camera (Fig. 1b) for the organization of the swirl aerodynamics (allowing to provide combustion of coarse fuel at its repeated circulation) and reconstruction of dust preparation system components (for coursing the grind). In the lower aerodynamic ledge of fire chamber eight direct-flow rhomboid torches of solid fuel which inclination to the horizon of axis makes 45° are established. Under solid-fuel torches on the vertical site of the front screen four gas torches of GMPV-13 which are at the same time used for kindling are established. The furnace camera of boiler is completely replaced with gas-dense.

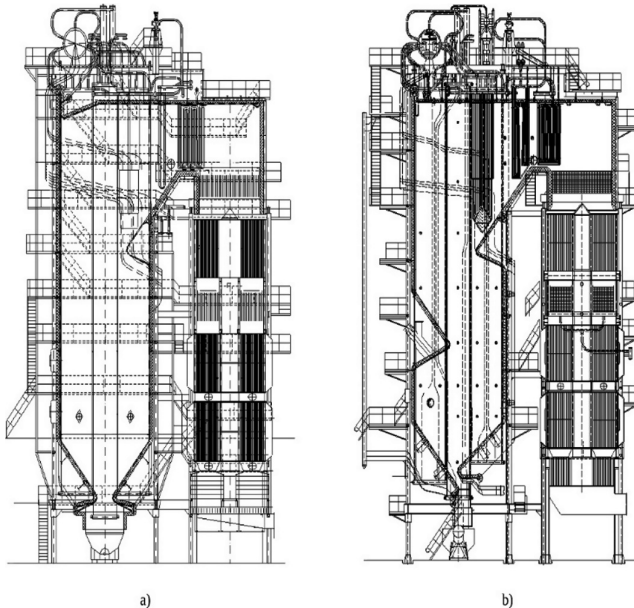


Fig. 1. Boiler of BKZ-220-9,8 (No. 15) of the Novomoskovsk state district power plant: (a) – before reconstruction; (b) – after reconstruction

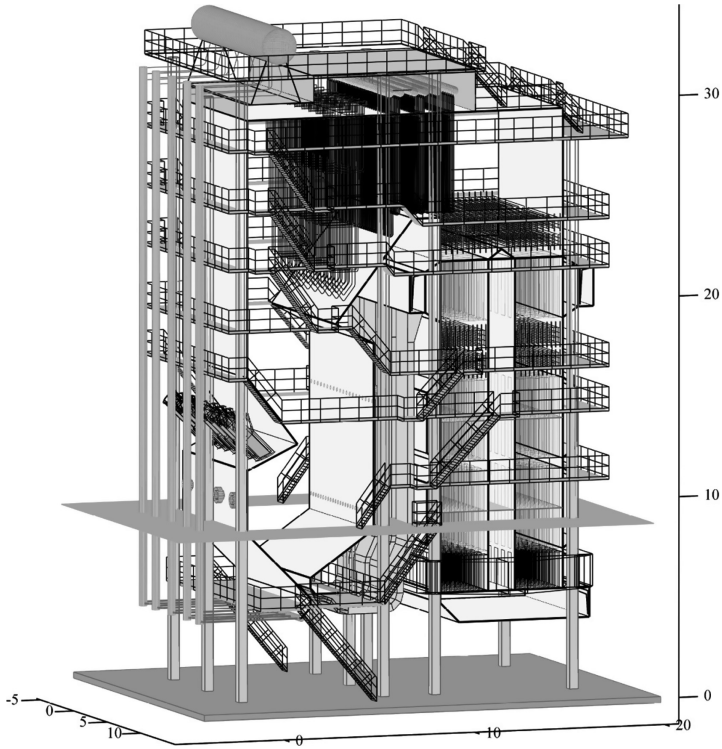


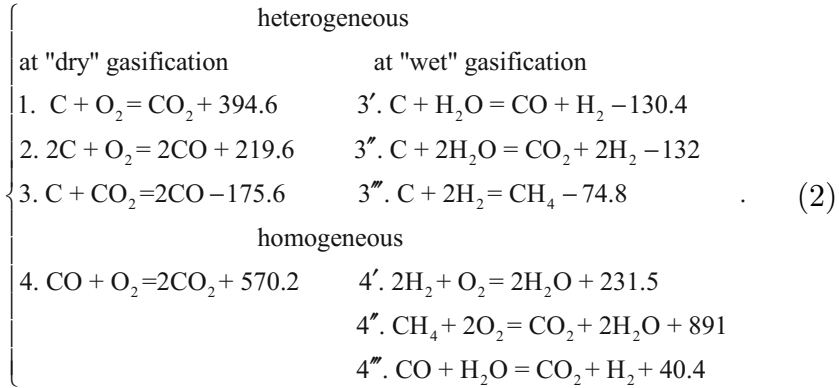
Fig. 2. BKZ-220 boiler model with low-temperature swirl technology of burning

For numerical research of LTS-furnace process, the model of boiler BKZ-220-9,8 of the Novomoskovsk state district power plant (Fig. 2) which is completely reflecting the made constructive decisions, the principles and features of LTS technology, and also allowing to make necessary changes for optimization of constructive characteristics and regime parameters of work is developed.

The model of furnace process is based on the diffusion and kinetic theory of burning, considers generation and transformation of gaseous pollutants, has possibility of change qualitative (look and composition of solid fuel, its grinding and so forth) and quantitative characteristics of process (fuel consumption, speeds of burner air, air of the lower and tertiary blasting and so forth), and allows to carry out quantitative estimates of emissions of gaseous pollutants during the work of boiler. Consideration of process of burning from diffusion and kinetic positions has allowed to make system of the nonlinear differential equations of diffusion and kinetics of type:

$$dG_j = -(D/RT) \cdot (d^2p_j/dx^2)dx; G_j = (\alpha_D/RT) \cdot (p_j - p_{j0}); dG_i/d\tau = C_i \cdot k_i, \quad (1)$$

considering oxidizing and recovery reactions of the particles going on surfaces, and the homogeneous reactions proceeding within interface:



Change of constants of speed of chemical reactions from temperature submits to Arrhenius's dependence:

$$k_i = k_{0i} \cdot \exp[-E_i/(RT)], \quad (3)$$

where k_0 – preexponential multiplier of dependence of Arrhenius (in m/s for heterogeneous and in 1/sec with for homogeneous reactions); E – the seeming energy of activation, J/mol.

For calculation of communication of energy of activation (E_i) and preexponential multiplier (k_{0i}) the pole offered by S. M. Shestakov is used:

$$\lg k_{0i} = 0.2 \cdot 10^{-4} \cdot E_i + 2. \quad (4)$$

The significant difference of values of the energy of activation obtained when processing of experimental data even on one type of carbon material is caused not only by inhomogeneity of carbon materials, but also insufficiently strict accounting of diffusion influence. It complicates the choice of k_0 values and E. L.A. Vulis's researches, V.V. Pomerantseva, etc. show that between values of energy of activation of different reactions of carbon with O₂ and CO₂ for the same coke there is certain communication. On the basis of the analysis of the experimental data the following ratios between values of energy of activation of different reactions are recommended:

$$\left\{ \begin{array}{l}
 E_{C+O_2=CO}/E_{C+O_2=CO_2} = 1.1 \\
 E_{C+CO_2=2CO}/E_{C+O_2=CO_2} = 2.2 \\
 E_{C+H_2O=CO}/E_{C+O_2=CO_2} = 1.6
 \end{array} \right. \quad (5)$$

For assessment of extent of influence of reaction No. 4 of system (1) in burning out of carbon particle Se criterion characterizing the relation of flow of the substance absorbed by homogeneous reaction of afterburning 4 to its diffusion flow is used:

$$Se = (k_4 \Delta^2 / D)^{1/2}, \quad (6)$$

where k_4 – constant of speed of reaction No. 4 of system (1); $\Delta = \delta / \text{Nu}D$ – thickness of the given boundary film, m; D – coefficient of diffusion, sq.m/sec.

For the accounting of mass exchange near carbon surface the method of “the given film” is used. The diffusion coefficient in multi-component mixture is defined from Uilk’s ratio:

$$D_{1,n} = (1 - x_1) / (x_2 / D_{1,2} + x_3 / D_{1,3} + x_4 / D_{1,4} + \dots) \quad (7)$$

where $x_1 = p_1/P$; $x_2 = p_2/P$, etc. – mole fractions of components in mix; $D_{1,2}$, $D_{1,3}$, $D_{1,4}$ – the coefficients of mutual diffusion of substances under real conditions determined by Vinkelman’s dependence:

$$D_{1,2} = D_{0,1,2} (T/T_0)^{1.75} \cdot (P/P_0), \quad (8)$$

where $D_{0,1,2}$ – coefficient of mutual diffusion of substances at N at. ($P_0 = 101.3$ kPa, $T_0 = 273$ K).

Calculations have shown that process of burning proceeds in intermediate area according to the scheme of the double burning interface ($Se > 100$), (case of “wet” gasification), [20].

Expression for flow of the carbon which is burning out from surface of particles, ($\text{kmol/m}^2 \cdot \text{s}$) of is received was result of the solution of system (2):

$$G_c = \frac{\alpha_D}{RT} \left[\frac{N_3}{1 + N_3} p_{CO_2\Delta} + \frac{N_{3'}}{1 + N_{3'}} (p_{O_2\Delta} + 0.5 p_{H_2O\Delta}) + \frac{N_5}{1 + N_5} p_{NO\Delta} \right], \quad (9)$$

and at the same time to calculate decrease of weight and size of particle on expressions:

$$\begin{aligned} \frac{dm}{d\tau} &= \frac{dm_w}{d\tau} + \frac{dm_{let}}{d\tau} + \frac{dm_c}{d\tau}, \quad \text{kg/s}; \quad \frac{dm_c}{d\tau} = -G_c \cdot M_C \cdot \pi \cdot \delta^2, \quad \text{kg}/(\text{m}^2 \cdot \text{s}); \quad \frac{d\delta}{d\tau} \\ &= -\frac{2M_C}{\rho_C} \cdot G_c, \quad \text{m/s}, \end{aligned} \quad (10)$$

where $M_C = 12$ kg/kmol – the molar mass of carbon; $m = \pi/6 \cdot \delta^3 \text{ eq} \cdot \rho_C$ – mass of spherical particle; $f = \pi/6 \cdot \delta^2 \text{ eq}$ – the external surface area, m².

Distribution of concentrations of NO on the furnace section (concentrations field) in the known field of gas flow velocity, was defined by the numerical solution (scheme “against flow”) of the differential equation of mass exchange in the presence of the source (NO generation zone):

$$\frac{\partial}{\partial \tau} (\rho \cdot C_{NO}) + \nabla \cdot (\rho \vec{w} C_{NO}) = \rho D_{NO} \nabla^2 C_{NO} + J_{NO}, \quad (11)$$

where C_{NO} – mass concentration of nitrogen oxides; w – gas flow velocity; D_{NO} – average effective coefficient of diffusion of NO in the mixture of furnace gases; J_{NO} – intensity of nitrogen oxides generation (NO source output).

Power of source of J_{NO} is defined in the assumption of fuel nitrogen oxides generation ($T_{max} < 1600$ K) occurring at the volatile output stage and is solved from the solution of following equations system:

$$J_{NO} = \begin{cases} dN_{2i}/d\tau_i = k_{01} \exp[-E_1/(RT_i)][N_i]^2 \\ dNO_{xi}/d\tau_i = k_{02} \exp[-E_2/(RT_i)](1/T_i)[O_2]_i^{1.8}[N_i] \end{cases}, \quad (12)$$

where $[N]_i$ – concentration of atomic nitrogen.

The amount of the nitrogen oxides which have decayed is designed for surfaces of the burning carbon particles from balance of reaction:



Distribution of concentration of SO_2 on the fire chamber section (the field of concentration) at the known speeds of gas flow, was defined by the numerical solution of the differential equation of mass exchange:

$$\frac{\partial}{\partial \tau} (\rho \cdot C_{SO_2}) + \nabla \cdot (\rho \vec{w} C_{SO_2}) = \rho D_{SO_2} \nabla^2 C_{SO_2} + J_{SO_2}, \quad (14)$$

where C_{SO_2} – mass concentration of sulfur oxides; D_{SO_2} – average effective coefficient of diffusion of SO_2 in mix of furnace gases) in the presence of the source member (zone of generation of SO_2) which is written down in look:

$$J_{SO_2} = dG_{SO_2}/d\tau = (G_C \cdot S^{daf}) / (V \cdot 100), \quad (15)$$

where J_{SO_2} – power of source of SO_2 , kg/m^3c ; G_C – speed of burning out of carbon of coke, kg/s ; S^{daf} – sulfur content in the dry ashless mass of fuel, %; V – volume of settlement cell, m^3 .

The amount of the sulfur oxides which have reacted with fuel ashes CaO was calculated on reaction:



For the solution of problem of binding of sulfur oxides with fuel ashes CaO, the polydisperse particle system of ashes breaks into fractions on fineness; within each fraction the quantity (with CaO share in fuel sol) particles of CaO of average radius of R_i which does not change in the course of sulfurization is defined. In each timepoint the quantity of SO_2 in gas (mol/cm^3), is from the known field of concentration of sulfur oxides. For each fraction i ($i = 1, 2, \dots, n$) the system of the equations for concentration of SO_2 in particle of C_i and radius of not reacted CaO kernel in r_i grain decides (G.D. Silcox, D.M. Slaughter, D.W. Pershing):

$$\begin{cases} \left(\frac{d^2 C_i}{dR^2} + \left(\frac{2}{R} + \frac{d \cdot \ln D_{\text{eff},i}}{dR} \right) \cdot \frac{dC_i}{dR} = A_i \frac{k_{\text{eff},i}}{D_{\text{eff},i}} \right. \\ \left. \frac{dR_i}{d\tau} = - \left(\frac{M_{\text{CaO}}}{\rho_{\text{CaO}}} \right) \cdot k_{\text{eff},i} \right. \end{cases} \quad (17)$$

where C_i – concentration of SO_2 in particle of fraction i ; $D_{\text{eff}, i}$ – effective coefficient of diffusion of SO_2 in particle of fraction i ; A_i – the surface of reaction carried to the volume of porous particle; $k_{\text{eff},i}$ – effective constant of speed of reaction; M_{CaO} and ρ_{CaO} – the molecular weight and density of CaO .

Boundary conditions of system (18):

$$dC_i/dR = 0, R = 0; C_i = C_0(\tau), R = R_i; r_i = r_{\text{grain}}, \tau = 0 \quad (18)$$

where $C_0(\tau)$ – concentration of SO_2 in gas; R_i – the radius of particles of lime of fraction i ; r_i – the radius of not reacted CaO kernel in grain; r_{grain} – the initial radius of grains.


By the developed technique the algorithm and the program of calculation is made, its debugging and testing on the experimental data on LTS to burning, and also with use of the results received by other authors are made.

References

1. Hodakov, Yu.S.: Nitrogen Oxides and Heat-and-power Engineering: Problems and Decision. LLC EST-M Publishing house, Moscow, p. 428 (2001)
2. Shulman, V.L.: Thermal Power Plants in the Environment of the Modern World. Socrates Publishing house, Yekaterinburg, p. 376 (2010)
3. Salamov, A.A.: J. Heat-and-power Eng. **2**, 76–80 (2002)
4. Solomatov, B.B.: Nature Protection Technologies on the Thermal and Nuclear Power Plants. NGTU Publishing house, Novosibirsk, p. 852 (2006)
5. Abramov, A.I., Yelizarov, D.P., Remezov, A.N.: Increase in Ecological Safety of Thermal Power Plants. MEI Publishing house, Moscow, p. 378 (2001)
6. Kotler, V.R.: J. Heat-and-power Eng. **12**, 69–71 (2005)
7. Ezhov, V.S.: J. Ind. Power **12**, 44–47 (2006)
8. Boyadjiev, C.B.: J. Heat-power Eng. **9**, 76–80 (2014)
9. Putilov, V.Y.: Ecology of Power Engineering. MEI Publishing house, Moscow, p. 716 (2003)
10. Zhikhar, G.I.: Boiler Installations of Thermal Power Plants. Vysheyshaya school, Minsk, p. 532 (2015)
11. Rundygin, Yu.A., Grigoriev, K.A., Skuditsky, V.E., Shestakov, S.M.: Victor Vladimirovich Pomerantsev. To the 100 Anniversary Since Birth, Publishing house Politekhn, Saint Petersburg, pp. 133–149 (2006)
12. Grigoriev, K.A., Rundygin, Yu.A., Skuditsky, V.E., Trinchenko A.A.: Formation of the technical policy of innovative high technology. In: Materials Science-practice Conference and Workshop Schools, Publishing house Politekhn, Saint Petersburg, pp. 216–222 (2003)
13. Grigoriev, K.A., Rundygin, Yu.A., Skuditsky, V.E., Trinchenko, A.A.: Sat. Doc. Thematic Seminar “Ecology in Power Engineering–2004”, Publishing house of the All-Russia Exhibition Centre, Moscow, pp. 108–109 (2004)

14. Grigoriev, K.A., Rundygin, Yu.A., Skuditsky, V.E., Trinchenko, A.A.: Sat. Doc. IV International Scientific-technical Conference "Achievements and prospects for the development of Siberia's energy industry", Publishing house of SIBVTI, Krasnoyarsk, pp. 144–147 (2005)
15. Grigoriev, K.A., Rundygin, Yu.A., Skuditsky, V.E., Trinchenko, A.A.: Increasing the efficiency of production and use of energy in the far east. In: Proceedings of the 4th Seminar of the Higher Schools of Siberia and the Far East on Thermal Physics and Heat Power Engineering, DVG TU Publishing house, Vladivostok, pp. 83–89 (2006)
16. Trinchenko, A.A.: Mat. of the Day of the Young Scientist at the Polytechnic University. Publishing house Politekhn, Saint Petersburg, pp. 17–18 (2007)
17. Grigoriev, K.A., Skuditsky, V.E., Rundygin, Yu.A., Trinchenko, A.A.: Swirling-type furnace Patent of 2253801 Russia. Publ. 10.06.2005. Bulletin No. 16
18. Grigoriev, K.A., Skuditsky, V.E., Rundygin, Yu.A., Trinchenko, A.A.: Swirling-type furnace Eurasian Patent of 008691. Publ. 29.06.2007. Bulletin No. 3
19. Grigoriev, K.A., Skuditsky, V.E., Rundygin, Yu.A., Trinchenko, A.A.: Swirling-type furnace Patent of 83761 Ukraine. Publ. 11.08.2008. Bulletin No. 15
20. Trinchenko, A.A., Shestakov, S.M.: J. Sci. Tech. Sheets SPbSTU **54**, 149–156 (2008)
21. Grigoriev, K.A., Rundygin, Yu.,A., Skuditsky, V.E., Anoshin, R.G., Paramonov, A.P., Trinchenko, A.A.: Proceedings of the 7th International Symposium Coal Combustion. University Press Beijing, Tsinghua and Springer, Heidelberg, pp. 662–665 (2012)
22. Trinchenko, A.A., Paramonov, A.P.: J. Sci. Tech. Sheets SPbSTU **231**, 72–81 (2015)
23. Trinchenko, A.A.: J. Sci. Tech. Sheets SPbSTU **207**, 61–70 (2004)

Low-Temperature Swirl Burning as Technological Method of Simultaneous Decrease in Emissions of Nitrogen and Sulfur Oxides (Part 2. Results of Modeling, Their Practical Implementation and Analysis)

Aleksey Trinchenko^(✉)  and Aleksandr Paramonov 

Peter the Great St. Petersburg Polytechnic University,
Polytechnicheskaya, 29, St. Petersburg 195251, Russia
trinchenko@spbstu.ru

Abstract. The results of energy efficiency increase reached due to implementation of low-temperature swirl technology on boiler of BKZ-220 of the Novomoskovsk state district power plant are given in the work. With use of the developed model numerical researches of generation and transformation during burning fuel of gaseous nitrogen oxides are conducted and assessment of their concentration in combustion gases of the reconstructed boiler is gray, executed. Results of reconstruction and the analysis of the obtained experimental data have confirmed advantages of low-temperature swirl burning when using low-grade high-ash fuels.

Keywords: Boiler plant · Emissions of pollutants · Nitrogen oxide

1 Results

The brown coals of the pool situated near Moscow arriving to the Novomoskovsk state district power plant have humidity of $W_t^r = 30...40\%$ and ash content of $A^d = 35.0...40.0\%$. Content in fuel of S^r sulfur changes within $1.6...2.3\%$. Range of change of heat of combustion (Q_t^r) makes $1716...2089$ kcal/kg [1]. At combustion of powdered fuel of rather high milling ($R_{90} < 40...50\%$, $R_{1000} < 1.0\%$) in the conditions of direct-flow torch, the maximum temperature in fire chamber reaches $1350...1370$ °C that causes intensive slagging of surfaces of heating of fire chamber. Problems of operation of boilers are complicated by the high level of emissions: nitrogen oxides (in view of high temperature of torch) and sulfur oxides, because of the raised sulfur content ($\sim 2\%$) in coal situated near Moscow.

Calculations of process of burning to fire chamber are carried out to LTS in relation to the boiler of BKZ-220-9,8 station No. 15 of the Novomoskovsk state district power plant planned for modernization for LTS technology of combustion [2–8] of brown coal [9, 10] situated near Moscow.

The characteristics of fuel accepted for calculations are provided in Table 1, characteristics of ashes of fuel are provided in Table 2.

Table 1. Characteristics of brown coal situated near Moscow of the B2R brand

Elementary composition of fuel on working weight	Symbol	Dimension	Value
Moisture	W^r	%	28.9
Ashes	A^r	%	34.6
Sulfur (pyritic + organic)	S^r	%	1.9 (1.1 + 0.8)
Carbon	C^r	%	23.3
Hydrogen	H^r	%	2.0
Nitrogen	N^r	%	0.4
Oxygen	O^r	%	8.9
The lowest heat of combustion	Q_i^r	kcal/kg	1997
		kJ/kg	8361

Table 2. Characteristics of ashes of brown coal situated near Moscow of the B2R brand

<i>Composition of ashes on sulfate-free weight, %</i>							
SiO ₂	Al ₂ O ₃	TiO ₂	Fe ₂ O ₃	CaO	MgO	K ₂ O	Na ₂ O
47.5	38.5	0.5	8.5	3.5	0.5	0.7	0.3
<i>Ash fusibility characteristics</i>							
Name of the indicator	Symbol	Dimension	Value				
Deformation start temperature	t_A	°C	1350				
Softening start temperature	t_B	°C	1500				
Temperature of the liquid state onset	t_C	°C	1500				
Slagging start temperature	$t_{sl.st}$	°C	1090				

The consumption of the natural solid fuel with polyfractional structure given to the furnace camera was recalculated for equivalent expense of spherical particles [11]. The sieving curve broke into $N = 10$ fractions, each of which is characterized by the average diameter.

The sizes of fuel particles, their number on 1 kg of settlement fuel, weight within each fraction and the area of initial surface of reaction, were by processing of sieving curve of initial fuel. Particle distribution of initial dust by the sizes (Fig. 1) was described by dependence Rozin-Rammler-Bennet:

$$R_{0i} = \exp(-b\delta_{0i}^n), \quad (1)$$

where b and n – the pilot coefficients characterizing respectively subtlety of grinding and uniformity of grain structure.

For this purpose the sieving curve broke into 10 fractions, each of which was characterized by the average diameter:

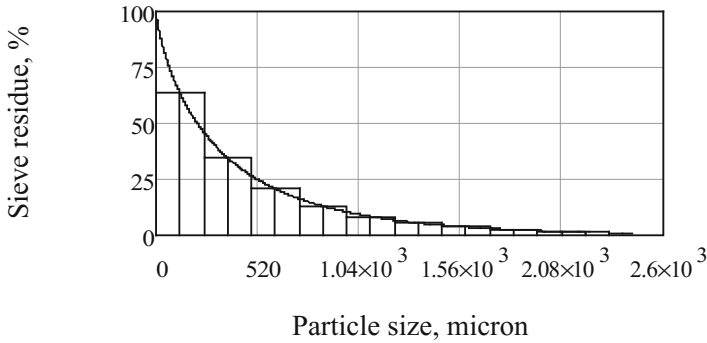


Fig. 1. Processing of sieving curve of brown coal situated near Moscow of the B2R brand: $W^r = 12\%$, $A^r = 13.2\%$, $R_{90} = 70\%$, $R_{1000} = 10\%$.

$$\delta_i = 0.5 \cdot (d_i + d_{i+1}), \quad (2)$$

where: δ_i – average diameter of particle i -th fractions, m; d_i, d_{i+1} – the maximum and minimum particle size i -th fractions, m.

Giving frequency i -th fractions (piece/c) was defined as:

$$n_i = \frac{6}{\pi} \cdot \frac{B}{\rho_{\text{coal}} \cdot \delta_i^3} \cdot \frac{R_i - R_{i-1}}{100} \quad (3)$$

where B - fuel consumption, kg/s; R_i, R_{i+1} - full remains on sets with sizes of cells d_i and d_{i+1} , %.

For burning in boiler of BKZ-220-9.8 fuel of coarsen grind with particle size distribution of $R_{90} = 70\%$, $R_{1000} = 10\%$, which polydispersion indicator determined by dependence is supposed:

$$n = \frac{\lg[\ln(100/R_{90})] - \lg[\ln(100/R_{1000})]}{\lg(90/1000)} \quad (4)$$

makes 0.775, and the size of the most coarsened particle determined from ratio:

$$\delta_{01} = (m/b)^{1/n} \quad (5)$$

makes $\delta_{01} = 2150$ microns.

Temperatures in the furnace camera received by zonal thermal calculation (Fig. 2 (a)) do not exceed 1800 K that indicates lack of formation of “thermal” nitrogen oxides.

Settlement fields of concentration of nitrogen oxides and sulfur oxides were from the solution of the differential equations of their generation for each of elementary cells of irregular curvilinear grid (Fig. 2(b)). Generation of pollutants in elementary cells of fire chamber (source members), was defined by summing of number of NO and SO₂ allocated in these cells during stay in them of the reacting particles.

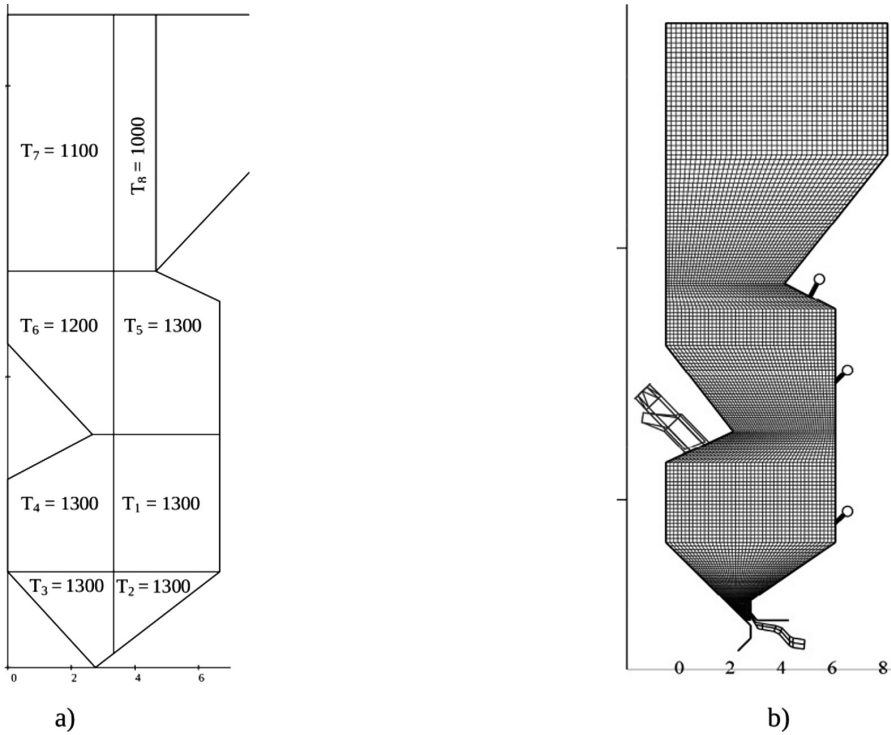


Fig. 2. (a) – Temperatures in zones of LTS-furnace of boiler BKZ-220-9,8, C°; (b) – elementary cells in LTS fire chamber of boiler of BKZ-220-9,8

For the solution of problem of modeling of LTS-furnace process in boiler fire chamber BKZ-220 has applied concepts of “the given film” ($\Delta/\delta = 1/(\text{Nu}_D - 2)$); dimensionless coordinate ($\xi = x/\Delta$); Semenov’s criterion ($\text{Se} = (k_4 \cdot \Delta/D)^{0.5}$); diffusion and chemical criterion ($N_i = k_i/\alpha_D$); Arrhenius’s dependences for constants of speeds of reactions ($k_i = k_{0i} \cdot \exp(-E_i/RT)$); “poles” with coordinates of $k^* = 100 \text{ m/c}$, $T^* = 2600 \text{ K}$; energy of activation. At the same time the following assumptions are made: 1. The Stefanovsky flow has no significant effect on thickness of the given film; 2. The given film is considered as flat; 3. Thermal diffusion on thickness of the given film is absent; 4. Speed of homogeneous reactions and coefficient of diffusion are calculated on the average temperature of the given film; 5. For diffusion in multi-component gas mixture the average coefficient of diffusion is accepted; 6. Temperature of particle is accepted to the equal temperature of flow.

Calculations of trajectories of the movement of the reacting particles were made by the numerical solution of the equation of the movement which is written down in projections to axes of the Cartesian system of coordinates which considers action on particle of two main forces on particle – gravity and forces of aerodynamic resistance:

$$\begin{cases} m \frac{dV_x}{d\tau} = \frac{cf\rho}{2} (W_x - V_x) \left[(W_x - V_x)^2 + (W_y - V_y)^2 + (W_z - V_z)^2 \right]^{1/2} \\ m \frac{dV_y}{d\tau} = \frac{cf\rho}{2} (W_y - V_y) \left[(W_x - V_x)^2 + (W_y - V_y)^2 + (W_z - V_z)^2 \right]^{1/2} \\ m \frac{dV_z}{d\tau} = \frac{cf\rho}{2} (W_z - V_z) \left[(W_x - V_x)^2 + (W_y - V_y)^2 + (W_z - V_z)^2 \right]^{1/2} - mg \end{cases}, \quad (6)$$

where V and W – particle velocity and gas flow; m, f – respectively a weight and the area of middle section of particle; ρ – density of gas flow; $c = f(\text{Re})$ – coefficient of resistance of the burning particles.

Speeds of air-gas flows for the solution of the equation of the movement were in the nodal points shown in Fig. 3 and. The received settlement aerodynamic picture of currents (Fig. 3) was used for finding of trajectories of the movement (the solution of system 5) and calculations of burning out of the reacting fuel particles (Fig. 4) with simultaneous definition of the resulting concentration of the nitrogen oxides formed in the course of burning and decaying on the surface of the burning carbon in the course of repeated circulation in the lower swirl zone of LTS of fire chamber.

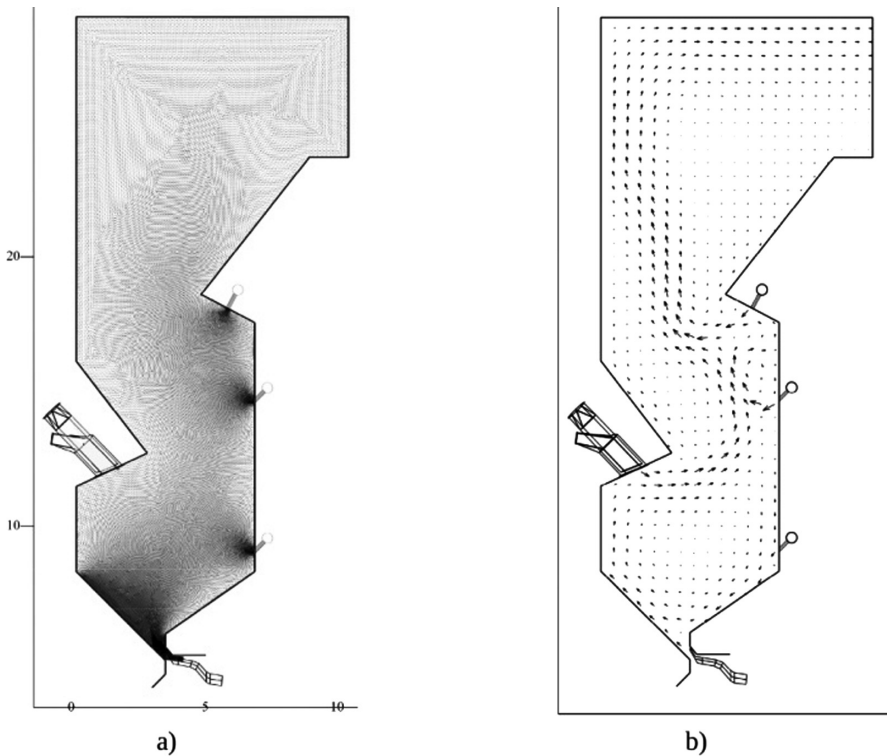


Fig. 3. (a) – Nodal points for definition of vectors of speed of gas-air flows in BKZ-220 boiler LTS fire chamber; (b) – vectors of speed of gas-air flows

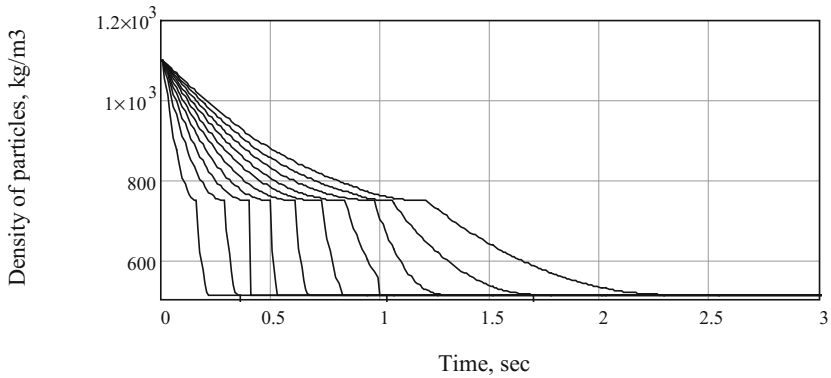


Fig. 4. Change of particle density in the course of drying and exit of flying

Time of warming up of particles until ignition flying ($\tau_{v.l.}$) in the environment $O_2 = 10...21\%$ and temperature of gas flow of $T_g = 1173...1373$ K were calculated with concentration on empirical dependence:

$$\tau_{v.l.} = k_{v.l.} \cdot 10^{13} \cdot T_g^{n_{v.l.}} \cdot \delta^{m_{v.l.}} \cdot \left(1 + w_{rel}^{\bar{n}_{v.l.}}\right), \text{ c,} \tag{7}$$

and time of visible burning flying ($\tau_{g.l.}$) on dependence:

$$\tau_{g.l.} = k_{g.l.} \cdot 10^8 \cdot T_g^{n_{g.l.}} \cdot \delta^{m_{g.l.}} \cdot \left(1 + w_{rel}^{\bar{n}_{g.l.}}\right), \text{ c,} \tag{8}$$

where w_{rel} – particle flow speed flow, in m/s; $k_{v.l.}$, $n_{v.l.}$, $m_{v.l.}$, $c_{v.l.}$, $k_{g.l.}$, $n_{g.l.}$, $m_{g.l.}$, $c_{g.l.}$ – experimental coefficients.

Results of calculation for dependences (6) and (7) changes of particle density of the different sizes, are given in Fig. 4 where two characteristic time intervals are visible: drying of fuel particles and exit and burning of volatiles of fuel.

Reduction of particle size of fuel in the course of burning out is shown in Fig. 5.

In general for particles with sizes of $\delta = 3.1 \cdot 10^{-5}...2.15 \cdot 10^{-3}$ m it makes from 0.35 to 45 s.

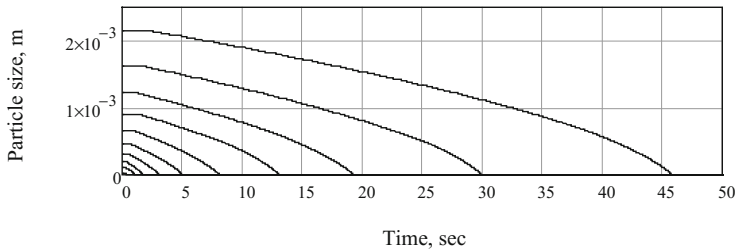


Fig. 5. Change of particle size in the course of burning out

At the same time fine particles burn out practically at once in direct-flow part of torch (Fig. 6a), and coarse particles during burning do several turns in the lower swirl zone (Fig. 6b).

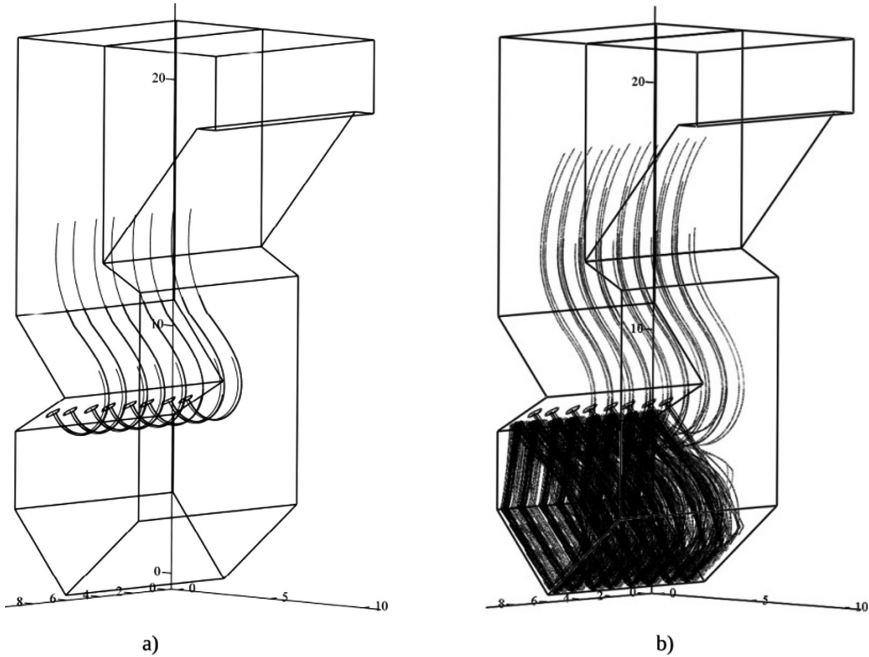


Fig. 6. Separation of the reacting fuel particles and their burning out in LTS fire chamber: (a) – fine particles ($\delta = 3.1 \cdot 10^{-5} \dots 4.56 \cdot 10^{-4}$ m); (b) – coarse particles ($\delta = 6.52 \cdot 10^{-4} \dots 2.15 \cdot 10^{-3}$ m)

2 Discussion

Reaction of the formed nitrogen oxides with carbon of coke leads to decrease in their concentration in fire chamber and to reduction of their content in the leaving gases of boiler [12]. The settlement field of concentration of nitrogen oxides taking into account their decomposition on coke particles is shown in Fig. 7. To exit average concentration of nitrogen oxides in combustion gases of fire chamber makes 180...240 mg/nm³ that is 30% lower, than at similar boilers of NGRES with direct-flow coal-dust torch.

Intensive generation of sulfur oxides happens in the lower swirl zone of fire chamber at burning out of bulk of carbon of coke. Reaction of SO₂ with fuel ashes CaO in LSZ LTS-furnace leads to decrease in concentration of sulfur oxides in the leaving gases of boiler [13, 14].

The average size of the reacting particles of CaO decides on use of dependence (1) for what the sieving characteristic of ashes ($R_{90} = 35\%$, $R_{200} = 20\%$) breaks into 10 intervals, within each of which (taking into account CaO share in fuel sol) are: quantity

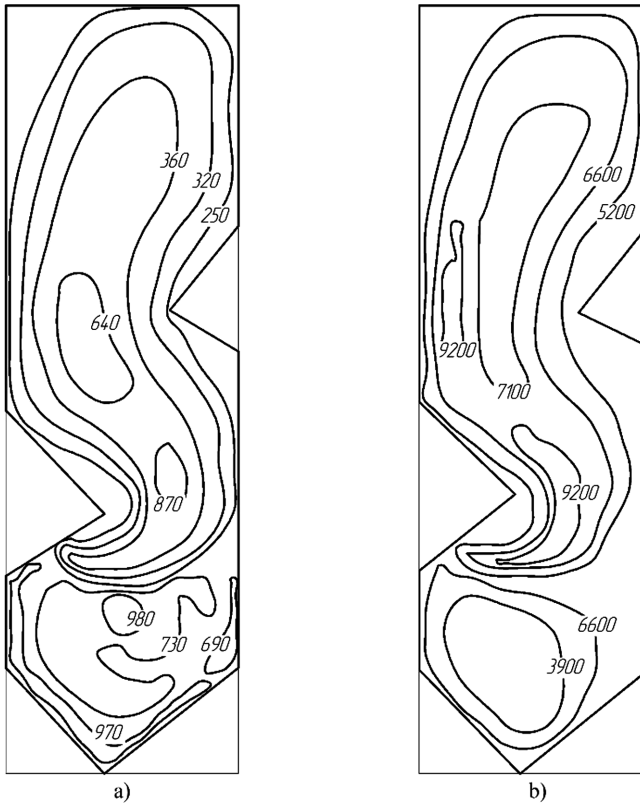


Fig. 7. The settlement field of concentration of nitrogen oxides (a) taking into account decomposition of NO on coke particles and sulfur oxides (b) taking into account reaction with fuel ashes CaO in BKZ-220 boiler LTS fire chamber

of the reacting particles, their average size, volume, weight and the area of the reacting surface taking into account porous structure of material.

Fine particles having made one turn in the lower swirl zone are taken out in direct-flow part of torch and leave fire chamber, and coarse particles of ashes during stay in LSZ LTS-furnace manage to make from 2 to 7...10 turns. The average settlement field of concentration of sulfur oxides (taking into account their reaction with fuel ashes CaO) in LTS fire chamber of boiler of BKZ-220 is shown in Fig. 7. Reaction of SO₂ with CaO of ashes of fuel reduces concentration of sulfur oxides in the leaving boiler gases by ~35% in comparison with the generation of sulfur oxides received from balance of reaction of burning of sulfur on condition of its full combustion.

Thus, is confirmed by results of settlement researches that at reconstruction of boiler of BKZ-220 of the Novomoskovsk state district power plant on low-temperature swirl technology, at combustion of brown coals situated near Moscow it is necessary to expect decrease in emissions of nitrogen oxides (on 25... 30%) and sulfur oxides (on 30... 40%) in comparison with traditional coal-dust burning.

3 Conclusions

Reconstruction of boiler of E-220-9,8 of the Novomoskovsk state district power plant is carried out during its capital repairs; commissioning [15] is carried out in two steps [16].

During the first stage, testing of boiler were carried out on loadings from 100 to 172 t/h during the work on coal (with characteristics on working weight: $W_t^r = 26.8...30.7\%$, $A^r = 36.4...39.4\%$, $Q_i^r = 6.8...8.8$ MJ/kg (1600...2100 kcal/kg)). The consumption of coal varied within 30...70 t/h, and the particle size distribution of the ground fuel corresponded to calculated values (Fig. 1) and changed in the range: $R_{90} = 70...90\%$; $R_{1000} = 7...21\%$. The second stage of commissioning was carried out at combustion of coal situated near Moscow with characteristics: $W_t^r = 22...30\%$, $A^r = 35...41\%$, $Q_i^r = 6.79...7.12$ MJ/kg (1620...1700 kcal/kg) and natural gas with the lowest specific heat of combustion of $Q_i^r = 33.58$ MJ/nm³ (8014 kcal/nm³).

The main results of reconstruction checked during commissioning and regime and adjustment tests was the following:

1. The boiler steadily, in the absence of slagging, burns brown coal situated near Moscow without torch illumination in the range of loadings of $D = (0.57...1.0) \cdot D_n$ with ensuring temperature of overheat in required limits (785 ± 5) K. The slag-free power of boiler has increased from $0.73 \cdot D_n$ to nominal.
2. The efficiency (gross) of boiler has increased on 2...4% to level $\eta_k = 89...91\%$, (at q_4 values = 1...1.5% are lower than normative).
3. Concentration of nitrogen oxides in the leaving gases (brought to normal conditions and $\alpha = 1.4$ (content of oxygen of 6%) during the work on coal have made 200...250 mg/nm³, and carbon oxide – no more than 150 mg/nm³ that satisfies to modern standards. Extent of binding of sulfur oxides in boiler at the expense of the main oxides of own ashes of fuel reaches 40...45%.

Thus, implementation of LTS technology has allowed to provide effective high-economic combustion of brown coal situated near Moscow with complete elimination of slagging, to increase efficiency of boiler, to improve ecological [17] and economic indicators of its work.

References

1. Thermal calculation of boilers (normative method), p. 432. Publishing house NPO CKTI, Saint Petersburg (1998)
2. Anoshin, R.G., Grigoriev, K.A., Mikhaylov, D.N.: Burning of solid fuel: saturday. In: Reports of VI Conference Novosibirsk, Publishing House of Institute of Thermophysics of the Siberian Branch of the Russian Academy of Science, pp. 128–135 (2006)
3. Grigoriev, K.A., Rundygina, Y.A., Skuditsky, V.E., Trichenko, A.A.: Increasing the efficiency of production and use of energy in the far east. In: Proceedings of the IV Seminar of the Universities of Siberia and the Far East on Thermal Physics and Thermal Power, pp. 83–89, VTI Publishing house. Novosibirsk (2006)

4. Grigoriev, K.A., Rundygin, Y.A., Skuditsky, V.E., Trinchenko, A.A.: Sat. Doc. IV Int. Scientific-technical. In: Conference on "Achievements and Prospects for the Development of Siberia's Energy Industry", pp. 144–147 (2005)
5. Trinchenko, A.A.: Mat. of the Day of the Young scientist at the Polytechnic University, pp. 17–18 (2007)
6. Grigoriev, K.A., Skuditsky, V.E., Rundygin, Y.A., Trinchenko, A.A.: Swirling-type furnace. Patent of 2253801 Russia, Publ. 10.06.2005, Bulletin No. 16 (2005)
7. Grigoriev, K.A., Skuditsky, V.E., Rundygin, Y.A., Trinchenko, A.A.: Swirling-type furnace. Eurasian patent of 008691, Publ. 29.06.2007, Bulletin No. 3 (2007)
8. Grigoriev, K.A., Skuditsky, V.E., Rundygin, Y.A., Trinchenko, A.A.: Swirling-type furnace. Patent of 83761 Ukraine, Publ. 11.08.2008, Bulletin No. 15 (2008)
9. Rundygin, Y.A., Grigoriev, K.A., Skuditsky, V.E., Shestakov, S.M.: Victor Vladimirovich Pomerantsev, pp. 133–149. Publishing house Politekhn, Saint Petersburg (2006). To the 100 anniversary since birth
10. Trinchenko, A.A., Shestakov, S.M.: J. Sci. Tech. Sheets SPbSTU **54**, 149–156 (2008)
11. Trinchenko, A.A.: J. Sci. Tech. Sheets SPbSTU **207**, 61–70 (2014)
12. Trinchenko, A.A., Paramonov, A.P.: J. Sci. Tech. Sheets SPbSTU **231**, 72–81 (2015)
13. Grigoriev, K.A., Rundygin, Y.A., Skuditsky, V.E., Trinchenko, A.A.: Formation of the technical policy of innovative high technology. In: Mat. Sci.-Pract. Conf. and Workshop Schools, pp. 216–222. Publishing house Politekhn, Saint Petersburg (2003)
14. Grigoriev, K.A., Rundygin, Y.A., Skuditsky, V.E., Trinchenko, A.A.: Sat. Doc. Thematic Seminar "Ecology in Power Engineering–2004", pp. 108–109. Publishing house of the All-Russia Exhibition Centre, Moscow (2004)
15. RD 153-34.1-26.303-98: Methodical instructions for conducting operational tests of boiler plants, p. 36. IPK Publishing house, Moscow (1998)
16. Rundygin, Y.A., Grigoriev, K.A., Skuditsky, V.E.: Mat. National. Conf. on NKTE-2006 Heat-and-Power Engineering, pp. 160–162. Publishing House Issl. Center of Problems Energy KASNZ RAHN, Kazan (2006)
17. GOST P 50831-95 Boiler plants. Heatmechanical equipment. General technical requirements, p. 23. IPK Publishing house, Moscow

Problems of Magnesium Oxide Wallboard Usage in Construction

Marina Gravit¹(✉) , Olga Zybina¹ , Artem Vaitickii¹ ,
and Anna Kopytova² 

¹ Peter the Great St. Petersburg Polytechnic University,
Politekhnicheskaya st., 29, 195251 St. Petersburg, Russia
marina.gravit@mail.ru

² Industrial University of Tyumen,
Volodarskogo str., 38, 625001 Tyumen, Russia

Abstract. Magnesium oxide wallboard is the building and finishing material, which has a reputation of new generational ecological constructing material. It has a wide range of uses: as a revetment in ventilated facades' production, as a decorative material, as different types of formworks for a foundation filling and as a protector against a fire threat. During the study it was considered that magnesium oxide wallboards have some defects, such as moisture formation as a concentrated brine on the surface under special climatic conditions and absence of clear distinguishing between different types of magnesia boards. Usage of this material can become a cause of frame's corrosion and origin of mold on wooden details. Authors provide the information from a foreign data source about negative consequences of SML usage. In conclusion researchers state that it is necessary to provide a clear magnesium wallboards classification and define technical requirements, which will, in their opinion, lead to Russian standard formulation.

Keywords: Magnesium oxide wallboard · Decorative material
Transport buildings and structures

1 Introduction

Portland cement, the most common binder that is used in construction, has several substantial drawbacks, for example, necessity to spend 1 t of HRC to produce to 300 kg of fossil fuels (in this process exudes to 0.8 tons of CO and CO₂ – the root cause of the greenhouse effect). Therefore, people are searching the alternatives for this material, and one of them is magnesia binder. In its simplest form, it is a binder consisting of caustic magnesium oxide and magnesium salts aqueous solution, preferably chloride or sulfate.

Magnesium oxide wallboard is sheet construction and designing material based on magnesia binder. It consists of caustic magnesite, magnesium chloride, expanded perlite and glass fiber as a reinforcing material. Magnesia binder also named Sorel cement is based on magnesium oxide offered by the French engineer C. Sorel in 1866 [1–5]. Magnesium oxide wallboard are mainly used as a construction substrate in the

manufacture of building facades both in new construction and in repair of already constructed objects. Also in some cases, magnesium sheets are used as facade materials or rain screen. Sometimes magnesium sheets can serve as a foundation for plaster application. The magnesia boards almost are not produced in Russia. The bulk of manufacturers are located in China, South Korea [6].

One of the most significant disadvantages of this compound is low water resistance of articles, turn to cause corrosion in franked steel constructions. All these factors lead to formation of mold on wooden constructions, made on its basis [7, 8]. Exists variety of investigations oriented to lowering of negative features of glass magnesium sheets exploitable in high humidity conditions [9–12].

In research [9], the authors suggest to increase the water resistance of products made of CF, with adding to them minerals such as wollastonite, diopside, and zeolite in a form of powder. At the same time, it increases the strength and decreases the magnitude of shrinkage during solidification. The addition of wollastonite in an amount of 60–80 fraction of total mass leads to an increase in strength in high humidity (over 95%). In addition, a diopside can be used to increase the water resistance.

In the research [10] investigated the possibility of increasing the water resistance of the CA product by introducing dunite and serpentinite. A study [11] describes the possibility of reducing the cases of the appearance of efflorescence on the surface of products by adding a part of the binder diabase. The author of the research [12] proposes to use the crystalline hemihydrate of calcium sulfate (plaster of the brand G-5AP), which allows to reduce water consumption and lengthen the timing of setting the mixed binder.

2 Results and Discussion

Typical chemical composition of magnesium sheets studied in the work [8]. In studies of the Danish Institute stated [7, 8]:

- the content of magnesium chloride salt (MgCl_2) leads to the absorption of moisture;
- after about 7 days exudation of moisture is observed on the surface of the sheet (at 90% relative humidity);
- eventually binding substances, that are used in sheets construction for their connection, decompose with relative humidity increasing;
- magnesite sheets cause corrosion on adjoining non-stainless metal parts of structures;
- magnesium sheets lead to the fact that the adjoining wooden parts begin to absorb moisture more intensively than ordinary wood, so they may cause the spread of mold.

Negative moisture-absorbing features of magnesium sheets are associated with the fact that they contain free magnesium chloride (MgCl_2), which is very hygroscopic. Furthermore, Sorel cement is unstable at a relative humidity of 93%. The presence of salt in the sheets leads to the fact that they begin to absorb moisture from the air when the relative humidity in environment reaches a certain level (Fig. 1).



Fig. 1. The formation of traces of moisture on the surface.

Theoretically, magnesium chloride already begins to absorb moisture at a relative humidity of 33%, but in practice, the panels begin to absorb moisture in a large amount at a high humidity.

In the technical literature clearly indicates that Sorel cement (magnesia binder) is not a moisture resistant at a high humidity [13–15]. In 1947 has been found that the level of relative humidity of 93% is its critical limit. Materials on this subject were published in 2011 [16].

In Denmark were done few experiments wherein magnesium sheets were placed in an environment with a relative humidity of 93% [7, 8]. Sheets absorb moisture from the air in considerable quantities and absorption process was observed within one month or more. Another important effect which can be stated as a result of the experiments is that on the surface of a sheet between the 7th to the 14th day with a relative humidity of 93% were formed water drops. The Danish Technical University conducted a series of samples for moisture, and these tests fully confirmed the results of initial experiments. Experiments were also carried out at a humidity of 85% - they have shown the similar results.

In experiments at a relative humidity of 95% magnesite binders and sheets decompose the material loses its cohesive force. Salts transferred from the sheet into the timber when magnesite sheets come into direct contact with a wood. Since, as mentioned, contain high amounts of magnesium chloride, which in turn leads to increased moisture absorption wood [17]. This phenomenon has long been known in China and called the «crying boards», and there are special building materials brand «anti-crying boards». It is found that the mold can develop on magnesite sheets themselves, that including, caused by a relatively high content of wood fiber sheets (Figs. 2 and 3).

When magnesium sheets emit moisture, it absorbs by surrounding parts of the wood. That leads to its putrefaction and further damage. This applies to both: to remote sheets for covering the facades and to located underneath wooden core.

The liquid, which collects in the magnesite sheets and penetrates into their surface when they “cry” – is water with a high content of magnesium chloride. This fluid is very corrosive and causes corrosion on fasteners and metal plating (Fig. 4), which come in contact with the sheets [18].



Fig. 2. Dew drops on the wooden structures.



Fig. 3. Dew drops on the wooden structures.



Fig. 4. Formation of the metal structure corrosion.

In some product passports for magnesite sheets it is indicated that they have a sufficiently high pH – about 10.

Typically, the pH of 10 is considered as sufficient protection against mold.

Measurements made on magnesium sheets, however, have shown that they have a much lower pH, usually 7–8, and, accordingly, cannot be protected from the mold formation. This value also eventually decreases due to the fact that the sheets absorb carbon dioxide from the air. Magnesium sheets partially dry in summer, when the

relative humidity slightly reduces. Magnesium sheets can create the risk of corrosion of steel skeleton that is located beneath the sheets and consists in thin galvanized sheets [18]. In the long term, it will lead to the fact that the screws that hold the cover will lose their functionality [19, 20].

Also, found moisturizing wooden window constructions in facades where magnesium sheets used as building substrates. Fireproof properties of magnesium sheets eventually reduce to the extent that they are decomposed by moisture.

Magnesite sheets with appropriate quality control and formulation are non-combustible. It has a low thermal conductivity and enhanced resistance to high temperatures, which allows their use as structural fire protection to enhance fire resistance of building structures. However, fasteners elements for wallboards should have high reliability and don't deteriorate when exposed to extremes of temperature and humidity because sheets can quite change the geometrical dimensions and may cause corrosion on ferrous and non-ferrous metals fasteners (Figs. 5, 6).



Fig. 5. Corrosion on fasteners elements.

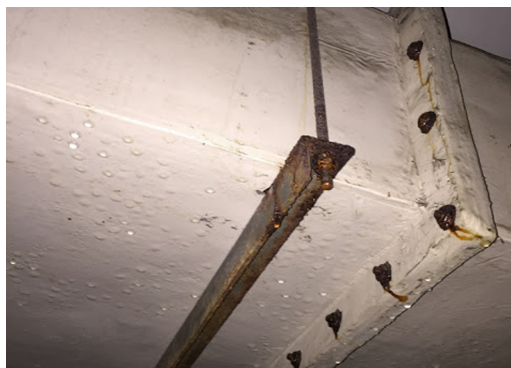


Fig. 6. Corrosion on fasteners elements.

Studies that were made by Bunch NGO institute about magnesium sheets in Denmark in 2015 had a great response [21]. The study was initiated after collapse and

corrosion of magnesium wallboards that were used as facade panels for Dokk1 library. The library was opened in June 2015 and became the largest in Scandinavia. It has an area of 35.6 thousand m² (Fig. 7). In June 2016, the media reported that the construction of the external facade of the building is damaged by corrosion. About 3,000–4,000 m² facades' surface fell into disrepair. The cost of replacement is estimated at 19–26 million kroner (Fig. 8). Experts believe that the cause is marine and wet climate of Denmark.



Fig. 7. The Dokk1 library.



Fig. 8. Corrosion on the facades of Dokk1.

Problems arise with magnesium sheets due to the weather conditions in which they are used [22–26]. Thus, the ski complex in Rezh Sverdlovsk region was constructed using magnesium oxide wallboards as the facing material (Fig. 9).

Organization that was implementing construction did not consider climatic conditions of this region. Magnesium oxide wallboards absorbed moisture and after turning on the heating system were destroyed. Therefore, the ski complex was not even put into operation (Figs. 10, 11).



Fig. 9. Ski complex in Sverdlovsk region.



Fig. 10. Cracked ceiling.



Fig. 11. Destroyed wallboards.

3 Conclusions

Naturally, complexity of using this material will exist in other territories with analogous climatic conditions. Negative impact of magnesium oxide wallboard's exploitation on building structures calls into question of expediency of it's usage. Especially, if


it is exploited in conditions of high humidity. It is necessary to undertake a fundamental and long-term study based on full-scaled observations and material exposition in near-operational conditions. It is advisable to create normative documents constituting magnesium oxide wallboard's classification, terminology, study methods and quality specifications for different makes of the wallboards. Specifications should contain clear indications for exploitation regime and control methods to avoid low-quality magnesium oxide wallboards' import. Order of Ros Standard No. 2034 dated 30 December 2016 formed the Technical Standardization Committee TC 144 "Construction materials, products and engineering structures", particularly Subcommittee SC4 with insulating and finishing materials and products falling within its' competence. These Committee and Subcommittee were formed on the basis of the Institute of Civil Engineering of The Federal State Autonomous Educational Institution of Higher Education "Peter the Great St. Petersburg Polytechnic University". It is envisaged that major Russian scientific groups in construction field will be involved in standards evaluating. Also, in order to harmonize Russian and international standards in particular export oriented industries, leading foreign scientific centers are planning to be involved. The development of standard, harmonized with Chinese standard PRC JC688-2006, considering climatic zones of Russia and national regulatory requirements about finishing materials, is the necessary orientation keeping in mind the current situation with the perspective but insufficiently explored new finishing material - magnesium oxide wallboards.

References

1. Huziahmetov, A.: Methods of assessment «activity» of MgO in magnesia binders Herald Kazan Technological University, pp. 58–64 (2013)
2. Tolkachev, C., Kozlov, A., Deviatkin, D.: To a question about how to reduce the reactivity of magnesia cements for safe handling them in cementing casing in oil and gas wells. Bull. Perm Natl. Res. Polytech. Univ. Geol. Oil Gas Min. **9**, 49–56 (2013)
3. Kiyanets, A.: Hardening of the construction of composite materials based on magnesia binder in various temperature conditions. Bull. South Ural State Univ. Constr. Archit **1**, 29–32 (2015)
4. Jurišová, J., Fellner, P., Pach, L.: Characteristics of Sorel cement prepared from impure materials. Acta Chim. Slovaca **8**(2), 87–90 (2015)
5. Ustinova, Yu., Nikiforova, T., Nasonova, A., Sidorov, V.: Environmental assessment plate materials based on magnesia astringent their life cycle. Vestnik MGSU **1**, 288–293 (2010)
6. Matthew, C.: Reactions of compounds occurring in Sorel's cement. Cem. Concr. Res. **7**, 575–583 (2003)
7. Orlov, A., Trofimov, B., Chernyh, T., Kramar, L., Zimich, V.: A complete system for interior with Mg materials. Bull. South Ural State Univ. Constr. Eng. Archit. **35**, 33–37 (2011)
8. El-Gammal, M., Ayman, M., Mohamed, N.: Using magnesium oxide wallboard as an alternative building façade cladding material in modern cairo buildings. J. Appl. Sci. Res. **8**, 2024–2032 (2012)
9. BYG-ERFA Fugtsugende vindspærreplader Erfaringsblad (2005). www.byg-erfa.dk/fugtsugende-vindspærreplader

10. Epshtein, S.A., Adamtsevich, A.O., Gavrilova, D.I., Kossovich, E.L.: Thermal methods exploitation for coals propensity to oxidation and self-ignition study. *Gornyi Zhurnal* **7**, 100–104 (2016). <https://doi.org/10.17580/gzh.2016.07.22>
11. Zyryanov, V., Lytkina, E., Byrd, T.: Increased mechanical strength and water resistance of magnesia binders with the introduction of mineral fillers. *Proc. Univ.* **3**, 21–26 (2010)
12. Zyryanov, V., Bird, T., Vereshchagin, V.: Magnesium cementing of waste sludge magniyhloridnyh. *Proc. Univ.* **8**, 21–25 (2009)
13. Lytkina, E.: Xylolite kostrolitovye and building materials using composite magnesia binder containing diabase. *Proc. Univ.* **9**, 26–29 (2010)
14. Miryuk, O.: Influence of material composition on the properties sulfamagnezialnyh compositions. *Proc. Univ.* **2**, 31–36 (2011)
15. Golovnev, S., Kiyansets, A., Dyakov, K.: New high-performance energy- and resource- saving construction technologies and materials base on magnesia binding. *Acad. Bull. Uralniiproekt RAASN* **3**, 86–87 (2009)
16. Mathur, R., Chandrawat, M., Sanjay, K.: Effects on setting, strength, moisture resistance and linear changes of Sorel's cement on mixing portland cement as an additive. *E-J. Chem.* **6**, 412–418 (2009)
17. Gravit, M., Nedryshkin, O., Vaititckii, A.: Aspect of using magnesium oxide wallboard in construction. *Archit. Constr. Russia* **1**(223), 110–115 (2017)
18. Wojtowicz, V., Spirin, G.: The possibility of using magnesia binders in construction The head of a construction company (2011). <http://base.garant.ru/58101344>
19. Pukhal, V., Tanic, M., Vatin, N., Murgul, V.: Studying humidity conditions in the design of building envelopes of “passive house”. *Procedia Eng.* **117**, 859–864 (2015)
20. Bonić, Z., Topličić Ćurčić, G., Trivunić, M., Davidović, N., Vatin, N.: Some methods of protection of concrete and reinforcement of reinforced-concrete foundations exposed to environmental impacts. *Procedia Eng.* **117**, 419–430 (2015)
21. BUNCH Byggningsfysik. MgO-plader Undersogelse af problemer med fug tog corrosion (2015). <http://bsf.dk/media/1559/mgo-rapport.pdf>
22. Krivtsov, A., Gravit, M., Zimin, S., Nedryshkin, O., Pershakov, V.: Calculation of limits of fire resistance for structures with fire retardant coating. In: *MATEC Web of Conference*, vol. 53 (2016)
23. Artiukh, V., Mazur, V., Adamtsevich, A.: Priority influence of horizontal forces at rolling on operation of main sheet rolling equipment. In: *MATEC Web of Conferences*, vol. 106 (2017). Article no. 04001. <https://doi.org/10.1051/mateconf/201710604001>
24. Pustovgar, A., Tanasoglo, A., Garanzha, I., Shilova, L., Adamtsevich, A.: Optimal design of lattice metal constructions of overhead power transmission lines. In: *MATEC Web of Conferences*, vol. 86 (2016). Article no. 04003. <https://doi.org/10.1051/mateconf/20168604003>
25. Shilova, L., Soloviev, D., Timatkov, V., Adamtsevich, A.: About the territorial potential of the construction of battery-charging stations for autonomous electric motor vehicles in the regions. In: *MATEC Web of Conferences*, vol. 73 (2016). Article no. 02017. <https://doi.org/10.1051/mateconf/20167302017>
26. Solovyev, A., Pustovgar, A., Shilova, L., Adamtsevich, A., Solovev, D.: Simulating power efficiency of heat transfer agent cooling recirculation systems at power plants. *Procedia Eng.* **165**, 1275–1280 (2016). <https://doi.org/10.1016/j.proeng.2016.11.850>

Additive Technologies in Construction of Temporary Housing for Victims of Natural Disasters and Other Emergencies

Alexander Lanko^(✉) 

Peter the Great St. Petersburg Polytechnic University,
Polytechnicheskaya str., 29, 195251 St. Petersburg, Russia
alexandr.lancko@yandex.ru

Abstract. The article considers the possibility of applying modern additive technologies in construction of temporary housing for victims of natural disasters and other emergencies. A number of technologies for printing sheltering structures using mobile 3D printers is discussed. The suggested examples present not only a fundamentally different technology of construction, but also show how differently materials can be used for 3D printing of temporary housing facilities. There is proposed a construction of dome shape structures, that are the most resistant to possible disasters and demonstrate the possibilities of additive technologies. Special attention is paid to the state and ways of development of material science in the field of 3D printing.

Keywords: Additive technology · 3D printing · Rapid prototyping
Emergency · Victims · Domed constructions · Mobile 3D printers

1 Introduction

Man-caused emergency situation is a temporary condition when:

- normal living conditions and activities of people are violated;
- their life and health are threatened;
- damage to property of the population, national economy and environment is dealt.

Emergencies resulting from human activities include: terrorist acts, auto, aviation, railway accidents, industrial accidents, fires, etc. The resulting natural elements: floods, hurricanes, droughts, and other environmental disasters and epidemics. Temporary structures in emergency situations are involved in overcoming their consequences. Placement of the suffered population from emergency situations is carried out at the rescue points and temporary accommodation as well as temporary camps [1, 2].

Typologically, these are rescue camps, health facilities, temporary shelter and catering facilities. The time of the existence of these temporary structures in a stationary condition is due to the duration of rescue activities and does not always fit into a few days. Sometimes, rescue work lasts for several months, especially if, due to an emergency, the victims have lost their main housing. Deployment of temporary camps can be carried by construction and operation organizations, public service and logistics

agencies. In the field conditions, military units and other specialized groups can be enlisted to deploy tent camps [3, 4]. The main criteria that determine the choice of structures and materials for these temporary structures are:

- speed of construction;
- versatility;
- ability to respond to new emergencies.

This affects people's lives and the possibility to provide them immediate medical care. Today, shelters are generally used in case of emergency. Temporary structures for accommodation of victims and rescuers are needed in different climatic and geological conditions.

One of the main factors that determine the deployment of temporary accommodation is the expected duration of residence of the population [5], therefore, when planning the camp for a period longer than one month more robust and durable structures should be considered.

Inflated structures have several disadvantages:

- not always are able to respond to new emergencies;
- are subject to wear and require maintenance when used for extended periods of time (e.g., air-inflated structures require constant pumping);
- have a low fire resistance class;
- are low comfort for long-term stays, from a practical and a psychological point of view.

With the planned placement of victims of emergencies for a longer period (more than 1 month), stronger and more reliable structures are required. At the same time, these structures should comply with the main criteria applied to facilities for temporary accommodation of victims and rescuers. The construction of classical buildings is not always possible because of the terms of their construction. In this case, building using a mobile 3d construction printer is a good alternative. The technology of creating three-dimensional objects with the help of material growth has been actively developing since 1980s, and at the initial stage it is called "rapid prototyping" or additive construction [6]. Additive technologies (AM - Additive Manufacturing) have developed slowly for quite a long period of time and a real breakthrough has been noted since about 2010 [7].

Printing domed buildings of small size practically does not require the use of additional materials and equipment. Moreover, the domed buildings are extremely durable and able to withstand a natural disaster. Advantages of a house printed on a 3d printer for the long-term placement of people affected by natural disasters, in comparison with classical buildings are:

- high speed of construction;
- ability to use various types of construction mixtures;
- versatility - use one equipment and the type of printing materials for the whole house, free choice of thickness and configuration of walls;
- maximum efficiency of the used materials, no construction waste;
- walls can be insulated with any appropriate material;
- low cost.

2 Analysis of Existing Technologies

As an example of such technology, the Russian development of APIS COR can be cited. This mobile 3D-printer is capable of creating a house of 100 square meters in size within 24 h, meeting construction standards and capable of standing for 175 years on the assurances of the manufacturer's company. In February 2017, near Moscow, the capabilities of a mobile 3d printer were demonstrated and a 38 m² residential house was printed per day.

The main difference of the device from other existing construction printers is that APIS COR prints the building, being inside it. The overall dimensions (4000 × 1600 × 1500 mm) and weight (2000 kg) of this printer allow it to be transported on a small truck with a manipulator. All start-up and adjustment works take no more than 30 min. The maximum printable area is 132 m². In order to operate the printer requires a mobile automated complex for preparing and delivering concrete, dimensions and weight of which also make it easy for transportation. Dry construction mixture is fed into the mobile system of preparation and feed of the mixture and then goes to the printer [8–14] (Fig. 1).



Fig. 1. APIS COR printer (<http://www.apis-cor.com>).

The main drawback of this technology is the need to extract the printer from the printed house using lifting equipment. In addition, there is a need to print the building in two phases if it has a dome. At the first stage house is printed from inside and then the printer should be placed outside of the building to print the final domed roof.

Researchers from the Massachusetts Institute of Technology offer another option for a mobile construction 3D printer [15]. They managed to create a self-propelled platform that can move freely around the construction site. Of course, the weight and dimensions of this platform make it very difficult to transport it to the construction site, but its reach parameters allow printing small domed buildings from outside. For the first test, the researchers erected a foam insulated domed structure, used to form a ready-made concrete structure. This method is similar to traditional insulation and

concrete formwork technologies. Its advantage is high building speed and the possibility to create formwork of complex shape.

Scientists have been working on the complex since 2011, setting an ambitious goal of creating a standalone printer capable of working in harsh environmental conditions and even in space. High automation and robotization of the process allows implementing projects in hostile environments [8], without endangering the personnel.

According to the project manager Stephen Keating, such system can be sent to the Antarctic or Mars, to build a house. Next goal is to use the system in remote regions of developing countries or assistance in the construction of long-term shelters for disaster victims (Fig. 2).



Fig. 2. Digital construction platform (<http://matter.media.mit.edu/>).

Another example of the use of 3d printing in the construction of temporary shelters is the architectural firm DUS, that printed a small house in Amsterdam with a volume of 25 m³. The authors of the project demonstrated the ability to quickly 3D print shelters in areas of disaster. The Urban Cabin printed of biodegradable plastic based on flax. The building has a honeycomb structure that allows to achieve a sufficient strength at low material and time costs. The used plastic can be granulated and turned into a material for new projects. A 3D printer of its own design called the “KamerMaker” was used to manufacture the house, a device with a height of three feet, which fits in a conventional shipping container that allows quickly delivering it to the site of the future camp and beginning construction. The printer is more limited in the sizes of the finished products than the above-described system and allows printing large buildings only in part. Lightweight honeycomb structure allows placing the building in the right place using a small crane or even manually. This technology also allows printing a house of domed shape, making them more durable and resistant to environmental influence (Fig. 3).



Fig. 3. Urban Cabin by DUS company.

Currently, there is a rejection of traditional concepts in the field of construction, and modern trends are focused specifically on additive technologies of erection [9]. Studies aimed at solving the problems of 3D construction printing are being carried out in many institutes around the world. Much attention is paid both to mixtures for printers [10–13], and to technologies and equipment [14–16]. Interest in additive technologies is caused by the following factors:

- high automation of production, including the creation of fully autonomous printers to work in dangerous conditions;
- significant reduction of time expenses;
- the absence of “human factor” excluding mistakes of builders during the construction process;
- the possibility to optimize CAD models;
- the most effective use of “construction materials”;
- environmentally friendly production through a significant reduction of construction waste.

3 Materials

One of the most critical issues remains the material for 3d printing. Cement compositions which harden long cannot meet the performance requirements. The composition should be thixotropic, that is, to reduce the viscosity from mechanical impact and to increase the viscosity in the resting state [17], with the reduced shrinkage and creep parameters [18].

Dispersed reinforcement qualitatively improves the mechanical characteristics of concrete, allows to reduce the working cross-section of the structure and, in some cases, to give up on using the core reinforcement [19]. Together with the Russian-Italian company Renka Rus, APIS COR engineers are exploring the possibility to use geopolymeric materials that are more environmentally friendly [20].

The demand for serious research in the field of material science for the needs of 3d printing is confirmed by many authors [21, 22]. With regard to the provision of traditional requirements, known methods and approaches in the technology of concretes and other construction mixtures should be used. Further development of formulations can consist in the use of special mineral binders (for example, expanding [23, 24], and the use of industrial waste, including construction industry [25, 26], etc.

4 Conclusion

The above examples of additive technologies in the construction of temporary shelters for victims of natural disasters show a huge variation of technologies, equipment and materials. Today, most of the developments are at the testing stage and do not find a large scale of application. Substantial problem remains the material for additive printing, the possibility of reinforcement of structures. Nevertheless, the use of mobile 3d printers for erecting temporary housing for victims of emergencies is a good alternative in context of the need for long-term accommodation.






References

1. Sednev, V., Voronov, S., Lysenko, I., Sergeenkova, N.: Engineering protection of the population. Akademiya GPS MCHS Rossii, Moscow (2015)
2. Sednev, V., Teterina, N., Alyaev, P.: A study of major problems of engineering protection of population and territories from emergency situations in peace and war: report on the research work. Akademiya GPS MCHS Rossii, Moscow (2015)
3. Methodical recommendations on the organization of primary life support of population in emergency situations and the work of the temporary accommodation of the affected population. MCHS Rossii, Moscow (2013)
4. Recommendations on equipment and life support field camp for the temporary accommodation of the evacuees and refugees. GKCHS Rossii, Moscow (1992)
5. Durnev, R., Trofimov, A., Durnev, R., Trofimov, A.: Method of evaluating an emergency situation to deploy the temporary accommodation of the population affected by accidents, catastrophes and natural disasters and system for its implementation. Patent RF na izobretenie № 2537878 28.02.2013. Byull. Izobretenij № 1 (2015)
6. Litovkin, S., Pet'kova, Y.: The use of 3D printing in the engineering and construction industry. In: International Scientific-Practical Conference "Actual Problems of Modern Engineering". FGA OU «NI TPU» (2015)
7. Barkovskaya, N.: The issues of standardization of 3D-printing technology. In: Science – Education, Production, Economy: Materials of the 12th International Scientific and Technical Conference. BNTU, Minsk (2014)
8. Ramachandran, N., Gale, A.: Space colonization. *Aerosp. Am.* **46**(12), 77 (2008)
9. Val'ter, A.: Reinforced layer-by-layer synthesis of bulk products. *Gornyj Informacionno-Analiticheskij Byulleten'* **2**(12) (2011)
10. Xi-Qiang, L., Jing-Fang, L., Tao, Z., Liang, H., Nan, Z., Juan, L., Guoyou, L.: Cement-based composite material used for 3D printing technology as well as preparation method and application thereof. Pat. CN104310918A (2014)

11. Tianrong, Y., Qiaoling, L.: 3D printing cement-based material and preparation method thereof. Pat. CN104891891A (2015)
12. Peng, F., Xinmiao, M.: Fiber reinforced composite material reinforced 3D (three-dimensional) printing structure. Pat. CN104309126A (2014)
13. Fu-Cai, L., Yi-Yuan, W., Min, X., Bin, L., Xin-Zhen, Z., Ming, H.: High-performance powder concrete for 3D (threedimensional) printing. Pat. CN104961411A (2015)
14. Khoshnevis, B.: Contour crafting extrusion nozzles. Pat. US14/961,071 (2015)
15. Dini, E.: Method for automatically producing a conglomerate structure and apparatus therefor. Pat. US8337736 (2012)
16. Dini, E., Chiarugi, M., Nannini, R.: Method and device for building automatically conglomerate structures. Pat. 11/908,993 (2006)
17. Vatin, N., Chumadova, L., Goncharov, I., Zykhova, V., Karpenya, A., Kim, A., Finashenkov, E.: 3D printing in construction. *Stroitel'stvo Unikal'nykh Zdanij i Sooruzheniy* **1**(52), 27–46 (2017)
18. Barabanshchikov, Yu., Arkharova, A., Ternovskiy, M.: Beton s ponizhennoy usadkoy i polzuchestyu. *Stroitelstvo Unikalnykh Zdanij i Sooruzheniy* **7**(22), 152–165 (2014)
19. Klyuev, A., Klyuev, S., Ntrebenko, A., Durachenko, A.: Fine-grained fiber concrete reinforced with polypropylene fiber. *Vestnik BGTU im. V.G. SHuhova* **4**, 67–72 (2014)
20. Habert, G., De Lacaillerie, J., Roussel, N.: An environmental evaluation of geopolymer based concrete production: reviewing current research trends. *J. Clean. Prod.* **19**(11), 1229–1238 (2011)
21. Stepanova, E., Barsukov, G., Stepanov, Y.: Breakthrough technology the new generation of shaping a spatially complex surfaces of scientific products. *Izvestiya Tul'skogo Gosudarstvennogo Universiteta Tekhnicheskie Nauki* **8–2**, 243–249 (2016)
22. Grahov, V., Mohnachev, S., Borozdov, O.: The impact of 3D technology on construction Economics. *Fundamental'nye Issledovaniya* **11–12**, 2673–2676 (2014)
23. Nesvetaev, G., Potapova, Y.: Management of own deformations of cement stone by changing the composition and quantity of expanding agents. *Nauchnoe Obozrenie* **11**, 46–49 (2013)
24. Nesvetaev, G., Udodov, S., Bychkova, O.: On the impact of the modified gipoglikemical expanding cement strength and hardening rate. *Internet-Zhurnal Naukovedenie* **7**(6)(31), 122 (2015)
25. Udodov, S., Chernyh, V.: The particular properties of dry mixes with the use of porous fillers. *Stroitel'nye Materialy* **3**, 15–17 (2006)
26. Sajdumov, M.: Screenings from the concrete crushing and rock to obtain concrete composites. *Dissertaciya na soiskanie uchenoj stepeni kandidata tekhnicheskikh nauk. Belgorodskij gosudarstvennyj tekhnologicheskij universitet im. V.G. SHuhova, Groznyj* (2012)

**Management, Analysis, Monitoring,
Organizational and Technological
Solutions**

Management and Monitoring of Urban Environment in the Integrated Development of Underground Space

Galina Romanova¹ , Michael Pleshko^{2,3} ,
Marina Rossinskaya^{1,3} , Nelli Saveleva¹ ,
and Alexander Pankratenko⁴ 

¹ Sochi State University, Russia Sovetskaya Street 26a,
Sochi City, Krasnodar Krai 354000, Russia

² Rostov State Transport University, Rostovskogo Strelkovogo polka sq., 2,
Rostov-on-Don 344038, Russia
mixail-stepan@mail.ru

³ Don State Technical University, pl. Gagarina, 1,
Rostov-on-Don 344022, Russia

⁴ National University of Science and Technology (MISiS),
Leninskij Av., 4, Moscow 119991, Russia

Abstract. The paper presents the results of developing the system of managing and monitoring the urban environment in the integrated development of the underground space. Its main elements are a block of geotechnical management and monitoring, a block of energy management and monitoring of life support systems, a block of ecological and socio-economic monitoring. The essentials and principles of construction of each block are considered. The key attention is paid to geotechnical monitoring in the construction of underground structures with the use of protective screens. The features of stress distribution in the span tubes and the side walls of the protective screen are established based on the analysis of monitoring data. By means of numerical simulation by the finite element method, the stresses in the span pipes and vertical deformations of the soil mass are obtained over the span from the rigidity of the pipe section area. An improved design of a protective screen with the possibility of regulating its vertical resistance by means of hydraulic jacks is proposed. The effectiveness of this technology in the development of underground space is determined not only by economic, but also by social and environmental aspects.

Keywords: Transport infrastructure · Underground space
Geotechnical monitoring

1 Introduction

The intensive development of Russian cities is characterized by a constant increase in transportation and passenger traffic volume, the density of urban saturation, impacts on utilities and communications, environmental degradation, the growth of social tension and other unfavorable factors. A comprehensive analysis of international experience in

the development of the urban environment shows that the way out of this situation is, primarily, possible with the integrated development of underground space [1, 2], as well as improving the energy efficiency of construction and operational technologies.

Recently, a fundamentally new approach to the concept of the underground space of the city has been formed, which is reflected both in foreign and domestic research.

The underground space of the city is considered as a natural resource, which civilized development and application allows solving many ecological and socio-economic issues, predetermining the extensive development of infrastructure [3]. The potential of such a resource consists of spatial-territorial, geoenergetic and mineral raw materials factors [4–6].

However, it should be emphasized that the underground space of a large city is no longer a natural resource but a natural resource that intensively interacts with the homosphere and, at the same time, is a part of the city noxosphere. This approach requires an interdisciplinary approach [3], and a simultaneous consideration of many components of a dynamic urban environment.

The importance of improving technical and technological solutions for the development of the underground space of cities is confirmed by the development of guidelines [7]. New trends in the development of underground space are systematically analyzed in the research [8].

The critical influence on the underground space development and the development of transport, energy and municipal systems of the city is based on ensuring anthropogenic security. The operational experience of these systems shows that they are characterized by a high percentage of failures and accidents resulting in both individual accidents and major man-made accidents and catastrophes. In this case, insufficient reliability of the systems usually appears at the design stage [9].

One of the main reasons for this situation is insufficient funding [10]. Excessive system deterioration leads to an increase in the additional costs of repair and restoration work. It is necessary change from the practice of eliminating accidents to the implementation of advanced measures on the basis of integrated monitoring of life support systems and construction projects.

At this stage, energy policy traditionally underestimates the benefits of energy efficiency for society, environment and labor. The achieved levels of the introduction of energy-efficient technologies depend on the stage of industrialization, mechanization, electrification, human capital assets and politics [11]. The neglect of energy-efficient technologies and the declaration of intentions instead of real affairs only aggravate the gap between the developing countries and the world's leading economic powers. In addition to the directions outlined above, a fundamental improvement in the situation is possible if the trends in town planning policies change from investment orientation to social orientation. It is necessary to apply a social planning, as the implementation of modern holistic views on the development of society [12].

Thus, the complex development of the underground space requires the organization of effective management and monitoring of the main elements of the urban environment and must solve the following tasks:

- compactly place buildings and structures for various purposes in conditions of cramped buildings;

- improve the transport services of the population with a significant increase in the speed of communication;
- provide optimal conditions for the development, operation and repair of urban engineering networks;
- solve the problem of permanent and temporary storage of the park of cars and other types of transport;
- provide significant savings in fuel and energy resources [7].

The development of the basic elements of the management and monitoring system of the urban environment in the development of the underground space is very relevant and represent the goal of the authors' research.

2 Methods

A complex research method was used in the paper: analysis and generalization of scientific and technical achievements on the problem; stochastic analysis; the performance of the full-scale experiments; numerical modeling of underground structures by the finite elements method, elements of technical and economic analysis.

3 Results

The main constituent parts of the proposed management and monitoring system for the urban environment in the integrated development of the underground space are:

- a block of geotechnical management and monitoring;
- an energy management and monitoring of life support systems;
- a block of ecological and socio-economic monitoring.

Taking into account the limited scope of this paper, we will consider the main elements of each block and dig deeper into the block of geotechnical management and monitoring.

The block of geotechnical management and monitoring is based on the system-complex approach with consideration of three components of the combined natural and man-made system of the city:

1. The ground part with buildings, structures, monuments of architecture, roads, engineering infrastructure, water and air environment.
2. The underground part, which includes underground objects of any purpose, underground communications, roads, underground parts of buildings and structures.
3. Geological and hydrogeological environment, including primary rocks, quaternary deposits, pressure groundwater horizons, subsurface waters.

These subsystems constantly interact with each other and have their own hierarchy. The underground part of the modern city is currently represented by:

- underground transportation facilities (road and railway tunnels, tunnels and subway stations, pedestrian crossings);

- facilities and networks of engineering equipment (water supply and sewage networks, power supply and gas supply, heating networks, boiler houses, pumping stations and reservoirs, common through manifolds, transformer stations, gas distribution stations, etc.);
- underground parts of buildings and structures (underground floors, basements, foundations, natural and artificial bases) [13];
- military objects (bomb shelter with approaches and communications);
- underground parts of the liquidated mining enterprises (vertical, inclined and horizontal workings, chambers, mined-out space) [14].

The effective management at the first stage requires the development of a general layout for the allocation of underground transportation facilities and a scheme of the spatial structure of the city on the basis of an analysis of the existing transport network, a city development plan, and engineering geological and geoecological survey data.

The main goal of the first stage is to eliminate the existing contradictions between the space planning development and its transport infrastructure. Its achievement is provided due to the organization of effective interaction of the transport system with the planned and spatial structure of the city, both in the functional and in the structural aspect. The main emphasis is placed on the improvement of transportation in the central district of the city, its connection with peripheral suburban areas, the issues of differentiated placement of transport systems in urban areas; the organization and planning interaction between urban and suburban transportation; the modeling of transport systems at the initial stages of urban planning; the influence of urban factors on the development and formation of mass transportation facilities, etc.

The development of the spatial structure of the city provides the effective insertion of new underground objects into the urban environment by the application of optimal space-planning solutions developed on individual projects, taking into consideration the characteristics of urban development, the branching of underground engineering networks and the geological and hydrogeological conditions of construction. Determination of the main parameters of underground structures: the extent and depth of the location, the sizes and shapes of the cross sections, the schemes of exits to the surface etc., is based on a system analysis of the influencing factors, which are formed as a result of the interaction of the previously allocated structural elements of a metropolis.

At the second stage of the research, the construction geotechnologies for the development of underground space are established, which are as safe as possible for the combined natural and man-made city system. The following factors influence their choice:

- the dimensions of the underground structure in plan and depth;
- the location of the underground structure (construction on a free territory or in the conditions of the existing compact planning);
- the engineering-geological and hydro-geological conditions of the construction area;
- the necessity to comply with environmental requirements on environmental protection;
- economic considerations;
- the possibilities of a construction organization.

The objects of underground transport infrastructure are usually located in the central part of the city, which is characterized by a high building density, the presence of architectural monuments and busy roads, which long-run overlap can't be proposed. Under these conditions, the following basic requirements can be presented to geotechnologies for the development of underground space:

- the reduction of the volume of works performed by the open method;
- the avoidance of the development of excessive surface subsidence;
- the avoidance of negative influence of underground objects on neighboring buildings, structures, roads and other objects of urban infrastructure;
- the reduction of the volume of excavation and groundwater pumping that alter the hydrogeological situation;
- the application of environmentally friendly materials and technologies for underground construction;
- the increase of the technical and economic effect from the introduction of underground objects of the transport infrastructure.

Open, semi-closed and closed methods of the construction of underground structures are known today. The closed methods meet the above requirements.

The following basic approaches of work are applied for the erection of underground structures with the help of the closed method:

- rock tunneling - in strong and stable soils, and with the use of the “New Austrian” method (NATM) and in soils of medium and weak stability;
- shield method - in soft and weak soils;
- thrust-bore method - mainly in embankments, folded by compacted and drained incoherent soils, as well as in weak moist ground, drained by water depletion. In the most complex engineering geological, topographical and town planning conditions, rock tunneling and shielding methods of work are used in combination with special types of work that ensure the preliminary stabilization of the soil mass (chemical sealing and soil freezing, jet grouting, outstripping protective supports, etc.) [15].

The analysis of known construction methods shows that they, as a rule, can't completely exclude the impact on interacting elements of the combined natural and man-made city system. The reasons for this situation are: the absence of an integrated approach in the development and implementation of geotechnologies, the basis of their individual elements independently of each other, the insufficient consideration of technology and possible changes in the physical and mechanical properties of soils in the construction and operation of hoisting facilities, low variability and adaptability of geotechnologies to dynamically changing natural and technogenic system of a metropolis.

The effective reduction of the impact of constructing underground facilities on the urban environment can be achieved by the application of combined traditional and innovative building geotechnologies, the main elements of which are:

- the technique of analysing the stress-strain state of objects in the underground space in the process of its development;

- the unified system of automated control of geotechnical monitoring during construction;
- the system of advanced active anchoring of underground structures and fixing the surrounding mass of soils on the basis of advanced anchor system, screens, high-strength materials and reinforcements;
- the adaptive technology and the organization of mining operations with changing parameters of a sinking cycle, stages of face digging, lining design;
- the complex hydroprotection of underground objects using new composite materials based on local economical raw materials.

The implementation of combined geotechnologies involves a transition to a two-stage design scheme.

At the first stage, the basic parameters of construction technologies are substantiated, taking into account all the influencing factors. For this purpose, within the framework of the research, a technique is developed for analyzing the stress-strain state of objects in the underground space in the process of its development, taking into account:

- the spatial geometry and properties of underground and surface facilities in the construction zone;
- the nonlinearity of soil deformation, the possibility of their physical and mechanical characteristics in the process of construction;
- the stability and work performance behaviour over time;
- the joint work of active systems of advanced soil nailing of underground structures, soil solidification and basic lining;
- the behaviour of change in the properties of building materials in time;
- the dynamics of groundwater flow, etc.

The implementation of the adopted parameters of geotechnologies in the construction of underground facilities is accompanied by geotechnical, engineering-geological and environmental monitoring with the use of the developed unified system of automated control. On the basis of processing and analysis of incoming data, whenever necessary, an operative adjustment of the basic design solutions is carried out, aimed at ensuring maximum safety of construction.

Consider the following example.

With the participation of the authors, an innovative solution has been developed for constructing subaqueous crossing of a rectangular cross-section with mitigation of the impact mitigation. The work is carried out without any pauses in the traffic flow and with an application of constant geotechnical monitoring.

The construction of the crossing is carried out under the protection of the leading screen. The structure of the protective screen is implemented by sequential metal pipe sections ramming with subsequent excavation of soil, web bar bending and filling with monolithic concrete. The sections of two or three pipes fix the entire span and the side walls of the tunneling. A tunnel lining is being constructed under the cover of the protective screen as well as portals of the tunnel. The movement is organized in two levels at the intersection. The pipes can also be used for the construction of supply lines.

While performing the works, a complex automated system for monitoring the “advanced screen-massive” system is used, which controls four groups of parameters:

1. Parameters of the stress-strain state (SSS) of the constructions of the advanced support: tension and deformation.
2. Indirect parameters of SSS support: the pressure of the ground mass on the pipes of the advanced support.
3. Technological parameters of the state of the object: mutual displacement of sections, translational displacement and roll of sections from the design position.
4. Environmental parameters: the displacement and subsidence of the soil massive and the ground surface.

There are four basic types of sensors: pressure sensors; strain gauge sensors; displacement sensors; crack sensors.

Based on the described types of sensors, a monitoring system is formed. It consists of:

- central device for data collection and processing;
- automated workplace of the monitoring system operator;
- measuring equipment (sensors);
- recording unit (registrars).

The interaction structure of this system is organized in the following way: the final measuring equipment is connected to the registration units that collect and perform initial processing of information. The registrars transmit the data that has passed the primary processing to the monitoring system server. On the server, through special software, the information received from the registrars is processed, the technical condition of the structures is evaluated, the information is stored in the monitoring system database and the system self-diagnostics. The automated workplace requests information about the state of the elements of the design from the server and displays it to the operator in a graphical form.

In Fig. 1 shows examples of diagrams of maximum principal stresses in the pipes of the advanced screen. They occur after excavation in the section of the tunnel intersection under the action of permanent and temporary tension, obtained as a result

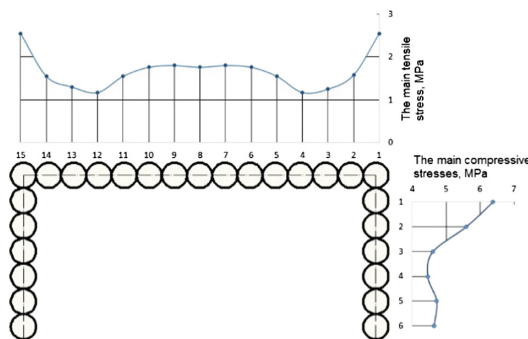


Fig. 1. Diagrams of the maximum principal stress in sections of the pipes of the advanced screen of the tunnel intersection.

of monitoring. The tensile stress arises in the span tube, the maximum reaches value of 2.6 MPa. In the pipes of the side walls, there is compressive stress with the maximum value of 6.3 MPa. It is observed in the section of the upper pipe of the side wall.

The figure shows that the stress distributions in a section of pipe protective screen characterized by considerable unevenness. In order to evaluate the effect of the screening parameters on the stress-strain state of the system, calculations are carried out with the help of a finite-element spatial model of tunnel intersection in response to the different rigidity of the screen tubes determined by formula

$$B = \frac{Et}{r^2} \tag{1}$$

where E is the elastic modulus of the pipe steel, MPa; t is the thickness of the pipe, m; r is the radius of the neutral axis of the pipe section, m. The calculations yielded a parabolic dependence of maximum principal compressive stress (Fig. 2) in the corner section of pipe and the power dependence of the maximum vertical shift of the soil mass (Fig. 3) in the center of the tunnel span of the intersection on a parameter of rigidity.

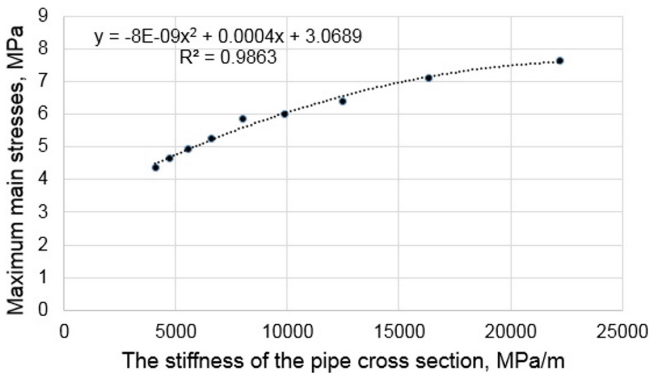


Fig. 2. The dependence of the maximum principal stress on the rigidity of the tube cross section of the protective screen.

The obtained dependences make possible to deduce an inference that by varying the characteristics of the rigidity of the protective screen, it is possible to create the prerequisites for controlling the stress-strain state of the “support-massive” system.

For this purpose, active control elements are additionally included in the construction of the protective screen (Fig. 4). Firstly, the pipes of the advance support of the usual construction of 1 side walls are installed bottom-up. They are connected to each other by means of mounts 2. Two-section pipes with internal elements of active regulation 3 in the form of hydraulic jacks are adjusted last.

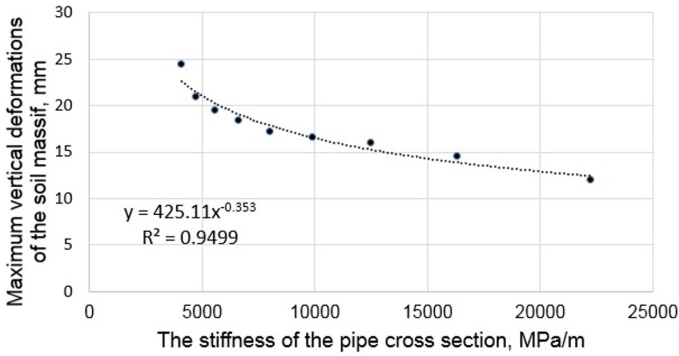


Fig. 3. The dependence of the maximum vertical shifts on the rigidity of the protective screensection.

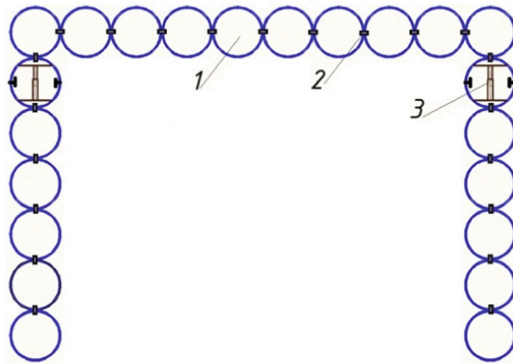


Fig. 4. Layout of the protective screen elements

Afterwards, the pipes of the advance support of the tunnel intersection are installed, which, as the side pipes, are connected by mounts 2.

The sinking is carried out under the subaqueous crossing through the use of the protection of the advanced support. In case of the progression of the surface subsidence, it is compensated by the activation of the elements of active regulation of the advanced support. If necessary, on the basis of monitoring data, the dimensions of the drifting face, the speed of movement and other technological parameters can be corrected. Thus, the minimization of the influence of construction on the related environments and the ground achieves.

After the completion of the construction the life support systems of the city are located in the underground space. They are specified by the general lay-out of the city development. Thus, the implementation phase of the energy management and monitoring block of life support systems comes forward.

Energy management is a complex of management methods for increasing energy efficiency. Energy efficiency in the broad sense of the word can be considered as an effective use of energy resources. However, only the maximum of management methods can't achieve a result. Simultaneous introduction of administrative and technical measures is necessary. The reserve for application of this approach in Russia is truly enormous. Only in the scale of a city of 200 thousand people the economy at the expense of reducing costs is 150–200 million rubles per year.

Energy management is carried out on the basis of the following initial data:

- the analysis of project documentation (analysis of the compliance of the actual installed equipment, engineering communications, structural elements of design documentation);
- the analysis of the results obtained during the visual inspection;
- the analysis of the results obtained during the instrumental survey;
- the analysis of the energy consumption dynamics by type (hot water supply, heating, ventilation, electrical energy, cold water supply);
- the definition of specific indicators of energy consumption and their comparison with normative values.

Based on the results of the energy survey, an energy performance certificate for each facility is developed with a report on the mandatory energy audit (explanatory note to the energy performance certificate), which determines the amount of planned energy savings and a list of management decisions to improve energy efficiency.

To improve the efficiency of data collection and the development of the most effective management solutions, an automated monitoring system for life support systems is being introduced. The system provides automated collection of information from engineering systems located in the underground space of the city, accounting and control of resource consumption, control of the emergence of destabilizing factors and the transfer of operational information for the prevention and elimination of their consequences into a single center of operational dispatch management.

The main elements of the system are:

- specific sensors and data logging units;
- specific drivers for interaction with engineering systems of a certain class;
- servers for the integration and message processing by pre-configured algorithms;
- the control system for setting up the system operation rules;
- the geoinformation system for mapping and modelling the work of engineering systems;
- the system-transmitter of the data array.

The Centre for Operational Dispatch Control includes the following sectors:

- informational and analytical;
- analytical;
- prognostic;
- monitoring and administrative;
- executive.

The informational and analytical sector should contain the following documents:

- the information about distribution networks and volumes of consumption;
- the energy consumption standards;
- the technical and technological requirements for processes and equipment;
- the technical operating instructions;
- the environmental standards.

The analytical sector should include instructional materials:

- the methods for assessing the parameters of systems and technological processes and the state of equipment;
- the methodical manuals for the application of measuring equipment;
- the methods of analysis of the environmental situation in the controlled area.

The functions of the prognostic sector are:

- the forecast of the state of life support systems;
- the assessment of the dynamics of the development of the ecological situation in the municipal service area of responsibility;
- the preparation of information for making management decisions by the management of the relevant administrative or economic structure.

The monitoring and administrative sector should ensure the preparation of the necessary orders and regulations, as well as supervise and monitor the implementation of management decisions. An important element of the work of this subsystem is the adjustment of decisions when the current situation in the city changes.

The functions of the executive sector:

- the implementation of accepted management decisions;
- the implementation of a set of necessary measurements and the transfer of factual information to the employees of the analytical sector.

The information models of life support systems are formed as a result of the work of all sectors:

- the structural model of the distribution network;
- the model of the process of consumers energy supply;
- the specific models of distribution centres of nodes;
- the level model of the system with the indication of critical points;
- the mathematical models (equations of balances), etc.

The comparison of the model and actual data of the city life support state systems allows the most accurate assessment of technological and technical condition risks. On the basis of it timely administrative decisions which provide the maximum energy efficiency and resource-saving are made.

Capital investments for the creation of a territorial monitoring system, as shows the experience of the introduction of similar systems in the practice of other industries, pays off within several years [16].

At the same time, the effectiveness of the underground space development, energy management and monitoring of life support systems is determined not only by

economic, but also by social and environmental aspects. They are accounted for using a block of ecological and socio-economic monitoring.

Ecological and socio-economic monitoring is a complex study in which social, environmental (natural-technogenic) and economic conditions of the cycle “society - economy - ecology” are considered as equally important components of the functioning of each of its components. With reference to the present object of the research, ecological and socio-economic monitoring is a specially organized target systematic observation and short-term forecasting of the progress of the most important processes within the urban environment in the exploration of the underground space with the purpose of analysis and identification a range of regulating factors for decision-making.

The objects of the monitoring are the elements of the homosphere and the noxosphere interacting with the underground space of the city or forming part of it, the reaction of the natural and man-made environment, as well as the health and socio-economic well-being of the population to the changes that occur during the stage-by-stage development of the underground space.

The purpose of the monitoring is ensuring management of timely and reliable information. Its structural links are:

- the measuring system;
- the information system that includes databases of legal, technical-economic, social, sanitary-hygienic, medical and biological data;
- the systems of modelling and optimizing the performance of observables;
- the restoration and forecasting system of fields of ecological, economic and social factors;
- the system of decisions preparation.

The practical implement of the monitoring unit is based on the integration of geographical information system (GIS) and SCADA (Supervisory Control And Data Acquisition) software and hardware complex, which performs dispatching and data collection and their subsequent visualization of monitoring system data in GIS, so that all information from distant stationary posts of data collection about the environment, given out by the SCADA system, is displayed with an exact binding to spatial location.

It results in formation of an integrated information field of ecological and socio-economic monitoring, which ensures the operative information interactions of information producers through the introduction of discrete and continuous monitoring data, as well as the satisfaction of information needs of users through the information and telecommunications system in the existing information infrastructure.

The integrated information field of ecological and socio-economic monitoring is dynamically filled with diverse data of economic, social and environmental branches, links them together and provides a comprehensive assessment of urban development efficiency in the development of the underground space with visual representation of the results in the form of a “development scheme”.

The creation of such “scheme” will allow to effectively manage the main factors of sustainable development of the city in the development of the underground space and take into consideration all the influencing factors and aspects.

4 Discussion

The scientific novelty and significance of the received results consists in the following:

- for the first time an approach to the development of the city underground space with the introduction of a management and monitoring system for the urban environment, which includes blocks of geotechnical management and monitoring, energy management and monitoring of life support systems, ecological and socio-economic monitoring.
- Theoretical and practical aspects of the implementation of each block are considered, considering the specific features of the solvable tasks;
- The technology of underground space development was improved with the application of a protective screen made of pipes with adjustable resistance; the parameters of the stress-strain state of the system “advanced screen-massive” depends on the rigidity of the screen tubes section;
- The proposal of the ecological and socio-economic monitoring of the urban environment in the development of the underground space with the creation of an integrated information field and a visual representation of the results in the form of a “development scheme”. It allows to effectively manage the main factors of sustainable development of the city.

5 Conclusions

In accordance with the goal and on the basis of a set of studies carried out, the main elements of a management and monitoring system for the urban environment in the development of underground space were developed. It is aimed at solving two inter-related tasks: the increase of technical and economic and energy efficiency and the improvement of the urban environment quality.

The primary task of further research of the authors is to inform the municipal authorities about the advantages of this system, as well as to adjust and actively implement the system on the territory of the Russian Federation.

References

1. Korotaev, V.P.: *Gradostroitel'stvo* **6**(40), 38–48 (2015)
2. Denisova, Ju.V., Korenkova, G.V.: *Vestnik Belgorodskogo gosudarstvennogo tehnologicheskogo universiteta im. V.G. Shuhova*. 11, pp. 99–103 (2016)
3. Dashko, R.Je.: *Sovremennye problemy gidrogeologii, inzhenernoj geologii i gidrogeologoj Evrazii. Materialy Vserossijskoj konferencii s mezhdunarodnym uchastiem cjelementami nauchnoj shkoly. Nacional'nyj issledovatel'skij Tomskij politehnicheskij universitet*, pp. 150–155 (2015)
4. Parriaux, A., Blunier, P., Maire, P., Tacher, L.: *The DEEP CITY project: a global concept for a sustainable urban underground management*. In: 11th ACUUS International Conference, Underground Space Expanding the Frontiers. 10–13 September 2007, Athens, Greece, pp. 255–260 (2007)

5. Li, H., Parriaux, A., et al.: The way to plan a viable Deep City: from economic and institutional aspects. In: The Joint HKIE-HKIP Conference on Planning and Development of Underground Space. The Hong Kong Institution of Engineers and The Hong Kong Institution of Planners. Hong Kong, pp. 53–60 (2011)
6. Ou, C.-Y.: Deep Excavation Theory and Practice, p. 532. Taylor & Francis, London (2006)
7. Ilyichev, V.A., Golubev, G.E., Zamaraev, A.V., et al.: V sbornike: Rossijskaja arhitekturno-stroitel'naja jenciklopedija, pp. 118–120 (2008)
8. Kartozija, B.A.: Gornyj informacionno-analiticheskij bjulleten' (nauchno-tehnicheskij zhurnal) **1**, pp. 615–630 (2015)
9. Kulikova, E.Ju.: Gornyj informacionno-analiticheskij bjulleten' (nauchno-tehnicheskij zhurnal) **6**, pp. 222–226 (2014)
10. Kaloshina, S.V.: Vestnik Permskogo nacional'nogo issledovatel'skogo politehnicheskogo universiteta. Stroitel'stvo i arhitektura **7**(3), 78–90 (2016)
11. Bhatt, M.: J. Siberian Fed. Univ. Humanit. Soc. Sci. **2**(6), 257–264 (2013)
12. Semjonova, O.S., Kolomasova, S.A.: Gradostroitel'stvo **3**(31), 53–60 (2014)
13. Prokopov, A., Prokopova, M., Rubtsova, Y.: Year the Document was Publish 2017 Source of the Document MATEC Web of Conferences. vol. 106, p. 02001 (2017)
14. Rossinskaya, M.V., Rossinskiy, N.P.: Year the Document was Publish 2014 Source of the Document Life Science Journal. 11 (SPEC. ISSUE 11), 43, pp. 198–200 (2014)
15. Pleshko, M.S., Stradanchenko, S.G., Maslennikov, S.A., Pashkov, O.V.: ARPN J. Eng. Appl. Sci. **10**(1), 14–19 (2015)
16. Molev, M.D., Stradanchenko, S.G., Maslennikov, S.A.: ARPN J. Eng. Appl. Sci. **10**(16), 6787–6792 (2015)

Integrated Approach to the Improvement of the Information Support of Management During the Transporting and Distribution of Heat

Natalia Verstina¹  and Evgeny Evseev² 

¹ Moscow State University of Civil Engineering,
Yaroslavskoye Shosse, 26, Moscow 129337, Russia
verstina@mail.ru

² Moscow Institute of Physics and Technology (State University),
9, Institutskiy per., Dolgoprudny, Moscow Region 141701, Russian Federation

Abstract. The current performance of heating systems of the centralized heat supply does not provide reliability of heat transportation and distribution processes due to existence of considerable wear. The analysis of damageability of the heating systems is submitted, where the authors noted the prevailing type of the reasons of their emergence, which are the corrosion processes. The matter of defining methods of their diagnostics, which were established within the Russian practice by hydraulic tests, is considered depending on the identified types of damages. The research of their positive and negative aspects allowed to present the integrated approach to the improvement of information support of managing transportation and distribution of heat. It is suggested to form it on the basis of joint consideration of technical, organizational and economic aspects of the organization of information formation processes in heat-supply organizations. At the same time, the authors pointed out the need of the use of the economic indicators along with the data of technical control.

Keywords: Transporting of Heat · Distribution of heat · Energy Management
Transport Buildings and Structures · Energy Efficiency

1 Introduction

Considering the use and producing resources, the subjects of energy industry in the Russian Federation are on the leading positions and have the world's largest resource power supply sources, which in case of energy saving, will be able to provide the needs of our country and to provide export inquiries from other countries in the long term of three next decades, bringing up to 70 percent of export revenue of Russia. The supply of the consumers with heat making object of activity of the heat supply organizations (HSO) draw special attention of the professional community in the field of preservations of energy resources during the transporting and distribution of heat [1–3]. Many changes which are constantly arising because of the introduction of new programmes of development and reforming of housing-and-communal services in the Russian

Federation, adoption of various regulations on power supply, long-term state programmes of the development of the industry in the Russian Federation, relevant toughening of the responsibility of subjects of power supply and also the growth of the competition between the suppliers of energy resources cause the need of changes in the sphere of management of modern HSO [4]. First of all, that affects the development of the competition in the Russian Federation between the almost monopolistic structures, which exist in the previous years (HSO of systems of the centralized heat supply, which perform the delivery of heat from the combined heat and power plant to consumers) and the subjects, which belong to the decentralized heat supply and which have received the increasing spread recently. Actually the development of “big power system” and the centralized heat supply in Russia has stopped for the last two decades: heat supply by the combined heat and power plant was reduced by 35%, the contribution of the branch to economy of Russia has decreased to 2.5% of GDP [5, 6].

In this regard the providing of desirable competitive positions of the suppliers of heat directly depends on the quality of management in the organization, on the existence of opportunities of the complex approach to the improvement of management during the transporting and distribution of heat, to adequately assess current situation and to react to it. [7–9] As a rule, the analysis of conditions of activity and the formation of the new principles of management demanded by the current situation of energy saving on HSO make up the core of all the decisions on improvement. However, as the researches of authors prove, HSO of systems of the centralized heat supply are rather conservative, concerning the applied management tools. According to some expert data in 2014 to 3% of sources of heat and 70% of heating systems were operated outside standard service life and that became the reason of losses of resources because of the growth of accident rate and low efficiency of the operated equipment. In particular, losses of the valuable resource – heat when transporting on heating systems reach by different estimates 30% reach that several times exceeds the similar indicator in the developed countries. In this regard the energy saving potential concluded in activity of the Russian HSO which by expert estimates makes up to 20–25% of all volume of the delivered resources now that, is at least three times higher, than the actual losses on the similar profile the foreign enterprises is obvious.

High losses of heat at the Russian enterprises of heat supply are the consequence of numerous damages of heating systems due to which the term of their service decreases by 1.5–2.5 times over the standard term. Even in the organizations, which joined large modern power holdings as a result of transactions in the markets of corporate control, the motivation to updating of the principles of management is not always observed. Traditional approaches, especially regarding power management of the primary production activity are mainly used.

2 Materials and Methods

Considering the matters of improvement of management during the transporting and distribution of heat authors offer the approach, which is based on the analysis of service conditions of heating systems, and also by definition of nature of information support of management on the basis of control methods of their performance. Nowadays

domestic and foreign practice of monitoring procedure of technical condition of heating systems recognizes a significant amount of the methods, based on various technical and technological base of carrying out, which provides various results on the main substantial characteristics. These provisions make possible the comparison of control methods, allowing to carry out the definition of the best methods of the destroying and nondestructive control depending on the specifics of the heating system under maintenance.

The analysis of damageability of the HSO heating systems, which make possible the transportation and distribution of heat was taken as the initial materials of a research. The materials, received as the result of the research, confirmed the pessimistic estimates, which were stated by other experts: more than a half from 200 thousand km of backbone heating systems already exhausted the maintenance period, at the same time approximately to 20% are in the critical performance, that requires the annual changeover of the pipelines of 10–12% of the general expansion of the heating systems [10].

Besides, high losses of heat at the Russian HSO are the consequence of numerous damages of heating systems due to which the period of their service decreases by 1.5–2.5 times over normative. The reasons of such essential distinctions - are obvious: they are the poor quality of the spacer of heating systems during the socialist and transition periods of our history, the existence of hostile environment of operation and other reasons of the technical plan. We should mention, that the heating systems of such a large capital megalopolis represent the most characteristic pattern of the domestic centralized heat supply according to types of constructions of engineering systems, conditions of their operation, and also the “history” of the centralized heat supply numbering nearly hundred years. Comparing with other developed countries proved that the Russian HSO of the centralized heat supply take the leading positions on the expansion and on the volume of the delivered heat, their share is more than 40 percent of volume of the deliveries on a global scale. The group of the capital cities of Denmark, Sweden, Finland is evidently selected among the most comparable, for example, with the Moscow operating conditions of heating systems. However, the expansion of networks of the centralized heat supply is rather small and makes respectively 2, 5 and 7% in comparison with the general expansion of heating systems of Moscow. The number of the combined heat and power plant generating heat differs more that by 5 times: there are 15 plants in Moscow, while there are 3 plants in Stockholm and Helsinki, there are 4 plants in Copenhagen. At the same time the damageability significantly differs to the best. This circumstance generated the paradox found by the authors - the analysis of control methods is the most demonstrative for the more “abnormal” Russian experience [11].

The technical methods of diagnostics of heating systems, the positive and negative aspects of their application on the example of operation of backbone heating systems of Moscow were analyzed, considering information support of management. The total characteristic of the damageability of heating systems from the corrosion during the transporting and distribution of heat, which is the basic reason, is presented in Table 1.

Despite the obvious prevalence of corrosion damages it is impossible to neglect the damages of not corrosion character (up to 10% of total amount), which also need to be diagnosed. Their quantitative characteristics, presented in Table, 2 were revealed.

Table 1. Distribution of types of damages from outside and internal corrosion, depending on types of a spacer of backbone heating systems

Type of laying of pipelines	External corrosion			Internal corrosion		
	Fistulas	Gaps	Cracks of a welded seam	Fistulas	Gaps	Cracks of a welded seam
1. Chanceless channel	85.6%	14.3%	0.1%	91.5%	8.4%	0.1%
2. Semi-chanceless channel	84.8%	30.7%	0.2%	87.7%	10.9%	1.4%
3. Channelless polyurethane foam	80.32%	19.68%	–	76.48%	11.76%	11.76%
4. Channelless reinforced foam concrete	68.4%	31.6%	–	66.67%	33.33%	–
5. Sleeve case	85.5%	14.5%	–	100%	–	–

Table 2. Types of not corrosion damages of heating systems, which should be necessarily warned by the methods of technical diagnostics

Pattern of damage	Number of damages (%) of total corrosion damages
1. Cracks of a welded seam	18.3%
2. Through crack of a welded seam	15.5%
3. Fistula because of defect of welding	43.5%
4. Mechanical deformation of a pipe without leak	2.2%
5. Mechanical deformation of a pipe with the advent of leak	14.2%
6. Defect of a pipe metal	0.3%

We can conclude according to the Tables 1 and 2 the fistulas and gaps from defect of welding and mechanical deformation of the pipe exist beside the fistulas and gaps from corrosion. According to the results of the considered materials we have concluded that there are some principles of the choice of control methods for information ensuring management during the transporting and distribution of heat [12]: (Table 3)

It is possible to call the rest of not revealed defective zones in heat network economy of HSO the error of the method. The additional positive effect of HT is the fact that the repairs, made during the summer period will not pass into the heating period with big losses of more hot network water which will cause additional losses of heat. In this case it is possible to consider that HT reveals the weak points which are inevitably demanding further repair. The disadvantage of pressure testing, as diagnostics method, it is possible to consider, the fact that only the pipeline zones which are in the margin performance are found. It is important that in technical aspect it is provided when carrying out HT implementation application of the uniform technological modes of excessive pressure at the HSO one and all the network including

Table 3. Data on the gaps by years of maintenance for the period of 2011–2015

Mode	Quantity of damages (fistulas and gaps) on the giving pipeline to 24 kgfs/cm ² ; on the return pipeline to 20 kgfs/cm ²							
	15.05.11 - 30.09.11	01.10.11 - 15.05.12	15.05.12 - 30.09.12	01.10.12 - 15.05.13	15.05.13 - 30.09.13	01.10.13 - 15.05.14	15.05.14 - 30.09.14	01.10.14 - 15.05.15
during pressure testing	2511	408	2124	217	1583	224	1825	75
during maintenance	33	141	84	99	41	118	76	102
during hydrolic tests	60	0	36	1	77	0	124	2
per 1 year	3153		2561		2043		2204	
total per 4 years and average per 1 year	9961 and 2490.25							

those, which have been under maintenance (with the term from 1 to 10 years of service) [13]. This technologically caused association within HT negatively affects certain parts of pipelines of smaller diameters: on sites of heating system with wall thickness to 1 mm pressure of 2.5–3.0 MPas (25–30 kgfs/cm²) will be required, small diameters of pipes demand considerably greater pressure.

Such technical disadvantages of HT have caused a question of their efficiency, even taking into account the universality of workmanship of the method. The need of gradual exception of HT form practice of the Russian HSO became obvious. The analysis of foreign practice and the specifications and technical documents regarding the regulation of the approaches to the improvement of the maintenance has proved that standard provisions allow pressure testing by elevated pressure only at the stage of test of pipes during production and during acceptance of ready structures. Therefore the question of full or partial refusal of pipelines of heating systems are for a long time discussed considering the traditional approach to ensuring energy saving [14, 15].

However, in our opinion, the unilaterality of such approach excluded a possibility of receiving definite answer to a question of full information support of management during the transporting and distribution of heat [4, 5].

3 Results

According the materials of statistics of damages of heating systems during the transporting and distribution of heat, and also according the research of the market of devices of diagnostics and control methods on their basis, the number of results which allow to pass to an integrated approach to information support of management to HSO by minimization of volume of application of HT has been obtained. When carrying out HT, the HSO are guided by the identification of the greatest possible number of damages to the preventive mode [16–19]. We will record it as a final reference point and we will define its providing on the basis of other approach - from positions of carrying out the complex of actions. As it was mentioned earlier - the most popular expert belief consists that possible technical solutions in this direction have to provide when replacing HT with the methods of nondestructive 100% control of the surface of pipelines regarding identification of damages. In our opinion, the is a rather “narrow” vision the solution of the matter, raised in the research. As a result of the expansion of the range of the matter it is possible to note that there are several necessary conditions of refusal of carrying out HT of heat conductors which are differentiated into three groups. They are also make up the basis of full information support of management during the transporting and distribution of heat in the condition of minimization of volume of HT:

- the first, “technical” group of conditions includes:
 1. Carrying out nondestructive control including continuous control of thickness of the pipe wall and continuous control of the intense deformed performance on the basis of a certain combination of various technical methods, guaranteeing information, comparable to HT, and necessary for the managerial decisions making, which is based on the standard requirements to the heating system maintenance;
 2. Identification of 100% of defective sites by nondestructive control of heating systems. The elimination of those defective sites will allow to increase the maintenance interval without refusals and tests on the checked site up to 5–7 years (this term is accepted approximately by analogy with the successful practice of maintenance of gas systems where in-line inspection is carried out once in 5–7 years). That also allows to provide phased transition to full inspection of all the economy of the heat supply enterprise in the prospect.
- the second, “organizational” group of conditions includes:
 1. Providing of managerial decisions on carrying out local repair of complex character according the results of nondestructive control [20]. Those decisions include volume, structure of works, which will include elimination of consequences and

reasons of the corrosion factors operating on the surveyed network site and also the available factors during the transporting and distribution of thermal energy, the defiant critical intense deformed pipeline conditions. Thus it will become possible to provide the complex of managerial decisions, connected with the elimination of the reasons of losses of heat on HSO;

2. The organization of system control of technical performance of heating systems with the accumulation of retrospective database, their statistical processing and the analysis, which results will allow to carry out reliable forecasting of the performance of heating system, providing the opportunity to obtaining objective information on transportation and distribution of heating systems in scales of the whole HSO for managerial decisions making on ensuring energy saving in the advancing mode on the basis of modeling of processes of emergence of damages at the HSO heating systems.

– the third, “economic” group of conditions include:

1. Concentration of enough investment financial resources (including credit resources) for ensuring financing of actions for repair for achievement of reduction of the saved-up wear more in high gear, than it is carried out on the basis of carrying out HT in the scales of the whole heat supply enterprise.
2. Obtaining of economic effect of application of the certain methods of nondestructive control, replacing HT on the selection of sites of heating systems, allocated according to certain principles in the scales of all operated HSO of systems which is defined on the basis of comparison of values of a complex of technical-and-economic indicators them characterizing them.

As for authors, the combination of a complex of these conditions allows to carry out the improvement of information support of management during the transporting and distribution of heat in modern conditions. We will characterize in details the integrated approach in the aforesaid aspects: technical, organizational, economic.

The first group (specifications) are in priority and have to be considered during the transporting and distribution of heat first of all. Their application resolves “the matter of replacement of HI” at the level of the current activities for the heating systems maintenance. But at the same time the second and third groups can provide a new foreshortening of the solution of the matter, transferring it from “plane” perception as replacement of one technology (destroying) to others (nondestructive) within technical system of the heat supplying enterprise - in “volume” vision of the perspective at higher level of the decisions made at HSO within its organizational-and-economic systems. The feature of the new integrated approach is the following: the analysis of the current situation of transportation and distribution of heat has proved that the accounting of data on the heating systems maintenance in the most various forms is carried out, however, the essential dissonance between the character of information which has HSO and the opportunity to receive some realistic assessment of energy saving and to take the appropriate measures is observed. The lack of the expressed target orientation of systems of data collection is the reason of the situation. The idea of the use of data for forecasting of a condition of all the economy of HSO actually is

implemented in the most perspective options from the point of view of management. Within orientation of such systems to creation of new quality of information support of management – beginning from standard requirements for transportation and distribution of heat, finishing with planning of actions for minimization of losses of energy in scales of all economy of HSO for the account planning of actions for the stage-by-stage replacement of unreliable sites it is possible to pass reasonably and gradually to the replacement of HT.

The substantial characteristic of monitoring of the data on transportation and distribution of heat has been published earlier by authors, therefore in this research presents its new aspect, which is economic, detailing the 2nd group position [21]. During the choice by economic criteria of the methods of monitoring procedure of technical performance of the heating systems, alternative to HI it is necessary, having recorded the quantitative characteristics of damageability of the heating systems, to create a complex of the technical means, allowing to perform the required measurements and to determine expenses by these two options which structure owing to technological features of methods will differ evidently on various types of laying. The carried-out calculations have proved that the use of a number of methods of nondestructive control as HI alternatives for the off-channel laying and chanceless channel laying is justified at damageability counting on 1 km at the level of 3–4 units on diameters of 600–1400 mm. A bit different results dismiss similar character on so-called “small diameters” - in the presence of a small amount of damages by the most economic there are HI. We will note that the received results cannot act as the exhaustive economic justification for the improvement of information support of management during the transporting and distribution of thermal energy on the basis of monitoring of the heating systems given about a state, but at the same time they allow to start the process of the transfer of “centre of gravity” in the solution of “long-term” questions in activity of HSO from the technical aspect to the management aspect [22].

4 Discussion

According to the established practices of management during the transporting and distribution of heat on domestic HSO the question of the organization of its information support on the constant basis including the analysis of foreign and domestic experience of a regulation of this activity regarding search of additional reserves of improvement was not considered. According to the authors, the core of the development of regulations is the certain backbone idea, universal for all the HSO which are carrying out transportation and distribution of heat to consumers. In this aspect the Russian experience, as well as regarding the analysis of prospects of replacement of HI, can be used for the development of the integrated approach to the information support of management at HSO.

The analysis has proved that only in two countries using the developed systems of the centralized heat supply (Russia, Belarus), the standards of the state level have fixed requirements for ensuring the industrial safety (IS) of the heating systems obliging the HSO in the legislative order to carry out any expertize of the heating systems

performance by the means of the external expert organizations.” [23]. It can act as “common denominator” for the development of regulations of HSO. We will note that the research completed by the authors has proved that in other countries there are no requirements from the state for providing IS of heating systems. The greatest number of the countries using the systems of the centralized heat supply is concentrated in Europe - up to 85 percent from the total number. The main document for these countries is the Directive on the use of the working equipment [24]. According to it the safety during the transporting and distribution of heat is the responsibility of the HSO only. In each EU country, there is its own option of the performance for example, such law in Great Britain is called PUWER, in France it is called - Décret No 93-40, and in Germany it is called Own rules of the industrial safety [Betriebssicherheitsverordnung (BetrSichV)]; in Austria it is the Act of occupational health and safety measures [Arbeitnehmer Innenschutzgesetz (ASchG)]. In the countries of the former Soviet Union there is no state regulation of IS. For example, in Kazakhstan the approach of the EU, concerning regulation of fire safety, fixed at the legislative level, has been apprehended. Moreover, the text of the law On civil protection N 188-V dated 11.04. 2014 do not include the heating systems in the two types of hazardous production facilities (the enterprises and technical devices) [25, 27, 28]. For this reason the uniform approach to the providing the reality in the regulation of control of processes transportation and distribution of heat is absent in these countries, the information in open access is not enough, while the Russian practice is rather well presented and suitable for any generalizations.

Providing the IS on the vast majority of domestic HSO is characterized by the existence of internal regulations according to IS, which is created on the basis of generalization of practical experience of personnel of the enterprise. However, modern conditions define absolutely other trend of the development of management during the transporting and distribution of heat. Its novelty consists in the definition as a part of internal regulations of HSO obligatory to the execution and the requirements to the accuracy of the taken measurements of the guaranteeing IS, to establishment of the nomenclature of the data and rules of their interpretation, received during conducting examination of the heating systems performance, recommended for the prospect and, above all the accurate regulation of the purpose of examination of IS and the directions of its achievement. Now such statement have not been presented in the regulations of the HSO level of the requirements. We consider the expedient to offer to discussion the following offers on their substantial filling taking into account the practice of conducting examinations of IS:

- regulations provide the existence of the passport of the pipeline (with the scheme of the heating systems) in which we should note systematically: the flooded sites of pipelines; sites where the turn was made; sites where corrosion and other damages of pipelines were observed; places where shurfing was carried out or were opened pipelines for external examination, other engineering constructions which are available near the considered site of thermal network have to be applied on the scheme;
- it is necessary to create the characteristics of technical performance of each element of heating systems from the positions of effective and timely holding recovery

- actions in case of recognized need for an operational assessment of results of control of processes of transportation and distribution of heat to develop in the regulation;
- as the element of preliminary preparation for conducting examination, it is important to have the technique uniting an assessment of technical condition of heating systems, according to the damageability and an assessment of technical performance of heating systems, according to control of processes of transportation and distribution of heat demanded information.

The aforesaid positions are not, in our opinion, exhaustive, however, can be the basis for the further discussions concerning contents of regulations of HSO in the aspect of the improvement of the information support of management during the transporting and distribution of heat.

5 Conclusions

Thus, the carried-out analysis of the opportunities and directions of the improvement of information support of management during the transporting and distribution of heat has been caused by the objective requirements of modern domestic heat supply in which structure of subjects the shift of preferences of consumers of energy resources from large HSO of systems of the centralized heat supply to local sources of thermal energy is observed. The main reason for the developed situation -is the high damageability of heating systems caused first of all by the saved-up wear of heating systems of the centralized heat supply which constantly collects is noted. Overcoming such negative situation is possible first of all due to improvement of information support of management of HSO objective information on the processes of transportation and distribution of heat which has to be based on the objective data of control of technical condition of heating systems. The carried-out analysis of damageability of heating systems has allowed to define quantitatively the ratio of corrosion and not corrosion damages of heating systems, at the same time an important condition of objectivity of an assessment is also diagnostics of the reasons of not corrosion damages despite their low share in the general structure of refusals during the transporting and distribution of heat. The research of practice of application of the hydraulic tests (HT) characteristic of the Russian practice of control of the performance of heating systems have allowed to define their advantages and disadvantages. These results have formed the basis for the development of the integrated approach to the improvement of information support of management during the transporting and distribution of heat which according to offers to authors has been based on the joint accounting of technical, organizational and economic aspects of the organization of processes of formation of information in HSO. The provisions on the organization of internal regulations of HSO are presented, which are created on the basis of the analysis of experience of ensuring the industrial safety regulated in the Russian conditions from the state which oblige to exercise control of technical condition of heating systems on the constant basis are offered.

References

1. Arseniev, D.G., Rechinskiy, A.V., Shvetsov, K.V., Vatin, N.I., Gamayunova, O.S.: Appl. Mech. Mater. **635–637**, 2076–2080 (2014). <https://doi.org/10.4028/www.scientific.net/AMM.635-637.2076>
2. Četković, J., Rutešić, S., Zarković, M., Knežević, M., Vatin, N.: Primary directions and advancements in competitiveness of montenegrin construction sector. *Procedia Eng.* **117**, 775–785 (2015)
3. Porter, M.: *Competition*. Williams, Moscow, p. 608 (2014)
4. Verstina, N., et al: *Open Access J. Naukovedenie.* **85**(36), 12 (2016)
5. Verstina, N., et al.: *J. Econ. Entrepr.* **9**(74), 967–972 (2016)
6. Kubyshkin, Y., et al.: *Aktual'nye problemy gumanitarnykh i estestvennykh nauk*, vol. 12-2, pp. 4–7 (2015)
7. Chulkova, A., Lukiche, S., Romanovich, M.: *MATEC Web of Conferences*, vol. 86, p. 02019 (2016). <https://doi.org/10.1051/mateconf/20168602019>
8. Verstina, N., Meshcheryakova, T.: *Biosciences Biotechnology Research Asia*, vol. 12-2 (2015)
9. Jevric, M., Romanovich, M.: *Procedia Eng.* **165**, 1478–1482 (2016). <https://doi.org/10.1016/j.proeng.2016.11.882>
10. Simankina, T., Romanovich, M., Tsvetkov, O.: *MATEC Web of Conferences*, vol. 53, p. 01054 (2016). <https://doi.org/10.1051/mateconf/20165301054>
11. Romanovich, R., Vilinskaya, A.: *MATEC Web of Conferences*, vol. 53, p. 01052 (2016). <https://doi.org/10.1051/mateconf/20165301052>
12. Panteleeva, M., Borozdina, S.: *MATEC Web of Conferences*, vol. 106, p. 080471 (2017)
13. Meshcheryakova, T.: *MATEC Web of Conferences*, vol. 106, p. 06021 (2017)
14. Mottaeva, A.: *Methodological approaches to identification of clusters in regional economy system*. In: *MATEC Web of Conferences*, p. 08071 (2017). <https://doi.org/10.1051/mateconf/201710608071>
15. Rozhentsova, I., Mottaeva, A.: *Terms of orientation on customer needs in the housing sector*. In: *MATEC Web of Conferences*, p. 08076 (2017). <https://doi.org/10.1051/mateconf/201710608076>
16. Priadko, I.N., Mushchanov, V.P., Bartolo, H., Vatin, N.I., Rudnieva, I.N.: *Mag. Civ. Eng.* **65** (5), 27–41 (2016). <https://doi.org/10.5862/MCE.65.3>
17. Chibisova, E., Zinatullin, A.: *Strategy of sustainable development of regions of Russia*. vol. 5, pp. 324–328 (2011)
18. Akimova, E.: *MATEC Web of Conferences*, vol. 106, p. 01043 (2017)
19. Verstina, N.: *MATEC Web of Conferences*, vol. 106, p. 08091 (2017)
20. Miroshnikova, T., Taskaeva, N.: *MATEC Web of Conferences*, vol. 106, p. 08093 (2017)
21. Kisel, T.: *MATEC Web of Conferences*, vol. 106, p. 08094 (2017)
22. Glazkova, V.: *MATEC Web of Conferences*, vol. 106, p. 08095 (2017)
23. Vasilyeva, E., Polyakova, I.: *MATEC Web of Conferences*, vol. 106, p. 08097 (2017)
24. Karakozova, I., Pavlov, A.I.: *MATEC Web of Conferences*, vol. 106, p. 08046 (2017)
25. Stein, E.: *MATEC Web of Conferences*, vol. 106, p. 01036 (2017)
26. Saari, J., Sermiyagina, E., Kaikko, J., Vakkilainen, E., Sergeev, V.: *Energy* **113**, 574–585 (2016). <https://doi.org/10.1016/j.energy.2016.06.102>
27. Sergeev, V.V., Aleshina, A.S.: *Thermal Eng.* **58**(3), 268–270 (2011). <https://doi.org/10.1134/S0040601511030116>

Methodic Approach to Energy Costs Reduction on the Basis of the Energy Service Contract

Tatiana Meshcheriakova^(✉)  and Natalia Verstina 

Moscow State University of Civil Engineering,
Yaroslavskoe Sh., 26, 129337 Moscow, Russia
t.meshcheryakova@mail.ru

Abstract. On the basis of energy consumption management process studies under conditions of ESC use at the industrial enterprise it was revealed that in contrast to the traditional approach to energy saving, the approach based on ESC allows imposing the responsibility for the implementation of required activities and risks in achieving the declared results on ESCO. With account of this, authors decided to lay in the basis of economical evaluation of ESC the mathematical model for estimating the real option cost, which allowed considering its specifics. The calculated data on the real option cost allow concluding that ESC cost grows significantly. The article presents the following highlights: the analysis of energy saving issue and energy efficiency enhancement in the Russian Federation on the basis of Federal documents; the process of energy consumption management organization is based on Deming cycle of continuous improvement in accordance with ISO-50001 principles; justification of energy saving procedures as part of the Energy Service Contract using three calculation options: withholding activities, timely performance of activities, multistage performance of activities; application of real options method when evaluating a multi-stage project, which allows consideration the specific risks of energy service.

Keywords: Energy Service Contract · Energy Management · Energy efficiency

1 Introduction

The key engine of the global energy demand is the growth of population and income. Demographic studies over the last two decades show a population growth 1.6 billion people. Based on forecasts of international organizations in the field of power engineering and energy cooperation, the global Gross Domestic Product (GDP) growth is predicted to accelerate from 3.2% per year to 3.7% till 2030. This trend assumes enhancing per capita income growth. In this context, energy efficiency, defined by energy consumption per unit of GDP should enhance at a growing rate. Such acceleration requires the containment of the total growth of primary energy resources consumption. By energy resources of an industrial enterprise are meant all available resources consumed in the functioning and production processes of an enterprise and involved in mutual settlements between subdivisions and with external suppliers. They comprise: electric energy, thermal energy, various industrial gases, special fluids and others.

Based on the concept of long-term socio-economic development of the Russian Federation till 2020, a change of the national economy from the source-based to source-innovative type of development takes place. This assumes, among others the stimulation of strategic initiatives in the field of energy saving. Active attraction of investments for implementation of activities in the field of energy saving and energy efficiency enhancement is one of the main tasks of the State Program "Energy saving and energy efficiency enhancement". In this matter, a state-of-the-art mechanism of the implementation of energy saving procedures merits special attention - the Energy Service Contract, which implementation practice in the territory of the Russian Federation does not have yet pronounced character, despite the reasonable relevance of the mechanism, set in the Energy Strategy of the Russian Federation [1]. The developed approach to implementation of the Energy Service Contract includes an organizational component and justification model of activities as part of the project with the use of real options method and Blake-Scholz mathematical model for multi-stage performance of energy-saving procedures. A mathematical model allows determining the potential economic effect of the Energy Service Contract taking into account possible risks of an energy service company.

Following the analysis of official data and scientific research on the costs of energy resources and development trends of various economy sectors, it was determined that the industrial sector has the greatest potential for energy saving. The energy-efficient industrial sector development is one of priority tasks of the state policy.

According to British Petroleum forecasts, until 2030 almost all demand for energy resources (about 96%) falls on the countries, which are not members of the Organization for Economic Co-operation and Development (OECD), where the energy consumption for the predicted period (until 2035) will grow by 2.2% per year, compared with 0.1% per year in the countries which are members of the OECD, where from 2030 the level of primary energy resources consumption will begin to decrease [1]. The growth of energy consumption mainly provides countries which are not members of the Organization for Economic Cooperation and Development (OECD) countries, including Russia. In the OECD countries by 2030 the energy consumption is predicted by 4% higher, and in countries which are not members of the OECD by 69% higher compared to the level of 2010.

According to researches, the tendency of industry influence on macroeconomic indicators of the economies power consumption is weakened. Since 2000, the industrial sector was the fastest growing sector in terms of power consumption indicators (annual growth was 2.7%). However, the reduction of annual energy consumption growth in the industry is forecasted to be 1.4% by 2035. Energy consumption indicators will grow in the service sector, municipal sector and agriculture up to 1.6% per year. Energy consumption indicators in the transport sector have not expressed changing tendency, a steady growth in consumption by 1.2% per year is predicted. Thus, the transport does not play a significant part in the overall growth of the global energy consumption.

The economic development of the Russian Federation and other countries beyond the OECD is ensured due to the increase in consumption of all types of fuel resources [2]. The energy intensity of the Russian economy is significantly higher than in the states-members of the OECD, as shown by tendencies of change in the energy demand by sectors (Fig. 1) [3–5]:

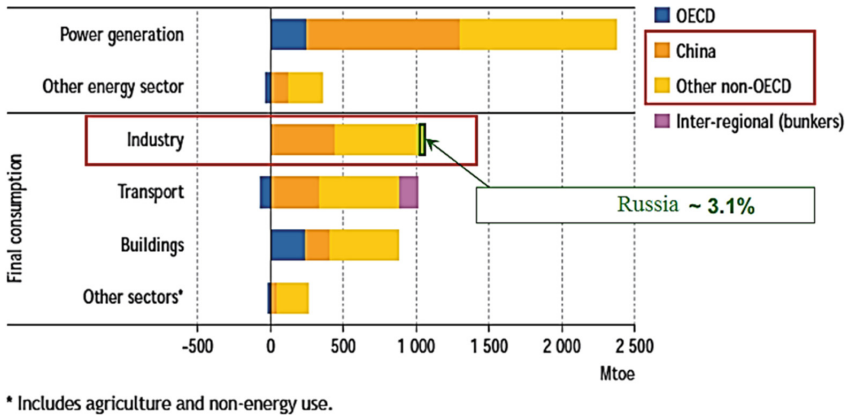


Fig. 1. Energy demand by sectors and countries, 2008–2035.

High volumes of global power consumption and significant energy resources costs have led to the fact that the issues of energy efficiency enhancement, production energy intensity reduction and widespread implementation of energy saving technologies currently obtained the particular relevance. Modern development of the national economies is focused on innovative modernization, which must take place under conditions of the most rational use of energy resources, increasing energy efficiency of the existing equipment and, therefore, increasing effectiveness of technological processes in power systems.

At the present time, the volume of inefficient use of energy in the Russian Federation is equal to the annual consumption of primary energy in France. Investments of governmental and private organizations, as well as households in the amount of US\$320 billion will be needed for the realization of power efficiency enhancement potential. These investments will result in annual savings for end consumers in the amount of about US\$80 billion and could be paid back in just four years. Annual economic effect from savings in energy resources and additional revenues on the gas export is significantly higher: US\$120–150 billion. By realizing the potential of energy efficiency enhancement, the Russian Federation will be able to save: 240 billion cubic meters of natural gas, 340 billion kWh of electric energy, 89 million tons of coal, 43 million tons of crude oil and its equivalent in the form of refined petroleum products [3–5].

In accordance with the plan of the Ministry of Energy of the Russian Federation, its key objective is to improve the management system that ensure the effective implementation of the state policy in the field of energy saving and energy efficiency enhancement, including due to stimulation of mechanisms of extra-budgetary funds attraction in the implementation of energy saving activities and energy efficiency enhancement [6]. The basic investment mechanism of energy saving can become the Energy Service Contract, which approved itself in Europe and the USA a long time ago. The cost-effectiveness evaluation of the energy service company funds use, which differs by the specific technical and financial risks for energy-saving projects, takes on the important significance.

2 Materials and Methods

Use of the developed model of the energy consumption management organization makes it possible to use the set of methods for practical implementation of energy saving procedures taking into account current conditions and tendencies enterprise development.

On the basis of the implementation stages of the package of energy saving procedures, four blocks of the energy consumption management organization model:

- determination of power consumption economy reserves;
- forming a complete list of possible energy saving activities;
- implementation of energy saving activities on the basis of the Energy Service Contract;
- energy saving results monitoring (Figs. 2 and 3) [7].

As a result of the energy audit carrying out, as a rule, ESCO proposes to the enterprise sufficiently large number of energy saving measures (ESM). In practice, the decision making on composition of activities and sequence of their fulfilment is subjective until now. In this regard, the author proposed the methodical approach to the formation of the composition of activities, based on the selection of preliminary grouped variants, evaluation of which is carried out iteratively. It allows taking into account to the full extent equipment operation features in combination with possible terms and stages of the ESC fulfilment.

Calculation of the planned effectiveness of energy-saving activities shall be carried out taking into account modern methods of investment evaluation. The sequence of the ESM effectiveness calculation is developed on the basis of NPV comparison for different cash flow variants [7–12]: variant 1 (Z1) – static system (consideration of a case of forecasting energy consumption for the power system without ESM); variant 2 (Z2) – dynamic system (one-time investment in one or several energy efficient procedures); option 3 (Z3) – dynamic system (step-by-step investment in energy efficient procedures, taking into account the scale of a project) (Fig. 4).

Comparison of 3 implementation options of energy saving activities consists of sequential steps:

1. Input of calculation parameters characterizing ESC proposed by the author:
 - Nyear – predicted number of years of the energy saving procedures implementation;
 - Ny1 – number of fixed points for simulation of the energy saving procedures implementation schedule (usually 12, that corresponds to the number of months in the year, however, quarterly calculations are also used);
 - zdiscount – discount rate;
 - nopt – number of time lags for option conducting (for how many stages it is planned to divide the project);
 - iyearopa(I) – i-th year, at the end of which the option is realized;
 - alphopa(I) – share of the equipment, replaced in the i-th option;
 - z1 – annual energy consumption of the operating equipment unit, in rubles;
 - c1 – cost of the equipment unit;

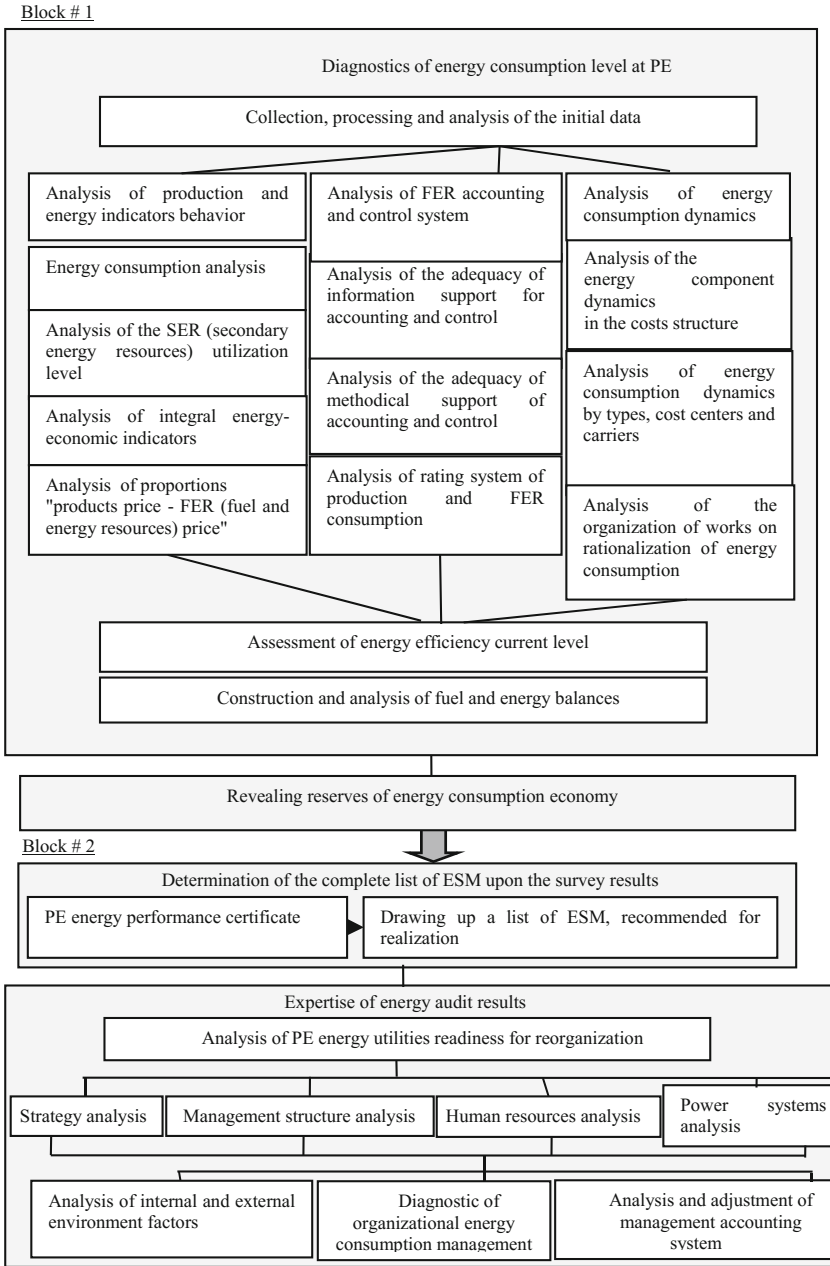


Fig. 2. Policy of energy consumption management organization.

Block # 3

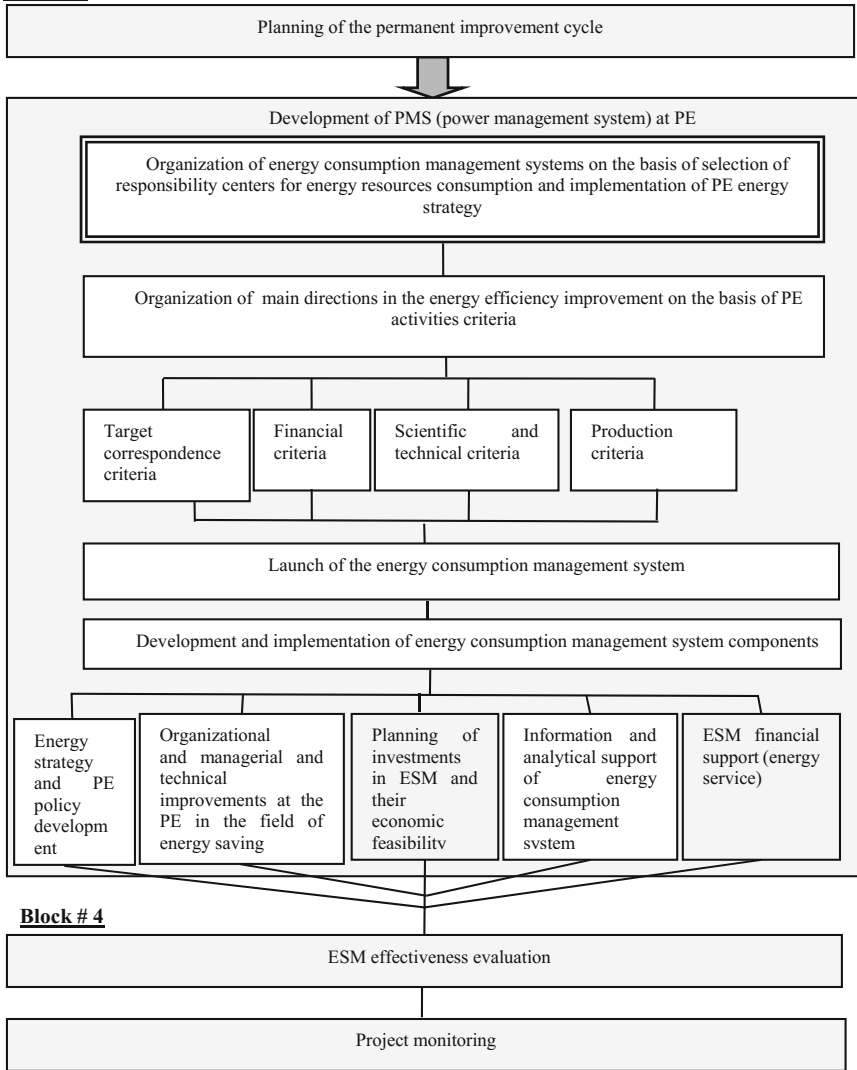


Fig. 3. Policy of energy consumption management organization (continued).

- ca2 – cost of tools (additional component parts) required for installation of the energy-saving equipment;
- term1b1p1, term1b1p2 – minimum and maximum operational life of the operated equipment, years;
- term2b1p1, term2b1p2 – minimum and maximum operational life of the energy saving equipment, years;
- z2 – energy consumption of the energy-saving equipment, in rubles;
- c2– cost of the energy-saving equipment;

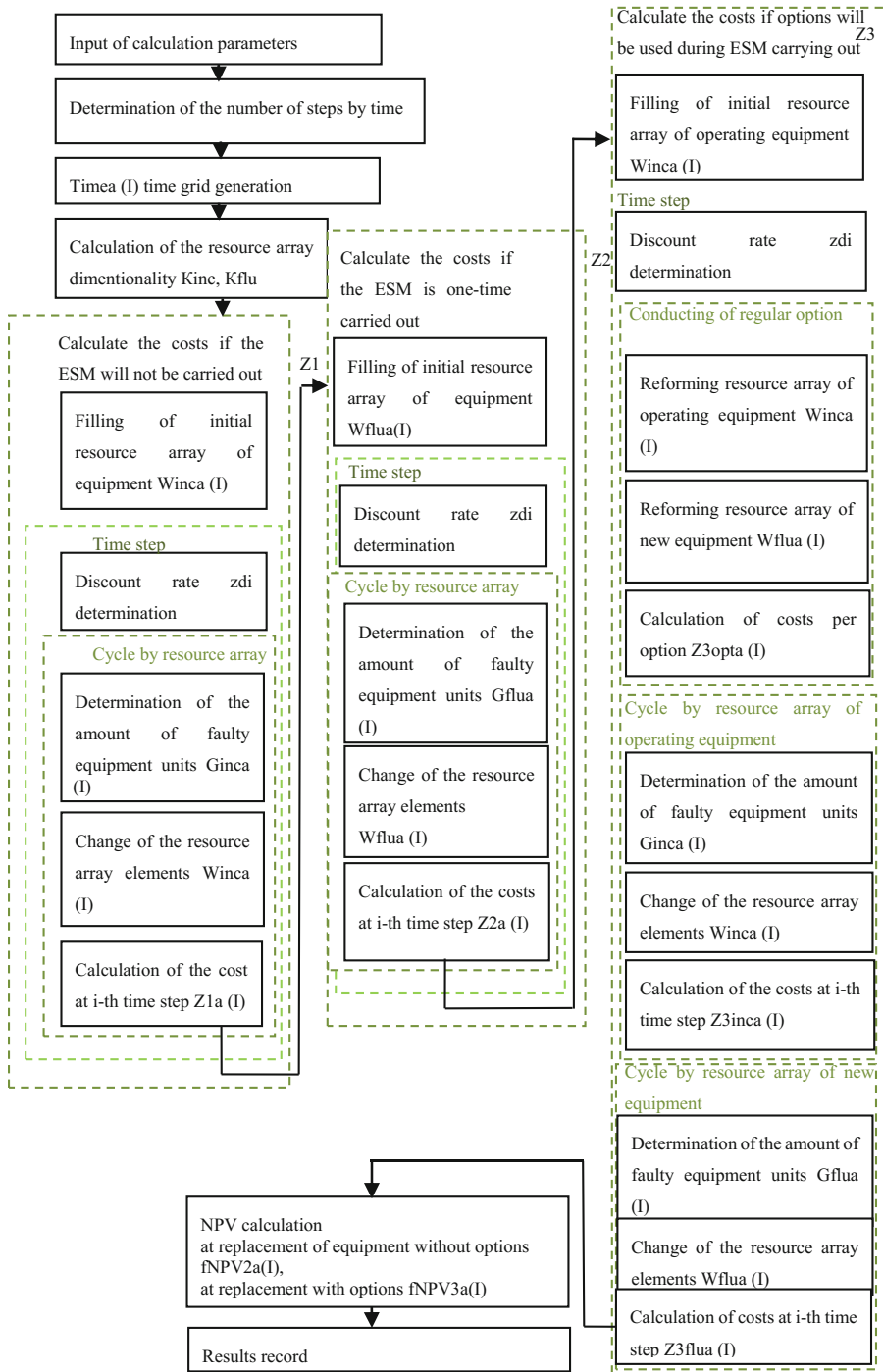


Fig. 4. Diagram of implementation variants of energy-saving activities.

2. The number of time steps is determined in the calculation of the project.
 3. Timea (I) time grid is generated: $N_{date} = N_{year} \times N_{month} + 1$.
 4. The dimensionality of resource array for operated energy-saving equipment is calculated: $K_{inc} = \text{term1}b1p2/dt$; $K_{flu} = \text{term2}b1p2$; $dt = 1.0/N_{month}$.
 5. Based on initial parameters the costs by three variants of energy-saving activities implementation are calculated ($Z1$, $Z2$, $Z3$).
- The calculation of operated equipment costs is performed in accordance with time distribution of the operational life. It is assumed that at the initial time distribution of the equipment by the operational life is uniform. In case of equipment failure, it is replaced by similar new equipment (non energy-saving). Thus, this variant of ESC implementation provides for the refusal of specific energy-saving procedures ($Z1$).
 - At the second stage ($Z2$) the calculation of costs is carried out similarly to the first stage. At that, it is taken into account that all supplied energy saving equipment is new and, accordingly, has a maximum operational life.
 - The calculation of costs is carried out taking into account that the equipment replacement project is multi-stage in accordance with the number of options. When old operated energy-saving equipment fails, it is replaced by similar equipment ($Z3$).

The decision on expediency of energy saving procedures is made on the basis of comparison of these variants. When specified the mandatory modernization of capacities (non-conformance to current regulations and standards of energy efficiency, environmental compatibility, etc.), it is necessary to select the second or the third variant of the project implementation. Such selection can be made on the basis of preliminary analysis of equipment technical specifications and source of investment assets. In exceptional cases of one-time special-purpose financing and limitedness of applied technologies or equipment the second variant should be selected.

The total ESM effectiveness indicator should be adjusted to the “real option” cost value (1):

$$W = \int_{t=0}^{t_n} CF(t)dt + C \quad (1)$$

where

- W – value of the project, expressed in money terms;
 CF – cash flows, including the costs of ESM, current operation expenditure savings in the course of the operational life of energy-saving equipment, outsourcing costs (maintenance of engineering systems and ESCO equipment);
 $t_n - t_0$ – standard service life of the equipment;
 C – “real option” value [12].

To determine the “real options” value the premium assessment model according to European Black-Scholes call option is used (2), (3), (4):

$$C = N(d_1) \times S - N(d_2) \times X \times e^{-rt} \quad (2)$$

where

$N(d)$ – integral function of normal distribution,

$$d_1 = \frac{\ln(S/X) + (r + \sigma^2/2) \times t}{\sigma\sqrt{t}} \quad (3)$$

$$d_2 = d_1 - (\sigma\sqrt{t}) \quad (4)$$

where

σ – “volatility” of expected return (calculated by extracting a square-root from the standard deviation of the expected return logarithms);

S – current value of the underlying asset (present value of cash flows from the realization of that investment opportunity which the company will get as a result of the investment project implementation);

X – option strike price (for “real options” it is the costs of the project implementation)

e – number that is the base of the natural logarithm (rounded value of e number is 2.71828);

r – short-term risk-free rate of return;

t – time before the expiry date of option exercise (implementation of opportunities contained in the option) or time till the next time point of decision making [13]

“Real option” value (C) will be the higher:

- the NPV value is higher;
- the exercise price X is lower;
- t value is higher;
- the risk is higher.

The present value of the expected cash flows has the greatest impact on the increase of option value.

Application of the developed methodological approach will allow ensuring energy consumption management effectiveness enhancement in the enterprise at the various stages: enterprise diagnostics, energy saving procedures carrying out, energy-saving equipment operation [14–16].

3 Results

When calculating by options method normative and actual operational time limits of the equipment should be considered. Thus, it is necessary to determine the operational life of the new equipment or expected actual operational life of the equipment, energy effectiveness of which is planned to be improved.

The calculation is given for energy saving procedures of boiler's internal surfaces scaling by alkali-free acid-free method [17].

Based on the initial data of the energy performance certificate it is known that the expected fuel consumption for thermal energy production is 7550.94 m³/year.

Let the project is designed for 3 years. Let us calculate costs in accordance with the given above variants of energy-saving activities implementation.

Variant 1. Heating expenses, if the energy saving procedures would not be carried out, are calculated for each month using the following Eq. 5:

$$Z1_i = Z1_{i-1} + \frac{z1}{k_i} \cdot \Delta t, \quad i = 1, \dots, N \tag{5}$$

where:

- N – number of months in the project (in this case, N = 36),
- Z1₀ = 0 – initial expenses;
- Δt – time step (in this case Δt = 1 month);
- z1 – heating expenses per unit time (per 1 month), if boilers would not be cleaned;
- k_i – discounting coefficient

Discounting coefficient varies over years, and within the first year it is assumed to be equal k_i = 1.

Variant 2. Cleaning of all boilers at the enterprise will be carried out at the same time, then the expenses are calculated for each month and determined by the following formulas (6), (7):

$$Z2_0 = C2 + Ca2 \tag{6}$$

$$Z2_i = Z2_{i-1} + \frac{z2'}{k_i} \cdot \Delta t \tag{7}$$

$$z2' = z2 + (z1 - z2) \cdot \frac{t}{T_w}, \quad \text{at } t < T_w; \quad z2' = z1 \text{ at } t \geq T_w,$$

where:

- C2 – boiler cleaning cost;
- Ca2 – cost of additional equipment required for cleaning;
- z2' – heating charges per unit time in case of cleaned boilers with account of gradual scaling.
- z2 – heating charges per unit time (for 1 month) immediately after boiler cleaning.

Variant 3. Boilers cleaning will conducted using options. Heating charges are calculated according to the Eqs. (8), (9):

$$Z3_1 = (C2 + Ca2) \cdot \xi_1 \tag{8}$$

$$Z3_i = Z3_{i-1} + \frac{[z2'_i + z1 \cdot (1 - \Xi_i)]}{k_i} \cdot \Delta t + (C2 + Ca2) \cdot \xi_j \cdot \delta_{ij} \tag{9}$$

where:

- ξ_0 – part of boilers, cleaned in the 1st option (at the project start);
- ξ_j – part of boilers, cleaned in jth option;
- $z2$ – heating charges per unit time (for 1 month) immediately after boiler cleaning

The summation is made by all exercised options (10), (11):

$$z2'_i = \sum_{j=0}^k \xi_j \cdot z2''_j \tag{10}$$

$$z2''_j = z2 + (z1 - z2) \cdot \frac{\tau_j}{T_w} \text{ at } \tau_j < T_w \text{ and } z2''_j = z1 \text{ at } \tau_j \geq T_w \tag{11}$$

where:

- $\tau_j = t - t_j$ – time since the execution of jth option,
- Ξ_i – part of boilers, cleaned to the ith time step;

$\delta_{ij} = 1$, if the beginning of ith time step coincides with the jth option and $\delta_{ij} = 0$ in the opposite case (if there is no coincidence of ith time step start with either option).

Next, let us make a comparison of expenses in cases of cleaning with or without options. For this purpose let us calculate NPV value for 2 and 3 variants of ESM implementation:

NPV for cleaning without options: $NPV2_i = Z1_i - Z2_i, i = 1, N_{month}$.

NPV for cleaning with options: $NPV3_i = Z1_i - Z3_i, i = 1, N_{month}$.

In view of the above initial values of power system parameters of boiler rooms, let us calculate $Z1_i, Z2_i, Z3_i$ with cumulative total for the first few months:

1. For the first variant only the energy resources costs are taken into account:

$$Z1_0 = 0 \text{ thousand rubles}$$

$$Z1_1 = 0 + \frac{35171/12}{1} \times 1 = 2931 \text{ thousand rubles}$$

$$Z1_2 = 2931 + \frac{35171/12}{1} \times 1 = 5862 \text{ thousand rubles}$$

$$Z1_3 = 5862 + \frac{35171/12}{1} \times 1 = 8793 \text{ thousand rubles etc.}$$

It should be taken into account that from the second year (starting from 13th month - $Z1_{12}$) in the denominator the discount rate k will have a value of 0.12:

$$Z1_{12} = 32240 + \frac{35171/12}{1.12} \times 1 = 34857 \text{ thousand rubles}$$

Similarly, costs for all 3 years were obtained.

2. For the second variant investment costs are accounted at the basic time point, and in subsequent periods the operational energy costs $Z2_0 = 942.6$ thousand rubles

$$Z2_1 = 942.6 + \frac{33413/12 + (35171/12 - 33413/12) \cdot \frac{1}{120}}{1} \times 1 = 3728 \text{ thousand rubles}$$

$$Z2_2 = 3728 + \frac{33413/12 + (35171/12 - 33413/12) \cdot \frac{2}{120}}{1} \times 1 = 6515 \text{ thousand rubles etc.}$$

3. For the third variant the cleaning is carried out step-by-step: at the beginning of each period the cleaning of 1/3 of all the equipment is made (since there are 3 boiler rooms at the enterprise, duration of works will be 3 years).

$$Z3_0 = \frac{942.6}{3} = 314.3 \text{ thousand rubles}$$

$$\begin{aligned} Z3_1 &= 314,3 + \frac{35171/12}{1} \times \frac{2}{3} + \frac{33413/12 + (35171/12 - 33413/12) \cdot \frac{1}{120}}{1} \times \frac{1}{3} \\ &= 3197 \text{ thousand rubles} \end{aligned}$$

$$\begin{aligned} Z3_2 &= 3200 + \frac{35171/12}{1} \times \frac{2}{3} + \frac{33413/12 + (35171/12 - 33413/12) \cdot \frac{2}{120}}{1} \times \frac{1}{3} \\ &= 6080 \text{ thousand rubles} \end{aligned}$$

$$\begin{aligned} Z3_3 &= 6090 + \frac{35171/12}{1} \times \frac{2}{3} + \frac{33413/12 + (35171/12 - 33413/12) \cdot \frac{3}{120}}{1} \times \frac{1}{3} \\ &= 8963 \text{ thousand rubles} \end{aligned}$$

In 13th month the cleaning of the second third of boilers shall be carried out, i.e. already 2/3 boilers will be energy efficient:

$$\begin{aligned} Z3_{13} &= 34555 + 273 + \frac{35171/12}{1} \times \frac{1}{3} \\ &+ \frac{33413/12 + (35171/12 - 33413/12) \cdot \frac{13}{120}}{1.12} \times \frac{1}{3} \\ &+ \frac{33413/12 + (35171/12 - 33413/12) \cdot \frac{1}{120}}{1.12} \times \frac{1}{3} = 37297 \text{ thousand rubles etc.} \end{aligned}$$

In the 25th month the cleaning of the third boiler room shall be carried out, i.e. already in the 3rd year all the boilers will be energy efficient:

$$\begin{aligned} Z3_{25} &= 64176 + 273 + \frac{33413/12 + (35171/12 - 33413/12) \cdot \frac{25}{120}}{1, 12} \times \frac{1}{3} \\ &+ \frac{33413/12 + (35171/12 - 33413/12) \cdot \frac{13}{120}}{1.12} \times \frac{1}{3} \\ &+ \frac{33413/12 + (35171/12 - 33413/12) \cdot \frac{1}{120}}{1.12} \times \frac{1}{3} = 66531 \text{ thousand rubles etc.} \end{aligned}$$

Let us calculate the real option cost for energy-saving procedure on the basis of the formulas given above 1–4:

$$d_1 = \frac{\ln(1740/942.06) + (0.06 + 0.72^2/2) \times 1}{0.72\sqrt{1}} = 1.91$$

$$d_2 = 1.91 - 0.72\sqrt{1} = 1.19$$

Cumulative function of normal distribution is:

$$N(d_1) = 0.5 + 0.4719 = 0.9719$$

$$N(d_2) = 0.5 - 0.383 = 0.117$$

The real option cost is equal to:

$$C = 0.9719 \times 1740 - 0.117 \times 942.6 \times 2.718^{-0.06} = 1574 \text{ thousand rubles}$$

4 Discussion

ESCO often focuses on high-yield projects. This is due to the fact that such projects are highly expensive. General ESC diagram does not anticipate the risk distribution between the project participants; all risks should undertake ESCO. In view of the above, the special attention should be paid to risks that so far have not been proved in the ESC system. Risk management determines particular complex specifics of interaction with financial institutions. That narrow segment of banking structures which show activity in the energy service sector, usually impose strict requirements to investment contract conditions.

The issue related to the ECS risks is taken into account in the development and appraisal of economic-mathematical evaluation model. The use of “real options” theory in the evaluation model increases the value of the project because:

1. There takes place a distribution of financial flows into several stages, and therefore the – reduction in terms of return on the investment (payback of separate option).
2. Short payback period leads to the risks reduction, and hence simplifies the investment procedure itself.
3. In case of success of the project at the first stage, the guarantee of successful implementation of ECM package increases.

Indicators for decision making on ESC start at the enterprise may differ depending on the industry specifics of the main production. It is important to take into account not only the economic effectiveness but technical capabilities, environmental and social aspects too.

The analysis revealed the relevance of the following complementary indicators when decision making on the project start:

- possible maximum technical potential of energy resources economy;
- sufficiency of energy-saving effect to meet 261-FZ requirements;

- value of capital investments and amount of operating expenditures, payback period of investments;
- percentage of possible resources economy relative to the total consumption of this resource by the facility;
- aesthetic propriety and up-to-date decisions applied;
- environmental, fire, biological and other security of the decisions;

Indicators of the third party investor's activity at the assistance to ESC development are:

- The maximum amount of credit for one organization, reliability of its justification (confirmed by economic calculations), payback period from the economic effect of investments (rarely exceeds 5 years);
- Annual savings of financial resources (preferably not less than 25% of investment expenditures);
- Significant ecological effect;
- Well-developed feasibility study according to bank requirements, design and estimate documentation;
- Loss-free borrower's activity in the last 2–3 years.

It is important to note that the fundamental point is the stimulation of energy saving activities and energy efficiency enhancement for energy-intensive activities by providing state guarantees of the Russian Federation for loans for the project's implementation in the field of energy saving and energy efficiency enhancement. Loans are granted to the attracted organizations which are selected according to the procedure established by the Government of the Russian Federation. It is also possible to stimulate the implementation of standard projects in the field of energy saving and energy efficiency improvement by using economic mechanisms as required by the Law, used mainly within regional programs in the field of energy saving and energy efficiency improvement.

From the aforementioned facts, it can be concluded that implementation of energy saving programs is possible only in the presence of a highly efficient organizational-economic mechanism.

It should be taken into account that additional costs associated with a change in ESM composition are inevitable. This is an additional confirmation in favor of Black-Scholes model applied in the evaluation of ESC, which takes into account the option value as part of ESC.

5 Conclusions

Based on the study of status and tendencies of energy resources consumers development under conditions of ESC application it was found that, unlike the traditional approach to energy saving, the approach on the basis of ESC allows provision of financing and execution of ESM at ESCO account.

The application of proposed methodological approach to reduction of energy consumption at the enterprise allows optimization of the energy resources management due to the continuous improvement system with ESC use.

The developed methodical approach to the evaluation of cost-effectiveness of energy saving procedures makes it possible to justify the ESC composition. In the implementation of energy saving procedures in several phases the value of the project increases on the basis of capabilities of decision making (cancellation or suspension of the project, change the pace and scope of the project), providing “flexibility” of the investments strategic management system, that is reflected in the mathematical evaluation model.

References

1. Jakšić, Ž., Trivunić, M., Adamtsevich, A.: MATEC Web of Conferences, vol. 106, art. no. 01001 (2017). <https://doi.org/10.1051/mateconf/201710601001>
2. Sergeev, V., Aleshina, A.: Therm. Eng. **58**(3), 268–270 (2011). <https://doi.org/10.1134/S0040601511030116>
3. Vatin, N., Chechevichkin, V., Chechevichkin, A., Shilova, Y.: Mag. Civ. Eng. **37**(2), 81–88 and 127–129 (2013). <https://doi.org/10.5862/MCE.37.12>
4. Bashmakov, I.: Costs and Benefits of Low-Carbon Economy and Society Transformation in Russia 2050 Perspective (2014)
5. Usmanov, R., Vatin, N., Murgul, V.: Appl. Mech. Mater. **633–634**, 1082–1085 (2014). <https://doi.org/10.4028/www.scientific.net/AMM.633-634.1082>
6. Romanovich, R., Vilinskaya, A.: MATEC Web of Conferences, vol. 53, p. 01052 (2016). <https://doi.org/10.1051/mateconf/20165301052>
7. Mescheryakova, T.: Econ. Entrep. **3**, 663–666 (2015)
8. Pimenova, A., Kuzmina, S., Morozova, N., Mottaeva, A.: The functional model approach to the consulting for vertically-integrated construction group. In: MATEC Web of Conferences, p. 07018 (2016). <https://doi.org/10.1051/mateconf/20167307018>
9. Simankina, T., Romanovich, M., Tsvetkov, O.: MATEC Web of Conferences, vol. 53, p. 01054 (2016). <https://doi.org/10.1051/mateconf/20165301054>
10. Rozhentsova, I., Mottaeva, A.: Terms of orientation on customer needs in the housing sector. In: MATEC Web of Conferences, p. 08076 (2017). <https://doi.org/10.1051/mateconf/201710608076>
11. Taskaeva, N., Silantyeva, T.: Nauchnoye Obozrenie **4**, 444–448 (2013)
12. Mescheryakova, T., Samarin, O.: Econ. Entrep. **8**, 647–651 (2014)
13. Rutešić, S., Četković, J., Knežević, M., Žarcković, M., Vatin, N.: Institutional framework, current investments and future strategic direction for development of construction sector in Montenegro. Procedia Eng. **117**, 637–645 (2015)
14. Mescheryakova, T., Verstina, N.: Econ. Entrepr. **3**, 697–700 (2015)
15. Mescheryakova, T., Verstina, N.: Biosci. Biotechnol. Res. Asia **12**, 1411–1423 (2015)
16. Priadko, I., Mushchanov, V., Bartolo, H., Vatin, N., Rudnieva, I.: Mag. Civ. Eng. **65**(5), 27–41 (2016). <https://doi.org/10.5862/MCE.65.3>
17. Jevric, M., Romanovich, M.: Procedia Eng. **165**, 1478–1482 (2016). <https://doi.org/10.1016/j.proeng.2016.11.882>

Influence of the Sustainable Development of the Fuel Power Complex on the Formation of Competitiveness of the Region

Angela Mottaeva^{1,2}  and Jasmina Četković³ 

¹ Moscow State University of Civil Engineering,
Yaroslavskoe shosse, 26, Moscow 129337, Russia
angela-1309.m@yandex.ru

² Moscow Regional State University, Radio str. 10, Moscow 129125, Russia

³ Faculty of Economics Podgorica, University of Montenegro,
Jovana Tomaševića 37, 81000 Podgorica, Montenegro

Abstract. Various criteria for the evaluation of competitive capacity of territories, considering first of all economic infrastructure and innovative development, human potential and the standard of living of the population, are considered in the article. The study is dedicated to the resource potential as the objective basis of the formation of competitiveness of the region. The author studies the role of sustainable development of the fuel-and-energy complex on the formation of competitiveness of the region. The author proves that the leading element in the development of energy industry is the natural capital because of the high material capacity of products and services of the complex, while the lack of any real competition in the energy industry of regions creates all the complex of the social-and-economic problems, peculiar for exclusive market structures.

Keywords: Fuel power complex · Competitiveness · Energy management

1 Introduction

The driving force of self-development of social-and-economic systems is the intra-organizational, intra-branch, intermarket competition and also the interindustry competition for production factors. The competition is the key category of the market economy which is deeply investigated in economic literature. Classics of the theory of the competition, such as Kotler and Keller [1], Porter [2] have put the theoretic-and-methodological base of research of the firm's competition.

Globalization of the economy has strengthened the integration processes and at the same time it has generated the amplifying tendencies of self-identification of the states and national economies, of fight for natural resources, for qualitative human resources that has led to growth of the intercountry competition. Coen [3], M. Porter, J. Saks's devoted their works to these problems [4]. It is also necessary to call A. Dynkin, S.V. Kuznetsov and S.A. Ivanov, etc. as Russian researchers of the competition at the macrolevel.

Competitiveness problems at the mesolevel and at the level of regions are the least studied ones, however the interest of researchers in the matters has amplified recently. This tendency is explained by the change of the role of the region in the Russian social-and-economic system, emphasizing that regions in fact had no interests, which would differ from the interests of the central power, up to the beginning of the 90th years. At the same time, it is necessary to recognize that the region became the independent economic agent in the competitive processes, taking place at different levels.

The leading element in the development of energy industry is the natural capital because the high material capacity of products and services of the complex.

The lack of the real competition in the energy industry of regions creates all the complex of the social-and-economic problems, which are peculiar for exclusive market structures: increase in prices for the delivered services, social inequality, social responsibility of business, low in comparison with the income taken from natural wealth.

High extent of monopolization of the fuel and energy markets causes a considerable share of the state participation in the activity of the energy industries enterprises, and it is justified because of the need of preservation of the state control over reproduction, distribution and consumption of backbone resources of national social-and-economic system. Besides, “the major is the role of the state in regulation of tariffs at the federal and regional levels, directed to increase in prices control, the achievement of balance of economic interests of producers and consumers of production, increase in efficiency of functioning of energy industry of the country” [5–7].

Besides the regulating and controlling role, the state acts as the equal partner in relationship with energy industries corporations.

The foreign policy situation, connected with the Ukrainian crisis and expansion of sanctions opposition between the countries of EEC, the USA, Canada, Australia, on the one hand, and Russia which significantly has become complicated on the other hand is a very serious call for development of energy industry which already have real consequences. It was proved, in the form of decrease in volumes of supplies of equipment for development of energy industry.

2 Methodological Approaches and Analysis

Nowadays there is no conventional methodology and tools for the assessment of competitiveness of regions, which would form information basis for the development of the reasonable managerial decisions aimed on the increase in competitiveness of Russia. The offered hierarchy of levels of competitiveness is added with communications of influence of competitive structure of energy industry on competitiveness levels (Fig. 1).

This competitiveness characterizes the results and quality of management of the regional economy” [8, 9].

The dynamics of the development of branches of energy industry can serve as the indirect characteristic of the efficiency of regions.

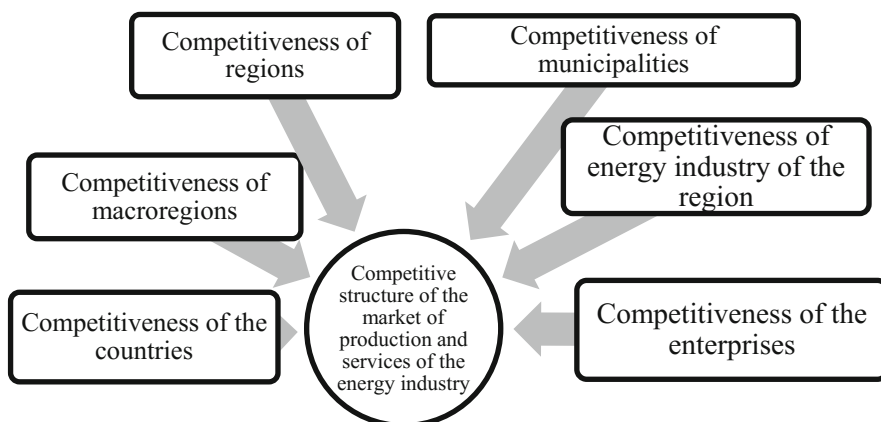


Fig. 1. Hierarchy of levels of competitiveness

It is possible to accept the average index of growth in the region, calculated as an average geometrical, as the indicator defining the average level of economic activity in the field of production and distribution of the electric energy, gas and water. The deviation of this indicator from the average for the Russian Federation is the indirect characteristic of the use of resources of energy industry in the region. The carried-out analysis proves that, about a half of territorial subjects of the federation exceed the average Russian level according this indicator.

The classical economic theory distinguishes four main types of competitive structures of the markets.

The market of production and services of energy industries classified as an oligopoly and true monopoly, and according to high extent of monopolization of this market it is the subject to rigid state regulation and makes impact on all levels - from the microlevel (the enterprise, corporation) to macrolevel (national economy) and the megalevel (the economic unions). Heterogeneity of the competitive structure of the fuel and energy markets is known; even without infrastructure and auxiliary productions of energy industry this market is characterized by oligopoly and true monopoly.

Regional competitiveness is formed at the expense of competitiveness of the energy industries enterprises, by formation of competitive advantages.

In turn formation and realization of competitive advantages cannot be considered in a separation from the processes of “the rent relations”, as the concept “competition” consists of the concept “rivalry” and the concept “rent” (obtaining some income having an exclusive component). That generally means the relations of rents or the rent relations.

The rent, its formation, distribution and influence on the development of regional social-and-economic systems are the key questions in the research in the field of regional economy. At the same time classical economics proves that the development of regional energy industries is based on the natural resources maintenance. Therefore, the natural rent is the fundamental theoretical category which is the core of the research

of problems of development of energy industry. Kulikov [10] names the following group of approaches to the definition of a natural rent (Fig. 2).

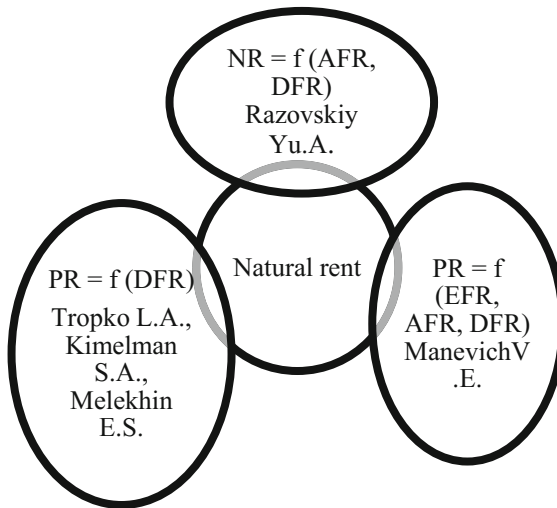


Fig. 2. Approaches to sources of formation of natural rent. NR – a natural rent; AFR – an absolute part of a full rent; DFR – a differential part of a full rent; EFR – an exclusive part of a full rent.

As the figure proves, the inclusion of differential part of the full rent having as a source educations mainly natural resources of the region into the structure of the natural rent is indisputable. The natural rent can exert double impact on the competitiveness of the region.

It is necessary to recognize that Russia, which is the first in oil production in Europe and the recognized leader in the world oil production, in case of lack of access to creation and management of the international standards is almost discharged of mechanisms of pricing for oil and gas resources in the foreign markets. In the conditions of the development of the economic crisis that leads to growth of the level of uncertainty in obtaining the income, to the decrease in efficiency of mechanisms of fiscal policy and as a result that leads to the decrease in the level of social-and-economic development of certain regions and the whole states.

According to the idea of the institutional environment of formation of regional competitiveness along with the natural rent, the rent relations are formed by the mechanisms of the economic rent which is in turn presented in the form of production and institutional rent (Fig. 3).

The production rent arises in the corporations possessing higher than on average on have grown the level of production technologies of production and services that provides lower costs of production and, as a result, - a possibility of receiving additional profit. The main form production rents is the production and technological rent.

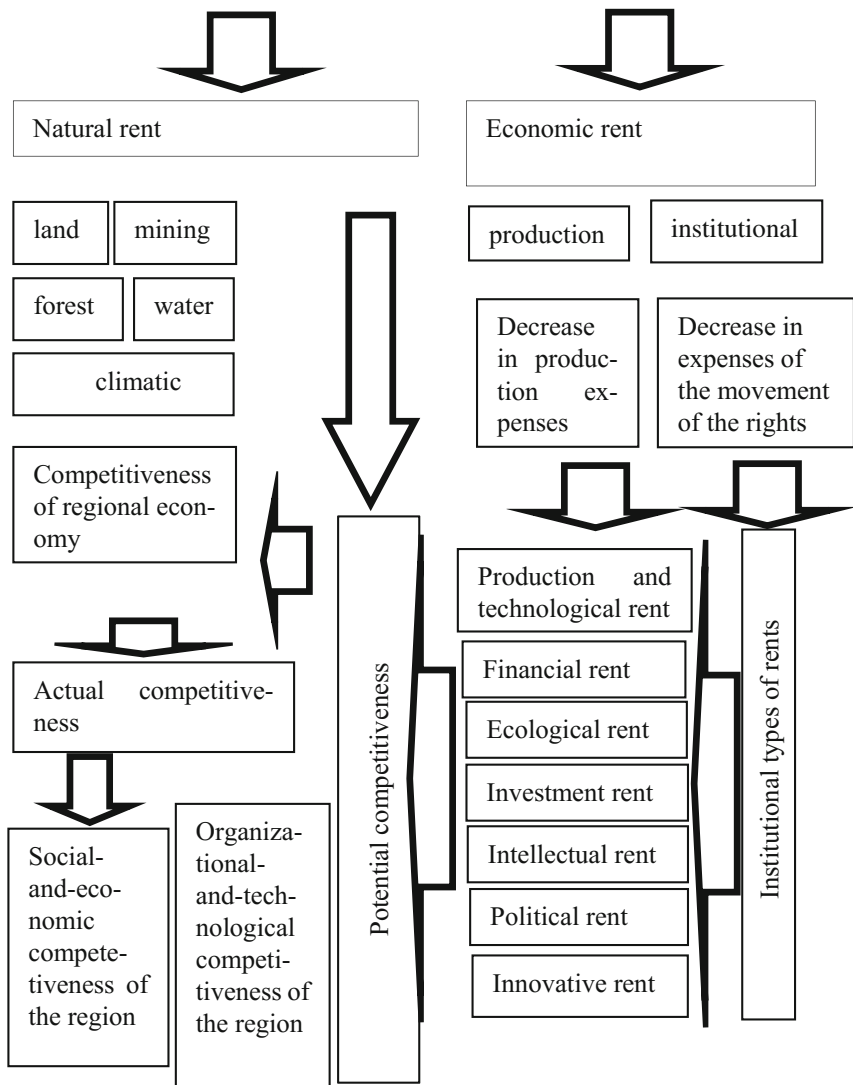


Fig. 3. Rent relations as the source of formation of regional competitiveness.

3 Results

The study, completed by the author allows to state the following.

Emergence of such institutes as rules and norms determining the order of interaction between the subjects of the relations is always connected:

- with absolute desire of subjects as much as possible to reduce uncertainty level in these relations on the one hand;
- with relative desire of subjects to fulfill fully the undertaken obligations on the other hand.

In other words, when forming the institutes, it is always supposed that the subjects of the economic relations, forming “rules of the game” can be inclined to the implementation of opportunistic behavior for the purpose of creation of competitive advantages, first of all, by not execution of separately undertaken obligations at realization of the general for all rules.

Therefore, competitive advantages of activity of an institute and the subjects, forming it, are forced to agree about the mutually binding and mutually advantageous exceptions to the rules which take the form of personal privileges, or a privileged position unofficially. The author of this research considers that the increase in level of privileges most often, leads to decrease in efficiency of institute from the point of view of development of society, at the same time creates exclusive participants additional opportunities of monopolization of separate types of the institutional rent. It fully belongs to the formation of the market of monopolies, oligopoly and the market of the monopolistic competition of activity of the energy industries enterprises. The institutional rent is formed both in the sphere of direct production activity, and in various spheres providing production of the economic benefits. The main types of the institutional rent, having significant effect both on regional social and economic development in general and on development of activity of energy industry in particular, are the following:

- the financial rent arising in the branches and energy industries corporations having access to cheap credit resources that gives the chance of faster, in comparison with competitors, the development, the decrease in expenses regarding service of credit resources and, as a result, the possibility of receiving additional profit [11, 12];
- the ecological rent, which represents “expression of all natural resources of the territory in the form of set of the public benefits and resources of joint consumption of this territory. Natural resources of joint consumption are as well the public benefits necessary for life of the population of the territory. Thus, natural ecosystems provide a high ecological rent of land resources of the territory that, in turn, promotes a stable socio-political situation and investment appeal of the region, development of economy” [11–14];
- the investment rent, which arises as a result of strategically right decision about the location of enterprises of the energy industry, which activity in the medium-term and long-term period is transformed to the steady income in conditions of basic change political and economic and social-and-economic factors of the institutional environment of the development of the energy industry;
- the innovative rent which arises in the branches and energy industries corporations having big, than on average on a complex, innovative potential that allows to receive super profit owing to high mobility and ability to territorial expansion and lower, in comparison with industry average, costs of production and product sales and services [15–18];
- the intellectual rent arising in educational and research sector of energy industry (the research organizations and universities) due to development of the human capital, realization of the property rights to patents and inventions in the sphere of power;

- the political rent which arises according to the development of the political institutes capable with the minimum transactional expenses to create and realize economic institutes. Political rules are the cornerstone of the formation of economic rules which establish admissible forms of economic activity within which economic agents cooperate or compete; restrictions for access for other persons to use of property in the form of limited resources; system of the specification and protection of the property rights.

It is possible to distinguish two main types of rent: formal and informal institutional rent. The formal institutional rent arises, when the activity of the organization for the decrease in transactional expenses of the market relations and intra-corporate communication expenses coincides with the activity of the formal institutes directed to creation of the effective institutional environment.

The informal institutional rent arises in the conditions of the positive relation of the population of the concrete territory to the activity of the formal institutes and informal restrictions, aimed on the decrease in level of uncertainty in the rent relations by the decrease in various types of transactional expenses. At the same time the author considers that the arisen informal institutional rent is offered to be designated as an informal quasi-rent.

4 Discussion

Still there is very serious problem of the decrease in the level of the rent-directed behavior, which is exerting negative impact on the processes of social-and-economic development of regions. Now there are various interpretations of this phenomenon and different approaches to the solution of this problem.

Investigating this phenomenon, D. Nort noted that the institutes, working in the society are non-uniform: formally they can be divided into formal institutes and informal institutes [19–22].

However, the problems of interregional inequality remain at rather high level, because of inefficiency, and sometimes because of mutually exclusive orientation of the formal institutes. A.V. Vinogradova fairly specifies that the problems of redistribution of the income from the natural rent unresolved so far root in uncertainty of the property rights in the Russian Federation [23–26]. There is a certain contradiction between the Act of the Russian Federation “About a subsoil”, in which the state ownership on the subsoil, and the Constitution of the Russian Federation which allows to consider any subject as the subject of private property is approved.

In recent years the terms “natural capital”, “natural capital of the territory”, have gained distribution in the economic science, one of tools of an assessment of which is the system of the ecological-and-economic accounting, recommended by the World Bank and the United Nations Organization [27–29].

5 Conclusions

Taking into account the aforesaid facts, the author can conclude, that the formation of the institutional environment of social and economic development demands a detailed research of the complicated structured interrelations between the formal and informal institutes creating different types of the rent relations. Generally social-and-economic development of society has the positive focus guaranteeing social stability, cultural development and the human capital of the region when formal and informal institutes form a uniform positive trend. Therefore, the most important task of the state and municipal authority is the creation of conditions of coherence in actions of formal and informal institutes. The decrease in level of the formal and informal quasi-rent by the energy industries enterprises becomes the priority in the course of formation of social responsibility of business, aimed on providing the social standards meaning the high level of social-and-economic safety, steady improvement of quality of life and social development of the population of the region. Further social and economic development of the country, her regions and municipalities is in many respects caused by transformation of proportions of distribution of a formal and informal institutional rent and minimization of sizes of a formal and informal quasi-rent. This difficult process refers to tax regulation, budgetary process and the inter-budgetary relations the objective advantages of development by energy industry corporation based on operation of the natural capital of the country by them to use for covering of the state needs understood as needs of the social performance.

Thus, the natural rent is the classical economic category which allows to carry out scientific research of the influence of fuel and energy complexes according to the competitiveness of regions.

Having conducted the research of theoretical, analytical and statistical sources, the author proved, that sustainable development of fuel-and-energy complex significantly influences the formation of competitiveness of the region. According to the results of the research, the author offers suggests, that the creation of high level of competitiveness and sustainable social-and-economic development of the region should set the following requirements:






1. to create some conditions for the formation of the institutional environment for the interaction between formal and informal energy institutes, creating various types of the rent relations and providing social stability of the region;
2. to transform the proportions of distribution of the formal and informal rent, established by the enbergy enterprises and to minimize its amount;
3. to develop the reduction of quasirent by the power industrial enterprises both on the formal and informal level as the priority direction;
4. to determine the level of social responsibility of the business, providing social standards, high level of social-and-economic safety, steady improvement of quality of life and social development of the population of the region.

Thus, the presented conclusions will allow to carry out regular further scientific research within the influence of fuel-and-energy complexes on competitiveness of regions.

References

1. Kotler, F., Keller, K.: Marketing Management. Piter, Saint-Petersburg (2008)
2. Porter, M.: Competitiveness, Moscow, Saint-Petersburg, Kiev (2005)
3. Coen, S.: Failure of a Crusade: USA and Tragedy of Post-communist Russia. AIRO-XX, Moscow (2001)
4. Saks, J.: Price of the civilization, Moscow (2012)
5. Arseniev, D.: Applied Mechanics and Materials, vol. 635–637, pp. 2076–2080 (2014). <https://doi.org/10.4028/www.scientific.net/AMM.635-637.2076>
6. Nikolova, L.: Int. J. Econ. Financ. Issues **6**(S3), 1–7 (2016)
7. Murgul, V.: MATEC Web of Conferences, p. 02001 (2016). <http://doi.org/10.1051/mateconf/20167302001>
8. Panteleeva, M., Borozdina, S.: MATEC Web of Conferences, vol. 106, p. 080471 (2017)
9. Meshcheryakova, T.: MATEC Web of Conferences, vol. 106, p. 06021 (2017)
10. Kulikov, A.: Scientific works: institute of economic forecasting of RAS scientific works. Inst. Econ. Forecast. RAS **2**, 398–419 (2016)
11. Rozhentsova, I., Mottaeva, A.: MATEC Web of Conferences, p. 08076 (2017). <http://doi.org/10.1051/mateconf/201710608076>
12. Glazkova, V.: MATEC Web of Conferences, vol. 106, p. 08095 (2017)
13. Vasilyeva, E., Polyakova, I.: MATEC Web of Conferences, vol. 106, p. 08097 (2017)
14. Isaev, S.: Tech. Phys. Lett. **40**(8), 653–656 (2014). <https://doi.org/10.1134/S1063785014080057>
15. Mottaeva, A.: MATEC Web of Conferences, p. 07018 (2016). <http://doi.org/10.1051/mateconf/20167307018>
16. Vasilyeva, E., Polyakova, I.: MATEC Web of Conferences, vol. 106, p. 08097 (2017)
17. Polyakova, I., Vasilyeva, E.: Procedia Eng. **165**, 1380–1387 (2016)
18. Romanovich, R., Vilinskaya, A.: MATEC Web of Conferences, vol. 53, p. 01052 (2016). <http://doi.org/10.1051/mateconf/20165301052>
19. Chulkova, A., Lukiche, S., Romanovich, M.: MATEC Web of Conferences, vol. 86, p. 02019 (2016). <http://doi.org/10.1051/mateconf/20168602019>
20. Chibisova, E.: J. Int. Sci. Publ.: Econ. Bus. **5**(2), 600 (2015)
21. Priadko, I.: Mag. Civil Eng. **65**(5), 27–41 (2016). <https://doi.org/10.5862/MCE.65.3>
22. Chechevichkin, V., Vatin, N.: Mag. Civil Eng. **50**(6), 67–74 (2014). <https://doi.org/10.5862/MCE.50.7>
23. Dudin, M.: Mag. Civil Eng. **54**(2), 33–45 (2015). <https://doi.org/10.5862/MCE.54.4>
24. Dražić, J., Peško, I., Mučenski, V., Dejić, A., Romanovich, M.: Procedia Eng. **165**, 898–905 (2016). <https://doi.org/10.1016/j.proeng.2016.11.790>
25. Gorshkov, A.: Mag. Civil Eng. **52**(8), 38–48, 65–66 (2014). <https://doi.org/10.5862/MCE.52.5>
26. Jevric, M., Romanovich, M.: Procedia Eng. **165**, 1478–1482 (2016). <https://doi.org/10.1016/j.proeng.2016.11.882>

Organizational-Technological Reliability of Monolithic Construction

Alexander Ginzburg¹(✉) , Alina Bolotova¹ ,
Andrey Dolganov² , Ivan Vedyakov¹ ,
and Michael Vaynshteyn¹ 

¹ Moscow State University of Civil Engineering,
Yaroslavskoye Sh. 26, 129337 Moscow, Russia
ginav@mgsu.ru

² LLC Expert, 14, Pohodniy pr., 125373 Moscow, Russia

Abstract. Reliability and quality of the organization of work at the transport infrastructure facilities is determined through the analysis of the system of preparation for the implementation of certain technological operations, the establishment and maintenance of a common order, the timing of work, and the supply of all types of resources. During the execution of construction and installation work are conducted periodic inspections of compliance with construction norms and rules. Nonconformities issued in the form of regulations, which indicate the time of elimination of this violation. The calendar plan does not provide for the time spent on eliminating violations. For this reason, the actual period of construction of transport infrastructure are often considerably longer than planned. In this connection, the task was to assess the degree of influence of violations on the efficiency of the functioning and quality of the organization of production processes in transport infrastructure. Analytic studies of this problem concluded that it is necessary to develop a mathematical model for estimating the construction period, taking into account the random nature of the appearance of violations. The study contains a diagram of the technological operations in monolithic construction, the Pareto chart for the number of violations identified by the construction supervision, the main factors affecting the duration of construction.

Keywords: Transport buildings and structures · Technology of construction
Organizational-technological reliability
Technology of monolithic construction · Construction monitoring

1 Introduction

In modern construction, the most promising technology of construction of buildings and structures is a monolithic construction. The houses built on this technology occupy most of the cities of the whole world. According to world statistics in many developed countries, the monolithic technology has completely occupied the leading place in the construction industry. For example, in Europe, America and China, the share of monolithic construction is more than 50%, while in major cities it can reach 80% [3, 6].

In Russia, monolithic technology is widely used both in housing and in industrial construction. It is particularly active in the construction of transport buildings and structures [3]. Meanwhile, improving the quality and organization of production in the construction of reinforced concrete is the basic strategic problem of the Russian enterprises, as evidenced by the annual statistics of service of state construction supervision and examination of defects and violations revealed in the process of construction and operation. On average, in the year on the territory of the Russian Federation, the supervisory authorities issue 100,000 prescriptions, of which 20,000 are for the suspension of construction due to the threat of an accident. The result is an increase in the cost of contract services, non-compliance with construction deadlines, and most importantly there is a need to work in emergency mode, which negatively affects the quality of the final product. According to the results of annual checks of the Moscow state construction supervision revealed that the number of violations recorded in Moscow in 2016 has increased by 8.6% in comparison with the results of the previous year. More than a third of the total number of violations relates to the quality of construction works.

The issues of quality assurance of construction, improvement of organizational and technological processes of erection of monolithic buildings with the purpose of increasing their efficiency and quality were dealt with many specialists [7, 8, 10–12]. Analysis of research data showed that the majority of projects under construction technology and organization of construction and installation works at construction of transport buildings and structures of reinforced concrete, and the existing system of organization of production and quality control of work performed does not guarantee the required level of quality. The required quality and reliability of buildings and structures depends on the implementation of the set technical, economical and organizational measures to control creation of object of capital construction. It should be noted that violations in the organization of production processes create the risk of failure to complete the construction phase within a specified period, reduce the quality of work, and, consequently, the reliability of the structure of the facility and, accordingly, reduce the efficiency of construction organizations and, in general, all participants in the project.

The rate of organizational-technological reliability (OTR) significantly affects the efficiency of construction. The organizational-technological reliability is the ability of technological, organizational, management decisions to ensure the achievement of a given result of construction production in the conditions of random perturbations inherent in construction as a complex stochastic system. The works of famous Russian scientists are devoted to the increase of organizational and technological reliability - mainly industrial construction projects [1, 2, 4, 5]. This index takes into account the statistical characteristics of efficiency and organizational risks that arise in the process of functioning of objects of monolithic construction. Despite the large number of works devoted to the improvement of organizational-technological processes in construction and organizational-technological reliability, availability and analysis of the relationship between the index of OTR and the inconsistencies and deviations in the production process has so far not been studied.

We assume that due to the operational evaluation of organizational-technological reliability of monolithic construction, it is possible to solve the problems of efficiency of production and quality of organization of production processes.

The purpose of this research paper is using statistical data to form a list of the most important factors affecting the quality of the production system. Based on the list of important factors is planned to develop an information database for objects of transport infrastructure.

For this purpose, the following tasks have been accomplished:

- analysis of activity of bodies of building control in the manufacture of monolithic works;
- collection of data on discrepancies and violations revealed as a result of quality control on construction sites for the period from 2012 to 2016;
- classification of the main types of deviation when performing works on monolithic technology;

Statistical processing and systematic analysis of the requirements of building control and selection of the most important factors influencing the quality management of works in monolithic construction.

2 Method

The degree of reliability of the calculated results. As the primary method of obtaining information used the results of a system analysis and statistical processing of data on violations identified in the quality control process at construction sites for the period from 2012 to 2016 [6]. Based on statistical methods of quality management and methodology of General quality management the main factors affecting the quality of the monolithic reinforced concrete structures. On each technological operation disturbances may occur, entailing the total or partial failure of the production system. To determine the possible impact of the root causes for the failure of the system is required to represent the relative importance of all damage. For this, we use the method of constructing the Pareto chart. The statistical method of quality management will establish the main factors to identify the most frequent causes of disorders in the production process for priority elimination [13–15]. To determine the factors of greatest impact, the study uses the method of expert evaluations. Using the method of expert evaluations quantified the impact of these factors on organizational and technological reliability of the object of monolithic construction.

3 Results

Building control in transport infrastructure is conducted for each type of work, from the beginning of their execution and receipt of material to the acceptance of object in operation. Results and performance of works and check for compliance with regulatory, project and working documentation, engineering surveys. For each of the construction, design and regulatory and technical documentation is determined by: the list

of monitored parameters, frequency of inspection, methods of control, measuring equipment. The collection of information and the recording of events that affect the functioning of the production process in monolithic construction consists of fixing:

- moments of occurrence of nonconformities and failures,
- time for correcting the violation,
- causes and circumstances of loss of efficiency,
- deviation of the intensity of construction flows from specified design values,

Deviations in the terms of the planned scope of work, the completion of technological stages and stages of work.

Based on the violations and the regulations issued on the results of scientific and practical activities of the MSSU STROY-TEST a Pareto chart was constructed. This material was systematized by the nature of the violations in the additional groups:

- Irregularities in the implementation of the preparatory work;
- Impairment in carrying out excavation works;
- Irregularities in the implementation of piling works;
- Irregularities in the execution of shuttering work;
- Violations during the execution of reinforcement works;
- Violations while performing concrete works.

The results of the calculations needed to construct a Pareto chart, shown in Table 1.

Table 1. Percentage distribution of violations identified during construction monitoring of construction organizations

Identified violations (inconsistencies)	The percentage of each discrepancy	Accumulated percent
Concrete work	29%	29%
Reinforcement works	27%	57%
Excavation work	22%	79%
Shuttering work	11%	89%
Piling works	7%	96%
Preparatory work	3%	99%
Other	1%	100%
Total	100%	

As can be seen from Fig. 1, about 80% of the discrepancies arises from 20% of causes, the removal of which will significantly improve the quality and efficiency of construction using monolithic technology.

In this case, the 80/20 rule shows that the main effect on the result is provided by:

- Violations while performing concrete works,
- Violations during the execution of reinforcement works;
- Impairment in carrying out excavation works.

Building control have identified more abnormalities in the organization and production of concrete work. Typically, the stage of concrete including input control of materials and training equipment to the process of pouring concrete has the highest duration of performance of work relative to everyone else. The violations discovered at the stage of concrete casting, can greatly increase the total construction period. Thus, the causes of violations and inconsistencies detected in the process of execution of concrete works, will allow us to improve the quality and organization of works on construction of monolithic reinforced concrete.

In addition, to the serious defects of monolithic reinforced concrete structures can lead to weak control over the quality of reinforcement of structures. The most common violations of the transport buildings and structures are:

- inconsistency with the design of reinforcement structures,
- poor-quality welding of structural components and joints of reinforcement,
- Application of highly corroded reinforcement.

Earthwork, in turn, must made under strict geodetic control. The quality of the supporting structure significantly affected by the development of the excavation. In addition, the failure to date can occur for reasons beyond the participants in the construction of reasons. For example, when excavation work may show objects that represent cultural and historical value – in this case, all construction work will suspended indefinitely. In the implementation of earthworks on the site of the future home may be engineering communications that are not marked on any map, will have to spend time on unplanned work on their transfer [9–13].

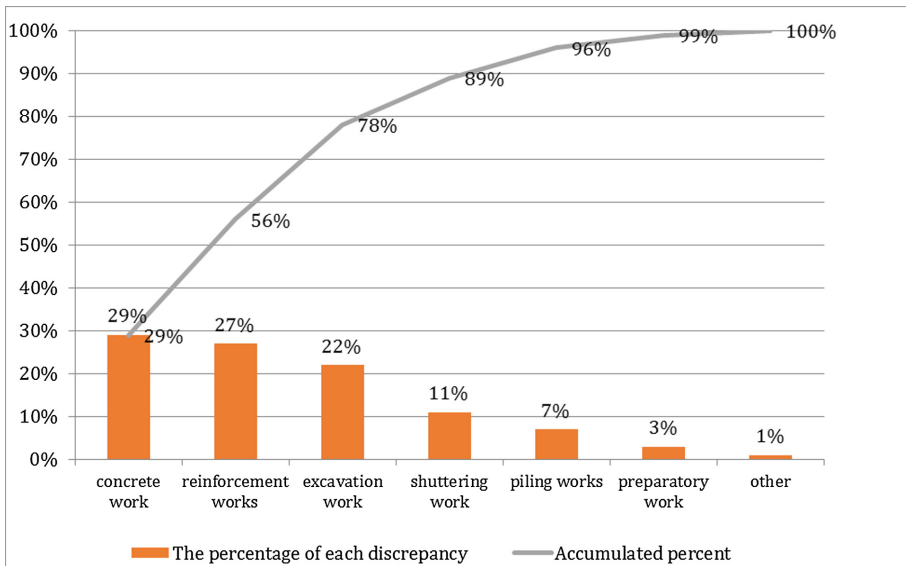


Fig. 1. Pareto chart.

However, the combination of various causes of deviations can lead to a complete or partial failure of the production system. Therefore, in order to identify the root causes of failures in the production system, it is necessary to quantify the degree of their influence on the organizational and technological reliability of monolithic construction. With the help of assessing the reliability of construction, we classify the main types of nonconformities and failures of the production system in terms of the degree of influence on the operable state of the facility. The main factors determining the probabilistic nature of the production process in transport construction is shown in Diagram cause-and-effect relationships (Ishikawa Diagram). The Ishikawa Diagram shown in Fig. 2.

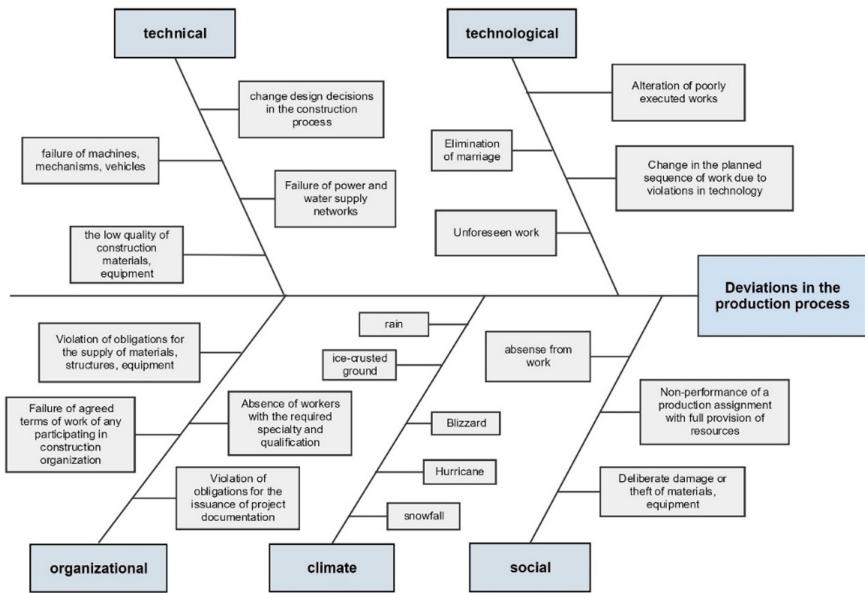


Fig. 2. Ishikawa Diagram.

4 Conclusions

- A systematic analysis of the requirements of the construction control showed that the following technological stages are the vulnerable place in the production system of transport construction: concrete works, reinforcement works and excavation.
- The following groups of factors influence the deviations in the production process: technological, technical, organizational, climatic, and social. The influence of external and internal random factors leads to the fact that the course of the production process deviates from the previously planned one.
- The analysis showed that at present the most vulnerable place of the existing organization of monolithic construction is the efficiency of the activity of

construction organizations and all project participants. Failure to comply with the construction phase within a specified period, the decline in the quality of work, the high labor intensity of technological operations - all this affects the reliability of the construction site as a whole.

Accordingly, the most important direction of improvement of the technology of monolithic construction is the development and implementation of organizational and technological solutions that:

- provide reduction of the duration of the most time consuming operations during the construction of monolithic buildings and structures,
- improved use of machinery, mechanisms and tooling,
- increasing productivity,
- Improving the quality of performed construction and installation works.

References

1. Ginzburg, A.: Building life cycle information modelling. *Promyshlennoe i grazhdanskoe stroitelstvo* **9** (2016)
2. Ginzburg, A.: Queuing systems in management construction. *Appl. Mech. Mater.* **405–408**, 3352–3355 (2013)
3. Bolotova, A., Ginzburg, A.: Analysis of organizational and technological reliability (OTR) of monolithic construction. *Econ. Entrep.* **10**(1), 647–651 (2016)
4. Volkov, A.: General information models of intelligent building control systems: basic concepts, determination and the reasoning. *Appl. Mech. Mater.* **838–841**, 2973 (2014)
5. Volkov, A., Chulkov, V., Kazaryan, R., Gazaryan, R.: Cycle reorganization as model of dynamics change and development norm in every living and artificial beings. *Appl. Mech. Mater.* **584–586**, 2685 (2014)
6. Bolotova, A., Treskina, G.: Research of technological features monolithic construction on the basis of system analysis. *Bull. Tomsk State Univ. Archit. Civ. Eng.* **2**(55), 176–183 (2016)
7. Lapidus, A.: Efficiency potential of organizational and technological solutions of a construction object. *Sci. Eng. J. Constr. Archit.* **1**, 175–180 (2014)
8. Garyaeva, V., Garyaev, N.: Integrated assessment of the technical condition of the housing projects on the basis of computer technology. In: *Proceedings of the International Conference on Computing in Civil and Building Engineering*, p. 1336 (2014)
9. Bargstädt, H., Nasir, A., Ignatova, E.: Can BIM support better working conditions for low-skilled labor? In: *14th International Conference on Construction Applications of Virtual Reality, CONVR 2014*, pp. 44–51 (2014)
10. Vajnshtejn, M., Zhadanovskij, B., Sinenko, S., Afanas'ev, A., Pavlov, A., Efimenko, A., Dolganov, A.: Evaluation of the effectiveness of organizational and technological solutions in the choice of means of mechanization of construction and installation works. *Sci. Rev.* **13**, 123–128 (2015)
11. Ignatova, E., Kirschke, H., Tauscher, A., Smarsly, K.: Parametric geometric modeling in construction planning using industry foundation classes. In: *The 20th International Conference on the Applications of Computer Science and Mathematics in Architecture and Civil Engineering, Bauhaus University Weimar, Weimar, Germany*, pp. 68–75 (2015)

12. Bajburin, A.: Reliability as a criterion for the classification of defects in construction. *Ind. Civ. Eng.* **10**, 25–26 (2000)
13. Kuzina, O.: Components of functional information model of city environment reorganization in interactive mode. In: *MATEC Web of Conferences*, vol. 73, p. 07013 (2016)
14. Rubcov, I., Treskina, G., Bolotova, A.: Classification of defects in the construction of monolithic concrete structures and their impact on the quality. *Sci. Rev.* **18**, 58–63 (2015)
15. Volkov, A., Chulkov, V., Kazaryan, R., Fachratov, M., Kyzina, O.: Possibility quantitative appraise components and guidance for constructional rearrangement of buildings attached to their confrontation. *Adv. Mater. Res.* **1065–1069**, 2585–2588 (2015)
16. Gumerova, E., Gamayunova, O., Shilova, L.: The optimal decision of insulation in cladding structures for energy efficient buildings. In: *MATEC Web of Conferences*, vol. 106, p. 06020 (2017)

Automation of Roof Construction Management by Means Artificial Neural Network

Azary Lapidus  and Alexander Makarov 

Moscow State University of Civil Engineering,
Yaroslavskoye Sh. 26, 129337 Moscow, Russia
anmakarov@yandex.ru

Abstract. To enable efficient managerial decisions in planning and generation of construction process, we need technologies to analyze and evaluate their conditions and to predict their further evolution. One of advanced methods to generate them is based on artificial neural networks (ANN). This paper represents the outcome from a research in construction process organization and management to build roof structures at the planning and operation stage, assisted by the ANN methodology. Relying on systems analysis and expert survey, the authors have designed a 4-layer feedforward ANN with a node pattern of 15-6-3-1. The authors used the concept of fuzzy sets to measure input and output of the network. The paper clearly illustrates the function of ANN and describes the learning algorithm by the backward propagation of errors relative to the resulting ANN. The authors have identified problems related to generation of the labeled training data in the researched field and developed a network learning approach that combines extraction of expert knowledge about the system with learning on training examples from real-life construction project.

Keywords: Artificial neural network · Organization of construction
Decision making support · Fuzzy sets · Roofing · Training data
Learning algorithm

1 Introduction

Currently, the procedure used to organize and manage construction processes is poorly formalized, and their evaluation and regulation mainly remains the prerogative of contractor engineering personnel (EP) and project managers, also the heuristic approach to problem solution is practiced frequently. This is because few efficient software solutions are able to reliably assess and predict a construction process, with sufficiently broad application range and rapid rate of implementation. Such problems exist also because it is hard to recover regressions in the field of construction organization and technology that features multiple parameters, defies quantitative evaluation, and tends to have a strong human factor and labor-intensive field experiments. For two decades now, software developed on the basis of artificial neural networks (ANN) has been actively implemented in different domains and activities, including construction [1–3]. This is first of all because ANN is multipurpose thanks to its free architecture that can comprise several levels with various sets of component links – thus the ANN can be used with nearly any property tree built as a result of systems

analysis of the object. Secondly, relatively simple and easily programmable network training algorithms help to get target dependencies under different conditions and in short time, thus ensuring low labor-intensity and high adaptability of the ANN. Thirdly, access to specific tools such as the threshold, activation function, feedback channels, storage memory, and others make the ANN able to approximate a dependency within multi-factor tasks that are difficult to formalize [4]. Both academic and practical research of different ANN-assisted processes has demonstrated that the approach, if adopted for dependency recovery tasks, is not inferior to and oftentimes excels the classical regression analysis method [5–7]. Neural networks developed and tested for construction project organization and management now can support decision making for construction process safety [8] and project management [9], they are also able to predict and evaluate specific construction processes such as: building underground structures [10], road building [11], earthwork [12], and other [13]. At this time, ANN has been used to study engineering features for roof design [14], included wind load problem [15], and deterioration process on the stage of roof maintenance [16]. This paper's main purpose is to create an ANN-based tool that can evaluate and forecast the construction process to build roof structures, meant to support administrative, technological, and managerial decision-making at the stage of construction project planning and implementation. The paper presents the results of the authors' studies on creation of the ANN architecture, formulating its working principles, methodology and training techniques. The authors lay down a theoretical basis for successful network training in real-life construction projects.

2 ANN Structure

The ANN structure (Fig. 1) is built around 6 key parameters: Cs – construction supervision, Qw – qualification of workers, Cc – construction crew, Mr – material resources, Wc – weather condition, It – information technology; and also the system's key variables (evaluation criteria): Q – quality, T – time, S – safety. The authors obtained the above parameters and criteria through systems analysis of the object and expert survey [17].

The first ANN layer (the entry layer) is comprised of sensors that harvest information from the construction site and translate it to the system's language. The layer consists of elementary administrative and production factors of the construction process. In this way, each second-layer neuron has a unique set of factors so that Cs: g1 – master, g2 – foreman, g3 – technical supervision inspector, g4 – chief engineer; Qw: g5 – working experience and competencies, g6 – labor discipline (this factor combines such notions as seniority, careful use of tools and construction materials, no irregular breaks, and such like); Cc: g7 – team staffing (to meet labor code and planned activities), g8 – production flowcharts (to meet the production time schedule); Mr: g9 – building materials, g10 – tools and inventory; Wc: g11 – immediate weather condition, g12 – taking extra steps to support production in specific weather conditions as necessary; It: g13 – project documents (including operational planning documents, work schedule), g14 – executive documents, g15 – digital document flow (also includes all necessary computer equipment and visual control for the construction site).

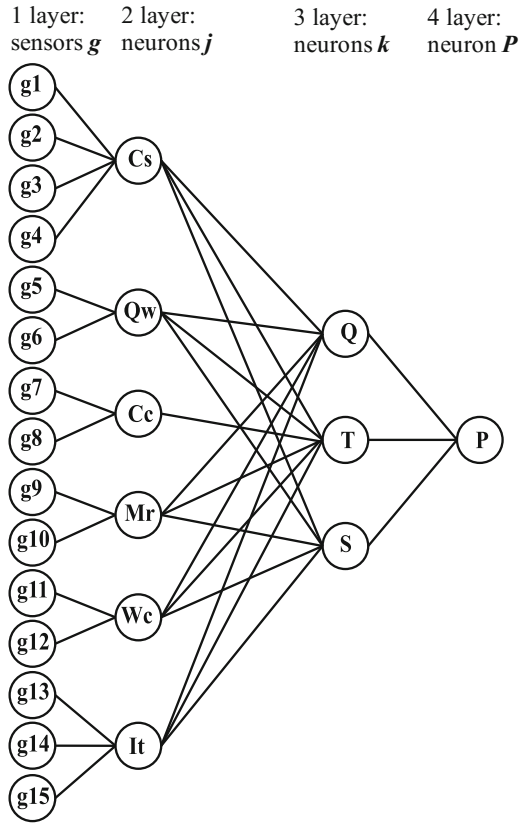


Fig. 1. ANN architecture.

Each sensor g is a basic administrative and technological factor. To measure it, we used the “System Component Measurement Device” SCMD (Fig. 2) that previously designed by these authors [18] using fuzzy sets.

SCMD consist of three linguistic variables preset as a fuzzy set, the membership function of which included the interval of stable equilibrium and the uncertainty interval. The operator – an expert in the field – should process data on each elemental factor collected from the real system, and then uses the SCMD to evaluate it: first by determining the linguistic term, and then by selecting the interval of membership function. Then acquired information to convert to numerical signal x_g by operation of defuzzification, according that input of network is abscissa of a point representing the average value over the selected interval of membership function. This is how the chain of steps occurs to encode inputs from the construction site into the system language. Let us express the vector of ANN input signals as $\{x_g\}$, where g - sensor index.

Each neuron for the ANN is designed based on the classic structure of the McCulloch-Pitts artificial neuron with the exception of bias. The operation of the second network layer is presented in Fig. 3. Thus signals generated by second-layer

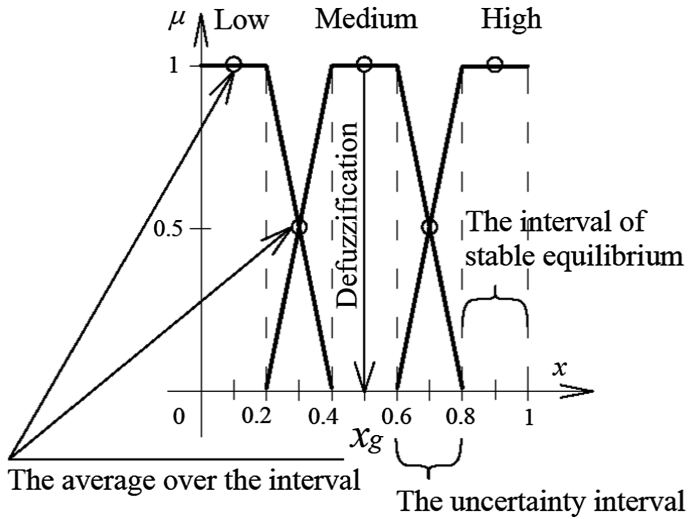


Fig. 2. System Component Measurement Device (SCMD).

neurons are transmitted up to the third layer of neurons, which functioning are identical to that of the lower layer. This layer processes inputs about system parameters and generates output vector $\{y_k\}$ based on key criteria of the construction process. The resulted converted functional signals are sent from the third layer to the network's last (exit) layer that has only one linear neuron: the construction process potential (P), which is an integral evaluation of the entire system.

This neuron compresses all information extracted from an object, which the ANN converts into a single value that is the network's output. The output signal y_p received by P is made at a point by defuzzification (the process of sensor defuzzification mirrored), which belongs to one of the graphs in the SCMD, to determine the linguistic term of the construction process potential P and its membership function value.

3 Concept of ANN Learning

ANN training is a process whereby weight coefficients of synaptic links are tuned within the network. A number of approaches to ANN training exist. Supervised learning with the backward propagation of errors is one tried and trusted approach [19]. This algorithm needs a training data comprised of an input signal vector $\{x\}$ and a corresponding output signal vector $\{y\}$ for system responses. The process to generate the first part of the training set was described in the previous chapter, it corresponds to the vector of ANN input signals $\{x_g\}$ after they have passed defuzzification. However, potential P is an integrated comprehensive descriptor of the construction process, and it is rather difficult to measure accurately, even in linguistic terms, and particularly when its key variables have different values. Evaluation of potential P is a task that is difficult to formalize, because it can have different values under the same internal and external

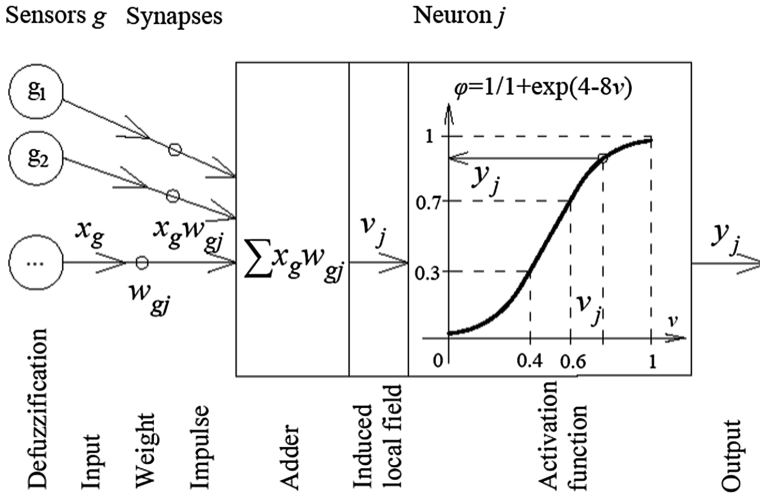


Fig. 3. Neuron structure.

conditions, depending on which construction process criteria (key variables) are preferable in the circumstances. If key variable S has roughly the same weight on any construction site, the weights of variables Q and T do depend on how critical the project is, as well as on project deadlines, goals, opportunities, and the developer’s administrative machine, including the key decision maker (DM). Such factors are always project-specific and can evolve within the project cycle, so determining the weights of synapses for key variables Q, T, S relative to P defies formalization and remains the task to be handled by the DM in the specific environment of each construction project. This is why we decided to leave them beyond the array of learning parameters. Unlike the construction process potential P , main variables Q, T, S are more easily measurable. Virtually each construction project does such measurements nearly every day. For example, technical supervision inspector will assess construction process quality Q , chief engineer/foreman/master acting within their respective job descriptions will file reports on time T according of the work schedule and safety S in the course of construction. But such assessments are linguistic by nature, issued as instructions, reports, letters and oral presentations. Therefore, to measure the system’s key variables and elementary administrative and production factors the authors use the SCMD based on the concept of linguistic variable [20]. We can express the training data in the following way

$$\{(x_g, y)_n\}_{n=1}^N \tag{1}$$

where y – vector of values of the construction process key variables measured with the SCMD and then subjected to defuzzification,

- N – number of example in the training data, or the sample complexity,
- n – ID number of the training example.

There are two ways to generate a training data (1). In the first method we extract knowledge about the item by mobilizing competent expert teams, and then launch multilevel expert assessment, the second method consist in direct observation of the real-life system. The first way has certain disadvantages: it is rather expensive, and each expert opinion is subjective and abstract possibly resulting in low concordance coefficients by Kendall or poor rank correlation by Spearman, so the expert panel needs to be expanded to overcome this weakness. Another disadvantage is a limited effective life of data received by expert survey. Extracted expert knowledge stands for accumulated experiences of different construction projects in the specific environment of the building sector at a certain point in time, which is always in the past by the time of survey. Also, considering the continuous dynamics of existing construction materials, technologies and methods, such knowledge tends to become less valuable with the lapse of time, and therefore any model they underlie will be relatively obsolete.

ANN learning relying on data obtained immediately from the construction site in question is free of such shortcomings, nor does sampling call for extra financing, because evaluation of process components is one of the key functions of the EP in any construction project. One major flaw of the method is the need to collect a multitude of training examples with approximately the same density within the interval of all possible values [0, 1], to ensure good generalization of the ANN and statistical reliability of ultimate results. Determining enough training examples to make the training algorithm statistically reliable is a key objective in the theory of machine learning [21], which solution presented in our other works. Another serious disadvantage is the lack of access to construction sites for outside researchers, to obtain training data it is necessary to be an employee of a construction company that is interested in learning and implementing ANN.

In this research, these authors chose to combine the two above methods, as they can be complementary, each addressing the other's problems. Expert survey – the results were covered in some previous papers – found weight coefficients for connecting links, and this considerably limited the number of necessary training examples, and their purpose was no to weigh but to adjust them in the conditions of real-life projects.

3.1 Learning Algorithm

Let us examine a network learning algorithm that uses backpropagation – part of the algorithm family that minimize a simple network error (SEM algorithm), as applied to the created ANN. The signal vector $\{x_g\}$ is sent to the network's input from the first example of the training data, and the system's response is registered: the output vector of signals from the network's third layer $\{y_k\}$, which is then compares to the respective vector of the training example $\{y\}$. Thus, for the output signal of each neuron in Layer 3, the system finds error $e_k = y - y_k$. To evaluate error level of the entire ANN by this training example uses a function which merges errors from all neurons in Layer 3

$$E = \frac{1}{2} \sum_k e_k^2 = \frac{1}{2} \sum_k [y - \varphi(v_k)]^2 = \frac{1}{2} \sum_k \{y - \varphi[(\sum_j w_{jk} \varphi(\sum_g x_g w_{gj}))]\}^2 \quad (2)$$

The purpose of training is to adjust free parameters of the ANN – synaptic weights $w + \Delta w$ in a way that minimizes the function (2). The point of backpropagation is to find value Δw for each synaptic weight, where the function (2) will change away towards its gradient. So this method actually realizes the gradient descent with steps found as

$$\Delta w = -\eta \frac{\partial E}{\partial w}, \quad (3)$$

where η - coefficient of the gradient descent rate.

If we use the chain rule of differentiation for the function (2) with respect to w_{jk} the expression (3) for synaptic weights of the links between Layer 2 and Layer 3 will appear as:

$$\Delta w_{jk} = -\eta \frac{\partial E}{\partial w_{jk}} = \eta e_k \varphi'(v_k) y_j = \eta \delta_k y_j, \quad (4)$$

where δ_k - local gradient of neuron k.

Let us now differentiate activation function for argument v_k to get

$$\varphi'(v_k) = \frac{8 \exp(4 - 8v_k)}{(1 + \exp(4 - 8v_k))^2} = 8y_k(1 - y_k), \quad (5)$$

and then for the local gradient of neuron k, the expression will appear as:

$$\delta_k = 8e_k y_k (1 - y_k) \quad (6)$$

To find Δw_{gj} of synaptic weights of the links between the network's Layer 1 and Layer 2, in the same way we find the partial derivative of function (2) with respect to w_{gj} and we get

$$\Delta w_{gj} = -\eta \frac{\partial E}{\partial w_{gj}} = \eta \delta_j x_g, \quad (7)$$

where δ_j - local gradient of neuron j, which in the light of (5) will appear as:

$$\delta_j = 8y_j(1 - y_j) \sum_k \delta_k w_{jk}. \quad (8)$$

Parameter η describes the rate of ANN learning, since its value determines the step Δw used to approach the minimum of function (2). Parameter η may be shared by the entire ANN, or it can be selected individually for each link of the network, as this will raise speed of convergence notably. For larger η values, there is likelihood of missing the extremum of function (2), thus losing stability of the algorithm. At smaller values of η the ANN will take much time to converge to the minimum error values. The value of η should be selected based on the curvature of a graph of function (2) that is hard to

know theoretically before ANN learning begins. To speed up ANN learning by backpropagation, the momentum from the previous example can be added successfully [22]. Thus weight correction value w_{jk} for example $n + 1$ from the training data (1) will appear as this

$$\Delta w_{jk}^{n+1} = \eta \delta_k y_j + \alpha \Delta w_{jk}^n, \quad (9)$$

where α - the momentum to describe the contribution of past iteration n .

The stopping criterion used to evaluate the quality of learning algorithm can be the average squared error of the network within the recent training sample

$$\frac{1}{N_e} \sum_{N_e} \sum_k e_k^2 \leq c, \quad (10)$$

Where c - constant to describe the high limit of error,

N_e - number of examples in the recent training sample, $N_e \subset N$.

Finding the sample complexity N enough for high-quality ANN learning is an important objective which the authors solved in another paper.

4 Conclusions





The final stage of learning for the created ANN understands its test run on real-life construction projects. The authors are currently working to design a software solution that will automate ANN operation and learning. This article demonstrates that to introduce it the construction company will not require any extra financing to expand its staff or respective employees' jobs descriptions. In the course of ANN learning, defining the inputs and outputs is a natural process where the project manager gathers data on construction progress from reports filed by the company's EP and supervising agencies, and the ANN makes this process more structured. Soon after the learning, the company begins to wield a tool that enables highly reliable forecasts of development of roofing building process based on information about the key administrative and production factors. Therefore, with automation, all information from construction site are instantaneously processed to generate accurate estimates, and this accelerates and facilitates the process of managerial decision-making, during both planning and implementation of the construction process. Ultimately, once built into the construction company's system, the ANN will ensure more efficient management of the roofing construction processes, while also cutting the respective time period and costs, and better structuring the data flow from the construction site.

References

1. Moon, J., Jung, S.: Algorithm for optimal application of the setback moment in the heating season using an artificial neural network model. *Energy Build.* **127**, 859–869 (2016)

2. Taffese, W., Sistonen, E.: Neural network based hygrothermal prediction for deterioration risk analysis of surface-protected concrete facade element. *Constr. Build. Mater.* **113**, 34–48 (2016)
3. Silva, A., Dias, J., Gaspar, P., de Brito, J.: Statistical models applied to service life prediction of rendered facades. *Autom. Constr.* **30**, 151–160 (2013)
4. Cybenko, G.: Approximation by superpositions of a sigmoidal function. *Math. Control Signals Syst.* **2**, 303–314 (1989)
5. Fernandez, F., de Palacios, P., Esteban, L., Garcia-Iruela, A., Rodrigo, B., Menasalvas, E.: Prediction of MOR and MOE of structural plywood board using an artificial neural network and comparison with a multivariate regression model. *Compos. Part B: Eng.* **43**, 3528–3533 (2012)
6. Khademi, F., Jamal, S., Deshpande, N., Londhe, S.: Predicting strength of recycled aggregate concrete using artificial neural network, adaptive neuro-fuzzy inference system and multiple linear regression. *Int. J. Sustain. Built Environ.* **5**, 355–369 (2016)
7. Pombeiro, H., Santos, R., Carreira, P., Silva, C., Sousa, J.: Comparative assessment of low-complexity models to predict electricity consumption in an institutional building: linear regression vs. fuzzy modeling vs. neural networks. *Energy Build.* **146**, 141–151 (2017)
8. Patel, D., Jha, K.: Evaluation of construction projects based on the safe work behavior of co-employees through a neural network model. *Saf. Sci.* **89**, 240–248 (2016)
9. Costantino, F., Gravio, G., Nonino, F.: Project selection in project portfolio management: an artificial neural network model based on critical success factors. *Int. J. Proj. Manag.* **33**, 1744–1754 (2015)
10. Siami-Irdemoosa, E., Dindarloo, S., Sharifzadeh, M.: Work breakdown structure (WBS) development for underground construction. *Autom. Constr.* **58**, 85–94 (2015)
11. Li, M., Chen, W.: Application of BP neural network algorithm in sustainable development of highway construction projects. *Phys. Procedia* **25**, 1212–1217 (2012)
12. Hola, B., Schabowicz, K.: Estimation of earthworks execution time cost by means of artificial neural networks. *Autom. Constr.* **19**, 570–579 (2010)
13. Akhavian, R., Behzadan, A.: Smartphone-based construction workers activity recognition and classification. *Autom. Constr.* **71**, 198–209 (2016)
14. Chong, W., Al-Mamoon, A., Poh, S., Saw, L., Shamshirband, S., Mojumder, J.: Sensitivity analysis of heat transfer rate for smart roof design by adaptive neuro-fuzzy technique. *Energy Build.* **124**, 112–119 (2016)
15. Fu, J., Liang, S., Li, Q.: Prediction of wind-induced pressures on a large gymnasium roof using artificial neural networks. *Comput. Struct.* **85**, 179–192 (2007)
16. Attoh-Okine, N., Appea, A.: Comparative analysis of artificial neural networks and evolutionary programming in roof deterioration modeling. *Constr. Build. Mater.* **13**, 311–320 (1999)
17. Lapidus, A., Makarov, A.: Model for the potential manufacture of roof structures for residential multi-storey buildings. *Procedia Eng.* **153**, 378–383 (2016)
18. Lapidus, A., Makarov, A.: Fuzzy sets on step of planning of experiment for organization and management of construction processes. In: *MATEC Web of Conferences*, vol. 86, p. 05003 (2016)
19. Rumelhart, D., Hinton, G., Williams, R.: Learning representations by back-propagating errors. *Nature* **323**, 533–536 (1986)
20. Zadeh, L.: The concept of a linguistic variable and its application to approximate reasoning – I. *Inf. Sci.* **8**, 199–249 (1975)
21. Anthony, M.: Aspects of discrete mathematics and probability in the theory of machine learning. *Discret. Appl. Math.* **156**, 883–902 (2008)
22. Plaut, D., Hinton, G.: Learning sets of filters using back-propagation. *Comput. Speech Lang.* **2**, 35–61 (1987)

Organization of Concrete Works on the Bases of the Information System of Tracking

Alexander Ginzburg^(✉) , Sophia Kozhevnikova ,
Alexander Afanas'ev , and Vitaliy Stepanov 

Moscow State University of Civil Engineering,
Yaroslavskoye sh., 26, 129337 Moscow, Russia
ginav@mgsu.ru

Abstract. Classification of the origins of refusals of structural elements, depending on the character of their origin is presented in the article. The approach to the quality assessment of the performed works and the enterprises, carrying out the works on construction of artificial structures, which is based on the mark assessment according to four categories is offered. Detailing has been completed for each category and the main features of the controlled elements have been described. The most admissible points are determined depending on filling of the verification processes and according to the criteria and controlled parameters for each group, which are included. The results of practical implementation of the offered approach to the capital construction project in the field of bridge construction, displaying summary quality assessment of the works performance on the basis of the analysis of two construction enterprises and three concrete plants are provided. According to the practical use of the developed approach the analysis in comparison with the process of the organization of construction production, developed in practice, is carried out, the benefits of the first are established as well. Values of specific weight of each criterion for the purpose of carrying out the most qualitative and rational analysis are also obtained.

Keywords: Construction of road-and-transport network
Organization of works · Installation-and-construction works
Quality control · Information system of tracking

1 Introduction

The road-and-transport network plays the important role in the development of the country. The special place is allocated to the artificial constructions, which are included. The problems, connected with the increase in the performance indicators of the organization of construction production, the choice of potential participants of the construction process, the increase in qualitative level of construction projects and their components have a great relevance [1]. The existing quality control system of construction means the assessment of documentation, materials, equipment, works and fixing of the results of check, and also the revealed discrepancies [2]. The service of construction supervision performs complex control, concerning the aforesaid

parameters, and provides the Customer with the reports on the results of check, being the only participant of construction production by, whose problem is the owning of complex information on a construction project. There are no uniform provisions on the operations procedure during the control in construction, however there are separate standards in the organizations or the recommendation for specific projects. Due to the specific features of construction of different structures there are no generalizing provisions on control of contract organizations and their assessment.

The considerable share in the variety of structural elements of artificial structures is occupied by the precast and monolithic concrete structures, that defines the list of the key parameters under control [3]. In the modern conditions the particular interest is attracted by the development of the integrated approach to the assessment of producers and suppliers of raw materials as well as of the construction organizations for the rational organization of works on construction of road-and-transport artificial structures and the improvement of quality of the works performed [4, 5].

2 Materials and Methods

According to the analysis of the results of laboratory research, completed for construction and reconstruction projects both by National Research Moscow State University of Civil Engineering, Research Centre “MSUCE SYSTEM-TEST” and by Research Institute of Transport Construction (Joint Stock Company), the origins of refusals of structural elements were classified into groups depending on the character of their origin [6–10]. The main groups are the following:

1. Organizational reasons: terms of conduction works in the changing conditions, the necessity of concreting of volume constructs, rates of works;
2. Organizational-and-technology reasons: the lack of operational management, carried out by any construction laboratory, insufficient equipment supply, violation of stages and requirements of the production schedules;
3. Constructive reasons: mistakes in calculations;
4. The reasons, connected with information insufficiency: the lack of data on the influence of the complex of factors on the reliability of structures and the lack of scientific maintenance of the construction production.

The implementation of the approach, based on the ball assessment according to the categories, is suggested during the assessment of quality of the construction works performance within the construction of artificial structures.

Four groups of the principle controlled processes are distinguished:

- the choice of suppliers of concrete mixes (group A);
- the production organization of concrete works (group B);
- the organization of quality control of concrete mixes and the finished construct (group C).
- forming and maintaining of the executive documents (group D).

Each group is divided into subgroups, which contain their lists of controlled parameters. Group A. Success of the production of monolithic concrete works during

the construction strongly depends on that, how accurately the suppliers of the concrete mix perform their functions [11]. The choice of the “correct” supplier is the basis of successful functioning and creation of the steady base of supply. Only professionals are able to make the proper decision on a supplier, having only limited subjective information [12]. The necessity to prove the decision before the heads of the enterprise complicates the task in addition, because some persons, who are responsible for making decisions on the purchase, often act intuitively.

The field of creation of the effective relations with suppliers in Russia is studied rather poorly, especially in the construction industry. There had been no prerequisites for that before the stabilization, which took place during the last years and allowed to shift the horizon of economic planning at the enterprises for 3–5 years ahead [13]. Until the market is weak and chaotic, the only tactics of creation of the relations is mostly the bargaining on the price. The effective organization of works on choosing of suppliers and the creation of the competent relations leads to the decrease in risk of the appearance of defects and discrepancies during the acceptance of mixes [14] and structures within the construction project. We suggest to follow the process, presented in the Fig. 1, during the choice of suppliers of concrete mixes and to make the comparative analysis of suppliers by the following criteria:

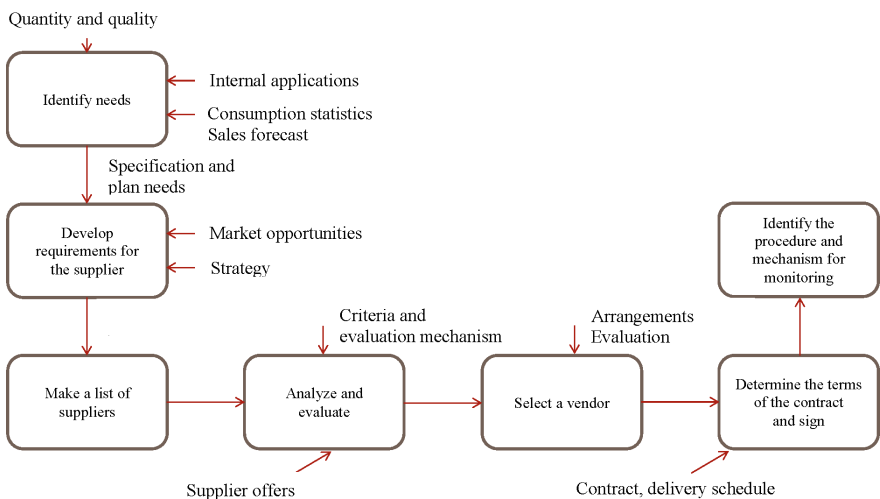


Fig. 1. The process of choosing of a plant as a supplier of concrete mixes.

1. Quality (compliance of the mixes to the standard-and-design requirements during the delivery);
2. Price (production and transportation costs);
3. Remoteness of the supplier from the enterprise (taking into account keeping of properties during the definite period);
4. Reliability of the supplier (the experience of production of road mixes, absence of claims);

5. Terms of payment (the possibility of flexible payments);
6. Delivery (the possibility of the round-the-clock and long-term supply of mixes without quality loss);
7. The condition of production (the equipment, existence of Quality Management System, certificates for the mixes, the conclusions for the raw materials).

We recommend to create the three-leveled hierarchy during the assessment of the supplier. In this hierarchy the 1st level contains the purpose (the choice of the supplier), the 2nd level includes some private criteria for the evaluation of suppliers, the 3rd level concludes some alternatives for the plants, concerning the production of concrete mixes. Then it is necessary to estimate the criteria with the use of various methods (particularly the method of rating estimates). Specific weights for the pointed out criteria of the choice of suppliers of concrete mixes are stated for this method on the basis of the carried out works. After choosing of suppliers, the most suitable for a certain construction project, the necessary stage is the check of the possibility of concreting along with other plants, as well as the analysis of raw materials on compatibility (Fig. 1).

Group B. It is important to control the accompanying processes, connected with the carried out works, during the production organization of monolithic concrete works [15, 16]. The processes, preceding the concrete works are also the subject to the detailed analysis and the check of compliance to requirements of technological documents, including projects of the construction enterprises [17]. At this stage, according to the revealed discrepancies, there is the possibility of adoption of the organizational-and-technological solutions, aimed on the correction of the works process, on the observance of the terms of construction, provided by the schedule of works. It is suggested to make control of the following elements for the assessment of this type of works:

1. Warehousing and storage of materials.
2. Performance of the processing equipment;
3. Production of the preparatory works (reinforcing and shuttering works);
4. Laying of concrete mix;
5. Care of the concrete of the structure;

Group C. The organization of control of concrete mixes quality as well as the finished construct quality is the most important stage of carrying out the concrete works. It is necessary to consider that road concrete mixes with non-standard frost resistance are applied for the objects of transport construction. Thus, some additional parameters and test methods are applied to such concrete mixes. The features of such products provides the use of various additives, which effect can vary, depending on many factors. The responsibility for the implementation of this stage increases, as in the sake of the economy of material and temporary resources, this stage is very seldom made in full [18]. This violation leads to the formation of defects, discrepancies, violation of the bearing ability of a structure and even to a collapse. Timely detection of any discrepancy and the management of the process of the return of inappropriate materials makes it possible to prevent any future defects and accidents [19, 20]. During the assessment of the parameters on this group the following items are distinguished:

1. Control of indicators of the concrete mix quality;
2. Frequency of the quality control;
3. Definition of indicators of quality of a concrete (or reinforced concrete) structure.

Group D. Correct maintaining of technical documents and the formation of executive documents are the major tasks, which are aimed on the confirmation of the fact of performance of construction-and-installation works. Both participants of the construction process and external auditors from Federal executive authorities pay great attention on the analysis and assessment of documents. Executive documents have to reflect the actual indicators of the created structures, including their deviations from the project, and they also have to conform to requirements of the standard documents in the field of construction [21].

The following items can be named as the main evaluation criteria:

1. Working drawings;
2. Project of works;
3. Production schedules of works;
4. Provision with the urgent standard documents;
5. Presence of workers' journals;
6. Existence of accompanying documentation on materials;
7. Existence and registration of acts of acceptance of work.

The ball mark is put down according to the number of the parameters of the third group, which are contained in each of the criteria. The determination of the level of controlled parameters is carried out as follows:

- 0 points – at least one requirement of the standard or project documents to a certain parameter is not carried out;
- 0.5 points – boundary value;
- 1 point – all the requirements are fulfilled.

3 Results

The results of the application of the offered approach to the assessment of the controlled processes of construction-and-installation works in the aspect of monolithic concrete works have been obtained within the construction project of the bridge-crossing through the Volga River in the Moscow region. These results are presented in the Fig. 2.

Within carrying out the research works the number of the plants, supplying road concrete mixes, has been limited to 3, the number of the analyzed construction enterprises was limited to 2. The duration of works, which have undergone the multi-criteria assessment, has made up six months.

In the sake of the possibility of carrying out the comprehensive assessment and adoption of the most rational relevant decision, connected with the choice of suppliers of road concrete mixes the weight values for each criterion have been revealed in the research. (Table 1).



Fig. 2. Schedules of the controlled processes assessment.

Table 1. Ratio of the criteria and specific weight.

№	Criteria	Specific weight of the criteria
1	Quality	0.21
2	Price	0.11
3	Remoteness of the supplier from the enterprise	0.17
4	Reliability of the supplier	0.15
5	Term of payment	0.05
6	Delivery	0.18
7	Performance of production	0.13

4 Discussion

The organization of concrete operations using the approach based on an assessment of the A-D groups and subgroups gives the chance to carry out the qualitative analysis of the actual situation, concerning the construction as well as to inform the stakeholders, participating in the construction. The information, created during the application of the offered monitoring technique gives the chance of the implementation of tracking of the works correctness and also tracking of the influence of mismatches on finite characteristics of a construction product.

This approach allows to analyze the activity of the plants, supplying concrete compounds as well as the activity of construction enterprises, and also to carry out the assessment of all the production processes of the concrete operations within construction projects. The development and enhancement of the methodology requires carrying out further scientific research in this direction, statistics collection, extension of the database on the contractors and plants for limiting of time of the organizational component of works and also the acceptance of managerial decisions.

5 Conclusion

The information system of tracking during the organization of concrete works is made up by the results, obtained within the research, namely:

- the classification of the causes of refusals of structural elements, depending on the character of their origin;
- the approach based on the ball assessment in the categories (the choice of the supplier of concrete mix, the organization of production of concrete works, the organization of quality control of concrete mixes and the finished construct, the formation and maintaining executive documents);
- the process of the choice of suppliers of concrete mixes according to the set criteria with the use of specific weight of each criterion.

Acknowledgments. The research in this scientific direction was performed with the assistance of “MSUCE SYSTEM-TEST” Research Centre of National Research Moscow State University


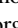
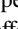

of Civil Engineering. The equipment, necessary for carrying out the research, is provided by “M-Certification Ltd”.

References

1. Eremin, V., Cao, V.: Automating the evaluation of riding quality of bridges. *Mag. Civ. Eng.* **3**(29), 83–88 (2012)
2. Volkov, A., Petrova, S., Ginzburg, A., et al.: *Information Management Systems and Data Processing Technologies in Civil Engineering*. MGSU Publication, Moscow (2015)
3. Ignatova, E., Kirschke, H., Tauscher, A., Smarsly, K.: Parametric geometric modeling in construction planning using industry foundation classes. In: *The 20th International Conference on the Applications of Computer Science and Mathematics in Architecture and Civil Engineering*, Weimar, Germany, pp. 68–75 (2015)
4. Ignatov, V., Ignatova, E.: Intelligent technologies in construction design. *Vestnik MGSU* **2**, 237–238 (2009)
5. Volkov, A., Chulkov, V., Kazaryan, R., Fachratov, M., Kyzina, O., Gazaryan, R.: Components and guidance for constructional rearrangement of buildings and structures within reorganization cycles. *Appl. Mech. Mater.* **580–583**, 2281–2284 (2014)
6. Scott, R., Deb, S., Dutta, A.: Strain distributions in external reinforced concrete beam-column joints subjected to cyclic loading. *Concrete* **44**(6), 57–59 (2010). (London)
7. Kan, L., Shi, H., Sakulich, A., Li, V.: Self-healing characterization of engineered cementitious composite materials. *ACI Mater. J.* **107**(6), 617–624 (2010)
8. Dao, V., Dux, P., Morris, P., Carse, A.: Performance of permeability-reducing admixtures in marine concrete structures. *ACI Mater. J.* **107**(3), 291–296 (2010)
9. Yang, K., Ashour, A., Lee, J.: Shear strength of reinforced concrete dapped-end beams using mechanism analysis. *Mag. Concr. Res.* **63**(2), 81–97 (2011)
10. Scerrato, D., Giorgio, I., Della Corte, A., Madeo, A., Dowling, N., Darve, F.: Towards the design of an enriched concrete with enhanced dissipation performances. *Cem. Concr. Res.* **84**, 48–61 (2016)
11. Kozhevnikov, M., Kozhevnikova, S., Sviridov, V.: Application of the QFD method for concrete products manufacturing enterprises. *Sci. Rev.* **11**, 17–21 (2016)
12. Kozhevnikova, S., Kozhevnikov, M., Sviridov, V.: Prospects for applying statistical methods in the field of quality management of concrete mixes. *Sci. Rev.* **11**, 66–71 (2016)
13. Pugachev, V.: *Internal audit and control. Organization of internal audit in the context of economic crisis. Case and Service*, Moscow (2010)
14. Ginzburg, A.: Queuing systems in management construction. *Appl. Mech. Mater.* **405–408**, 3352–3355 (2013)
15. Ginzburg, A., Kozhevnikov, M.: Features of the organization of construction and control of bridge structures in modern conditions. *Bulletin BSTU named after V.G. Shoukhov*, vol. 6, pp. 58–61 (2017)
16. Kozhevnikov, M.: Evaluation of the application of information modeling technologies in the organization of bridge construction. *Econ. Entrepreneurship* **5**(1), 640–643 (2017)
17. Badaguev, B.: *Organization of construction production. Production and technical documentation*. Alpha Press, Moscow (2013)
18. Kiryuhin, S., Kozhevnikov, M., Sviridov, V.: Quality management system of an organization or project in construction and the role of leadership in policy and decision-making. In: *Modern Russian Management: State, Problems, Development: XXIV International Scientific and Practical Conference*, pp. 19–23 (2016)

19. Volkov, A.: General information models of intelligent building control systems: basic concepts, determination and the reasoning. *Appl. Mech. Mater.* **838–841**, 2973 (2014)
20. Garyaeva, V., Garyaev, N.: Integrated assessment of the technical condition of the housing projects on the basis of computer technology. In: *Computing in Civil and Building Engineering Proceedings International Conference*, p. 1336 (2014)
21. Kuzina, O.: Components of functional information model of city environment reorganization in interactive mode. In: *MATEC Web of Conferences*, vol. 73, p. 07013 (2016)

Information Support for the Operational Management of the Construction Organization

Nataly Knyazeva¹ , Vitaliy Chulkov¹  , and Mark Abelev² 

¹ Moscow State University of Civil Engineering,

Yaroslavskoye Sh. 26, 129337 Moscow, Russia

nknyazeva@mgsu.ru, vitolch@gmail.com

² National Research University Higher School of Economics,

20, Myasnitskaya, 101000 Moscow, Russia

Abstract. The technology and efficiency of the organization of construction industry largely depend on the timely provision of all internal processes with the optimal amount of information sufficient for making managerial decisions. The operational management of construction and production activities includes planning and accounting of works, control of execution, logistics and logistics. Information support defines the basis of the information technology application platform. The life cycle of any building object is extremely informationally saturated. With the introduction of innovative materials and technologies, with the connection of a large number of process participants at different stages, more information is required for prompt decision-making, pressure on time and resources is increasing. The distribution of information flows along the stages of the life cycle of a construction site, its spread over time and among the involved specialists is the main task of information support, on the basis of which the effectiveness of operational management is increased by building an information model for the construction of the facility and automation of the issuance of organizational and technical documentation.

Keywords: Information support · Operational management

Transport buildings and structures · Efficiency of the organization · Life cycle

1 Introduction

Today, the practice of introducing information models has shown the inadequacy of the development of only the design model. The information model of the construction site at each stage of its implementation is transformed and supplemented taking into account the amount of information needed for the specificity of the new activity (Ignatiev 2007). The use of information models allows for effective control over the construction process. For example, it is possible to organize an automated monitoring system for the construction of buildings and structures in real time and integrate it with corporate management systems, that is, the posting of comments and the issuance of tasks in an electronic system with tracking capabilities (Tarasenko and Ostroukh 2007). All this in combination with the availability of a set of information on the project makes it possible to improve the quality of management decisions (Kaneman 2005).

The object of this work are companies of all organizational typologies of property, acting as participants in the construction market. As a subject, the system of operational management of the organization and planning of construction production is singled out.

The main purpose of the article is to formulate and formulate a list of theses on the most relevant tendencies in the field of information support for the operational management systems of the construction organization.

Achieving the goal implies the solution of the list of tasks:

- categorization of elements of information support for operational management systems for construction companies;
- theoretical analysis of existing software and allocation of functionality;
- development of an algorithm for the formation of information support for operational management systems of a construction organization.

The basis of operational management is planning, which in turn represents one of the procedures for project management. A. Fayol defined five basic principles of planning: unity, continuity, flexibility, accuracy. R. Akoff justified another key principle - participation (Sheldrake 2001).

Since the 1950s, automation elements have been used in the field of project management to develop schedules for large work packages based on the Critical Path Method (M. Walker and D. Kelly). To date, the evaluation of the effectiveness of informatization of the operational management of the construction organization, convenient for use in construction companies with various organizational structures, participants of the process (Farwick et al. 2016) has not been fully studied. The criteria for the evaluation of project management systems in construction have been determined, and based on them, a system of indicators has been developed for a comprehensive assessment of the effectiveness of informatization of building management systems (Mrugalska et al. 2016). The system consists of: an indicator of the quality of technical solutions, which reflects the quality of the design of objects at the first stages of the life cycle of the project; An indicator of the quality of organizational and technological solutions, showing the degree of informatization of the system in the development of the construction project, as well as the project for the production of works; An indicator of the quality of integrated software solutions reflecting the ability of an automated system used to support a number of information data structures and different levels of user access rights; The indicator of the number of staff, expressed as a percentage reduction in personnel involved in project management (Itskovich 2016). These directions, inherent in the construction industry and reflecting the main aspects of management in the implementation of construction projects, allow us to fully appreciate the effectiveness of informatization of the operational management system of the construction organization in terms of the use of automated systems (Pezeshki and Ivani 2016).

Methods. In a market economy, both the circle of consumers of scientific and technical information and the range of information about its sources of search are significantly expanding. Information acquires a multifunctional character that requires constant improvement of methods of its processing, classification and efficiency of use (Underwood et al. 2016). In general, information support for management of innovative

processes in the organizations of the construction complex can be represented by the following scheme:

- analysis of the general innovation situation in the country's construction sector;
- specification of target indicators of innovative activity of firms, companies of a building complex;
- forming a list of problems that must be solved by the company to ensure innovative development;
- analysis of information capabilities of the company to ensure the solution of the list of problems;
- identification of additional information problems to ensure preferential indicators of the company's innovation activity;
- search, systematization, selection and classification of additional sources of scientific and technical information;
- formation of information bank of technologies of the construction company;
- evaluation of the priorities of information technologies that are in the sphere of the company's activities;
- evaluation and selection of the company's innovative strategy in accordance with the target model.

2 Results and Discussion

The practice of implementing information models has shown the inadequacy of the development of only the design model. The information model of the building object at each stage of its implementation is transformed and supplemented taking into account the amount of information required for the specificity of the new activity. The use of information models allows for effective control over the construction process. For example, it is possible to organize an automated monitoring system for the construction of buildings and structures in real time and integrate it with corporate management systems, that is, the issuing of comments and the issuance of tasks in an electronic system with traceability capabilities. All this, together with the availability of a set of information on the project, makes it possible to improve the quality of management decisions.

Investigation of information flows is expedient with the help of constructing logical-information models (LIM) of processes, where information about input and output information, documents, routes, their movements, tasks and participants should be reflected for each stage (Figs. 1 and 2).

One of the most important tasks, partially automated in various software complexes, is the scheduling of construction, with the help of which relations are established between the participants in the construction industry concerning the amount of work and resources (temporary, human, material). The calendar plan is the basis for planning the activities of the enterprise (Gumba 2012). If we consider the LIM of the construction of the calendar plan from the point of view of the traditional approach to the development of the Organization of construction section in the project documentation, the whole process is divided into 5 stages (Oleinik 2015):

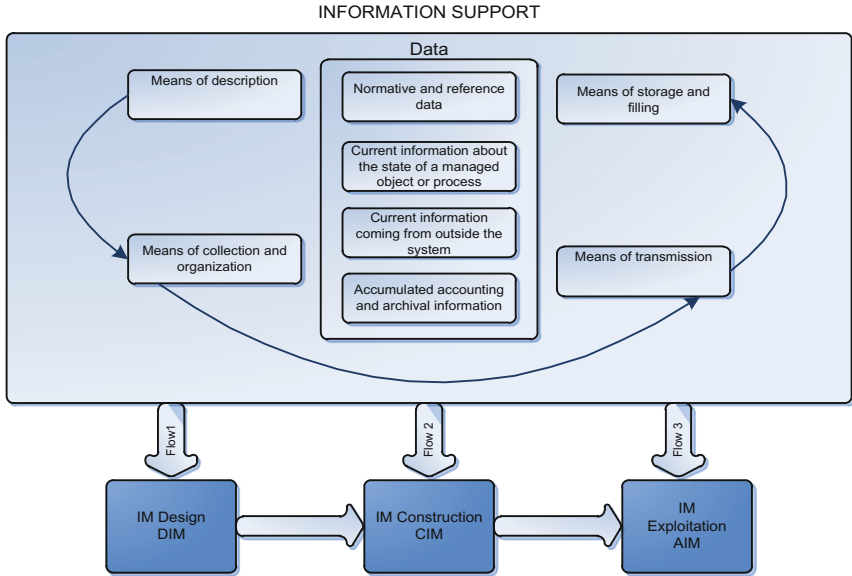


Fig. 1. Scheme of information support of information models of design, construction and operation processes.

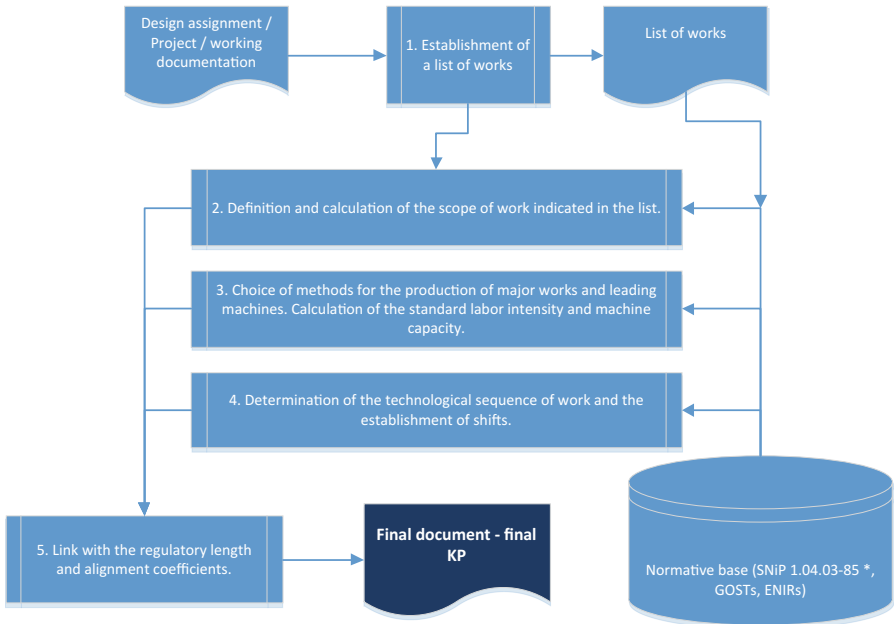


Fig. 2. LIM construction of the calendar plan.

1. Drawing up a list of construction works, based on architectural, space-planning and constructive solutions.
2. Calculation of the scope of work according to this list.
3. Selection of methods for the production of major works and leading machines from the relevant databases. Calculation of labor intensity of work using normative documents (GESN, ENR).
4. Determining the technological sequence of work and the establishment of shifts.
5. Linkage with the normative duration and leveling of the coefficients.

The basis of such a calculation scheme is a list of construction works without a direct relationship with the structural elements of the building. Even the use of automation tools, for example, the software complex NanoCad Construction Site or Hector: the Designer-Builder, does not allow to avoid collisions that arise when making changes to the sections of the AR, KR, etc.

Does not solve this problem and the development of IM construction (CIM), because it is based on object-oriented design. In the design of MI, the following changes are made:

1. Complex designs are decomposed into elements, on which the main work is carried out;
2. Add temporary structures and devices;
3. Building equipment is added;
4. Added (determined for all elements) of the stage of erection;
5. Define the capture;
6. Element-wise pricing is added;
7. Elements are added with logistic information.

The ideology of developing MI construction from MI design is the following: a list of works that reflects a variety of technological options for erecting or erecting is placed in accordance with the elements of the material applied for this element of the building. Each work is characterized by a normative amount of labor per unit of work volume, as well as a set of machines and mechanisms by which this work will be performed. After the list of basic and associated works is formed, the task of determining “temporary” and “cost” parameters is solved. IM construction must also solve the issues of operational management of construction production: on the basis of the adopted technology to ensure rhythmicity, shorter work periods, uniform loading of machines and equipment, reflect changes caused by deviations from previously planned indicators. Existing solutions for the management of construction processes solve local or sectoral planning and dispatching tasks without offering an integrated approach and linking with MI design (Solution “TRIM-Construction Monitoring”, System for monitoring and operational management of capital construction on Microsoft Silverlight 5.0 platforms, SAS Business Intelligence, InterView (NEOLANT), DevalVR player.

The main role in operational planning and management is given to the competent formation of organizational and technological documentation that touches on the issues of modeling of construction processes and their coordination in space and time, logistics, organization of transport, construction, installation and special works, selection of methods and means of implementation Design solutions for buildings and

structures. Among the basic documents of operational management, there are monthly plans and weekly schedules. The operational plans include schedules for construction and installation works, production of building materials and structures, construction machinery and vehicles (Buzirev et al. 2016). The complex of software solutions for operational management of construction production includes:

1. Weekly daily charts
2. Resource support for construction
3. Quality control
4. Maintenance and storage of executive documentation.

Planning in modern conditions is associated with a high degree of uncertainty, depending on a variety of external factors, faced with which all participants in the organization of construction production are at risk of an adverse event leading to loss. To reduce them, it is important to create an information model of construction and think over the flow of information flows (Kostyuchenko 2015).

In the market there are some ready-made solutions for the organization of operational management of construction, which are implemented with the aim of improving the efficiency of managing production activities and optimizing the use of available financial and material resources.

The system, which is created directly for the construction industry, is «1C: Construction Contractor 3.0. Management of construction production». The functional capabilities of this system are intended for the compilation of calendar plans for construction and for monitoring the performance of work (Stringam et al. 2016). The system is operated in production and technical units and directly at construction sites. The system allows you to exchange data with budgeting programs, as well as with systems such as “1C: Construction Contractor 4.0. Financial Management “and” 1C: Salary and Human Resources Management 8”. Formed calendar plans can be integrated with MS Project and MS Excel programs, after which the specified files can be transferred to authorized employees for execution or review and agreement (Chefetz and Howard 2007).

The control system “PARUS” is suitable for automation of the main lines of financial and economic activity of the construction company. As applied to the specifics of the construction industry, the system allows to solve the tasks of forming production plans, planning the requirements for raw materials, materials, components, equipment, labor, operational management of construction production and record keeping, as well as multifactor analysis of logistics costs in several projects, which allows for taking into account And highlight the profitability of each project (Kučera and Pitner 2016).

Another solution is “Management of development projects in capital construction” on the basis of SAP ERP is intended for construction companies. This solution allows companies to reduce the risks of unforeseen situations, reduce project implementation time and costs through quality planning, control of financial and material resources. It is important that this solution can be integrated with the company’s existing planning systems, specialized programs for working with project and estimate documentation, with geoinformation systems. (Cho et al. 2016) The system consists of the following modules: project management, material flow management, real estate management,

planning and budgeting, accounting and management accounting of costs and revenues, management of records archive, document circulation (Cordeiro et al. 2016).

However, all the listed software products require specially prepared input data that are uniquely identifiable, sufficient and subject to updating throughout the entire period of construction, depending on changes in external conditions, from adjustments made to project documentation or from management decisions related to technology or organization of construction production (Erdogan et al. 2014).

The use of automated workplaces in construction under innovative development forms the information flow management system (Karpushko et al. 2016).

3 Conclusions

Information support for the operational management of the construction organization allows to achieve the following results:

- automation of calculation algorithms;
- Invariance of planning;
- accounting for production efficiency;
- formation of a single data warehouse;
- the ability to automate the generation of reports.

A distinctive feature of the systems of production automation in construction is that the measurements are made using simple and simple algorithms, but the derivation of results is inherently a very costly process, in view of the vast volumes and various types of reducible data.

The development and use of MI construction gives an opportunity in case of failure or failure of system elements (organizational and technological resources of construction production) to replace them with alternative ones, while ensuring a slight deviation from the specified performance indicators of construction production.

It is this property of building systems that determines their high degree of adaptability under the influence of destabilizing factors and high possibilities for managing the reliability of building processes, i.e. Maintenance of the set results of building production.

During the study of the object and the subject of the study was:


- the sequence of solving individual tasks of the organization of construction production is clarified;
- algorithms of settlement procedures are defined;
- the scheme of information flows is drawn up;
- sets of design and management documents, both paper and paperless, used by the system.

The materials obtained as a result of the study form the basis for the development of an automated system for the design, organization or management of construction.

References

- Ignatiev, O.: Information models in construction. *Bull. Volgogr. State Archit. Constr. Univ.* **6**, 24–30 (2007)
- Tarasenko, D., Ostroukh, A.: On the issue of automation of calculation of construction work schedules. *Bull. Russ. New Univ.* **2**, 121–124 (2007)
- Kaneman, S.: *Tversky Decision Making in Uncertainty: Rules and Prejudices*. Humanitarian Center, Moscow (2005)
- Sheldrake, J.: The theory of management: from Taylorizma to Japanization. Transaction with English. In: Spivak, V.P. (ed.) *St. Petersburg* (2001)
- Farwick, M., Schweda, C., Breu, R., Hanschke, I.: A situational method for semi-automated enterprise architecture documentation. *Softw. Syst. Model.* **15**(2), 397–426 (2016). <https://doi.org/10.1007/s10270-014-0407-3>
- Mrugalska, B., Wyrwicka, M., Zasada, B.: Human-automation manufacturing industry system: current trends and practice. In: Rebelo, F., Soares, M. (eds.) *Advances in Ergonomics in Design: Proceedings of the AHFE 2016 International Conference on Ergonomics in Design*. Springer International Publishing, Cham (2016)
- Itskovich, E.: Basics of MES construction concept for production industries. *Autom. Remote Control* **77**(11), 2035–2043 (2016). <https://doi.org/10.1134/s0005117916110126>
- Pezeshki, Z., Ivani, S.: Applications of BIM: a brief review and future outline. *Arch. Comput. Methods Eng.* 1–40 (2016). <http://doi.org/10.1007/s11831-016-9204-1>
- Underwood, S., Bartz, D., Kade, A., Crawford, M.: Truck Automation: Testing and Trusting the Virtual Driver. In: Meyer, G., Beiker, S. (eds.) *Springer International Publishing, Cham*, vol. 3, pp. 91–109 (2016)
- Gumba, H.: *Planning in Construction: Educational-practical Guide*. ASV, Moscow (2012)
- Oleinik, P.: *Organization of Planning and Management in Construction: Textbook*. ASV, Moscow (2015)
- Buzirev, V., Selyutina, L., Martynov, V.: Modern methods of managing housing construction: a training manual on the direction of preparation 080200 “Management” for the master’s program “Entrepreneurship and construction management”. INFRA-M, Moscow (2016)
- Kostyuchenko, V.: Bases of the formation of organizational and technological construction systems. *Internet-Vestnik VolgGASU* **1**(37), 15 (2015). <http://www.vestnik.vgasu.ru/>
- Stringam, B., Gill, T., Sauer, B.: Integration of irrigation. *Irrig. Sci.* **34**(1), 33–40 (2016). <https://doi.org/10.1007/s00271-015-0477-1>
- Chefetz, G., Howard, D.: *Managing Enterprise Projects using Microsoft Project Server 2007*. Computercollectief BV, Engels (2007)
- Kučera, A., Pitner, T.: *Semantic BMS: Ontology for Analysis of Building Automation Systems Data*. Springer International Publishing, Costa de Caparica (2016)
- Cho, J., Vosgien, T., Prante, T., Gerhard, D.: *KBE-PLM Integration Schema for Engineering Knowledge Re-use and Design Automation*. Springer International Publishing, Columbia (2016)
- Cordeiro, E., Barbosa, G., Trabasso, L.: A customized QFD (quality function deployment) applied to management of automation projects. *Int. J. Adv. Manufact. Technol.* **87**(5), 2427–2436 (2016). <https://doi.org/10.1007/s00170-016-8626-0>
- Erdogan, B., Anumba, C., Bouchlaghem D., Nielsen Y.: Collaboration environments for construction: management of organizational changes. *J. Manag. Eng.* 1943–5479, 0742–597X (2014). 10.1061/(ASCE)ME
- Karpushko, M., Karpushko E., Bartolomei I.: World experience of operational management in construction. In: *Globalization and its socio-economic consequences* (2016)
- Ginzburg, A.: Building life cycle information modelling (BLC IM). *Ind. Civ. Eng.* **9** (2016)

Production Skills and the PC in Training of Students

Il'ja Cipurskij^(✉) 

Moscow State University of Civil Engineering,
Yaroslavskoye Sh. 26, 129337 Moscow, Russia
cil@bk.ru

Abstract. The paper evaluates the impact of innovations on the practical level of workforce training for the construction and transportation sector. It has been established that students' practice skills tend to deteriorate due to economic issues of cooperation with real-life production. It is apparent that the shift of emphasis between manufacturing businesses and schools from partnerships to market relations has become an adverse factor. It is proposed to engage the pedagogical experiences of the sector's researchers as regards imparting practical skills to students in the environment of academic laboratories. As an example, the paper examines the chair faculty's working experience in preserving computer-based practice-oriented training processes. It presents a laboratory complex where students of mechanical engineering gain practical skills by using a scale model of working equipment to learn the production technology of topsoil excavation. The paper describes a methodology for a construction student to learn academic knowledge and hands-down skills by engaging their understanding of physical substance of production process components in construction in order to convert their knowledge to a socially useful product, including during construction of transportation facilities and utilities lines. The methodology comprises two stages: practical fieldwork, gaining experimental data, and academic (manual and computer-assisted) calculation of the parameters of the working organ and technological performance. The paper obviously demonstrates how basic safety products can be used efficiently to complement experimental activities with mathematical computation.

Keywords: Transportation sector · Training · Production
Laboratory workshop · Workbench · Excavation · Skill · Mathematical model

1 Introduction

The process of academic training for future construction engineering specialists is directly related to future outlooks of organizing competent management of production technology components in the construction sector as a whole and transportation facilities in particular.

Existential issues with R&D in the construction sector that commenced in the late 1980s became an immediate impact on the quality of student training in a number of Russia's engineering colleges, including construction personnel – mechanical engineers, to be more specific. The Ministry for Transportation Construction started out by

cutting financing for the sector's R&D schools, which used to act as testing grounds to run in advanced construction equipment and technologies. This step prevented the students from accessing experimental advanced production equipment and gaining their practical skills [1, 2].

Other problems also existed: training methodology novelties, including ones related to the use of an exceptional power tool such as the PC. Meanwhile, Russian colleges changed their bearings towards the two - and three-level training system of the Bologna Convention. The old faculty – the main champions of mandatory basic knowledge and skills – were confronted with the challenge of PC competence, even though some of them managed to switch to the computer-assisted teaching of academic courses. However, the new computer-competent generation of teachers – still young and few – had yet to gain any practical trade skills prerequisite to teach the future construction engineers.

The students of mechanical engineering at the Moscow State University for Construction (MGSU) now had no chance of internship they previously received at the testing grounds of such providers as VNIISstroydormash, CNIISK experimental laboratories, pilot works and plants in the cities of Tver, Dmitrov, etc., and this had an adverse effect on the competencies of the new generation of construction engineers who were thus deprived of hands-down apprenticeship experience with construction design and production problems. The best Russian professors have always known how critical this is for a construction engineer [2, 3].

Even as early as in 1920 and 1930s, students of construction engineering at the MVTU (the school's name during the period, further known as VISU, then 'Construction Training Center', and finally MISI) attended the lectures read by the Dean of the Department, Prof. P.P. Velikhov, who deliberately used graphical methods to solve problems of construction mechanics, helping his students first to grasp the physical essence of the problem, and only then to support the resulting concepts with mathematical models.

To identify the content/substance of any process, the student has to perform a whole series of various functions that call for acquired practical skills to be realized. On the other hand, the teacher needs to ensure that information is covered comprehensively (with the assistance of the PC). Under the circumstances at hand, it seems best that the skills required for the future career in employment should be acquired during the college years [6, 7, 9].

Incidentally, many industrially developed nations practice interruption of school studies after the students have acquired basic academic competencies, in order to gain purely hands-down skills of production, and only later to continue their studies after years of employment and subsequent qualifications upon graduation. Perhaps the division between "Bachelor of applied arts/science" and "academic bachelor" currently being adopted by this nation may at least partly diminish the problem with gaining practical skills.

2 Materials and Methods

The engineer's academic training must also tend to adapt him to the equipment and the tasks to be addressed. In other words, the student must gain his first engineering skills on the shop floor rather than as a passive PC user. This being impossible, today the Construction Mechanization Department at MGSU has partly covered this lack of construction work practice (also necessary for the student's science research) by building a mini center, where different situations are simulated in variant digital models [4, 5].

Here is a concrete example. The Department's laboratory of earth excavating machines has test benches that precisely model the field operation conditions of certain construction machines engaged in production processes.

One of such test benches is an operating model with a clamshell bucket that can be replaced at any time with a chain bucket. The laboratory's earth strip is used to teach students the practical skills and the design, structure and operation principles of the clamshell as a standalone earth-moving machine and as integral implements of an excavator (see Fig. 1) [8, 15].

As they learn to operate any machine, including an excavator, young specialists need to get an experience in establishing the machine's output and the difficulty of the

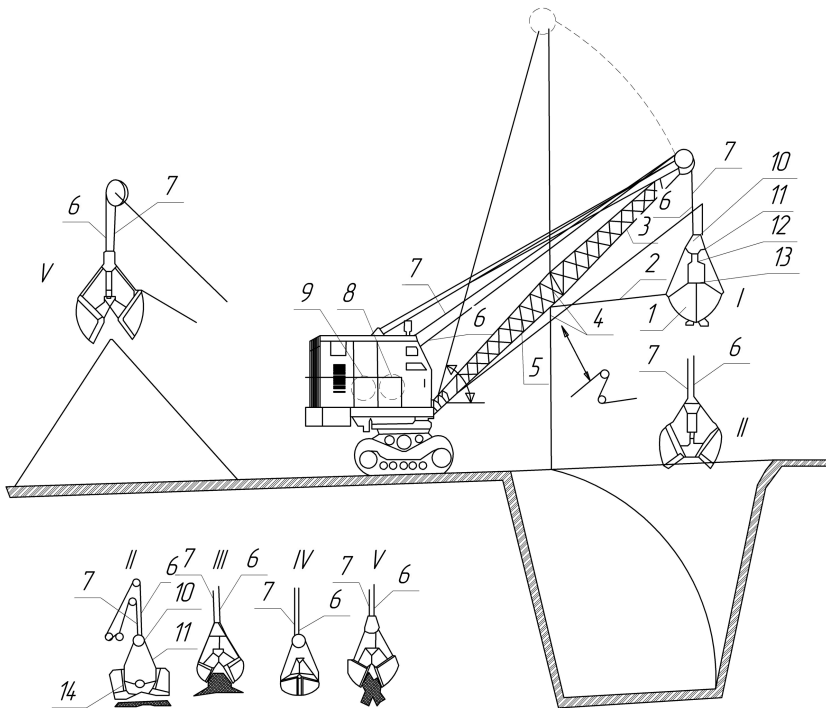


Fig. 1. Clamshell excavator: I – grapple start; II – lowering to the developed soil; III – bucket filling; IV – moving the loaded bucket; V – bucket unloading; 1 – double-jaw clamshell bucket; 2 – rope; 3 – extended lattice boom; 4 – block; 5 – pulling device; 6 – closing rope; 7 – hoist rope; 8, 9 – drum; 10 – top head; 11 – thrust; 12 – bottom head of the grapple; 13 – hinge; 14 – jaws

soil at hand. This experiment's methodology is intended to address exactly such skills. The test bench experiment helps the student to clearly perceive and physically sense this part of the construction technology – pit excavation – and thus to expand and secure the range of academic and practical skills related to earthworks. In addition, during their laboratory session the students can access fact-based data needed to know the operation output capacity of the specific bucket-chain (clamshell rope) excavator model, and they also have to decide the soil difficulty category – something necessary to rate the excavator's standard performance and output.

The technology of earth excavation using a clamshell power shovel includes a cyclic alteration of operations such as: scooping – full bucket traveling to the unloading area – bucket unloading – empty bucket returning to workface.

To begin operation, the clamshell in position I (Fig. 1) suspended on the hoisting rope goes down to rest on the pit floor (position II). For a deep scoop, the clamshell should be dropped down. By pulling the locking rope to close the shell slowly, the bucket separates a layer from the floor (position III – bucket filling). With the shell closed completely, the clamshell hanging on both the locking and hoisting ropes (position IV – loaded bucket in motion) travels to the unloading area. To empty the clamshell (position V – bucket unloading), it is suspended on the hoisting rope while the locking rope is released, so that the shell opens and spills the load. To turn the bucket for unloading and moving back to the workface, the machine's rotary section pivots in relation to the undercarriage that remains put throughout the operation cycle. Except motion of the machine itself, part of the steps can be concurrent with the swivel of the rotary table. Throughout the operation cycle, manual control of the clamshell boils down to alternate activation of drive drums thereby pulling tight either the hoisting rope, or the locking rope, or both at the same time.

The laboratory complex (Fig. 2) consists of a mockup of a clamshell rope (or bucket-chain) excavator, a set of controls, and an earth strip [10, 11].

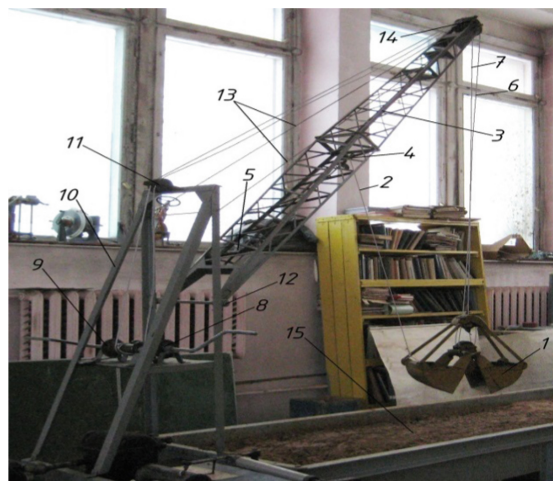


Fig. 2. Laboratory complex with a clamshell rope (or bucket-chain) excavator mockup.

The equipment set of the laboratory complex includes: 1 – clamshell; 2 – pull-back rope; 3 – boom; 4 – back rope pulley; 5 – pull-back device; 6 – locking rope; 7 – hoisting rope; 8 – manual-drive drum for locking rope; 9 – manual-drive drum for hoisting rope; 10 – shear legs; 11 – support pulleys; 12 – tailpiece of boom; 13 – boom raising rope; 14 – boom head pulleys; 15 – earth strip [12–14].

As the result of a test bench experiment, the team (4–5 students) must establish the following operation parameters: total cycle time; bucket filling time; loaded bucket traveling time; bucket unloading time; return time (idle run); bucket load volume per cycle; bucket load weight per cycle; bucket capacity. The time used for the cycle steps is taken using a stopwatch; a measuring box is used to know the bucket load volume; a weighing scale measures the weight of earth processed; the bucket capacity is found by dimensional measuring.

During experimental excavation using a clamshell model, the value of normal component P_{02} for earth's resistance to excavation P_0 depends on how earth responds to each grab bucket shell at the time of closing, when a strip layer of maximum thickness is torn off, and it equals the sum of clamshell half-weight ($G/2$) and the weight of earth in the shell volume ($Gg/2$). For ratio ψ_1 of the normal and tangential P_{01} components of the force of earth resistance to excavation being 0.5, we find the value of the tangential component active on the cutting edge of the clamshell's one rim:

$$P_{01} = G + G_g, \text{ kN} \quad (1)$$

The methodology to calculate the difficulty category for earth excavation by a bucket-chain is based on the excavation theory offered by Prov. N.G. Dombrovskiy, according to whom the criterion for the excavation difficulty category is K_1 as specific resistance of earth to digging, found as the quotient of the tangential P_{01} of resistance to digging divided by the area ($b \cdot c$) of the b by c ($W \times D$) earth strip being separated from the floor:

$$K_1 = P_{01}/b \cdot c, \text{ kPa} \quad (2)$$

After they fill up the clamshell by excavating the earth strip on the laboratory test bench, the team moves the full bucket to the unloading area. There they measure the excavated strip to record its greatest thickness c_{max} , excavation width b and chordal length L . Each student then uses these figures to independently calculate the value of specific resistance of earth in the earth strip (K_1) actually obtained after the experiment, and compares it with the data from reference tables to establish the excavation difficulty category for the clamshell operation.

3 Results

Test excavation with a bucket-chain (Fig. 3) follows the same methodology as the clamshell.



Fig. 3. Bucket-chain model at the end of an excavation run.

Here the student gets clear knowledge of the main provisions of the excavation theory, to find the bucket filling length L_h with drag force P_t and traction mechanism power N_t , lifting force P_f and lifting

Running length of bucket filling is found using this formula (Fig. 4a):

$$L_h = L_c \frac{\cos\alpha_c}{\cos\beta_3} - L_{t.c} - L_k, \tag{3}$$

where L_c - boom length; $L_{t.c}$ - length of bucket's pulling chains; L_k - bucket length; α_c - boom inclination angle; β_3 - pit floor slope angle. The filling runway is approximated as $L_h = (3-5) L_k$.

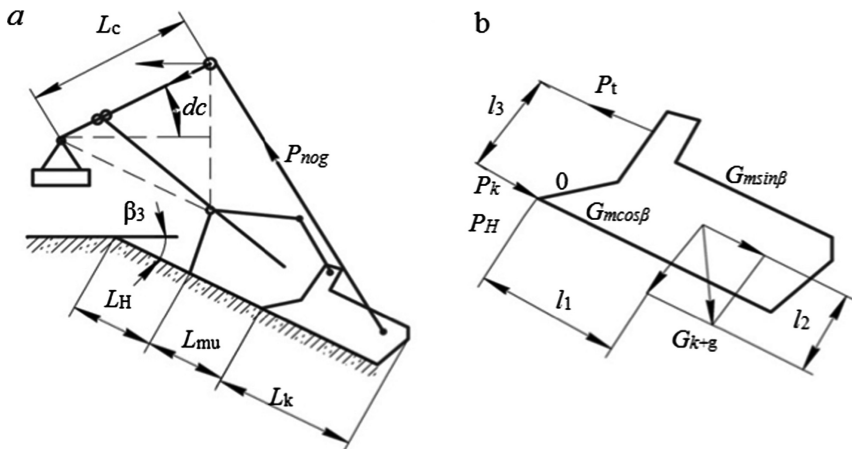


Fig. 4. Illustration for calculation of traction and lifting forces in a bucket-chain: *a* – bucket operation diagram; *b* – diagram of forces on the bucket.

Traction force P_t is found from an equation to project all forces effective on the bucket, in the traction force vector (Fig. 4b).

$$\Sigma P = P_k + G_{k+g} \sin \beta_3 + f G_{k+g} \cos \beta_3 - P_t = 0, \quad (4)$$

where f —constant of friction for the bucket against the earth.

We convert this expression to find:

$$P_t = P_k + G_{k+g} (\sin \beta_3 + f \cos \beta_3). \quad (5)$$

The greatest value of the tangential of resistance of earth to excavation P_k is found from the greatest dimension of the excavated strip along the bucket run length L_h , assuming its volume equal to that of earth held inside the bucket q_k (for $K_h = 1$) and to that in the dragging wedge q_d :

$q_k + q_d = b c_{\max} L_h K_p$ (below, substitute c_{\max} with h_{\max}),

Whence:

$$h_{\max} = \frac{q_k + q_d}{b L_h K_p}, \quad (6)$$

Therefore:

$$P_k = K_1 b h_{\max} = \frac{K_1 (q_k + q_d)}{L_h K_p}, \quad (7)$$

where K_1 —specific resistance to excavation.

For a bucket-chain, the normal component of resistance to excavation is 0.4÷0.6 of the tangential, namely

$$P_h = \psi_1 P_k = (0.4-0.6) P_k \quad (8)$$

The equation of the forces impacting the bucket projected on the normal component vector P_h , helps to find its value (Fig. 4b)

$P_h = G_{k+g} \cos \beta_3$ thus:

$$G_{k+g} = \frac{P_h}{\cos \beta_3} = \frac{\psi_1 P_k}{\cos \beta_3} \quad (9)$$

Now we substitute expression (9) in (5) to get:

$$P_t = P_k + \frac{\psi_1 P_k}{\cos \beta_3} (\sin \beta_3 + f \cos \beta_3) \quad (10)$$

or else, converted:

$$P_t = P_k [1 + \psi_1 (\operatorname{tg} \beta_3 + f)] \quad (11)$$

Lifting force P_p , based on calculated and experimental data, amounts to 0.7–0.8 of the traction force, and thus $P_f = (0.7-0.8) P_t$.

The power of the dragging and hoisting drives can be found through these expressions:

$$N_t = \frac{P_t V_t}{\eta_t}, N_f = \frac{P_f V_f}{\eta_f} \quad (12)$$

An important parameter in bucket-chain calculations is the lever of traction chain pin l_3 (Fig. 4), which determines possible movement of the bucket bottom along the pit floor slope without tipping. To find the lever we can use the equation of the sum of forces acting on the bucket respective to point O:

$$\Sigma M_0 = P_t l_3 - G_{k+g}(l_1 \cos \beta_3 + l_2 \sin \beta_3) = 0$$

hence, we substitute the values of P_t and G_{k+g} ,

$$l_3 = \frac{\psi_1 P_k (l_1 \cos \beta_3 + l_2 \sin \beta_3)}{\cos \beta_3 P_k [l + \psi_1 (tg \beta_3 + f)]} \quad (13)$$

or else, converted:

$$l_3 = \frac{l_1 + l_2 tg \beta_3}{tg \beta_3 + f + \frac{1}{\psi_1}}, \quad (14)$$

To calculate the above parameters of the bucket-chain operation process, the values of certain characteristics can be borrowed from reference values quoted in the engineering literature.

Structurally, rated capacity of a single-bucket excavator is found using this expression:

$$P_{tech} = q_g / t_r, \quad (15)$$

where P_{tech} —rated output capacity; q_g —average volume of earth in solid shape processed per cycle; t_r —mean work cycle runtime under specific working conditions.

It is known that the value of q_g is different from that of q as the bucket volume/capacity:

$$q_g = q k_1 / k_m, \quad (16)$$

where k_1 , k_m —respectively, coefficients for bucket filling and earth looseness.

The said coefficients are used in:

$$P_b = P_{tech} K_d = q \frac{k_1 \cdot k_d}{k_m \cdot t_r}; \quad (17)$$

where P_b —output capacity; k_d —excavator runtime coefficient describing time costs of off-cycle operations, always $k_d < 1.0$

Theoretical capacity P_{theory} —particular case of actual output provided that in expression (19) $q_g = q$, while $t_r = t_n$ is:

$$P_n = q/t_n, \quad (18)$$

For a bucket-chain, duration $t_{b\text{-ch}}$ of the stripping (excavation) process proper, according to N.G. Dombrovskiy may be approximated using this formula:

$$T_{b\text{-ch}} = L_{b\text{-ch}}/V_t \quad (19)$$

where $L_{b\text{-ch}}$ —normal length of excavation, from experimental data $L_{b\text{-ch}} = (3.6 - 3.8) \sqrt[3]{q}$, (q —bucket holding capacity) or $L_{b\text{-ch}} = (3-5)L_{bl}$; L_{bl} —bucket length; V_t —mean velocity of the traction rope.

At the field experiment stage, the student uses a stopwatch to record the time of both the entire cycle t_r , and individual time intervals, as necessary and sufficient, to establish the duration of the work cycle of the bucket model, with this expression:

$$t_r = t_k + t_n + t_p + t_b, \text{ sec.} \quad (20)$$

where t_k – time to fill bucket; t_n – traveling time to unload; t_p – unloading time; t_b – traveling time to the excavation area (idle run); all measured in seconds.

4 Discussion

All manipulations are done manually by the student team. Under real-life working conditions, extra operations may arise such as: shaking the bucket to drop off stuck soil; control passes in a low pit; removing large lumps from the pit floor, etc. Such operations add to the duration of the work cycle and reduce the machine's output.

Each student independently uses the actual cycle duration and the resulting excavation volume to build a report on the output capacity of the clamshell excavator model.

To conclude, all teams within the training group must establish their own respective hourly output rates and then declare the team that achieved the highest hourly output rate by using their skills and competencies and by optimizing the steps within the operation cycle.

Only from this point, the use of the PC to establish performance parameters of the field model of power shovel equipment becomes fully justified. The computer can be instrumental to obtain optimal final results using the similarity method, variant functional parameters that determine the output, and calculations to verify the duration of the machine's work cycle. At this time, work is in progress on a Mathcad computation algorithm to process resulting outputs, possibly taking into consideration certain solutions for structural design of transportation vehicles.

Such experimental work materializes such concepts as “equipment output capacity” and “earth excavation difficulty”; it also secures the student's skills of learning the physical nature of the process of excavation [11, 14, 15].

5 Conclusions

Seemingly a paradox, but swapping the priorities while a subject is being studied, namely by placing computer studies and engineering design computation first, only to allow respective physical perceptions at a later stage, has an adverse effect on the specialist's purely engineering qualities (although this can be justified in certain global problems) [15]. This alarming trend was reported at the dawn of cybernetics by its engineering ideologues, even by Norbert Wiener himself, the forefather of cybernetics, who said, "If man proves less able than the machine, the outcome will be deplorable... This will qualify as a defeat through man's own fault... The computer's value only depends on how reasonably man will use it".

Today, this is also the opinion of our faculty and construction sector's executives.

References

1. Bogomolov, A.: Machine for the Production of Excavation Work. Publishing house BGTU, Belgorod (2011)
2. Verigin, Yu., Sevryugina, N.: Synergetic basis of processes and technologies - a new course in the training of masters in the direction 270800 "Building". FGBOU VPO, Barnaul (2012)
3. Glagolev, S., Duyun, T., Sevryugina, N.: Problems of Engineering Education in the Field of Engineering and Technology. Publishing house BGTU, Belgorod (2013)
4. Balovnev, V.: Road Construction Machines and Systems. Publishing house SibADI, Moscow-Omsk (2001)
5. Drozdov, A.: Construction Machinery And Equipment: Textbook for Studies of Institutions of Higher Education. Academy, Moscow (2012)
6. Kazakov, N.: Qualifying certification of specialists of construction. *Age Qual.* **1**, 22–24 (2014)
7. Kazakov, N.: Implementation model for competency assessment of specialists – builders in terms of industry self-regulatory organization. *Mech. Constr.* **10**, 35–38 (2014)
8. Balovnev, V., Glagolev, S., Danilov, R.: Machines for Earthworks: Design, Calculation, Consumer Properties. Publishing house BGTU, Belgorod (2011)
9. Nikulin, A., Sevryugina, N.: Logistic model of educational institutions as building systems. In: Proceedings of Orel State Technical University. SERIES: Construction and Transport 1–2, pp. 47–49 (2006)
10. Zipursky, I.: Excavator with the Working Equipment Dragline and Grapple. MGSU, Moscow (2011)
11. Zipursky, I.: Increase traction rail stroke model of excavator. *Mech. Constr.* **11**(857), 7–8 (2015)
12. Zipursky, I., Cherkasova, D., Mozhaev, E.: Mechanization in the construction of the bridge at Hoover dam. *Mech. Constr.* **7**(T.77), 32–35 (2016)
13. Zipursky, I.: Digging grapple, hinged on the universal excavator. *Mech. Constr.* **4**, 20–22 (2010)
14. Zipursky, I. The influence of external teeth on the milling capacity of the rotor. In: *Interstroyemeh*, pp. 124–126 (2016)
15. Zipursky, I.: Settings digging and recruitment earthmoving machines: textbook. Publisher ASV, Moscow (2016)

Labor Management in Organizational Structures of Russian Energy Enterprises

Natalia Zotkina¹ , Miroslava Gusarova^{1,2} ,
and Anna Kopytova¹ 

¹ Tyumen Industrial University, Volodarskogo str., 38, Tyumen 625000, Russia
a.copytowa@yandex.ru

² Tyumen State University, Volodarskogo str., 6, Tyumen 625001, Russia

Abstract. The article is devoted to designing the organizational structure of labor management service and determining its location in general management structure of organization. Basing on the analysis of scientific publications, the author assessed existing developments in field of forming labor management system at the enterprise, and substantiated the necessity of their further development in accordance with the concept of modern management. It is established that labor management in accordance with theses of the modern management concept should be based on the management system, i.e., the complex of functions and powers necessary to implement the management impact; mechanism of management as a set of tools for implementing a targeted impact on the organization personnel, the management process - the sequence of actions of the management subject in the field of work. Recommendations are given on formation of labor management mechanism. Logical model of their interaction is presented. The typical organizational structure of the labor management service of a large organization is proposed based on a survey of Russian enterprises in the Tyumen region, its location in the management system is determined, variants of modification are considered depending on the specifics and scope of activity, recommendations for redistribution of functional responsibilities of the labor management service are given.

Keywords: Labor management · Concept of modern management
Command control

1 Introduction

The totality of labor management problems affects the vital interests of millions of employees and their families. The innovative vector of the Russian economy development determines new tasks for management of labor resources at the enterprise, presenting qualitatively different requirements to their structure and composition, the format of work of the management subject.

One of the strategic enterprises development directions is nowadays undoubtedly formation of such a labor management system, which functioning contributes to the achievement of their stable competitiveness in corresponding market of goods and services.

In retrospect, the objective necessity of labor managing appeared simultaneously with the emergence, formation and development of joint labor, its cooperation. However, the goals, content, functions of management itself changed along with the development of productive forces, labor itself, and were conditioned, first of all, by the social structure of labor inherent in a particular mode of production [3, 6].

Labor management issues should be considered at all levels of government. In some cases, they can be solved only at the state level, since they require taking into account the actual socio-economic and political situation. However, most often, these issues are solvable at the level of individual economic entities, based on the prevailing specificity of their production and social and labor relations.

Some problems of the labor management system formation at the enterprise have been investigated by many authors. The essence of the provisions was reduced to the labor management as a system consisting of three subsystems: labor organization, personnel management and payment management in the works of MS Gusarova. [12, 17, 19, 21]. The management process corresponding to this system is represented by its classical functions: planning, organization, motivation and control [18]. These functions encompass all of the above subsystems by their action, tend to cycle through time. The purpose of implementing these functions is to justify the management decisions taken. These decisions should be based on a system of reliable information, which data sets need to be expanded and deepened, as new problems arise in the labor management.

In general, we positively evaluate the approaches used by the above-mentioned authors, we consider it necessary to note that they need further development. Prospective directions of their development and improvement should be innovative approaches based on the concept of modern management, comprehensively, systematically considering and solving the problems of labor management.

Labor management is a functional area of the economic and administrative services of the enterprise. The main structural units for managing employees in the organization are personnel departments, which, as a rule, are neither a methodical, nor information, nor a coordinating center for personnel work. They are structurally separated from production and technical services, from the organization of labor and wages services, etc., which clearly does not contribute to the effective functioning of the enterprise. Social research services etc. are additionally created in organizations to solve social problems. But there do not exist yet special services that comprehensively perform functions of labor management in the organizational structures of the management of Russian enterprises. It determines the urgency of developing typical organizational structure that corresponds to the concept of modern management.

2 Methods

Forming of the mechanism of labor management is carried out in the following sequence, taking into account specific conditions of production activity of each organization.

1. Designation of the aims of the labor management mechanism formation at the enterprise. The recommended aims are: the most rational and effective use of personnel, living and materialized labor, the expenditure of funds for payment and

financial incentives for employees, the observance of constitutional rights and duties of citizens or one complex aim.

2. Setting the tasks of labor management, which, above all, include improving the efficiency and quality of work, ensuring the balance and proportionality of economic development, reducing the socio-economic differences in labor, creating conditions for the comprehensive development of man, the development of labor collectives and increasing their role in management, etc.
3. Determination of the object of labor management. In general, the objects are immediate process of labor, relationship between people in the labor process, reproduction of labor. As applied to the management activities of the enterprise, the objects can be specified and singled out as separate objects: management of the personnel of the enterprise, management of organizational support of personnel labor activity, management of productivity and labor quality, etc.
4. Selection of labor management tools, i.e. means or levers, which help to implement the mechanism of labor management.
5. Formation of the organizational structure of labor management should include the following stages:
 - structuring the goals of the labor management system;
 - determining the composition of the management functions that allow you to actualize goals of the system;
 - forming of the composition of the organizational structure subsystems;
 - establishing links between the organizational structure subsystems;
 - determining of rights and responsibilities of subsystems;
 - calculating of labor intensity of functions and number of subsystems;
 - building the configuration of the organizational structure.

3 Results

Proceeding from the modern conception of the methodology of management, its leading components are [16]:

- Management system or set of functions and powers necessary to implement management impact;
- Management mechanism as a set of tools, methods, instruments to influence people's activities;
- Management process, i.e. the sequence of actions which form the corresponding impact.

Labor management can be carried out only in case when there is a really functioning system that solves management tasks. The labor management system is a real form of implementing managerial relationships. The labor management system can be viewed from two sides. On the one hand, it is a set of managerial relations in field of labor (functional form). In this case, the labor management system is represented by

such functions as personnel management, organizational management of labor activity, productivity management and labor quality, motivation and labor incentives management, social and labor relations management. And on the other hand, all these sub-systems are characterized by specific forms of relations.

They are manifested in form of a real substance, that allows management to acquire concrete content and manifestation. These relations are implemented and organized by special services that form the system of labor management in general (institutional form). The links of the institutional form of labor management are the Department of Labor and Wages, the Department of Labor Organization, the Personnel Department, the Personnel Management Service, etc. [2, 7–14].

Formation of the mechanism of labor management is based on universally recognized elements of production systems, namely: production personnel, means and objects of labor, as well as methods of organizing labor and production [15]. Therefore, it would be logical to propose three units of the formed mechanism of labor management. The first unit is personnel management, the second is organization of the labor process, in the third unit, it seems expedient to authors to combine all the means and instruments of activity on the management of wages in the enterprise.

The unit “personnel management”. Personnel management should be designed in such a way that solution of any issue necessary for the employer’s position would be beneficial to the employee. Nowadays the personnel management system uses diverse arsenal of means of influencing the personal interests of the employee in the interests of the enterprise and society with an increase in the range of his rights and duties. Consequently, the basis for personnel management is human motivation and interdependence of personal, collective, public interests.

The motivation for work is related to the nature of the incentives for work and involves the establishment of relationship in the “needs - interests - incentives - reward” scheme. These categories help to understand how the person’s motivation for active work occurs.

Participating in labor activity, a person, as a rule, has a number of diverse needs, interests, value orientations, that can be significant or insignificant, of varying degrees of significance and relevance. In the course of correlation of needs, interests, values with the labor situation through motives, the most important of them are selected. Motives in the workplace perform a variety of functions that are implemented in behavior of the employee. These functions include the following: orienting, meaning-forming, mediating, mobilizing, justifying function.

Knowledge of the dynamics of work motivation is a condition of mandatory requirements to the employee and his correct expectations of correct and timely choice of incentive methods. After all, motivation is the process of encouraging an individual employee or groups to act, leading to the implementation of the organization’s goals. Thus, the personnel management unit is responsible for the formation of the right direction of employee’s labor behavior through the motivation mechanism.

The unit “Labor Organization.” The labor organization represents the forms and methods of uniting the efforts of people and technology in the labor process to achieve the beneficial effect of labor activity. Traditionally, it includes the following components: separation, cooperation, setting norms and improving labor methods, recruiting

and training personnel, maintaining jobs and creating safe working conditions, planning, accounting, paying for and stimulating of work, and educating a disciplined and creatively active worker in the work process.

To date, an effective tool for labor management is in theory and practice of management the strategic and project management within the framework of modern (innovative) model of labor management. Project teams implemented in the organization as subjects of management may be structural elements of the organization and target-setting entities, which in the context of responsibility is an important and significant factor. Currently in Russia you can meet such management bodies as committees, various task groups, brigades, commissions, project teams, like Western teams, [1, 6].

The unit “Managing the payment”. The market mechanism of payment management at the enterprise consists of a multi-level contractual system, system for ensuring minimum guarantees, tax regulatory system, information system on the level and dynamics of wages, etc. There is determined the need to allocate the labor costs management in a separate unit in the formation of modern mechanism of labor management at the enterprise by the most important role of wages both in the system of organization of social labor at the macro level and at the level of an individual enterprise. In addition, it is important to note that the pay management system, being a complex system [5], requires special attention and control, since any negative deviations in it directly affect overall performance of the enterprise. The general schematic diagram (logical model) of interaction between the units of the mechanism of labor management at the enterprise in the authors’ view is structured as follows. All the units of the mechanism of labor management are closely related and mutually complementary. In this case, each of the units carries its target load and does not overlap completely with other units.

The organization of the labor management process of the enterprise consists of establishing the sequence of actions of the management subject and depends on objective and subjective factors. The objective factors include: size of the enterprise, products manufactured, complexity of the technological process, nature and type of production, qualifications of managers and other factors. The subjective factor is different approach to the labor problems among managers (Fig. 1).

A survey conducted by the authors in the period 2011–2016 showed that at most of Russia’s enterprises until recently the implementation of labor management functions was concentrated mainly in four subdivisions: the Personnel Department, the Labor Organization Department, the Labor and Wages Department and the Safety Engineering and Labor protection Department. The options for building such services were very diverse. They differed in structure, functions, subordination and strength. In larger enterprises, bureaux, laboratories were allocated within the departments, and there were created separate departments for physiology, psychology and sociology of labor and independent positions of organizational engineers, standardization engineers in workshops. At medium-sized enterprises, one department for labor and wages was most often created, its structure was made up of various bureaux (a bureau of tariff rationing, a labor organization bureau, etc.) or the posts of a rationer or organizer were introduced.

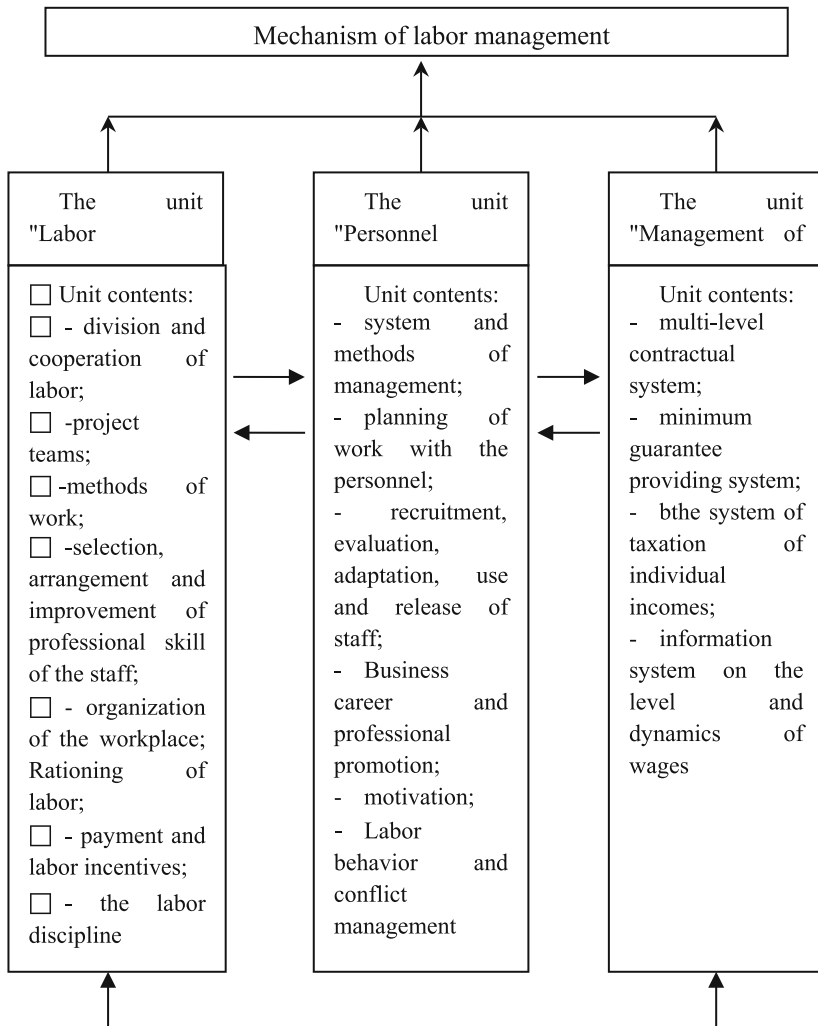


Fig. 1. The interaction scheme of the labor management mechanism units in the enterprise

In small enterprises, individual labor management services, as a rule, were not created, and persons who dealt with these issues were part of other economic or technical services.

Often the services involved in labor management had different subordination. Thus, the personnel department was subordinate to the director or deputy director for cadres; The department of labor and wages was subordinate to the director or deputy director for economic affairs, or to the chief economist, etc. Thus, we see that for the solution of interrelated issues on labor management, structural units were subordinated to persons at different levels of the hierarchy.

Recently, at Russian enterprises, new systems of personnel management began to be formed in order to provide an integrated approach to labor management, in which the Human Resources Department, the Labor and Wages Department, the Department of Social Development are subordinate to the Deputy Director for Human Resources Management [3, 5].

The structural location of the labor management service depends on the development degree and characteristics of the organization. In the practice, by analogy with personnel services, there are several options:

1. Labor management services are structurally subordinated to the head of administration;
2. Labor management services as a staff department are structurally subordinated to the general management of the organization;
3. Labor management services as a staff department are structurally subordinated to the top management;
4. Labor management services are organizationally included in the management of the organization.

It is the option presented in point “d” that can be considered as the most typical for fairly large firms with the allocation of the labor management service sphere as an equivalent subsystem among other structural units that have equal influence on strategic management issues.

The composition of the subsystems of the labor management system, formed on the basis of system of goals and functional division of labor, is shown in Fig. 2. The names of subsystems are formulated in the most part roughly, characterizing the main target task that is decided by this or that subdivision, a number of units or a post. The number of employees of the subdivision is determined by complexity and laboriousness of the tasks to be accomplished, which in turn depends to a large extent on the number of employees of the organization and the structural composition of staff.

The proposed organizational structure of labor management system is focused on organization with large financial resources. In general, this structural construction can be considered not only as an organizational consolidation of various subsystems, but also as a possible structuring of the basic functions performed by the labor management system.

Features of this or that organization, and mainly its size, determine the modification of the organizational structure of labor management. Options for the modification of the organizational structure may depend on the ability of the organization (primarily financial) to form a particular unit. Important role is played by the methodological and personnel potential that has been achieved, which affects the participation degree of external advisory firms in the implementation of a particular target.

The composition of functions of the organizational structure subsystems of the labor management system is determined on the basis of goals structuring, as well as formulation of criteria for achieving the goals and determining the form of the goals achieving results presentation.

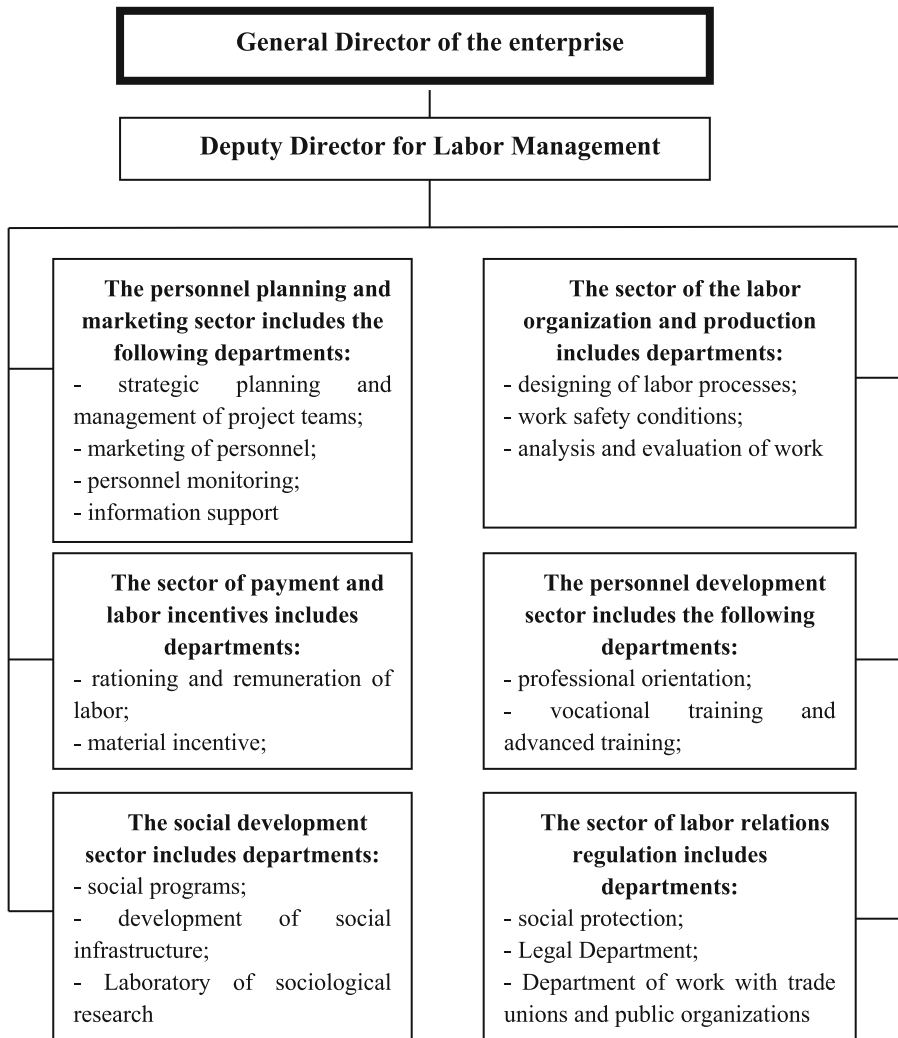


Fig. 2. Typical organizational structure of the labor management system

4 Discussion

The main problem of building the structure of labor management is the question of formation of a unified management service as an independent structural unit. In Russia, it is common to form a single service for personnel management, which does not assume the implementation of all functions for labor management. In practice, foreign companies are, increasingly tending to create a single multifunctional structural unit [21, 22]. As the study of management experience of organizations and relevant literature shows, there are possible the following options for some changes in organizational structure of the labor management service. Individual tasks can be assigned to a

specific specialist rather than to a department, if you have a few staff and, correspondingly, an insignificant total labor intensity of the labor management system functions. In any case, regardless of the organization characteristics, the composition of the labor management system functions remains constant. Only the laboriousness of their fulfillment changes. In large organizations, you can observe further structuring of the internal units of the labor management system. The most typical example is allocation of intermediate units in the departments, for example, in the training department there can be singled out groups or bureaus for the training of pupils, additional training of specialists, training and retraining of managers. The role and organizational status of the labor management service will be largely determined by the level of organizational and financial status, the potential development of the organization, as well as the position of its leadership in relation to the labor management service. In this case, the organizational form has less impact on the status of labor management system than other factors listed above. However, organizational form influences features of building a labor management system. In this case, the organizational form implies a combination of two important concepts: organizational and legal form of the organization; parameters of organizational structure (type of structure, capacity of individual units, structural configuration peculiarities, etc.). It may be proposed to improve the functional labor division of labor administration specialists as a perspective direction for development of organizational structures of labor management.

5 Conclusions


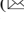
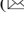

The current realities of the Russian economy urgently require activation of a system of factors and realization of reserves to increase the productivity of social labor, which is impossible without existence of effective system of labor management at macro and micro levels. Labor management is a special kind of managerial activity, which includes the whole set of relations of a purposeful influence on the reproduction cycle of labor resources. Central to this cycle is the phase of labor consumption. In the labor process takes place the combination of material and personal factors of production. This combination focuses on technical, organizational and socio-economic aspects of production. The total labor management tasks include: involvement of employees in labor, their involvement in the process of production, the organization of interaction with other components of labor process when creating products, goods and services.

In accordance with the concept of modern management, labor management is implemented through a system, mechanism and management process. The system defines the functions and forms of labor management. The mechanism is formed from three interrelated units (personnel management, labor organization, payment management) with the necessary set of management tools. The process establishes the sequence of actions of subject of management at the appropriate level of labor management. Formation of effective labor management system in the enterprise to meet modern requirements, and the implementation of its basic functions through establishment of appropriate organizational structure will provide the necessary conditions for productive work of the staff, help to boost the productivity of social labor.

References

1. Urheim, R., Rypdal, K., Melkevik, O., Hoff, H.A., Mykletun, A., Palmstierna, T.: *Crim. Behav. Mental Health* **24**, 141 (2014)
2. Jakubowska, A., Woolga, M.J., et al.: *Eat. Disord.* **21**, 16 (2013)
3. Kopytova, A.: *Procedia Eng.* **165**, 1132 (2016)
4. Nemirovskiy, V.G., Polovinko, V.S.: *Sotsiologicheskie Issledovaniya.* **1**, 27 (2015)
5. Kopytova, A.: Modern problems of science and education, p. 1 (2015). <https://doi.org/10.17513/spno.18700>
6. Simonova, M.V., Sankova, L.V., Mirzabalaeva, F.I., Shchipanova, D.Y., Dorozhkin, V.E.: *Int. J. Environ. Sci. Educ.* **11**, 7608 (2016)
7. Sturikova, M.V., Albrekht, N.V., Kondyurina, I.M., et al.: *Int. J. Environ. Sci. Educ.* **11**, 7826 (2016)
8. Saver, C.: *OR Manag.* **32**, 18 (2016)
9. Bansal, R.N., Malhotra, M.: *Biomed. Pharmacol. J.* **9**, 585 (2016)
10. Kukla, M., McGuire, A.B., Salyers, M.P.: *Psychiatr. Serv.* **67**, 412 (2016)
11. Nilsen, E.R., Olafsen, A.H., Steinsvåg, A.G., Halvari, H., Grov, E.K.: *J. Multidiscip. Healthc.* **9**, 153 (2016)
12. Westcott, L.: *J. Clin. Nurs.* **25**, 2669 (2016)
13. Kreye, M.E.: *Prod. Plan. Control* **27**, 1249 (2016)
14. Engbers, R., Fluit, C.R.M.G., Bolhuis, S., Sluiter, R., Stuyt, P.M.J., Laan, R.F.J.M.: *Adv. Health Sci. Educ.* **20**, 969 (2014)
15. Yuan, Z., Li, Y., Tetrack, L.E.: *Appl. Ergon.* **51**, 163 (2015)
16. Uzhakhova, L.M.: *Basics of Management: A Textbook.* 2nd edn., Revised and Additional. pp. 55, 388. Tyumen State University Publishing House, Tyumen (2010)
17. Saka, K.A., Haruna, I.: *Mediterr. J. Soc. Sci.* **4**, 9 (2013)
18. Osakwe, R.N.: *Int. Educ. Stud.* **7**, 43 (2014)
19. Edwards, R.A., Kirwin, J., Gonyeau, M., Matthews, S.J., Lancaster, J., DiVall, M.: *Am. J. Pharm. Educ.* **78**, 103 (2014)
20. Bartle, E., Thistlethwaite, J.: *BMC Med. Educ.* **14**, 110 (2014)
21. Kopytova, A.V.: *MATEC Web of Conferences*, vol. 106, p. 08056 (2017)
22. Zotkina, N., Kopytova, A., Zenkina, M., Zhigunjva, O.: *MATEC Web of Conferences*, vol. 106, p. 08058 (2017)

Enterprise Architecture Analysis for Energy Efficiency of Saint-Petersburg Underground

Igor Ilin , Anastasia Levina  , and Oxana Iliashenko 

Graduate School of Business Technologies,
Peter the Great Saint-Petersburg Polytechnic University,
Polytechnicheskaya str. 29, 195251 St. Petersburg, Russia
alyovina@gmail.com

Abstract. Energy efficiency is one of the important factors of efficient performance of municipal passenger transport. An implementation of energy efficient solutions, as any other organizational changes, require a systematic approach in order to be fulfilled effectively. A systematic approach to the development and/or reengineering of business management system is realized by means of an enterprise architecture concept. The latter enables to create a holistic management solution, which provide effective operations of the enterprise today and create conditions for its sustainable development for the future. A proper process reengineering enables to adjust a number of managerial aspect, including resource consumption control. The paper describes the process reengineering project in Saint Petersburg Underground, which was aimed at adjustment of the company performance to the requirements of energy legislation. The process reengineering was performed using enterprise architecture analysis of the problem area. The example of the Saint Petersburg Underground proved the efficiency of using enterprise architecture approach for process analysis and reengineering during energy audit.

Keywords: Energy management · Energy efficiency · Underground

1 Introduction

Energy saving in transport is not only economically justified and profitable, but extremely urgent and necessary in view of a reduction of the world's reserves of natural energy resources. Public municipal passenger transport belongs to the category of regulated types of activities in Russia. According to the legislation of the Russian Federation [1–4], organizations with the participation of the state or municipal entity and organization that carry out regulated types of activities should approve and implement energy saving and energy saving programs containing:

- target indicators of energy saving and energy efficiency increase,
- measures to save energy and improve energy efficiency, including the economic impact of these activities.

The main result of implementing the energy saving program should be a reduction in energy consumption and costs. The structure of energy resource consumption [5]

shows that oil products are considered to be the key energy source for transport in general (around 60%). Concerning such a specific kind of municipal transport as underground railway, the main energy source for it is electricity, which is used both directly (for railway operation) and indirectly – for producing of other energy sources (for example, compressed air). The paper describes the ways of reduction of the latter type of energy consumption by means of revealing potential for process reengineering (based on the case study of Saint-Petersburg Underground). The latter is a subject of a strict state control, including energy efficiency aspect the its activity.

Saint-Petersburg Underground (hereinafter referred as the Underground) is an enterprise that provides express off-street passenger transportation in Saint-Petersburg and serves about 5 million residents of the city. Currently the Underground is actively developing as 6 out of 18 city districts are poorly covered by subway network. [6] In this regard, not only the units of the Underground engaged in core activity (i.e. passenger transportation) are actively developing, but support services as well in order to ensure reliable and uninterrupted functioning of the core units. The paper is focused on the “Compressed air provision” process of Saint-Petersburg underground.

Compressed air is an important energy source for the underground, which is used to provide both train operations and supporting processes. Compressed air is produced by one of the departments of the Underground and is sold (distributed) to operation departments. There were two reasons to establish the process reengineering project: the external reason – change of energy efficiency law, and the internal one – need to bring the compressed air system in accordance with the modernized rolling stock, manufacturing equipment and air distributing system involved in the process of production and distribution of compressed air. Management of the company recognized the need to reengineer the existing processes of compressed air production and distribution for the purposes of future sustainable development and effective and reliable operations of the underground. Previously implemented energy-saving-oriented activities (modernization of rolling stock, air producing equipment and air distributing system) did not cause the desired outcome as the mentioned changes were not properly coordinated with each other. It resulted in:

- the lack of integration of new processes with existing information systems and technological equipment;
- the ineffective information exchange between the compressed air production department and management divisions;
- non transparent procedure of compressed air pricing.

As a result of the issues mentioned above, the energy is consumed uncontrollably: there is no clear vision of real energy consumption by the “Compressed air provision” process and, as a sequence, the price of the final product (compressed air) can not be calculated correctly. As a solution to these management concerns the service-oriented enterprise architecture analysis was used for developing the holistic solution for process reengineering and related areas.

1.1 Enterprise Architecture as a Systematic Approach to Process Reengineering – Literature Overview

To manage an enterprise effectively the holistic management model is required. To provide both effective routine operations and sustainable future development, it is necessary to build an effective enterprise architecture model that will enable effective and strategically focused management system. Enterprise architecture is one of the mainstream concepts in enterprise management nowadays, which can be successfully applied to other economic and social system. Systematic approach to managing enterprise means that a management system is defined by all its components, their interrelations and interdependencies. [7] The architecture model can be used to analyse the current state and to design the future state of the system, as well as to present alternative development scenarios. [examples can be found in 8–10]

Currently, there are a number of generally accepted descriptions, definitions and approaches to the enterprise architecture modelling and development, which are formalized in various standards or manuals (the overview can be found in [11–14]). The names and groupings of architectural elements can differ in different sources, but the idea is almost the same. Traditionally, the components of the enterprise architecture are presented as a set of layers, composed of the elements of a single managerial nature. Such sort of representation of the enterprise architecture allows to specify the relationships between the main components of the system.

The introduction of energy efficiency solutions to the enterprise architecture of the system inevitably influences seriously to all the architecture layers. Thus, the current architecture should be carefully reengineered using service-oriented analyses approach [8, 15] in order to provide effective change management while the components of the system are being restructured. Service oriented architecture (SOA) [11, 16, 17, 19] intends to consider an enterprise as a system of components each of which produces and provides certain services to each other. From this point of view, effective change management starts from the analysis of new service requirements and service changes, needed to provide them. [15] Then the analysis of changes in the appropriate architecture components is carried out.

The paper describes the application of the systematic approach to the process reengineering project in Saint-Petersburg Underground and shows its results from the energy efficiency point of view.

2 Case Study

Before starting development an energy-saving program it needs to collect base values of energy consumption and define energy-saving actions. [3, 4] Thus, the first step of energy efficiency implementation activity involves examination of all the facilities of the enterprise, collecting data on the amount of energy consumption, the technical equipment of the facility, the provision of meters, collect information on the status and effectiveness of energy consumption systems, determining the causes of energy losses and factors that impede energy efficiency. The main task of this stage is to determine the list of causes leading to irrational use of energy.

The authors of the paper, involved in the process analysis and reengineering project in the Underground [18], defined the following criteria for “Compressed air provision” process:

- Elimination of operations duplicating;
- Elimination of the dead end branches;
- Minimization of organizational interfaces;
- Clear roles and responsibilities in processes;
- Efficiency of information exchange.

The analysis of “Compressed air provision” process in its as-is state, its optimization and reengineering was carried out in the following aspects:

1. Interaction of sub processes of “Compressed air provision” process – as-is analysis:

For effective realization of production, distribution and consumption of compressed air activities it is necessary to provide not only the technological process organization, but also management and support (auxiliary processes) of the main process. During the examination of the as-is state of “Compressed air provision” process it has been revealed that there is a lack of timely and full information exchange between the main technological processes and processes of the accounting, planning and control. The accounting process obtains information on compressed air production and the consumed resources post factum once a month (at the beginning of the next month), but doesn’t obtain data from processes of distribution and compressed air consumption. As a result, control and analysis of the actual indicators deviations from planned ones does not performed quickly (monthly), and the account and control of distribution and consumption is carried out by means of indirect (settlement) methods. Besides, the account process does not operate with actual data about the volume of produced compressed air, but with the data calculated from a compressor operating time.

The impossibility of immediate control and analysis is a consequence of failure of compressed air production process monitoring in real-time. It makes the management of the production process less flexible and less effective and it can exert negative impact on safety during process performance.

Planning is carried out mostly by all-in-one method (but not on separate objects), operates with the aggregated indicators, and it is made in a monthly section, so operating scheduling isn’t implemented. The service and repair of equipment processes are examined in detail however they are not automated entirely and this makes such planning less effective.

2. Automation of processes, information exchange and integration of information systems – as-is analysis:

The system of dispatching management KASDU is not integrated with metering devices of inventory in divisions of Saint Petersburg Underground regarding compressed air. As a result manual control by the processing equipment is involved in a process of manufacture of compressed air. At the same time KASDU is integrated with out-of-service record system (ACS ARLM).

The system of the energy resources accounting (KUCER) is not integrated with compressor metering devices, as a result, data on the consumed electric power and the

produced compressed air monthly are entered into the system manually and also manually taken from KUCER for further input in the SAP ERP system. The result is duplication of operations by personnel at data transmission, inefficient paper document flow.

The out-of-service record system ACS ARLM is not integrated with compressor metering devices, data on refusals are entered into system manually. Information from ACS ARLM is not transferred further to other information systems and it is stored as

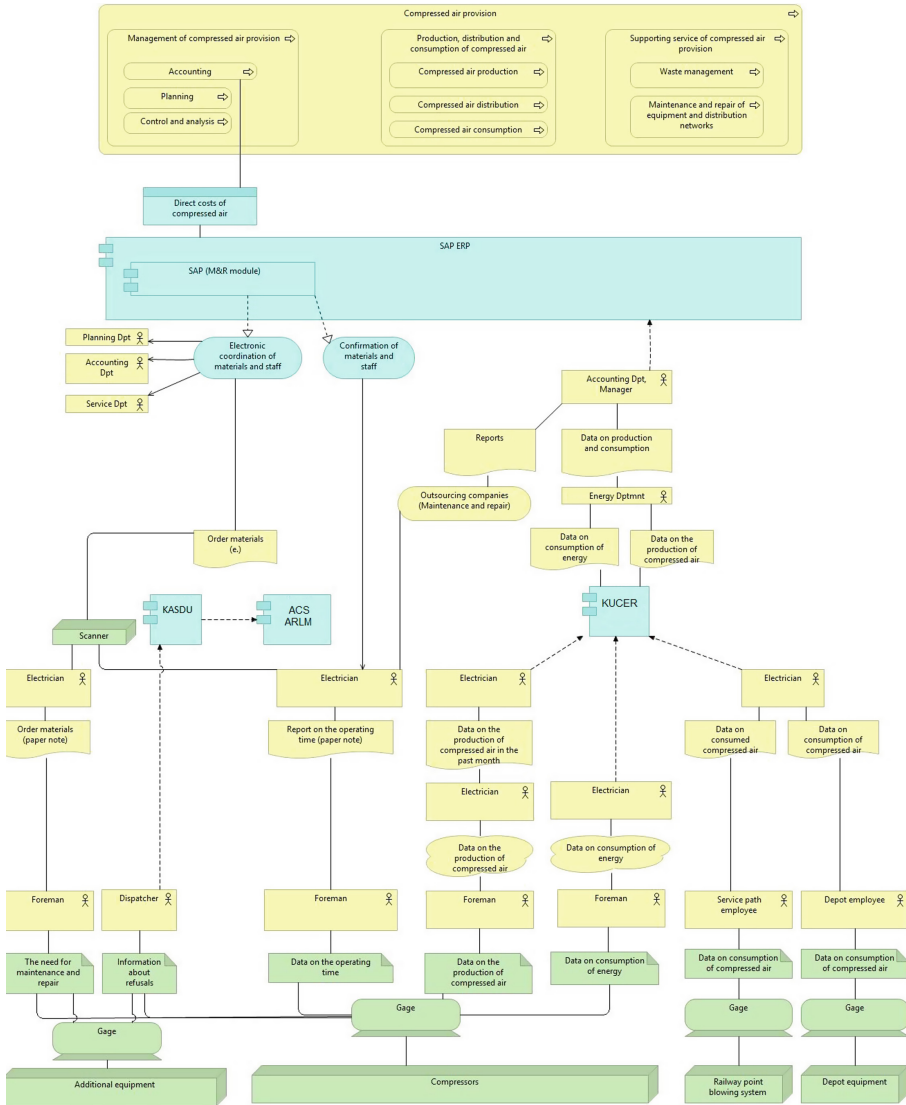


Fig. 1. Architecture model of the “Compressed air provision” process.

archive of observations. Such work of the out-of-service record system can cause threat to security of all business process realization.

The Maintenance and Repair (MR) module of the SAP ERP system allows to automate technical upkeep and maintenance planning inventories on the basis the actual operating time data and its comparison to the registration certificate requirements of an inventory entered into the system. Metering devices of compressors are not integrated with the SAP ERP system that makes automatic data recording about a compressors operating time impossible. Planning of compressors' maintenance and repair in SAP ERP is carried out "manually" by means of extrapolation of previous maintenance and repair information, i.e. it is rather theoretical and often does not coincide with terms of actually required maintenance and repair.

The analysis of subprocesses interaction and process automation resulted in the architecture model of compressed air provision system (Fig. 1). The current state of compressed air provision process discourages the energy efficiency activities as there is no means of effective monitoring and control of the resource consumption. The architecture model, presented on Fig. 1, demonstrates the bottlenecks of the process: poor automation, including lack of the appropriate IT system integration, unclear roles and responsibilities, unclear document flow. All these factors negatively influence on the process performance, including resource consumption. As the electricity is the core resource for the analyzed activity, its proper accounting is a crucially important factor in compressed air pricing and costs calculation. The process reengineering is supposed to make the process more transparent and more controlled, including through the use of a proper IT support tools.

3 Results and Discussion

The "Compressed air provision" process analysis revealed the need of the following changes to be implemented:

- It is needed to introduce two additional sub processes – "The accounting of compressed air distribution" and "The accounting of compressed air consumption" – to ensure monitoring and control of actual data about compressed air volumes on all the resource transfer chain from the producer to the consumer.
- It is advisable to introduce system of operating scheduling, operating control and the analysis of realization of production, distribution and consumption of compressed air technological process. Operational efficiency means obtaining urgent data of management processes from the main processes up to real time. The possibility of operational management realization mainly depends on the chosen scheme of process automation.
- Implementation of the system of operational data accounting on production will provide clear actual data about the produced compressed air volume. That will increase the accuracy of settlements with consumers, and also will create prerequisites for better planning.

As a part of an offer on process reengineering it is necessary to propose the monitoring mechanism of process realization efficiency. In the future a KPI system can

be this monitoring mechanism. For a “Providing with compressed air” business process realization assessment it is expedient to use the following KPI according to the top level processes:

- Management of compressed air providing:
 - KPI1 – the minimum deviation of planned compressed air cost from the actual cost for the period
- Production, distribution and consumption with compressed air:
 - KPI2 – factor cost on production of 1 cubic meter of compressed air (rubles for a cubic meter) for the period
 - KPI3 – electric power costs of production of 1 cubic meter of compressed air (kilowatt-cubic meter) for the period
- Servicing of compressed air providing process:
 - KPI4 – cumulative cost of the equipment (compressors) ownership.

The proposed KPI characterize efficiency of process performance in general. If necessary, the complete KPI system with indicators can be developed for each sub process according to levels of specification of processes up to operational level. There can be following examples of KPI for processes of compressed air production, distribution and consumption: pressure of compressed air on escaping of compressor (kp/cm^2), pressure of compressed air at the consumer (kp/cm^2), difference of pressure of compressed air between outlet pressure from compressor and inlet pressure at the consumer (kp/cm^2), etc. Introduction of the KPI system mainly depends on a level of process automation as efficiency indicators calculation needs correct up-to-date data which are possible to collect, to analyze and store only in the presence of the processes IT support.

Effects of business process reengineering:

1. From the point of energy efficiency:

- Compressed air as an energy resource for consumers: Energy efficiency means rational use of energy resources. For consumers compressed air is the power supply allowing performing particular work. The account and monitoring of energy resources consumption, and also detection and elimination of unproductive losses are necessary conditions of energy efficiency. The offered reengineering assumes to keep account, monitoring, the analysis and scheduling of not only compressed air production, but also its distribution and consumption that will provide more rational approach to production and use of this energy resource.
- The electric power for production of compressed air: As the produced compressed air is used for the different purposes, consumers make different demands. This is why Track maintenance requires compressed air with the parameter of 4 kp/cm^2 and the Nevsky depot requires 7.2 kp/cm^2 . Now consumers receive compressed air from uniform network of distribution therefore compressed air production has reference point at most required pressure – 7.2 kp/cm^2 .

Now compressors work in the given range of the pressure parameter (depending on the period – from 7.0 to 7.5 kp/cm^2 or from 7.1 to 7.6 kp/cm^2): on an upper bound of an interval of the fissile intake of compressed air periods from network and reducing pressure when air in network is enough. The given range of compressor operation is

explained partly by requirements to an operational duty of compressors, partly by need to create pressure stock in network of distribution. Inertia of system in case of sharp increase in consumption is compensated by the volumes of compressed air which are in network and air collectors, and also exuberant in comparison with the required pressure of compressed air. Such duty of the compressor (recommended by the producer) allows to regulate smoothly loading, alternating the periods of the fissile work with the unloading periods.

Producing compressed air with the specified characteristics on pressure the compressor consumes 85–90% of the design capacity. Dependence of power consumption on pressure of the produced compressed air not the linear: the higher the pressure is, the larger power should be involved. It is possible to assume that on a piece from 7.0 to 7.5 kp/cm² of each padding 0.1 kp/cm² of pressure leads to increase in power consumption by 1% that counting on the main compressor design capacity of 110 kW makes 1.1 kW. In case of implementation of compressor operating control system by operation on requirement there will be a possibility of the instantaneous response of the compressor to signals of the metering stations established at consumers. That makes reduction of compressor operation range in the pressure parameter possible.

It is important to note that an opportunity to produce compressed air with different characteristics for different consumers makes implementation of management system for compressed air providing even more urgent.

2. From the point of technology:

For ensuring efficient process (from the point of the consumed resources – the electric power, oil, etc.) it is needed to support an optimum operational duty of an inventory when the specific resources expense level is minimum. Achievement and maintenance of such mode is possible only expeditious and correct technological indexes process monitoring is up-to-date and correct.

4 Conclusion

A systematic approach to the development and/or reengineering of business management system is realized by means of an enterprise architecture concept. The latter enables to create a holistic management solution, which provide effective operations of the enterprise today and create conditions for its sustainable development for the future. A proper process reengineering enables to adjust a number of managerial aspect, including resource consumption control.

The case of Saint Petersburg Underground, described in the paper, highlights that for energy efficient performance the modern equipment is not enough if the accounting processes are not performed properly. Only the systematic approach, which takes into account all the components of the enterprise architecture (processes, IT systems, document flows and procedures, roles and responsibilities, equipment and facilities), can provide an effective implementation of organizational changes. Process analysis and reengineering is an important part of energy audit, but it can be performed really effectively if processes are considered as a part of a broader managerial entity (i.e. enterprise architecture).

The further step of the development of the subject, discussed in the paper, can be development of an architecture-oriented energy audit procedure for transport sector or other industries. The uniform procedure can be beneficial for all representatives of the particular industry as it is considered to be based on the best practices and industry specific.

References

1. “On Energy Saving and on Improving Energy Efficiency and on Amending Certain Legislative Acts of the Russian Federation” Federal Law No. 261-FZ of 23 November 2009 (2016)
2. “On approval of the requirements for the form of programs in the field of energy conservation and improving the energy efficiency of organizations with the participation of the state and the municipal entity, organizations that carry out regulated activities and reporting on the progress of their implementation”. Order of the Ministry of Energy of Russia, Moscow, p. 398, 30 June 2014
3. “On approval of the methodology for calculating the values of targets in the field of energy conservation and improving energy efficiency, including in comparable conditions”. Order of the Ministry of Energy of the Russian Federation, p. 399, 30 June 2014
4. “On approval of an approximate list of activities in the field of energy conservation and energy efficiency, which can be used to develop regional, municipal programs in the field of energy conservation and energy efficiency”. Order of the Ministry of Economic Development of the Russian Federation, p. 61, 17 February 2010
5. AfterShock Information Center: Energy Efficiency in Transport. <https://aftershock.news/?q=node/68471&full>
6. On the State Program of St. Petersburg Development of St. Petersburg transport system St. Petersburg Government Decree of 6/30/2014 number 552 for 2015–2020
7. Ilin, I.V., Lyovina, A.I., Antipin, A.R.: Business architecture development and process and project maturity. In: *Emerging Trends in Information Systems Recent Innovations, Results and Experiences*, Switzerland, pp. 51–63 (2016)
8. Kozin, E.G., Ilin, I.V., Levina, A.I.: Service-oriented approach to enterprise architecture solution analysis. *St. Petersburg State Polytech. Univ. J. Econ.* **4**(246), 162–172 (2016)
9. Bril, A., Kalinina, O., Valebnikova, O.: Innovation venture financing projects in information technology. In: *Lecture Notes in Computer Science (including subseries Lecture Notes in Artificial Intelligence and Lecture Notes in Bioinformatics)*, vol. 9870, pp. 766–775. Springer (2016)
10. Rodionov, D.G., Kudryavtseva, T.J.: Factors of the effective development of the St. Petersburg instrument engineering cluster. *Int. J. Econ. Finan. Issues* **6**(2), 298–306 (2016)
11. Lankhorst, M.: *Enterprise Architecture at Work. Modelling, Communication, Analysis*. Springer (2013)
12. Op’t Land, M., Proper, E., Waage, M., Cloo, J., Steghuis, C.: *Enterprise architecture. Creating Value by Informed Governance*. Springer, Berlin (2009)
13. Kudryavcev, D.V., Arzumanyan, M.Yu., Grigorev, L.Yu.: *Business Engineering Technologies: Study Guide*. Saint Petersburg, Polytechnic University Publishing, p. 427 (2014)
14. Kalyanov, G.: *Enterprise architecture and instruments of its modeling*. National Institute Higher School of Management (2011). <http://www.vshu.ru/files/IR01a.pdf>. Accessed 25 Jan 2014

15. Ilin, I.V., Iliashenko, O.Yu., Levina, A.I.: Application of service-oriented approach to business process reengineering. In: Proceedings of the 28th International Business Information Management Association Conference, Vision 2020: Innovation Management, Development Sustainability, and Competitive Economic Growth, Spain, Seville, pp. 768–781, 9–10 November 2016
16. MacLennan, E., Van Belle, J.-P.: Factors affecting the organizational adoption of service-oriented architecture (SOA). *Inf. Syst. e-Business Manag.* **12**(1), 71–100 (2014)
17. Kistasamy, C., van der Merwe, A., de La Harpe, A.: The relationship between service-oriented architecture and enterprise architecture. In: 14th IEEE International Enterprise Distributed Object Computing Conference Workshops, 25–29 October 2010
18. Ilin, I.V., Kalinina, O.V., Iliashenko, O.Yu., Levina, A.I.: IT-architecture re-engineering as a prerequisite for sustainable development in saint petersburg urban underground procedia engineering 15. In: 15th International Scientific Conference ‘Underground Urbanisation as a Prerequisite for Sustainable Development’, ACUUS 2016, pp. 1683–1692 (2016)
19. Shilova, L., Soloviev, D., Timatkov, V., Adamtsevich, A.: About the territorial potential of the construction of battery-charging stations for autonomous electric motor vehicles in the regions. In: MATEC Web of Conferences, vol. 73, Article no. 02017 (2016). <https://doi.org/10.1051/mateconf/20167302017>

The Energy Saving Motivation of Certain Categories of Personnel in the Company

Anna Minnullina¹ and Rais Abdrazakov²

¹ Tyumen Industrial University, Volodarskogo St., 38, Tyumen 625000, Russia
minnullinaay@yandex.ru

² Northern Trans-Ural State Agricultural University,
Respublika St., 7, Tyumen 625003, Russia

Abstract. The problems of energy saving in Russian companies are studied in this article. The possibilities of reducing the consumption of energy resources through the motivation of the personnel within the company are considered by the authors. The expert evaluation of the importance of the human capital factors affecting the motivation of energy saving in the company is proposed in the article for this purpose. The expert evaluation allows determining the certain categories of the company personnel, requiring the development of the incentive measures for energy saving, as well as the most significant human capital factors affecting the certain categories of the company's personnel. To confirm the applied nature of the proposed methodology, the opinions of 40 experts who are the employees in large construction companies of the Tyumen region, in some way related to the process of energy consumption in the company, are assessed by the authors.

Keywords: Energy saving · Expert evaluation · Motivation of the personnel

1 Introduction

Currently, the tightening of the requirements for energy management in any company in Russia is based on the adopted Federal Law “On Energy Saving and Introduction of Changes to Certain Legislative Acts of the Russian Federation” [1].

Moreover, the energy policy of companies of various organizational and legal forms is subject to state control in accordance with the rules established by the Government of the Russian Federation, and the data on total costs for payment for the energy resources used during a calendar year should be included in the explanatory note to annual financial statements.

The issues of the development of the energy strategy of the Russian Federation, the methods of system research in the energy sector, the energy policy and the creation of new energy management systems in companies are studied in the scientific papers of Andrizhievsky, Volodin, Bushuev, Voropai, Gitelman, Dmitriev, Grebneva, Ya. Kaminskaya, Kuznetsov, Novikova, Lyubimov, Melnyk, Sadriev, Ya. Shchelokov, Danilov, Yavorsky et al. [2–11].

The analysis of some works [2, 3, 9, 10] on energy saving management and energy efficiency improvement of the companies showed that currently used energy

management mechanisms and means not to the fullest extent take into account the possibilities of economic integration of the participants in the energy saving business process in the implementation of the energy saving measures, in some cases preventing the implementation of the scientifically-grounded recommendations for the improvement of the energy efficiency, and reducing the energy efficiency indicators of the companies as one of the important conditions for their competitiveness.

According to the Energy Strategy of the Russian Federation until 2030 [12], the potential for the organizational and technological energy saving in the Russian industry is up to 40% of the total energy consumption. Moreover, at the meeting of the Presidium of the Government of the Russian Federation held on February 17, 2010, it was planned to reduce the energy intensity of GDP by at least 40% by the year of 2020 [13]. The foreign experience shows that the industrial companies, which had paid serious attention to energy management, managed to reduce actually the energy costs by 30% or more [14].

Foreign scientists Thomson, Infield, Glifford, Nuttali, Tan, Tsang, Hu, Wang and many others have successfully solved the problem of forming the system of accounting and operational control over the power consumption in companies [15–21]. For example, Tsang, Nuttali, Hu, and Wang paid more attention to the accuracy of the existing system in the field of energy accounting in order to improve the efficiency of the “supplier-consumer” economic relations.

In order to improve the energy efficiency of the company, the company’s energy management system plays a significant role in the system of motivation of the personnel for energy saving, which allows increasing the efficiency of the company’s activity without significant financial expenses, reducing the costs of production of goods and services, and increasing the efficiency of the personnel.

In energy saving, the motivation of the personnel is a component of the energy management policy of any company. At the corporate level, the energy management defines the responsibility for energy consumption, includes the structural changes, related to the redistribution of the authority for energy control, the formulation of the corporate energy policy and the formation of an interest in energy saving on the part of the company’s top management.

To evaluate the energy management potential of a particular company, Worrell, and Galitsky in their work [14] proposed the use of the energy management matrix. This energy management matrix allows identifying and describing the priorities in various aspects of the company’s energy policy, as well as identifying the alternative ways to increase the energy efficiency.

Unfortunately, only a small percentage of companies in Russia form a policy in the field of personnel management and implement this process in accordance with the international quality management standards ISO 9000. Most often, they do not pay attention to this issue, and therefore the human capital of the company degrades, which negatively affects the efficiency of production, the quality and effectiveness of innovation. Some authors in their works [2, 22] note that the integration of energy management into the organizational structure of the company is carried out through certain aspects associated with the introduction of a system of motivation of the personnel for the purpose of energy saving: the allocation of responsibility for energy consumption; the introduction of the energy manager on energy efficiency; the development of a

mechanism for the control over the energy saving; the development of the information system for notification on the tasks, actual consumption of the energy resources and energy saving results for the whole company, and for each unit; the sources of financing of the motivation system.

The main groups of personnel at which the system of motivation for energy saving should be aimed are the heads of the subdivisions, the junior management and the ordinary personnel of the company, whose actions and decisions determine the amount of consumed energy resources. It is important to use the real incentives for each of the groups involved in the production and consumption of the energy resources [7, 10, 23].

Given the importance of the development of the energy management within the company, it is advisable to study the factors affecting the efficiency of energy saving in the conditions of developed system of motivation of the personnel of the company. For this purpose, it is advisable to conduct the evaluation of the energy management of the company in terms of individual categories of personnel.

2 Methods

To study the effectiveness of energy saving motivation among the certain categories of personnel in the company, the authors proposed a methodology based on the expert evaluation [24] of the set of human capital factors taken into account in energy management:

1. The level of participation in energy consumption. This factor takes into account the volume of direct consumption of the energy resources in the process of the main activity of the employee.
2. The level of participation in energy saving. This factor assesses the possibility of saving of the energy resources in the process of the main activity of the employee. At the same time, the employees who are not directly involved in the process of energy consumption can participate in the development of the energy-efficient projects, the formation of energy policy.
3. The level of awareness of energy saving. This factor provides for the dissemination to each employee of the information on the need to solve the energy saving problems, the information on the energy saving activities performed by the company.
4. The culture of energy saving in the company. This factor characterizes the attitude of the employees towards the energy saving problems and the understanding of the importance of their solution for the company. The culture of energy saving in the company is at a high level if the employees associate the energy saving with the company's successes, its development, as well as with their own stable position in the company, career growth and salary increase.
5. The culture of energy consumption of the employee. This factor takes into account that each employee is a member of society, social environment. Without changing the mentality, common human habits, awareness of national interests, it is practically impossible to implement the energy saving policy.

6. The level of education of the employee. This factor is one of the key factors in the energy saving motivation of the personnel. The energy saving projects are of an innovative nature, while their management is a complex and multifaceted process, requiring a certain level of knowledge and competence for each category of personnel.
7. The accumulated period of work and the experience of the employee. This factor is important for almost all categories of personnel, but there are categories for which it is indispensable. For example, for the key personnel it includes the ability to work in economic modes, for designers it is the experience in the development of energy-efficient design solutions, for technologists and standardizers it is the skills of correlating the requirements for technological regimes and energy saving.
8. The level of relevance of an employee in the company. This factor is important first of all for the “individual” specialists or leaders, on whom the decision-making depends – the proactivity, the respect of the team, the ability to set and to solve the important tasks.

Initially, the experts are proposed to evaluate the importance of each human capital factor, taken into account in the energy saving motivation, on a 5-point scale for each category of personnel (1 point for the least important factor, 5 points for the most important factor). Each expert must have the necessary professional qualification and form his assessments independently of other participants in the expert evaluation and free from any external influence. The results of the expert evaluation are presented in the form of a matrix $F = (a_{ij}^k)$, ($i = \overline{1, n}$; $j = \overline{1, m}$), which has the following expanded form (1):

$$F^a = \left\{ \begin{matrix} a_{11}^k a_{12}^k \dots a_{1m}^k \\ a_{21}^k a_{22}^k \dots a_{2m}^k \\ \dots \\ a_{n1}^k a_{n2}^k \dots a_{nm}^k \end{matrix} \right\} \tag{1}$$

- a_{ij}^k – evaluation by the k – expert of the importance of j – the human capital factor for i – category of personnel;
- m – the number of human capital factors considered in the energy saving motivation;
- n – the number of categories of personnel

It should be borne in mind that the number of categories of personnel should be no less than the number of human capital factors.

In the course of the expert evaluation, the degree of consistency of the expert opinions in the context of each category of personnel should be determined using the Kendall Concordance Ratio (W) according to the formula (2):

$$W = \frac{12S}{K^2(m^3 - m)} \tag{2}$$

- K – the number of experts;
- m – the number of human capital factors considered in the energy saving motivation;
- S – the sum of the squares of the differences in ranks (deviations), calculated by the formula (3):

$$S = \sum_{j=1}^m \left(\sum_{k=1}^K x_{ij}^k - \frac{1}{2}K(m+1) \right)^2 \tag{3}$$

x_{ij}^k – the rank of evaluation, assigned by k – expert to j – human capital factor for the personnel.

The value of the Concordance Ratio can be in the range from 0 to 1. If the value of the Concordance Ratio lies in the interval (0.5; 1), then the expert evaluations are considered fully consistent. Otherwise, it is proposed to re-conduct the expert evaluation with a possible change in the set of human capital factors that are taken into account in the energy saving motivating or the categories of the company’s personnel.

Upon the determination of the degree of agreement between the experts, the values of the expert evaluations of the importance of the human capital factors taken into account in the energy saving motivation are aggregated. The results of the aggregation of the expert evaluations are represented in the form of a matrix $F = (A_{ij})$, ($i = \overline{1, n}; j = \overline{1, m}$), which has the following expanded view (4):

$$F^A = \left\{ \begin{array}{l} A_{11}A_{12} \dots A_{1m} \\ A_{11}A_{22} \dots A_{2m} \\ \dots \\ A_{n1}A_{n2} \dots A_{nm} \end{array} \right\} \tag{4}$$

A_{ij} – average expert evaluation of the importance of j – human capital factor for i – category of personnel

The total group evaluation of the factors A_j calculated by the formula (5):

$$A_j = \frac{\sum_{i=1}^n A_{ij}}{n} \tag{5}$$

The total group evaluation of the categories of the personnel A_i calculated by the formula (6):

$$A_i = \frac{\sum_{j=1}^m A_{ij}}{m} \tag{6}$$

The identification of the general patterns in the context of different categories of the personnel in the course of assessment of the factors, taken into account in the energy saving motivation, is based on the total group evaluations A_i and A_j .

3 Assessment and Results

Based on the proposed methodology for the evaluation of the level of energy saving motivation in the company, the expert evaluation of the opinions of 40 employees from 16 large construction companies of the Tyumen region of Russia was conducted. The experts were the employees occupying the different positions, one way or another related to the process of energy consumption in the company.

The values of the Concordance Ratio ranged from 0.59 to 0.84, and were equal to 0.79 on average, which indicates a high degree of consistency among the experts. The statistical significance of the Concordance Ratios was confirmed by the Pearson criterion (χ^2) at the 5% error level.

Table 1. The matrix of the aggregated values of the expert evaluation of the importance of the human capital factors, taken into account in the energy saving motivation

Human capital factors	Categories of the personnel						
	Top and senior managers	Unit managers	Key personnel	General and support personnel	Energy management personnel	Procurement personnel	Total evaluation of the factor (A_j)
Level of participation in energy consumption	3.6	4.2	4.82	3.8	4.02	3.8	4.07
Level of participation in energy saving	4.2	4.3	4.5	3.6	4.8	3.9	4.22
Level of awareness of energy saving	4.1	4.02	4.2	4	4.4	4.08	4.13
Culture of energy saving in the company	4.3	4.2	4.2	4.1	4.3	4.1	4.2
Culture of energy consumption of the employee	4.04	4	4.4	4	4	3.9	4.06
Level of education of the employee	4.1	4.1	3.8	3.7	3.9	4	3.93
Accumulated period of work and the experience	4.2	4.1	4.5	3.8	3.96	3.7	4.04
Level of relevance of an employee in the company	4.1	4.06	4	3.8	4.2	3.9	4.01
Total evaluation of the category of personnel (A_i)	4.08	4.12	4.30	3.88	4.2	3.45	

The results of the aggregation of the values of the expert evaluations of the importance of human capital factors, taken into account in the energy saving motivating, are presented in Table 1.

The expert opinion on the importance of the factors of the energy saving motivation is fairly homogeneous. The average expert evaluations exceed the average value of the scale used, equal to 3 points, and vary from 3.6 to 4.82 points.

For the category “Top and senior managers”, almost all factors are important (except for participation in energy consumption, which is related to the type of activity of the employees occupying the managerial positions in the company). The unit managers are responsible for energy consumption and energy saving (the level of participation in energy consumption, the level of participation in energy saving, the level of awareness of energy saving) at the workplaces. Moreover, in assessing this category of personnel it is important to take into account such factors as the accumulated period of work and experience, the level of education and the culture of energy consumption of the employee.

The energy consumption and the energy saving highly depend on the key personnel of the company, because, as a rule, these employees use the power energy equipment. In this regard, the experts noted a high assessment of such factors as the level of participation in energy consumption, the level of participation in energy saving, and the level of awareness of energy saving. Moreover, the awareness of the culture of energy consumption and developed energy saving culture in the company are important for this category.

General personnel (all other employees). The experts noted the importance of such human capital factors as the participation in energy consumption, awareness of energy saving, the culture of energy saving in the company.

An energy manager is a specific and unique profession in the company. Energy managers participate in the organization of the whole process of energy saving, they interact with the personnel of various categories, including the management. The experts noted that not every Russian company has this category of personnel. However, the functions of this employee (a group of employees) are performed by a unit under the supervision of an employee who holds the position of a “chief power engineer”. For this category of personnel, the importance of such factors as the participation in energy saving, the awareness of energy saving, the culture of energy saving in the company and the relevance of the employee in the company are highly appreciated.

The employees of the procurement personnel category are responsible for procurement of new energy-efficient equipment, so the factors such as the energy saving culture in the company, the awareness of energy saving and the level of education are important for them.

As a result of the expert evaluation performed, the most significant factors for different categories of personnel were identified. According to the experts, the greatest impact on the energy saving process in general for all groups of personnel is provided by: the level of participation in energy conservation; the culture of energy consumption of the employee; the level of participation in energy consumption and the level of awareness of energy saving (Fig. 1). These factors should be considered first of all when developing the measures aimed at increasing the level of motivation for energy saving.

At the same time, it is advisable to impact mainly such categories of company personnel as: the key personnel, the energy management personnel and the unit managers (Fig. 2).

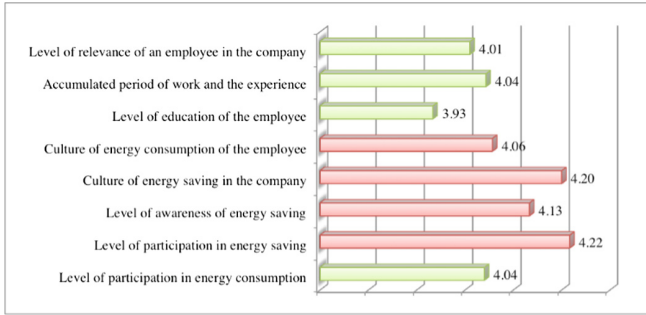


Fig. 1. The average expert assessment of the level of importance of human capital factors taken into account in energy saving motivation (on a 5-point scale).

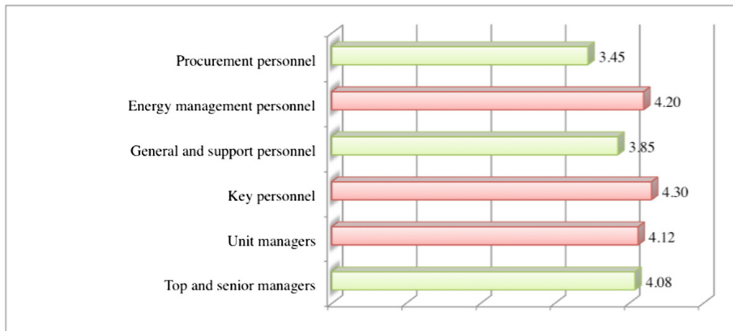


Fig. 2. The average expert evaluation of the key categories of personnel taken into account in the energy saving motivation (on a 5-point scale).

The motivation of the employees in the field of energy saving should be integrated into the overall motivation system in the company and aimed at the support of the energy efficiency improvement, and also at the encouraging of the improvement of production indicators, the reduction of the turnover of staff, while it should not result in the decline of the product quality, safety of production, labor efficiency.

4 Discussion

As a recommendation for the further studies it can be noted that the method of principal components can be applied to the aggregated results of the expert evaluation of the factors influencing the energy saving motivation. The method of the principal components allows assessing the general pattern in the evaluation of the importance and completeness of the set of motivation factors for energy saving and revealing the latent factors. As a result of the implementation of the computational procedures of the method of principal components, the matrix of factor loads, the principal components and their eigenvalues are calculated.

It should be emphasized that the proposed set of factors affecting the energy saving motivation in the company is not the only true one. The application of the methodology allows changing the set of human capital factors that are taken into account in the energy saving motivation of the personnel, as well as the personnel category depending on the organizational structure of the company.

5 Conclusions

The results of the evaluation of the importance of the human capital factors taken into account in the energy saving motivation have shown that, according to the experts, the process of energy saving in general for all groups of personnel depends on: the level of participation in the energy saving; the culture of energy consumption of the employee; the level of participation in energy consumption and the level of awareness of energy saving. These factors should be considered first of all when developing the measures aimed at improvement of the level of energy saving motivation. In this case, it is advisable to impact mainly such categories of company personnel as: the key personnel, the energy management personnel and the unit managers. This is due to the fact that the employees of these categories of personnel are most involved in the process of consumption of the energy resources of the company and have a high potential for energy saving.

The evaluation of the experts' opinions revealed the importance of introduction of an employee of the "Energy manager" category into the organizational structure of the company, whose main duties will include the improvement of the level of awareness of the personnel of the possibilities of energy saving and maintenance of the culture of energy saving in the company.

Thus, the motivation of the personnel for energy saving should be carried out on an ongoing basis, as the human capital cannot be preserved, an employee's attitude to the company takes a long time to develop, it is important to form a positive attitude of an employee to the company, to create the conditions in which an employee could be confident in the future.

References

1. The Federal Law of the Russian Federation: On Energy Saving and Introduction of Changes to Certain Legislative Acts of the Russian Federation, N 261-FZ
2. Andrizhievsky, A., Volodin, V.: Energy saving and energy management, High School, Minsk, p. 296 (2005)
3. Bushuev, V.: The Concept of the Intelligent Electric Power System of Russia with an Active-Adaptive Network. Scientific and Technical Center of Federal Grid Company of Unified Energy System, Moscow (2012). p. 219
4. Voropai, N., Podkakovnikov, S., Trufanov, V.: The substantiation of the development of the electric power systems: methodology, models, methods, their use, Science, Moscow, p. 448 (2015)
5. Dmitriev, A., Grebneva, I.: *Innov. Investments*. 7, 213–216 (2013)
6. Kaminskaya, Ya.: Energy of Russia, Prospection, Energy, Moscow, p. 612 (2012)

7. Kuznetsov, E., Novikova, O., Dyachenko, A.: *Economics and Management of Energy Saving*. SPb, SPbPU, p. 591 (2010)
8. Melnyk, A., Sadriev, A.: *Creative Econ.* **12**(48), 82–86 (2010)
9. Shchelokov, Ya., Danilov, N.: *Energy Saving in the Budgetary Sphere*. EnergyPress, Ekaterinburg (2012)
10. Yavorsky, M.: *Energy Saving in Industrial Enterprises*. Tomsk, TPU, p. 134 (2000)
11. Lyubimova, N.: *Vestnik Universiteta*, vol. 9, p. 352–356 (2015)
12. Draft of the Energy Strategy of Russia until 2035. http://www.energystrategy.ru/ab_ins/source/ES-2035_09_2015.pdf. Accessed 27 Aug 2017
13. Putin, V.: It is necessary to build a unified effective management system in the sphere of energy saving. <http://rosinvest.com/novosti/651491>. Accessed 27 Aug 2017
14. Worrell, E., Galitsky, C.: *Energy efficiency improvement and cost saving opportunities for cement making* Berkeley, p. 77 (2008)
15. Tan, Z., Zhang, J., Xu, J., Wang, J.: *Appl. Energy* **87**(11), 3606–3610 (2010)
16. Boute, A.: *Energy Policy* **46**, 68–77 (2012)
17. Zhang, T., Nuttall, W.: *IEEE Trans. Power Syst.* **28**(2), 169–186 (2011)
18. Korppoo, A., Korobova, N.: *Energy Policy.* **42**, 213–220 (2012)
19. Ochoa, L., Harrison, G.: *IEEE Trans. Power Syst.* **26**(1), 198–205 (2011)
20. Richardson, I., Thomson, M., Infield, D., Clifford, C.: *Energy Build.* **42**(10), 1878–1887 (2010)
21. Wayne, C., Doty, W.S.: *Energy Management Handbook*. Fairmont Press, Boca Raton (2007). p. 758
22. Popkova, E., Mitrahovich, E.: *Economics* **2**(63), 108–111 (2010)
23. Kopytova, A.: *Procedia Eng.* **165**, 1132 (2016)
24. Beshelev, S., Gurvich, F.: *Mathematical and Statistical Methods of Expert Evaluation, Statistic*, p. 265, Moscow (1980)

The Problems of Market Orientation of Russian Innovative Products (Electric Cars as a Case Study)

Svetlana Bozhuk^(✉)  and Natal'ya Pletneva 

Peter the Great St. Petersburg Polytechnic University,
Politechnicheskaya st., 29, St. Petersburg 194064, Russia
bojuk.svetlana@yandex.ru

Abstract. The aim of this research is to analyze the results of realizing the market-oriented concept in Russian car market and to determine the impact of marketing on its development. M. Porter and R. Grant's model of competitive forces was used to assess the prospects for changing the situation and the main moving forces which determine the state of the car market. The analysis of the empirical data, characterizing the electric and hybrid car markets in separate countries and in the world, as a whole, was done. Using the method of expert assessments allowed to identify the following key attributes of the competitiveness in Russian market: the acquisition cost, the rapidity, the economy of travel, the duration of travel and the capacity of the trunk. For the competitive analysis, we applied the calculation methods, which allowed to determine the individual and weighted indicators of competitiveness for each characteristic of the considered models of electric cars in Russian market. As a result, it was revealed that the impact of complementary goods and services: fuel (energy sources), car insurance, car loans, car parking, maintenance and repair services is the main moving force in the car market. The car manufacturers should build their market orientation on the balance between innovation and marketing competences.

Keywords: Car market · Electric car · Hybrid car · Marketing

1 Introduction

The fundamental principle of marketing, consumer orientation, has many interpretations in related research papers; however, most recently, it has not always been recognized as the right focus, and the priority of marketing in determining market orientation has been increasingly challenged. Most large companies, holding leading positions in their respective market sectors, dismiss their marketing departments, replacing them with departments for development and innovation.

The existing priorities are due to many factors. High competition in existing markets encourages companies to create new markets. In order to create a new market, a new way to meet the consumer demand has to be offered or a new technology has to be applied (more cost-effective, allowing to attract new segments), providing value innovation for consumers. However, while ensuring the satisfaction of its customers, an

organization can not act in isolation and is forced to factor in other market participants, such as distributors, competitors, decision-makers in procurement [1]. Therefore, each company requires a polycentric focus on many market players, not just consumers. The concept of market orientation contributes to the evolution of the philosophy of business and the organizational culture based thereupon towards value innovation for consumers. However, weakening marketing orientation can hinder implementation of innovative products.

The purpose of this study is to analyze the problems of excessive concentration of Russian manufacturers based on the concept of market orientation in the market of passenger electric vehicles.

In this regard, the following objectives are established: to identify the major factors that determine the transformation of the passenger car market towards electric vehicles, to assess the prospects of the Russian automotive industry in terms of value innovation for consumers and the influence of marketing factors on the success of an innovative product in the market.

Market orientation has determined the main world trends in the automotive industry: expectations of greater value are manifested in terms of energy efficiency and environmental friendliness, automation and intellectual functions of both the car itself (unmanned driving) and accessories (alarms, video recorders, etc.), with combinations of functions providing the consumer with universal mobility.

It is fair to assume that in countries with a high level of motorization (in Europe and North America), further renewal of cars will be carried out in favor of models offering greater value at a lower price. The most active development in recent years has been demonstrated by the trend towards increased environmental friendliness of cars, which ensures both personal benefits (in the form of more cost-efficient operation) and public values (preservation of the environment). In 2016, investments in this sector worldwide amounted to \$2 billion, twice as much as in 2015 and \$650 million more than in the previous three years combined. The volume of the market has grown ten times over the past five years and amounted to 1.26 million cars in 2015. The number of cars fully operating due to electric traction in 2015 was approximately 700 th. cars [2].

AvtoVAZ is represented in the market of passenger electric vehicles with only one model, VAZ-1817 ELLADA. The choice of a Russian consumer when buying a car is influenced by many factors: the tradition of consumption, poor awareness of the advantages of an electric vehicle and the underdeveloped infrastructure of charging stations. However, as shown by the practice of other countries, this situation can be overcome by appropriate state regulation. Improvements in the manufacturing technology for electric vehicles will, in the near future, help to find solutions to eliminate the essential disadvantages of electric cars. After that, marketing factors will become the main drivers determining the competitiveness of Russian electric vehicles. In this area, the Russian automotive industry is lagging far behind foreign manufacturers. Market success is ensured by market orientation simultaneously on two development vectors: innovations and marketing.

2 Materials and Methods

Empirical sources of the initial data for the study were represented by reports and analytical articles characterizing the state of the markets for electric and hybrid cars in individual countries and in the world as a whole, as well as previous research by the authors [6, pp. 96–109].

Assessment of the change prospects and the main driving forces determining the state of the car market is performed based on the model of competitive forces proposed by Michael Porter and specified by Robert M. Grant [3].

Successful implementation of the market orientation concept was evaluated on the basis of key features of the competitive profile of electric car manufacturers according to the methodology for determining unit and integral competitiveness indicators.

Unit competitiveness indicators were determined using the following formulas.

If customer satisfaction for the feature is maximized by increasing its value (the more, the better), for example, as seen for the fuel endurance, the calculation of the unit indicator is carried out according to the formula of:

$$q_i = P_i/P_0 \quad (1)$$

where

- q_i is the single competitiveness indicator for the i -th feature;
- P_i is the value of the i -th feature obtained by the competitor in question;
- P_0 is the value of the i -th feature for the base option.

If customer satisfaction for the feature is maximized by reducing its value (as seen for energy consumption, acceleration time up to 100 km/h, base price), the calculation of the unit competitiveness indicator is carried out according to the formula of:

$$q_i = P_0/P_i \quad (2)$$

where

- q_i is the single competitiveness indicator for the i -th feature;
- P_i is the value of the i -th feature obtained by the competitor in question;
- P_0 is the value of the i -th feature for the base option.

The significance of the features and their implementation were determined by consumer surveys

When ranking the significance, the following condition was met:

$$\sum_{i=1}^N a_i = 1 \quad (3)$$

where a_i is the significance of the i -th feature (weight coefficient);

i is the number of the feature under consideration (index); N is the total number of features considered.

Implementation of the key features with a subjective nature of evaluation was measured in points on a scale of 1 to 5, where 1 is extremely poor implementation; 2 is unsatisfactory implementation; 3 is satisfactory implementation; 4 is good implementation; 5 is maximum implementation.

Given the different significance of various features, unit competitiveness indicators were refined by calculating the weighted values by the formula.

$$Q_i = a_i \times q_i \quad (4)$$

where Q_i is the weighted value of the unit competitiveness indicator;

a_i is the significance of the i -th feature (weight coefficient).

The value of the final indicator is determined as the sum of weighted values of unit competitiveness indicators:

$$I = \sum_{i=1}^N Q_i \quad (5)$$

where I is the final competitiveness indicator.

Strategic significance of each feature in terms of value provision to the consumer was carried out based on the results of surveys conducted by the authors [4, 8], with account of data obtained from other sources [5, 6].

3 Results

The main results of the study cover the assessment of the key features reflecting the marketing and innovative performance of companies producing electric vehicles, the values of weight coefficients as assessed by consumers and the final indicators that characterize the competitive positions of companies producing electric vehicles obtained through market orientation.

The overall competitive situation for the car market is quite dramatic (see Fig. 1). Cars with internal combustion engines (ICEs) and electric cars meet the same demand of consumers, but in different ways, i.e. are substitute goods. Competition between substitute goods continues to develop with further attempts to create cars operating on alternative fuels, such as hydrogen fuel. Hybrid cars are the most successful in terms of sales. Being an environmentally friendly alternative to a car with an internal combustion engine, hybrid vehicles provide the owner with savings in operating costs, while being less dependent on the battery runtime than electric vehicles.

ICE cars create a significant competitive threat to electric vehicles, as the amount of money required to purchase an electric vehicle is sufficient for acquiring a higher-class car with a gasoline engine.

A promising technology for environmentally friendly transport is PHEV (plug-in hybrid electric vehicle). The advantages of plug-in hybrid cars are that they can operate on conventional fuel, charging the electric battery while driving. This solves the

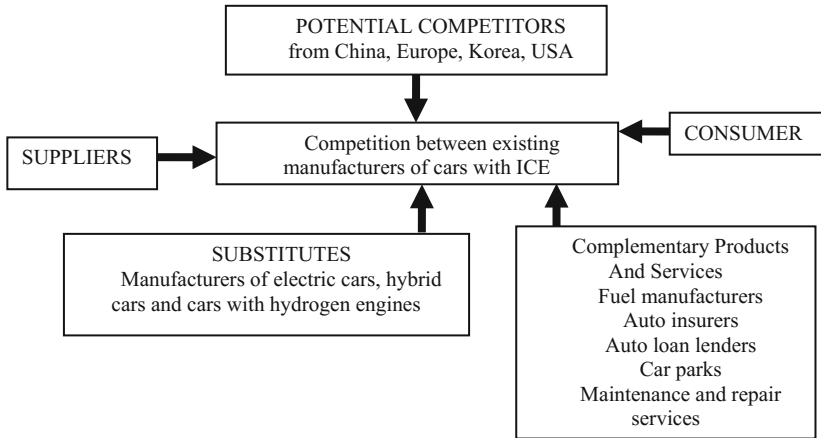


Fig. 1. Model of competition forces in the car market

problem of the driving range limitation by the battery capacity and enables the owner to charge batteries from the mains in a convenient location.

The expanded model of competitive forces demonstrates that the cost of owning a car is not limited to the price that the customer pays at the car dealership. The influence of such complementary goods and services as fuel (energy sources), car insurance, car loans, parking, maintenance and repair services may also be noted in the car market. The related system of taxes and fees may also be added. Therefore, the total cost of ownership of a car, in addition to the cost of the car with the ordered specifications, includes: mandatory costs for insurance, maintenance and repair, refueling or other energy recharge, as well as additional costs that can vary in different conditions, such as payment for parking, additional insurance, property tax, transport tax, interest on loans, travel on toll roads, etc.

Obviously, when comparing the total cost of ownership for automotive substitutes in Russia, such components as the cost of the car in the basic configuration, the cost of fuel, maintenance and repairs should be compared in combination. This is due to the fact that in Russia the remaining components do not vary for the owner depending on the environmental characteristics of the vehicle.

4 Discussion

The main problems preventing the spread of electric vehicles in Russia are the high cost and the short travel range. Studies show that, in the first quarter of 2017, the average car cost for the Russian consumer was RUR 1.3 million [7]. The base price of an ELLADA car corresponds to the average statistical level, i.e. the price level may be considered acceptable for Russian middle-class consumers.

Direct competitors offering electric vehicles in the price category similar to that of ELLADA are the manufacturers of Renault ZOE and Kia Soul EV (see Table 1).

Table 1. Characteristics of electric vehicles [8]

	ELLADA	Renault ZOE	Kia Soul EV	Nissan Leaf	VW e-Golf	Mercedes Clase B Electric	BMW i3	Tesla Model S
Maximum power (hp)	80	88	110	109	115	177	170	302
Maximum power (kW)		65	82	80	85	132	127	225
Battery capacity (kW/h)	14	41	27	24	26.5	28	22	70
Fuel endurance (km)	150	210	190	175	190	200	130	400
Power consumption per 100 km	9.3	19.5	14.2	13.7	13.9	14	16.9	17.5
Maximum speed (km/h)	130	135	144	145	140	160	150	190
Acceleration to 100 km/h (s)	12	12	12	10.5	10.4	7.9	7.2	6.2
Full/fast recharging time (h)	7/1	9/0.5	4/0.5	8/0.5	8/0.5	4/-	6/0.5	5.3/2
Number of seats	5	5	5	5	5	5	4	5
Number of doors	5	5	5	5	5	5	5	5
Trunk volume (l)	350	338	250	330	170	488	200	790
Warranty (years/thousand km)		8/160	8/160	8/160	8/160	8/160	8/160	8/200
Base price (th. RUR)	1200	1280	1500	2066	2556	2943	3000	5000

The calculations show that, by its technical and economic characteristics, ELLADA is a competitive innovation of AvtoVAZ. Comparison of technical and economic characteristics was performed using such criteria as travel duration, cost-efficiency, speed and cost of acquisition [8, p. 102].

However, electric vehicles as a whole are still losing to hybrid models and ICE cars, which are highly popular with consumers. Nissan X-TRAIL, Fiat 500, Ford EcoSport Toyota Corolla and the hybrid BYD Qin are in the near-price category to ELLADA. The manufacturer of the BYD Qin hybrid left the Russian market due to lack of demand for its models, therefore popular hybrid Toyota Prius was used in the comparison. In order to compare the characteristics of cars with different engine types, the data were reduced to a comparable form based on fuel consumption in terms of value at the rate of RUR 4.0 per 1 kWh and RUR 36.0 per 1 L, without consideration of electricity losses during charging and operation of batteries. The result is shown in Table 2.

Table 2. Implementation of key features competing models

	ELLADA	Renault ZOE	Kia Soul EV	Nissan X-TRAIL	Fiat 500	Ford EcoSport	Toyota Corolla	Toyota Prius
Travel distance (km)	150	210	190	800	1140	750	850	600
Travel cost-efficiency per 100 km (RUR)	37.2	78.0	56.8	270.0	219.6	248.4	230.4	108
Speed (km/h)	140	135	144	183	182	172	195	180
Purchase price (th. RUR)	1200	1280	1500	1279	1015	900	985	2200
Information support (point)	1	4	1	5	5	5	5	5
Infrastructure development (point)	1	1	1	5	5	5	5	5
Service level (point)	3	4	5	4	4	5	5	5
Popularity level (point)	1	4	4	5	5	5	5	5
Reputation of the manufacturer (%)	16	45	35	40	11	37	56	56

The criteria for comparison were selected with account of the benefits expected by the consumer and the competencies that enable the manufacturer to differentiate its offer in the market.

The success of market orientation of car manufacturers in the field of marketing competencies was assessed by the criteria of information support, service level and infrastructure development, reputation of the manufacturer, and popularity of the model.

Implementation of the key features by marketing competencies was measured in points on a scale of 1 to 5, where 1 is extremely poor implementation; 2 is unsatisfactory implementation;

3 is satisfactory implementation; 4 is good implementation; 5 is maximum implementation.

Such key characteristics as the number of seats, acceleration dynamics, design and manufacturer's warranty were excluded from consideration. The number of passenger seats, the acceleration dynamics for up to 10 km/h and the warranty provided are the same for all models, and therefore may be excluded from the comparison. Design is a very important attribute in selection of a car, however, its assessment by the consumer is always subjective. Considering that electric car manufacturers use modern design or copy the designs of popular ICE models, this feature may also be omitted.

The cost of acquisition has the highest weight for Russian consumers. The results of ranking of the key features of the competitive profile and competitiveness calculations are summarized in Table 3.

The final competitiveness indicator may be interpreted both by its absolute value and in comparison with competitors. If the value of the final competitiveness indicator exceeds 1, then the car manufacturer may be deemed competitive; if it is less than 1, the manufacturer is not competitive. A comparison against competitors demonstrates the

Table 3. Values of unit indicators with account of weight and final competitiveness indicators

Item no.	Benefit for consumer, product attribute	Significance of feature (weight)	ELLADA	Renault ZOE	Kia Soul EV	Nissan X-TRAIL	Fiat 500	Ford EcoSport	Toyota Prius
1	Travel distance	0.15	0.026	0.037	0.034	0.141	0.201	0.132	0.106
2	Travel cost-efficiency	0.14	0.867	0.414	0.568	0.119	0.147	0.130	0.299
3	Speed	0.10	0.072	0.069	0.074	0.094	0.093	0.088	0.092
4	Purchase price	0.20	0.164	0.154	0.131	0.154	0.194	0.219	0.090
5	Information support	0.05	0.010	0.040	0.010	0.050	0.050	0.050	0.050
6	Infrastructure development	0.05	0.010	0.010	0.010	0.050	0.050	0.050	0.050
7	Service level	0.07	0.042	0.056	0.070	0.056	0.070	0.070	0.070
8	Popularity	0.11	0.022	0.088	0.088	0.110	0.110	0.110	0.110
9	Reputation of the manufacturer	0.13	0.037	0.104	0.081	0.093	0.026	0.086	0.130
	FINAL INDICATOR	1.00	1.251	0.972	1.066	0.867	0.927	0.935	0.996

existing gaps between the estimates, which enables identification of the most dangerous competitor with an analysis of its strengths and weaknesses.

It can be noted that ELLADA is a competitive model as compared to similar vehicles; however, the gap is extremely small. The manufacturer loses the margin of benefits obtained through innovative competencies due to marketing mistakes. The benefits of an ELLADA electric car are its relatively (as compared to other electric vehicles) low price, high cost- efficiency and good travel distance to full battery discharge. The car manufacturer's focus on innovation has brought certain positive results, however, in the absence of developed marketing competencies, consumers remain unaware thereof.

When evaluating the results, it should be noted that the values of competitiveness indicators for ICE cars were determined based on the significance of the key features of electric vehicles. In an isolated assessment of the competitiveness of cars with internal combustion engines, the set of key features and their significance levels would change. Obviously, the travel distance ensured by the tank capacity may be excluded from consideration, since the existing developed network of gas stations ensures the total freedom for consumers. It should also be reminded that determination of the weight of the key features was guided by the requirements of the "average" consumer and did not take into account the opinions of individual segments of consumers, for example, of those adhering to the LOHAS lifestyle (Lifestyle of Health and Sustainability). If we evaluate the competitiveness of electric vehicles taking into account the opinion of the "green" segment (which is still very weak in Russia), ICE cars may "lose" their advantages. In addition, the calculations took into account the data on technical and operational characteristics provided by the manufacturers and information portals for ideal operating conditions. In practice, their actual values may deviate significantly from those declared.

5 Conclusions

Market orientation of a car manufacturer shall be based on a balance between innovative and marketing competencies. The experience of European countries demonstrates that environmentally friendly innovations in the automotive industry enable car manufacturers to form a new market, which is now entering a growth phase. Further expansion of the market largely depends on marketing tools. Marketing competencies consolidate the success of technical achievements, creating value for the consumer in the field of intangible assets, such as reputation, positive image, popularity of electric vehicle models. An electric car should become a fashionable city car.

The prospects of electric vehicles in the Russian market are highly dependent on macro- environment drivers, mainly of the legislative, economic and cultural nature.

Cultural factors characterize the imbalance of values and opportunities of consumers in the Russian car market. Environmental protection has not yet become a significant mission for Russian consumers. Savings in car refueling costs attract those consumers who can not afford acquisition of a new premium-class car. ELLADA electric cars have an opportunity to fit into the difficult market situation due to their attractive technical and economic characteristics.

References

1. Evdokimov, K.V.: The main stages of the evolution of the entrepreneurship theory. *Econ. Manag.* **6**(68), 21–24 (2011)
2. The main trends of development of global oil market up to 2030 year (Electronic Materials). <http://www.ey.com/ru/ru/industries/automotive/ey-russia-automotive-survey>. Accessed 29 Aug 2017
3. Information portal Cleantechnica.com (Electronic Materials). <https://cleantechnica.com/2017/05/17/us-doe-plug-electric-vehicles-captured-23-5-share-norways-total-auto-market-2016/>. Accessed 29 Aug 2017
4. Bojuk, S.G., Pletneva, N.A.: Impact of ecological and social initiatives of companies on the forming of consumers loyalty. *Pract. Mark.* **2–1**(240), 11–18 (2017)
5. Khvoryh, G.: The car's buyer behavior. Who evaluates whom? (Electronic Materials). www.AutoMarketolog.ru
6. Information portal ZR (Electronic Materials). <https://www.zr.ru/content/news/656859-kakie-factory-vliyayut-na-vybor-avtomobilya/>. Accessed 29 Aug 2017
7. Information portal E-Vesti. Electronic Materials. <http://www.e-vesti.ru/ru>. Accessed 29 Aug 2017
8. Bojuk, S.G., Pletneva, N.A., Evdokimov, K.V.: Impact of ecological innovations on consumers' preferences (Russian car market as a case study). *Vestn. Belgorod Univ. Coop. Econ. Leg.* **3**, 96–109 (2017)

Automation of Calculations for Selecting Construction Equipment Purchasing Techniques

Zalina Tuskaeva^(✉) , Gevork Aslanov , and Zalina Alikova 

Federal State Budgetary Educational Institution of Higher Education,
North-Caucasian Institute of Mining and Metallurgy
(State Technological University),
Nikolaeva Street, 44, 362021 Vladikavkaz, Russia
tuskaevazalina@yandex.ru

Abstract. Considering high material consumption and the wide range of performed construction works, and the resulting variety of required construction machinery, it is essential to define the most beneficial way of purchasing the machinery and to establish its most efficient lifetime for effective operation of both a certain construction company and a whole construction complex. To reduce material consumption, increase accuracy and optimize calculation time it is recommended to develop a software product allowing to evaluate the efficiency of any purchasing technique. The proposed method and correspondingly the developed software product makes it possible to compare the methods visually and having analyzed them to make a reasonable decision. They also provide an opportunity to perform complex analysis of the methods of purchasing construction equipment.

Keywords: Techniques of purchasing construction equipment
Software product · Interface

1 Introduction

Studies showed that currently there exist three most widespread methods of purchasing construction equipment for the needs of construction companies: direct purchase, credit purchase, leasing. In the complicated financial situation of most organizations in the construction sphere and in view of the general investment reduction this situation requires searching and finding the most acceptable purchase option in the given condition [16–19]. Therefore, it is necessary to develop methods providing a base for a software product securing a quick and reasonable selection of a purchase technique, providing financial saving for the company.

The ideas, concepts, methodological, methodical and applied conditions of this problem have been dealt with in the works of Asaul V.V., Volkov D.P., Afanasyev V. A., Gusakov A.A., Kollegaev R.N., Vasilyeva V.M., Panibratov Y.P., Repin S.V., Dikman L.G., Grabovoi P.G., Tsai T.N., Ivakin E.K., Kazakov O.B., Shreiber A.K. and others.

2 Methodology

Three options of purchasing construction equipment are compared: direct purchase (buying at the company's own expense), credit purchase and leasing. When buying at the company's own expense the organization has now credit dealings with the bank. Cash outflows are equal to the cost of equipment. In this case depreciation is charged on equipment, but it should be noted that during depreciation the acceleration ratio is not applied, while in leasing it is recommended. The retirement period of the equipment in this purchasing option is equal to depreciation period, thus accordingly the property tax, paid out by the asset holder, is increased. Total costs of this purchasing option are presented in Table 1.

Table 1. Total costs of direct purchase (thousands of rubbles)

Accounting period	Net assets value	Depreciation	Property tax	Advance payment	Transport expenses	Costs for taxation purposes	Income tax recovery	VAT recoverable
0				1800000	1800000			
1	1 525 423.73	25 423.73	2796.61	0.00	2796.61	28220.34	5644.07	274576.27
2	1500000	25 423.73	2750	0.00	2750	28173.73	5634.75	
...						
36	635593.18	25 423.73	1165.25	0.00	1165.25	26588.98	5317.8	
Total		915254.28	71268.02	1800 000.00	1871268.02	986522.3	197304.5	274576.27

The equipment bought on credit becomes the property of the organization immediately as in the first case. But we should consider that it is pledged as a secure repayment of the loan. The organization depreciates as in direct purchase. It is not recommended to use the acceleration ratio in this case either.

The amount of the "included" VAT is presented to budget; therefore, the total costs are reduced by this amount. The results of total costs of credit purchase are summarized in Table 2.

In leasing purchase the lease holder makes regular leasing payments to refund the equipment cost. The structure of leasing payment includes: the annual debt payments or out of the equity capital, the property tax amount (the equipment is on the balance sheet of the lessor), commission fees in % from the amount of the leasing payment. The VAT in the equipment cost is excluded from leasing payment and the less or transfers this amount to budget. The calculations of leasing payments are presented in Table 3.

Table 2. Total costs of credit purchase (thousands of rubbles)

Accounting period	Net assets value	Depreciation	Property tax	Advance payment	Credit	Credit debt	Debt repayment	Debt interest payment (16,5%)	Transport expenses	Costs for taxation purposes	Income tax recovery	VAT recoverable
0				630000	1170000				630 000			
1	1 525 423.73	25 423.73	2796.61	0.00		1 144 664.37	32 500.00	16 087.50	51384.11	44307.84	8861.568	274576.27
2	1500000	25 423.73	2750	0.00		1 118 980.38	32 500.00	15 640.63	50890.63	43814.36	8762.872	
...												
36	635593.18	25 423.73	1165.25			0.00	32 500.00	446.88	34112.13	27035.86	5407.172	
Total		915254.28	71268.02	630000	1 170 000.00	1 144 664.37	1 170 000.00	297 618.75	2168886.86		256748.2	274576.27

Table 3. Total costs of leasing (thousands of rubles)

Accounting period	Leasing installment (payable)	Including VAT	Leasing payment (assessed)	Including VAT	Income tax recovery	VAT recoverable
0	630 000	96101.69				
1	43000	6559.32	60500	9228.81	10254.24	9228.81
2	43000	6559.32	60500	9228.81	10254.24	9228.81
...						
36	43000	6559.32	60500	9228.81	10254.24	9228.81
Total	2178000	332237.21	2178000	332237.16	369152.64	332237.16

3 Results

The basic algorithm of the developed software product is consistently presented in 4 pictures (Fig. 1 – the basic algorithm of the program; Fig. 2 –direct purchase algorithm; Fig. 3 credit purchase algorithm; Fig. 4 – leasing algorithm).

To facilitate calculations a software program was developed [20–22], allowing to calculate the cost of construction equipment purchase in three ways. To perform calculations, it is necessary to run the program and input all the basic values. The program interface consists of one window with all the basic controls. The main window (see Fig. 5) includes pages which present the results of calculation for each option. The main page is divided into 4 zones for basic values input. The first zone contains values

The basic algorithm of the program

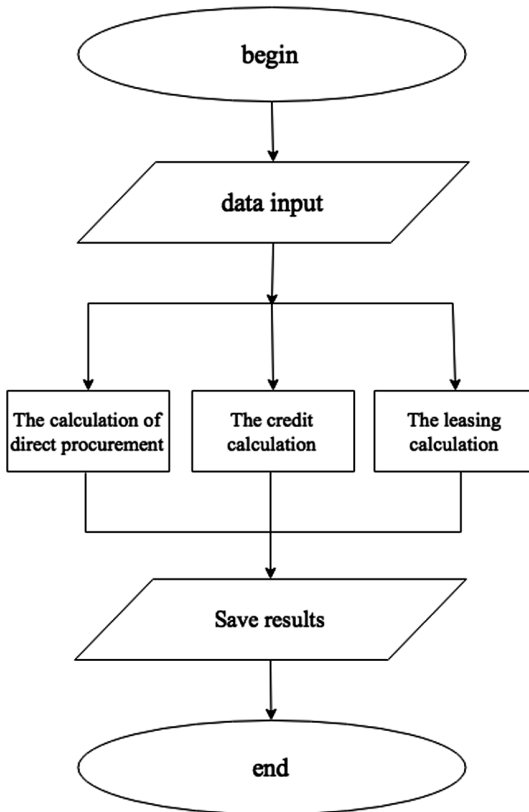
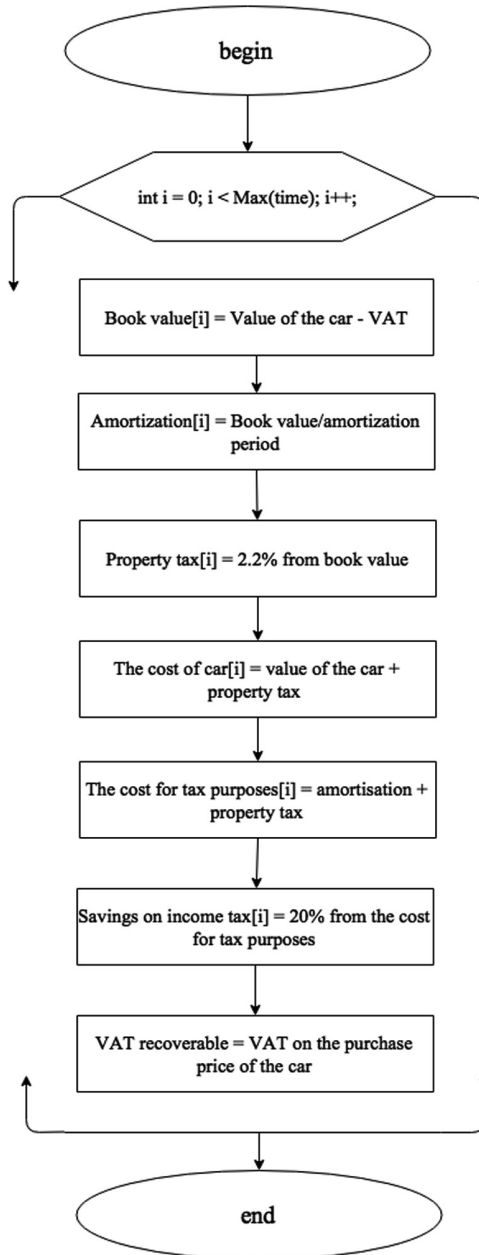


Fig. 1. Basic algorithm of the program.

Algorithm of direct purchase**Fig. 2.** Direct purchase algorithm.

Algorithm of credit purchase

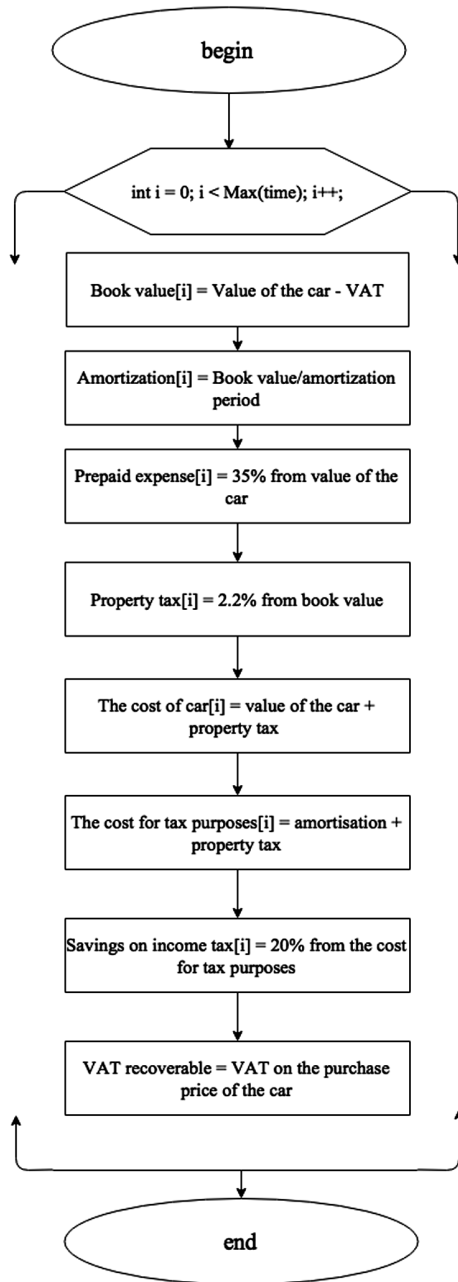
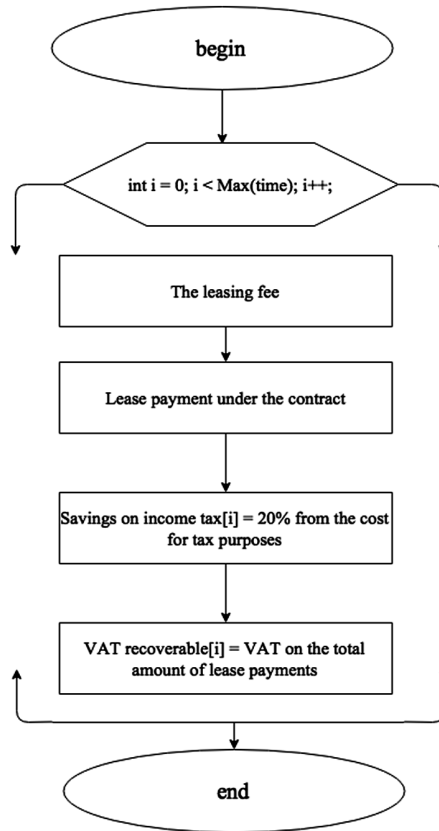


Fig. 3. Credit purchase algorithm.

Purchase algorithm in leasing**Fig. 4.** Leasing algorithm.

common for every method (cost of transport, amortization period etc.). The second zone includes values which refer only to direct purchase method. The third and the fourth zones have information related with credit purchase and leasing correspondingly.

After inputting all the necessary information press the “Start” button and the application will start calculations. After finishing calculation, the panel disappears and the user can see the results on other pages in the main from (see Figs. 6, 7 and 8).

On page «Notes» there is summarized information on all the three types of calculations. If necessary, the results can be saved as a file for quick browsing. In order to do that open menu «File/Save». To open saved files select menu «File/Open» (Fig. 9).

Ways of acquisition of the construction equipment

General

Calculate Clear

Calculation

Input Data Calculation of direct procurement Calculation when buying on credit Calculation for buying leasing Notes

Common parameters

Car price, rub 1800000

VAT, % 18

Depreciation period, month 60

Property tax, % 2,2

Direct purchase parameters

Prepaid expense, rub 1800000

Settlement period, month 36

Savings on income tax, % 20

Credit options

Prepaid expense, % 35

Interest rate, % 16,5

Savings on income tax, % 20

Settlement period, month 36

Leasing parameters

Prepaid expense, % 35

Rise in price, % 7

Savings on income tax, % 20

Settlement period, month 36

Fig. 5. The program main page.

Ways of acquisition of the construction equipment

General

Calculate Clear

Calculation

Input Data Calculation of direct procurement Calculation when buying on credit Calculation for buying leasing Notes

Estimated period	Book value	Depreciation	Property tax	Prepaid expense	The cost of car	Costs for taxation purposes
0				1800000	1800000	
1	1525423,729	25423,729	2796,61	0	2796,61	28220,338
2	1500000	25000	2750	0	2750	27750
3	1475000	24583,333	2704,167	0	2704,167	27287,5
4	1450416,667	24173,611	2659,097	0	2659,097	26832,706
5	1426243,056	23770,718	2614,779	0	2614,779	26385,491
6	1402472,338	23374,539	2571,199	0	2571,199	25945,738
7	1379097,799	22984,963	2528,346	0	2528,346	25513,305
8	1356112,836	22601,881	2486,207	0	2486,207	25088,083
9	1333510,955	22225,183	2444,77	0	2444,77	24669,951
10	1311285,773	21854,763	2404,024	0	2404,024	24258,781
11	1289431,01	21490,517	2363,957	0	2363,957	23854,477
12	1267940,493	21132,342	2324,558	0	2324,558	23456,895
13	1246808,151	20780,136	2285,815	0	2285,815	23065,951
14	1226028,015	20433,8	2247,718	0	2247,718	22681,518
15	1205594,215	20093,237	2210,256	0	2210,256	22303,491
16	1185500,978	19758,35	2173,418	0	2173,418	21931,766
17	1165747,639	19429,044	2137,195	0	2137,195	21566,798

Fig. 6. Calculation results.

Ways of acquisition of the construction equipment

General

Calculate Clear

Calculation

Input Data Calculation of direct procurement Calculation when buying on credit Calculation for buying leasing Notes

Estimated period	Book value	Depreciation	Property tax	Prepaid expense	Credit	The balanc of the loa debt
0				630000	1170000	
1	1525423,729	25423,729	2796,61	0		1137500
2	1500000	25000	2750	0		1105000
3	1475000	24583,333	2704,167	0		1072500
4	1450416,667	24173,611	2659,097	0		1040000
5	1426243,056	23770,718	2614,779	0		1007500
6	1402472,338	23374,539	2571,199	0		975000
7	1379097,799	22984,963	2528,346	0		942500
8	1356112,836	22601,881	2486,207	0		910000
9	1333510,955	22225,183	2444,77	0		877500
10	1311285,773	21854,763	2404,024	0		845000
11	1289431,01	21490,517	2363,957	0		812500
12	1267940,493	21132,342	2324,558	0		780000
13	1246808,151	20780,136	2285,815	0		747500
14	1226028,015	20433,8	2247,718	0		715000
15	1205594,215	20093,237	2210,256	0		682500
16	1185500,978	19758,35	2173,418	0		650000
17	1165747,629	19429,044	2137,105	0		617500

Fig. 7. Calculation results.

Ways of acquisition of the construction equipment

General

Calculate Clear

Calculation

Input Data Calculation of direct procurement Calculation when buying on credit Calculation for buying leasing Notes

Costs for the car:
At direct purchase of the car: 1871268,02 rub.
When buying a car on credit: 2168886,86 rub.
When buying a car for leasing: 2178000 rub.

Savings on income tax:
With direct purchase of a car: 197304,5 rub.
When buying a car on credit: 256748,2 rub.
When buying a car for leasing: 369152,64 rub.

VAT recoverable:
At direct purchase of the car: 274576,27 rub.
When buying a car on credit: 274576,27 rub.
At purchase of the car in leasing: 332237,16 rub.

Method	Expense (rub.)
Direct purchase	1,871,268.02
Buying on credit	2,168,886.86
Leasing	2,178,000.00

Fig. 8. Calculation results

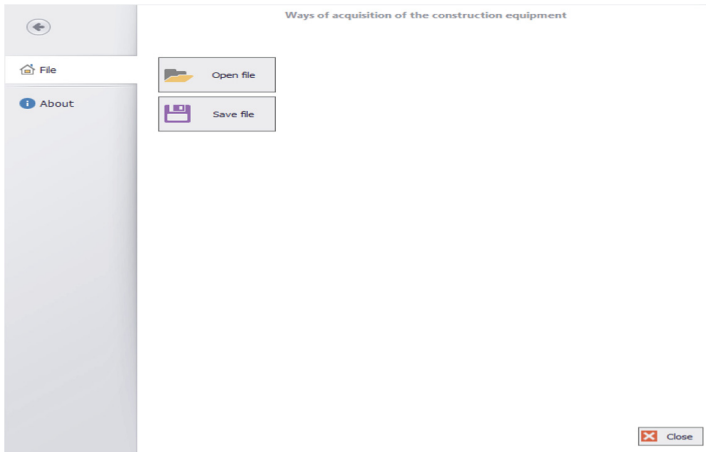


Fig. 9. Program menu.

4 Discussion

For reasonable decisions on the method of purchasing construction equipment it is necessary to consider the opportunities of the organization in the given period and the peculiarities covered above. The more accurately are considered the peculiarities of any method, the higher the possibility of choosing the best option for purchasing certain unit of construction equipment. Therefore, the development of a software program is of great practical value. Firstly, this is determined by high labor intensity of calculations. The developed software product allows to perform multiple-choice calculations, and to take a reasonable approach to purchasing method, which significantly reduces the probability of serious mistakes in the financial activities of the organization.

5 Conclusion

The current situation with various construction organizations functioning at different levels under the conditions of crisis and severe competition, demand finding and mobilizing the reserves for purchasing construction equipment. This situation determined the importance of correct evaluation of the purchasing methods.

The proposed method and correspondingly the developed software product makes it possible to compare the methods visually and having analyzed them to make a reasonable decision. They also provide an opportunity to perform complex analysis of the methods of purchasing construction equipment.

The developed method and software product allow to conclude that it is extremely important to select purchasing method reasonably, considering economical peculiarities and tax policy of the government in the given period.

References

1. Asaul, V.V.: Analysis of the competitive construction market. *Constr. Econ.* **1**, 14–25 (2005)
2. Asaul, A.N., Starovoitov, M.K., Faltinskiy, R.A.: *Cost Management in Construction*. IPAV, Saint Petersburg (2009)
3. Buttaeva, S.M.: The condition and trends in guaranteeing of reproduction of main funds. *Bull. Russ. State Soc. Univ.* **2**(54), 119–130 (2007)
4. Volkov, D.P., Nikolaev, S.N.: *Reliability of Construction Machinery and Equipment*. Highschool, Moscow (1979)
5. Voschanov, P.I.: *Balance Between Construction Plans and Construction Organizations Capacity*. Stroyizdat, Moscow (1993)
6. Gusakov, A.A.: *Organizational-Technological Reliability of Construction (Under the Conditions of Automated Design Systems)*. Stroyizdat, Moscow (1974)
7. Katz, G.B., Kovalev, A.P.: *Technical - Economic Analysis and Optimization of Machinery Construction*. Machinebuilding, Moscow (1981)
8. Kamenetskiy, M.I., Kostetskiy, M.F.: Inventory and reevaluation of production und son the basis of construction modernization. *Constr. Econ.* **4**, 17–22 (2010)
9. Kovalev, A.P.: Property management at an enterprise Moscow. ZAO “Finsttatin form” (2002)
10. Kontorer, S.E.: *Building Machines and the Economics of Their Application (Details, Construction and the Economics of Application)*. High School, Moscow (1973)
11. Korolevskiy, K.Y.: Criteria of efficiency evaluation of innovations in construction. *Constr. Econ.* **5**, 58–61 (2012)
12. Pankratov, E.P., Pankratov, O.E.: *Main Construction Funds: Reproduction and Renewal*. Economics, Moscow (2014)
13. Pankratov, E.P., Pankratov, O.E.: Problems of increasing production potential of building enterprises. *Constr. Econ.* **3**(33), 4–17 (2015)
14. Repin, S.V., Savelyev, A.V.: Mechanization of construction works and problems of using construction equipment. *Constr. Equip.* 31–35 (2006)
15. Tuskaeva, Z.R.: Problems and perspectives of managing technical potential in construction. *Sustain. Dev. Mt. Territ.* **1**(7), 84–89 (2011)
16. Sharapova, I.V., Tuskaeva, Z.R.: Evaluation of main funds effective exploitation. *Tambov State Technical University Bulletin Issue 1t* (1990)
17. Tuskaeva, Z.: Criteria for the building machinery units alternatives. *Int. J. Appl. Eng. Res.* Number **6**, 4369–4376 (2016)
18. Tuskaeva, Z., Aslanov, G.: Software product development for the construction equipment selection. *Procedia Eng.* **165**, 1184–1191 (2016)
19. Tuskaeva, Z.R.: Leasing – as a perspective method for renewing the material and technical resources of construction. *Real Estate: Econ. Manag.* **1**, 32–35 (2015)
20. Gerbert, S.: *A Comprehensive Reference Book on Construction*. Publishing House “Williams”, 748 p. (2004)
21. <https://www.devexpress.com/>. Accessed 29 Aug 2017
22. Throelsen, A.: *C# and platform .NET (Piter)*, 1154 p. (2007)

Analysis of the Reproduction of Generating Capacities of Electric Power Industry of the Russian Federation

Lyubov Manukhina^(✉) 

Moscow State University of Civil Engineering,
Yaroslavskoe shosse, 26, Moscow 129337, Russia
4804107@mail.ru

Abstract. To achieve sustainable growth in electricity consumption is possible by a more intensive use of the existing facilities of generating equipment of power plants (PP) and/or through the construction and commissioning of new power plants, reconstruction, modernization and technical re-equipment of existing PP, i.e. by the use of extensive factors of development. The article discusses trends in reproduction of the BPA (Basic Production Assets) of Russian power plants for the period of market reforms, evaluated execution of the assignment phase of the Program for modernization of electric power in the country until 2020, lists the reasons influencing the insufficient construction level of new and modernization of existing power generation capacities of power plants. The article also contains recommendations on accelerated development of electric power in comparison with other sectors through the construction of new and modernization of existing power plants. The paper calculates summary rates of inflation growth and electricity tariffs over the last 7 years. The author came up with recommendations for radical improvement of the pricing policy for electricity in Russia and an increase in investment in the fixed capital for the construction and modernization of power plants on an innovative basis.

Keywords: Reproduction · Generation capacity · Electric power industry

1 Introduction

One of the most important prerequisites for achieving the country's economic growth is the outrunning the increase in electricity production over the rates of GDP growth. A steady increase in electricity production can be achieved by a more intensive use of available capacities of the power plant (PP) generating equipment and/or by the way of extensive construction and commissioning of new power plants, reconstruction, technical re-equipment, modernization of the existing PP. In the adopted Energy Strategy of Russia for the Period until 2030, an innovative energy policy of the country for the modernization of electricity has been set forth. Reproduction of PP basic production assets planned to produce by the construction of new and modernization (technical upgrading) of existing power plants. The paper calculates summary rates of inflation growth and electricity tariffs over the last 7 years, and concludes that the growth of

tariffs is ahead of inflation, and the prices for electricity “stimulate” an additional increase in inflation. Despite the measures adopted by the Russian Government, electric energy efficiency remains below the level of 1990.

The author develops recommendations for radical improvement of the pricing policy for electricity in Russia and an increase in investment in the fixed capital for the construction and modernization of power plants on an innovative basis. An innovative option of development of national power industry at the expense of rational combination of extensive and intensive factors of economic growth was chosen [1–4].

The article analyzes the data of the Energy Strategy of Russia for the Period up to 2030, the Russian Power Industry Modernization Program for the Period up to 2020, network operator reports on the functioning of the UES, reports on the socio-economic situation in Russia, data of the Federal State Statistics Service, the International Monetary Fund, the World Bank, the International Energy agency, the works of Russian and foreign scientists economists.

2 Experimental Section

Methodically, the article is based on the application of methods and techniques of economic analysis (comparative analysis and value analysis), the method of specific indicators, the method of elasticity, optimization method (dynamic programming).

In recent years—since 1991—the global electric power industry has at least doubled (according to the data of the International Energy Agency), and the Russian power sector grew by only 10.7% in the rated power of power plants, whereas by other indicators, it showed a negative growth (Table 1).

Table 1. Dynamics of development electric power industry of Russia 1991–2016 years

No.	Indicators	Units of measurement	Years				Growth for the 2009–2016 years	
			1990	2009	2014	2016	Absolute value	in %
1	Capacity of power plants	GW	213.3	211.8	232.5	236.15	24.35	11.5
	Including the NPP	GW	20.2	23.4	27.1	27.9	4.5	19.2
2	Produced electricity	Billion kW per hour	1082	957	1029	1048	91	9.5
	Including NPP	Billion kW per hour	118	163	172	196	33	20.2
3	Consumed electricity	Billion kW per hour	1074	943	1014	1027	84	8.9
4	GDP at current prices	Trillion rubles	0.644	39.02	70.98	85.88	46.86	120
5	The annual rate of inflation	%	1.2	8.8	11.4	5.4	-3.4	-38.6
6	GDP electric capacity	Kopeks/RUB. GDP	6.7	7.3	6.4	6.0	-1.3	-17.8

Over the last 26 years, the rated power of electric power industry of the Russian Federation has been developing at a slow pace. The increase amounted to only 10.7%, with the exception of nuclear energy, whose power grew by 38.1%. Electricity generation in the industry as a whole has not reached the level of 1990 [4]. The installed capacity utilization rate (load factor) also dropped from 60.5% in 1990 to 50.3% in 2015, or by almost 17%. On the other hand, nuclear power industry showed positive tendencies: power generation increased by 65.3% and the load factor by 25.5% [5].

Positive growth of the nuclear power sector of the Russian Federation is largely caused by the fact that the state owns NPP and government capital investments go to the construction of new nuclear power plants. During the privatization period of 1992–1998, most thermal power plants and hydropower plants passed into the ownership of private investors, mostly foreign companies. The main aim of shareholders is to maximize the profits rather than develop the industry. All these years, there is a growth in electricity tariffs, and besides, the final tariff for the consumer is several times higher than the selling price of wholesale power plants. For example, the average selling price of 1 kWh of a PP is 1.07 rubles, and the single rate for the population of Moscow to 01.01.2016 is 5.03 rubles. The final rates are raised by private organizations who intermediate in the transmission and distribution of electricity.

The basis of the effectiveness of the planned economy are low electricity tariffs for end consumers for 1 kWh - 2 kopeks for the population, and 4 kopeks for organizations. Now at market economy, prices for all consumers are the same, but the specific electric capacity Russian products (1 rbl. of GDP) in the last 5 years (except 2015) reached 10–12%, which is higher than similar indicators in Europe and the US (6–8%) at the higher (1.5–2 times) electric capacity GDP measured in watts per hour [6–8].

Since 1991, electricity generation in the Russian Federation kWh decreased from 1082 billion kWh in 1990 to 1027 billion kWh in 2015 (5%); PP basic overall wear of equipment increased from 51% to 60% as input of new generating capacity was reduced by 3 times compared with the planned period of operation, the country's economy (annual input of new capacity for the period amounted to 2.42 GW years from 1991–2015, instead of the 7.0 GW in planning period); 1.5 times increased power losses and the specific number of PP staff; 2.5 times decreased the effectiveness of capital investments. There has been a significant increase in electricity tariffs, which is ahead of inflation in the economy of country.

It should be noted that following the adoption of the Energy Strategy of Russia a positive changes have taken place in 2008 year in the rate of reproduction of the basic production assets of power plants (reactors, units, turbines, power plants, they increased by an annual average of 1.4 GW (for the period 1991–2008) to 4.9 GW (for the period 2009–2015), i.e. 3.5 times. Nevertheless, the annual volume of construction and installation of the main equipment and commissioning remains less than 30% of similar investments in the main capital of the planning period of the economy [9–11] (Table 2).

Table 2. Dynamics of reproduction of generating capacity for Russian power plants for the years of 2009-2016 (GW)

Direction of reproduction	2009	2010	2011	2012	2013	2014	2015	2016	Total for 2009–2016 years
New construction of PP	1.27	2.89	4.69	6.13	3.74	7.3	4.71	4.26	30.73
Modernization of PP (modernization, reconstruction, expansion, re-marking)	0.25	1.14	0.19	0.61	0.34	0.44	0.50	0.34	3.47
Decommissioning of PP	0.29	1.01	1.51	1.91	0.68	1.76	2.35	3.75	9.51
Increase in generation capacity	1.23	3.02	3.37	4.83	3.40	5.98	2.86	0.85	24.59
Installed capacity of PP									
- For the beginning of the year	210.62	211.85	214.87	218.24	223.07	226.47	232.45	235.31	25.54
- At the end of the year	211.85	214.87	218.24	223.07	226.47	232.45	235.31	236.16	24.59

3 Result Section

The rate of expanded reproduction BPA of power plants can be estimated by generating capacity growth factor (W_{gr}), which is calculated, by the formula:

$$W_{gr} = (W_{re} - W_{dis})/W_b \quad (1)$$

where W_{re} , W_{dis} - received and disposed of PP capacity;

W_b - mounted of PP capacity at the beginning of the accounting period.

For 1991–2008 years, total installed capacity of PP fell to 213.3 GW in 1990 up to 210.6 GW in 2008. The outflow capacity went faster than their input. Consequently, the value growth rate was negative: -2.7 :

$$213.3 = -0.013 \text{ or } -1.3\%;$$

$(-1.3\%): 18 \text{ years} = -0.072\%$ per year, i.e. there was a process for disposal of BPA 0.072% per year.

Since the adoption of the Energy Development Strategy (for the last 7 years 2009–2015), the situation has changed positively, growth rate was:

$$W_{gr} = (38.8 - 13.26)/210.62 = 0.1213 \text{ or } 12.3\%$$

Or $12.13\%:8 \text{ years} = 1.52\%$ per year, that is, of PP capacity installed annually increased by 1.52%

Measures taken by the Russian Government in the field of expanded reproduction BPA of PP allowed stopping the process of narrowed reproduction BPA and going to expanded reproduction. The annual increase of generating capacity amounts to 1.52% , but this is not enough to enter the required level of simple reproduction BPA of power plants -2.5% per year.

Most types of the main PP equipment serve no more than 40 years (turbine power units, units, etc.), so the normative value of the coefficient is 2.5% per year considering that the of PP generating capacities have deterioration 60% or more, with the exception of nuclear of PP, where 35% of aged deterioration, it is recommended, due to the significant deterioration of PP BPA, adjust annual growth rate upwards to 3.5% .

According to energy reserves Russia is among the top ten countries in the world, and for the consumption of electricity per person (6431KVt/h) in 2011, occupies the 28th place, with our northern neighbors consume more: Norway 3.9 more, Sweden 2.3 times. Russia produces electricity 5 times less than China's, 4 times less than the United States. There is a correlation. [12, 13] The most objective indicator of power industry development (data from the International Energy Agency) and the modernization of the country's electricity is the produced and consumed volume of electricity (Table 3).

Table 3. Dynamics of production and consumption of electricity in Russia for the period of 1990–2015 years, bln. KWh

	1990	2010	2012	2014	2015	2016	% Growth in 1990/2015	% Growth in 2010/2016
Electricity generation	1082	1019	1032	1025	1027	1048	94.9	104.4
Electricity consumption	1074	1000	1016	1014	1008	1027	93.9	103.8
Balance	8	19	16	11	19	21	At 2.4 fold	140
The percentage of under-consumption of energy pos. 3/pos. 1 * 100%	0.7	1.9	1.6	1.1	1.9	2	At 2.7 fold	133.3

From these data, it is evident that the maximum volume of electricity production and consumption were in 2016, and the minimum volumes were in 2010. A more significant drop in electricity consumption volumes occurred in 1998 year - 779.9 billion kWh (year greatest downturn and contraction of GDP due to falling world energy prices and the collapse of the Russian GKO). Maximum power consumption in 2016, 1027 billion. KWh amounts to 95.61% from 1990 levels, the last year of the planned economy. State electricity largely affect the level of GDP, the size of the development of productive forces, labor productivity and comfort of homes and other macroeconomic indicators of the country's economy. Electricity is also the public service (free highlights streets, cities, roads, free supply of electricity for the needs of the Army and Navy) and product (realized at the cost to businesses and the public), so power development is essential for State to grant to public goods and services, and for private sector.

The main premise of the increase in GDP growth is outpacing the value of generating capacity, length and size of electric distribution grid facilities in the electricity.

The growth in electricity consumption, depending on the growth of 1% called as the coefficient of elasticity of energy consumption on the GDP. Its value in the calculations shall be equal to 0.3 [6]. Let us analyze the correlation of GDP and electricity consumption in Russia in recent years.

If according to the forecast of the World Bank (WB), Russia's GDP will grow by 1.7% in 2017, then in 2016 it is recommended to create an energy reserve by increasing electricity generation capacity and electricity production $1.7 \times 0.3 = 0.51\%$.

In 2016, 1048.0 billion kWh being produced, and consumed 1008 billion KWh (98.1% of the generated electricity) in Russia, and then in 2017 it should be to develop at least 1053.2 billion kWh. In 2017, the Russian economy may remain in recession, GDP will decrease by approximately 1% (World Bank estimate) [13]. GDP electric capacity is an important characteristic of the state of the economy. Russia's Energy Strategy is foreseen specific electric capacity reduction in industrial production by increasing the share of low power sectors in the economy. Let us analyze the progress of the strategy situation (Table 4).

Table 4. Dynamics of GDP electric capacity in Russia

Years	GDP in trillion Rub. in prices	Electricity consumption in billion KWh	Specific electric capacity kWh/RUB GDP
2008	41.54	990	0.024
2009	38.3	943	0.025
2010	40.0	989	0.025
2011	41.7	1000	0.024
2012	43.1	1016	0.024
2013	43.7	1009	0.023
2014	43.9	1014	0.023
2015	42.7	1008	0.024
2016	42.6	1027	0.024
2017	43.3	1032.2	0.024
Forecast	Growth +1.7%	Growth +1.05%	

The data above shows that the specific electric capacity of GDP has remained largely unchanged throughout the analyzed period (average 0.024), indicating the same power consumption structure. The structure-manufactured products, works and services for the past 9 years in Russia remains the same and structural changes in the economy does not occur. Specific electric capacity products in terms of money is growing all the time due to progressive rates of tariff growth over inflation growth, but it is a subject of another research. Compare the rates of growth of GDP and the growth rate of production and consumption of electricity, and the calculated value of the coefficient of elasticity of energy consumption on the GDP (Table 5).

The period from 2009 to 2016, GDP growth in Russia was equal to 11.2%, and of electricity consumption, growth (ΔGEC) was 8.9%, hence the annual average of electricity consumption elasticity coefficient on GDP growth (Cel):

$$Cel = \Delta GEC / \Delta GPD = 8.9 / 11.2 = 0.79 \quad (2)$$

Which is 2 times more than the recommended value of this coefficient (0.3).

Table 5. Dynamics of the elasticity coefficient in electricity consumption in GDP

Years	Of GDP in 2008 prices trillion rub.	Growth in% of GDP the previous year.	Electricity consumption billion kW/h	Growth in% compared to last year	The elasticity coefficient in electricity consumption in GDP
2008	41.54	105.25	990	102.0	0.38
2009	38.3	92.2	943	95.3	-0.60
2010	40.0	104.5	989	104.9	1.09
2011	41.7	104.3	1000	101.1	0.26
2012	43.1	103.4	1016	101.6	0.47
2013	43.7	101.3	1009	99.3	-0.54
2014	43.9	100.6	1014	100.5	0.83
2015	42.7	97.2	1008	99.4	-0.16
2016	42.6	99.8	1013	100.5	-0.83
2017 forecast	43.3	101.7	1023	101.0	0.59

4 Discussion Section

The discrepancy of recommended values and the actual of electricity consumption elasticity coefficient in GDP caused due to:

1. factor of higher consumption per unit of national income produced in Russia It is 2 times higher than in Europe because of the long winter;
2. long-term extensive development of electric power industry of the Russian Federation and the late transition (since 2010) on the an intensive path on the basis of innovation;
3. development in the Russian Federation over the past 20 years on energy resources and energy intensive industries sectors: ferrous and nonferrous metallurgy; the petrochemical industry; development of new hydrocarbon deposits in the Far North and Far East coal and construction of new power plants and power transmission lines, pipelines and pumping stations;
4. presence in the Russian economy of a large sector of the “shadow” economy, the volume of which are not included in official statistics, and the power consumption can not be hidden and therefore, reflected in the reporting of power supply companies;
5. increase in electricity losses during its transmission to end-users by 1.5 times due to the limit depreciation of basic assets and industry of outbound electricity transmissions in Russia compared to European or American States;
6. uneven annual commissioning of new generating capacities in operation and outputting of the number of operating. Input-variation coefficient - 5.75 and the output of order 8.1;

In 2008–2011, the government adopted several important documents for the removal of the country’s electricity from its pre-crisis state and its development:

1. In 2009, approved the «Energy Strategy of Russia up to 2030»;
2. In 2010, was developed the «Russian electric power modernization program until 2020»;
3. In 2011, was developed «scheme and development program of the Unified Energy System of Russia for 2011–2017 (Order of the Ministry of the Russian Federation from 29.08.2011) ».

The first two documents complement each other, and the order of the Ministry of Energy of the Russian Federation from 29.08.2011 №380 clarified the development program for UES of Russia for the period until 2017.

Russian electric power modernization program until 2020 divided into two sub-program execution deadlines:

- sub-program for 2011–2015 (I stage);
- sub-program for the period 2016–2020 (II stage).

It is now possible to summarize implementation of the Stage I of “Electricity Modernization Program of Russia for the period till 2020”, in which the control tasks for the construction, modernization and commissioning of power generating capacities operation were given. In general, benchmarks of Stage I «Program of modernization of electric power industry of the Russian Federation for the period till 2020» not fulfilled.

The level of performance tasks on commissioning of new capacity will be approximately 61%, and construction of solar, wind power (renewable energy) was conducted on the residual principle of financing and was introduced only 18% of the project tasks [11–13]. Construction of stations on renewable energy well developed in Europe, the US, Japan, and only the first steps made in Russia (Table 6).

Table 6. Implementation of Stage I for the period of 2011–2015 «Russian electric power modernization program until 2020»

№	Indicators	Task of the program, GW	In fact fulfilled, GW	% performing
1	Construction and commissioning of new generating capacity of PP – all including RES	43.8 0.761	26.57 0.14	60.7 18.4
2	Modernization of PP existing generating capacity(modernization, reconstruction, re-marking of existing facilities)	Task undefined	2.08	X
3	Decommissioning of PP generating capacity	5.17	8.21	158.8
4	The growth of PP capacity	38.63	20.44	52.9

The main reason is the low efficiency of power plants on the renewable energy (17%) due to the lack of solar and windy days in Russia, as well as the high cost of investment projects. For example, the construction of Orsk SES will cost investors at 3

billion rubles, its capacity will be 40 MW, thus the unit cost of 1 MW will be 75 million rubles or 1.15 million US dollars (exchange rate taken \$ = 65 rub.).

For comparison, the construction and commissioning of the combined cycle gas turbine power plant of the same capacity, according to the IEA estimates, is 900 thousands \$, and its efficiency will be 38% [12]. Therefore, to build in Russia PP running on renewable energy sources (RES) today is unprofitable and inefficient. Exceptions are remote from utilities settlements, enterprises, which cannot be connect to the central power grid. Task for the modernization of the electric power Russia for the years 2011–2015 is not fulfilled for the following reasons:

1. reductions due to funding crisis of the state (for example from 2014 the halted construction of the Baltic nuclear power plant) and private investors
2. lack of foreign long-term loans due to Western sanctions;
3. rise in price 2–3 times of the investment projects due to the increase of 2.5 times the cost of imported equipment;
4. lack of new innovative technologies to reduce electricity losses during transmission over long distances;
5. lack of capacity in building and the construction industry enterprises in undeveloped regions of Eastern Siberia and the Far East;
6. unplanned decommissioning of the new generated capacities of a number of power plants (the actual output exceeds forecast by 1.6 times).

At the same time, during the analyzed period, the annual rate of commissioning of new generating capacity has increased almost 4 times with 1.47 GW (for the period 1991–2010gg) to 5.73 GW (for the period 2011–2015), or 3.7 times. If in 20 years in the Russian Federation due to the development of capital investments is put into operation the generating capacity of 29.35 GW, it is only in the last five years, almost the same amount of 28.65 GW [16, 17].

5 Conclusions

These numbers of development of the Russian power for the period 2011–2015 years inspire some optimism that if the pace of construction and modernization of the PP in the last 5 years will be maintained, the industry modernization program for the period up to 2020 will be executed. The main reason for the increase in electricity tariffs for end users was the privatization of infrastructure enterprises of Russia that engaged in electricity transmission, sales and distribution of electricity. The pricing policy of the industry infrastructure, enabling them to impunity, as a monopolist, to increase the selling price of electricity up to several times. For example, the average sales prices of the Russian Federation power plants located in the European part of the country in 2014 were at the level of 1.11 rubles/Kwh, and for end-users in Moscow, they amounted to 4.5 rubles per 1 kWh, that is, become more expensive than 4 times.

Basic tariffs for industry amount to approximately 70% of the installed tariffs for the population. Empirically it found that with an increase in specific energy capacity of GDP by more than 10% [18], the economy is prerequisites for the crisis. Consequently,

high electricity tariffs in Russia were one of the factors for occurrence of the economic crisis, so for out of the recession it is necessary to reduce tariffs is about 3 times.

For the implementation of this process, should be established the following preconditions:

1. It is recommended following the example of France, Germany, and the United States to nationalize companies, distributing and transmitting electricity. Electricity on the one hand is a product, and, on the other hand, a public service and therefore it is necessary government administration for tariff policy.
2. Set the maximum permissible rates (extra charge) at the industry service infrastructure, depending on the complexity and importance of the work that they perform, the services, but the overall extra charge must be no more than 50% of the selling price of electric power.
3. Set state control over electricity tariffs for final consumers in the entire technological chain, starting with gas, coal, electricity generation, before it is receiving by the end users.
4. To oblige every private energy company to send the necessary investments (capital investments) for expanded reproduction of the basic production assets of electric power on the innovative basis.





If the proposed recommendations will be adopted and implemented, it will create additional prerequisites for the development of electric power industry for the period until 2030 year.

References

1. Russian Federation Government Decree 2009 on Russia's energy strategy for the period until 2030
2. Doroshenko, Y.A., Salmina, O.I.: Bulletin of BSTU named after Shukhov, V.G., vol. 3 (2013)
3. Koneva, O.I., Doroshenko, Y.A.: Bulletin of BSTU named after Shukhov, V.G., vol. 1 (2013)
4. Order of the Ministry of Energy of the Russian Federation 2011 Driving program and development of the Unified Energy System of Russia for 2011–2017
5. Chizhova, E.N.: Bulletin of BSTU named after Shukhov, V.G., vol. 2, pp. 99–106 (2007)
6. Bukhonova, S.M., Klimashevsky, K.A.: Bulletin of BSTU named after Shukhov, V.G., vol. 3, pp. 100–104 (2013)
7. Kamenetsky, M.I.: Probl. Forecast. **3**, 249–258 (2013)
8. Negnevitsky, M., Tomin, N., Panasetsky, D., Voropai, N., Kurbatsky, V., Hager, U., Rehtanz, C.: Proceedings - 2014 Power Systems Computation Conference 7038340 (2014)
9. Grabovyi, P.G., Avilova, I.P.: Life Sci. J. **12**, 610–615 (2014)
10. Fedotova, G.A., Voropai, N.I.: Chinese Society for Electrical Engineering (CSEE), pp. 1121–1126 (2008)
11. Kamenetskii, M.I.: Stud. Russ. Econ. Dev. **1**, 55–63 (2011)
12. Lukinov, V.A., Mottaeva, A.B.: Sci. Sci. **2**, 54–69 (2014)
13. Lukinov, V.A., Manuhina, L.A.: Sci. Bull. VGASU **4**, 196–202 (2011)

14. Panasetsky, D.A., Etingov, P.V., Voropai, N.I.: Chinese Society for Electrical Engineering (CSEE), pp. 2157–2161 (2008)
15. The data of the European Environment Agency: Access: www.eea.europa.eu/ru. Accessed 17 Aug 2017
16. The data of the International Energy Agency (IEA): Access: www.iea.org/statics. Accessed 17 Aug 2017
17. World Bank data (World Bank): Access: www.worldbank.org. Accessed 17 Aug 2017

Green (Ecological) Marketing in Terms of Sustainable Development and Building a Healthy Environment

Boban Melovic¹ , Slavica Mitrovic² , Biljana Rondovic¹ ,
and Irina Alpackaya³ 

¹ Faculty of Economics, University of Montenegro,
Jovana Tomaševića, 37, Podgorica 81000, Montenegro
bobanm@ac.me

² Faculty of Technical Sciences,
Trg Dositeja Obradovića, 6, Novi Sad 21000, Serbia

³ Moscow State University of Civil Engineering,
Yaroslavskoye Shosse, 26, Moscow 129337, Russia

Abstract. The environmental (ecological) marketing is increasingly present issue at the global level while environmental changes have created a new segment of environmentally responsible consumers, known as green consumers. Previously said, led to the emergence of new forms of marketing, also known as green marketing, which means that the production processes, products, services, and all marketing activities are created and implemented in accordance with the impact that can have on building a healthy environment and society as a whole. In this paper, besides theoretical basis of understanding key terms related to the segment of green marketing and green consumer, we will present the results of primary data from our own research, which aims to determine the awareness and attitudes about green marketing, green consumers and products. The conclusion to which the authors come states that although there is a relatively large consumer awareness about the concept of green marketing, it is still a very small percentage of those who regularly buy these products, which is largely a consequence of higher prices that green products have over conventional (traditional) ones.

Keywords: Green marketing · Green consumer · Sustainable development
Healthy environment · Corporate social responsibility

1 Introduction

In modern business conditions, marketing as a concept should be seen not only in the term to sales, but broader in the new context, which refers to customer satisfaction in the long term. Modern manufacturers continually develop new technologies regarding production while, on the other hand, consumers are constantly searching for obtaining reliable and accurate information about the products they buy (Hunt 2011). Hence the discussions at the academic level, as well as activities of many companies that give more importance to marketing with the prefix ecological, or green. The reaction to the

strengthening of the movement on sustainable development, environment protection and building a healthy environment, resulted in the emergence of new marketing activities, and the creation of green marketing (Belz and Peattie 2012). A recent study conducted in the US showed that over 80% of respondents will participate in simple environmental actions, such as recycling and reducing energy consumption, while 73% of them will buy an environmentally friendly product (Ghanadan 2014). Similar to the above information, Levinson (Levinson 2007) points out that an increasing number of consumers prefer buying green products, and that even 83% of loyal consumers are willing to change the product, if it is established that a company from which they purchase goods is not socially responsible. Proceeding from the above, it is clear that modern manufacturers are increasingly creating their strategies starting and based on socially responsible business when they make profit (Anderson and Gaile-Sarkane 2010). In the context of the problem that is being treated, corporate social responsibility (CSR) is seen as a business concept in which economic entities integrate the care for society and environment within their business (Kotler and Lee 2009). Therefore, foreign and domestic companies, are realizing that the role related to the dilemma of retaining customers over the long term in the future increasingly lies in activities related to ecology (Melovic et al. 2014), and thus to green (environmentally friendly) marketing. Modern marketing-oriented companies must define the concept of ecological marketing starting from the mission, through the general objectives, to individual tasks. The implementation of policies, strategies and tactics of ecological (environmental) marketing is a very important segment of modern companies. Therefore, the world requires the concept of sustainable development, just like the concept of sustainable development requires green marketing.

The fact is that in the modern theory and practice, we can encounter much often thesis on the necessity of implementing the environmental principles in the marketing strategy, in order to meet new consumer segment, the so-called, green consumers. Green marketing implies cooperation with a large number of stakeholders, and even with competitors, in order to make profit, but with ecologically sustainable development and the creation of a healthy environment (Adams 2006). On the other hand, it is evident that, regardless the level of market development that we talk about, on each of them there is an environmentally responsible consumer segment (Saxena and Khandelwal 2010). The market segment of green consumers offers new opportunities to manufacturers, but new requirements as well, which are reflected in society as a whole. In fact, meeting the needs of green consumers imposes manufacturers' need to develop specific strategies of segmentation, differentiation and positioning, in order to meet the requirements of this category of consumers. In accordance with the previously mentioned, the authors start from the *hypothesis that the concept of production of green products, followed by green marketing activities, are in a direct positive correlation with sustainable development and the construction of a healthy environment*. The goal of this paper is to highlight the importance of green marketing, to identify attitudes of consumers in relation to this concept, as well as to analyse the influence that green consumers (products) have on sustainable development and the creation of a healthy environment.

The use of green marketing involves the fulfilment of certain conditions, primarily, economic, legal and political (Bhaskar 2013). Marking a critical mass, or a base of

green consumers, represents the basis for the creation of the strategy and intensive development of the concept of green marketing in any society. The incentive about the development of organic farming and the production of green products, represent a strong factor in strengthening competitiveness in today's global market. In modern business conditions, environmentally responsible producers have the opportunity to realize (actualize) a key competitive advantage in the market, because the environmental awareness is gradually integrated into all aspects of social and business activity.

2 Closer Definition of the Concept of Green Marketing

Historically green marketing appeared during the seventies of the twentieth century, when the first theoretical discussion of this phenomenon began (Omkareshwar 2013). Seen in the narrow sense, green marketing belongs to socially responsible marketing, while in a broader sense, this type of marketing fits into the concept of corporate social responsibility. Analysing literature, we can find different terms that are used as synonyms of green marketing, such as “*Ecological-Marketing*”, “*Eco-Marketing*”, “*Sustainable Marketing*”, “*Environmentally Responsible Marketing*”, etc. Practice has shown that the term of green marketing is in use in Europe since the eighties of the twentieth century (European Commission 2013). Etymologically speaking, green marketing has evolved from a movement for protection of the human environment called *environmentalism* (environmentalism is an organized movement of citizens and government institutions/agencies to protect and improve the environment of people). Despite some similarities and some common elements, green marketing is different from similar terms related to ecology, sustainable development, through the development of the concept, which as a goal has the environmental protection, labour and life environment.

Author Polonsky (Polonsky 1994) states that the first definition of green marketing was established in 1975, by the *American Marketing Association* (AMA 2015), according to which the green marketing represents “*a study of the positive and negative aspects of marketing activities to pollution, depletion of energy and exhaustion of non-energy resources.*” Almost in the same period Henon and Kinnear (Hanon and Kinnear 1976), on the basis of their research, offered the definition of ecological marketing: “*Ecological marketing involves all marketing activities: (1) those that appear as causes of environmental problems, and (2) those that assist in solving environmental problems. In this way, environmental marketing studies both positive and negative aspects of marketing activities in connection with pollution, exhaustion of energy sources and depletion of non-renewable resources.*” Also, authors Dujak and Ham (Dujak and Ham 2008) come out with one of the first definition of green marketing that comes from Stanton and Futrell's (Stanton and Futrell 1987) and according to them, green marketing is defined as “*a set of activities designed to create and facilitate any exchanges intended for the satisfaction of human needs and desires, in the way to fulfilment of those needs and desires causes minimal negative impact on the natural environment.*” Sometime later, authors Mintu and Lozada (Mintu and Lozada 1993) defined the green marketing as: “*the application of marketing tools in order to facilitate the exchange that should meet the goals of the organization and individuals in*

order to maintain the protection of the environment.” There are also authors such as Coddington’s (Coddington 1993) that defined the environmental (ecological) marketing under a different name “marketing of the life” environment as: “Marketing activity that recognizes environmental concerns as a responsibility in the development and growth of business activities.” Author Donald Fuller (Fuller 1999) gave another definition stating the term “sustainable marketing”, which means: “the process of planning, implementing and controlling development, pricing policies, promotion and distribution of products in a way that meets the following three criteria: (1) needs of the customers are fulfilled; (2) organization goals are achieved and (3) the process is compatible with the ecosystem.” Starting from the above explanation, we can conclude that green marketing is a form of socially responsible marketing in which production processes, products, services, and all marketing activities are created and implemented in accordance with the impact that they have on creating a healthy environment and society as a whole.

Today it is widely accepted that the green marketing notion is based on a 3R formula (*reduce - reuse - recycle*), which represents three steps to preserve the environment (Prakash 2002):

- Reduce - the reduced use of natural resources (replacement of natural resources with artificially produced and/or non-renewable with renewable resources) and reducing of the consumption of energy sources into the process of production and other business processes;
- Reuse – reuse packages or its parts in production;
- Recycle - producers collect unused products and/or its packaging for the recycling process; recycling of waste generated in the production process.

In accordance with the foregoing, the green marketing requires a proactive corporate strategies will benefit to both consumers and companies. Such strategies must be directed towards redefining the needs and desires of consumers according to ecologically healthy products and services, then provide them (consumer) socio-ecological products.

Ecological marketing is consisted of five major strategies known as 5C (Fuller 1999):

1. *Clarity* is an important strategy of ecological marketing. Information on the ecological issues that companies give, should clear and credible;
2. *Cooperation* with third parties, such as government agencies and ecological organizations;
3. *Communication* with the public. Many companies realize that they are being pressured to make environmentally friendly products, and in order to avoid time wasting in the development of entirely new alternative products, they create new advertising message. In these messages, the requirements for eco-friendly products are highlighted on the packaging, in order to create the desired image;
4. *Commence* action without hesitation. Companies should motivate their customers to buy their products, in the way that they will convince them in the benefits of the products. Customers should be aware of the contribution that derives by using of this product, in relation to solving ecological problems.

5. *Continuously regard* your company as ecological. The company thus should be overviewed not only by customers, but also by the whole environment and those who live and work around the company.

Application of the green marketing requires a proactive approach to consumers, key stakeholders, to the legislation and numerous institutions. Activities that companies implement using green marketing are diverse. However, each of these activities must be in accordance with possible impact on the environment (European Commission 2008). Some of them are:

- *Introduce ecological packaging,*
- *Reduction of pollution caused by transportation,*
- *Rational use of all forms of energy,*
- *Reduce waste through reduction, recycling,*
- *Usage of natural resources,*
- *Protection of animals, water, earth and air.*

The green marketing during its existence must satisfy and improve the following two objectives: (1) improve the ecological quality of the product, and (2) improve the customer satisfaction in the long term.

3 Ecological Marketing Mix

The main feature of ecological marketing mix is that decisions in all areas must be made from the standpoint of the environmental protection. Just like the traditional marketing mix, ecological marketing contains four elements: *product, price, distribution/place and promotion*. One product can be defined as an *ecological product* if its harmful impacts on environment during the production, usage and distribution are minimized. Research (Prakash 2002) has shown that organic products have a higher *price*, with other words, they are more expensive than their traditional versions, since they usually require additional investments to modify production processes and replace resources with ecological alternatives. Ecological adaptation of business means greater initial investment, in order to prevent additional costs in the future, and/or to ensure the long-term market share in and profit. For this reason, it is necessary to make a good estimation while determining prices - *are consumers willing to pay more for environmentally friendly products, and how much would they pay more for it?* Distribution should ensure the availability of products/services to target market in the best possible way. Decisions regarding the distribution are related to the choice of distribution channels, selection of participants in certain channels, the choice of types and locations of retail outlets, transportation methods and inventory levels that should be kept. Ecological marketing requires that these decisions should be made from the standpoint of environmental protection. Attitude towards the environment of all participants in the distribution chain. Ecological distribution should perceive the attitude of all participants in the distribution chain. The main task of ecological promotion is to inform the market about its engagement in the field of environment protection and thus help in creating a corporate ecological image of the company. The second task of the

promotion is to introduce customers with the ecological attributes of new and/or ecologically adaptable products/services. Ecological promotion is not always focused on making profit. Ecological promotion can also be in the function of developing environmental awareness of consumers and the adoption of ecologically suitable behaviour in consumption. The most common elements of environmental promotions are advertisements/advertising and public relations. One of the aspects of communication with customers is the specific labelling of products. In the end, it is important to create a specific ecological promotional messages for customers.

Having in consideration the previous mentioned, some authors point out that instruments of green marketing mix are (Tolušić et al. 2013):

- *Green products/services* - production of environmentally friendly products/services (e.g., McDonald's was the first one to start using napkins, boxes, cups and bags of biodegradable and recyclable materials);
- *Green price* - although consumers are willing to pay more for ecological (environmentally friendly) products, ecological elements of the product should not be the basis for determining the higher price of the product;
- *Green packaging* - recycled, returnable, minimal;
- *Green communication* - deception of consumers is not permitted in terms of propagating non-existent "green" features. Identifiable and protected designations of organic products must be a guarantee of quality and method of production of the product.

In addition to these instruments, ecological marketing includes some new elements/activities (Sheth and Parvatiyar 1995):

- *Re-consumption* – approach towards the promotion of possibilities for reusing the product in total or in parts (more usable cycles);
- *Redirect* - Induce customers to use less harmful products and services;
- *Reorientation* - a comprehensive approach to marketing mix changes starting from products and packaging to positioning and promotion;
- *Pre-labelling* – add new information which identifies environmentally friendly product;
- *Positioning* - approach to positioning products to whom have been added ecological contents, which results with a new position comparing to the competition;
- *Reorganization* – approach of introducing changes in the organizational concept of the process and parts of the organization so that it is directed towards ecological business concept.

Based on all aforesaid, we can conclude that the creation of ecological marketing mix more complex compared to the traditional one, mainly because of many specifics that must be fulfilled in order to meet the expectations of very demanding ecological consumers.

4 Definition and Segmentation of Green Consumers

Different approaches in understanding the green consumer has led to the fact that there are many definitions related to this term. The difference in the definitions of the green consumers depends on various criteria. In the main, green consumers are defined as those that meet their needs and wishes, seeking a product/service that has a minimal negative impact on the human environment. Green consumer, and any other consumer, buys products and services to meet their needs, but the fact is that green consumers are ecologically conscious and educated enough. Thus, for example, the *Business Dictionary* (Business Dictionary 2010) defines green consumers as: “Consumers who are intensely thinking about matters related to the environment, they support environmental objectives and actions, and are willing to move to another manufacturer or supplier due to ecological reasons, even if it means higher costs.” Similar to the definition above, the author Ham (Ham 2009) cites the opinion of Elkington’s (Elkington 1994) which defines green consumers through features that are undesirable for him: “Green consumer is the consumer who avoids products that are likely to threaten his health or the health of others; that can cause significant harm to the environment during production, usage and disposal; that consumes more energy; that creates unnecessary waste; that contains materials derived from endangered species or the environment; that include unnecessary use of animals or cruelty towards animals; that create negative consequences for other countries.” If though the market of classical (passive) consumers is more comprehensive towards the men environment, the market of green consumers represents a much more interesting market potential for modern companies. The purchasing power of green consumers and their future potential is what makes them as desirable consumers in the future. Hereof the growing reorientation of modern companies to this market segment.

When we talk about segmentation of green consumers, today a classification given by the company *Roper Starch Worldwide* is generally accepted. According to the research of the company *Roper Starch Worldwide* (Roper Starch Worldwide 1995), consumers can be divided into five segments according to their interest regarding environmental issues and activities that are undertaken because of it:

1. *True-Blue Greens* – very caring for the environment and actively want to achieve positive change: four times more likely to boycott products or organizations that are not responsible or in care of the protection of the environment; within this group there are three subgroups: passionate guardians of the planet, health fanatics, and animal lovers.
2. *Greenback Greens* – they are not politically active, but are very likely to buy more environmentally friendly product than the average consumers.
3. *Sprouts* – these are consumers that believe in caring for the environment in theory, but not in practice; they rarely buy green products, but it is easy to persuade them to move in any direction.
4. *Grouzers* – this is group in which consumers are sceptical and ignorant when it comes to the environment and cynical about the positive changes they may bring; they believe that green products are overpriced and inferior compering to traditional ones.

5. *Basic Browns* – they are burdened with everyday problems and do not care about social issues and the environment.

Recent approaches to segmentation of green consumers show that consumers during the purchase of green products are primarily driven by concern for their own health and well-being, but not a dominantly by the concern for the environment (Ottman 2011). For this reason, newer models of segmentation based on lifestyle consumer have been developed.

5 Research Methodology

The empirical part of the paper is consisted of a primary research conducted through an online survey in order to determine awareness of green marketing and green products, as well as consumer attitudes about such a category of product and their interest in purchasing (consumption) them. The study sample is consisted of 1,100 respondents, which, having in consideration the geographic coverage of all parts of Montenegro, is considered as appropriate structured sample, which is used for this type of research in Montenegro. Questions are given in the form of “open”, “dichotomous” and “questions with multiple choice answers”, while the questionnaire contained three sections: general part that is related to the structure of the sample, awareness about the concept of green marketing, and consumption (usage) and attitudes about green products. It was attempted to prove the initial hypothesis by using statistical analysis. Data processing was done in SPSS.

6 Research Results

Through testing conducted via surveys, we wanted to ascertain consumer awareness about green marketing, as well as factors that affect the purchase of ecological products, and consumers’ perceptions and attitudes about them, which, moreover, reflects positively on sustainable development and the creation a healthy environment. Namely, starting from a defined research goal, in this section of the paper we tried to find answers to the following questions: *Are consumers familiar with the concept of green marketing? Who are green consumers in Montenegro? How often do they buy green products? Do they react to promotional messages that are related to green products? Are they willing to pay a higher price for green products? Do they believe that companies should undertake “green marketing activities”?* Thanks to under-segmental analysis it was possible to get certain indirect answers relevant to decision-making and future research.

Out of the total respondents (1,100), 52% were females and 48% were males. Such gender structure of respondents can be considered as adequate, due to an approximately same gender representation in the procurement or purchase of products in general. Gender structure is shown in the graph below (Fig. 1):

The study sample included all age segments, in the manner shown in the following graph (Fig. 2).

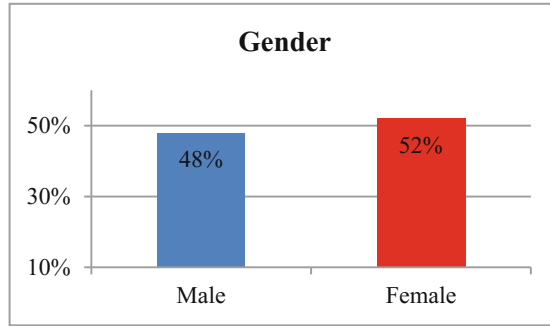


Fig. 1. Gender structure of respondents

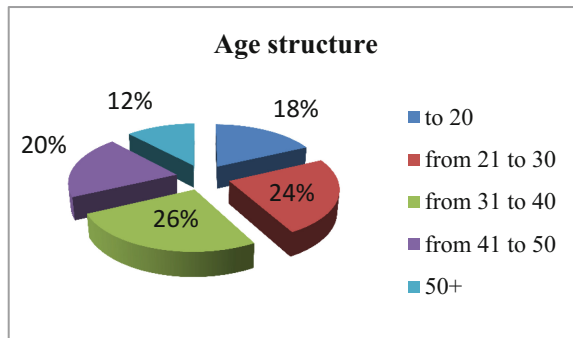


Fig. 2. Age structure of respondents

Most of the respondents included in samples were young and middle-aged persons, that should be familiar the most with new concepts, and thus with the concept of green marketing. Anyhow, even older consumers, who are increasingly cautious and who give great importance to tradition, are interesting for analysis, therefore, they are represented in the sample as well. Status of respondents included all categories of younger consumers, from students, to pensioners, in the manner as provided in the following graph (Fig. 3).

After the introductory part of the questionnaire, which concerned the general information regarding the structure of the respondents, in the second half we wanted to determine the awareness of green marketing and consumer attitudes about buying green products. Figure 4 shows respondents' familiarity with the concept of green marketing.

The survey showed that 68% of respondents are familiar with the concept of green marketing, while almost a third of respondents (32%) are not familiar with it. This data shows that a relatively large number of consumers is aware of the concept of green marketing. On the other hand, unawareness about the concept of green marketing is also presented by a significant number of consumers (nearly one third of respondents) which is of a particular concern because of various possibilities for modern consumers to get informed and the fact that this phenomenon "is on the air" on a global level.

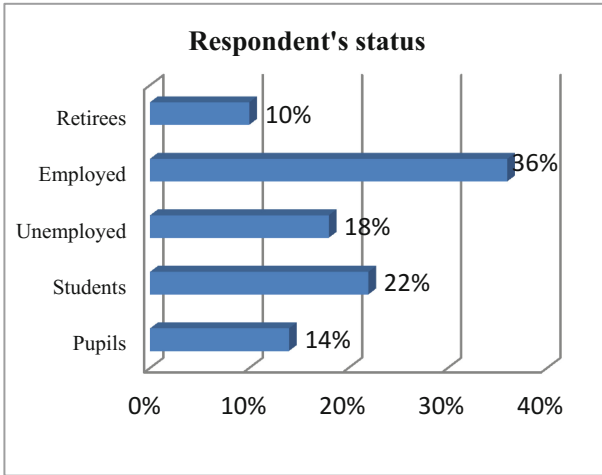


Fig. 3. Respondents' status

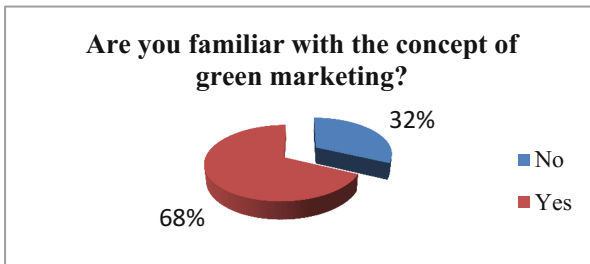


Fig. 4. Respondents' familiarity with the concept of green marketing

With a detailed under-segment analysis of the respondents we wanted to determine the profile of a green consumer in Montenegro, taking into account the key determinants, such as age, level of incomes, education and status (Fig. 5).

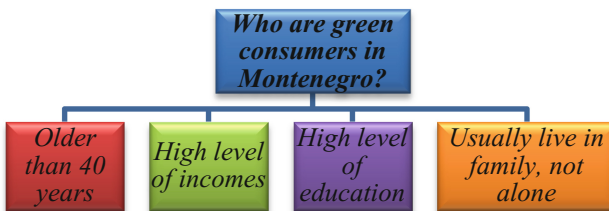


Fig. 5. Author's research

Results of the research describe the general green consumer in Montenegro, as a person older than 40 years with high level of incomes, with a secondary or higher level of education, who usually lives in the family (matrimony), and not alone.

The next segment of the research is related to the frequency, precisely the frequency of purchasing green products, as well as key factors of purchase (non-purchase) of these products. Frequency of buying green products is shown in the following graph (Fig. 6).

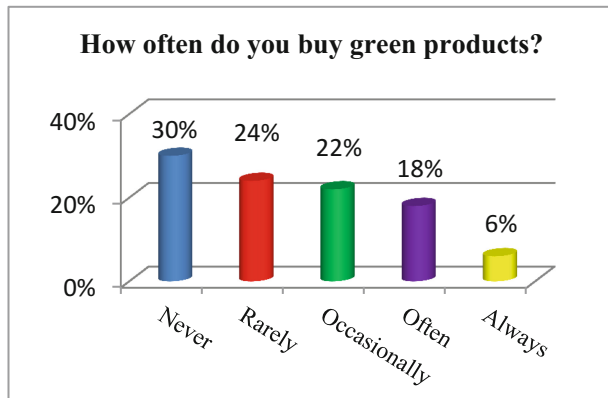


Fig. 6. Frequency of purchasing green products

Only 6% of respondents always buy green products, while 30% of them never buy this type of product. The under-segment analysis showed that the key reason of non-purchasing green products are prices, which in these products are, on average, higher by 30%, and in some cases even more. Green consumer in Montenegro, on average, is willing to pay 25–30% higher price for an environmentally friendly product. The impact of the price on consumers that are committed to green products is shown in the following graph (Fig. 7).

Also, the under-segmental analysis in this part of the study showed that more than half of respondents (52%) believe that the price is a key factor for (non)purchase of green products, while 32% of respondents consider the quality as the main factor. As factors that influence the purchase are the clear declaration of the origin of products, packaging design, as well as the lack of consumers' information.

Promotion plays a significant role on consumers that are committed to green products. Namely, 78% of consumers, to some extent, respond (react) to promotional messages and advertising, while 22% of them do not react. Structure of response of respondents to the promotional message is presented in the following graph (Fig. 8).

When we talk about promotion, it is important to consider the impact of certain media and promotional tools, which are used as ways of advertising of green products, as shown in the following graph (Fig. 9).

The biggest influence on decision making regarding purchase of green products have TV's (32%), Internet (30%) and recommendations - "word of mouth" (20%).

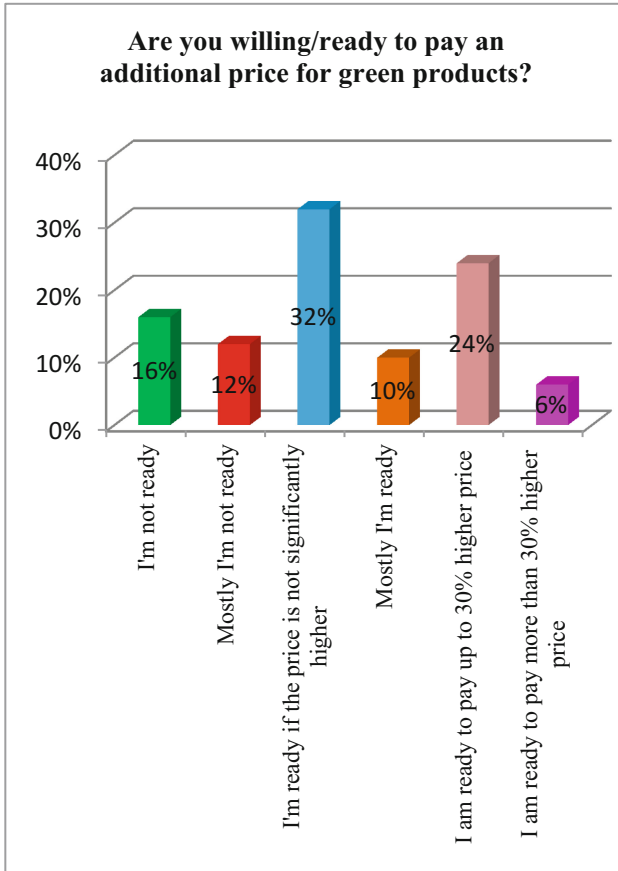


Fig. 7. The impact of prices on consumers that are committed to green products

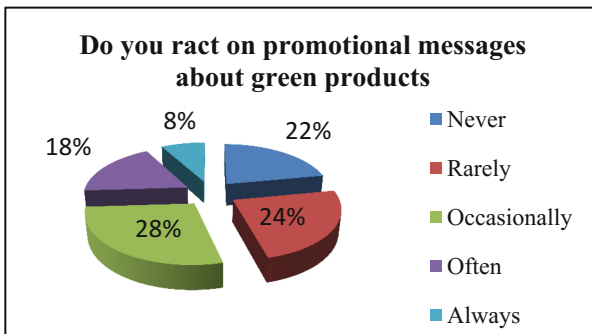


Fig. 8. Responding to promotional messages about green products

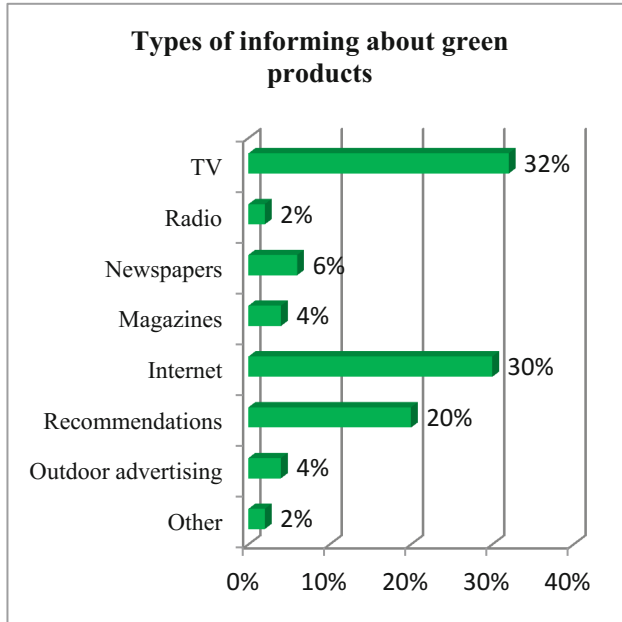


Fig. 9. Types of informing about green products

Also, under-segmental analysis in this part of the study showed that a significant number of consumers respond a lot on promotional messages on which is stated that the product is safe for the environment and their health, and they occasionally or frequently make buying decisions under such decisions.

In the last part of the research we wanted to determine on which category of green consumers, in accordance with the division given by the company *Roper Starch Worldwide*, which is elaborated in the theoretical part, do our respondents belong. The research results are shown in the graph below (Fig. 10).

The survey showed that only 6% of respondents declared themselves as “*truly green*”, meaning that they extremely care for the environment and actively want to achieve changes in this regard. 26% of the sample is consisted of consumers that in theory believe in the environment care, but not in practice (“*sprouts*”) and rarely buy green products, while the largest number of respondents belongs to the “*brown*” category (29%), who are burdened with everyday problems and do not care about social issues and the environment.

At the end, respondents were asked to give an opinion on whether the company in creating future business strategies should be more oriented to the green marketing activities or not (Fig. 11).

A very large number of respondents (87%) believe that companies should undertake green marketing activities in the future. It is interesting to note that even those who identified themselves as someone that does not buy green products, think that companies should develop this type of business concept in the future, which confirms the initial assumptions about the direct correlation of green marketing, sustainable

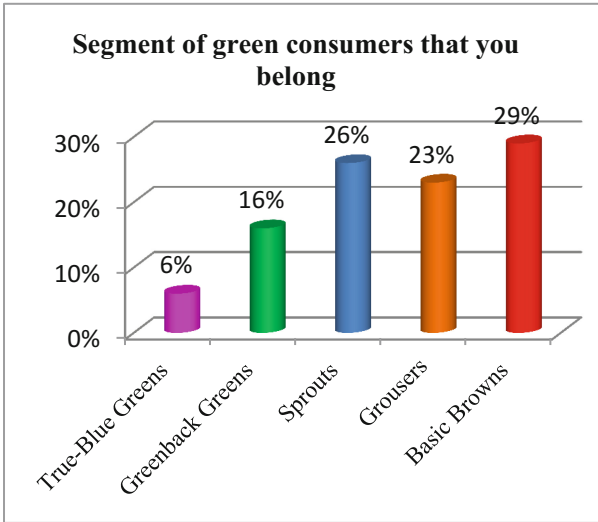


Fig. 10. Segment of green consumers that you belong?

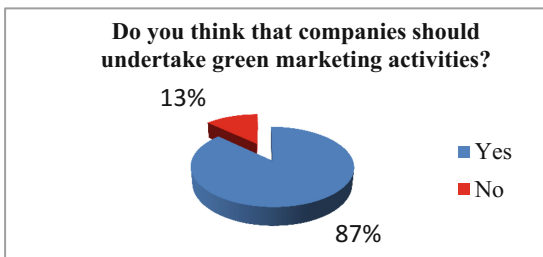


Fig. 11. The future orientation of the company towards green marketing activities

development and competitiveness of modern companies. On the other hand, although their presence is at a low lever, green consumers are designated and marked as a growing and potentially very profitable and attractive segment. In the end, empirical research has shown that there is still present a non-sufficient level of knowledge about green consumers and the level of environmental awareness in general.

7 Conclusion

The epicentre of the overall marketing activity has always been and remains the customer. The interdisciplinary of marketing is particularly evident in contemporary society, where as a separate segment evolves the field of green marketing. The modern market has recognized the growing and potentially profitable segment of green consumers which take into account all available information when purchasing and make decisions not only to satisfy their own needs, but to benefit to the environment and

society as well (Bhaskar 2013). The concept of green marketing can be successfully implemented in the business concept of modern companies, which strengthens their competitive advantage.

Realized primary research aimed to contribute to the creation of a clearer picture of green marketing and green consumer. Despite certain limitations of the research, the results obtained are suitable for general conclusions about the level of the ecological awareness of consumers and can serve as an important basis for decision-making by individual economic entities.

The survey showed that 68% of respondents are familiar with the concept of green marketing, while almost a third of respondents (32%) are not familiar with it. This data implies a relatively large nonawareness of a significant number of consumers about the concept of green marketing, which is particularly worrying due to various possibilities for modern consumers to get informed and the fact that about this phenomenon people are speaking worldwide. Research results describe the average green consumer in Montenegro as a person older than 40 years with high level of income, with a secondary or a higher level of education, who usually lives in the family (matrimony), and not alone. Such a consumer reacts to a lot of promotional messages which state that the product is safe for the environment, and they occasionally or frequently make purchasing decisions under the influence of such messages. Also, such a consumer is willing to pay 25–30% higher price for an environmentally friendly product. The under-segment analysis showed that the key reason of non-purchasing green products are price. Also, the under-segmental analysis in this part of the study showed that more than half of respondents (52%) believe that the price is a key factor for purchase of green products, while 32% of respondents consider the quality as the main factor. On the other hand, although their presence is at a low lever, green consumers are designated and marked as a growing and potentially very profitable and attractive segment. In the end, empirical research has shown that there is still present a non-sufficient level of knowledge about green consumers and the level of environmental awareness in general.

Based on the research it is possible to conclude that green consumers in Montenegro are still making a very small market segment. On the other hand, this category of consumers becomes more and more active and willing to react, in accordance with their environmental convictions. Often promotional activities related to green products indicate to the increasing interest of manufacturers to find a way to loyal customers. On the other hand, the possibility of defining premium prices is also an important factor to decide for the field of production of green products.






Finally, a relatively low standard of living and poor economic situation affects small purchase of green products, and as a limitation appears the lack of awareness regarding the care and the protection of the environment. Therefore, all participants of the economic and social life should act jointly in the promotion and implementation of the concept of green marketing, which appears as an important determinant of sustainable development and creation of a healthy environment in the modern era.

References

- Adams, W.M.: The Future of Sustainability: Re-thinking Environment and Development in the Twenty-first Century, The World Conservation Union, Report of the IUCN Renowned Thinkers Meeting, 29–31 January, Gland, Switzerland, pp. 1–18 (2006). <http://www.iucn.org>. Accessed 17 Oct 2015
- AMA - American Marketing Association. Dictionary. <https://archive.ama.org>. Accessed 11 Sept 2015
- Andersonse, I., Gaile-Sarkane, E.: Socially responsible marketing for sustainable development. *Hum. Resour. - Main Factor Reg. Dev. J. Soc. Sci.* **3**, 197–205 (2010)
- Belz, F.M., Peattie, K.: *Sustainability Marketing – A Global Perspective*, 2nd edn. Wiley, New York (2012)
- Bhaskar, H.L.: Green marketing: a tool for sustainable development. *Int. J. Res. Commer. Manag.* **4**(6), 142–145 (2013)
- Business Dictionary: What is green consumer? (2010). <http://www.businessdictionary.com/definition/green-consumer.html>. Accessed 17 Oct 2015
- Coddington, W.: Environmental marketing: a call for action. *Mark. Educ. Rev.* **2**(5), 2 (1993)
- Dujak, D., Ham, M.: Integrating green marketing principles in the supply chain. In: *Proceedings VIII International Scientific Conference Business Logistics in Modern Management*. Faculty of Economics Osijek, Osijek (2008)
- Elkington, J.: Toward the sustainable corporation: win-win-win business strategies for sustainable development. *Calif. Manag. Rev.* **36**(2), 92 (1994)
- European Commission, Eurobarometer: Attitudes of European citizens towards the environment (2008). http://ec.europa.eu/public_opinion/index_en.htm. Accessed 12 Oct 2015
- European Commission, Eurobarometer: Attitudes of Europeans Towards Building The Single Market For Green Products (2013). http://ec.europa.eu/publicopinion/flash/fl_367en.pdf. Accessed 13 Oct 2015
- Fuller, A.D.: *Sustainable Marketing: Managerial-Ecological Issue*, p. 111. Sage Publications, Thousand Oaks (1999)
- Ghanadan, H.: Greening Up the Lab - Part 3: Five Opportunities to Differentiate with Environmentally Friendly Value Propositions-A Quantitative Survey. <http://www.thelinusgroup.com/greening-up-the-lab-part-3-five-opportunities-to-differentiate-with-environmentally-friendly-value-propositions-a-quantitative-survey/>. Accessed 14 Oct 2015 (2014)
- Ham, M.: Segmentation of consumers based on the level of environmental responsibility. *Mark. - J. Mark. Theory Pract.* **2**, 183–202 (2009)
- Henion, K., Kinnear, C.T.: *A Guide to Ecological Marketing*, p. 1. American Marketing Association, Chicago (1976)
- Hunt, S.H.: Sustainable marketing, equity, and economic growth: a resource-advantage, economic freedom approach. *J. Acad. Mark. Sci.* **39**(1), 7–20 (2011)
- Kotler, P., Lee, N.: *CSR - Corporate Social Responsibility: Contemporary Theory and Best Practices*, p. 5. MEP, Zagreb (2009)
- Levinson, J.C.: *Guerrilla Marketing: Easy and Inexpensive Strategies for Making Big Profits from Your Small Business*, p. 44. Houghton Mifflin Harcourt, Wilmington (2007)
- Melović, B., Radović, M., Babić, R.: Corporate social responsibility and business ethics through the prism of global operating - experience from Montenegro. In: *3rd International Scientific Conference Contemporary Issues in Economics, Business and Management – EBM 2014*, pp. 135–148. Faculty of Economics, Kragujevac (2014)
- Mintu, A.T., Lozada H.R.: Green marketing education: a call for action. *Mark. Educ. Rev.* **3**(3), 2 (1993)

- Omkareshwar, M.: Green marketing initiatives by corporate world: a study. *Adv. Manag.* **6**(3), 20–26 (2013)
- Ottman, J.A.: *The New Rules of Green Marketing: Strategies, Tools, and Inspiration for Sustainable Branding*. Berrett-Koehler Publishers, Inc., San Francisco (2011)
- Polonsky, M.J.: Green marketing regulation in the US and Australia: the Australian checklist. *Greener Manag. Int.* (5), 44–53 (1994)
- Prakash, A.: Green marketing, public policy and managerial strategies. *Bus. Strategy Environ.* **11** (5), 22–31 (2002)
- Roper Starch Worldwide, *Green Gauge* (1995). http://www.greenmarketing.com/Green_Marketing_Book/Chapter02.html. Accessed 20 Oct 2015
- Saxena, P.R., Khandelwal, K.P.: Sustainable development through green marketing. *Ind. Perspect. Int. J. Environ. Econ. Soc. Sustain.* **6**(6), 59–79 (2010)
- Sheth, J.N., Parvatiyar, A.: Ecological imperatives and the role of marketing. In: Polonsky, M.J., Mintu-Wimsatt, A.T. (eds.) *Environmental Marketing: Strategies, Practice, Theory, and Research*, pp. 3–20. Hawarth Press, New York (1995)
- Stanton, W.J., Futrell, C.: *Fundamentals of Marketing*, 8th edn., pp. 127–128. McGraw-Hill, New York (1987)
- Tolušić, M., Dumančić, L., Tolušić, Z.: Application of green marketing in Vukovar-Srijem County. *Pract. Manag.* **4**(2), 43–49 (2013)

Quality as a Determinant of the Customer's Satisfaction on the Mobile Communication Market

Boban Melović¹  , Biljana Rondović¹ , Slavica Mitrović² ,
and Vitaly Shoshinov³ 

¹ Faculty of Economics Podgorica, University of Montenegro,
Jovana Tomaševića, 37, Podgorica 81000, Montenegro
bobanm@ac.me

² Faculty of Technical Sciences,
Trg Dositeja Obradovića, 6, 21000 Novi Sad, Serbia

³ Moscow State University of Civil Engineering,
Yaroslavskoye Shosse, 26, Moscow 129337, Russia

Abstract. The telecommunication market is characterized by continuous growth in the last fifteen years, especially in the field of mobile telephony and internet communications. The aim of this paper is to examine the level of users' satisfaction regarding the quality of services that is offered by mobile operators in the Montenegrin market of mobile communications, as well as to provide guidance to mobile operators in which direction should the improving of the quality of services go. The proposed process, research methodology and research results may be important for mobile operators, who operate not only on the Montenegrin market. Research has shown that users of mobile communications have clearly defined views regarding the quality of the service that is being provided. On the basis of the research, it can be concluded that if mobile operators understand market demands and requests, transform their knowledge into appropriate service as well as deliver the service with the least possible difference between the delivered and what was promised to customers, the positive effects of service quality management will be multiple.

Keywords: Quality · Customer · Satisfaction · Loyalty
Mobile communications

1 Introduction

Modern business conditions, especially in the transition and developing countries, set a range of new demands with their companies (Mitrović et al. 2013), and based upon that, company managers are more aware that they can maintain existing and attract new users only through satisfaction. Customer centricity has long been propagated as the most important approach to understanding what businesses should do to succeed (Drucker 1954; Levitt 1960). The perception of quality could be different because of the various reasons. Firstly, the consumer could be influenced by his/her vision or his/her experience of a low quality product. Therefore, a consumer does not have to

believe in any new fact about the quality or he/she does not plan to devote his/her time to the verification aims. Secondly, the company can achieve quality in the areas, which are not important to be perceived by consumers. Thirdly, the consumers seldom have the necessary information, in the point of the rational and objective valuation of the product quality. If they own these information, they very often do not have time and the motivation to assess them. In the end, they count on one or two impulses, which are related to the quality (Horska *et al.* 2011).

The business world today is in the process of very rapid and numerous changes (globalization of the economy, the swift growth of electronic commerce, the increasing pace of business operations, rapid obsolescence of technological novelties, the rapid expansion of new companies in the world market), which inevitably imposes the need for the development of new models and forms of business (Mitrovic *et al.* 2013), which entails the different treatment and users, in order to ensure the highest possible level of their satisfaction and loyalty.

Telecommunications services dominate the world economy and their quality is a key factor for generating value for their customers and for society (OECD 2007). Mobile communications represent one of the most developed and dynamic segments of telecommunication sector in Montenegro. Dynamic development of this sector was brought by continuous innovations in technology, as well as new trends and structural shifts in regular framework which is characterized by bigger technical standardization and liberalization in the approach towards telecommunication infrastructure. Information technology (IT) has an increasing importance and development in business life. Importance of IT arises because the businesses have tendencies to reach their customers through mobile services lately (Özer *et al.* 2013).

Liberalization at telecommunication markets conditioned numerous changes in mobile providers' operations. There are almost no monopolies at this market. The number of users in certain mobile telecommunication networks is growing relatively quickly. Telecommunication services have always been regarded as services which the user need and for which he is ready to pay additionally in order to use them.

Competitive relation among providers of telecommunication services have brought to reducing prices at these markets and posted new challenges. Competition encourages telecommunications operators to be more efficient and to offer greater quality (Johnson and Kong 2011) so as not to lose market share. High competitive conditions of doing business condition constant effort of telecommunication service providers to find new ways of differentiation with regards to competition, as well as ways to keep existing users. Saturation of telecommunication market leads to slowing down their growth, and thus in such circumstances service providers have to focus on the fight for each user, by creating new values and new ways how to keep them.

Montenegrin market of mobile communication is treated as competitive market which has all characteristics of the saturated market. According to the comparative assessment of *European Bank for Reconstruction and Development*, which was done during 2012, Monte Negro is on the first position with regards to other countries in the region for penetration of mobile subscribers, penetration of mobile broadband approach and total broadband approach (www.mid.gov.me/vijesti/). Mobile broadband is growing rapidly and from 13.7 to 100 people (www.mid.gov.me/vijesti/) is bigger than

double average value from the surrounding countries (Serbia, Bosnia and Herzegovina, Croatia, Macedonia, Albania, Turkey).

Operators have to fight for each user under the circumstances at the market such as Montenegrin. Namely, a big percentage of penetration shows that mobile operators have to direct their strategies towards keeping existing users, since there are actually no new users. New users at the market such as Montenegrin can be regarded those who are more sensitive to pricing and thus buy cards because they are looking for lower prices. A big percentage of penetration at the Montenegrin market of mobile telephony proves that all or majority of users have more mobile phones, i.e. two or more SIM (*Subscriber Identity Module*) cards and that they simply use promotion offers from all three operators in Montenegro. This has a further consequence of reducing traffic towards competitive networks, and operators mark reduced consumption and profit per user.

In an intense competitive environment, the provision of high-quality service is one of the crucial factors for success (Wang et al. 2004; Kelly 2005). The importance of service quality has grown in the telecommunications sector (Weisman 2005). Undoubtedly, the quality of service is one of the essential factors of success at the mobile communication market in Montenegro. Offering high quality services is vital for successful business results, as well as for profitable achieving business goals of mobile providers which are concerned with the users' satisfaction, growth of market participation and getting new users.

2 Quality as a Determinant of Satisfaction of Modern Users

Determining significance and essence of quality in service providing sector is a more complex issue with the essence of quality of physically tangible products. The basic understanding while realizing quality in service providing sector is to start from the user when define and determine quality, i.e. his understanding of quality. In that sense, the most used definition is the one given by *Parasuraman, Berry and Zeithaml*, who define the quality of the service the client perceives as “*measure and direction of deviation between clients' perception and anticipation* (Parasuraman et al. 1988).

Taking into account understanding of the quality in the service context, we can deduce that the quality is everything the user regards it is, and it is the ability of the service to fulfill or overcome user's expectations. Service users will be satisfied when their perception of services coincides with expectations and needs. If the noticed performance of the service is out of their expectations, they will be especially satisfied (delighted). The user assesses the service quality during its offer/usage, and thus the degree of the quality will be assessed through his satisfaction (Melović 2012). Since the degree of the service quality is a result of the user's comparison between the expected and obtained, it is clear that we cannot speak about the quality service if the user's satisfaction hasn't been achieved, and that there is also no satisfaction with the user if the quality has not been obtained.

If we take into account a range of positive effects which emerge from the strategic approach to the issue of quality, we can regard the concept of quality in the service providing sector as one of great importance for each market oriented company. Strategic approach to the issue of quality contributes to the company image, helps it to

gain bigger profit and competitive advantage, as well as loyalty of the users. From the above mentioned reasons, the company must realize these quality dimensions which dominantly influence the user to be satisfied.

Widely accepted model of understanding dimensions of the quality service is *Servqual* (Since it was first published in 1985, its creators *Parasuraman, Zeithamal* and *Berry* have been working on its further improvement and the promoted the instrument through a series of publications) model, which represents one of the most frequently used methods for determining users' satisfaction with the service quality. It is design to measure the service quality in various organizational models of the service providing sector. There is almost no service providing activity in which this instrument is not applied.

Variables (dimensions) of perceived service quality according to the *SERVQUAL* scales are (Nefat and Paus 2008):

- **Tangible elements** – presence of tangible, physical elements such as environment where the service is being offered, equipment which is used, personnel's appearance, promotive material etc.;
- **Reliability** – anticipates ability to deliver the promised service in appropriate way;
- **Responsibility** – anticipates readiness to help the user and offer a quick service;
- **Certainty** – anticipates knowledge and politeness of the service provider personnel and ability to gain user's confidence.
- **Empathy** – is reflected through offering individualized service through realizing and respecting special demands by the user and regarding the user as an individual.

By investigating above mentioned variables on users' perception and setting up questions on their expectations with regards to the same dimensions of the quality service, companies can obtain a whole range of useful information which they can use for different purposes. This primarily relates to (Grubor 2007):

- Determining average deviation of the perception and expectation per each service determinant;
- Assessment quality service of the company per all service determinants;
- Following users' expectations and perceptions, i.e. service quality during the course of time;
- Comparison the obtained results with the competition;
- Identifying user segments with significant differences with regards to the issue of satisfaction with the performances of the company services;
- Determining intern quality standards (between subsidiaries, departments within the company etc.).

Upon the obtained results, the company can carry out corrective actions and in that way to improve the service quality.

Experts of academic research in the field of service providing quote ten guidelines for service marketing managers, for which they think are of key importance for improving service quality in to the total service providing branch and they are:

- **Listening** – to understand what users wish through constant education on expectations and perceptions of the users and those who haven't become such;
- **Reliability** – the most important dimension of service quality in fulfilling expectations of the user which must have a priority when we talk about services;
- **Basic service** – service providing companies must deliver basic and do what they are expected to do, and it is to keep promises, to listen to users, to inform them and to be decisive in attempting to deliver the value to the users;
- **Service design** – to develop a holistic approach towards services and to pay attention to the details which these services consist of at the same time;
- **Correction** – in order to satisfy users who are faced with problem with regards to service providing, service providing companies should encourage users and to enable them to submit their complaints, to reply to them swiftly and personally, and to develop the system for solving issues;
- To surprise users – dimensions of process (persuasiveness, responsibility and empathy) are the most important when we talk about exceeding users' expectations. For example, to surprise the user with unexpected speed, style, politeness, competitiveness and understanding.
- **Fairness** – service providing companies have to make efforts to be fair and to show that fairness both to the users and the employees;
- **Team work** – enables big companies to offer services carefully and attentively, because in that way they improve motivation and ability of the employees;
- **Researches among the employees** – with the aim to reveal why there are issues and what the company has to do in order to solve them;
- **Associated leadership** – service quality derives from encouraging leadership at the level of the whole organization, from excellent design of the service system, to efficient application of information and technology, from established corporate culture.

Implementing above mentioned principles and procedures by the marketing managers of mobile operators is very significant, since their application enables the improvement of the service quality. Establishing and satisfying high standards with regards to service and its delivery, the commitment to users with monitoring their satisfaction and continuous improving the service quality are practices that mobile operators would always have in mind, and what is more important – to regularly carry them out and improve in order to have satisfied users. So, it is clear and continuous and regular researches of users' expectations and perceptions, respecting their opinion have to be the basics for taking corrective measures and bringing business decisions connected with services and service quality which are offered to the customers.

Ultimately, only those products and services which have ability to provide “what is wanted up to the point that it is enough” can obtain satisfaction (Oliver 1997). It means to the point that it is not too much, i.e. that too much is not necessarily desirable. Companies that put consumer's satisfaction in the first plan do it based on experience. It is regarded that customer's satisfaction increases loyalty, intention to buy again, positive reactions and reduces the number of complaints. On the other hand, dissatisfaction of the customers increases the brand change, brings to negative reactions and bigger

number of complaints. In that way the customers' satisfaction has a very strong influence on profit gain and expenses of modern companies.

3 Materials and Methods

Subject of the research – Subject of this paper is analysis of users' perception with regards to quality service of mobile operators in Montenegro, by implementation of the Servqual model.

Aim of the research – Aim of the research is to examine the level of users' satisfaction of the service quality offered by mobile operators at the Montenegrin market of mobile communication by using the *Servqual* model, and also to offer guidelines to mobile operators in which direction they should go in order to improve the level of the service quality.

Research task – In order to identify the fields for improving service quality at the market of mobile communications in Montenegro, the basic research task of this paper is analysis of existing level of users' satisfaction with the service quality of mobile operators, so that they can recognize basic failures and problems in service quality which are offered by Montenegrin mobile operators, and to offer recommendation for further decisions in terms of improving the level of the service quality and its research.

Basic hypothesis – Starting from the subject and objective of the research, it is possible to set the basic hypothesis in the following way: *(H1) Service quality represents a significant index of users' satisfaction and success of mobile operators in satisfying users' expectations, as well as the guidepost to show in which direction and in what way the operators can improve the level of the service they are offering.* Above mentioned hypothesis further anticipates that today marketing efforts of the companies have to be oriented towards creating and delivering superior value to the users so that they can satisfy their bigger demands and expectations with regards to the demanded service. The level of the users' satisfaction will depend on the delivered value and the quality.

Instrument and research sample – In order to show the process of the research of service quality at the market of mobile communication in Montenegro by using *Servqual* model, a research which included analysis of bigger number of variables was carried out and it comprised 620 interviewees. The questionnaire which was used for researching service quality is shown in the following Table 1.

The questionnaire which was implemented in the research consists of three parts. The first part of the questionnaire consists of questions which collected details on demographic features (gender, age, education) of individual users of mobile operator services. The second part is questioning perceived level of service offered by the mobile operator whose services the interviewee is using, whereas the third part is about questioning users in the sector of mobile communications.

States contained in the questionnaire were designed so that they can be grouped in one of the five variables (dimensions) of service quality according to the *Servqual* model. Individual criteria, i.e. claims connected to them are distributed in the following way: 1–4 *tangibility*, 5–9 *reliability*, 10–13 *responsibility*, 14–17 *certainty* and 18–22 *empathy*. Each claim is followed by the scale of 5 values, starting from 1 (I totally

Table 1. Servqual questionnaire for researching service quality at the market of mobile communications

Second part: perception of the service quality		
Assess the following 22 claims of Servqual model by circling the number which corresponds to the assessment from “I totally disagree = 1” to “I totally agree = 5” according to the perception of service quality which you get from mobile operator whose services you are using		
Perception examining		
1	Show room is modernly equipped	1...2...3...4...5
2	Exterior and interior of the show room are visually appealing	1...2...3...4...5
3	Staff in the show room seems to be tidy	1...2...3...4...5
4	Materials connected to the service (flyers, forms) are visually attractive	1...2...3...4...5
5	Mobile operator fulfills given jobs in the agreed deadline	1...2...3...4...5
6	When a user has a problem, mobile operator shows honest efforts to solve it	1...2...3...4...5
7	Mobile operator offered appropriate service to the user from the first meeting onwards	1...2...3...4...5
8	Mobile operator offers a service in the period he/she promised to offer it	1...2...3...4...5
9	Mobile operator insists on service without an error	1...2...3...4...5
10	Staff of the mobile operator is able to say when precisely the service will be offered	1...2...3...4...5
11	Staff of the mobile operator offers quick (timely) service	1...2...3...4...5
12	Staff of the mobile operator is always ready to help the user	1...2...3...4...5
13	Staff of the mobile operator is never too busy to answer the user’s questions	1...2...3...4...5
14	Mobile operator staff’s behaviour gives confidence to the users	1...2...3...4...5
15	Users feel safe during the transactions	1...2...3...4...5
16	Staff of the mobile operator is always polite with users	1...2...3...4...5
17	Staff of the mobile operator is competent to answer the user’s questions	1...2...3...4...5
18	Staff of the mobile operator devotes attention to the user as an individual	1...2...3...4...5
19	Working hours of the mobile operator is adjusted to all users	1...2...3...4...5
20	Mobile operator has staff which shows personal attention to the users	1...2...3...4...5
21	Mobile operator is always focused on what is the best for the user	1...2...3...4...5
22	Staff of the mobile operator understands specific requests and needs of the user	1...2...3...4...5
Third part: expectation of the service quality		
Assess the following 22 claims of Servqual model by circling the number which corresponds to the assessment from “I totally disagree = 1” to “I totally agree = 5” according to the expectation of the service quality which you get from an ideal mobile operator		
Examining expectations		
	Mobile operator’s show room must be modernly equipped	1...2...3...4...5
	Exterior and interior of the show room should be visually appealing	1...2...3...4...5
	Staff in the show room should look tidy	1...2...3...4...5
	Materials connected to the service (flyers, forms) should be visually attractive	1...2...3...4...5
	Mobile operator should fulfill given jobs in the agreed deadline	1...2...3...4...5
	When a user has a problem, mobile operator will show honest efforts to solve it	1...2...3...4...5
	Mobile operator will offer appropriate service to the user from the first meeting onwards	1...2...3...4...5
	Mobile operator will offer a service in the period he/she promised to offer it	1...2...3...4...5
	Mobile operator always insists on service without an error	1...2...3...4...5
	Staff of the mobile operator is able to say when precisely the service will be offered	1...2...3...4...5

(continued)

Table 1. (continued)

Staff of the mobile operator will offer quick (timely) service	1...2...3...4...5
Staff of the mobile operator will always be ready to help the user	1...2...3...4...5
Staff of the mobile operator will never be too busy to answer the user's questions	1...2...3...4...5
Mobile operator staff's behaviour should give confidence to the users	1...2...3...4...5
Users should feel safe during the transactions	1...2...3...4...5
Staff of the mobile provider should always be polite with the users	1...2...3...4...5
Staff of the mobile operator should be competent to answer the user's questions	1...2...3...4...5
Staff of the mobile operator should devote attention to the user as an individual	1...2...3...4...5
Working hours of the mobile operator should be adjusted to all users	1...2...3...4...5
Mobile operator should have staff which shows personal attention to the users	1...2...3...4...5
Mobile operator should be always focused on what is the best for the user	1...2...3...4...5
Staff of the mobile operator should understand specific requests and needs of the user	1...2...3...4...5

disagree) till 5 (I totally agree). The highest value on the scale is about high expectations and high level of perception. Good quality service is a result of fulfilled expectations (or exceeded), whereas the gap appears when the expectations have not been fulfilled. The gap is counted as a difference between values of perception and expectation. Positive difference is when the expectation is achieved or exceeded, and negative when the expectation is not achieved. Gaps can be analyzed for each claim and they can be collected so that we can get the total result for each dimension. In the following part, the results obtained by the research which was carried out are shown.

4 Analysis and Discussion of Obtained Results

The research of quality service offered by mobile operators at the Montenegrin market was carried out in 2016. The following table shows basic data on the characteristics of the interviewees comprised by the sample (Table 2).

Table 2. Sample characteristics

Factor	Category	Percentage
Gender	(a) Male	46%
	(b) Female	54%
Age	(c) 25 and less	46%
	(a) 26–35	38%
	(b) 36–46	4%
	(c) 46 years and more	12%
Education	(a) Primary school	0%
	(b) Secondary school	14%
	(c) College, faculty	70%
	(d) Master degree, doctorate	16%

As you can see from the above table, in the sample of the users who assessed service quality of the mobile operators, there are more females (54%) and more people with degree of college or faculty (70%). Additionally, majority of the interviewees' age is 25 years or less (46%). From the above given, it is obvious that younger and more educated population is more involved in using services of mobile communications.

After analyzing the sample characteristics, data on perceptions of the quality services and users' expectations were analyzed. Mean values of the users' expectation and perception for each of the claims from the questionnaire can be seen in Table 3. Negative *Servqual* result of the claim means that users' expectations are bigger than the perception, thus the perceived quality is not satisfactory, because of which a quality gap emerges. In the opposite case, when the *Servqual* result is positive, users' expectation is achieved or exceeded, and in that case we can talk about satisfactorily perceived quality service.

As we can see from the above given table, interviewees mostly assessed the claim 19 (*Working hours of the mobile operator is adjusted to all users*) with the highest grade. With regards to expectations, the claims 12 (*Staff of the mobile operator will always be ready to help the user*) and 21 (*Mobile operator should be always focused on what is the best for the user*) were assessed with the highest grades. The claim 13 got

Table 3. Average *Servqual* grades of the interviewees

Variable (dimension)	Claim from the questionnaire	Perception	Expectation	<i>Servqual</i> grade
Tangibility	1	3.38	4.24	-0.86
	2	3.20	4.10	-0.90
	3	3.52	4.52	-1.00
	4	3.36	4.08	-0.72
Reliability	5	2.88	4.48	-1.60
	6	2.38	4.56	-2.18
	7	2.26	4.22	-1.96
	8	2.46	4.42	-1.96
	9	2.08	4.24	-2.16
Responsibility	10	1.80	3.96	-2.16
	11	2.10	4.30	-2.20
	12	2.50	4.60	-2.10
	13	1.68	4.18	-2.50
Certainty	14	2.36	4.44	-2.08
	15	2.82	4.56	-1.74
	16	2.88	4.56	-1.68
	17	2.72	4.54	-1.82
Empathy	18	2.80	4.26	-1.46
	19	3.62	4.30	-0.68
	20	2.66	4.20	-1.54
	21	2.32	4.60	-2.28
	22	2.32	4.30	-1.98

the smallest grade by the users (*Staff of the mobile operator is never too busy to answer the users' questions*), whereas the claim 10 (*Staff of the mobile operator is able to say when precisely the service will be offered*) got the least grade with regards to expectations. The biggest gap appeared with the claim 13 (*Staff of the mobile operator is never too busy to answer the users' questions*). Contrary to that, the smallest gap appeared with the claim 19 (*Working hours of the mobile operator is adjusted to all users*).

The following table shows the average grades of perception and expectation of the quality service, together with the *Servqual* grades for each individual dimension (Table 4).

Table 4. Average grades for Servqual dimensions of the service quality

Dimension	Perception	Expectation	<i>Servqual</i> grade
Tangibility	3.37	4.24	-0.87
Reliability	2.41	4.38	-1.97
Responsibility	2.02	4.26	-2.24
Certainty	2.67	4.53	-1.86
Empathy	2.74	4.33	-1.59

We can notice from the previous table that expectation and perception of the service quality are different for all five variables (dimensions). The biggest gap appeared with the dimension for responsibility, whereas it was the least for the dimension for tangibility. Based upon the results which have been shown in the previous tables, we can conclude that the interviewees negatively scored dimensions of the service quality, which means that users' expectations are bigger than their perception, perceived quality is not satisfactory, and that is why we have a gap in the quality service. Obtained results show the fact that all mobile operators, for who the perception regarding quality differs, would improve the quality of their services so that they can fulfill their users' expectations and ensure their satisfaction.

5 Conclusion

For successful internationalization the company must know the environment of the target market and understand the consumer behaviour and needs of local consumers to choose the right entry mode (Galova 2014).

In modern business, satisfaction is connected with the consumers' effort to achieve content by using goods and services in any sector. Telecommunication sector has marked continuous growth in the last ten years. This is especially true in the field of mobile telephony (Melovic et al. 2014). The telecommunications industry has changed radically in recent years. The new structure of the market and technological improvements has increased the volume of telecommunications services (OECD 2005) and customers have become more aware of their rights and demand better quality (Pina et al. 2014). Users' satisfaction is an extraordinary index and barometer of the future

incomes and profit. The satisfaction is influenced firstly by the individual expectations of the visitors and secondly by the destination and its characteristics itself (Vajčnerova et al. 2014). Satisfaction is an indicator which looks ahead about business success which measures how the consumers react to the future of the company. In that way, consumers' satisfaction significantly influences the financial flows of the company.

Constant changes and competitiveness at the market of mobile communications require good knowledge about users. This change in behaviour has forced telecommunications operators to redefine their strategy (Rienzner and Testa 2003), including a new approach to customers. Users are no longer forced to be tied to only one service and one operator, but they have a wide range of offers which enables them to choose those offers that suit them best. Intensifying competitive relationships at the market of mobile communications complicate offer differentiation and gaining competitive advantage, but it also influence the users with regards to their expectations. Users are becoming more demanding and expect a higher degree of care by the mobile operators when it is about their wishes, needs and total satisfaction.

The research showed that mobile communication users in Montenegro have clearly expressed attitudes regarding the service quality that is offered to them. Namely, the research showed that the interviewees negatively assess all dimensions of the service quality. It means that their expectations with regards to the service quality have not been fulfilled and that the service quality they are getting is perceived as not satisfactory. Obtained results are a signal to the mobile operators that the service quality is not on the satisfactory level and that they have to take measures for their improvement.

It is clear that continuous delivery of higher service quality regarding the competitive companies is one of the basic ways for differentiation. In that sense, the objective of the mobile operators must be fulfilling and exceeding the level of service quality which the user expects. In this regard, all that contributes the value with users also influences their perception and it has to be inbuilt in the quality system. Possibilities of improving the quality are big, and the task of the mobile operator is to choose those characteristics which are especially important for the users and to improve them. That is why the service quality management has to be based on the following (Živković 2009):

- Continuous marketing researches so that they can identify the factors which influence the quality service;
- Innovativeness with regards to offer differentiation;
- Establishing integrated marketing communication with recognized target segments;
- Designing the service according to the users' requests and according to the requests of the employees (service environment, physical elements, service standardization);
- Human resource management (internal marketing – motivation, training);
- Adjusting the offer and demand and
- Setting up the monitoring i.e. service process control.

Taking into account the importance and complexity of researching users' satisfaction, as well as specificity of the service sector, it is clear that the procedure of researching satisfaction of the users must be based upon the researching users so that it can result with obtaining valid and good quality information. Since the user's satisfaction with the company service represents subjective perception of the user, its

quantifying demands a special attention. The procedure of measuring satisfaction is a very complex process which requires precise activity planning and continuous data collection, when it is necessary to take into account its subjective reference.

As the research objective is users' satisfaction, it is actually objectifying and quantifying subjective users' perception (Tse and Wilton 1988), it is necessary that the researches include all those variables which are in cause-and-effect relationship with it. Traditional research approach, which anticipates to ask the user what he thinks is important, does not obtain the answer to the question whether he is satisfied or not. Frequent error that is made during the research on users' satisfaction is that the users are offered the answer to the question and based upon that to conclude whether they are satisfied or not, but they do not examine the degree of satisfaction or connections between satisfaction and other variables that it is influenced by. That is why have to have in mind that satisfaction is not one-dimensional binary concept, but that it is the matter of degree (Kostić 2010). However, customer satisfaction lacks to include many other factors such as social norm, image, privacy, and security, which found to be important by other studies (Abbas 2013; Rouibah and Abbas 2010; Roubiah *et al.* 2011).

There was a similar research on the users' satisfaction in the field of information technologies with the *Servqual* model which was carried out in the world and it gave the following results (Kettinger and Choong 1994): Recognizing the need to improve existing MIS (*Marketing Information System*) measures of user satisfaction with the ISF (*Information System Function*), that study adapts the *Servqual* measure from marketing to provide more specific information about user satisfaction with the information service function. It was found that, while the three original dimensions of the traditional *user information satisfaction* (UIS) measure remain strong predictors of overall ISF user satisfaction, two aspects of IS (Information System) service quality, "reliability" and "empathy," are also significant predictors. The results suggest that the original dimensions of UIS may not be comprehensive enough to capture the more detailed dimensions of ISF service quality in *Servqual*, and that the reliability and empathy dimensions of service quality may be needed to supplement the traditional UIS measure in determining user satisfaction with the information services function. Similar recommendations can be useful for decision makers in the area of telecommunication (mobile communications). Namely, subject research of the satisfaction with quality of mobile communications in Montenegro confirmed that the users classify "reliability" and "certainty" as an important dimension of quality that they receive from a certain operator.




Based upon all above mentioned, we can conclude that if mobile operators understand the market demands, convert the knowledge into appropriate service and deliver the service with the least possible difference between the delivered and what was promised to the user, positive effects of quality service management based on previously mentioned procedures will be multiplied.

References

- Abbas, H.: Quality as determinant factor of customer satisfaction. Case study of Zain-Kuwait. *Sci. Res.* **5**(3), 182–189 (2013)
- Drucker, P.F.: *The Practice of Management*. Harper Collier, New York (1954)
- Galova, J.: Selected business aspects of the emerging market of Ukraine. *J. Cent. Eur. Green Innov.* **2**(1), 51–59 (2014)
- Grubor, A.: Service marketing competitiveness in the new economy. *Montenegrin J. Econ.* **4**(7), 103–110 (2007)
- Horska, E., Ūrgeová, J., Prokeinova, R.: Consumers' food choice and quality perception: comparative analysis of selected Central European countries. *Agric. Econ.* **10**, 493–499 (2011)
- Johnston, R., Kong, X.: The customer experience: a road-map for improvement. *Manag. Serv. Qual.* **21**(1), 5–24 (2011)
- Kelly, J.M.: The dilemma of the unsatisfied customer. *Public Adm. Rev.* **65**(1), 76–84 (2005)
- Kettinger, W., Choong, C.: Perceived service quality and user satisfaction with the information services function. *Decis. Sci.* **25**(5/6), 737–766 (1994)
- Kostić, E.: Merenje zadovoljstva korisnika usluge na primeru Delta DMD-a. *Marketing* **41**(4), 268–276 (2010)
- Levitt, T.: Marketing myopia. *Harv. Bus. Rev.* **38**, 45–56 (1960)
- Melovic, B., Mitrovic, S., Markovic, T., Nestic, A., Vajčnerova, I.: Satisfaction as a determinant of customer loyalty towards mobile communication. *Acta Universitatis Agriculturae et Silviculturae Mendelianae Brunensi* **62**(6), 1363–1371 (2014)
- Melović, B.: Unapređenje poslovanja kroz Customer Relationship Management. *Preduzetnik*, broj 7, Ekonomski fakultet Podgorica, 31–34 (2012)
- Mitrović, S., Borocki, J., Sokolovski, V., Nešić, A., Melović, B.: Potential of young entrepreneurs: is there any possibility of their development through education? *New Educ. Rev.* **32**(2), 288–298 (2013)
- Nefat, A., Paus, N.: Determinants of customer satisfaction with service encounter. *Tržište* **20**(2), 195–210 (2008)
- OECD: *Communications Outlook*, Paris (2005)
- OECD: *Communications Outlook*, Paris (2007)
- Oliver, L.R.: *Satisfaction*. McGraw-Hill Companies, New York (1997)
- Özer, A., Argan, M.T., Argan, M.: The effect of mobile service quality dimensions on customer satisfaction. *Procedia-Soc. Behav. Sci.* **99**, 428–438 (2013)
- Parasuraman, A., Berry, L., Zeithaml, V.: Servqual: a multiple - item scale for measuring consumer perceptions of service quality. *J. Retail.* **64**(1), 12–40 (1988)
- Pina, V., Torres, L., Bachiller, P.: Service quality in utility industries: the european telecommunications sector. *Manag. Serv. Qual.* **24**(1), 2–22 (2014)
- Rienzner, R., Testa, F.: The captive consumer no longer exists. Creating customer loyalty to compete on the new deregulated markets of public utilities. *Total Qual. Manag. Bus. Excell.* **14**(2), 171–187 (2003)
- Rouibah, K., Abbas, H.: Effect of personal innovativeness, attachment motivation, and social norms on the acceptance of cameral mobile phones. *Int. J. Handheld Comput. Res.* **1**(4), 41–62 (2010)
- Rouibah, K., Abbas, H., Rouibah, S.: factors affecting camera mobile phone adoption before e-shopping in the Arab world. *Technol. Soc.* **33**, 271–283 (2011)
- Tse, D., Wilton, P.: Models of consumer satisfaction: an extension. *J. Market. Res.* **25**(2), 204–212 (1988)

- Živković, R.: Ponašanje i zaštita potrošača u turizmu. Univerzitet Singidunum, Beograd (2009)
- Vajčnerova, I., Žiaran, P., Ryglova, K., Andraško, I.: Quality management of the tourist destination in the context of visitors' satisfaction. In: Enterprise and the Competitive Environment 2014 conference, ECE 2014, 6–7 March 2014, Brno, Czech Republic (2014)
- Wang, Y., Lo, H., Yang, Y.: An integrated framework for service quality, customer value, satisfaction evidence from China's communication industry. *Inf. Syst. Front.* **6**(4), 325–340 (2004)
- Weisman, D.L.: Price regulation and quality. *Inf. Econ. Policy* **17**, 165–174 (2005)

Methodological Approaches to a Substantiation Resurso - and Energetically Effective Economic Model of Object of Placing of a Waste

Edward Tshovrebov¹ , Evgeniy Velichko² ,
and Andrey Shevchenko³ 

¹ FGAU Scientific Research Institute «The Center of Ecological Industrial Policy», Olympic prospectus, 42, Mytishi 142000, Russia

² Moscow State University of Civil Engineering,
Yaroslavskoye Sh., 26, Moscow 129337, Russia
pct44@yandex. ru

³ National Engineering Company «GK NATEC»,
Gorbunova street, 2, Moscow 121596, Russia

Abstract. In article questions of the feasibility report saving up energy and resources of economic model of object of placing of a waste of housing and communal services, industrial, civil and transport building, various industries are considered; the organisation and activity planning in sphere of recycling of a waste, manufactures of various kinds of production from secondary raw materials. Parametres of activity of proving grounds of housing of a waste saving up resources, economic productivity in the field of the reference with a waste are offered and resulted at economic activities realization.

Keywords: Waste of production and consumption · Waste management Utilization · Economic efficiency · Resource saving

1 Introduction

Now in connection with increasing volumes of waste burial on active proving grounds and not authorised dumps more and more actual and significant for ecology and economy of Russia there is a question on increase in a share of waste recycling in connection with universal exhaustion of power of such installations and absence of the new squares under the legal entombment, matching to natural-landscape, hydro-geological conditions, town-planning, technical, ecological and sanitary-and-epidemiologic demands, size standards and normatives. A unique exit from the developed situation menacing to ecological and economic safety of the country, on the one hand - use saving up energy and resources of technologies in the various branches, allowing to involve a technological waste: losses and marriage directly in secondary economic circulation, on the other hand - processing of already formed waste, first of all, municipal, building and transport - in secondary raw materials, materials, products, excepting their hit in the form of a buried waste in an environment.

2 Problem Statement

With allowance for last declarations and demands of heads of bodies legislative and an executive power of Russia on tuning up and maintenance of system of an ecological security, resource and power savings, rehash and waste recycling there is a necessity for basic new approach to the organisation of branch of the reference with a waste in our country, revising of demands and standards to the factories which are engaged in gathering, housing, entombment, salvaging, destruction of a waste.

The developed ecological situation in Russia, connected with necessity of closing produced an expected life of the majority of active proving grounds and liquidation of not authorised dumps will essentially increase loading by the remained authorised installations of entombment and destruction of a waste and thus will demand designing, building of new analogous installations. Therefore necessity of revising of ecologically proved technical and economic demands, on the one hand, to active, designed and under construction installations of housing of a waste regarding the organisation and activity activation on resource saving, salvaging and a waste processing, with another, to managing subjects - to sources of formation industrial and a domestic wastes aimed, in the final reckoning, on the power and resource savings, maintenance of economic efficiency of business designs and observance of demands of the ecological legislation already has already matured. The huge parcels on all country, occupied under proving grounds and dumps, instead of the enormous ecological harm put to a natural habitat and washing up of “garbage billions”, should bring economic result in the form of the prevented ecological-economic damage, profit on production new necessary for various economic branches ecologically and hygienic safety products and job creation [1–3].

Within the limits of creation of an ecological-economic model of installations of housing of a waste saving up resources working out for each installation of target estimated parametres of activity not only on a buried waste within the limits of legislation demands, but also on their salvaging, the organisation of production from them on the basis of the best accessible production engineering or their implementation in the capacity of a secondary material after matching rehash is represented actual.

3 Results and Discussion

Environmentally sound for a concrete application conditions technical-and-economic indexes of savings of resources and a waste processing in secondary products in a standard order are expedient for proving on blueprint stages of new installations - in the project documentation, and also at the stage of exploitation with allowance for redesign and modernisation of active proving grounds with creation of manufactures recycling a waste.

Such productive and economic parametres can be counted proceeding from following parametres:

- The square and expected lifes of installations, the capacity, fixed limits of housing of a waste;

- A morphological componental compound, physical and chemical characteristics of the arriving waste directly influencing volumes and quality of the taken secondary material from a waste;
- Reception quantity indicators on proving ground for salvaging of a secondary material, building and some sorts of industrial wastes 3–5 class-rooms of hazard (allowed to reception on proving ground and not liable to destruction);
- The squares of territory of the region served by given installation on gathering and a waste disposal and economically expedient distance of transportation of a waste;
- Optimal utilisation and a combination of production engineering of a waste processing;
- The list and price parametres of made products or an implemented secondary material from the waste, having demand in region or behind its limits.

Analysing formation of quantity indicators of the waste addressing on proving ground, including communal, building and others, it is necessary to differentiate accurately parametres of directly entombment and separately - housings of the waste which is subject to the subsequent salvaging, recurrings in secondary economic circulation.

The mass allowed to the reception, a placed waste on proving ground (M_{hous}) develops of following components:

$$M_{\text{hous}} = M_{\text{ent}_1} + M_{\text{reh}}, \quad (1)$$

M_{ent_1} - The mass of a waste accepted on proving ground, not subject to salvaging and buried in a body of proving ground without conducting of any other production operations;

M_{reh} - mass of a waste (communal, building, a secondary material), directed on production processes: storage, machining (preliminary disassembling, the classifying, clearing), a coarse crushing, separation with a view of the further salvaging.

Last parametre reflects quantity indicators of the waste directed on the further salvaging:

$$M_{\text{reh}} = M_{\text{util}} + M_{\text{ent}_2} + M_{\text{neutr}}, \quad (2)$$

M_{ent_2} - Mass of not reutilizable waste formed as a result of production operations of machining, crushing, the separation, directed on entombment in a proving ground body;

M_{neutr} - mass of not reutilizable waste formed as a result of production operations of machining, crushing, the separation, not subject under the characteristics and hazard extent to entombment and directed on neutralisation, destruction on installation of entombment or transferred to other subjects of economic activities for these purposes;

M_{util} - the mass of a waste which on the properties, to characteristics, extent of toxicity, ecological hazard is suitable for the further salvaging (recycling, recuperations, regenerations) after preparative treatment, crushing, separation.

$$M_{\text{util}} = M_{\text{reg}} + M_{\text{recycl}} + M_{\text{rec}}, \quad (3)$$

M_{reg} - mass of a refunded waste in a production cycle after matching preparation;

M_{recycl} - mass of repeatedly applied waste on straight appointment;

M_{rec} - mass of taken useful ingredients for their repetitive application.

As a result the mass of a placed waste on proving ground will develop of following components:

$$M_{\text{hous}} = M_{\text{util}} + M_{\text{ent}_1} + M_{\text{ent}_2} + M_{\text{neutr}}. \quad (4)$$

Then the parametre of productivity of process of resource saving in the course of housing of a waste ($Pres$) will be defined from a relationship:

$$Pres = M_{\text{util}} / M_{\text{hous}} \quad (5)$$

With allowance for a time spacing on a heading and development of new production engineering recycling a waste, their pay-back periods, it is expedient to ration parametres of efficiency from the beginning of realisation of the activity which is saving up material and natural resources. In particular, on achievements of the first five years to instal an average minimum parametre - 50%, with 6 for 10 year - 60%, with 11 for 15 year - 70–75%. It is in parallel expedient to instal target parametres on the various groups of a waste recycled in a secondary material and products: for example, on a board and paper for recycling waste - 70–80%, to empties and a broken glass - 65–75%, to a wood waste – 85–90%, to a polymeric waste - not less than 50%.

Proceeding from the analysis of a morphological compound of a waste the useful mass of various types of the recycled secondary resources directed on a reuse in the capacity of a secondary material or materials for manufacturing of products is predicted. Having data on development of various types of products from unit of a used secondary material ($M_{s.m}$), i.e. about economic result of return of the secondary resources, defined by the corresponding figure - factor of secondary return of resources (K_r) for a concrete secondary material, it is expedient to define the integrated estimated target parametres of the production program of exhaust of various sorts of products ($M_{b.p}$) from various types of the recycled secondary resources:

$$K_r = M_{b.p} / M_{s.m} \quad (6)$$

$$M_{b.p} = M_{s.m} * K_r. \quad (7)$$

The given parametres are of great importance as from the economic point of view - process realisation to volplane productive forces and released products in region, and from the point of view of an ecological evaluation of activity of managing subjects in the field of the reference with a waste and resource saving.

The analysis of foreign experience [2, 4–10] shows, that the considerable part of volumes of a formed waste (to 80% in countries of Western Europe) is recycled by the small and average industrial, building and other factories which have been had

including in boundary lines of installation of housing of a waste. To the factors influencing efficiency and expediency of realisation of such business designs refer to:

- Possibility of the state support and decrease in administrative parting layers;
- Profitableness of the design with allowance for level capital and carrying costs, fluctuation of prices, a rate of inflation, fixed rates of discounting, tax loading, cost of power resources, etc. parametres;
- Presence of the matching squares for the organisation recycling production wastes, warehousings of a secondary material, a finished product in territory of installation of waste burial;
- Economically expedient shoulder of transportation of a waste (distance from a place of their formation to installation of housing);
- Presence of stable goods turnover, demand and commodity markets of products from a secondary material and a waste.

The nomenclature of released products with waste utilisation is rather various and is defined by quality and safety as secondary material in the form of a waste, and a finished product from it, and also a price relation and local features of demand for interchangeable sorts of products from primary and a secondary material.

Scientists and specialists FBU «NITSPURO» (nowadays - FGAU “Scientific research institute «The Center of industrial ecological policy», the Moscow state building university, Academy of safety and special programs, National Engineering Company «GK NATEC», and the Moscow state university of means of communication in a current of several years work on a substantiation of methodological approaches to an ekologo-economic estimation of new innovative business designs in sphere of the industry of building materials, transport building, rehash and waste recycling is guided. The great value is given to the analysis of ekologo-economic indicators at an investment estimation under construction, technically re-equipped, redesigned installations of the real property. Analysis basis estimated, comparative, economic-mathematical methods, geoinformation technologies, methods of distant sounding, ecological rationing, instrumental-analytical monitoring of natural, anthropogenous installations (make proving grounds of a waste and so forth), a technical condition of installations of the real property, level of their ecological hazard. The considerable volume of the modern information on ecologically safety manufactures on rehash of various sorts building, transport and a domestic wastes [11–15] is collected and generalised. The list of some ecologically safe manufactures of secondary production (on an example of a waste of transport building) is presented in Table 1.

Besides, technical-and-economic indexes of rehash of various sorts of a waste, now, unfortunately, in a total storage of a solid communal waste buried on proving grounds - in the concrete goods, products, materials are developed: rubber plastic coatings, industrial and economic stock, bags-refrigerators, heat-insulating products, fertilizers from sediments of the cleared sewage, neutralising acidity of soils and toxic joints in it, non-load-bearing and garden designs from a waste of plastic bottles. Similar indicators are defined and on development of thermal energy from the installations developed NEC «GK NATEC» on clearing of filtrational (drainage) runoffs of ranges of a hard communal waste. In Moscow suburbs is realised by Common efforts the design of an independent energetic complex «Ecological Dwelling» with innovative

Table 1. Waste processing production engineering in secondary products.

Type of taken raw materials from a waste	Rehash production engineering	End production	Pay-back period, years
Sediment of treatment facilities	Thermoichesky and biological machining	Organic fertilizer	2–3
Scraps woody The wood rests, wood pieces	Crushing	Wood concrete	1.5–2
Scraps woody Chip woody	Crushing, Pressing	The oriented slabs from a chip	1.5–2
Rasplings woody Chip woody	Powdering, Pressing	Fuel cakes	1–1.5
Paper and board	Powdering, Pressing	Cellulose heaters	1–1.5
Auto-tyre casing rubber scrap	Powdering, Pressing Thermal processing	Rubber tile, Filling material for fibrous concrete	2–3
Waste of a granulated slag, slag of ash, brick, haydite, rubble	Crushing, Pressing	Filling material for cinder betons; cinder blocks	1–1.5
Waste of cement the Chip woody	Powdering Pressing Thermal processing	Cement slabs from a chip	1.5–2
Waste reinforced-concrete, concrete articles	Two-stage breaking	Filling material for concrete mixtures	4–6
Waste of plastic bottles, plastic materials, polysterene, poly-propylene and so forth	Powdering, fractionation, Thermal processing	Filling material for polymeric betons, a polymeric sandy tile	3–5
Waste of a stoneware	Powdering, pressing	Additives for production of fire-resistant products	3–5

treatment facilities and the production engineering of exploitation which is saving up natural and material resources.

Efficiency of a model of installation of placement of a waste saving up resources is defined by set of measures of support as economic and is standard-reguljativnoj. According to enterprise community, use saving material both natural resources of production engineering and output from a secondary material fixed practice of reception of government subsidies and subsidies essentially brakes. Within the limits of matching techniques and methodical recommendations giving of investments in the form of budgetary investments assumes pay-back period of capital outlays no more than 2 years. By calculations FBU NITSPURO, real pay-back period of investments for the majority of widespread production engineering of waste recycling (switching on not only powdering and pressing, and more difficult and expensive - multiphase crushing,

separation, thermal moulding (an extrusion, injection moulding, milling, pneumovacuum blowing, a spraying of plastic), chemical methods (depolymerisation, regeneration of polymers), thermal decomposition (pyrolysis, cracking)), is sized up in 3–6 years (without recovery of percent on credits). Necessity of recovery of budgetary funds for a short time forces a commodity producer to raise the price for products made of a secondary material that does its noncompetitive in the market, and the business design in waste recycling sphere, as a result - economically inexpedient [2, 16].

Revising of approaches to an estimation of the discounted pay-back period of designs in waste processing sphere in secondary ecologically safety products, rates per hundred and factors (rates) of discounting is represented actual. Use of the high rates per hundred characterising speed of a capital gain without ecological-business factors result ins a negligible current value of intermediate term and long-term designs and does not promote fluidized optimum solutions on investment of designs with a high level of financial risk. The rate of discounting used at an estimation of pay-back period and economic efficiency of investments, for discounting of cash flows, i.e. for recalculation of cost of streams of the future incomes and charges in cost for the present moment, depends on flock of factors and can vary in significant limits. For streamlining of calculations of the rate with allowance for remoteness in a time of act of environmental factors working out of recommendations by definition optimum spacings of a market risk premium for business designs with various levels of ecological, financial and economic risk and on separate groups of business designs of ecological directivity is expedient: rehash and waste recycling, production from a waste of scarce products for the yielded region, resource and energetic production engineering, re-using of material resources, manufacturing of ecologically safety products [17–19].

By the made estimations with the help for the first time specially developed multipurpose programm complex of the analysis of ekologo-economic indicators of business designs on platform Exel-2007, the real discounted pay-back period of observed designs with application of standard production engineering of pressing, crushing, powdering fluctuates within 1.5–3 years, and with use of difficult production engineering of salvaging with allowance for all complex of nature protection costs can already attain 5–7 years. But stability, safety of the production, working, a circumambient, economic growth, production of pollution-free products, minimisation of ecological risk and problems with the legislation will be thus provided. However nevertheless without revising of financial and economic aspects of the state investment and stimulation of without waste, ecologically safety production engineering development in a total storage of branch manufacturing a waste and businesses in the yielded sphere is not represented perspectiv.

Authors it is investigated and defined, that the complex problem of optimisation and effectivization of work of a manufacturing complex should dare at following stages.

1. The organisation of process of transportation of the waste, the traffic stream connected with optimisation, timeliness and uninterrupted operation of delivery of a waste in necessary quantity for maintenance of continuum of a flow process on a waste processing in a secondary material. The quantity, hoisting capacity and operative conditions of trasport facilities is selected on the basis of alternativeness

between the basic criteria: in distance, in cost of conveyance and quantity of a carried waste. The criterion characterises efficiency of transport process with allowance for the resultant purpose - minimisation of expenses for transportation of a waste. With other things being equal, efficiency of transportation building and a domestic wastes is defined by real hoisting capacity of trasport facilities which as show researches, makes 70–80% from nominal that is a consequence of an insufficient degree of compaction of a waste in a body of a garbage truck because of inhomogeneity of morphological composition, the sizes of a waste and insufficient possibilities of pressing in a real application conditions of the technics transporting a waste. Charges on transportation of a waste from a place of formation to proving ground can be optimised with allowance for:

- Organizational provisions: the rational scheme of moving, minimisation of idle times, traffic without weights, application of containers of great volume, decrease of frequency of a waste disposal;
 - Technological provisions: applications of pressing devices, measures on maintenance of tightness of transported dangerous goods [20].
2. The organisation of an effective flow process of a waste processing in secondary products. As show calculations, the most expedient alternative of rehash of a building waste from a pulling down of buildings on proving ground is placement of manufacturing production so that the material was forwarded from a formation place, passed coarse crushing on separately had storage platform and only after the yielded production process moved on separating installation. For example, optimum flow diagramme of basic processes of rehash of a building waste (a large-sized lumpy waste of panels of wall, blocks, interfloor floorings, stairways, the bases from a waste of beton, ferro-concrete, a brick) are: preparation of a material for coarse crushing; metal partitioning off; crushed fines siftings, siftings of a woody and plastic waste, crushed fines clearing; a regrinding (the open or closed cycles); metal partitioning off; the classifying on fractions [14].
 3. The rational and effective organisation of industrial planning and marketing researches of goods turnover, demand and products commodity market. Competitiveness of products from the processed waste in comparison, for example, with ordinary building products from primary mined raw materials is specific by two major factors: the price and the quality, characterised by high tehniko-performance properties and safety for health of people. For optimisation of all system as a whole and receptions of the maximum economic benefit it is necessary to size up and schedule parametres of work of each production process - the classifying, pressing, powdering, crushing, transportations, a warehouse complex and so forth with allowance for technological limiting factors to organise the entering supervisory control of morphological, physical and chemical and other indexes and characteristics of an entering waste for rehash. To basic restricting factors should refer to mass and recurrence of receipt of a feed stock - a waste on proving ground. At sampling of production engineering and optimisation of the production program of the classifying and rehash of building, household and some sorts of industrial wastes in the capacity of an optimality criterion expediently use of extent (factor) of salvaging of valuable ingredients - raw materials for involving in secondary

economic circulation owing to that the maintenance of valuable ingredients in manufactured raw materials on installation of the classifying is a limiting factor for volume of output from it. An important limiting factor is quality of initial technogenic raw materials (including its ecological hazard, toxicity), directly influencing the cost price of made products - expenses on maintenance of quality of end production, its conformity ecological, sanitary-and-hygienic, technical, to fire protection regulations, rules, demands, standards, normatives. Major factor of such production is its ecological and sanitary-and-hygienic safety, minimisation of negative impact on a natural habitat and health of people.

4 Conclusion




Offered methodological approaches to creation saving up energy and resources of economic model of object of placing of a waste, according to authors of the given research, can become scientifically-methodical base of a substantiation of organizational-administrative and technical and economic decisions of actual problems of maintenance of ecological safety, economy natural, material and power resources, recycling and processing of a waste in secondary production in various industries, civil, industrial and transport building, housing and communal services without which realisation steady innovative development of the Russian state now is impossible.

References

1. Tshovrebov, E., Sadov, A.: Paths of the solution of a problem of reversion with a waste in the order region. *Bull. RAEN* **5**, 29–31 (2011)
2. Golubin, A., Shubov, L.: *The Concept of Management of a Domestic Wastes*. GU NITSPURO, Moscow (2000)
3. Zheltobryuhova, V., Rybalsky, N.: *Activity on Reversion with a Hazwaste*, vol. 2. NIA-Nature, REFIA, Moscow (2003)
4. Tihotsky, I.: Japan: the innovative approach to management solid waste. *Solid Domest. Wastes* **6**, 52–57 (2013)
5. Jackson, K.: The “Garbage” policy of EU: instruments of control. *Solid Domest. Wastes* **1**, 54–55 (2013)
6. Bani, M., Rashid, Z., Hamid, K.: The development of decision support system for waste management: a review. *World Acad. Sci. Eng. Technol.* **25**, 161–168 (2009)
7. Celik, N., Antmann, E., Hayton, B.: *Simulation-based optimisation for planning of effective waste reduction, diversion, and recycling programs*. Department of Industrial Engineering, University of Miami (2012)
8. Galante, G., Aiello, G., Enea, M., Panascia, E.: A multi-objective approach to solid waste management. *Waste Manag.* **30**, 1720–1728 (2006)
9. *Measuring the environmental impact of waste management system: Integrated Solid Waste Management Tools*. University of Waterloo, Canada (2004)
10. Fiorucci, P., Minciardi, R., Robba, M., Sacile, R.: Solid waste management in urban areas development and application of decision support system. *Resour. Conserv. Recycl.* **37**, 301–328 (2003)

11. EUROSTAT: data about material recycling of solid waste for 15 years. European Statistical System. <http://epp.eurostat.ec.europa.eu/tgm/refreshTableAction>
12. Secondary material resources of the nomenclature of State Logistics Committee: Formation and use. Economy, Moscow (1987)
13. Shubov, L., Stavrovsky, M., Shehirev, D.: Production engineering of a megacity waste. Production processes in service. Publishing house "News", Moscow (2002)
14. Tshovrebov, E., Chetvertakov, G., Shcanov, S.: Ecological securit in the building industry. The monography. Alpha-M, Moscow (2014)
15. Methodical recommendations according to volumes of formation of production wastes and consumption. GU NITSPURO, Moscow (2003)
16. Golubin, A.: Development of market relations in system of reversion with a waste. In: Golubin, A., Klepatsky, I. (eds.) The Carrying Trade of Russia, vol. 4, pp. 104–106 (2009)
17. Isaenko, L., Samsonov, M.: The account of environmental factors in business planning as implementation of optimum ekologo-economic strategy of firm. Bull. URGGU (NPI) **2**, 162–165 (2013)
18. Nuzhina, I.: Performance evaluation of the investment design as the instrument of ekologo-economic regulating investitsionno - building activity in region. Reg. Econ.: Theory Pract. **34**, 67–70 (2014)
19. Malenkov, J.: A new methods of investment management. Publishing House - Dwelling «Business Press», SPb (2002)
20. Tshovrebov, E., Velichko, E.: Scientifically approaches to creation of a model of a complex guidance system by streams of a building waste. Bull. MGSU **9**, 95–110 (2015)

Analysis of Factors, Defining Software Development Approach

Igor Ilin , Aleksandr Lepekhin , Anastasia Levina  ^(✉),
and Oksana Iliashenko 

Peter the Great Saint-Petersburg Polytechnic University,
Polytechnicheskaya str., 29, 195251 St. Petersburg, Russia
alyovina@gmail.com

Abstract. The issue of software development approach choice is one of the most controversial in software engineering research. Different authors argue whether Agile or Waterfall practices could be potentially admitted as efficient for developing software or there might be a place for their combination. Currently, the software engineering research is full of studies, describing the differences between these two baseline approaches, comparison of their characteristics and analysis of suitability. But the issue of reasoning why the specific approach has been chosen is potentially undiscovered area. This research paper addresses the analysis of difference between the ways how companies perceive the problem at hand. Specifically, the focus is put on requirements aspects and which factors do the companies consider, when defining the software development approach.

Keywords: Software development · Requirements engineering
Project approach · Factors · Agile · Waterfall

1 Introduction

The primary measure of success of a software system is the degree to which it meets the purpose for which it was intended [1]. Fast-changing technology and increased competition are placing increasing pressure on the development process. Establishing the requirements enables the stakeholders to agree on and visualize the “right product”.

There are different definitions of the term “requirement”, emphasizing its different aspects. The IEEE 610.12- 1990 standard defines a requirement as:

1. A condition or capability needed by a user to solve a problem or achieve an objective;
2. A condition or capability that must be met or possessed by a system or system component to satisfy a contract, standard, specification, or other formally imposed documents.

A documented representation of a condition or capability as in 1 or 2 [2]. Summarizing the definition, requirements consist of needs of different stakeholders: users, organization, industry (dictating standards) and others, which need to be addressed and met properly.

There are other requirements definitions differ in the existing literature, aside from the standard [3]. The researchers state that requirements must be determined and agreed to by the customers, users, and suppliers of a software product before the software can be built, which would provide services, which would be valuable for the stakeholders [4]. The requirements define the “what” of a software product:

- What the software must do to add value for its stakeholders. These functional requirements define the capabilities of the software product.
- What the software must be to add value for its stakeholders. These nonfunctional requirements define the characteristics, properties, or qualities that the software product must possess. They define how well the product performs its functions.
- What limitations there are on the choices that developers have when implementing the software. The external interface definitions and other constraints define these limitations [5].

Requirements addressing throughout their whole lifecycle, independently from their type, is captured by the discipline of Requirements engineering. Requirements engineering (RE) is the process of discovering, documenting and managing the requirements for a computer-based system. The goal of requirements engineering is to produce a set of system requirements which, as far as possible, is complete, consistent, relevant and reflects what the customer actually wants [6].

The importance of RE activity is extremely high in software development process and different aspects need to be mindfully addressed [7]. One of the best-known investigations of the economics of software development was a series of studies conducted in the 1970’s by Barry Boehm. Boehm investigated the cost to fix errors in the development of large software systems.

The way how requirements are managed define the overall approach to the software development project management. The baseline approaches in software development industry, which are commonly addressed and compared between each other are Agile and Traditional (Waterfall) approaches. Traditional software development methodologies grew out of a need to control large development projects. Waterfall approach inherited a deterministic, reductionist approach that relied on task breakdown, and was predicated on stability – stable requirements, analysis and stable design [8]. The official definition of Agile Software Development was contained in a form of “manifesto” in February 2001 by a group of 17 noted software process methodologists, who attended a summit meeting to advocate for a better way of developing software and then formed the Agile Alliance [9]. This is a project management approach, which is flexible and responsive. It seeks for customers’ feedback and appreciates changes as a source of requirements definition.

The approach choice is likely to be affected by a number of contextual factors and surroundings characteristics. These context-driven factors in general are addressed by the complexity theory, which has emerged in software development field of study due to the influence of different types of managerial uncertainty. Understanding uncertainty as a basis of complexity, project managers can then manage technical and structural complexity to control time and cost constraints [10]. There is strong evidence of a link between ‘project management style’ and complexity arising out of uncertainties. Management of technology and structural complexity are associated with an increased

ability to adjust and adapt to emerging contexts [11]. Further, project management maturity models and project complexity have been explored in controlling the cost overruns and reaping business benefits [12].

The way, how complexity of the underlining problem is addressed in scopes of the specific software development project is analyzed in this research. The analysis is potentially important and applicable for managing complex software projects, which concern IT architecture development [13]. The study seeks for understanding how do the companies choose whether Waterfall or Agile project management approach should be applied for the specific situation and what are the factors, affecting this choice.

2 Methodology

The questionnaire was used in order to get more relevant data on the requirements engineering complexity perception. The data gathering with use of questionnaire was organized in the following way:

- Formulating the questionnaire on RE features;
- Contacting the representatives;
- Sending the questionnaire to the representatives;
- Collecting and analysing the data.

The companies for the survey were different IT companies, which are focused on different types of software projects. Each representative was asked to pick one project to discuss it in scopes of the interview. The information about representatives is listed in the Table 1.

Table 1. Interviews information.

Project №	Representative title	Chosen approach
1	Developer	Agile
2	Business analyst	Waterfall
3	Lead business analyst	Agile
4	Business analyst	Waterfall
5	Process orchestration, process integration analyst	Agile
6	Technical product manager	Agile

In order to find out how the companies perceive the RE activity, the analysis of the projects was dedicated to investigating which parameters do companies distinguish in requirements engineering for each specific project.

The parameters of RE complexity have been divided into simple and complex groups based on a well-known framework [14]. In the baseline study, the simple group stands for the “old requirements features”, and the complex stands for “new complex requirements”, represented in the chosen framework. Table 2 summarized the RE features.

Table 2. Requirements features description.

Requirement feature	Feature group	Definition
Volume	Simple	The size of the requirements pool influencing the scope of the work
Veracity	Simple	To what extent requirements express the needs of the stakeholders and are consistent
Volatility	Complex	The rate at which the requirements change over a given period of time
Vagueness	Complex	To what extent designers and other stakeholders understand the content and consequences of the requirement
Variance	Complex	The variation in the design scope and consequences of the requirement pool and the heterogeneity of design components involved
Velocity	Complex	The rate at which requirements are changing over time

The 6 V's of requirements engineering concept, proposed by [14], was investigated for each project in order to analyze whether the companies distinguish how complex the RE activity is.

All the aspects got the following rating based on the questionnaire:

- There was need for consideration indicated, the need is marked as High – 2
- There was need for consideration indicated, the need is marked as Low – 1
- There was no need for consideration indicated or the team did not take the aspect into account - 0.

3 Results and Discussion

The results, which were derived from the questionnaire are represented in the Tables 3, 4, 5, 6, 7 and 8 for each company.

The considerable complex RE feature among the companies, which practice Agile approaches, appeared to be the volatility of requirements, which stands for the rate at which the requirements change over a given period of time, and is close to velocity in its meaning. The requirements volatility have been previously indicated as the key aspect to investigate project complexity in one row with team composition and performance; urgency and flexibility of cost, time and scope; clarity of problem and many other project aspects [15]. The rate of this complex feature consideration can be also explained by its direct influence on project constraints and, as a result, high attention to this aspect on an intuitive level [16]. The previous researches indicate that there is a negative relationship between requirements volatility and software project performance, measured by project completing on time and on budget. There is a clear indication that the more unstable requirements become the more likely it is that the project will be completed behind schedule and over budget [17].

Table 3. RE features recognition in project 1.

Requirement feature	Need for consideration	Level	Rate
Volume	There are the high level tasks and a number of smaller tasks which constantly refreshes, there more than 80 tasks in the backlog. It has to be planned to have a bug picture of the project and plan it	High	2
Veracity	Reaching the same level of understanding and correct formulation of the requirements by continuous communication. You have to pay attention to it in order to avoid doing extra job	High	2
Volatility	15–20% of requirements change after getting to production, because the user understands better what he wants. The key point here is to deliver the basic version as soon as possible	Low	1
Vagueness	The connections are always checked carefully to ensure integration when the requirement is implemented. It might happen in 5–7% of implemented requirements. Very urgent aspect, because there were no analyst who check the comprehensiveness of the requirement	High	2
<i>Variance</i>	<i>We did not pay much attention to this aspect</i>		
Velocity	The company is continuously growing and the needs are growing over time	Low	1

Table 4. RE features recognition in project 2.

Requirement feature	Need for consideration	Level	Rate
Volume	There were about 120 high level requirements from one business direction and 60–70 from another. This is highly important aspect to consider	High	2
Veracity	The business requirements are continuously negotiated to reach the same level understanding and represent the needs of stakeholders	High	2
<i>Volatility</i>	<i>We do not take it much into consideration</i>		0
Vagueness	The work is organized based on specification, everything is clear	Low	1
<i>Variance</i>	<i>The aspect is not clearly perceived, but all the processes, which concern the variation of the design scope, are regulated</i>		0
Velocity	For the changes after a period of time there are prescribed procedures to manage changes, the aspect addressed	Low	1

As for velocity of requirements, it seems to be addressed among all the studied companies, despite the fact that its meaning is considerably close to volatility. This aspect was indicated in previous studies as highly important for being aligned with changing and evolving business needs of users. It was stated that evolutionary complexity of the systems results from the evolution of user requirements and needs, named

Table 5. RE features recognition in project 3.

Requirement feature	Need for consideration	Level	Rate
Volume	Initially there was a vast amount of requirements, they were all tracked. This refreshing backlog gave us the understanding of the project scope	High	2
Veracity	All the meeting protocols were written down in order to keep all the desired requirements. We had only face to face communication with the users to get deeper understanding	High	2
Volatility	The tasks were constantly refreshing. We totally engaged users in the implementation right from the beginning, so we had to work with it	High	2
<i>Vagueness</i>	<i>Did not pay much attention to this aspect</i>		0
<i>Variance</i>	<i>Did not pay much attention to this aspect</i>		0
Velocity	The project was fast, express-implementation, so most concentration was on volatility	Low	1

Table 6. RE features recognition in project 4.

Requirement feature	Need for consideration	Level	Rate
Volume	The number of requirements were derived from the accounting documentation lines. The aspect is considered as important, because it helps to get the system structure and internal interaction	High	2
Veracity	Highly urgent aspect, because it is important understand the real need in the requirement and be able to propose solution	High	2
<i>Volatility</i>	<i>We do not take it much into consideration</i>		0
Vagueness	Very important in one row with Veracity, here it is also important to have the person in the team with the knowledge of context (of customer’s business)	High	2
Variance	Not much important, can be achieved through constant communication	Low	1
Velocity	We worked with it. Everything changes and you should work with it. You need to organize the contracting in a correct way and work	Low	1

evolved complexity, and there is strong need for the software to be co-evolved with it [17]. The reason why it is addressed more carefully than the volatility aspect, no matter which approach the company practices, could be the issue of long-term vision. This means that Waterfall-oriented companies seem to seek for being aligned with business needs, but for the larger time-horizons. They do not tend to be focused on following-up with changing business needs within specific project, but still understand importance of this issue.

Table 7. RE features recognition in project 5.

Requirement feature	Need for consideration	Level	Rate
Volume	There were about 400–500 tasks on the board. This was the highly important aspect	High	2
Veracity	The requirements were rarely understood incorrectly, because it was more technical project, but we did pay much attention to it	High	2
Volatility	The process model changes, everything changes, many underwater stones, we had to react fast, because there were many ongoing projects in parallel. The aspect though is less important, because the project was more technical	Low	1
Vagueness	It often happens when the requirement implementation affects somehow other requirements and we control it. One of the most urgent aspects	High	2
Variance	Very important aspect to take into consideration to get the comprehensive product	High	2
Velocity	We prepared a process for changes when the product was ready. You just had to follow it	High	2

Table 8. RE features recognition in project 6.

Requirement feature	Need for consideration	Level	Rate
Volume	There were about 15 high level requirements, we track the amount of them	High	2
Veracity	The requirements are often perceived in a wrong way, but explained afterwards why they have been executed in this way	High	2
Volatility	All the changes are welcome on the iterative development after delivering the MVP. The changes can be done within 1 spring	High	2
Vagueness	We write user-stories to get comprehensive understanding of requirement place and influence	High	2
<i>Variance</i>	<i>We do not take it much into consideration</i>		0
Velocity	The product stays on our support at 25–30% of it are changing, because the needs are changing	High	2

Simple RE features are all addressed by the companies, which practice Agile or Waterfall approaches. This might be potentially due to the fact that their influence on project scopes is much easier to diagnose than for the complex RE aspects.

4 Conclusion

The research provided an overview of the way how companies perceive the complexity of problem within software development project and suggested a linkage between this perception and the project management approach choice. It was argued that simple

factors and aspects of requirements do not affect the choice between Agile and Waterfall, but are more likely to be addressed by different companies. Though, the analysis of more complex aspects revealed the potential difference between Agile-oriented and Waterfall-oriented companies. It seems that both types tend to pay attention to changing business-needs and importance of being up-to-date with them, but companies, which tend to choose Agile approaches, seem to address this issue within short-term and long-term periods.



The key limitation of the current research appeared to be a number of the analyzed companies, which could be expanded for the future research in order to provide more comprehensive analysis of the factors, affecting the choice of software project management approach.

References

1. Nuseibeh, B., Easterbrook, S.: Requirements engineering: a roadmap (2000)
2. IEEE Standards Committee: IEEE std 610.12-1990 IEEE standard glossary of software engineering terminology. Online Httpst-Dards IEEE Org reading IEEE Std public descriptions 61012 (1990)
3. Robertson, S., Robertson, J.: Mastering the Requirements Process: Getting Requirements Right. Addison-wesley, Boston (2012)
4. Ilin, I., Iliashenko, O., Levina, A.: Application of service-oriented approach to business process reengineering. In: Vision 2020: Innovation Management, Development Sustainability and Competitive Economic Growth, Spain (2014)
5. Westfall, L.: Software requirements engineering: what, why, who, when, and how. *Softw. Qual. Prof.* **7**(4), 17 (2005)
6. Sommerville, I., Sawyer, P.: Requirements Engineering: A Good Practice Guide. Wiley, New York (1999)
7. Ilin, I., Frolov, K., Lepekhin, A.: From business processes model of the company to software development: MDA business extension. In: Sustainable Economic Growth, Education Excellence and Innovation Management Through Vision 2020. Austria (2014)
8. Fitsilis, P.: Comparing PMBOK and Agile project management software development processes. In: Advances in Computer and Information Sciences and Engineering. Springer (2008)
9. Chow, T., Cao, D.: A survey study of critical success factors in agile software projects. *J. Syst. Softw.* **81**(6), 961–971 (2008)
10. Macheridis, N., Nilsson, C.: Managing project complexity-a managerial view (2004)
11. Camci, A., Kotnour, T.: Technology complexity in projects: does classical project management work? *PICMET* **5**, 2181–2186 (2006)
12. Christoph, A., Konrad, S.: Project complexity as an influence factor on the balance of costs and benefits in project management maturity modeling. *Proc.-Soc. Behav. Sci.* **119**, 162–171 (2014)
13. Ilin, I., Kalinina, O., Iliashenko, O., Levina, A.: IT-architecture reengineering as a prerequisite for sustainable development in Saint Petersburg urban underground. *Proc. Eng.* **165**, 1683–1692 (2016)
14. Jarke, M., Lyytinen, K.: Complexity of systems evolution: requirements engineering perspective. *ACM Trans. Manag. Inf. Syst.* **5**(3), 1–7 (2015)

15. Araujo, A., França, C., de Moura, H.: Complexity within software development projects: an exploratory overview. *Gest. Org. Rev. Eletrôn. Gest. Organ.* **13** (2015)
16. Ferreira, S., Collofello, J., Shunk, D., Mackulak, G.: Understanding the effects of requirements volatility in software engineering by using analytical modeling and software process simulation. *J. Syst. Softw.* **82**(10), 1568–1577 (2009)
17. Zowghi, D., Nurmuliani, N.: A study of the impact of requirements volatility on software project performance. In: Ninth Asia-Pacific Software Engineering Conference, pp. 3–11 (2002)

Human Capital Management as Innovation Technologies for Municipal Organization

Olga Kalinina^(✉)  and Olga Valebnikova 

Peter the Great St. Petersburg Polytechnic University,
Politechnicheskaya st., 29, 195251 St. Petersburg, Russia
olgakalinina@bk.ru

Abstract. Effective human capital management system is one of the key factors of business success of any enterprise. Human capital is very important part of each person. During the whole life, people invest in it, both consciously and unconsciously. To become successful, people have to develop in professional way. Municipal enterprises show less ways for professional development, and consequently have more problems with competitive staff. Article defines ways for improvement of human capital system in municipal enterprise to attain competitive advantages and grow effectiveness.

Keywords: Management · Innovation technologies · Municipal organization

1 Introduction

Modern tendencies such as globalization, innovative economy, integration, technological evolution motive countries and companies to finding new ways of keeping competitive advantages. In this regard, human resources play key role in successful performance, an employee with high level of personal competency. Humans became an eligible asset and now considered in terms of human capital. Concept of human capital, generally, is a mix of human and capital.

Human capital is a main factor of professional success. Career growth is strictly dependent from human capital.

Companies use different methods of recruitment, some of them recruited staff with existing and suitable skills, others are developing the system of education and training for newly arrived staff. All this is done in order to use the staff as a competitive advantage.

In an era of information technology, human capital is becoming a desirable factor. To create new advantages, the search for new factors that may be increased or improved begins. Human capital is precisely one of the most promising factors. Human resources - one of the most important assets of the enterprise. Human capital determines the successful development of other constituent elements of the company. Human capital - is the main element that affects the increase in intellectual capital and the prosperity of the entire company.

2 Materials and Methods

Human capital for the individual - the most important and valuable asset. Human capital - is a set of skills, knowledge, abilities and experience that allows a person to occupy a place in the company, in the community, to position themselves on one level or another. Various scholars in different periods saw different concepts of origin and the definition of human capital. For the first time the term was used by Theodore Schultz [1]. It was he thinking, that there is a set, which later included the experience, knowledge and skills, which is the human capital. For his achievements, in 1979 T. Schultz received the Nobel Prize in economics.

Initially, under the human capital we understood only professional skills, that is, the concept of human capital has started to develop in terms of its effectiveness in relation to the organization. Further, various scientists have formed their own idea, consider their theories.

The concept of human capital attracts a lot of attention in modern history. Human capital was defined as knowledge, skills, abilities, skills and acquired traits in manufacturing by Goode in 1969 [2]. As can be seen, the author is close to the definition of human capital to its ancestor, Theodore Schultz. The second half of the XX century affects the unilateral perception of human capital as a set of economic characteristics acquired during operation.

Gary Becker, another economist who won the Nobel Prize in 1992 in the field of economics, and a follower of Theodore Schultz, in his work "Human capital", 1964 defines human capital as a store of knowledge, motivation, skills that can be extended through investments in education, work experience, health, information retrieval [3]. Gary Becker developed the theory of Schulz and proved the effectiveness of investments in human capital and formulated an economic approach to human behavior.

Bontis in 1999 defined human capital as the human factor in the organization, education, skills and abilities that give the organization its distinctive character [4]. Thus, the author speaks about the place of human capital in the organization. As known, human capital represents a set of personal qualities of the worker, his opportunities to create additional value for the organization. Ultimately, the total human capital of all employees generates intellectual capital.

Davenport in his research in 1999 suggests that human capital consists of "intangible" that workers provide for their companies [5]. The author considers the human capital as an integral part of the organization, that creates benefits for it, and in total affects the activities of the organization.

According to Blundell (2000), there are two major components of human capital: the initial abilities (congenital or acquired) and skills acquired through formal education or training on the job [6]. Thus, the author combined the concept of innate qualities and learning by creating an aggregated concept which holds a fairly wide range of elements.

Skills represent the individual capacity to facilitate the production of an argument in the production function, defined Bowles in 2001 [7]. Here, he returned to the idea of the original concept of human capital. He talked about human capital as a power that contributes to the development of the organization.

Ishikawa and Ryan (2002) suggest, the stock of human capital is what defines income of people [8]. The authors have moved away from defining the elements of human capital, and considered it in terms of impact, the results of what he gives to person.

Armstrong in his book “Human resource management practice” in 2006 defined human capital as a universal human possibility, either congenital or acquired, the value of which can be increased with the help of the necessary investment [9]. Armstrong didn’t combined human capital with organization, on the contrary, he spoke about human development. By investing in training, education, and even a hobby, a person learns and forms its own human capital. It creates for individuals those features and advantages which will position themselves in society.

From the review of the concepts, visible evolution of human capital can be seen. Initially, under the human capital only the knowledge and skills required for the company were meant, now human capital refers to the whole range of traits and characteristics, knowledge and skills, experience and capabilities that define a person.

To conclude, consideration of human capital is possible in terms of the different areas and levels (Table 1). And in each time period, there was a specific vision of human capital, see Table 2.

Table 1. Level and the direction of human capital [10].

Level/direction	Politics	Economics	Sociology	Psychology
Individual	Increase in skill level	Increase in income	Strengthening society positions	Strengthening in self-assurance
Enterprise level	Compliance with external environment	Increase of competitiveness	Strengthening of company’s image	Improvement of working conditions
State level	Creation of labor market and HR policies	Allocation of education and training related costs	Implementation of lifelong learning concept	Idea of dynamic country and society

Table 1 illustrates the value of human capital at all levels as well as the ratio of each level with a certain direction. Thus, it is clear that at the individual level, human capital is the direction of improving the personal traits and characteristics, skills and knowledge of an individual, in terms of the level of the state, it covers a fairly wide range of problems to be solved on a global level, and is not inherent in one person. In economic terms, the most interesting for consideration is the enterprise level. There, human capital continues to strengthen its position for independent person, but also works to benefit the organization, which in the modern world is the main objective of increasing human capital.

These table illustrates the evolution of approaches to the management of human capital on the initial review of its employees as costs to date evaluation activities based on indicators. Like any science, management is evolving and taking new forms, and

Table 2. Main approaches to human capital concept.

	Calculation of costs for HR policy, beginning 1960s	Calculation of human capital, middle 1960s	Management of human capital, end 1970s	Strategic management, beginning 1990s
Main representatives	E. Mayo, T. Schultz	G. Becker	D. Kendrick	E. Sveiby
Characteristic	The monetary approach to recruitment	The financial value of the human capital of the organization	Education and dissemination of knowledge - the main internal administrative strategy	The total of financial performance, human capital, internal business processes, customer relationships and innovation
Accepted methods	Utility analysis	Human resource accounting	Organization of education, knowledge management	Balanced scorecard
Reporting	Counting the cost benefit	Financial reporting	Managerial accounting	Cross-functional performance indicators

human capital management started their way back in the 1960s and is becoming more powerful tool in the hands of companies to gain competitive advantage.

This article is considering human capital within the state level. For non-profit organizations which activity is directed towards achievement of the social, charitable, cultural, educational, scientific and management goals, towards the development and increase of the human capital quality, health of its citizens, development of fitness and sports, meeting of the spiritual and other non-material needs of citizens, protection of rights, legal interests of citizens and organizations, resolution of disputes and conflicts, provision of legal assistance as well as other goals directed towards achievement of creation of public benefit.

In Russian Federation Concept of human capital is not considering to be crucial, but experience of transnational companies has shown that the future of competence is people and specifically talents.

In this connection, talent management as a tool to increase human capital is highly important.

Deficit in qualified staff is caused by high speed of globalization, informatization, tough competition between industries and sectors, these factors stimulate headhunting. It's time for a new war for talent, but the methods of struggle for the best employees will be completely different.

The most frequent reason for the lack of qualified and talented workers is a problem of generations:

- young qualified personnel is less Interested in traditional employment and see themselves as free agents, and it is difficult to adapt to such an interaction scheme for companies management. This problem is obvious in municipal enterprises, as

young specialists don't assess this field as attractive. Municipal enterprises involve high rate of bureaucracy, not high salaries and less opportunities to grow;

- lack of people with the necessary skills for new occupations, is perceived as the most acute shortage in the market.

Today, not all companies unreservedly believe that standard practices of talent management as part of human capital management system, based on the search and retention of employees with high productivity, contribute to improving business performance. Analysis of the practice of followers of the “war for talents” strategy showed that the past 15 years did not lead to an increase in the performance of companies and did not improve their ability to survive.

Only 25% of the companies can be called successful in their industry, and a third of organizations has already completely ceased to exist.

It is time to move on to a new, more holistic strategy for managing talent:

- It is important to focus on the talent development needs of all employees in accordance with the business strategy and conditions.
- The strategy of attracting employees with high potential to the detriment of the interests of the team puts the business at risk.

The three most successful methods of combating the scarcity of necessary knowledge and skills:

- to enlist the support of management and ensure its active participation in solving this issue together with HR specialists;
- focus on developing a clear career path for employees;
- apply a holistic approach to talent management for all employees in the organization.

It is very difficult to quantify the non-financial benefits that the company derives from the effective operation of the HR function. However, new technologies allow gathering accurate data and conducting a thorough analysis, on the basis of which the HR-service will subsequently be able to make decisions that positively influence the business.

Instead of following industry trends or adapting ready solutions, companies should strive to:

- a global view of the search and retention of talents;
- development of talent management strategies taking into account the characteristics of its product, market and business objectives;
- application of a more thoughtful system approach, measuring return on investment;
- application of new data analysis capabilities for assessing performance and improving HR-practitioner;
- monitoring and evaluating talent management strategies and adjusting them to improve outcomes, meet future business demands, and create opportunities for staff to contribute in the company's business [11].

The business practice in municipal enterprises is under though tension, as Government seeks way to improve performance and harden regulation. Also, there is a problem of competitive employees, as compared with business structures, they are either less

benefits or less opportunities for employees in municipal organizations. In this connection, human capital management is crucial for improving performance of these enterprises.

To adopt system of human capital management, a program was developed. The program is the following.

1st stage. Assessment. To implement any innovation technology, first current state of the object should be assessed. The following actions should be made:

- analysis of business processes in the organization and definition of human requirements for each process.
- analysis of current human capital for each process by different classifications (see Table 3).

Table 3. Analysis of human capital.

Classification feature	The evaluation methodologies considered (evaluation indicators)
Human capital structure	In the structure of human capital, two components are distinguished: the basic and developed human capital, which differ in the methods of formation, content and, as a consequence, in the methods of evaluation used [12]
Depreciation by type of asset	Considers human capital as an inseparable intangible asset of the second category, accordingly applying to its assessment methods for valuing intangible assets [13]
Human capital assessment	It is connected with an estimation of amortization of each kind of investments into the human capital multiplied for the time of their real turnover. Asset models; Assume the accounting of capital expenditures (by analogy with fixed capital) and its depreciation [14]
Type of assessment: quantitative and qualitative	Methods are divided into monetary (monetary valuation) and non-monetary (qualitative assessment of human capital). One of the basic monetary methods is the model of net added value [15]
Kinds of assessment	An economic assessment is an estimate of the incomes generated by a human capital (individual); Price estimation of human capital by the volume of investments; Reflection of the total value in the balance sheet of the firm (enterprise). Integral assessment of human capital includes both natural and value indicators of human capital assessment [16]
Type of costs incurred	The method of assessing human capital based on the calculation of costs for human capital; Method of determining initial and replacement costs for staff; Method of measuring the individual value of an employee, etc. [17]
Type of income received	Utility models. Allow to assess the economic consequences of changes in the labor behavior of employees as a result of certain measures, as well as the ability of the employee to bring a greater or lesser surplus value in the enterprise [18]

As a result of assessment, organization will clearly define needs and potential for growth and development.

2nd stage. Implementation. After needs of organization defined, system of human capital management should be implemented. Implementation implies regular assessment of human capital, talent management, improve of motivation system, creation of non-monetary benefits for employees (professional development, ways to self-realization of employees), coaching, intellectually-oriented consulting.

3d stage. Assessment. System should be assessed at every stage and with its development, This assessment should be made regularly, and planed for future periods. [19, 20] Each Technology needs planning, to define results and pursuing them. Only comprehensive evaluation will lead to success.

3 Conclusions

Implementation of innovation requires comprehensive approach within the organization. Human capital management is poorly developed in municipal organizations, so effectiveness of its improvement will be obvious on very early stages. The program of implementation, as proposed in this paper will create clear structure for actions to be taken by top-management.



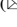
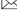

Specific methods of human capital management are beyond of the scope of this article, as it requires deep approach and analysis of organization's needs and opportunities.

References

1. Schultz, T.: Human Resources (Human Capital: Policy Issues and Research Opportunities). National Bureau of Economic Research, New York (1972)
2. Goode, R.: *Am. Econ. Rev.* **49**(2), 147–155 (1959)
3. Becker, G.: Human Capital: A Theoretical and Empirical Analysis, with Special Reference to Education. National Bureau of Economic Research, New York (1975)
4. Bontis, N.: *The Strategic Management of Intellectual Capital and Organizational Knowledge*. Oxford University Press, New York (2002)
5. Davenport, T.: *Human Capital: What It is and Why People Invest It*. Davenport and Jossey-Bass Inc., San-Francisco (1990)
6. Blundell, R.: *Effective Organisational Communication: Perspectives, Principles and Practices*. Piter, Saint-Petersburg (2000)
7. Bowles, S., Gintis, H.: *Walrasian Economics in Retrospect*. ID GU HSE, Moscow (2001)
8. Ishikawa, M., Ryan, D.: *Econ. Edu. Rev.* **21**(3), 231–243 (2002)
9. Armstrong, M.: *A Handbook of Human Resource Management Practice*. Kogan Page, London (2003)
10. Singh, A., Rastogi, L.: *Delhi Bus. Rev.* **2**(1), 1–14 (2001)
11. Michaels, E., Handfield-Jones, H., Axelrod, B.: *The War for Talent*. Harvard Business School Press, Brighton (1997)
12. Stukach, F., Lalova, E.: *Omsk Sci. Bull.* **4**(111), 32–39 (2012)

13. Leontiev, B., Mamadzhanov, Kh.: Management of intellectual property in the enterprise, Yekaterinburg (2011)
14. Tuguskina, G.: Basic approaches and methods for assessing human capital in business value (2009). http://www.Rusnauka.com/20_AND_2009/Economics/49162.doc.htm. Accessed 29 Aug 2017
15. Noskova, K.: Actual issues of economic sciences. Summer, Ufa (2013)
16. Milost, F.: Eur. Sci. J. **1**, 23–28 (2014)
17. Kastyulina, Yu.: Analysis of methods for estimating the value of human capital of economic entities (2013). <http://economics.ihbt.Ifmo.ru/file/article/19.pdf>. Accessed 29 Aug 2017
18. Cracow, I.: Econ. Anal. Theor. Pract. **19**, 41–50 (2008)
19. Ilin, I., Koposov, V., Levina, A.: Life Sci. J. **11**(11), 265–269 (2014)
20. Shilova, L., Soloviev, D., Timatkov, V., Adamtsevich, A.: About the Territorial Potential of the Construction of Battery-Charging Stations for Autonomous Electric Motor Vehicles in the Regions. In: MATEC Web of Conferences, vol. 73, art. no. 02017 (2016). <https://doi.org/10.1051/mateconf/20167302017>

Financial Literacy as a Driver for Responsible Energy Consumption

Mariia Sigova , Inna Kruglova , Marina Vlasova  ,
and Irina Shashina 

International Banking Institute,
Nevsky pr., 60, St. Petersburg 191011, Russia
vms68@yandex.ru

Abstract. The article examines the linkages between the interrelation of financial literacy of the population in questions of household use of the electric power and energy efficiency. This relationship is illustrated by the example of different countries grouped by the standard of living of the population. To classify countries that fall into the sample, the happiness index was used. The analysis was carried out for such indicators as GDP per unit of consumed electricity, consumption of renewable electricity and electricity consumption (kWh per capita), and financial literacy of the population in points. It is noted that a higher correlation between energy consumption and financial literacy is observed in countries with a higher standard of living. The author gives recommendations on the basis of the revealed regularities for a comprehensive impact on the level of household energy saving by including the information on the possibility of reducing household expenditure by the way of saving energy in the financial literacy programs.

Keywords: Responsible energy consumption · Energy efficiency
Financial literacy · Happiness index · Renewable energy consumption

1 Introduction

The problem of energy saving is one of the most urgent in the modern world. Despite the scientific and technical progress and the introduction of energy-saving equipment and technologies in all sectors of the economy of many countries the irrational use of resources has led to depletion of world reserves and had actualized the need for alternative energy sources. The need for more efficient use of energy sources is also noted at various levels of government. Particularly the Sustainable Energy for All Initiative (SE4All) with the participation of the World Bank aims to one of three goals by 2030 and calls for doubling the rate of energy efficiency.

For Russia, this problem is also relevant because the energy saving potential of Russia is colossal, but it is not fully used, which has led to a high energy intensity of Russia's GDP. Increasing of the energy efficiency of the Russian economy by rationalizing the consumption of heat and energy resources, by the use of energy-saving technologies and equipment is one of the main priorities of the Energy Strategy of Russia for the period up to 2020, approved in 2003 [1]. Within the

framework of the government's anti-crisis measures program for 2009, the policy of increasing the energy efficiency of the economy was included in the list of seven main priorities of the federal executive power. It should be noted that in times of crisis, energy efficiency can be increased mainly through energy saving.

The issue of energy intensity and energy efficiency in the sphere of production is raised up quite often. Energy conservation in the sphere of consumption, which is also an important reserve for energy saving, is studied much more rarely in the scientific literature. The population is affected by a variety of factors: from its actual availability and cost up to mentality and cultural traditions. The issue of the need to improve the financial literacy of the population is just as obvious, as it contributes to raising the standard of living of the population, as well as to increasing the level of citizens' responsibility for the decisions making and, accordingly, contributes the reducing of the state's expenses for social support to citizens who find themselves in a difficult life situation.

In this regard, we formulated the hypothesis that financial literacy stimulates energy efficiency, primarily by improving the level of energy saving by the population.

The aim of the study is to assess the impact of financial literacy on the energy efficiency and energy intensity. The object of the study is the level of financial literacy of the population, the subject of research is the relationship between financial literacy and energy efficiency.

2 Materials and Methods

The study carried out a comparative analysis of the financial literacy of the population, estimated in the framework of The Organisation for Economic Co-operation and Development «International Network on Financial Education» OECD/INFE International Survey of Adult Financial Literacy Competencies in October 2016 and data on consumption of the electricity, presented on the World Bank's website [2–5].

Since a different standard of living implies a fundamentally different amount of energy consumption and sometimes even the access to electricity, it became necessary to group countries by their standard of living. We used the happiness level index for the classification of countries, since not only economic indicators such as the GDP level was taken into account, but also public opinion polls were taken into account. Since the active use of electricity in everyday life significantly affects the level of comfort and, as a consequence, the assessment of the standard of living. Based on the happiness index, the surveyed countries were divided into four groups with an index above 7, ranging from 6 to 7, from 5.5 to 6 and below 5.5. In order to bring the analyzed data into a comparable form, we calculated the deviations from the average values of the indicators for the groups of studied countries.

The analysis of the improving financial literacy practice in different countries was conducted to develop recommendations aimed at improving energy efficiency.

3 Results

Of the total sample of 30 countries in which the OECD carried out a study of the financial literacy level, South Africa and the British Virgin Islands were excluded due to the absence for these countries of the complete data required for further research. The indicators of the overall assessment of financial behavior (in points), as well as the assessment of financial behavior, the fact of managing a family budget were chosen for the analysis of financial literacy. At the same time, in order to assess the energy efficiency of the economy, only the data of the 2014 year were taken into account; as not all countries included in the OECD study provided the necessary information in 2015. The indicators such as GDP per unit of energy, the consumption of renewable electricity and electricity consumption (kWh per capita) were selected for analysis (Tables 1 and 2).

As a result of the analysis, there was no significant correlation between the indicators of financial literacy and electricity consumption, except for a high level of energy consumption per capita in countries with a high level of financial literacy. In our opinion, this is largely explained by the fact that countries with a high standard of living are characterized by a higher level of energy consumption, as well as a high level of financial literacy. We separately analyzed the correlation of financial literacy and energy efficiency among groups of countries to exclude the influence of this factor (Table 3).

The highest correlation between the studied indicators is observed in the group of countries with the highest index of happiness. At the same time the extremely strong negative correlation is observed between the population, managing the family budget and GDP per unit of energy consumed. This dependence, in our opinion, is due to the fact that a significant number of countries in this group are located in the climatic zone, which requires additional costs for heating and electricity to ensure a comfortable life (Finland, Canada, Norway, etc.). At the same time, a high level of financial literacy of the population directly contributes to the raising of the well-being level and enables the disposal of large amounts of resources. This explains the relatively high correlation of financial literacy with the consumption of electricity per capita.

Also in countries with a fairly high happiness index (6 to 7), there is a significant correlation between the overall level of financial literacy and the electricity consumption per capita. This state of affairs, in our opinion can be explained on the one hand, by the high standard of living and the corresponding active use of various devices that consume electricity in countries such as France and the UK, on the other hand, by the active use of financial instruments by the population and, accordingly, by a high level of financial literacy. At the same time, in a number of countries of this group, less economically developed, such as Malaysia, Thailand and Brazil, the level of financial literacy is much lower and at the same time there are high energy consumption indicators, which support the hypothesis that the level of financial literacy is generally positive affects the energy efficiency.

In the group of countries with an index of happiness from 5.5 to 6, it should be noted a significant correlation between the proportion of respondents who are managing the family budget and GDP per unit of energy consumed. In our opinion, this

Table 1. The evaluation of financial literacy, energy consumption and energy efficiency

Country	Mean total score of the financial literacy level (in points)	Share of respondents managing the family budget	GDP per unit of energy use (constant 2011 PPP \$ per kg of oil equivalent)	Renewable energy consumption (% of total final energy consumption)	Electric power consumption (kWh per capita)	Happiness index
Albania	12.7	71%	13.25412	38.6895	2305.735	4.644
Austria	12.4	64%	7.427945	31.89298	2688.489	4.286
Belarus	14	72%	12.79111	3.455932	4662.601	5.195
Belgium	12	70%	10.62404	33.64664	3.714.383	5.293
Brazil	12.4	25%	10.37647	10.36064	3965.958	5.324
Canada	12.6	64%	9.285.983	3.130.499	2242.828	5.336
Croatia	14.4	61%	26.76559	1.792585	6073.022	5.472
Czech Republic	12.5	78%	12.11436	11.57817	2565.515	5.5
Estonia	11.7	77%	5.929137	9.038057	3679.979	5.569
Finland	13.4	43%	5.869691	25.24914	6732.367	5.611
France	14.4	77%	6.319.521	2.838098	10563.69	5.838
Georgia	13.3	90%	10.23593	40.23606	3507.405	5.85
Hong Kong, China	13.5	65%	10.9964	28.07217	3821.145	5.902
Hungary	12.2	50%	5.113004	16.58715	6602.658	5.963
Jordan	11.6	66%	9.843187	30.49879	3971.8	5.973
Korea	12.1	86%	8.153519	4.769774	4646.446	6.084
Latvia	12.8	77%	7.526654	23.58597	4228.861	6.424
United Kingdom	14.9	85%	10.22852	13.13264	6944.457	6.442
Malaysia	12.6	40%	7.437745	12.75267	6258.891	6.609
Netherlands	12.1	43%	10.35135	41.81093	2577.826	6.635
New Zealand	13.1	53%	13.67853	7.294445	2836.407	6.714
Norway	14.3	47%	8.783782	36.54404	7693.915	6.891
Poland	14.2	31%	11.71781	35.78393	8360.519	7.006
Portugal	14.4	59%	7.599594	30.86475	9026.321	7.314
Russian Federation	14.6	63%	5.454163	22.57581	15541.5	7.316
Thailand	13.4	40%	10.5579	5.668.454	6712.775	7.377
Turkey	14.8	63%	6.279622	41.19126	15249.99	7.469
United Kingdom	14.6	33%	11.30997	11.54736	22999.93	7.537
Average value	13.25	60%	9.858059	20.52102	6434.836	6.128

dependence indicates that the management of the family budget encourages to monitor the use of electricity for domestic needs more carefully, but also in the long term it promotes to transfer this approach to the sphere of the entrepreneurship. A striking example in this group of countries is Latvia, in which 90% of households manage a family budget (which is 31.87% higher than the average for the group), while the GDP per unit of energy consumption in this country is 23.29% higher than in this group of

Table 2. The correlation of indicators of financial literacy and energy efficiency

	GDP per unit of the consumed energy	Renewable energy consumption (% of total energy consumption)	Electric power consumption (kWh per capita)
Total score of the financial literacy level (points)	0.159801	-0.01101	0.677495
Share of respondents managing the family budget	-0.03237	-0.04274	-0.29198

Table 3. The correlation of indicators for groups of countries financial literacy and energy efficiency

	GDP per unit of the consumed energy	Renewable energy consumption (% of total energy consumption)	Electric power consumption (kWh per capita)
Countries with a happiness index above 7			
Total score of the financial literacy level (points)	-0.51604	0.581982	0.690933
Share of respondents managing the family budget	-0.98382	0.420565	0.0158
Countries with an index of happiness from 6 to 7			
Total score of the financial literacy level (points)	0.180351	0.036893	0.703429
Share of respondents managing the family budget	-0.15578	-0.48659	0.09097
Countries with an index of happiness from 5.5 to 6			
Total score of the financial literacy level (points)	-0.01304	-0.05329	0.595375
Share of respondents managing the family budget	0.491118	-0.00594	-0.29822
Countries with an index of happiness below 5.5			
Total score of the financial literacy level (points)	0.797698	-0.64171	0.753078
Share of respondents managing the family budget	0.071946	0.284343	-0.11488

countries, the indicator of renewable energy consumption is 96% higher than the average, and the per capita electricity consumption index is 32.3% lower than the average for this group. In the Russian Federation only 50% of households manage a family budget (26.74% lower than in the group), while the GDP per unit of energy consumption in this country is 38.42 lower than the average for this group, the consumption of renewable electricity is for 19.4 below the average, and the electricity consumption per capita rate is 27.45% lower than the average for this group.

In the group of surveyed countries with an index of happiness below 5.5 the correlation between the level of financial literacy and GDP per unit of energy is much higher, at 0.8. Also there can be seen a significant correlation between the level of electricity consumption per capita, and financial literacy. It should be noted that this group includes quite different countries in terms of economic development: in Hong Kong there is the highest level of financial literacy in the group and the highest GDP per unit of energy consumed, Croatia has the lowest level of financial literacy in the group, with one of the highest indicators for the proportion of households that manage the family budget. This fact is undoubtedly one of the prerequisites for a rather high level of consumption of renewable energy (120.24% higher than the average for the group), and in many respects causes a relatively low level of electricity consumption per capita (37.08% lower than the average by group) (Table 4).

Table 4. Average values by country group of indicators to measure the financial literacy and energy efficiency

Indicators	Happiness index				
	Average sample	More than 7	6 to 7	5.5 to 6	Less than 5
Total score of the level of financial literacy (points)	13.250	14.333	13.129	12.825	12.929
Share of respondents managing the family budget	0.605	0.482	0.616	0.683	0.610
GDP per unit of energy consumed	9.858	8.820	9.451	8.303	12.932
Renewable energy consumption (% of total energy consumption)	20.521	24.605	19.984	20.512	17.567
Electric power consumption (kWh per capita)	6434.836	12981.841	5026.686	5180.570	3664.717

The result of the comparative analysis of the average values of the indicators for groups of countries showed that in countries with a happiness index higher than 7, the deviation of the average value of the electricity consumption per capita for the sample is more than 101.74% from the average per group, which indicates an extremely high level of energy consumption, also caused by a high standard of living. In the group of

countries with a significantly lower level of happiness (from 5 to 5.5) and, accordingly, the welfare of the population, there is the lowest electricity consumption per capita, which is confirmed by previous conclusions. At the same time, in countries with the highest level of happiness, the overall assessment of the level of financial literacy is above the average, which in our opinion is due to the high level of education, including financial and long-term experience in the use of financial instruments. In addition, the proportion of respondents who manage the family budget in these countries is quite low (20.33% below the average for the sample), which, among other things, contributes to a high level of electricity consumption. Also, in countries with a high standard of living, the highest result is achieved in terms of the consumption of renewable energy, which is not only because of a competent energy policy at the national level, but also because of the fact that citizens consciously choose the “green” sources of energy, as evidenced by the performance correlation of financial literacy and renewable energy. In the groups of countries with a lower standard of living (index of happiness from 5 to 6), there is the lowest indicators for the level of financial literacy and the lowest indicators for the consumption of renewable energy (countries with an index of happiness from 5 to 5.5) and GDP per unit consumed Energy (countries with an index of happiness 5.5–6).

4 Discussion

According to experts, energy consumption in apartment buildings, on average, can be reduced by 30–35% solely by increasing the competence of household consumers in matters of energy conservation. All the energy consumed in everyday life, mostly spent on heating the premises, in addition, about 10% is spent on heating water, and on electricity consumption (electrical household appliances and lighting). And each of these areas has significant reserves for energy conservation. But for this, the population should be aware of the need for energy conservation, even if it requires to give up some established habits (Fig. 1).

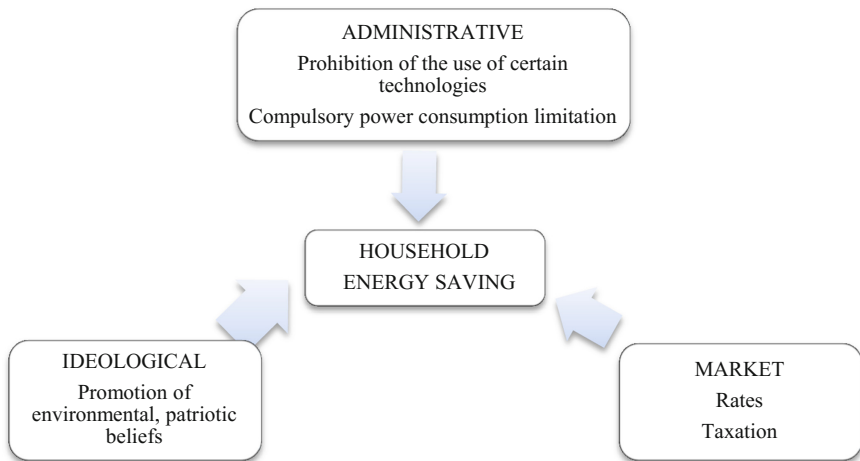


Fig. 1. The factors influencing household energy savings

Thanks to the analysis of factors affecting household energy saving, it became possible to separate into a the groups the factors based on market mechanisms, including differentiation of tariffs for energy consumption, preferential taxation of organizations using energy-efficient technologies [6]. In addition, historically important key role is played by ideological factors, as the population tends to take a much more responsible attitude to energy saving if it realizes the scale of consequences of waste of electricity.

The improvement of the financial literacy of the population will have a complex impact in the framework of two groups of factors: on the one hand, it is necessary to plan the incomes and expenditures, and in this case it is expedient to dwell on the possibilities of reducing the expenditure part of the budget due to:

1. Installations of the counters and use of energy-intensive household instrumentation at nighttime;
2. Reduction of inexpedient energy costs (including the all rooms light, working household appliances, lack of control over charging phones and tablets);
3. More careful use of water;
4. Use of household appliances with a high class of energy saving, etc.

In addition, the improvement of the financial literacy is relevant in terms of energy saving ideology as the way to form the new world citizens responsible for their decisions and able to calculate their effects. In the long term the economical attitude to energy will spread also in to the sphere of business, both in terms of planning the enterprise energy costs, and within the framework of energy saving in the workplace. There by we will get the synergistic effect, and the energy savings will increase in many times.

In our opinion, to implement this integrated approach, it is advisable to start with the senior classes in school. Within the framework of educational or extra-curricular activities in a number of schools lessons on drawing up a family budget are already conducted. In our opinion, already in the framework of these lessons is useful to consider the energy savings not only as a tool for reducing the family budget, but also for the saving of natural resources.

The seniors are a priority target group for a number of reasons:

1. Improving the financial literacy of children is a catalyst for improving the financial literacy of parents, while the students, especially in the European countries, are already beginning to live separately from their families, the majority of students live with their parents.
2. Consumer habits that contribute to energy savings or use it in vain laid in childhood, and as the older the person is, the harder it is to change, even if the need for change is objectively determined.
3. From an organizational point of view of the school children it is easier to gather and convey to them some information, while the majority of workers are not willing to spend the time and energy to receive information, even helpful, after working hours. A significant proportion of students also worked after school and does not always have free time, and sometimes the desire. Of course this information is able and must use the distance learning technologies, but to give the volume of information

available on the network it is need to centrally deliver information about the opportunities to reduce costs through energy savings.

In addition to working with high school students in the study of Economics students of non-core areas and specialties it is also advisable to conduct sessions on management of the family budget and consider them the opportunities to reduce costs through energy conservation.

5 Conclusions

As part of the research on energy efficiency trends we primarily focuses on energy efficiency technologies, production, public policy, and standardization, etc. In this case, we much less considered the human factor, including improving energy efficiency on the part of individuals, while on private consumption accounts for a significant amount of the energy consumption.

In our opinion, while the development of energy efficiency and dealing with financial literacy materials it should do the emphasis on an integrated approach, since electricity specificity is shown including its almost zero elasticity of demand at the current price. That is, when the amount of increase in the price of the current demand for it does not change significantly. This is due to the fact that the power consumption is the foundation of the modern information society and is an important part of everyday life. Consumer usefulness and significance of the use of household appliances is so great, which makes it virtually impossible to avoid the use of already purchased equipment.

Thus, financial literacy is a quite promising direction of activity of authorities, since it helps to improve the level of welfare of citizens and to reduce the burden on the budget of the social benefits at the expense of a more literate population disposition of their resources, as well as to reduce social tension [7]. In our opinion, the improvement of the financial literacy of the family budget necessity and rules will promote energy conservation in the framework of domestic electricity consumption. First of all, it should be implemented at training students in the upper grades - telling them about the rules of building a family budget, and within the framework of the possibility to reduce the energy costs. However, it should be noted that not all of the schools have such an opportunity, so that it is logical to attract Russian educational institutions of higher education for financial literacy in the field of effective energy consumption. The ANO HE “International business institute” can offer everything you need for such training: and educational programs, and opportunities [8].

References

1. Energy Strategy of Russia up to 2035 [electronic resource]. http://www.energystrategy.ru/ab_ins/source/ES-2035_09_2015.pdf. Accessed 09 Mar 2017
2. OECD/INFE International Survey of Adult Financial Literacy Competencies (2016)
3. The World Bank Group Renewable energy consumption is the share of renewables energy in total final energy consumption (2016)

4. The World Bank Group GDP per unit of energy use (constant 2011 PPP \$ per kg of oil equivalent) (2016)
5. The World Bank Group Electric power consumption (kWh per capita) (2016)
6. Vlasova, M.S., et al.: The impact of taxation on the sustainability of machine-building enterprises: a case study. In: Proceedings of the 10th International Conference of DAAAM Baltic, Industrial Engineering, 12–13 May 2015, Tallinn, Estonia (2015)
7. Sigova, M.V., Kruglova, I.A., Kluchnikov, I.K.: Approaches to the classification and measurement of financial security prospects. *Bank. Law* **6**, 29–35 (2016)
8. Sigova, M.V., Kruglova, I.A., Ignatova, A.A.: International standards in vocational education and training for financial services sector to ensure sustainable development and environmental safety. In: MATEC Web of Conferences 15. Ser. “15th International Conference” Topical Problems of Architecture, Civil Engineering, Energy Efficiency and Ecology 2016, pp. 7–17 (2016)

Matrix Tool for Efficiency Assessment of Production of Building Materials and Constructions in the Digital Economy

Tamara Kuladzi¹ , Aleksandr Babkin² ,
and Said-Alvi Murtazaev³ 

¹ Northern Arctic Federal University named after M.V. Lomonosov,
Northern Dvina Embankment, 17, 163002 Arkhangelsk, Russia
kuladzhit@list.ru

² St. Petersburg Polytechnic University named after Peter the Great,
Polytechnicheskaya, 29, 195251 St. Petersburg, Russia

³ Grozny State Oil Technical University named after academician
MD Millionshtchikov, H. Isaeva prospect, 100, 364061 Grozny, Russia
al-vas@mail.ru

Abstract. The construction industry, in the global trends, determines the level of economy development and production capacity increase in the country. The article reveals the modern approaches to the evaluation of the production of innovative construction products. Professor M.D. Kargopolov's universal matrix formula is proposed, allowing to identify the efficiency of production of both the finished construction products, and the effectiveness of the use of intermediate production components, including the transport component of micro- and macro-logistics produced by different economic entities. This approach is especially useful for assessing the efficiency of production in an innovation cluster that is located in a macro-region with different production conditions that affect the cost indices of products produced under market conditions.

Keywords: Transport buildings and structures
Building materials and constructions
Prime cost of building materials production
Production efficiency · Logistics costs

1 Introduction

Currently, the program called “Digital Economy of the Russian Federation” (Program [1]), which was noted on 1.12.2016 in the President’s Message to the Federal Assembly [2] is in effect. The program [1] complements the materials on strategic planning: “Strategy of scientific and technological development of the Russian Federation” [3], “Forecast of scientific and technological development of the Russian Federation for the period until 2030” [4] and other documents, including papers on coordinated development of digital economy in the territory of the countries participating in the Eurasian Economic Union [1].

According to the “Strategy for the Development of the Information Society in the Russian Federation for 2017–2030”, the digital economy is an economic activity where the key factors of production are represented by data in digital form, and “processing large volumes and application of analysis results in comparison with traditional forms of management allow to significantly increase the efficiency of various types of production, technology, equipment, storage, sale, delivery of goods and services” [5].

After the American computer scientist Nicholas Negroponte (University of Massachusetts) introduced the term “digital economy” [6] in 1995, the questions of developing new approaches to the economics of enterprises and organisations reflecting economic activities in the digital space are being constantly investigated. Since they are under the influence of digitalisation, changes in the configuration of global markets are currently being considered, where “many traditional industries lose their significance in the structure of the world economy against the background of the rapid growth of new sectors generating fundamentally new needs” [1]. At the meeting of the “Council for Strategic Development and Priority Projects” on 5 July 2017 in Novo-Ogaryovo, V.V. Putin stressed that “the digital economy is not a separate industry, in fact it is a way of life, a new basis for the development of the system of public administration, economy, business, social sphere, the whole society. And of course, the formation of the digital economy is a matter of national security and independence of Russia, the competitiveness of domestic companies, the country’s position in the world arena for a long-term perspective” [7], and at a meeting on August 15, D.A. Medvedev also noted that “the digital economy is not a project of the Ministry of Communications, the Ministry of Economic Development or any other agency. This is a space for the joint work of all government bodies, business, science and also people, in general, who deal with these problems” [8].

Implementation of the Program [1] by economic sectors is primarily planned in such fields and spheres as healthcare, the creation of “smart cities”, public administration, including control and supervision activities, with the development of specific “road maps”, etc. Thus, in the Ministry of Construction of Russia in accordance with § 5.4.87 [9], digital topographic maps and plans are being developed for planning documentation of territories. In the world practice, the building industry and the industry of building materials and structures determine the level of development of the economy and the country’s productive capacity. During the years of economic reforms in Russia in this industry, there have been changes related to changes in state regulation and the introduction of self-regulation in the activities of construction organizations, etc. At the meeting of the State Council of the Russian Federation “On the development of the construction complex and the improvement of urban development in the Russian Federation” [10] in the speech of the President of the Russian Federation it was noted that construction in Russia represents the most important strategic direction of the country’s development, accounting for almost 6% of the country’s GDP. Simultaneously V.V. Putin pointed out that “the current estimate and regulatory framework has long been obsolete, there are no clear, valid and reliable data on expenditures in both design and construction.” In his report, the Minister of the Ministry of Construction of Russia M.A. Men noted that “for the first time in 20 years, within the framework of the reform of the pricing system, the Government of the Russian Federation decided to implement the state task on developing and updating estimate norms that meet modern

construction technologies and real market conditions and ensuring the reliable value of construction products” [10]. At present, the Ministry of Industry of Russia is responsible for the development of state policy and normative-legal regulation in the sphere of construction materials (products) industry and building constructions field [11]. And according to point 6 of the “Action plan for implementation in the state information system of industry” [12], proposals are being prepared “on the feasibility of developing an information industry subsystem related to the construction materials industry, including an information map concerning the construction materials industry and a section on innovative building materials (products) and constructions and the technologies for their production.”

Therefore, in the management of construction at the present stage, the issues of introduction of digital economy technologies into management accounting for the analysis of the efficiency of production of building materials and constructions, as well as transport and logistics costs for their delivery to construction sites are considered. It should be noted that at the First European Congress (1974) the term “logistics” was for the first time given a new definition, from the point of view of its application in the non-military area, “logistics - the doctrine of systematic planning and control of material, energy, information and passenger flows, and their management” [13]. According to [14] by early 2015, Russia had 226,800 construction organizations, including 223,200 small businesses, of which 86.1% were micro-enterprises with an average strength of up to 15 people, the total scope of work amounted to 5945.5 billion rubles. The share of the gross added value of construction products - 4264.2 billion rubles. in current basic prices or - 5.9%. in the total volume of the Russian Federation’s GDP in 2015. In 2015, the average volume of construction work by medium-sized enterprises was about 6.9%, and by large organizations - 44.6%. This article shows an example of calculation taking into account real production costs for the cost of production of construction products - reinforced concrete slabs with complex binders for the production of innovative products - concrete composites, introduced by FSFEI HPE “Millionshchikov GGNTU”, performed on Professor M.D. Kargopolov’s matrix formula [15–17], considered as an instrument of digital economy [18–20].

2 Statement of a Question

In section III “The Russian Federation in the global digital market” [1] it is shown that our country ranks 41st in the availability and use of the digital economy, and on economic and innovative results of using digital technologies “takes the 38th place with a large gap from leading countries such as Finland, Switzerland, Sweden, Israel, Singapore, the Netherlands, the United States of America, Norway, Luxembourg and Germany”, due to gaps in the regulatory framework for the digital economy and “inadequate environment for running business and innovation and, as a result, a low level of application of digital technologies by business structures” [1]. Professor O.B. Vakhrusheva noted that [21] “managerial accounting is not only an information system and it only exchanges information with other components of management - in large companies it synthesizes the system”, and it is important that information is formed “in optimal time, enabling management decisions at the right time.” With the purpose of

effective development of the enterprise, the author [21] recommended such methods as “economic-mathematical modeling, balance, program-target, fixed and flexible budget” for the subsystem of planning. In the work of Alekseev [22] it was stated that “the mathematization of economic science is the process of introducing mathematical methods into it, one of the forms of formalization understood in the broadest sense as the separation of the form of an object from content”. And to assess the efficiency of production of building materials and constructions, taking into account market factors, especially within the framework of the management accounting mechanism, such economic and mathematical methods that meet the modern requirements of the digital economy are in demand. Therefore, in [18–20, 23–30, 51–52] for calculating the prime cost and production efficiency of building materials, the Professor M.D. Kargopolov’s matrix formula, voiced in the report: “The matrix formula of the production prime cost and unit prices of products (works, services)” at the international conference “Mathematics, economics, management: 100 years since the birth of L.V. Kantorovich” in St. Petersburg State University [15], is recommended.

3 Method and Results of the Study

The Program [1] pre-plans “the establishment of at least 10 national leader companies - high-tech enterprises developing “end-to-end” technologies and managing digital platforms.” In section III “Quality management and management of building materials range” (item 21 [12]), there is a demand factor noted and that is a demand for the analysis of practices of “creating innovative building materials (products) and constructions, including using composite materials, as well as technologies for the production of building materials (products) with the use of production and consumption wastes or raw materials obtained as a result of processing of production and consumption wastes”, and trigger the relevance factor of sectoral action plans and plans of related industries (including mechanical engineering), that are in industrial cooperation aimed for import substitution to include them into the action plan of import substitution of the most prioritised types of products (item 2 [12]), and the development of inventories of innovative and energy-efficient building materials (products), building constructions and technologies for their production (art. 3 [12]). In the Strategy [14], the main consumers of building materials are: “construction industry, building materials industry, road industry, railway track facilities, housing and communal services, oil and gas industry”, etc. [14].

It is important to take into account the information noted in [31] that “the specific weight of the cost of building materials in the total cost of construction and installation works, as well as in many spheres of the economy, and depending on the type of construction work, construction objects can be up to 85% of all estimated costs.”

The activity of the building materials industry, according to [14], is carried out “within the framework of class 08” Extraction of other minerals” of section B “Mining Operations”, class 16 “Wood processing and production of wood products and cork, except furniture, production of straw products and materials for weaving” and class 23 “Production of other non-metallic mineral products” of section C “Processing industries”, determined in accordance with the All-Russian Classification of Economic

Activities OK 029-2014 (NACE Rev. 2)”. In this industry are produced such materials as: cement, small-piece wall materials, prefabricated reinforced concrete structures and products, building metal structures and products, sawn timber, wooden building structures, heat-insulating products, roofing and waterproofing materials, sheet glass, slate, gravel, sand, clay, etc. The author in [32] it is shown that the building complex is a set of self-managing subjects, including:

- on the resource principle of the enterprise sectors “construction” and “construction materials industry”, as well as other sub-sectors to ensure the construction of objects, means of labor and services;
- by the target principle as construction and construction materials industry, and design and survey and research, procurement of construction and educational institutions of the building profile.

The introduction in the domestic practice of innovative technological and design solutions using modern production of building materials that meet the requirements of world standards has always been aimed at reducing the funds and terms of construction of facilities. Professor Kondrakov [33] emphasises that in the course of carrying out economic activities, “deviations from planned for performance of work occur, for example, as a result of violation of plans for the supply of raw materials and materials,” and solutions are needed to ensure further effective activity. And for the adoption of the “managerial decision, the head conducts a comparative evaluation of alternative options and chooses the best of them,” taking into account the cost of production and their sales, taking into account the planned profit. In the article “Mathematical Methods in Economic Science: Evolution and Prospects” [34], authors noted that economic science has not yet developed methods that would lead to sustainable crisis-free management and long-term forecasting of the economic system, and the development of more sophisticated mathematical methods capable of adequately describing occurring processes, is only in the initial stage [36]. In the Soviet era, the economic and mathematical school, formed in the 50–60’s of XX century., was represented by the works of A.G. Aganbegyan, A.G. Granberg, L.V. Kantorovich, B.S. Nemchinova, V.V. Novozhilova, N.Ya. Petrakova, Ya.S. Pontryagin, N.P. Fedorenko, S.S. Shatalin and many others who have implemented the game theory model, econometrics analysis, general market equilibrium, economic growth, interindustry balance, linear and dynamic programming, optimal management, etc.

Particularly noted are the approaches to economics of the Nobel Prize laureate in economics V.V. Leontief “as a quantitative science, where the methods of quantitative analysis are not just a methodological device used by the researcher, but in themselves become the subject of study” [35]. In the Professor M.D. Kargopolov’s matrix formula, developed taking into account the work of Leontiev [35, 36], Kossova [37], etc., the basic tool of economic calculations are the inter-operational balances of costs and outputs of production at the enterprise, calculated by balance methods on the basis of a strict relationship between costs and output, both between production and consumption of products, laid down in the balance-sheet “costs - production” B.B. Leontief.

In the production of products in [15–17] the following concepts are used: “simple products”, under which products (work, service) are considered that use only primary resources purchased by the enterprise (PR), and complex products designate products

(work, service), in the production of which both primary resources and own resources (OPR), that is, various n-types of products (works, services) produced at the enterprise are used.

In the well-known balance equation of Leontief [36]: $X = (E - A) - 1 Y$, in matrix form the main and possible is the solution variant, where the levels of production of final (commodity) output (Y) are known (preset), and the levels of production of gross output (X) are the sought (calculated) ones.

The Professor Kargopolov's matrix formula to determine the production prime cost of products has the form [17, p. 37]:

$$P = (E - AT) - 1 * DT * C,$$

where: $P = \|p_j\|$; $j = \overline{1, n}$ — the required (calculated) vector-column of the production (full) production cost of a unit of output (works, services); E — the identity matrix $n \times n$; $A = \|a_{ij}\|$, $i = \overline{1, n}$, $j = \overline{1, n}$ — matrix $n \times n$ norms of consumption of resources of own production; $D = \|d_{ij}\|$, $i \in L \cup R$, $j = \overline{1, n}$ — the matrix of norms of consumption of primary resources (L - variables, R - constants), $C = \|c_i\|$, $i \in L \cup R$, — vector-column of wholesale and procurement prices of primary resources; T – transpose sign for matrices A and D.

To calculate the unit cost of production according to the Professor M.D. Kargopolov's matrix formula, two groups are required in the cost items: the costs of own resources (OPR) and primary resources (PR), with the allocation of variables (L-types) and constants (R-types), with flow rates dl_j - for resource variables that do not depend on production volumes, and dr_j - for constants that depend on them.

The required (calculated) values of the elements of the vector P in the matrix formula in the Microsoft Office Excel environment are defined as follows [15–17]: =MMULT (MMULT(MINVERSE(E-TRANPOSE(A));TRANPOSE(D));C).

According to this matrix formula of Professor M.D. Kargopolov all calculations of the cost of production of a unit of n-types of products (works) of any complexity are carried out simultaneously and with absolute accuracy.

Examples of calculations using the matrix formula are disclosed in [23–30, 51–52].

It can be noted that for the management accounting technique for calculating the cost of manufactured construction products according to the Professor M.D. Kargopolov's matrix formula allows to carry out all calculations simultaneously taking into account market factors and to allocate corresponding (variably required) changes in variables (direct) and constant costs according to multi-stage (multi-tier) chains of added value in the manufacture of products. This approach is important for the digital economy and the development of Industry 4.0 technologies.

On the new requirements of the time Smirnov in [40] showed that the process of digitalization is “a fundamentally transforming industrial production, when it becomes possible that the machines (equipment) exchange information with each other, self-organization of various processes occurs, and individual preferences of consumers are automatically included in the production process.... What is Industry 4.0? This is when in the manufacturing plant the machines autonomously coordinate production processes, service robots work together with people at the stages of clever assemblies, vehicles without a driver control the tasks of logistics...” [40].

Minister of Investment and Development of the Republic of Kazakhstan Kasymbek Zhenis Makhmuduly noted [41] that “in various countries appropriate medium- and long-term initiatives and concepts for the introduction of” Industry 4.0. “:” Industrie 4.0 “in Germany,” Industrie du Futur “in France, Manufacturing Innovation 3.0 in South Korea, Made in India in India, Industria Conectada 4.0 in Spain, National Technology Initiative in Russia, The New Robot Strategy in Japan, Manifattura Italia in Italy, China Manufacturing 2025 in China, etc.” [41].

It should be noted that in domestic practice, the definition of cost indicators and the identification of the effectiveness of innovative building materials and structures in digital form with the use of existing documents is difficult to perform because when determining the cost of innovative construction products (regardless of funding sources), the provisions of “Methodology for determining the value of construction products in the territory of the Russian Federation” [42] are recommended.

When calculating the cost of scientific and technical products, “Typical methodological recommendations for the planning, accounting and calculation of the cost of scientific and technical products [43], as well as” Basic provisions for the planning, accounting and calculation of production costs in industrial enterprises “[44] and industry methods developed with these provisions in mind.

Thus, according to paragraph 17 [44] when planning, accounting costs, forming the cost of production, groups of expenses are applied: at the place of origin (production, shops, sites, etc.); by types of products, works; by types of expenses (articles and elements of costs). It was noted in [44] that in connection with the calculation of the cost price for technical and economic factors, the costs are grouped into conditional-constant and conditionally variable, with the identification of a link with various production conditions or changes in technology, technology, and organization. So, conditional-constant costs are incurred, the absolute value of which, when the output volume changes, does not change significantly, and the conditional variable includes expenses, the amounts of which increase or decrease in connection with the change in output: the cost of raw materials and basic materials, fuel and energy, wages of workers, etc.

In the article, Suvorova and Boytsova [45] for accounting of costs, from the point of view of the concept of a single accounting information and from systemic accounting positions (financial, managerial and tax), it was proposed to solve problems: the use by managers of processed information on costs, including data reflected in accounting, including production and supply and marketing costs of competitors, average costs for the industry at the regional level, etc.; monitoring of current costs to monitor their compliance with indicators of strategic and current plans, identifying deviations and adjusting development strategies; to determine internal and external reserves to reduce current production costs, as well as efficient allocation and use of resources, etc.; introduction for the management of advanced methods of calculating the cost of production, etc. And in the conclusions the authors noted [45] that in Russian practice, the main element of the cost accounting in construction is the calculation, as the costing system accumulates all costs, giving managers the opportunity to decide before them the tasks in the fields of cost management, planning, control, pricing, etc.

At present, the formation of favorable conditions in the territories of advanced social and economic development (TASED) is topical for Russia [46], TASED are parts of the territory of the subjects of the Russian Federation, where for 70 years a

special legal regime is established for carrying out entrepreneurial and other activities with the formation of favorable conditions for attract investments, ensure accelerated socio-economic development and create comfortable conditions for ensuring the livelihoods of the population, Therefore, in these territories they decide (item 2–7 article10 [46]) on the construction and operation of highways; placement of infrastructure objects of TASED; transport services at TASED; power supply, heat supply, gas supply, cold and hot water supply, water disposal at TASED; collection, transportation of solid municipal waste, construction of facilities used to house and dispose of these wastes, as well as improvement of TASED; creation of conditions for the development of communication services, catering, trade and consumer services, leisure organization, etc. to ensure the life of people in TASED.

In the opinion of prof. Chebotayev in [47] the spread of logistics in the 80's. XX century. “The world economy was facilitated by the transition of the world's leading companies, including transnational ones, to strategic management based on the principles of modern management (MRP) and quality based on the developed standards ISO-9000-2001, and CALS - technologies (computer process support deliveries from the beginning of production and to the disposal of the goods)”, therefore, the job description of the “logistics manager” [48] indicates what he should know as the principles of forecasting and planning of logistics and production, and own the fundamentals of economic cybernetics, the economy, and to know the methods of mathematical modeling and formalization of the problems with the development of algorithms, etc. In the Strategy for the Development of the Construction Materials Industry for the Period to 2020 and Further Prospects until 2030, the state information system is considered as the basis for an interactive map on which the “geoinformation system of the building materials industry will allow to reflect in an actual manner the location of enterprises of the industry for each region countries, which will help to more quickly identify and assess the problems of the industry, identify priority areas for the deployment of new businesses If it is in the territory of the Russian Federation, it will also expand the opportunities for intra- and inter-branch technological, investment and marketing cooperation. The result will be the creation and development of the most efficient production and logistics chains both between enterprises and between producers and consumers” [14].

The program “Development of the transport system of Russia (2010–2020)” [49] noted that “regional uneven development of transport infrastructure limits the development of the single economic space of the country and does not allow to fully master the resources of the regions. The most significant differences between the European part of the Russian Federation and the regions of Siberia and the Far East, “while the differences between individual subjects of the Russian Federation” in density of paved roads per 1000 sq. M. km reach 450 times, “and Russia's losses due to” low capacity of the road network make up 3% of the gross domestic product, which is 6 times higher than in the countries of the European Union” [49].

Therefore, calculations on revealing, taking into account the raw material base and minimization of both the production cost and logistics costs for transportation to the construction site, options for the optimal planning of the production of building materials and structures, are becoming topical. In the conditions of the digital economy, this approach is especially relevant for determining the value indicators of products

manufactured at TASED [46] or for calculating the cost of final products in an innovation-territorial cluster [23, 27–29].

Further in Tables 1–4, the options for calculating the prime cost of reinforced concrete structures with initial data are shown [50]. In the example given, the calculation of the cost parameters of innovative products - reinforced concrete slabs (w/w slabs) differ: the amount of cement in the concrete and the components of binders, logistics costs Data on the manufacture of innovative structures - reinforced concrete slabs with complex binders (“Biotech-NM”, which increase the resistance of concrete when operating in an aggressive environment) made in helioforms with SWITAP coatings, allowing up to 70% of the design strength in reinforced concrete products to be obtained within one day, are accepted according to the Tables 4.1, 5.1, 5.3–5.7 [50] (Tables 1 and 2).

Table 1. The matrix A of resource consumption rates own production (7 × 7) (Part 1) and Matrix P_{m-m-1} (Part 2).

Part 1							Part 2		
Own production resources (OPR)- water	Dry concrete mix			R/C products with solar thermal image					
	KB 100	KBZ 50	KBP 50	KB 100	KBZ 50	KBP 50			
1	2	3	4	5	6	7			
0	0	0	0	0.14	0.152	0.162	1.	Water	0.0804
0	0	0	0	1	0	0	2.	KB 100	3.095
0	0	0	0	0	1	0	3.	KBZ 50	2.1437
0	0	0	0	0	0	1	4.	KBP 50	2.1357
0	0	0	0	0	0	0	5.	KB 100	5.1277
0	0	0	0	0	0	0	6.	KBZ 50	4.1774
0	0	0	0	0	0	0	7.	KBP 50	4.1702

For the example of calculation according to the Professor M.D. Kargopolov’s matrix formula the following matrices are formed:

- Part 1: matrix A (with a dimension of 7 × 7) of the norms of consumption of resources of own production (water, concrete mixes: KV 100, KVZ 50 and KVP 50), shows the norms of consumption of the i-th resource for the production of a j-th product according to [50].
- Part 2: matrix P_{m-m-1} - matrix of the calculated vector column, with production indicators of the values of the components of the dry mixture KV 100, KVZ 50, KVP 50 and reinforced concrete plates manufactured in helioforms, taking into account the costs of micro- and macro-logistics.
- Part 3: matrix D_{m-m-1} - the matrix of the norms of primary resources (OL) and wholesale prices of composite concrete according to the data of [50], with conditional costs for micro- and macro-logistics (due to the lack of these data in [50]), where the primary resources are divided into two groups of primary resources:

Table 2. The matrix D_{m-m-1} of the norms of expenditure of primary resources, including purchased, for the production of reinforced concrete products (Part 3) and S_{m-m-1} (Part 4).

Part 3									Part 4	
Naming of expenditures by levels and cost elements										
		OPR	Dry concrete mix			R/C products with solar thermal image				
		Water	KB 100	KBZ 50	KBP 50	KB 100	KBZ 50	KBP 50		
		1	2	3	4	5	6	7		
Conditional variable costs ^(*)	Material costs	Capital investments in helioforms thous. rubs	0	0	0	0	0.012	0.012	0.012	1
		Cement, thous. rub/t	0	0.5	0.254	0.254	0	0	0	5
		Screening of crushing thous. rub/t	0	1.5	1.524	1.492	0	0	0	0.25
		Filler thous.rub/t	0	0	0.254	0.254	0	0	0	1.5
		BIO-FILLER, thous.rub/t	0	0.01	0.005	0.005	0	0	0	22
		Armature, thous.rub/t	0	0	0	0	0.065	0.065	0.065	5
		Water, thous. r	0.0237	0	0	0	0	0	0	1
		Electricity + fuel thous.rubs	0.0124	0	0	0	0.2794	0.2794	0.2794	1
	Salary, thous.r	0.01	0	0	0	0.3439	0.3439	0.3439	1	
	Deductions for insurance contributions - 34% of the salary,thous.rub (2011)	0.0034	0	0	0	0.1169	0.1169	0.1169	1	
Expenses for operation. Equipment - 127,8% of w/fee, thousand rubles	0.01278	0	0	0	0.4395	0.4395	0.4395	1		
Other costs thousand rubles	0.0137	0	0	0	0	0	0	1		
Conditional-fixed costs ^(*)	Shop costs - 25% from salary (thousand rubles)		0.0025	0	0	0	0.086	0.086	0.086	1
	General plant costs - 20% from payment, thousand rubles		0.002	0	0	0	0.06878	0.06878	0.06878	1
Micrologistics	Loading and unloading costs of work (thousand rub/tonne)		0	0	0	0	0.1	0.1	0.1	1
Macrologistics	Loading and unloading costs of work (thousand rubles/tonne)		0	0	0	0	0.1	0.1	0.1	1
	The cost of transportation (thousand rubles/tonne)		0	0	0	0	0.15	0.15	0.15	1

conditional variables^(*) with L-types and conditionally-constant^(*) resources, with the number of R-types.

- Part 4: matrix $S_{m-m-1} = [c1 \dots cL \dots cr \dots cR]L + R$ - vector-column of wholesale prices of primary resources (where l - conditionally-variable, r - conditionally-constant), that is, the acquisition price vector (or the creation) of primary resources (in the matrix D, the data was taken by [50]), and containing the value units that are the same for production resources and manufactured products in thousand rubles, which include indicators and costs for micro- and macro-logistics.

For Part 4, it is important to note: if in the matrix D individual costs are taken in rubles, then in Table 4 they are denoted - 1 (unit).

The identity matrix E has the dimension of the matrix A (7×7) (not shown).

In matrix P_{m-m-1} the calculated values of all components of the reinforced concrete slab are calculated, taking into account the cost of the composition of materials with the addition of the conventional costs for micro- and macro-logistics (in practice, real values should be taken for logistical costs).

4 Conclusions

1. In accordance with the Message of the President of the Russian Federation to the Federal Assembly (01.12.2016), the “Strategy for Scientific and Technological Development of the Russian Federation” (01.12.2016) and the program “Digital Economy of the Russian Federation” (July 28, 2017), now in Russia a course is taken for a large-scale formation of the national digital economy, which digitizes the implementation of sectoral strategies and government development programs of the country, including the areas of advanced social and economic development in the Russian Federation in Daln the Eastern Federal District and other regions, where it is required to make effective decisions on production and logistics chains between producers and consumers, and, accordingly, the development of enterprises of the construction materials industry, road transport and other territorial and branch enterprises in the region.
2. For the purposes of digital forecasting of cost indicators of products (for example, the production of innovative products - reinforced concrete slabs with the use of complex binders (“Biotech-NM”, increasing the resistance of concrete in aggressive environments) and manufactured in helioforms with SWITAP coatings, allowing up to 70% design strength in reinforced concrete products to be obtained within one day), it is recommended to use Professor M.D. Kargopolov’s matrix formula as an economic and mathematical model of the interoperational balance of costs and results of production of building materials.
3. At the present stage, the Professor M.D. Kargopolov’s matrix formula should be considered as a tool of the digital economy, allowing to perform calculations of the value of construction products taking into account all factors necessary for comparison, affecting the final cost of production. Calculations of the cost (cost price) of products according to the Professor M. D. Kargopolov’s matrix formula allow you to differentiate, as well as analyze and take into account all the pricing conditions of the final product, ie. take into account all the objective conditions associated with various territorial factors (district coefficients for wages) or the cost of road transport (taking into account distances, etc.) conditions of production.
4. Calculations using the Professor M.D. Kargopolov’s matrix formula is recommended to be used in management, internal audit and controlling when calculations are required to analyze the factors affecting the final price of production, taking into account the added costs in the production chain and the delivery of products to the consumer, which is especially important for determining the cost of final cluster products to account for the production efficiency of components products by different manufacturers.

References

1. About the approval of the program “Digital Economy of the Russian Federation”. Order of the Government of the Russian Federation № 1632-r (2017). <http://base.consultant.ru/>
2. Message from the President of the Russian Federation to the Federal Assembly (2016). <http://base.consultant.ru/>
3. Strategy of scientific and technological development of the Russian Federation. Decree of the President of the Russian Federation of December 1, 642 (2016). <http://base.consultant.ru/>
4. Forecast of scientific and technological development of the Russian Federation for the period until 2030 (approved by the Government of the Russian Federation). <http://base.consultant.ru/>
5. On the Strategy for the Development of the Information Society in the Russian Federation for 2017–2030. Decree of the President of the Russian Federation № 203 (2017). <http://base.consultant.ru/>
6. Urmantseva, A.: Digital economy: as specialists understand this term. <https://ria.ru/science/20170616/1496663946.html>
7. Meeting of the Council for Strategic Development and Priority Projects. <http://kremlin.ru/events/president/news/54983>
8. On the tool for operational management of the implementation of the program “Digital Economy of the Russian Federation”. <http://government.ru/docs/28824/>
9. About the Ministry of Construction and Housing and Communal Services of the Russian Federation. Decree of the Government of the Russian Federation № 1038 (2017). <http://base.consultant.ru>
10. About development of a building complex and perfection of town-planning activity in the Russian Federation. Materials of the meeting of the State Council of the Russian Federation (2016). <http://kremlin.ru/events/president/news/51926>
11. About the Ministry of Industry and Trade of the Russian Federation. Decree of the Government of the Russian Federation № 438 (2017). <http://base.consultant.ru/>
12. On the approval of the plan of measures for the implementation of the Strategy for the Development of the Building Materials Industry for the period to 2020 and further prospects until 2030. Order of the Government of the Russian Federation № 630-r (2017). <http://base.consultant.ru/>
13. Anikin, B.: Logistics: Training Manual. In: Anikina, B., Rodkinoy, T. (eds.) Publishing House: Prospect, Moscow (2005)
14. On the Strategy for the Development of the Construction Materials Industry for the Period to 2020 and Further Prospects until 2030. Ordinance of the Government of the Russian Federation № 868-r (2016). <http://base.consultant.ru/>
15. Kargopolov, M.: Matrix formula for the production cost and unit price of products (works, services). Materials of the International Scientific Conference Mathematics, Economics. St. Petersburg State University, St. Petersburg (2012)
16. Kargopolov, M.: Inter-operational Balances of Costs and Production Results: Theory and Practice. Publishing House of ASTU, Arkhangelsk (2001)
17. Kargopolov, M.: Balanced Methods in Economic Calculations at the Enterprise: Textbook. CPI SAFU, Arkhangelsk (2012)
18. Kuladzhi, T., Babkin, A., Murtazaev, S.: Recommendations on the digital matrix micro-forecasting of the cost of innovative products. Economics and management in the conditions of nonlinear dynamics. Publishing house of the Polytechnical University, St. Petersburg (2017). <https://doi.org/10.18720/IEP/2017.2/29>

19. Kuladzhi, T., Babkin, A., Murtazaev, S.: Digital Economy: Product Costing Calculations Based on the Matrix Approach. Digital Economy and “Industry 4.0.”: Problems and Prospects. Publishing house of the Polytechnical University, St. Petersburg (2017)
20. Kuladzhi, T.: Digital matrix micro forecasting of the rationalization proposal evaluation in construction. *Compet. Glob. World: Econ. Sci. Technol.* **4**(6), 51–61 (2017)
21. Vakhrusheva, O.: Formation of management accounting on the basis of harmonization of accounting, analysis, budgeting and control. *Auditor* **11** (2014). <http://base.consultant.ru>
22. Alekseev, B.: Philosophical problems of formalization. L. (1981)
23. Kuladzhi, T.: Algorithm of micro-forecasting of organization of production of competitive building products in a cluster. *Vestnik MGSU* **12**, **3**(102), 273–283 (2017). <https://doi.org/10.22227/1997-0935.2017.3>
24. Kuladzhi, T., Murtazaev, S.: Use in micro - macrologistics of the construction of the matrix formula of Professor MD. Kargopolova. *Compet. Glob. World: Econ. Sci. Technol.* **7**(1), 176–183 (2016)
25. Kuladzhi, T., Kutukova, E., Murtazaev, S., Idilov, I.: Increase of efficiency of the managerial accounting with use of modern approaches of calculation of cost of innovative building production. *Quest. Econ. Right* **9**, 80–84 (2015)
26. Kuladzhi, T., Kutukova, E., Murtazaev, S., Taymaskhanov, Z.: A matrix approach to the evaluation of innovative building products in controlling. *Issues Econ. Law* **2**, 98–102 (2016)
27. Kuladzhi, T.: Cluster Economy: A Matrix Tool for Assessing the Efficiency of Production: Monograph. Publishing House of the SAFUIM. M.V. Lomonosov, Arkhangelsk (2014)
28. Kuladzhi, T.: Methodology for Evaluating the Effectiveness of Constructive Solutions in the Building Complex: Monograph. Publishing House of Safuu. M.V. Lomonosov, Arkhangelsk (2014)
29. Kuladzhi, T., Iskichekova, N.: Clusters as the most important tool for promoting innovation. *Bull. Univ. “Turan”* **4**(64), 57–63 (2014)
30. Murtazaev, S., Kuladzhi, T.: Use of the matrix formula M.D. Kargopolova in the calculation of the cost of construction materials. Information technologies in the study of the Northern and Arctic territories: materials of the NPK. CPI CAFU, Arkhangelsk (2012)
31. Galenko, V.: Thematic issue: accounting and tax accounting of materials in the construction organization. *Econ. Leg. Bull.* **8** (2015). <http://base.consultant.ru/>
32. Tserpento, S.: Accounting in construction: uch. Allowance. KNORUS, Moscow (2011)
33. Kondrakov, N.: Accounting (Financial, Managerial) Accounting: A Textbook. Prospekt, Moscow (2013)
34. Barlybaev, A., Yunusova, G.: Mathematical methods in economic science: evolution and perspectives. *Econ. Anal.: Theory Pract.* **23** (2009). <http://base.consultant.ru>
35. Leontiev, V.: Economic essays. Theory, research, facts and politics. Political Literature, Moscow (1990)
36. Leontiev, V.: Interindustry Economics. Publishing House “Economics”, Moscow (1997)
37. Kossov, V.: Interindustry Models. Economics, Moscow (1973)
38. Smirnov, F.: Transformation of the world financial system: blockage, “smart contracts” and off-exchange derivatives. *The Auditor* **6** (2017). <http://base.consultant.ru>
39. Mahmuduly, K.: Industry 4.0. <http://eenergy.media/2017/02/08/industriya-4-0>
40. On the approval and implementation of the Methodology for determining the value of construction products on the territory of the Russian Federation Decree of the State Construction Committee of Russia № 15/1 (2014). <http://base.consultant.ru>
41. Typical methodological recommendations for planning, accounting and calculating the cost of scientific and technical products № OR-22-2-46ю (1994). <http://base.consultant.ru>

42. The main provisions for the planning, accounting and calculation of the cost of production in industrial enterprises (1970). <http://base.consultant.ru>
43. Suvorova, S., Boytsova, N.: Accounting for the production costs of construction organizations for the purposes of strategic management. *Constr.: Tax. Acc.* **2** (2006). <http://base.consultant.ru/>
44. About the territories of advanced social and economic development in the Russian Federation. Federal Law № 473-FZ (2016). <http://base.consultant.ru>
45. Chebotaev, A.: Logistics and Marketing (Marketinglogistics). Ekonomika, Moscow (2005)
46. Liberman, K.: Instruction instructions. In: Shalaeva, A. (ed.) GrossMedia. ROSBUKH (2017). <http://base.consultant.ru/>
47. About the Federal Target Program “Development of the Transport System of Russia (2010–2020)”. Decree of the Government of the Russian Federation № 848 (2017). <http://base.consultant.ru>
48. Aliev, S.: Concrete composites based on technogenic raw materials for dry hot climate conditions. Diss. to the soot. candidate of science, Makhachkala (2011)
49. Kuladzi, T., Murtazaev, S., Taimaskhanov, K., Aliiev, S., MintsaeV, M.: Professor M.D. Kargopolov’s matrix formula-an effective tool to find the cost of construction products. *Indian J. Sci. Technol.* **8**(29), 0974–6846 (2015). <https://doi.org/10.17485/ijst/2015/v8i29/IPL0975>
50. Taimaskhanov, K., Kuladzi, T., MintsaeV, M., Salgiriev, R., Khuriev, R.: Calculating the innovative construction products cost by using professor M.D. Kargopolov’s matrix formula. *Int. J. Environ Sci. Educ.* **11**(18), 12737–12751 (2016). ISSN 1306-3065

Author Index

A

Abaidullina, Tatiana, 980
Abdrzakov, Rais, 1224
Abelev, Mark, 1186
Adamtsevich, Aleksey, 402, 608
Afanas'ev, Alexander, 1177
Agapov, Vladimir, 1009
Akhtiamov, Midkhat, 987
Akopyan, Vladimir, 647
Aksenov, Nikolay, 536
Aksenov, Vladimir, 536
Alekseeva, Tatyana, 120
Alikova, Zalina, 1243
Alimov, Lev, 601
Alpackaya, Irina, 1265
Alwahab, Yaser Abd, 634
Anisimov, Aleksandr, 177
Anisimov, Alexandr, 31
Anisimov, Vladimir, 177
Antonov, Valery, 915
Artiukh, Viktor, 201, 212, 220, 1065
Aslanov, Gevork, 1243
Astrakhantsev, Leonid, 120
Atamaniuk, Iryna, 555
Averkeev, Ilya, 391

B

Babkin, Aleksandr, 1333
Bagautdinov, Ruslan, 1036
Bajramukov, Salis, 902
Balalayeveva, Elena, 220
Bardin, Alexey, 818
Barinov, Sergey, 830
Bayramukov, Salis, 885
Bekkiev, Mukhtar, 869, 877
Belentsov, Yuri, 640
Belyaev, Alexey, 529
Beresneva, Natalia, 739
Beskopylny, Alexey, 184

Bezgodov, Igor, 440
Blagodatskaya, Angelina, 739
Bobyashov, Victor, 801
Bogdanovičs, Raimonds, 543
Bolotova, Alina, 1160
Bondarenko, Valery, 894
Borodinecs, Anatolijs, 543
Bozhuk, Svetlana, 1234
Braila, Natalia, 356
Bushuev, Nikolay, 801
Buslov, Anatoly, 769
Butyrin, Andrey, 201, 212, 473, 482

C

Ćetković, Jasmina, 1151
Chepur, Petr, 936, 962, 980
Chepurmenko, Anton, 808
Cheremisin, Vasily, 83
Cherepanov, Aleksandr, 91, 100
Cherevatova, Alla, 776
Chetvergov, Vitaly, 31
Chulkov, Vitaliy, 367, 1186
Chusov, Alexander, 908, 921, 1046
Cipurskij, Il'ja, 1194

D

Danilina, Nina, 299
Davydov, Boris, 236
Davydov, Roman, 915
Derevianko, Oleg, 1024
Didikov, Roman, 192
Divac, Ljubo, 1055
Dmitrenko, Elena, 440
Dmitriev, Sergey, 655
Dobretsov, Roman, 192
Dolganov, Andrey, 1160
Dolzhiikov, Peter, 647
Drozd, Vladimir, 1017
Drozdov, Anatoly, 750

Dulskiy, Evgeny, 109
Dunichkin, Ilya, 446

E

Efimenko, Anatoly, 367
Epifanova, Marina, 921
Evseev, Evgeny, 1125

F

Fedyukhin, Alexander, 1024
Fomin, Alexander, 520
Fomina, Ekaterina, 520
Frishter, Lyudmila, 837
Frolova, Anastasya, 498

G

Gabitova, Gulnara, 830
Galyshev, Yuriy, 192
Gamayunova, Olga, 432
Gilemkanov, Rustam, 1036
Ginzburg, Alexander, 1160, 1177
Glasunov, Andrey, 801
Glazko, Vladyslav, 220
Golokhvast, Kirill, 1017
Golovanov, Roman, 1009
Goncharova, Elena, 145
Goncharuk, Sergey, 177
Gopkalo, Vadim, 236
Gorshkov, Aleksandr, 577
Goryunov, Vladimir, 12
Gravit, Marina, 739, 818, 1093
Gribach, Dmitry, 490
Gruchenkova, Alesya, 936, 962
Gulkova, Svetlana, 1017
Gumba, Khuta, 326
Gumerova, Eliza, 432, 818
Gusarova, Miroslava, 1204
Gutman, Svetlana, 453

H

Haritonova, Larisa, 700
Harmathy, Norbert, 563

I

Iliashenko, Oksana, 1306
Iliashenko, Oxana, 1214
Ilin, Igor, 1214, 1306
Ishkov, Alexey, 655
Ivanov, Pavel, 109

K

Kadyshev, Nikolay, 776
Kalinina, Olga, 453, 1315

Kankhva, Vadim, 220, 1036
Kapustyan, Mikhail, 69
Karanina, Elena, 318
Kashtanov, Alexey, 83
Katasonov, Alexander, 655
Katin, Viktor, 987
Kazharsky, Aleksey, 145
Kharitonov, Alexey, 640
Kharlamov, Viktor, 24, 76
Kholodov, Aleksei, 1017
Khudonogov, Anatoliy, 109
Kim, Marina, 998
Kim, Vyacheslav, 998
Kiselev, Arkadiy, 367
Klochko, Aleksey, 615
Klochko, Asmik, 615
Knyazeva, Nataly, 1186
Kondratenko, Tatyana, 710
Konjević, Nikola, 345
Kontra, Jenő, 563
Kopytova, Anna, 1093, 1204
Korolchenko, Dmitry, 783
Korotkin, Viktor, 184
Korovyakov, Vasilii, 601
Kostenko, Dmitry, 845
Kosygin, Vladimir, 987
Kovshun, Vyacheslav, 953
Kozhevnikova, Sophia, 1177
Kozhukhova, Natalia, 520, 776
Kravchenko, Galina, 845
Kruglova, Inna, 1323
Kryukov, Andrey, 91, 100
Kubenin, Alexander, 490
Kudryavtsev, Sergey, 145, 953
Kukhar, Volodymyr, 201, 220
Kuladzhi, Tamara, 1333
Kuzina, Ekaterina, 410
Kuznetsova, Tatiana, 555
Kvitko, Alexandr, 859

L

Lanko, Alexander, 1102
Lapidus, Azary, 1168
Larsen, Oksana, 601
Lazarević, Luka, 3, 791
Lepekhin, Aleksandr, 1306
Levina, Anastasia, 1214, 1306
Linkov, Aleksey, 134
Litvinov, Stepan, 885, 902
Lukinov, Vitaly, 818
Lukmanova, Liliya, 852
Lushin, Kirill, 776

M

Magyar, Zoltán, 563
 Mailyan, Dmitry, 529, 536
 Makarov, Alexander, 1168
 Makasheva, Svetlana, 154, 162
 Malikov, Vladimir, 655
 Maloyan, Garrik, 367
 Malyavina, Elena, 498
 Malysheva, Olga, 170
 Manukhina, Lyubov, 1254
 Manukhina, Olga, 1046
 Margolin, Vladimir, 769
 Marjanović, Miloš, 625
 Maslikov, Vladimir, 908, 1046
 Matveeva, Larisa, 640
 Mazur, Vladlen, 212, 1065
 Melnichenko, Oleg, 134
 Melović, Boban, 1265, 1282
 Meshcheriakova, Tatiana, 1136
 Meshcheryakova, Tatiana, 432
 Minnullina, Anna, 1224
 Mirković, Nikola, 3, 1055
 Mirković, Uroš, 1055
 Miroshnikova, Tatyana, 256, 334
 Mitrović, Slavica, 1265, 1282
 Molodtsov, Dmitry, 915, 1046
 Mordvintsev, Konstantin, 634
 Moskalev, Yuriy, 76
 Mottaeva, Angela, 1151
 Mukhametrakhimov, Rustem, 852
 Murgul, Vera, 563, 577
 Murtazaev, Said-Alvi, 1333
 Musorina, Tatiana, 417, 473, 482
 Mut, Aleksandra, 953

N

Narezhnaya, Tamara, 247
 Nedevska, Ivana, 247
 Nedviga, Ekaterina, 739
 Nesterova, Natalia, 177
 Nesvetaev, Grigory, 529
 Neumerzhitskaya, Natalia, 808
 Nidziy, Elena, 1065
 Nikiforov, Mikhail, 83
 Nikolenko, Maxim, 710

O

Obradović, Nikola, 1055
 Ognjenovic, Slobodan, 247
 Onishkov, Nikolay, 184
 Orlov, Alexandr, 282
 Orlov, Vladimir, 391, 689
 Ostrovaia, Anastasia, 417

P

Pankratenko, Alexander, 1111
 Paramonov, Aleksandr, 1074, 1083
 Peiyu, Shi, 265
 Pelipenko, Alexey, 391
 Peresyppkin, Evgeniy, 869, 877
 Philippov, Victor, 59
 Pigurin, Andrey, 783
 Pinchukov, Pavel, 154, 162
 Plavelsky, Evgeny, 760
 Pleshko, Michael, 1111
 Pletneva, Natal'ya, 1234
 Poddaeva, Olga, 490
 Podgornaya, Svetlana, 48
 Politaeva, Natalia, 555
 Politi, Violetta, 289
 Popov, Denis, 76
 Popović, Zdenka, 3, 791, 1055
 Prokopov, Albert, 647
 Prysiaznyi, Andrii, 201, 220
 Pshennikov, Kirill, 356
 Pujević, Veljko, 625
 Pukhkal, Viktor, 379, 512
 Pushenko, Sergey, 710
 Pustovgar, Andrey, 608

R

Radovanović, Slobodan, 1055
 Radović, Goran, 345
 Razov, Igor, 666
 Rimshin, Vladimir, 410
 Romanov, Petr, 463
 Romanova, Galina, 1111
 Romanova, Irina, 463
 Romanovich, Marina, 265
 Rondović, Biljana, 1265, 1282
 Rossinskaya, Marina, 1111
 Ryabchyonok, Natalya, 120
 Ryabova, Antonina, 640
 Ryazanova, Olesya, 318

S

Sagalakov, Anatoly, 655
 Salya, Ilya, 12
 Saveleva, Nelli, 1111
 Selezneva, Anna, 473
 Sergievskaya, Natalia, 417
 Sergina, Natalia, 710
 Sevryugina, Nadezhda, 273
 Shagimuratova, Anna, 299
 Shangina, Nina, 640

Shantarenko, Sergei, 69
 Sharapov, Rashid, 760
 Shashina, Irina, 1323
 Shendrik, Viktor, 859
 Shestakov, Ignat, 24
 Shevchenko, Andrey, 1296
 Shilova, Liubov, 402, 608
 Shirokov, Lev, 310
 Shirokova, Olga, 310
 Shishkin, Alexander, 921
 Shkodun, Pavel, 24
 Shoshinov, Vitaly, 1282
 Sidorov, Oleg, 12, 59
 Sidorova, Elena, 48
 Sigova, Mariia, 1323
 Silka, Dmitriy, 921
 Simonyan, Vladimir, 729
 Skuratov, Sergey, 877, 894
 Smirnov, Anatoly, 592
 Smyatskaya, Yulia, 555
 Sokolov, Vladimir, 666
 Soloviev, Vyacheslav, 170
 Solovyev, Dmitry, 402
 Statsenko, Elena, 417
 Šteinerte, Kristīne, 543
 Stepanov, Vitaliy, 750, 1177
 Stepanova, Tatiana, 1024
 Stratiy, Pavel, 970
 Strogonov, Konstantin, 1024
 Sukhanov, Kirill, 592
 Sukhorukov, Sergei, 170
 Supchinsky, Oleg, 69
 Synitsyn, Denis, 720

T

Tarasenko, Alexander, 936, 944, 962
 Tarasenko, Mikhail, 944
 Taskaeva, Natalia, 256, 334
 Taurit, Voldemar, 379
 Timin, Alexander, 318
 Tomilov, Valery, 12
 Trebukhin, Anatoliy, 915
 Trinchenko, Aleksey, 1074, 1083
 Trukhina, Elena, 555
 Trush, Lyubov, 885
 Tshovrebov, Edward, 1296
 Tsurikov, Sergey, 845
 Turko, Michael, 808
 Turko, Mikhail, 869

Tuskaeva, Zalina, 1243
 Tuzenko, Olga, 220

U

Ugay, Sergey, 1017
 Ushakov, Sergey, 83
 Utkina, Ekaterina, 356
 Uvarova, Svetlana, 326

V

Vaititckii, Artem, 1093
 Valebnikova, Olga, 1315
 Valtseva, Tatiana, 145
 Vasilyeva, Olga, 908
 Vaynshteyn, Michael, 1160
 Vedyakov, Ivan, 1160
 Velichko, Evgeniy, 1296
 Verstina, Natalia, 1125, 1136
 Vieira, Gabriel, 482
 Vilotijević, Milica, 3, 791
 Vlasov, Denis, 299
 Vlasova, Marina, 1323
 Voitovich, Elena, 520, 776
 Vol'khin, Igor, 987
 Voronin, Victor, 601
 Vukićević, Mirjana, 625
 Vysokovsky, Dmitry, 877

Y

Yagovkin, Dmitry, 134
 Yastremsky, Dmitry, 980
 Yazyev, Serdar, 869, 894, 902
 Yazyeva, Svetlana, 894

Z

Zaborova, Daria, 473, 482, 830
 Zafirovski, Zlatko, 247
 Zajacs, Aleksandrs, 543
 Zakaryukin, Vasilii, 91, 100
 Zakieva, Nadezhda, 885
 Zaychenko, Irina, 453
 Zemenkova, Maria, 679
 Zhazhkov, Viacheslav, 908
 Zhila, Victor, 615
 Zhuravlev, Alexander, 902
 Ziyue, Wang, 265
 Zotkin, Sergey, 689
 Zotkina, Natalia, 1204
 Zybina, Olga, 1093